



Provided by the author(s) and University of Galway in accordance with publisher policies. Please cite the published version when available.

Title	A Mathematical and Numerical Examination of Wave-Current Interaction and Wave-Driven Hydrodynamics
Author(s)	Newell, Carl
Publication Date	2010-04-28
Item record	http://hdl.handle.net/10379/1966

Downloaded 2024-04-25T00:30:31Z

Some rights reserved. For more information, please see the item record link above.





NUI Galway
OÉ Gaillimh

A Mathematical and Numerical Examination of Wave-Current Interaction and Wave-Driven Hydrodynamics

CARL NEWELL

carl@newelleng.ie

*Civil Engineering,
National University of Ireland, Galway*

**Professor of Civil Engineering:
Prof. Padraic O' Donoghue**

**Research Supervisor:
Dr. Thomas Mullarkey**

**Ph.D. Thesis
April 2010**

Contents

CONTENTS.....	III
ABSTRACT	IX
DECLARATION.....	X
ACKNOWLEDGEMENTS	XI
NOMENCLATURE.....	XII
CHAPTER 1: INTRODUCTION	1
CHAPTER 2: LITERATURE AND STATE-OF-THE-ART REVIEW	5
2.1 Introduction	5
2.2 Coastal Zone Processes.....	6
2.2.1 Gravity Waves	6
2.2.2 Wave Behaviour.....	7
2.2.2.1 Reflection.....	7
2.2.2.2 Shoaling	8
2.2.2.3 Refraction	8
2.2.2.4 Diffraction	9
2.2.2.5 Breaking.....	10
2.2.2.5.1 Spilling Breakers	10
2.2.2.5.2 Plunging Breakers	11
2.2.2.5.3 Collapsing Breakers	11
2.2.2.5.4 Surging Breakers	12
2.2.3 Water Particle Velocity	13
2.2.4 Set-up/Set-down.....	14
2.2.5 Wave Generated Currents	15
2.2.6 Wave-Current Interaction	16
2.2.7 Turbulent Diffusion / Lateral Mixing	17
2.2.8 Bottom Friction.....	17
2.3 Mathematical Description of Coastal Zone Processes	18
2.3.1 Wave Theories	18
2.3.1.1 Regular Wave Theory.....	18
2.3.1.1.1 Linear (Airy) Theory.....	19
2.3.1.1.2 Non-Linear Theory	20
2.3.1.1.2.1 Finite Amplitude Wave Theories	20
2.3.1.1.2.1.1 Stokes Theory	20
2.3.1.1.2.1.2 Cnoidal Theory	22
2.3.1.1.2.1.3 Boussinesq Theory	22
2.3.1.1.2.1.4 Solitary Wave Theory	23
2.3.1.1.2.2 Numerical Wave Theories	24
2.3.1.2 Irregular Wave Theory.....	24
2.3.2 Wave Breaking	25
2.3.3 Set-up/Set-down.....	26
2.3.4 Wave Generated Currents	27
2.3.5 Wave-Current Interaction	27
2.4 State-of-the-Art Modelling of Coastal Zone Processes	29
2.4.1 Wave Models	29
2.4.1.1 Introduction to Computer Wave Models.....	29
2.4.1.2 Energy Balanced Wave Models.....	29
2.4.1.3 Phase Resolving Wave Models.....	29
2.4.1.3.1 Introduction to Phase Resolving Wave Models	29
2.4.1.3.2 Steady State Phase Resolving Wave Models.....	30
2.4.1.3.3 Historical Development of Phase Resolving Models	31
2.4.1.3.3.1 Ray Tracing Techniques	31
2.4.1.3.3.2 Elliptic Mild-Slope Equation	32
2.4.1.3.3.3 Parabolic Approximation to Mild-Slope Equation	37
2.4.1.3.4 Examples of Steady State Phase Resolving Wave Models based on Linear Theory.....	38
2.4.1.3.4.1 RCPWAVE.....	38
2.4.1.3.4.2 REF/DIF.....	38

2.4.1.3.4.3 CGWAVE	39
2.4.1.3.4.4 Clyne (2008).....	40
2.4.1.3.4.5 MIKE 21.....	40
2.4.1.3.4.6 PHAROS.....	40
2.4.2 Models of Nearshore Currents and Set-up/Set-down	42
2.4.2.1 Introduction	42
2.4.2.2 Analytical Calculation of Wave-Driven Currents	42
2.4.2.3 Cross Shore Profile of Longshore Currents	43
2.4.2.4 Analytical Calculation of Set-up/Set-down	44
2.4.2.5 Bed Friction	44
2.4.2.6 Numerical Models for Wave-Generated Currents and Set-up/Set-down	45
2.4.2.6.1 Introduction.....	45
2.4.2.6.2 NMLONG	45
2.4.2.6.3 MIKE 21 HD	46
2.4.2.6.4 TELEMAC-3D.....	46
2.4.2.6.5 Newell et al. (2005b)	46
2.5 Research Decisions based on Literature and State of the Art Review.....	47
2.5.1 Newell Mullarkey Wave-Current Interaction Model (NM-WCIM)	47
2.5.2 Newell Mullarkey Wave-Driven Hydrodynamic Model (NM-WDHM).....	47
CHAPTER 3: WAVE CURRENT INTERACTION MODEL	49
3.1 Introduction.....	49
3.2 Equations of Continuity and Momentum	51
3.2.1 Continuity Equation	51
3.2.2 Momentum Equation	52
3.3 Application of Velocity Potential to Continuity and Momentum Equations	57
3.3.1 Application of Velocity Potential to the Continuity Equation.....	57
3.3.2 Separation of Velocity and Free Surface Height into Steady and Unsteady Components	57
3.3.3 Laplace's Equation.....	58
3.3.4 Application of Velocity Potential to the Momentum Equation	58
3.4 Non-Linear Boundary Conditions	64
3.4.1 Kinematic Free Surface Boundary Condition for Laplacian Equation.....	64
3.4.2 Dynamic Free Surface Boundary Condition for Laplace's Equation	68
3.4.3 Combined Free Surface Boundary Condition for the Laplace Equation	69
3.4.4 Kinematic Seabed Boundary Condition	69
3.4.5 Summary of Laplace's Equation and Non-Linear Boundary Conditions	72
3.5 Harmonic Form of Wave Equations.....	73
3.5.1 Laplace's Equation	73
3.5.2 Dynamic Free Surface Boundary Condition.....	74
3.5.3 Combined Free Surface Boundary Condition.....	74
3.5.4 Kinematic Seabed Boundary Condition	76
3.5.5 Summary of Harmonic Wave Equations	77
3.6 Vertical Function for Two-Dimensional Laplace Equation.....	78
3.6.1 Propagation of Simple Harmonic Waves on a Constant Depth.....	78
3.6.2 Governing Equations for Vertical Function	79
3.6.2.1 Laplace's Equation	79
3.6.2.2 Combined Free Surface Boundary Condition applied to Vertical Function.....	80
3.6.2.3 Kinematic Seabed Boundary Condition applied to Vertical Function	83
3.6.2.4 Summary of Governing Equations for Vertical Function	83
3.6.3 Solving for the form of the Vertical Function	83
3.6.3.1 Kinematic Seabed Boundary Condition.....	84
3.6.3.2 Combined Free Surface Boundary Condition	84
3.6.3.3 Further Manipulation of the Vertical Function	86
3.7 Derivation of Mild-Slope Equation.....	87
3.7.1 Vertical Integration of Weighted Laplace Equation	88
3.7.2 Gradients of the vertical function in Equation (3.213).....	90
3.7.3 Use of dispersion relation to obtain gradients of the wave number.....	93
3.7.3.1 Horizontal derivatives of κ	94
3.7.3.2 Derivatives of G_2 with respect to κ and x	97
3.7.3.3 Further expansion of the horizontal derivatives of κ	101
3.7.3.4 Derivatives of the vertical function.....	109
3.7.3.4.1 Derivatives of the vertical function with respect to \mathbf{h}' :	109

3.7.3.4.2 Derivatives of the vertical function with respect to \mathbf{K} :	111
3.7.3.4.3 Cross derivatives of the vertical function with respect to \mathbf{K} and \mathbf{h}' :	114
3.7.3.4.4 Derivatives of the vertical function with respect to z :	118
3.7.3.4.5 Cross derivative of the vertical function with respect to \mathbf{K} and z :	119
3.7.3.4.6 Cross derivative of the vertical function with respect to \mathbf{h}' and z :	119
3.7.4 Summary of Equations developed to date for Mild Slope Equation	120
3.7.5 Evaluating terms of the Mild-Slope Equation	123
3.7.5.1 Combined Free Surface Boundary Condition	123
3.7.5.2 Evaluation of Remaining Mild-Slope Equation Terms	131
3.7.6 Complete Mild-Slope Equation	145
3.7.6.1 Summary of Mild-Slope Equations	149
3.7.7 Integral Summary	152
3.8 One Dimensional Finite Element Mild-Slope Wave Model	160
3.8.1 Simplification of two dimensional terms to one dimension	160
3.8.2 Integration over a finite element	165
3.8.3 Parabolic mild slope boundary condition	169
3.8.3.1 Parabolisation of Elliptic Mild-Slope Equation	169
3.8.3.2 Comparison of Parabolic Approximation with that of Booij (1981)	172
3.8.3.3 Parabolic Boundary Condition for 1d-NM-WCIM	173
3.8.3.4 Generalised Parabolic Boundary Condition with Gradient of Phase	175
3.8.4 Complete One-Dimensional Finite Element Wave Driven Hydrodynamic Model	177
3.8.5 Complete One-Dimensional Finite Element Wave Driven Hydrodynamic Model with Gradients of Wave Phase on Boundary	180
3.9 Two-Dimensional Cartesian Finite Element Mild-Slope Wave-Current Interaction Model	183
3.10 Helmholtz Equation for Finite Element Mild-Slope Wave-Current Interaction Model	195
3.10.1 Derivatives of Wave Celerity and Group Velocity	207
3.11 Boundary Conditions for 2d-NM-WCIM	213
3.11.1 Parabolic absorbing mild slope boundary condition for Non-Helmholtz 2d-NM-WCIM	214
3.11.2 Complete Two-Dimensional Finite Element Wave Driven Hydrodynamic Model	220
3.11.3 A Generalised Curvilinear Downwave Absorbing Boundary Condition	225
3.11.3.1 Generalised Curvilinear Coordinate System	225
3.11.3.2 Transformation of the Helmholtz Type Elliptic Mild-Slope Wave Equation to a Generalised Curvilinear Coordinate System	227
3.11.3.3 Transformation of the Non-Helmholtz Type Elliptic Mild-Slope Wave Equation to a Generalised Curvilinear Coordinate System	231
3.11.3.4 Parabolisation of Elliptic Mild-Slope Wave Equation in Generalised Curvilinear Coordinate System	234
3.11.3.5 Alternative Parabolisation in General Coordinate System	238
3.11.3.6 Parabolisation of Non-Helmholtz Elliptic Mild-Slope Wave Equation in Generalised Curvilinear Coordinate System	239
3.11.3.7 Absorbing Parabolic Downwave Boundary Condition	242
3.11.3.8 Absorbing Parabolic Downwave Boundary Condition for Simpler Condition	244
3.11.4 Radiation Boundary Condition	245
3.11.4.1 Incident Potential and Gradients	248
3.11.5 Reflecting Boundary Condition	252
3.11.6 Full Helmholtz form of the 2d-NM-WCIM finite element solution scheme	253
3.11.6.1 Special Case – Simple Progressive Wave with No Obstacles	261
3.12 Wave Breaking in the One-Dimensional and Two-Dimensional Wave-Current Interaction Models	277
3.12.1 Energy Dissipation in 1d-NM-WCIM	277
3.12.2 Energy dissipation in 2d-NM-WCIM	279
3.12.3 Expressing energy dissipation in terms of the parameters of wave breaking	280
3.12.3.1 Battjes and Janssen (1978) breaking solution	280
3.12.3.2 Massel (1992) breaking solution	281
3.12.3.3 Chawla <i>et al.</i> (1998) breaking solution	282
3.13 NM-WCIM in Operation	283
3.13.1 Iteration of NM-WCIM for Solution of Wave Current Interaction	283
3.13.2 Iteration of NM-WCIM for Energy Dissipation	283

CHAPTER 4: WAVE-DRIVEN HYDRODYNAMIC MODEL.....	285
4.1 Introduction.....	285
4.2 Initial Definitions.....	285
4.3 Depth and Time-Averaged Equations for Mean Motion of Water Body	287
4.3.1 Averaged Equation for Conservation of Mass.....	290
4.3.2 Averaged Equation for Conservation of Momentum	293
4.3.2.1 Complete Momentum Balance Equation including time	293
4.3.2.2 Horizontal Momentum Balance Equation including Time Integrated over Depth.....	294
4.3.3 Some Simplifications of the Horizontal Momentum Balance Equation.....	306
4.3.3.1 Preliminary Orders of Magnitude	306
4.3.3.2 Viscous Stress Terms.....	307
4.3.3.3 Bottom Stress Terms.....	308
4.3.3.4 Integration of Vertical Momentum Equation	309
4.3.3.5 Use of Dimensional Analysis to Simplify the Mean Water Pressure	311
4.3.4 Radiation Stress.....	314
4.4 Summary of Approximate Equations of Motion	321
4.5 Radiation Stress expressed in terms of Velocity Potential.....	322
4.5.1 Expression of wave orbital velocity in terms of velocity potential	322
4.5.2 First term of Equation (4.201) in terms of velocity potential	324
4.5.3 Second term of Equation (4.201) in terms of velocity potential.....	327
4.5.5 Fourth term of Equation (4.201) in terms of velocity potential	335
4.5.6 Complete Expression of Radiation Stress in terms of Velocity Potential.....	339
4.6 Bottom Friction	340
4.7 Turbulent term in Hydrodynamic Equation	342
4.7.1 Turbulent Diffusion Term in NM-WDHM	342
4.7.2 Relating lateral mixing to Wave Breaking	344
4.8 Finite Element Solution of NM-WDHM.....	345
CHAPTER 5: WAVE ENERGY RAYS.....	349
5.1 Introduction.....	349
5.2 Development of Wave Energy Equation	350
5.3 Relating Amplitudes and Phases of Velocity Potential and Physical Waves.....	355
5.4 Expression of Energy Equation in terms of Wave Components	359
5.5 Obtaining Eddy Viscosity from Wave Energy Equation	360
5.6 Obtaining Wave Heights using Wave Energy Rays	362
5.6.1 Battjes and Janssen (1978) Wave Breaking Solution in the Wave Energy Ray Method.....	364
5.6.2 Dally <i>et al.</i> (1985) Wave Breaking Solution in the Wave Energy Ray Method.....	365
5.7 Selection of Insipience Criterion for Wave Breaking In Wave Energy Methodology.....	368
5.7.1 Simple relationship between Water Depth and Wave Height	368
5.7.2 Miche (1954) Insipience Criterion	368
5.7.3 Miche (1954) Insipience Criterion including the effects of Wave Steepness	369
5.7.4 Dally (1990) Insipience Criterion.....	369
5.8 Calculation of Input Terms Required for Wave Energy Methodology	370
CHAPTER 6: RESULTS AND DISCUSSION.....	375
6.1 Introduction.....	375
6.2 Wave Height vs. Analytical	375
6.2.1 Introduction	375
6.2.2 Results	375
6.2.3 Discussion	377
6.3 Wave Current Interaction vs. Mei <i>et al.</i> (2005) and Brevik and Aas (1980)	378
6.3.1 Introduction	378
6.3.2 Waves approaching a current at an angle	378
6.3.3 Waves with a Co-linear Current	382
6.3.4 Discussion	384
6.4 Different Breaker Methods	385
6.4.1 Introduction	385
6.4.2 Results	385

6.4.3 Discussion.....	387
6.5 Turbulent Diffusion in NM-WDHM	389
6.5.1 Introduction.....	389
6.5.2 Results.....	389
6.5.3 Discussion.....	395
6.6 Comparison of Set-up/Set-down with Bowen <i>et al.</i> (1968)	397
6.6.1 Introduction.....	397
6.6.2 Results.....	397
6.6.3 Discussion.....	398
6.7 Iteration between NM-WCIM and NM-WDHM	399
6.7.1 Introduction.....	399
6.7.2 Results.....	399
6.7.3 Discussion.....	400
6.8 Wave Breaking and Recovery over an Offshore Bar	401
6.8.1 Introduction.....	401
6.8.2 Results.....	401
6.8.3 Discussion.....	403
6.9 Detached Breakwater of Liu and Mei (1976)	404
6.9.1 Introduction.....	404
6.9.2 Results.....	404
6.9.3 Discussion.....	412
6.10 Detached Breakwater of Liu and Mei (1976) – Waves at an Angle.....	414
6.10.1 Introduction.....	414
6.10.2 Results.....	414
6.10.3 Discussion.....	425
6.11 Detached Breakwater after Péchon <i>et al.</i> (1997)	427
6.11.1 Introduction.....	427
6.11.2 Results.....	427
6.11.3 Discussion.....	435
6.12 Comparison of Radiation Stress with Watanabe and Maruyama (1986)	437
6.12.1 Introduction.....	437
6.12.2 Results.....	437
6.12.3 Discussion.....	446
6.13 Comparison with Attached Breakwater of Liu and Mei (1976)	447
6.13.1 Introduction.....	447
6.13.2 Results.....	447
6.13.3 Discussion.....	457
6.14 Currents around a Conical Island after Mei and Angelides (1977).....	459
6.14.1 Introduction.....	459
6.14.2 Results.....	459
6.14.3 Discussion.....	469
6.15 Wave-Current Interaction of Chen <i>et al.</i> (2005) and Kostense <i>et al.</i> (1988)	470
6.15.1 Introduction.....	470
6.15.2 Results.....	470
6.15.3 Discussion.....	474
6.16 Energy Rays vs. Wave Rays.....	476
6.16.1 Introduction.....	476
6.16.2 Results.....	476
6.16.3 Discussion.....	477
6.17 Case Study – Casheen Bay	479
6.17.1 Introduction.....	479
6.17.2 Casheen Bay – Location and Bathymetry	479
6.17.3 Wave Propagation in Casheen Bay	482
6.17.4 Wave Current Interaction in Casheen Bay	488
6.17.5 Wave-Driven Hydrodynamic Behaviour In Casheen Bay	497
6.17.6 Discussion	505

CHAPTER 7: CONCLUSION & RECOMMENDATIONS.....	507
7.1 Conclusion.....	507
7.2 Recommendations for Future Work.....	509
APPENDIX A: FINITE ELEMENT METHODOLOGY	511
A.1 Introduction	511
A.2 Finite Element Technique.....	511
A.3 Method of Weighted Residuals	511
A.3 Galerkin Method	512
A.4 Shape Functions.....	514
A.4.1 Introduction	514
A.4.2 One-Dimensional Linear Shape Function.....	514
A.4.3 Two-Dimensional Linear Shape Function.....	515
APPENDIX B: COMPARISON OF NOMENCLATURE WITH CLYNE (2008)	517
REFERENCES	525
Primary References.....	525
Secondary References	531

Abstract

A new derivation of an elliptic extended mild-slope wave equation, including the effects of energy dissipation and current, has been accomplished. A Galerkin-Eigenfunction method was used for this derivation and the final equation has been used to create a Finite Element Wave-Current Interaction Model (NM-WCIM). The NM-WCIM solves for the complex value of velocity potential, from which all other wave properties can be obtained. An iterative solution scheme based on the gradient of wave phase is implemented to solve for wave-current interaction. A novel post-processing technique for the NM-WCIM has been developed to obtain wave energy rays and hence breaking wave heights and eddy viscosity values. The model has been calibrated and tested against measured data and published results of similar models. The NM-WCIM was used to examine scenarios with complex wave-current interaction and bathymetry, including a case study of Casheen Bay on the west coast of Ireland. The NM-WCIM has proven itself to be an advancement over previous similar models in terms of efficiency and accuracy.

Equations for the conservation of mass and momentum have been derived to examine wave-driven hydrodynamics in and around the surf-zone. These equations use a radiation stress driving force obtained, using a unique formula, from the velocity potential results of the NM-WCIM. The conservation equations also include turbulent diffusion terms based on eddy viscosity and a general bottom friction term for flow in any direction. The conservation of mass and momentum formulae have been used to develop a depth-integrated Finite Element Wave-Driven Hydrodynamic Model (NM-WDHM) which iterates to a converged solution using a finite difference time-stepping procedure. This model was calibrated against measured data and published results of similar models and has been used in a coupled system with the NM-WCIM to examine many scenarios with complex bathymetric and wave conditions, including those in Casheen Bay. The NM-WDHM has proven itself to be both accurate and computationally efficient.

Declaration

I certify that this thesis, in whole or in part, has not been submitted to any other university as an exercise or to obtain a degree. Except where specific reference is made to the work of others, this thesis is my own work.

Carl Newell, April 2010

Acknowledgements

I would like to thank my supervisor Dr. Thomas Mullarkey for his invaluable assistance throughout this project. His mathematical guidance in the derivation of the extended elliptic mild-slope equation including currents, the wave-driven hydrodynamic equations and the wave energy ray equations was essential to their completion. I would also like to thank him for his assistance in finite element and computer coding techniques during the creation of the NM-WCIM and the NM-WDHM and his great help in assessing and examining the results of both.

I would like to thank IRCSET (Irish Research Council for Science and Engineering Technology) for the Embark Scholarship I received to pursue this project.

My gratitude is also due to my parents Paddy Joe and Maura, my family, close friends and my girlfriend for the support they have shown throughout my PhD studies. Without their tireless support this project would not have been possible.

Finally I would like to express my gratitude to the staff, students and my fellow post-graduate students and researchers in the Dept. of Civil Engineering at NUI, Galway. The camaraderie, both professionally and socially, of all within the department has made the sometimes solitary research process enjoyable. I would like to specially thank my colleague Dr. Mark Clyne who initiated research on a finite element wave model and without who's work this project would not be possible. My gratitude is also due to Dr. Michael Hartnett and Dr. Tomasz Dabrowski who provided measured data of Casheen Bay for testing of the models created in this thesis.

My thanks to all.

Nomenclature

A	=	Area
A	=	Wave Amplitude
A_D	=	Area between Energy Rays and Perpendicular Lines to Rays
A_ξ	=	Amplitude of Instantaneous Set-Up (Wave Amplitude)
A_ϕ	=	Amplitude of Velocity Potential
a_m^m	=	Divergence of the Vector \mathbf{A}

B	=	Empirical Wave Breaking Constants
b	=	Width between Rays

C	=	Constant
C	=	Relative Wave Celerity
$C_{precise}$	=	Absolute Wave Celerity
C_g	=	Relative Wave Group Velocity

$$\mathbf{C}_{Gj} = CC_g \sigma \frac{\partial S_\phi}{\partial x_j}$$

cn	=	Jacobian Elliptic Function
------	---	----------------------------

$$D = -\frac{\partial}{\partial s}(EnC)$$

E	=	Energy
\mathbf{E}_x	=	Basis Vector
$\hat{\mathbf{e}}$	=	Unit Vector

$$\{E_{U_1}\} = [KI] \left\{ \frac{dU_1}{dt} \right\}$$

$$\{E_{U_2}\} = [KI] \left\{ \frac{dU_2}{dt} \right\}$$

$$\{E_{\bar{\eta}}\} = [KI] \left\{ \frac{d\bar{\eta}}{dt} \right\}$$

\mathbf{F}	=	External Force per unit Volume
f_B	=	Friction Coefficient
f	=	Vertical Function such that $\tilde{\phi}(x, y, z) = f(z)\phi(x, y)$
$G^{\alpha(i)}$	=	The Cofactor of $g_{\alpha\beta}$
g	=	Gravitational Acceleration
g_{xx}	=	Metric Tensor
g^{ij}	=	Conjugate Metric Tensor
g	=	Determinant of the Metric Tensor Matrix
H_{st}	=	Stable Wave Height
H_0	=	Deep-Water Wave Height
H_b	=	Breaking Height
H_m	=	Maximum Sustainable Wave Height
H	=	Wave Height
h	=	Depth
h'	=	$h + \bar{\eta}$
I	=	Integral of Various Functions
i	=	$\sqrt{-1}$
K	=	Effective Wave Number
\mathbf{K}	=	Pressure Vector
K_{cn}	=	Parameter of Jacobian Elliptic Function
$[KI]$	=	Mass Matrix
L'	=	One-Dimensional Shape Function
L	=	Wave Length
L_j	=	Lateral Mixing Term
L_0	=	Deep-Water Wave Length
l	=	Length of Element

M = Mass

M = Empirical Turbulence Coefficient

m_b = Slope of Beach

N = Empirical Turbulence Coefficient

N^I = Two-Dimensional Shape Function

\mathbf{n} = Outward Unit Normal to Surface

NM-WCIM = Newell Mullarkey Wave-Current Interaction Model

NM-WDHM = Newell Mullarkey Wave-Driven Hydrodynamic Model

p = Pressure

\mathbf{p} = Momentum

Q_b = $e^{\frac{-(1-Q_b)}{r^2}}$

R_{ij} = Radiation Stress

∂R = Boundary Curve

R_E = Reynolds Number

$\mathbf{r}(s)$ = Positional Vector

r = $\frac{H}{\sqrt{2}H_m}$

$\{R_{U_j}\}$ and $\{R_{\eta_j}\}$ = Residual Vectors

S = Surface

S_ϕ = Phase of Velocity Potential

s_0 = Wave Steepness

T = Period

t = Time

\mathbf{t} = Tangent

Δt = Time Step

U = Steady Component of Instantaneous Velocity

$\mathbf{u} = (u_1, u_2, u_3)$ = Instantaneous Velocity

$\tilde{\mathbf{u}}$ = Unsteady Component of Instantaneous Velocity

\mathbf{u}' = Wave Fluctuation of Velocity

\mathbf{u}'' = Turbulent Fluctuation of Velocity

u_1, u_2 = Horizontal Velocity

V = Volume

W^I = Weighting Function

W_v = Steady Component of Instantaneous Vertical Velocity

w = Vertical Velocity = u_3

\tilde{w} = Unsteady Component of Instantaneous Vertical Velocity

w' = Wave Fluctuation of Vertical Velocity

w'' = Turbulent Fluctuation of Vertical Velocity

$\mathbf{x} = (x, y)$ = Horizontal Coordinates

x_1, x_2 = Horizontal Coordinates

z = Vertical Coordinates

z' = $z - \bar{\eta}$

$A_x, B_x, C_x, D_x, E_x, H_x, J_x,$

$M_x, P_x, W_x, Q_x, Q', Q'', Q_U, \tilde{Q}''$ = Various Functions of $h', \lambda', \kappa, \bar{\eta}, I$ and z'

α = An Empirical Wave Breaking Constant

Γ = Empirical Parameter Relating Wave Height to Water Depth

Γ_x	=	Boundary
γ	=	Energy Dissipation Factor
γ_0	=	Wave Breaking and Insipience Constant
$\hat{\gamma}$	=	Breaker Index
δ_{ij}	=	Kroneker Delta
δ	=	Boundary Layer Thickness
ε_{ij}	=	Eddy Viscosity
$\tilde{\zeta}$	=	Complex Wave Set-up
ζ'	=	Wave Fluctuation of Free Surface
	=	$\text{Re}(\tilde{\zeta}) = \text{Re}(\xi e^{-i\omega t})$
ζ''	=	Turbulent Fluctuation of Free Surface
$\eta(x, y, t)$	=	Free Surface in the absence of turbulence
	=	$\zeta' + \bar{\eta}$
$\eta''(x, y, t)$	=	Free Surface
	=	$\zeta' + \zeta'' + \bar{\eta} = \zeta'' + \eta$
$\bar{\eta}(x, y)$	=	Steady Component of Free Surface
κ	=	Wave Number
λ	=	Empirical Wave Breaking Constants
λ'	=	$\frac{\sigma^2}{g}$
μ	=	Viscosity

$$\nu = \frac{\mu}{\rho}$$

$$\xi = \text{Complex Instantaneous Set-Up}$$

$$\rho = \text{Density}$$

$$\sigma = \text{Intrinsic/Relative Frequency}$$

$$\sigma'_{ij} = \text{A Stress Tensor}$$

$$\tau_j^B = \text{Bottom Stress}$$

$$\tau_j^F = \text{Stress at the Free Surface}$$

$$\Upsilon = \mathbf{t} \cdot \frac{d\mathbf{n}}{ds}$$

$$\begin{aligned} \tilde{\Phi}(x, y, z, t) &= \text{Velocity Potential in Three-Dimensional and Time Space} \\ &= \text{Re}(\tilde{\phi}(x, y, z)e^{-i\omega t}) \end{aligned}$$

$$\begin{aligned} \tilde{\phi}(x, y, z) = \tilde{\phi}_1 + i\tilde{\phi}_2 &= \text{Velocity Potential in Three-Dimensional Space} \\ &= f(z)\phi(x, y) \end{aligned}$$

$$\phi(x, y) = \phi_1 + i\phi_2 = \text{Velocity Potential in Two-Dimensional Space}$$

$$\phi' = \phi\sqrt{CC_g} = \text{Scaled Helmholtz Style Velocity Potential}$$

$$\hat{\phi} = A_\phi e^{iS_\phi} = \text{One-Dimensional Velocity Potential}$$

$$\psi = \frac{1}{\left(\mathbf{t} \cdot \frac{d\mathbf{n}}{ds}\right)^2 + 4\left(\frac{\partial S_\phi}{\partial n}\right)^2}$$

$$\hat{\psi} = \frac{1}{\Upsilon^2 + 4\kappa^2}$$

$$\Omega = \text{External Force Potential}$$

$$\omega = \text{Angular Frequency (in rad/s)}$$

$$\nabla = \frac{\partial}{\partial x} + \frac{\partial}{\partial y} + \frac{\partial}{\partial z}$$

$$\nabla_h = \frac{\partial}{\partial x} + \frac{\partial}{\partial y}$$

Chapter 1: Introduction

“How inappropriate to call this planet Earth when it is clearly Ocean,” Arthur C. Clarke.

The annals of human history are fraught with attempts to control, tame or otherwise master the seas. Some human endeavours on the sea such as the empire building of the Conquistadores and more recently the search for offshore oil deposits in the North Sea have met with “success.” Yet it is clear from the myth of Odysseus being ship-wrecked by Poseidon to modern events such as the Asian tsunami of 2004 that we cannot even claim to understand the workings of the sea much less be masters of it.

Having acknowledged one’s ignorance with respect to the machinations of the sea it should be pointed out that in recent times much effort has been expended to increase our understanding of the sea and that these efforts have not been in vain. At the present time humans can claim to have a deeper understanding of the processes that occur in the Earth’s seas and oceans than ever before. However, this understanding is by no means complete and further research will undoubtedly improve the way mankind interacts with the sea.

Although human interaction with the sea occurs in many places by many means, from deep sea fishing in the cold North Atlantic to pleasure scuba diving in the warmer climate of the Great Barrier Reef, it is arguably along the world’s coastlines that most of our collective interaction with the sea occurs. The processes that occur along the coast affect us deeply. Not only do these coastal processes shape the coastline near which many of us live, but they also provide recreational amenity, scenic beauty, transport possibilities, processes to aid effluent treatment and a host of other effects we often take for granted.

Waves are present to some degree at all coastlines and at many they are a dominant process. They contribute to the effects of erosion and accretion on the coast, they can be used for recreational processes such as surfing, they generate secondary processes such as longshore and rip currents and they impart forces on manmade structures such as ports, harbours and piers. Over the past few decades a large amount of research has been carried out with regard to wave behaviour in the coastal zone. More recently much of this research has been applied to methods to predict wave behaviour and wave generated

behaviour near the coast. The increasing computational power provided by modern computer systems has allowed complex scenarios and solutions to be examined.

A detailed examination of the research completed in this area led me to believe that a more efficient succinct computer methodology, which would provide results as accurately and in some cases more accurately than existing prediction techniques and models, could be created. The underlying aim of my PhD research can therefore be stated as the creation of a new computer modelling system to examine wave behaviour and wave-generated effects in the coastal zone. It is my hope that this research will assist the coastal engineering community in examining the effects of waves, such as generated currents, applied forces, erosion, accretion etc. in the coastal zone and hence, will allow for an improved collective understanding of the sea. Such understanding will in turn allow us to interact in a responsible, sustainable and, most importantly, safe way with the sea.

In order to discuss the scope of this project it is necessary to briefly examine wave processes and wave generated behaviour in the coastal zone. Waves approaching a shore undergo a number of processes. Waves approaching a shoreline at an angle gradually refract as they get closer to the shoreline, that is they gradually turn to align themselves with the contours of the sea-bed. As they approach shallower water waves also shoal; this means they increase in height as the water depth decreases. At some point they will increase to a height that is unsustainable and at this point (known as the breaking point) the wave collapses in a process known as breaking. The region between this breaking point and the shore is known as the surf zone. In the surf zone the wave height decreases from its height at breaking to zero. The breaking of waves leads to a momentum flux in both the onshore and longshore direction. The physical manifestation of this momentum flux in the onshore direction is a slight increase in mean sea level at the shore, known as set-up and a slight decrease in mean sea-level at the breaking point; this is known as set-down. The longshore component of the momentum flux physically manifests itself as currents known as longshore and rip currents.

It should be noted that in the presence of a current the direction of wave propagation will be altered by the direction and magnitude of the current. However, as discussed above, some currents are generated by waves. This leads to a circular relationship between the waves and wave-generated currents. The only way to accurately examine such a relationship is by using an iterative process.

It was decided that to provide a detailed analysis of waves and wave generated behaviour this project would examine the behaviour of monochromatic waves (waves of uniform period) approaching a coastline and would also examine the behaviour generated by the presence of these waves. It was decided that this examination would be carried out by using, or deriving where necessary, mathematical equations to describe wave and wave-generated behaviour in the coastal zone. These mathematical developments are then applied to a computer model to simulate and predict a complete solution for wave and wave-generated behaviour in a variety of complex situations in the coastal zone.

Initially an extensive literature review was carried out to examine existing research in the area and the state of the art for existing computer simulations of the type proposed by this project. Chapter 2 details this literature and state of the art review. Based on the research carried out in Chapter 2 it was then possible to select a detailed methodology for carrying out the proposed research. The subsequent chapters then detail how the research was carried out, the results obtained and the significance of these results.

It was decided that two separate sub-models were needed to provide a full examination of waves, wave-current interaction and wave-generated currents in the surf zone. These were titled the Newell Mullarkey Wave-Current Interaction Model (NM-WCIM), which examines the behaviour of waves in the presence of a current, and the Newell Mullarkey Wave-Driven Hydrodynamic Model (NM-WDHM), which uses the principles of hydrodynamics to model wave-generated currents and wave-generated set-up and set-down

Chapter 3 of this thesis gives details of the formulation of the Newell Mullarkey Wave-Current Interaction Model (NM-WCIM). A full derivation, using the Galerkin-Eigenfunction method, of the elliptic mild-slope equation including the effects of current is provided. This equation is then used to form the basic equations of the finite element computer model to examine wave-current interaction. The necessary boundary conditions are derived for the model. Derivation of energy dissipation terms and their inclusion in the basic equations of the NM-WCIM are also presented in this chapter.

The formulation of the Newell Mullarkey Wave-Driven Hydrodynamic Model (NM-WDHM) is discussed in Chapter 4. The mathematical basis for the model is presented and then adapted for use in the finite element numerical model. This chapter also presents the key driving term of the hydrodynamic model, namely radiation stress, obtained from the velocity potential results of the previously discussed NM-WCIM. Mathematical expressions are derived for the energy dissipation effects of turbulence and bottom friction. These expressions are applied to the basic equations of the NM-WDHM to provide a complete numerical scheme for model solution.

Chapter 5 of this thesis examines a new use for Wave Rays. In this thesis wave energy rays are generated from the results of the NM-WCIM and then used to calculate and plot the progression of wave energy through a domain. This wave energy calculation is used to obtain a number of parameters such as breaking wave height and eddy viscosity which are necessary for the energy dissipation terms of the NM-WDHM. Chapter 5 provides a full mathematical formulation of the basic equations used to generate wave rays from wave potential values and a discussion of how this is implemented numerically.

Chapter 6 of this thesis examines the use of the developed NM-WCIM, NM-WDHM and Wave Ray techniques to examine various phenomena occurring in the coastal zone. Discussion is provided of each result obtained. The chapter examines the use of the models in both one-dimensional and two-dimensional circumstances and discusses the results obtained. Results are initially compared to existing data to ensure accurate calibration and then a number of complex bathymetric scenarios are examined. In the two dimensional cases the bathymetry and obstacles vary in both the longshore and cross-shore directions. The final part of Chapter 6 is a case study of Casheen Bay in Co. Galway, Ireland. The NM-WCIM, NM-WDHM and Wave Ray techniques are applied to the bay to obtain a detailed description of wave behaviour in the bay. The results obtained are then discussed with a view to the practical uses for the results data obtained.

Overall conclusions drawn from the literature review, mathematical derivations, numerical model formulations and modelled results of the thesis are presented in Chapter 7. This chapter discusses the advantages of the NM-WCIM and the NM-WDHM as well as briefly discussing possible future applications and extensions of the models.

Chapter 2: Literature and State-of-the-Art Review

“Research is the act of going up alleys to see if they are blind,” Plutarch.

2.1 Introduction

As discussed in Chapter 1 the overall aim of this project is to examine wave-current interaction and wave-generated effects in the coastal zone. As such it was necessary to carry out an extensive examination of literature regarding waves and coastal zone processes as well as a detailed examination of the current “state of the art” in computer modelling of such processes. This chapter initially discusses the physical processes at work in the coastal zone and then moves on to examine the various mathematical formulations that have been derived to describe these processes. The “state of the art” in terms of computer models using the discussed mathematical formulations is detailed. The final section of this chapter then discusses, based on this research, the methodology that has been undertaken for this project.

2.2 Coastal Zone Processes

2.2.1 Gravity Waves

At sea a surface gravity wave is caused by some external force causing a vertical disturbance in the water column. This external force can be wind, a vessel, seismic activity or the gravitational pull of the moon or sun. When the water column is disturbed vertically gravity acts upon the water column to return the column to its equilibrium position. The surface of the water has inertia as it returns towards its equilibrium position and therefore will progress past it. Each time the water column returns towards equilibrium it will pass its equilibrium position due to inertia. This oscillatory effect is known as a gravity wave.

Gravity waves acquire energy from their exciting force and transmit it across the surface of the water body. This transmission of energy is known as wave propagation. Waves will propagate until they reach an obstacle which causes a reflection or dissipation of the wave's energy. As a wave propagates it will also dissipate some energy due to interaction at the air-water interface and in shallower water at the sea-bed interface.

As waves oscillate the water particles within them are continuously accelerating and decelerating. This produces dynamic pressure gradients in the water column which must be superimposed on the hydrostatic pressure to obtain a full description of the water pressure at any point in the column.

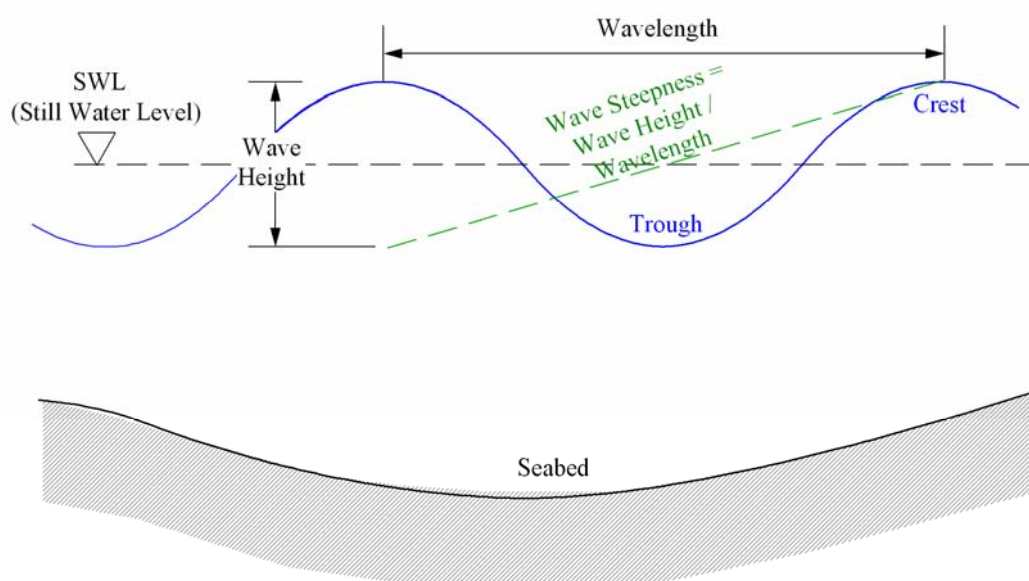


Figure 2.1 – Sketch of Gravity Wave Properties

2.2.2 Wave Behaviour

A visual examination of wave behaviour shows a number of important principles that are discussed in below.

2.2.2.1 Reflection

When a propagating wave collides with an obstacle a percentage of the wave's energy may be reflected off the obstacle thus producing a wave travelling in a different direction to the original wave. This reflected wave may in some circumstances travel in exactly the opposite direction to the original wave. The percentage of reflection that occurs is usually dependant on properties of the obstacle such as shape and construction material.

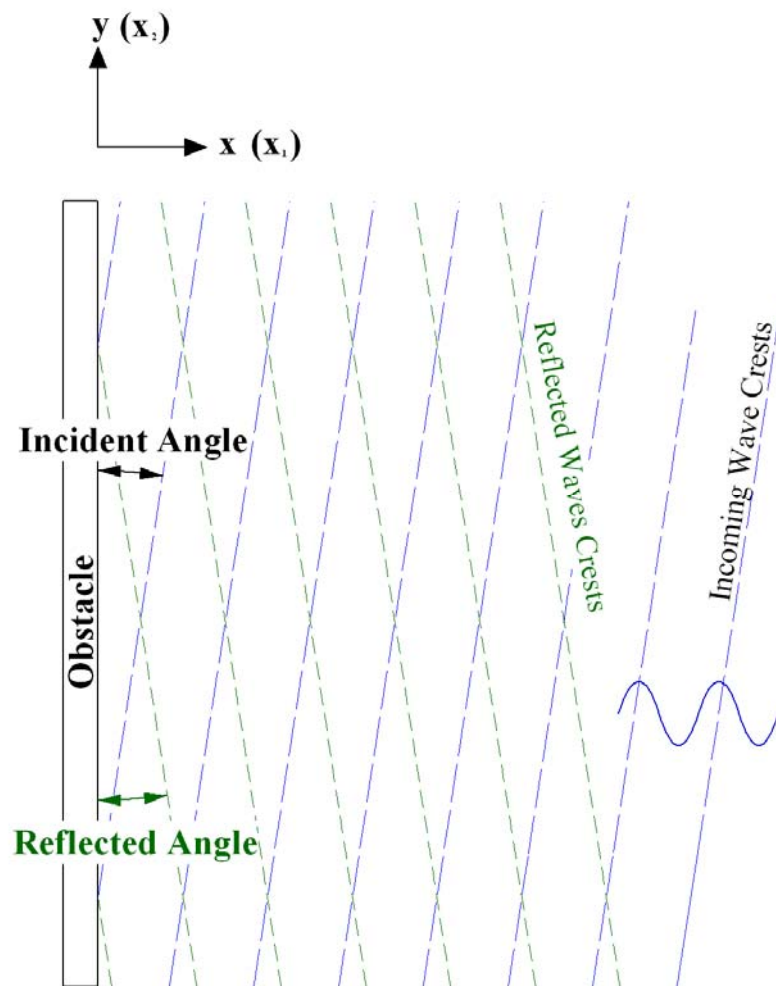


Figure 2.2 – Diagram of Wave Reflection off an Obstacle

2.2.2.2 Shoaling

Shoaling is the gradual increase of wave height and reduction of wavelength as the wave propagates in increasingly shallow water. The celerity (speed of propagation) of the wave also decreases.

2.2.2.3 Refraction

Refraction of a surface gravity wave occurs when the wave propagates into shallower water. As a wave propagates into shallower water the direction of propagation changes so that the wave crest gradually aligns itself to be parallel with the contours of the sloping sea-bed. This occurs because if a wave approaches the shallower region at an angle the wavelength and celerity decreases for the portion of the wave that enters the shallower region first. This causes a turn in the direction of the wave because the portion of the wave still in deeper water does not suffer this change in wavelength and celerity. Refraction of a wave can also be caused by the presence of a current.

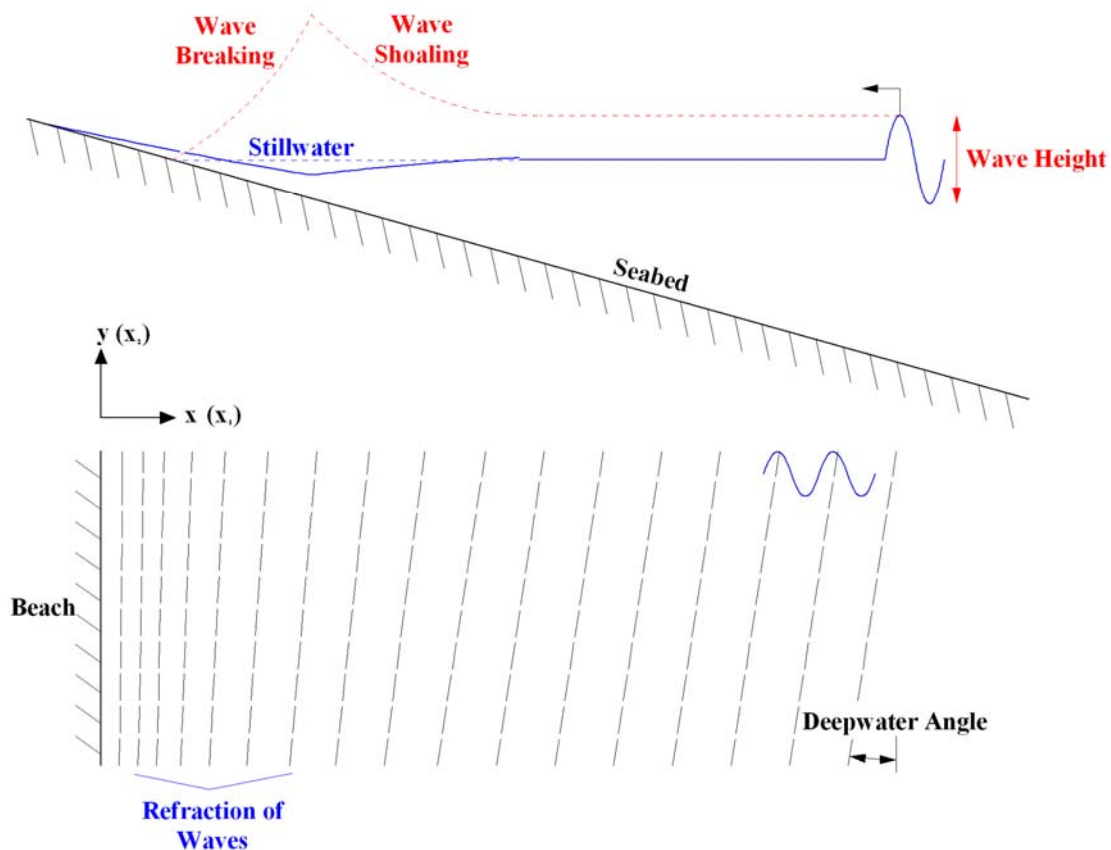


Figure 2.3 – Diagram showing Refraction, Shoaling and Breaking of Waves

2.2.2.4 Diffraction

When the height of a wave is higher at one point along its crest than at a neighbouring point the wave will undergo a process called diffraction. Diffraction is the transfer of energy along the crest of the wave from regions of higher wave height to regions of lower wave height. Therefore as a wave move forwards undergoing diffraction its height will change; decreasing in some locations and increasing in others. An example of diffraction would be when a wave passes an obstacle that creates a sheltered zone behind it. The wave will diffract into this zone once it passes the obstacle. It is worth noting that diffraction also occurs in cases where the wave height is affected by refraction. The diffraction experienced by the wave in this case is usually small compared to other causes of diffraction.

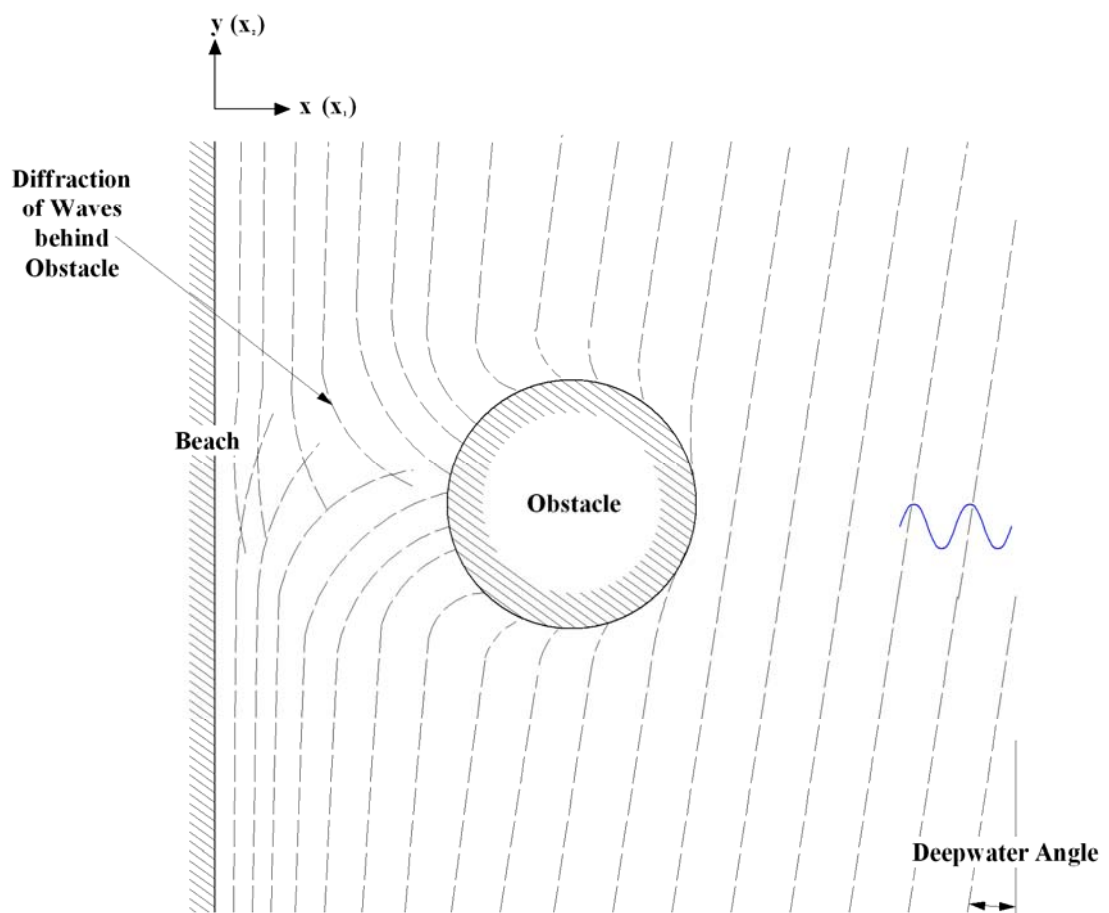


Figure 2.4 – Diagram showing Diffraction of Waves

2.2.2.5 Breaking

Breaking is a process through which a wave dissipates energy. The water particle velocity at the crest of a wave is proportional the wave height. Hence the greater the height of the wave the greater the crest particle velocity. If the crest particle velocity becomes equal to the celerity of the wave the wave becomes unstable and it breaks. This means that the wave collapses. This process can occur in any water depth if the wave height is large enough, however, it most frequently occurs as waves approach the shoreline because the effects of shoaling cause wave height to increase and celerity to decrease.

Smith (2003) describes four different types of breaking wave after Galvin (1968). These are spilling, plunging, collapsing and surging.

2.2.2.5.1 Spilling Breakers

A spilling breaker can be described as one where turbulence and foam first appear at the top of the wave and then spread down the shoreward face of the wave as it breaks. Sorenson (2006) describes the energy dissipation from this breaker type as “relatively uniform” across the surf zone. Komar (1998) states that spilling breakers usually occur on beaches of gentle slope with waves of high steepness.

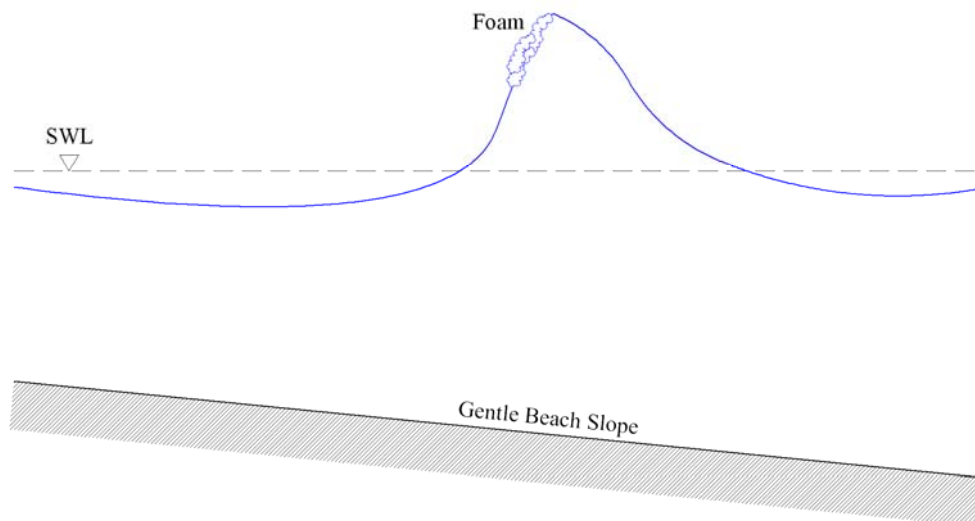


Figure 2.5 – Sketch of a Spilling Breaker

2.2.2.5.2 Plunging Breakers

A plunging breaker occurs when the crest of the wave develops a tongue which curls over the shoreward face of the wave and then collapses into the base of the wave. This type of breaking may lead to a series of irregular waves that propagate towards the shore and break also. Sorenson (2006) states that the energy dissipation for plunging breakers is “more confined” to the breaking point than spilling breakers. Komar (1998) states that plunging breakers usually occur on steeper beaches with waves of intermediate steepness.

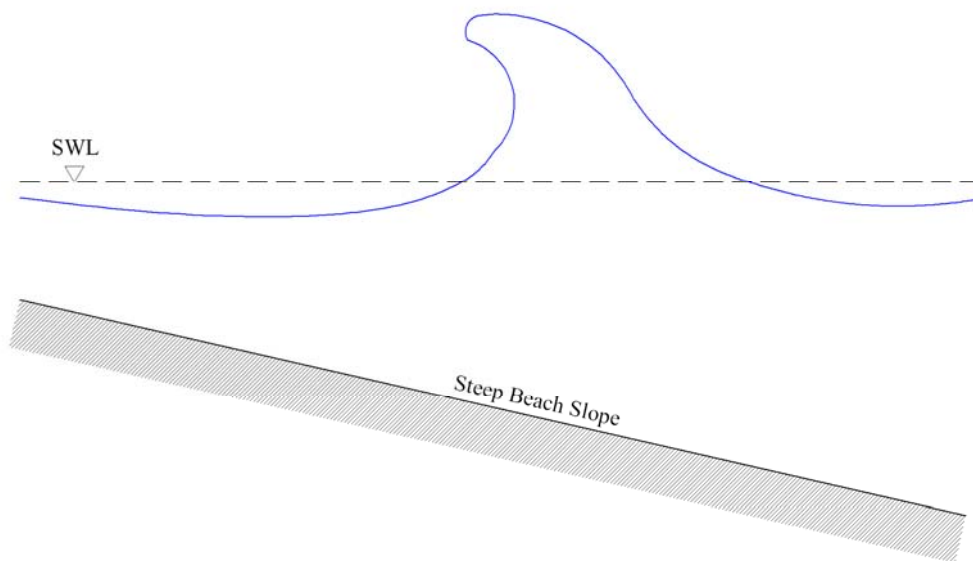


Figure 2.6 – Sketch of a Plunging Breaker

2.2.2.5.3 Collapsing Breakers

Collapsing breakers are described by some authors such as Sorenson (2006) as a transitional class of breakers that occur between plunging and surging breakers. Other authors such as the Smith (2003) describe them as a separate type of breaker in their own right. A collapsing breaking wave is one where the crest of the wave remains unbroken as the lower portion of the wave on the shoreward side becomes steeper until it reaches a point at which it collapses. Figure 2.7 on the following page shows a sketch of a collapsing breaker.

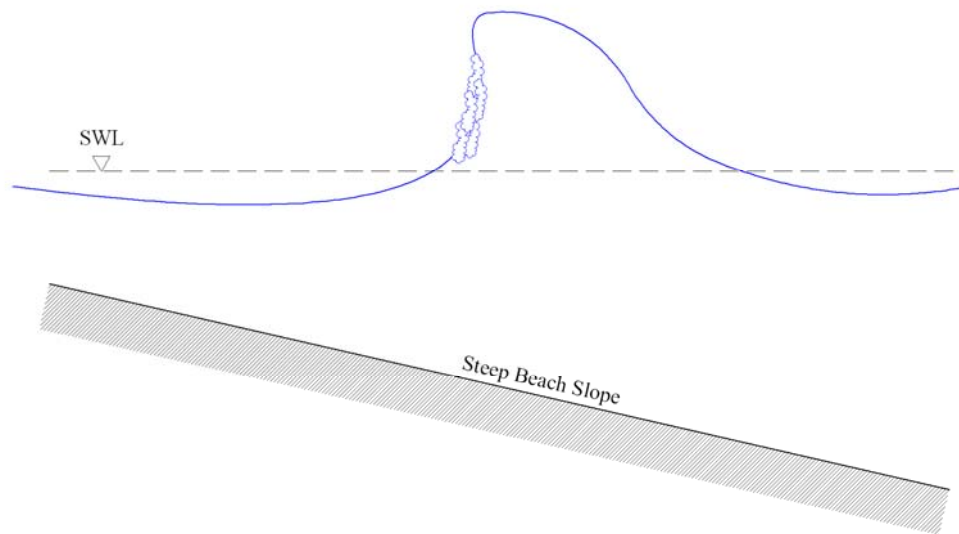


Figure 2.7 – Sketch of a Collapsing Breaker

2.2.2.5.4 Surging Breakers

A surging breaker is one where the crest of the wave remains unbroken and the shoreward face of the wave progresses up the slope of the beach where some minor breaking may occur. Sorenson (2006) states that this form of breaking is a progression towards a standing wave that could occur due to reflection of the wave by the beach. . Komar (1998) states that surging breakers usually occur on beaches of high gradient with waves of low steepness.

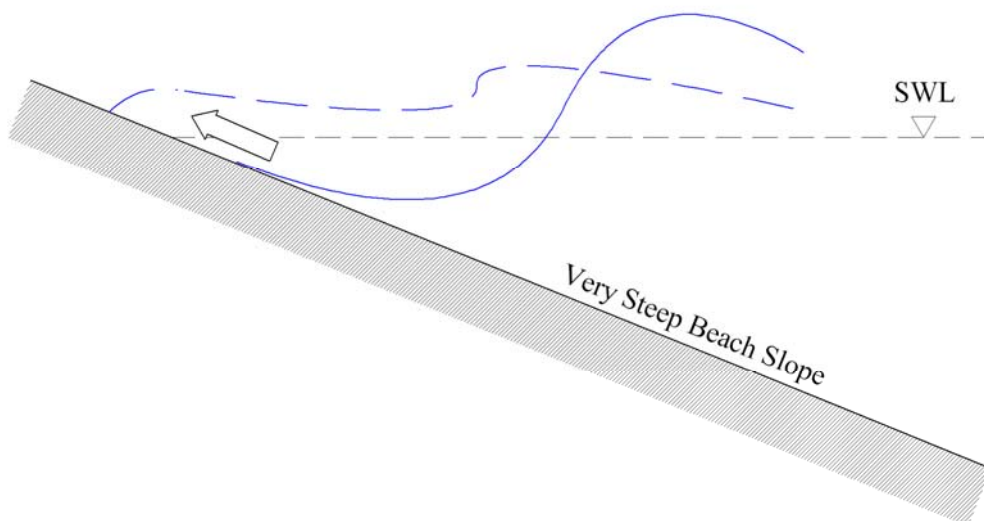


Figure 2.8 – Sketch of a Surging Breaker

2.2.3 Water Particle Velocity

It has been discovered experimentally and later explained mathematically that as a wave propagates in deep water it causes an approximately circular motion of the water particles beneath its surface. The diameters of the circles decrease with increasing depth and go to zero at a depth approximately equal to half the wave length. The geometry of these particle orbits is such that when a wave crest passes a certain point in the water body the particle velocity at that point is in the direction of wave propagation whereas when a trough passes the same point the particle velocity will be counteracting the direction of wave propagation. When a wave moves into shallow water the particle orbits change from circular shape towards an elliptical shape, the reduction in water depth reduces the vertical components of the orbit. At the seabed a linear horizontal particle velocity dominates. This is self-evident because water cannot flow through the sea-bed. The wave particles generally progress slowly in the direction of wave propagation as they rotate, this process is known as mass transport.

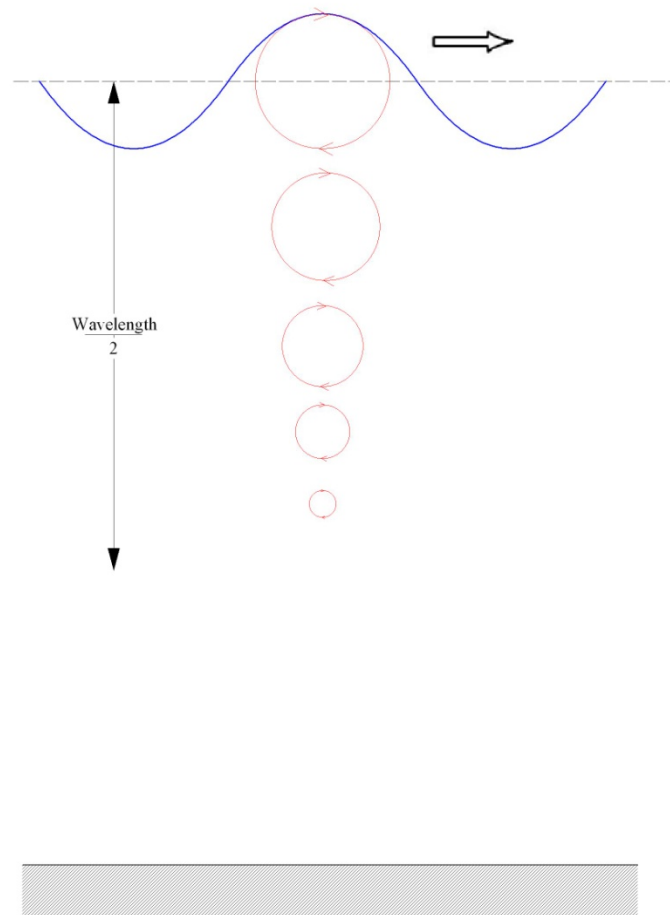


Figure 2.9 – Sketch of Circular Water Particle Motion in Deep Water. Wave propagating from left to right.

2.2.4 Set-up/Set-down

Waves breaking on a beach generate an excess momentum flux. This excess flux comes about due to the difference in momentum between the particle velocity in the direction of wave propagation at a crest of a wave and the particle velocity opposing wave propagation at the trough. This excess momentum flux is called radiation stress after Longuet-Higgins and Stewart (1964). In the cross shore direction equilibrium is maintained against this momentum flux by a rise in the mean sea level at the shore and a corresponding decrease in sea-level at the breaker point known as set-up and set-down respectively.

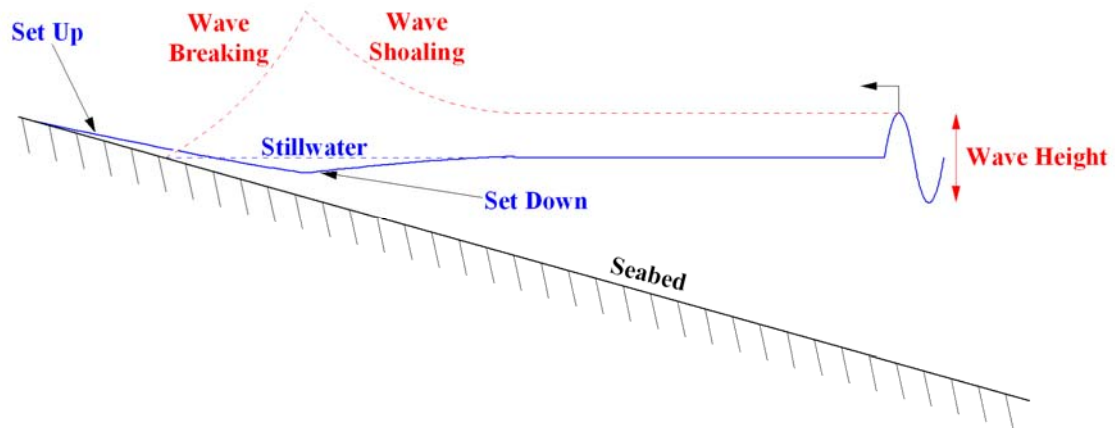


Figure 2.10 – Sketch of Set-up and Set-down

2.2.5 Wave Generated Currents

When waves break on a beach at an angle both a cross-shore and longshore component of radiation stress is generated. As described in Section 2.2.4 the physical manifestation of the cross-shore radiation stress is set-up and set-down. In the longshore direction the excess momentum flux may drive a current. This is the wave generated portion of longshore current. Depending on bottom topography and obstacles waves may generate currents in any direction. Currents generated perpendicular to the coastline are called rip currents.

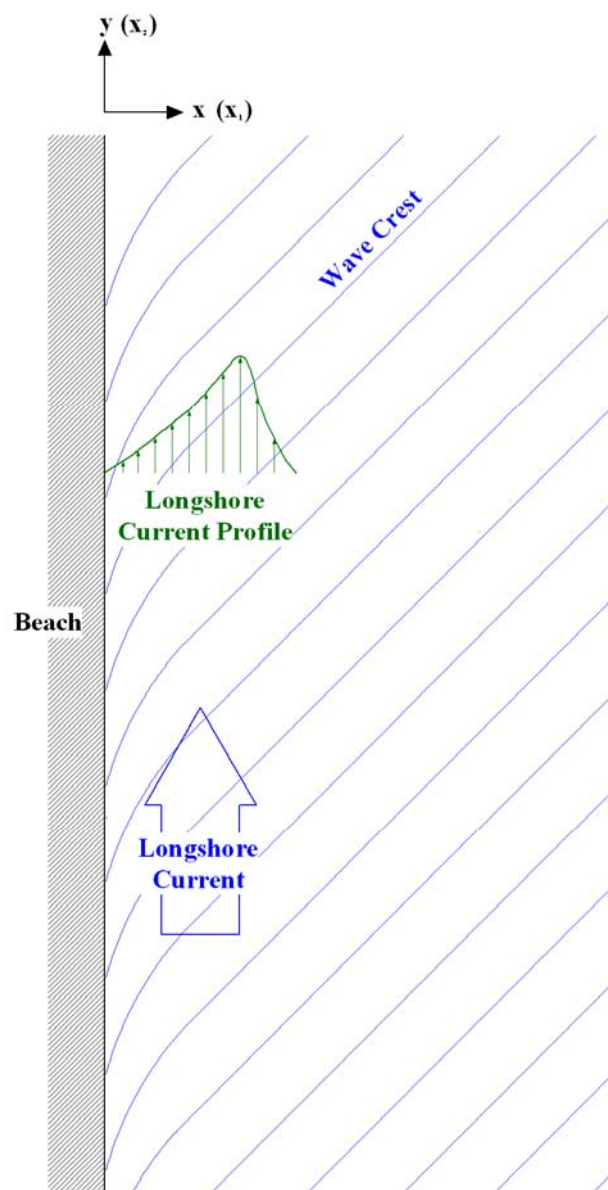


Figure 2.11 – Sketch of Longshore Current generated by Obliquely Incident Waves

2.2.6 Wave-Current Interaction

The presence of a current in any domain across which waves propagate will affect the direction of wave propagation. Depending on the magnitude and direction of the current, the group velocity may decrease, thus increasing the wave amplitude, or it may increase thus reducing the wave amplitude. The refraction of waves caused by the presence of a current is a similar phenomenon to that which occurs when the direction of light is changed as it passes through a glass block. In some extreme cases the presence of a very strong current may cause the majority of wave energy to be reflected. When the presence of a current causes a change in wave behaviour this will also affect any wave generated currents which in turn influence the waves. This circular relationship is very complex and can be difficult to examine numerically.

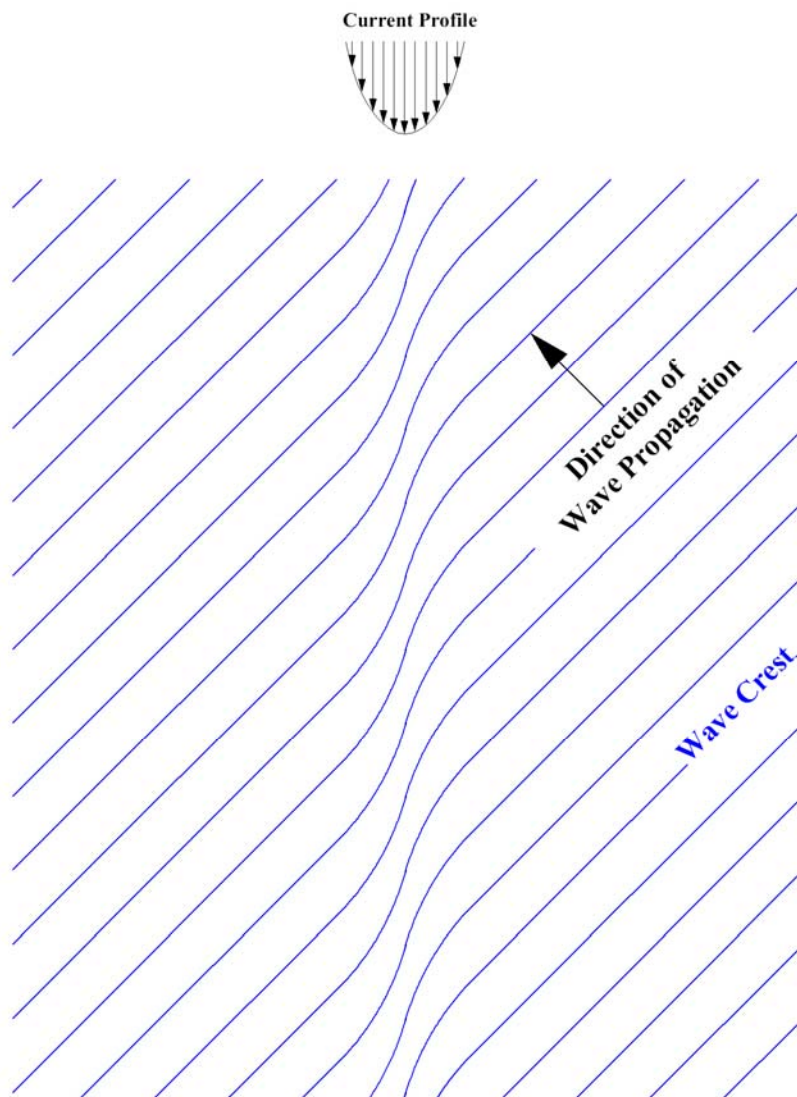


Figure 2.12 – Sketch of Change in Wave Crest Behaviour due to Wave-Current Interaction

2.2.7 Turbulent Diffusion / Lateral Mixing

Turbulent diffusion and lateral mixing are two terms used to describe the same process. Smith (2003) describes the process as “The exchange of momentum caused by turbulent eddies which tend to "spread out" the effect of wave forcing beyond the region of steep gradients in wave decay.” Conceptually this means that the effects of any wave generated phenomenon (e.g. longshore current) occur in a larger area than the particular area where the wave is forcing the generation of the phenomenon. This spreading of the wave effects is caused by small eddies which develop in the water body.

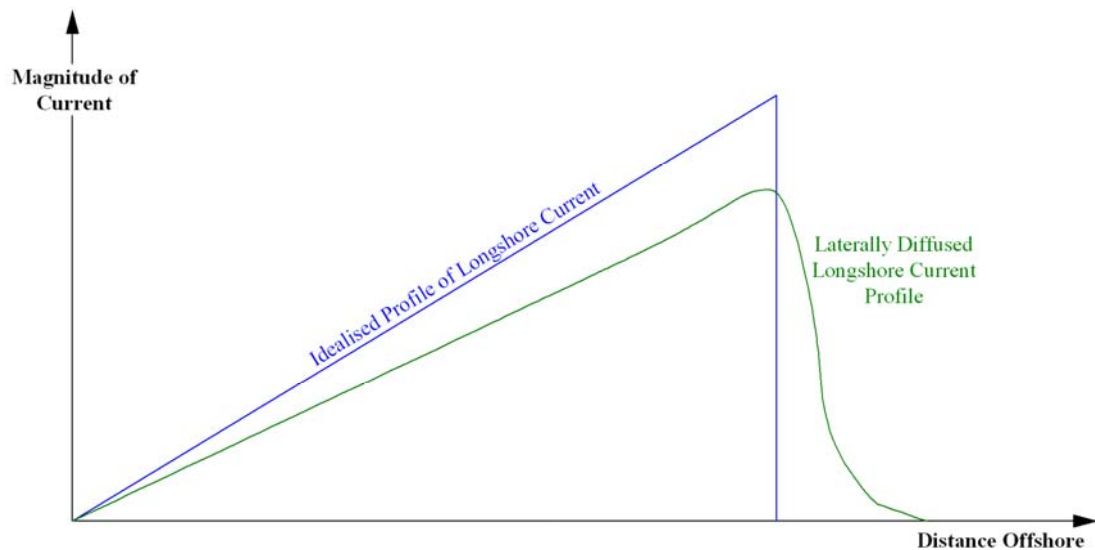


Figure 2.13 – Cross-Shore Profile of Longshore Current showing the effects of Lateral Diffusion

2.2.8 Bottom Friction

The roughness of the sea bed is analogous to the roughness of a river bed in open channel flow. Just as the velocity of the water passing over a river bed is affected by frictional forces between it and the bed so are wave and longshore current velocities damped by friction with the sea-bed. The magnitude of this frictional effect is governed by the material of the sea-bed and its in-situ conditions. For example a sandy sea-bed would be expected to have a more significant frictional effect than a smooth sea-bed made of rock.

2.3 Mathematical Description of Coastal Zone Processes

Section 2.2 gives a brief description of the main processes occurring in the coastal zone. Without a mathematical theory for how these processes occur it would be impossible to predict or model the processes. In many cases a number of theories exist and it is incumbent upon the users to select the most appropriate theory or combination of theories for their specific requirements.

2.3.1 Wave Theories

Wave theories can be broken down into two distinct types; regular wave theory and irregular wave theory. Regular wave theory (often termed monochromatic wave theory) assumes all the waves being examined satisfy a single set of criteria with regards to wave height, period and direction. The waves are assumed to be almost sinusoidal in shape. Due to the regularity of this assumed wave it is possible to carry out detailed mathematical analyses of regular waves to calculate wave kinematics and dynamics. Irregular wave theory acknowledges the fact that real bodies of water consist of a series of waves of different heights and periods travelling in different directions. As such irregular waves must be treated using statistical methods to approximate the varying wave conditions. It is important to select the appropriate wave theory for a given purpose. Demerbilek and Vincent (2002) explain that irregular wave theories are usually used to determine a range of wave conditions and from that select a representative wave height, direction and period for use with regular wave theory to calculate specific kinematics and dynamics. It is evident that for the purposes of this project regular, monochromatic waves should be used for modelling purposes with the particular individual wave properties being obtained from irregular wave theory if necessary.

2.3.1.1 Regular Wave Theory

No mathematical theory can fully describe every wave process. Some theories are more useful for examining certain criteria than others so the onus is on the user to select the most appropriate theory or set of theories for use in any given application. Developed monochromatic wave theories range from the simplest linear wave theory to perturbation methods and Fourier-series approximations for non-linear wave theory.

2.3.1.1.1 Linear (Airy) Theory

The simplest linear theory for describing wave motion was presented by Airy (1845). Linear theory is the easiest wave theory to apply and provides quite accurate results in a wide variety of circumstances. Some assumptions are made in the derivation of Linear Theory (also sometimes referred to as small amplitude theory due to assumption number 9). These assumptions are listed by Demerbilek and Vincent (2002):

1. The fluid is homogeneous and incompressible; therefore, the density ρ is a constant.
2. Surface tension can be neglected.
3. The coriolis effect due to the earth's rotation can be neglected.
4. Pressure at the free surface is uniform and constant.
5. The fluid is ideal or inviscid (lacks viscosity).
6. The flow is irrotational so that water particles do not rotate (only normal forces are important and shearing forces are negligible).
7. The particular wave being considered does not interact with any other water motions.
8. The bed is a horizontal, fixed, impermeable boundary, which implies that the vertical velocity at the bed is zero.
9. The wave amplitude is small with respect to the water depth and the waveform is invariant in time and space.
10. Waves are plane or long-crested (two-dimensional).

Assumptions 1, 2 and 3 are common assumptions for almost all coastal engineering applications and pose no problem for the application of linear theory to a wide variety of scenarios. Assumptions 4 and 5 are appropriate for the vast majority of coastal engineering problems. In some specialised cases it may be necessary to examine their effect on results, however these cases are beyond the scope of this project and will not be considered here. Assumptions 6 and 7 are not strictly accurate in cases where wave generated vortices or other phenomena such as the presence of a current effect the wave field. The author's method for dealing with this issue when it occurs is outlined in the text. Assumption 8 is frequently relaxed and Linear Wave theory is very useful in many cases with sloping sea-beds where the bed is considered to slope "mildly" and thus does not produce reflection of waves. Many models, including the NM-WCIM developed in

this work, include extended terms in the mild-slope derivation to further address the assumption of a mild slope. Assumption 9 although true in deep water is not true in shallow water and thus linear theory does not provide appropriate wave shapes for shoaling waves; however, it has been shown to still provide accurate results for phase and energy flux in these zones as stated by Clyne (2008). Further evidence of this is provided by the widespread use of linear wave theory in existing wave models discussed by Vincent *et al.* (2002) such as RCPWAVE by Ebersole (1985) and Ebersole *et al.* (1986) and STWAVE by Resio (1993) and the widespread use of mild-slope wave models for coastal engineering problems in models such as MIKE 21 –Danish Hydraulic Institute (2008b, c)

Linear Wave Theory describes internal motion using the Laplace equation. This coupled with equations for the conservation of mass and momentum provides sufficient equations to solve for the water-particle velocities, local pressures and all other wave properties. The assumptions listed above can then be applied to obtain the equations for Linear Wave Theory in deep, transitional and shallow water. Linear Wave Theory can be used a number of times and superposition of results used to obtain a more accurate overall result of wave behaviour where required.

2.3.1.1.2 Non-Linear Theory

In many cases Linear Wave Theory will not provide accurate enough results for the particular application in question. In these cases a more complex solution is required in order to obtain more accurate results for wave behaviour. Several finite amplitude non-linear wave theories have been developed, these include Stokes Theory, Boussinesq Theory, Cnoidal Theory and Solitary Wave Theory (a special case of Cnoidal Theory). However in cases where numerical solutions can be used it is suggested by Demerbilek and Vincent (2002) that these finite amplitude wave theories have all been superseded by the Fourier Series Approximation of Fenton (1988).

2.3.1.1.2.1 Finite Amplitude Wave Theories

2.3.1.1.2.1.1 Stokes Theory

Stokes (1847, 1880) recognised the failing of Assumption 9 in Linear Wave Theory (Section 2.3.1.1.1) that wave height is small compared to water depth. This is clearly not the case in shallow water. Stokes provided second and third order solutions to the wave

equations which more accurately represented the behaviour of waves in the shoaling zone. The equations developed by Stokes have initial terms that correspond with those of Linear Wave Theory but extra second and third order terms are added to more accurately describe the wave behaviour.

Modern forms of the Stokes perturbation method usually contain up to fifth order terms, such as that of Fenton (1985). One author, Cokelet (1977) experimented with 110th order Stokes Theory. Komar (1998) states that in general the effect of these extra terms is to widen the trough and narrow the crest of the wave as it propagates into increasingly shallow water. This peaking of wave crests is more in line with observed wave behaviour in shallow water. It is worth noting that higher order Stokes Theories prove to be inaccurate in deep water when compared to Linear Wave Theory.

A corresponding difference is evident in water particle velocity, the velocity under a crest is increased in magnitude but shortened in duration whereas the exact opposite occurs to the velocity under a trough. The water particle motion in Stokes theory does not form a closed loop like Linear Wave Theory. Instead a slow advancement of particles in direction of wave propagation occurs. This phenomenon occurs in nature and is known as mass transport velocity. It can also be referred to as Stokes drift in this case. Stokes drift does not account for any return flow and is in the direction of wave propagation at all depths, which is not entirely accurate.

As water depth gets shallower the effect of Stokes Theory is to extend the trough more and thus make it flatter. Sorenson (2006) states that any increase in wave steepness after the trough becomes horizontal causes a hump to form at the wave trough. This hump does not occur in nature. Hence Stokes Theory has a specific limit on the height a wave may approach in shallow water. This can cause problems with its implementation in shallow regions. The maximum wave height allowed in shallow water by second order Stokes Theory is approximately half of the water depth according to the Demerbilek and Vincent (2002) and Fenton (1985). It is recommended that beyond this depth another theory such as Cnoidal Theory, and in very shallow water Solitary Wave Theory, be used.

In deep water the difference between Linear Wave Theory (essentially first order Stokes Theory) and Stokes Theories of lower orders is quite small but in transitional and shallow

water Stokes Theory provides more accurate results with the penalty of increased computational expense. As stated it is still not completely accurate in shallow water and hence further theories have been developed.

2.3.1.1.2.1.2 Cnoidal Theory

Cnoidal Theory is a wave theory developed by Korteweg and de Vries (1895). The theory is a non-linear wave theory that includes dispersion. It can only be used for waves progressing in one direction. Cnoidal Theory is defined using a Jacobian Elliptic function, cn , hence the name cnoidal. The mathematical implementation of Cnoidal Theory is very complex which somewhat limits its use. The Jacobian Elliptic function is defined in terms of a parameter K (termed K_{cn} here for the sake of clarity). At the limiting values of K_{cn} equal to zero and K_{cn} equal to one, Cnoidal theory simplifies to Linear Wave Theory and Solitary Wave Theory, respectively.

The difficulty in implementing Cnoidal Theory usually means that it is only used where strictly necessary. Usually, as stated by Sorenson (2006), this means the range where higher order Stokes Theory becomes inaccurate and Solitary Wave Theory is not yet useful. Due to its mathematical complexity Cnoidal Theory is usually utilised with the aid of pre-calculated graphs such as those of Wiegel (1960) and Masch and Wiegel (1961).

2.3.1.1.2.1.3 Boussinesq Theory

If the assumption is made that the pressure at any point in the water column is hydrostatic and that the water velocity potential increases polynomially from the seabed to the water surface it is possible to derive an easily solvable set of mathematical wave equations. These equations are termed the Boussinesq type equations after Boussinesq (1871, 1872). Chen *et al.* (2005) states that the assumptions made meant that Boussinesq type equations were “traditionally limited to shallow water.” However, they did allow the Boussinesq equations to be solved for two dimensions only, thus cutting the calculation work required for examining waves.

Sukardi (2008) carries out a detailed examination of Boussinesq type equations. The original equations of Boussinesq were derived solely for a flat seabed but the work of authors such as Mei and LeMehaute (1966) and Peregrine (1967) extended the theory to

sloping sea-beds. The major difference between their respective works is the selected parameter to quantify horizontal particle velocity. Although this further work provided a version of the Boussinesq Theory that was valid for sloping seabeds it was still limited to shallow water and also limited in the maximum wave height it could model thus limiting the extent to which the model could be used in shallow water. To keep errors in the phase velocity less than 5%, the water depth has to be less than about one-fifth of the equivalent deep-water wavelength according to McCowan (1987). More recent work by Madsen *et al.* (1991) and Nwogu (1993) provided further extensions to the Boussinesq approach to allow it to be used in deeper water. The Nwogu (1993) approach has become quite popular because it is relatively simple to apply and allows non-linear wave modelling using Boussinesq Theory into intermediate water depths.

2.3.1.1.2.1.4 Solitary Wave Theory

A solitary wave is the simplest solution to the Boussinesq Theory. It simply approximates a single crest progressive wave. The wave is assumed to be entirely above the Still Water level and hence has no trough. It is a lone wave so there is no period or wavelength associated with it. Sorenson (2006) describes Solitary Wave Theory as translatory rather than oscillatory. When ocean waves enter very shallow water they become sharp crests separated by wide troughs. Munk (1949) suggested that waves in this stage could be accurately modelled using Solitary Wave Theory. Solitary Wave Theory is therefore often considered appropriate for use in water that is too shallow for the application of Stokes or Cnoidal Theory.

Due its non-oscillatory nature Solitary Wave Theory cannot be used to directly calculate wave period or wave length. Values for these parameters can be inferred from different wave theories used in the shallow zone approaching the region where Solitary Wave Theory is used.

It is notable that Smith (2003) states that laboratory measured wave heights obtained by solitary waves just prior to breaking are often used as an indicator for the incipient point of ocean waves.

2.3.1.1.2.2 Numerical Wave Theories

In addition to the Linear and Finite Amplitude Wave Theories discussed above a number of numerical methods have been developed to approximate wave propagation. Numerical methods can give quite accurate results especially when utilising modern computer systems to their full extent. Examples of numerical wave theory are the Stream Function Theory of Dean (1965, 1974) and the Fourier Series approach adopted by Fenton (1988). Both of these numerical theories take the approach of calculating coefficients of a series expansion to obtain a best fit solution to the non-linear free surface condition. The results provided by these numerical methods are very accurate and are widely used in the coastal engineering community because they can be used to obtain results in both shallow and deep water.

2.3.1.2 Irregular Wave Theory

A detailed discussion of irregular wave theory would be beyond the scope of this project. The main concerns of this project are with estimating specific dynamic and kinematic properties of given wave events. This is exclusively the domain of monochromatic wave theory. In some cases however, irregular wave theory is used to select appropriate wave parameters to examine using regular wave theory. It is hence beneficial to give a short description of the general principles of irregular wave theory.

Irregular wave theory acknowledges that at any given time the wave field at a particular offshore location will consist of a variety of different wave heights, periods and directions. Longer period waves (swell) will generally be ones created elsewhere that have travelled to the given region whereas shorter period waves (wind sea) would more likely be generated at closer locations by atmospheric conditions. These “wind sea” waves often have very short crest lengths leading to a very confused water surface. The overall wave field will hence be a complex system and if the wave height at a given point is measured over a given time frame the series of crests and troughs will not be uniform. In most scenarios the scatter of this data will not be predictable as the number of interacting wave fields will be too difficult to separate from each other. The field of irregular wave theory is therefore based on the interpretation of this irregular data to obtain some useful parameters that may be used to describe wave behaviour at the point in question. Many statistical methods can be used to derive various parameters. Perhaps

the most commonly discussed is significant wave height. Significant wave height is a parameter introduced by Sverdrup and Munk (1947) and was initially selected as a parameter to tally with what sailors would classify as the wave height if they were examining a sea by eye. The most common way of calculating significant wave height from a set or irregular wave data is to calculate the average height of the highest one third of waves.

Regular wave theory is often linked to irregular wave theory through the inclusion of empirical coefficients such as those to model breaking and turbulent effects. These parameters cannot be completely mathematically explained and hence in many cases must rely on some degree of empirical evidence which can only be obtained from irregular wave data sets.

2.3.2 Wave Breaking

As discussed in Section 2.2.2.5 above, there are a number of different ways in which a wave can break. It is understood by science that when any wave reaches a certain height (which varies depending on the given circumstances) it will be unstable and will break. However, the exact water particle behaviour that causes this process is not well understood. Traditionally the change in wave height due to breaking was assumed to be linear once breaking had been instigated. This method is discussed by Smith (2003) and was used successfully to calculate set-up and set-down and longshore current values by Longuet-Higgins and Stewart (1963), Bowen *et al.* (1968), Bowen (1969), Thornton (1970), Longuet-Higgins (1970a, b), Liu and Mei (1976), Mei and Angelides (1977), Péchon *et al.* (1997) and Newell *et al.* (2005b). Smith (2003) states that this over-predicts wave heights for slopes steeper than 1/30 and under predicts wave height for shallower slopes or barred bathymetry.

Smith (2003) states that a more general model for wave height in the breaking zone is to solve a steady state energy equation in the surf-zone. Divoky *et al.* (1970) states that the breaking wave behaves like a bore and carries out an energy comparison using a wave height upwave of the breaker “bore” and the height downwave of the bore. Dally *et al.* (1985) uses an energy balance equation to examine wave breaking. Energy dissipation is assumed to be a function of excess wave energy over a stable wave height. Empirical

parameters are selected to provide the function of excess wave energy for a specific beach. Dally *et al.* (1985) allows for the continuation of breaking until a stable wave height is obtained even in situations where the sea bed becomes level after a period of breaking. It is impossible for the similarity method discussed above to treat this phenomenon correctly. Authors such as Battjes and Janssen (1978) provide equations for energy dissipation based on statistical wave breaking. This method can in some cases be used for monochromatic wave breaking by substitution of the monochromatic wave height being examined for the statistical wave height implied in the formula. Zhao *et al.* (2001) examined the Dally *et al.* (1985) solution, the Battjes and Janssen (1978) solution and solutions by Massel (1992), Chawla *et al.* (1998) and Isobe (1999). Newell and Mullarkey (2007a) examine the use of these solutions examined by Zhao *et al.* (2001) as a method for driving set-up/set-down.

Most modern computer models include wave breaking as an energy dissipation effect. Zhao *et al.* (2001), Newell and Mullarkey (2007a) and Clyne (2008) all provide examples of how to include an energy dissipative term in the elliptic mild-slope equation discussed in Section 2.4.1.3.3.2. In all of these cases a general energy dissipation term was included in the mild-slope equation to be solved by the computer model. The including of a general energy dissipation term allows the examination of different breaking wave criteria such as those of Dally *et al.* (1985), Battjes and Janssen (1978), Massel (1992), Chawla *et al.* (1998) and Isobe (1999). With the selection of an appropriate energy dissipation term within the solution scheme it was shown that broken wave results could be obtained using the same iterative solution scheme for a number of different breaking criteria.

2.3.3 Set-up/Set-down

The physical process causing set-up/set-down is discussed in Section 2.2.4. Longuet-Higgins and Stewart (1963, 1964) introduced the concept of radiation stress and provided an equation for its calculation with respect to causing set-up/set-down. The use of this description of radiation stress as a driving force in basic hydrodynamic equations has become widely accepted as the appropriate means to calculate set-up/set-down. Komar (1998) mentions that there may be some uncertainties with the Longuet-Higgins and Stewart (1963, 1964) method because it is based on linear wave theory which may not describe high waves in the surf-zone very well. However, Komar (1998) acknowledges that the fundamental cause of set-up/set-down is well described by Longuet-Higgins and

Stewart (1963, 1964) and has been verified by both laboratory and field studies. It has been discussed and accepted by authors such as Smith (2003) and Mei *et al.* (2005). Péchon *et al.* (1997) shows that gradients of radiation stress have been used as a driving force in many existing wave-generated current models. Accurate values of set-up/set-down have been obtained using this principle by Newell and Mullarkey (2007b), Newell *et al.* (2005b), , Mei and Angelides (1977) and Liu and Mei (1976). The methodology used to include radiation stress in general hydrodynamic models is discussed further below.

2.3.4 Wave Generated Currents

Bowen (1969), Longuet-Higgins (1970a, b) and Thornton (1970) used the formula for radiation stress to examine wave driven currents on a beach. The overall methodology is similar for all the authors. Komar (1998) suggests that the main difference between the approaches was the frictional affects applied to currents resulting from radiation stress and in the horizontal mixing of the fluid across the surf zone. The derivation of Longuet-Higgins (1970a, b) has gained widespread acceptance and is the starting point for all modern investigations into radiation stress and the resulting wave driven currents. Authors such as Mei *et al.* (2005) and Smith (2003) show the continued use of the Longuet-Higgins (1970a, b) approach to calculate wave-driven currents. Newell and Mullarkey (2007b), Newell *et al.* (2005b), Mei and Angelides (1977) and Liu and Mei (1976) are examples of models where wave-generated currents have been calculated on foot of calculated radiation stress values. Péchon *et al.* (1997) examines a number of state of the art wave-driven current models that use gradients of radiation stress. The use of radiation stress in computer models to calculate wave-driven currents is discussed in Section 2.4.2 below.

2.3.5 Wave-Current Interaction

The presence of a current as waves propagate can affect the way in which waves propagate. The inclusion of terms to take account of current in basic wave equations is addressed by authors such as Booij (1981) and Kirby (1984), who discuss the inclusion of current terms in the mild-slope equations based on linear wave theory. In practice it proved difficult to implement and many wave models disregarded wave-current interaction. Péchon *et al.* (1997) examined seven different wave models and found only two that included the effects of wave-current interaction. Newell and Mullarkey (2007b)

examine the effects of wave-current interaction in a finite element wave model based on the mild-slope equation including currents. Many existing state-of-the-art computer models such as MIKE 21 — Danish Hydraulic Institute (2008b, c) — still do not account for wave current interaction in their basic equations. It is evident that if the effects of current are not included in the original derivation of a basic wave equation, wave-current interaction will be ignored by any model using such an equation as its basis.

2.4 State-of-the-Art Modelling of Coastal Zone Processes

2.4.1 Wave Models

2.4.1.1 Introduction to Computer Wave Models

A number of different computer models have been created to simulate wave propagation. The choice of wave propagation model depends mainly on what properties of the wave the user envisages as most important in their given circumstances. Wave propagation models broadly fall into two categories. These are phase resolving and energy balanced (phase averaged) models. In general phase resolving models are more likely to be used in the coastal zone where the water is shallow and the modelled domain is of the order of a few kilometres. Phase resolving models are more useful for dealing with domains where wave-growth is not important and bottom topography governs wave behaviour. In these coastal models the water depth rarely exceeds 20m. Energy balanced models are more likely to be used in areas where wave growth effects are important and bottom topography does not have a dominant influence on wave behaviour.

2.4.1.2 Energy Balanced Wave Models

Energy balanced models examine a spectrum of wave heights and periods. Nwogu and Demirbilek (2001) consider these models appropriate where “wind-input, shoaling and refraction are dominant.” Chen *et al.* (2005) describes energy balanced models as suited to “large scale wave growth and wave transformation applications.” Models such as SWAN — Booij *et al.* (1999) — and STWAVE — Resio (1993) — are phase-averaged models. The phase averaging properties of these energy balanced models makes them unsuitable for circumstances where changes in domain properties such as changes in depth or domain shape lead to abrupt changes in the wave field within the range of a wavelength. Extensive meteorological data is usually required for the accurate implementation of an energy balanced model to a specific domain.

2.4.1.3 Phase Resolving Wave Models

2.4.1.3.1 Introduction to Phase Resolving Wave Models

The second type of wave propagation model is the phase resolving type. This model is run independently for any given wave phase in a spectrum. Chen *et al.* (2005) describe phase resolving models as “better suited to domains with complex bathymetry and geometric features, where the effects of wave diffraction and reflection can be important.” The aims of this project are more in keeping with this type of wave model because it can

be applied to complex bathymetry and indeed the effects of diffraction and reflection will undoubtedly be important in the coastal regions being examined, especially considering the presence of various obstacles in the domain. It was hence decided that for this project a phase resolving type wave model would be used to simulate wave propagation.

Phase resolving models can be either steady state or time dependant in nature. Time dependant models allow for change in sea level and incoming wave field for the model. Time dependant models are required if the change in water level within the domain or the wave field entering the domain is significant within the time it takes for a wave to propagate across the domain; Clyne (2008). In many cases it can be assumed that the variation in wave field and water depth is negligible when compared with the time taken for a wave to propagate across the modelled domain. In these cases a steady state model is sufficient. Vincent *et al.* (2002) gives examples of time-dependant phase resolving models for shallow water. These are by Jensen *et al.* (1987) and Demirbilek and Webster (1992a, b). However, Vincent *et al.* (2002) also state that these models “require extensive sets of meteorological data” and “cannot easily be applied.” In this project a general examination of waves, currents and wave-current interaction in the coastal zone is being carried out without reference to a specific location and hence it was deemed appropriate to use a steady-state model where external environmental conditions do not have a significant effect on the coastal zone to be examined.

2.4.1.3.2 Steady State Phase Resolving Wave Models

There are many different types of steady state phase-resolving wave propagation models and it was necessary to select an appropriate one for use in this project. Any of the wave theories discussed in Section 2.3.1 can be used as the mathematical basis for a numerical steady-state phase-resolving wave propagation mode. However, in most cases the phase-resolving models are based on Linear Theory or Boussinesq Theory. These include Linear models such as RCPWAVE by Ebersole (1985) and Ebersole *et al.* (1986), REF/DIF by Kirby and Dalrymple (1984) and CGWAVE by Demirbilek and Panchang (1998) and Boussinesq models such as BOUSS-2D as described by Nwogu and Demirbilek (2001) and the models of Madsen and Sorenson (1992) and Wei *et al.* (1995).

As described in Section 2.3.1.1.2.1.3 the traditional Boussinesq equations assumed a quadratic variation of wave velocity potential over the depth and were only suitable for

use in water of shallow depth. Although significant work has been completed by authors such as Nwogu (1993) to extend the effectiveness of Boussinesq Theory into the intermediate zone its usefulness for an overall model that can examine waves propagating in water of any depth is still limited. In comparison phase resolving wave models based on Linear Theory, which assume a hyperbolic cosine variation of the same property over the depth of the water column, are valid in water of all depths.

This project examines wave propagation, reflection and refraction in the coastal zone for varying bathymetry. No assumption is made with regard to the water depth being shallow and in some cases the water depth is transitional or deep. Hence, the author decided that a steady state phase resolving wave model based on Linear Theory is more appropriate for the aims of this project. The computer model created in this work is not limited to examining shallow water waves. This decision is made by a number of other authors with similar research interests, such as Chen *et al.* (2005).

2.4.1.3.3 Historical Development of Phase Resolving Models

Over the years engineers and scientists have used various methods to examine the effects of wave propagation. The increasing availability of computer processing power in recent years has led to a gradual change away from approximate graphical techniques towards increasingly more accurate numerical solution schemes for wave theories. As discussed in Section 2.3.1.3.2 the scope of this project is concerned with models based on linear theory so the following discussing will be limited to that theory.

2.4.1.3.3.1 Ray Tracing Techniques

Early wave models were based on graphical techniques. A simplified linear refraction theory was usually developed for these models and then wave rays were drawn to trace the behaviour of a specific wave across a spatial domain. The effects of shoaling could also be included. Vincent *et al.* (2002) provides a development of a wave ray theory following the development of Dean and Dalrymple (1991). These wave rays were lines drawn perpendicular to the wave crest. One of the main principles of ray theory is that energy between the wave rays remains constant. Hence the rays tend to move closer together in areas of wave focusing and further apart when the opposite occurs. Ray tracing techniques are limited by a number of factors. Most wave ray theories cannot model reflected waves so any obstacles within a modelled domain cannot be reflecting. In

regions where complex bathymetry causes the occurrence of amphidromic points classic wave ray theory tends to break down because the wave rays cross leading to a physically impossible situation. Wave rays also tend to behave erratically in domains with rapidly varying bathymetry and Vincent *et al.* (2002) highlight the problems that may occur even when smoothing techniques are used for the seabed. Wave rays are usually drawn by a progressive method that goes from deep to shallow water, hence any inaccuracies early in the drawing process will be magnified downstream. In more recent times computer programs have been developed to draw wave rays, these include those of Harrison and Wilson (1964), Dobson (1967) and Noda *et al.* (1974).

Wave ray techniques have mainly been superseded by numerical methods such as the mild-slope equation discussed in Sections 2.4.1.3.3.2 and 2.4.1.3.3.3; however, many authors have noted their usefulness as a speedy approach to obtain approximate solutions in simple circumstances. Clyne (2008) examines a new application of wave ray techniques for the simulation of wave breaking and recovery and for use in the construction of finite element solution meshes for more complex problems solved using the mild-slope equation. This method utilises a wave potential solution from an elliptic mild-slope wave model to draw progressive wave rays for the particular wave in question.

2.4.1.3.3.2 Elliptic Mild-Slope Equation

With the evident limitations on wave ray techniques and the increasing power of desktop computers numerical solution of wave behaviour has become significantly more popular than wave ray techniques. Various different numerical solutions have been derived based on the various wave theories described in Section 2.3.1. As discussed in Section 2.3.1.3.2 Linear Theory has shown itself to be the most suitable for the current project. One numerical solution based on linear theory that includes the effects of refraction, diffraction and reflection has been adopted in various forms by most computer based numerical models used to examine wave behaviour. This solution is the Mild-Slope Equation originally developed by Berkhoff (1972).

In the case of water waves of small amplitude it can be assumed that the fluid behaves in an incompressible, irrotational and inviscid manner. The use of such assumptions reduces the governing Navier-Stokes equations of motion for the fluid to a three dimensional Laplace equation. It would be possible to solve this three-dimensional Laplace equation

for wave behaviour but only in a very small domain due to the numerical intensity of the solution. A suggested method of more efficiently treating this three-dimensional Laplace equation is to integrate it vertically thus removing one degree of freedom from the system that must be solved. The vertically integrated Laplace equation for fluid motion is known as the mild-slope equation due to the assumption of a slowly varying seabed that is required to carry out the integration.

Berkhoff (1972) was the first to carry out this vertical integration procedure and thus developed a combined refraction-diffraction numerical solution known as the mild-slope equation. The Mild-Slope Equation is sometimes referred to as the Elliptic Mild-Slope Equation in order to distinguish its full elliptic form as derived by Berkhoff (1972) from some of the approximations that were later used to make the solution of the equation more computationally efficient.

The elliptic mild-slope equation developed by Berkhoff (1972) has been extended by a number of authors since. In general the alterations have included extra terms in the equation in order to account for the effects of various physical phenomena. These include the addition of terms to account for energy dissipation, both due to friction by Chen (1986), Dalrymple *et al.* (1984) and Liu (1994), and due to wave breaking by Dally *et al.* (1985) and De Girolamo *et al.* (1988).

Extra terms have also been included in the Elliptic Mild-Slope equation to counteract the “mild slope” assumption made during its derivation. Although these terms don’t remove this assumption they allow for the mild-slope equation to be used in domains with a steeper seabed. These “Extended Mild-Slope” terms allow the use of the now Extended Mild-Slope Equation on slopes steeper than the 1 in 3 slope that Booij (1983) states is the limit of accuracy for the mild-slope equation. Authors that have addressed the extension of the Mild-Slope Equation to steeper slopes are Massel (1993, 1994), Chamberlain and Porter (1995), Porter and Staziker (1995) and Clyne and Mullarkey (2008). The wave equations developed as part of this work also include extended terms to address the mild slope assumption.

The effects of wave-current interaction have also been included in some extensions to the Mild-Slope Equation. The effect of currents on the wave solution of the mild-slope equation was examined by Booij (1981) and subsequently corrected by Kirby (1984). It was also examined by Kostense *et al.* (1988). Panchang *et al.* (1999) mentions that for implementation of the current terms in any solution to the Mild-Slope Equation including the current terms developed by the authors listed here it is necessary to know the specific wave direction at any given point. This may not always be available for complex models involving obstacles or rapidly varying bathymetry. Panchang *et al.* (1999) highlights the inclusion of terms that model the effect of currents on waves in the Mild-Slope Equation as an area where further research is required. Chen *et al.* (2005) and Kostense *et al.* (1988) use an iterative scheme that updates on the gradient of phase to address the problem of unknown wave direction.

In order to make use of any variant of the Mild-Slope Equation an appropriate solution scheme is required. For most modern models this takes the form of either a finite difference or a finite element model. The complex nature of the equation is such that the discretisation of the equation over the domain in question and subsequent solving of the resulting system of equations is the most efficient solution. Due to its scalability and arbitrary unmapped meshing possibilities the finite element method has enjoyed increased favour in recent times. The programming of a finite element solution to the system of equations is, however, significantly more difficult than that of a finite difference scheme. Tsay and Liu (1983), Chen and Houston (1987), Demirbilek and Panchang (1998) and Clyne (2008) all developed finite element models for the Elliptic Mild-Slope Equation. Some of these models are discussed further in Section 2.3.1.3.4.

The solution scheme used to solve the discretised Mild-Slope Equation within a finite element domain is the key factor in determining the efficiency of the finite element model. Earlier models such as Tsay and Liu (1983) and Chen and Houston (1987) were restricted to the use of Gaussian elimination for solving the systems of equations. Later models more efficiently deal with the solution process. The model of Demirbilek and Panchang (1998) used the conjugate gradient method, and Clyne (2008) used a forward elimination and back substitution with upper and lower triangular matrices method after Zienkiewicz (1977). Both of these models significantly reduce the computational intensity of the finite element solution to the mild-slope equation.

The Mild-Slope Equation within the domain is largely the same in all the models discussed. However the types of boundary conditions used on the boundaries of the domain vary from model to model. The selection of appropriate boundary conditions is of vital importance to the accuracy of the solution obtained. In some cases the same model may require different boundary conditions depending on the wave conditions and physical makeup of the domain being examined.

Generally on the downstream (beach) boundary of the finite element a fully absorbing or partially reflecting boundary condition will be used. Berkhoff (1976) developed a boundary condition that allowed partial reflection based on a parameter that varied from 0 to 1 where 0 was fully absorbing and 1 was completely reflecting. The assumption is made that the wave is travelling perpendicular to the reflecting obstacle when reflection occurs. A phase lag term is also included in the Berkhoff (1976) partial reflection solution. Both Isaacson and Qu (1990) and Steward and Panchang (2000) investigate the inclusion of a non-perpendicular wave angle at reflection in the Berkhoff (1976) partial reflection method. In both cases this involves iteration of the solution compared to the single step solution of the Berkhoff (1976) method. Although the Steward and Panchang (2000) method has been shown to give quite accurate results the Berkhoff (1976) method is still used in many computer models such as those of Xu and Panchang (1993), Thompson *et al.* (1996), Xu *et al.* (1996), and Demirbilek and Panchang (1998), because of its simplicity. The Clyne (2008) model incorporates a similar scaling factor to Berkhoff (1976) but for increased accuracy includes it with an absorbing boundary condition based on the parabolic approximation to the Mild-Slope Equation after Booij (1981).

On the upstream (open) boundary a condition is required that specifies the input values of various wave properties and in the case of most models the upstream boundary condition is required to allow backscattered and reflected wave energy to escape from the domain so as not to pollute the results. A number of different boundary conditions have been developed to achieve this aim. Panchang *et al.* (1991) use a simple radiation condition that was derived assuming a constant depth outside the domain and assuming the crests of back scattered waves are parallel to the boundary. Berkhoff (1972) developed a modelling method which uses a Sommerfeld radiation boundary condition which uses Hankel functions to represent the radiated wave field. The Hankel functions are solved as part of the overall system of equations. Zienkiewicz (1977) developed a radiation

condition using infinite elements. These infinite elements have shape functions that are applied on the open boundary and decay to zero at infinity. A method that combines the main points of Berkhoff (1972) and Zienkiewicz (1977) is used by Thompson *et al.* (1996). A hybrid grid is created using a main domain of conventional finite elements and a second semi-infinite domain using an analytical solution for constant depth with Hankel functions. Other authors such as Houston (1981), Tsay and Liu (1983) and Xu *et al.* (1996) use a super-element technique to link open boundary points to points at infinity where the backscattered wave field is known. This method requires the use of Bessel functions to describe the backscattered waves.

More recently Kirby (1989) and Xu *et al.* (1996) investigate the use of a parabolic approximation to the Mild-Slope Equation as a radiation boundary condition. This method has the advantage of being more accurate when waves do not approach the boundary with crests parallel to that boundary. This is likely to be the case in most models. Clyne (2008) states that the radiation condition using a parabolic approximation to the Mild-Slope Equation is accurate for waves making small angles to the boundary and that this is the case in most models. Xu *et al.* (1996) compare the results of this method to the more traditional super-element method described above and find that the parabolic approximation method is not sensitive to the size of the domain and provides a more accurate result in cases where the super-element conditions have not been appropriately tuned to the problem being analysed.

Panchang *et al.* (2000), Zhao *et al.* (2001), Clyne and Mullarkey (2004, 2008) and Clyne (2008) investigate a radiation boundary condition where initially the cross shore domain is solved using a one dimensional elliptic mild-slope wave model and then the results of this model are interpolated as an incident wave field in conjunction with the parabolic approximation to the Mild-Slope Equation on to the open boundary of a two-dimensional model. Panchang *et al.* (2000) obtains results superior to those of the traditional super element method using this technique and Zhao *et al.* (2001) obtained results better than the traditional method of Xu *et al.* (1996). The parabolic approximation used by Clyne and Mullarkey (2004, 2008) and Clyne (2008) is based on the original parabolic approximation of Radder (1979) and it corresponds to a simple version of that used by Booij (1981).

2.4.1.3.3.3 Parabolic Approximation to Mild-Slope Equation

The increasing power of desktop computing in recent years has led to the creation of many computer models based on the Elliptic Mild-Slope Equation; however, in the recent past the computational intensity of such models prohibited their use in all but the smallest domains with the simplest bathymetry. At that time it was necessary to create approximate models that could reasonably accurately simulate the results of the Elliptic Mild-Slope Equation. Radder (1979) derived a parabolic approximation to the Elliptic Mild-Slope Equation, this parabolic approximation proved significantly less computationally intense and required less nodes per wavelength within the domain than a corresponding elliptic model. This improved efficiency was obtained with a corresponding loss in accuracy. The parabolic approximation does not include the effects of forward diffraction i.e. diffraction is only considered along the wave crest. It is also impossible to model wave reflection with the parabolic approximation and hence no reflecting obstacles could be included within a domain being examined using this method. Since the Radder (1979) derivation of the parabolic approximation other authors have included extra terms in the parabolic equation both to improve its accuracy and to allow it to model extra physical effects such as current interaction and breaking. Examples include Booij (1981), Berkhoff *et al.* (1982), Kirby and Dalrymple (1984), Kirby (1986), Kirby (1989) and Kirby *et al.* (1994). A large number of computer models were based on the parabolic approximation to the Mild-Slope Equation because of its efficiency. A selection of these is discussed in Section 2.4.1.3.4 below. The parabolic approximation to the Mild-Slope Equation has also proved itself to be very useful as a boundary condition for models based on the complete Elliptic Mild-Slope Equation. This is discussed in Section 2.3.1.3.3.2 above.

2.4.1.3.4 Examples of Steady State Phase Resolving Wave Models based on Linear Theory

There are a vast number of steady state phase resolving computer wave models available based on Linear Theory. It would be beyond the scope of this project to examine every available model. However, a selection of state of the art models is examined in the following sections.

2.4.1.3.4.1 RCPWAVE

RCPWAVE is a finite difference steady state phase resolving model based on linear wave theory. Full details of RCPWAVE can be found in Ebersole (1985) and Ebersole *et al.* (1986). RCPWAVE is based on the parabolic simplification of the elliptic mild-slope equation discussed in Section 2.4.1.3.3.3 above. For this model the mild-slope equation is separated into real and imaginary components and used with an explicit form of the irrotationality equation to obtain three coupled equations that can be solved for wave height, direction and phase gradient. RCPWAVE solves these coupled equations using a forward marching scheme that starts with specific input wave conditions at the deep boundary of the domain being examined and calculates the solution towards the beach. This solution method can only be used in cases where no reflection occurs and refraction is only in the advancing wave direction. This precludes the presence of reflecting obstacles within the domain being examined. Vincent *et al.* (2002) discuss this fact and mention that this limitation allows larger mesh sizes to be used by RCPWAVE, hence it can be used to examine larger domains more efficiently than other models. Panchang *et al.* (1999) also examine RCPWAVE and mention that for certain frequencies and grid layouts a solution does not converge and hence in many cases it is necessary to carry out a stability analysis on an engineering problem prior to solving it with RCPWAVE. For wave breaking RCPWAVE calculates a limiting wave height using the method of Weggel (1972) beyond this limit the model initiates the breaking wave model of Dally *et al.* (1985) If during breaking wave height falls below the stable value discussed by Dally *et al.* (1985) the energy dissipation term that instigates breaking is switched off.

2.4.1.3.4.2 REF/DIF

REF/DIF, based on the equations of Kirby (1984) is a weakly non-linear wave refraction diffraction model. REF/DIF is based on a wide angle parabolic solution of the mild-slope equation. The full elliptic solution to the mild-slope equation and its parabolic

approximation are discussed in Section 2.4.1.3.3.2 and 2.4.1.3.3.3 above. REF/DIF also includes third order non-linear Stokes Theory terms to provide more accurate results for wave behaviour in the intermediate water. The inclusion of these third order terms in very shallow water would cause inaccurate results and hence REF/DIF includes a smooth correction between Stokes Theory and an approximation to linear theory by Hedges (1976) to provide smoother more accurate results in the surf zone. The inclusion of higher order terms can also cause numerical noise to occur in the solution especially in the vicinity of breaker points and obstacles such as islands. A noise filtering subroutine has been included in REF/DIF to counteract the occurrence of this noise. The smooth correction and noise filtering subroutines are discussed in Vincent *et al.* (2002) and in Kirby and Dalrymple (1986a, b) respectively. REF/DIF examines wave height with respect to a specific limit beyond which height it instigates a breaking wave energy flux decay model detailed by Dally *et al.* (1985). A spectral version of the REF/DIF model has also been developed. The basic mild-slope equations of the REF/DIF model include the effects of currents. Hence according to Vincent *et al.* (2002) “The model can simulate aspects of propagation associated with simple currents.”

2.4.1.3.4.3 CGWAVE

CGWAVE contrasts with RCPWAVE and REF/DIF in that instead of being based on the Parabolic Approximation of the mild-slope equation it is based on the full elliptic solution to the mild-slope equation. CGWAVE is developed in detail in Demirbilek and Panchang (1998) and is also examined by Panchang *et al.* (1999). The increased complexity of the elliptic mild-slope equation compared to the parabolic approximation allows CGWAVE to solve for refraction, diffraction, reflections by bathymetry and structures, dissipation due to friction and breaking, and nonlinear amplitude dispersion. The examination of all the effects means that in some places a very refined solution grid is required. CGWAVE uses a finite element solution scheme which provides a more scalable grid than a finite difference method. The conjugate gradient method developed by Panchang *et al.* (1991) is used to solve the system of equations developed using the finite element method. CGWAVE uses energy dissipation terms based on the equations of Dally *et al.* (1985), Demirbilek (1994) and Briggs *et al.* (1996) for wave breaking. CGWAVE does not yet include the effects of wave-current interaction.

2.4.1.3.4.4 Clyne (2008)

The Clyne (2008) model is an updated version of the previous models by the same author discussed in Clyne and Mullarkey (2004, 2008). This is a finite element model based on the complete Elliptic Mild-Slope Equation extended to include the effects of a steep bottom. As with CGWAVE the superiority of the elliptic mild-slope equation above the parabolic approximation allows the Clyne (2008) model to solve for refraction, diffraction, reflections by bathymetry and structures and dissipation due to breaking. Clyne (2008) examines the use of this model for a wide variety of scenarios and compares it with both measured results and other models. The results are very favourable. The Clyne (2008) model uses a forward elimination and back substitution with upper and lower triangular matrices method after Zienkiewicz (1977) for solution of the system of matrices. Breaking is carried out in the model using an energy dissipation term after Dally *et al.* (1985) and Battjes and Janssen (1978). Wave-current interaction is not examined by the Clyne (2008) model.

2.4.1.3.4.5 MIKE 21

MIKE 21 is a state of the art finite difference computer model incorporating both a wave model and a hydrodynamic model. The MIKE 21 wave model can be run either using the parabolic approximation to the mild-slope equation discussed in Danish Hydraulic Institute (2008b), or using the complete elliptic solution to the mild-slope equation discussed in Danish Hydraulic Institute (2008c). Neither version of the MIKE 21 wave model includes the effects of wave current interaction. The model equations listed by Danish Hydraulic Institute (2008b, c) are based on the mild-slope equation in the absence of currents. The MIKE 21 wave model includes an energy dissipation term for wave breaking based on the work of Battjes and Janssen (1978). There is also a term included for the dissipation of energy due to bottom friction which for monochromatic waves is based on the work of Putnam and Johnson (1949). A spectral wave version of the MIKE 21 model is available.

2.4.1.3.4.6 PHAROS

PHAROS is a finite element computer model based on the Berkhoff (1972) solution to the elliptic mild slope equation and extended to account for the presence of ambient currents. PHAROS includes terms for energy dissipation from wave breaking based on the work of Battjes and Janssen (1978) and energy dissipation terms due to bed friction are also

included after the work of Putnam and Johnson (1949). The PHAROS model can utilise reflection, partial reflection and transmission boundary conditions. Wave diffraction, refraction and shoaling due to bathymetry and ambient currents and wave reflection can be examined by PHAROS.

2.4.2 Models of Nearshore Currents and Set-up/Set-down

2.4.2.1 Introduction

Currents in the near shore region can be driven by tidal effects, wave breaking or wind effects. In general nearshore currents can be split into two distinct categories; those that travel parallel to the shore, known as longshore currents and those that travel perpendicular to the shore, known as cross-shore or rip currents. A current in any direction can be defined by its longshore and cross-shore components. In many cases circulation cells may form in the coastal region that comprises sections of coastline where a longshore current is dominant and interspersed with rip currents. Currents caused by wind may occur in any direction dependant on meteorological conditions. Currents caused by tidal effects are always a property of the tidal range and bathymetry at the location being examined. Wave-driven currents are caused by radiation stress, an effect of breaking waves which has been discussed in Sections 2.2.5 and 2.3.4 above. Obliquely breaking waves on a beach will create a longshore current which at abrupt bathymetric changes will give rise to a rip current. Waves breaking directly perpendicular to a beach may in some cases generate circulation cells depending on the bathymetry of the beach. Second order nearshore currents occur in cases where the set-up/set-down caused by cross-shore radiation stress varies along a coastline. This variation in set-up/set-down leads to a difference in water pressures and hence a hydrostatic flow of fluid from one location to another. Sorenson (2006) discusses the magnitude of longshore currents. The results of Szuwalski (1970) are quoted. Szuwalski (1970) produced results of a very large number of longshore current measurements off the California coast taken at a number of different sites. The values of longshore current were generally below 0.5m/s but in some extreme cases reached values of approximately 1m/s.

2.4.2.2 Analytical Calculation of Wave-Driven Currents

The only nearshore currents that lend themselves to possible analytical calculation are wave-driven longshore currents. Longuet-Higgins (1970a, b) developed his work on Radiation Stress into a simple analytical formula for longshore current. The assumptions made in this derivation were uniformity of bathymetry and wave behaviour in the alongshore direction, no lateral mixing and a small angle of wave incidence. Komar and Inman (1970) also develop a formula for prediction of longshore current. Smith (2003) provides the equation of the Komar and Inman (1970) solution and shows that a value for longshore current can only be obtained at the midpoint of the surf zone using this method.

The solution is independent of both beach slope and bottom roughness which would indicate an assumed relationship between the two which leads to a constant value.

2.4.2.3 Cross Shore Profile of Longshore Currents

An idealised solution for longshore current would have a linear profile across the surf-zone from zero at the beach to a maximum velocity at the breaker point beyond which the longshore velocity would be zero. The formula of Longuet-Higgins (1970a, b) provides this triangular profile exactly. In nature, however, the presence of turbulent diffusion has a mixing effect which smoothes this profile. The selection of the turbulent diffusion term is important for quantifying the degree of longshore current outside the surf zone and the peak value of longshore current within the surf zone.

Physically the turbulent diffusion or lateral mixing is caused by horizontal eddies developed by wave breaking. Bowen (1969) assumed that a constant eddy coefficient could be used across the surf zone to model this process. Longuet-Higgins (1970b) developed a formula for calculating the eddy coefficient that linked the value of the coefficient with the distance offshore. Battjes (1975) suggests that the eddy coefficient is actually governed by the depth and hence its relationship to distance offshore is only valid for uniformly sloping beaches. Battjes (1975) derived a method based on beach slope and local rate of wave-energy dissipation, this relationship is very similar to that of Longuet-Higgins (1970b) for uniform beaches but shows a difference for non-uniform ones. Thornton (1970) and Jonsson *et al.* (1974) based their calculation of the eddy coefficient on wave orbital motions a methodology which Battjes (1975) criticised because the main source of turbulence in the surf zone is wave breaking and not orbital motions. Church and Thornton (1993) discuss the use of an equation linking the eddy coefficient with turbulent kinetic energy. This methodology links the eddy viscosity directly to the dissipation of wave energy.

The selection of an appropriate methodology for calculation of the eddy coefficient can depend largely on the scenarios being examined by the model in question. All the methodologies discussed in this section can be found in present state of the art models. Mei *et al.* (2005) suggest the use of the Longuet-Higgins (1970b) model. The NMLONG model of Larson and Kraus (1991) uses a methodology based on orbital motions. Kuriyama and Nakatsukasa (2000) and the TIDEFLOW-2D and University of Liverpool

models examined by Péchon *et al.* (1997) use the Battjes (1975) method. The CIRCO and University of Thessaloniki models examined by Péchon *et al.* (1997) use the method based on turbulent kinetic energy. Leont'yev (1997) found that after examining various types of horizontal eddy viscosity coefficients the best agreement with available longshore current data was obtained from using a uniform value throughout the surf zone. The MIKE 21 HD model examined by Péchon *et al.* (1997) also uses a uniform value throughout the surf zone, however it is stated by Danish Hydraulic Institute (2008b) that the newer version of MIKE 21 also allows the user the option of applying the eddy viscosity as “A time-varying function of the local gradients in the velocity field.” After examination of the principles involved it was decided for this project it would be best to select appropriate turbulent diffusion and energy dissipation methods for each given circumstance as opposed to deciding on one overall method. It would then be possible to examine the results to determine the appropriateness of each method.

2.4.2.4 Analytical Calculation of Set-up/Set-down

The physical process of set-up/set-down has been discussed in Section 2.2.4 and the available mathematical descriptions of the process have been examined in Section 2.3.3. Smith (2003) provides an analytical formula, after Longuet-Higgins and Stewart (1963), for calculating set-up and set-down in the case of simple waves approaching a beach with unvarying bathymetry in the alongshore direction. However, most modern calculation of set-up/set-down is focused on using numerical models that combine the effects of radiation stress with the governing equations for momentum and conservation of mass that define hydrodynamic behaviour of fluids.

2.4.2.5 Bed Friction

In the presence of both waves and current the friction between the water column and the sea-bed is a significant factor in the dissipation of energy. Indeed in the case of some wave-generated currents the bottom friction combined with turbulence effects are the only factors resisting the flow. Jonsson *et al.* (1974) proposed a formula for bottom friction in the presence of both waves and current. Mei *et al.* (2005) presents this quadratic law as appropriate for use in the presence of waves and current. Kraus and Larson (1991) also present the same formula for use in the presence of a large current and small waves. There is no indication provided, however, of the range of magnitudes of current for which it is valid. Péchon *et al.* (1997) examine a number of different wave-driven current models

and find that all but one of the seven models examined use a quadratic law of wave driven velocity to model bottom friction. This model is also used by Newell *et al.* (2005b). Some of the models examined by P  chon *et al.* (1997) also include a wave orbital velocity component in the bottom friction term similar to that included in the Newell *et al.* (2005b) model.

2.4.2.6 Numerical Models for Wave-Generated Currents and Set-up/Set-down

2.4.2.6.1 Introduction

Set-up/set-down and wave generated currents have proved much easier to examine with the use of modern numerical models solved by computer. Although the early analytical and empirical formulae discussed above can be used in some simple circumstances it is necessary to run numerical models to obtain values of currents and set-up/set-down where complex bathymetry and wave scenarios are being examined. These numerical computer models are based on the conservation of mass and Navier-Stokes momentum equations that describe the hydrodynamic behaviour of fluids. The momentum equations can include terms to model bed friction, turbulent diffusion and the driving force of radiation stress generated by a wave field. In most cases the momentum equations are developed in a vertically averaged form that allows the model to be solved in two dimensions as opposed to a more computationally intensive solution in three dimensions.

2.4.2.6.2 NMLONG

The NMLONG model of Kraus and Larson (1991) and Larson and Kraus (2002) is a one dimensional, depth-averaged, finite difference model that solves for set-up/set-down and longshore currents for waves approaching a beach with non-varying bathymetry in the longshore direction. NMLONG uses gradients of radiation stress as a driving force within the momentum equations. The lateral dispersion term in the NMLONG model is based on energy dissipation as a function of eddy viscosity which in turn is taken as a function of characteristic wave orbital velocity. The bottom friction term in the NMLONG model is a quadratic law of wave driven velocity.

2.4.2.6.3 MIKE 21 HD

MIKE 21 is a series of both wave and hydrodynamic models that examine behaviour in the coastal zone. The depth averaged hydrodynamic portion of the model that calculates set-up/set-down and wave-driven currents using a finite difference solution scheme in two dimensions is titled MIKE 21 HD. The basic equations of the MIKE 21 HD model are discussed by Danish Hydraulic Institute (2008a, b). The MIKE 21 HD model includes a quadratic law of wave driven velocity to model bottom friction and has the option of using a uniform value of eddy viscosity throughout the surf zone for lateral dispersion. However MIKE 21 HD also allows the user the option to apply the eddy viscosity as “A time-varying function of the local gradients in the velocity field.” Gradients of radiation stress are used by the MIKE 21 HD model as a driving force for wave generated effects.

2.4.2.6.4 TELEMAC-3D

TELEMAC-3D was examined by P  chon *et al.* (1997) and compared with a number of other wave driven models. TELEMAC-3D includes a constant viscosity coefficient and a wave energy dissipation term to model turbulent diffusion. It also includes a quadratic equation of wave driven velocity to model bottom friction. TELEMAC-3D uses an expression of radiation stress developed by Dingemans *et al.* (1987). It was noted by P  chon *et al.* (1997) that in order to obtain accurate results using the TELEMAC-3D model it was necessary to apply a correction coefficient to the driving terms obtained by the model. TELEMAC-3D does not adopt a depth averaged solution and must therefore be solved in three dimensions.

2.4.2.6.5 Newell *et al.* (2005b)

Newell *et al.* (2005b) is a publication of earlier work of this thesis. As such the model presented in the paper is an earlier version of final model presented in this thesis. The model uses gradients of radiation stress as the driving term in the momentum equations. The bottom friction is modelled using a quadratic law developed after Mei *et al.* (2005) and including the effects of wave orbital velocity. No turbulent diffusion had been included in the model at the 2005 stage. The Newell *et al.* (2005b) model is a depth-averaged model and hence solutions are obtained for set-up/set-down and current over two depth-averaged dimensions.

2.5 Research Decisions based on Literature and State of the Art Review

As stated in Chapter 1 the aim of this project was to examine the behaviour of waves in the presence of obstacles and complex bathymetry in the coastal zone and to examine the effects generated by these waves.

2.5.1 Newell Mullarkey Wave-Current Interaction Model (NM-WCIM)

It was apparent from the literature review carried out in this chapter that considering the stated aims of this project, monochromatic waves should be examined. The complexity of the bathymetry to be examined and the range of depths being examined lead to the conclusion that the most efficient wave theory to use for the broad range of scenarios being examined was linear wave theory. The extended elliptic solution to the mild-slope equation including the effects of currents is the most accurate solution available for linear wave theory and was therefore selected for use in this project. The inclusion of extended terms will address the assumption of a mild slope in the derivation of the elliptic equation. The wide availability and complexity of wave breaking methodologies led to the conclusion that it was not appropriate to limit the model to one breaking methodology. A better solution was to select an appropriate breaking methodology for each individual scenario being examined. It was apparent also from the state of the art numerical wave models examined in this chapter that the use of a finite element technique for numerical solution allowed more scalability. A finite element solution scheme was chosen for this project on the basis that it would allow a concentration of the results of the model in locations that were of interest without the necessity for detailed computationally intensive calculations in regions of little interest.

2.5.2 Newell Mullarkey Wave-Driven Hydrodynamic Model (NM-WDHM)

Use of the Navier-Stokes momentum equations and conservation of mass are considered the most appropriate way of examining wave-generated behaviour. From the literature review carried out above it was apparent the most widespread and favoured method of including a wave driving force in the momentum equations was using the gradients of radiation stress obtained from the wave field. It was considered appropriate to use this method for the current project. The use of a quadratic law including wave orbital terms is seen as the most accurate way to simulate bottom friction and it was decided that this project would include such a method. There is a wide range of methodologies available to describe turbulent diffusion effects and it was considered necessary to examine more than

one. The two most widespread and most scientifically viable methods were examined in detail in this project; namely the energy dissipation method based on eddy viscosity of Battjes (1975) and the methodology of Longuet-Higgins (1970b). Using the information discussed in this chapter it was decided to use a depth-integrated wave driven hydrodynamic model. It was considered that the increased computational load that would result from a three-dimensional model would have a serious detrimental effect on the possible range and number of scenarios that could be examined which would not be outweighed by the increase in accuracy of results. Section 2.5.1 discusses the use of a finite element solution technique in the NM-WCIM. The same arguments apply here and hence it was deemed appropriate to use a finite element solution technique for the NM-WDHM.

Chapter 3: Wave Current Interaction Model

“Do not worry about your difficulties in mathematics, I assure you that mine are greater,” Albert Einstein.

3.1 Introduction

This chapter presents the derivation of the basic equations for the NM-WCIM. Berkhoff (1976) developed an elliptic solution to the mild-slope equation that excludes the effects of current. Booij (1981) developed a mild-slope equation including the effects of current (subsequently corrected by Kirby (1984) for inaccuracies in the current terms) using a variational calculus approach. Massel (1993) and Clyne (2008) developed an elliptic solution to the mild-slope wave equation using a Galerkin-Eigenfunction method, excluding the effects of current. This chapter presents a similar derivation using the Galerkin-Eigenfunction method of Massel (1993) for the formulation of an elliptic solution to the mild-slope equation including the effects of current. After derivation of this solution it will be adjusted for use in a finite element wave current interaction model. The adjustments include the incorporation of appropriate boundary conditions and integration of the solution over a triangular finite element.

The progression of Chapter 3 is as follows:

- Initially the governing equations of continuity and momentum for fluid motion are discussed and the continuity equation is used to develop a Laplacian equation in terms of velocity potential – Sections 3.2 and 3.3
- A set of non-linear boundary conditions at the free surface and sea-bed are developed using the kinematic and momentum equations – Section 3.4
- The developed Laplacian and boundary conditions are used to obtain a set of harmonic wave equations – Section 3.5
- A vertical eigenfunction is derived by solving the Laplacian equation and its boundary conditions on a flat sea bed with a constant current – Section 3.6
- A Laplacian equation weighted by the vertical equation is then integrated over the depth. Using integration by parts combined with the free surface and seabed boundary conditions results in the two-dimensional extended mild-slope wave equation – Section 3.7

- The developed mild-slope equation is used to create a one-dimensional and two-dimensional finite element model (NM-WCIM) – Sections 3.8 and 3.9
- A Helmholtz form of the finite element mild-slope wave current interaction model is developed – Section 3.10
- Boundary conditions for the finite element model are examined – Section 3.11
- Energy dissipation in the NM-WCIM is discussed – Section 3.12
- Practical aspects of the iterative use of the NM-WCIM are discussed – Section 3.13

3.2 Equations of Continuity and Momentum

This section discusses the governing equations of fluid motion, known as the Navier-Stokes Equations for conservation of mass and momentum, within a system following closely the work of Berkhoff (1976) and Clyne (2008).

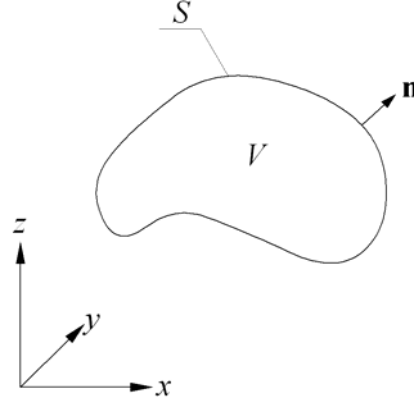


Figure 3.1 – Fixed Volume of Water in Three-Dimensional Space

Figure 3.1 describes a fixed volume of fluid V with a surface S and an outward normal to that surface \mathbf{n} . Moving fluid is considered to have an instantaneous velocity $\mathbf{u} = (u_1, u_2, u_3)$ and a density ρ .

3.2.1 Continuity Equation

To formulate any equation for continuity (also known as conservation of mass) within a system the mass of that system must first be examined. Mass is defined as the product of volume and density. Therefore the mass of the fixed volume described in Figure 3.1 is as follows:

$$M = \iiint_V \rho dV \quad (3.1)$$

To examine the change in mass of a fixed volume of fluid with respect to time one must examine both a possible change in density within the volume and the flow of fluid through the surface of the volume. Hence the derivative of mass with respect to time may be expressed as follows:

$$\frac{dM}{dt} = \iiint_V \frac{\partial \rho}{\partial t} dV + \iint_S \rho \mathbf{u} \cdot \mathbf{n} dS \quad (3.2)$$

If the mass is assumed to remain constant then the following is clearly true:

$$\frac{dM}{dt} = 0 \quad (3.3)$$

It is convenient at this stage to examine the divergence theory of Gauss. This states that if a vector $\mathbf{a}(x, y, z)$ is a continuous function and its first partial derivatives are continuous within the domain containing V then the following identity holds true:

$$\iiint_V \nabla \cdot \mathbf{a} dV = \iint_S \mathbf{n} \cdot \mathbf{a} dS \quad (3.4)$$

The Gauss divergence theorem can be used with the second term on the right hand side of Equation (3.2) leading to the following expression:

$$\frac{\partial M}{\partial t} = \iiint_V \frac{\partial \rho}{\partial t} dV + \iiint_V \nabla \cdot (\rho \mathbf{u}) dV \quad (3.5)$$

Combining Equation (3.5) with the assumption of Equation (3.3) gives:

$$0 = \iiint_V \left(\frac{\partial \rho}{\partial t} + \nabla \cdot (\rho \mathbf{u}) \right) dV \quad (3.6)$$

The volume V selected for this derivation is arbitrary in nature and hence the following simplification of Equation (3.6) can be made:

$$\frac{\partial \rho}{\partial t} + \nabla \cdot \rho \mathbf{u} = 0 \quad (3.7)$$

Equation (3.7) is the Continuity Equation. The first term is the change in density with respect to time and the second term is the divergence of the mass flux density vector.

3.2.2 Momentum Equation

Momentum \mathbf{p} is defined as the vector resulting from the product of mass and velocity.

Thus working with Equation (3.1) the following definition can be made:

$$\mathbf{p} = \iiint_V \rho \mathbf{u} dV \quad (3.8)$$

The rate of change of momentum with respect to time (known as impulse) can then be obtained using Equation (3.2):

$$\frac{d\mathbf{p}}{dt} = \iiint_V \frac{\partial \rho \mathbf{u}}{\partial t} dV + \iint_S \rho (\mathbf{u} \cdot \mathbf{n}) \mathbf{u} dS \quad (3.9)$$

Newton's principle is that the rate of change of momentum per unit time acting on a volume V is equal to the total force exerted on the volume. In the case of this derivation shear forces acting on the body are ignored due to the assumption of negligible viscosity. Therefore the forces acting on the body consist of the force of gravity, described as an external force vector per unit volume \mathbf{F} , and the pressure, described as a vector \mathbf{K} (including shear stresses and other stresses) acting on the volume's surface.

$$\iiint_V \frac{\partial \rho \mathbf{u}}{\partial t} dV + \iint_S \rho (\mathbf{u} \cdot \mathbf{n}) \mathbf{u} dS = \iiint_V \rho \mathbf{F} dV + \iint_S \mathbf{K} dS \quad (3.10)$$

The pressure can be defined as a pressure p acting normal to the surface. The pressure vector hence takes on a negative sign as the normal \mathbf{n} is defined earlier in this section as positive in the outward direction from the surface, whereas the pressure acts inwards on the surface.

$$\mathbf{K} = -p\mathbf{n} + \boldsymbol{\sigma}' \cdot \mathbf{n} \quad (3.11)$$

Where $\boldsymbol{\sigma}' \cdot \mathbf{n}$ is a general stress term.

Using the result of Equation (3.11) with Equation (3.10) yields the following:

$$\iiint_V \frac{\partial \rho \mathbf{u}}{\partial t} dV + \iint_S \rho (\mathbf{u} \cdot \mathbf{n}) \mathbf{u} dS - \iiint_V \rho \mathbf{F} dV + \iint_S p \mathbf{n} dS - \iint_S \boldsymbol{\sigma}' \cdot \mathbf{n} dS = 0 \quad (3.12)$$

An inner product of Equation (3.12) and a constant vector \mathbf{a} gives:

$$\iiint_V \mathbf{a} \cdot \frac{\partial \rho \mathbf{u}}{\partial t} dV + \iint_S \rho (\mathbf{u} \cdot \mathbf{n}) \mathbf{a} \cdot \mathbf{u} dS - \iiint_V \rho \mathbf{F} \cdot \mathbf{a} dV + \iint_S p \mathbf{n} \cdot \mathbf{a} dS - \iint_S \mathbf{a} \cdot \boldsymbol{\sigma}' \cdot \mathbf{n} dS = 0 \quad (3.13)$$

Expressing the last term of Equation (3.13) in tensor notation gives:

$$-\iint_S \mathbf{a} \cdot \boldsymbol{\sigma}' \cdot \mathbf{n} dS = -\iint_S a_i \sigma'_{ij} n_j dS \quad (3.14)$$

Equation (3.14) can also be expressed as follows using the Gauss divergence theorem:

$$-\iint_S \mathbf{a} \cdot \boldsymbol{\sigma}' \cdot \mathbf{n} dS = -\iiint_V \frac{\partial}{\partial x_i} a_i \sigma'_{ij} dV \quad (3.15)$$

Exploiting the fact that $\sigma'_{ij} = \sigma'_{ji}$ in this case allows Equation (3.15) to be written as follows:

$$-\iint_S \mathbf{a} \cdot \boldsymbol{\sigma}' \cdot \mathbf{n} dS = -\iiint_V \nabla \cdot (\mathbf{a} \cdot \boldsymbol{\sigma}') dV \quad (3.16)$$

Applying the Gauss divergence theorem from Equation (3.4) on the second and fourth terms of Equation (3.13) gives:

$$\begin{aligned} & \iiint_V \mathbf{a} \cdot \frac{\partial \rho \mathbf{u}}{\partial t} dV + \iiint_V \nabla \cdot [\rho \mathbf{u} (\mathbf{u} \cdot \mathbf{a})] dV \\ & - \iiint_V \rho \mathbf{F} \cdot \mathbf{a} dV + \iiint_V \nabla \cdot (p \mathbf{a}) dV - \iiint_V \nabla \cdot (\mathbf{a} \cdot \boldsymbol{\sigma}') dV = 0 \end{aligned} \quad (3.17)$$

$$\iiint_V \left(\mathbf{a} \cdot \frac{\partial \rho \mathbf{u}}{\partial t} + \nabla \cdot [\rho \mathbf{u} (\mathbf{u} \cdot \mathbf{a})] - \rho \mathbf{F} \cdot \mathbf{a} + \nabla \cdot (p \mathbf{a}) - \nabla \cdot (\mathbf{a} \cdot \boldsymbol{\sigma}') \right) dV = 0 \quad (3.18)$$

The second term of Equation (3.18) can be expanded as follows:

$$\begin{aligned} \nabla \cdot [\rho \mathbf{u} (\mathbf{u} \cdot \mathbf{a})] &= \frac{\partial}{\partial x_i} (\rho u_i u_j a_j) = u_j a_j \frac{\partial}{\partial x_i} (\rho u_i) + \rho a_j u_i \frac{\partial u_j}{\partial x_i} + \rho u_j u_i \frac{\partial a_j}{\partial x_i} \\ \nabla \cdot [\rho \mathbf{u} (\mathbf{u} \cdot \mathbf{a})] &= (\mathbf{u} \cdot \mathbf{a}) \nabla \cdot (\rho \mathbf{u}) + \rho \mathbf{a} \cdot (\mathbf{u} \cdot \nabla \mathbf{u}) + \rho \mathbf{u} \cdot (\mathbf{u} \cdot \nabla \mathbf{a}) \end{aligned} \quad (3.19)$$

The vector \mathbf{a} is a constant vector. Hence:

$$\nabla \mathbf{a} = 0 \quad (3.20)$$

Therefore using Equation (3.20) in Equation (3.19) gives:

$$\nabla \cdot [\rho \mathbf{u} (\mathbf{u} \cdot \mathbf{a})] = (\mathbf{u} \cdot \mathbf{a}) \nabla \cdot (\rho \mathbf{u}) + \rho \mathbf{a} \cdot (\mathbf{u} \cdot \nabla \mathbf{u}) \quad (3.21)$$

Using Equation (3.21) with Equation (3.18) yields:

$$\iiint_V \left(\mathbf{a} \cdot \frac{\partial \rho \mathbf{u}}{\partial t} + (\mathbf{u} \cdot \mathbf{a}) \nabla \cdot (\rho \mathbf{u}) + \rho \mathbf{a} \cdot (\mathbf{u} \cdot \nabla \mathbf{u}) - \rho \mathbf{F} \cdot \mathbf{a} + \nabla \cdot (p \mathbf{a}) - \nabla \cdot (\mathbf{a} \cdot \boldsymbol{\sigma}') \right) dV = 0 \quad (3.22)$$

The vector \mathbf{a} can now be isolated:

$$\iiint_V \mathbf{a} \cdot \left(\frac{\partial \rho \mathbf{u}}{\partial t} + \mathbf{u} \nabla \cdot (\rho \mathbf{u}) + \rho \mathbf{u} \cdot (\nabla \mathbf{u}) - \rho \mathbf{F} + \nabla p \right) dV - \iiint_V \nabla \cdot (\mathbf{a} \cdot \boldsymbol{\sigma}') dV = 0 \quad (3.23)$$

The vector \mathbf{a} and volume V are arbitrary in nature and provide neither is zero the Equation (3.23) reduces to:

$$\frac{\partial \rho \mathbf{u}}{\partial t} + \mathbf{u} \nabla \cdot (\rho \mathbf{u}) + \rho \mathbf{u} \cdot (\nabla \mathbf{u}) - \rho \mathbf{F} + \nabla p - \nabla \cdot (\boldsymbol{\sigma}') = 0 \quad (3.24)$$

Expanding the first term of Equation (3.24) yields:

$$\rho \frac{\partial \mathbf{u}}{\partial t} + \mathbf{u} \frac{\partial \rho}{\partial t} + \mathbf{u} \nabla \cdot (\rho \mathbf{u}) + \rho \mathbf{u} \cdot (\nabla \mathbf{u}) - \rho \mathbf{F} + \nabla p - \nabla \cdot (\boldsymbol{\sigma}') = 0 \quad (3.25)$$

Equation (3.25) can also be expressed as:

$$\mathbf{u} \left(\frac{\partial \rho}{\partial t} + \nabla \cdot (\rho \mathbf{u}) \right) + \rho \frac{\partial \mathbf{u}}{\partial t} + \rho \mathbf{u} \cdot (\nabla \mathbf{u}) - \rho \mathbf{F} + \nabla p - \nabla \cdot (\boldsymbol{\sigma}') = 0 \quad (3.26)$$

Using Equation (3.7) with Equation (3.26) gives:

$$\rho \frac{\partial \mathbf{u}}{\partial t} + \rho \mathbf{u} \cdot (\nabla \mathbf{u}) - \rho \mathbf{F} + \nabla p - \nabla \cdot (\boldsymbol{\sigma}') = 0 \quad (3.27)$$

Equation (3.27) can now be divided across by ρ :

$$\frac{\partial \mathbf{u}}{\partial t} + \mathbf{u} \cdot (\nabla \mathbf{u}) - \mathbf{F} + \frac{\nabla p}{\rho} - \frac{\nabla \cdot (\boldsymbol{\sigma}')}{\rho} = 0 \quad (3.28)$$

Moving the general stress term in Equation (3.28) to the right hand side of the equation yields:

$$\frac{\partial \mathbf{u}}{\partial t} + \mathbf{u} \cdot (\nabla \mathbf{u}) - \mathbf{F} + \frac{\nabla p}{\rho} = \frac{\nabla \cdot (\boldsymbol{\sigma}')}{\rho} \quad (3.29)$$

The product rule for vectors can be expressed as follows:

$$\nabla (\mathbf{u} \cdot \mathbf{v}) = (\mathbf{u} \cdot \nabla) \mathbf{v} + (\mathbf{v} \cdot \nabla) \mathbf{u} + \mathbf{u} \times (\nabla \times \mathbf{v}) + \mathbf{v} \times (\nabla \times \mathbf{u}) \quad (3.30)$$

In the case where $\mathbf{u} = \mathbf{v}$ this becomes:

$$\nabla (\mathbf{u} \cdot \mathbf{u}) = 2(\mathbf{u} \cdot \nabla) \mathbf{u} + 2[\mathbf{u} \times (\nabla \times \mathbf{u})] \quad (3.31)$$

Equation (3.31) can then be rearranged to give:

$$(\mathbf{u} \cdot \nabla) \mathbf{u} = \frac{1}{2} \nabla (\mathbf{u} \cdot \mathbf{u}) - [\mathbf{u} \times (\nabla \times \mathbf{u})] \quad (3.32)$$

The second term in Equation (3.29) can be replaced by the result of Equation (3.32):

$$\frac{\partial \mathbf{u}}{\partial t} + \frac{1}{2} \nabla (\mathbf{u} \cdot \mathbf{u}) - \mathbf{u} \times (\nabla \times \mathbf{u}) - \mathbf{F} + \frac{\nabla p}{\rho} = \frac{\nabla \cdot (\boldsymbol{\sigma}')}{\rho} \quad (3.33)$$

When \mathbf{F} represents a conservative vector field the following is true:

$$\mathbf{F} = -\nabla \Omega \quad (3.34)$$

Equation (3.33) can now be rewritten taking account of Equation (3.34):

$$\frac{\partial \mathbf{u}}{\partial t} + \frac{1}{2} \nabla (\mathbf{u} \cdot \mathbf{u}) - \mathbf{u} \times (\nabla \times \mathbf{u}) + \frac{\nabla p}{\rho} + \nabla \Omega = \frac{\nabla \cdot (\boldsymbol{\sigma}')}{\rho} \quad (3.35)$$

The external force potential representing gravity can be expressed as:

$$\Omega = gz \quad (3.36)$$

Using Equations (3.34) and (3.36) with Equation (3.29) yields:

$$\frac{\partial \mathbf{u}}{\partial t} + \mathbf{u} \cdot (\nabla \mathbf{u}) + \nabla gz + \frac{\nabla p}{\rho} = \frac{\nabla \cdot (\boldsymbol{\sigma}')}{\rho} \quad (3.37)$$

Equation (3.37) can be expressed as follows:

$$\left(\frac{\partial}{\partial t} + \mathbf{u} \cdot \nabla \right) \mathbf{u} = -\nabla \left(\frac{p}{\rho} + gz \right) + \frac{\nabla \cdot (\boldsymbol{\sigma}')}{\rho} \quad (3.38)$$

This form of the momentum equation in the absence of viscosity is given by many authors including Mei *et al.* (2005).

3.3 Application of Velocity Potential to Continuity and Momentum Equations

3.3.1 Application of Velocity Potential to the Continuity Equation

In the coastal zone properties of fluid flow are often expressed in terms of a scalar quantity called the velocity potential $\tilde{\Phi}$. The gradient of the velocity potential is the velocity. In order to model coastal flow in terms of velocity potential it is necessary to assume irrotational flow. This assumption is justified for an ideal fluid where the onset of motion has no tendency to cause rotation. The assumption of irrotational flow can be expressed mathematically by setting the curl of the water particle velocity to zero:

$$\nabla \times \mathbf{u}' = 0 \quad (3.39)$$

Wave orbital velocity is real component of the gradient of velocity potential:

$$\mathbf{u}' = \text{Re}(\nabla \tilde{\Phi}) \quad (3.40)$$

If the fluid is assumed to be incompressible and homogeneous Equation (3.7) reduces to:

$$\nabla \cdot \mathbf{u} = 0 \quad (3.41)$$

3.3.2 Separation of Velocity and Free Surface Height into Steady and Unsteady Components

The instantaneous velocity of the particle \mathbf{u} can be separated into a steady and oscillatory portion:

$$\mathbf{u} = \mathbf{U} + \tilde{\mathbf{u}} \quad (3.42)$$

where \mathbf{U} is the steady component and $\tilde{\mathbf{u}}$ is the unsteady component. The unsteady component can be further separated as follows:

$$\tilde{\mathbf{u}} = \mathbf{u}' + \mathbf{u}'' \quad (3.43)$$

where \mathbf{u}' is the wave fluctuation and \mathbf{u}'' is the turbulent fluctuation.

Equations (3.42) and (3.43) may be combined as follows:

$$\mathbf{u} = \mathbf{U} + \mathbf{u}' + \mathbf{u}'' \quad (3.44)$$

Equation (3.44) can be expressed in tensor notation as:

$$u_j = U_j + u_j' + u_j'' \quad , \quad j = 1, 2, 3 \quad (3.45)$$

The free surface height η can also be separated into an unsteady and steady component:

$$\eta = \zeta + \bar{\eta} \quad (3.46)$$

where ζ is the unsteady component and $\bar{\eta}$ is the steady component.

3.3.3 Laplace's Equation

It is not unreasonable to assume that if \mathbf{u} is split into its steady and unsteady components these components will individually satisfy Equation (3.41). This gives the following equations for the unsteady wave component and the steady component:

$$\nabla \cdot \mathbf{u}' = 0 \quad (3.47)$$

$$\nabla \cdot \mathbf{U} = 0 \quad (3.48)$$

Substitution of Equation (3.40) into Equation (3.47) leads to the following Laplace Equation:

$$\nabla \cdot \nabla \tilde{\Phi} = \nabla^2 \tilde{\Phi} = 0 \quad (3.49)$$

3.3.4 Application of Velocity Potential to the Momentum Equation

Equation (3.38) is the Momentum Equation and can be expressed in tensor notation as follows:

$$\rho \left(\frac{\partial u_i}{\partial t} + u_j \frac{\partial u_i}{\partial x_j} \right) + \frac{\partial}{\partial x_i} (p + \rho g z) + \frac{\partial \sigma'_{ij}}{\partial x_j} = 0, \quad j = 1, 2, 3 \quad (3.50)$$

Substituting Equation (3.45) into Equation (3.50) separates the velocity terms into their steady and unsteady components.

$$\begin{aligned} & \rho \left(\frac{\partial}{\partial t} (U_i + u'_i + u''_i) + (U_j + u'_j + u''_j) \frac{\partial}{\partial x_j} (U_i + u'_i + u''_i) \right) \\ & + \frac{\partial}{\partial x_i} (p + \rho g z) + \frac{\partial \sigma'_{ij}}{\partial x_j} = 0, \quad j = 1, 2, 3 \end{aligned} \quad (3.51)$$

In the absence of a time average turbulent effects in Equation (3.51) can safely be neglected giving:

$$\rho \left(\frac{\partial}{\partial t} (u'_i + U_i) + (u'_j + U_j) \frac{\partial}{\partial x_j} (u'_i + U_i) \right) + \frac{\partial}{\partial x_i} (p + \rho g z) + \frac{\partial \sigma'_{ij}}{\partial x_j} = 0, \quad j = 1, 2, 3 \quad (3.52)$$

The steady component of velocity is constant or slowly varying throughout time. Hence the following identity is appropriate:

$$\frac{\partial U_i}{\partial t} = 0, \quad i = 1, 2, 3 \quad (3.53)$$

Using Equation (3.53) with Equation (3.52) gives:

$$\rho \left(\frac{\partial u_i}{\partial t} + (u_j' + U_j) \left(\frac{\partial u_i'}{\partial x_j} + \frac{\partial U_i}{\partial x_j} \right) \right) + \frac{\partial}{\partial x_i} (p + \rho g z) + \frac{\partial \sigma'_{ij}}{\partial x_j} = 0, \quad j = 1, 2, 3 \quad (3.54)$$

Carrying out further expansion on Equation (3.54) gives:

$$\begin{aligned} & \rho \frac{\partial u_i'}{\partial t} + \rho u_j' \frac{\partial u_i'}{\partial x_j} + \rho u_j' \frac{\partial U_i}{\partial x_j} + \rho U_j \frac{\partial u_i'}{\partial x_j} \\ & + \rho U_j \frac{\partial U_i}{\partial x_j} + \frac{\partial p}{\partial x_i} + \frac{\partial}{\partial x_i} (\rho g z) + \frac{\partial \sigma'_{ij}}{\partial x_j} = 0 \end{aligned}, \quad j = 1, 2, 3 \quad (3.55)$$

Using Equation (3.40) with Equation (3.55) gives:

$$\begin{aligned} & \rho \frac{\partial}{\partial t} \left(\frac{\partial \tilde{\Phi}}{\partial x_i} \right) + \rho \frac{\partial \tilde{\Phi}}{\partial x_j} \frac{\partial}{\partial x_j} \left(\frac{\partial \tilde{\Phi}}{\partial x_i} \right) + \rho \frac{\partial \tilde{\Phi}}{\partial x_j} \frac{\partial U_i}{\partial x_j} \\ & + \rho U_j \frac{\partial}{\partial x_j} \left(\frac{\partial \tilde{\Phi}}{\partial x_i} \right) + \rho U_j \frac{\partial U_i}{\partial x_j} + \frac{\partial p}{\partial x_i} + \frac{\partial}{\partial x_i} (\rho g z) + \frac{\partial \sigma'_{ij}}{\partial x_j} = 0 \end{aligned}, \quad j = 1, 2, 3 \quad (3.56)$$

Again following Booij (1981) in relation to the product of wave variables the second term on the left hand side will also be removed as it not considered significant. Its contribution is considered negligible because it is the product of a spatial derivative of $\tilde{\Phi}$ and a second order spatial derivative of $\tilde{\Phi}$. This leaves the following equation:

$$\begin{aligned} & \rho \frac{\partial}{\partial t} \left(\frac{\partial \tilde{\Phi}}{\partial x_i} \right) + \rho \frac{\partial \tilde{\Phi}}{\partial x_j} \frac{\partial U_i}{\partial x_j} + \rho U_j \frac{\partial}{\partial x_j} \left(\frac{\partial \tilde{\Phi}}{\partial x_i} \right) \\ & + \rho U_j \frac{\partial U_i}{\partial x_j} + \frac{\partial p}{\partial x_i} + \frac{\partial}{\partial x_i} (\rho g z) + \frac{\partial \sigma'_{ij}}{\partial x_j} = 0 \end{aligned}, \quad j = 1, 2, 3 \quad (3.57)$$

In order to examine the unsteady boundary condition any term that includes all steady terms can be removed from Equation (3.56). The fifth and sixth terms on the left hand side of Equation (3.57) contain both steady and unsteady portions. Figure 3.2, below, examines these terms.

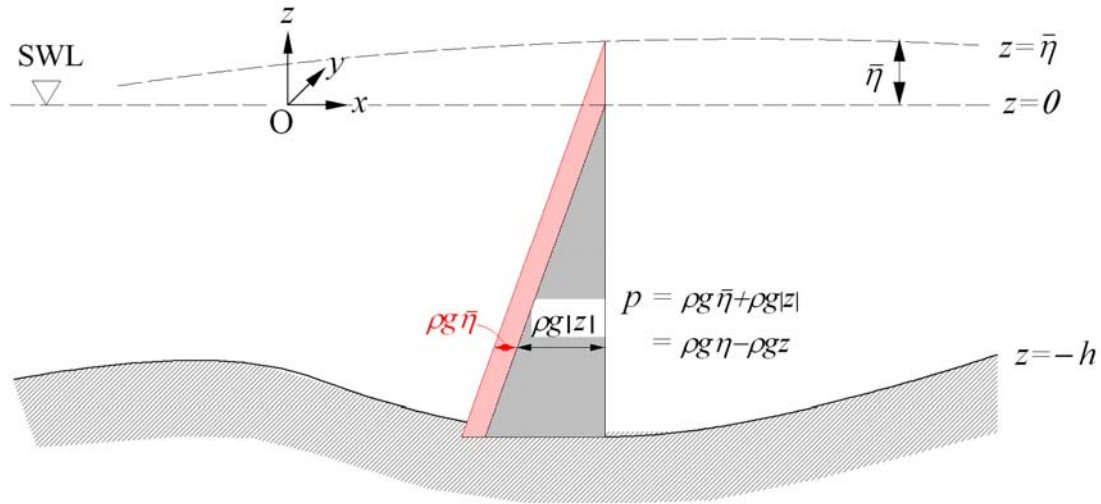


Figure 3.2 - Diagram of Steady and Unsteady Pressure components in water column

The steady part of $p + \rho g z$ amounts to $\rho g \bar{\eta}$ where $\bar{\eta}$ is the set-up. Hence the unsteady portion may be defined as:

$$p + \rho g z - \rho g \bar{\eta} = p + \rho g (z - \bar{\eta}) \quad (3.58)$$

It is now possible to remove the steady portion of Equation (3.57) by removing the fourth term on the left hand side and using the result of Equation (3.58). At this point it will also be necessary to introduce a wave energy dissipation term as a replacement for the general stress term. A force is applied within the momentum equation that opposes the direction of flow of the particles. It is assumed that this force is proportional to the instantaneous velocity of the particles.

$$\begin{aligned} & \rho \frac{\partial}{\partial t} \left(\frac{\partial \tilde{\Phi}}{\partial x_i} \right) + \rho \frac{\partial \tilde{\Phi}}{\partial x_j} \frac{\partial U_i}{\partial x_j} + \rho U_j \frac{\partial}{\partial x_j} \left(\frac{\partial \tilde{\Phi}}{\partial x_i} \right) \\ & + \frac{\partial p}{\partial x_i} + \frac{\partial}{\partial x_i} \left(\rho g (z - \bar{\eta}) \right) + \rho \gamma \left(\frac{\partial \tilde{\Phi}}{\partial x_i} \right) = 0 \end{aligned} \quad , i, j = 1, 2, 3 \quad (3.59)$$

Booij (1981) replaces $\frac{\partial U_i}{\partial x_j}$ in this case with $\frac{\partial U_j}{\partial x_i}$. Booij (1981) states that this would not

normally be the case but the mean flow varies slowly spatially so the replacement is one small term with another one. This changes Equation (3.59) to be:

$$\begin{aligned} & \rho \frac{\partial}{\partial t} \left(\frac{\partial \tilde{\Phi}}{\partial x_i} \right) + \rho \frac{\partial \tilde{\Phi}}{\partial x_j} \frac{\partial U_j}{\partial x_i} + \rho U_j \frac{\partial}{\partial x_j} \left(\frac{\partial \tilde{\Phi}}{\partial x_i} \right) \\ & + \frac{\partial p}{\partial x_i} + \frac{\partial}{\partial x_i} \left(\rho g (z - \bar{\eta}) \right) + \rho \gamma \left(\frac{\partial \tilde{\Phi}}{\partial x_i} \right) = 0 \end{aligned}, \quad i, j = 1, 2, 3 \quad (3.60)$$

Equation (3.60) can now be rewritten as follows. A small term, $\rho \tilde{\Phi} \left(\frac{\partial \gamma}{\partial x_i} \right)$, is added to the equation in order to allow the spatial derivative to be isolated. The gradient of γ is significantly smaller than the gradient of $\tilde{\Phi}$ or $(z - \bar{\eta})$ and hence the new term will not affect the accuracy of the equation. The same method was used by Clyne (2008).

$$\begin{aligned} & \rho \frac{\partial}{\partial t} \left(\frac{\partial \tilde{\Phi}}{\partial x_i} \right) + \rho \frac{\partial}{\partial x_i} \left(U_j \frac{\partial \tilde{\Phi}}{\partial x_j} \right) + \frac{\partial p}{\partial x_i} \\ & + \frac{\partial}{\partial x_i} \left(\rho g (z - \bar{\eta}) \right) + \rho \gamma \left(\frac{\partial \tilde{\Phi}}{\partial x_i} \right) + \rho \tilde{\Phi} \left(\frac{\partial \gamma}{\partial x_i} \right) = 0 \end{aligned}, \quad i, j = 1, 2, 3 \quad (3.61)$$

Isolating the spatial derivatives in Equation (3.61) gives the following:

$$\begin{aligned} & \frac{\partial}{\partial x_i} \left(\rho \frac{\partial \tilde{\Phi}}{\partial t} \right) + \frac{\partial}{\partial x_i} \left(\rho U_j \frac{\partial \tilde{\Phi}}{\partial x_j} \right) + \frac{\partial}{\partial x_i} (p) \\ & + \frac{\partial}{\partial x_i} \left(\rho g (z - \bar{\eta}) \right) + \frac{\partial}{\partial x_i} (\rho \gamma \tilde{\Phi}) = 0 \end{aligned}, \quad i, j = 1, 2, 3 \quad (3.62)$$

Taking a spatial derivative outside brackets Equation (3.62) can be written as:

$$\frac{\partial}{\partial x_i} \left[\rho \frac{\partial \tilde{\Phi}}{\partial t} + \rho U_j \frac{\partial \tilde{\Phi}}{\partial x_j} + p + \rho g (z - \bar{\eta}) + \rho \gamma \tilde{\Phi} \right] = 0, \quad i, j = 1, 2, 3 \quad (3.63)$$

Equation (3.63) is valid throughout the fluid including on the free surface.

Integrating Equation (3.63) gives the following equation which is valid throughout the fluid:

$$\rho \frac{\partial \tilde{\Phi}}{\partial t} + \rho U_j \frac{\partial \tilde{\Phi}}{\partial x_j} + p + \rho g (z - \bar{\eta}) + \rho \gamma \tilde{\Phi} = C(t), \quad j = 1, 2, 3 \quad (3.64)$$

Equation (3.64) can also be written as:

$$\frac{\partial \tilde{\Phi}}{\partial t} + \mathbf{U} \cdot \nabla \tilde{\Phi} + \frac{p}{\rho} + g(z - \bar{\eta}) + \gamma \tilde{\Phi} = C(t) \quad (3.65)$$

Equation (3.65) is an equation for waves on a current similar to the Bernoulli Equation in the absence of waves.

The constant $C(t)$ is arbitrary in time and constant spatially. The addition of a constant term to the velocity potential will not affect the velocity field and hence it is appropriate to set $C(t)$ equal to zero. Equation (3.64) becomes:

$$\rho \frac{\partial \tilde{\Phi}}{\partial t} + \rho U_j \frac{\partial \tilde{\Phi}}{\partial x_j} + p + \rho g(z - \bar{\eta}) + \rho \gamma \tilde{\Phi} = 0, \quad j = 1, 2, 3 \quad (3.66)$$

Re-expressing Equation (3.66) in terms of pressure leads to an equation where the first two terms on the right hand side represent the hydrodynamic pressure components and the third term is the static component:

$$p = -\rho \frac{\partial \tilde{\Phi}}{\partial t} - \rho U_j \frac{\partial \tilde{\Phi}}{\partial x_j} - \rho g(z - \bar{\eta}) - \rho \gamma \tilde{\Phi}, \quad j = 1, 2, 3 \quad (3.67)$$



3.4 Non-Linear Boundary Conditions

In order to solve Equation (3.49) boundary conditions must be obtained for the domain being examined. In this case the domain is bounded by the free surface of the water column and the sea bed.

3.4.1 Kinematic Free Surface Boundary Condition for Laplacian Equation

The following derivation obtains a kinematic boundary condition at the free surface. It follows the work of Mei *et al.* (2005) and Clyne (2008). Figure 3.3, above, shows the free surface and seabed boundaries of the water column in the presence of wave and turbulent effects. Figure 3.3 shows that the order of magnitude of the turbulent wave effects is significantly less than the oscillatory portion of the waves. It is hence considered appropriate to disregard the turbulent effects in the selection of boundary conditions. Figure 3.4 shows a simplified version of Figure 3.3 in the absence of turbulence.

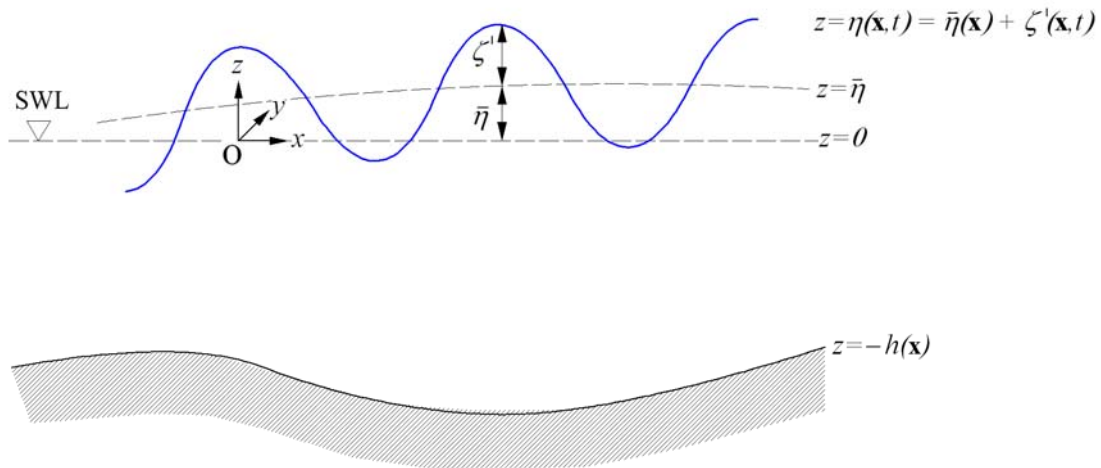


Figure 3.4 – Diagram of Free Surface and Sea-bed Boundaries in the absence of Turbulence

In the presence of turbulent effects the water surface is defined from Figure 3.3 as:

$$z = \eta'' \quad (3.68)$$

Therefore:

$$z - \eta'' = 0 \quad (3.69)$$

Define a function $F(\mathbf{x}, t)$ where $\mathbf{x} = (x, y)$:

$$F(\mathbf{x}, t) = z - \eta''(\mathbf{x}, t) = 0 \quad (3.70)$$

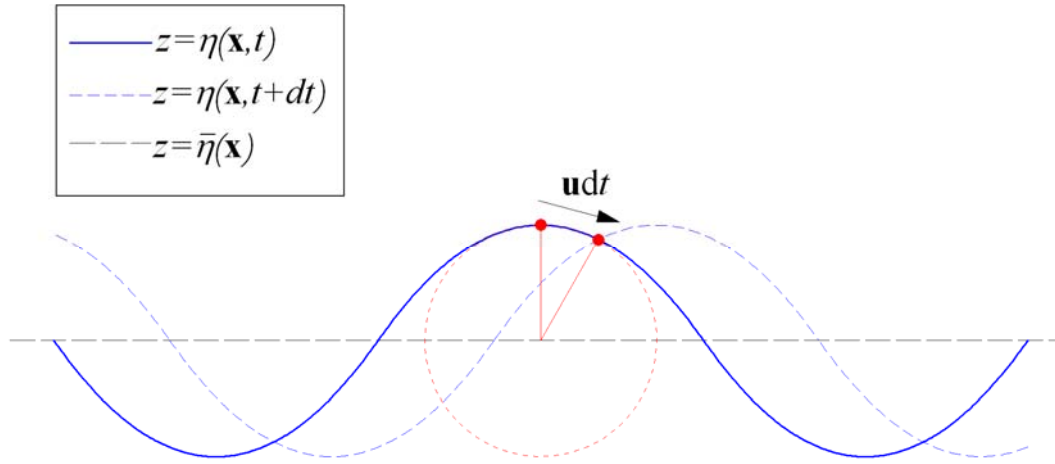


Figure 3.5 – Following the motion of a particle on the free surface

Assuming a water particle on the free surface moves at a velocity \mathbf{u} . The position of the free surface after a short time dt becomes:

$$F(\mathbf{x} + \mathbf{u}dt, t + dt) = 0 \quad (3.71)$$

Employing a Taylor series expansion of Equation (3.71) gives:

$$F(\mathbf{x} + \mathbf{u}dt, t + dt) = F(\mathbf{x}, t) + \left(\frac{\partial F}{\partial t} + \mathbf{u} \cdot \nabla F \right) dt + O(dt)^2 + \dots \quad (3.72)$$

Individually each term on the right hand side of Equation (3.72) is equal to zero. The higher order terms need not be considered and the first term has been set up to equal zero in Equation (3.70). This leaves:

$$\frac{\partial F}{\partial t} + \mathbf{u} \cdot \nabla F = 0 \quad (3.73)$$

Examining spatial and temporal gradients of the function F gives the following:

$$\frac{\partial F}{\partial t} = \frac{\partial}{\partial t}(z - \eta'') = -\frac{\partial \eta''}{\partial t} \quad (3.74)$$

$$\nabla F = \left(\frac{\partial F}{\partial x}, \frac{\partial F}{\partial y}, \frac{\partial F}{\partial z} \right) = \left(-\frac{\partial \eta''}{\partial x}, -\frac{\partial \eta''}{\partial y}, 1 \right) \quad (3.75)$$

Equation (3.73) can be rewritten as follows using the results of Equations (3.74) and (3.75):

$$\frac{\partial \eta''}{\partial t} + u_1 \frac{\partial \eta''}{\partial x} + u_2 \frac{\partial \eta''}{\partial y} - u_3 = 0 \quad \text{at } z = \eta'' \quad (3.76)$$

Substituting Equations (3.42) and (3.46) into Equation (3.76) gives the following equation where steady and unsteady components of both velocity and free surface height are separated:

$$\begin{aligned} & \frac{\partial \zeta'}{\partial t} + \frac{\partial \zeta''}{\partial t} + (\tilde{u}_1 + U_1) \frac{\partial \zeta'}{\partial x} + (\tilde{u}_1 + U_1) \frac{\partial \zeta''}{\partial x} + (\tilde{u}_1 + U_1) \frac{\partial \bar{\eta}}{\partial x} \\ & + (\tilde{u}_2 + U_2) \frac{\partial \zeta'}{\partial y} + (\tilde{u}_2 + U_2) \frac{\partial \zeta''}{\partial y} + (\tilde{u}_2 + U_2) \frac{\partial \bar{\eta}}{\partial y} - (\tilde{u}_3 + U_3) = 0 \end{aligned} \quad \text{at } z = \eta'' \quad (3.77)$$

Expressing Equation (3.77) more explicitly and multiplying across by -1 for simplicity:

$$\begin{aligned} & -\frac{\partial \zeta'}{\partial t} - \frac{\partial \zeta''}{\partial t} - \tilde{u}_1 \frac{\partial \zeta'}{\partial x} - \tilde{u}_1 \frac{\partial \zeta''}{\partial x} - \tilde{u}_1 \frac{\partial \bar{\eta}}{\partial x} - \tilde{u}_2 \frac{\partial \zeta'}{\partial y} - \tilde{u}_2 \frac{\partial \zeta''}{\partial y} - \tilde{u}_2 \frac{\partial \bar{\eta}}{\partial y} + \tilde{u}_3 \\ & - U_1 \frac{\partial \zeta'}{\partial x} - U_1 \frac{\partial \zeta''}{\partial x} - U_1 \frac{\partial \bar{\eta}}{\partial x} - U_2 \frac{\partial \zeta'}{\partial y} - U_2 \frac{\partial \zeta''}{\partial y} - U_2 \frac{\partial \bar{\eta}}{\partial y} + U_3 = 0 \end{aligned} \quad \text{at } z = \eta'' \quad (3.78)$$

Using Equation (3.43) gives:

$$\begin{aligned} & -\frac{\partial \zeta'}{\partial t} - \frac{\partial \zeta''}{\partial t} - (u_1' + u_1'') \frac{\partial \zeta'}{\partial x} - (u_1' + u_1'') \frac{\partial \zeta''}{\partial x} - (u_1' + u_1'') \frac{\partial \bar{\eta}}{\partial x} \\ & - (u_2' + u_2'') \frac{\partial \zeta'}{\partial y} - (u_2' + u_2'') \frac{\partial \zeta''}{\partial y} - (u_2' + u_2'') \frac{\partial \bar{\eta}}{\partial y} + (u_3' + u_3'') \quad \text{at } z = \eta'' \quad (3.79) \\ & - U_1 \frac{\partial \zeta'}{\partial x} - U_1 \frac{\partial \zeta''}{\partial x} - U_1 \frac{\partial \bar{\eta}}{\partial x} - U_2 \frac{\partial \zeta'}{\partial y} - U_2 \frac{\partial \zeta''}{\partial y} - U_2 \frac{\partial \bar{\eta}}{\partial y} + U_3 = 0 \end{aligned}$$

In the absence of a time-averaged component to Equation (3.79) it is possible to ignore the turbulent terms because as shown in Figure 3.3 they are an order of magnitude less than the oscillatory components. This leads to the following equation:

$$\begin{aligned} & -\frac{\partial \zeta'}{\partial t} - u_1' \left(\frac{\partial \bar{\eta}}{\partial x} \right) - u_1' \left(\frac{\partial \zeta'}{\partial x} \right) - u_2' \left(\frac{\partial \bar{\eta}}{\partial y} \right) - u_2' \left(\frac{\partial \zeta'}{\partial y} \right) + u_3' \\ & - U_1 \left(\frac{\partial \bar{\eta}}{\partial x} \right) - U_1 \left(\frac{\partial \zeta'}{\partial x} \right) - U_2 \left(\frac{\partial \bar{\eta}}{\partial y} \right) - U_2 \left(\frac{\partial \zeta'}{\partial y} \right) + U_3 = 0 \end{aligned} \quad \text{at } z = \eta \quad (3.80)$$

The steady terms will be eliminated at this point to apply Equation (3.80) approximately to the free surface:

$$\begin{aligned} & -\frac{\partial \zeta'}{\partial t} - u_1' \left(\frac{\partial \bar{\eta}}{\partial x} \right) - u_1' \left(\frac{\partial \zeta'}{\partial x} \right) - u_2' \left(\frac{\partial \bar{\eta}}{\partial y} \right) \\ & - u_2' \left(\frac{\partial \zeta'}{\partial y} \right) + u_3' - U_1 \left(\frac{\partial \zeta'}{\partial x} \right) - U_2 \left(\frac{\partial \zeta'}{\partial y} \right) = 0 \end{aligned} \quad \text{at } z = \bar{\eta} \quad (3.81)$$

Booij (1981) removes terms consisting of the product of two unsteady parameters because their contribution is not significant. These terms may now be removed from Equation (3.81) yielding:

$$-\frac{\partial \zeta'}{\partial t} - u_1' \left(\frac{\partial \bar{\eta}}{\partial x} \right) - u_2' \left(\frac{\partial \bar{\eta}}{\partial y} \right) + u_3' - U_1 \left(\frac{\partial \zeta'}{\partial x} \right) - U_2 \left(\frac{\partial \zeta'}{\partial y} \right) = 0 \quad \text{at } z = \bar{\eta} \quad (3.82)$$

In order to further the derivation at this stage it is necessary to assume that the horizontal gradients of the mean free surface are small. Booij (1981) considers this acceptable as the gradients of the mean free surface are expected to be of the same order as the slope of the seabed and the consideration of a mild slope is essential to the formulation of the mild-slope equation. The drawbacks caused by this assumption will be addressed by the inclusion of extended terms in the developed mild-slope equation. This leads to the further simplification of Equation (3.82):

$$-\frac{\partial \zeta'}{\partial t} - U_1 \left(\frac{\partial \zeta'}{\partial x} \right) - U_2 \left(\frac{\partial \zeta'}{\partial y} \right) + u_3' = 0 \quad \text{at } z = \bar{\eta} \quad (3.83)$$

Multiplying Equation (3.83) by -1 and expressing the remaining unsteady term as a function of velocity potential leads to the following expression of the Kinematic Free Surface Boundary Condition:

$$\frac{\partial \zeta'}{\partial t} + U_1 \frac{\partial \zeta'}{\partial x} + U_2 \frac{\partial \zeta'}{\partial y} - \frac{\partial \Phi}{\partial z} = 0 \quad \text{at } z = \bar{\eta} \quad (3.84)$$

Expressing Equation (3.48) with $j = 1, 2$ gives:

$$\frac{\partial U_j}{\partial x_j} + \frac{\partial U_3}{\partial x_3} = 0 \quad \text{at } z = \bar{\eta} \quad (3.85)$$

An assumption will be made at this stage that the vertical variation of the steady component of vertical velocity is small in the vicinity of the free surface. This assumption is necessary to obtain a suitable Kinematic Free Surface Boundary Condition and is

required to obtain a condition similar to that of authors such as Panchang *et al.* (1999) and Kirby (1984). This assumption gives:

$$\frac{\partial U_j}{\partial x_j} = 0, \quad j = 1, 2 \quad \text{at } z = \bar{\eta} \quad (3.86)$$

Thus the Kinematic Free Surface Boundary Condition of Equation (3.84) may be rewritten as:

$$\frac{\partial \zeta'}{\partial t} + \frac{\partial}{\partial x_j} (U_j \zeta') - \frac{\partial \tilde{\Phi}}{\partial z} = 0, \quad j = 1, 2 \quad \text{at } z = \bar{\eta} \quad (3.87)$$

3.4.2 Dynamic Free Surface Boundary Condition for Laplace's Equation

A Dynamic Free Surface Boundary Condition can be obtained by applying Equation (3.66) at $z = \eta$ ($= \zeta' + \bar{\eta}$), where $p=0$. This includes the assumption as before that the effects of turbulence are negligible and hence η defines the free surface.

$$\rho \frac{\partial \tilde{\Phi}}{\partial t} + \rho U_j \frac{\partial \tilde{\Phi}}{\partial x_j} + \rho g \zeta' + \rho \gamma \tilde{\Phi} = 0 \quad \text{at } z = \eta, \quad j = 1, 2, 3 \quad (3.88)$$

It is considered that if Equation (3.64) is applied at $z = \bar{\eta}$ it will be approximately the same as Equation (3.88):

$$\rho \frac{\partial \tilde{\Phi}}{\partial t} + \rho U_j \frac{\partial \tilde{\Phi}}{\partial x_j} + \rho g \zeta' + \rho \gamma \tilde{\Phi} = 0 \quad \text{at } z = \bar{\eta}, \quad j = 1, 2, 3 \quad (3.89)$$

Equation (3.89) can then be divided by the density to give:

$$\frac{\partial \tilde{\Phi}}{\partial t} + U_j \frac{\partial \tilde{\Phi}}{\partial x_j} + g \zeta' + \gamma \tilde{\Phi} = 0 \quad \text{at } z = \bar{\eta}, \quad j = 1, 2, 3 \quad (3.90)$$

The vertical component of U at the free surface is very small and hence the subscript j need only be used to symbolise the two horizontal directions. This gives the Dynamic Free Surface Boundary Condition:

$$\frac{\partial \tilde{\Phi}}{\partial t} + U_j \frac{\partial \tilde{\Phi}}{\partial x_j} + g \zeta' + \gamma \tilde{\Phi} = 0 \quad \text{at } z = \bar{\eta}, \quad j = 1, 2 \quad (3.91)$$

Equation (3.91) can also be rearranged to obtain an expression for ζ' :

$$\zeta' = -\frac{1}{g} \left[\frac{\partial \tilde{\Phi}}{\partial t} + U_j \frac{\partial \tilde{\Phi}}{\partial x_j} + \gamma \tilde{\Phi} \right] \quad \text{at } z = \bar{\eta}, \quad j = 1, 2 \quad (3.92)$$

3.4.3 Combined Free Surface Boundary Condition for the Laplace Equation

Equation (3.87), the Kinematic Free Surface Boundary Condition, can be expressed in tensor notation as:

$$\frac{\partial \zeta'}{\partial t} + \frac{\partial}{\partial x_j} (U_j \zeta') - \frac{\partial \tilde{\Phi}}{\partial z} = 0, \quad j = 1, 2 \quad \text{at } z = \bar{\eta} \quad (3.93)$$

Multiplying Equation (3.93) by g gives:

$$\frac{\partial}{\partial t} (g \zeta') + \frac{\partial}{\partial x_j} (g U_j \zeta') - g \frac{\partial \tilde{\Phi}}{\partial z} = 0, \quad j = 1, 2 \quad \text{at } z = \bar{\eta} \quad (3.94)$$

Substituting Equation (3.91) into Equation (3.94) gives:

$$\begin{aligned} & \frac{\partial}{\partial t} \left(-\frac{\partial \tilde{\Phi}}{\partial t} - U_k \frac{\partial \tilde{\Phi}}{\partial x_k} - \gamma \tilde{\Phi} \right) \\ & + \frac{\partial}{\partial x_j} \left(-U_j \frac{\partial \tilde{\Phi}}{\partial t} - U_j U_k \frac{\partial \tilde{\Phi}}{\partial x_k} - \gamma U_j \tilde{\Phi} \right) - g \frac{\partial \tilde{\Phi}}{\partial z} = 0 \end{aligned}, \quad j = 1, 2 \quad \text{at } z = \bar{\eta} \quad (3.95)$$

Multiplying Equation (3.95) by -1 gives the Combined Free Surface Boundary condition:

$$\begin{aligned} & \frac{\partial}{\partial t} \left(\frac{\partial \tilde{\Phi}}{\partial t} + U_k \frac{\partial \tilde{\Phi}}{\partial x_k} + \gamma \tilde{\Phi} \right) + \frac{\partial}{\partial x_j} \left(U_j \frac{\partial \tilde{\Phi}}{\partial t} + U_j U_k \frac{\partial \tilde{\Phi}}{\partial x_k} + \gamma U_j \tilde{\Phi} \right) + g \frac{\partial \tilde{\Phi}}{\partial z} = 0 \\ & \text{at } z = \bar{\eta}, \quad j = 1, 2, \quad k = 1, 2 \end{aligned} \quad (3.96)$$

3.4.4 Kinematic Seabed Boundary Condition

To fully describe the state of wave behaviour a boundary condition at the interface between the water column and the seabed is required.

At the seabed:

$$z = -h \quad (3.97)$$

Therefore:

$$z + h = 0 \quad (3.98)$$

Define a function $F'(\mathbf{x})$ where $\mathbf{x} = (x, y)$:

$$F'(\mathbf{x}) = z + h(\mathbf{x}) = 0 \quad (3.99)$$

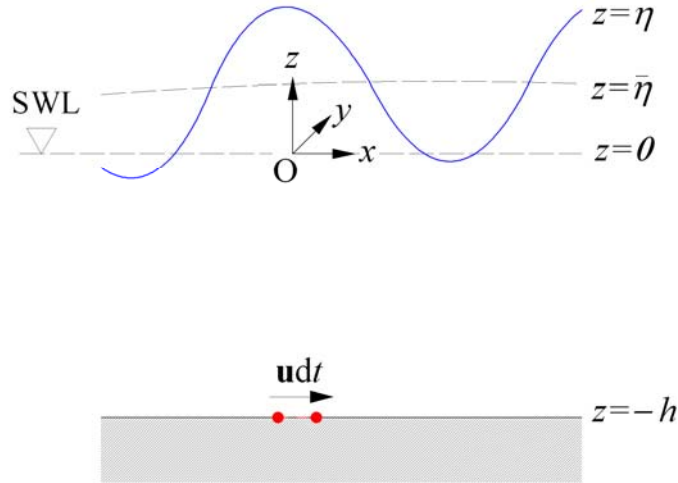


Figure 3.6 – Following the motion of a particle on the seabed

Assuming a water particle on the seabed moves at a velocity \mathbf{u} . After a short time dt the function becomes:

$$F'(\mathbf{x} + \mathbf{u}dt) = 0 \quad (3.100)$$

Employing a Taylor series expansion:

$$F'(\mathbf{x} + \mathbf{u}dt) = F'(\mathbf{x}) + (\mathbf{u} \cdot \nabla F') dt + O(dt)^2 + \dots \quad (3.101)$$

Individually each term on the right hand side of Equation (3.101) is equal to zero. The higher order terms need not be considered and the first term has been set up to equal zero in Equation (3.99). This leaves:

$$\mathbf{u} \cdot \nabla F' = 0 \quad (3.102)$$

Equation (3.102) can be expressed in tensor notation as follows:

$$u_i \frac{\partial}{\partial x_i} F' = u_i \frac{\partial}{\partial x_i} (z + h) = 0 \quad (3.103)$$

Expressing the spatial derivative in Equation (3.103) more explicitly gives:

$$u_i \frac{\partial}{\partial x_i} F' = u_i \frac{\partial z}{\partial x_i} + u_i \frac{\partial h}{\partial x_i} = 0, \quad i = 1, 2, 3 \quad (3.104)$$

Acknowledging the fact that $\frac{\partial z}{\partial x_i}$ is only non-zero in the vertical direction Equation

(3.104) can be rewritten as follows:

$$u_i \frac{\partial}{\partial x_i} F' = \left(w + u_i \frac{\partial h}{\partial x_i} \right) = 0, \quad i = 1, 2, 3 \quad (3.105)$$

where $w = u_3$

Using Equation (3.42) and acknowledging that the boundary condition is valid for the steady and unsteady components independently gives the following boundary condition for wave particle velocity:

$$\mathbf{u}' \cdot \nabla F' = 0 \quad (3.106)$$

Equation (3.106) can be written more explicitly using the identity of Equation (3.40):

$$\left(\frac{\partial \tilde{\Phi}}{\partial x}, \frac{\partial \tilde{\Phi}}{\partial y}, \frac{\partial \tilde{\Phi}}{\partial z} \right) \left(\frac{\partial h}{\partial x}, \frac{\partial h}{\partial y}, 1 \right) = 0 \quad (3.107)$$

Rewriting Equation (3.107) in tensor form gives the Kinematic Seabed Boundary Condition:

$$\frac{\partial \tilde{\Phi}}{\partial x_k} \frac{\partial h}{\partial x_k} + \frac{\partial \tilde{\Phi}}{\partial z} = 0 \text{ at } z = -h, \quad k = 1, 2 \quad (3.108)$$

3.4.5 Summary of Laplace's Equation and Non-Linear Boundary Conditions

Laplace's Equation and the Non-Linear Boundary Conditions developed in this section are summarised in Table 3.1 below.

Table 3.1 – Non-Linear Boundary Conditions for Laplace's Equation

	Boundary Condition	Equation
(a)	<i>Laplace's Equation</i>	$\nabla \cdot \nabla \tilde{\Phi} = \nabla^2 \tilde{\Phi} = 0$ (3.49)
(b)	<i>Kinematic Free Surface Boundary Condition</i>	$\frac{\partial \zeta'}{\partial t} + \frac{\partial}{\partial x_j} (U_j \zeta) - \frac{\partial \tilde{\Phi}}{\partial z} = 0$ at $z = \bar{\eta}$, $j = 1, 2$ (3.87)
(c)	<i>Dynamic Free Surface Boundary Condition</i>	$\zeta' = -\frac{1}{g} \left[\frac{\partial \tilde{\Phi}}{\partial t} + U_j \frac{\partial \tilde{\Phi}}{\partial x_j} + \gamma \tilde{\Phi} \right]$ at $z = \bar{\eta}$, $j = 1, 2$ (3.92)
(d)	<i>Combined Free Surface Boundary Condition</i>	$\frac{\partial}{\partial t} \left(\frac{\partial \tilde{\Phi}}{\partial t} + U_k \frac{\partial \tilde{\Phi}}{\partial x_k} + \gamma \tilde{\Phi} \right) + g \frac{\partial \tilde{\Phi}}{\partial z}$ $+ \frac{\partial}{\partial x_j} \left(U_j \frac{\partial \tilde{\Phi}}{\partial t} + U_j U_k \frac{\partial \tilde{\Phi}}{\partial x_k} + \gamma U_j \tilde{\Phi} \right) = 0$ at $z = \bar{\eta}$, $j = 1, 2$, $k = 1, 2$ (3.96)
(e)	<i>Kinematic Seabed Boundary Condition</i>	$\frac{\partial \tilde{\Phi}}{\partial x_k} \frac{\partial h}{\partial x_k} + \frac{\partial \tilde{\Phi}}{\partial z} = 0$ at $z = -h$, $k = 1, 2$ (3.108)

3.5 Harmonic Form of Wave Equations

3.5.1 Laplace's Equation

In order to obtain a harmonic solution to the wave equations discussed in Sections 3.2 to 3.4, above, it is necessary to select a harmonic solution for velocity potential. Berkhoff (1976), Booij (1981), Mei (2005) and Clyne (2007) as well as many other authors all select the same criteria:

$$\tilde{\Phi}(x, y, z, t) = \text{Re}(\tilde{\phi}(x, y, z)e^{-i\omega t}) \quad (3.109)$$

where $i^2 = -1$, ω is angular frequency and t is time. $\tilde{\phi}$ is a three-dimensional spatial form of velocity potential that is complex:

$$\tilde{\phi} = \tilde{\phi}_1 + i\tilde{\phi}_2 \quad (3.110)$$

Similarly a real component of the complex variable for set-up must also be defined.

$$\zeta' = \text{Re}(\tilde{\zeta}) = \text{Re}(\xi e^{-i\omega t}) \quad (3.111)$$

Using Equation (3.109) it is possible to convert the necessary equations derived in Sections 3.2 to 3.4 into harmonic forms.

Equation (3.49) can be expressed as follows using Equation (3.109):

$$\text{Re}[\nabla^2(\tilde{\phi}e^{-i\omega t})] = 0 \quad (3.112)$$

The harmonic term can be taken outside the derivative completely as it does not vary spatially:

$$\text{Re}[e^{-i\omega t}\nabla^2\tilde{\phi}] = 0 \quad (3.113)$$

Dividing across by the harmonic function yields a harmonic Laplace equation:

$$\nabla^2\tilde{\phi} = 0 \quad (3.114)$$

3.5.2 Dynamic Free Surface Boundary Condition

Equation (3.109) can be used to express Equation (3.92) as follows:

$$\zeta' = -\frac{1}{g} \left[\frac{\partial [\operatorname{Re}(\tilde{\phi} e^{-i\omega t})]}{\partial t} + U_j \frac{\partial [\operatorname{Re}(\tilde{\phi} e^{-i\omega t})]}{\partial x_j} + \gamma [\operatorname{Re}(\tilde{\phi} e^{-i\omega t})] \right] \text{ at } z = \bar{\eta}, j = 1, 2 \quad (3.115)$$

Expanding the derivatives within Equation (3.115) gives:

$$\zeta' = -\frac{1}{g} \left[\operatorname{Re}(-i\omega \tilde{\phi} e^{-i\omega t}) + U_j \left[\operatorname{Re} \left(e^{-i\omega t} \frac{\partial \tilde{\phi}}{\partial x_j} \right) \right] + \gamma [\operatorname{Re}(\tilde{\phi} e^{-i\omega t})] \right] \text{ at } z = \bar{\eta}, j = 1, 2 \quad (3.116)$$

Cancelling $e^{-i\omega t}$ gives:

$$\zeta' = -\frac{1}{g} \left[-i\omega \tilde{\phi} + U_j \left(\frac{\partial \tilde{\phi}}{\partial x_j} \right) + \gamma \tilde{\phi} \right] \text{ at } z = \bar{\eta}, j = 1, 2 \quad (3.117)$$

Equation (3.117) may be rewritten as follows:

$$i\omega \tilde{\phi} - U_j \left(\frac{\partial \tilde{\phi}}{\partial x_j} \right) - \gamma \tilde{\phi} - g\zeta' = 0 \text{ at } z = \bar{\eta}, j = 1, 2 \quad (3.118)$$

3.5.3 Combined Free Surface Boundary Condition

Equation (3.96) can be expressed as follows using Equation (3.109):

$$\begin{aligned} & \frac{\partial}{\partial t} \left(\frac{\partial}{\partial t} [\operatorname{Re}(\tilde{\phi} e^{-i\omega t})] + U_k \frac{\partial}{\partial x_k} [\operatorname{Re}(\tilde{\phi} e^{-i\omega t})] + \gamma [\operatorname{Re}(\tilde{\phi} e^{-i\omega t})] \right) \\ & + \frac{\partial}{\partial x_j} \left(U_j \frac{\partial}{\partial t} [\operatorname{Re}(\tilde{\phi} e^{-i\omega t})] + U_j U_k \frac{\partial}{\partial x_k} [\operatorname{Re}(\tilde{\phi} e^{-i\omega t})] + \gamma U_j [\operatorname{Re}(\tilde{\phi} e^{-i\omega t})] \right) \\ & + g \frac{\partial}{\partial z} [\operatorname{Re}(\tilde{\phi} e^{-i\omega t})] = 0 \end{aligned} \quad (3.119)$$

at $z = \bar{\eta}, j = 1, 2, k = 1, 2$

Separating Equation (3.119) into more explicit components yields:

$$\begin{aligned} & \frac{\partial}{\partial t} \left(\frac{\partial}{\partial t} [\operatorname{Re}(\tilde{\phi} e^{-i\omega t})] \right) + \frac{\partial}{\partial t} \left(U_k \frac{\partial}{\partial x_k} [\operatorname{Re}(\tilde{\phi} e^{-i\omega t})] \right) + \frac{\partial}{\partial t} (\gamma [\operatorname{Re}(\tilde{\phi} e^{-i\omega t})]) \\ & + \frac{\partial}{\partial x_j} \left(U_j \frac{\partial}{\partial t} [\operatorname{Re}(\tilde{\phi} e^{-i\omega t})] \right) \\ & + \frac{\partial}{\partial x_j} \left(U_j U_k \frac{\partial}{\partial x_k} [\operatorname{Re}(\tilde{\phi} e^{-i\omega t})] \right) + \frac{\partial}{\partial x_j} (\gamma U_j [\operatorname{Re}(\tilde{\phi} e^{-i\omega t})]) \\ & + g \frac{\partial}{\partial z} [\operatorname{Re}(\tilde{\phi} e^{-i\omega t})] = 0 \end{aligned} \quad (3.120)$$

at $z = \bar{\eta}, j = 1, 2, k = 1, 2$

Equation (3.120) can be re-expressed as follows:

$$\begin{aligned}
& -\operatorname{Re}\left[\omega^2 \tilde{\phi} e^{-i\omega t}\right] - \operatorname{Re}\left[i\omega e^{-i\omega t} U_k \frac{\partial \tilde{\phi}}{\partial x_k}\right] \\
& - \operatorname{Re}\left[i\omega e^{-i\omega t} \frac{\partial U_j}{\partial x_j} \tilde{\phi}\right] - \operatorname{Re}\left[i\omega e^{-i\omega t} U_j \frac{\partial \tilde{\phi}}{\partial x_j}\right] - \operatorname{Re}\left[i\omega e^{-i\omega t} \gamma \tilde{\phi}\right] \\
& + \operatorname{Re}\left[e^{-i\omega t} \frac{\partial U_j}{\partial x_j} U_k \frac{\partial \tilde{\phi}}{\partial x_k}\right] + \operatorname{Re}\left[e^{-i\omega t} U_j \frac{\partial U_k}{\partial x_j} \frac{\partial \tilde{\phi}}{\partial x_k}\right] + \operatorname{Re}\left[e^{-i\omega t} U_j U_k \frac{\partial^2 \tilde{\phi}}{\partial x_j \partial x_k}\right] \\
& + \operatorname{Re}\left[e^{-i\omega t} \tilde{\phi} U_j \frac{\partial \gamma}{\partial x_j}\right] + \operatorname{Re}\left[e^{-i\omega t} \gamma \tilde{\phi} \frac{\partial U_j}{\partial x_j}\right] + \operatorname{Re}\left[e^{-i\omega t} \gamma U_j \frac{\partial \tilde{\phi}}{\partial x_j}\right] + g \operatorname{Re}\left[e^{-i\omega t} \frac{\partial \tilde{\phi}}{\partial z}\right] = 0
\end{aligned} \tag{3.121}$$

at $z = \bar{\eta}$, $j = 1, 2$, $k = 1, 2$

At this stage the term with $\frac{\partial \gamma}{\partial x_k}$ can be ignored because the value of $\frac{\partial \gamma}{\partial x_k}$ is significantly smaller in magnitude than the other terms in Equation (3.121):

$$\begin{aligned}
& -\operatorname{Re}\left[\omega^2 \tilde{\phi} e^{-i\omega t}\right] - \operatorname{Re}\left[i\omega e^{-i\omega t} U_k \frac{\partial \tilde{\phi}}{\partial x_k}\right] \\
& - \operatorname{Re}\left[i\omega e^{-i\omega t} \frac{\partial U_j}{\partial x_j} \tilde{\phi}\right] - \operatorname{Re}\left[i\omega e^{-i\omega t} U_j \frac{\partial \tilde{\phi}}{\partial x_j}\right] - \operatorname{Re}\left[i\omega e^{-i\omega t} \gamma \tilde{\phi}\right] \\
& + \operatorname{Re}\left[e^{-i\omega t} \frac{\partial U_j}{\partial x_j} U_k \frac{\partial \tilde{\phi}}{\partial x_k}\right] + \operatorname{Re}\left[e^{-i\omega t} U_j \frac{\partial U_k}{\partial x_j} \frac{\partial \tilde{\phi}}{\partial x_k}\right] + \operatorname{Re}\left[e^{-i\omega t} U_j U_k \frac{\partial^2 \tilde{\phi}}{\partial x_j \partial x_k}\right] \\
& + \operatorname{Re}\left[e^{-i\omega t} \gamma \tilde{\phi} \frac{\partial U_j}{\partial x_j}\right] + \operatorname{Re}\left[e^{-i\omega t} \gamma U_j \frac{\partial \tilde{\phi}}{\partial x_j}\right] + g \operatorname{Re}\left[e^{-i\omega t} \frac{\partial \tilde{\phi}}{\partial z}\right] = 0
\end{aligned} \tag{3.122}$$

at $z = \bar{\eta}$, $j = 1, 2$, $k = 1, 2$

Assuming the imaginary part of Equation (3.122) is also zero the following can be stated:

$$\begin{aligned}
& -\left[\omega^2 \tilde{\phi} e^{-i\omega t}\right] - \left[i\omega e^{-i\omega t} U_k \frac{\partial \tilde{\phi}}{\partial x_k}\right] \\
& - \left[i\omega e^{-i\omega t} \frac{\partial U_j}{\partial x_j} \tilde{\phi}\right] - \left[i\omega e^{-i\omega t} U_j \frac{\partial \tilde{\phi}}{\partial x_j}\right] - \left[i\omega e^{-i\omega t} \gamma \tilde{\phi}\right] \\
& + \left[e^{-i\omega t} \frac{\partial U_j}{\partial x_j} U_k \frac{\partial \tilde{\phi}}{\partial x_k}\right] + \left[e^{-i\omega t} U_j \frac{\partial U_k}{\partial x_j} \frac{\partial \tilde{\phi}}{\partial x_k}\right] + \left[e^{-i\omega t} U_j U_k \frac{\partial^2 \tilde{\phi}}{\partial x_j \partial x_k}\right] \\
& + \left[e^{-i\omega t} \gamma \tilde{\phi} \frac{\partial U_j}{\partial x_j}\right] + \left[e^{-i\omega t} \gamma U_j \frac{\partial \tilde{\phi}}{\partial x_j}\right] + g \left[e^{-i\omega t} \frac{\partial \tilde{\phi}}{\partial z}\right] = 0
\end{aligned} \tag{3.123}$$

at $z = \bar{\eta}$, $j = 1, 2$, $k = 1, 2$

Dividing Equation (3.123) by $e^{-i\omega t}$ gives:

$$\begin{aligned} & -\omega^2 \tilde{\phi} - 2i\omega U_k \frac{\partial \tilde{\phi}}{\partial x_k} - i\omega \frac{\partial U_j}{\partial x_j} \tilde{\phi} + \frac{\partial U_j}{\partial x_j} U_k \frac{\partial \tilde{\phi}}{\partial x_k} + U_j \frac{\partial U_k}{\partial x_j} \frac{\partial \tilde{\phi}}{\partial x_k} \\ & + U_j U_k \frac{\partial^2 \tilde{\phi}}{\partial x_j \partial x_k} + g \frac{\partial \tilde{\phi}}{\partial z} + \gamma \frac{\partial U_j}{\partial x_j} \tilde{\phi} + \gamma U_j \frac{\partial \tilde{\phi}}{\partial x_j} - i\omega \gamma \tilde{\phi} = 0 \end{aligned} \quad (3.124)$$

at $z = \bar{\eta}$, $j = 1, 2$, $k = 1, 2$

An expression for $\frac{\partial \tilde{\phi}}{\partial z}$ at the surface can be obtained using the harmonic form of the

combined free surface boundary condition:

$$\frac{\partial \tilde{\phi}}{\partial z} = \frac{1}{g} \left[\begin{aligned} & \omega^2 \tilde{\phi} + 2i\omega U_k \frac{\partial \tilde{\phi}}{\partial x_k} + i\omega \frac{\partial U_j}{\partial x_j} \tilde{\phi} - \frac{\partial U_j}{\partial x_j} U_k \frac{\partial \tilde{\phi}}{\partial x_k} \\ & - U_j \frac{\partial U_k}{\partial x_j} \frac{\partial \tilde{\phi}}{\partial x_k} - U_j U_k \frac{\partial^2 \tilde{\phi}}{\partial x_j \partial x_k} - \gamma \frac{\partial U_j}{\partial x_j} \tilde{\phi} - \gamma U_j \frac{\partial \tilde{\phi}}{\partial x_j} + i\omega \gamma \tilde{\phi} \end{aligned} \right] \quad (3.125)$$

at $z = \bar{\eta}$, $j = 1, 2$, $k = 1, 2$

3.5.4 Kinematic Seabed Boundary Condition

Substituting Equation (3.112) into Equation (3.108) gives:

$$\frac{\partial}{\partial x_k} \left[\text{Re} \left(\tilde{\phi} e^{-i\omega t} \right) \right] \frac{\partial h}{\partial x_k} + \frac{\partial}{\partial z} \left[\text{Re} \left(\tilde{\phi} e^{-i\omega t} \right) \right] = 0 \quad \text{at } z = -h, \quad k = 1, 2 \quad (3.126)$$

The harmonic term can be taken outside the spatial derivatives completely as it does not vary spatially:

$$\text{Re} \left[e^{-i\omega t} \frac{\partial \tilde{\phi}}{\partial x_k} \frac{\partial h}{\partial x_k} \right] + \text{Re} \left[e^{-i\omega t} \frac{\partial \tilde{\phi}}{\partial z} \right] = 0 \quad \text{at } z = -h, \quad k = 1, 2 \quad (3.127)$$

Dividing Equation (3.127) by $e^{-i\omega t}$ gives an expression for $\frac{\partial \tilde{\phi}}{\partial z}$ at the seabed using the

harmonic form of the kinematic seabed boundary condition:

$$\frac{\partial \tilde{\phi}}{\partial z} = - \frac{\partial \tilde{\phi}}{\partial x_k} \frac{\partial h}{\partial x_k} \quad \text{at } z = -h, \quad k = 1, 2 \quad (3.128)$$

3.5.5 Summary of Harmonic Wave Equations

Laplace's Equation and the Non-Linear Boundary Conditions developed in this section are summarised in Table 3.2 below.

Table 3.2 – Summary of Harmonic Wave Equations

Boundary Condition		Equation
(a)	<i>Laplace's Equation</i>	$\nabla^2 \tilde{\phi} = 0$ (3.114)
(b)	<i>Dynamic Free Surface Boundary Condition</i>	$i\omega \tilde{\phi} - U_j \left(\frac{\partial \tilde{\phi}}{\partial x_j} \right) - \gamma \tilde{\phi} - g\zeta = 0$ <p style="text-align: center;">at $z = \bar{\eta}$, $j = 1, 2$</p>
(c)	<i>Combined Free Surface Boundary Condition</i>	$\frac{\partial \tilde{\phi}}{\partial z} = \frac{1}{g} \left[\begin{aligned} &\omega^2 \tilde{\phi} + 2i\omega U_k \frac{\partial \tilde{\phi}}{\partial x_k} + i\omega \frac{\partial U_j}{\partial x_j} \tilde{\phi} \\ &- \frac{\partial U_j}{\partial x_j} U_k \frac{\partial \tilde{\phi}}{\partial x_k} - U_j \frac{\partial U_k}{\partial x_j} \frac{\partial \tilde{\phi}}{\partial x_k} \\ &- U_j U_k \frac{\partial^2 \tilde{\phi}}{\partial x_j \partial x_k} - \gamma \frac{\partial U_j}{\partial x_j} \tilde{\phi} - \gamma U_j \frac{\partial \tilde{\phi}}{\partial x_j} + i\omega \gamma \tilde{\phi} \end{aligned} \right]$ <p style="text-align: center;">at $z = \bar{\eta}$, $j = 1, 2$, $k = 1, 2$</p>
(d)	<i>Kinematic Seabed Boundary Condition</i>	$\frac{\partial \tilde{\phi}}{\partial z} = - \frac{\partial \tilde{\phi}}{\partial x_k} \frac{\partial h}{\partial x_k}$ <p style="text-align: center;">at $z = -h$, $k = 1, 2$</p>

3.6 Vertical Function for Two-Dimensional Laplace Equation

Using separation of variables and a vertical function f it is possible to develop a Laplacian equation in terms of a two-dimensional velocity potential. This section examines the form of the vertical function and the form of the two-dimensional velocity potential term. In order to make the development of a vertical term possible it will be necessary for the derivation to assume propagation of simple harmonic waves on a constant depth. A similar process is carried out by authors such as Clyne (2008) and Booij (1981).

3.6.1 Propagation of Simple Harmonic Waves on a Constant Depth

On a constant depth the seabed boundary condition of Equation (3.128) reduces to:

$$\frac{\partial \tilde{\phi}}{\partial z} = 0 \text{ at } z = -h, \quad k = 1, 2 \quad (3.129)$$

Table 3.3 below summarises the harmonic wave equations for a progressive wave on a constant depth.

Table 3.3 – Summary of Harmonic Wave Equations on a Constant Depth

	Boundary Condition	Equation
(a)	<i>Laplace's Equation</i>	$\nabla^2 \tilde{\phi} = 0$ (3.114)
(b)	<i>Combined Free Surface Boundary Condition</i>	$\frac{\partial \tilde{\phi}}{\partial z} = \frac{1}{g} \left[\begin{aligned} &\omega^2 \tilde{\phi} + 2i\omega U_k \frac{\partial \tilde{\phi}}{\partial x_k} + i\omega \frac{\partial U_j}{\partial x_j} \tilde{\phi} \\ & - \frac{\partial U_j}{\partial x_j} U_k \frac{\partial \tilde{\phi}}{\partial x_k} - U_j \frac{\partial U_k}{\partial x_j} \frac{\partial \tilde{\phi}}{\partial x_k} \\ & - U_j U_k \frac{\partial^2 \tilde{\phi}}{\partial x_j \partial x_k} - \gamma \frac{\partial U_j}{\partial x_j} \tilde{\phi} - \gamma U_j \frac{\partial \tilde{\phi}}{\partial x_j} + i\omega \gamma \tilde{\phi} \end{aligned} \right]$ $\text{at } z = \bar{\eta}, \quad j = 1, 2, \quad k = 1, 2$ (3.125)
(c)	<i>Kinematic Seabed Boundary Condition</i>	$\frac{\partial \tilde{\phi}}{\partial z} = 0$ $\text{at } z = -h, \quad k = 1, 2$ (3.129)

3.6.2 Governing Equations for Vertical Function

3.6.2.1 Laplace's Equation

In order to reduce the velocity potential from a three-dimensional form to a two-dimensional velocity potential using separation of variables a function f is defined as follows using the Laplace Equation (3.114):

$$\nabla^2 [\tilde{\phi}(x, y, z)] = \nabla^2 [f(z)\phi(x, y)] = f \frac{\partial^2 \phi}{\partial x^2} + \phi \frac{\partial^2 f}{\partial z^2} = 0 \quad (3.130)$$

for $-h < z < 0$

Equation (3.130) can be rearranged as follows with the definition of κ^2 :

$$\frac{\frac{\partial^2 \phi}{\partial x^2} + \frac{\partial^2 \phi}{\partial y^2}}{\phi} = -\frac{\frac{\partial^2 f}{\partial z^2}}{f} = -\kappa^2 \quad (3.131)$$

It is assumed that using a negative value of the κ^2 variable in Equation (3.131) will provide a propagating wave where κ is the eigenvalue called wave number in this case.

This leads to the following definitions:

$$\frac{\partial^2 \phi}{\partial x^2} + \frac{\partial^2 \phi}{\partial y^2} = -\kappa^2 \phi \quad (3.132)$$

$$\frac{\partial^2 f}{\partial z^2} = f \kappa^2 \quad (3.133)$$

$$\frac{\partial^2 f}{\partial z^2} - f \kappa^2 = 0 \quad (3.134)$$

At this stage it is necessary to examine a solution for velocity potential. The following form of velocity potential is selected by Booij (1981), Mei *et al.* (2005) and Clyne (2008):

$$\phi = A_\phi e^{iS_\phi} \quad (3.135)$$

where A_ϕ is the amplitude of velocity potential and S_ϕ is its phase.

For waves on a constant depth the phase can be expressed as follows:

$$S_\phi = \kappa_1 x + \kappa_2 y \quad (3.136)$$

where

$$\kappa_1^2 + \kappa_2^2 = \kappa^2 \quad (3.137)$$

If κ_1 and κ_2 are constant the wave they describe is a plane wave. i.e. A wave with an infinitely straight crest.

Substituting Equation (3.136) into Equation (3.132) gives the following:

$$\frac{\partial^2}{\partial x^2} (A_\phi e^{iS_\phi}) + \frac{\partial^2}{\partial y^2} (A_\phi e^{iS_\phi}) = -\kappa^2 (A_\phi e^{iS_\phi}) \quad (3.138)$$

Using Equation (3.136) this becomes:

$$A_\phi \frac{\partial^2}{\partial x^2} (e^{i\kappa_1 x + i\kappa_2 y}) + A_\phi \frac{\partial^2}{\partial y^2} (e^{i\kappa_1 x + i\kappa_2 y}) = -\kappa^2 A_\phi e^{iS_\phi} \quad (3.139)$$

Dividing Equation (3.139) by A_ϕ gives:

$$\frac{\partial^2}{\partial x^2} (e^{i\kappa_1 x + i\kappa_2 y}) + \frac{\partial^2}{\partial y^2} (e^{i\kappa_1 x + i\kappa_2 y}) = -\kappa^2 e^{iS_\phi} \quad (3.140)$$

Assuming a plane wave as discussed above gives the following simplification of Equation (3.140):

$$-\kappa_1^2 e^{iS_\phi} - \kappa_2^2 e^{iS_\phi} = -\kappa^2 e^{iS_\phi} \quad (3.141)$$

Dividing Equation (3.141) by e^{iS_ϕ} gives:

$$\kappa_1^2 + \kappa_2^2 = \kappa^2 \quad (3.142)$$

Equation (3.142) is identical to Equation (3.137) thus proving that the chosen solution for wave potential in Equation (3.135) satisfies Equation (3.132) and also that the selected eigenvalue has been chosen correctly as the wave number of a propagating wave.

Use can now be made of the vertical function f of Equation (3.130) to obtain a useful solution to wave behaviour for the two-dimensional simplification of velocity potential. An assumption of constant current on a constant depth will be required to obtain this dispersion relation.

3.6.2.2 Combined Free Surface Boundary Condition applied to Vertical Function

Using Equation (3.130) with the combined free surface boundary condition of Equation (3.125) in the case of a constant depth, slowly varying current with no energy dissipation terms yields:

$$\phi \frac{df}{dz} = \frac{1}{g} \left[\omega^2 f \phi + 2i\omega U_j f \frac{\partial \phi}{\partial x_j} - U_j f \frac{\partial U_k}{\partial x_j} \frac{\partial \phi}{\partial x_k} - U_j U_k f \frac{\partial^2 \phi}{\partial x_j \partial x_k} \right] \quad (3.143)$$

at $z = \bar{\eta}$, $j = 1, 2$, $k = 1, 2$

Expression of Equation (3.143) explicitly yields:

$$\phi \frac{df}{dz} = \frac{\omega^2 f \phi}{g} + \frac{2i\omega U_j f}{g} \frac{\partial \phi}{\partial x_j} - \frac{U_j U_k f}{g} \frac{\partial^2 \phi}{\partial x_j \partial x_k} \quad (3.144)$$

at $z = \bar{\eta}$, $j = 1, 2$, $k = 1, 2$

Expanding the tensor terms of Equation (3.144) into a more explicit form gives the following:

$$\begin{aligned} \phi \frac{df}{dz} = & \frac{\omega^2 f \phi}{g} + \frac{2i\omega U_1 f}{g} \frac{\partial \phi}{\partial x} + \frac{2i\omega U_2 f}{g} \frac{\partial \phi}{\partial y} - \frac{U_1 U_1 f}{g} \frac{d^2 \phi}{dx^2} \\ & - \frac{U_1 U_2 f}{g} \frac{d^2 \phi}{dx dy} - \frac{U_2 U_1 f}{g} \frac{d^2 \phi}{dy dx} - \frac{U_2 U_2 f}{g} \frac{d^2 \phi}{dy^2} \end{aligned} \quad \text{at } z = \bar{\eta} \quad (3.145)$$

Combining similar terms gives the following:

$$\begin{aligned} \phi \frac{df}{dz} = & \frac{\omega^2 f \phi}{g} + \frac{2i\omega U_1 f}{g} \frac{\partial \phi}{\partial x} + \frac{2i\omega U_2 f}{g} \frac{\partial \phi}{\partial y} \\ & - \frac{U_1^2 f}{g} \frac{d^2 \phi}{dx^2} - \frac{2U_1 U_2 f}{g} \frac{d^2 \phi}{dx dy} - \frac{U_2^2 f}{g} \frac{d^2 \phi}{dy^2} \end{aligned} \quad \text{at } z = \bar{\eta} \quad (3.146)$$

Equations (3.147) to (3.161) describe some necessary gradients of velocity potential using the identity in Equation (3.135):

$$\frac{d\phi}{dx} = A_\phi \frac{d}{dx} (e^{i\kappa_1 x + i\kappa_2 y}) \quad (3.147)$$

$$\frac{d\phi}{dx} = i\kappa_1 A_\phi e^{i\kappa_1 x} e^{i\kappa_2 y} \quad (3.148)$$

$$\frac{d\phi}{dx} = i\kappa_1 \phi \quad (3.149)$$

$$\frac{d^2 \phi}{dx^2} = i\kappa_1 A_\phi e^{i\kappa_2 y} \frac{d}{dx} (e^{i\kappa_1 x}) \quad (3.150)$$

$$\frac{d^2 \phi}{dx^2} = -\kappa_1^2 A_\phi e^{i\kappa_2 y} e^{i\kappa_1 x} \quad (3.151)$$

$$\frac{d^2 \phi}{dx^2} = -\kappa_1^2 \phi \quad (3.152)$$

$$\frac{d^2 \phi}{dx dy} = i\kappa_1 A_\phi e^{i\kappa_1 x} \frac{d}{dy} (e^{i\kappa_2 y}) \quad (3.153)$$

$$\frac{d^2 \phi}{dx dy} = -\kappa_1 \kappa_2 A_\phi e^{i\kappa_1 x} e^{i\kappa_2 y} \quad (3.154)$$

$$\frac{d^2\phi}{dx dy} = -\kappa_1 \kappa_2 \phi \quad (3.155)$$

$$\frac{d\phi}{dy} = A_\phi \frac{d}{dy} (e^{i\kappa_1 x} e^{i\kappa_2 y}) \quad (3.156)$$

$$\frac{d\phi}{dy} = i\kappa_2 A_\phi e^{i\kappa_1 x} e^{i\kappa_2 y} \quad (3.157)$$

$$\frac{d\phi}{dy} = i\kappa_2 \phi \quad (3.158)$$

$$\frac{d^2\phi}{dy^2} = i\kappa_2 A_\phi e^{i\kappa_1 x} \frac{d}{dy} (e^{i\kappa_2 y}) \quad (3.159)$$

$$\frac{d^2\phi}{dy^2} = i\kappa_2 i\kappa_2 A_\phi e^{i\kappa_1 x} e^{i\kappa_2 y} \quad (3.160)$$

$$\frac{d^2\phi}{dy^2} = -\kappa_2^2 \phi \quad (3.161)$$

Using Equations (3.149), (3.152), (3.155), (3.158), (3.161) with Equation (3.146) yields:

$$\begin{aligned} \phi \frac{df}{dz} = & \frac{\omega^2 f \phi}{g} + \frac{2i\omega U_1 f}{g} (i\kappa_1 \phi) + \frac{2i\omega U_2 f}{g} (i\kappa_2 \phi) \\ & - \frac{U_1^2 f}{g} (-\kappa_1^2 \phi) - \frac{2U_1 U_2 f}{g} (-\kappa_1 \kappa_2 \phi) - \frac{U_2^2 f}{g} (-\kappa_2^2 \phi) \end{aligned} \quad \text{at } z = \bar{\eta} \quad (3.162)$$

Diving Equation (3.162) by ϕ gives the following equation:

$$\begin{aligned} \frac{df}{dz} = & \frac{\omega^2 f}{g} + \frac{2i\omega U_1 f}{g} (i\kappa_1) + \frac{2i\omega U_2 f}{g} (i\kappa_2) \\ & - \frac{U_1^2 f}{g} (-\kappa_1^2) - \frac{2U_1 U_2 f}{g} (-\kappa_1 \kappa_2) - \frac{U_2^2 f}{g} (-\kappa_2^2) \end{aligned} \quad \text{at } z = \bar{\eta} \quad (3.163)$$

Equation (3.163) can be simplified to:

$$\frac{df}{dz} = \frac{f}{g} \left[\omega^2 - 2\omega U_1 \kappa_1 - 2\omega U_2 \kappa_2 + U_1^2 \kappa_1^2 + 2U_1 U_2 \kappa_1 \kappa_2 + U_2^2 \kappa_2^2 \right] \quad \text{at } z = \bar{\eta} \quad (3.164)$$

Writing Equation (3.164) in vector form gives:

$$\frac{df}{dz} = \frac{f}{g} \left[\omega - (\mathbf{U} \cdot \boldsymbol{\kappa}) \right]^2 \quad \text{at } z = \bar{\eta} \quad (3.165)$$

3.6.2.3 Kinematic Seabed Boundary Condition applied to Vertical Function

On the assumption of a constant depth the kinematic seabed boundary condition from (3.128) simplifies to the following:

$$\frac{\partial \tilde{\phi}}{\partial z} = 0 \text{ at } z = -h \quad (3.166)$$

Using the function f , defined in Equation (3.130), with Equation (3.166) yields:

$$\frac{\partial f}{\partial z} = 0 \text{ at } z = -h \quad (3.167)$$

3.6.2.4 Summary of Governing Equations for Vertical Function

Table 3.4 below summarises the governing equations developed in this section for the vertical function. The equations form a boundary value problem in homogenous ordinary differential equations.

Table 3.4 – Summary of Governing Equations for Vertical Function

	Boundary Condition	Equation
(a)	<i>Laplace's Equation</i>	$\frac{\partial^2 f}{\partial z^2} - f\kappa^2 = 0$ (3.134)
(b)	<i>Combined Free Surface Boundary Condition</i>	$\frac{df}{dz} = \frac{f}{g} [\omega - (\mathbf{U} \cdot \boldsymbol{\kappa})]^2$ at $z = \bar{\eta}$ (3.165)
(c)	<i>Kinematic Seabed Boundary Condition</i>	$\frac{\partial f}{\partial z} = 0$ at $z = -h$ (3.167)

3.6.3 Solving for the form of the Vertical Function

Equations (3.134), (3.165) and (3.167) form the basis of an eigenvalue problem. The solution to an eigenvalue problem for f is:

$$f = Ce^{mz} \quad (3.168)$$

Therefore:

$$\frac{d^2 f}{dz^2} = m^2 Ce^{mz} \quad (3.169)$$

Substituting Equations (3.168) and (3.169) into Equation (3.134) gives the following:

$$m^2 C e^{mz} - \kappa^2 C e^{mz} = 0 \quad (3.170)$$

$$m^2 C e^{mz} = \kappa^2 C e^{mz} \quad (3.171)$$

$$m = \pm \kappa \quad (3.172)$$

The function f can now be updated using Equation (3.172):

$$f = C_1 e^{\kappa z} + C_2 e^{-\kappa z} \quad (3.173)$$

$$\frac{df}{dz} = C_1 \kappa e^{\kappa z} - C_2 \kappa e^{-\kappa z} \quad (3.174)$$

3.6.3.1 Kinematic Seabed Boundary Condition

At the seabed $z = -h$ and Equation (3.167) applies. Using Equation (3.174) at the seabed yields:

$$C_1 \kappa e^{\kappa z} - C_2 \kappa e^{-\kappa z} = 0 \text{ at } z = -h \quad (3.175)$$

$$C_1 \kappa e^{-\kappa h} - C_2 \kappa e^{\kappa h} = 0 \quad (3.176)$$

$$C_1 = C_2 e^{2\kappa h} \quad (3.177)$$

Once again the function f can now be updated, this time using Equation (3.177):

$$f = C_2 e^{2\kappa h} e^{\kappa z} + C_2 e^{-\kappa z} \quad (3.178)$$

$$\frac{df}{dz} = C_2 \kappa e^{2\kappa h} e^{\kappa z} - C_2 \kappa e^{-\kappa z} \quad (3.179)$$

3.6.3.2 Combined Free Surface Boundary Condition

At the free surface $z = \bar{\eta}$ and Equation (3.165) apply. Letting $z = \bar{\eta}$ in Equation (3.178) and (3.179) gives:

$$f = C_2 e^{2\kappa h} e^{\kappa \bar{\eta}} + C_2 e^{-\kappa \bar{\eta}} \quad (3.180)$$

$$\frac{df}{dz} = C_2 \kappa e^{2\kappa h} e^{\kappa \bar{\eta}} - C_2 \kappa e^{-\kappa \bar{\eta}} \quad (3.181)$$

Substitution of Equations (3.180) and (3.181) into Equation (3.165) yields:

$$C_2 \kappa e^{2\kappa h} e^{\kappa \bar{\eta}} - C_2 \kappa e^{-\kappa \bar{\eta}} = \frac{C_2 e^{2\kappa h} e^{\kappa \bar{\eta}} + C_2 e^{-\kappa \bar{\eta}}}{g} [\omega - (\mathbf{U} \cdot \mathbf{\kappa})]^2 \quad (3.182)$$

$$\kappa e^{2\kappa h} e^{2\kappa \bar{\eta}} - \kappa = \frac{e^{2\kappa h} e^{2\kappa \bar{\eta}} + 1}{g} [\omega - (\mathbf{U} \cdot \mathbf{\kappa})]^2 \quad (3.183)$$

Defining h' as the depth of the fluid column from the mean free surface to the seabed gives:

$$h' = h + \bar{\eta} \quad (3.184)$$

Using Equation (3.184) with Equation (3.183) gives the following:

$$\kappa(e^{2\kappa h'} - 1) = \frac{e^{2\kappa h'} + 1}{g} [\omega - (\mathbf{U} \cdot \boldsymbol{\kappa})]^2 \quad (3.185)$$

$$\kappa \frac{e^{2\kappa h'} - 1}{e^{2\kappa h'} + 1} = \frac{1}{g} [\omega - (\mathbf{U} \cdot \boldsymbol{\kappa})]^2 \quad (3.186)$$

$$g\kappa \tanh(\kappa h') = [\omega - (\mathbf{U} \cdot \boldsymbol{\kappa})]^2 \quad (3.187)$$

Upon development of the mild-slope equation in Section 3.7, $\boldsymbol{\kappa}$ will be defined as follows:

$$\boldsymbol{\kappa} = \kappa \frac{\nabla S_\phi}{|\nabla S_\phi|} \quad (3.188)$$

For a constant depth S_ϕ is defined in Equation (3.136).

Equation (3.187) is the two-dimensional dispersion equation and is identical to the one developed by Booij (1981). Although this dispersion relation has been obtained for a constant depth it is considered suitable by authors such as Booij (1981), Mei *et al.* (2005) and Clyne (2008) for use with slowly varying (mild slope) bathymetry. Berkhoff (1976) also uses this relation in the absence of current. Equation (3.187) may also be written as:

$$\sigma^2 = [\omega - (\mathbf{U} \cdot \boldsymbol{\kappa})]^2 \quad (3.189)$$

Where:

$$\sigma^2 = g\kappa \tanh(\kappa h') \quad (3.190)$$

In this case σ is referred to as the intrinsic frequency and ω as the absolute frequency.

During implementation of the NM-WCIM the presence of a product of current and a $\boldsymbol{\kappa}$ vector on the right hand side of Equation (3.189) introduces the need for an iterative approach to solving the dispersion equation. This process is discussed in Section 3.13.

3.6.3.3 Further Manipulation of the Vertical Function

It is now possible to manipulate the equation for the vertical function to get an explicit form of f . Multiplying both terms on the right hand side of Equation (3.178) by a term amounting to unity yields:

$$f = C_2 \left(\frac{e^{-\kappa h}}{e^{-\kappa h}} \right) e^{2\kappa h} e^{\kappa z} + C_2 \left(\frac{e^{-\kappa h}}{e^{-\kappa h}} \right) e^{-\kappa z} \quad (3.191)$$

The constant C_2 can be changed to incorporate $\left(\frac{1}{e^{-\kappa h}} \right)$ without affecting the equation.

This leaves:

$$f = C_2' e^{\kappa h} e^{\kappa z} + C_2' e^{-\kappa h} e^{-\kappa z} \quad (3.192)$$

Expressing the exponential values in (3.192) more succinct form gives:

$$f = C_2' e^{\kappa(h+z)} + C_2' e^{-\kappa(h+z)} \quad (3.193)$$

Incorporating a further factor of 0.5 into the C_2 constant allows Equation (3.193) to be expressed as follows:

$$f = C_2'' \cosh[\kappa(h+z)] \quad (3.194)$$

At this point the following definition can be made:

$$z'(x, y) = z(x, y) - \bar{\eta}(x, y) \quad (3.195)$$

Using Equation (3.184) and Equation (3.195) with Equation (3.194) gives:

$$f = C_2'' \cosh[\kappa(h' + z')] \quad (3.196)$$

C_2'' can now be selected as an appropriate term to set $f=1$ when $z' = 0$:

$$f = \frac{\cosh[\kappa(h' + z')]}{\cosh[\kappa h']} \quad (3.197)$$

Berkhoff (1976), Booij (1981), Mei *et al.* (2005) and Clyne (2008) all use a vertical function similar to that of Equation (3.197).

3.7 Derivation of Mild-Slope Equation

To obtain a two-dimensional wave solution the Laplace equation described in Equation (3.114) is multiplied by the vertical function of Equation (3.130) and Equation (3.197) and integrated over the depth of the water column. In Section 3.6 a constant depth and constant current are assumed when examining the vertical function. In the case of the derivation to follow the current and depth are both assumed to vary. The method followed is similar to the Galerkin-Eigenfunction method of Massel (1993) but in this case the effects of currents will not be neglected.

Table 3.2 from Section 3.5.4 (reproduced below) summarises the harmonic wave equations for a varying current and depth that will be utilised in this section.

Table 3.2 – Summary of Harmonic Wave Equations

Boundary Condition			Equation
(a)	Laplace's Equation	$\nabla^2 \tilde{\phi} = 0$	(3.114)
(b)	Combined Free Surface Boundary Condition	$\frac{\partial \tilde{\phi}}{\partial z} = \frac{1}{g} \left[\begin{aligned} &\omega^2 \tilde{\phi} + 2i\omega U_k \frac{\partial \tilde{\phi}}{\partial x_k} + i\omega \frac{\partial U_j}{\partial x_j} \tilde{\phi} \\ &- \frac{\partial U_j}{\partial x_j} U_k \frac{\partial \tilde{\phi}}{\partial x_k} - U_j \frac{\partial U_k}{\partial x_j} \frac{\partial \tilde{\phi}}{\partial x_k} \\ &- U_j U_k \frac{\partial^2 \tilde{\phi}}{\partial x_j \partial x_k} - \gamma \frac{\partial U_j}{\partial x_j} \tilde{\phi} - \gamma U_j \frac{\partial \tilde{\phi}}{\partial x_j} + i\omega \gamma \tilde{\phi} \end{aligned} \right]$ <p style="text-align: center;">at $z = \bar{\eta}$, $j = 1, 2$, $k = 1, 2$</p>	(3.125)
(c)	Kinematic Seabed Boundary Condition	$\frac{\partial \tilde{\phi}}{\partial z} = - \frac{\partial \tilde{\phi}}{\partial x_k} \frac{\partial h}{\partial x_k}$ <p style="text-align: center;">at $z = -h$, $k = 1, 2$</p>	(3.128)

3.7.1 Vertical Integration of Weighted Laplace Equation

In this case the values of depth and current may vary so the application of the vertical function to the velocity potential may be expressed as follows:

$$\tilde{\phi}(x, y, z) = f(z', \kappa(h'), h'(x, y))\phi(x, y) \quad (3.198)$$

Utilising the vertical function f with Equation (3.114) and integrating the product over the depth of the fluid column yields:

$$\int_{-h}^{\bar{\eta}} f(z, \kappa(h), h(x, y)) \nabla^2 \tilde{\phi}(x, y, z) dz = 0 \quad (3.199)$$

Equation (3.199) can be expressed more explicitly as:

$$\int_{-h}^{\bar{\eta}} f(z) \left(\frac{\partial^2 \tilde{\phi}}{\partial x^2} + \frac{\partial^2 \tilde{\phi}}{\partial y^2} + \frac{\partial^2 \tilde{\phi}}{\partial z^2} \right) dz = 0 \quad (3.200)$$

Separating Equation (3.200) into horizontal and vertical components gives:

$$\int_{-h}^{\bar{\eta}} f(z) \nabla_h^2 \tilde{\phi} dz + \int_{-h}^{\bar{\eta}} f(z) \frac{\partial^2 \tilde{\phi}}{\partial z^2} dz = 0 \quad (3.201)$$

where

$$\nabla_h^2 = \frac{\partial}{\partial x} + \frac{\partial}{\partial y} \quad (3.202)$$

Integration by parts of the second term of Equation (3.201) gives the following:

$$\int_{-h}^{\bar{\eta}} f(z) \frac{\partial^2 \tilde{\phi}}{\partial z^2} dz = - \int_{-h}^{\bar{\eta}} \frac{\partial f}{\partial z} \frac{\partial \tilde{\phi}}{\partial z} dz + f(z) \frac{\partial \tilde{\phi}}{\partial z} \Big|_{-h}^{\bar{\eta}} \quad (3.203)$$

Substitution of Equation (3.203) for the second term of Equation (3.201) gives:

$$\int_{-h}^{\bar{\eta}} f \nabla_h^2 \tilde{\phi} dz - \int_{-h}^{\bar{\eta}} \frac{\partial f}{\partial z} \frac{\partial \tilde{\phi}}{\partial z} dz + f \frac{\partial \tilde{\phi}}{\partial z} \Big|_{-h}^{\bar{\eta}} = 0 \quad (3.204)$$

Examining the first term in Equation (3.204):

$$\nabla_h^2 \tilde{\phi} = \frac{\partial}{\partial x_k} \frac{\partial}{\partial x_k} \tilde{\phi}, \quad k=1,2 \quad (3.205)$$

Substituting Equation (3.198) into Equation (3.205) gives:

$$\nabla_h^2 \tilde{\phi} = \frac{\partial}{\partial x_k} \frac{\partial}{\partial x_k} (f \phi), \quad k=1,2 \quad (3.206)$$

The vertical function f , as defined in Equation (3.197), is only a function of the horizontal coordinates so the derivative of f in Equation (3.207) is not a partial derivative.

$$\nabla_h^2 \tilde{\phi} = \frac{\partial}{\partial x_k} \left(\frac{df}{dx_k} \phi + f \frac{\partial \phi}{\partial x_k} \right) \quad (3.207)$$

Equation (3.207) can be expanded to:

$$\nabla_h^2 \tilde{\phi} = \phi \frac{d^2 f}{dx_k dx_k} + \frac{df}{dx_k} \frac{\partial \phi}{\partial x_k} + \frac{df}{dx_k} \frac{\partial \phi}{\partial x_k} + f \frac{\partial^2 \phi}{\partial x_k \partial x_k} \quad (3.208)$$

Therefore:

$$\int_{-h}^{\bar{\eta}} f \nabla_h^2 \tilde{\phi} dz = \int_{-h}^{\bar{\eta}} f \phi \frac{d^2 f}{dx_k dx_k} dz + \int_{-h}^{\bar{\eta}} 2f \frac{df}{dx_k} \frac{\partial \phi}{\partial x_k} dz + \int_{-h}^{\bar{\eta}} f^2 \frac{\partial^2 \phi}{\partial x_k \partial x_k} dz \quad (3.209)$$

Examining the second term in Equation (3.204) gives:

$$\int_{-h}^{\bar{\eta}} \frac{\partial f}{\partial z} \frac{\partial \tilde{\phi}}{\partial z} dz = \int_{-h}^{\bar{\eta}} \frac{\partial f}{\partial z} \frac{\partial f}{\partial z} \phi dz \quad (3.210)$$

Examining the third term in Equation (3.204):

$$f \frac{\partial \tilde{\phi}}{\partial z} \Big|_{-h}^{\bar{\eta}} = f \frac{\partial \tilde{\phi}}{\partial z} \Big|_{\bar{\eta}} - f \frac{\partial \tilde{\phi}}{\partial z} \Big|_{-h} \quad (3.211)$$

As shown in Equation (3.197) $f=1$ when $z=\bar{\eta}$ hence:

$$f \frac{\partial \tilde{\phi}}{\partial z} \Big|_{-h}^{\bar{\eta}} = \frac{\partial \tilde{\phi}}{\partial z} \Big|_{\bar{\eta}} - f \frac{\partial \tilde{\phi}}{\partial z} \Big|_{-h} \quad (3.212)$$

Substituting Equations (3.212), (3.210) and (3.209) into (3.204) gives:

$$\int_{-h}^{\bar{\eta}} f \phi \frac{d^2 f}{dx_k dx_k} dz + \int_{-h}^{\bar{\eta}} 2f \frac{df}{dx_k} \frac{\partial \phi}{\partial x_k} dz + \int_{-h}^{\bar{\eta}} f^2 \frac{\partial^2 \phi}{\partial x_k \partial x_k} dz - \int_{-h}^{\bar{\eta}} \frac{\partial f}{\partial z} \frac{\partial f}{\partial z} \phi dz + \frac{\partial \tilde{\phi}}{\partial z} \Big|_{\bar{\eta}} - f \frac{\partial \tilde{\phi}}{\partial z} \Big|_{-h} = 0 \quad (3.213)$$

It is evident that the fifth term of Equation (3.213) can be defined using combined free surface boundary condition in Equation (3.125):

$$\left. \frac{\partial \tilde{\phi}}{\partial z} \right|_{\bar{\eta}} = \frac{1}{g} \left[\begin{aligned} &\omega^2 \tilde{\phi} + 2i\omega U_k \frac{\partial \tilde{\phi}}{\partial x_k} + i\omega \frac{\partial U_j}{\partial x_j} \tilde{\phi} - \frac{\partial U_j}{\partial x_j} U_k \frac{\partial \tilde{\phi}}{\partial x_k} \\ &- U_j \frac{\partial U_k}{\partial x_j} \frac{\partial \tilde{\phi}}{\partial x_k} - U_j U_k \frac{\partial^2 \tilde{\phi}}{\partial x_j \partial x_k} - \gamma \frac{\partial U_j}{\partial x_j} \tilde{\phi} - \gamma U_j \frac{\partial \tilde{\phi}}{\partial x_j} + i\omega \gamma \tilde{\phi} \end{aligned} \right]_{\bar{\eta}} \quad (3.214)$$

The sixth term of Equation (3.213) can be defined using the seabed boundary condition in Equation (3.128):

$$\left. \frac{\partial \tilde{\phi}}{\partial z} \right|_{-h} = - \frac{\partial \tilde{\phi}}{\partial x_k} \frac{\partial h}{\partial x_k} \quad (3.215)$$

3.7.2 Gradients of the vertical function in Equation (3.213)

Equation (3.213) contains horizontal gradients of the vertical function f . These are non-zero if depth and current are varying. Equations for these can be obtained using the dispersion equation listed in Equation (3.187). Initially the required gradients will be expressed symbolically. The first horizontal derivative of the vertical function is:

$$\frac{df}{dx_k} = \frac{\partial f}{\partial \kappa} \frac{\partial \kappa}{\partial x_k} + \frac{\partial f}{\partial h'} \frac{\partial h'}{\partial x_k} + \frac{\partial f}{\partial z'} \frac{\partial z'}{\partial \bar{\eta}} \frac{\partial \bar{\eta}}{\partial x_k}, \quad k=1,2 \quad (3.216)$$

It should be noted that this derivation is carried out for the mean free surface including set-up, where:

$$h' = h'(x, y) = h(x, y) + \bar{\eta}(x, y) \quad (3.217)$$

κ is also a function of the horizontal derivatives

$$\kappa = \kappa(x, y) \quad (3.218)$$

At this point Equation (3.195) should also be recalled:

$$z' = z'(x, y) = z(x, y) - \bar{\eta}(x, y) \quad (3.219)$$

The second horizontal derivatives of the vertical function may be expressed as follows:

$$\frac{d^2 f}{dx_k dx_k} = \frac{\partial}{\partial x_k} \left[\frac{\partial f}{\partial \kappa} \frac{\partial \kappa}{\partial x_k} + \frac{\partial f}{\partial h'} \frac{\partial h'}{\partial x_k} + \frac{\partial f}{\partial z'} \frac{\partial z'}{\partial \bar{\eta}} \frac{\partial \bar{\eta}}{\partial x_k} \right] \quad (3.220)$$

Similarly the cross-derivative is:

$$\frac{d^2 f}{dx_j dx_k} = \frac{\partial}{\partial x_j} \left[\frac{\partial f}{\partial \kappa} \frac{\partial \kappa}{\partial x_k} + \frac{\partial f}{\partial h'} \frac{\partial h'}{\partial x_k} + \frac{\partial f}{\partial z'} \frac{\partial z'}{\partial \bar{\eta}} \frac{\partial \bar{\eta}}{\partial x_k} \right] \quad (3.221)$$

Isolating the terms containing the vertical function in Equation (3.224) gives:

$$\begin{aligned}
\frac{d^2 f}{dx_k dx_k} &= \frac{\partial f}{\partial h'} \frac{\partial^2 h'}{\partial x_k \partial x_k} + \frac{\partial f}{\partial \kappa} \frac{\partial^2 \kappa}{\partial x_k \partial x_k} + \frac{\partial f}{\partial z'} \frac{\partial z'}{\partial \bar{\eta}} \frac{\partial^2 \bar{\eta}}{\partial x_k \partial x_k} \\
&+ \frac{\partial^2 f}{\partial h'^2} \left(\frac{\partial h'}{\partial x_k} \right)^2 + \frac{\partial^2 f}{\partial \kappa^2} \left(\frac{\partial \kappa}{\partial x_k} \right)^2 + \frac{\partial^2 f}{\partial z'^2} \left(\frac{\partial z'}{\partial \bar{\eta}} \right)^2 \left(\frac{\partial \bar{\eta}}{\partial x_k} \right)^2 \\
&+ 2 \frac{\partial^2 f}{\partial h' \partial \kappa} \frac{\partial \kappa}{\partial x_k} \frac{\partial h'}{\partial x_k} + 2 \frac{\partial^2 f}{\partial h' \partial z'} \frac{\partial z'}{\partial \bar{\eta}} \frac{\partial \bar{\eta}}{\partial x_k} \frac{\partial h'}{\partial x_k} + 2 \frac{\partial^2 f}{\partial z' \partial \kappa} \frac{\partial z'}{\partial \bar{\eta}} \frac{\partial \bar{\eta}}{\partial x_k} \frac{\partial \kappa}{\partial x_k}
\end{aligned} \tag{3.226}$$

Similarly isolating the terms containing the vertical function in Equation (3.225) gives:

$$\begin{aligned}
\frac{d^2 f}{dx_j dx_k} &= \frac{\partial f}{\partial h'} \frac{\partial^2 h'}{\partial x_j \partial x_k} + \frac{\partial f}{\partial \kappa} \frac{\partial^2 \kappa}{\partial x_j \partial x_k} + \frac{\partial f}{\partial z'} \frac{\partial z'}{\partial \bar{\eta}} \frac{\partial^2 \bar{\eta}}{\partial x_j \partial x_k} \\
&+ \frac{\partial^2 f}{\partial h'^2} \frac{\partial h'}{\partial x_k} \frac{\partial h'}{\partial x_j} + \frac{\partial^2 f}{\partial \kappa^2} \frac{\partial \kappa}{\partial x_k} \frac{\partial \kappa}{\partial x_j} + \frac{\partial^2 f}{\partial z'^2} \frac{\partial z'}{\partial \bar{\eta}} \frac{\partial \bar{\eta}}{\partial x_k} \frac{\partial z'}{\partial \bar{\eta}} \frac{\partial \bar{\eta}}{\partial x_j} \\
&+ \frac{\partial^2 f}{\partial \kappa \partial h'} \frac{\partial h'}{\partial x_k} \frac{\partial \kappa}{\partial x_j} + \frac{\partial^2 f}{\partial \kappa \partial h'} \frac{\partial \kappa}{\partial x_k} \frac{\partial h'}{\partial x_j} + \frac{\partial^2 f}{\partial z' \partial h'} \frac{\partial z'}{\partial \bar{\eta}} \frac{\partial \bar{\eta}}{\partial x_k} \frac{\partial h'}{\partial x_j} + \frac{\partial^2 f}{\partial h' \partial z'} \frac{\partial h'}{\partial x_k} \frac{\partial z'}{\partial \bar{\eta}} \frac{\partial \bar{\eta}}{\partial x_j} \\
&\frac{\partial^2 f}{\partial z' \partial \kappa} \frac{\partial z'}{\partial \bar{\eta}} \frac{\partial \bar{\eta}}{\partial x_k} \frac{\partial \kappa}{\partial x_j} + \frac{\partial^2 f}{\partial \kappa \partial z'} \frac{\partial \kappa}{\partial x_k} \frac{\partial z'}{\partial \bar{\eta}} \frac{\partial \bar{\eta}}{\partial x_j}
\end{aligned} \tag{3.227}$$

Equation (3.226) is the corresponding equation in this derivation to Equation 26 in the Massel (1993) derivation. This derivation includes the effects of set-up, $\bar{\eta}$, its effects are neglected in the Massel (1993) derivation.

3.7.3 Use of dispersion relation to obtain gradients of the wave number

Examining Equation (3.187) gives:

$$\omega^2 - g\kappa \tanh \kappa h' + (\mathbf{\kappa} \cdot \mathbf{U})^2 - 2\omega(\mathbf{\kappa} \cdot \mathbf{U}) = 0 \quad (3.228)$$

Where $\mathbf{\kappa}$ is defined as discussed in Equation (3.188):

$$\mathbf{\kappa} = \kappa \frac{\nabla S_\phi}{|\nabla S_\phi|}$$

A function G can be selected as follows:

$$G = \omega^2 - g\kappa \tanh \kappa h' + (\mathbf{\kappa} \cdot \mathbf{U})^2 - 2\omega(\mathbf{\kappa} \cdot \mathbf{U}) \quad (3.229)$$

By setting:

$$G_1 = \omega^2 - g\kappa \tanh \kappa h' \quad (3.230)$$

$$G_2 = (\mathbf{\kappa} \cdot \mathbf{U})^2 - 2\omega(\mathbf{\kappa} \cdot \mathbf{U}) = \left(\kappa \frac{\nabla S_\phi}{|\nabla S_\phi|} \cdot \mathbf{U} \right)^2 - 2\omega \left(\kappa \frac{\nabla S_\phi}{|\nabla S_\phi|} \cdot \mathbf{U} \right) \quad (3.231)$$

The G function can be expressed as:

$$G = G_1 + G_2 \quad (3.232)$$

where:

$$G_1 = G_1(\kappa, h') = G_1(\kappa, h'(x_1, x_2))$$

$$G_2 = G_2(\kappa, x_1, x_2)$$

Equation (3.229) can also be expressed as follows:

$$\lambda' = \frac{\omega^2 + G_2}{g} = \kappa \tanh \kappa h' \quad (3.233)$$

Where λ' can be defined in terms of the σ from Equation (3.190) as follows:

$$\lambda' = \frac{\sigma^2}{g} \quad (3.234)$$

3.7.3.1 Horizontal derivatives of κ

The horizontal partial derivatives of G can be used to obtain first and second horizontal derivatives of the function with respect to κ and h' . Using Equation (3.228) with Equation (3.230) and (3.231) gives:

$$G_1(\kappa(x_1, x_2), h'(x_1, x_2)) + G_2(\kappa, x_1, x_2) = 0 \quad (3.235)$$

Initially examining the first horizontal derivative of G :

$$\frac{dG}{dx_k} = \frac{\partial G_1}{\partial x_k} + \frac{dG_2}{dx_k} = 0 \quad (3.236)$$

G_2 will be obtained numerically throughout the modelling of this project. For any step in an iterative scheme G_2 will be calculated based on the results of the previous iteration. Hence G_2 and its derivatives will be isolated from G_1 for this derivation.

$$\frac{dG}{dx_k} = \left(\frac{\partial G_1}{\partial x_k} \right) + \frac{dG_2}{dx_k} = \left(\frac{\partial G_1}{\partial \kappa} \frac{\partial \kappa}{\partial x_k} + \frac{\partial G_1}{\partial h'} \frac{\partial h'}{\partial x_k} \right) + \frac{dG_2}{dx_k} = 0 \quad (3.237)$$

Rearranging Equation (3.237) to obtain the horizontal derivative of κ gives:

$$\frac{\partial \kappa}{\partial x_k} = - \frac{\frac{\partial G_1}{\partial h'} \frac{\partial h'}{\partial x_k} + \frac{dG_2}{dx_k}}{\frac{\partial G_1}{\partial \kappa}} \quad (3.238)$$

Examining the second horizontal derivative of G gives:

$$\frac{d^2 G}{dx_k dx_k} = \frac{\partial^2 G_1}{\partial x_k \partial x_k} + \frac{d^2 G_2}{dx_k dx_k} = 0 \quad (3.239)$$

Using Equation (3.237) with Equation (3.239) gives:

$$\frac{d^2 G}{dx_k dx_k} = \left[\frac{\partial^2 G_1}{\partial x_k \partial x_k} \right] + \frac{d^2 G_2}{dx_k dx_k} = \left[\begin{aligned} & \frac{\partial}{\partial \kappa} \left(\frac{\partial G_1}{\partial \kappa} \frac{\partial \kappa}{\partial x_k} + \frac{\partial G_1}{\partial h'} \frac{\partial h'}{\partial x_k} \right) \frac{d\kappa}{dx_k} \\ & + \frac{\partial}{\partial h'} \left(\frac{\partial G_1}{\partial \kappa} \frac{\partial \kappa}{\partial x_k} + \frac{\partial G_1}{\partial h'} \frac{\partial h'}{\partial x_k} \right) \frac{dh'}{dx_k} \\ & + \frac{\partial}{\partial x_k} \left(\frac{\partial G_1}{\partial \kappa} \frac{\partial \kappa}{\partial x_k} + \frac{\partial G_1}{\partial h'} \frac{\partial h'}{\partial x_k} \right) \end{aligned} \right] + \frac{d^2 G_2}{dx_k dx_k} = 0 \quad (3.240)$$

Equation (3.240) can be expanded to:

$$\begin{aligned} & \left(\frac{\partial^2 G_1}{\partial \kappa^2} \frac{\partial \kappa}{\partial x_k} + \frac{\partial^2 G_1}{\partial \kappa \partial h'} \frac{\partial h'}{\partial x_k} \right) \frac{\partial \kappa}{\partial x_k} + \left(\frac{\partial^2 G_1}{\partial h' \partial \kappa} \frac{\partial \kappa}{\partial x_k} + \frac{\partial^2 G_1}{\partial h'^2} \frac{\partial h'}{\partial x_k} \right) \frac{\partial h'}{\partial x_k} \\ & + \left(\frac{\partial G_1}{\partial \kappa} \frac{\partial^2 \kappa}{\partial x_k \partial x_k} + \frac{\partial G_1}{\partial h'} \frac{\partial^2 h'}{\partial x_k \partial x_k} \right) + \frac{d^2 G_2}{dx_k dx_k} = 0 \end{aligned} \quad (3.241)$$

Isolation of the second horizontal derivative of κ gives:

$$\frac{\partial^2 \kappa}{\partial x_k \partial x_k} = \frac{\left(\frac{\partial^2 G_1}{\partial \kappa^2} \frac{\partial \kappa}{\partial x_k} + \frac{\partial^2 G_1}{\partial \kappa \partial h'} \frac{\partial h'}{\partial x_k} \right) \frac{\partial \kappa}{\partial x_k} + \left(\frac{\partial^2 G_1}{\partial h' \partial \kappa} \frac{\partial \kappa}{\partial x_k} + \frac{\partial^2 G_1}{\partial h'^2} \frac{\partial h'}{\partial x_k} \right) \frac{\partial h'}{\partial x_k} + \frac{\partial G_1}{\partial h'} \frac{\partial^2 h'}{\partial x_k \partial x_k} + \frac{d^2 G_2}{dx_k dx_k}}{-\frac{\partial G_1}{\partial \kappa}} \quad (3.242)$$

Expansion and separation of the explicit G_2 term as before gives:

$$\frac{\partial^2 \kappa}{\partial x_k \partial x_k} = \frac{-\frac{\partial^2 G_1}{\partial \kappa^2} \left(\frac{\partial \kappa}{\partial x_k} \right)^2 - \frac{\partial^2 G_1}{\partial h'^2} \left(\frac{\partial h'}{\partial x_k} \right)^2 - \frac{\partial G_1}{\partial h'} \frac{\partial^2 h'}{\partial x_k \partial x_k} - \frac{\partial^2 G_1}{\partial \kappa \partial h'} \left(2 \frac{\partial h'}{\partial x_k} \frac{\partial \kappa}{\partial x_k} \right) - \frac{d^2 G_2}{dx_k dx_k}}{\frac{\partial G_1}{\partial \kappa}} - \frac{\frac{d^2 G_2}{dx_k dx_k}}{\frac{\partial G_1}{\partial \kappa}} \quad (3.243)$$

3.7.3.2 Derivatives of G_I with respect to κ and h'

In order to complete the symbolic derivations listed in Section 3.7.3.2 above it is necessary to individually calculate each of the components as follows:

$$\frac{\partial G_1}{\partial \kappa} = \frac{\partial}{\partial \kappa} (\omega^2 - g \kappa \tanh \kappa h') \quad (3.244)$$

$$\frac{\partial G_1}{\partial \kappa} = -h' g \kappa \operatorname{sech}^2 \kappa h' - g \tanh \kappa h' \quad (3.245)$$

$$\frac{\partial^2 G_1}{\partial \kappa^2} = \frac{\partial}{\partial \kappa} (-h' g \kappa \operatorname{sech}^2 \kappa h') - \frac{\partial}{\partial \kappa} (g \tanh \kappa h') \quad (3.246)$$

The first term in Equation (3.246) may be written as:

$$\frac{\partial}{\partial \kappa} (-h' g \kappa \operatorname{sech}^2 \kappa h') = -h' g \operatorname{sech}^2 \kappa h' - h'^2 g \kappa 2 \operatorname{sech} \kappa h' (-\operatorname{sech} \kappa h' \tanh \kappa h') \quad (3.247)$$

$$\frac{\partial}{\partial \kappa} (-h' g \kappa \operatorname{sech}^2 \kappa h') = -h' g \operatorname{sech}^2 \kappa h' + h'^2 g \kappa 2 \operatorname{sech}^2 \kappa h' \tanh \kappa h' \quad (3.248)$$

Examining the second term of Equation (3.246) gives:

$$\frac{\partial}{\partial \kappa} (g \tanh \kappa h') = g h' \operatorname{sech}^2 \kappa h' \quad (3.249)$$

Combining Equations (3.248) and (3.249):

$$\frac{\partial^2 G_1}{\partial \kappa^2} = -h'g \operatorname{sech}^2 \kappa h' + h'^2 g \kappa^2 \operatorname{sech}^2 \kappa h' \tanh \kappa h' - gh' \operatorname{sech}^2 \kappa h' \quad (3.250)$$

$$\frac{\partial^2 G_1}{\partial \kappa^2} = 2g \kappa h'^2 \operatorname{sech}^2 \kappa h' \tanh \kappa h' - 2gh' \operatorname{sech}^2 \kappa h' \quad (3.251)$$

$$\frac{\partial^2 G_1}{\partial \kappa \partial h'} = \frac{\partial}{\partial h'} (-h'g \kappa \operatorname{sech}^2 \kappa h') - \frac{\partial}{\partial h'} (g \tanh \kappa h') \quad (3.252)$$

The first term in Equation (3.252) may be written as:

$$\frac{\partial}{\partial h'} (-h'g \kappa \operatorname{sech}^2 \kappa h') = -g \kappa \operatorname{sech}^2 \kappa h' - h'g \kappa^2 2 \operatorname{sech} \kappa h' (-\operatorname{sech} \kappa h' \tanh \kappa h') \quad (3.253)$$

$$\frac{\partial}{\partial h'} (-h'g \kappa \operatorname{sech}^2 \kappa h') = -g \kappa \operatorname{sech}^2 \kappa h' + 2h'g \kappa^2 \operatorname{sech}^2 \kappa h' \tanh \kappa h' \quad (3.254)$$

Examining the second term of Equation (3.252) gives:

$$\frac{\partial}{\partial h'} (g \tanh \kappa h') = g \kappa \operatorname{sech}^2 \kappa h' \quad (3.255)$$

Combining Equations (3.254) and (3.255):

$$\frac{\partial^2 G_1}{\partial \kappa \partial h'} = 2h'g \kappa^2 \operatorname{sech}^2 \kappa h' \tanh \kappa h' - 2g \kappa \operatorname{sech}^2 \kappa h' \quad (3.256)$$

$$\frac{\partial G_1}{\partial h'} = \frac{\partial}{\partial h'} (\omega^2 - g \kappa \tanh \kappa h') \quad (3.257)$$

$$\frac{\partial G_1}{\partial h'} = -g \kappa^2 \operatorname{sech}^2 \kappa h' \quad (3.258)$$

$$\frac{\partial^2 G_1}{\partial h'^2} = \frac{\partial}{\partial h'} (-g \kappa^2 \operatorname{sech}^2 \kappa h') \quad (3.259)$$

$$\frac{\partial^2 G_1}{\partial h'^2} = 2g \kappa^3 \operatorname{sech}^2 \kappa h' \tanh \kappa h' \quad (3.260)$$

$$\frac{\partial^2 G_1}{\partial h' \partial \kappa} = \frac{\partial}{\partial \kappa} (-g \kappa^2 \operatorname{sech}^2 \kappa h') \quad (3.261)$$

$$\frac{\partial^2 G_1}{\partial h' \partial \kappa} = 2g h' \kappa^2 \operatorname{sech}^2 \kappa h' \tanh \kappa h' - 2g \kappa \operatorname{sech}^2 \kappa h' \quad (3.262)$$

Equation (3.262) is identical to Equation (3.256) as expected.

3.7.3.2 Derivatives of G_2 with respect to κ and x

The gradient of G_2 with respect to x can be expanded as follows:

$$\frac{dG_2}{dx_k} = \frac{\partial G_2}{\partial x_k} + \frac{\partial G_2}{\partial \kappa} \frac{\partial \kappa}{\partial x_k} \quad (3.263)$$

The second differential of G_2 with respect to x becomes:

$$\frac{d^2 G_2}{dx_k dx_k} = \frac{d}{dx_k} \left(\frac{\partial G_2}{\partial x_k} + \frac{\partial G_2}{\partial \kappa} \frac{\partial \kappa}{\partial x_k} \right) \quad (3.264)$$

This may be expanded as:

$$\frac{d^2 G_2}{dx_k dx_k} = \frac{\partial^2 G_2}{\partial x_k \partial x_k} + \frac{\partial G_2}{\partial \kappa} \frac{\partial^2 \kappa}{\partial x_k \partial x_k} \quad (3.265)$$

Equation (3.231) can be expressed in index notation as follow:

$$G_2 = \left(\frac{\kappa U_k \frac{\partial S_\phi}{\partial x_k}}{\left| \frac{\partial S_\phi}{\partial x_j} \hat{\mathbf{e}}_j \right|} \right)^2 - 2\omega \left(\frac{\kappa U_k \frac{\partial S_\phi}{\partial x_k}}{\left| \frac{\partial S_\phi}{\partial x_j} \hat{\mathbf{e}}_j \right|} \right) \quad (3.266)$$

Further expansion of (3.266) gives:

$$G_2 = \frac{\kappa^2 U_k U_k \frac{\partial S_\phi}{\partial x_k} \frac{\partial S_\phi}{\partial x_k}}{\left| \frac{\partial S_\phi}{\partial x_j} \hat{\mathbf{e}}_j \right|^2} - \frac{2\omega \kappa U_k \frac{\partial S_\phi}{\partial x_k}}{\left| \frac{\partial S_\phi}{\partial x_j} \hat{\mathbf{e}}_j \right|} \quad (3.267)$$

The partial derivative of G_2 with respect to x can be calculated as follows:

$$\frac{\partial G_2}{\partial x_k} = \frac{\partial}{\partial x} \left(\frac{\kappa^2 U_k U_k}{\left| \frac{\partial S_\phi}{\partial x_j} \hat{\mathbf{e}}_j \right|^2} \frac{\partial S_\phi}{\partial x_k} \frac{\partial S_\phi}{\partial x_k} \right) - \frac{\partial}{\partial x} \left(\frac{2\omega \kappa U_k}{\left| \frac{\partial S_\phi}{\partial x_j} \hat{\mathbf{e}}_j \right|} \frac{\partial S_\phi}{\partial x_k} \right) \quad (3.268)$$

Equation (3.268) can be rewritten as:

$$\frac{\partial G_2}{\partial x_k} = \frac{\kappa^2}{\left| \frac{\partial S_\phi}{\partial x_j} \hat{\mathbf{e}}_j \right|^2} \frac{\partial}{\partial x_k} \left(U_k U_k \frac{\partial S_\phi}{\partial x_k} \frac{\partial S_\phi}{\partial x_k} \right) - \frac{2\omega \kappa}{\left| \frac{\partial S_\phi}{\partial x_j} \hat{\mathbf{e}}_j \right|} \frac{\partial}{\partial x_k} \left(U_k \frac{\partial S_\phi}{\partial x_k} \right) \quad (3.269)$$

Equation (3.269) may be expressed more explicitly as:

$$\frac{\partial G_2}{\partial x_k} = \frac{\kappa^2}{\left| \frac{\partial S_\phi}{\partial x_j} \hat{\mathbf{e}}_j \right|^2} \left(2 \frac{\partial U_k}{\partial x_k} U_k \frac{\partial S_\phi}{\partial x_k} \frac{\partial S_\phi}{\partial x_k} + 2 U_k U_k \frac{\partial^2 S_\phi}{\partial x_k \partial x_k} \frac{\partial S_\phi}{\partial x_k} \right) - \frac{2\omega \kappa}{\left| \frac{\partial S_\phi}{\partial x_j} \hat{\mathbf{e}}_j \right|} \left(U_k \frac{\partial^2 S_\phi}{\partial x_k \partial x_k} + \frac{\partial U_k}{\partial x_k} \frac{\partial S_\phi}{\partial x_k} \right) \quad (3.270)$$

Full expansion of Equation (3.270) gives:

$$\frac{\partial G_2}{\partial x_k} = \frac{2U_k \kappa^2}{\left| \frac{\partial S_\phi}{\partial x_j} \hat{\mathbf{e}}_j \right|^2} \frac{\partial U_k}{\partial x_k} \frac{\partial S_\phi}{\partial x_k} \frac{\partial S_\phi}{\partial x_k} + \frac{2U_k U_k \kappa^2}{\left| \frac{\partial S_\phi}{\partial x_j} \hat{\mathbf{e}}_j \right|^2} \frac{\partial^2 S_\phi}{\partial x_k \partial x_k} \frac{\partial S_\phi}{\partial x_k} - \frac{2U_k \omega \kappa}{\left| \frac{\partial S_\phi}{\partial x_j} \hat{\mathbf{e}}_j \right|} \frac{\partial^2 S_\phi}{\partial x_k \partial x_k} + \frac{\partial U_k}{\partial x_k} \frac{\partial S_\phi}{\partial x_k} \quad (3.271)$$

The partial derivative of G_2 with respect to κ can be expressed as follows:

$$\frac{\partial G_2}{\partial \kappa} = \frac{2\kappa U_k U_k}{\left| \frac{\partial S_\phi}{\partial x_j} \hat{\mathbf{e}}_j \right|^2} \frac{\partial S_\phi}{\partial x_k} \frac{\partial S_\phi}{\partial x_k} - \frac{2\omega U_k}{\left| \frac{\partial S_\phi}{\partial x_j} \hat{\mathbf{e}}_j \right|} \frac{\partial S_\phi}{\partial x_k} \quad (3.272)$$

Using Equations (3.271) and (3.272) with Equation (3.263) gives the following:

$$\frac{dG_2}{dx_k} = \left(\begin{aligned} & \frac{2U_k \kappa^2}{\left| \frac{\partial S_\phi}{\partial x_j} \hat{\mathbf{e}}_j \right|^2} \frac{\partial U_k}{\partial x_k} \frac{\partial S_\phi}{\partial x_k} \frac{\partial S_\phi}{\partial x_k} \\ & + \frac{2U_k U_k \kappa^2}{\left| \frac{\partial S_\phi}{\partial x_j} \hat{\mathbf{e}}_j \right|^2} \frac{\partial^2 S_\phi}{\partial x_k \partial x_k} \frac{\partial S_\phi}{\partial x_k} \\ & - \frac{2U_k \omega \kappa}{\left| \frac{\partial S_\phi}{\partial x_j} \hat{\mathbf{e}}_j \right|} \frac{\partial^2 S_\phi}{\partial x_k \partial x_k} + \frac{\partial U_k}{\partial x_k} \frac{\partial S_\phi}{\partial x_k} \end{aligned} \right) + \left(\begin{aligned} & \frac{2\kappa U_k U_k}{\left| \frac{\partial S_\phi}{\partial x_j} \hat{\mathbf{e}}_j \right|^2} \frac{\partial S_\phi}{\partial x_k} \frac{\partial S_\phi}{\partial x_k} \\ & - \frac{2\omega U_k}{\left| \frac{\partial S_\phi}{\partial x_j} \hat{\mathbf{e}}_j \right|} \frac{\partial S_\phi}{\partial x_k} \end{aligned} \right) \frac{\partial \kappa}{\partial x_k} \quad (3.273)$$

A second derivative of Equation (3.271) produces:

$$\frac{\partial^2 G_2}{\partial x_k \partial x_k} = \frac{\partial}{\partial x_k} \left(\begin{aligned} & \frac{2U_k \kappa^2}{\left| \frac{\partial S_\phi}{\partial x_j} \hat{\mathbf{e}}_j \right|^2} \frac{\partial U_k}{\partial x_k} \frac{\partial S_\phi}{\partial x_k} \frac{\partial S_\phi}{\partial x_k} \\ & + \frac{2U_k U_k \kappa^2}{\left| \frac{\partial S_\phi}{\partial x_j} \hat{\mathbf{e}}_j \right|^2} \frac{\partial^2 S_\phi}{\partial x_k \partial x_k} \frac{\partial S_\phi}{\partial x_k} \\ & - \frac{2U_k \omega \kappa}{\left| \frac{\partial S_\phi}{\partial x_j} \hat{\mathbf{e}}_j \right|} \frac{\partial^2 S_\phi}{\partial x_k \partial x_k} + \frac{\partial U_k}{\partial x_k} \frac{\partial S_\phi}{\partial x_k} \end{aligned} \right) \quad (3.274)$$

Further expansion of Equation (3.274) gives:

$$\frac{\partial^2 G_2}{\partial x_k \partial x_k} = \left(\begin{aligned} & \frac{2\kappa^2}{\left| \frac{\partial S_\phi}{\partial x_j} \hat{\mathbf{e}}_j \right|^2} \frac{\partial U_k}{\partial x_k} \frac{\partial U_k}{\partial x_k} \frac{\partial S_\phi}{\partial x_k} \frac{\partial S_\phi}{\partial x_k} + \frac{2U_k \kappa^2}{\left| \frac{\partial S_\phi}{\partial x_j} \hat{\mathbf{e}}_j \right|^2} \frac{\partial^2 U_k}{\partial x_k \partial x_k} \frac{\partial S_\phi}{\partial x_k} \frac{\partial S_\phi}{\partial x_k} \\ & + \frac{4U_k \kappa^2}{\left| \frac{\partial S_\phi}{\partial x_j} \hat{\mathbf{e}}_j \right|^2} \frac{\partial U_k}{\partial x_k} \frac{\partial^2 S_\phi}{\partial x_k \partial x_k} \frac{\partial S_\phi}{\partial x_k} + \frac{4U_k \kappa^2}{\left| \frac{\partial S_\phi}{\partial x_j} \hat{\mathbf{e}}_j \right|^2} \frac{\partial U_k}{\partial x_k} \frac{\partial^2 S_\phi}{\partial x_k \partial x_k} \frac{\partial S_\phi}{\partial x_k} \\ & + \frac{2U_k U_k \kappa^2}{\left| \frac{\partial S_\phi}{\partial x_j} \hat{\mathbf{e}}_j \right|^2} \frac{\partial^3 S_\phi}{\partial x_k \partial x_k \partial x_k} \frac{\partial S_\phi}{\partial x_k} + \frac{2U_k U_k \kappa^2}{\left| \frac{\partial S_\phi}{\partial x_j} \hat{\mathbf{e}}_j \right|^2} \frac{\partial^2 S_\phi}{\partial x_k \partial x_k} \frac{\partial^2 S_\phi}{\partial x_k \partial x_k} \\ & - \frac{2\omega \kappa}{\left| \frac{\partial S_\phi}{\partial x_j} \hat{\mathbf{e}}_j \right|^2} \frac{\partial U_k}{\partial x_k} \frac{\partial^2 S_\phi}{\partial x_k \partial x_k} - \frac{2U_k \omega \kappa}{\left| \frac{\partial S_\phi}{\partial x_j} \hat{\mathbf{e}}_j \right|^2} \frac{\partial^3 S_\phi}{\partial x_k \partial x_k \partial x_k} + \frac{\partial^2 U_k}{\partial x_k \partial x_k} \frac{\partial S_\phi}{\partial x_k} + \frac{\partial U_k}{\partial x_k} \frac{\partial^2 S_\phi}{\partial x_k \partial x_k} \end{aligned} \right) \quad (3.275)$$

Using Equations (3.275) and (3.272) with (3.265) gives:

$$\begin{aligned} \frac{d^2 G_2}{dx_k dx_k} = & \left(\begin{aligned} & \frac{2\kappa^2}{\left| \frac{\partial S_\phi}{\partial x_j} \hat{\mathbf{e}}_j \right|^2} \frac{\partial U_k}{\partial x_k} \frac{\partial U_k}{\partial x_k} \frac{\partial S_\phi}{\partial x_k} \frac{\partial S_\phi}{\partial x_k} + \frac{2U_k \kappa^2}{\left| \frac{\partial S_\phi}{\partial x_j} \hat{\mathbf{e}}_j \right|^2} \frac{\partial^2 U_k}{\partial x_k \partial x_k} \frac{\partial S_\phi}{\partial x_k} \frac{\partial S_\phi}{\partial x_k} \\ & + \frac{4U_k \kappa^2}{\left| \frac{\partial S_\phi}{\partial x_j} \hat{\mathbf{e}}_j \right|^2} \frac{\partial U_k}{\partial x_k} \frac{\partial^2 S_\phi}{\partial x_k \partial x_k} \frac{\partial S_\phi}{\partial x_k} + \frac{4U_k \kappa^2}{\left| \frac{\partial S_\phi}{\partial x_j} \hat{\mathbf{e}}_j \right|^2} \frac{\partial U_k}{\partial x_k} \frac{\partial^2 S_\phi}{\partial x_k \partial x_k} \frac{\partial S_\phi}{\partial x_k} \\ & + \frac{2U_k U_k \kappa^2}{\left| \frac{\partial S_\phi}{\partial x_j} \hat{\mathbf{e}}_j \right|^2} \frac{\partial^3 S_\phi}{\partial x_k \partial x_k \partial x_k} \frac{\partial S_\phi}{\partial x_k} + \frac{2U_k U_k \kappa^2}{\left| \frac{\partial S_\phi}{\partial x_j} \hat{\mathbf{e}}_j \right|^2} \frac{\partial^2 S_\phi}{\partial x_k \partial x_k} \frac{\partial^2 S_\phi}{\partial x_k \partial x_k} \\ & - \frac{2\omega \kappa}{\left| \frac{\partial S_\phi}{\partial x_j} \hat{\mathbf{e}}_j \right|^2} \frac{\partial U_k}{\partial x_k} \frac{\partial^2 S_\phi}{\partial x_k \partial x_k} - \frac{2U_k \omega \kappa}{\left| \frac{\partial S_\phi}{\partial x_j} \hat{\mathbf{e}}_j \right|^2} \frac{\partial^3 S_\phi}{\partial x_k \partial x_k \partial x_k} + \frac{\partial^2 U_k}{\partial x_k \partial x_k} \frac{\partial S_\phi}{\partial x_k} + \frac{\partial U_k}{\partial x_k} \frac{\partial^2 S_\phi}{\partial x_k \partial x_k} \end{aligned} \right) \\ & + \left(\begin{aligned} & \frac{2\kappa U_k U_k}{\left| \frac{\partial S_\phi}{\partial x_j} \hat{\mathbf{e}}_j \right|^2} \frac{\partial S_\phi}{\partial x_k} \frac{\partial S_\phi}{\partial x_k} - \frac{2\omega U_k}{\left| \frac{\partial S_\phi}{\partial x_j} \hat{\mathbf{e}}_j \right|^2} \frac{\partial S_\phi}{\partial x_k} \frac{\partial^2 \kappa}{\partial x_k \partial x_k} \end{aligned} \right) \quad (3.276) \end{aligned}$$

During computer modelling $\frac{\partial S_\phi}{\partial x_k}$ and its magnitude will be obtained numerically from the previous iterations.

3.7.3.3 Further expansion of the horizontal derivatives of κ

Equation (3.273) can be used with Equation (3.238) to give:

$$\frac{\partial \kappa}{\partial x_k} = \frac{-\frac{\partial G_1}{\partial h'} \frac{\partial h'}{\partial x_k} + \left(\frac{2U_k \kappa^2}{\left| \frac{\partial S_\phi}{\partial x_j} \hat{\mathbf{e}}_j \right|^2} \frac{\partial U_k}{\partial x_k} \frac{\partial S_\phi}{\partial x_k} \frac{\partial S_\phi}{\partial x_k} + \frac{2U_k U_k \kappa^2}{\left| \frac{\partial S_\phi}{\partial x_j} \hat{\mathbf{e}}_j \right|^2} \frac{\partial^2 S_\phi}{\partial x_k \partial x_k} \frac{\partial S_\phi}{\partial x_k} - \frac{2U_k \omega \kappa}{\left| \frac{\partial S_\phi}{\partial x_j} \hat{\mathbf{e}}_j \right|} \frac{\partial^2 S_\phi}{\partial x_k \partial x_k} + \frac{\partial U_k}{\partial x_k} \frac{\partial S_\phi}{\partial x_k} \right)}{\frac{\partial G_1}{\partial \kappa}} + \left(\frac{2\kappa U_k U_k}{\left| \frac{\partial S_\phi}{\partial x_j} \hat{\mathbf{e}}_j \right|^2} \frac{\partial S_\phi}{\partial x_k} \frac{\partial S_\phi}{\partial x_k} - \frac{2\omega U_k}{\left| \frac{\partial S_\phi}{\partial x_j} \hat{\mathbf{e}}_j \right|} \frac{\partial S_\phi}{\partial x_k} \right) \frac{\partial \kappa}{\partial x_k} \quad (3.277)$$

Isolating the $\frac{\partial \kappa}{\partial x_k}$ terms on one side of the equation yields:

$$\frac{\partial \kappa}{\partial x_k} \left[1 - \frac{\left(\frac{2\kappa U_k U_k}{\left| \frac{\partial S_\phi}{\partial x_j} \hat{\mathbf{e}}_j \right|^2} \frac{\partial S_\phi}{\partial x_k} \frac{\partial S_\phi}{\partial x_k} - \frac{2\omega U_k}{\left| \frac{\partial S_\phi}{\partial x_j} \hat{\mathbf{e}}_j \right|} \frac{\partial S_\phi}{\partial x_k} \right)}{\frac{\partial G_1}{\partial \kappa}} \right] = \frac{-\frac{\partial G_1}{\partial h'} \frac{\partial h'}{\partial x_k} + \left(\frac{2U_k \kappa^2}{\left| \frac{\partial S_\phi}{\partial x_j} \hat{\mathbf{e}}_j \right|^2} \frac{\partial U_k}{\partial x_k} \frac{\partial S_\phi}{\partial x_k} \frac{\partial S_\phi}{\partial x_k} + \frac{2U_k U_k \kappa^2}{\left| \frac{\partial S_\phi}{\partial x_j} \hat{\mathbf{e}}_j \right|^2} \frac{\partial^2 S_\phi}{\partial x_k \partial x_k} \frac{\partial S_\phi}{\partial x_k} - \frac{2U_k \omega \kappa}{\left| \frac{\partial S_\phi}{\partial x_j} \hat{\mathbf{e}}_j \right|} \frac{\partial^2 S_\phi}{\partial x_k \partial x_k} + \frac{\partial U_k}{\partial x_k} \frac{\partial S_\phi}{\partial x_k} \right)}{\frac{\partial G_1}{\partial \kappa}} \quad (3.278)$$

Dividing across by the coefficient of $\frac{\partial \kappa}{\partial x_k}$ gives:

$$\frac{\partial \kappa}{\partial x_k} = \frac{-\frac{\partial G_1}{\partial h'} \frac{\partial h'}{\partial x_k} - \left(\frac{2U_k \kappa^2}{\left| \frac{\partial S_\phi}{\partial x_j} \hat{\mathbf{e}}_j \right|^2} \frac{\partial U_k}{\partial x_k} \frac{\partial S_\phi}{\partial x_k} \frac{\partial S_\phi}{\partial x_k} + \frac{2U_k U_k \kappa^2}{\left| \frac{\partial S_\phi}{\partial x_j} \hat{\mathbf{e}}_j \right|^2} \frac{\partial^2 S_\phi}{\partial x_k \partial x_k} \frac{\partial S_\phi}{\partial x_k} \right) - \frac{2U_k \omega \kappa}{\left| \frac{\partial S_\phi}{\partial x_j} \hat{\mathbf{e}}_j \right|} \frac{\partial^2 S_\phi}{\partial x_k \partial x_k} + \frac{\partial U_k}{\partial x_k} \frac{\partial S_\phi}{\partial x_k}}{\frac{\partial G_1}{\partial \kappa} \left[1 - \frac{\left(\frac{2\kappa U_k U_k}{\left| \frac{\partial S_\phi}{\partial x_j} \hat{\mathbf{e}}_j \right|^2} \frac{\partial S_\phi}{\partial x_k} \frac{\partial S_\phi}{\partial x_k} - \frac{2\omega U_k}{\left| \frac{\partial S_\phi}{\partial x_j} \hat{\mathbf{e}}_j \right|} \frac{\partial S_\phi}{\partial x_k} \right)}{\frac{\partial G_1}{\partial \kappa}} \right]} \quad (3.279)$$

Simplifying Equation (3.279) gives:

$$\frac{\partial \kappa}{\partial x_k} = \frac{-\frac{\partial G_1}{\partial h'} \frac{\partial h'}{\partial x_k} - \left(\frac{2U_k \kappa^2}{\left| \frac{\partial S_\phi}{\partial x_j} \hat{\mathbf{e}}_j \right|^2} \frac{\partial U_k}{\partial x_k} \frac{\partial S_\phi}{\partial x_k} \frac{\partial S_\phi}{\partial x_k} + \frac{2U_k U_k \kappa^2}{\left| \frac{\partial S_\phi}{\partial x_j} \hat{\mathbf{e}}_j \right|^2} \frac{\partial^2 S_\phi}{\partial x_k \partial x_k} \frac{\partial S_\phi}{\partial x_k} \right) - \frac{2U_k \omega \kappa}{\left| \frac{\partial S_\phi}{\partial x_j} \hat{\mathbf{e}}_j \right|} \frac{\partial^2 S_\phi}{\partial x_k \partial x_k} + \frac{\partial U_k}{\partial x_k} \frac{\partial S_\phi}{\partial x_k}}{\frac{\partial G_1}{\partial \kappa} \left[\frac{2\kappa U_k U_k}{\left| \frac{\partial S_\phi}{\partial x_j} \hat{\mathbf{e}}_j \right|^2} \frac{\partial S_\phi}{\partial x_k} \frac{\partial S_\phi}{\partial x_k} - \frac{2\omega U_k}{\left| \frac{\partial S_\phi}{\partial x_j} \hat{\mathbf{e}}_j \right|} \frac{\partial S_\phi}{\partial x_k} \right]} \quad (3.280)$$

Equation (3.280) can now be written as follows using Equations (3.245) and (3.258):

$$\frac{\partial \kappa}{\partial x_k} = \frac{\left(\left(g \kappa^2 \operatorname{sech}^2 \kappa h' \right) \frac{\partial h'}{\partial x_k} - \frac{2U_k \kappa^2}{\left| \frac{\partial S_\phi}{\partial x_j} \hat{\mathbf{e}}_j \right|^2} \frac{\partial U_k}{\partial x_k} \frac{\partial S_\phi}{\partial x_k} \frac{\partial S_\phi}{\partial x_k} \right.}{-h' g \kappa \operatorname{sech}^2 \kappa h' - g \tanh \kappa h' - \frac{2\kappa U_k U_k}{\left| \frac{\partial S_\phi}{\partial x_j} \hat{\mathbf{e}}_j \right|^2} \frac{\partial S_\phi}{\partial x_k} \frac{\partial S_\phi}{\partial x_k} + \frac{2\omega U_k}{\left| \frac{\partial S_\phi}{\partial x_j} \hat{\mathbf{e}}_j \right|} \frac{\partial S_\phi}{\partial x_k}} \quad (3.281)$$

Equation (3.243) can be rewritten using the results of Section 3.7.3.2:

$$\frac{\partial^2 \kappa}{\partial x_k \partial x_k} = \frac{-\frac{\partial^2 G_1}{\partial \kappa^2} \left(\frac{\partial \kappa}{\partial x_k} \right)^2 - \frac{\partial^2 G_1}{\partial h'^2} \left(\frac{\partial h'}{\partial x_k} \right)^2 - \frac{\partial G_1}{\partial h'} \frac{\partial^2 h'}{\partial x_k \partial x_k} - \frac{\partial^2 G_1}{\partial \kappa \partial h'} \left(2 \frac{\partial h'}{\partial x_k} \frac{\partial \kappa}{\partial x_k} \right)}{\frac{\partial G_1}{\partial \kappa}} \quad (3.282)$$

$$+ \frac{\left(\frac{2\kappa^2}{\left| \frac{\partial S_\phi}{\partial x_j} \hat{\mathbf{e}}_j \right|^2} \frac{\partial U_k}{\partial x_k} \frac{\partial U_k}{\partial x_k} \frac{\partial S_\phi}{\partial x_k} \frac{\partial S_\phi}{\partial x_k} + \frac{2U_k \kappa^2}{\left| \frac{\partial S_\phi}{\partial x_j} \hat{\mathbf{e}}_j \right|^2} \frac{\partial^2 U_k}{\partial x_k \partial x_k} \frac{\partial S_\phi}{\partial x_k} \frac{\partial S_\phi}{\partial x_k} \right.}{\frac{\partial G_1}{\partial \kappa}} \left(\frac{2\kappa U_k U_k}{\left| \frac{\partial S_\phi}{\partial x_j} \hat{\mathbf{e}}_j \right|^2} \frac{\partial^3 S_\phi}{\partial x_k \partial x_k \partial x_k} \frac{\partial S_\phi}{\partial x_k} + \frac{2U_k U_k \kappa^2}{\left| \frac{\partial S_\phi}{\partial x_j} \hat{\mathbf{e}}_j \right|^2} \frac{\partial^2 S_\phi}{\partial x_k \partial x_k} \frac{\partial^2 S_\phi}{\partial x_k \partial x_k} \right. \right.$$

Bringing the terms containing $\frac{\partial^2 \kappa}{\partial x_k \partial x_k}$ to one side yields:

$$\left(\frac{\partial^2 \kappa}{\partial x_k \partial x_k} \right) \left(\frac{2\kappa U_k U_k \frac{\partial S_\phi}{\partial x_k} \frac{\partial S_\phi}{\partial x_k}}{\left| \frac{\partial S_\phi}{\partial x_j} \hat{\mathbf{e}}_j \right|^2} - \frac{2\omega U_k \frac{\partial S_\phi}{\partial x_k}}{\left| \frac{\partial S_\phi}{\partial x_j} \hat{\mathbf{e}}_j \right|} \right) \frac{\partial^2 \kappa}{\partial x_k \partial x_k} = \frac{-\frac{\partial^2 G_1}{\partial \kappa^2} \left(\frac{\partial \kappa}{\partial x_k} \right)^2 - \frac{\partial^2 G_1}{\partial h'^2} \left(\frac{\partial h'}{\partial x_k} \right)^2 - \frac{\partial G_1}{\partial h'} \frac{\partial^2 h'}{\partial x_k \partial x_k} - \frac{\partial^2 G_1}{\partial \kappa \partial h'} \left(2 \frac{\partial h'}{\partial x_k} \frac{\partial \kappa}{\partial x_k} \right)}{\frac{\partial G_1}{\partial \kappa}}$$

$$\left(\frac{2\kappa^2}{\left| \frac{\partial S_\phi}{\partial x_j} \hat{\mathbf{e}}_j \right|^2} \frac{\partial U_k}{\partial x_k} \frac{\partial U_k}{\partial x_k} \frac{\partial S_\phi}{\partial x_k} \frac{\partial S_\phi}{\partial x_k} + \frac{2U_k \kappa^2}{\left| \frac{\partial S_\phi}{\partial x_j} \hat{\mathbf{e}}_j \right|^2} \frac{\partial^2 U_k}{\partial x_k \partial x_k} \frac{\partial S_\phi}{\partial x_k} \frac{\partial S_\phi}{\partial x_k} \right.$$

$$+ \frac{4U_k \kappa^2}{\left| \frac{\partial S_\phi}{\partial x_j} \hat{\mathbf{e}}_j \right|^2} \frac{\partial U_k}{\partial x_k} \frac{\partial^2 S_\phi}{\partial x_k \partial x_k} \frac{\partial S_\phi}{\partial x_k} + \frac{4U_k \kappa^2}{\left| \frac{\partial S_\phi}{\partial x_j} \hat{\mathbf{e}}_j \right|^2} \frac{\partial U_k}{\partial x_k} \frac{\partial^2 S_\phi}{\partial x_k \partial x_k} \frac{\partial S_\phi}{\partial x_k}$$

$$+ \frac{2U_k U_k \kappa^2}{\left| \frac{\partial S_\phi}{\partial x_j} \hat{\mathbf{e}}_j \right|^2} \frac{\partial^3 S_\phi}{\partial x_k \partial x_k \partial x_k} \frac{\partial S_\phi}{\partial x_k} + \frac{2U_k U_k \kappa^2}{\left| \frac{\partial S_\phi}{\partial x_j} \hat{\mathbf{e}}_j \right|^2} \frac{\partial^2 S_\phi}{\partial x_k \partial x_k} \frac{\partial^2 S_\phi}{\partial x_k \partial x_k}$$

$$- \frac{2\omega \kappa}{\left| \frac{\partial S_\phi}{\partial x_j} \hat{\mathbf{e}}_j \right|} \frac{\partial U_k}{\partial x_k} \frac{\partial^2 S_\phi}{\partial x_k \partial x_k} - \frac{2U_k \omega \kappa}{\left| \frac{\partial S_\phi}{\partial x_j} \hat{\mathbf{e}}_j \right|} \frac{\partial^3 S_\phi}{\partial x_k \partial x_k \partial x_k} + \frac{\partial^2 U_k}{\partial x_k \partial x_k} \frac{\partial S_\phi}{\partial x_k}$$

$$\left. + \frac{\partial U_k}{\partial x_k} \frac{\partial^2 S_\phi}{\partial x_k \partial x_k} \right) \frac{\partial G_1}{\partial \kappa}$$

(3.283)

Isolating the $\frac{\partial^2 \kappa}{\partial x_k \partial x_k}$ term gives:

$$\begin{aligned}
 \frac{\partial^2 \kappa}{\partial x_k \partial x_k} \left[1 - \frac{\left(\frac{2\kappa U_k U_k}{\left| \frac{\partial S_\phi}{\partial x_j} \hat{\mathbf{e}}_j \right|^2} \frac{\partial S_\phi}{\partial x_k} \frac{\partial S_\phi}{\partial x_k} - \frac{2\omega U_k}{\left| \frac{\partial S_\phi}{\partial x_j} \hat{\mathbf{e}}_j \right|} \frac{\partial S_\phi}{\partial x_k} \right)}{\frac{\partial G_1}{\partial \kappa}} \right] &= \frac{-\frac{\partial^2 G_1}{\partial \kappa^2} \left(\frac{\partial \kappa}{\partial x_k} \right)^2 - \frac{\partial^2 G_1}{\partial h'^2} \left(\frac{\partial h'}{\partial x_k} \right)^2}{\frac{\partial G_1}{\partial \kappa}} \\
 &\quad - \frac{\frac{\partial G_1}{\partial h'} \frac{\partial^2 h'}{\partial x_k \partial x_k} - \frac{\partial^2 G_1}{\partial \kappa \partial h'} \left(2 \frac{\partial h'}{\partial x_k} \frac{\partial \kappa}{\partial x_k} \right)}{\frac{\partial G_1}{\partial \kappa}} \\
 &= \frac{\left(\frac{2\kappa^2}{\left| \frac{\partial S_\phi}{\partial x_j} \hat{\mathbf{e}}_j \right|^2} \frac{\partial U_k}{\partial x_k} \frac{\partial U_k}{\partial x_k} \frac{\partial S_\phi}{\partial x_k} \frac{\partial S_\phi}{\partial x_k} + \frac{2U_k \kappa^2}{\left| \frac{\partial S_\phi}{\partial x_j} \hat{\mathbf{e}}_j \right|^2} \frac{\partial^2 U_k}{\partial x_k \partial x_k} \frac{\partial S_\phi}{\partial x_k} \frac{\partial S_\phi}{\partial x_k} \right.}{\frac{\partial G_1}{\partial \kappa}} \\
 &\quad + \frac{4U_k \kappa^2}{\left| \frac{\partial S_\phi}{\partial x_j} \hat{\mathbf{e}}_j \right|^2} \frac{\partial U_k}{\partial x_k} \frac{\partial^2 S_\phi}{\partial x_k \partial x_k} \frac{\partial S_\phi}{\partial x_k} + \frac{4U_k \kappa^2}{\left| \frac{\partial S_\phi}{\partial x_j} \hat{\mathbf{e}}_j \right|^2} \frac{\partial U_k}{\partial x_k} \frac{\partial^2 S_\phi}{\partial x_k \partial x_k} \frac{\partial S_\phi}{\partial x_k} \\
 &\quad + \frac{2U_k U_k \kappa^2}{\left| \frac{\partial S_\phi}{\partial x_j} \hat{\mathbf{e}}_j \right|^2} \frac{\partial^3 S_\phi}{\partial x_k \partial x_k \partial x_k} \frac{\partial S_\phi}{\partial x_k} + \frac{2U_k U_k \kappa^2}{\left| \frac{\partial S_\phi}{\partial x_j} \hat{\mathbf{e}}_j \right|^2} \frac{\partial^2 S_\phi}{\partial x_k \partial x_k} \frac{\partial^2 S_\phi}{\partial x_k \partial x_k} \\
 &\quad - \frac{2\omega \kappa}{\left| \frac{\partial S_\phi}{\partial x_j} \hat{\mathbf{e}}_j \right|} \frac{\partial U_k}{\partial x_k} \frac{\partial^2 S_\phi}{\partial x_k \partial x_k} - \frac{2U_k \omega \kappa}{\left| \frac{\partial S_\phi}{\partial x_j} \hat{\mathbf{e}}_j \right|} \frac{\partial^3 S_\phi}{\partial x_k \partial x_k \partial x_k} \\
 &\quad \left. + \frac{\partial^2 U_k}{\partial x_k \partial x_k} \frac{\partial S_\phi}{\partial x_k} + \frac{\partial U_k}{\partial x_k} \frac{\partial^2 S_\phi}{\partial x_k \partial x_k} \right) \\
 &= \frac{\partial G_1}{\partial \kappa}
 \end{aligned} \tag{3.284}$$

Dividing both sides by the coefficient of the $\frac{\partial^2 \kappa}{\partial x_k \partial x_k}$ term gives:

$$\frac{\partial^2 \kappa}{\partial x_k \partial x_k} = \left[-\frac{\partial^2 G_1}{\partial \kappa^2} \left(\frac{\partial \kappa}{\partial x_k} \right)^2 - \frac{\partial^2 G_1}{\partial h'^2} \left(\frac{\partial h'}{\partial x_k} \right)^2 - \frac{\partial G_1}{\partial h'} \frac{\partial^2 h'}{\partial x_k \partial x_k} \right. \\ \left. - \frac{\partial^2 G_1}{\partial \kappa \partial h'} \left(2 \frac{\partial h'}{\partial x_k} \frac{\partial \kappa}{\partial x_k} \right) - \left(\frac{2\kappa^2}{\left| \frac{\partial S_\phi}{\partial x_j} \hat{\mathbf{e}}_j \right|^2} \frac{\partial U_k}{\partial x_k} \frac{\partial U_k}{\partial x_k} \frac{\partial S_\phi}{\partial x_k} \frac{\partial S_\phi}{\partial x_k} + \frac{2U_k \kappa^2}{\left| \frac{\partial S_\phi}{\partial x_j} \hat{\mathbf{e}}_j \right|^2} \frac{\partial^2 U_k}{\partial x_k \partial x_k} \frac{\partial S_\phi}{\partial x_k} \frac{\partial S_\phi}{\partial x_k} \right. \right. \\ \left. + \frac{4U_k \kappa^2}{\left| \frac{\partial S_\phi}{\partial x_j} \hat{\mathbf{e}}_j \right|^2} \frac{\partial U_k}{\partial x_k} \frac{\partial^2 S_\phi}{\partial x_k \partial x_k} \frac{\partial S_\phi}{\partial x_k} + \frac{4U_k \kappa^2}{\left| \frac{\partial S_\phi}{\partial x_j} \hat{\mathbf{e}}_j \right|^2} \frac{\partial U_k}{\partial x_k} \frac{\partial^2 S_\phi}{\partial x_k \partial x_k} \frac{\partial S_\phi}{\partial x_k} \right. \\ \left. + \frac{2U_k U_k \kappa^2}{\left| \frac{\partial S_\phi}{\partial x_j} \hat{\mathbf{e}}_j \right|^2} \frac{\partial^3 S_\phi}{\partial x_k \partial x_k \partial x_k} \frac{\partial S_\phi}{\partial x_k} + \frac{2U_k U_k \kappa^2}{\left| \frac{\partial S_\phi}{\partial x_j} \hat{\mathbf{e}}_j \right|^2} \frac{\partial^2 S_\phi}{\partial x_k \partial x_k} \frac{\partial^2 S_\phi}{\partial x_k \partial x_k} \right. \\ \left. - \frac{2\omega \kappa}{\left| \frac{\partial S_\phi}{\partial x_j} \hat{\mathbf{e}}_j \right|^2} \frac{\partial U_k}{\partial x_k} \frac{\partial^2 S_\phi}{\partial x_k \partial x_k} - \frac{2U_k \omega \kappa}{\left| \frac{\partial S_\phi}{\partial x_j} \hat{\mathbf{e}}_j \right|^2} \frac{\partial^3 S_\phi}{\partial x_k \partial x_k \partial x_k} + \frac{\partial^2 U_k}{\partial x_k \partial x_k} \frac{\partial S_\phi}{\partial x_k} \right. \\ \left. + \frac{\partial U_k}{\partial x_k} \frac{\partial^2 S_\phi}{\partial x_k \partial x_k} \right) \\ \left. \frac{\partial G_1}{\partial \kappa} \left[1 - \frac{\left(\frac{2\kappa U_k U_k}{\left| \frac{\partial S_\phi}{\partial x_j} \hat{\mathbf{e}}_j \right|^2} \frac{\partial S_\phi}{\partial x_k} \frac{\partial S_\phi}{\partial x_k} - \frac{2\omega U_k}{\left| \frac{\partial S_\phi}{\partial x_j} \hat{\mathbf{e}}_j \right|^2} \frac{\partial S_\phi}{\partial x_k} \right)}{\frac{\partial G_1}{\partial \kappa}} \right] \right] \quad (3.285)$$

Equation (3.285) may be simplified as follows:

$$\begin{aligned}
 \frac{\partial^2 \kappa}{\partial x_k \partial x_k} = & \left[-\frac{\partial^2 G_1}{\partial \kappa^2} \left(\frac{\partial \kappa}{\partial x_k} \right)^2 - \frac{\partial^2 G_1}{\partial h'^2} \left(\frac{\partial h'}{\partial x_k} \right)^2 - \frac{\partial G_1}{\partial h'} \frac{\partial^2 h'}{\partial x_k \partial x_k} \right. \\
 & \left. - \frac{\partial^2 G_1}{\partial \kappa \partial h'} \left(2 \frac{\partial h'}{\partial x_k} \frac{\partial \kappa}{\partial x_k} \right) - \left(\begin{aligned} & \frac{2\kappa^2}{\left| \frac{\partial S_\phi}{\partial x_j} \hat{\mathbf{e}}_j \right|^2} \frac{\partial U_k}{\partial x_k} \frac{\partial U_k}{\partial x_k} \frac{\partial S_\phi}{\partial x_k} \frac{\partial S_\phi}{\partial x_k} + \frac{2U_k \kappa^2}{\left| \frac{\partial S_\phi}{\partial x_j} \hat{\mathbf{e}}_j \right|^2} \frac{\partial^2 U_k}{\partial x_k \partial x_k} \frac{\partial S_\phi}{\partial x_k} \frac{\partial S_\phi}{\partial x_k} \\ & + \frac{4U_k \kappa^2}{\left| \frac{\partial S_\phi}{\partial x_j} \hat{\mathbf{e}}_j \right|^2} \frac{\partial U_k}{\partial x_k} \frac{\partial^2 S_\phi}{\partial x_k \partial x_k} \frac{\partial S_\phi}{\partial x_k} + \frac{4U_k \kappa^2}{\left| \frac{\partial S_\phi}{\partial x_j} \hat{\mathbf{e}}_j \right|^2} \frac{\partial U_k}{\partial x_k} \frac{\partial^2 S_\phi}{\partial x_k \partial x_k} \frac{\partial S_\phi}{\partial x_k} \\ & + \frac{2U_k U_k \kappa^2}{\left| \frac{\partial S_\phi}{\partial x_j} \hat{\mathbf{e}}_j \right|^2} \frac{\partial^3 S_\phi}{\partial x_k \partial x_k \partial x_k} \frac{\partial S_\phi}{\partial x_k} + \frac{2U_k U_k \kappa^2}{\left| \frac{\partial S_\phi}{\partial x_j} \hat{\mathbf{e}}_j \right|^2} \frac{\partial^2 S_\phi}{\partial x_k \partial x_k} \frac{\partial^2 S_\phi}{\partial x_k \partial x_k} \\ & - \frac{2\omega \kappa}{\left| \frac{\partial S_\phi}{\partial x_j} \hat{\mathbf{e}}_j \right|^2} \frac{\partial U_k}{\partial x_k} \frac{\partial^2 S_\phi}{\partial x_k \partial x_k} - \frac{2U_k \omega \kappa}{\left| \frac{\partial S_\phi}{\partial x_j} \hat{\mathbf{e}}_j \right|^2} \frac{\partial^3 S_\phi}{\partial x_k \partial x_k \partial x_k} + \frac{\partial^2 U_k}{\partial x_k \partial x_k} \frac{\partial S_\phi}{\partial x_k} \\ & + \frac{\partial U_k}{\partial x_k} \frac{\partial^2 S_\phi}{\partial x_k \partial x_k} \end{aligned} \right) \right] \\
 & \left[\frac{\partial G_1}{\partial \kappa} - \frac{2\kappa U_k U_k}{\left| \frac{\partial S_\phi}{\partial x_j} \hat{\mathbf{e}}_j \right|^2} \frac{\partial S_\phi}{\partial x_k} \frac{\partial S_\phi}{\partial x_k} + \frac{2\omega U_k}{\left| \frac{\partial S_\phi}{\partial x_j} \hat{\mathbf{e}}_j \right|^2} \frac{\partial S_\phi}{\partial x_k} \right]
 \end{aligned} \tag{3.286}$$

Using the results of Section 3.7.3.2 with Equation (3.286) gives the following:

$$\begin{aligned}
 \frac{\partial^2 \kappa}{\partial x_k \partial x_k} = & \left[\begin{aligned}
 & - \left(\begin{aligned}
 & -2h'g \operatorname{sech}^2 \kappa h' \\
 & +2h'^2 g \kappa \operatorname{sech}^2 \kappa h' \tanh \kappa h'
 \end{aligned} \right) \left(\frac{\partial \kappa}{\partial x_k} \frac{\partial \kappa}{\partial x_k} \right) - \left(2g \kappa^3 \operatorname{sech}^2 \kappa h' \tanh \kappa h' \right) \left(\frac{\partial h'}{\partial x_k} \frac{\partial h'}{\partial x_k} \right) \\
 & - \left(-g \kappa^2 \operatorname{sech}^2 \kappa h' \right) \frac{\partial^2 h'}{\partial x_k \partial x_k} \\
 & - \left(\begin{aligned}
 & 2gh' \kappa^2 \operatorname{sech}^2 \kappa h' \tanh \kappa h' \\
 & -2g \kappa \operatorname{sech}^2 \kappa h'
 \end{aligned} \right) \left(2 \frac{\partial h'}{\partial x_k} \frac{\partial \kappa}{\partial x_k} \right) \\
 & \left(\begin{aligned}
 & \frac{2\kappa^2}{\left| \frac{\partial S_\phi}{\partial x_j} \hat{\mathbf{e}}_j \right|^2} \frac{\partial U_k}{\partial x_k} \frac{\partial U_k}{\partial x_k} \frac{\partial S_\phi}{\partial x_k} \frac{\partial S_\phi}{\partial x_k} + \frac{2U_k \kappa^2}{\left| \frac{\partial S_\phi}{\partial x_j} \hat{\mathbf{e}}_j \right|^2} \frac{\partial^2 U_k}{\partial x_k \partial x_k} \frac{\partial S_\phi}{\partial x_k} \frac{\partial S_\phi}{\partial x_k} \\
 & + \frac{4U_k \kappa^2}{\left| \frac{\partial S_\phi}{\partial x_j} \hat{\mathbf{e}}_j \right|^2} \frac{\partial U_k}{\partial x_k} \frac{\partial^2 S_\phi}{\partial x_k \partial x_k} \frac{\partial S_\phi}{\partial x_k} + \frac{4U_k \kappa^2}{\left| \frac{\partial S_\phi}{\partial x_j} \hat{\mathbf{e}}_j \right|^2} \frac{\partial U_k}{\partial x_k} \frac{\partial^2 S_\phi}{\partial x_k \partial x_k} \frac{\partial S_\phi}{\partial x_k} \\
 & + \frac{2U_k U_k \kappa^2}{\left| \frac{\partial S_\phi}{\partial x_j} \hat{\mathbf{e}}_j \right|^2} \frac{\partial^3 S_\phi}{\partial x_k \partial x_k \partial x_k} \frac{\partial S_\phi}{\partial x_k} + \frac{2U_k U_k \kappa^2}{\left| \frac{\partial S_\phi}{\partial x_j} \hat{\mathbf{e}}_j \right|^2} \frac{\partial^2 S_\phi}{\partial x_k \partial x_k} \frac{\partial^2 S_\phi}{\partial x_k \partial x_k} \\
 & - \frac{2\omega \kappa}{\left| \frac{\partial S_\phi}{\partial x_j} \hat{\mathbf{e}}_j \right|^2} \frac{\partial U_k}{\partial x_k} \frac{\partial^2 S_\phi}{\partial x_k \partial x_k} - \frac{2U_k \omega \kappa}{\left| \frac{\partial S_\phi}{\partial x_j} \hat{\mathbf{e}}_j \right|^2} \frac{\partial^3 S_\phi}{\partial x_k \partial x_k \partial x_k} + \frac{\partial^2 U_k}{\partial x_k \partial x_k} \frac{\partial S_\phi}{\partial x_k} + \frac{\partial U_k}{\partial x_k} \frac{\partial^2 S_\phi}{\partial x_k \partial x_k}
 \end{aligned} \right)
 \end{aligned} \right] \\
 & \left[\begin{aligned}
 & -h'g \kappa \operatorname{sech}^2 \kappa h' - g \tanh \kappa h' - \frac{2\kappa U_k U_k}{\left| \frac{\partial S_\phi}{\partial x_j} \hat{\mathbf{e}}_j \right|^2} \frac{\partial S_\phi}{\partial x_k} \frac{\partial S_\phi}{\partial x_k} + \frac{2\omega U_k}{\left| \frac{\partial S_\phi}{\partial x_j} \hat{\mathbf{e}}_j \right|^2} \frac{\partial S_\phi}{\partial x_k}
 \end{aligned} \right]
 \end{aligned} \quad (3.287)$$

3.7.3.4 Derivatives of the vertical function

The vertical function f was defined in Equation (3.197) as follows:

$$f = \frac{\cosh[\kappa(h' + z')]}{\cosh[\kappa h']}$$

where:

$$z' = z - \bar{\eta} \text{ and } h' = h + \bar{\eta}$$

Massel (1993) selects a representation using trigonometric functions for this term but the more accepted practice in the coastal engineering field is the use of hyperbolic functions as derived in Section 3.6.3.3. Berkhoff (1976), Booij (1981), Mei *et al.* (2005) and Clyne (2008) all use this function.

In order to evaluate the various terms discussed in Section 3.7.3.3 it is necessary to obtain first and second derivatives of the vertical function with respect to h' , κ and z' .

3.7.3.4.1 Derivatives of the vertical function with respect to h' :

The derivative of f from Equation (3.197) with respect to h' is calculated as follows:

$$\frac{\partial f}{\partial h'} = \frac{\partial}{\partial h'} \left[\frac{\cosh[\kappa(h' + z')]}{\cosh[\kappa h']} \right] \quad (3.288)$$

Expanding (3.288) gives:

$$\frac{\partial f}{\partial h'} = \frac{\cosh \kappa h' \frac{\partial}{\partial h'} (\cosh[\kappa(h' + z')]) - \cosh[\kappa(h' + z')] \frac{\partial}{\partial h'} (\cosh \kappa h')}{\cosh^2 \kappa h'} \quad (3.289)$$

$$\frac{\partial f}{\partial h'} = \frac{\kappa \cosh \kappa h' \sinh[\kappa(h' + z')] - \cosh[\kappa(h' + z')] \sinh \kappa h'}{\cosh^2 \kappa h'} \quad (3.290)$$

Dividing the numerator and the denominator by $\cosh \kappa h'$ gives:

$$\frac{\partial f}{\partial h'} = \frac{\kappa \sinh[\kappa(h' + z')] - \cosh[\kappa(h' + z')] \tanh \kappa h'}{\cosh \kappa h'} \quad (3.291)$$

Equation (3.291) may be rewritten as:

$$\frac{\partial f}{\partial h'} = \frac{\kappa \sinh[\kappa(h' + z')] - \lambda' \cosh[\kappa(h' + z')]}{\cosh \kappa h'} \quad (3.292)$$

The second derivative of f with respect to h' is approached the same way:

$$\frac{\partial^2 f}{\partial h'^2} = \frac{1}{(\cosh^2 \kappa h')^2} \left(\cosh^2 \kappa h' \frac{\partial}{\partial h'} \left[\begin{array}{c} \kappa \cosh \kappa h' \sinh [\kappa(h' + z')] \\ -\kappa \cosh [\kappa(h' + z')] \sinh \kappa h' \end{array} \right] - \left[\begin{array}{c} \kappa \cosh \kappa h' \sinh [\kappa(h' + z')] \\ -\kappa \cosh [\kappa(h' + z')] \sinh \kappa h' \end{array} \right] \frac{\partial}{\partial h'} \cosh^2 \kappa h' \right) \quad (3.293)$$

Isolating a term from Equation (3.293) to be expanded on its own gives:

$$\frac{\partial}{\partial h'} \left[\begin{array}{c} \kappa \cosh \kappa h' \sinh [\kappa(h' + z')] \\ -\kappa \cosh [\kappa(h' + z')] \sinh \kappa h' \end{array} \right] = \kappa \frac{\partial}{\partial h'} \cosh \kappa h' \sinh [\kappa(h' + z')] - \kappa \frac{\partial}{\partial h'} \cosh [\kappa(h' + z')] \sinh \kappa h' \quad (3.294)$$

$$\begin{aligned} \frac{\partial}{\partial h'} \left[\begin{array}{c} \kappa \cosh \kappa h' \sinh [\kappa(h' + z')] \\ -\kappa \cosh [\kappa(h' + z')] \sinh \kappa h' \end{array} \right] &= \kappa^2 \cosh \kappa h' \cosh [\kappa(h' + z')] + \kappa^2 \sinh [\kappa(h' + z')] \sinh \kappa h' \\ &\quad - \kappa^2 \cosh [\kappa(h' + z')] \cosh \kappa h' - \kappa^2 \sinh \kappa h' \sinh [\kappa(h' + z')] \end{aligned} \quad (3.295)$$

$$\frac{\partial}{\partial h'} \left[\begin{array}{c} \kappa \cosh \kappa h' \sinh [\kappa(h' + z')] \\ -\kappa \cosh [\kappa(h' + z')] \sinh \kappa h' \end{array} \right] = 0 \quad (3.296)$$

Isolating the second term containing a derivative from Equation (3.293) gives:

$$\frac{\partial}{\partial h'} \cosh^2 \kappa h' = 2\kappa \cosh \kappa h' \sinh \kappa h' \quad (3.297)$$

Using Equations (3.296) and (3.297) with Equation (3.293) gives:

$$\frac{\partial^2 f}{\partial h'^2} = \frac{1}{(\cosh^2 \kappa h')^2} \left(\cosh^2 \kappa h' [0] - \left[\begin{array}{c} \kappa \cosh \kappa h' \sinh [\kappa(h' + z')] \\ -\kappa \cosh [\kappa(h' + z')] \sinh \kappa h' \end{array} \right] 2\kappa \cosh \kappa h' \sinh \kappa h' \right) \quad (3.298)$$

This can be expanded as:

$$\frac{\partial^2 f}{\partial h'^2} = \frac{-2\kappa^2 \cosh^2 \kappa h' \sinh \kappa h' \sinh [\kappa(h' + z')] + 2\kappa^2 \cosh \kappa h' \sinh^2 \kappa h' \cosh [\kappa(h' + z')]}{\cosh^4 \kappa h'} \quad (3.299)$$

Dividing the numerator and denominator by $\cosh^3 \kappa h'$ gives:

$$\frac{\partial^2 f}{\partial h'^2} = \frac{-2\kappa^2 \tanh \kappa h' \sinh[\kappa(h' + z')] + 2\kappa^2 \tanh^2 \kappa h' \cosh[\kappa(h' + z')]}{\cosh \kappa h'} \quad (3.300)$$

Equation (3.300) can then be written as:

$$\frac{\partial^2 f}{\partial h'^2} = \frac{-2\kappa \lambda' \sinh[\kappa(h' + z')] + 2\lambda'^2 \cosh[\kappa(h' + z')]}{\cosh \kappa h'} \quad (3.301)$$

3.7.3.4.2 Derivatives of the vertical function with respect to κ :

The derivative of f from Equation with respect to κ is calculated as follows:

$$\frac{\partial f}{\partial \kappa} = \frac{\partial}{\partial \kappa} \left[\frac{\cosh[\kappa(h' + z')]}{\cosh[\kappa(h')]} \right] \quad (3.302)$$

Expanding Equation (3.302) yields:

$$\frac{\partial f}{\partial \kappa} = \frac{\cosh \kappa h' \frac{\partial}{\partial \kappa} \cosh[\kappa(h' + z')] - \cosh[\kappa(h' + z')] \frac{\partial}{\partial \kappa} \cosh \kappa h'}{\cosh^2 \kappa h'} \quad (3.303)$$

$$\frac{\partial f}{\partial \kappa} = \frac{(h' + z') \cosh \kappa h' \sinh[\kappa(h' + z')] - h' \cosh[\kappa(h' + z')] \sinh \kappa h'}{\cosh^2 \kappa h'} \quad (3.304)$$

Dividing the numerator and denominator by $\cosh \kappa h'$ gives:

$$\frac{\partial f}{\partial \kappa} = \frac{(h' + z') \sinh[\kappa(h' + z')] - h' \cosh[\kappa(h' + z')] \tanh \kappa h'}{\cosh \kappa h'} \quad (3.305)$$

Equation (3.305) may also be written as:

$$\frac{\partial f}{\partial \kappa} = \frac{(h' + z') \sinh[\kappa(h' + z')] - \frac{h' \lambda'}{\kappa} \cosh[\kappa(h' + z')]}{\cosh \kappa h'} \quad (3.306)$$

The second derivative of f with respect to κ is approached the same way:

$$\frac{\partial^2 f}{\partial \kappa^2} = \frac{1}{(\cosh^2 \kappa h')^2} \left[\cosh^2 \kappa h' \frac{\partial}{\partial \kappa} \left(\begin{array}{l} (h' + z') \cosh \kappa h' \sinh [\kappa (h' + z')] \\ -h' \cosh [\kappa (h' + z')] \sinh \kappa h' \end{array} \right) - \left(\begin{array}{l} (h' + z') \cosh \kappa h' \sinh [\kappa (h' + z')] \\ -h' \cosh [\kappa (h' + z')] \sinh \kappa h' \end{array} \right) \frac{\partial}{\partial \kappa} \cosh^2 \kappa h' \right] \quad (3.307)$$

Examining the first term on the right hand side of Equation (3.293) containing a derivative gives

$$\begin{aligned} \frac{\partial}{\partial \kappa} \left(\begin{array}{l} (h' + z') \cosh \kappa h' \sinh [\kappa (h' + z')] \\ -h' \cosh [\kappa (h' + z')] \sinh \kappa h' \end{array} \right) &= (h' + z') \frac{\partial}{\partial \kappa} \cosh \kappa h' \sinh [\kappa (h' + z')] \\ &\quad - h' \frac{\partial}{\partial \kappa} \cosh [\kappa (h' + z')] \sinh \kappa h' \end{aligned} \quad (3.308)$$

Equation (3.308) can be expanded to give:

$$\begin{aligned} \frac{\partial}{\partial \kappa} \left(\begin{array}{l} (h' + z') \cosh \kappa h' \sinh [\kappa (h' + z')] \\ -h' \cosh [\kappa (h' + z')] \sinh \kappa h' \end{array} \right) &= (h' + z')^2 \cosh \kappa h' \cosh [\kappa (h' + z')] \\ &\quad + h' (h' + z') \sinh [\kappa (h' + z')] \sinh \kappa h' \\ &\quad - h'^2 \cosh [\kappa (h' + z')] \cosh \kappa h' \\ &\quad - h' (h' + z') \sinh \kappa h' \sinh [\kappa (h' + z')] \end{aligned} \quad (3.309)$$

Equation (3.309) simplifies to:

$$\frac{\partial}{\partial \kappa} \left(\begin{array}{l} (h' + z') \cosh \kappa h' \sinh [\kappa (h' + z')] \\ -h' \cosh [\kappa (h' + z')] \sinh \kappa h' \end{array} \right) = z'^2 \cosh \kappa h' \cosh [\kappa (h' + z')] \quad (3.310)$$

Examining the second term on the right hand side of Equation (3.293) containing a derivative gives:

$$\frac{\partial}{\partial \kappa} \cosh^2 \kappa h' = 2h' \cosh \kappa h' \sinh \kappa h' \quad (3.311)$$

So Equation (3.307) can be rewritten using Equations (3.310) and (3.311):

$$\frac{\partial^2 f}{\partial \kappa^2} = \frac{1}{(\cosh^2 \kappa h')^2} \left[\cosh^2 \kappa h' \left(\begin{aligned} &z'^2 \cosh \kappa h' \cosh [\kappa(h' + z')] \\ &+ 2h'z' \cosh \kappa h' \cosh [\kappa(h' + z')] \end{aligned} \right) \right. \\ \left. - \left(\begin{aligned} &(h' + z') \cosh \kappa h' \sinh [\kappa(h' + z')] \\ &- h' \cosh [\kappa(h' + z')] \sinh \kappa h' \end{aligned} \right) (2h' \cosh \kappa h' \sinh \kappa h') \right] \quad (3.312)$$

In a more explicit form this becomes:

$$\frac{\partial^2 f}{\partial \kappa^2} = \frac{\left[\begin{aligned} &z'^2 \cosh^3 \kappa h' \cosh [\kappa(h' + z')] + 2h'z' \cosh^3 \kappa h' \cosh [\kappa(h' + z')] + \\ &- 2h'(h' + z') \cosh^2 \kappa h' \sinh \kappa h' \sinh [\kappa(h' + z')] \\ &+ 2h'^2 \cosh \kappa h' \sinh^2 \kappa h' \cosh [\kappa(h' + z')] \end{aligned} \right]}{\cosh^4 \kappa h'} \quad (3.313)$$

Dividing the numerator and denominator by $\cosh^3 \kappa h'$ gives:

$$\frac{\partial^2 f}{\partial \kappa^2} = \frac{\left[\begin{aligned} &z'^2 \cosh [\kappa(h' + z')] + 2h'z' \cosh [\kappa(h' + z')] \\ &- 2h'(h' + z') \tanh \kappa h' \sinh [\kappa(h' + z')] + 2h'^2 \tanh^2 \kappa h' \cosh [\kappa(h' + z')] \end{aligned} \right]}{\cosh \kappa h'} \quad (3.314)$$

Equation (3.314) can be rewritten as follows:

$$\frac{\partial^2 f}{\partial \kappa^2} = \frac{\left[\begin{aligned} &z'^2 \cosh [\kappa(h' + z')] + 2h'z' \cosh [\kappa(h' + z')] \\ &- 2h'(h' + z') \frac{\lambda'}{\kappa} \sinh [\kappa(h' + z')] + 2h'^2 \frac{\lambda'^2}{\kappa^2} \cosh [\kappa(h' + z')] \end{aligned} \right]}{\cosh \kappa h'} \quad (3.315)$$

$$\frac{\partial^2 f}{\partial \kappa^2} = \frac{\left[\begin{aligned} &-\frac{2h'\lambda'}{\kappa} (h' + z') \sinh [\kappa(h' + z')] + \left(z'^2 + \frac{2h'^2 \lambda'^2}{\kappa^2} + 2h'z' \right) \cosh [\kappa(h' + z')] \end{aligned} \right]}{\cosh \kappa h'} \quad (3.316)$$

3.7.3.4.3 Cross derivatives of the vertical function with respect to κ and h' :

The derivative with respect to κ of Equation (3.290) is:

$$\frac{\partial^2 f}{\partial h' \partial \kappa} = \frac{1}{(\cosh^2 \kappa h')^2} \left(\cosh^2 \kappa h' \frac{\partial}{\partial \kappa} \left[\frac{\kappa \cosh \kappa h' \sinh [\kappa (h' + z')]}{-\kappa \cosh [\kappa (h' + z')] \sinh \kappa h'} \right] - \left[\frac{\kappa \cosh \kappa h' \sinh [\kappa (h' + z')]}{-\kappa \cosh [\kappa (h' + z')] \sinh \kappa h'} \right] \frac{\partial}{\partial \kappa} \cosh^2 \kappa h' \right) \quad (3.317)$$

Examining the first term containing a derivative on the right hand side of Equation (3.317) gives:

$$\begin{aligned} \frac{\partial}{\partial \kappa} \left[\frac{\kappa \cosh \kappa h' \sinh [\kappa (h' + z')]}{-\kappa \cosh [\kappa (h' + z')] \sinh \kappa h'} \right] &= \kappa \frac{\partial}{\partial \kappa} \cosh \kappa h' \sinh [\kappa (h' + z')] \\ &\quad - \kappa \frac{\partial}{\partial \kappa} \cosh [\kappa (h' + z')] \sinh \kappa h' \\ &\quad + \cosh \kappa h' \sinh [\kappa (h' + z')] \\ &\quad - \cosh [\kappa (h' + z')] \sinh \kappa h' \end{aligned} \quad (3.318)$$

$$\begin{aligned} \frac{\partial}{\partial \kappa} \left[\frac{\kappa \cosh \kappa h' \sinh [\kappa (h' + z')]}{-\kappa \cosh [\kappa (h' + z')] \sinh \kappa h'} \right] &= \kappa ((h' + z') \cosh \kappa h' \cosh [\kappa (h' + z')] + h' \sinh \kappa h' \sinh [\kappa (h' + z')]) \\ &\quad - \kappa (h' \cosh \kappa h' \cosh [\kappa (h' + z')] + (h' + z') \sinh \kappa h' \sinh [\kappa (h' + z')]) \\ &\quad + \cosh \kappa h' \sinh [\kappa (h' + z')] - \cosh [\kappa (h' + z')] \sinh \kappa h' \end{aligned} \quad (3.319)$$

$$\begin{aligned} \frac{\partial}{\partial \kappa} \left[\frac{\kappa \cosh \kappa h' \sinh [\kappa (h' + z')]}{-\kappa \cosh [\kappa (h' + z')] \sinh \kappa h'} \right] &= \kappa z' \cosh \kappa h' \cosh [\kappa (h' + z')] - \kappa z' \sinh \kappa h' \sinh [\kappa (h' + z')] \\ &\quad + \cosh \kappa h' \sinh [\kappa (h' + z')] - \cosh [\kappa (h' + z')] \sinh \kappa h' \end{aligned} \quad (3.320)$$

Examining the second term containing a derivative on the right hand side of Equation (3.317) gives:

$$\frac{\partial}{\partial \kappa} \cosh^2 \kappa h' = 2h' \cosh \kappa h' \sinh \kappa h' \quad (3.321)$$

Equation (3.317) can be rewritten using Equations (3.320) and (3.321):

$$\frac{\partial^2 f}{\partial h' \partial \kappa} = \frac{1}{(\cosh^2 \kappa h')^2} \left(\cosh^2 \kappa h' \left(\kappa z' \cosh \kappa h' \cosh [\kappa(h' + z')] - \kappa z' \sinh \kappa h' \sinh [\kappa(h' + z')] \right) + \cosh \kappa h' \sinh [\kappa(h' + z')] - \cosh [\kappa(h' + z')] \sinh \kappa h' \right) - \left[\begin{array}{c} \kappa \cosh \kappa h' \sinh [\kappa(h' + z')] \\ -\kappa \cosh [\kappa(h' + z')] \sinh \kappa h' \end{array} \right] 2h' \cosh \kappa h' \sinh \kappa h' \right) \quad (3.322)$$

Expanding Equation (3.322) gives:

$$\frac{\partial^2 f}{\partial h' \partial \kappa} = \frac{\left(\begin{array}{c} \kappa z' \cosh^3 \kappa h' \cosh [\kappa(h' + z')] - \kappa z' \cosh^2 \kappa h' \sinh \kappa h' \sinh [\kappa(h' + z')] \\ + \cosh^3 \kappa h' \sinh [\kappa(h' + z')] - \cosh^2 \kappa h' \cosh [\kappa(h' + z')] \sinh \kappa h' \\ - 2h' \kappa \cosh^2 \kappa h' \sinh \kappa h' \sinh [\kappa(h' + z')] + 2h' \kappa \cosh \kappa h' \sinh^2 \kappa h' \cosh [\kappa(h' + z')] \end{array} \right)}{\cosh^4 \kappa h'} \quad (3.323)$$

Dividing the numerator and denominator by $\cosh^3 \kappa h'$ gives:

$$\frac{\partial^2 f}{\partial h' \partial \kappa} = \frac{\left(\begin{array}{c} \kappa z' \cosh [\kappa(h' + z')] - \kappa z' \tanh \kappa h' \sinh [\kappa(h' + z')] \\ + \sinh [\kappa(h' + z')] - \cosh [\kappa(h' + z')] \tanh \kappa h' \\ - 2h' \kappa \tanh \kappa h' \sinh [\kappa(h' + z')] + 2h' \kappa \tanh^2 \kappa h' \cosh [\kappa(h' + z')] \end{array} \right)}{\cosh \kappa h'} \quad (3.324)$$

Equation (3.324) may be rewritten and simplified as follows:

$$\frac{\partial^2 f}{\partial h' \partial \kappa} = \frac{\left(\begin{array}{c} \kappa z' \cosh [\kappa(h' + z')] - z' \lambda' \sinh [\kappa(h' + z')] \\ + \sinh [\kappa(h' + z')] - \frac{\lambda'}{\kappa} \cosh [\kappa(h' + z')] \\ - 2h' \lambda' \sinh [\kappa(h' + z')] + \frac{2h' \lambda'^2}{\kappa} \cosh [\kappa(h' + z')] \end{array} \right)}{\cosh \kappa h'} \quad (3.325)$$

$$\frac{\partial^2 f}{\partial h' \partial \kappa} = \frac{\left(\begin{array}{c} \left(\kappa z' - \frac{\lambda'}{\kappa} + \frac{2h' \lambda'^2}{\kappa} \right) \cosh [\kappa(h' + z')] \\ (1 - 2h' \lambda' - z' \lambda') \sinh [\kappa(h' + z')] \end{array} \right)}{\cosh \kappa h'} \quad (3.326)$$

In order to provide confirmation of the result of Equation (3.326) the same derivative can be obtained from Equation (3.304):

$$\frac{\partial^2 f}{\partial \kappa \partial h'} = \frac{1}{(\cosh^2 \kappa h')^2} \left(\cosh^2 \kappa h' \frac{\partial}{\partial h'} \left[\begin{array}{l} (h' + z') \cosh \kappa h' \sinh [\kappa (h' + z')] \\ -h' \cosh [\kappa (h' + z')] \sinh \kappa h' \end{array} \right] - \left[\begin{array}{l} (h' + z') \cosh \kappa h' \sinh [\kappa (h' + z')] \\ -h' \cosh [\kappa (h' + z')] \sinh \kappa h' \end{array} \right] \frac{\partial}{\partial h'} \cosh^2 \kappa h' \right) \quad (3.327)$$

Examining the first term containing a derivative on the right hand side of Equation (3.327):

$$\begin{aligned} \frac{\partial}{\partial h'} \left[\begin{array}{l} (h' + z') \cosh \kappa h' \sinh [\kappa (h' + z')] \\ -h' \cosh [\kappa (h' + z')] \sinh \kappa h' \end{array} \right] &= \kappa (h' + z') \cosh \kappa h' \cosh [\kappa (h' + z')] \\ &\quad + \kappa (h' + z') \sinh \kappa h' \sinh [\kappa (h' + z')] \\ &\quad - \kappa h' \cosh [\kappa (h' + z')] \cosh \kappa h' \\ &\quad - \kappa h' \sinh [\kappa (h' + z')] \sinh \kappa h' \\ &\quad + \cosh \kappa h' \sinh [\kappa (h' + z')] \\ &\quad - \cosh [\kappa (h' + z')] \sinh \kappa h' \end{aligned} \quad (3.328)$$

Equation (3.328) simplifies as follows:

$$\begin{aligned} \frac{\partial}{\partial h'} \left[\begin{array}{l} (h' + z') \cosh \kappa h' \sinh [\kappa (h' + z')] \\ -h' \cosh [\kappa (h' + z')] \sinh \kappa h' \end{array} \right] &= \kappa z' \cosh \kappa h' \cosh [\kappa (h' + z')] \\ &\quad + \kappa z' \sinh \kappa h' \sinh [\kappa (h' + z')] \end{aligned} \quad (3.329)$$

Examining the second term containing a derivative on the right hand side of Equation (3.327) gives:

$$\frac{\partial}{\partial h'} \cosh^2 \kappa h' = 2\kappa \cosh \kappa h' \sinh \kappa h' \quad (3.330)$$

Equation (3.328) can be rewritten using Equations (3.329) and (3.330):

$$\frac{\partial^2 f}{\partial \kappa \partial h'} = \frac{1}{(\cosh^2 \kappa h')^2} \left(\begin{array}{c} \cosh^2 \kappa h' \left(\begin{array}{c} \kappa z' \cosh \kappa h' \cosh [\kappa (h' + z')] \\ + \kappa z' \sinh \kappa h' \sinh [\kappa (h' + z')] \\ + \cosh \kappa h' \sinh [\kappa (h' + z')] \\ - \cosh [\kappa (h' + z')] \sinh \kappa h' \end{array} \right) \\ - \left[\begin{array}{c} (h' + z') \cosh \kappa h' \sinh [\kappa (h' + z')] \\ - h' \cosh [\kappa (h' + z')] \sinh \kappa h' \end{array} \right] 2\kappa \cosh \kappa h' \sinh \kappa h' \end{array} \right) \quad (3.331)$$

$$\frac{\partial^2 f}{\partial \kappa \partial h'} = \frac{\left(\begin{array}{c} \kappa z' \cosh^3 \kappa h' \cosh [\kappa (h' + z')] - \kappa z' \cosh^2 \kappa h' \sinh \kappa h' \sinh [\kappa (h' + z')] \\ + \cosh^3 \kappa h' \sinh [\kappa (h' + z')] - \cosh [\kappa (h' + z')] \sinh \kappa h' \cosh^2 \kappa h' \\ - 2\kappa h' \cosh^2 \kappa h' \sinh \kappa h' \sinh [\kappa (h' + z')] + 2\kappa h' \cosh \kappa h' \sinh^2 \kappa h' \cosh [\kappa (h' + z')] \end{array} \right)}{\cosh^4 \kappa h'} \quad (3.332)$$

As expected Equation (3.332) is identical to Equation (3.323).

3.7.3.4.4 Derivatives of the vertical function with respect to z :

Examination of Equation (3.219) yields:

$$\frac{\partial z'}{\partial \bar{\eta}} = -1 \quad (3.333)$$

where:

$$\frac{\partial z'}{\partial z} = 1 \quad (3.334)$$

Vertical integration of the vertical function described in Equation (3.197) gives:

$$\frac{\partial f}{\partial z} = \frac{\partial f}{\partial z'} = \frac{\partial}{\partial z'} \left[\frac{\cosh[\kappa(h' + z')]}{\cosh \kappa h'} \right] \quad (3.335)$$

Equation (3.335) can be expanded to give:

$$\frac{\partial f}{\partial z} = \frac{1}{\cosh \kappa h'} \frac{\partial}{\partial z'} (\cosh[\kappa(h' + z')]) \quad (3.336)$$

$$\frac{\partial f}{\partial z} = \frac{\kappa \sinh[\kappa(h' + z')]}{\cosh \kappa h'} \quad (3.337)$$

It is possible to obtain the second derivative with respect to z of the vertical function from Equation (3.337):

$$\frac{\partial^2 f}{\partial z^2} = \frac{\partial}{\partial z'} \left[\frac{\kappa \sinh[\kappa(h' + z')]}{\cosh \kappa h'} \right] \quad (3.338)$$

Equation (3.338) can be expanded and simplified as follows:

$$\frac{\partial^2 f}{\partial z^2} = \frac{\cosh \kappa h' \frac{\partial}{\partial z'} [\kappa \sinh[\kappa(h' + z')]] - [\kappa \sinh[\kappa(h' + z')]] \frac{\partial}{\partial z} \cosh \kappa h'}{\cosh^2 \kappa h'} \quad (3.339)$$

$$\frac{\partial^2 f}{\partial z^2} = \frac{\kappa^2 \cosh \kappa h' \cosh[\kappa(h' + z')]}{\cosh^2 \kappa h'} \quad (3.340)$$

$$\frac{\partial^2 f}{\partial z^2} = \frac{\kappa^2 \cosh[\kappa(h' + z')]}{\cosh \kappa h'} \quad (3.341)$$

3.7.3.4.5 Cross derivative of the vertical function with respect to κ and z :

Working with Equation (3.337) gives:

$$\frac{\partial^2 f}{\partial \kappa \partial z'} = \frac{\partial}{\partial \kappa} \left(\frac{\kappa \sinh [\kappa (h' + z')]}{\cosh \kappa h'} \right) \quad (3.342)$$

Equation (3.342) may be expanded to give:

$$\frac{\partial^2 f}{\partial \kappa \partial z'} = \frac{\cosh \kappa h' \frac{\partial}{\partial \kappa} (\kappa \sinh [\kappa (h' + z')]) - (\kappa \sinh [\kappa (h' + z')]) \frac{\partial}{\partial \kappa} \cosh \kappa h'}{(\cosh \kappa h')^2} \quad (3.343)$$

After differentiation Equation (3.343) becomes:

$$\frac{\partial^2 f}{\partial \kappa \partial z'} = \frac{\cosh \kappa h' \left[\kappa \frac{\partial}{\partial \kappa} (\sinh [\kappa (h' + z')]) + (\sinh [\kappa (h' + z')]) \frac{\partial}{\partial \kappa} \kappa \right] - (\kappa \sinh [\kappa (h' + z')]) \frac{\partial}{\partial \kappa} \cosh \kappa h'}{(\cosh \kappa h')^2} \quad (3.344)$$

Equation (3.344) can be expanded as follows:

$$\frac{\partial^2 f}{\partial \kappa \partial z'} = \frac{\kappa (h' + z') \cosh \kappa h' \cosh [\kappa (h' + z')] + \cosh \kappa h' \sinh [\kappa (h' + z')] - \kappa h' \sinh \kappa h' \sinh [\kappa (h' + z')]}{\cosh^2 \kappa h'} \quad (3.345)$$

3.7.3.4.6 Cross derivative of the vertical function with respect to h' and z :

Working with Equation (3.337) gives:

$$\frac{\partial^2 f}{\partial h' \partial z'} = \frac{\partial}{\partial h'} \left(\frac{\kappa \sinh [\kappa (h' + z')]}{\cosh \kappa h'} \right) \quad (3.346)$$

Equation (3.346) may be expanded as follows:

$$\frac{\partial^2 f}{\partial h' \partial z'} = \frac{\cosh \kappa h' \frac{\partial}{\partial h'} \{ \kappa \sinh [\kappa (h' + z')] \} - \kappa \sinh [\kappa (h' + z')] \frac{\partial}{\partial h'} \cosh \kappa h'}{(\cosh \kappa h')^2} \quad (3.347)$$

Equation (3.347) may be simplified as follows:

$$\frac{\partial^2 f}{\partial h' \partial z'} = \frac{(\cosh \kappa h') \kappa^2 \cosh [\kappa (h' + z')] - \kappa^2 \sinh [\kappa (h' + z')] \sinh \kappa h'}{\cosh^2 \kappa h'} \quad (3.348)$$

3.7.4 Summary of Equations developed to date for Mild Slope Equation

Table 3.5 gives details of the integrated version of the Laplace Equation and gradients of vertical function and wave numbers that will be used to construct the mild slope equation.

Table 3.5 - Summary of Integrated Laplace Equation and Derivatives of the Vertical Function and Wave Number

		Boundary Condition	Equation
(a)	Development of Laplace's Equation	$\int_{-h}^{\bar{\eta}} f \phi \frac{d^2 f}{dx_k dx_k} dz + \int_{-h}^{\bar{\eta}} 2f \frac{df}{dx_k} \frac{\partial \phi}{\partial x_k} dz + \int_{-h}^{\bar{\eta}} f^2 \frac{\partial^2 \phi}{\partial x_k \partial x_k} dz$ $- \int_{-h}^{\bar{\eta}} \frac{\partial f}{\partial z} \frac{\partial f}{\partial z} \phi dz + \left. \frac{\partial \phi}{\partial z} \right _{\bar{\eta}} - f \left. \frac{\partial \phi}{\partial z} \right _{-h} = 0$	(3.213)
(b)	Derivatives of the Vertical Function	$\frac{\partial^2 f}{\partial h' \partial z'} = \frac{\left(\cosh \kappa h' \kappa^2 \cosh [\kappa(h' + z')] \right)}{\cosh^2 \kappa h'}$	(3.348)
(c)		$\frac{\partial^2 f}{\partial \kappa \partial z'} = \frac{\left(\kappa(h' + z') \cosh \kappa h' \cosh [\kappa(h' + z')] \right)}{\cosh^2 \kappa h'}$	(3.345)
(d)		$\frac{\partial f}{\partial z'} = \frac{\partial f}{\partial z} = \frac{\kappa \sinh [\kappa(h' + z')]}{\cosh \kappa h'}$	(3.337)
(e)		$\frac{\partial^2 f}{\partial \kappa^2} = \frac{\left(z'^2 \cosh [\kappa(h' + z')] + 2h' z' \cosh [\kappa(h' + z')] \right)}{\cosh \kappa h'}$	(3.314)
(f)		$\frac{\partial f}{\partial \kappa} = \frac{\left((h' + z') \cosh \kappa h' \sinh [\kappa(h' + z')] \right)}{\cosh^2 \kappa h'}$	(3.304)
(g)		$\frac{\partial^2 f}{\partial h' \partial \kappa} = \frac{\left(\left(\kappa z' - \frac{\lambda'}{\kappa} + \frac{2h' \lambda'^2}{\kappa} \right) \cosh [\kappa(h' + z')] \right)}{\cosh \kappa h'}$	(3.326)
(h)		$\frac{\partial^2 f}{\partial h'^2} = \frac{-2\kappa \lambda' \sinh [\kappa(h' + z')] + 2\lambda'^2 \cosh [\kappa(h' + z')]}{\cosh \kappa h'}$	(3.301)

(i)		$\frac{\partial f}{\partial h'} = \frac{\kappa \sinh[\kappa(h' + z')] - \lambda' \cosh[\kappa(h' + z')]}{\cosh \kappa h'}$	(3.292)
(l)		$\frac{\partial^2 f}{\partial z^2} = \frac{\kappa^2 \cosh[\kappa(h' + z')]}{\cosh \kappa h'}$	(3.341)
(j)	Derivatives of the Wave Number	$\frac{\partial \kappa}{\partial x_k} = \frac{\left(\begin{aligned} & \left(g \kappa^2 \operatorname{sech}^2 \kappa h' \right) \frac{\partial h'}{\partial x_k} - \frac{2U_k \kappa^2}{\left \frac{\partial S_\phi}{\partial x_j} \hat{\mathbf{e}}_j \right ^2} \frac{\partial U_k}{\partial x_k} \frac{\partial S_\phi}{\partial x_k} \frac{\partial S_\phi}{\partial x_k} \\ & - \frac{2U_k U_k \kappa^2}{\left \frac{\partial S_\phi}{\partial x_j} \hat{\mathbf{e}}_j \right ^2} \frac{\partial^2 S_\phi}{\partial x_k \partial x_k} \frac{\partial S_\phi}{\partial x_k} \\ & + \frac{2U_k \omega \kappa}{\left \frac{\partial S_\phi}{\partial x_j} \hat{\mathbf{e}}_j \right } \frac{\partial^2 S_\phi}{\partial x_k \partial x_k} - \frac{\partial U_k}{\partial x_k} \frac{\partial S_\phi}{\partial x_k} \end{aligned} \right)}{\left(\begin{aligned} & -h' g \kappa \operatorname{sech}^2 \kappa h' - g \tanh \kappa h' \\ & - \frac{2\kappa U_k U_k}{\left \frac{\partial S_\phi}{\partial x_j} \hat{\mathbf{e}}_j \right ^2} \frac{\partial S_\phi}{\partial x_k} \frac{\partial S_\phi}{\partial x_k} + \frac{2\omega U_k}{\left \frac{\partial S_\phi}{\partial x_j} \hat{\mathbf{e}}_j \right } \frac{\partial S_\phi}{\partial x_k} \end{aligned} \right)}$	(3.281)

(k)		$ \begin{aligned} & - \left(-2h'g \operatorname{sech}^2 \kappa h' \right. \\ & \quad \left. + 2h'^2 g \kappa \operatorname{sech}^2 \kappa h' \tanh \kappa h' \right) \left(\frac{\partial \kappa}{\partial x_k} \frac{\partial \kappa}{\partial x_k} \right) \\ & - \left(2g \kappa^3 \operatorname{sech}^2 \kappa h' \tanh \kappa h' \right) \left(\frac{\partial h'}{\partial x_k} \frac{\partial h'}{\partial x_k} \right) \\ & - \left(-g \kappa^2 \operatorname{sech}^2 \kappa h' \right) \frac{\partial^2 h'}{\partial x_k \partial x_k} \\ & - \left(\begin{array}{l} 2gh' \kappa^2 \operatorname{sech}^2 \kappa h' \tanh \kappa h' \\ -2g \kappa \operatorname{sech}^2 \kappa h' \end{array} \right) \left(2 \frac{\partial h'}{\partial x_k} \frac{\partial \kappa}{\partial x_k} \right) \\ & \left(\begin{array}{l} \frac{2\kappa^2}{\left \frac{\partial S_\phi}{\partial x_j} \hat{\mathbf{e}}_j \right ^2} \frac{\partial U_k}{\partial x_k} \frac{\partial U_k}{\partial x_k} \frac{\partial S_\phi}{\partial x_k} \frac{\partial S_\phi}{\partial x_k} \\ + \frac{2U_k \kappa^2}{\left \frac{\partial S_\phi}{\partial x_j} \hat{\mathbf{e}}_j \right ^2} \frac{\partial^2 U_k}{\partial x_k \partial x_k} \frac{\partial S_\phi}{\partial x_k} \frac{\partial S_\phi}{\partial x_k} \\ + \frac{4U_k \kappa^2}{\left \frac{\partial S_\phi}{\partial x_j} \hat{\mathbf{e}}_j \right ^2} \frac{\partial U_k}{\partial x_k} \frac{\partial^2 S_\phi}{\partial x_k \partial x_k} \frac{\partial S_\phi}{\partial x_k} \\ + \frac{4U_k \kappa^2}{\left \frac{\partial S_\phi}{\partial x_j} \hat{\mathbf{e}}_j \right ^2} \frac{\partial U_k}{\partial x_k} \frac{\partial^2 S_\phi}{\partial x_k \partial x_k} \frac{\partial S_\phi}{\partial x_k} \\ + \frac{2U_k U_k \kappa^2}{\left \frac{\partial S_\phi}{\partial x_j} \hat{\mathbf{e}}_j \right ^2} \frac{\partial^3 S_\phi}{\partial x_k \partial x_k \partial x_k} \frac{\partial S_\phi}{\partial x_k} \\ + \frac{2U_k U_k \kappa^2}{\left \frac{\partial S_\phi}{\partial x_j} \hat{\mathbf{e}}_j \right ^2} \frac{\partial^2 S_\phi}{\partial x_k \partial x_k} \frac{\partial^2 S_\phi}{\partial x_k \partial x_k} \\ - \frac{2\omega \kappa}{\left \frac{\partial S_\phi}{\partial x_j} \hat{\mathbf{e}}_j \right } \frac{\partial U_k}{\partial x_k} \frac{\partial^2 S_\phi}{\partial x_k \partial x_k} - \frac{2U_k \omega \kappa}{\left \frac{\partial S_\phi}{\partial x_j} \hat{\mathbf{e}}_j \right } \frac{\partial^3 S_\phi}{\partial x_k \partial x_k \partial x_k} \\ + \frac{\partial^2 U_k}{\partial x_k \partial x_k} \frac{\partial S_\phi}{\partial x_k} + \frac{\partial U_k}{\partial x_k} \frac{\partial^2 S_\phi}{\partial x_k \partial x_k} \end{array} \right) \\ & \frac{\partial^2 \kappa}{\partial x_k \partial x_k} = \left[\begin{array}{l} -h'g \kappa \operatorname{sech}^2 \kappa h' - g \tanh \kappa h' \\ - \frac{2\kappa U_k U_k}{\left \frac{\partial S_\phi}{\partial x_j} \hat{\mathbf{e}}_j \right ^2} \frac{\partial S_\phi}{\partial x_k} \frac{\partial S_\phi}{\partial x_k} + \frac{2\omega U_k}{\left \frac{\partial S_\phi}{\partial x_j} \hat{\mathbf{e}}_j \right } \frac{\partial S_\phi}{\partial x_k} \end{array} \right] \end{aligned} $	(3.287)
-----	--	--	---------

3.7.5 Evaluating terms of the Mild-Slope Equation

The results summarised in Section 3.7.4 are now combined.

3.7.5.1 Combined Free Surface Boundary Condition

Equation (3.214) may be expressed as follows using the result of Equation (3.130):

$$\left. \frac{\partial \tilde{\phi}}{\partial z} \right|_{\bar{\eta}} = \frac{1}{g} \left[\begin{aligned} &\omega^2 (f\phi) + 2i\omega U_k \frac{\partial (f\phi)}{\partial x_k} + i\omega \frac{\partial U_j}{\partial x_j} (f\phi) - \frac{\partial U_j}{\partial x_j} U_k \frac{\partial (f\phi)}{\partial x_k} \\ &- U_j \frac{\partial U_k}{\partial x_j} \frac{\partial (f\phi)}{\partial x_k} - U_j U_k \frac{\partial^2 (f\phi)}{\partial x_j \partial x_k} - \gamma \frac{\partial U_j}{\partial x_j} (f\phi) - \gamma U_j \frac{\partial (f\phi)}{\partial x_j} + i\omega \gamma (f\phi) \end{aligned} \right]_{\bar{\eta}} \quad (3.349)$$

The derivative in the sixth term of Equation (3.349) can be expanded as follows:

$$\frac{\partial^2 (f\phi)}{\partial x_j \partial x_k} = \frac{\partial}{\partial x_j} \left(f \frac{\partial \phi}{\partial x_k} + \phi \frac{\partial f}{\partial x_k} \right) = f \frac{\partial^2 \phi}{\partial x_j \partial x_k} + \frac{\partial f}{\partial x_j} \frac{\partial \phi}{\partial x_k} + \phi \frac{\partial^2 f}{\partial x_j \partial x_k} + \frac{\partial f}{\partial x_k} \frac{\partial \phi}{\partial x_j} \quad (3.350)$$

Substitution of Equation (3.350) into Equation (3.349) yields:

$$\left. \frac{\partial \tilde{\phi}}{\partial z} \right|_{\bar{\eta}} = \frac{1}{g} \left[\begin{aligned} &\omega^2 f\phi + 2i\omega U_k \phi \frac{\partial f}{\partial x_k} + 2i\omega U_k f \frac{\partial \phi}{\partial x_k} + i\omega \frac{\partial U_j}{\partial x_j} f\phi \\ &- \frac{\partial U_j}{\partial x_j} f U_k \frac{\partial \phi}{\partial x_k} - \frac{\partial U_j}{\partial x_j} U_k \phi \frac{\partial f}{\partial x_k} - U_j \frac{\partial U_k}{\partial x_j} \phi \frac{\partial f}{\partial x_k} \\ &- U_j \frac{\partial U_k}{\partial x_j} f \frac{\partial \phi}{\partial x_k} - U_j U_k f \frac{\partial^2 \phi}{\partial x_j \partial x_k} - U_j U_k \frac{\partial f}{\partial x_j} \frac{\partial \phi}{\partial x_k} \\ &- U_j U_k \frac{\partial f}{\partial x_k} \frac{\partial \phi}{\partial x_j} - U_j U_k \phi \frac{\partial^2 f}{\partial x_j \partial x_k} \\ &- \gamma \frac{\partial U_j}{\partial x_j} \phi f - \gamma U_j \phi \frac{\partial f}{\partial x_j} - \gamma U_j \frac{\partial \phi}{\partial x_j} f + i\omega \gamma \phi f \end{aligned} \right]_{\bar{\eta}} \quad (3.351)$$

At $z = \bar{\eta}$:

$$f = 1 \quad (3.352)$$

Using Equation (3.216) and the results summarised in Section 3.7.4 gives the following:

$$\begin{aligned} \frac{df}{dx_k} = & \left(\frac{(h' + z') \cosh \kappa h' \sinh [\kappa(h' + z')]}{-h' \cosh [\kappa(h' + z')] \sinh \kappa h'} \right) \frac{\partial \kappa}{\partial x_k} \\ & + \left(\frac{\kappa \cosh \kappa h' \sinh [\kappa(h' + z')]}{-\kappa \cosh [\kappa(h' + z')] \sinh \kappa h'} \right) \frac{\partial h'}{\partial x_k} \\ & + \left(\frac{\kappa \sinh [\kappa(h' + z')]}{\cosh \kappa h'} \right) (-1) \frac{\partial \bar{\eta}}{\partial x_k} \end{aligned} \quad (3.353)$$

Equation (3.353) and the equations summarised in Section 3.7.4 may now be calculated at the free surface.

Equation (3.353) at $z = \bar{\eta}$:

$$\frac{df}{dx_k} = - \left(\frac{\kappa \sinh \kappa h'}{\cosh \kappa h'} \right) \frac{\partial \bar{\eta}}{\partial x_k} \quad (3.354)$$

$$\frac{df}{dx_k} = -\kappa \tanh \kappa h' \frac{\partial \bar{\eta}}{\partial x_k} \quad (3.355)$$

$$\frac{df}{dx_k} = -\lambda' \frac{\partial \bar{\eta}}{\partial x_k} \quad (3.356)$$

Equation (3.292) at $z = \bar{\eta}$:

$$\frac{\partial f}{\partial h'} = \frac{\kappa \sinh \kappa h' - \lambda' \cosh \kappa h'}{\cosh \kappa h'} \quad (3.357)$$

$$\frac{\partial f}{\partial h'} = \lambda' - \lambda' \quad (3.358)$$

$$\frac{\partial f}{\partial h'} = 0 \quad (3.359)$$

Equation (3.301) at $z = \bar{\eta}$:

$$\frac{\partial^2 f}{\partial h'^2} = \frac{-2\kappa\lambda' \sinh[\kappa(h' + z')] + 2\lambda'^2 \cosh[\kappa(h' + z')]}{\cosh \kappa h'} \quad (3.360)$$

$$\frac{\partial^2 f}{\partial h'^2} = \frac{-2\kappa\lambda' \sinh \kappa h' + 2\lambda'^2 \cosh \kappa h'}{\cosh \kappa h'} \quad (3.361)$$

$$\frac{\partial^2 f}{\partial h'^2} = -2\lambda'^2 + 2\lambda'^2 \quad (3.362)$$

$$\frac{\partial^2 f}{\partial h'^2} = 0 \quad (3.363)$$

Equation (3.304) at $z = \bar{\eta}$:

$$\frac{\partial f}{\partial \kappa} = \frac{(h' + z') \sinh[\kappa(h' + z')] - \frac{h'\lambda'}{\kappa} \cosh[\kappa(h' + z')]}{\cosh \kappa h'} \quad (3.364)$$

$$\frac{\partial f}{\partial \kappa} = \frac{h' \sinh \kappa h' - \frac{h'\lambda'}{\kappa} \cosh \kappa h'}{\cosh \kappa h'} \quad (3.365)$$

$$\frac{\partial f}{\partial \kappa} = \frac{h'\lambda'}{\kappa} - \frac{h'\lambda'}{\kappa} \quad (3.366)$$

$$\frac{\partial f}{\partial \kappa} = 0 \quad (3.367)$$

Equation (3.337) at $z = \bar{\eta}$:

$$\frac{\partial f}{\partial z} = \frac{\kappa \sinh[\kappa(h' + z')]}{\cosh \kappa h'} \quad (3.368)$$

$$\frac{\partial f}{\partial z} = \frac{\kappa \sinh \kappa h'}{\cosh \kappa h'} \quad (3.369)$$

$$\frac{df}{dz} = \lambda' \quad (3.370)$$

Equation (3.341) at $z = \bar{\eta}$:

$$\frac{\partial^2 f}{\partial z^2} = \frac{\kappa^2 \cosh[\kappa(h' + z')]}{\cosh \kappa h'} \quad (3.371)$$

$$\frac{\partial^2 f}{\partial z^2} = \frac{\kappa^2 \cosh \kappa h'}{\cosh \kappa h'} \quad (3.372)$$

$$\frac{d^2 f}{dz^2} = \kappa^2 \quad (3.373)$$

Equation (3.314) at $z = \bar{\eta}$:

$$\frac{\partial^2 f}{\partial \kappa^2} = \frac{\left[-\frac{2h'\lambda'}{\kappa}(h' + z') \sinh[\kappa(h' + z')] + \left(z'^2 + \frac{2h'^2\lambda'^2}{\kappa^2} + 2h'z' \right) \cosh[\kappa(h' + z')] \right]}{\cosh \kappa h'} \quad (3.374)$$

$$\frac{\partial^2 f}{\partial \kappa^2} = \frac{\left[-\frac{2h'\lambda'}{\kappa}(h') \sinh \kappa h' + \left(\frac{2h'^2\lambda'^2}{\kappa^2} \right) \cosh \kappa h' \right]}{\cosh \kappa h'} \quad (3.375)$$

$$\frac{\partial^2 f}{\partial \kappa^2} = -\frac{2h'^2\lambda'^2}{\kappa^2} + \frac{2h'^2\lambda'^2}{\kappa^2} \quad (3.376)$$

$$\frac{\partial^2 f}{\partial \kappa^2} = 0 \quad (3.377)$$

Equation (3.326) at $z = \bar{\eta}$:

$$\frac{\partial^2 f}{\partial h' \partial \kappa} = \frac{\left(\left(\kappa z' - \frac{\lambda'}{\kappa} + \frac{2h'\lambda'^2}{\kappa} \right) \cosh[\kappa(h' + z')] \right)}{(1 - 2h'\lambda' - z'\lambda') \sinh[\kappa(h' + z')]} \quad (3.378)$$

$$\frac{\partial^2 f}{\partial h' \partial \kappa} = \frac{\left(\left(-\frac{\lambda'}{\kappa} + \frac{2h'\lambda'^2}{\kappa} \right) \cosh \kappa h' \right)}{(1 - 2h'\lambda') \sinh \kappa h'} \quad (3.379)$$

$$\frac{\partial^2 f}{\partial h' \partial \kappa} = -\frac{\lambda'}{\kappa} + \frac{2h'\lambda'^2}{\kappa} + \frac{\lambda'}{\kappa} - \frac{2h'\lambda'^2}{\kappa} \quad (3.380)$$

$$\frac{\partial^2 f}{\partial h' \partial \kappa} = 0 \quad (3.381)$$

Equation (3.345) at $z = \bar{\eta}$:

$$\frac{\partial^2 f}{\partial \kappa \partial z'} = \frac{\kappa(h' + z') \cosh \kappa h' \cosh[\kappa(h' + z')] + \cosh \kappa h' \sinh[\kappa(h' + z')] - \kappa h' \sinh \kappa h' \sinh[\kappa(h' + z')]}{\cosh^2 \kappa h'} \quad (3.382)$$

$$\frac{\partial^2 f}{\partial \kappa \partial z'} = \frac{\kappa h' \cosh^2 \kappa h' + \cosh \kappa h' \sinh \kappa h' - \kappa h' \sinh^2 \kappa h'}{\cosh^2 \kappa h'} \quad (3.383)$$

$$\frac{\partial^2 f}{\partial \kappa \partial z'} = \kappa h' + \frac{\lambda'}{\kappa} - \frac{h\lambda'^2}{\kappa} \quad (3.384)$$

Equation (3.348) at $z = \bar{\eta}$:

$$\frac{\partial^2 f}{\partial h' \partial z'} = \frac{\cosh \kappa h' \kappa^2 \cosh[\kappa(h' + z')] - \kappa^2 \sinh[\kappa(h' + z')] \sinh \kappa h'}{\cosh^2 \kappa h'} \quad (3.385)$$

$$\frac{\partial^2 f}{\partial h' \partial z'} = \frac{\kappa^2 \cosh^2 \kappa h' - \kappa^2 \sinh^2 \kappa h'}{\cosh^2 \kappa h'} \quad (3.386)$$

$$\frac{\partial^2 f}{\partial h' \partial z'} = \kappa^2 - \lambda'^2 \quad (3.387)$$

Substituting the results of Equations (3.354) to (3.387) into Equation (3.226) gives:

$$\begin{aligned}
\frac{d^2 f}{dx_k dx_k} = & 0 \left[\frac{\partial^2 \kappa}{\partial x_k \partial x_k} \right] + 0 \left[\frac{\partial^2 h'}{\partial x_k \partial x_k} \right] + \lambda \left[\frac{\partial z'}{\partial \bar{\eta}} \frac{\partial^2 \bar{\eta}}{\partial x_k \partial x_k} \right] \\
& + 0 \left[\frac{\partial \kappa}{\partial x_k} \frac{\partial \kappa}{\partial x_k} \right] + 0 \left[\frac{\partial h'}{\partial x_k} \frac{\partial h'}{\partial x_k} \right] + \kappa^2 \left[\frac{\partial z'}{\partial \bar{\eta}} \frac{\partial \bar{\eta}}{\partial x_k} \frac{\partial z'}{\partial \bar{\eta}} \frac{\partial \bar{\eta}}{\partial x_k} \right] \\
& + 0 \left[\frac{\partial h'}{\partial x_k} \frac{\partial \kappa}{\partial x_k} + \frac{\partial \kappa}{\partial x_k} \frac{\partial h'}{\partial x_k} \right] \quad \text{at } z = \bar{\eta} \\
& + \left(\kappa h' + \frac{\lambda'}{\kappa} - \frac{h \lambda'^2}{\kappa} \right) \left[\frac{\partial z'}{\partial \bar{\eta}} \frac{\partial \bar{\eta}}{\partial x_k} \frac{\partial \kappa}{\partial x_k} + \frac{\partial \kappa}{\partial x_k} \frac{\partial z'}{\partial \bar{\eta}} \frac{\partial \bar{\eta}}{\partial x_k} \right] \\
& + (\kappa^2 - \lambda'^2) \left[\frac{\partial z'}{\partial \bar{\eta}} \frac{\partial \bar{\eta}}{\partial x_k} \frac{\partial h'}{\partial x_k} + \frac{\partial h'}{\partial x_k} \frac{\partial z'}{\partial \bar{\eta}} \frac{\partial \bar{\eta}}{\partial x_k} \right]
\end{aligned} \tag{3.388}$$

Similarly the cross-derivative becomes:

$$\begin{aligned}
\frac{d^2 f}{dx_j dx_k} = & \lambda' \frac{\partial z'}{\partial \bar{\eta}} \frac{\partial^2 \bar{\eta}}{\partial x_j \partial x_k} \\
& + \kappa^2 \left(\frac{\partial z'}{\partial \bar{\eta}} \right)^2 \frac{\partial \bar{\eta}}{\partial x_k} \frac{\partial \bar{\eta}}{\partial x_j} \quad \text{at } z = \bar{\eta} \\
& + (\kappa^2 - \lambda'^2) \left(\frac{\partial z'}{\partial \bar{\eta}} \frac{\partial \bar{\eta}}{\partial x_k} \frac{\partial h'}{\partial x_j} + \frac{\partial h'}{\partial x_k} \frac{\partial z'}{\partial \bar{\eta}} \frac{\partial \bar{\eta}}{\partial x_j} \right) \\
& + \left(\kappa h' + \frac{\lambda'}{\kappa} - \frac{h \lambda'^2}{\kappa} \right) \left(\frac{\partial z'}{\partial \bar{\eta}} \frac{\partial \bar{\eta}}{\partial x_k} \frac{\partial \kappa}{\partial x_j} + \frac{\partial \kappa}{\partial x_k} \frac{\partial z'}{\partial \bar{\eta}} \frac{\partial \bar{\eta}}{\partial x_j} \right)
\end{aligned} \tag{3.389}$$

Equation (3.388) can then be simplified as follows using Equation (3.333):

$$\begin{aligned}
\frac{d^2 f}{dx_k dx_k} = & -\lambda \left[\frac{\partial^2 \bar{\eta}}{\partial x_k \partial x_k} \right] + \kappa^2 \left[\frac{\partial \bar{\eta}}{\partial x_k} \frac{\partial \bar{\eta}}{\partial x_k} \right] \\
& - \left(\kappa h' + \frac{\lambda'}{\kappa} - \frac{h \lambda'^2}{\kappa} \right) \left[2 \frac{\partial \bar{\eta}}{\partial x_k} \frac{\partial \kappa}{\partial x_k} \right] \quad \text{at } z = \bar{\eta} \\
& - (\kappa^2 - \lambda'^2) \left[2 \frac{\partial \bar{\eta}}{\partial x_k} \frac{\partial h'}{\partial x_k} \right]
\end{aligned} \tag{3.390}$$

Similarly the cross-derivative can be simplified as:

$$\begin{aligned} \frac{d^2 f}{dx_j dx_k} = & -\lambda' \frac{\partial^2 \bar{\eta}}{\partial x_j \partial x_k} + \kappa^2 \frac{\partial \bar{\eta}}{\partial x_k} \frac{\partial \bar{\eta}}{\partial x_j} \\ & + (\kappa^2 - \lambda'^2) \left(-\frac{\partial \bar{\eta}}{\partial x_k} \frac{\partial h'}{\partial x_j} - \frac{\partial h'}{\partial x_k} \frac{\partial \bar{\eta}}{\partial x_j} \right) \quad \text{at } z = \bar{\eta} \\ & + \left(\kappa h' + \frac{\lambda'}{\kappa} - \frac{h \lambda'^2}{\kappa} \right) \left(-\frac{\partial \bar{\eta}}{\partial x_k} \frac{\partial \kappa}{\partial x_j} - \frac{\partial \kappa}{\partial x_k} \frac{\partial \bar{\eta}}{\partial x_j} \right) \end{aligned} \quad (3.391)$$

Equation (3.351) can be rewritten using f from Equations (3.356) and (3.390):

$$\begin{aligned} \frac{\partial \tilde{\phi}}{\partial z} \Big|_{\bar{\eta}} = & \frac{1}{g} \left[\begin{aligned} & \omega^2 \phi - 2i\omega U_k \phi \lambda' \frac{\partial \bar{\eta}}{\partial x_k} + 2i\omega U_k \frac{\partial \phi}{\partial x_k} + i\omega \frac{\partial U_j}{\partial x_j} \phi - \frac{\partial U_j}{\partial x_j} U_k \frac{\partial \phi}{\partial x_k} \\ & + \frac{\partial U_j}{\partial x_j} U_k \phi \lambda' \frac{\partial \bar{\eta}}{\partial x_k} + U_j \frac{\partial U_k}{\partial x_j} \phi \lambda' \frac{\partial \bar{\eta}}{\partial x_k} - U_j \frac{\partial U_k}{\partial x_j} \frac{\partial \phi}{\partial x_k} - U_j U_k \frac{\partial^2 \phi}{\partial x_j \partial x_k} \\ & + 2U_j U_k \lambda' \frac{\partial \bar{\eta}}{\partial x_j} \frac{\partial \phi}{\partial x_k} - \gamma \frac{\partial U_j}{\partial x_j} \phi + \lambda' \gamma U_j \phi \frac{\partial \bar{\eta}}{\partial x_k} - \gamma U_j \frac{\partial \phi}{\partial x_j} + i\omega \gamma \phi \\ & - U_j U_k \phi \left(-\lambda' \frac{\partial^2 \bar{\eta}}{\partial x_j \partial x_k} + \kappa^2 \frac{\partial \bar{\eta}}{\partial x_k} \frac{\partial \bar{\eta}}{\partial x_j} \right. \\ & \quad \left. + (\kappa^2 - \lambda'^2) \left(-\frac{\partial \bar{\eta}}{\partial x_k} \frac{\partial h'}{\partial x_j} - \frac{\partial h'}{\partial x_k} \frac{\partial \bar{\eta}}{\partial x_j} \right) \right. \\ & \quad \left. + \left(\kappa h' + \frac{\lambda'}{\kappa} - \frac{h \lambda'^2}{\kappa} \right) \left(-\frac{\partial \bar{\eta}}{\partial x_k} \frac{\partial \kappa}{\partial x_j} - \frac{\partial \kappa}{\partial x_k} \frac{\partial \bar{\eta}}{\partial x_j} \right) \right) \end{aligned} \right]_{\bar{\eta}} \end{aligned} \quad (3.392)$$

Simplification of Equation (3.392) yields:

$$\begin{aligned} \frac{\partial \tilde{\phi}}{\partial z} \Big|_{\bar{\eta}} = & \frac{1}{g} \left[\begin{aligned} & \omega^2 \phi - 2i\omega \lambda' U_k \frac{\partial \bar{\eta}}{\partial x_k} \phi + 2i\omega U_k \frac{\partial \phi}{\partial x_k} + i\omega \frac{\partial U_j}{\partial x_j} \phi - U_k \frac{\partial U_j}{\partial x_j} \frac{\partial \phi}{\partial x_k} \\ & + \lambda' U_k \frac{\partial U_j}{\partial x_j} \frac{\partial \bar{\eta}}{\partial x_k} \phi + \lambda' U_j \frac{\partial \bar{\eta}}{\partial x_k} \frac{\partial U_k}{\partial x_j} \phi - U_j \frac{\partial U_k}{\partial x_j} \frac{\partial \phi}{\partial x_k} - U_j U_k \frac{\partial^2 \phi}{\partial x_j \partial x_k} \\ & + 2\lambda' U_j U_k \frac{\partial \bar{\eta}}{\partial x_j} \frac{\partial \phi}{\partial x_k} - \gamma \frac{\partial U_j}{\partial x_j} \phi + \lambda' \gamma U_j \phi \frac{\partial \bar{\eta}}{\partial x_k} - \gamma U_j \frac{\partial \phi}{\partial x_j} + i\omega \gamma \phi \\ & - U_j U_k \phi \left(-\lambda' \frac{\partial^2 \bar{\eta}}{\partial x_j \partial x_k} + \kappa^2 \frac{\partial \bar{\eta}}{\partial x_k} \frac{\partial \bar{\eta}}{\partial x_j} \right. \\ & \quad \left. + (\kappa^2 - \lambda'^2) \left(-\frac{\partial \bar{\eta}}{\partial x_k} \frac{\partial h'}{\partial x_j} - \frac{\partial h'}{\partial x_k} \frac{\partial \bar{\eta}}{\partial x_j} \right) \right. \\ & \quad \left. + \left(\kappa h' + \frac{\lambda'}{\kappa} - \frac{h \lambda'^2}{\kappa} \right) \left(-\frac{\partial \bar{\eta}}{\partial x_k} \frac{\partial \kappa}{\partial x_j} - \frac{\partial \kappa}{\partial x_k} \frac{\partial \bar{\eta}}{\partial x_j} \right) \right) \end{aligned} \right]_{\bar{\eta}} \end{aligned} \quad (3.393)$$

3.7.5.2 Kinematic Seabed Boundary Condition

Equation (3.215) multiplied by the vertical function may be expanded as follows using Equation (3.198):

$$f \frac{\partial \tilde{\phi}}{\partial z} \Big|_{-h} = -f \frac{\partial (f\phi)}{\partial x_k} \frac{\partial h}{\partial x_k} \Big|_{-h} \quad (3.394)$$

Expansion of Equation (3.394) gives:

$$f \frac{\partial \tilde{\phi}}{\partial z} \Big|_{-h} = -f^2 \frac{\partial \phi}{\partial x_k} \frac{\partial h}{\partial x_k} \Big|_{-h} - f\phi \frac{\partial f}{\partial x_k} \frac{\partial h}{\partial x_k} \Big|_{-h} \quad (3.395)$$

Substitution of Equation (3.395) into Equation (3.213) gives:

$$\begin{aligned} & \int_{-h}^{\bar{\eta}} f\phi \frac{d^2 f}{dx_k dx_k} dz + \int_{-h}^{\bar{\eta}} 2f \frac{df}{dx_k} \frac{\partial \phi}{\partial x_k} dz + \int_{-h}^{\bar{\eta}} f^2 \frac{\partial^2 \phi}{\partial x_k \partial x_k} dz - \int_{-h}^{\bar{\eta}} \frac{\partial f}{\partial z} \frac{\partial f}{\partial z} \phi dz + \frac{\partial \tilde{\phi}}{\partial z} \Big|_{\bar{\eta}} \\ & + f^2 \frac{\partial \phi}{\partial x_k} \frac{\partial h}{\partial x_k} \Big|_{-h} + f\phi \frac{\partial f}{\partial x_k} \frac{\partial h}{\partial x_k} \Big|_{-h} = 0 \end{aligned} \quad (3.396)$$

Equation (3.396) can be rewritten as:

$$\begin{aligned} & \int_{-h}^{\bar{\eta}} f\phi \frac{d^2 f}{dx_k dx_k} dz + \int_{-h}^{\bar{\eta}} \frac{df^2}{dx_k} \frac{\partial \phi}{\partial x_k} dz + f^2 \frac{\partial \phi}{\partial x_k} \frac{\partial h}{\partial x_k} \Big|_{-h} + \int_{-h}^{\bar{\eta}} f^2 \frac{\partial^2 \phi}{\partial x_k \partial x_k} dz - \int_{-h}^{\bar{\eta}} \frac{\partial f}{\partial z} \frac{\partial f}{\partial z} \phi dz \\ & + \frac{\partial \tilde{\phi}}{\partial z} \Big|_{\bar{\eta}} + f\phi \frac{\partial f}{\partial x_k} \frac{\partial h}{\partial x_k} \Big|_{-h} = 0 \end{aligned} \quad (3.397)$$

Isolating the horizontal derivative of velocity potential in the second and third terms of Equation (3.397) gives:

$$\begin{aligned} & \int_{-h}^{\bar{\eta}} f\phi \frac{d^2 f}{dx_k dx_k} dz + \frac{\partial \phi}{\partial x_k} \left(\int_{-h}^{\bar{\eta}} \frac{df^2}{dx_k} dz + f^2 \frac{\partial h}{\partial x_k} \Big|_{-h} \right) + \int_{-h}^{\bar{\eta}} f^2 \frac{\partial^2 \phi}{\partial x_k \partial x_k} dz - \int_{-h}^{\bar{\eta}} \frac{\partial f}{\partial z} \frac{\partial f}{\partial z} \phi dz \\ & + \frac{\partial \tilde{\phi}}{\partial z} \Big|_{\bar{\eta}} + f\phi \frac{\partial f}{\partial x_k} \frac{\partial h}{\partial x_k} \Big|_{-h} = 0 \end{aligned} \quad (3.398)$$

Leibniz's Rule states that:

$$D \int_b^a Y dz = \int_b^a DY dz + (Da) Y_{z=a} - (Db) Y_{z=b} \quad (3.399)$$

where $D = \frac{\partial}{\partial x}, \frac{\partial}{\partial y}, \frac{\partial}{\partial t}$

In this case let the function Y be the same as f^2 :

$$D \int_b^a f^2 dz = \int_b^a D f^2 dz + (Da) f^2_{z=a} - (Db) f^2_{z=b} \quad (3.400)$$

$$\frac{\partial}{\partial x_k} \int_b^a f^2 dz = \int_b^a \frac{\partial(f^2)}{\partial x_k} dz + \left(\frac{\partial a}{\partial x_k} \right) f^2_{z=a} - \left(\frac{\partial b}{\partial x_k} \right) f^2_{z=b} \quad (3.401)$$

If we choose limits of $\bar{\eta}$ and $-h$:

$$\frac{\partial}{\partial x_k} \int_{-h}^{\bar{\eta}} f^2 dz = \int_{-h}^{\bar{\eta}} \frac{\partial(f^2)}{\partial x_k} dz + \left(\frac{\partial \bar{\eta}}{\partial x_k} \right) f^2_{z=\bar{\eta}} - \left(\frac{\partial(-h)}{\partial x_k} \right) f^2_{z=-h} \quad (3.402)$$

Rearranging gives:

$$\int_{-h}^{\bar{\eta}} \frac{\partial(f^2)}{\partial x_k} dz = \frac{\partial}{\partial x_k} \int_{-h}^{\bar{\eta}} f^2 dz - \left(\frac{\partial \bar{\eta}}{\partial x_k} \right) f^2_{z=\bar{\eta}} + \left(\frac{\partial h}{\partial x_k} \right) f^2_{z=-h} \quad (3.403)$$

$$\int_{-h}^{\bar{\eta}} \frac{\partial(f^2)}{\partial x_k} dz + \left(\frac{\partial h}{\partial x_k} \right) f^2_{z=-h} = \frac{\partial}{\partial x_k} \int_{-h}^{\bar{\eta}} f^2 dz - \left(\frac{\partial \bar{\eta}}{\partial x_k} \right) f^2_{z=\bar{\eta}} \quad (3.404)$$

Using Equation (3.404) with Equation (3.398) gives:

$$\begin{aligned} & \int_{-h}^{\bar{\eta}} f \phi \frac{d^2 f}{dx_k dx_k} dz + \frac{\partial \phi}{\partial x_k} \left(\frac{\partial}{\partial x_k} \int_{-h}^{\bar{\eta}} f^2 dz - \left(\frac{\partial \bar{\eta}}{\partial x_k} \right) f^2_{z=\bar{\eta}} \right) + \int_{-h}^{\bar{\eta}} f^2 \frac{\partial^2 \phi}{\partial x_k \partial x_k} dz - \int_{-h}^{\bar{\eta}} \frac{\partial f}{\partial z} \frac{\partial f}{\partial z} \phi dz \\ & + \left. \frac{\partial \tilde{\phi}}{\partial z} \right|_{\bar{\eta}} + f \phi \left. \frac{\partial f}{\partial x_k} \frac{\partial h}{\partial x_k} \right|_{-h} = 0 \end{aligned} \quad (3.405)$$

Expanding Equation (3.405) yields:

$$\begin{aligned} & \frac{\partial^2 \phi}{\partial x_k \partial x_k} \int_{-h}^{\bar{\eta}} f^2 dz + \frac{\partial \phi}{\partial x_k} \frac{\partial}{\partial x_k} \int_{-h}^{\bar{\eta}} f^2 dz + \phi \int_{-h}^{\bar{\eta}} f \frac{d^2 f}{dx_k dx_k} dz - \phi \int_{-h}^{\bar{\eta}} \frac{\partial f}{\partial z} \frac{\partial f}{\partial z} dz - \frac{\partial \phi}{\partial x_k} \left(\frac{\partial \bar{\eta}}{\partial x_k} \right) f^2_{z=\bar{\eta}} \\ & + \left. \frac{\partial \tilde{\phi}}{\partial z} \right|_{\bar{\eta}} + f \phi \left. \frac{\partial f}{\partial x_k} \frac{\partial h}{\partial x_k} \right|_{-h} = 0 \end{aligned} \quad (3.406)$$

3.7.5.2 Evaluation of Remaining Mild-Slope Equation Terms

Working with the following part of Equation (3.406) gives:

$$\int_{-h}^{\bar{\eta}} f^2 dz = \frac{1}{\cosh^2 \kappa h'} \left[\int_{-h}^{\bar{\eta}} \cosh^2 \kappa (h' + z') dz \right] \quad (3.407)$$

where:

$$\cosh^2 x = \frac{1}{2} [1 + \cosh 2x] \quad (3.408)$$

Therefore:

$$\int_{-h}^{\bar{\eta}} f^2 dz = \frac{1}{\cosh^2 \kappa h'} \left[\int_{-h}^{\bar{\eta}} \frac{1}{2} [1 + \cosh 2\kappa (h' + z')] dz \right] \quad (3.409)$$

$$\int_{-h}^{\bar{\eta}} f^2 dz = \frac{1}{2 \cosh^2 \kappa h'} \left[z + \frac{\sinh 2\kappa (h' + z')}{2\kappa} \right]_{-h}^{\bar{\eta}} \quad (3.410)$$

Recalling the definition of (3.217) :

$$h' = h + \bar{\eta}$$

Acknowledging that:

$$z' = z - \bar{\eta} \quad (3.411)$$

$$\int_{-h}^{\bar{\eta}} f^2 dz = \frac{1}{2 \cosh^2 \kappa h'} \left[\left(\bar{\eta} + \frac{\sinh 2\kappa h'}{2\kappa} \right) - \left(-h + \frac{\sinh 2\kappa(0)}{2\kappa} \right) \right] \quad (3.412)$$

$$\int_{-h}^{\bar{\eta}} f^2 dz = \frac{1}{2 \cosh^2 \kappa h'} \left[\bar{\eta} + h + \frac{\sinh 2\kappa h'}{2\kappa} \right] \quad (3.413)$$

$$\int_{-h}^{\bar{\eta}} f^2 dz = \frac{1}{2 \cosh^2 \kappa h'} \left[h' + \frac{\sinh 2\kappa h'}{2\kappa} \right] \quad (3.414)$$

$$\int_{-h}^{\bar{\eta}} f^2 dz = \frac{\frac{1}{2} \kappa h' + \frac{1}{4} \sinh 2\kappa h'}{\kappa \cosh^2 \kappa h'} \quad (3.415)$$

It is possible to define Relative Wave Celerity, C , for a plane wave on a current undergoing refraction as follows:

$$C = \frac{\sigma}{\kappa} \quad (3.416)$$

In the case of waves experiencing the effects diffraction also the exact relative wave celerity would be:

$$C_{precise} = \frac{\sigma}{|\nabla S|} \quad (3.417)$$

It would be impossible to use this definition of wave celerity without applying some sort of iterative mathematical scheme which in turn would also be inaccurate. Hence, the plane wave solution of relative wave celerity defined in (3.416) is deemed sufficiently accurate for present purposes. Using Equation (3.190) with Equation (3.416) gives:

$$C = \frac{\sqrt{g\kappa \tanh \kappa h'}}{\kappa} \quad (3.418)$$

Relative Wave Group Velocity, C_g , is defined by:

$$C_g = \frac{1}{2} \left[1 + \frac{\frac{4\pi h'}{L}}{\sinh\left(\frac{4\pi h'}{L}\right)} \right] C \quad (3.419)$$

$$C_g = \frac{1}{2} \left[1 + \frac{2\kappa h'}{\sinh 2\kappa h'} \right] C \quad (3.420)$$

Working with Equations (3.418) and (3.420) gives the following development:

$$CC_g = \frac{1}{2} \left[1 + \frac{2\kappa h'}{\sinh 2\kappa h'} \right] C^2 \quad (3.421)$$

$$CC_g = \frac{1}{2} \left[1 + \frac{2\kappa h'}{\sinh 2\kappa h'} \right] \left[\frac{g \tanh \kappa h'}{\kappa} \right] \quad (3.422)$$

$$CC_g = \frac{1}{2} \left[1 + \frac{2\kappa h'}{\sinh 2\kappa h'} \right] \cdot \left[\frac{g}{\kappa \tanh \kappa h'} \frac{\sinh^2 \kappa h'}{\cosh^2 \kappa h'} \right] \quad (3.423)$$

$$CC_g = \left[\frac{g \sinh^2 \kappa h'}{2 \tanh \kappa h'} + \frac{\kappa h' g \sinh^2 \kappa h'}{\tanh \kappa h' \sinh 2\kappa h'} \right] \frac{1}{\kappa \cosh^2 \kappa h'} \quad (3.424)$$

$$CC_g = \left[\frac{g \sinh^2 \kappa h' \sinh 2\kappa h' + 2\kappa h' g \sinh^2 \kappa h'}{2 \tanh \kappa h' \sinh 2\kappa h'} \right] \frac{1}{\kappa \cosh^2 \kappa h'} \quad (3.425)$$

$$CC_g = \left[\frac{g \sinh^2 \kappa h' \sinh 2\kappa h' + 2\kappa h' g \sinh^2 \kappa h'}{2 \frac{\sinh \kappa h'}{\cosh \kappa h'} 2 \sinh \kappa h' \cosh \kappa h'} \right] \frac{1}{\kappa \cosh^2 \kappa h'} \quad (3.426)$$

$$CC_g = \left[\frac{g \sinh^2 \kappa h' \sinh 2\kappa h' + 2\kappa h' g \sinh^2 \kappa h'}{4 \sinh^2 \kappa h'} \right] \frac{1}{\kappa \cosh^2 \kappa h'} \quad (3.427)$$

$$CC_g = \left[\frac{g \sinh 2\kappa h' + 2\kappa h' g}{4} \right] \frac{1}{\kappa \cosh^2 \kappa h'} \quad (3.428)$$

$$CC_g = g \frac{\frac{1}{4} \sinh 2\kappa h' + \frac{1}{2} \kappa h'}{\kappa \cosh^2 \kappa h'} \quad (3.429)$$

Therefore using Equations (3.415) and (3.429):

$$\int_{-h}^{\bar{\eta}} f^2 dz = \frac{\frac{1}{2} \kappa h' + \frac{1}{4} \sinh 2\kappa h'}{\kappa \cosh^2 \kappa h'} = \frac{CC_g}{g} \quad (3.430)$$

Substituting Equation (3.430) in Equation (3.406) gives:

$$\begin{aligned} & \frac{\partial^2 \phi}{\partial x_k \partial x_k} \frac{CC_g}{g} + \frac{\partial \phi}{\partial x_k} \frac{\partial}{\partial x_k} \left(\frac{CC_g}{g} \right) + \phi \int_{-h}^{\bar{\eta}} f \frac{d^2 f}{dx_k dx_k} dz - \phi \int_{-h}^{\bar{\eta}} \frac{\partial f}{\partial z} \frac{\partial f}{\partial z} dz - \frac{\partial \phi}{\partial x_k} \left(\frac{\partial \bar{\eta}}{\partial x_k} \right) \\ & + \frac{\partial \tilde{\phi}}{\partial z} \Big|_{\bar{\eta}} + f \phi \frac{\partial f}{\partial x_k} \frac{\partial h}{\partial x_k} \Big|_{-h} = 0 \end{aligned} \quad (3.431)$$

Examining the fourth term of Equation (3.431) in conjunction with Equation (3.337) gives the following development:

$$\int_{-h}^{\bar{\eta}} \frac{\partial f}{\partial z} \frac{\partial f}{\partial z} dz = \frac{1}{\cosh^2 \kappa h'} \int_{-h}^{\bar{\eta}} \kappa^2 \sinh^2 [\kappa(h' + z')] dz \quad (3.432)$$

$$\int_{-h}^{\bar{\eta}} \frac{\partial f}{\partial z} \frac{\partial f}{\partial z} dz = \frac{1}{\cosh^2 \kappa h'} \frac{\kappa^2}{2} \int_{-h}^{\bar{\eta}} (\cosh [2\kappa(h' + z')] - 1) dz \quad (3.433)$$

$$\int_{-h}^{\bar{\eta}} \frac{\partial f}{\partial z} \frac{\partial f}{\partial z} dz = \frac{1}{\cosh^2 \kappa h'} \frac{\kappa^2}{2} \left[\frac{1}{2\kappa} \sinh [2\kappa(h' + z')] - z \right]_{-h}^{\bar{\eta}} \quad (3.434)$$

$$\int_{-h}^{\bar{\eta}} \frac{\partial f}{\partial z} \frac{\partial f}{\partial z} dz = \frac{1}{\cosh^2 \kappa h'} \frac{\kappa^2}{2} \left[\frac{1}{2\kappa} \sinh 2\kappa h' - \bar{\eta} \right] - \frac{1}{\cosh^2 \kappa h'} \frac{\kappa^2}{2} \left[\frac{1}{2\kappa} \sinh [0] + h \right] \quad (3.435)$$

$$\int_{-h}^{\bar{\eta}} \frac{\partial f}{\partial z} \frac{\partial f}{\partial z} dz = \frac{1}{\cosh^2 \kappa h'} \frac{\kappa^2}{2} \left[-\bar{\eta} - h + \frac{1}{2\kappa} \sinh 2\kappa h' \right] \quad (3.436)$$

$$\int_{-h}^{\bar{\eta}} \frac{\partial f}{\partial z} \frac{\partial f}{\partial z} dz = \frac{1}{\cosh^2 \kappa h'} \frac{\kappa^2}{2} \left[-h' + \frac{1}{2\kappa} \sinh 2\kappa h' \right] \quad (3.437)$$

$$\int_{-h}^{\bar{\eta}} \frac{\partial f}{\partial z} \frac{\partial f}{\partial z} dz = \frac{h' \kappa^2}{2 \cosh^2 \kappa h'} \left[\frac{\sinh 2\kappa h'}{2h' \kappa} - 1 \right] \quad (3.438)$$

$$\int_{-h}^{\bar{\eta}} \frac{\partial f}{\partial z} \frac{\partial f}{\partial z} dz = \frac{h' \kappa^2}{2 \cosh^2 \kappa h'} \left[\frac{\frac{\sinh 2\kappa h'}{h' \kappa} - 2}{2} \right] \quad (3.439)$$

$$\int_{-h}^{\bar{\eta}} \frac{\partial f}{\partial z} \frac{\partial f}{\partial z} dz = \frac{\kappa \sinh 2\kappa h' - 2h' \kappa^2}{4 \cosh^2 \kappa h'} \quad (3.440)$$

$$\int_{-h}^{\bar{\eta}} \frac{\partial f}{\partial z} \frac{\partial f}{\partial z} dz = \frac{-\kappa \sinh 2\kappa h' - 2h' \kappa^2}{4 \cosh^2 \kappa h'} + \frac{2\kappa \sinh 2\kappa h'}{4 \cosh^2 \kappa h'} \quad (3.441)$$

$$\int_{-h}^{\bar{\eta}} \frac{\partial f}{\partial z} \frac{\partial f}{\partial z} dz = -\kappa^2 \frac{\frac{1}{4} \sinh 2\kappa h' + \frac{1}{2} h' \kappa}{\kappa \cosh^2 \kappa h'} + \frac{4\kappa \sinh \kappa h' \cosh \kappa h'}{4 \cosh^2 \kappa h'} \quad (3.442)$$

$$\int_{-h}^{\bar{\eta}} \frac{\partial f}{\partial z} \frac{\partial f}{\partial z} dz = -\kappa^2 \frac{\frac{1}{4} \sinh 2\kappa h' + \frac{1}{2} h' \kappa}{\kappa \cosh^2 \kappa h'} + \kappa \tanh \kappa h' \quad (3.443)$$

Using the results of Equation (3.430) with Equation (3.443) gives:

$$\int_{-h}^{\bar{\eta}} \frac{\partial f}{\partial z} \frac{\partial f}{\partial z} dz = \frac{-\kappa^2 C C_g}{g} + \lambda' \quad (3.444)$$

Equation (3.444) may also be written as:

$$\int_{-h}^{\bar{\eta}} \frac{\partial f}{\partial z} \frac{\partial f}{\partial z} dz = \frac{-\kappa^2 C C_g}{g} + \frac{\omega^2 + G_2}{g} \quad (3.445)$$

Working with the third term of Equation (3.431) using Equation (3.226) gives:

$$\begin{aligned} \int_{-h}^{\bar{\eta}} f \frac{d^2 f}{dx_k dx_k} dz &= \left(\int_{-h}^{\bar{\eta}} f \frac{\partial f}{\partial h'} dz \right) \frac{\partial^2 h'}{\partial x_k \partial x_k} + \left(\int_{-h}^{\bar{\eta}} f \frac{\partial f}{\partial \kappa} dz \right) \frac{\partial^2 \kappa}{\partial x_k \partial x_k} + \frac{\partial z'}{\partial \bar{\eta}} \frac{\partial^2 \bar{\eta}}{\partial x_k \partial x_k} \int_{-h}^{\bar{\eta}} f \frac{\partial f}{\partial z'} dz \\ &+ \left[\int_{-h}^{\bar{\eta}} f \frac{\partial^2 f}{\partial h'^2} dz \right] \left(\frac{\partial h'}{\partial x_k} \frac{\partial h'}{\partial x_k} \right) + \left[\int_{-h}^{\bar{\eta}} f \frac{\partial^2 f}{\partial \kappa^2} dz \right] \left(\frac{\partial \kappa}{\partial x_k} \frac{\partial \kappa}{\partial x_k} \right) \\ &+ \left(\frac{\partial z'}{\partial \bar{\eta}} \right)^2 \left(\frac{\partial \bar{\eta}}{\partial x_k} \frac{\partial \bar{\eta}}{\partial x_k} \right) \int_{-h}^{\bar{\eta}} f \frac{\partial^2 f}{\partial z'^2} dz + 2 \left(\int_{-h}^{\bar{\eta}} f \frac{\partial^2 f}{\partial h' \partial \kappa} dz \right) \frac{\partial \kappa}{\partial x_k} \frac{\partial h'}{\partial x_k} \\ &+ 2 \left(\int_{-h}^{\bar{\eta}} f \frac{\partial^2 f}{\partial h' \partial z'} dz \right) \frac{\partial z'}{\partial \bar{\eta}} \frac{\partial h'}{\partial x_k} \frac{\partial \bar{\eta}}{\partial x_k} + 2 \left(\int_{-h}^{\bar{\eta}} f \frac{\partial^2 f}{\partial z' \partial \kappa} dz \right) \frac{\partial z'}{\partial \bar{\eta}} \frac{\partial \bar{\eta}}{\partial x_k} \frac{d\kappa}{dx_k} \end{aligned} \quad (3.446)$$

Each of the integrals in Equation (3.446) is now examined in turn with reference to the various equations described in the summary section above, Equations (3.213), (3.281), (3.287), (3.292), (3.301), (3.326), (3.304), (3.313), (3.337), (3.345) and (3.348):

$$\int_{-h}^{\bar{\eta}} f \frac{\partial f}{\partial \kappa} dz = \frac{1}{\cosh^2 \kappa h'} \int_{-h}^{\bar{\eta}} \left((h' + z') \sinh [\kappa (h' + z')] \cosh [\kappa (h' + z')] \right) dz \quad (3.447)$$

$$\int_{-h}^{\bar{\eta}} f \frac{\partial f}{\partial \kappa} dz = \frac{1}{\cosh^2 \kappa h'} \left[\int_{-h}^{\bar{\eta}} (h' + z') \sinh [\kappa (h' + z')] \cosh [\kappa (h' + z')] dz \right] \quad (3.448)$$

$$\int_{-h}^{\bar{\eta}} f \frac{\partial f}{\partial \kappa} dz = \frac{1}{\cosh^2 \kappa h'} \left[I_3 - \frac{h' \lambda'}{\kappa} I_1 \right] \quad (3.449)$$

$$\int_{-h}^{\bar{\eta}} f \frac{\partial f}{\partial h'} dz = \frac{1}{\cosh^2 \kappa h'} \int_{-h}^{\bar{\eta}} \left(\kappa \sinh[\kappa(h' + z')] \cosh[\kappa(h' + z')] \right. \\ \left. - \lambda' \cosh^2[\kappa(h' + z')] \right) dz \quad (3.450)$$

$$\int_{-h}^{\bar{\eta}} f \frac{\partial f}{\partial h'} dz = \frac{1}{\cosh^2 \kappa h'} \left(\kappa \int_{-h}^{\bar{\eta}} \sinh[\kappa(h' + z')] \cosh[\kappa(h' + z')] dz \right. \\ \left. - \lambda' \int_{-h}^{\bar{\eta}} \cosh^2[\kappa(h' + z')] dz \right) \quad (3.451)$$

$$\int_{-h}^{\bar{\eta}} f \frac{\partial f}{\partial h'} dz = \frac{1}{\cosh^2 \kappa h'} [\kappa I_2 - \lambda' I_1] \quad (3.452)$$

$$\int_{-h}^{\bar{\eta}} f \frac{\partial^2 f}{\partial \kappa^2} dz = \frac{1}{\cosh^2 \kappa h'} \int_{-h}^{\bar{\eta}} \left(-\frac{2h' \lambda'}{\kappa} (h' + z') \sinh[\kappa(h' + z')] \cosh[\kappa(h' + z')] \right. \\ \left. + \left(z'^2 + \frac{2h'^2 \lambda'^2}{\kappa^2} + 2h' z' \right) \cosh^2[\kappa(h' + z')] \right) dz \quad (3.453)$$

$$\int_{-h}^{\bar{\eta}} f \frac{\partial^2 f}{\partial \kappa^2} dz = \frac{1}{\cosh^2 \kappa h'} \left(-\frac{2h' \lambda'}{\kappa} \int_{-h}^{\bar{\eta}} (h' + z') \sinh[\kappa(h' + z')] \cosh[\kappa(h' + z')] dz \right. \\ \left. + \left(\frac{2h'^2 \lambda'^2}{\kappa^2} - h'^2 \right) \int_{-h}^{\bar{\eta}} \cosh^2[\kappa(h' + z')] dz \right. \\ \left. + \int_{-h}^{\bar{\eta}} (h' + z')^2 \cosh^2[\kappa(h' + z')] dz \right) \quad (3.454)$$

$$\int_{-h}^{\bar{\eta}} f \frac{\partial^2 f}{\partial \kappa^2} dz = \frac{1}{\cosh^2 \kappa h'} \left(-\frac{2h' \lambda'}{\kappa} I_3 + \left(\frac{2h'^2 \lambda'^2}{\kappa^2} - h'^2 \right) I_1 + I_5 \right) \quad (3.455)$$

$$\int_{-h}^{\bar{\eta}} f \frac{\partial^2 f}{\partial h'^2} dz = \frac{1}{\cosh^2 \kappa h'} \int_{-h}^{\bar{\eta}} \left(-2\kappa \lambda' \sinh[\kappa(h' + z')] \cosh[\kappa(h' + z')] \right. \\ \left. + 2\lambda'^2 \cosh^2[\kappa(h' + z')] \right) dz \quad (3.456)$$

$$\int_{-h}^{\bar{\eta}} f \frac{\partial^2 f}{\partial h'^2} dz = \frac{1}{\cosh^2 \kappa h'} \left(\begin{aligned} &2\lambda'^2 \int_{-h}^{\bar{\eta}} \cosh^2 [\kappa(h' + z')] dz \\ &-2\kappa\lambda' \int_{-h}^{\bar{\eta}} \sinh [\kappa(h' + z')] \cosh [\kappa(h' + z')] dz \end{aligned} \right) \quad (3.457)$$

$$\int_{-h}^{\bar{\eta}} f \frac{\partial^2 f}{\partial h'^2} dz = \frac{1}{\cosh^2 \kappa h'} (2\lambda'^2 I_1 - 2\kappa\lambda' I_2) \quad (3.458)$$

$$\int_{-h}^{\bar{\eta}} f \frac{\partial^2 f}{\partial h' \partial \kappa} dz = \frac{1}{\cosh^2 \kappa h'} \int_{-h}^{\bar{\eta}} \left(\begin{aligned} &\left(\kappa z' - \frac{\lambda'}{\kappa} + \frac{2h'\lambda'^2}{\kappa} \right) \cosh^2 [\kappa(h' + z')] \\ &(1 - 2h'\lambda' - z'\lambda') \sinh [\kappa(h' + z')] \cosh [\kappa(h' + z')] \end{aligned} \right) dz \quad (3.459)$$

$$\int_{-h}^{\bar{\eta}} f \frac{\partial^2 f}{\partial h' \partial \kappa} dz = \frac{1}{\cosh^2 \kappa h'} \left[\begin{aligned} &\left(\frac{2h'\lambda'^2}{\kappa} - \frac{\lambda'}{\kappa} - \kappa h' \right) \int_{-h}^{\bar{\eta}} \cosh^2 [\kappa(h' + z')] dz \\ &+ \kappa \int_{-h}^{\bar{\eta}} (h' + z') \cosh^2 [\kappa(h' + z')] dz \\ &+ (1 - h'\lambda') \int_{-h}^{\bar{\eta}} \sinh [\kappa(h' + z')] \cosh [\kappa(h' + z')] dz \\ &- \lambda' \int_{-h}^{\bar{\eta}} (z' + h') \sinh [\kappa(h' + z')] \cosh [\kappa(h' + z')] dz \end{aligned} \right] \quad (3.460)$$

$$\int_{-h}^{\bar{\eta}} f \frac{\partial^2 f}{\partial h' \partial \kappa} dz = \frac{1}{\cosh^2 \kappa h'} \left[\left(\frac{2h'\lambda'^2}{\kappa} - \frac{\lambda'}{\kappa} - \kappa h' \right) I_1 + \kappa I_4 + (1 - h'\lambda') I_2 - \lambda' I_3 \right] \quad (3.461)$$

$$\int_{-h}^{\bar{\eta}} f \frac{\partial f}{\partial z'} dz = \frac{1}{\cosh^2 \kappa h'} \int_{-h}^{\bar{\eta}} \kappa \sinh [\kappa(h' + z')] \cosh [\kappa(h' + z')] dz \quad (3.462)$$

$$\int_{-h}^{\bar{\eta}} f \frac{\partial f}{\partial z'} dz = \frac{1}{\cosh^2 \kappa h'} \left(\kappa \int_{-h}^{\bar{\eta}} \sinh [\kappa(h' + z')] \cosh [\kappa(h' + z')] dz \right) \quad (3.463)$$

$$\int_{-h}^{\bar{\eta}} f \frac{\partial f}{\partial z'} dz = \frac{1}{\cosh^2 \kappa h'} (\kappa I_2) \quad (3.464)$$

$$\int_{-h}^{\bar{\eta}} f \frac{\partial^2 f}{\partial z'^2} dz = \frac{1}{\cosh^2 \kappa h'} \int_{-h}^{\bar{\eta}} \kappa^2 \cosh^2 [\kappa(h' + z')] dz \quad (3.465)$$

$$\int_{-h}^{\bar{\eta}} f \frac{\partial^2 f}{\partial z'^2} dz = \frac{1}{\cosh^2 \kappa h'} \left(\kappa^2 \int_{-h}^{\bar{\eta}} \cosh^2 [\kappa(h' + z')] dz \right) \quad (3.466)$$

$$\int_{-h}^{\bar{\eta}} f \frac{\partial^2 f}{\partial z'^2} dz = \frac{1}{\cosh^2 \kappa h'} (\kappa^2 I_1) \quad (3.467)$$

$$\int_{-h}^{\bar{\eta}} f \frac{\partial^2 f}{\partial \kappa \partial z'} dz = \frac{1}{\cosh^3 \kappa h'} \int_{-h}^{\bar{\eta}} \begin{pmatrix} \kappa(h' + z') \cosh \kappa h' \cosh^2 [\kappa(h' + z')] \\ + \cosh \kappa h' \sinh [\kappa(h' + z')] \cosh [\kappa(h' + z')] \\ - \kappa h' \sinh \kappa h' \sinh [\kappa(h' + z')] \cosh [\kappa(h' + z')] \end{pmatrix} dz \quad (3.468)$$

$$\int_{-h}^{\bar{\eta}} f \frac{\partial^2 f}{\partial \kappa \partial z'} dz = \frac{1}{\cosh^3 \kappa h'} \begin{pmatrix} \kappa \cosh \kappa h' \int_{-h}^{\bar{\eta}} (h' + z') \cosh^2 [\kappa(h' + z')] dz \\ + \cosh \kappa h' \int_{-h}^{\bar{\eta}} \sinh [\kappa(h' + z')] \cosh [\kappa(h' + z')] dz \\ - \kappa h' \sinh \kappa h' \int_{-h}^{\bar{\eta}} \sinh [\kappa(h' + z')] \cosh [\kappa(h' + z')] dz \end{pmatrix} \quad (3.469)$$

$$\int_{-h}^{\bar{\eta}} f \frac{\partial^2 f}{\partial \kappa \partial z'} dz = \frac{1}{\cosh^2 \kappa h'} \begin{pmatrix} \kappa \int_{-h}^{\bar{\eta}} (h' + z') \cosh^2 [\kappa(h' + z')] dz \\ + \int_{-h}^{\bar{\eta}} \sinh [\kappa(h' + z')] \cosh [\kappa(h' + z')] dz \\ - \kappa h' \tanh \kappa h' \int_{-h}^{\bar{\eta}} \sinh [\kappa(h' + z')] \cosh [\kappa(h' + z')] dz \end{pmatrix} \quad (3.470)$$

$$\int_{-h}^{\bar{\eta}} f \frac{\partial^2 f}{\partial \kappa \partial z'} dz = \frac{1}{\cosh^2 \kappa h'} \begin{pmatrix} \kappa \int_{-h}^{\bar{\eta}} (h' + z') \cosh^2 [\kappa(h' + z')] dz \\ + \int_{-h}^{\bar{\eta}} \sinh [\kappa(h' + z')] \cosh [\kappa(h' + z')] dz \\ - h' \lambda \int_{-h}^{\bar{\eta}} \sinh [\kappa(h' + z')] \cosh [\kappa(h' + z')] dz \end{pmatrix} \quad (3.471)$$

$$\int_{-h}^{\bar{\eta}} f \frac{\partial^2 f}{\partial \kappa \partial z'} dz = \frac{1}{\cosh^2 \kappa h'} \left(\kappa \int_{-h}^{\bar{\eta}} (h' + z') \cosh^2 [\kappa(h' + z')] dz + (1 - h' \lambda') I_2 \right) \quad (3.472)$$

$$\int_{-h}^{\bar{\eta}} f \frac{\partial^2 f}{\partial \kappa \partial z'} dz = \frac{1}{\cosh^2 \kappa h'} (\kappa I_4 + (1 - h' \lambda') I_2) \quad (3.473)$$

$$\int_{-h}^{\bar{\eta}} f \frac{\partial^2 f}{\partial z' \partial h'} dz = \frac{1}{\cosh^3 \kappa h'} \int_{-h}^{\bar{\eta}} \left(\kappa^2 \cosh \kappa h' \cosh^2 [\kappa(h' + z')] \right. \\ \left. - \kappa^2 \sinh \kappa h' \sinh [\kappa(h' + z')] \cosh [\kappa(h' + z')] \right) dz \quad (3.474)$$

$$\int_{-h}^{\bar{\eta}} f \frac{\partial^2 f}{\partial z' \partial h'} dz = \frac{1}{\cosh^3 \kappa h'} \left(\kappa^2 \cosh \kappa h' \int_{-h}^{\bar{\eta}} \cosh^2 [\kappa(h' + z')] dz \right. \\ \left. - \kappa^2 \sinh \kappa h' \int_{-h}^{\bar{\eta}} \sinh [\kappa(h' + z')] \cosh [\kappa(h' + z')] dz \right) \quad (3.475)$$

$$\int_{-h}^{\bar{\eta}} f \frac{\partial^2 f}{\partial z' \partial h'} dz = \frac{1}{\cosh^3 \kappa h'} (\kappa^2 \cosh \kappa h' I_1 - \kappa^2 \sinh \kappa h' I_2) \quad (3.476)$$

$$\int_{-h}^{\bar{\eta}} f \frac{\partial^2 f}{\partial z' \partial h'} dz = \frac{1}{\cosh^2 \kappa h'} (\kappa^2 I_1 - \kappa^2 \tanh \kappa h' I_2) \quad (3.477)$$

$$\int_{-h}^{\bar{\eta}} f \frac{\partial^2 f}{\partial z' \partial h'} dz = \frac{1}{\cosh^2 \kappa h'} (\kappa^2 I_1 - \kappa \lambda' I_2) \quad (3.478)$$

Where:

$$I_1 = \int_{-h}^{\bar{\eta}} \cosh^2 [\kappa(h' + z')] dz \quad (3.479)$$

$$I_2 = \int_{-h}^{\bar{\eta}} \cosh [\kappa(h' + z')] \sinh [\kappa(h' + z')] dz \quad (3.480)$$

$$I_3 = \int_{-h}^{\bar{\eta}} (h' + z') \cosh [\kappa(h' + z')] \sinh [\kappa(h' + z')] dz \quad (3.481)$$

$$I_4 = \int_{-h}^{\bar{\eta}} (h' + z') \cosh^2 [\kappa(h' + z')] dz \quad (3.482)$$

$$I_5 = \int_{-h}^{\bar{\eta}} (h' + z')^2 \cosh^2 [\kappa(h' + z')] dz \quad (3.483)$$

The integrals from I_1 to I_5 are expanded in detail in Section 3.7.7.

Substituting Equations (3.449), (3.452), (3.455), (3.458), (3.461), (3.464), (3.467), (3.470), (3.473) and (3.478) into Equation (3.446) gives:

$$\begin{aligned}
\int_{-h}^{\bar{\eta}} f \frac{d^2 f}{dx_k dx_k} dz = & \left(\frac{1}{\cosh^2 \kappa h'} [\kappa I_2 - \lambda' I_1] \right) \frac{\partial^2 h'}{\partial x_k \partial x_k} + \left(\frac{1}{\cosh^2 \kappa h'} \left[I_3 - \frac{h' \lambda'}{\kappa} I_1 \right] \right) \frac{\partial^2 \kappa}{\partial x_k \partial x_k} \\
& + \frac{\partial z'}{\partial \bar{\eta}} \frac{\partial^2 \bar{\eta}}{\partial x_k \partial x_k} \left[\frac{1}{\cosh^2 \kappa h'} (\kappa I_2) \right] + \left[\frac{1}{\cosh^2 \kappa h'} (2\lambda'^2 I_1 - 2\kappa \lambda' I_2) \right] \left(\frac{\partial h'}{\partial x_k} \frac{\partial h'}{\partial x_k} \right) \\
& + \left[\frac{1}{\cosh^2 \kappa h'} \left(-\frac{2h' \lambda'}{\kappa} I_3 + \left(\frac{2h'^2 \lambda'^2}{\kappa^2} - h'^2 \right) I_1 + I_5 \right) \right] \left(\frac{\partial \kappa}{\partial x_k} \frac{\partial \kappa}{\partial x_k} \right) \\
& + \left(\frac{\partial z'}{\partial \bar{\eta}} \right)^2 \left(\frac{\partial \bar{\eta}}{\partial x_k} \frac{\partial \bar{\eta}}{\partial x_k} \right) \left[\frac{1}{\cosh^2 \kappa h'} (\kappa^2 I_1) \right] \\
& + 2 \left(\frac{1}{\cosh^2 \kappa h'} \left[\left(\frac{2h' \lambda'^2}{\kappa} - \frac{\lambda'}{\kappa} - \kappa h' \right) I_1 + \kappa I_4 + (1 - h' \lambda') I_2 - \lambda' I_3 \right] \right) \frac{\partial \kappa}{\partial x_k} \frac{\partial h'}{\partial x_k} \\
& + 2 \left(\frac{1}{\cosh^2 \kappa h'} (\kappa^2 I_1 - \kappa \lambda' I_2) \right) \frac{\partial z'}{\partial \bar{\eta}} \frac{\partial h'}{\partial x_k} \frac{\partial \bar{\eta}}{\partial x_k} \\
& + 2 \left(\frac{1}{\cosh^2 \kappa h'} (\kappa I_4 + (1 - h' \lambda') I_2) \right) \frac{\partial z'}{\partial \bar{\eta}} \frac{\partial \bar{\eta}}{\partial x_k} \frac{\partial \kappa}{\partial x_k}
\end{aligned} \tag{3.484}$$

Equation (3.484) can be rewritten as follows:

$$\begin{aligned}
\int_{-h}^{\bar{\eta}} f \frac{d^2 f}{dx_k dx_k} dz = & \frac{\lambda'}{\cosh^2 \kappa h'} \left(-I_1 + \frac{\kappa}{\lambda'} I_2 \right) \frac{\partial^2 h'}{\partial x_k \partial x_k} + \frac{\lambda'}{\cosh^2 \kappa h'} \left(-\frac{h'}{\kappa} I_1 + \frac{1}{\lambda'} I_3 \right) \frac{\partial^2 \kappa}{\partial x_k \partial x_k} \\
& + \frac{\lambda'}{\cosh^2 \kappa h'} \left[\frac{\kappa}{\lambda'} \frac{\partial z'}{\partial \bar{\eta}} I_2 \right] \frac{\partial^2 \bar{\eta}}{\partial x_k \partial x_k} + \frac{\lambda'}{\cosh^2 \kappa h'} [2\lambda' I_1 - 2\kappa I_2] \left(\frac{\partial h'}{\partial x_k} \frac{\partial h'}{\partial x_k} \right) \\
& + \frac{\lambda'}{\cosh^2 \kappa h'} \left[\left(\frac{2h'^2 \lambda'}{\kappa^2} - \frac{h'^2}{\lambda'} \right) I_1 - \frac{2h'}{\kappa} I_3 + \frac{1}{\lambda'} I_5 \right] \left(\frac{\partial \kappa}{\partial x_k} \frac{\partial \kappa}{\partial x_k} \right) \\
& + \frac{\lambda'}{\cosh^2 \kappa h'} \left[\frac{\kappa^2}{\lambda'} \left(\frac{\partial z'}{\partial \bar{\eta}} \right)^2 I_1 \right] \left(\frac{\partial \bar{\eta}}{\partial x_k} \frac{\partial \bar{\eta}}{\partial x_k} \right) \\
& + \frac{\lambda'}{\cosh^2 \kappa h'} \left(\left(\frac{4h' \lambda'}{\kappa} - \frac{2}{\kappa} - \frac{2\kappa}{\lambda'} h' \right) I_1 + \left(\frac{2}{\lambda'} - 2h' \right) I_2 - 2I_3 + \frac{2\kappa}{\lambda'} I_4 \right) \frac{\partial \kappa}{\partial x_k} \frac{\partial h'}{\partial x_k} \\
& + \frac{\lambda'}{\cosh^2 \kappa h'} \left(\frac{2\kappa^2}{\lambda'} \frac{\partial z'}{\partial \bar{\eta}} I_1 - 2\kappa \frac{\partial z'}{\partial \bar{\eta}} I_2 \right) \frac{\partial h'}{\partial x_k} \frac{\partial \bar{\eta}}{\partial x_k} \\
& + \frac{\lambda'}{\cosh^2 \kappa h'} \left(\left(\frac{2}{\lambda'} - 2h' \right) \frac{\partial z'}{\partial \bar{\eta}} I_2 + \frac{2\kappa}{\lambda'} \frac{\partial z'}{\partial \bar{\eta}} I_4 \right) \frac{\partial \bar{\eta}}{\partial x_k} \frac{\partial \kappa}{\partial x_k}
\end{aligned} \tag{3.485}$$

Selecting a set of coefficients yields:

$$\begin{aligned}
\int_{-h}^{\bar{\eta}} f \frac{d^2 f}{dx_k dx_k} dz = & \frac{\lambda'}{\cosh^2 \kappa h'} (A_1 I_1 + A_2 I_2) \frac{\partial^2 h'}{\partial x_k \partial x_k} + \frac{\lambda'}{\cosh^2 \kappa h'} (B_1 I_1 + B_3 I_3) \frac{\partial^2 \kappa}{\partial x_k \partial x_k} \\
& + \frac{\lambda'}{\cosh^2 \kappa h'} [C_2 I_2] \frac{\partial^2 \bar{\eta}}{\partial x_k \partial x_k} + \frac{\lambda'}{\cosh^2 \kappa h'} [D_1 I_1 + D_2 I_2] \left(\frac{\partial h'}{\partial x_k} \frac{\partial h'}{\partial x_k} \right) \\
& + \frac{\lambda'}{\cosh^2 \kappa h'} [E_1 I_1 + E_3 I_3 + E_5 I_5] \left(\frac{\partial \kappa}{\partial x_k} \frac{\partial \kappa}{\partial x_k} \right) \\
& + \frac{\lambda'}{\cosh^2 \kappa h'} [H_1 I_1] \left(\frac{\partial z'}{\partial \bar{\eta}} \right)^2 \left(\frac{\partial \bar{\eta}}{\partial x_k} \frac{\partial \bar{\eta}}{\partial x_k} \right) \\
& + \frac{\lambda'}{\cosh^2 \kappa h'} (J_1 I_1 + J_2 I_2 + J_3 I_3 + J_4 I_4) \frac{\partial \kappa}{\partial x_k} \frac{\partial h'}{\partial x_k} \\
& + \frac{\lambda'}{\cosh^2 \kappa h'} (M_1 I_1 + M_2 I_2) \frac{\partial h'}{\partial x_k} \frac{\partial \bar{\eta}}{\partial x_k} \\
& + \frac{\lambda'}{\cosh^2 \kappa h'} (P_2 I_2 + P_4 I_4) \frac{\partial \bar{\eta}}{\partial x_k} \frac{\partial \kappa}{\partial x_k}
\end{aligned} \tag{3.486}$$

Where

$$A_1 = -1 \tag{3.487}$$

$$A_2 = \frac{\kappa}{\lambda'} \tag{3.488}$$

$$B_1 = -\frac{h'}{\kappa} \tag{3.489}$$

$$B_3 = \frac{1}{\lambda'} \tag{3.490}$$

$$C_2 = \frac{\kappa}{\lambda'} \frac{\partial z'}{\partial \bar{\eta}} \tag{3.491}$$

$$D_1 = 2\lambda' \tag{3.492}$$

$$D_2 = -2\kappa \tag{3.493}$$

$$E_1 = \frac{2h'^2 \lambda'}{\kappa^2} - \frac{h'^2}{\lambda'} \tag{3.494}$$

$$E_3 = -\frac{2h'}{\kappa} \tag{3.495}$$

$$E_5 = \frac{1}{\lambda'} \tag{3.496}$$

$$H_1 = \frac{\kappa^2}{\lambda'} \left(\frac{\partial z'}{\partial \bar{\eta}} \right)^2 \tag{3.497}$$

$$J_1 = \frac{4h' \lambda'}{\kappa} - \frac{2}{\kappa} - \frac{2\kappa}{\lambda'} h' \tag{3.498}$$

$$J_2 = \frac{2}{\lambda'} - 2h' \quad (3.499)$$

$$J_3 = -2 \quad (3.500)$$

$$J_4 = \frac{2\kappa}{\lambda'} \quad (3.501)$$

$$M_1 = \frac{2\kappa^2}{\lambda'} \frac{\partial z'}{\partial \bar{\eta}} \quad (3.502)$$

$$M_2 = -2\kappa \frac{\partial z'}{\partial \bar{\eta}} \quad (3.503)$$

$$P_2 = \left(\frac{2}{\lambda'} - 2h' \right) \frac{\partial z'}{\partial \bar{\eta}} \quad (3.504)$$

$$P_4 = \frac{2\kappa}{\lambda'} \frac{\partial z'}{\partial \bar{\eta}} \quad (3.505)$$

Examining the last term of Equation (3.431) gives:

$$f\phi \frac{\partial f}{\partial x_k} \frac{\partial h}{\partial x_k} \bigg|_{-h} = \phi \frac{\partial h}{\partial x_k} \left(f \frac{\partial f}{\partial x_k} \bigg|_{-h} \right) \quad (3.506)$$

Using the definitions of (3.217) and (3.219):

$$h' = h + \bar{\eta}$$

$$z' = z - \bar{\eta}$$

when $z = -h$

$$z' = -h'$$

From Equation (3.353) the horizontal derivative of the vertical function can be obtained at the seabed, where $z' = -h'$:

$$\begin{aligned} \frac{df}{dx_k} = & \left(\frac{-h' \cosh[0] \sinh \kappa h'}{\cosh^2 \kappa h'} \right) \frac{\partial \kappa}{\partial x_k} \\ & + \left(\frac{\kappa \cosh \kappa h' \sinh[0]}{\cosh^2 \kappa h'} \right) \frac{\partial h'}{\partial x_k} \\ & + \left(\frac{\kappa \sinh[0]}{\cosh \kappa h'} \right) (-1) \frac{\partial \bar{\eta}}{\partial x_k} \end{aligned} \quad (3.507)$$

Simplification of Equation (3.507) gives:

$$\frac{df}{dx_k} = \left(\frac{-h' \sinh \kappa h'}{\cosh^2 \kappa h'} \right) \frac{\partial \kappa}{\partial x_k} + \left(\frac{-\kappa \sinh \kappa h'}{\cosh^2 \kappa h'} \right) \frac{\partial h'}{\partial x_k} \quad (3.508)$$

Calculation of the vertical function from Equation (3.197) at $z' = -h'$ gives:

$$f = \frac{1}{\cosh \kappa h'} \quad (3.509)$$

Equation (3.506) can be rewritten using Equations (3.508) and (3.509):

$$f \phi \frac{\partial f}{\partial x_k} \frac{\partial h}{\partial x_k} \Big|_{-h} = \phi \frac{\partial h}{\partial x_k} \frac{1}{\cosh \kappa h'} \left(\left(\frac{-h' \sinh \kappa h'}{\cosh^2 \kappa h'} \right) \frac{\partial \kappa}{\partial x_k} + \left(\frac{-\kappa \sinh \kappa h'}{\cosh^2 \kappa h'} \right) \frac{\partial h'}{\partial x_k} \right) \quad (3.510)$$

Equation (3.510) can be rewritten as follows:

$$f \phi \frac{\partial f}{\partial x_k} \frac{\partial h}{\partial x_k} \Big|_{-h} = \phi \frac{\partial h}{\partial x_k} \frac{1}{\cosh^2 \kappa h'} \left((-h' \tanh \kappa h') \frac{\partial \kappa}{\partial x_k} + (-\kappa \tanh \kappa h') \frac{\partial h'}{\partial x_k} \right) \quad (3.511)$$

Equation (3.511) can be written more symbolically as:

$$f \phi \frac{\partial f}{\partial x_k} \frac{\partial h}{\partial x_k} \Big|_{-h} = \phi \frac{\partial h}{\partial x_k} \frac{\lambda'}{\cosh^2 \kappa h'} \left(\frac{-h'}{\kappa} \frac{\partial \kappa}{\partial x_k} - \frac{\partial h'}{\partial x_k} \right) \quad (3.512)$$

Selecting a coefficient W_6 in Equation (3.512) gives:

$$f \phi \frac{\partial f}{\partial x_k} \frac{\partial h}{\partial x_k} \Big|_{-h} = \phi \left(\frac{\partial h'}{\partial x_k} - \frac{\partial \bar{\eta}}{\partial x_k} \right) \frac{\lambda'}{\cosh^2 \kappa h'} W_6 \quad (3.513)$$

Expanding Equation (3.513) gives:

$$f \phi \frac{\partial f}{\partial x_k} \frac{\partial h}{\partial x_k} \Big|_{-h} = \phi \frac{\lambda'}{\cosh^2 \kappa h'} \left(\frac{\partial h'}{\partial x_k} \right) W_6 - \phi \frac{\lambda'}{\cosh^2 \kappa h'} \left(\frac{\partial \bar{\eta}}{\partial x_k} \right) W_6 \quad (3.514)$$

Combining Equations (3.514) and (3.486) gives:

$$\begin{aligned}
 \int_{-h}^{\bar{\eta}} f \frac{d^2 f}{dx_k dx_k} dz + f \frac{\partial f}{\partial x_k} \frac{\partial h}{\partial x_k} \Big|_{-h} &= \frac{\lambda'}{\cosh^2 \kappa h'} (A_1 I_1 + A_2 I_2) \frac{\partial^2 h'}{\partial x_k \partial x_k} + \frac{\lambda'}{\cosh^2 \kappa h'} (B_1 I_1 + B_3 I_3) \frac{\partial^2 \kappa}{\partial x_k \partial x_k} \\
 &+ \frac{\lambda'}{\cosh^2 \kappa h'} [C_2 I_2] \frac{\partial^2 \bar{\eta}}{\partial x_k^2} + \frac{\lambda'}{\cosh^2 \kappa h'} [D_1 I_1 + D_2 I_2 + W_6] \left(\frac{\partial h'}{\partial x_k} \frac{\partial h'}{\partial x_k} \right) \\
 &+ \frac{\lambda'}{\cosh^2 \kappa h'} [E_1 I_1 + E_3 I_3 + E_5 I_5] \left(\frac{\partial \kappa}{\partial x_k} \frac{\partial \kappa}{\partial x_k} \right) \\
 &+ \frac{\lambda'}{\cosh^2 \kappa h'} [H_1 I_1 + W_6] \left(\frac{\partial z'}{\partial \bar{\eta}} \right)^2 \left(\frac{\partial \bar{\eta}}{\partial x_k} \frac{\partial \bar{\eta}}{\partial x_k} \right) \\
 &+ \frac{\lambda'}{\cosh^2 \kappa h'} (J_1 I_1 + J_2 I_2 + J_3 I_3 + J_4 I_4) \frac{\partial \kappa}{\partial x_k} \frac{\partial h'}{\partial x_k} \\
 &+ \frac{\lambda'}{\cosh^2 \kappa h'} (M_1 I_1 + M_2 I_2 - 2W_6) \frac{\partial h'}{\partial x_k} \frac{\partial \bar{\eta}}{\partial x_k} \\
 &+ \frac{\lambda'}{\cosh^2 \kappa h'} (P_2 I_2 + P_4 I_4) \frac{\partial \bar{\eta}}{\partial x_k} \frac{\partial \kappa}{\partial x_k} \\
 &+ \frac{\lambda'}{\cosh^2 \kappa h'} (W_6) \frac{\partial h'}{\partial x_k} - \frac{\lambda'}{\cosh^2 \kappa h'} (W_6) \frac{\partial \bar{\eta}}{\partial x_k}
 \end{aligned} \tag{3.515}$$

Selecting appropriate symbolic notation for the coefficients of Equation (3.515) gives:

$$\int_{-h}^{\bar{\eta}} f \frac{d^2 f}{dx_k dx_k} dz + f \frac{\partial f}{\partial x_k} \frac{\partial h}{\partial x_k} \Big|_{-h} = \frac{\lambda'}{\cosh^2 \kappa h'} \left(\begin{aligned} &Q_1 \frac{\partial^2 h'}{\partial x_k \partial x_k} + Q_2 \frac{\partial^2 \kappa}{\partial x_k^2} + Q_3 \frac{\partial^2 \bar{\eta}}{\partial x_k \partial x_k} + Q_4 \left(\frac{\partial h'}{\partial x_k} \frac{\partial h'}{\partial x_k} \right) \\ &+ Q_5 \left(\frac{\partial \kappa}{\partial x_k} \frac{\partial \kappa}{\partial x_k} \right) + Q_6 \left(\frac{\partial \bar{\eta}}{\partial x_k} \frac{\partial \bar{\eta}}{\partial x_k} \right) + Q_7 \frac{\partial \kappa}{\partial x_k} \frac{\partial h'}{\partial x_k} \\ &+ Q_8 \frac{\partial h'}{\partial x_k} \frac{\partial \bar{\eta}}{\partial x_k} + Q_9 \frac{\partial \bar{\eta}}{\partial x_k} \frac{\partial \kappa}{\partial x_k} + W_6 \frac{\partial h'}{\partial x_k} - W_6 \frac{\partial \bar{\eta}}{\partial x_k} \end{aligned} \right) \tag{3.516}$$

Where:

$$Q_1 = A_1 I_1 + A_2 I_2 \tag{3.517}$$

$$Q_2 = B_1 I_1 + B_3 I_3 \tag{3.518}$$

$$Q_3 = C_2 I_2 \tag{3.519}$$

$$Q_4 = D_1 I_1 + D_2 I_2 \tag{3.520}$$

$$Q_5 = E_1 I_1 + E_3 I_3 + E_5 I_5 \tag{3.521}$$

$$Q_6 = H_1 I_1 \tag{3.522}$$

$$Q_7 = J_1 I_1 + J_2 I_2 + J_3 I_3 + J_4 I_4 \tag{3.523}$$

$$Q_8 = M_1 I_1 + M_2 I_2 \tag{3.524}$$

$$Q_9 = P_2 I_2 + P_4 I_4 \tag{3.525}$$

3.7.6 Complete Mild-Slope Equation

To assemble the complete Mild-Slope Equation it is necessary to substitute Equations (3.393), (3.445) and (3.516) into Equation (3.431) as follows:

$$\begin{aligned}
& \frac{\partial^2 \phi}{\partial x_k \partial x_k} \frac{CC_g}{g} + \frac{\partial \phi}{\partial x_k} \frac{\partial}{\partial x_k} \left(\frac{CC_g}{g} \right) + \frac{\phi \lambda'}{\cosh^2 \kappa h'} \left(\begin{aligned} & Q_1 \frac{\partial^2 h'}{\partial x_k \partial x_k} + Q_2 \frac{\partial^2 \kappa}{\partial x_k^2} + Q_3 \frac{\partial^2 \bar{\eta}}{\partial x_k \partial x_k} + Q_4 \left(\frac{\partial h'}{\partial x_k} \frac{\partial h'}{\partial x_k} \right) \\ & + Q_5 \left(\frac{\partial \kappa}{\partial x_k} \frac{\partial \kappa}{\partial x_k} \right) + Q_6 \left(\frac{\partial \bar{\eta}}{\partial x_k} \frac{\partial \bar{\eta}}{\partial x_k} \right) + Q_7 \frac{\partial \kappa}{\partial x_k} \frac{\partial h'}{\partial x_k} \\ & + Q_8 \frac{\partial h'}{\partial x_k} \frac{\partial \bar{\eta}}{\partial x_k} + Q_9 \frac{\partial \bar{\eta}}{\partial x_k} \frac{\partial \kappa}{\partial x_k} + W_6 \frac{\partial h'}{\partial x_k} - W_6 \frac{\partial \bar{\eta}}{\partial x_k} \end{aligned} \right) \\
& - \phi \left(\frac{-\kappa^2 CC_g}{g} + \lambda' \right) - \frac{\partial \phi}{\partial x_k} \left(\frac{\partial \bar{\eta}}{\partial x_k} \right) + \frac{1}{g} \left[\begin{aligned} & \omega^2 \phi - 2i\omega \lambda' U_k \frac{\partial \bar{\eta}}{\partial x_k} \phi + 2i\omega U_k \frac{\partial \phi}{\partial x_k} + i\omega \frac{\partial U_j}{\partial x_j} \phi \\ & - U_k \frac{\partial U_j}{\partial x_j} \frac{\partial \phi}{\partial x_k} + \lambda' U_k \frac{\partial U_j}{\partial x_j} \frac{\partial \bar{\eta}}{\partial x_k} \phi + \lambda' U_j \frac{\partial \bar{\eta}}{\partial x_k} \frac{\partial U_k}{\partial x_j} \phi \\ & - U_j \frac{\partial U_k}{\partial x_j} \frac{\partial \phi}{\partial x_k} - U_j U_k \frac{\partial^2 \phi}{\partial x_j \partial x_k} + 2\lambda' U_j U_k \frac{\partial \bar{\eta}}{\partial x_j} \frac{\partial \phi}{\partial x_k} \\ & - U_j U_k \phi + \left(\kappa^2 - \lambda'^2 \right) \left(-\frac{\partial \bar{\eta}}{\partial x_k} \frac{\partial h'}{\partial x_j} - \frac{\partial h'}{\partial x_k} \frac{\partial \bar{\eta}}{\partial x_j} \right) \\ & + \left(\kappa h' + \frac{\lambda'}{\kappa} - \frac{h\lambda'^2}{\kappa} \right) \left(-\frac{\partial \bar{\eta}}{\partial x_k} \frac{\partial \kappa}{\partial x_j} - \frac{\partial \kappa}{\partial x_k} \frac{\partial \bar{\eta}}{\partial x_j} \right) \end{aligned} \right] \\
& + \frac{1}{g} \left[-\gamma \frac{\partial U_j}{\partial x_j} \phi + \lambda' \gamma U_j \phi \frac{\partial \bar{\eta}}{\partial x_k} - \gamma U_j \frac{\partial \phi}{\partial x_j} + i\omega \gamma \phi \right] = 0
\end{aligned} \tag{3.526}$$

Multiplying Equation (3.526) by g yields:

$$\begin{aligned}
 & \frac{\partial^2 \phi}{\partial x_k \partial x_k} CC_g + \frac{\partial \phi}{\partial x_k} \frac{\partial (CC_g)}{\partial x_k} + \frac{\phi \sigma^2}{\cosh^2 \kappa h'} \left(Q_1 \frac{\partial^2 h'}{\partial x_k \partial x_k} + Q_2 \frac{\partial^2 \kappa}{\partial x_k^2} + Q_3 \frac{\partial^2 \bar{\eta}}{\partial x_k \partial x_k} + Q_4 \left(\frac{\partial h'}{\partial x_k} \frac{\partial h'}{\partial x_k} \right) \right. \\
 & \quad \left. + Q_5 \left(\frac{\partial \kappa}{\partial x_k} \frac{\partial \kappa}{\partial x_k} \right) + Q_6 \left(\frac{\partial \bar{\eta}}{\partial x_k} \frac{\partial \bar{\eta}}{\partial x_k} \right) + Q_7 \frac{\partial \kappa}{\partial x_k} \frac{\partial h'}{\partial x_k} \right. \\
 & \quad \left. + Q_8 \frac{\partial h'}{\partial x_k} \frac{\partial \bar{\eta}}{\partial x_k} + Q_9 \frac{\partial \bar{\eta}}{\partial x_k} \frac{\partial \kappa}{\partial x_k} + W_6 \frac{\partial h'}{\partial x_k} - W_6 \frac{\partial \bar{\eta}}{\partial x_k} \right) \\
 & + \phi \kappa^2 CC_g - \phi \sigma^2 - g \frac{\partial \phi}{\partial x_k} \left(\frac{\partial \bar{\eta}}{\partial x_k} \right) + \left[\begin{aligned} & \omega^2 \phi - 2i\omega \lambda' U_k \frac{\partial \bar{\eta}}{\partial x_k} \phi + 2i\omega U_k \frac{\partial \phi}{\partial x_k} + i\omega \frac{\partial U_j}{\partial x_j} \phi \\ & - U_k \frac{\partial U_j}{\partial x_j} \frac{\partial \phi}{\partial x_k} + \lambda' U_k \frac{\partial U_j}{\partial x_j} \frac{\partial \bar{\eta}}{\partial x_k} \phi + \lambda' U_j \frac{\partial \bar{\eta}}{\partial x_k} \frac{\partial U_k}{\partial x_j} \phi \\ & - U_j \frac{\partial U_k}{\partial x_j} \frac{\partial \phi}{\partial x_k} - U_j U_k \frac{\partial^2 \phi}{\partial x_j \partial x_k} + 2\lambda' U_j U_k \frac{\partial \bar{\eta}}{\partial x_j} \frac{\partial \phi}{\partial x_k} \\ & - U_j U_k \phi + \left(\kappa^2 - \lambda'^2 \right) \left(-\frac{\partial \bar{\eta}}{\partial x_k} \frac{\partial h'}{\partial x_j} - \frac{\partial h'}{\partial x_k} \frac{\partial \bar{\eta}}{\partial x_j} \right) \\ & + \left(\kappa h' + \frac{\lambda'}{\kappa} - \frac{h \lambda'^2}{\kappa} \right) \left(-\frac{\partial \bar{\eta}}{\partial x_k} \frac{\partial \kappa}{\partial x_j} - \frac{\partial \kappa}{\partial x_k} \frac{\partial \bar{\eta}}{\partial x_j} \right) \end{aligned} \right] \\
 & + \left[i\omega \gamma \phi - \gamma \frac{\partial}{\partial x_j} (U_j \phi) + \lambda' \gamma U_j \phi \frac{\partial \bar{\eta}}{\partial x_k} \right] = 0
 \end{aligned} \tag{3.527}$$

Equation (3.527) is the Complete Extended Mild-Slope Equation including current and energy dissipation.

If $\frac{\partial \bar{\eta}}{\partial x_k}$, $\frac{\partial^2 h'}{\partial x_k \partial x_k}$, $\frac{\partial^2 \kappa}{\partial x_k \partial x_k}$, $\left(\frac{\partial \kappa}{\partial x_k} \frac{\partial \kappa}{\partial x_k}\right)$ and $\left(\frac{\partial h'}{\partial x_k} \frac{\partial h'}{\partial x_k}\right)$ are considered negligible the

Unextended (traditional) Mild-Slope Equation including current and dissipation is obtained. This is the same as the equation of Kirby (1984) with the addition of the energy dissipation terms:

$$\begin{aligned} & \frac{\partial^2 \phi}{\partial x_k \partial x_k} CC_g + \frac{\partial \phi}{\partial x_k} \frac{\partial (CC_g)}{\partial x_k} + \phi \kappa^2 CC_g - \phi \sigma^2 + \omega^2 \phi \\ & + \left[2i\omega U_k \frac{\partial \phi}{\partial x_k} + i\omega \frac{\partial U_j}{\partial x_j} \phi - U_k \frac{\partial U_j}{\partial x_j} \frac{\partial \phi}{\partial x_k} - U_j \frac{\partial U_k}{\partial x_j} \frac{\partial \phi}{\partial x_k} - U_j U_k \frac{\partial^2 \phi}{\partial x_j \partial x_k} \right] \\ & + \left[i\omega \gamma \phi - \gamma \frac{\partial}{\partial x_j} (U_j \phi) \right] = 0 \end{aligned} \quad (3.528)$$

In the absence of current Equation (3.528) becomes the traditional Mild-Slope Equation including breaking of Clyne (2008):

$$\frac{\partial^2 \phi}{\partial x_k \partial x_k} CC_g + \frac{\partial \phi}{\partial x_k} \frac{\partial}{\partial x_k} CC_g + \phi \kappa^2 CC_g + i\omega \gamma \phi = 0 \quad (3.529)$$

In the absence of energy dissipation:

$$\gamma=0 \quad (3.530)$$

Therefore Equation (3.527) can be used to obtain the Complete Extended Mild-Slope Equation including current with no energy dissipation:

$$\begin{aligned} & \frac{\partial^2 \phi}{\partial x_k \partial x_k} CC_g + \frac{\partial \phi}{\partial x_k} \frac{\partial (CC_g)}{\partial x_k} + \frac{\phi \sigma^2}{\cosh^2 \kappa h'} \left(\begin{aligned} & Q_1 \frac{\partial^2 h'}{\partial x_k \partial x_k} + Q_2 \frac{\partial^2 \kappa}{\partial x_k^2} + Q_3 \frac{\partial^2 \bar{\eta}}{\partial x_k \partial x_k} + Q_4 \left(\frac{\partial h'}{\partial x_k} \frac{\partial h'}{\partial x_k} \right) \\ & + Q_5 \left(\frac{\partial \kappa}{\partial x_k} \frac{\partial \kappa}{\partial x_k} \right) + Q_6 \left(\frac{\partial \bar{\eta}}{\partial x_k} \frac{\partial \bar{\eta}}{\partial x_k} \right) + Q_7 \frac{\partial \kappa}{\partial x_k} \frac{\partial h'}{\partial x_k} \\ & + Q_8 \frac{\partial h'}{\partial x_k} \frac{\partial \bar{\eta}}{\partial x_k} + Q_9 \frac{\partial \bar{\eta}}{\partial x_k} \frac{\partial \kappa}{\partial x_k} + W_6 \frac{\partial h'}{\partial x_k} - W_6 \frac{\partial \bar{\eta}}{\partial x_k} \end{aligned} \right) \\ & + \phi \kappa^2 CC_g - \phi \sigma^2 - g \frac{\partial \phi}{\partial x_k} \left(\frac{\partial \bar{\eta}}{\partial x_k} \right) + \left[\begin{aligned} & \omega^2 \phi - 2i\omega \lambda' U_k \frac{\partial \bar{\eta}}{\partial x_k} \phi + 2i\omega U_k \frac{\partial \phi}{\partial x_k} + i\omega \frac{\partial U_j}{\partial x_j} \phi \\ & - U_k \frac{\partial U_j}{\partial x_j} \frac{\partial \phi}{\partial x_k} + \lambda' U_k \frac{\partial U_j}{\partial x_j} \frac{\partial \bar{\eta}}{\partial x_k} \phi + \lambda' U_j \frac{\partial \bar{\eta}}{\partial x_k} \frac{\partial U_k}{\partial x_j} \phi \\ & - U_j \frac{\partial U_k}{\partial x_j} \frac{\partial \phi}{\partial x_k} - U_j U_k \frac{\partial^2 \phi}{\partial x_j \partial x_k} + 2\lambda' U_j U_k \frac{\partial \bar{\eta}}{\partial x_j} \frac{\partial \phi}{\partial x_k} \\ & - \lambda' \frac{\partial^2 \bar{\eta}}{\partial x_j \partial x_k} + \kappa^2 \frac{\partial \bar{\eta}}{\partial x_k} \frac{\partial \bar{\eta}}{\partial x_j} \\ & - U_j U_k \phi + \left(\kappa^2 - \lambda'^2 \right) \left(-\frac{\partial \bar{\eta}}{\partial x_k} \frac{\partial h'}{\partial x_j} - \frac{\partial h'}{\partial x_k} \frac{\partial \bar{\eta}}{\partial x_j} \right) \\ & + \left(\kappa h' + \frac{\lambda'}{\kappa} - \frac{h \lambda'^2}{\kappa} \right) \left(-\frac{\partial \bar{\eta}}{\partial x_k} \frac{\partial \kappa}{\partial x_j} - \frac{\partial \kappa}{\partial x_k} \frac{\partial \bar{\eta}}{\partial x_j} \right) \end{aligned} \right] = 0 \end{aligned} \quad (3.531)$$

Equation (3.528) can be used to obtain the traditional unextended Mild-Slope Equation including current with no energy dissipation, following Kirby (1984):

$$\begin{aligned} & \frac{\partial^2 \phi}{\partial x_k \partial x_k} CC_g + \frac{\partial \phi}{\partial x_k} \frac{\partial (CC_g)}{\partial x_k} + \phi \kappa^2 CC_g - \phi \sigma^2 + \omega^2 \phi \\ & + \left[2i\omega U_k \frac{\partial \phi}{\partial x_k} + i\omega \frac{\partial U_j}{\partial x_j} \phi - U_k \frac{\partial U_j}{\partial x_j} \frac{\partial \phi}{\partial x_k} - U_j \frac{\partial U_k}{\partial x_j} \frac{\partial \phi}{\partial x_k} - U_j U_k \frac{\partial^2 \phi}{\partial x_j \partial x_k} \right] = 0 \end{aligned} \quad (3.532)$$

Equation (3.529) can be used to obtain the Mild-Slope Equation in the absence of current.

This corresponds exactly to the equations of Berkhoff (1976) and Clyne (2008):

$$\frac{\partial^2 \phi}{\partial x_k \partial x_k} CC_g + \frac{\partial \phi}{\partial x_k} \frac{\partial}{\partial x_k} CC_g + \phi \kappa^2 CC_g = 0 \quad (3.533)$$

3.7.6.1 Summary of Mild-Slope Equations

Table 3.6 summarises the various mild-slope wave equations developed Section 3.7.6.

Table 3.6 – Summary of Mild Slope Wave Equations

	Boundary Condition	Equation
(a) <i>Extended Elliptic Mild-Slope Equation Including Current and Energy Dissipation</i>	$ \begin{aligned} & \frac{\partial^2 \phi}{\partial x_k \partial x_k} C C_g + \frac{\partial \phi}{\partial x_k} \frac{\partial (C C_g)}{\partial x_k} + \phi \kappa^2 C C_g - \phi \sigma^2 - g \frac{\partial \phi}{\partial x_k} \left(\frac{\partial \bar{\eta}}{\partial x_k} \right) \\ & + \frac{\phi \sigma^2}{\cosh^2 \kappa h'} \left(\begin{aligned} & Q_1 \frac{\partial^2 h'}{\partial x_k \partial x_k} + Q_2 \frac{\partial^2 \kappa}{\partial x_k^2} + Q_3 \frac{\partial^2 \bar{\eta}}{\partial x_k \partial x_k} \\ & + Q_4 \left(\frac{\partial h'}{\partial x_k} \frac{\partial h'}{\partial x_k} \right) + Q_5 \left(\frac{\partial \kappa}{\partial x_k} \frac{\partial \kappa}{\partial x_k} \right) \\ & + Q_6 \left(\frac{\partial \bar{\eta}}{\partial x_k} \frac{\partial \bar{\eta}}{\partial x_k} \right) + Q_7 \frac{\partial \kappa}{\partial x_k} \frac{\partial h'}{\partial x_k} \\ & + Q_8 \frac{\partial h'}{\partial x_k} \frac{\partial \bar{\eta}}{\partial x_k} + Q_9 \frac{\partial \bar{\eta}}{\partial x_k} \frac{\partial \kappa}{\partial x_k} \\ & + W_6 \frac{\partial h'}{\partial x_k} - W_6 \frac{\partial \bar{\eta}}{\partial x_k} \end{aligned} \right) \\ & + \left[\begin{aligned} & \omega^2 \phi - 2i\omega \lambda' U_k \frac{\partial \bar{\eta}}{\partial x_k} \phi + 2i\omega U_k \frac{\partial \phi}{\partial x_k} + i\omega \frac{\partial U_j}{\partial x_j} \phi \\ & - U_k \frac{\partial U_j}{\partial x_j} \frac{\partial \phi}{\partial x_k} + \lambda' U_k \frac{\partial U_j}{\partial x_j} \frac{\partial \bar{\eta}}{\partial x_k} \phi + \lambda' U_j \frac{\partial \bar{\eta}}{\partial x_k} \frac{\partial U_k}{\partial x_j} \phi \\ & - U_j \frac{\partial U_k}{\partial x_j} \frac{\partial \phi}{\partial x_k} - U_j U_k \frac{\partial^2 \phi}{\partial x_j \partial x_k} + 2\lambda' U_j U_k \frac{\partial \bar{\eta}}{\partial x_j} \frac{\partial \phi}{\partial x_k} \\ & - U_j U_k \phi + \left(\kappa^2 - \lambda'^2 \right) \left(-\frac{\partial \bar{\eta}}{\partial x_k} \frac{\partial h'}{\partial x_j} - \frac{\partial h'}{\partial x_k} \frac{\partial \bar{\eta}}{\partial x_j} \right) \\ & + \left(\kappa h' + \frac{\lambda'}{\kappa} - \frac{h \lambda'^2}{\kappa} \right) \left(-\frac{\partial \bar{\eta}}{\partial x_k} \frac{\partial \kappa}{\partial x_j} - \frac{\partial \kappa}{\partial x_k} \frac{\partial \bar{\eta}}{\partial x_j} \right) \end{aligned} \right] \\ & + \left[i\omega \gamma \phi - \gamma \frac{\partial}{\partial x_j} (U_j \phi) + \lambda' \gamma U_j \phi \frac{\partial \bar{\eta}}{\partial x_k} \right] = 0 \end{aligned} $	(3.534)

(b)	<i>Elliptic Mild-Slope Equation Including Current and Energy Dissipation</i>	$ \begin{aligned} & \frac{\partial^2 \phi}{\partial x_k \partial x_k} CC_g + \frac{\partial \phi}{\partial x_k} \frac{\partial (CC_g)}{\partial x_k} + \phi \kappa^2 CC_g - \phi \sigma^2 + \omega^2 \phi \\ & + \left[2i\omega U_k \frac{\partial \phi}{\partial x_k} + i\omega \frac{\partial U_j}{\partial x_j} \phi - U_k \frac{\partial U_j}{\partial x_j} \frac{\partial \phi}{\partial x_k} \right] \\ & + \left[-U_j \frac{\partial U_k}{\partial x_j} \frac{\partial \phi}{\partial x_k} - U_j U_k \frac{\partial^2 \phi}{\partial x_j \partial x_k} \right] \\ & + \left[i\omega \gamma \phi - \gamma \frac{\partial}{\partial x_j} (U_j \phi) \right] = 0 \end{aligned} $	(3.535)
(c)	<i>Elliptic Mild-Slope Equation Including Energy Dissipation</i>	$ \frac{\partial^2 \phi}{\partial x_k \partial x_k} CC_g + \frac{\partial \phi}{\partial x_k} \frac{\partial}{\partial x_k} CC_g + \phi \kappa^2 CC_g + i\omega \gamma \phi = 0 $	(3.536)

(d)	Extended Elliptic Mild-Slope Equation Including Current	$ \begin{aligned} & \frac{\partial^2 \phi}{\partial x_k \partial x_k} CC_g + \frac{\partial \phi}{\partial x_k} \frac{\partial (CC_g)}{\partial x_k} + \phi \kappa^2 CC_g - \phi \sigma^2 - g \frac{\partial \phi}{\partial x_k} \left(\frac{\partial \bar{\eta}}{\partial x_k} \right) \\ & + \frac{\phi \sigma^2}{\cosh^2 \kappa h'} \left(\begin{aligned} & Q_1 \frac{\partial^2 h'}{\partial x_k \partial x_k} + Q_2 \frac{\partial^2 \kappa}{\partial x_k^2} + Q_3 \frac{\partial^2 \bar{\eta}}{\partial x_k \partial x_k} \\ & + Q_4 \left(\frac{\partial h'}{\partial x_k} \frac{\partial h'}{\partial x_k} \right) + Q_5 \left(\frac{\partial \kappa}{\partial x_k} \frac{\partial \kappa}{\partial x_k} \right) \\ & + Q_6 \left(\frac{\partial \bar{\eta}}{\partial x_k} \frac{\partial \bar{\eta}}{\partial x_k} \right) + Q_7 \frac{\partial \kappa}{\partial x_k} \frac{\partial h'}{\partial x_k} \\ & + Q_8 \frac{\partial h'}{\partial x_k} \frac{\partial \bar{\eta}}{\partial x_k} + Q_9 \frac{\partial \bar{\eta}}{\partial x_k} \frac{\partial \kappa}{\partial x_k} \\ & + W_6 \frac{\partial h'}{\partial x_k} - W_6 \frac{\partial \bar{\eta}}{\partial x_k} \end{aligned} \right) \\ & + \left[\begin{aligned} & \omega^2 \phi - 2i\omega \lambda' U_k \frac{\partial \bar{\eta}}{\partial x_k} \phi + 2i\omega U_k \frac{\partial \phi}{\partial x_k} + i\omega \frac{\partial U_j}{\partial x_j} \phi \\ & - U_k \frac{\partial U_j}{\partial x_j} \frac{\partial \phi}{\partial x_k} + \lambda' U_k \frac{\partial U_j}{\partial x_j} \frac{\partial \bar{\eta}}{\partial x_k} \phi + \lambda' U_j \frac{\partial \bar{\eta}}{\partial x_k} \frac{\partial U_k}{\partial x_j} \phi \\ & - U_j \frac{\partial U_k}{\partial x_j} \frac{\partial \phi}{\partial x_k} - U_j U_k \frac{\partial^2 \phi}{\partial x_j \partial x_k} + 2\lambda' U_j U_k \frac{\partial \bar{\eta}}{\partial x_j} \frac{\partial \phi}{\partial x_k} \\ & - \lambda' \frac{\partial^2 \bar{\eta}}{\partial x_j \partial x_k} + \kappa^2 \frac{\partial \bar{\eta}}{\partial x_k} \frac{\partial \bar{\eta}}{\partial x_j} \\ & - U_j U_k \phi + (\kappa^2 - \lambda'^2) \left(-\frac{\partial \bar{\eta}}{\partial x_k} \frac{\partial h'}{\partial x_j} - \frac{\partial h'}{\partial x_k} \frac{\partial \bar{\eta}}{\partial x_j} \right) \\ & + \left(\kappa h' + \frac{\lambda'}{\kappa} - \frac{h \lambda'^2}{\kappa} \right) \left(-\frac{\partial \bar{\eta}}{\partial x_k} \frac{\partial \kappa}{\partial x_j} - \frac{\partial \kappa}{\partial x_k} \frac{\partial \bar{\eta}}{\partial x_j} \right) \end{aligned} \right] = 0 \end{aligned} $	(3.537)
(e)	Elliptic Mild-Slope Equation Including Current	$ \begin{aligned} & \frac{\partial^2 \phi}{\partial x_k \partial x_k} CC_g + \frac{\partial \phi}{\partial x_k} \frac{\partial (CC_g)}{\partial x_k} + \phi \kappa^2 CC_g - \phi \sigma^2 + \omega^2 \phi \\ & + \left[\begin{aligned} & 2i\omega U_k \frac{\partial \phi}{\partial x_k} + i\omega \frac{\partial U_j}{\partial x_j} \phi - U_k \frac{\partial U_j}{\partial x_j} \frac{\partial \phi}{\partial x_k} \\ & - U_j \frac{\partial U_k}{\partial x_j} \frac{\partial \phi}{\partial x_k} - U_j U_k \frac{\partial^2 \phi}{\partial x_j \partial x_k} \end{aligned} \right] = 0 \end{aligned} $	(3.538)
(f)	Elliptic Mild-Slope Equation	$ \frac{\partial^2 \phi}{\partial x_k \partial x_k} CC_g + \frac{\partial \phi}{\partial x_k} \frac{\partial (CC_g)}{\partial x_k} + \phi \kappa^2 CC_g = 0 $	(3.539)

3.7.7 Integral Summary

In order to implement the extended mild-slope wave equation in a finite element model it is necessary to evaluate the integrals I_1 to I_6 from Equations (3.479) to (3.483) as follows:

$$I_1 = \int_{-h}^{\bar{\eta}} \cosh^2 [\kappa(h' + z')] dz$$

let $[\kappa(h' + z')] = [\kappa(h + \bar{\eta} + z - \bar{\eta})] = [\kappa(h + z)] = x$
therefore the limits go to $\kappa h'$ and 0
 $\frac{dx}{dz} = \kappa$
 $\frac{1}{\kappa} dx = dz$

$$I_1 = \frac{1}{\kappa} \int_0^{\kappa h'} \cosh^2 x dx \quad (3.540)$$

$$I_1 = \frac{1}{\kappa} \int_0^{\kappa h'} \left(\frac{e^x + e^{-x}}{2} \right)^2 dx \quad (3.541)$$

$$I_1 = \frac{1}{4\kappa} \int_0^{\kappa h'} e^{2x} + 2 + e^{-2x} dx \quad (3.542)$$

$$I_1 = \frac{1}{4\kappa} \left[\frac{e^{2x}}{2} + 2x - \frac{e^{-2x}}{2} \right]_0^{\kappa h'} \quad (3.543)$$

$$I_1 = \frac{1}{4\kappa} \left[\left(\frac{e^{2\kappa h'}}{2} + 2\kappa h' - \frac{e^{-2\kappa h'}}{2} \right) - \left(\frac{e^0}{2} + 0 - \frac{e^{-0}}{2} \right) \right] \quad (3.544)$$

$$I_1 = \frac{1}{4\kappa} \left[\frac{e^{2\kappa h'} - e^{-2\kappa h'}}{2} + 2\kappa h' \right] \quad (3.545)$$

$$I_1 = \frac{\sinh 2\kappa h' + 2\kappa h'}{4\kappa} \quad (3.546)$$

$$I_2 = \int_{-h}^{\bar{\eta}} \cosh[\kappa(h' + z')] \sinh[\kappa(h' + z')] dz$$

let $[\kappa(h' + z')] = [\kappa(h + \bar{\eta} + z - \bar{\eta})] = [\kappa(h + z)] = x$
therefore the limits go to $\kappa h'$ and 0

$$\frac{dx}{dz} = \kappa$$

$$\frac{1}{\kappa} dx = dz$$

$$I_2 = \frac{1}{\kappa} \int_0^{\kappa h'} \cosh x \sinh x dx \quad (3.547)$$

$$I_2 = \frac{1}{\kappa} \int_0^{\kappa h'} \cosh x \sinh x dx \quad (3.548)$$

$$I_2 = \frac{1}{\kappa} \int_0^{\kappa h'} \frac{(e^x + e^{-x})(e^x - e^{-x})}{4} dx \quad (3.549)$$

$$I_2 = \frac{1}{4\kappa} \int_0^{\kappa h'} (e^{2x} - e^{-2x}) dx \quad (3.550)$$

$$I_2 = \frac{1}{4\kappa} \left[\frac{e^{2x}}{2} + \frac{e^{-2x}}{2} \right]_0^{\kappa h'} \quad (3.551)$$

$$I_2 = \frac{1}{4\kappa} \left[\left(\frac{e^{2\kappa h'} + e^{-2\kappa h'}}{2} \right) - \left(\frac{e^0 + e^0}{2} \right) \right] \quad (3.552)$$

$$I_2 = \frac{1}{4\kappa} \left[\frac{e^{2\kappa h'} + e^{-2\kappa h'}}{2} - 1 \right] \quad (3.553)$$

$$I_2 = \frac{1}{4\kappa} [\cosh 2\kappa h' - 1] \quad (3.554)$$

$$I_3 = \int_{-h}^{\bar{\eta}} (h' + z') \cosh[\kappa(h' + z')] \sinh[\kappa(h' + z')] dz$$

$$\text{let } [\kappa(h' + z')] = [\kappa(h + \bar{\eta} + z - \bar{\eta})] = [\kappa(h + z)] = x$$

therefore the limits go to $\kappa h'$ and 0

$$\frac{dx}{dz} = \kappa$$

$$\frac{1}{\kappa} dx = dz$$

$$I_3 = \int_0^{\kappa h'} \frac{x}{\kappa} \frac{1}{\kappa} \cosh x \sinh x dx \quad (3.555)$$

$$I_3 = \frac{1}{\kappa^2} \int_0^{\kappa h'} x \cosh x \sinh x dx \quad (3.556)$$

$$I_3 = \frac{1}{\kappa^2} \int_0^{\kappa h'} x \frac{(e^x + e^{-x})(e^x - e^{-x})}{4} dx \quad (3.557)$$

$$I_3 = \frac{1}{4\kappa^2} \int_0^{\kappa h'} x (e^{2x} - e^{-2x}) dx \quad (3.558)$$

$$I_3 = \frac{1}{4\kappa^2} \int_0^{\kappa h'} (xe^{2x} - xe^{-2x}) dx \quad (3.559)$$

$$I_3 = \frac{1}{4\kappa^2} \int_0^{\kappa h'} xe^{2x} dx - \frac{1}{4\kappa^2} \int_0^{\kappa h'} xe^{-2x} dx \quad (3.560)$$

For the first term in Equation (3.560)

$$\text{let } u = x \text{ and } dv = e^{2x} dx$$

$$\frac{du}{dx} = 1$$

$$du = dx$$

$$v = \int e^{2x} dx$$

$$v = \frac{e^{2x}}{2}$$

$$\int_0^{\kappa h'} xe^{2x} dx = \left[\frac{xe^{2x}}{2} \right]_0^{\kappa h'} - \int_0^{\kappa h'} \frac{e^{2x}}{2} dx \quad (3.561)$$

$$\int_0^{\kappa h'} xe^{2x} dx = \left[\frac{xe^{2x}}{2} \right]_0^{\kappa h'} - \frac{1}{2} \int_0^{\kappa h'} e^{2x} dx \quad (3.562)$$

$$\int_0^{\kappa h'} xe^{2x} dx = \left[\frac{xe^{2x}}{2} \right]_0^{\kappa h'} - \frac{1}{2} \left[\frac{e^{2x}}{2} \right]_0^{\kappa h'} \quad (3.563)$$

$$\int_0^{\kappa h'} xe^{2x} dx = \left[\frac{\kappa h' e^{2\kappa h'}}{2} \right] - \frac{1}{2} \left[\frac{e^{2\kappa h'}}{2} - \frac{1}{2} \right] \quad (3.564)$$

$$\int_0^{\kappa h'} x e^{2x} dx = \left[\frac{2\kappa h' e^{2\kappa h'}}{4} \right] - \left[\frac{e^{2\kappa h'} - 1}{4} \right] \quad (3.565)$$

$$\int_0^{\kappa h'} x e^{2x} dx = \frac{2\kappa h' e^{2\kappa h'} - e^{2\kappa h'} + 1}{4} \quad (3.566)$$

Similarly for the second term in equation (3.560):

$$\text{let } u = x \text{ and } dv = e^{-2x} dx$$

$$\frac{du}{dx} = 1$$

$$du = dx$$

$$v = \int e^{-2x} dx$$

$$v = -\frac{e^{-2x}}{2}$$

$$\int_0^{\kappa h'} x e^{-2x} dx = \left[-\frac{x e^{-2x}}{2} \right]_0^{\kappa h'} + \int_0^{\kappa h'} \frac{e^{-2x}}{2} dx \quad (3.567)$$

$$\int_0^{\kappa h'} x e^{-2x} dx = \left[-\frac{x e^{-2x}}{2} \right]_0^{\kappa h'} + \frac{1}{2} \int_0^{\kappa h'} e^{-2x} dx \quad (3.568)$$

$$\int_0^{\kappa h'} x e^{-2x} dx = \left[-\frac{x e^{-2x}}{2} \right]_0^{\kappa h'} - \frac{1}{2} \left[\frac{e^{-2x}}{2} \right]_0^{\kappa h'} \quad (3.569)$$

$$\int_0^{\kappa h'} x e^{-2x} dx = \left[-\frac{\kappa h' e^{-2\kappa h'}}{2} \right] - \frac{1}{2} \left[\frac{e^{-2\kappa h'}}{2} - \frac{1}{2} \right] \quad (3.570)$$

$$\int_0^{\kappa h'} x e^{-2x} dx = \left[\frac{-2\kappa h' e^{-2\kappa h'}}{4} \right] - \left[\frac{e^{-2\kappa h'} - 1}{4} \right] \quad (3.571)$$

$$\int_0^{\kappa h'} x e^{-2x} dx = \frac{-2\kappa h' e^{-2\kappa h'} - e^{-2\kappa h'} + 1}{4} \quad (3.572)$$

Using Equations (3.566) and (3.572) in Equation (3.560) gives:

$$I_3 = \frac{1}{4\kappa^2} \left[\left(\frac{2\kappa h' e^{2\kappa h'} - e^{2\kappa h'} + 1}{4} \right) - \left(\frac{-2\kappa h' e^{-2\kappa h'} - e^{-2\kappa h'} + 1}{4} \right) \right] \quad (3.573)$$

$$I_3 = \frac{1}{16\kappa^2} [2\kappa h' e^{2\kappa h'} - e^{2\kappa h'} + 1 + 2\kappa h' e^{-2\kappa h'} + e^{-2\kappa h'} - 1] \quad (3.574)$$

$$I_3 = \frac{1}{16\kappa^2} [2\kappa h' e^{2\kappa h'} + 2\kappa h' e^{-2\kappa h'} - e^{2\kappa h'} + e^{-2\kappa h'}] \quad (3.575)$$

$$I_3 = \frac{\kappa h'}{4\kappa^2} \left(\frac{e^{2\kappa h'} + e^{-2\kappa h'}}{2} \right) - \frac{1}{8\kappa^2} \left(\frac{e^{2\kappa h'} - e^{-2\kappa h'}}{2} \right) \quad (3.576)$$

$$I_3 = \frac{\kappa h'}{4\kappa^2} (\cosh 2\kappa h') - \frac{1}{8\kappa^2} (\sinh 2\kappa h') \quad (3.577)$$

$$I_3 = \frac{1}{8\kappa^2} (2\kappa h' \cosh 2\kappa h' - \sinh 2\kappa h') \quad (3.578)$$

$$I_4 = \int_{-h}^{\bar{\eta}} (h' + z') \cosh^2 [\kappa(h' + z')] dz$$

$$\text{let } [\kappa(h' + z')] = [\kappa(h + \bar{\eta} + z - \bar{\eta})] = [\kappa(h + z)] = x$$

therefore the limits go to $\kappa h'$ and 0

$$\frac{dx}{dz} = \kappa$$

$$\frac{1}{\kappa} dx = dz$$

$$I_4 = \frac{1}{\kappa^2} \int_0^{\kappa h'} x \cosh^2 x dx \quad (3.579)$$

$$I_4 = \frac{1}{\kappa^2} \int_0^{\kappa h'} x \frac{(e^x + e^{-x})(e^x + e^{-x})}{4} dx \quad (3.580)$$

$$I_4 = \frac{1}{4\kappa^2} \int_0^{\kappa h'} x (e^{2x} + 2 + e^{-2x}) dx \quad (3.581)$$

$$I_4 = \frac{1}{4\kappa^2} \left[\int_0^{\kappa h'} x e^{2x} dx + \int_0^{\kappa h'} 2x dx + \int_0^{\kappa h'} x e^{-2x} dx \right] \quad (3.582)$$

$$\int_0^{\kappa h'} 2x dx = [x^2]_0^{\kappa h'} \quad (3.583)$$

$$\int_0^{\kappa h'} 2x dx = [\kappa^2 h'^2 - 0] \quad (3.584)$$

$$\int_0^{\kappa h'} 2x dx = \kappa^2 h'^2 \quad (3.585)$$

From Equations (3.566) and (3.572):

$$\int_0^{\kappa h'} x e^{2x} dx = \frac{2\kappa h' e^{2\kappa h'} - e^{2\kappa h'} + 1}{4} \quad (3.586)$$

$$\int_0^{\kappa h'} x e^{-2x} dx = \frac{-2\kappa h' e^{-2\kappa h'} - e^{-2\kappa h'} + 1}{4} \quad (3.587)$$

$$I_4 = \frac{1}{4\kappa^2} \left[\frac{2\kappa h' e^{2\kappa h'} - e^{2\kappa h'} + 1}{4} + \kappa^2 h'^2 + \frac{-2\kappa h' e^{-2\kappa h'} - e^{-2\kappa h'} + 1}{4} \right] \quad (3.588)$$

$$I_4 = \frac{1}{4\kappa^2} \left(\frac{2\kappa h' e^{2\kappa h'} - 2\kappa h' e^{-2\kappa h'}}{4} \right) + \frac{1}{4\kappa^2} \left(\frac{-e^{2\kappa h'} - e^{-2\kappa h'}}{4} \right) + \frac{1}{4\kappa^2} \left(\frac{2}{4} \right) + \frac{\kappa^2 h'^2}{4\kappa^2} \quad (3.589)$$

$$I_4 = \frac{\kappa h'}{4\kappa^2} \left(\frac{e^{2\kappa h'} - e^{-2\kappa h'}}{2} \right) - \frac{1}{8\kappa^2} \left(\frac{e^{2\kappa h'} + e^{-2\kappa h'}}{2} \right) + \frac{1}{8\kappa^2} + \frac{2\kappa^2 h'^2}{8\kappa^2} \quad (3.590)$$

$$I_4 = \frac{2\kappa h'}{8\kappa^2} (\sinh 2\kappa h') - \frac{1}{8\kappa^2} (\cosh 2\kappa h') + \frac{1}{8\kappa^2} + \frac{2\kappa^2 h'^2}{8\kappa^2} \quad (3.591)$$

$$I_4 = \frac{1}{8\kappa^2} (2\kappa h' \sinh 2\kappa h' - \cosh 2\kappa h' + 1 + 2\kappa^2 h'^2) \quad (3.592)$$

$$I_5 = \int_{-h}^{\bar{\eta}} (h' + z')^2 \cosh^2 [\kappa(h' + z')] dz$$

$$\text{let } [\kappa(h' + z')] = [\kappa(h + \bar{\eta} + z - \bar{\eta})] = [\kappa(h + z)] = x$$

therefore the limits go to $\kappa h'$ and 0

$$\frac{dx}{dz} = \kappa$$

$$\frac{1}{\kappa} dx = dz$$

$$I_5 = \frac{1}{\kappa^3} \int_0^{\kappa h'} x^2 \cosh^2 x dx \quad (3.593)$$

$$I_5 = \frac{1}{\kappa^3} \int_0^{\kappa h'} x^2 \frac{(e^x + e^{-x})(e^x + e^{-x})}{4} dx \quad (3.594)$$

$$I_5 = \frac{1}{4\kappa^3} \int_0^{\kappa h'} x^2 (e^{2x} + 2 + e^{-2x}) dx \quad (3.595)$$

$$I_5 = \frac{1}{4\kappa^3} \left[\int_0^{\kappa h'} x^2 e^{2x} dx + \int_0^{\kappa h'} 2x^2 dx + \int_0^{\kappa h'} x^2 e^{-2x} dx \right] \quad (3.596)$$

For the first term in Equation (3.596):

$$\text{let } u = x^2 \text{ and } dv = e^{2x} dx$$

$$\frac{du}{dx} = 2x$$

$$du = 2x dx$$

$$v = \int e^{2x} dx$$

$$v = \frac{e^{2x}}{2}$$

$$\int_0^{\kappa h'} x^2 e^{2x} dx = \left[\frac{x^2 e^{2x}}{2} \right]_0^{\kappa h'} - \int_0^{\kappa h'} x e^{2x} dx \quad (3.597)$$

From Equation (3.566):

$$\int_0^{\kappa h'} x e^{2x} dx = \frac{2\kappa h' e^{2\kappa h'} - e^{2\kappa h'} + 1}{4}$$

Therefore Equation (3.597) becomes:

$$\int_0^{\kappa h'} x^2 e^{2x} dx = \left[\frac{x^2 e^{2x}}{2} \right]_0^{\kappa h'} - \left[\frac{2\kappa h' e^{2\kappa h'} - e^{2\kappa h'} + 1}{4} \right] \quad (3.598)$$

$$\int_0^{\kappa h'} x^2 e^{2x} dx = \left[\frac{\kappa^2 h'^2 e^{2\kappa h'}}{2} \right] - \left[\frac{2\kappa h' e^{2\kappa h'} - e^{2\kappa h'} + 1}{4} \right] \quad (3.599)$$

$$\int_0^{\kappa h'} x^2 e^{2x} dx = \frac{2\kappa^2 h'^2 e^{2\kappa h'} - 2\kappa h' e^{2\kappa h'} + e^{2\kappa h'} - 1}{4} \quad (3.600)$$

Similarly for the third term in Equation (3.596):

$$\text{let } u = x^2 \text{ and } dv = e^{-2x} dx$$

$$\frac{du}{dx} = 2x$$

$$du = 2x dx$$

$$v = \int e^{-2x} dx$$

$$v = -\frac{e^{-2x}}{2}$$

$$\int_0^{\kappa h'} x^2 e^{-2x} dx = \left[-\frac{x^2 e^{-2x}}{2} \right]_0^{\kappa h'} + \int_0^{\kappa h'} x e^{-2x} dx \quad (3.601)$$

From Equation (3.572):

$$\int_0^{\kappa h'} x e^{-2x} dx = \frac{-2\kappa h' e^{-2\kappa h'} - e^{-2\kappa h'} + 1}{4}$$

Therefore Equation (3.601) becomes:

$$\int_0^{\kappa h'} x^2 e^{-2x} dx = \left[-\frac{x^2 e^{-2x}}{2} \right]_0^{\kappa h'} + \left[\frac{-2\kappa h' e^{-2\kappa h'} - e^{-2\kappa h'} + 1}{4} \right] \quad (3.602)$$

$$\int_0^{\kappa h'} x^2 e^{-2x} dx = \left[-\frac{\kappa^2 h'^2 e^{-2\kappa h'}}{2} \right] + \left[\frac{-2\kappa h' e^{-2\kappa h'} - e^{-2\kappa h'} + 1}{4} \right] \quad (3.603)$$

$$\int_0^{\kappa h'} x^2 e^{-2x} dx = \frac{-2\kappa^2 h'^2 e^{-2\kappa h'} - 2\kappa h' e^{-2\kappa h'} - e^{-2\kappa h'} + 1}{4} \quad (3.604)$$

For the second term in Equation (3.596):

$$\int_0^{\kappa h'} 2x^2 dx = \left[\frac{2x^3}{3} \right]_0^{\kappa h'} \quad (3.605)$$

$$\int_0^{\kappa h'} 2x^2 dx = \frac{2\kappa^3 h'^3}{3} \quad (3.606)$$

Therefore using Equations (3.600), (3.604) and (3.606) Equation (3.596) now becomes:

$$I_5 = \frac{1}{4\kappa^3} \left[\frac{2\kappa^2 h'^2 e^{2\kappa h'} - 2\kappa h' e^{2\kappa h'} + e^{2\kappa h'} - 1}{4} + \frac{2\kappa^3 h'^3}{3} + \frac{-2\kappa^2 h'^2 e^{-2\kappa h'} - 2\kappa h' e^{-2\kappa h'} - e^{-2\kappa h'} + 1}{4} \right] \quad (3.607)$$

$$I_5 = \frac{1}{4\kappa^3} \left[\frac{2\kappa^2 h'^2 e^{2\kappa h'} - 2\kappa^2 h'^2 e^{-2\kappa h'} - 2\kappa h' e^{2\kappa h'} - 2\kappa h' e^{-2\kappa h'} + e^{2\kappa h'} - e^{-2\kappa h'}}{4} + \frac{2\kappa^3 h'^3}{3} \right] \quad (3.608)$$

$$I_5 = \frac{1}{4\kappa^3} \left[\kappa^2 h'^2 \left(\frac{e^{2\kappa h'} - e^{-2\kappa h'}}{2} \right) - \kappa h' \left(\frac{e^{2\kappa h'} + e^{-2\kappa h'}}{2} \right) + \frac{1}{2} \left(\frac{e^{2\kappa h'} - e^{-2\kappa h'}}{2} \right) + \frac{2\kappa^3 h'^3}{3} \right] \quad (3.609)$$

$$I_5 = \frac{1}{4\kappa^3} \left[\kappa^2 h'^2 \sinh 2\kappa h' - \kappa h' \cosh 2\kappa h' + \frac{1}{2} \sinh 2\kappa h' + \frac{2\kappa^3 h'^3}{3} \right] \quad (3.610)$$

Summarising the results of the above integrals I_1 to I_5 from Equations (3.546), (3.554), (3.578), (3.592) and (3.610) gives:

$$I_1 = \frac{\sinh 2\kappa h' + 2\kappa h'}{4\kappa}$$

$$I_2 = \frac{1}{4\kappa} [\cosh 2\kappa h' - 1]$$

$$I_3 = \frac{1}{8\kappa^2} (2\kappa h' \cosh 2\kappa h' - \sinh 2\kappa h')$$

$$I_4 = \frac{1}{8\kappa^2} (2\kappa h' \sinh 2\kappa h' - \cosh 2\kappa h' + 1 + 2\kappa^2 h'^2)$$

$$I_5 = \frac{1}{4\kappa^3} \left[\kappa^2 h'^2 \sinh 2\kappa h' - \kappa h' \cosh 2\kappa h' + \frac{1}{2} \sinh 2\kappa h' + \frac{2\kappa^3 h'^3}{3} \right]$$

3.8 One Dimensional Finite Element Mild-Slope Wave Model

Initially the finite element formulation for a one-dimensional finite element wave-current interaction model is examined (1d-NM-WCIM). This model can examine wave behaviour along a line of linear finite elements.

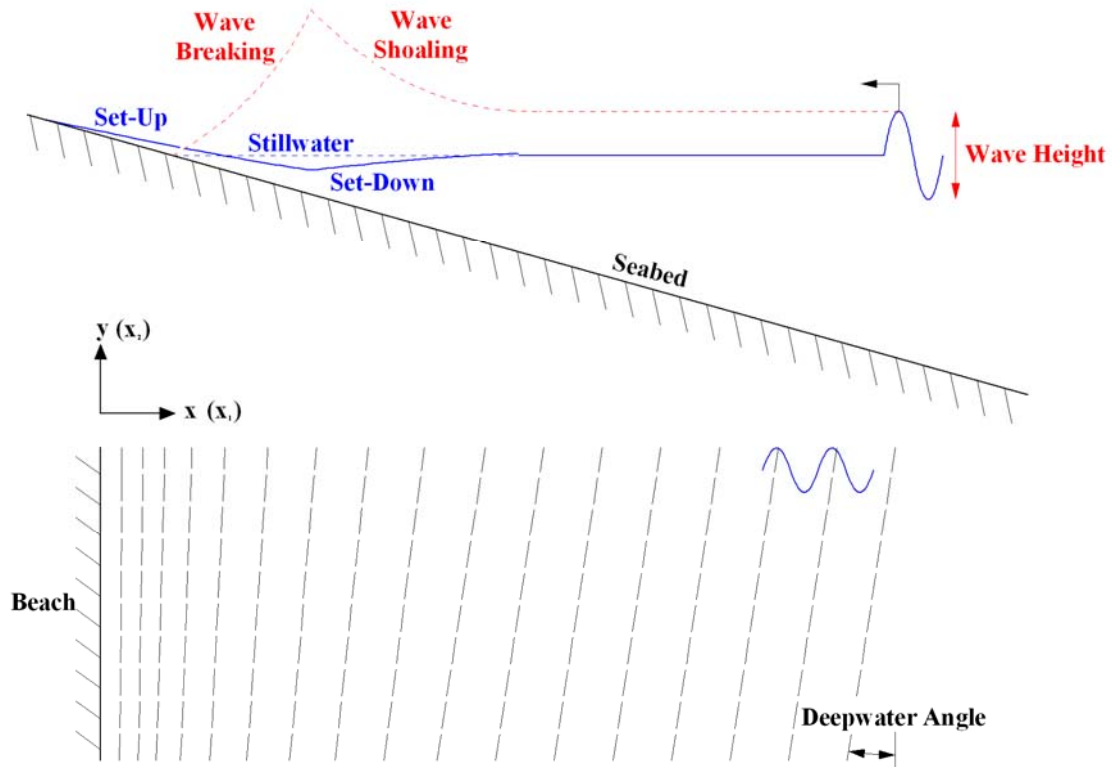


Figure 3.7 – Definition Sketch of Wave Behaviour for One-Dimensional Situation

3.8.1 Simplification of two dimensional terms to one dimension

In the case of a longshore (shore parallel) current:

$$U_1 = 0$$

Therefore for a longshore current Equation (3.531) becomes:

$$\begin{aligned}
 & \frac{\partial^2 \phi}{\partial x_k \partial x_k} CC_g + \frac{\partial \phi}{\partial x_k} \frac{\partial (CC_g)}{\partial x_k} + \frac{\phi \sigma^2}{\cosh^2 \kappa h'} \left(\begin{aligned} & Q_1 \frac{\partial^2 h'}{\partial x_k \partial x_k} + Q_2 \frac{\partial^2 \kappa}{\partial x_k^2} + Q_3 \frac{\partial^2 \bar{\eta}}{\partial x_k \partial x_k} + Q_4 \left(\frac{\partial h'}{\partial x_k} \frac{\partial h'}{\partial x_k} \right) \\ & + Q_5 \left(\frac{\partial \kappa}{\partial x_k} \frac{\partial \kappa}{\partial x_k} \right) + Q_6 \left(\frac{\partial \bar{\eta}}{\partial x_k} \frac{\partial \bar{\eta}}{\partial x_k} \right) + Q_7 \frac{\partial \kappa}{\partial x_k} \frac{\partial h'}{\partial x_k} \\ & + Q_8 \frac{\partial h'}{\partial x_k} \frac{\partial \bar{\eta}}{\partial x_k} + Q_9 \frac{\partial \bar{\eta}}{\partial x_k} \frac{\partial \kappa}{\partial x_k} + W_6 \frac{\partial h'}{\partial x_k} - W_6 \frac{\partial \bar{\eta}}{\partial x_k} \end{aligned} \right) \\
 & + \phi \kappa^2 CC_g - \phi \sigma^2 - g \frac{\partial \phi}{\partial x_k} \left(\frac{\partial \bar{\eta}}{\partial x_k} \right) + \left[\begin{aligned} & \omega^2 \phi - 2i\omega \lambda' U_2 \frac{\partial \bar{\eta}}{\partial x_2} \phi + 2i\omega U_2 \frac{\partial \phi}{\partial x_2} + i\omega \frac{\partial U_2}{\partial x_2} \phi \\ & - U_2 \frac{\partial U_2}{\partial x_2} \frac{\partial \phi}{\partial x_2} + \lambda' U_2 \frac{\partial U_2}{\partial x_2} \frac{\partial \bar{\eta}}{\partial x_2} \phi + \lambda' U_2 \frac{\partial \bar{\eta}}{\partial x_2} \frac{\partial U_2}{\partial x_2} \\ & - U_2 \frac{\partial U_2}{\partial x_2} \frac{\partial \phi}{\partial x_2} - U_2 U_2 \frac{\partial^2 \phi}{\partial x_2 \partial x_2} + 2\lambda' U_2 U_2 \frac{\partial \bar{\eta}}{\partial x_2} \frac{\partial \phi}{\partial x_2} \\ & - U_2 U_2 \phi + \left(\kappa^2 - \lambda'^2 \right) \left(-\frac{\partial \bar{\eta}}{\partial x_2} \frac{\partial h'}{\partial x_2} - \frac{\partial h'}{\partial x_2} \frac{\partial \bar{\eta}}{\partial x_2} \right) \\ & + \left(\kappa h' + \frac{\lambda'}{\kappa} - \frac{h \lambda'^2}{\kappa} \right) \left(-\frac{\partial \bar{\eta}}{\partial x_2} \frac{\partial \kappa}{\partial x_2} - \frac{\partial \kappa}{\partial x_2} \frac{\partial \bar{\eta}}{\partial x_2} \right) \end{aligned} \right] = 0
 \end{aligned}
 \tag{3.611}$$

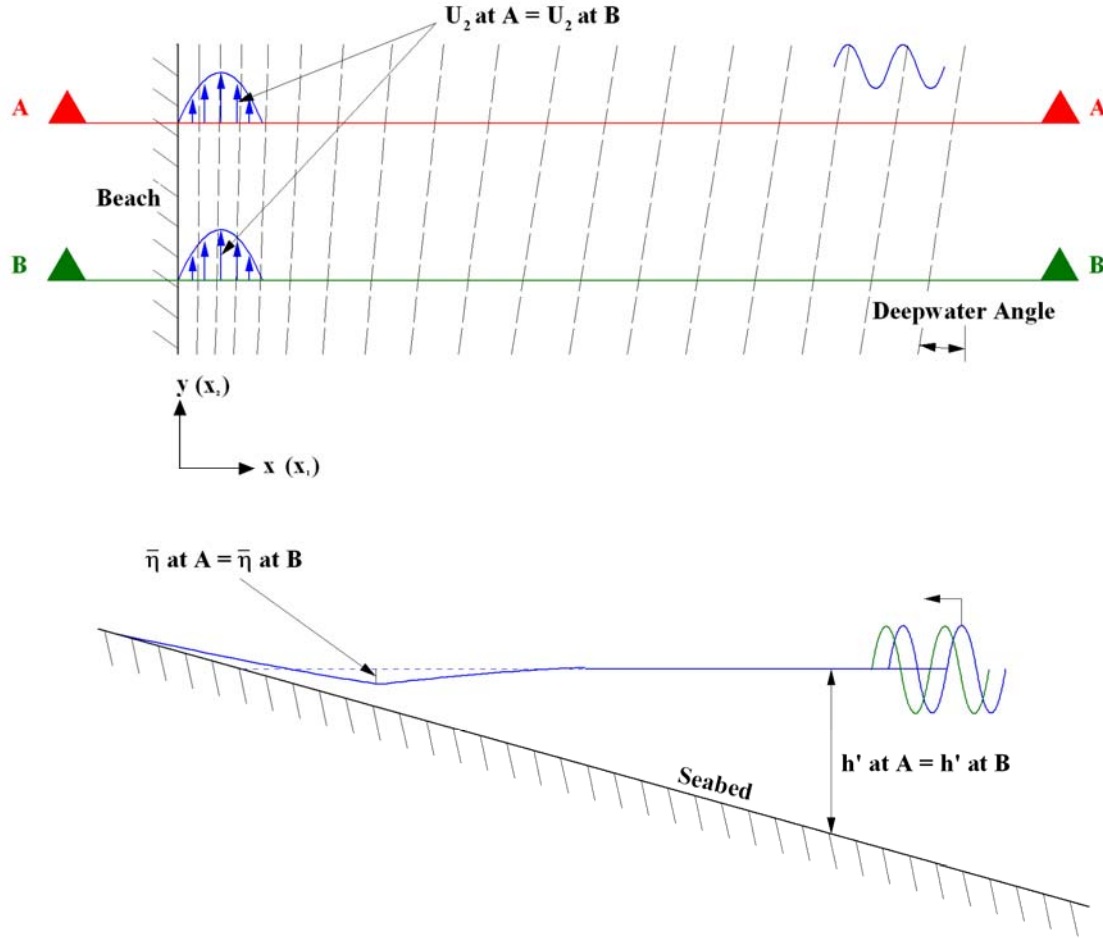


Figure 3.8 - Sketch showing terms that do not vary in x_2 for One-Dimensional Model

As shown in Figure 3.8 for a one dimensional model U_2 , κ , $\bar{\eta}$, and h' will not vary in the x_2 direction. Hence Equation (3.611) reduces to:

$$\begin{aligned}
 & \frac{\partial}{\partial x_k} \left(CC_g \frac{\partial \phi}{\partial x_k} \right) + \frac{\phi \sigma^2}{\cosh^2 \kappa h'} \left(Q_1 \frac{\partial^2 h'}{\partial x_1 \partial x_1} + Q_2 \frac{\partial^2 \kappa}{\partial x_1^2} + Q_3 \frac{\partial^2 \bar{\eta}}{\partial x_1 \partial x_1} + Q_4 \left(\frac{\partial h'}{\partial x_1} \frac{\partial h'}{\partial x_1} \right) \right. \\
 & \quad \left. + Q_5 \left(\frac{\partial \kappa}{\partial x_1} \frac{\partial \kappa}{\partial x_1} \right) + Q_6 \left(\frac{\partial \bar{\eta}}{\partial x_1} \frac{\partial \bar{\eta}}{\partial x_1} \right) + Q_7 \frac{\partial \kappa}{\partial x_1} \frac{\partial h'}{\partial x_1} \right. \\
 & \quad \left. + Q_8 \frac{\partial h'}{\partial x_1} \frac{\partial \bar{\eta}}{\partial x_1} + Q_9 \frac{\partial \bar{\eta}}{\partial x_1} \frac{\partial \kappa}{\partial x_1} + W_6 \frac{\partial h'}{\partial x_1} - W_6 \frac{\partial \bar{\eta}}{\partial x_1} \right) \\
 & + \phi \kappa^2 CC_g - \phi \sigma^2 - g \frac{\partial \phi}{\partial x_1} \left(\frac{\partial \bar{\eta}}{\partial x_1} \right) + \omega^2 \phi + 2i\omega U_2 \frac{\partial \phi}{\partial x_2} - U_2^2 \frac{\partial^2 \phi}{\partial x_2 \partial x_2} = 0
 \end{aligned} \tag{3.612}$$

Equation (3.612) may be expanded to give:

$$\begin{aligned} & \frac{\partial}{\partial x_1} \left(CC_g \frac{\partial \phi}{\partial x_1} \right) + \frac{\partial CC_g}{\partial x_2} \frac{\partial \phi}{\partial x_2} + CC_g \frac{\partial^2 \phi}{\partial x_2 \partial x_2} + \frac{\phi \sigma^2}{\cosh^2 \kappa h'} \left(Q_1 \frac{\partial^2 h'}{\partial x_1 \partial x_1} + Q_2 \frac{\partial^2 \kappa}{\partial x_1^2} + Q_3 \frac{\partial^2 \bar{\eta}}{\partial x_1 \partial x_1} + Q_4 \left(\frac{\partial h'}{\partial x_1} \frac{\partial h'}{\partial x_1} \right) \right. \\ & \left. + Q_5 \left(\frac{\partial \kappa}{\partial x_1} \frac{\partial \kappa}{\partial x_1} \right) + Q_6 \left(\frac{\partial \bar{\eta}}{\partial x_1} \frac{\partial \bar{\eta}}{\partial x_1} \right) + Q_7 \frac{\partial \kappa}{\partial x_1} \frac{\partial h'}{\partial x_1} \right. \\ & \left. + Q_8 \frac{\partial h'}{\partial x_1} \frac{\partial \bar{\eta}}{\partial x_1} + Q_9 \frac{\partial \bar{\eta}}{\partial x_1} \frac{\partial \kappa}{\partial x_1} + W_6 \frac{\partial h'}{\partial x_1} - W_6 \frac{\partial \bar{\eta}}{\partial x_1} \right) \\ & + \phi \kappa^2 CC_g - \phi \sigma^2 - g \frac{\partial \phi}{\partial x_1} \left(\frac{\partial \bar{\eta}}{\partial x_1} \right) + \omega^2 \phi + 2i\omega U_2 \frac{\partial \phi}{\partial x_2} - U_2^2 \frac{\partial^2 \phi}{\partial x_2 \partial x_2} = 0 \end{aligned} \quad (3.613)$$

CC_g does not vary in the x_2 direction hence Equation (3.613) may be simplified to give the following equation for a one dimensional hydrodynamic model:

$$\begin{aligned} & \frac{\partial}{\partial x_1} \left(CC_g \frac{\partial \phi}{\partial x_1} \right) + CC_g \frac{\partial^2 \phi}{\partial x_2 \partial x_2} + \frac{\phi \sigma^2}{\cosh^2 \kappa h'} \left(Q_1 \frac{\partial^2 h'}{\partial x_1 \partial x_1} + Q_2 \frac{\partial^2 \kappa}{\partial x_1^2} + Q_3 \frac{\partial^2 \bar{\eta}}{\partial x_1 \partial x_1} + Q_4 \left(\frac{\partial h'}{\partial x_1} \frac{\partial h'}{\partial x_1} \right) \right. \\ & \left. + Q_5 \left(\frac{\partial \kappa}{\partial x_1} \frac{\partial \kappa}{\partial x_1} \right) + Q_6 \left(\frac{\partial \bar{\eta}}{\partial x_1} \frac{\partial \bar{\eta}}{\partial x_1} \right) + Q_7 \frac{\partial \kappa}{\partial x_1} \frac{\partial h'}{\partial x_1} \right. \\ & \left. + Q_8 \frac{\partial h'}{\partial x_1} \frac{\partial \bar{\eta}}{\partial x_1} + Q_9 \frac{\partial \bar{\eta}}{\partial x_1} \frac{\partial \kappa}{\partial x_1} + W_6 \frac{\partial h'}{\partial x_1} - W_6 \frac{\partial \bar{\eta}}{\partial x_1} \right) \\ & + \phi \kappa^2 CC_g - \phi \sigma^2 - g \frac{\partial \phi}{\partial x_1} \left(\frac{\partial \bar{\eta}}{\partial x_1} \right) + \omega^2 \phi + 2i\omega U_2 \frac{\partial \phi}{\partial x_2} - U_2^2 \frac{\partial^2 \phi}{\partial x_2 \partial x_2} = 0 \end{aligned} \quad (3.614)$$

Equation (3.135) can be rewritten as:

$$\phi = A_\phi e^{iS_\phi} = A_\phi e^{i(S_{\phi 1} x_1 + \kappa_2 x_2)} \quad (3.615)$$

A new one dimensional velocity potential term, $\hat{\phi}$, may now be defined as follows:

$$\hat{\phi} = A_\phi e^{iS_{\phi 1} x_1} \quad (3.616)$$

Hence:

$$\phi = e^{i\kappa_2 x_2} \hat{\phi} \quad (3.617)$$

Use of Equation (3.617) yields the following version of Equation (3.614):

$$\begin{aligned}
 & \frac{\partial}{\partial x_1} \left(CC_g e^{i\kappa_2 x_2} \frac{\partial \hat{\phi}}{\partial x_1} \right) + CC_g \left(-\kappa_2^2 e^{i\kappa_2 x_2} \hat{\phi} \right) + \frac{e^{i\kappa_2 x_2} \hat{\phi} \sigma^2}{\cosh^2 \kappa h'} \left(\begin{aligned} & Q_1 \frac{\partial^2 h'}{\partial x_1 \partial x_1} + Q_2 \frac{\partial^2 \kappa}{\partial x_1^2} + Q_3 \frac{\partial^2 \bar{\eta}}{\partial x_1 \partial x_1} + Q_4 \left(\frac{\partial h'}{\partial x_1} \frac{\partial h'}{\partial x_1} \right) \\ & + Q_5 \left(\frac{\partial \kappa}{\partial x_1} \frac{\partial \kappa}{\partial x_1} \right) + Q_6 \left(\frac{\partial \bar{\eta}}{\partial x_1} \frac{\partial \bar{\eta}}{\partial x_1} \right) + Q_7 \frac{\partial \kappa}{\partial x_1} \frac{\partial h'}{\partial x_1} \\ & + Q_8 \frac{\partial h'}{\partial x_1} \frac{\partial \bar{\eta}}{\partial x_1} + Q_9 \frac{\partial \bar{\eta}}{\partial x_1} \frac{\partial \kappa}{\partial x_1} + W_6 \frac{\partial h'}{\partial x_1} - W_6 \frac{\partial \bar{\eta}}{\partial x_1} \end{aligned} \right) \\
 & + e^{i\kappa_2 x_2} \hat{\phi} \kappa^2 CC_g - e^{i\kappa_2 x_2} \hat{\phi} \sigma^2 - g e^{i\kappa_2 x_2} \frac{\partial \hat{\phi}}{\partial x_1} \left(\frac{\partial \bar{\eta}}{\partial x_1} \right) + \omega^2 e^{i\kappa_2 x_2} \hat{\phi} + 2i\omega U_2 \left(i\kappa_2 e^{i\kappa_2 x_2} \hat{\phi} \right) - U_2^2 \left(-\kappa_2^2 e^{i\kappa_2 x_2} \hat{\phi} \right) = 0
 \end{aligned} \tag{3.618}$$

Dividing Equation (3.618) by $e^{i\kappa_2 x_2}$ gives:

$$\begin{aligned}
 & \frac{\partial}{\partial x_1} \left(CC_g \frac{\partial \hat{\phi}}{\partial x_1} \right) + CC_g \left(-\kappa_2^2 \hat{\phi} \right) + \frac{\hat{\phi} \sigma^2}{\cosh^2 \kappa h'} \left(\begin{aligned} & Q_1 \frac{\partial^2 h'}{\partial x_1 \partial x_1} + Q_2 \frac{\partial^2 \kappa}{\partial x_1^2} + Q_3 \frac{\partial^2 \bar{\eta}}{\partial x_1 \partial x_1} + Q_4 \left(\frac{\partial h'}{\partial x_1} \frac{\partial h'}{\partial x_1} \right) \\ & + Q_5 \left(\frac{\partial \kappa}{\partial x_1} \frac{\partial \kappa}{\partial x_1} \right) + Q_6 \left(\frac{\partial \bar{\eta}}{\partial x_1} \frac{\partial \bar{\eta}}{\partial x_1} \right) + Q_7 \frac{\partial \kappa}{\partial x_1} \frac{\partial h'}{\partial x_1} \\ & + Q_8 \frac{\partial h'}{\partial x_1} \frac{\partial \bar{\eta}}{\partial x_1} + Q_9 \frac{\partial \bar{\eta}}{\partial x_1} \frac{\partial \kappa}{\partial x_1} + W_6 \frac{\partial h'}{\partial x_1} - W_6 \frac{\partial \bar{\eta}}{\partial x_1} \end{aligned} \right) \\
 & + \hat{\phi} \kappa^2 CC_g - \hat{\phi} \sigma^2 - g \frac{\partial \hat{\phi}}{\partial x_1} \left(\frac{\partial \bar{\eta}}{\partial x_1} \right) + \omega^2 \hat{\phi} + 2i\omega U_2 \left(i\kappa_2 \hat{\phi} \right) - U_2^2 \left(-\kappa_2^2 \hat{\phi} \right) = 0
 \end{aligned} \tag{3.619}$$

Simplification of Equation (3.619) yields:

$$\begin{aligned}
 & \frac{\partial}{\partial x_1} \left(CC_g \frac{\partial \hat{\phi}}{\partial x_1} \right) - \kappa_2^2 CC_g \hat{\phi} + \frac{\hat{\phi} \sigma^2}{\cosh^2 \kappa h'} \left(\begin{aligned} & Q_1 \frac{\partial^2 h'}{\partial x_1 \partial x_1} + Q_2 \frac{\partial^2 \kappa}{\partial x_1^2} + Q_3 \frac{\partial^2 \bar{\eta}}{\partial x_1 \partial x_1} + Q_4 \left(\frac{\partial h'}{\partial x_1} \frac{\partial h'}{\partial x_1} \right) \\ & + Q_5 \left(\frac{\partial \kappa}{\partial x_1} \frac{\partial \kappa}{\partial x_1} \right) + Q_6 \left(\frac{\partial \bar{\eta}}{\partial x_1} \frac{\partial \bar{\eta}}{\partial x_1} \right) + Q_7 \frac{\partial \kappa}{\partial x_1} \frac{\partial h'}{\partial x_1} \\ & + Q_8 \frac{\partial h'}{\partial x_1} \frac{\partial \bar{\eta}}{\partial x_1} + Q_9 \frac{\partial \bar{\eta}}{\partial x_1} \frac{\partial \kappa}{\partial x_1} + W_6 \frac{\partial h'}{\partial x_1} - W_6 \frac{\partial \bar{\eta}}{\partial x_1} \end{aligned} \right) \\
 & + \kappa^2 CC_g \hat{\phi} - \sigma^2 \hat{\phi} - g \frac{\partial \hat{\phi}}{\partial x_1} \left(\frac{\partial \bar{\eta}}{\partial x_1} \right) + \omega^2 \hat{\phi} - 2\omega \kappa_2 U_2 \hat{\phi} + \kappa_2^2 U_2^2 \hat{\phi} = 0
 \end{aligned} \tag{3.620}$$

Equation (3.620) is a restructured form of the Extended Mild-Slope Equation including Currents that is suitable for use in a one-dimensional model (linear finite elements) of wave propagation in the presence of a shore-parallel current.

The following abbreviation will be used at this stage:

$$Q' = \frac{1}{\cosh^2 \kappa h'} \left(Q_1 \frac{\partial^2 h'}{\partial x_1 \partial x_1} + Q_2 \frac{\partial^2 \kappa}{\partial x_1^2} + Q_3 \frac{\partial^2 \bar{\eta}}{\partial x_1 \partial x_1} + Q_4 \left(\frac{\partial h'}{\partial x_1} \frac{\partial h'}{\partial x_1} \right) \right. \\ \left. + Q_5 \left(\frac{\partial \kappa}{\partial x_1} \frac{\partial \kappa}{\partial x_1} \right) + Q_6 \left(\frac{\partial \bar{\eta}}{\partial x_1} \frac{\partial \bar{\eta}}{\partial x_1} \right) + Q_7 \frac{\partial \kappa}{\partial x_1} \frac{\partial h'}{\partial x_1} \right. \\ \left. + Q_8 \frac{\partial h'}{\partial x_1} \frac{\partial \bar{\eta}}{\partial x_1} + Q_9 \frac{\partial \bar{\eta}}{\partial x_1} \frac{\partial \kappa}{\partial x_1} + W_6 \frac{\partial h'}{\partial x_1} - W_6 \frac{\partial \bar{\eta}}{\partial x_1} \right) \quad (3.621)$$

3.8.2 Integration over a finite element

Equation (3.620) can now be multiplied by a weighting function (W^I) and the product integrated over the length of the element. In the interest of maintaining consistency with previous authors the equation will also be multiplied by -1 at this stage:

$$-\int_0^l \frac{\partial}{\partial x_1} \left(CC_g \frac{\partial \hat{\phi}}{\partial x_1} \right) W^I dx + \int_0^l \kappa^2 CC_g \hat{\phi} W^I dx - \int_0^l \hat{\phi} \sigma^2 Q' W^I dx - \int_0^l \kappa^2 CC_g \hat{\phi} W^I dx + \int_0^l \sigma^2 \hat{\phi} W^I dx \\ + \int_0^l g \frac{\partial \bar{\eta}}{\partial x_1} \frac{\partial \hat{\phi}}{\partial x_1} W^I dx - \int_0^l \omega^2 \hat{\phi} W^I dx + \int_0^l 2\omega \kappa_2 U_2 \hat{\phi} W^I dx - \int_0^l \kappa_2^2 U_2^2 \hat{\phi} W^I dx = 0 \quad (3.622)$$

Examining the first term of Equation (3.622) in more detail using Green's Theorem gives:

$$-\int_0^l \frac{\partial}{\partial x_1} \left(CC_g \frac{\partial \hat{\phi}}{\partial x_1} \right) W^I dx = -\int_0^l \frac{\partial}{\partial x_1} \left(CC_g \frac{\partial \hat{\phi}}{\partial x_1} W^I \right) dx + \int_0^l CC_g \frac{\partial \hat{\phi}}{\partial x_1} \frac{\partial W^I}{\partial x_1} dx \quad (3.623)$$

$$-\int_0^l \frac{\partial}{\partial x_1} \left(CC_g \frac{\partial \hat{\phi}}{\partial x_1} \right) W^I dx = -CC_g \frac{\partial \hat{\phi}}{\partial x_1} W^I \Big|_0^l + \int_0^l CC_g \frac{\partial \hat{\phi}}{\partial x_1} \frac{\partial W^I}{\partial x_1} dx \quad (3.624)$$

$$-\int_0^l \frac{\partial}{\partial x_1} \left(CC_g \frac{\partial \hat{\phi}}{\partial x_1} \right) W^I dx = -CC_g \frac{\partial \hat{\phi}}{\partial x_1} W^I \Big|_l + CC_g \frac{\partial \hat{\phi}}{\partial x_1} W^I \Big|_0 + \int_0^l CC_g \frac{\partial \hat{\phi}}{\partial x_1} \frac{\partial W^I}{\partial x_1} dx \quad (3.625)$$

Substituting Equation (3.625) into Equation (3.622) gives:

$$\int_0^l 2\omega \kappa_2 U_2 \hat{\phi} W^I dx - \int_0^l \kappa_2^2 U_2^2 \hat{\phi} W^I dx - CC_g \frac{\partial \hat{\phi}}{\partial x_1} W^I \Big|_l + CC_g \frac{\partial \hat{\phi}}{\partial x_1} W^I \Big|_0 \\ + \int_0^l CC_g \frac{\partial \hat{\phi}}{\partial x_1} \frac{\partial W^I}{\partial x_1} dx + \int_0^l \kappa^2 CC_g \hat{\phi} W^I dx + \int_0^l \sigma^2 \hat{\phi} W^I dx - \int_0^l \omega^2 \hat{\phi} W^I dx \\ - \int_0^l \kappa^2 CC_g \hat{\phi} W^I dx - \int_0^l \hat{\phi} \sigma^2 Q' W^I dx + \int_0^l g \frac{\partial \bar{\eta}}{\partial x_1} \frac{\partial \hat{\phi}}{\partial x_1} W^I dx = 0 \quad (3.626)$$

Expressing $\hat{\phi}$ in terms of shape functions L^J gives:

$$\hat{\phi} = \hat{\phi}^J L^J \quad (3.627)$$

$$\begin{aligned} & \int_0^l 2\omega\kappa_2 U_2 \hat{\phi}^J L^J W^I dx - \int_0^l \kappa_2^2 U_2^2 \hat{\phi}^J L^J W^I dx - CC_g \left. \frac{\partial \hat{\phi}}{\partial x_1} W^I \right|_l + CC_g \left. \frac{\partial \hat{\phi}}{\partial x_1} W^I \right|_0 \\ & + \int_0^l CC_g \frac{\partial(\hat{\phi}^J L^J)}{\partial x_1} \frac{\partial W^I}{\partial x_1} dx + \int_0^l \kappa_2^2 CC_g \hat{\phi}^J L^J W^I dx + \int_0^l \sigma^2 \hat{\phi}^J L^J W^I dx - \int_0^l \omega^2 \hat{\phi}^J L^J W^I dx \\ & - \int_0^l \kappa^2 CC_g \hat{\phi}^J L^J W^I dx - \int_0^l \sigma^2 Q' \hat{\phi}^J L^J W^I dx + \int_0^l g \frac{\partial \bar{\eta}}{\partial x_1} \frac{\partial(\hat{\phi}^J L^J)}{\partial x_1} W^I dx = 0 \end{aligned} \quad (3.628)$$

Rearranging Equation (3.628) gives:

$$\begin{aligned} & \int_0^l 2\omega\kappa_2 U_2 W^I L^J \hat{\phi}^J dx - \int_0^l \kappa_2^2 U_2^2 W^I L^J \hat{\phi}^J dx - CC_g \left. \frac{\partial \hat{\phi}}{\partial x_1} W^I \right|_l + CC_g \left. \frac{\partial \hat{\phi}}{\partial x_1} W^I \right|_0 \\ & + \int_0^l CC_g \frac{\partial W^I}{\partial x_1} \frac{\partial L^J}{\partial x_1} \hat{\phi}^J dx + \int_0^l \kappa_2^2 CC_g W^I L^J \hat{\phi}^J dx + \int_0^l \sigma^2 W^I L^J \hat{\phi}^J dx - \int_0^l \omega^2 W^I L^J \hat{\phi}^J dx \\ & - \int_0^l \kappa^2 CC_g W^I L^J \hat{\phi}^J dx - \int_0^l \sigma^2 Q' W^I L^J \hat{\phi}^J dx + \int_0^l g \frac{\partial \bar{\eta}}{\partial x_1} W^I \frac{\partial L^J}{\partial x_1} \hat{\phi}^J dx = 0 \end{aligned} \quad (3.629)$$

The superscript I is a free superscript and varies between one and two. Hence Equation (3.629) is actually two equations. Where $I = 1$ Equation (3.629) becomes:

$$\begin{aligned} & \int_0^l 2\omega\kappa_2 U_2 W^1 L^J \hat{\phi}^J dx - \int_0^l \kappa_2^2 U_2^2 W^1 L^J \hat{\phi}^J dx - CC_g \left. \frac{\partial \hat{\phi}}{\partial x_1} W^1 \right|_l + CC_g \left. \frac{\partial \hat{\phi}}{\partial x_1} W^1 \right|_0 \\ & + \int_0^l CC_g \frac{\partial W^1}{\partial x_1} \frac{\partial L^J}{\partial x_1} \hat{\phi}^J dx + \int_0^l \kappa_2^2 CC_g W^1 L^J \hat{\phi}^J dx + \int_0^l \sigma^2 W^1 L^J \hat{\phi}^J dx - \int_0^l \omega^2 W^1 L^J \hat{\phi}^J dx \\ & - \int_0^l \kappa^2 CC_g W^1 L^J \hat{\phi}^J dx - \int_0^l \sigma^2 Q' W^1 L^J \hat{\phi}^J dx + \int_0^l g \frac{\partial \bar{\eta}}{\partial x_1} W^1 \frac{\partial L^J}{\partial x_1} \hat{\phi}^J dx = 0 \end{aligned} \quad (3.630)$$

Where $I = 2$ Equation (3.629) becomes:

$$\begin{aligned} & \int_0^l 2\omega\kappa_2 U_2 W^2 L^J \hat{\phi}^J dx - \int_0^l \kappa_2^2 U_2^2 W^2 L^J \hat{\phi}^J dx - CC_g \left. \frac{\partial \hat{\phi}}{\partial x_1} W^2 \right|_l + CC_g \left. \frac{\partial \hat{\phi}}{\partial x_1} W^2 \right|_0 \\ & + \int_0^l CC_g \frac{\partial W^2}{\partial x_1} \frac{\partial L^J}{\partial x_1} \hat{\phi}^J dx + \int_0^l \kappa_2^2 CC_g W^2 L^J \hat{\phi}^J dx + \int_0^l \sigma^2 W^2 L^J \hat{\phi}^J dx - \int_0^l \omega^2 W^2 L^J \hat{\phi}^J dx \\ & - \int_0^l \kappa^2 CC_g W^2 L^J \hat{\phi}^J dx - \int_0^l \sigma^2 Q' W^2 L^J \hat{\phi}^J dx + \int_0^l g \frac{\partial \bar{\eta}}{\partial x_1} W^2 \frac{\partial L^J}{\partial x_1} \hat{\phi}^J dx = 0 \end{aligned} \quad (3.631)$$

This means that the variable I provides a row number so Equation (3.630) and Equation (3.631) can now be put together as a vector equation:

$$\begin{aligned}
& \int_0^l 2\omega\kappa_2 U_2 \left\{ \frac{W^1}{W^2} \right\} L^J \hat{\phi}^J dx - \int_0^l \kappa_2^2 U_2^2 \left\{ \frac{W^1}{W^2} \right\} L^J \hat{\phi}^J dx - CC_g \frac{\partial \hat{\phi}}{\partial x_1} \left\{ \frac{W^1}{W^2} \right\} \Big|_l + CC_g \frac{\partial \hat{\phi}}{\partial x_1} \left\{ \frac{W^1}{W^2} \right\} \Big|_0 \\
& + \int_0^l CC_g \left\{ \frac{\partial W^1}{\partial x_1} \right\} \frac{\partial L^J}{\partial x_1} \hat{\phi}^J dx + \int_0^l \kappa_2^2 CC_g \left\{ \frac{W^1}{W^2} \right\} L^J \hat{\phi}^J dx + \int_0^l \sigma^2 \left\{ \frac{W^1}{W^2} \right\} L^J \hat{\phi}^J dx - \int_0^l \omega^2 \left\{ \frac{W^1}{W^2} \right\} L^J \hat{\phi}^J dx \\
& - \int_0^l \kappa^2 CC_g \left\{ \frac{W^1}{W^2} \right\} L^J \hat{\phi}^J dx - \int_0^l \sigma^2 Q' \left\{ \frac{W^1}{W^2} \right\} L^J \hat{\phi}^J dx + \int_0^l g \frac{\partial \bar{\eta}}{\partial x_1} \left\{ \frac{W^1}{W^2} \right\} \frac{\partial L^J}{\partial x_1} \hat{\phi}^J dx = 0
\end{aligned} \tag{3.632}$$

The superscript J may also be one or two and hence defines the row number of a matrix:

$$\begin{aligned}
& \int_0^l 2\omega\kappa_2 U_2 \left\{ \frac{W^1}{W^2} \right\} \begin{bmatrix} L^1 & L^2 \end{bmatrix} \begin{Bmatrix} \hat{\phi}^1 \\ \hat{\phi}^2 \end{Bmatrix} dx - \int_0^l \kappa_2^2 U_2^2 \left\{ \frac{W^1}{W^2} \right\} \begin{bmatrix} L^1 & L^2 \end{bmatrix} \begin{Bmatrix} \hat{\phi}^1 \\ \hat{\phi}^2 \end{Bmatrix} dx \\
& - CC_g \frac{\partial \hat{\phi}}{\partial x_1} \left\{ \frac{W^1}{W^2} \right\} \Big|_l + CC_g \frac{\partial \hat{\phi}}{\partial x_1} \left\{ \frac{W^1}{W^2} \right\} \Big|_0 + \int_0^l CC_g \left\{ \frac{\partial W^1}{\partial x_1} \right\} \begin{bmatrix} \frac{\partial L^1}{\partial x_1} & \frac{\partial L^2}{\partial x_1} \end{bmatrix} \begin{Bmatrix} \hat{\phi}^1 \\ \hat{\phi}^2 \end{Bmatrix} dx \\
& + \int_0^l \kappa_2^2 CC_g \left\{ \frac{W^1}{W^2} \right\} \begin{bmatrix} L^1 & L^2 \end{bmatrix} \begin{Bmatrix} \hat{\phi}^1 \\ \hat{\phi}^2 \end{Bmatrix} dx + \int_0^l \sigma^2 \left\{ \frac{W^1}{W^2} \right\} \begin{bmatrix} L^1 & L^2 \end{bmatrix} \begin{Bmatrix} \hat{\phi}^1 \\ \hat{\phi}^2 \end{Bmatrix} dx \\
& - \int_0^l \omega^2 \left\{ \frac{W^1}{W^2} \right\} \begin{bmatrix} L^1 & L^2 \end{bmatrix} \begin{Bmatrix} \hat{\phi}^1 \\ \hat{\phi}^2 \end{Bmatrix} dx - \int_0^l \kappa^2 CC_g \left\{ \frac{W^1}{W^2} \right\} \begin{bmatrix} L^1 & L^2 \end{bmatrix} \begin{Bmatrix} \hat{\phi}^1 \\ \hat{\phi}^2 \end{Bmatrix} dx \\
& - \int_0^l \sigma^2 Q' \left\{ \frac{W^1}{W^2} \right\} \begin{bmatrix} L^1 & L^2 \end{bmatrix} \begin{Bmatrix} \hat{\phi}^1 \\ \hat{\phi}^2 \end{Bmatrix} dx + \int_0^l g \frac{\partial \bar{\eta}}{\partial x_1} \left\{ \frac{W^1}{W^2} \right\} \begin{bmatrix} \frac{\partial L^1}{\partial x_1} & \frac{\partial L^2}{\partial x_1} \end{bmatrix} \begin{Bmatrix} \hat{\phi}^1 \\ \hat{\phi}^2 \end{Bmatrix} dx = 0
\end{aligned} \tag{3.633}$$

Equation (3.633) can be reduced to:

$$\begin{aligned}
& \int_0^l 2\omega\kappa_2 U_2 \begin{bmatrix} W^1 L^1 & W^1 L^2 \\ W^2 L^1 & W^2 L^2 \end{bmatrix} \begin{Bmatrix} \hat{\phi}^1 \\ \hat{\phi}^2 \end{Bmatrix} dx - \int_0^l \kappa_2^2 U_2^2 \begin{bmatrix} W^1 L^1 & W^1 L^2 \\ W^2 L^1 & W^2 L^2 \end{bmatrix} \begin{Bmatrix} \hat{\phi}^1 \\ \hat{\phi}^2 \end{Bmatrix} dx \\
& - CC_g \frac{\partial \hat{\phi}}{\partial x_1} \begin{Bmatrix} W^1 \\ W^2 \end{Bmatrix} \bigg|_l + CC_g \frac{\partial \hat{\phi}}{\partial x_1} \begin{Bmatrix} W^1 \\ W^2 \end{Bmatrix} \bigg|_0 + \int_0^l CC_g \begin{bmatrix} \frac{\partial W^1}{\partial x_1} \frac{\partial L^1}{\partial x_1} & \frac{\partial W^1}{\partial x_1} \frac{\partial L^2}{\partial x_1} \\ \frac{\partial W^2}{\partial x_1} \frac{\partial L^1}{\partial x_1} & \frac{\partial W^2}{\partial x_1} \frac{\partial L^2}{\partial x_1} \end{bmatrix} \begin{Bmatrix} \hat{\phi}^1 \\ \hat{\phi}^2 \end{Bmatrix} dx \\
& + \int_0^l \kappa_2^2 CC_g \begin{bmatrix} W^1 L^1 & W^1 L^2 \\ W^2 L^1 & W^2 L^2 \end{bmatrix} \begin{Bmatrix} \hat{\phi}^1 \\ \hat{\phi}^2 \end{Bmatrix} dx + \int_0^l \sigma^2 \begin{bmatrix} W^1 L^1 & W^1 L^2 \\ W^2 L^1 & W^2 L^2 \end{bmatrix} \begin{Bmatrix} \hat{\phi}^1 \\ \hat{\phi}^2 \end{Bmatrix} dx \\
& - \int_0^l \omega^2 \begin{bmatrix} W^1 L^1 & W^1 L^2 \\ W^2 L^1 & W^2 L^2 \end{bmatrix} \begin{Bmatrix} \hat{\phi}^1 \\ \hat{\phi}^2 \end{Bmatrix} dx - \int_0^l \kappa^2 CC_g \begin{bmatrix} W^1 L^1 & W^1 L^2 \\ W^2 L^1 & W^2 L^2 \end{bmatrix} \begin{Bmatrix} \hat{\phi}^1 \\ \hat{\phi}^2 \end{Bmatrix} dx \\
& - \int_0^l \sigma^2 Q' \begin{bmatrix} W^1 L^1 & W^1 L^2 \\ W^2 L^1 & W^2 L^2 \end{bmatrix} \begin{Bmatrix} \hat{\phi}^1 \\ \hat{\phi}^2 \end{Bmatrix} dx + \int_0^l g \frac{\partial \bar{\eta}}{\partial x_1} \begin{bmatrix} W^1 \frac{\partial L^1}{\partial x_1} & W^1 \frac{\partial L^2}{\partial x_1} \\ W^2 \frac{\partial L^1}{\partial x_1} & W^2 \frac{\partial L^2}{\partial x_1} \end{bmatrix} \begin{Bmatrix} \hat{\phi}^1 \\ \hat{\phi}^2 \end{Bmatrix} dx = 0
\end{aligned} \tag{3.634}$$

The finite element model created for this project will be using the Galerkin method in which the weighting function is equal to the shape functions being used. Hence, at this stage W^I will be replaced with L^I . The Galerkin method and shape functions for both the one-dimensional and two-dimensional models are discussed in Appendix A.

$$\begin{aligned}
& \int_0^l 2\omega\kappa_2 U_2 \begin{bmatrix} L^1 L^1 & L^1 L^2 \\ L^2 L^1 & L^2 L^2 \end{bmatrix} \begin{Bmatrix} \hat{\phi}^1 \\ \hat{\phi}^2 \end{Bmatrix} dx - \int_0^l \kappa_2^2 U_2^2 \begin{bmatrix} L^1 L^1 & L^1 L^2 \\ L^2 L^1 & L^2 L^2 \end{bmatrix} \begin{Bmatrix} \hat{\phi}^1 \\ \hat{\phi}^2 \end{Bmatrix} dx \\
& + \int_0^l CC_g \begin{bmatrix} \frac{\partial L^1}{\partial x_1} \frac{\partial L^1}{\partial x_1} & \frac{\partial L^1}{\partial x_1} \frac{\partial L^2}{\partial x_1} \\ \frac{\partial L^2}{\partial x_1} \frac{\partial L^1}{\partial x_1} & \frac{\partial L^2}{\partial x_1} \frac{\partial L^2}{\partial x_1} \end{bmatrix} \begin{Bmatrix} \hat{\phi}^1 \\ \hat{\phi}^2 \end{Bmatrix} dx + \int_0^l \kappa_2^2 CC_g \begin{bmatrix} L^1 L^1 & L^1 L^2 \\ L^2 L^1 & L^2 L^2 \end{bmatrix} \begin{Bmatrix} \hat{\phi}^1 \\ \hat{\phi}^2 \end{Bmatrix} dx \\
& + \int_0^l \sigma^2 \begin{bmatrix} L^1 L^1 & L^1 L^2 \\ L^2 L^1 & L^2 L^2 \end{bmatrix} \begin{Bmatrix} \hat{\phi}^1 \\ \hat{\phi}^2 \end{Bmatrix} dx - \int_0^l \omega^2 \begin{bmatrix} L^1 L^1 & L^1 L^2 \\ L^2 L^1 & L^2 L^2 \end{bmatrix} \begin{Bmatrix} \hat{\phi}^1 \\ \hat{\phi}^2 \end{Bmatrix} dx \\
& - \int_0^l \kappa^2 CC_g \begin{bmatrix} L^1 L^1 & L^1 L^2 \\ L^2 L^1 & L^2 L^2 \end{bmatrix} \begin{Bmatrix} \hat{\phi}^1 \\ \hat{\phi}^2 \end{Bmatrix} dx - \int_0^l \sigma^2 Q' \begin{bmatrix} L^1 L^1 & L^1 L^2 \\ L^2 L^1 & L^2 L^2 \end{bmatrix} \begin{Bmatrix} \hat{\phi}^1 \\ \hat{\phi}^2 \end{Bmatrix} dx \\
& + \int_0^l g \frac{\partial \bar{\eta}}{\partial x_1} \begin{bmatrix} L^1 \frac{\partial L^1}{\partial x_1} & L^1 \frac{\partial L^2}{\partial x_1} \\ L^2 \frac{\partial L^1}{\partial x_1} & L^2 \frac{\partial L^2}{\partial x_1} \end{bmatrix} \begin{Bmatrix} \hat{\phi}^1 \\ \hat{\phi}^2 \end{Bmatrix} dx - CC_g \frac{\partial \hat{\phi}}{\partial x_1} \begin{Bmatrix} L^1 \\ L^2 \end{Bmatrix} \bigg|_l + CC_g \frac{\partial \hat{\phi}}{\partial x_1} \begin{Bmatrix} L^1 \\ L^2 \end{Bmatrix} \bigg|_0 = 0
\end{aligned} \tag{3.635}$$

3.8.3 Parabolic mild slope boundary condition

With the exception of the last two terms Equation (3.635) may now be used with the finite element computer solution scheme of Zienkiewicz (1977) to solve for the unknown values of $\hat{\phi}'$ (that is the value of $\hat{\phi}$ at node J) bearing in mind that $\hat{\phi}$ is complex and will have two components at each node. Examination of the last two terms shows that within the domain they cancel each other out at each node. Hence they need only be examined at the boundary node at either end of the model.

3.8.3.1 Parabolisation of Elliptic Mild-Slope Equation

At the boundary nodes the last two terms must now be converted into a form that the solution scheme can control. At this point the parabolic approximation to the mild-slope equation will be used. Equation (3.533) can be expressed as follows:

$$\frac{\partial^2 \phi}{\partial n^2} CC_g + \frac{\partial^2 \phi}{\partial s^2} CC_g + \frac{\partial \phi}{\partial n} \left(\frac{\partial}{\partial n} CC_g \right) + \frac{\partial \phi}{\partial s} \left(\frac{\partial}{\partial s} CC_g \right) + \phi \kappa^2 CC_g = 0 \quad (3.636)$$

The parabolic approximation to the mild-slope equation assumes there is no diffraction in the direction of wave propagation. In order to remove the forward diffraction terms it is necessary to rewrite Equation (3.636) in terms of (3.135); $\phi = A_\phi e^{iS_\phi}$.

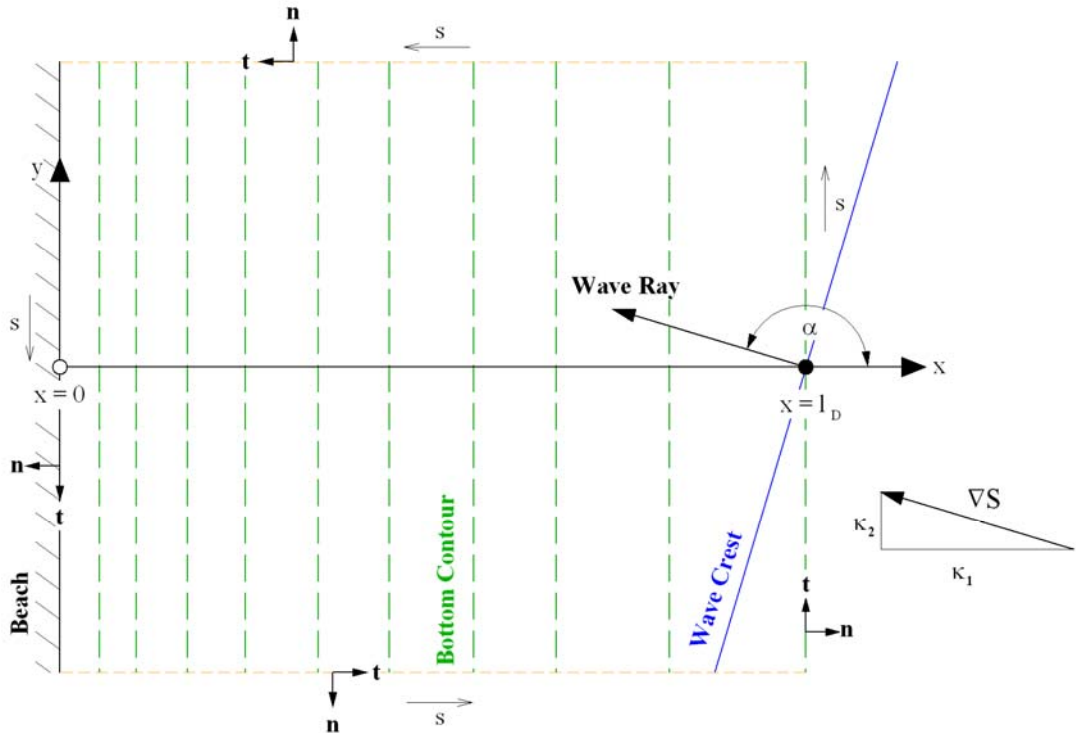


Figure 3.9 – Definition Sketch of Domain showing Boundary treatment

It is necessary to examine the derivatives of this equation assuming in this case that n is the direction perpendicular to the boundary through which the wave is exiting and s is parallel to that boundary:

$$\frac{\partial \phi}{\partial n} = \frac{\partial A_\phi}{\partial n} e^{iS_\phi} + iA_\phi \frac{\partial S_\phi}{\partial n} e^{iS_\phi} \quad (3.637)$$

Equation (3.637) can be rewritten as:

$$\frac{\partial A_\phi}{\partial n} e^{iS_\phi} = \frac{\partial \phi}{\partial n} - i\phi \frac{\partial S_\phi}{\partial n} \quad (3.638)$$

Substitution of Equation (3.135) into Equation (3.637) yields:

$$\frac{\partial \phi}{\partial n} = \frac{\partial A_\phi}{\partial n} \frac{\phi}{A_\phi} + i\phi \frac{\partial S_\phi}{\partial n} \quad (3.639)$$

The second derivative of velocity potential with respect to n is:

$$\frac{\partial^2 \phi}{\partial n^2} = \frac{\partial^2 A_\phi}{\partial n^2} e^{iS_\phi} + 2i \frac{\partial A_\phi}{\partial n} \frac{\partial S_\phi}{\partial n} e^{iS_\phi} + iA_\phi \frac{\partial^2 S_\phi}{\partial n^2} e^{iS_\phi} - A_\phi \frac{\partial S_\phi}{\partial n} \frac{\partial S_\phi}{\partial n} e^{iS_\phi} \quad (3.640)$$

Substitution of Equations (3.638) and (3.135) into Equation (3.640) gives:

$$\frac{\partial^2 \phi}{\partial n^2} = \frac{\partial^2 A_\phi}{\partial n^2} \frac{\phi}{A_\phi} + 2i \left(\frac{\partial \phi}{\partial n} - i\phi \frac{\partial S_\phi}{\partial n} \right) \frac{\partial S_\phi}{\partial n} + i\phi \frac{\partial^2 S_\phi}{\partial n^2} - \phi \frac{\partial S_\phi}{\partial n} \frac{\partial S_\phi}{\partial n} \quad (3.641)$$

$$\frac{\partial^2 \phi}{\partial n^2} = \frac{\partial^2 A_\phi}{\partial n^2} \frac{\phi}{A_\phi} + 2i \frac{\partial \phi}{\partial n} \frac{\partial S_\phi}{\partial n} + \phi \left(\frac{\partial S_\phi}{\partial n} \right)^2 + i\phi \frac{\partial^2 S_\phi}{\partial n^2} \quad (3.642)$$

It is now possible to remove the effects of forward diffraction from the equations. The removal of the derivatives of the amplitude of velocity potential from Equations (3.642) and (3.639) yields:

$$\frac{\partial^2 \phi}{\partial n^2} = 2i \frac{\partial \phi}{\partial n} \frac{\partial S_\phi}{\partial n} + \phi \left(\frac{\partial S_\phi}{\partial n} \right)^2 + i\phi \frac{\partial^2 S_\phi}{\partial n^2} \quad (3.643)$$

$$\frac{\partial \phi}{\partial n} = i\phi \frac{\partial S_\phi}{\partial n} \quad (3.644)$$

Substitution of Equations (3.643) and (3.644) into the elliptic solution of Equation (3.636) gives the following:

$$\left[2i \frac{\partial \phi}{\partial n} \frac{\partial S_\phi}{\partial n} + \phi \left(\frac{\partial S_\phi}{\partial n} \right)^2 + i\phi \frac{\partial^2 S_\phi}{\partial n^2} \right] CC_g + \frac{\partial^2 \phi}{\partial s^2} CC_g + \left(i\phi \frac{\partial S_\phi}{\partial n} \right) \left(\frac{\partial}{\partial n} CC_g \right) + \frac{\partial \phi}{\partial s} \left(\frac{\partial}{\partial s} CC_g \right) + \phi \kappa^2 CC_g = 0 \quad (3.645)$$

The one remaining term containing the derivative of velocity potential with respect to n may now be isolated on one side of the equation:

$$2i \frac{\partial \phi}{\partial n} \frac{\partial S}{\partial n} CC_g = - \left(i\phi \frac{\partial S}{\partial n} \right) \frac{\partial (CC_g)}{\partial n} - \phi \left(\frac{\partial S}{\partial n} \right)^2 CC_g - i\phi \frac{\partial^2 S}{\partial n^2} CC_g - \frac{\partial^2 \phi}{\partial s^2} CC_g - \frac{\partial \phi}{\partial s} \frac{\partial (CC_g)}{\partial s} - \phi \kappa^2 CC_g \quad (3.646)$$

$$2i \frac{\partial \phi}{\partial n} \frac{\partial S}{\partial n} = - \frac{1}{CC_g} \left(i\phi \frac{\partial S}{\partial n} \right) \frac{\partial (CC_g)}{\partial n} - \phi \left(\frac{\partial S}{\partial n} \right)^2 - i\phi \frac{\partial^2 S}{\partial n^2} - \frac{\partial^2 \phi}{\partial s^2} - \frac{1}{CC_g} \frac{\partial \phi}{\partial s} \frac{\partial (CC_g)}{\partial s} - \phi \kappa^2 \quad (3.647)$$

It can be assumed that at the downwave boundary where the wave is exiting the domain the shoaling and refraction process has caused the wave to be parallel to the beach boundary. This means the following assumption can be made:

$$\frac{\partial S}{\partial n} = \kappa \quad (3.648)$$

Using Equation (3.648) with Equation (3.647) gives:

$$2i \frac{\partial \phi}{\partial n} \kappa = - \frac{i\kappa \phi}{CC_g} \frac{\partial (CC_g)}{\partial n} - \phi \kappa^2 - i\phi \frac{\partial \kappa}{\partial n} - \frac{\partial^2 \phi}{\partial s^2} - \frac{1}{CC_g} \frac{\partial \phi}{\partial s} \frac{\partial (CC_g)}{\partial s} - \phi \kappa^2 \quad (3.649)$$

$$\frac{\partial \phi}{\partial n} = - \frac{\phi}{2CC_g} \frac{\partial (CC_g)}{\partial n} + \frac{i\phi \kappa}{2} - \frac{\phi}{2\kappa} \frac{\partial \kappa}{\partial n} + \frac{i}{2\kappa} \frac{\partial^2 \phi}{\partial s^2} + \frac{i}{2\kappa CC_g} \frac{\partial \phi}{\partial s} \frac{\partial (CC_g)}{\partial s} + \frac{i\phi \kappa}{2} \quad (3.650)$$

$$\frac{\partial \phi}{\partial n} = - \frac{1}{2\kappa} \frac{\partial \kappa}{\partial n} \phi - \frac{1}{2CC_g} \frac{\partial (CC_g)}{\partial n} \phi + i\kappa \phi + \frac{i}{2\kappa} \frac{\partial^2 \phi}{\partial s^2} + \frac{i}{2\kappa CC_g} \frac{\partial \phi}{\partial s} \frac{\partial (CC_g)}{\partial s} \quad (3.651)$$

$$\frac{\partial \phi}{\partial n} = - \frac{1}{2\kappa} \frac{\partial \kappa}{\partial n} \phi - \frac{1}{2CC_g} \frac{\partial CC_g}{\partial n} \phi + i\kappa \phi + \frac{i}{2CC_g \kappa} \left[CC_g \frac{\partial^2 \phi}{\partial s^2} + \frac{\partial CC_g}{\partial s} \frac{\partial \phi}{\partial s} \right] \quad (3.652)$$

$$\frac{\partial \phi}{\partial n} = - \frac{1}{2\kappa} \frac{\partial \kappa}{\partial n} \phi - \frac{1}{2CC_g} \frac{\partial CC_g}{\partial n} \phi + i\kappa \phi + \frac{i}{2CC_g \kappa} \left[\frac{\partial}{\partial s} \left(CC_g \frac{\partial \phi}{\partial s} \right) \right] \quad (3.653)$$

Equation (3.653) is the Parabolic Approximation to the Elliptic Equation in the absence of currents.

3.8.3.2 Comparison of Parabolic Approximation with that of Booij (1981)

Equation 6.17 of Booij (1981) in the absence of a current is:

$$M\phi = \frac{\partial}{\partial s} \left(CC_g \frac{\partial \phi}{\partial s} \right) \quad (3.654)$$

Then using the following identities:

$$P_1 = 0 \quad (3.655)$$

$$P_2 = 0.5 \quad (3.656)$$

A simplified expression is obtained for Equation 6.19 of Booij (1981). The wave will be propagating normal to the boundary due to shoaling.

$$\frac{\partial}{\partial n} \left[(CC_g \kappa)^{\frac{1}{2}} \phi \right] - i\kappa (CC_g \kappa)^{\frac{1}{2}} \phi - i \frac{(CC_g \kappa)^{-\frac{1}{2}}}{2} \left[\frac{\partial}{\partial s} \left(CC_g \frac{\partial \phi}{\partial s} \right) \right] = 0 \quad (3.657)$$

Equation (3.657) may now be manipulated as follows to isolate the gradient of velocity potential with respect to n :

$$\phi \frac{\partial (CC_g \kappa)^{\frac{1}{2}}}{\partial n} + (CC_g \kappa)^{\frac{1}{2}} \frac{\partial \phi}{\partial n} - i\kappa (CC_g \kappa)^{\frac{1}{2}} \phi - i \frac{(CC_g \kappa)^{-\frac{1}{2}}}{2} \left[\frac{\partial}{\partial s} \left(CC_g \frac{\partial \phi}{\partial s} \right) \right] = 0 \quad (3.658)$$

$$(CC_g \kappa)^{\frac{1}{2}} \frac{\partial \phi}{\partial n} = -\phi \frac{\partial (CC_g \kappa)^{\frac{1}{2}}}{\partial n} + i\kappa (CC_g \kappa)^{\frac{1}{2}} \phi + i \frac{(CC_g \kappa)^{-\frac{1}{2}}}{2} \left[\frac{\partial}{\partial s} \left(CC_g \frac{\partial \phi}{\partial s} \right) \right] \quad (3.659)$$

$$\frac{\partial \phi}{\partial n} = -\phi (CC_g \kappa)^{-\frac{1}{2}} \frac{\partial (CC_g \kappa)^{\frac{1}{2}}}{\partial n} + i\kappa \phi + \frac{i}{2a\kappa} \left[\frac{\partial}{\partial s} \left(CC_g \frac{\partial \phi}{\partial s} \right) \right] \quad (3.660)$$

$$\frac{\partial \phi}{\partial n} = -\phi (CC_g \kappa)^{-\frac{1}{2}} \left[\frac{(CC_g \kappa)^{-\frac{1}{2}}}{2} \left(CC_g \frac{\partial \kappa}{\partial n} + \kappa \frac{\partial a}{\partial n} \right) \right] + i\kappa \phi + \frac{i}{2a\kappa} \left[\frac{\partial}{\partial s} \left(CC_g \frac{\partial \phi}{\partial s} \right) \right] \quad (3.661)$$

$$\frac{\partial \phi}{\partial n} = \frac{-1}{2CC_g \kappa} \left(CC_g \frac{\partial \kappa}{\partial n} + \kappa \frac{\partial a}{\partial n} \right) \phi + i\kappa \phi + \frac{i}{2CC_g \kappa} \left[\frac{\partial}{\partial s} \left(CC_g \frac{\partial \phi}{\partial s} \right) \right] \quad (3.662)$$

$$\frac{\partial \phi}{\partial n} = -\frac{1}{2\kappa} \frac{\partial \kappa}{\partial n} \phi - \frac{1}{2CC_g} \frac{\partial CC_g}{\partial n} \phi + i\kappa \phi + \frac{i}{2CC_g \kappa} \left[\frac{\partial}{\partial s} \left(CC_g \frac{\partial \phi}{\partial s} \right) \right] \quad (3.663)$$

Equation (3.663) is identical to (3.653). This shows agreement between the parabolic approximations of this project and of Booij (1981) in the absence of a current. Clyne (2008) shows that both the Clyne (2008) and Radder (1979) parabolic approximations also match that of Booij (1981) in the absence of a current. Thus all four of the above mentioned parabolic approximations concur.

3.8.3.3 Parabolic Boundary Condition for 1d-NM-WCIM

In Equation (3.653) n is the direction of wave propagation and s is the normal to the direction of wave propagation. An examination of the beach boundary shows that at this boundary:

$$n = -x_1 \quad (3.664)$$

$$\frac{d}{dn} = -\frac{d}{dx_1} \quad (3.665)$$

$$s = -x_2 \quad (3.666)$$

$$\frac{d}{ds} = -\frac{d}{dx_2} \quad (3.667)$$

Therefore Equation (3.653) becomes:

$$-\frac{\partial}{\partial x_1} \left[(CC_g \kappa)^{\frac{1}{2}} \phi \right] - i\kappa (CC_g \kappa)^{\frac{1}{2}} \phi - i \frac{(CC_g \kappa)^{-\frac{1}{2}}}{2} \left[\frac{\partial}{\partial x_2} \left(CC_g \frac{\partial \phi}{\partial x_2} \right) \right] = 0 \quad (3.668)$$

As before $\frac{\partial CC_g}{\partial x_2} = 0$ for the one dimensional model. This leads to the following:

$$-\frac{\partial}{\partial x_1} \left[(CC_g \kappa)^{\frac{1}{2}} \phi \right] - i\kappa (CC_g \kappa)^{\frac{1}{2}} \phi - i \frac{(CC_g \kappa)^{-\frac{1}{2}}}{2} \left[CC_g \frac{\partial^2 \phi}{\partial x_2^2} \right] = 0 \quad (3.669)$$

Using Equation (3.617) with Equation (3.669) gives:

$$-\frac{\partial}{\partial x_1} \left[(CC_g \kappa)^{\frac{1}{2}} \hat{\phi} e^{i\kappa_2 x_2} \right] - i\kappa (CC_g \kappa)^{\frac{1}{2}} \hat{\phi} e^{i\kappa_2 x_2} - i \frac{(CC_g \kappa)^{-\frac{1}{2}}}{2} \left[-CC_g \kappa_2^2 \hat{\phi} e^{i\kappa_2 x_2} \right] = 0 \quad (3.670)$$

Dividing across by $e^{i\kappa_2 x_2}$ yields:

$$-\frac{\partial}{\partial x_1} \left[(CC_g \kappa)^{\frac{1}{2}} \hat{\phi} \right] - i\kappa (CC_g \kappa)^{\frac{1}{2}} \hat{\phi} - i \frac{(CC_g \kappa)^{-\frac{1}{2}}}{2} \left[-CC_g \kappa_2^2 \hat{\phi} \right] = 0 \quad (3.671)$$

Expanding the first term in Equation (3.671) gives:

$$-\frac{\partial (CC_g \kappa)^{\frac{1}{2}}}{\partial x_1} \hat{\phi} - \frac{\partial \hat{\phi}}{\partial x_1} (CC_g \kappa)^{\frac{1}{2}} - i\kappa (CC_g \kappa)^{\frac{1}{2}} \hat{\phi} - i \frac{(CC_g \kappa)^{-\frac{1}{2}}}{2} \left[-CC_g \kappa_2^2 \hat{\phi} \right] = 0 \quad (3.672)$$

Isolating the $\frac{\partial \hat{\phi}}{\partial x_1}$ term on one side of the equation gives:

$$\frac{\partial \hat{\phi}}{\partial x_1} (CC_g \kappa)^{\frac{1}{2}} = -\frac{\partial (CC_g \kappa)^{\frac{1}{2}}}{\partial x_1} \hat{\phi} - i\kappa (CC_g \kappa)^{\frac{1}{2}} \hat{\phi} + i \frac{(CC_g \kappa)^{\frac{1}{2}} CC_g \kappa^2}{2} \hat{\phi} \quad (3.673)$$

Dividing Equation (3.673) by $(CC_g \kappa)^{-\frac{1}{2}}$ gives:

$$\frac{\partial \hat{\phi}}{\partial x_1} = -(CC_g \kappa)^{-\frac{1}{2}} \frac{\partial (CC_g \kappa)^{\frac{1}{2}}}{\partial x_1} \hat{\phi} - i\kappa \hat{\phi} + i \frac{CC_g \kappa^2}{2CC_g \kappa} \hat{\phi} \quad (3.674)$$

The last term may be reduced to give:

$$\frac{\partial \hat{\phi}}{\partial x_1} = -(CC_g \kappa)^{-\frac{1}{2}} \frac{\partial (CC_g \kappa)^{\frac{1}{2}}}{\partial x_1} \hat{\phi} - i\kappa \hat{\phi} + \frac{i\kappa^2}{2\kappa} \hat{\phi} \quad (3.675)$$

Expanding the derivative in the first term on the right hand side of Equation (3.675) gives:

$$\frac{\partial \hat{\phi}}{\partial x_1} = -(CC_g \kappa)^{-\frac{1}{2}} \left[\frac{(CC_g \kappa)^{\frac{1}{2}}}{2} \left(CC_g \frac{\partial \kappa}{\partial x_1} + \kappa \frac{\partial CC_g}{\partial x_1} \right) \right] \hat{\phi} - i\kappa \hat{\phi} + \frac{i\kappa^2}{2\kappa} \hat{\phi} \quad (3.676)$$

Equation (3.676) can be reduced to give:

$$\frac{\partial \hat{\phi}}{\partial x_1} = -\frac{1}{2CC_g \kappa} \left(CC_g \frac{\partial \kappa}{\partial x_1} + \kappa \frac{\partial CC_g}{\partial x_1} \right) \hat{\phi} - i\kappa \hat{\phi} + \frac{i\kappa^2}{2\kappa} \hat{\phi} \quad (3.677)$$

Further simplifying Equation (3.677) yields:

$$\frac{\partial \hat{\phi}}{\partial x_1} = -\frac{1}{2\kappa} \frac{\partial \kappa}{\partial x_1} \hat{\phi} - \frac{1}{2CC_g} \frac{\partial a}{\partial x_1} \hat{\phi} - i\kappa \hat{\phi} + \frac{i\kappa^2}{2\kappa} \hat{\phi} \quad (3.678)$$

Hence:

$$CC_g \frac{\partial \hat{\phi}}{\partial x_1} = -\frac{CC_g}{2\kappa} \frac{\partial \kappa}{\partial x_1} \hat{\phi} - \frac{1}{2} \frac{\partial CC_g}{\partial x_1} \hat{\phi} - iCC_g \kappa \hat{\phi} + \frac{iCC_g \kappa^2}{2\kappa} \hat{\phi} \quad (3.679)$$

Isolating the velocity potential gives the following equation:

$$CC_g \frac{\partial \hat{\phi}}{\partial x_1} = \left(-\frac{CC_g}{2\kappa} \frac{\partial \kappa}{\partial x_1} - \frac{1}{2} \frac{\partial CC_g}{\partial x_1} - iCC_g \kappa + \frac{iCC_g \kappa^2}{2\kappa} \right) \hat{\phi} \quad (3.680)$$

3.8.3.4 Generalised Parabolic Boundary Condition with Gradient of Phase

The methodology undertaken in Section 3.8.3.3 can also be carried out on the more general form of the parabolic equation given in Equation (3.647). Isolating the gradient of velocity potential with respect to n in Equation (3.647) yields:

$$\frac{\partial \phi}{\partial n} = -\frac{\left[\frac{\partial^2 S_\phi}{\partial n^2}\right]}{2\left[\frac{\partial S_\phi}{\partial n}\right]}\phi - \frac{1}{2CC_g}\frac{\partial(CC_g)}{\partial n}\phi + \frac{i\left[\frac{\partial S_\phi}{\partial n}\right]}{2}\phi - \frac{i\kappa^2}{2\left[\frac{\partial S_\phi}{\partial n}\right]}\phi - \frac{i}{2\left[\frac{\partial S_\phi}{\partial n}\right]}\frac{\partial^2 \phi}{\partial s^2} + \frac{i}{2CC_g\left[\frac{\partial S_\phi}{\partial n}\right]}\frac{\partial \phi}{\partial s}\frac{\partial(CC_g)}{\partial s} \quad (3.681)$$

Combining the final two terms of Equation (3.681) gives:

$$\frac{\partial \phi}{\partial n} = -\frac{\left[\frac{\partial^2 S_\phi}{\partial n^2}\right]}{2\left[\frac{\partial S_\phi}{\partial n}\right]}\phi - \frac{1}{2CC_g}\frac{\partial(CC_g)}{\partial n}\phi - \frac{i\left[\frac{\partial S_\phi}{\partial n}\right]}{2}\phi - \frac{i\kappa^2}{2\left[\frac{\partial S_\phi}{\partial n}\right]}\phi + \frac{i}{2\left[\frac{\partial S_\phi}{\partial n}\right]}\left[CC_g\frac{\partial^2 \phi}{\partial s^2} + \frac{\partial \phi}{\partial s}\frac{\partial(CC_g)}{\partial s}\right] \quad (3.682)$$

Equation (3.682) can be expressed as:

$$\frac{\partial \phi}{\partial n} = -\frac{\left[\frac{\partial^2 S_\phi}{\partial n^2}\right]}{2\left[\frac{\partial S_\phi}{\partial n}\right]}\phi - \frac{1}{2CC_g}\frac{\partial(CC_g)}{\partial n}\phi - \frac{i\left[\frac{\partial S_\phi}{\partial n}\right]}{2}\phi - \frac{i\kappa^2}{2\left[\frac{\partial S_\phi}{\partial n}\right]}\phi + \frac{i}{2\left[\frac{\partial S_\phi}{\partial n}\right]}\left[\frac{\partial}{\partial s}\left(CC_g\frac{\partial \phi}{\partial s}\right)\right] \quad (3.683)$$

Substituting Equations (3.665) and (3.667) into Equation (3.683) gives:

$$-\frac{\partial \phi}{\partial x_1} = \frac{\left[\frac{\partial^2 S_\phi}{\partial x_1 \partial x_1}\right]}{2\left[\frac{\partial S_\phi}{\partial x_1}\right]}\phi + \frac{1}{2CC_g}\frac{\partial(CC_g)}{\partial x_1}\phi + \frac{i\left[\frac{\partial S_\phi}{\partial x_1}\right]}{2}\phi + \frac{i\kappa^2}{2\left[\frac{\partial S_\phi}{\partial x_1}\right]}\phi - \frac{i}{2\left[\frac{\partial S_\phi}{\partial x_1}\right]}\left[\frac{\partial}{\partial x_2}\left(CC_g\frac{\partial \phi}{\partial x_2}\right)\right] \quad (3.684)$$

As before $\frac{\partial CC_g}{\partial x_2} = 0$ for the one dimensional model. This leads to the following:

$$-\frac{\partial \phi}{\partial x_1} = \frac{\left[\frac{\partial^2 S_\phi}{\partial x_1 \partial x_1}\right]}{2\left[\frac{\partial S_\phi}{\partial x_1}\right]}\phi + \frac{1}{2CC_g}\frac{\partial(CC_g)}{\partial x_1}\phi + \frac{i\left[\frac{\partial S_\phi}{\partial x_1}\right]}{2}\phi + \frac{i\kappa^2}{2\left[\frac{\partial S_\phi}{\partial x_1}\right]}\phi - \frac{i}{2\left[\frac{\partial S_\phi}{\partial x_1}\right]}\left[CC_g\frac{\partial^2 \phi}{\partial x_2 \partial x_2}\right] \quad (3.685)$$

Using Equation (3.617) with Equation (3.685) gives:

$$\begin{aligned}
 -\frac{\partial(\hat{\phi}e^{i\kappa_2 x_2})}{\partial x_1} &= \frac{\left[\frac{\partial^2 S_\phi}{\partial x_1 \partial x_1}\right]}{2\left[\frac{\partial S_\phi}{\partial x_1}\right]} \hat{\phi}e^{i\kappa_2 x_2} + \frac{1}{2CC_g} \frac{\partial(CC_g)}{\partial x_1} \hat{\phi}e^{i\kappa_2 x_2} + \frac{i\left[\frac{\partial S_\phi}{\partial x_1}\right]}{2} \hat{\phi}e^{i\kappa_2 x_2} \\
 &+ \frac{i\kappa^2}{2\left[\frac{\partial S_\phi}{\partial x_1}\right]} \hat{\phi}e^{i\kappa_2 x_2} - \frac{i}{2\left[\frac{\partial S_\phi}{\partial x_1}\right]} \left[-CC_g \kappa_2^2 \hat{\phi}e^{i\kappa_2 x_2}\right]
 \end{aligned} \tag{3.686}$$

Dividing across by $-e^{i\kappa_2 x_2}$ yields:

$$\frac{\partial \hat{\phi}}{\partial x_1} = -\frac{\left[\frac{\partial^2 S_\phi}{\partial x_1 \partial x_1}\right]}{2\left[\frac{\partial S_\phi}{\partial x_1}\right]} \hat{\phi} - \frac{1}{2CC_g} \frac{\partial(CC_g)}{\partial x_1} \hat{\phi} - \frac{i\left[\frac{\partial S_\phi}{\partial x_1}\right]}{2} \hat{\phi} - \frac{i\kappa^2}{2\left[\frac{\partial S_\phi}{\partial x_1}\right]} \hat{\phi} + \frac{CC_g \kappa_2^2 \hat{\phi}}{2\left[\frac{\partial S_\phi}{\partial x_1}\right]} \tag{3.687}$$

Therefore:

$$CC_g \frac{\partial \hat{\phi}}{\partial x_1} = \left(-\frac{CC_g \frac{\partial^2 S_\phi}{\partial x_1 \partial x_1}}{2\frac{\partial S_\phi}{\partial x_1}} - \frac{1}{2} \frac{\partial(CC_g)}{\partial x_1} - \frac{iCC_g \frac{\partial S_\phi}{\partial x_1}}{2} - \frac{iCC_g \kappa^2}{2\frac{\partial S_\phi}{\partial x_1}} + \frac{(CC_g)^2 \kappa_2^2}{2\frac{\partial S_\phi}{\partial x_1}} \right) \hat{\phi} \tag{3.688}$$

3.8.4 Complete One-Dimensional Finite Element Wave Driven Hydrodynamic Model

Now at the beach boundary Equation (3.635) can be expressed as follows using the result of Equation (3.680):

$$\begin{aligned}
& \int_0^l 2\omega\kappa_2 U_2 \begin{bmatrix} L^1 L^1 & L^1 L^2 \\ L^2 L^1 & L^2 L^2 \end{bmatrix} \begin{Bmatrix} \hat{\phi}^1 \\ \hat{\phi}^2 \end{Bmatrix} dx - \int_0^l \kappa_2^2 U_2^2 \begin{bmatrix} L^1 L^1 & L^1 L^2 \\ L^2 L^1 & L^2 L^2 \end{bmatrix} \begin{Bmatrix} \hat{\phi}^1 \\ \hat{\phi}^2 \end{Bmatrix} dx \\
& + \int_0^l CC_g \begin{bmatrix} \frac{\partial L^1}{\partial x_1} \frac{\partial L^1}{\partial x_1} & \frac{\partial L^1}{\partial x_1} \frac{\partial L^2}{\partial x_1} \\ \frac{\partial L^2}{\partial x_1} \frac{\partial L^1}{\partial x_1} & \frac{\partial L^2}{\partial x_1} \frac{\partial L^2}{\partial x_1} \end{bmatrix} \begin{Bmatrix} \hat{\phi}^1 \\ \hat{\phi}^2 \end{Bmatrix} dx + \int_0^l \kappa_2^2 CC_g \begin{bmatrix} L^1 L^1 & L^1 L^2 \\ L^2 L^1 & L^2 L^2 \end{bmatrix} \begin{Bmatrix} \hat{\phi}^1 \\ \hat{\phi}^2 \end{Bmatrix} dx \\
& + \int_0^l \sigma^2 \begin{bmatrix} L^1 L^1 & L^1 L^2 \\ L^2 L^1 & L^2 L^2 \end{bmatrix} \begin{Bmatrix} \hat{\phi}^1 \\ \hat{\phi}^2 \end{Bmatrix} dx - \int_0^l \omega^2 \begin{bmatrix} L^1 L^1 & L^1 L^2 \\ L^2 L^1 & L^2 L^2 \end{bmatrix} \begin{Bmatrix} \hat{\phi}^1 \\ \hat{\phi}^2 \end{Bmatrix} dx \\
& - \int_0^l \kappa^2 CC_g \begin{bmatrix} L^1 L^1 & L^1 L^2 \\ L^2 L^1 & L^2 L^2 \end{bmatrix} \begin{Bmatrix} \hat{\phi}^1 \\ \hat{\phi}^2 \end{Bmatrix} dx - \int_0^l \sigma^2 Q' \begin{bmatrix} L^1 L^1 & L^1 L^2 \\ L^2 L^1 & L^2 L^2 \end{bmatrix} \begin{Bmatrix} \hat{\phi}^1 \\ \hat{\phi}^2 \end{Bmatrix} dx \\
& + \int_0^l g \frac{\partial \bar{\eta}}{\partial x_1} \begin{bmatrix} L^1 \frac{\partial L^1}{\partial x_1} & L^1 \frac{\partial L^2}{\partial x_1} \\ L^2 \frac{\partial L^1}{\partial x_1} & L^2 \frac{\partial L^2}{\partial x_1} \end{bmatrix} \begin{Bmatrix} \hat{\phi}^1 \\ \hat{\phi}^2 \end{Bmatrix} dx - CC_g \frac{\partial \hat{\phi}}{\partial x_1} \begin{Bmatrix} L^1 \\ L^2 \end{Bmatrix} \bigg|_l \\
& + \left\{ \begin{bmatrix} L^1 \\ L^2 \end{bmatrix} \right\} \left(-\frac{CC_g}{2\kappa} \frac{\partial \kappa}{\partial x_1} - \frac{1}{2} \frac{\partial CC_g}{\partial x_1} - iCC_g \kappa + \frac{iCC_g \kappa^2}{2\kappa} \right) \begin{bmatrix} L^1 & L^2 \end{bmatrix} \begin{Bmatrix} \hat{\phi}^1 \\ \hat{\phi}^2 \end{Bmatrix} \bigg|_0 = 0
\end{aligned} \tag{3.689}$$

This leads to:

$$\begin{aligned}
& \int_0^l 2\omega\kappa_2 U_2 \begin{bmatrix} L^1 L^1 & L^1 L^2 \\ L^2 L^1 & L^2 L^2 \end{bmatrix} \begin{Bmatrix} \hat{\phi}^1 \\ \hat{\phi}^2 \end{Bmatrix} dx - \int_0^l \kappa_2^2 U_2^2 \begin{bmatrix} L^1 L^1 & L^1 L^2 \\ L^2 L^1 & L^2 L^2 \end{bmatrix} \begin{Bmatrix} \hat{\phi}^1 \\ \hat{\phi}^2 \end{Bmatrix} dx \\
& + \int_0^l CC_g \begin{bmatrix} \frac{\partial L^1}{\partial x_1} \frac{\partial L^1}{\partial x_1} & \frac{\partial L^1}{\partial x_1} \frac{\partial L^2}{\partial x_1} \\ \frac{\partial L^2}{\partial x_1} \frac{\partial L^1}{\partial x_1} & \frac{\partial L^2}{\partial x_1} \frac{\partial L^2}{\partial x_1} \end{bmatrix} \begin{Bmatrix} \hat{\phi}^1 \\ \hat{\phi}^2 \end{Bmatrix} dx + \int_0^l \kappa_2^2 CC_g \begin{bmatrix} L^1 L^1 & L^1 L^2 \\ L^2 L^1 & L^2 L^2 \end{bmatrix} \begin{Bmatrix} \hat{\phi}^1 \\ \hat{\phi}^2 \end{Bmatrix} dx \\
& + \int_0^l \sigma^2 \begin{bmatrix} L^1 L^1 & L^1 L^2 \\ L^2 L^1 & L^2 L^2 \end{bmatrix} \begin{Bmatrix} \hat{\phi}^1 \\ \hat{\phi}^2 \end{Bmatrix} dx - \int_0^l \omega^2 \begin{bmatrix} L^1 L^1 & L^1 L^2 \\ L^2 L^1 & L^2 L^2 \end{bmatrix} \begin{Bmatrix} \hat{\phi}^1 \\ \hat{\phi}^2 \end{Bmatrix} dx \\
& - \int_0^l \kappa^2 CC_g \begin{bmatrix} L^1 L^1 & L^1 L^2 \\ L^2 L^1 & L^2 L^2 \end{bmatrix} \begin{Bmatrix} \hat{\phi}^1 \\ \hat{\phi}^2 \end{Bmatrix} dx - \int_0^l \sigma^2 Q' \begin{bmatrix} L^1 L^1 & L^1 L^2 \\ L^2 L^1 & L^2 L^2 \end{bmatrix} \begin{Bmatrix} \hat{\phi}^1 \\ \hat{\phi}^2 \end{Bmatrix} dx \\
& + \int_0^l g \frac{\partial \bar{\eta}}{\partial x_1} \begin{bmatrix} L^1 \frac{\partial L^1}{\partial x_1} & L^1 \frac{\partial L^2}{\partial x_1} \\ L^2 \frac{\partial L^1}{\partial x_1} & L^2 \frac{\partial L^2}{\partial x_1} \end{bmatrix} \begin{Bmatrix} \hat{\phi}^1 \\ \hat{\phi}^2 \end{Bmatrix} dx - CC_g \frac{\partial \hat{\phi}}{\partial x_1} \begin{Bmatrix} L^1 \\ L^2 \end{Bmatrix} \Big|_l \\
& + \left(-\frac{CC_g}{2\kappa} \frac{\partial \kappa}{\partial x_1} - \frac{1}{2} \frac{\partial CC_g}{\partial x_1} - iCC_g \kappa + \frac{iCC_g \kappa_2^2}{2\kappa} \right) \begin{bmatrix} L^1 L^1 & L^1 L^2 \\ L^2 L^1 & L^2 L^2 \end{bmatrix} \begin{Bmatrix} \hat{\phi}^1 \\ \hat{\phi}^2 \end{Bmatrix} \Big|_0 = 0
\end{aligned} \tag{3.690}$$

Evaluating the terms not inside integrals gives:

$$\begin{aligned}
& \int_0^l 2\omega\kappa_2 U_2 \begin{bmatrix} L^1 L^1 & L^1 L^2 \\ L^2 L^1 & L^2 L^2 \end{bmatrix} \begin{Bmatrix} \hat{\phi}^1 \\ \hat{\phi}^2 \end{Bmatrix} dx - \int_0^l \kappa_2^2 U_2^2 \begin{bmatrix} L^1 L^1 & L^1 L^2 \\ L^2 L^1 & L^2 L^2 \end{bmatrix} \begin{Bmatrix} \hat{\phi}^1 \\ \hat{\phi}^2 \end{Bmatrix} dx \\
& + \int_0^l CC_g \begin{bmatrix} \frac{\partial L^1}{\partial x_1} \frac{\partial L^1}{\partial x_1} & \frac{\partial L^1}{\partial x_1} \frac{\partial L^2}{\partial x_1} \\ \frac{\partial L^2}{\partial x_1} \frac{\partial L^1}{\partial x_1} & \frac{\partial L^2}{\partial x_1} \frac{\partial L^2}{\partial x_1} \end{bmatrix} \begin{Bmatrix} \hat{\phi}^1 \\ \hat{\phi}^2 \end{Bmatrix} dx + \int_0^l \kappa_2^2 CC_g \begin{bmatrix} L^1 L^1 & L^1 L^2 \\ L^2 L^1 & L^2 L^2 \end{bmatrix} \begin{Bmatrix} \hat{\phi}^1 \\ \hat{\phi}^2 \end{Bmatrix} dx \\
& + \int_0^l \sigma^2 \begin{bmatrix} L^1 L^1 & L^1 L^2 \\ L^2 L^1 & L^2 L^2 \end{bmatrix} \begin{Bmatrix} \hat{\phi}^1 \\ \hat{\phi}^2 \end{Bmatrix} dx - \int_0^l \omega^2 \begin{bmatrix} L^1 L^1 & L^1 L^2 \\ L^2 L^1 & L^2 L^2 \end{bmatrix} \begin{Bmatrix} \hat{\phi}^1 \\ \hat{\phi}^2 \end{Bmatrix} dx \\
& - \int_0^l \kappa^2 CC_g \begin{bmatrix} L^1 L^1 & L^1 L^2 \\ L^2 L^1 & L^2 L^2 \end{bmatrix} \begin{Bmatrix} \hat{\phi}^1 \\ \hat{\phi}^2 \end{Bmatrix} dx - \int_0^l \sigma^2 Q' \begin{bmatrix} L^1 L^1 & L^1 L^2 \\ L^2 L^1 & L^2 L^2 \end{bmatrix} \begin{Bmatrix} \hat{\phi}^1 \\ \hat{\phi}^2 \end{Bmatrix} dx \\
& + \int_0^l g \frac{\partial \bar{\eta}}{\partial x_1} \begin{bmatrix} L^1 \frac{\partial L^1}{\partial x_1} & L^1 \frac{\partial L^2}{\partial x_1} \\ L^2 \frac{\partial L^1}{\partial x_1} & L^2 \frac{\partial L^2}{\partial x_1} \end{bmatrix} \begin{Bmatrix} \hat{\phi}^1 \\ \hat{\phi}^2 \end{Bmatrix} dx - CC_g \frac{\partial \hat{\phi}}{\partial x_1} \begin{Bmatrix} 0 \\ 1 \end{Bmatrix} \Big|_l \\
& + \left(-\frac{CC_g}{2\kappa} \frac{\partial \kappa}{\partial x_1} - \frac{1}{2} \frac{\partial CC_g}{\partial x_1} - iCC_g \kappa + \frac{iCC_g \kappa_2^2}{2\kappa} \right) \begin{bmatrix} 1 & 0 \\ 0 & 0 \end{bmatrix} \begin{Bmatrix} \hat{\phi}^1 \\ \hat{\phi}^2 \end{Bmatrix} \Big|_0 = 0
\end{aligned} \tag{3.691}$$

Equation (3.691) is the complete elliptic equation to be solved using the finite element solution scheme for the boundary element. In a more general form for every element the equation is:

$$\begin{aligned}
& \int_0^l 2\omega\kappa_2 U_2 \begin{bmatrix} L^1 L^1 & L^1 L^2 \\ L^2 L^1 & L^2 L^2 \end{bmatrix} \begin{Bmatrix} \hat{\phi}^1 \\ \hat{\phi}^2 \end{Bmatrix} dx - \int_0^l \kappa_2^2 U_2^2 \begin{bmatrix} L^1 L^1 & L^1 L^2 \\ L^2 L^1 & L^2 L^2 \end{bmatrix} \begin{Bmatrix} \hat{\phi}^1 \\ \hat{\phi}^2 \end{Bmatrix} dx \\
& + \int_0^l CC_g \begin{bmatrix} \frac{\partial L^1}{\partial x_1} \frac{\partial L^1}{\partial x_1} & \frac{\partial L^1}{\partial x_1} \frac{\partial L^2}{\partial x_1} \\ \frac{\partial L^2}{\partial x_1} \frac{\partial L^1}{\partial x_1} & \frac{\partial L^2}{\partial x_1} \frac{\partial L^2}{\partial x_1} \end{bmatrix} \begin{Bmatrix} \hat{\phi}^1 \\ \hat{\phi}^2 \end{Bmatrix} dx + \int_0^l \kappa_2^2 CC_g \begin{bmatrix} L^1 L^1 & L^1 L^2 \\ L^2 L^1 & L^2 L^2 \end{bmatrix} \begin{Bmatrix} \hat{\phi}^1 \\ \hat{\phi}^2 \end{Bmatrix} dx \\
& + \int_0^l \sigma^2 \begin{bmatrix} L^1 L^1 & L^1 L^2 \\ L^2 L^1 & L^2 L^2 \end{bmatrix} \begin{Bmatrix} \hat{\phi}^1 \\ \hat{\phi}^2 \end{Bmatrix} dx - \int_0^l \omega^2 \begin{bmatrix} L^1 L^1 & L^1 L^2 \\ L^2 L^1 & L^2 L^2 \end{bmatrix} \begin{Bmatrix} \hat{\phi}^1 \\ \hat{\phi}^2 \end{Bmatrix} dx \\
& - \int_0^l \kappa^2 CC_g \begin{bmatrix} L^1 L^1 & L^1 L^2 \\ L^2 L^1 & L^2 L^2 \end{bmatrix} \begin{Bmatrix} \hat{\phi}^1 \\ \hat{\phi}^2 \end{Bmatrix} dx - \int_0^l \sigma^2 Q' \begin{bmatrix} L^1 L^1 & L^1 L^2 \\ L^2 L^1 & L^2 L^2 \end{bmatrix} \begin{Bmatrix} \hat{\phi}^1 \\ \hat{\phi}^2 \end{Bmatrix} dx \\
& + \int_0^l g \frac{\partial \bar{\eta}}{\partial x_1} \begin{bmatrix} L^1 \frac{\partial L^1}{\partial x_1} & L^1 \frac{\partial L^2}{\partial x_1} \\ L^2 \frac{\partial L^1}{\partial x_1} & L^2 \frac{\partial L^2}{\partial x_1} \end{bmatrix} \begin{Bmatrix} \hat{\phi}^1 \\ \hat{\phi}^2 \end{Bmatrix} dx - CC_g \frac{\partial \hat{\phi}}{\partial x_1} \begin{Bmatrix} 0 \\ 1 \end{Bmatrix} \bigg|_l + CC_g \frac{\partial \hat{\phi}}{\partial x_1} \begin{Bmatrix} 1 \\ 0 \end{Bmatrix} \bigg|_0 = 0
\end{aligned} \tag{3.692}$$

Equation (3.692) may also be expressed as:

$$\begin{aligned}
& \int_0^l 2\omega\kappa_2 U_2 L^I L^J \hat{\phi}^J dx - \int_0^l \kappa_2^2 U_2^2 L^I L^J \hat{\phi}^J dx + \int_0^l CC_g \frac{\partial L^I}{\partial x_1} \frac{\partial L^J}{\partial x_1} \hat{\phi}^J dx + \int_0^l \kappa_2^2 CC_g L^I L^J \hat{\phi}^J dx \\
& + \int_0^l \sigma^2 L^I L^J \hat{\phi}^J dx - \int_0^l \omega^2 L^I L^J \hat{\phi}^J dx - \int_0^l \kappa^2 CC_g L^I L^J \hat{\phi}^J dx - \int_0^l \sigma^2 Q' L^I L^J \hat{\phi}^J dx \\
& + \int_0^l g \frac{\partial \bar{\eta}}{\partial x_1} L^I \frac{\partial L^I}{\partial x_1} \hat{\phi}^J dx - CC_g \frac{\partial \hat{\phi}}{\partial x_1} L^I \bigg|_l + CC_g \frac{\partial \hat{\phi}}{\partial x_1} L^I \bigg|_0 = 0
\end{aligned} \tag{3.693}$$

3.8.5 Complete One-Dimensional Finite Element Wave Driven Hydrodynamic Model with Gradients of Wave Phase on Boundary

At the beach boundary Equation (3.635) can be expressed as follows using the result of Equation (3.688):

$$\begin{aligned}
& \int_0^l 2\omega\kappa_2 U_2 \begin{bmatrix} L^1 L^1 & L^1 L^2 \\ L^2 L^1 & L^2 L^2 \end{bmatrix} \begin{Bmatrix} \hat{\phi}^1 \\ \hat{\phi}^2 \end{Bmatrix} dx - \int_0^l \kappa_2^2 U_2^2 \begin{bmatrix} L^1 L^1 & L^1 L^2 \\ L^2 L^1 & L^2 L^2 \end{bmatrix} \begin{Bmatrix} \hat{\phi}^1 \\ \hat{\phi}^2 \end{Bmatrix} dx \\
& + \int_0^l CC_g \begin{bmatrix} \frac{\partial L^1}{\partial x_1} \frac{\partial L^1}{\partial x_1} & \frac{\partial L^1}{\partial x_1} \frac{\partial L^2}{\partial x_1} \\ \frac{\partial L^2}{\partial x_1} \frac{\partial L^1}{\partial x_1} & \frac{\partial L^2}{\partial x_1} \frac{\partial L^2}{\partial x_1} \end{bmatrix} \begin{Bmatrix} \hat{\phi}^1 \\ \hat{\phi}^2 \end{Bmatrix} dx + \int_0^l \kappa_2^2 CC_g \begin{bmatrix} L^1 L^1 & L^1 L^2 \\ L^2 L^1 & L^2 L^2 \end{bmatrix} \begin{Bmatrix} \hat{\phi}^1 \\ \hat{\phi}^2 \end{Bmatrix} dx \\
& + \int_0^l \sigma^2 \begin{bmatrix} L^1 L^1 & L^1 L^2 \\ L^2 L^1 & L^2 L^2 \end{bmatrix} \begin{Bmatrix} \hat{\phi}^1 \\ \hat{\phi}^2 \end{Bmatrix} dx - \int_0^l \omega^2 \begin{bmatrix} L^1 L^1 & L^1 L^2 \\ L^2 L^1 & L^2 L^2 \end{bmatrix} \begin{Bmatrix} \hat{\phi}^1 \\ \hat{\phi}^2 \end{Bmatrix} dx \\
& - \int_0^l \kappa^2 CC_g \begin{bmatrix} L^1 L^1 & L^1 L^2 \\ L^2 L^1 & L^2 L^2 \end{bmatrix} \begin{Bmatrix} \hat{\phi}^1 \\ \hat{\phi}^2 \end{Bmatrix} dx - \int_0^l \sigma^2 Q' \begin{bmatrix} L^1 L^1 & L^1 L^2 \\ L^2 L^1 & L^2 L^2 \end{bmatrix} \begin{Bmatrix} \hat{\phi}^1 \\ \hat{\phi}^2 \end{Bmatrix} dx \\
& + \int_0^l g \frac{\partial \bar{\eta}}{\partial x_1} \begin{bmatrix} L^1 \frac{\partial L^1}{\partial x_1} & L^1 \frac{\partial L^2}{\partial x_1} \\ L^2 \frac{\partial L^1}{\partial x_1} & L^2 \frac{\partial L^2}{\partial x_1} \end{bmatrix} \begin{Bmatrix} \hat{\phi}^1 \\ \hat{\phi}^2 \end{Bmatrix} dx - CC_g \frac{\partial \hat{\phi}}{\partial x_1} \begin{Bmatrix} L^1 \\ L^2 \end{Bmatrix} \bigg|_l \\
& + \left\{ \begin{matrix} L^1 \\ L^2 \end{matrix} \right\} \left(-\frac{CC_g \frac{\partial^2 S_\phi}{\partial x_1 \partial x_1}}{2 \frac{\partial S_\phi}{\partial x_1}} - \frac{1}{2} \frac{\partial (CC_g)}{\partial x_1} - \frac{iCC_g \frac{\partial S_\phi}{\partial x_1}}{2} - \frac{iCC_g \kappa^2}{2 \frac{\partial S_\phi}{\partial x_1}} + \frac{(CC_g)^2 \kappa_2^2}{2 \frac{\partial S_\phi}{\partial x_1}} \right) \begin{bmatrix} L^1 & L^2 \end{bmatrix} \begin{Bmatrix} \hat{\phi}^1 \\ \hat{\phi}^2 \end{Bmatrix} \bigg|_0 = 0
\end{aligned}
\tag{3.694}$$

This leads to:

$$\begin{aligned}
& \int_0^l 2\omega\kappa_2 U_2 \begin{bmatrix} L^1 L^1 & L^1 L^2 \\ L^2 L^1 & L^2 L^2 \end{bmatrix} \begin{Bmatrix} \hat{\phi}^1 \\ \hat{\phi}^2 \end{Bmatrix} dx - \int_0^l \kappa_2^2 U_2^2 \begin{bmatrix} L^1 L^1 & L^1 L^2 \\ L^2 L^1 & L^2 L^2 \end{bmatrix} \begin{Bmatrix} \hat{\phi}^1 \\ \hat{\phi}^2 \end{Bmatrix} dx \\
& + \int_0^l CC_g \begin{bmatrix} \frac{\partial L^1}{\partial x_1} \frac{\partial L^1}{\partial x_1} & \frac{\partial L^1}{\partial x_1} \frac{\partial L^2}{\partial x_1} \\ \frac{\partial L^2}{\partial x_1} \frac{\partial L^1}{\partial x_1} & \frac{\partial L^2}{\partial x_1} \frac{\partial L^2}{\partial x_1} \end{bmatrix} \begin{Bmatrix} \hat{\phi}^1 \\ \hat{\phi}^2 \end{Bmatrix} dx + \int_0^l \kappa_2^2 CC_g \begin{bmatrix} L^1 L^1 & L^1 L^2 \\ L^2 L^1 & L^2 L^2 \end{bmatrix} \begin{Bmatrix} \hat{\phi}^1 \\ \hat{\phi}^2 \end{Bmatrix} dx \\
& + \int_0^l \sigma^2 \begin{bmatrix} L^1 L^1 & L^1 L^2 \\ L^2 L^1 & L^2 L^2 \end{bmatrix} \begin{Bmatrix} \hat{\phi}^1 \\ \hat{\phi}^2 \end{Bmatrix} dx - \int_0^l \omega^2 \begin{bmatrix} L^1 L^1 & L^1 L^2 \\ L^2 L^1 & L^2 L^2 \end{bmatrix} \begin{Bmatrix} \hat{\phi}^1 \\ \hat{\phi}^2 \end{Bmatrix} dx \\
& - \int_0^l \kappa^2 CC_g \begin{bmatrix} L^1 L^1 & L^1 L^2 \\ L^2 L^1 & L^2 L^2 \end{bmatrix} \begin{Bmatrix} \hat{\phi}^1 \\ \hat{\phi}^2 \end{Bmatrix} dx - \int_0^l \sigma^2 Q' \begin{bmatrix} L^1 L^1 & L^1 L^2 \\ L^2 L^1 & L^2 L^2 \end{bmatrix} \begin{Bmatrix} \hat{\phi}^1 \\ \hat{\phi}^2 \end{Bmatrix} dx \\
& + \int_0^l g \frac{\partial \bar{\eta}}{\partial x_1} \begin{bmatrix} L^1 \frac{\partial L^1}{\partial x_1} & L^1 \frac{\partial L^2}{\partial x_1} \\ L^2 \frac{\partial L^1}{\partial x_1} & L^2 \frac{\partial L^2}{\partial x_1} \end{bmatrix} \begin{Bmatrix} \hat{\phi}^1 \\ \hat{\phi}^2 \end{Bmatrix} dx - CC_g \frac{\partial \hat{\phi}}{\partial x_1} \begin{Bmatrix} L^1 \\ L^2 \end{Bmatrix} \bigg|_l \\
& + \left(-\frac{CC_g}{2} \frac{\partial^2 S_\phi}{\partial x_1 \partial x_1} - \frac{1}{2} \frac{\partial(CC_g)}{\partial x_1} - \frac{iCC_g}{2} \frac{\partial S_\phi}{\partial x_1} - \frac{iCC_g \kappa^2}{2 \frac{\partial S_\phi}{\partial x_1}} + \frac{(CC_g)^2 \kappa_2^2}{2 \frac{\partial S_\phi}{\partial x_1}} \right) \begin{bmatrix} L^1 L^1 & L^1 L^2 \\ L^2 L^1 & L^2 L^2 \end{bmatrix} \begin{Bmatrix} \hat{\phi}^1 \\ \hat{\phi}^2 \end{Bmatrix} \bigg|_0 = 0
\end{aligned}
\tag{3.695}$$

Evaluating the terms not inside integrals gives:

$$\begin{aligned}
& \int_0^l 2\omega\kappa_2 U_2 \begin{bmatrix} L^1 L^1 & L^1 L^2 \\ L^2 L^1 & L^2 L^2 \end{bmatrix} \begin{Bmatrix} \hat{\phi}^1 \\ \hat{\phi}^2 \end{Bmatrix} dx - \int_0^l \kappa_2^2 U_2^2 \begin{bmatrix} L^1 L^1 & L^1 L^2 \\ L^2 L^1 & L^2 L^2 \end{bmatrix} \begin{Bmatrix} \hat{\phi}^1 \\ \hat{\phi}^2 \end{Bmatrix} dx \\
& + \int_0^l CC_g \begin{bmatrix} \frac{\partial L^1}{\partial x_1} \frac{\partial L^1}{\partial x_1} & \frac{\partial L^1}{\partial x_1} \frac{\partial L^2}{\partial x_1} \\ \frac{\partial L^2}{\partial x_1} \frac{\partial L^1}{\partial x_1} & \frac{\partial L^2}{\partial x_1} \frac{\partial L^2}{\partial x_1} \end{bmatrix} \begin{Bmatrix} \hat{\phi}^1 \\ \hat{\phi}^2 \end{Bmatrix} dx + \int_0^l \kappa_2^2 CC_g \begin{bmatrix} L^1 L^1 & L^1 L^2 \\ L^2 L^1 & L^2 L^2 \end{bmatrix} \begin{Bmatrix} \hat{\phi}^1 \\ \hat{\phi}^2 \end{Bmatrix} dx \\
& + \int_0^l \sigma^2 \begin{bmatrix} L^1 L^1 & L^1 L^2 \\ L^2 L^1 & L^2 L^2 \end{bmatrix} \begin{Bmatrix} \hat{\phi}^1 \\ \hat{\phi}^2 \end{Bmatrix} dx - \int_0^l \omega^2 \begin{bmatrix} L^1 L^1 & L^1 L^2 \\ L^2 L^1 & L^2 L^2 \end{bmatrix} \begin{Bmatrix} \hat{\phi}^1 \\ \hat{\phi}^2 \end{Bmatrix} dx \\
& - \int_0^l \kappa^2 CC_g \begin{bmatrix} L^1 L^1 & L^1 L^2 \\ L^2 L^1 & L^2 L^2 \end{bmatrix} \begin{Bmatrix} \hat{\phi}^1 \\ \hat{\phi}^2 \end{Bmatrix} dx - \int_0^l \sigma^2 Q' \begin{bmatrix} L^1 L^1 & L^1 L^2 \\ L^2 L^1 & L^2 L^2 \end{bmatrix} \begin{Bmatrix} \hat{\phi}^1 \\ \hat{\phi}^2 \end{Bmatrix} dx \\
& + \int_0^l g \frac{\partial \bar{\eta}}{\partial x_1} \begin{bmatrix} L^1 \frac{\partial L^1}{\partial x_1} & L^1 \frac{\partial L^2}{\partial x_1} \\ L^2 \frac{\partial L^1}{\partial x_1} & L^2 \frac{\partial L^2}{\partial x_1} \end{bmatrix} \begin{Bmatrix} \hat{\phi}^1 \\ \hat{\phi}^2 \end{Bmatrix} dx - CC_g \frac{\partial \hat{\phi}}{\partial x_1} \begin{Bmatrix} 0 \\ 1 \end{Bmatrix} \bigg|_l \\
& + \left(-\frac{CC_g \frac{\partial^2 S_\phi}{\partial x_1 \partial x_1}}{2 \frac{\partial S_\phi}{\partial x_1}} - \frac{1}{2} \frac{\partial (CC_g)}{\partial x_1} - \frac{iCC_g \frac{\partial S_\phi}{\partial x_1}}{2} - \frac{iCC_g \kappa^2}{2 \frac{\partial S_\phi}{\partial x_1}} + \frac{(CC_g)^2 \kappa_2^2}{2 \frac{\partial S_\phi}{\partial x_1}} \right) \begin{bmatrix} 1 & 0 \\ 0 & 0 \end{bmatrix} \begin{Bmatrix} \hat{\phi}^1 \\ \hat{\phi}^2 \end{Bmatrix} \bigg|_0 = 0 \quad (3.696)
\end{aligned}$$

Equation (3.696) is the complete elliptic equation to be solved using the finite element solution scheme for the boundary element with a more general boundary condition than that of (3.691). In a more general form for every element the equation is the same as that of Equation (3.693).

3.9 Two-Dimensional Cartesian Finite Element Mild-Slope Wave-Current Interaction Model

The finite element formulation of a full two-dimensional finite element wave current interaction model is examined (2d-NM-WCIM). This two-dimensional model uses triangular finite elements to examine wave behaviour over a two dimensional spatial domain.

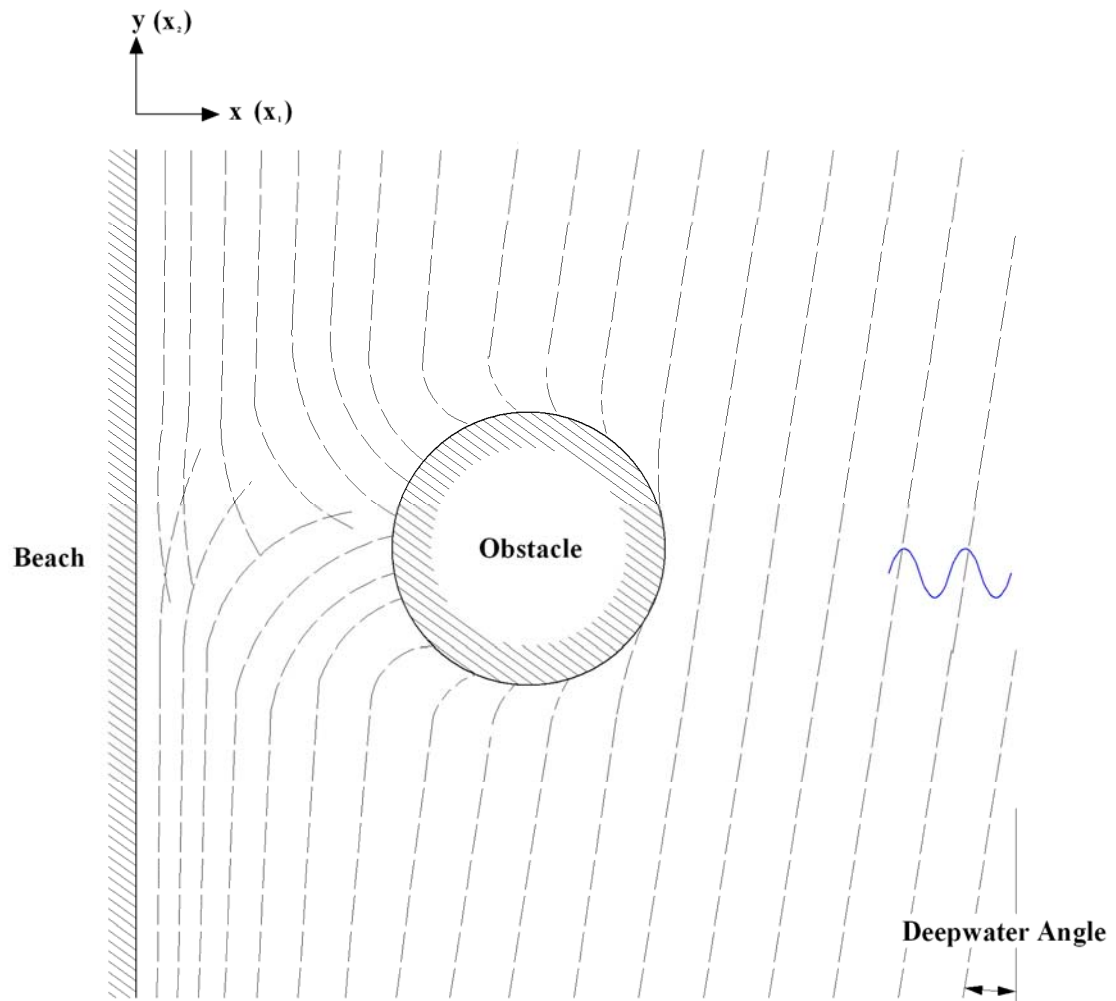


Figure 3.10 – Sketch of Scenario where 1d Wave Model would be Insufficient and a 2d Wave Model would be required

The simplest form of the 2d-NM-WCIM is a wave model with an absorbing downstream boundary condition and specified values of wave potential on the boundary with no energy dissipation. Initially this will be examined. The application of more complex boundary conditions is discussed in the following sections.

A similar process to that used in Section 3.8 may be carried out for the two-dimensional finite element wave equation. Firstly the following abbreviations may be defined:

$$Q'' = \frac{1}{\cosh^2 \kappa h'} \left(\begin{aligned} &Q_1 \frac{\partial^2 h'}{\partial x_k \partial x_k} + Q_2 \frac{\partial^2 \kappa}{\partial x_k^2} + Q_3 \frac{\partial^2 \bar{\eta}}{\partial x_k \partial x_k} + Q_4 \left(\frac{\partial h'}{\partial x_k} \frac{\partial h'}{\partial x_k} \right) \\ &+ Q_5 \left(\frac{\partial \kappa}{\partial x_k} \frac{\partial \kappa}{\partial x_k} \right) + Q_6 \left(\frac{\partial \bar{\eta}}{\partial x_k} \frac{\partial \bar{\eta}}{\partial x_k} \right) + Q_7 \frac{\partial \kappa}{\partial x_k} \frac{\partial h'}{\partial x_k} \\ &+ Q_8 \frac{\partial h'}{\partial x_k} \frac{\partial \bar{\eta}}{\partial x_k} + Q_9 \frac{\partial \bar{\eta}}{\partial x_k} \frac{\partial \kappa}{\partial x_k} + W_6 \frac{\partial h'}{\partial x_k} - W_6 \frac{\partial \bar{\eta}}{\partial x_k} \end{aligned} \right) \quad (3.697)$$

$$(Q''_{U})_{kj} = - \left(\kappa h' + \frac{\lambda'}{\kappa} - \frac{h \lambda'^2}{\kappa} \right) \left[\frac{\partial \bar{\eta}}{\partial x_k} \frac{\partial \kappa}{\partial x_j} + \frac{\partial \kappa}{\partial x_k} \frac{\partial \bar{\eta}}{\partial x_j} \right] - (\kappa^2 - \lambda'^2) \left[\frac{\partial \bar{\eta}}{\partial x_k} \frac{\partial h'}{\partial x_j} + \frac{\partial h'}{\partial x_k} \frac{\partial \bar{\eta}}{\partial x_j} \right] \quad (3.698)$$

Equation (3.531) may be expressed using Equations (3.697) and (3.698) and assuming that when the current varies in a direction it varies slowly in that direction (i.e.

$$\frac{\partial U_j}{\partial x_j} = 0):$$

$$\begin{aligned} &-2i\omega U_j \frac{\partial \phi}{\partial x_j} + U_j U_k \frac{\partial^2 \phi}{\partial x_j \partial x_k} + U_j \frac{\partial U_k}{\partial x_j} \frac{\partial \phi}{\partial x_k} - \frac{\partial}{\partial x_k} \left(CC_g \frac{\partial \phi}{\partial x_k} \right) \\ &- \phi \kappa^2 CC_g + \phi \sigma^2 - \omega^2 \phi \\ &+ g \frac{\partial \phi}{\partial x_k} \left(\frac{\partial \bar{\eta}}{\partial x_k} \right) - \phi \sigma^2 Q'' + 2i\omega \phi \lambda' U_j \frac{\partial \bar{\eta}}{\partial x_j} - \phi \lambda' U_j \frac{\partial U_k}{\partial x_j} \frac{\partial \bar{\eta}}{\partial x_k} \\ &- U_j U_k \lambda' \frac{\partial \bar{\eta}}{\partial x_j} \frac{\partial \phi}{\partial x_k} - U_j U_k \lambda' \frac{\partial \bar{\eta}}{\partial x_k} \frac{\partial \phi}{\partial x_j} - U_j U_k \phi \lambda' \frac{\partial^2 \bar{\eta}}{\partial x_j \partial x_k} + U_j U_k \phi \kappa^2 \frac{\partial \bar{\eta}}{\partial x_k} \frac{\partial \bar{\eta}}{\partial x_j} + U_j U_k (Q''_{U})_{kj} \phi = 0 \end{aligned} \quad (3.699)$$

Equation (3.699) can now be multiplied by a weighting function and the product integrated over the finite element area:

$$\begin{aligned}
& -\iint_A W^I 2i\omega U_j \frac{\partial \phi}{\partial x_j} dA + \iint_A W^I U_j U_k \frac{\partial^2 \phi}{\partial x_k \partial x_k} dA + \iint_A W^I U_j \frac{\partial U_k}{\partial x_j} \frac{\partial \phi}{\partial x_k} dA - \iint_A W^I \frac{\partial}{\partial x_k} \left(CC_g \frac{\partial \phi}{\partial x_k} \right) dA \\
& + \iint_A W^I \phi \sigma^2 dA - \iint_A W^I \omega^2 \phi dA - \iint_A W^I \phi \kappa^2 CC_g dA + \iint_A W^I g \frac{\partial \phi}{\partial x_k} \left(\frac{\partial \bar{\eta}}{\partial x_k} \right) dA \\
& - \iint_A W^I \phi \sigma^2 Q'' dA + \iint_A W^I 2i\omega \phi \lambda' U_j \frac{\partial \bar{\eta}}{\partial x_j} dA - \iint_A W^I \phi \lambda' U_j \frac{\partial U_k}{\partial x_j} \frac{\partial \bar{\eta}}{\partial x_k} dA - \iint_A W^I 2\lambda' U_j U_k \frac{\partial \bar{\eta}}{\partial x_j} \frac{\partial \phi}{\partial x_k} dA \\
& - \iint_A W^I U_j U_k \phi \lambda' \frac{\partial^2 \bar{\eta}}{\partial x_k \partial x_j} dA + \iint_A W^I U_j U_k \phi \kappa^2 \left(\frac{\partial \bar{\eta}}{\partial x_k} \frac{\partial \bar{\eta}}{\partial x_j} \right) dA + \iint_A W^I U_j U_k (Q''_{kj}) \phi dA = 0
\end{aligned} \tag{3.700}$$

Examining the second term in Equation (3.700) using Green's Theorem:

$$\begin{aligned}
\iint_A W^I U_j U_k \frac{\partial^2 \phi}{\partial x_j \partial x_k} dA &= \iint_A \frac{\partial}{\partial x_j} \left(W^I U_j U_k \frac{\partial \phi}{\partial x_k} \right) dA - \iint_A \frac{\partial W^I}{\partial x_j} U_j U_k \frac{\partial \phi}{\partial x_k} dA \\
& - \iint_A W^I \frac{\partial U_j}{\partial x_j} U_k \frac{\partial \phi}{\partial x_k} dA - \iint_A W^I U_j \frac{\partial U_k}{\partial x_j} \frac{\partial \phi}{\partial x_k} dA
\end{aligned} \tag{3.701}$$

$$\begin{aligned}
\iint_A W^I U_j U_k \frac{\partial^2 \phi}{\partial x_j \partial x_k} dA &= \int_S n_j W^I U_j U_k \frac{\partial \phi}{\partial x_k} dS - \iint_A \frac{\partial W^I}{\partial x_j} U_j U_k \frac{\partial \phi}{\partial x_k} dA \\
& - \iint_A W^I \frac{\partial U_j}{\partial x_j} U_k \frac{\partial \phi}{\partial x_k} dA - \iint_A W^I U_j \frac{\partial U_k}{\partial x_j} \frac{\partial \phi}{\partial x_k} dA
\end{aligned} \tag{3.702}$$

If there is no current at the boundary then Equation (3.702) becomes:

$$\begin{aligned}
\iint_A W^I U_j U_k \frac{\partial^2 \phi}{\partial x_j \partial x_k} dA &= - \iint_A \frac{\partial W^I}{\partial x_i} U_j U_k \frac{\partial \phi}{\partial x_k} dA \\
& - \iint_A W^I \frac{\partial U_j}{\partial x_j} U_k \frac{\partial \phi}{\partial x_k} dA - \iint_A W^I U_j \frac{\partial U_k}{\partial x_j} \frac{\partial \phi}{\partial x_k} dA
\end{aligned} \tag{3.703}$$

Examining the fourth term of Equation (3.700) in more detail using Green's Theorem gives:

$$- \iint_A W^I \frac{\partial}{\partial x_k} \left(CC_g \frac{\partial \phi}{\partial x_k} \right) dA = - \iint_A \frac{\partial}{\partial x_k} \left(W^I CC_g \frac{\partial \phi}{\partial x_k} \right) dA + \iint_A CC_g \frac{\partial W^I}{\partial x_k} \frac{\partial \phi}{\partial x_k} dA \tag{3.704}$$

$$-\iint_A W^I \frac{\partial}{\partial x_k} \left(CC_g \frac{\partial \phi}{\partial x_k} \right) dA = -\int_S n_k W^I CC_g \frac{\partial \phi}{\partial x_k} dS + \iint_A CC_g \frac{\partial W^I}{\partial x_k} \frac{\partial \phi}{\partial x_k} dA \quad (3.705)$$

$$-\iint_A W^I \frac{\partial}{\partial x_k} \left(CC_g \frac{\partial \phi}{\partial x_k} \right) dA = -\int_S W^I CC_g \frac{\partial \phi}{\partial n} dS + \iint_A CC_g \frac{\partial W^I}{\partial x_k} \frac{\partial \phi}{\partial x_k} dA \quad (3.706)$$

Substituting Equations (3.703) and (3.706) into Equation (3.700) gives:

$$\begin{aligned} & -\iint_A W^I 2i\omega U_j \frac{\partial \phi}{\partial x_j} dA - \iint_A \frac{\partial W^I}{\partial x_j} U_j U_k \frac{\partial \phi}{\partial x_k} dA - \iint_A W^I \frac{\partial U_j}{\partial x_j} U_k \frac{\partial \phi}{\partial x_k} dA \\ & -\iint_A W^I U_j \frac{\partial U_k}{\partial x_j} \frac{\partial \phi}{\partial x_k} dA + \iint_A W^I U_j \frac{\partial U_k}{\partial x_j} \frac{\partial \phi}{\partial x_k} dA - \int_S W^I CC_g \frac{\partial \phi}{\partial n} dS + \iint_A CC_g \frac{\partial W^I}{\partial x_k} \frac{\partial \phi}{\partial x_k} dA \\ & + \iint_A W^I \phi \sigma^2 dA - \iint_A W^I \omega^2 \phi dA - \iint_A W^I \phi \kappa^2 CC_g dA \\ & + \iint_A W^I g \frac{\partial \phi}{\partial x_k} \left(\frac{\partial \bar{\eta}}{\partial x_k} \right) dA - \iint_A W^I \phi \sigma^2 Q'' dA + \iint_A W^I 2i\omega \phi \lambda' U_j \frac{\partial \bar{\eta}}{\partial x_j} dA \\ & - \iint_A W^I \phi \lambda' U_j \frac{\partial U_k}{\partial x_j} \frac{\partial \bar{\eta}}{\partial x_k} dA - \iint_A W^I 2\lambda' U_j U_k \frac{\partial \bar{\eta}}{\partial x_j} \frac{\partial \phi}{\partial x_k} dA - \iint_A W^I U_j U_k \phi \lambda' \frac{\partial^2 \bar{\eta}}{\partial x_k \partial x_j} dA \\ & + \iint_A W^I U_j U_k \phi \kappa^2 \left(\frac{\partial \bar{\eta}}{\partial x_k} \frac{\partial \bar{\eta}}{\partial x_j} \right) dA + \iint_A W^I U_j U_k (Q''_{kj}) \phi dA = 0 \end{aligned} \quad (3.707)$$

Expressing ϕ in terms of shape functions N^J gives:

$$\phi = \phi^J N^J \quad (3.708)$$

$$\begin{aligned} & -\iint_A W^I 2i\omega U_j \frac{\partial (\phi^J N^J)}{\partial x_j} dA - \iint_A \frac{\partial W^I}{\partial x_j} U_j U_k \frac{\partial (\phi^J N^J)}{\partial x_k} dA - \iint_A W^I \frac{\partial U_j}{\partial x_j} U_k \frac{\partial (\phi^J N^J)}{\partial x_k} dA \\ & -\iint_A W^I U_j \frac{\partial U_k}{\partial x_j} \frac{\partial (\phi^J N^J)}{\partial x_k} dA + \iint_A W^I U_j \frac{\partial U_k}{\partial x_j} \frac{\partial (\phi^J N^J)}{\partial x_k} dA - \int_S W^I CC_g \frac{\partial \phi}{\partial n} dS \\ & + \iint_A CC_g \frac{\partial W^I}{\partial x_k} \frac{\partial (\phi^J N^J)}{\partial x_k} dA + \iint_A W^I \sigma^2 \phi^J N^J dA - \iint_A W^I \omega^2 \phi^J N^J dA - \iint_A W^I \kappa^2 CC_g \phi^J N^J dA \\ & + \iint_A W^I g \left(\frac{\partial \bar{\eta}}{\partial x_k} \right) \frac{\partial (\phi^J N^J)}{\partial x_k} dA - \iint_A W^I \sigma^2 Q'' \phi^J N^J dA + \iint_A W^I 2i\omega \lambda' U_j \frac{\partial \bar{\eta}}{\partial x_j} \phi^J N^J dA \\ & - \iint_A W^I \lambda' U_j \frac{\partial U_k}{\partial x_j} \frac{\partial \bar{\eta}}{\partial x_k} \phi^J N^J dA - \iint_A W^I 2\lambda' U_j U_k \frac{\partial \bar{\eta}}{\partial x_j} \frac{\partial (\phi^J N^J)}{\partial x_k} dA \\ & - \iint_A W^I U_j U_k \lambda' \frac{\partial^2 \bar{\eta}}{\partial x_k \partial x_j} \phi^J N^J dA + \iint_A W^I U_j U_k \kappa^2 \left(\frac{\partial \bar{\eta}}{\partial x_k} \frac{\partial \bar{\eta}}{\partial x_j} \right) \phi^J N^J dA + \iint_A W^I U_j U_k (Q''_{kj}) \phi^J N^J dA = 0 \end{aligned} \quad (3.709)$$

Equation (3.709) becomes:

$$\begin{aligned}
& -\iint_A 2i\omega U_j W^I \frac{\partial N^J}{\partial x_j} \phi^J dA - \iint_A U_j U_k \frac{\partial W^I}{\partial x_j} \frac{\partial N^J}{\partial x_k} \phi^J dA - \iint_A \frac{\partial U_j}{\partial x_j} U_k W^I \frac{\partial N^J}{\partial x_k} \phi^J dA \\
& - \iint_A U_j \frac{\partial U_k}{\partial x_j} W^I \frac{\partial N^J}{\partial x_k} \phi^J dA + \iint_A U_j \frac{\partial U_k}{\partial x_j} W^I \frac{\partial N^J}{\partial x_k} \phi^J dA - \int_S W^I C C_g \frac{\partial \phi}{\partial n} dS \\
& + \iint_A C C_g \frac{\partial W^I}{\partial x_k} \frac{\partial N^J}{\partial x_k} \phi^J dA + \iint_A \sigma^2 W^I N^J \phi^J dA - \iint_A \omega^2 W^I N^J \phi^J dA - \iint_A \kappa^2 C C_g W^I N^J \phi^J dA \\
& + \iint_A g \left(\frac{\partial \bar{\eta}}{\partial x_k} \right) W^I \frac{\partial N^J}{\partial x_k} \phi^J dA - \iint_A \sigma^2 Q'' W^I N^J \phi^J dA + \iint_A 2i\omega \lambda' U_j \frac{\partial \bar{\eta}}{\partial x_j} W^I N^J \phi^J dA \\
& - \iint_A \lambda' U_j \frac{\partial U_k}{\partial x_j} \frac{\partial \bar{\eta}}{\partial x_k} W^I N^J \phi^J dA - \iint_A 2\lambda' U_j U_k \frac{\partial \bar{\eta}}{\partial x_j} W^I \frac{\partial N^J}{\partial x_k} \phi^J dA \\
& - \iint_A U_j U_k \lambda' \frac{\partial^2 \bar{\eta}}{\partial x_k \partial x_j} W^I N^J \phi^J dA + \iint_A U_j U_k \kappa^2 \left(\frac{\partial \bar{\eta}}{\partial x_k} \frac{\partial \bar{\eta}}{\partial x_j} \right) W^I N^J \phi^J dA + \iint_A U_j U_k (Q''_{U'})_{kj} W^I N^J \phi^J dA = 0
\end{aligned} \tag{3.710}$$

In Equation (3.710) I is a free subscript that can be 1, 2 or 3. This means that Equation (3.710) is actually 3 equations:

$$\begin{aligned}
& -\iint_A 2i\omega U_j W^1 \frac{\partial N^J}{\partial x_j} \phi^J dA - \iint_A U_j U_k \frac{\partial W^1}{\partial x_j} \frac{\partial N^J}{\partial x_k} \phi^J dA - \iint_A \frac{\partial U_j}{\partial x_j} U_k W^1 \frac{\partial N^J}{\partial x_k} \phi^J dA \\
& - \iint_A U_j \frac{\partial U_k}{\partial x_j} W^1 \frac{\partial N^J}{\partial x_k} \phi^J dA + \iint_A U_j \frac{\partial U_k}{\partial x_j} W^1 \frac{\partial N^J}{\partial x_k} \phi^J dA - \int_S W^1 C C_g \frac{\partial \phi}{\partial n} dS \\
& + \iint_A C C_g \frac{\partial W^1}{\partial x_k} \frac{\partial N^J}{\partial x_k} \phi^J dA + \iint_A \sigma^2 W^1 N^J \phi^J dA - \iint_A \omega^2 W^1 N^J \phi^J dA - \iint_A \kappa^2 C C_g W^1 N^J \phi^J dA \\
& + \iint_A g \left(\frac{\partial \bar{\eta}}{\partial x_k} \right) W^1 \frac{\partial N^J}{\partial x_k} \phi^J dA - \iint_A \sigma^2 Q'' W^1 N^J \phi^J dA + \iint_A 2i\omega \lambda' U_j \frac{\partial \bar{\eta}}{\partial x_j} W^1 N^J \phi^J dA \\
& - \iint_A \lambda' U_j \frac{\partial U_k}{\partial x_j} \frac{\partial \bar{\eta}}{\partial x_k} W^1 N^J \phi^J dA - \iint_A 2\lambda' U_j U_k \frac{\partial \bar{\eta}}{\partial x_j} W^1 \frac{\partial N^J}{\partial x_k} \phi^J dA \\
& - \iint_A U_j U_k \lambda' \frac{\partial^2 \bar{\eta}}{\partial x_k \partial x_j} W^1 N^J \phi^J dA + \iint_A U_j U_k \kappa^2 \left(\frac{\partial \bar{\eta}}{\partial x_k} \frac{\partial \bar{\eta}}{\partial x_j} \right) W^1 N^J \phi^J dA + \iint_A U_j U_k (Q''_{U'})_{kj} W^1 N^J \phi^J dA = 0
\end{aligned} \tag{3.711}$$

$$\begin{aligned}
& -\iint_A 2i\omega U_j W^2 \frac{\partial N^J}{\partial x_j} \phi^J dA - \iint_A U_j U_k \frac{\partial W^2}{\partial x_j} \frac{\partial N^J}{\partial x_k} \phi^J dA - \iint_A \frac{\partial U_j}{\partial x_j} U_k W^2 \frac{\partial N^J}{\partial x_k} \phi^J dA \\
& -\iint_A U_j \frac{\partial U_k}{\partial x_j} W^2 \frac{\partial N^J}{\partial x_k} \phi^J dA + \iint_A U_j \frac{\partial U_k}{\partial x_j} W^2 \frac{\partial N^J}{\partial x_k} \phi^J dA - \int_S W^2 C C_g \frac{\partial \phi}{\partial n} dS \\
& + \iint_A C C_g \frac{\partial W^2}{\partial x_k} \frac{\partial N^J}{\partial x_k} \phi^J dA + \iint_A \sigma^2 W^2 N^J \phi^J dA - \iint_A \omega^2 W^2 N^J \phi^J dA - \iint_A \kappa^2 C C_g W^2 N^J \phi^J dA \\
& + \iint_A g \left(\frac{\partial \bar{\eta}}{\partial x_k} \right) W^2 \frac{\partial N^J}{\partial x_k} \phi^J dA - \iint_A \sigma^2 Q'' W^2 N^J \phi^J dA + \iint_A 2i\omega \lambda' U_j \frac{\partial \bar{\eta}}{\partial x_j} W^2 N^J \phi^J dA \quad (3.712) \\
& - \iint_A \lambda' U_j \frac{\partial U_k}{\partial x_j} \frac{\partial \bar{\eta}}{\partial x_k} W^2 N^J \phi^J dA - \iint_A 2\lambda' U_j U_k \frac{\partial \bar{\eta}}{\partial x_j} W^2 \frac{\partial N^J}{\partial x_k} \phi^J dA \\
& - \iint_A U_j U_k \lambda' \frac{\partial^2 \bar{\eta}}{\partial x_k \partial x_j} W^2 N^J \phi^J dA + \iint_A U_j U_k \kappa^2 \left(\frac{\partial \bar{\eta}}{\partial x_k} \frac{\partial \bar{\eta}}{\partial x_j} \right) W^2 N^J \phi^J dA \\
& + \iint_A U_j U_k (Q_U'')_{kj} W^2 N^J \phi^J dA = 0
\end{aligned}$$

$$\begin{aligned}
& -\iint_A 2i\omega U_j W^3 \frac{\partial N^J}{\partial x_j} \phi^J dA - \iint_A U_j U_k \frac{\partial W^3}{\partial x_j} \frac{\partial N^J}{\partial x_k} \phi^J dA - \iint_A \frac{\partial U_j}{\partial x_j} U_k W^3 \frac{\partial N^J}{\partial x_k} \phi^J dA \\
& -\iint_A U_j \frac{\partial U_k}{\partial x_j} W^3 \frac{\partial N^J}{\partial x_k} \phi^J dA + \iint_A U_j \frac{\partial U_k}{\partial x_j} W^3 \frac{\partial N^J}{\partial x_k} \phi^J dA - \int_S W^3 C C_g \frac{\partial \phi}{\partial n} dS \\
& + \iint_A C C_g \frac{\partial W^3}{\partial x_k} \frac{\partial N^J}{\partial x_k} \phi^J dA + \iint_A \sigma^2 W^3 N^J \phi^J dA - \iint_A \omega^2 W^3 N^J \phi^J dA - \iint_A \kappa^2 C C_g W^3 N^J \phi^J dA \\
& + \iint_A g \left(\frac{\partial \bar{\eta}}{\partial x_k} \right) W^3 \frac{\partial N^J}{\partial x_k} \phi^J dA - \iint_A \sigma^2 Q'' W^3 N^J \phi^J dA + \iint_A 2i\omega \lambda' U_j \frac{\partial \bar{\eta}}{\partial x_j} W^3 N^J \phi^J dA \quad (3.713) \\
& - \iint_A \lambda' U_j \frac{\partial U_k}{\partial x_j} \frac{\partial \bar{\eta}}{\partial x_k} W^3 N^J \phi^J dA - \iint_A 2\lambda' U_j U_k \frac{\partial \bar{\eta}}{\partial x_j} W^3 \frac{\partial N^J}{\partial x_k} \phi^J dA \\
& - \iint_A U_j U_k \lambda' \frac{\partial^2 \bar{\eta}}{\partial x_k \partial x_j} W^3 N^J \phi^J dA + \iint_A U_j U_k \kappa^2 \left(\frac{\partial \bar{\eta}}{\partial x_k} \frac{\partial \bar{\eta}}{\partial x_j} \right) W^3 N^J \phi^J dA \\
& + \iint_A U_j U_k (Q_U'')_{kj} W^3 N^J \phi^J dA = 0
\end{aligned}$$

Equations (3.711), (3.712) and (3.713) may be combined and written out vectorially as follows:

$$\begin{aligned}
& -\iint_A 2i\omega U_j \left\{ \frac{W^1}{W^2} \right\} \frac{\partial N^J}{\partial x_j} \phi^J dA - \iint_A U_j U_k \left\{ \frac{\frac{\partial W^1}{\partial x_j}}{\frac{\partial W^2}{\partial x_j}} \right\} \frac{\partial N^J}{\partial x_k} \phi^J dA - \iint_A \frac{\partial U_j}{\partial x_j} U_k \left\{ \frac{W^1}{W^2} \right\} \frac{\partial N^J}{\partial x_k} \phi^J dA \\
& -\iint_A U_j \frac{\partial U_k}{\partial x_j} \left\{ \frac{W^1}{W^2} \right\} \frac{\partial N^J}{\partial x_k} \phi^J dA + \iint_A U_j \frac{\partial U_k}{\partial x_j} \left\{ \frac{W^1}{W^3} \right\} \frac{\partial N^J}{\partial x_k} \phi^J dA - \int_S CC_g \frac{\partial \phi}{\partial n} \left\{ \frac{W^1}{W^2} \right\} dS \\
& + \iint_A CC_g \left\{ \frac{\frac{\partial W^1}{\partial x_k}}{\frac{\partial W^2}{\partial x_k}} \right\} \frac{\partial N^J}{\partial x_k} \phi^J dA + \iint_A \sigma^2 \left\{ \frac{W^1}{W^2} \right\} N^J \phi^J dA - \iint_A \omega^2 \left\{ \frac{W^1}{W^3} \right\} N^J \phi^J dA - \iint_A \kappa^2 CC_g \left\{ \frac{W^1}{W^2} \right\} N^J \phi^J dA \\
& + \iint_A g \left(\frac{\partial \bar{\eta}}{\partial x_k} \right) \left\{ \frac{W^1}{W^3} \right\} \frac{\partial N^J}{\partial x_k} \phi^J dA - \iint_A \sigma^2 Q'' \left\{ \frac{W^1}{W^3} \right\} N^J \phi^J dA + \iint_A 2i\omega \lambda' U_j \frac{\partial \bar{\eta}}{\partial x_j} \left\{ \frac{W^1}{W^2} \right\} N^J \phi^J dA \\
& - \iint_A \lambda' U_j \frac{\partial U_k}{\partial x_j} \frac{\partial \bar{\eta}}{\partial x_k} \left\{ \frac{W^1}{W^3} \right\} N^J \phi^J dA - \iint_A 2\lambda' U_j U_k \frac{\partial \bar{\eta}}{\partial x_j} \left\{ \frac{W^1}{W^3} \right\} \frac{\partial N^J}{\partial x_k} \phi^J dA \\
& - \iint_A U_j U_k \lambda' \frac{\partial^2 \bar{\eta}}{\partial x_k \partial x_j} \left\{ \frac{W^1}{W^3} \right\} N^J \phi^J dA + \iint_A U_j U_k \kappa^2 \left(\frac{\partial \bar{\eta}}{\partial x_k} \frac{\partial \bar{\eta}}{\partial x_j} \right) \left\{ \frac{W^1}{W^3} \right\} N^J \phi^J dA \\
& + \iint_A U_j U_k (Q''_{U})_{kj} \left\{ \frac{W^1}{W^3} \right\} N^J \phi^J dA = 0
\end{aligned} \tag{3.714}$$

The superscript J may also be 1, 2 or 3 and hence defines the column number of a matrix:

$$\begin{aligned}
& -\iint_A 2i\omega U_j \left\{ \begin{matrix} W^1 \\ W^2 \\ W^3 \end{matrix} \right\} \left[\begin{matrix} \frac{\partial N^1}{\partial x_j} & \frac{\partial N^2}{\partial x_j} & \frac{\partial N^3}{\partial x_j} \end{matrix} \right] \left\{ \begin{matrix} \phi^1 \\ \phi^2 \\ \phi^3 \end{matrix} \right\} dA - \iint_A U_j U_k \left\{ \begin{matrix} \frac{\partial W^1}{\partial x_j} \\ \frac{\partial W^2}{\partial x_j} \\ \frac{\partial W^3}{\partial x_j} \end{matrix} \right\} \left[\begin{matrix} \frac{\partial N^1}{\partial x_k} & \frac{\partial N^2}{\partial x_k} & \frac{\partial N^3}{\partial x_k} \end{matrix} \right] \left\{ \begin{matrix} \phi^1 \\ \phi^2 \\ \phi^3 \end{matrix} \right\} dA \\
& - \iint_A \frac{\partial U_j}{\partial x_j} U_k \left\{ \begin{matrix} W^1 \\ W^2 \\ W^3 \end{matrix} \right\} \left[\begin{matrix} \frac{\partial N^1}{\partial x_k} & \frac{\partial N^2}{\partial x_k} & \frac{\partial N^3}{\partial x_k} \end{matrix} \right] \left\{ \begin{matrix} \phi^1 \\ \phi^2 \\ \phi^3 \end{matrix} \right\} dA - \iint_A U_j \frac{\partial U_k}{\partial x_j} \left\{ \begin{matrix} W^1 \\ W^2 \\ W^3 \end{matrix} \right\} \left[\begin{matrix} \frac{\partial N^1}{\partial x_k} & \frac{\partial N^2}{\partial x_k} & \frac{\partial N^3}{\partial x_k} \end{matrix} \right] \left\{ \begin{matrix} \phi^1 \\ \phi^2 \\ \phi^3 \end{matrix} \right\} dA \\
& + \iint_A U_j \frac{\partial U_k}{\partial x_j} \left\{ \begin{matrix} W^1 \\ W^2 \\ W^3 \end{matrix} \right\} \left[\begin{matrix} \frac{\partial N^1}{\partial x_k} & \frac{\partial N^2}{\partial x_k} & \frac{\partial N^3}{\partial x_k} \end{matrix} \right] \left\{ \begin{matrix} \phi^1 \\ \phi^2 \\ \phi^3 \end{matrix} \right\} dA - \int_S CC_g \frac{\partial \phi}{\partial n} \left\{ \begin{matrix} W^1 \\ W^2 \\ W^3 \end{matrix} \right\} dS \\
& + \iint_A CC_g \left\{ \begin{matrix} \frac{\partial W^1}{\partial x_k} \\ \frac{\partial W^2}{\partial x_k} \\ \frac{\partial W^3}{\partial x_k} \end{matrix} \right\} \left[\begin{matrix} \frac{\partial N^1}{\partial x_k} & \frac{\partial N^2}{\partial x_k} & \frac{\partial N^3}{\partial x_k} \end{matrix} \right] \left\{ \begin{matrix} \phi^1 \\ \phi^2 \\ \phi^3 \end{matrix} \right\} dA + \iint_A \sigma^2 \left\{ \begin{matrix} W^1 \\ W^2 \\ W^3 \end{matrix} \right\} \left[\begin{matrix} N^1 & N^2 & N^3 \end{matrix} \right] \left\{ \begin{matrix} \phi^1 \\ \phi^2 \\ \phi^3 \end{matrix} \right\} dA \\
& - \iint_A \omega^2 \left\{ \begin{matrix} W^1 \\ W^2 \\ W^3 \end{matrix} \right\} \left[\begin{matrix} N^1 & N^2 & N^3 \end{matrix} \right] \left\{ \begin{matrix} \phi^1 \\ \phi^2 \\ \phi^3 \end{matrix} \right\} dA - \iint_A \kappa^2 CC_g \left\{ \begin{matrix} W^1 \\ W^2 \\ W^3 \end{matrix} \right\} \left[\begin{matrix} N^1 & N^2 & N^3 \end{matrix} \right] \left\{ \begin{matrix} \phi^1 \\ \phi^2 \\ \phi^3 \end{matrix} \right\} dA \\
& + \iint_A g \left(\frac{\partial \bar{\eta}}{\partial x_k} \right) \left\{ \begin{matrix} W^1 \\ W^2 \\ W^3 \end{matrix} \right\} \left[\begin{matrix} \frac{\partial N^1}{\partial x_k} & \frac{\partial N^2}{\partial x_k} & \frac{\partial N^3}{\partial x_k} \end{matrix} \right] \left\{ \begin{matrix} \phi^1 \\ \phi^2 \\ \phi^3 \end{matrix} \right\} dA - \iint_A \sigma^2 Q'' \left\{ \begin{matrix} W^1 \\ W^2 \\ W^3 \end{matrix} \right\} \left[\begin{matrix} N^1 & N^2 & N^3 \end{matrix} \right] \left\{ \begin{matrix} \phi^1 \\ \phi^2 \\ \phi^3 \end{matrix} \right\} dA \\
& + \iint_A 2i\omega \lambda' U_j \frac{\partial \bar{\eta}}{\partial x_j} \left\{ \begin{matrix} W^1 \\ W^2 \\ W^3 \end{matrix} \right\} \left[\begin{matrix} N^1 & N^2 & N^3 \end{matrix} \right] \left\{ \begin{matrix} \phi^1 \\ \phi^2 \\ \phi^3 \end{matrix} \right\} dA - \iint_A \lambda' U_j \frac{\partial U_k}{\partial x_j} \frac{\partial \bar{\eta}}{\partial x_k} \left\{ \begin{matrix} W^1 \\ W^2 \\ W^3 \end{matrix} \right\} \left[\begin{matrix} N^1 & N^2 & N^3 \end{matrix} \right] \left\{ \begin{matrix} \phi^1 \\ \phi^2 \\ \phi^3 \end{matrix} \right\} dA \\
& - \iint_A 2\lambda' U_j U_k \frac{\partial \bar{\eta}}{\partial x_j} \left\{ \begin{matrix} W^1 \\ W^2 \\ W^3 \end{matrix} \right\} \left[\begin{matrix} \frac{\partial N^1}{\partial x_k} & \frac{\partial N^2}{\partial x_k} & \frac{\partial N^3}{\partial x_k} \end{matrix} \right] \left\{ \begin{matrix} \phi^1 \\ \phi^2 \\ \phi^3 \end{matrix} \right\} dA - \iint_A U_j U_k \lambda' \frac{\partial^2 \bar{\eta}}{\partial x_k \partial x_j} \left\{ \begin{matrix} W^1 \\ W^2 \\ W^3 \end{matrix} \right\} \left[\begin{matrix} N^1 & N^2 & N^3 \end{matrix} \right] \left\{ \begin{matrix} \phi^1 \\ \phi^2 \\ \phi^3 \end{matrix} \right\} dA \\
& + \iint_A U_j U_k \kappa^2 \left(\frac{\partial \bar{\eta}}{\partial x_k} \frac{\partial \bar{\eta}}{\partial x_j} \right) \left\{ \begin{matrix} W^1 \\ W^2 \\ W^3 \end{matrix} \right\} \left[\begin{matrix} N^1 & N^2 & N^3 \end{matrix} \right] \left\{ \begin{matrix} \phi^1 \\ \phi^2 \\ \phi^3 \end{matrix} \right\} dA + \iint_A U_j U_k (Q''_{U})_{kj} \left\{ \begin{matrix} W^1 \\ W^2 \\ W^3 \end{matrix} \right\} \left[\begin{matrix} N^1 & N^2 & N^3 \end{matrix} \right] \left\{ \begin{matrix} \phi^1 \\ \phi^2 \\ \phi^3 \end{matrix} \right\} dA = 0
\end{aligned}
\tag{3.715}$$

Equation (3.715) reduces to:

The finite element model created for this project uses the Galerkin method in which the weighting function is equal to the shape functions being used. Hence at this stage W^I will be replaced with N^I . The Galerkin shape functions are discussed in Appendix A.

[illegible]

Equation (3.717) is the finite element solution scheme for the elliptic mild-slope equation including the effects of current. The third last term of the equation is a boundary integral which will be discussed in detail in Section 3.11 of this chapter.

3.10 Helmholtz Equation for Finite Element Mild-Slope Wave-Current Interaction Model

Clyne (2008) and many other authors use the Helmholtz form of the extended elliptic solution to the mild-slope equation. In the interests of brevity it was considered appropriate to produce a Helmholtz form of Equation (3.717) which includes currents. Initially the effects of energy dissipation will not be examined.

The process for obtaining the Helmholtz form of the extended elliptic mild-slope wave equation commences with Equation (3.699):

$$\begin{aligned}
& -2i\omega U_j \frac{\partial \phi}{\partial x_j} + U_j U_k \frac{\partial^2 \phi}{\partial x_j \partial x_k} + U_j \frac{\partial U_k}{\partial x_j} \frac{\partial \phi}{\partial x_k} - \frac{\partial}{\partial x_k} \left(CC_g \frac{\partial \phi}{\partial x_k} \right) \\
& -\phi \kappa^2 CC_g + \phi \sigma^2 - \omega^2 \phi \\
& + g \frac{\partial \phi}{\partial x_k} \left(\frac{\partial \bar{\eta}}{\partial x_k} \right) - \phi \sigma^2 Q'' + 2i\omega \phi \lambda' U_j \frac{\partial \bar{\eta}}{\partial x_j} - \phi \lambda' U_j \frac{\partial U_k}{\partial x_j} \frac{\partial \bar{\eta}}{\partial x_k} \\
& - U_j U_k \lambda' \frac{\partial \bar{\eta}}{\partial x_j} \frac{\partial \phi}{\partial x_k} - U_j U_k \lambda' \frac{\partial \bar{\eta}}{\partial x_k} \frac{\partial \phi}{\partial x_j} - U_j U_k \phi \lambda' \frac{\partial^2 \bar{\eta}}{\partial x_j \partial x_k} + U_j U_k \phi \kappa^2 \frac{\partial \bar{\eta}}{\partial x_k} \frac{\partial \bar{\eta}}{\partial x_j} + U_j U_k (Q_U)_{kj} \phi = 0
\end{aligned}$$

At this stage it can be assumed that the accuracy of the model will not suffer if the effects of the gradients of $\bar{\eta}$ are assumed to be negligible. This leads to the following equation:

$$\begin{aligned}
& -2i\omega U_j \frac{\partial \phi}{\partial x_j} + U_j U_k \frac{\partial^2 \phi}{\partial x_j \partial x_k} + U_j \frac{\partial U_k}{\partial x_j} \frac{\partial \phi}{\partial x_k} - \frac{\partial}{\partial x_k} \left(CC_g \frac{\partial \phi}{\partial x_k} \right) \\
& -\phi \kappa^2 CC_g + \phi \sigma^2 - \omega^2 \phi - \phi \sigma^2 \tilde{Q}'' = 0
\end{aligned} \tag{3.718}$$

Where:

$$\tilde{Q}'' = \frac{1}{\cosh^2 \kappa h'} \left(Q_1 \frac{\partial^2 h'}{\partial x_k \partial x_k} + Q_2 \frac{\partial^2 \kappa}{\partial x_k^2} + Q_4 \left(\frac{\partial h'}{\partial x_k} \frac{\partial h'}{\partial x_k} \right) + Q_5 \left(\frac{\partial \kappa}{\partial x_k} \frac{\partial \kappa}{\partial x_k} \right) + Q_7 \frac{\partial \kappa}{\partial x_k} \frac{\partial h'}{\partial x_k} + W_6 \frac{\partial h'}{\partial x_k} \right) \tag{3.719}$$

The Helmholtz form of a the mild-slope equation involves replacing the velocity potential with a scaled version of itself:

$$\phi' = \phi \sqrt{CC_g} \tag{3.720}$$

$$\frac{\phi'}{\sqrt{CC_g}} = \phi \tag{3.721}$$

Combining Equation (3.721) with Equation (3.718) and multiplying by -1 gives:

$$\begin{aligned}
 & CC_g \frac{\partial^2}{\partial x_k \partial x_k} \left(\frac{\phi'}{\sqrt{CC_g}} \right) + \frac{\partial}{\partial x_k} \left(\frac{\phi'}{\sqrt{CC_g}} \right) \frac{\partial (CC_g)}{\partial x_k} + \left(\frac{\phi'}{\sqrt{CC_g}} \right) \sigma^2 \tilde{Q}'' + \left(\frac{\phi'}{\sqrt{CC_g}} \right) \kappa^2 CC_g \\
 & - \left(\frac{\phi'}{\sqrt{CC_g}} \right) \sigma^2 + \omega^2 \left(\frac{\phi'}{\sqrt{CC_g}} \right) + 2i\omega U_j \frac{\partial}{\partial x_j} \left(\frac{\phi'}{\sqrt{CC_g}} \right) \\
 & - U_j \frac{\partial U_k}{\partial x_j} \frac{\partial}{\partial x_k} \left(\frac{\phi'}{\sqrt{CC_g}} \right) - U_j U_k \frac{\partial^2}{\partial x_j \partial x_k} \left(\frac{\phi'}{\sqrt{CC_g}} \right) = 0
 \end{aligned} \tag{3.722}$$

$$\begin{aligned}
 & CC_g \frac{\partial^2}{\partial x_k \partial x_k} \left(\frac{\phi'}{\sqrt{CC_g}} \right) + \frac{\partial}{\partial x_k} \left(\frac{\phi'}{\sqrt{CC_g}} \right) \frac{\partial (CC_g)}{\partial x_k} + \phi' \kappa^2 \sqrt{CC_g} + \frac{\sigma^2 \tilde{Q}'' \phi'}{\sqrt{CC_g}} - \frac{\sigma^2 \phi'}{\sqrt{CC_g}} \\
 & + \frac{\omega^2 \phi'}{\sqrt{CC_g}} + 2i\omega U_j \frac{\partial}{\partial x_j} \left(\frac{\phi'}{\sqrt{CC_g}} \right) - U_j \frac{\partial U_k}{\partial x_j} \frac{\partial}{\partial x_k} \left(\frac{\phi'}{\sqrt{CC_g}} \right) - U_j U_k \frac{\partial^2}{\partial x_j \partial x_k} \left(\frac{\phi'}{\sqrt{CC_g}} \right) = 0
 \end{aligned} \tag{3.723}$$

$$\begin{aligned}
 & \frac{\partial}{\partial x_k} \left[CC_g \frac{\partial}{\partial x_k} \left(\frac{\phi'}{\sqrt{CC_g}} \right) \right] + \phi' \kappa^2 \sqrt{CC_g} + \frac{\sigma^2 \tilde{Q}'' \phi'}{\sqrt{CC_g}} - \frac{\sigma^2 \phi'}{\sqrt{CC_g}} + \frac{\omega^2 \phi'}{\sqrt{CC_g}} \\
 & + 2i\omega U_j \frac{\partial}{\partial x_j} \left(\frac{\phi'}{\sqrt{CC_g}} \right) - U_j \frac{\partial U_k}{\partial x_j} \frac{\partial}{\partial x_k} \left(\frac{\phi'}{\sqrt{CC_g}} \right) - U_j U_k \frac{\partial^2}{\partial x_j \partial x_k} \left(\frac{\phi'}{\sqrt{CC_g}} \right) = 0
 \end{aligned} \tag{3.724}$$

The spatial derivative of Equation (3.721) is:

$$\frac{\partial}{\partial x_k} \left(\frac{\phi'}{\sqrt{CC_g}} \right) = \frac{\sqrt{CC_g} \frac{\partial \phi'}{\partial x_k} - \phi' \frac{\partial \sqrt{CC_g}}{\partial x_k}}{CC_g} \tag{3.725}$$

Expressing Equation (3.724) using Equation (3.725) gives the following:

$$\begin{aligned}
 & \frac{\partial}{\partial x_k} \left[CC_g \left(\frac{\sqrt{CC_g} \frac{\partial \phi'}{\partial x_k} - \phi' \frac{\partial \sqrt{CC_g}}{\partial x_k}}{CC_g} \right) \right] + \phi' \kappa^2 \sqrt{CC_g} + \frac{\sigma^2 \tilde{Q}'' \phi'}{\sqrt{CC_g}} - \frac{\sigma^2 \phi'}{\sqrt{CC_g}} + \frac{\omega^2 \phi'}{\sqrt{CC_g}} \\
 & + 2i\omega U_j \left(\frac{\sqrt{CC_g} \frac{\partial \phi'}{\partial x_j} - \phi' \frac{\partial \sqrt{CC_g}}{\partial x_j}}{CC_g} \right) - U_j \frac{\partial U_k}{\partial x_j} \left(\frac{\sqrt{CC_g} \frac{\partial \phi'}{\partial x_k} - \phi' \frac{\partial \sqrt{CC_g}}{\partial x_k}}{CC_g} \right) - U_j U_k \frac{\partial^2}{\partial x_j \partial x_k} \left(\frac{\phi'}{\sqrt{CC_g}} \right) = 0
 \end{aligned} \tag{3.726}$$

Equation (3.726) can be manipulated as follows:

$$\begin{aligned} & \frac{\partial}{\partial x_k} \left[\sqrt{CC_g} \frac{\partial \phi'}{\partial x_k} - \phi' \frac{\partial \sqrt{CC_g}}{\partial x_k} \right] + \phi' \kappa^2 \sqrt{CC_g} + \frac{\sigma^2 \tilde{Q}'' \phi'}{\sqrt{CC_g}} - \frac{\sigma^2 \phi'}{\sqrt{CC_g}} + \frac{\omega^2 \phi'}{\sqrt{CC_g}} \\ & + 2i\omega U_j \left(\frac{\sqrt{CC_g} \frac{\partial \phi'}{\partial x_j} - \phi' \frac{\partial \sqrt{CC_g}}{\partial x_j}}{CC_g} \right) - U_j \frac{\partial U_k}{\partial x_j} \left(\frac{\sqrt{CC_g} \frac{\partial \phi'}{\partial x_k} - \phi' \frac{\partial \sqrt{CC_g}}{\partial x_k}}{CC_g} \right) - U_j U_k \frac{\partial^2}{\partial x_j \partial x_k} \left(\frac{\phi'}{\sqrt{CC_g}} \right) = 0 \end{aligned} \quad (3.727)$$

$$\begin{aligned} & \frac{\partial}{\partial x_k} \left(\sqrt{CC_g} \frac{\partial \phi'}{\partial x_k} \right) - \frac{\partial}{\partial x_k} \left(\phi' \frac{\partial \sqrt{CC_g}}{\partial x_k} \right) + \phi' \kappa^2 \sqrt{CC_g} + \frac{\sigma^2 \tilde{Q}'' \phi'}{\sqrt{CC_g}} - \frac{\sigma^2 \phi'}{\sqrt{CC_g}} + \frac{\omega^2 \phi'}{\sqrt{CC_g}} \\ & + 2i\omega U_j \left(\frac{\sqrt{CC_g} \frac{\partial \phi'}{\partial x_j} - \phi' \frac{\partial \sqrt{CC_g}}{\partial x_j}}{CC_g} \right) - U_j \frac{\partial U_k}{\partial x_j} \left(\frac{\sqrt{CC_g} \frac{\partial \phi'}{\partial x_k} - \phi' \frac{\partial \sqrt{CC_g}}{\partial x_k}}{CC_g} \right) - U_j U_k \frac{\partial^2}{\partial x_j \partial x_k} \left(\frac{\phi'}{\sqrt{CC_g}} \right) = 0 \end{aligned} \quad (3.728)$$

$$\begin{aligned} & \sqrt{CC_g} \frac{\partial^2 \phi'}{\partial x_k \partial x_k} - \phi' \frac{\partial^2 \sqrt{CC_g}}{\partial x_k \partial x_k} + \phi' \kappa^2 \sqrt{CC_g} + \frac{\sigma^2 \tilde{Q}'' \phi'}{\sqrt{CC_g}} - \frac{\sigma^2 \phi'}{\sqrt{CC_g}} + \frac{\omega^2 \phi'}{\sqrt{CC_g}} \\ & + 2i\omega U_j \left(\frac{\sqrt{CC_g} \frac{\partial \phi'}{\partial x_j} - \phi' \frac{\partial \sqrt{CC_g}}{\partial x_j}}{CC_g} \right) - U_j \frac{\partial U_k}{\partial x_j} \left(\frac{\sqrt{CC_g} \frac{\partial \phi'}{\partial x_k} - \phi' \frac{\partial \sqrt{CC_g}}{\partial x_k}}{CC_g} \right) - U_j U_k \frac{\partial^2}{\partial x_j \partial x_k} \left(\frac{\phi'}{\sqrt{CC_g}} \right) = 0 \end{aligned} \quad (3.729)$$

$$\begin{aligned} & \sqrt{CC_g} \frac{\partial^2 \phi'}{\partial x_k \partial x_k} - \phi' \frac{\partial^2 \sqrt{CC_g}}{\partial x_k \partial x_k} + \phi' \kappa^2 \sqrt{CC_g} + \frac{\sigma^2 \tilde{Q}'' \phi'}{\sqrt{CC_g}} - \frac{\sigma^2 \phi'}{\sqrt{CC_g}} + \frac{\omega^2 \phi'}{\sqrt{CC_g}} \\ & + \frac{2i\omega U_j}{\sqrt{CC_g}} \frac{\partial \phi'}{\partial x_j} - \frac{2i\omega U_j \phi'}{CC_g} \frac{\partial \sqrt{CC_g}}{\partial x_j} - \frac{U_j}{\sqrt{CC_g}} \frac{\partial U_k}{\partial x_j} \frac{\partial \phi'}{\partial x_k} + \frac{U_j \phi'}{CC_g} \frac{\partial U_k}{\partial x_j} \frac{\partial \sqrt{CC_g}}{\partial x_k} - U_j U_k \frac{\partial^2}{\partial x_j \partial x_k} \left(\frac{\phi'}{\sqrt{CC_g}} \right) = 0 \end{aligned} \quad (3.730)$$

Examining the last term of Equation (3.730) shows that this substitution may be made:

$$\frac{\partial^2}{\partial x_j \partial x_k} \left(\frac{\phi'}{\sqrt{CC_g}} \right) = \frac{\partial}{\partial x_j} \left(\frac{1}{\sqrt{CC_g}} \frac{\partial \phi'}{\partial x_k} \right) - \frac{\partial}{\partial x_j} \left(\frac{\phi'}{CC_g} \frac{\partial \sqrt{CC_g}}{\partial x_k} \right) \quad (3.731)$$

$$\frac{\partial}{\partial x_j \partial x_k} \left(\frac{\phi'}{\sqrt{CC_g}} \right) = \left(\frac{\sqrt{CC_g} \frac{\partial^2 \phi'}{\partial x_j \partial x_k} - \frac{\partial \phi'}{\partial x_k} \frac{\partial \sqrt{CC_g}}{\partial x_j}}{CC_g} \right) - \phi' \left(\frac{CC_g \frac{\partial^2 \sqrt{CC_g}}{\partial x_j \partial x_k} - \frac{\partial \sqrt{CC_g}}{\partial x_k} \frac{\partial (CC_g)}{\partial x_j}}{(CC_g)^2} \right) - \left(\frac{1}{CC_g} \frac{\partial \sqrt{CC_g}}{\partial x_k} \right) \frac{\partial \phi'}{\partial x_j} \quad (3.732)$$

$$\frac{\partial}{\partial x_j \partial x_k} \left(\frac{\phi'}{\sqrt{CC_g}} \right) = \frac{1}{\sqrt{CC_g}} \frac{\partial^2 \phi'}{\partial x_j \partial x_k} - \frac{1}{CC_g} \frac{\partial \phi'}{\partial x_k} \frac{\partial \sqrt{CC_g}}{\partial x_j} - \frac{\phi'}{CC_g} \frac{\partial^2 \sqrt{CC_g}}{\partial x_j \partial x_k} + \frac{\phi'}{(CC_g)^2} \frac{\partial \sqrt{CC_g}}{\partial x_k} \frac{\partial (CC_g)}{\partial x_j} - \frac{1}{CC_g} \frac{\partial \sqrt{CC_g}}{\partial x_k} \frac{\partial \phi'}{\partial x_j} \quad (3.733)$$

Using Equation (3.733) with Equation (3.730) yields:

$$\begin{aligned} & \sqrt{CC_g} \frac{\partial^2 \phi'}{\partial x_k \partial x_k} - \phi' \frac{\partial^2 \sqrt{CC_g}}{\partial x_k \partial x_k} + \phi' \kappa^2 \sqrt{CC_g} + \frac{\sigma^2 \tilde{Q}'' \phi'}{\sqrt{CC_g}} - \frac{\sigma^2 \phi'}{\sqrt{CC_g}} + \frac{\omega^2 \phi'}{\sqrt{CC_g}} \\ & + \frac{2i\omega U_j}{\sqrt{CC_g}} \frac{\partial \phi'}{\partial x_j} - \frac{2i\omega U_j \phi'}{CC_g} \frac{\partial \sqrt{CC_g}}{\partial x_j} - \frac{U_j}{\sqrt{CC_g}} \frac{\partial U_k}{\partial x_j} \frac{\partial \phi'}{\partial x_k} + \frac{U_j \phi'}{CC_g} \frac{\partial U_k}{\partial x_j} \frac{\partial \sqrt{CC_g}}{\partial x_k} \\ & - U_j U_k \left(\frac{1}{\sqrt{CC_g}} \frac{\partial^2 \phi'}{\partial x_j \partial x_k} - \frac{1}{CC_g} \frac{\partial \phi'}{\partial x_k} \frac{\partial \sqrt{CC_g}}{\partial x_j} - \frac{\phi'}{CC_g} \frac{\partial^2 \sqrt{CC_g}}{\partial x_j \partial x_k} + \frac{\phi'}{(CC_g)^2} \frac{\partial \sqrt{CC_g}}{\partial x_k} \frac{\partial (CC_g)}{\partial x_j} - \frac{1}{CC_g} \frac{\partial \sqrt{CC_g}}{\partial x_k} \frac{\partial \phi'}{\partial x_j} \right) = 0 \end{aligned} \quad (3.734)$$

Which may be re-expressed as follows:

$$\begin{aligned} & \sqrt{CC_g} \frac{\partial^2 \phi'}{\partial x_k \partial x_k} - \phi' \frac{\partial^2 \sqrt{CC_g}}{\partial x_k \partial x_k} + \phi' \kappa^2 \sqrt{CC_g} + \frac{\sigma^2 \tilde{Q}'' \phi'}{\sqrt{CC_g}} - \frac{\sigma^2 \phi'}{\sqrt{CC_g}} + \frac{\omega^2 \phi'}{\sqrt{CC_g}} \\ & + \frac{2i\omega U_j}{\sqrt{CC_g}} \frac{\partial \phi'}{\partial x_j} - \frac{2i\omega U_j \phi'}{CC_g} \frac{\partial \sqrt{CC_g}}{\partial x_j} - \frac{U_j}{\sqrt{CC_g}} \frac{\partial U_k}{\partial x_j} \frac{\partial \phi'}{\partial x_k} + \frac{U_j \phi'}{CC_g} \frac{\partial U_k}{\partial x_j} \frac{\partial (CC_g)}{\partial x_k} \\ & - \frac{U_j U_k}{\sqrt{CC_g}} \frac{\partial^2 \phi'}{\partial x_j \partial x_k} + 2 \frac{U_j U_k}{CC_g} \frac{\partial \phi'}{\partial x_k} \frac{\partial \sqrt{CC_g}}{\partial x_j} + \frac{\phi' U_j U_k}{CC_g} \frac{\partial^2 \sqrt{CC_g}}{\partial x_j \partial x_k} \\ & - \frac{\phi' U_j U_k}{(CC_g)^2} \frac{\partial \sqrt{CC_g}}{\partial x_k} \frac{\partial (CC_g)}{\partial x_j} = 0 \end{aligned} \quad (3.735)$$

$$\begin{aligned}
& \sqrt{CC_g} \frac{\partial^2 \phi'}{\partial x_k \partial x_k} - \phi' \frac{\partial^2 \sqrt{CC_g}}{\partial x_k \partial x_k} + \phi' \kappa^2 \sqrt{CC_g} + \frac{\sigma^2 \tilde{Q}'' \phi'}{\sqrt{CC_g}} - \frac{\sigma^2 \phi'}{\sqrt{CC_g}} + \frac{\omega^2 \phi'}{\sqrt{CC_g}} - \frac{2i\omega U_k \phi'}{CC_g} \frac{\partial \sqrt{CC_g}}{\partial x_k} \\
& + \frac{U_j \phi'}{CC_g} \frac{\partial U_k}{\partial x_j} \frac{\partial \sqrt{CC_g}}{\partial x_k} + \frac{\phi' U_j U_k}{CC_g} \frac{\partial^2 \sqrt{CC_g}}{\partial x_j \partial x_k} - \frac{\phi' U_j U_k}{(CC_g)^2} \frac{\partial \sqrt{CC_g}}{\partial x_k} \frac{\partial (CC_g)}{\partial x_j} \\
& + \frac{2i\omega U_k}{\sqrt{CC_g}} \frac{\partial \phi'}{\partial x_k} - \frac{U_j}{\sqrt{CC_g}} \frac{\partial U_k}{\partial x_j} \frac{\partial \phi'}{\partial x_k} + 2 \frac{U_j U_k}{CC_g} \frac{\partial \phi'}{\partial x_k} \frac{\partial \sqrt{CC_g}}{\partial x_j} \\
& - \frac{U_j U_k}{\sqrt{CC_g}} \frac{\partial^2 \phi'}{\partial x_j \partial x_k} \\
& = 0
\end{aligned} \tag{3.736}$$

$$\begin{aligned}
& \frac{\partial^2 \phi'}{\partial x_k \partial x_k} - \frac{\phi'}{\sqrt{CC_g}} \frac{\partial^2 \sqrt{CC_g}}{\partial x_k \partial x_k} + \phi' \kappa^2 + \frac{\sigma^2 \tilde{Q}'' \phi'}{CC_g} - \frac{\sigma^2 \phi'}{CC_g} + \frac{\omega^2 \phi'}{CC_g} - \frac{2i\omega U_k \phi'}{(CC_g)^{\frac{3}{2}}} \frac{\partial \sqrt{CC_g}}{\partial x_k} \\
& + \frac{U_j \phi'}{(CC_g)^{\frac{3}{2}}} \frac{\partial U_k}{\partial x_j} \frac{\partial \sqrt{CC_g}}{\partial x_k} + \frac{\phi' U_j U_k}{(CC_g)^{\frac{3}{2}}} \frac{\partial^2 \sqrt{CC_g}}{\partial x_j \partial x_k} - \frac{\phi' U_j U_k}{(CC_g)^{\frac{5}{2}}} \frac{\partial \sqrt{CC_g}}{\partial x_k} \frac{\partial (CC_g)}{\partial x_j} \\
& + \frac{2i\omega U_k}{CC_g} \frac{\partial \phi'}{\partial x_k} - \frac{U_j}{CC_g} \frac{\partial U_k}{\partial x_j} \frac{\partial \phi'}{\partial x_k} + 2 \frac{U_j U_k}{(CC_g)^{\frac{3}{2}}} \frac{\partial \phi'}{\partial x_k} \frac{\partial \sqrt{CC_g}}{\partial x_j} \\
& - \frac{U_j U_k}{CC_g} \frac{\partial^2 \phi'}{\partial x_j \partial x_k} \\
& = 0
\end{aligned} \tag{3.737}$$

Isolating the derivatives of the new scaled velocity potential in Equation (3.737) gives:

$$\begin{aligned}
& \frac{\partial^2 \phi'}{\partial x_k \partial x_k} + \left(-\frac{1}{\sqrt{CC_g}} \frac{\partial^2 \sqrt{CC_g}}{\partial x_k \partial x_k} + \kappa^2 + \frac{\sigma^2 (\tilde{Q}'' - 1)}{CC_g} + \frac{\omega^2}{CC_g} - \frac{2i\omega U_k}{(CC_g)^{\frac{3}{2}}} \frac{\partial \sqrt{CC_g}}{\partial x_k} \right. \\
& \quad \left. + \frac{U_j}{(CC_g)^{\frac{3}{2}}} \frac{\partial U_k}{\partial x_j} \frac{\partial \sqrt{CC_g}}{\partial x_k} + \frac{U_j U_k}{(CC_g)^{\frac{3}{2}}} \frac{\partial^2 \sqrt{CC_g}}{\partial x_j \partial x_k} - \frac{U_j U_k}{(CC_g)^{\frac{5}{2}}} \frac{\partial \sqrt{CC_g}}{\partial x_k} \frac{\partial (CC_g)}{\partial x_j} \right) \phi' \\
& + \left(\frac{2i\omega U_k}{CC_g} - \frac{U_j}{CC_g} \frac{\partial U_k}{\partial x_j} + 2 \frac{U_j U_k}{(CC_g)^{\frac{3}{2}}} \frac{\partial \sqrt{CC_g}}{\partial x_j} \right) \frac{\partial \phi'}{\partial x_k} \\
& - \frac{U_j U_k}{CC_g} \frac{\partial^2 \phi'}{\partial x_j \partial x_k} \\
& = 0
\end{aligned} \tag{3.738}$$

$$\begin{aligned}
& \frac{\partial^2 \phi'}{\partial x_k \partial x_k} + \left(-\frac{1}{\sqrt{CC_g}} \frac{\partial^2 \sqrt{CC_g}}{\partial x_k \partial x_k} + \kappa^2 + \frac{\sigma^2 \tilde{Q}''}{CC_g} \right) \phi' + \frac{\omega^2}{CC_g} \phi' - \frac{\sigma^2}{CC_g} \phi' \\
& - \frac{U_j}{CC_g} \frac{\partial U_k}{\partial x_j} \frac{\partial \phi'}{\partial x_k} + 2 \frac{U_j U_k}{(CC_g)^{\frac{3}{2}}} \frac{\partial \sqrt{CC_g}}{\partial x_j} \frac{\partial \phi'}{\partial x_k} \\
& + \frac{U_j}{(CC_g)^{\frac{3}{2}}} \frac{\partial U_k}{\partial x_j} \frac{\partial \sqrt{CC_g}}{\partial x_k} \phi' + \frac{U_j U_k}{(CC_g)^{\frac{3}{2}}} \frac{\partial^2 \sqrt{CC_g}}{\partial x_j \partial x_k} \phi' - \frac{U_j U_k}{(CC_g)^{\frac{5}{2}}} \frac{\partial \sqrt{CC_g}}{\partial x_k} \frac{\partial \sqrt{CC_g}}{\partial x_j} \phi' \\
& - \frac{2i\omega U_k}{(CC_g)^{\frac{3}{2}}} \frac{\partial \sqrt{CC_g}}{\partial x_k} \phi' + \frac{2i\omega U_k}{CC_g} \frac{\partial \phi'}{\partial x_k} - \frac{U_j U_k}{CC_g} \frac{\partial^2 \phi'}{\partial x_j \partial x_k} \\
& = 0
\end{aligned} \tag{3.739}$$

A new term can now be introduced:

$$K^2 = -\frac{1}{\sqrt{CC_g}} \frac{\partial^2 \sqrt{CC_g}}{\partial x_k \partial x_k} + \kappa^2 + \frac{\sigma^2 \tilde{Q}''}{CC_g} \tag{3.740}$$

Using Equation (3.740) with Equation (3.739) gives:

$$\begin{aligned}
& \frac{\partial^2 \phi'}{\partial x_k \partial x_k} + K^2 \phi' + \frac{\omega^2}{CC_g} \phi' - \frac{\sigma^2}{CC_g} \phi' \\
& - \frac{U_j}{CC_g} \frac{\partial U_k}{\partial x_j} \frac{\partial \phi'}{\partial x_k} + 2 \frac{U_j U_k}{(CC_g)^{\frac{3}{2}}} \frac{\partial \sqrt{CC_g}}{\partial x_j} \frac{\partial \phi'}{\partial x_k} \\
& + \frac{U_j}{(CC_g)^{\frac{3}{2}}} \frac{\partial U_k}{\partial x_j} \frac{\partial \sqrt{CC_g}}{\partial x_k} \phi' + \frac{U_j U_k}{(CC_g)^{\frac{3}{2}}} \frac{\partial^2 \sqrt{CC_g}}{\partial x_j \partial x_k} \phi' - \frac{U_j U_k}{(CC_g)^{\frac{5}{2}}} \frac{\partial \sqrt{CC_g}}{\partial x_k} \frac{\partial \sqrt{CC_g}}{\partial x_j} \phi' \\
& - \frac{2i\omega U_k}{(CC_g)^{\frac{3}{2}}} \frac{\partial \sqrt{CC_g}}{\partial x_k} \phi' + \frac{2i\omega U_k}{CC_g} \frac{\partial \phi'}{\partial x_k} - \frac{U_j U_k}{CC_g} \frac{\partial^2 \phi'}{\partial x_j \partial x_k} = 0
\end{aligned} \tag{3.741}$$

Equation (3.741) is the Helmholtz Form of the Extended Elliptic Mild-Slope Wave Equation including Currents.

In order to obtain an equation which may be solved over a finite element Equation (3.741) can now be multiplied by a weighting function W^I and integrated over the finite element area:

$$\begin{aligned}
& \iint_A W^I \frac{\partial}{\partial x_k} \left(\frac{\partial \phi'}{\partial x_k} \right) dA + \iint_A W^I K^2 \phi' dA + \iint_A W^I \frac{\omega^2}{CC_g} \phi' dA - \iint_A W^I \frac{\sigma^2}{CC_g} \phi' dA \\
& - \iint_A W^I \frac{U_j}{CC_g} \frac{\partial U_k}{\partial x_j} \frac{\partial \phi'}{\partial x_k} dA + 2 \iint_A W^I \frac{U_j U_k}{(CC_g)^{\frac{3}{2}}} \frac{\partial \sqrt{CC_g}}{\partial x_j} \frac{\partial \phi'}{\partial x_k} dA \\
& + \iint_A W^I \frac{U_j}{(CC_g)^{\frac{3}{2}}} \frac{\partial U_k}{\partial x_j} \frac{\partial \sqrt{CC_g}}{\partial x_k} \phi' dA + \iint_A W^I \frac{U_j U_k}{(CC_g)^{\frac{3}{2}}} \frac{\partial^2 \sqrt{CC_g}}{\partial x_j \partial x_k} \phi' dA \\
& - \iint_A W^I \frac{U_j U_k}{(CC_g)^{\frac{5}{2}}} \frac{\partial \sqrt{CC_g}}{\partial x_k} \frac{\partial (CC_g)}{\partial x_j} \phi' dA - \iint_A W^I \frac{U_j U_k}{CC_g} \frac{\partial^2 \phi'}{\partial x_k \partial x_k} dA \\
& - \iint_A W^I \frac{2i\omega U_k}{(CC_g)^{\frac{3}{2}}} \frac{\partial \sqrt{CC_g}}{\partial x_k} \phi' dA + \iint_A W^I \frac{2i\omega U_k}{CC_g} \frac{\partial \phi'}{\partial x_k} dA = 0
\end{aligned} \tag{3.742}$$

Examining the ninth term in Equation (3.742) gives:

$$\begin{aligned}
\iint_A W^I \frac{U_j U_k}{CC_g} \frac{\partial^2 \phi'}{\partial x_j \partial x_k} dA &= \iint_A \frac{\partial}{\partial x_j} \left(W^I \frac{U_j U_k}{CC_g} \frac{\partial \phi'}{\partial x_k} \right) dA - \iint_A \frac{\partial W^I}{\partial x_j} \frac{U_j U_k}{CC_g} \frac{\partial \phi'}{\partial x_k} dA \\
& - \iint_A W^I \frac{\partial U_j}{\partial x_j} \frac{U_k}{CC_g} \frac{\partial \phi'}{\partial x_k} dA - \iint_A W^I \frac{U_j}{CC_g} \frac{\partial U_k}{\partial x_j} \frac{\partial \phi'}{\partial x_k} dA \\
& - \iint_A W^I U_k U_j \frac{\partial}{\partial x_j} \left(\frac{1}{CC_g} \right) \frac{\partial \phi'}{\partial x_k} dA
\end{aligned} \tag{3.743}$$

Using Green's Theorem with Equation (3.743) yields:

$$\begin{aligned}
\iint_A W^I \frac{U_j U_k}{CC_g} \frac{\partial^2 \phi'}{\partial x_j \partial x_k} dA &= \int_S n_j W^I \frac{U_j U_k}{CC_g} \frac{\partial \phi'}{\partial x_k} dS - \iint_A \frac{\partial W^I}{\partial x_j} \frac{U_j U_k}{CC_g} \frac{\partial \phi'}{\partial x_k} dA \\
& - \iint_A W^I \frac{\partial U_j}{\partial x_j} \frac{U_k}{CC_g} \frac{\partial \phi'}{\partial x_k} dA - \iint_A W^I \frac{U_j}{CC_g} \frac{\partial U_k}{\partial x_j} \frac{\partial \phi'}{\partial x_k} dA \\
& - \iint_A W^I U_k U_j \frac{\partial}{\partial x_j} \left(\frac{1}{CC_g} \right) \frac{\partial \phi'}{\partial x_k} dA
\end{aligned} \tag{3.744}$$

If there is no current at the boundary then Equation (3.744) becomes:

$$\begin{aligned} \iint_A W^I \frac{U_j U_k}{CC_g} \frac{\partial^2 \phi'}{\partial x_j \partial x_k} dA = & - \iint_A \frac{\partial W^I}{\partial x_j} \frac{U_j U_k}{CC_g} \frac{\partial \phi'}{\partial x_k} dA - \iint_A W^I \frac{\partial U_j}{\partial x_j} \frac{U_k}{CC_g} \frac{\partial \phi'}{\partial x_k} dA \\ & - \iint_A W^I \frac{U_j}{CC_g} \frac{\partial U_k}{\partial x_j} \frac{\partial \phi'}{\partial x_k} dA - \iint_A W^I U_k U_j \frac{\partial}{\partial x_j} \left[(CC_g)^{-1} \right] \frac{\partial \phi'}{\partial x_k} dA \end{aligned} \quad (3.745)$$

Substituting Equation (3.745) into Equation (3.742):

$$\begin{aligned} \iint_A W^I \frac{\partial}{\partial x_k} \left(\frac{\partial \phi'}{\partial x_k} \right) dA + \iint_A W^I K^2 \phi' dA + \iint_A W^I \frac{\omega^2}{CC_g} \phi' dA - \iint_A W^I \frac{\sigma^2}{CC_g} \phi' dA \\ - \iint_A W^I \frac{U_j}{CC_g} \frac{\partial U_k}{\partial x_j} \frac{\partial \phi'}{\partial x_k} dA + 2 \iint_A W^I \frac{U_j U_k}{(CC_g)^{\frac{3}{2}}} \frac{\partial \sqrt{CC_g}}{\partial x_j} \frac{\partial \phi'}{\partial x_k} dA \\ + \iint_A W^I \frac{U_j}{(CC_g)^{\frac{3}{2}}} \frac{\partial U_k}{\partial x_j} \frac{\partial \sqrt{CC_g}}{\partial x_k} \phi' dA + \iint_A W^I \frac{U_j U_k}{(CC_g)^{\frac{3}{2}}} \frac{\partial^2 \sqrt{CC_g}}{\partial x_j \partial x_k} \phi' dA \\ - \iint_A W^I \frac{U_j U_k}{(CC_g)^{\frac{5}{2}}} \frac{\partial \sqrt{CC_g}}{\partial x_k} \frac{\partial (CC_g)}{\partial x_j} \phi' dA \\ + \iint_A \frac{\partial W^I}{\partial x_j} \frac{U_j U_k}{CC_g} \frac{\partial \phi'}{\partial x_k} dA + \iint_A W^I \frac{\partial U_j}{\partial x_j} \frac{U_k}{CC_g} \frac{\partial \phi'}{\partial x_k} dA \\ + \iint_A W^I \frac{U_j}{CC_g} \frac{\partial U_k}{\partial x_j} \frac{\partial \phi'}{\partial x_k} dA + \iint_A W^I U_k U_j \frac{\partial}{\partial x_j} \left[(CC_g)^{-1} \right] \frac{\partial \phi'}{\partial x_k} dA \\ - \iint_A W^I \frac{2i\omega U_k}{(CC_g)^{\frac{3}{2}}} \frac{\partial \sqrt{CC_g}}{\partial x_k} \phi' dA + \iint_A W^I \frac{2i\omega U_k}{CC_g} \frac{\partial \phi'}{\partial x_k} dA = 0 \end{aligned} \quad (3.746)$$

Examining the first term of Equation (3.746) in more detail using Green's Theorem gives:

$$\iint_A W^I \frac{\partial}{\partial x_k} \left(\frac{\partial \phi'}{\partial x_k} \right) dA = \iint_A \frac{\partial}{\partial x_k} \left(W^I \frac{\partial \phi'}{\partial x_k} \right) dA - \iint_A \frac{\partial W^I}{\partial x_k} \frac{\partial \phi'}{\partial x_k} dA \quad (3.747)$$

$$\iint_A W^I \frac{\partial}{\partial x_k} \left(\frac{\partial \phi'}{\partial x_k} \right) dA = \int_S n_k W^I \frac{\partial \phi'}{\partial x_k} dS - \iint_A \frac{\partial W^I}{\partial x_k} \frac{\partial \phi'}{\partial x_k} dA \quad (3.748)$$

$$\iint_A W^I \frac{\partial}{\partial x_k} \left(\frac{\partial \phi'}{\partial x_k} \right) dA = \int_S W^I \frac{\partial \phi'}{\partial n} dS - \iint_A \frac{\partial W^I}{\partial x_k} \frac{\partial \phi'}{\partial x_k} dA \quad (3.749)$$

Substitution of Equation (3.749) into Equation (3.746) gives:

$$\begin{aligned}
& \int_S W^I \frac{\partial \phi'}{\partial n} ds - \iint_A \frac{\partial W^I}{\partial x_k} \frac{\partial \phi'}{\partial x_k} dA + \iint_A W^I K^2 \phi' dA + \iint_A W^I \frac{\omega^2}{CC_g} \phi' dA - \iint_A W^I \frac{\sigma^2}{CC_g} \phi' dA \\
& - \iint_A W^I \frac{U_j}{CC_g} \frac{\partial U_k}{\partial x_j} \frac{\partial \phi'}{\partial x_k} dA + 2 \iint_A W^I \frac{U_j U_k}{(CC_g)^{\frac{3}{2}}} \frac{\partial \sqrt{CC_g}}{\partial x_j} \frac{\partial \phi'}{\partial x_k} dA \\
& + \iint_A W^I \frac{U_j}{(CC_g)^{\frac{3}{2}}} \frac{\partial U_k}{\partial x_j} \frac{\partial \sqrt{CC_g}}{\partial x_k} \phi' dA + \iint_A W^I \frac{U_j U_k}{(CC_g)^{\frac{3}{2}}} \frac{\partial^2 \sqrt{CC_g}}{\partial x_j \partial x_k} \phi' dA \\
& - \iint_A W^I \frac{U_j U_k}{(CC_g)^{\frac{5}{2}}} \frac{\partial \sqrt{CC_g}}{\partial x_k} \frac{\partial (CC_g)}{\partial x_j} \phi' dA \\
& + \iint_A \frac{\partial W^I}{\partial x_j} \frac{U_j U_k}{CC_g} \frac{\partial \phi'}{\partial x_k} dA + \iint_A W^I \frac{\partial U_j}{\partial x_j} \frac{U_k}{CC_g} \frac{\partial \phi'}{\partial x_k} dA \\
& + \iint_A W^I \frac{U_j}{CC_g} \frac{\partial U_k}{\partial x_j} \frac{\partial \phi'}{\partial x_k} dA + \iint_A W^I U_k U_j \frac{\partial}{\partial x_j} \left[(CC_g)^{-1} \right] \frac{\partial \phi'}{\partial x_k} dA \\
& - \iint_A W^I \frac{2i\omega U_k}{(CC_g)^{\frac{3}{2}}} \frac{\partial \sqrt{CC_g}}{\partial x_k} \phi' dA + \iint_A W^I \frac{2i\omega U_k}{CC_g} \frac{\partial \phi'}{\partial x_k} dA = 0
\end{aligned} \tag{3.750}$$

In accordance with finite element methodology a shape function can now be applied to the unknown scaled velocity potential value:

$$\phi' = \phi'^J N^J \tag{3.751}$$

Applying Equation (3.751) to Equation (3.750) gives:

$$\begin{aligned}
& \int_S W^I \frac{\partial \phi'}{\partial n} ds - \iint_A \frac{\partial W^I}{\partial x_k} \frac{\partial (\phi'^J N^J)}{\partial x_k} dA + \iint_A W^I K^2 \phi'^J N^J dA + \iint_A W^I \frac{\omega^2}{CC_g} \phi'^J N^J dA - \iint_A W^I \frac{\sigma^2}{CC_g} \phi'^J N^J dA \\
& - \iint_A W^I \frac{U_j}{CC_g} \frac{\partial U_k}{\partial x_j} \frac{\partial (\phi'^J N^J)}{\partial x_k} dA + 2 \iint_A W^I \frac{U_j U_k}{(CC_g)^{\frac{3}{2}}} \frac{\partial \sqrt{CC_g}}{\partial x_j} \frac{\partial (\phi'^J N^J)}{\partial x_k} dA \\
& + \iint_A W^I \frac{U_j}{(CC_g)^{\frac{3}{2}}} \frac{\partial U_k}{\partial x_j} \frac{\partial \sqrt{CC_g}}{\partial x_k} \phi'^J N^J dA + \iint_A W^I \frac{U_j U_k}{(CC_g)^{\frac{3}{2}}} \frac{\partial^2 \sqrt{CC_g}}{\partial x_j \partial x_k} \phi'^J N^J dA \\
& - \iint_A W^I \frac{U_j U_k}{(CC_g)^{\frac{5}{2}}} \frac{\partial \sqrt{CC_g}}{\partial x_k} \frac{\partial (CC_g)}{\partial x_j} \phi'^J N^J dA \\
& + \iint_A \frac{\partial W^I}{\partial x_j} \frac{U_j U_k}{CC_g} \frac{\partial (\phi'^J N^J)}{\partial x_k} dA + \iint_A W^I \frac{\partial U_j}{\partial x_j} \frac{U_k}{CC_g} \frac{\partial (\phi'^J N^J)}{\partial x_k} dA \\
& + \iint_A W^I \frac{U_j}{CC_g} \frac{\partial U_k}{\partial x_j} \frac{\partial (\phi'^J N^J)}{\partial x_k} dA + \iint_A W^I U_k U_j \frac{\partial}{\partial x_j} \left[(CC_g)^{-1} \right] \frac{\partial (\phi'^J N^J)}{\partial x_k} dA \\
& - \iint_A W^I \frac{2i\omega U_k}{(CC_g)^{\frac{3}{2}}} \frac{\partial \sqrt{CC_g}}{\partial x_k} \phi'^J N^J dA + \iint_A W^I \frac{2i\omega U_k}{CC_g} \frac{\partial (\phi'^J N^J)}{\partial x_k} dA = 0
\end{aligned} \tag{3.752}$$

This can be rearranged as:

$$\begin{aligned}
& \int_S W^I \frac{\partial \phi'}{\partial n} ds - \iint_A \frac{\partial W^I}{\partial x_k} \frac{\partial N^J}{\partial x_k} \phi'^J dA + \iint_A K^2 W^I N^J \phi'^J dA + \iint_A W^I \frac{\omega^2}{CC_g} \phi'^J N^J dA - \iint_A W^I \frac{\sigma^2}{CC_g} \phi'^J N^J dA \\
& - \iint_A \frac{U_j}{CC_g} \frac{\partial U_k}{\partial x_j} W^I \frac{\partial N^J}{\partial x_k} \phi'^J dA + 2 \iint_A \frac{U_j U_k}{(CC_g)^{\frac{3}{2}}} \frac{\partial \sqrt{CC_g}}{\partial x_j} W^I \frac{\partial N^J}{\partial x_k} \phi'^J dA \\
& + \iint_A \frac{U_j}{(CC_g)^{\frac{3}{2}}} \frac{\partial U_k}{\partial x_j} \frac{\partial \sqrt{CC_g}}{\partial x_k} W^I N^J \phi'^J dA + \iint_A \frac{U_j U_k}{(CC_g)^{\frac{3}{2}}} \frac{\partial^2 \sqrt{CC_g}}{\partial x_j \partial x_k} W^I N^J \phi'^J dA \\
& - \iint_A \frac{U_j U_k}{(CC_g)^{\frac{5}{2}}} \frac{\partial \sqrt{CC_g}}{\partial x_k} \frac{\partial (CC_g)}{\partial x_j} W^I N^J \phi'^J dA \\
& + \iint_A \frac{U_j U_k}{CC_g} \frac{\partial W^I}{\partial x_j} \frac{\partial N^J}{\partial x_k} \phi'^J dA + \iint_A \frac{\partial U_j}{\partial x_j} \frac{U_k}{CC_g} W^I \frac{\partial N^J}{\partial x_k} \phi'^J dA \\
& + \iint_A \frac{U_j}{CC_g} \frac{\partial U_k}{\partial x_j} W^I \frac{\partial N^J}{\partial x_k} \phi'^J dA + \iint_A U_k U_j \frac{\partial}{\partial x_j} \left[(CC_g)^{-1} \right] W^I \frac{\partial N^J}{\partial x_k} \phi'^J dA \\
& - \iint_A \frac{2i\omega U_k}{(CC_g)^{\frac{3}{2}}} \frac{\partial \sqrt{CC_g}}{\partial x_k} W^I N^J \phi'^J dA + \iint_A \frac{2i\omega U_k}{CC_g} W^I \frac{\partial N^J}{\partial x_k} \phi'^J dA = 0
\end{aligned} \tag{3.753}$$

The finite element model created for this project uses the Galerkin method in which the weighting function is equal to the shape functions being used. Hence at this stage W^I will be replaced with N^I . The Galerkin method and shape functions are discussed in Appendix A.

$$\begin{aligned}
& \int_S W^I \frac{\partial \phi'}{\partial n} ds - \iint_A \frac{\partial N^I}{\partial x_k} \frac{\partial N^J}{\partial x_k} \phi'^J dA + \iint_A K^2 N^I N^J \phi'^J dA + \iint_A W^I \frac{\omega^2}{CC_g} \phi'^J N^I N^J dA - \iint_A W^I \frac{\sigma^2}{CC_g} \phi'^J N^I N^J dA \\
& - \iint_A \frac{U_j}{CC_g} \frac{\partial U_k}{\partial x_j} N^I \frac{\partial N^J}{\partial x_k} \phi'^J dA + 2 \iint_A \frac{U_j U_k}{(CC_g)^{\frac{3}{2}}} \frac{\partial \sqrt{CC_g}}{\partial x_j} N^I \frac{\partial N^J}{\partial x_k} \phi'^J dA \\
& + \iint_A \frac{U_j}{(CC_g)^{\frac{3}{2}}} \frac{\partial U_k}{\partial x_j} \frac{\partial \sqrt{CC_g}}{\partial x_k} N^I N^J \phi'^J dA + \iint_A \frac{U_j U_k}{(CC_g)^{\frac{3}{2}}} \frac{\partial^2 \sqrt{CC_g}}{\partial x_j \partial x_k} N^I N^J \phi'^J dA \\
& - \iint_A \frac{U_j U_k}{(CC_g)^{\frac{5}{2}}} \frac{\partial \sqrt{CC_g}}{\partial x_k} \frac{\partial (CC_g)}{\partial x_j} N^I N^J \phi'^J dA \\
& + \iint_A \frac{U_j U_k}{CC_g} \frac{\partial N^I}{\partial x_j} \frac{\partial N^J}{\partial x_k} \phi'^J dA + \iint_A \frac{\partial U_j}{\partial x_j} \frac{U_k}{CC_g} N^I \frac{\partial N^J}{\partial x_k} \phi'^J dA \\
& + \iint_A \frac{U_j}{CC_g} \frac{\partial U_k}{\partial x_j} N^I \frac{\partial N^J}{\partial x_k} \phi'^J dA + \iint_A U_k U_j \frac{\partial}{\partial x_j} \left[(CC_g)^{-1} \right] N^I \frac{\partial N^J}{\partial x_k} \phi'^J dA \\
& - \iint_A \frac{2i\omega U_k}{(CC_g)^{\frac{3}{2}}} \frac{\partial \sqrt{CC_g}}{\partial x_k} N^I N^J \phi'^J dA + \iint_A \frac{2i\omega U_k}{CC_g} N^I \frac{\partial N^J}{\partial x_k} \phi'^J dA = 0
\end{aligned} \tag{3.754}$$

The first term in Equation (3.754) is an integral around the boundary of the finite element. It is hence apparent that for all internal elements in the domain this term will cancel out. It is only necessary to examine this term on the boundary.

In the simplest case where the boundary is a reflecting one the gradient of velocity potential across the boundary is zero, i.e. $\frac{\partial \phi'}{\partial n} = 0$. Thus the Helmholtz type equation including currents, in the absence of energy dissipation, is similar for internal elements and perfectly reflecting boundary elements:

$$\begin{aligned}
& -\iint_A \frac{\partial N^I}{\partial x_k} \frac{\partial N^J}{\partial x_k} \phi'^J dA + \iint_A K^2 N^I N^J \phi'^J dA + \iint_A W^I \frac{\omega^2}{CC_g} \phi'^J N^I N^J dA - \iint_A W^I \frac{\sigma^2}{CC_g} \phi'^J N^I N^J dA \\
& -\iint_A \frac{U_j}{CC_g} \frac{\partial U_k}{\partial x_j} N^I \frac{\partial N^J}{\partial x_k} \phi'^J dA + 2 \iint_A \frac{U_j U_k}{(CC_g)^{\frac{3}{2}}} \frac{\partial \sqrt{CC_g}}{\partial x_j} N^I \frac{\partial N^J}{\partial x_k} \phi'^J dA \\
& + \iint_A \frac{U_j}{(CC_g)^{\frac{3}{2}}} \frac{\partial U_k}{\partial x_j} \frac{\partial \sqrt{CC_g}}{\partial x_k} N^I N^J \phi'^J dA + \iint_A \frac{U_j U_k}{(CC_g)^{\frac{3}{2}}} \frac{\partial^2 \sqrt{CC_g}}{\partial x_j \partial x_k} N^I N^J \phi'^J dA \\
& - \iint_A \frac{U_j U_k}{(CC_g)^{\frac{5}{2}}} \frac{\partial \sqrt{CC_g}}{\partial x_k} \frac{\partial (CC_g)}{\partial x_j} N^I N^J \phi'^J dA \\
& + \iint_A \frac{U_j U_k}{CC_g} \frac{\partial N^I}{\partial x_j} \frac{\partial N^J}{\partial x_k} \phi'^J dA + \iint_A \frac{\partial U_j}{\partial x_j} \frac{U_k}{CC_g} N^I \frac{\partial N^J}{\partial x_k} \phi'^J dA \\
& + \iint_A \frac{U_j}{CC_g} \frac{\partial U_k}{\partial x_j} N^I \frac{\partial N^J}{\partial x_k} \phi'^J dA + \iint_A U_k U_j \frac{\partial}{\partial x_j} \left[(CC_g)^{-1} \right] N^I \frac{\partial N^J}{\partial x_k} \phi'^J dA \\
& - \iint_A \frac{2i\omega U_k}{(CC_g)^{\frac{3}{2}}} \frac{\partial \sqrt{CC_g}}{\partial x_k} N^I N^J \phi'^J dA + \iint_A \frac{2i\omega U_k}{CC_g} N^I \frac{\partial N^J}{\partial x_k} \phi'^J dA = 0
\end{aligned} \tag{3.755}$$

However on boundaries that are not reflecting the first term of Equation (3.754) must be evaluated.

3.10.1 Derivatives of Wave Celerity and Group Velocity

Although gradients of CC_g can be obtained numerically during computer modelling in some cases it is helpful to have analytical derivatives where required. Recalling Equation (3.429):

$$CC_g = g \frac{\sinh 2\kappa h' + 2\kappa h'}{4\kappa \cosh^2 \kappa h'}$$

Equation (3.429) can also be expressed as follows:

$$CC_g = g \frac{\sinh(\kappa h') \cosh(\kappa h') + \kappa h'}{2\kappa \cosh^2 \kappa h'} \quad (3.756)$$

It can be seen from Equation (3.756) that CC_g is a function of κ and h' , i.e. $CC_g = CC_g(\kappa, h')$, where $\kappa = \kappa(h')$. In the interests of clarity the following abbreviation will be used:

$$a = CC_g \quad (3.757)$$

Hence the various derivatives of CC_g terms with respect to the horizontal coordinates can be expressed symbolically as follows:

$$\frac{da}{dx_j} = \frac{\partial a}{\partial \kappa} \frac{d\kappa}{dh'} \frac{dh'}{dx_j} + \frac{\partial a}{\partial h'} \frac{dh'}{dx_j} \quad (3.758)$$

$$\frac{\partial \sqrt{a}}{\partial x_j} = \frac{1}{2\sqrt{a}} \frac{\partial a}{\partial x_j} = \frac{1}{2\sqrt{a}} \left[\frac{\partial a}{\partial \kappa} \frac{d\kappa}{dh'} \frac{dh'}{dx_j} + \frac{\partial a}{\partial h'} \frac{dh'}{dx_j} \right] \quad (3.759)$$

$$\frac{\partial \sqrt{a}}{\partial x_j} = \frac{1}{2\sqrt{a}} \frac{\partial a}{\partial \kappa} \frac{d\kappa}{dh'} \frac{dh'}{dx_j} + \frac{1}{2\sqrt{a}} \frac{\partial a}{\partial h'} \frac{dh'}{dx_j} \quad (3.760)$$

$$\frac{\partial}{\partial x_j} [a^{-1}] = -\frac{1}{a^2} \frac{\partial (CC_g)}{\partial x_j} = -\frac{1}{a^2} \left[\frac{\partial a}{\partial \kappa} \frac{d\kappa}{dh'} \frac{dh'}{dx_j} + \frac{\partial a}{\partial h'} \frac{dh'}{dx_j} \right] \quad (3.761)$$

$$\frac{\partial}{\partial x_j} [a^{-1}] = -\frac{1}{a^2} \frac{\partial a}{\partial \kappa} \frac{d\kappa}{dh'} \frac{dh'}{dx_j} - \frac{1}{a^2} \frac{\partial a}{\partial h'} \frac{dh'}{dx_j} \quad (3.762)$$

$$\frac{\partial}{\partial x_j} \left[\frac{1}{\sqrt{a}} \right] = -\frac{1}{2} a^{-\frac{3}{2}} \frac{\partial a}{\partial x_j} = -\frac{1}{2} a^{-\frac{3}{2}} \left[\frac{\partial a}{\partial \kappa} \frac{d\kappa}{dh'} \frac{dh'}{dx_j} + \frac{\partial a}{\partial h'} \frac{dh'}{dx_j} \right] \quad (3.763)$$

$$\frac{\partial}{\partial x_j} \left[\frac{1}{\sqrt{a}} \right] = -\frac{1}{2a^{\frac{3}{2}}} \frac{\partial a}{\partial \kappa} \frac{d\kappa}{dh'} \frac{dh'}{dx_j} - \frac{1}{2a^{\frac{3}{2}}} \frac{\partial a}{\partial h'} \frac{dh'}{dx_j} \quad (3.764)$$

$$\frac{\partial^2 \sqrt{a}}{\partial x_j \partial x_k} = \frac{\partial}{\partial x_j} \left(\frac{\partial \sqrt{a}}{\partial x_k} \right) \quad (3.765)$$

Using Equation (3.760) gives:

$$\frac{\partial^2 \sqrt{a}}{\partial x_j \partial x_k} = \frac{\partial}{\partial x_j} \left(\frac{1}{2\sqrt{a}} \frac{\partial a}{\partial \kappa} \frac{d\kappa}{dh'} \frac{dh'}{dx_k} + \frac{1}{2\sqrt{a}} \frac{\partial a}{\partial h'} \frac{dh'}{dx_k} \right) \quad (3.766)$$

Equation (3.766) can be expanded to give:

$$\frac{\partial^2 \sqrt{a}}{\partial x_j \partial x_k} = \frac{1}{2} \frac{\partial}{\partial x_j} \left(\frac{1}{\sqrt{a}} \frac{\partial a}{\partial \kappa} \frac{d\kappa}{dh'} \frac{dh'}{dx_k} \right) + \frac{1}{2} \frac{\partial}{\partial x_j} \left(\frac{1}{\sqrt{a}} \frac{\partial a}{\partial h'} \frac{dh'}{dx_k} \right) \quad (3.767)$$

Using the product rule this becomes:

$$\begin{aligned} \frac{\partial^2 \sqrt{a}}{\partial x_j \partial x_k} &= \frac{1}{2} \frac{d\kappa}{dh'} \frac{dh'}{dx_k} \frac{1}{\sqrt{a}} \frac{\partial}{\partial x_j} \left(\frac{\partial a}{\partial \kappa} \right) + \frac{1}{2} \frac{d\kappa}{dh'} \frac{dh'}{dx_k} \frac{\partial a}{\partial \kappa} \frac{\partial}{\partial x_j} \left(\frac{1}{\sqrt{a}} \right) \\ &+ \frac{1}{2} \frac{dh'}{dx_k} \frac{1}{\sqrt{a}} \frac{\partial}{\partial x_j} \left(\frac{\partial a}{\partial h'} \right) + \frac{1}{2} \frac{dh'}{dx_k} \frac{\partial a}{\partial h'} \frac{\partial}{\partial x_j} \left(\frac{1}{\sqrt{a}} \right) \end{aligned} \quad (3.768)$$

Further expansion of Equation (3.768) yields:

$$\begin{aligned} \frac{\partial^2 \sqrt{a}}{\partial x_j \partial x_k} &= \frac{1}{2} \frac{d\kappa}{dh'} \frac{dh'}{dx_k} \frac{1}{\sqrt{a}} \left[\frac{\partial \left(\frac{\partial a}{\partial \kappa} \right)}{\partial \kappa} \frac{d\kappa}{dh'} \frac{dh'}{dx_j} + \frac{\partial \left(\frac{\partial a}{\partial \kappa} \right)}{\partial h'} \frac{dh'}{dx_j} \right] \\ &+ \frac{1}{2} \frac{d\kappa}{dh'} \frac{dh'}{dx_k} \frac{\partial a}{\partial \kappa} \left(-\frac{1}{2a^{\frac{3}{2}}} \frac{\partial a}{\partial \kappa} \frac{d\kappa}{dh'} \frac{dh'}{dx_j} - \frac{1}{2a^{\frac{3}{2}}} \frac{\partial a}{\partial h'} \frac{dh'}{dx_j} \right) \\ &+ \frac{1}{2} \frac{dh'}{dx_k} \frac{1}{\sqrt{a}} \left[\frac{\partial \left(\frac{\partial a}{\partial h'} \right)}{\partial \kappa} \frac{d\kappa}{dh'} \frac{dh'}{dx_j} + \frac{\partial \left(\frac{\partial a}{\partial h'} \right)}{\partial h'} \frac{dh'}{dx_j} \right] \\ &+ \frac{1}{2} \frac{dh'}{dx_k} \frac{\partial a}{\partial h'} \left(-\frac{1}{2a^{\frac{3}{2}}} \frac{\partial a}{\partial \kappa} \frac{d\kappa}{dh'} \frac{dh'}{dx_j} - \frac{1}{2a^{\frac{3}{2}}} \frac{\partial a}{\partial h'} \frac{dh'}{dx_j} \right) \end{aligned} \quad (3.769)$$

Re-expressing Equation (3.769) gives:

$$\begin{aligned}
 \frac{\partial^2 \sqrt{a}}{\partial x_j \partial x_k} = & \frac{1}{2} \frac{d\kappa}{dh'} \frac{dh'}{dx_k} \frac{1}{\sqrt{a}} \left[\frac{\partial^2 a}{\partial \kappa^2} \frac{d\kappa}{dh'} \frac{dh'}{dx_j} + \frac{\partial^2 a}{\partial \kappa \partial h'} \frac{dh'}{dx_j} \right] \\
 & + \frac{1}{2} \frac{d\kappa}{dh'} \frac{dh'}{dx_k} \frac{\partial a}{\partial \kappa} \left(-\frac{1}{2a^{\frac{3}{2}}} \frac{\partial a}{\partial \kappa} \frac{d\kappa}{dh'} \frac{dh'}{dx_j} - \frac{1}{2a^{\frac{3}{2}}} \frac{\partial a}{\partial h'} \frac{dh'}{dx_j} \right) \\
 & + \frac{1}{2} \frac{dh'}{dx_k} \frac{1}{\sqrt{a}} \left[\frac{\partial^2 a}{\partial h' \partial \kappa} \frac{d\kappa}{dh'} \frac{dh'}{dx_j} + \frac{\partial^2 a}{\partial h'^2} \frac{dh'}{dx_j} \right] \\
 & + \frac{1}{2} \frac{dh'}{dx_k} \frac{\partial a}{\partial h'} \left(-\frac{1}{2a^{\frac{3}{2}}} \frac{\partial a}{\partial \kappa} \frac{d\kappa}{dh'} \frac{dh'}{dx_j} - \frac{1}{2a^{\frac{3}{2}}} \frac{\partial a}{\partial h'} \frac{dh'}{dx_j} \right)
 \end{aligned} \tag{3.770}$$

Incorporating the terms outside brackets gives:

$$\begin{aligned}
 \frac{\partial^2 \sqrt{a}}{\partial x_j \partial x_k} = & \left[\frac{1}{2\sqrt{a}} \frac{\partial^2 a}{\partial \kappa^2} \frac{d\kappa}{dh'} \frac{dh'}{dx_j} \frac{dh'}{dx_k} + \frac{1}{2\sqrt{a}} \frac{\partial^2 a}{\partial \kappa \partial h'} \frac{d\kappa}{dh'} \frac{dh'}{dx_j} \frac{dh'}{dx_k} \right] \\
 & + \left(-\frac{1}{4a^{\frac{3}{2}}} \frac{\partial a}{\partial \kappa} \frac{\partial a}{\partial \kappa} \frac{d\kappa}{dh'} \frac{dh'}{dx_j} \frac{dh'}{dx_k} - \frac{1}{4a^{\frac{3}{2}}} \frac{\partial a}{\partial \kappa} \frac{\partial a}{\partial h'} \frac{d\kappa}{dh'} \frac{dh'}{dx_j} \frac{dh'}{dx_k} \right) \\
 & + \left[\frac{1}{2\sqrt{a}} \frac{\partial^2 a}{\partial h' \partial \kappa} \frac{d\kappa}{dh'} \frac{dh'}{dx_j} \frac{dh'}{dx_k} + \frac{1}{2\sqrt{a}} \frac{\partial^2 a}{\partial h'^2} \frac{dh'}{dx_j} \frac{dh'}{dx_k} \right] \\
 & + \left(-\frac{1}{4a^{\frac{3}{2}}} \frac{\partial a}{\partial \kappa} \frac{\partial a}{\partial h'} \frac{d\kappa}{dh'} \frac{dh'}{dx_j} \frac{dh'}{dx_k} - \frac{1}{4a^{\frac{3}{2}}} \frac{\partial a}{\partial h'} \frac{\partial a}{\partial h'} \frac{dh'}{dx_j} \frac{dh'}{dx_k} \right)
 \end{aligned} \tag{3.771}$$

Equation (3.771) may be reduced to give:

$$\begin{aligned}
 \frac{\partial^2 \sqrt{a}}{\partial x_j \partial x_k} = & \frac{1}{2\sqrt{a}} \frac{\partial^2 a}{\partial \kappa^2} \frac{d\kappa}{dh'} \frac{dh'}{dx_j} \frac{dh'}{dx_k} + \frac{1}{2\sqrt{a}} \frac{\partial^2 a}{\partial \kappa \partial h'} \frac{d\kappa}{dh'} \frac{dh'}{dx_j} \frac{dh'}{dx_k} \\
 & - \frac{1}{4a^{\frac{3}{2}}} \frac{\partial a}{\partial \kappa} \frac{\partial a}{\partial \kappa} \frac{d\kappa}{dh'} \frac{dh'}{dx_j} \frac{dh'}{dx_k} - \frac{1}{4a^{\frac{3}{2}}} \frac{\partial a}{\partial \kappa} \frac{\partial a}{\partial h'} \frac{d\kappa}{dh'} \frac{dh'}{dx_j} \frac{dh'}{dx_k} \\
 & + \frac{1}{2\sqrt{a}} \frac{\partial^2 a}{\partial h' \partial \kappa} \frac{d\kappa}{dh'} \frac{dh'}{dx_j} \frac{dh'}{dx_k} + \frac{1}{2\sqrt{a}} \frac{\partial^2 a}{\partial h'^2} \frac{dh'}{dx_j} \frac{dh'}{dx_k} \\
 & - \frac{1}{4a^{\frac{3}{2}}} \frac{\partial a}{\partial \kappa} \frac{\partial a}{\partial h'} \frac{d\kappa}{dh'} \frac{dh'}{dx_j} \frac{dh'}{dx_k} - \frac{1}{4a^{\frac{3}{2}}} \frac{\partial a}{\partial h'} \frac{\partial a}{\partial h'} \frac{dh'}{dx_j} \frac{dh'}{dx_k}
 \end{aligned} \tag{3.772}$$

The derivatives of CC_g with respect to κ and h' will now be examined so that they can be used in the symbolic equations derived above.

$$\frac{\partial(CC_g)}{\partial\kappa} = \frac{\partial a}{\partial\kappa} = g \frac{\left[2\kappa \cosh^2(\kappa h') \left[h' \cosh^2 \kappa h' + h' \sinh^2 \kappa h' + h' \right] + \left[-\sinh(\kappa h') \cosh(\kappa h') - \kappa h' \right] \left[2 \cosh^2(\kappa h') + 4\kappa h' \cosh(\kappa h') \sinh(\kappa h') \right] \right]}{4\kappa^2 \cosh^4 \kappa h'} \quad (3.773)$$

$$\frac{\partial a}{\partial\kappa} = g \frac{\cosh(\kappa h') \left[\kappa h' - \sinh(\kappa h') \cosh(\kappa h') \right] - 2\kappa^2 h'^2 \sinh(\kappa h')}{2\kappa^2 \cosh^3 \kappa h'} \quad (3.774)$$

$$\frac{\partial^2(CC_g)}{\partial\kappa^2} = \frac{\partial^2 a}{\partial\kappa^2} = g \frac{\left[2\kappa^2 \cosh^3(\kappa h') \left[h' \cosh \kappa h' - 2h' \cosh(\kappa h') \sinh^2(\kappa h') \right] - h' \cosh^3 \kappa h' - 3\kappa h'^2 \sinh \kappa h' - 2\kappa^2 h'^3 \cosh \kappa h' \right] + \left[\kappa h' \cosh(\kappa h') + \cosh^2(\kappa h') \sinh(\kappa h') \right] \left[4\kappa \cosh^3 \kappa h' + 6\kappa^2 h' \cosh(\kappa h') \sinh(\kappa h') \right] }{4\kappa^4 \cosh^6 \kappa h'} \quad (3.775)$$

$$\frac{\partial^2 a}{\partial\kappa^2} = g \frac{\left[-\kappa h' - 2\kappa^3 h'^3 + 2 \cosh(\kappa h') \sinh(\kappa h') - 2\kappa^2 h'^2 \tanh \kappa h' \right] - \kappa h' \cosh^2 \kappa h' + \kappa h' \sinh^2 \kappa h' + 6\kappa^3 h'^3 \tanh^2 \kappa h'}{2\kappa^3 \cosh^2 \kappa h'} \quad (3.776)$$

$$\frac{\partial(CC_g)}{\partial h'} = \frac{\partial a}{\partial h'} = g \frac{\left[2\kappa \cosh^2(\kappa h') \left[\kappa \cosh^2 \kappa h' + \kappa \sinh^2 \kappa h' + h' \right] + \left[-\sinh(\kappa h') \cosh(\kappa h') - \kappa h' \right] \left[4\kappa^2 \cosh(\kappa h') \sinh(\kappa h') \right] \right]}{4\kappa^2 \cosh^4 \kappa h'} \quad (3.777)$$

$$\frac{\partial a}{\partial h'} = g \frac{\cosh(\kappa h') - \kappa h' \sinh(\kappa h')}{\cosh^3 \kappa h'} \quad (3.778)$$

$$\frac{\partial^2(CC_g)}{\partial h'^2} = \frac{\partial^2 a}{\partial h'^2} = g \frac{\left[\cosh^3(\kappa h') \left[-\kappa^2 h' \cosh \kappa h' \right] + 3\kappa \cosh^2(\kappa h') \sinh(\kappa h') \left[-\cosh(\kappa h') - \kappa h' \sinh(\kappa h') \right] \right]}{\cosh^6 \kappa h'} \quad (3.779)$$

$$\frac{\partial^2(CC_g)}{\partial h' \partial \kappa} = \frac{\partial^2 a}{\partial h' \partial \kappa} = g \frac{\left[\cosh^3(\kappa h') \left[-\kappa h'^2 \cosh \kappa h' \right] + 3h' \cosh^2(\kappa h') \sinh(\kappa h') \left[-\cosh(\kappa h') + \kappa h' \sinh(\kappa h') \right] \right]}{\cosh^6 \kappa h'} \quad (3.780)$$

Table 3.7 below summarises the derivatives of CC_g obtained in this section.

Table 3.7 – Summary of Derivatives of Celerity and Group Velocity for Helmholtz Type Equations.

Symbolically:		
(a)	$\frac{da}{dx_j} = \frac{\partial a}{\partial \kappa} \frac{d\kappa}{dh'} \frac{dh'}{dx_j} + \frac{\partial a}{\partial h'} \frac{dh'}{dx_j}$	(3.758)
(b)	$\frac{\partial \sqrt{a}}{\partial x_j} = \frac{1}{2\sqrt{a}} \frac{\partial a}{\partial \kappa} \frac{d\kappa}{dh'} \frac{dh'}{dx_j} + \frac{1}{2\sqrt{a}} \frac{\partial a}{\partial h'} \frac{dh'}{dx_j}$	(3.760)
(c)	$\frac{\partial}{\partial x_j} [a^{-1}] = -\frac{1}{a^2} \frac{\partial a}{\partial \kappa} \frac{d\kappa}{dh'} \frac{dh'}{dx_j} - \frac{1}{a^2} \frac{\partial a}{\partial h'} \frac{dh'}{dx_j}$	(3.762)
(d)	$\frac{\partial}{\partial x_j} \left[\frac{1}{\sqrt{a}} \right] = -\frac{1}{2a^{\frac{3}{2}}} \frac{\partial a}{\partial \kappa} \frac{d\kappa}{dh'} \frac{dh'}{dx_j} - \frac{1}{2a^{\frac{3}{2}}} \frac{\partial a}{\partial h'} \frac{dh'}{dx_j}$	(3.764)
(e)	$\begin{aligned} \frac{\partial^2 \sqrt{a}}{\partial x_j \partial x_k} &= \frac{1}{2\sqrt{a}} \frac{\partial^2 a}{\partial \kappa^2} \frac{d\kappa}{dh'} \frac{dh'}{dx_j} \frac{dh'}{dx_k} + \frac{1}{2\sqrt{a}} \frac{\partial^2 a}{\partial \kappa \partial h'} \frac{d\kappa}{dh'} \frac{dh'}{dx_j} \frac{dh'}{dx_k} \\ &\quad - \frac{1}{4a^{\frac{3}{2}}} \frac{\partial a}{\partial \kappa} \frac{\partial a}{\partial \kappa} \frac{d\kappa}{dh'} \frac{dh'}{dx_j} \frac{dh'}{dx_k} - \frac{1}{4a^{\frac{3}{2}}} \frac{\partial a}{\partial \kappa} \frac{\partial a}{\partial h'} \frac{d\kappa}{dh'} \frac{dh'}{dx_j} \frac{dh'}{dx_k} \\ &\quad + \frac{1}{2\sqrt{a}} \frac{\partial^2 a}{\partial h' \partial \kappa} \frac{d\kappa}{dh'} \frac{dh'}{dx_j} \frac{dh'}{dx_k} + \frac{1}{2\sqrt{a}} \frac{\partial^2 a}{\partial h'^2} \frac{dh'}{dx_j} \frac{dh'}{dx_k} - \frac{1}{4a^{\frac{3}{2}}} \frac{\partial a}{\partial \kappa} \frac{\partial a}{\partial h'} \frac{d\kappa}{dh'} \frac{dh'}{dx_j} \frac{dh'}{dx_k} \\ &\quad - \frac{1}{4a^{\frac{3}{2}}} \frac{\partial a}{\partial h'} \frac{\partial a}{\partial h'} \frac{d\kappa}{dh'} \frac{dh'}{dx_j} \frac{dh'}{dx_k} \end{aligned}$	(3.772)

Where:		
(f)	$a = CC_g = g \frac{\sinh(\kappa h') \cosh(\kappa h') + \kappa h'}{2\kappa \cosh^2 \kappa h'}$	(3.756)
(g)	$\frac{\partial a}{\partial \kappa} = g \frac{\cosh(\kappa h') [\kappa h' - \sinh(\kappa h') \cosh(\kappa h')] - 2\kappa^2 h'^2 \sinh(\kappa h')}{2\kappa^2 \cosh^3 \kappa h'}$	(3.774)
(h)	$\frac{\partial^2 a}{\partial \kappa^2} = g \frac{\begin{bmatrix} -\kappa h' - 2\kappa^3 h'^3 + 2 \cosh(\kappa h') \sinh(\kappa h') - 2\kappa^2 h'^2 \tanh \kappa h' \\ -\kappa h' \cosh^2 \kappa h' + \kappa h' \sinh^2 \kappa h' + 6\kappa^3 h'^3 \tanh^2 \kappa h' \end{bmatrix}}{2\kappa^3 \cosh^2 \kappa h'}$	(3.776)
(i)	$\frac{\partial a}{\partial h'} = g \frac{\cosh(\kappa h') - \kappa h' \sinh(\kappa h')}{\cosh^3 \kappa h'}$	(3.778)
(j)	$\frac{\partial^2 (CC_g)}{\partial h'^2} = \frac{\partial^2 a}{\partial h'^2} = g \frac{\begin{bmatrix} \cosh^3(\kappa h') [-\kappa^2 h' \cosh \kappa h'] \\ + 3\kappa \cosh^2(\kappa h') \sinh(\kappa h') \begin{bmatrix} -\cosh(\kappa h') \\ -\kappa h' \sinh(\kappa h') \end{bmatrix} \end{bmatrix}}{\cosh^6 \kappa h'}$	(3.779)
(k)	$\frac{\partial^2 (CC_g)}{\partial h' \partial \kappa} = \frac{\partial^2 a}{\partial h' \partial \kappa} = g \frac{\begin{bmatrix} \cosh^3(\kappa h') [-\kappa h'^2 \cosh \kappa h'] \\ + 3h' \cosh^2(\kappa h') \sinh(\kappa h') \begin{bmatrix} -\cosh(\kappa h') \\ +\kappa h' \sinh(\kappa h') \end{bmatrix} \end{bmatrix}}{\cosh^6 \kappa h'}$	(3.780)

3.11 Boundary Conditions for 2d-NM-WCIM

There are a number of possible boundary conditions that may apply to the two-dimensional finite element domain being examined by the 2d-NM-WCIM model. These are detailed in Table 3.1 and Figure 3.11 below:

Table 3.8 – Boundary Conditions for Two-Dimensional Finite Element Wave Model

Boundary Title	Boundary Type	Boundary Description
Γ_1	Reflecting Boundary	Perfect reflection of all waves that occur at the boundary
Γ_2	Absorbing Boundary	Absorption of all waves that interact with boundary – waves exit domain at this point
Γ_3	Radiating Boundary	Backscattered or reflected waves may leave the domain along this boundary while specified waves may enter.

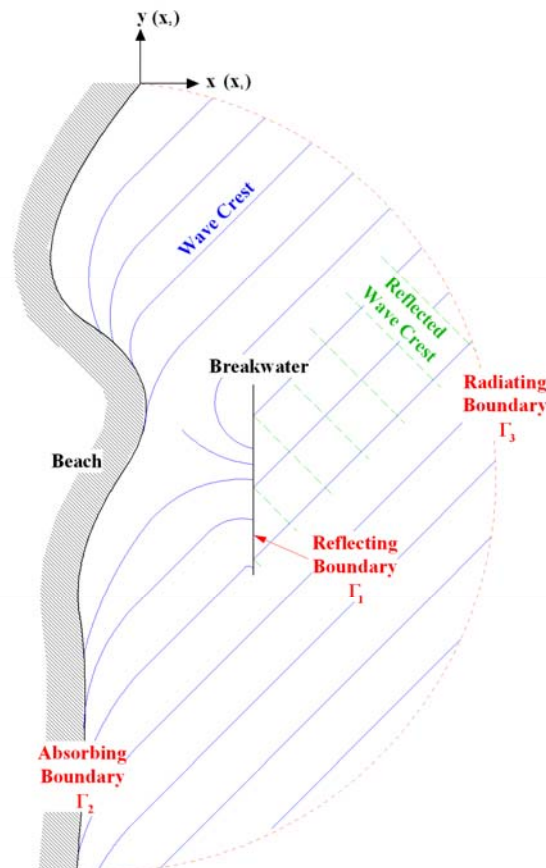


Figure 3.11 – Sketch of possible Boundary Conditions within a Domain

Each of these boundary conditions must be inspected in turn. Each boundary condition will then be applied to Equation (3.754) via the first term in the equation. Initially the simplest case of applying an absorbing boundary condition to the non-Helmholtz form of the 2d-NM-WCIM will be examined. Then the more complex case of applying various boundary conditions to the Helmholtz form of the equation will be examined.

3.11.1 Parabolic absorbing mild slope boundary condition for Non-Helmholtz 2d-NM-WCIM

In order to fully define the sixteenth term of Equation (3.717) it is necessary to once again use the parabolic solution to the mild-slope equation as defined in Equation (3.653) to obtain an absorbing boundary condition. Equation (3.653) can be multiplied by $-CC_g$ to give:

$$-CC_g \frac{\partial \phi}{\partial n} = \frac{CC_g}{2\kappa} \frac{\partial \kappa}{\partial n} \phi + \frac{1}{2} \frac{\partial CC_g}{\partial n} \phi - iCC_g \kappa \phi - \frac{i}{2\kappa} \left[\frac{\partial}{\partial s} \left(CC_g \frac{\partial \phi}{\partial s} \right) \right] \quad (3.781)$$

In the case the boundary under consideration is an absorbing boundary. Hence:

$$S = \Gamma_2 \quad (3.782)$$

Therefore:

$$\begin{aligned} -\int_S CC_g \frac{\partial \phi}{\partial n} W' ds &= \int_{\Gamma_2} \frac{CC_g}{2\kappa} \frac{\partial \kappa}{\partial n} \phi W' ds + \int_{\Gamma_2} \frac{1}{2} \frac{\partial CC_g}{\partial n} \phi W' ds \\ &\quad - \int_{\Gamma_2} iCC_g \kappa \phi W' ds - \int_{\Gamma_2} \frac{i}{2\kappa} \left[\frac{\partial}{\partial s} \left(CC_g \frac{\partial \phi}{\partial s} \right) \right] W' ds \end{aligned} \quad (3.783)$$

The last term of Equation (3.783) is:

$$-\int_{\Gamma_2} \frac{i}{2\kappa} \left[\frac{\partial}{\partial s} \left(CC_g \frac{\partial \phi}{\partial s} \right) \right] \left\{ \begin{matrix} W^1 \\ W^2 \\ W^3 \end{matrix} \right\} ds = -\int_{\Gamma_2} \frac{i}{2\kappa} \left[\frac{\partial}{\partial s} \left(CC_g \frac{\partial \phi}{\partial s} \right) \right] W' ds \quad (3.784)$$

This term can be expanded as follows using integration by parts:

$$-\int_{\Gamma_2} W^I \frac{i}{2\kappa} \left[\frac{\partial}{\partial s} \left(CC_g \frac{\partial \phi}{\partial s} \right) \right] ds = -W^I \frac{CC_g i}{2\kappa} \frac{\partial \phi}{\partial s} \Big|_0^l + \int_0^l \frac{\partial}{\partial s} \left(\frac{iW^I}{2\kappa} \right) CC_g \frac{\partial \phi}{\partial s} ds \quad (3.785)$$

$$\begin{aligned} -\int_{\Gamma_2} W^I \frac{i}{2\kappa} \left[\frac{\partial}{\partial s} \left(CC_g \frac{\partial \phi}{\partial s} \right) \right] ds &= -W^I \frac{CC_g i}{2\kappa} \frac{\partial \phi}{\partial s} \Big|_l + W^I \frac{CC_g i}{2\kappa} \frac{\partial \phi}{\partial s} \Big|_0 \\ &\quad + \int_0^l \frac{\partial}{\partial s} \left(\frac{iW^I}{2\kappa} \right) CC_g \frac{\partial \phi}{\partial s} ds \end{aligned} \quad (3.786)$$

$$\begin{aligned} -\int_{\Gamma_2} W^I \frac{i}{2\kappa} \left[\frac{\partial}{\partial s} \left(CC_g \frac{\partial \phi}{\partial s} \right) \right] ds &= -W^I \frac{CC_g i}{2\kappa} \frac{\partial \phi}{\partial s} \Big|_l + W^I \frac{CC_g i}{2\kappa} \frac{\partial \phi}{\partial s} \Big|_0 \\ &\quad + \int_0^l \frac{i}{2} \frac{\partial}{\partial s} \left(\frac{W^I}{\kappa} \right) CC_g \frac{\partial \phi}{\partial s} ds \end{aligned} \quad (3.787)$$

$$\begin{aligned} -\int_{\Gamma_2} W^I \frac{i}{2\kappa} \left[\frac{\partial}{\partial s} \left(CC_g \frac{\partial \phi}{\partial s} \right) \right] ds &= -W^I \frac{CC_g i}{2\kappa} \frac{\partial \phi}{\partial s} \Big|_l + W^I \frac{CC_g i}{2\kappa} \frac{\partial \phi}{\partial s} \Big|_0 \\ &\quad + \int_0^l \frac{i}{2} \left(\frac{\kappa \frac{\partial W^I}{\partial s} - W^I \frac{\partial \kappa}{\partial s}}{\kappa^2} \right) CC_g \frac{\partial \phi}{\partial s} ds \end{aligned} \quad (3.788)$$

$$\begin{aligned} -\int_{\Gamma_2} W^I \frac{i}{2\kappa} \left[\frac{\partial}{\partial s} \left(CC_g \frac{\partial \phi}{\partial s} \right) \right] ds &= -W^I \frac{CC_g i}{2\kappa} \frac{\partial \phi}{\partial s} \Big|_l + W^I \frac{CC_g i}{2\kappa} \frac{\partial \phi}{\partial s} \Big|_0 \\ &\quad + \int_0^l \frac{i}{2\kappa^2} \left(\kappa \frac{\partial W^I}{\partial s} \right) CC_g \frac{\partial \phi}{\partial s} ds + \int_0^l \frac{i}{2\kappa^2} \left(-W^I \frac{\partial \kappa}{\partial s} \right) CC_g \frac{\partial \phi}{\partial s} ds \end{aligned} \quad (3.789)$$

$$\begin{aligned} -\int_{\Gamma_2} W^I \frac{i}{2\kappa} \left[\frac{\partial}{\partial s} \left(CC_g \frac{\partial \phi}{\partial s} \right) \right] ds &= -W^I \frac{CC_g i}{2\kappa} \frac{\partial \phi}{\partial s} \Big|_l + W^I \frac{CC_g i}{2\kappa} \frac{\partial \phi}{\partial s} \Big|_0 \\ &\quad + \int_0^l \frac{iCC_g}{2\kappa} \frac{\partial W^I}{\partial s} \frac{\partial \phi}{\partial s} ds - \int_0^l \frac{iCC_g}{2\kappa^2} \frac{\partial \kappa}{\partial s} W^I \frac{\partial \phi}{\partial s} ds \end{aligned} \quad (3.790)$$

Substitution Equation (3.790) into Equation (3.783) gives:

$$\begin{aligned}
 -\int_{\Gamma_2} CC_g \frac{\partial \phi}{\partial n} W^I ds &= \int_0^l \frac{CC_g}{2\kappa} \frac{\partial \kappa}{\partial n} \phi W^I ds + \int_0^l \frac{1}{2} \frac{\partial CC_g}{\partial n} \phi W^I ds - \int_0^l iCC_g \kappa \phi W^I ds \\
 &\quad - W^I \left. \frac{CC_g i}{2\kappa} \frac{\partial \phi}{\partial s} \right|_l + W^I \left. \frac{CC_g i}{2\kappa} \frac{\partial \phi}{\partial s} \right|_0 + \int_0^l \frac{iCC_g}{2\kappa} \frac{\partial W^I}{\partial s} \frac{\partial \phi}{\partial s} ds \\
 &\quad - \int_0^l \frac{iCC_g}{2\kappa^2} \frac{\partial \kappa}{\partial s} W^I \frac{\partial \phi}{\partial s} ds
 \end{aligned} \tag{3.791}$$

With the application of the Galerkin method Equation (3.791) becomes:

$$\begin{aligned}
 -\int_{\Gamma_2} CC_g \frac{\partial \phi}{\partial n} W^I ds &= \int_0^l \frac{CC_g}{2\kappa} \frac{\partial \kappa}{\partial n} \phi L^I ds + \int_0^l \frac{1}{2} \frac{\partial CC_g}{\partial n} \phi L^I ds - \int_0^l iCC_g \kappa \phi L^I ds \\
 &\quad - L^I \left. \frac{CC_g i}{2\kappa} \frac{\partial \phi}{\partial s} \right|_l + L^I \left. \frac{CC_g i}{2\kappa} \frac{\partial \phi}{\partial s} \right|_0 + \int_0^l \frac{iCC_g}{2\kappa} \frac{\partial L^I}{\partial s} \frac{\partial \phi}{\partial s} ds \\
 &\quad - \int_0^l \frac{iCC_g}{2\kappa^2} \frac{\partial \kappa}{\partial s} L^I \frac{\partial \phi}{\partial s} ds
 \end{aligned} \tag{3.792}$$

Expressing ϕ in terms of shape functions L^J gives:

$$\phi = \phi^J L^J \tag{3.793}$$

$$\begin{aligned}
 -\int_{\Gamma_2} CC_g \frac{\partial \phi}{\partial n} W^I ds &= \int_0^l \frac{CC_g}{2\kappa} \frac{\partial \kappa}{\partial n} L^I L^J \phi^J ds + \int_0^l \frac{1}{2} \frac{\partial CC_g}{\partial n} L^I L^J \phi^J ds - \int_0^l iCC_g \kappa L^I L^J \phi^J ds \\
 &\quad - L^I \left. \frac{CC_g i}{2\kappa} \frac{\partial (L^J \phi^J)}{\partial s} \right|_l + L^I \left. \frac{CC_g i}{2\kappa} \frac{\partial (L^J \phi^J)}{\partial s} \right|_0 + \int_0^l \frac{iCC_g}{2\kappa} \frac{\partial L^I}{\partial s} \frac{\partial (L^J \phi^J)}{\partial s} ds \\
 &\quad - \int_0^l \frac{iCC_g}{2\kappa^2} \frac{\partial \kappa}{\partial s} L^I \frac{\partial (L^J \phi^J)}{\partial s} ds
 \end{aligned} \tag{3.794}$$

$$\begin{aligned}
-\int_{\Gamma_2} CC_g \frac{\partial \phi}{\partial n} W^I ds &= \int_0^l \frac{CC_g}{2\kappa} \frac{\partial \kappa}{\partial n} L^I L^J \phi^J ds + \int_0^l \frac{1}{2} \frac{\partial CC_g}{\partial n} L^I L^J \phi^J ds - \int_0^l iCC_g \kappa L^I L^J \phi^J ds \\
&\quad - \frac{CC_g i}{2\kappa} L^I \frac{\partial L^J}{\partial s} \phi^J \Big|_l + \frac{CC_g i}{2\kappa} L^I \frac{\partial L^J}{\partial s} \phi^J \Big|_0 + \int_0^l \frac{iCC_g}{2\kappa} \frac{\partial L^I}{\partial s} \frac{\partial L^J}{\partial s} \phi^J ds \quad (3.795) \\
&\quad - \int_0^l \frac{iCC_g}{2\kappa^2} \frac{\partial \kappa}{\partial s} L^I \frac{\partial L^J}{\partial s} \phi^J ds
\end{aligned}$$

$$\begin{aligned}
-\int_{\Gamma_2} CC_g \frac{\partial \phi}{\partial n} \begin{Bmatrix} W^1 \\ W^2 \\ W^3 \end{Bmatrix} ds &= \int_0^l \frac{CC_g}{2\kappa} \frac{\partial \kappa}{\partial n} \begin{Bmatrix} L^1 \\ L^2 \\ L^3 \end{Bmatrix} \begin{bmatrix} L^1 & L^2 & L^3 \end{bmatrix} \begin{Bmatrix} \phi^1 \\ \phi^2 \\ \phi^3 \end{Bmatrix} ds \\
&\quad + \int_0^l \frac{1}{2} \frac{\partial CC_g}{\partial n} \begin{Bmatrix} L^1 \\ L^2 \\ L^3 \end{Bmatrix} \begin{bmatrix} L^1 & L^2 & L^3 \end{bmatrix} \begin{Bmatrix} \phi^1 \\ \phi^2 \\ \phi^3 \end{Bmatrix} ds \\
&\quad - \int_0^l iCC_g \kappa \begin{Bmatrix} L^1 \\ L^2 \\ L^3 \end{Bmatrix} \begin{bmatrix} L^1 & L^2 & L^3 \end{bmatrix} \begin{Bmatrix} \phi^1 \\ \phi^2 \\ \phi^3 \end{Bmatrix} ds \\
&\quad - \frac{CC_g i}{2\kappa} \begin{Bmatrix} L^1 \\ L^2 \\ L^3 \end{Bmatrix} \begin{bmatrix} \frac{\partial L^1}{\partial s} & \frac{\partial L^2}{\partial s} & \frac{\partial L^3}{\partial s} \end{bmatrix} \begin{Bmatrix} \phi^1 \\ \phi^2 \\ \phi^3 \end{Bmatrix} \Big|_l \\
&\quad + \frac{CC_g i}{2\kappa} \begin{Bmatrix} L^1 \\ L^2 \\ L^3 \end{Bmatrix} \begin{bmatrix} \frac{\partial L^1}{\partial s} & \frac{\partial L^2}{\partial s} & \frac{\partial L^3}{\partial s} \end{bmatrix} \begin{Bmatrix} \phi^1 \\ \phi^2 \\ \phi^3 \end{Bmatrix} \Big|_0 \\
&\quad + \int_0^l \frac{iCC_g}{2\kappa} \begin{Bmatrix} \frac{\partial L^1}{\partial s} \\ \frac{\partial L^2}{\partial s} \\ \frac{\partial L^3}{\partial s} \end{Bmatrix} \begin{bmatrix} \frac{\partial L^1}{\partial s} & \frac{\partial L^2}{\partial s} & \frac{\partial L^3}{\partial s} \end{bmatrix} \begin{Bmatrix} \phi^1 \\ \phi^2 \\ \phi^3 \end{Bmatrix} ds \quad (3.796) \\
&\quad - \int_0^l \frac{iCC_g}{2\kappa^2} \frac{\partial \kappa}{\partial s} \begin{Bmatrix} L^1 \\ L^2 \\ L^3 \end{Bmatrix} \begin{bmatrix} \frac{\partial L^1}{\partial s} & \frac{\partial L^2}{\partial s} & \frac{\partial L^3}{\partial s} \end{bmatrix} \begin{Bmatrix} \phi^1 \\ \phi^2 \\ \phi^3 \end{Bmatrix} ds
\end{aligned}$$

$$\begin{aligned}
-\int_{\Gamma_2} CC_g \frac{\partial \phi}{\partial n} \begin{Bmatrix} W^1 \\ W^2 \\ W^3 \end{Bmatrix} ds &= \int_0^l \frac{CC_g}{2\kappa} \frac{\partial \kappa}{\partial n} \begin{bmatrix} L^1 L^1 & L^1 L^2 & L^1 L^3 \\ L^2 L^1 & L^2 L^2 & L^2 L^3 \\ L^3 L^1 & L^3 L^2 & L^3 L^3 \end{bmatrix} \begin{Bmatrix} \phi^1 \\ \phi^2 \\ \phi^3 \end{Bmatrix} ds + \int_0^l \frac{1}{2} \frac{\partial CC_g}{\partial n} \begin{bmatrix} L^1 L^1 & L^1 L^2 & L^1 L^3 \\ L^2 L^1 & L^2 L^2 & L^2 L^3 \\ L^3 L^1 & L^3 L^2 & L^3 L^3 \end{bmatrix} \begin{Bmatrix} \phi^1 \\ \phi^2 \\ \phi^3 \end{Bmatrix} ds \\
&\quad - \int_0^l iCC_g \kappa \begin{bmatrix} L^1 L^1 & L^1 L^2 & L^1 L^3 \\ L^2 L^1 & L^2 L^2 & L^2 L^3 \\ L^3 L^1 & L^3 L^2 & L^3 L^3 \end{bmatrix} \begin{Bmatrix} \phi^1 \\ \phi^2 \\ \phi^3 \end{Bmatrix} ds - \frac{CC_g i}{2\kappa} \left[\begin{array}{ccc} L^1 \frac{\partial L^1}{\partial s} & L^1 \frac{\partial L^2}{\partial s} & L^1 \frac{\partial L^3}{\partial s} \\ L^2 \frac{\partial L^1}{\partial s} & L^2 \frac{\partial L^2}{\partial s} & L^2 \frac{\partial L^3}{\partial s} \\ L^3 \frac{\partial L^1}{\partial s} & L^3 \frac{\partial L^2}{\partial s} & L^3 \frac{\partial L^3}{\partial s} \end{array} \begin{Bmatrix} \phi^1 \\ \phi^2 \\ \phi^3 \end{Bmatrix} \right]_l \\
&\quad + \frac{CC_g i}{2\kappa} \left[\begin{array}{ccc} L^1 \frac{\partial L^1}{\partial s} & L^1 \frac{\partial L^2}{\partial s} & L^1 \frac{\partial L^3}{\partial s} \\ L^2 \frac{\partial L^1}{\partial s} & L^2 \frac{\partial L^2}{\partial s} & L^2 \frac{\partial L^3}{\partial s} \\ L^3 \frac{\partial L^1}{\partial s} & L^3 \frac{\partial L^2}{\partial s} & L^3 \frac{\partial L^3}{\partial s} \end{array} \begin{Bmatrix} \phi^1 \\ \phi^2 \\ \phi^3 \end{Bmatrix} \right]_0 \\
&\quad + \int_0^l \frac{iCC_g}{2\kappa} \begin{bmatrix} \frac{\partial L^1}{\partial s} \frac{\partial L^1}{\partial s} & \frac{\partial L^1}{\partial s} \frac{\partial L^2}{\partial s} & \frac{\partial L^1}{\partial s} \frac{\partial L^3}{\partial s} \\ \frac{\partial L^2}{\partial s} \frac{\partial L^1}{\partial s} & \frac{\partial L^2}{\partial s} \frac{\partial L^2}{\partial s} & \frac{\partial L^2}{\partial s} \frac{\partial L^3}{\partial s} \\ \frac{\partial L^3}{\partial s} \frac{\partial L^1}{\partial s} & \frac{\partial L^3}{\partial s} \frac{\partial L^2}{\partial s} & \frac{\partial L^3}{\partial s} \frac{\partial L^3}{\partial s} \end{bmatrix} \begin{Bmatrix} \phi^1 \\ \phi^2 \\ \phi^3 \end{Bmatrix} dS \\
&\quad - \int_0^l \frac{iCC_g}{2\kappa^2} \frac{\partial \kappa}{\partial s} \begin{bmatrix} L^1 \frac{\partial L^1}{\partial s} & L^1 \frac{\partial L^2}{\partial s} & L^1 \frac{\partial L^3}{\partial s} \\ L^2 \frac{\partial L^1}{\partial s} & L^2 \frac{\partial L^2}{\partial s} & L^2 \frac{\partial L^3}{\partial s} \\ L^3 \frac{\partial L^1}{\partial s} & L^3 \frac{\partial L^2}{\partial s} & L^3 \frac{\partial L^3}{\partial s} \end{bmatrix} \begin{Bmatrix} \phi^1 \\ \phi^2 \\ \phi^3 \end{Bmatrix} ds
\end{aligned}
\tag{3.797}$$

L is a shape function for elements with two nodes. Hence L^3 will always be zero:

$$\begin{aligned}
-\int_{\Gamma_2} CC_g \frac{\partial \phi}{\partial n} \begin{Bmatrix} W^1 \\ W^2 \\ W^3 \end{Bmatrix} ds &= \int_0^l \frac{CC_g}{2\kappa} \frac{\partial \kappa}{\partial n} \begin{bmatrix} L^1 L^1 & L^1 L^2 & 0 \\ L^2 L^1 & L^2 L^2 & 0 \\ 0 & 0 & 0 \end{bmatrix} \begin{Bmatrix} \phi^1 \\ \phi^2 \\ \phi^3 \end{Bmatrix} dS + \int_0^l \frac{1}{2} \frac{\partial CC_g}{\partial n} \begin{bmatrix} L^1 L^1 & L^1 L^2 & 0 \\ L^2 L^1 & L^2 L^2 & 0 \\ 0 & 0 & 0 \end{bmatrix} \begin{Bmatrix} \phi^1 \\ \phi^2 \\ \phi^3 \end{Bmatrix} ds \\
&\quad - \int_0^l iCC_g \kappa \begin{bmatrix} L^1 L^1 & L^1 L^2 & 0 \\ L^2 L^1 & L^2 L^2 & 0 \\ 0 & 0 & 0 \end{bmatrix} \begin{Bmatrix} \phi^1 \\ \phi^2 \\ \phi^3 \end{Bmatrix} ds - \frac{CC_g i}{2\kappa} \begin{bmatrix} L^1 \frac{\partial L^1}{\partial s} & L^1 \frac{\partial L^2}{\partial s} & 0 \\ L^2 \frac{\partial L^1}{\partial s} & L^2 \frac{\partial L^2}{\partial s} & 0 \\ 0 & 0 & 0 \end{bmatrix} \begin{Bmatrix} \phi^1 \\ \phi^2 \\ \phi^3 \end{Bmatrix} \bigg|_l \\
&\quad + \frac{CC_g i}{2\kappa} \begin{bmatrix} L^1 \frac{\partial L^1}{\partial s} & L^1 \frac{\partial L^2}{\partial s} & 0 \\ L^2 \frac{\partial L^1}{\partial s} & L^2 \frac{\partial L^2}{\partial s} & 0 \\ 0 & 0 & 0 \end{bmatrix} \begin{Bmatrix} \phi^1 \\ \phi^2 \\ \phi^3 \end{Bmatrix} \bigg|_0 + \int_0^l \frac{iCC_g}{2\kappa} \begin{bmatrix} \frac{\partial L^1}{\partial s} \frac{\partial L^1}{\partial s} & \frac{\partial L^1}{\partial s} \frac{\partial L^2}{\partial s} & 0 \\ \frac{\partial L^2}{\partial s} \frac{\partial L^1}{\partial s} & \frac{\partial L^2}{\partial s} \frac{\partial L^2}{\partial s} & 0 \\ 0 & 0 & 0 \end{bmatrix} \begin{Bmatrix} \phi^1 \\ \phi^2 \\ \phi^3 \end{Bmatrix} ds \\
&\quad - \int_0^l \frac{iCC_g}{2\kappa^2} \frac{\partial \kappa}{\partial s} \begin{bmatrix} L^1 \frac{\partial L^1}{\partial s} & L^1 \frac{\partial L^2}{\partial s} & 0 \\ L^2 \frac{\partial L^1}{\partial s} & L^2 \frac{\partial L^2}{\partial s} & 0 \\ 0 & 0 & 0 \end{bmatrix} \begin{Bmatrix} \phi^1 \\ \phi^2 \\ \phi^3 \end{Bmatrix} ds
\end{aligned} \tag{3.798}$$

$$\begin{aligned}
-\int_{\Gamma_2} CC_g \frac{\partial \phi}{\partial n} \begin{Bmatrix} W^1 \\ W^2 \end{Bmatrix} ds &= \int_0^l \frac{CC_g}{2\kappa} \frac{\partial \kappa}{\partial n} \begin{bmatrix} L^1 L^1 & L^1 L^2 \\ L^2 L^1 & L^2 L^2 \end{bmatrix} \begin{Bmatrix} \phi^1 \\ \phi^2 \end{Bmatrix} ds + \int_0^l \frac{1}{2} \frac{\partial CC_g}{\partial n} \begin{bmatrix} L^1 L^1 & L^1 L^2 \\ L^2 L^1 & L^2 L^2 \end{bmatrix} \begin{Bmatrix} \phi^1 \\ \phi^2 \end{Bmatrix} ds \\
&\quad - \int_0^l iCC_g \kappa \begin{bmatrix} L^1 L^1 & L^1 L^2 \\ L^2 L^1 & L^2 L^2 \end{bmatrix} \begin{Bmatrix} \phi^1 \\ \phi^2 \end{Bmatrix} ds - \frac{CC_g i}{2\kappa} \begin{bmatrix} L^1 \frac{\partial L^1}{\partial s} & L^1 \frac{\partial L^2}{\partial s} \\ L^2 \frac{\partial L^1}{\partial s} & L^2 \frac{\partial L^2}{\partial s} \end{bmatrix} \begin{Bmatrix} \phi^1 \\ \phi^2 \end{Bmatrix} \bigg|_l \\
&\quad + \frac{CC_g i}{2\kappa} \begin{bmatrix} L^1 \frac{\partial L^1}{\partial s} & L^1 \frac{\partial L^2}{\partial s} \\ L^2 \frac{\partial L^1}{\partial s} & L^2 \frac{\partial L^2}{\partial s} \end{bmatrix} \begin{Bmatrix} \phi^1 \\ \phi^2 \end{Bmatrix} \bigg|_0 + \int_0^l \frac{iCC_g}{2\kappa} \begin{bmatrix} \frac{\partial L^1}{\partial s} \frac{\partial L^1}{\partial s} & \frac{\partial L^1}{\partial s} \frac{\partial L^2}{\partial s} \\ \frac{\partial L^2}{\partial s} \frac{\partial L^1}{\partial s} & \frac{\partial L^2}{\partial s} \frac{\partial L^2}{\partial s} \end{bmatrix} \begin{Bmatrix} \phi^1 \\ \phi^2 \end{Bmatrix} ds \\
&\quad - \int_0^l \frac{iCC_g}{2\kappa^2} \frac{\partial \kappa}{\partial s} \begin{bmatrix} L^1 \frac{\partial L^1}{\partial s} & L^1 \frac{\partial L^2}{\partial s} \\ L^2 \frac{\partial L^1}{\partial s} & L^2 \frac{\partial L^2}{\partial s} \end{bmatrix} \begin{Bmatrix} \phi^1 \\ \phi^2 \end{Bmatrix} dS
\end{aligned} \tag{3.799}$$

$$\begin{aligned}
-\int_{\Gamma_2} CC_g \frac{\partial \phi}{\partial n} \begin{Bmatrix} \mathcal{W}^1 \\ \mathcal{W}^2 \end{Bmatrix} ds &= \int_0^l \frac{CC_g}{2\kappa} \frac{\partial \kappa}{\partial n} \begin{bmatrix} L^1 L^1 & L^1 L^2 \\ L^2 L^1 & L^2 L^2 \end{bmatrix} \begin{Bmatrix} \phi^1 \\ \phi^2 \end{Bmatrix} ds + \int_0^l \frac{1}{2} \frac{\partial CC_g}{\partial n} \begin{bmatrix} L^1 L^1 & L^1 L^2 \\ L^2 L^1 & L^2 L^2 \end{bmatrix} \begin{Bmatrix} \phi^1 \\ \phi^2 \end{Bmatrix} ds \\
&\quad - \int_0^l iCC_g \kappa \begin{bmatrix} L^1 L^1 & L^1 L^2 \\ L^2 L^1 & L^2 L^2 \end{bmatrix} \begin{Bmatrix} \phi^1 \\ \phi^2 \end{Bmatrix} ds - \frac{CC_g i}{2\kappa} \begin{bmatrix} 0 & 0 \\ \frac{\partial L^1}{\partial s} & \frac{\partial L^2}{\partial s} \end{bmatrix} \begin{Bmatrix} \phi^1 \\ \phi^2 \end{Bmatrix} \bigg|_l \\
&\quad + \frac{CC_g i}{2\kappa} \begin{bmatrix} \frac{\partial L^1}{\partial s} & \frac{\partial L^2}{\partial s} \\ 0 & 0 \end{bmatrix} \begin{Bmatrix} \phi^1 \\ \phi^2 \end{Bmatrix} \bigg|_0 + \int_0^l \frac{iCC_g}{2\kappa} \begin{bmatrix} \frac{\partial L^1}{\partial s} \frac{\partial L^1}{\partial s} & \frac{\partial L^1}{\partial s} \frac{\partial L^2}{\partial s} \\ \frac{\partial L^2}{\partial s} \frac{\partial L^1}{\partial s} & \frac{\partial L^2}{\partial s} \frac{\partial L^2}{\partial s} \end{bmatrix} \begin{Bmatrix} \phi^1 \\ \phi^2 \end{Bmatrix} ds \\
&\quad - \int_0^l \frac{iCC_g}{2\kappa^2} \frac{\partial \kappa}{\partial s} \begin{bmatrix} L^1 \frac{\partial L^1}{\partial s} & L^1 \frac{\partial L^2}{\partial s} \\ L^2 \frac{\partial L^1}{\partial s} & L^2 \frac{\partial L^2}{\partial s} \end{bmatrix} \begin{Bmatrix} \phi^1 \\ \phi^2 \end{Bmatrix} ds
\end{aligned} \tag{3.800}$$

3.11.2 Complete Two-Dimensional Finite Element Wave Driven Hydrodynamic Model

Substituting Equation (3.800) into Equation (3.717) gives the following finite element matrix equation for the non-Helmholtz form of the 2d-NM-WCIM including an absorbing (downwave boundary) where 0 to l is the along the absorbing boundary:

$$\begin{aligned}
& -\iint_A U_j U_k \lambda' \frac{\partial^2 \bar{\eta}}{\partial x_j \partial x_k} \begin{bmatrix} N^1 N^1 & N^1 N^2 & N^1 N^3 \\ N^2 N^1 & N^2 N^2 & N^2 N^3 \\ N^3 N^1 & N^3 N^2 & N^3 N^3 \end{bmatrix} \begin{Bmatrix} \phi^1 \\ \phi^2 \\ \phi^3 \end{Bmatrix} dA - \int_{\Gamma_2} \frac{CC_g}{2\kappa} \frac{\partial \kappa}{\partial n} \begin{bmatrix} L^1 L^1 & L^1 L^2 & 0 \\ L^2 L^1 & L^2 L^2 & 0 \\ 0 & 0 & 0 \end{bmatrix} \begin{Bmatrix} \phi^1 \\ \phi^2 \\ \phi^3 \end{Bmatrix} ds \\
& + \int_{\Gamma_2} \frac{1}{2} \frac{\partial CC_g}{\partial n} \begin{bmatrix} L^1 L^1 & L^1 L^2 & 0 \\ L^2 L^1 & L^2 L^2 & 0 \\ 0 & 0 & 0 \end{bmatrix} \begin{Bmatrix} \phi^1 \\ \phi^2 \\ \phi^3 \end{Bmatrix} ds - \int_{\Gamma_2} iCC_g \kappa \begin{bmatrix} L^1 L^1 & L^1 L^2 & 0 \\ L^2 L^1 & L^2 L^2 & 0 \\ 0 & 0 & 0 \end{bmatrix} \begin{Bmatrix} \phi^1 \\ \phi^2 \\ \phi^3 \end{Bmatrix} ds \\
& - \frac{CC_g i}{2\kappa} \begin{bmatrix} 0 & 0 & 0 \\ \frac{\partial L^1}{\partial s} & \frac{\partial L^2}{\partial s} & 0 \\ 0 & 0 & 0 \end{bmatrix} \begin{Bmatrix} \phi^1 \\ \phi^2 \\ \phi^3 \end{Bmatrix} \Big|_l + \frac{CC_g i}{2\kappa} \begin{bmatrix} \frac{\partial L^1}{\partial s} & \frac{\partial L^2}{\partial s} & 0 \\ 0 & 0 & 0 \\ 0 & 0 & 0 \end{bmatrix} \begin{Bmatrix} \phi^1 \\ \phi^2 \\ \phi^3 \end{Bmatrix} \Big|_0 + \int_{\Gamma_2} \frac{iCC_g}{2\kappa} \begin{bmatrix} \frac{\partial L^1}{\partial s} \frac{\partial L^1}{\partial s} & \frac{\partial L^1}{\partial s} \frac{\partial L^2}{\partial s} & 0 \\ \frac{\partial L^2}{\partial s} \frac{\partial L^1}{\partial s} & \frac{\partial L^2}{\partial s} \frac{\partial L^2}{\partial s} & 0 \\ 0 & 0 & 0 \end{bmatrix} \begin{Bmatrix} \phi^1 \\ \phi^2 \\ \phi^3 \end{Bmatrix} ds \\
& - \int_{\Gamma_2} \frac{iCC_g}{2\kappa^2} \frac{\partial \kappa}{\partial s} \begin{bmatrix} L^1 \frac{\partial L^1}{\partial s} & L^1 \frac{\partial L^2}{\partial s} & 0 \\ L^2 \frac{\partial L^1}{\partial s} & L^2 \frac{\partial L^2}{\partial s} & 0 \\ 0 & 0 & 0 \end{bmatrix} \begin{Bmatrix} \phi^1 \\ \phi^2 \\ \phi^3 \end{Bmatrix} ds + \iint_A U_j U_k \kappa^2 \left(\frac{\partial \bar{\eta}}{\partial x_j} \frac{\partial \bar{\eta}}{\partial x_k} \right) \begin{bmatrix} N^1 N^1 & N^1 N^2 & N^1 N^3 \\ N^2 N^1 & N^2 N^2 & N^2 N^3 \\ N^3 N^1 & N^3 N^2 & N^3 N^3 \end{bmatrix} \begin{Bmatrix} \phi^1 \\ \phi^2 \\ \phi^3 \end{Bmatrix} dA \\
& + \iint_A U_j U_k (\mathcal{Q}_U'')_{kj} \begin{bmatrix} N^1 N^1 & N^1 N^2 & N^1 N^3 \\ N^2 N^1 & N^2 N^2 & N^2 N^3 \\ N^3 N^1 & N^3 N^2 & N^3 N^3 \end{bmatrix} \begin{Bmatrix} \phi^1 \\ \phi^2 \\ \phi^3 \end{Bmatrix} dA = 0
\end{aligned}
\tag{3.801}$$

Within the domain the boundary terms along the edge of each element will cancel each other out. In this model all other boundaries would have a specified velocity potential applied to them by means of a big-number method. Using the big number method the diagonal component of the mass matrix and the corresponding component of the right hand side vector for the node in question are multiplied by a large number so that the value in the right hand side vector is forced to be the solution at the given node.

Equation (3.801) may also be written as:

$$\begin{aligned}
& -\iint_A 2i\omega U_j N^I \frac{\partial N^J}{\partial x_j} \phi^J dA - \iint_A U_j U_k \frac{\partial N^I}{\partial x_j} \frac{\partial N^J}{\partial x_k} \phi^J dA - \iint_A \frac{\partial U_j}{\partial x_j} U_k N^I \frac{\partial N^J}{\partial x_k} \phi^J dA \\
& - \iint_A U_j \frac{\partial U_k}{\partial x_j} N^I \frac{\partial N^J}{\partial x_k} \phi^J dA + \iint_A U_j \frac{\partial U_k}{\partial x_j} N^I \frac{\partial N^J}{\partial x_k} \phi^J dA + \iint_A g \left(\frac{\partial \bar{\eta}}{\partial x_k} \right) N^I \frac{\partial N^J}{\partial x_k} \phi^J dA \\
& + \iint_A CC_g \frac{\partial N^I}{\partial x_k} \frac{\partial N^J}{\partial x_k} \phi^J dA - \iint_A 2\lambda' U_j U_k \frac{\partial \bar{\eta}}{\partial x_j} N^I \frac{\partial N^J}{\partial x_k} \phi^J dA - \iint_A \omega^2 N^I N^J \phi^J dA \\
& - \iint_A \kappa^2 CC_g N^I N^J \phi^J dA - \iint_A \sigma^2 Q'' N^I N^J \phi^J dA + \iint_A \sigma^2 N^I N^J \phi^J dA \\
& + \iint_A 2i\omega \lambda' U_j \frac{\partial \bar{\eta}}{\partial x_j} N^I N^J \phi^J dA - \iint_A \lambda' U_j \frac{\partial U_k}{\partial x_j} \frac{\partial \bar{\eta}}{\partial x_k} N^I N^J \phi^J dA - \iint_A U_j U_k \lambda' \frac{\partial^2 \bar{\eta}}{\partial x_j \partial x_k} N^I N^J \phi^J dA \\
& + \int_0^l \frac{CC_g}{2\kappa} \frac{\partial \kappa}{\partial n} L^I L^J \phi^J ds + \int_0^l \frac{1}{2} \frac{\partial CC_g}{\partial n} L^I L^J \phi^J ds - \int_0^l iCC_g \kappa L^I L^J \phi^J ds \\
& - \frac{CC_g i}{2\kappa} L^I \frac{\partial L^J}{\partial S} \phi^J \Big|_l + \frac{CC_g i}{2\kappa} L^I \frac{\partial L^J}{\partial S} \phi^J \Big|_0 + \int_0^l \frac{iCC_g}{2\kappa} \frac{\partial L^I}{\partial s} \frac{\partial L^J}{\partial s} \phi^J ds \\
& - \int_0^l \frac{iCC_g}{2\kappa^2} \frac{\partial \kappa}{\partial S} L^I \frac{\partial L^J}{\partial S} \phi^J ds + \iint_A U_j U_k \kappa^2 \left(\frac{\partial \bar{\eta}}{\partial x_j} \frac{\partial \bar{\eta}}{\partial x_k} \right) N^I N^J \phi^J dA + \iint_A U_j U_k (Q''_{U'})_{kj} N^I N^J \phi^J dA = 0
\end{aligned} \tag{3.802}$$

Equation (3.802) is the simplest form of the NM-WCIM. It can be solved for unbroken waves approaching a linear beach where there is no reflection of waves by obstacles. The following sections extend this equation to a form that can be used where the downwave boundary of the model area is varying in shape and where there are reflecting and radiating boundaries. To solve for velocity potential using Equation (3.802) it is necessary to isolate the real and imaginary components of the equation and solve an equation for the real components as follows:

$$\begin{aligned}
& \iint_A 2\omega U_j N^I \frac{\partial N^J}{\partial x_j} \phi_2' dA - \iint_A U_j U_k \frac{\partial N^I}{\partial x_j} \frac{\partial N^J}{\partial x_k} \phi_1' dA - \iint_A \frac{\partial U_j}{\partial x_i} U_k N^I \frac{\partial N^J}{\partial x_k} \phi_1' dA \\
& - \iint_A U_j \frac{\partial U_k}{\partial x_i} N^I \frac{\partial N^J}{\partial x_k} \phi_1' dA + \iint_A U_j \frac{\partial U_k}{\partial x_j} N^I \frac{\partial N^J}{\partial x_k} \phi_1' dA + \iint_A g \left(\frac{\partial \bar{\eta}}{\partial x_k} \right) N^I \frac{\partial N^J}{\partial x_k} \phi_1' dA \\
& + \iint_A CC_g \frac{\partial N^I}{\partial x_k} \frac{\partial N^J}{\partial x_k} \phi_1' dA - \iint_A 2\lambda' U_j U_k \frac{\partial \bar{\eta}}{\partial x_j} N^I \frac{\partial N^J}{\partial x_k} \phi_1' dA - \iint_A \omega^2 N^I N^J \phi_1' dA \\
& - \iint_A \kappa^2 CC_g N^I N^J \phi_1' dA - \iint_A \sigma^2 Q'' N^I N^J \phi_1' dA + \iint_A \sigma^2 N^I N^J \phi_1' dA \\
& - \iint_A 2\omega \lambda' U_j \frac{\partial \bar{\eta}}{\partial x_j} N^I N^J \phi_2' dA - \iint_A \lambda' U_j \frac{\partial U_k}{\partial x_j} \frac{\partial \bar{\eta}}{\partial x_k} N^I N^J \phi_1' dA - \iint_A U_j U_k \lambda' \frac{\partial^2 \bar{\eta}}{\partial x_j \partial x_k} N^I N^J \phi_1' dA \\
& + \int_0^l \frac{CC_g}{2\kappa} \frac{\partial \kappa}{\partial n} L^I L^J \phi_1' dS + \int_0^l \frac{1}{2} \frac{\partial CC_g}{\partial n} L^I L^J \phi_1' dS + \int_0^l CC_g \kappa L^I L^J \phi_2' dS \\
& + \frac{CC_g}{2\kappa} L^I \frac{\partial L^J}{\partial S} \phi_2' \Big|_l - \frac{CC_g}{2\kappa} L^I \frac{\partial L^J}{\partial S} \phi_2' \Big|_0 - \int_0^l \frac{CC_g}{2\kappa} \frac{\partial L^I}{\partial S} \frac{\partial L^J}{\partial S} \phi_2' dS \\
& + \int_0^l \frac{CC_g}{2\kappa^2} \frac{\partial \kappa}{\partial S} L^I \frac{\partial L^J}{\partial S} \phi_2' dS + \iint_A U_j U_k \kappa^2 \left(\frac{\partial \bar{\eta}}{\partial x_k} \frac{\partial \bar{\eta}}{\partial x_k} \right) N^I N^J \phi_1' dA + \iint_A U_j U_k (Q_U)_{kj} N^I N^J \phi_1' dA = 0
\end{aligned}
\tag{3.803}$$

3.11.3 A Generalised Curvilinear Downwave Absorbing Boundary Condition

A more useful absorbing boundary condition can be obtained for downwave conditions where the “beach” boundary is not a straight line shape. Clyne (2008) develops an absorbing downstream boundary condition using generalised curvilinear coordinates that can be used on any shape of downstream boundary. The usefulness and accuracy of this methodology is examined and proved in Clyne (2008). It is possible to apply the same type of absorbing boundary condition to the 2d-NM-WCIM of this project.

3.11.3.1 Generalised Curvilinear Coordinate System

In order to obtain a boundary condition in a set of generalised curvilinear coordinates the system of coordinates must first be defined, following Clyne (2008) :

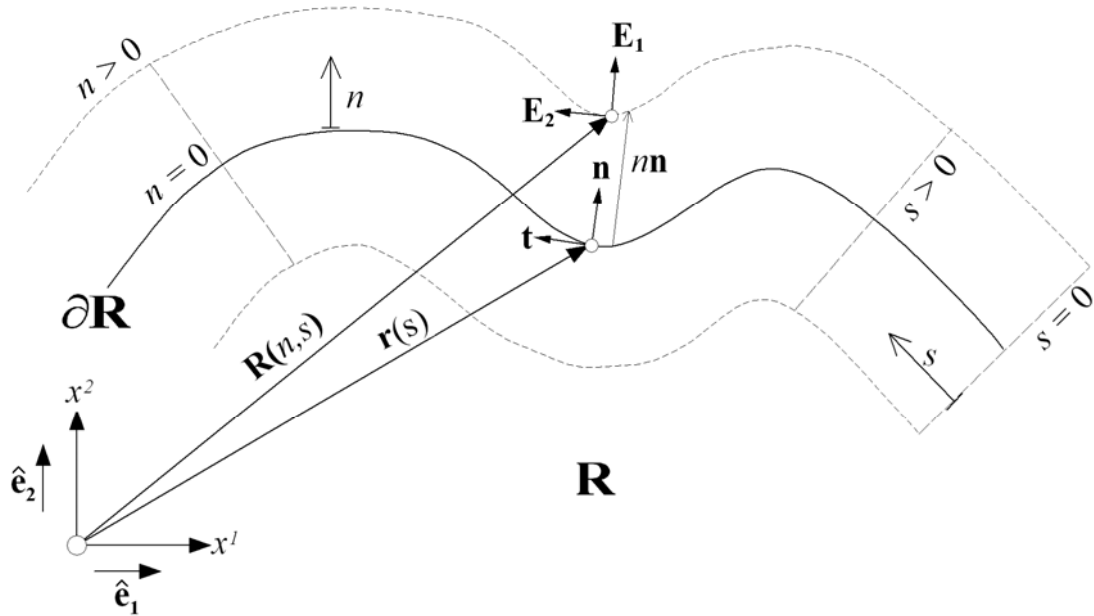


Figure 3.12 – Sketch of Boundary Curve ∂R to the region R

Figure 3.12 shows a boundary curve ∂R that represents the shoreline. The distance along this curve, or any of the family of curves parallel to it, can be defined using the variable s . A second family of curves can be defined as those perpendicular to the original boundary curves and its parallels. Each member of this family will have a fixed value of s and distance along them may be measured using the variable n . The curve ∂R can be represented by the vector \mathbf{r} as follows:

$$\mathbf{r}(s) = \hat{\mathbf{e}}_i x^i(s), \quad i = 1, 2 \quad (3.804)$$

Where $\hat{\mathbf{e}}$ is a unit vector.

The tangent to the boundary curve ∂R can also be defined:

$$\mathbf{t} = \frac{d\mathbf{r}}{ds}, \text{ where } \mathbf{t} \cdot \mathbf{t} = 1 \quad (3.805)$$

The unit normal vector \mathbf{n} points in the outward direction from the region enclosed by the curve ∂R and the unit tangent vector \mathbf{t} points in the direction of increasing values of s . Hence the position vector of any point in the domain, $\mathbf{R}(n, s)$, may be expressed as:

$$\mathbf{R}(n, s) = \mathbf{r}(s) + n\mathbf{n}(s) \quad (3.806)$$

The partial derivative of Equation (3.806) with respect to n gives a first basis vector for a set of generalised curvilinear coordinates:

$$\frac{\partial \mathbf{R}}{\partial n} = \mathbf{n} = \mathbf{E}_1 \quad (3.807)$$

Similarly the second basis vector can be obtained by taking the partial derivative with respect to s :

$$\frac{\partial \mathbf{R}}{\partial s} = \frac{d\mathbf{r}}{ds} + n \frac{d\mathbf{n}}{ds} = \mathbf{t} + n \frac{d\mathbf{n}}{ds} = \mathbf{E}_2 \quad (3.808)$$

Metric tensors can now be defined in terms of the basis vectors:

$$g_{11} = \mathbf{E}_1 \cdot \mathbf{E}_1 = \mathbf{n} \cdot \mathbf{n} = 1 \quad (3.809)$$

$$g_{22} = \mathbf{E}_2 \cdot \mathbf{E}_2 = \mathbf{t} \cdot \mathbf{t} + 2n\mathbf{t} \cdot \frac{d\mathbf{n}}{ds} + n^2 \frac{d\mathbf{n}}{ds} \cdot \frac{d\mathbf{n}}{ds} \quad (3.810)$$

$$g_{22} = 1 + 2n\mathbf{t} \cdot \frac{d\mathbf{n}}{ds} + n^2 \left(\frac{d\mathbf{n}}{ds} \right)^2 \quad (3.811)$$

$$g_{12} = g_{21} = \mathbf{E}_1 \cdot \mathbf{E}_2 = \mathbf{n} \cdot \mathbf{t} + n\mathbf{n} \cdot \frac{d\mathbf{n}}{ds} = 0 \quad (3.812)$$

$$g_{12} = g_{21} = 0 \quad (3.813)$$

The metric tensors g_{12} and g_{21} are zero because \mathbf{n} is perpendicular to \mathbf{t} and $\frac{d\mathbf{n}}{ds}$.

3.11.3.2 Transformation of the Helmholtz Type Elliptic Mild-Slope Wave Equation to a Generalised Curvilinear Coordinate System

The downwave boundary condition will be constructed for use in the absence of a current. In the absence of a current Equation (3.741) becomes the Helmholtz type elliptic solution to the mild-slope equation of Clyne (2008):

$$\frac{\partial^2 \phi'}{\partial x_k \partial x_k} + K^2 \phi' = 0 \quad (3.814)$$

Recalling from Equation (3.740):

$$K^2 = -\frac{1}{\sqrt{CC_g}} \frac{\partial^2 \sqrt{CC_g}}{\partial x_k \partial x_k} + \kappa^2 + \frac{\sigma^2 \tilde{Q}''}{CC_g}$$

The K of this project is different to that of Clyne (2008). If set-up was to be ignored the K value here would be the same as that of Clyne (2008).

Alternatively Equation (3.814) may be expressed as:

$$\nabla^2 \phi' + K^2 \phi' = 0 \quad (3.815)$$

In order to express Equation (3.815) in terms of the system of generalised curvilinear coordinates described above it will be necessary to use the tensor methods of Heinbockel (2001) and Clyne (2008). $\nabla \phi'$ can be expressed in tensor notation as the covariant vector:

$$\phi'_{,i} = \frac{\partial \phi'}{\partial x^i} \quad (3.816)$$

The contravariant form of this vector is then:

$$g^{ij} \frac{\partial \phi'}{\partial x^i} \quad (3.817)$$

Where g_{ij} is the metric tensor, and hence g^{ij} is the conjugate metric tensor.

Heinbockel (2001) and Clyne (2008) develop an expression for the divergence of any vector \mathbf{A} in the above set of generalised curvilinear coordinates. Using tensor notation this is as follows:

$$a^m_{,m} = \frac{1}{\sqrt{g}} \frac{\partial}{\partial x^m} (\sqrt{g} a^m) \quad (3.818)$$

Where $a^m_{,m}$ is the divergence of the vector \mathbf{A} and g is the determinant of the metric tensor matrix.

That is:

$$\mathbf{g} = g_{(i)\alpha} G^{\alpha(i)} \quad (3.819)$$

where $G^{\alpha(i)}$ is the cofactor of $g_{\alpha\beta}$.

The Laplacian term in Equation (3.815), $\nabla^2 \phi'$, can be expressed as $\nabla \cdot \nabla \phi'$, that is the divergence of $\nabla \phi'$. Hence the vector \mathbf{A} can be replaced by the contravariant form of ϕ'_i in order to get the divergence of $\nabla \phi'$ as follows:

$$a^j = g^{ij} \frac{\partial \phi'}{\partial x^i} \quad (3.820)$$

It is then possible to use Equation (3.818) to express $\nabla^2 \phi'$ as follows:

$$a^m_{,m} = \nabla^2 \phi' = \frac{1}{\sqrt{g}} \frac{\partial}{\partial x^j} \left(\sqrt{g} g^{ij} \frac{\partial \phi'}{\partial x^i} \right) \quad (3.821)$$

For an orthogonal two-dimensional system $g^{ij} = 0$ for $i \neq j$, $i, j = 1, 2$ and hence the determinant of the metric tensor matrix will be:

$$g = g_{11} g_{22} \quad (3.822)$$

Substituting Equation (3.822) into Equation (3.821) gives:

$$\nabla^2 \phi' = \frac{1}{\sqrt{g_{11} g_{22}}} \frac{\partial}{\partial x^j} \left(\sqrt{g_{11} g_{22}} g^{ij} \frac{\partial \phi'}{\partial x^i} \right) \quad (3.823)$$

Equation (3.823) may be expanded as:

$$\nabla^2 \phi' = \frac{1}{\sqrt{g_{11} g_{22}}} \left[\frac{\partial}{\partial x^1} \left(\sqrt{g_{11} g_{22}} \left(g^{11} \frac{\partial \phi'}{\partial x^1} + g^{21} \frac{\partial \phi'}{\partial x^2} \right) \right) + \frac{\partial}{\partial x^2} \left(\sqrt{g_{11} g_{22}} \left(g^{12} \frac{\partial \phi'}{\partial x^1} + g^{22} \frac{\partial \phi'}{\partial x^2} \right) \right) \right] \quad (3.824)$$

Further expansion and simplification of Equation (3.824) gives

$$\nabla^2 \phi' = \frac{1}{\sqrt{g_{11} g_{22}}} \left[\frac{\partial}{\partial x^1} \left(\sqrt{g_{11} g_{22}} g^{11} \frac{\partial \phi'}{\partial x^1} \right) + \frac{\partial}{\partial x^2} \left(\sqrt{g_{11} g_{22}} g^{22} \frac{\partial \phi'}{\partial x^2} \right) \right] \quad (3.825)$$

$$\nabla^2 \phi' = \frac{1}{\sqrt{g_{11}g_{22}}} \left[\frac{\partial}{\partial x^1} \left((g_{11})^{1/2} (g_{22})^{1/2} (g_{11})^{-1} \frac{\partial \phi'}{\partial x^1} \right) + \frac{\partial}{\partial x^2} \left((g_{11})^{1/2} (g_{22})^{1/2} (g_{22})^{-1} \frac{\partial \phi'}{\partial x^2} \right) \right] \quad (3.826)$$

$$\nabla^2 \phi' = \frac{1}{\sqrt{g_{11}g_{22}}} \left[\frac{\partial}{\partial x^1} \left((g_{11})^{-1/2} (g_{22})^{1/2} \frac{\partial \phi'}{\partial x^1} \right) + \frac{\partial}{\partial x^2} \left((g_{11})^{1/2} (g_{22})^{-1/2} \frac{\partial \phi'}{\partial x^2} \right) \right] \quad (3.827)$$

This gives the following expression of the Laplacian term of the Helmholtz form of the elliptic mild-slope equation in generalised curvilinear coordinates.

$$\nabla^2 \phi' = \frac{1}{\sqrt{g_{11}g_{22}}} \left[\frac{\partial}{\partial x^1} \left(\sqrt{\frac{g_{22}}{g_{11}}} \frac{\partial \phi'}{\partial x^1} \right) + \frac{\partial}{\partial x^2} \left(\sqrt{\frac{g_{11}}{g_{22}}} \frac{\partial \phi'}{\partial x^2} \right) \right] \quad (3.828)$$

Equation (3.828) can now be linked with the system of generalised curvilinear coordinates discussed in Section 3.11.3.1 above. Substituting Equation (3.809) into Equation (3.828) gives:

$$\nabla^2 \phi' = \frac{1}{\sqrt{g_{22}}} \left[\frac{\partial}{\partial x^1} \left(\sqrt{g_{22}} \frac{\partial \phi'}{\partial x^1} \right) + \frac{\partial}{\partial x^2} \left(\sqrt{\frac{1}{g_{22}}} \frac{\partial \phi'}{\partial x^2} \right) \right] \quad (3.829)$$

Expansion of Equation (3.829) yields:

$$\nabla^2 \phi' = \frac{1}{\sqrt{g_{22}}} \left[\sqrt{g_{22}} \frac{\partial^2 \phi'}{\partial (x^1)^2} + \frac{\partial \phi'}{\partial x^1} \frac{\partial \sqrt{g_{22}}}{\partial x^1} + \frac{\partial \phi'}{\partial x^2} \frac{\partial}{\partial x^2} \left(\sqrt{\frac{1}{g_{22}}} \right) + \sqrt{\frac{1}{g_{22}}} \frac{\partial^2 \phi'}{\partial (x^2)^2} \right] \quad (3.830)$$

Using Equation (3.811) the following relationships can be obtained:

$$\sqrt{g_{22}} = \left(1 + 2\mathbf{n} \cdot \frac{d\mathbf{n}}{ds} + n^2 \left(\frac{d\mathbf{n}}{ds} \right)^2 \right)^{1/2} \quad (3.831)$$

$$\frac{1}{\sqrt{g_{22}}} = \left(1 + 2\mathbf{n} \cdot \frac{d\mathbf{n}}{ds} + n^2 \left(\frac{d\mathbf{n}}{ds} \right)^2 \right)^{-1/2} \quad (3.832)$$

$$\frac{\partial}{\partial x^1} (\sqrt{g_{22}}) = \frac{\partial}{\partial n} \sqrt{1 + 2\mathbf{n} \cdot \frac{d\mathbf{n}}{ds} + n^2 \left(\frac{d\mathbf{n}}{ds} \right)^2} \quad (3.833)$$

$$\frac{\partial}{\partial x^1} (\sqrt{g_{22}}) = \frac{1}{2} \left(2\mathbf{n} \cdot \frac{d\mathbf{n}}{ds} + 2n \left(\frac{d\mathbf{n}}{ds} \right)^2 \right) \left(1 + 2\mathbf{n} \cdot \frac{d\mathbf{n}}{ds} + n^2 \left(\frac{d\mathbf{n}}{ds} \right)^2 \right)^{-1/2} \quad (3.834)$$

$$\frac{\partial}{\partial x^2} \left(\frac{1}{\sqrt{g_{22}}} \right) = \frac{\partial}{\partial s} \left(1 + 2n\mathbf{t} \cdot \frac{d\mathbf{n}}{ds} + n^2 \left(\frac{d\mathbf{n}}{ds} \right)^2 \right)^{-1/2} \quad (3.835)$$

$$\frac{\partial}{\partial x^2} \left(\frac{1}{\sqrt{g_{22}}} \right) = -\frac{1}{2} \frac{\partial}{\partial s} \left(1 + 2n\mathbf{t} \cdot \frac{d\mathbf{n}}{ds} + n^2 \left(\frac{d\mathbf{n}}{ds} \right)^2 \right) \left(1 + 2n\mathbf{t} \cdot \frac{d\mathbf{n}}{ds} + n^2 \left(\frac{d\mathbf{n}}{ds} \right)^2 \right)^{-3/2} \quad (3.836)$$

$$\frac{\partial}{\partial x^2} \left(\frac{1}{\sqrt{g_{22}}} \right) = -n \left(\frac{d\mathbf{t}}{ds} \cdot \frac{d\mathbf{n}}{ds} + \mathbf{t} \cdot \frac{d^2\mathbf{n}}{ds^2} + n \frac{d\mathbf{n}}{ds} \cdot \frac{d^2\mathbf{n}}{ds^2} \right) \left(1 + 2n\mathbf{t} \cdot \frac{d\mathbf{n}}{ds} + n^2 \left(\frac{d\mathbf{n}}{ds} \right)^2 \right)^{-3/2} \quad (3.837)$$

In this case the generalised equation will only be needed for the absorbing boundary condition and hence the terms above can be limited to the boundary ∂R where $n = 0$. Therefore Equation (3.831) becomes:

$$\sqrt{g_{22}} = 1 \text{ for } n = 0 \quad (3.838)$$

Equation (3.832) becomes:

$$\frac{1}{\sqrt{g_{22}}} = 1 \text{ for } n = 0 \quad (3.839)$$

Equation (3.834) becomes:

$$\frac{\partial}{\partial x^1} (\sqrt{g_{22}}) = \mathbf{t} \cdot \frac{d\mathbf{n}}{ds} \text{ for } n = 0 \quad (3.840)$$

Equation (3.837) becomes:

$$\frac{\partial}{\partial x^2} \left(\frac{1}{\sqrt{g_{22}}} \right) = 0 \text{ for } n = 0 \quad (3.841)$$

Substitution of Equations (3.838), (3.839), (3.840) and (3.841) into Equation (3.830) gives:

$$\nabla^2 \phi' = \frac{\partial^2 \phi'}{\partial (x^1)^2} + \frac{\partial^2 \phi'}{\partial (x^2)^2} + \mathbf{t} \cdot \frac{d\mathbf{n}}{ds} \frac{\partial \phi'}{\partial x^2} = \frac{\partial^2 \phi'}{\partial s^2} + \frac{\partial^2 \phi'}{\partial n^2} + \mathbf{t} \cdot \frac{d\mathbf{n}}{ds} \frac{\partial \phi'}{\partial n} \quad (3.842)$$

Equation (3.842) can now be substituted into Equation (3.815) to give an elliptic extended mild-slope equation in generalised curvilinear coordinates:

$$\frac{\partial^2 \phi'}{\partial s^2} + \frac{\partial^2 \phi'}{\partial n^2} + \mathbf{t} \cdot \frac{d\mathbf{n}}{ds} \frac{\partial \phi'}{\partial n} + K^2 \phi' = 0 \quad (3.843)$$

3.11.3.3 Transformation of the Non-Helmholtz Type Elliptic Mild-Slope Wave Equation to a Generalised Curvilinear Coordinate System

The downwave boundary condition will be constructed for use in the absence of a current.

In the absence of a current Equation (3.718) becomes:

$$-\frac{\partial}{\partial x_k} \left(CC_g \frac{\partial \phi}{\partial x_k} \right) - \phi \kappa^2 CC_g - \phi \sigma^2 \tilde{Q}'' = 0 \quad (3.844)$$

Equation (3.844) can be rewritten as follows:

$$\frac{\partial^2 \phi}{\partial x_k \partial x_k} + \frac{1}{CC_g} \frac{\partial CC_g}{\partial x_k} \frac{\partial \phi}{\partial x_k} + K'^2 \phi = 0 \quad (3.845)$$

where:

$$K'^2 = \kappa^2 + \frac{\sigma^2 \tilde{Q}''}{CC_g} \quad (3.846)$$

In order to express Equation (3.845) in terms of the system of generalised curvilinear coordinates described above it will be necessary to use the tensor methods of Heinbockel (2001) and Clyne (2008). $\nabla \phi$ can be expressed in tensor notation as the covariant vector:

$$\phi_{,i} = \frac{\partial \phi}{\partial x^i} \quad (3.847)$$

The contravariant form of this vector is then:

$$g^{ij} \frac{\partial \phi}{\partial x^i} \quad (3.848)$$

Where g_{ij} is the metric tensor, and hence g^{ij} is the conjugate metric tensor.

The Laplacian term in Equation (3.845), $\frac{\partial^2 \phi}{\partial x_k \partial x_k}$, can be expressed as $\nabla \cdot \nabla \phi$, that is the divergence of $\nabla \phi$. Hence the vector **A** in Equation (3.818) can be replaced by the contravariant form of $\phi_{,i}$ in order to get the divergence of $\nabla \phi$ as follows:

$$a^j = g^{ij} \frac{\partial \phi}{\partial x^i} \quad (3.849)$$

It is then possible to use Equation (3.818) to express $\nabla^2\phi$ as follows:

$$a_{,m}^m = \nabla^2\phi = \frac{1}{\sqrt{g}} \frac{\partial}{\partial x^j} \left(\sqrt{g} g^{ij} \frac{\partial \phi}{\partial x^i} \right) \quad (3.850)$$

For an orthogonal two-dimensional system $g^{ij} = 0$ for $i \neq j$, $i, j = 1, 2$ and hence the determinant of the metric tensor matrix will be:

$$g = g_{11}g_{22} \quad (3.851)$$

Substituting Equation (3.822) into Equation (3.850) gives:

$$\nabla^2\phi = \frac{1}{\sqrt{g_{11}g_{22}}} \frac{\partial}{\partial x^j} \left(\sqrt{g_{11}g_{22}} g^{ij} \frac{\partial \phi}{\partial x^i} \right) \quad (3.852)$$

Equation (3.852) may be expanded as:

$$\nabla^2\phi = \frac{1}{\sqrt{g_{11}g_{22}}} \left[\frac{\partial}{\partial x^1} \left(\sqrt{g_{11}g_{22}} \left(g^{11} \frac{\partial \phi}{\partial x^1} + g^{21} \frac{\partial \phi}{\partial x^2} \right) \right) + \frac{\partial}{\partial x^2} \left(\sqrt{g_{11}g_{22}} \left(g^{12} \frac{\partial \phi}{\partial x^1} + g^{22} \frac{\partial \phi}{\partial x^2} \right) \right) \right] \quad (3.853)$$

Further expansion and simplification of Equation (3.853) gives

$$\nabla^2\phi = \frac{1}{\sqrt{g_{11}g_{22}}} \left[\frac{\partial}{\partial x^1} \left(\sqrt{g_{11}g_{22}} g^{11} \frac{\partial \phi}{\partial x^1} \right) + \frac{\partial}{\partial x^2} \left(\sqrt{g_{11}g_{22}} g^{22} \frac{\partial \phi}{\partial x^2} \right) \right] \quad (3.854)$$

$$\nabla^2\phi = \frac{1}{\sqrt{g_{11}g_{22}}} \left[\frac{\partial}{\partial x^1} \left((g_{11})^{1/2} (g_{22})^{1/2} (g_{11})^{-1} \frac{\partial \phi}{\partial x^1} \right) + \frac{\partial}{\partial x^2} \left((g_{11})^{1/2} (g_{22})^{1/2} (g_{22})^{-1} \frac{\partial \phi}{\partial x^2} \right) \right] \quad (3.855)$$

$$\nabla^2\phi = \frac{1}{\sqrt{g_{11}g_{22}}} \left[\frac{\partial}{\partial x^1} \left((g_{11})^{-1/2} (g_{22})^{1/2} \frac{\partial \phi}{\partial x^1} \right) + \frac{\partial}{\partial x^2} \left((g_{11})^{1/2} (g_{22})^{-1/2} \frac{\partial \phi}{\partial x^2} \right) \right] \quad (3.856)$$

This gives the following expression of the Laplacian term of the Non-Helmholtz form of the elliptic mild-slope equation in generalised curvilinear coordinates.

$$\nabla^2\phi = \frac{1}{\sqrt{g_{11}g_{22}}} \left[\frac{\partial}{\partial x^1} \left(\sqrt{\frac{g_{22}}{g_{11}}} \frac{\partial \phi}{\partial x^1} \right) + \frac{\partial}{\partial x^2} \left(\sqrt{\frac{g_{11}}{g_{22}}} \frac{\partial \phi}{\partial x^2} \right) \right] \quad (3.857)$$

Equation (3.857) can now be linked with the system of generalised curvilinear coordinates discussed in Section 3.11.3.1 above. Substituting Equation (3.809) into Equation (3.857) gives:

$$\nabla^2 \phi' = \frac{1}{\sqrt{g_{22}}} \left[\frac{\partial}{\partial x^1} \left(\sqrt{g_{22}} \frac{\partial \phi'}{\partial x^1} \right) + \frac{\partial}{\partial x^2} \left(\sqrt{\frac{1}{g_{22}}} \frac{\partial \phi'}{\partial x^2} \right) \right] \quad (3.858)$$

Expansion of Equation (3.858) yields:

$$\nabla^2 \phi' = \frac{1}{\sqrt{g_{22}}} \left[\sqrt{g_{22}} \frac{\partial^2 \phi'}{\partial (x^1)^2} + \frac{\partial \phi'}{\partial x^1} \frac{\partial \sqrt{g_{22}}}{\partial x^1} + \frac{\partial \phi'}{\partial x^2} \frac{\partial}{\partial x^2} \left(\sqrt{\frac{1}{g_{22}}} \right) + \sqrt{\frac{1}{g_{22}}} \frac{\partial^2 \phi'}{\partial (x^2)^2} \right] \quad (3.859)$$

Substitution of Equations (3.838), (3.839), (3.840) and (3.841) into Equation (3.859) gives:

$$\nabla^2 \phi' = \frac{\partial^2 \phi'}{\partial (x^1)^2} + \frac{\partial^2 \phi'}{\partial (x^2)^2} + \mathbf{t} \cdot \frac{d\mathbf{n}}{ds} \frac{\partial \phi'}{\partial x^2} = \frac{\partial^2 \phi'}{\partial s^2} + \frac{\partial^2 \phi'}{\partial n^2} + \mathbf{t} \cdot \frac{d\mathbf{n}}{ds} \frac{\partial \phi'}{\partial n} \quad (3.860)$$

Using Equation (3.847) the following can be stated:

$$[\nabla \phi]_j = \phi_{,j} \quad (3.861)$$

The contravariant form of the tensor notation for gradients from Heinbockel (2001) can be used to state the following:

$$[\nabla(CC_g)]^i = g^{im} (CC_g)_{,m} \quad (3.862)$$

Using Equations (3.861) and (3.862) gives the following:

$$\nabla(CC_g) \cdot \nabla \phi = g^{im} (CC_g)_{,m} \phi_{,i} = g^{im} \frac{\partial(CC_g)}{\partial x^m} \frac{\partial \phi}{\partial x^i} \quad (3.863)$$

Equation (3.863) can be expanded as follows:

$$g^{im} \frac{\partial(CC_g)}{\partial x^m} \frac{\partial \phi}{\partial x^i} = g^{11} \frac{\partial(CC_g)}{\partial x^1} \frac{\partial \phi}{\partial x^1} + g^{12} \frac{\partial(CC_g)}{\partial x^2} \frac{\partial \phi}{\partial x^1} + g^{21} \frac{\partial(CC_g)}{\partial x^1} \frac{\partial \phi}{\partial x^2} + g^{22} \frac{\partial(CC_g)}{\partial x^2} \frac{\partial \phi}{\partial x^2} \quad (3.864)$$

Equation (3.864) can be rewritten to yield:

$$g^{im} \frac{\partial(CC_g)}{\partial x^m} \frac{\partial \phi}{\partial x^i} = (g_{11})^{-1} \frac{\partial(CC_g)}{\partial x^1} \frac{\partial \phi}{\partial x^1} + (g_{12})^{-1} \frac{\partial(CC_g)}{\partial x^2} \frac{\partial \phi}{\partial x^1} + (g_{21})^{-1} \frac{\partial(CC_g)}{\partial x^1} \frac{\partial \phi}{\partial x^2} + (g_{22})^{-1} \frac{\partial(CC_g)}{\partial x^2} \frac{\partial \phi}{\partial x^2} \quad (3.865)$$

Equation (3.865) can now be linked with the system of generalised curvilinear coordinates discussed in Section 3.11.3.1 above. Substituting Equations (3.809), (3.811) and (3.813) into Equation (3.865) gives:

$$g^{im} \frac{\partial(CC_g)}{\partial x^m} \frac{\partial \phi}{\partial x^i} = \frac{\partial(CC_g)}{\partial s} \frac{\partial \phi}{\partial s} + \left(1 + 2nt \cdot \frac{dn}{ds} + n^2 \left(\frac{dn}{ds} \right)^2 \right)^{-1} \frac{\partial(CC_g)}{\partial n} \frac{\partial \phi}{\partial n} \quad (3.866)$$

For $n=0$ this becomes:

$$g^{im} \frac{\partial(CC_g)}{\partial x^m} \frac{\partial \phi}{\partial x^i} = \frac{\partial(CC_g)}{\partial s} \frac{\partial \phi}{\partial s} + \frac{\partial(CC_g)}{\partial n} \frac{\partial \phi}{\partial n} \text{ at } n=0 \quad (3.867)$$

Using Equations (3.860) and (3.867) with Equation (3.845) gives a Non-Helmholtz elliptic extended mild-slope equation in generalised curvilinear coordinates:

$$\frac{\partial^2 \phi}{\partial s^2} + \frac{\partial^2 \phi}{\partial n^2} + t \cdot \frac{dn}{ds} \frac{\partial \phi}{\partial n} + (CC_g) \frac{\partial(CC_g)}{\partial s} \frac{\partial \phi}{\partial s} + (CC_g) \frac{\partial(CC_g)}{\partial n} \frac{\partial \phi}{\partial n} + K'^2 \phi = 0 \quad (3.868)$$

3.11.3.4 Parabolisation of Elliptic Mild-Slope Wave Equation in Generalised Curvilinear Coordinate System

The process for developing an absorbing downwave boundary for a generalised set of curvilinear coordinates is the same as that undertaken for Cartesian coordinates in Section 3.11.1. The elliptic equation in the generalised set of coordinates must be simplified into a parabolic approximation to the mild-slope equation in the generalised curvilinear coordinate system. A similar wave solution to that of Section 3.11.1 is examined. The same wave is selected although this time it must be expressed in Helmholtz form. Recalling Equation (3.135):

$$\phi = A_\phi e^{iS_\phi}$$

Also recalling Equation (3.721):

$$\frac{\phi'}{\sqrt{CC_g}} = \phi$$

Combining these two equations yields:

$$\frac{\phi'}{\sqrt{CC_g}} = A_\phi e^{iS_\phi} \quad (3.869)$$

Equation (3.869) may be rearranged as follows:

$$\phi' = \sqrt{CC_g} A_\phi e^{iS_\phi} \quad (3.870)$$

$$\phi' = A'_\phi e^{iS_\phi} \quad (3.871)$$

The first and second derivatives of the scaled velocity potential, ϕ' may now be obtained in the same fashion as those for the unscaled velocity potential, ϕ in Section 3.11.1.

$$\frac{\partial \phi'}{\partial n} = \frac{\partial A'_\phi}{\partial n} e^{iS_\phi} + i A'_\phi \frac{\partial S_\phi}{\partial n} e^{iS_\phi} \quad (3.872)$$

Equation (3.872) can be rewritten as:

$$\frac{\partial A'_\phi}{\partial n} e^{iS_\phi} = \frac{\partial \phi'}{\partial n} - i \phi' \frac{\partial S_\phi}{\partial n} \quad (3.873)$$

Substitution of Equation (3.871) into Equation (3.873) yields:

$$\frac{\partial \phi'}{\partial n} = \frac{\partial A'_\phi}{\partial n} \frac{\phi'}{A'_\phi} + i \phi' \frac{\partial S_\phi}{\partial n} \quad (3.874)$$

The second derivative of the scaled velocity potential with respect to n is:

$$\frac{\partial^2 \phi'}{\partial n^2} = \frac{\partial^2 A'_\phi}{\partial n^2} e^{iS_\phi} + 2i \frac{\partial A'_\phi}{\partial n} \frac{\partial S_\phi}{\partial n} e^{iS_\phi} + i A'_\phi \frac{\partial^2 S_\phi}{\partial n^2} e^{iS_\phi} - A'_\phi \frac{\partial S_\phi}{\partial n} \frac{\partial S_\phi}{\partial n} e^{iS_\phi} \quad (3.875)$$

Substitution of Equations (3.873) and (3.871) into Equation (3.875) gives:

$$\frac{\partial^2 \phi'}{\partial n^2} = \frac{\partial^2 A'_\phi}{\partial n^2} \frac{\phi'}{A'_\phi} + 2i \left(\frac{\partial \phi'}{\partial n} - i \phi' \frac{\partial S_\phi}{\partial n} \right) \frac{\partial S_\phi}{\partial n} + i \phi' \frac{\partial^2 S_\phi}{\partial n^2} - \phi' \frac{\partial S_\phi}{\partial n} \frac{\partial S_\phi}{\partial n} \quad (3.876)$$

$$\frac{\partial^2 \phi'}{\partial n^2} = \frac{\partial^2 A'_\phi}{\partial n^2} \frac{\phi'}{A'_\phi} + 2i \frac{\partial \phi'}{\partial n} \frac{\partial S_\phi}{\partial n} + \phi' \left(\frac{\partial S_\phi}{\partial n} \right)^2 + i \phi' \frac{\partial^2 S_\phi}{\partial n^2} \quad (3.877)$$

Substitution of Equation (3.877) into the Helmholtz form of the elliptic mild-slope solution of Equation (3.843) gives:

$$\frac{\partial^2 \phi'}{\partial s^2} + \frac{\partial^2 A'_\phi}{\partial n^2} \frac{\phi'}{A'_\phi} + 2i \frac{\partial \phi'}{\partial n} \frac{\partial S_\phi}{\partial n} + \phi' \left(\frac{\partial S_\phi}{\partial n} \right)^2 + i \phi' \frac{\partial^2 S_\phi}{\partial n^2} + \mathbf{t} \cdot \frac{d\mathbf{n}}{ds} \frac{\partial \phi'}{\partial n} + K^2 \phi' = 0 \quad (3.878)$$

Rearranging Equation (3.878) to isolate the derivative of the scaled velocity potential with respect to n yields:

$$\frac{\partial^2 \phi'}{\partial s^2} + \frac{\partial^2 A'_\phi}{\partial n^2} \frac{\phi'}{A'_\phi} + \frac{\partial \phi'}{\partial n} \left(2i \frac{\partial S_\phi}{\partial n} + \mathbf{t} \cdot \frac{d\mathbf{n}}{ds} \right) + \phi' \left(\frac{\partial S_\phi}{\partial n} \right)^2 + i \phi' \frac{\partial^2 S_\phi}{\partial n^2} + K^2 \phi' = 0 \quad (3.879)$$

$$\frac{\partial \phi'}{\partial n} \left(2i \frac{\partial S_\phi}{\partial n} + \mathbf{t} \cdot \frac{d\mathbf{n}}{ds} \right) = -\frac{\partial^2 \phi'}{\partial s^2} - \frac{\partial^2 A'_\phi}{\partial n^2} \frac{\phi'}{A'_\phi} - \phi' \left(\frac{\partial S_\phi}{\partial n} \right)^2 - i \phi' \frac{\partial^2 S_\phi}{\partial n^2} - K^2 \phi' \quad (3.880)$$

$$\frac{\partial \phi'}{\partial n} = \left(\mathbf{t} \cdot \frac{d\mathbf{n}}{ds} + 2i \frac{\partial S_\phi}{\partial n} \right)^{-1} \left[-\frac{\partial^2 A'_\phi}{\partial n^2} \frac{1}{A'_\phi} - \left(\frac{\partial S_\phi}{\partial n} \right)^2 - i \frac{\partial^2 S_\phi}{\partial n^2} - K^2 - \frac{\partial^2}{\partial s^2} \right] \phi' \quad (3.881)$$

Equation (3.881) may be rationalised by multiplying the right hand side of the equation by the complex conjugate of the inverse term in curved brackets:

$$\frac{\partial \phi'}{\partial n} = \psi \left(\mathbf{t} \cdot \frac{d\mathbf{n}}{ds} - 2i \frac{\partial S_\phi}{\partial n} \right) \left[-\frac{\partial^2 A'_\phi}{\partial n^2} \frac{1}{A'_\phi} - \left(\frac{\partial S_\phi}{\partial n} \right)^2 - i \frac{\partial^2 S_\phi}{\partial n^2} - K^2 - \frac{\partial^2}{\partial s^2} \right] \phi' \quad (3.882)$$

$$\psi = \frac{1}{\left(\mathbf{t} \cdot \frac{d\mathbf{n}}{ds} \right)^2 + 4 \left(\frac{\partial S_\phi}{\partial n} \right)^2} \quad (3.883)$$

As stated previously in Section 3.11.1. It can be assumed that at the downwave boundary where the wave is exiting the domain the shoaling and refraction process has caused the wave to be parallel to the beach boundary. This means the following assumption of Equation (3.648) can be made here also:

$$\frac{\partial S_\phi}{\partial n} = \kappa$$

Substituting Equation (3.648) into Equation (3.882) gives the following:

$$\frac{\partial \phi'}{\partial n} = \hat{\psi} \left(\mathbf{t} \cdot \frac{d\mathbf{n}}{ds} - 2i\kappa \right) \left[-\frac{\partial^2 A'_\phi}{\partial n^2} \frac{1}{A'_\phi} - \kappa^2 - i \frac{\partial \kappa}{\partial n} - K^2 - \frac{\partial^2}{\partial s^2} \right] \phi' \quad (3.884)$$

$$\hat{\psi} = \frac{1}{\left(\mathbf{t} \cdot \frac{d\mathbf{n}}{ds}\right)^2 + 4\kappa^2} \quad (3.885)$$

To finalise the creation of a parabolic approximation to the mild-slope equation the forward diffraction term in Equation (3.884) must now be dropped. This is the term containing the second derivative of the scaled amplitude of velocity potential (i.e. the first term inside the square brackets):

$$\frac{\partial \phi'}{\partial n} = \hat{\psi} \left(\mathbf{t} \cdot \frac{d\mathbf{n}}{ds} - 2i\kappa \right) \left[-\kappa^2 - i \frac{\partial \kappa}{\partial n} - K^2 - \frac{\partial^2}{\partial s^2} \right] \phi' \quad (3.886)$$

Equation (3.886) is an expression of $\frac{\partial \phi'}{\partial n}$ in a generalised set of curvilinear coordinates, after Clyne (2008), and hence can be used for absorbing downwave boundary condition where the boundary is not of straight line shape. Equation (3.886) may be expressed more succinctly as:

$$\frac{\partial \phi'}{\partial n} = \hat{\psi} (\Upsilon - 2i\kappa) \left[-\kappa^2 - i \frac{\partial \kappa}{\partial n} - K^2 - \frac{\partial^2}{\partial s^2} \right] \phi' \quad (3.887)$$

Where:

$$\Upsilon = \mathbf{t} \cdot \frac{d\mathbf{n}}{ds} \quad (3.888)$$

$$\hat{\psi} = \frac{1}{\Upsilon^2 + 4\kappa^2} \quad (3.889)$$

If Equation (3.648) was not substituted into Equation (3.882) a more general form of Equation (3.887) would be obtained:

$$\frac{\partial \phi'}{\partial n} = \hat{\psi} \left(\Upsilon - 2i \frac{\partial S_\phi}{\partial n} \right) \left[- \left(\frac{\partial S_\phi}{\partial n} \right)^2 - i \frac{\partial^2 S_\phi}{\partial n^2} - K^2 - \frac{\partial^2}{\partial s^2} \right] \phi' \quad (3.890)$$

3.11.3.5 Alternative Parabolisation in General Coordinate System

An alternative simpler parabolic solution can be obtained if the gradient of A'_ϕ with respect to n is considered negligible Equation (3.874). This would lead to the following equation:

$$\frac{\partial \phi'}{\partial n} = i\phi' \frac{\partial S_\phi}{\partial n} \quad (3.891)$$

Similarly the second derivative of the scaled velocity potential with respect to n would now become:

$$\frac{\partial^2 \phi'}{\partial n^2} = iA'_\phi \frac{\partial^2 S_\phi}{\partial n^2} e^{iS_\phi} - A'_\phi \frac{\partial S_\phi}{\partial n} \frac{\partial S_\phi}{\partial n} e^{iS_\phi} \quad (3.892)$$

Substitution of Equations (3.873) and (3.871) into Equation (3.892) gives:

$$\frac{\partial^2 \phi'}{\partial n^2} = i\phi' \frac{\partial^2 S_\phi}{\partial n^2} - \phi' \frac{\partial S_\phi}{\partial n} \frac{\partial S_\phi}{\partial n} \quad (3.893)$$

$$\frac{\partial^2 \phi'}{\partial n^2} = \phi' \left(\frac{\partial S_\phi}{\partial n} \right)^2 + i\phi' \frac{\partial^2 S_\phi}{\partial n^2} \quad (3.894)$$

Substitution of Equation (3.877) into the Helmholtz form of the elliptic mild-slope solution of Equation (3.843) gives:

$$\frac{\partial^2 \phi'}{\partial s^2} + \phi' \left(\frac{\partial S_\phi}{\partial n} \right)^2 + i\phi' \frac{\partial^2 S_\phi}{\partial n^2} + \mathbf{t} \cdot \frac{d\mathbf{n}}{ds} \frac{\partial \phi'}{\partial n} + K^2 \phi' = 0 \quad (3.895)$$

Rearranging Equation (3.895) to isolate the derivative of the scaled velocity potential with respect to n yields:

$$-\mathbf{t} \cdot \frac{d\mathbf{n}}{ds} \frac{\partial \phi'}{\partial n} = \frac{\partial^2 \phi'}{\partial s^2} + \phi' \left(\frac{\partial S_\phi}{\partial n} \right)^2 + i\phi' \frac{\partial^2 S_\phi}{\partial n^2} + K^2 \phi' \quad (3.896)$$

$$\frac{\partial \phi'}{\partial n} = \left(\mathbf{t} \cdot \frac{d\mathbf{n}}{ds} \right)^{-1} \left[-\frac{\partial^2 \phi'}{\partial s^2} - \phi' \left(\frac{\partial S_\phi}{\partial n} \right)^2 - i\phi' \frac{\partial^2 S_\phi}{\partial n^2} - K^2 \phi' \right] \quad (3.897)$$

Equation (3.897) is an slightly less computationally demanding expression of $\frac{\partial \phi'}{\partial n}$ than

Equation (3.886). It can also be used for absorbing downwave boundary conditions where the boundary is not of straight line shape. Equation (3.897) can be expressed as:

$$\frac{\partial \phi'}{\partial n} = \frac{1}{\Upsilon} \left[-\left(\frac{\partial S_\phi}{\partial n} \right)^2 - i \frac{\partial^2 S_\phi}{\partial n^2} - K^2 - \frac{\partial^2}{\partial s^2} \right] \phi' \quad (3.898)$$

3.11.3.6 Parabolisation of Non-Helmholtz Elliptic Mild-Slope Wave Equation in Generalised Curvilinear Coordinate System

The process for developing an absorbing downwave boundary for a generalised set of curvilinear coordinates is the same as that undertaken for Cartesian coordinates in Section 3.11.1. The Non-Helmholtz style elliptic equation in the generalised set of coordinates must be simplified into a parabolic approximation to the mild-slope equation in the generalised curvilinear coordinate system. A similar wave solution to that of Section 3.11.1 is examined. Recalling Equation (3.135):

$$\phi = A_\phi e^{iS_\phi}$$

The first and second derivatives of the velocity potential, ϕ may now be obtained as follows:

$$\frac{\partial \phi}{\partial n} = \frac{\partial A_\phi}{\partial n} e^{iS_\phi} + iA_\phi \frac{\partial S_\phi}{\partial n} e^{iS_\phi} \quad (3.899)$$

Equation (3.899) can be rewritten as:

$$\frac{\partial A_\phi}{\partial n} e^{iS_\phi} = \frac{\partial \phi}{\partial n} - i\phi \frac{\partial S_\phi}{\partial n} \quad (3.900)$$

Using Equation (3.135) with Equation (3.900) yields:

$$\frac{\partial \phi}{\partial n} = \frac{\partial A_\phi}{\partial n} \frac{\phi}{A_\phi} + i\phi \frac{\partial S_\phi}{\partial n} \quad (3.901)$$

The second derivative of the scaled velocity potential with respect to n is:

$$\frac{\partial^2 \phi}{\partial n^2} = \frac{\partial^2 A_\phi}{\partial n^2} e^{iS_\phi} + 2i \frac{\partial A_\phi}{\partial n} \frac{\partial S_\phi}{\partial n} e^{iS_\phi} + iA_\phi \frac{\partial^2 S_\phi}{\partial n^2} e^{iS_\phi} - A_\phi \frac{\partial S_\phi}{\partial n} \frac{\partial S_\phi}{\partial n} e^{iS_\phi} \quad (3.902)$$

Substitution of Equations (3.900) and (3.901) into Equation (3.902) gives:

$$\frac{\partial^2 \phi}{\partial n^2} = \frac{\partial^2 A_\phi}{\partial n^2} \frac{\phi}{A_\phi} + 2i \left(\frac{\partial \phi}{\partial n} - i\phi \frac{\partial S_\phi}{\partial n} \right) \frac{\partial S_\phi}{\partial n} + i\phi \frac{\partial^2 S_\phi}{\partial n^2} - \phi \frac{\partial S_\phi}{\partial n} \frac{\partial S_\phi}{\partial n} \quad (3.903)$$

$$\frac{\partial^2 \phi}{\partial n^2} = \frac{\partial^2 A_\phi}{\partial n^2} \frac{\phi}{A_\phi} + 2i \frac{\partial \phi}{\partial n} \frac{\partial S_\phi}{\partial n} + \phi \left(\frac{\partial S_\phi}{\partial n} \right)^2 + i\phi \frac{\partial^2 S_\phi}{\partial n^2} \quad (3.904)$$

Substitution of Equation (3.904) into the elliptic mild-slope solution of Equation (3.868) gives:

$$\begin{aligned} & \frac{\partial^2 \phi}{\partial s^2} + \frac{\partial^2 A_\phi}{\partial n^2} \frac{\phi}{A_\phi} + 2i \frac{\partial \phi}{\partial n} \frac{\partial S_\phi}{\partial n} + \phi \left(\frac{\partial S_\phi}{\partial n} \right)^2 + i \phi \frac{\partial^2 S_\phi}{\partial n^2} \\ & + \mathbf{t} \cdot \frac{d\mathbf{n}}{ds} \frac{\partial \phi}{\partial n} + (CC_g) \frac{\partial(CC_g)}{\partial s} \frac{\partial \phi}{\partial s} + (CC_g) \frac{\partial(CC_g)}{\partial n} \frac{\partial \phi}{\partial n} + K'^2 \phi = 0 \end{aligned} \quad (3.905)$$

Rearranging Equation (3.905) to isolate the derivative of the scaled velocity potential with respect to n yields:

$$\begin{aligned} & \frac{\partial^2 \phi}{\partial s^2} + \frac{\partial^2 A_\phi}{\partial n^2} \frac{\phi}{A_\phi} + \phi \left(\frac{\partial S_\phi}{\partial n} \right)^2 + i \phi \frac{\partial^2 S_\phi}{\partial n^2} + (CC_g) \frac{\partial(CC_g)}{\partial s} \frac{\partial \phi}{\partial s} + K'^2 \phi \\ & = -2i \frac{\partial \phi}{\partial n} \frac{\partial S_\phi}{\partial n} - \mathbf{t} \cdot \frac{d\mathbf{n}}{ds} \frac{\partial \phi}{\partial n} - (CC_g) \frac{\partial(CC_g)}{\partial n} \frac{\partial \phi}{\partial n} \end{aligned} \quad (3.906)$$

$$\begin{aligned} & \frac{\partial \phi}{\partial n} \left(2i \frac{\partial S_\phi}{\partial n} + \mathbf{t} \cdot \frac{d\mathbf{n}}{ds} + CC_g \frac{\partial(CC_g)}{\partial n} \right) \\ & = - \frac{\partial^2 \phi}{\partial s^2} - \frac{\partial^2 A_\phi}{\partial n^2} \frac{\phi}{A_\phi} - \phi \left(\frac{\partial S_\phi}{\partial n} \right)^2 - i \phi \frac{\partial^2 S_\phi}{\partial n^2} - (CC_g) \frac{\partial(CC_g)}{\partial s} \frac{\partial \phi}{\partial s} - K'^2 \phi \end{aligned} \quad (3.907)$$

$$\frac{\partial \phi}{\partial n} = \left(2i \frac{\partial S_\phi}{\partial n} + \mathbf{t} \cdot \frac{d\mathbf{n}}{ds} + CC_g \frac{\partial(CC_g)}{\partial n} \right)^{-1} \left[\begin{aligned} & - \frac{\partial^2 \phi}{\partial s^2} - \frac{\partial^2 A_\phi}{\partial n^2} \frac{\phi}{A_\phi} - \phi \left(\frac{\partial S_\phi}{\partial n} \right)^2 \\ & - i \phi \frac{\partial^2 S_\phi}{\partial n^2} - (CC_g) \frac{\partial(CC_g)}{\partial s} \frac{\partial \phi}{\partial s} - K'^2 \phi \end{aligned} \right] \quad (3.908)$$

As stated previously in Section 3.11.1. It can be assumed that at the downwave boundary where the wave is exiting the domain the shoaling and refraction process has caused the wave to be parallel to the beach boundary. This means the following assumption of Equation (3.648) can be made here also:

$$\frac{\partial S_\phi}{\partial n} = \kappa$$

Substituting Equation (3.648) into Equation (3.908) gives the following:

$$\frac{\partial \phi}{\partial n} = \left(2i\kappa + \mathbf{t} \cdot \frac{d\mathbf{n}}{ds} + CC_g \frac{\partial(CC_g)}{\partial n} \right)^{-1} \left[\begin{aligned} & - \frac{\partial^2 A_\phi}{\partial n^2} \frac{\phi}{A_\phi} - \phi \kappa^2 - i \phi \frac{\partial \kappa}{\partial n} \\ & - K'^2 \phi - \frac{\partial^2 \phi}{\partial s^2} - (CC_g) \frac{\partial(CC_g)}{\partial s} \frac{\partial \phi}{\partial s} \end{aligned} \right] \quad (3.909)$$

To finalise the creation of a parabolic approximation to the mild-slope equation the forward diffraction term in Equation (3.909) must now be dropped. This is the term containing the second derivative of the amplitude of velocity potential (i.e. the first term inside the square brackets):

$$\frac{\partial \phi}{\partial n} = \left(2i\kappa + \mathbf{t} \cdot \frac{d\mathbf{n}}{ds} + CC_g \frac{\partial(CC_g)}{\partial n} \right)^{-1} \begin{bmatrix} -\phi\kappa^2 - i\phi \frac{\partial \kappa}{\partial n} - K'^2 \phi - \frac{\partial^2 \phi}{\partial s^2} \\ -(CC_g) \frac{\partial(CC_g)}{\partial s} \frac{\partial \phi}{\partial s} \end{bmatrix} \quad (3.910)$$

Equation (3.910) is an expression of $\frac{\partial \phi}{\partial n}$ in a generalised set of curvilinear coordinates. It

can be used for absorbing downwave boundary condition where the boundary is not of straight line shape. Equation (3.910) may be expressed more succinctly as:

$$\frac{\partial \phi}{\partial n} = \left(2i\kappa + \Upsilon + CC_g \frac{\partial(CC_g)}{\partial n} \right)^{-1} \begin{bmatrix} -\phi\kappa^2 - i\phi \frac{\partial \kappa}{\partial n} - K'^2 \phi - \frac{\partial^2 \phi}{\partial s^2} \\ -(CC_g) \frac{\partial(CC_g)}{\partial s} \frac{\partial \phi}{\partial s} \end{bmatrix} \quad (3.911)$$

Where:

$$\Upsilon = \mathbf{t} \cdot \frac{d\mathbf{n}}{ds} \quad (3.912)$$

If Equation (3.648) was not substituted into Equation (3.908) a more general form of Equation (3.911) would be obtained:

$$\frac{\partial \phi}{\partial n} = \left(2i \frac{\partial S_\phi}{\partial n} + \Upsilon + CC_g \frac{\partial(CC_g)}{\partial n} \right)^{-1} \begin{bmatrix} -\phi \left(\frac{\partial S_\phi}{\partial n} \right)^2 - i\phi \frac{\partial^2 S_\phi}{\partial n^2} - K'^2 \phi - \frac{\partial^2 \phi}{\partial s^2} \\ -(CC_g) \frac{\partial(CC_g)}{\partial s} \frac{\partial \phi}{\partial s} \end{bmatrix} \quad (3.913)$$

3.11.3.7 Absorbing Parabolic Downwave Boundary Condition

Using Equation (3.887) it is now possible to examine how the boundary terms of Equation (3.754) would be affected by an absorbing parabolic downwave boundary condition in general curvilinear coordinates, Γ_2 :

$$\int_S W^I \frac{\partial \phi'}{\partial n} dS = \int_{\Gamma_2} W^I \left\{ \hat{\psi} (\Upsilon - 2i\kappa) \left[-\kappa^2 - i \frac{\partial \kappa}{\partial n} - K^2 - \frac{\partial^2}{\partial s^2} \right] \right\} \phi' dS \quad (3.914)$$

Equation (3.914) can be expanded to:

$$\int_S W^I \frac{\partial \phi'}{\partial n} dS = \int_{\Gamma_2} W^I \left\{ \hat{\psi} \left[\begin{aligned} &-\Upsilon \kappa^2 \phi' - i \Upsilon \frac{\partial \kappa}{\partial n} \phi' - \Upsilon K^2 \phi' - \Upsilon \frac{\partial^2 \phi'}{\partial s^2} \\ &+ 2i \kappa^3 \phi' - 2 \kappa \frac{\partial \kappa}{\partial n} \phi' + 2i \kappa K^2 \phi' + 2i \kappa \frac{\partial^2 \phi'}{\partial s^2} \end{aligned} \right] \right\} dS \quad (3.915)$$

Equation (3.915) can now be expanded to explicitly express the velocity potential in terms of its real and imaginary components:

$$\phi' = \phi'_1 + i \phi'_2 \quad (3.916)$$

Substituting Equation (3.916) into Equation (3.915) yields:

$$\int_S W^I \frac{\partial \phi'}{\partial n} dS = \int_{\Gamma_2} W^I \left\{ \hat{\psi} \left[\begin{aligned} &-\Upsilon \kappa^2 (\phi'_1 + i \phi'_2) - i \Upsilon \frac{\partial \kappa}{\partial n} (\phi'_1 + i \phi'_2) \\ &-\Upsilon K^2 (\phi'_1 + i \phi'_2) - \Upsilon \frac{\partial^2}{\partial s^2} (\phi'_1 + i \phi'_2) \\ &+ 2i \kappa^3 (\phi'_1 + i \phi'_2) - 2 \kappa \frac{\partial \kappa}{\partial n} (\phi'_1 + i \phi'_2) \\ &+ 2i \kappa K^2 (\phi'_1 + i \phi'_2) + 2i \kappa \frac{\partial^2}{\partial s^2} (\phi'_1 + i \phi'_2) \end{aligned} \right] \right\} dS \quad (3.917)$$

Expansion of Equation (3.917) gives the following:

$$\int_S W^I \frac{\partial \phi'}{\partial n} dS = \int_{\Gamma_2} W^I \left\{ \hat{\psi} \left[\begin{aligned} &-\Upsilon \kappa^2 \phi'_1 - i \Upsilon \kappa^2 \phi'_2 - i \Upsilon \frac{\partial \kappa}{\partial n} \phi'_1 + \Upsilon \frac{\partial \kappa}{\partial n} \phi'_2 \\ &-\Upsilon K^2 \phi'_1 - i \Upsilon K^2 \phi'_2 - \Upsilon \frac{\partial^2 \phi'_1}{\partial s^2} - i \Upsilon \frac{\partial^2 \phi'_2}{\partial s^2} \\ &+ 2i \kappa^3 \phi'_1 - 2 \kappa^3 \phi'_2 - 2 \kappa \frac{\partial \kappa}{\partial n} \phi'_1 - 2i \kappa \frac{\partial \kappa}{\partial n} \phi'_2 \\ &+ 2i \kappa K^2 \phi'_1 - 2 \kappa K^2 \phi'_2 + 2i \kappa \frac{\partial^2 \phi'_1}{\partial s^2} - 2 \kappa \frac{\partial^2 \phi'_2}{\partial s^2} \end{aligned} \right] \right\} dS \quad (3.918)$$

The real portion of Equation (3.918) may then be examined as it will be the only part required for the finite element solution scheme:

Real:

$$\int_S W^I \frac{\partial \phi'_1}{\partial n} dS = \int_{\Gamma_2} W^I \left\{ \hat{\psi} \begin{bmatrix} -\Upsilon \kappa^2 \phi'_1 + \Upsilon \frac{\partial \kappa}{\partial n} \phi'_2 - \Upsilon K^2 \phi'_1 - \Upsilon \frac{\partial^2 \phi'_1}{\partial s^2} \\ -2\kappa^3 \phi'_2 - 2\kappa \frac{\partial \kappa}{\partial n} \phi'_1 - 2\kappa K^2 \phi'_2 - 2\kappa \frac{\partial^2 \phi'_2}{\partial s^2} \end{bmatrix} \right\} dS \quad (3.919)$$

3.11.3.8 Absorbing Parabolic Downwave Boundary Condition for Simpler Condition

Using Equation (3.898) it is now possible to examine how the boundary terms of Equation (3.754) would be affected by an absorbing parabolic downwave boundary condition in general curvilinear coordinates, Γ_2 :

$$\frac{\partial \phi'}{\partial n} = \frac{1}{Y} \left[- \left(\frac{\partial S_\phi}{\partial n} \right)^2 - i \frac{\partial^2 S_\phi}{\partial n^2} - K^2 - \frac{\partial^2}{\partial s^2} \right] \phi'$$

$$\int_s W^I \frac{\partial \phi'}{\partial n} dS = \int_{\Gamma_2} W^I \left\{ \frac{1}{Y} \left[- \left(\frac{\partial S_\phi}{\partial n} \right)^2 - i \frac{\partial^2 S_\phi}{\partial n^2} - K^2 - \frac{\partial^2}{\partial s^2} \right] \right\} \phi' dS \quad (3.920)$$

Equation (3.920) can now be expanded to explicitly express the velocity potential in terms of its real and imaginary components:

$$\phi' = \phi'_1 + i\phi'_2 \quad (3.921)$$

Substituting Equation (3.921) into Equation (3.920) yields:

$$\int_s W^I \frac{\partial \phi'}{\partial n} dS = \int_{\Gamma_2} W^I \left\{ \frac{1}{Y} \left[- \left(\frac{\partial S_\phi}{\partial n} \right)^2 (\phi'_1 + i\phi'_2) - i \frac{\partial^2 S_\phi}{\partial n^2} (\phi'_1 + i\phi'_2) \right. \right. \\ \left. \left. - K^2 (\phi'_1 + i\phi'_2) - \frac{\partial^2}{\partial s^2} (\phi'_1 + i\phi'_2) \right] \right\} dS \quad (3.922)$$

Expansion of Equation (3.922) gives the following:

$$\int_s W^I \frac{\partial \phi'}{\partial n} dS = \int_{\Gamma_2} W^I \left\{ \frac{1}{Y} \left[- \left(\frac{\partial S_\phi}{\partial n} \right)^2 \phi'_1 - i \left(\frac{\partial S_\phi}{\partial n} \right)^2 \phi'_2 - i \frac{\partial^2 S_\phi}{\partial n^2} \phi'_1 + \frac{\partial^2 S_\phi}{\partial n^2} \phi'_2 \right. \right. \\ \left. \left. - K^2 \phi'_1 - i K^2 \phi'_2 - \frac{\partial^2 \phi'_1}{\partial s^2} - i \frac{\partial^2 \phi'_2}{\partial s^2} \right] \right\} dS \quad (3.923)$$

The real portion of Equation (3.923) may then be examined as it will be the only part required for the finite element solution scheme:

Real:

$$\int_s W^I \frac{\partial \phi'_1}{\partial n} dS = \int_{\Gamma_2} W^I \left\{ \frac{1}{Y} \left[- \left(\frac{\partial S_\phi}{\partial n} \right)^2 \phi'_1 + \frac{\partial^2 S_\phi}{\partial n^2} \phi'_2 - K^2 \phi'_1 - \frac{\partial^2 \phi'_1}{\partial s^2} \right] \right\} dS \quad (3.924)$$

3.11.4 Radiation Boundary Condition

The simplest way of applying a specific wave to a two-dimensional domain of this finite element wave model is to specify the velocity potential along any boundary through which waves are entering the domain. However, as discussed in Section 2.4.1.3.3.2 above, the elliptic solution to the mild-slope wave equation allows wave propagation (and therefore dissipation) in any direction. Hence some backscattered or reflected waves will be expected to approach any boundary through which waves are entering the domain. Clyne (2008) develops a radiation boundary condition that allows this backscattered wave energy to exit the modelled domain. Following the work of Kirby (1989) and Xu *et al.* (1996) this method utilises a parabolic approximation to the mild-slope equation to absorb excess wave energy above that of the incoming wave. This method assumes the crests of the backscattered waves are approximately parallel to the boundary in question. For an adequately sized finite element domain this is considered to be a reasonable assumption.

The basic concept on which the radiation condition is based is that the velocity potential along the boundary is a sum of the velocity potential of the incoming wave and that of the outgoing (backscattered) wave:

$$\phi' = \phi'^{in} + \phi'^{out} \quad (3.925)$$

Rearranging Equation (3.925) in terms of the outgoing velocity potential gives:

$$\phi'^{out} = \phi' - \phi'^{in} \quad (3.926)$$

The outgoing potential will be absorbed by using a parabolic equation. This is similar to the process used at the beach boundary except in that case the entire potential is absorbed, at the radiating boundary only the outgoing potential is absorbed.

Expressing the derivative of the outgoing velocity potential with respect to the outward pointing normal of the domain as a function f' yields:

$$\frac{\partial \phi'^{out}}{\partial n} = f'(\phi'^{out}) = \frac{\partial}{\partial n}(\phi' - \phi'^{in}) = f'(\phi' - \phi'^{in}) \quad (3.927)$$

Equation (3.927) may now be rewritten as:

$$\frac{\partial \phi'}{\partial n} - \frac{\partial \phi'^{in}}{\partial n} = f'(\phi'^{out}) \quad (3.928)$$

$$\frac{\partial \phi'}{\partial n} = f'(\phi') - f'(\phi'^{in}) + \frac{\partial \phi'^{in}}{\partial n} \quad (3.929)$$

Equation (3.887) is an absorbing boundary equation for ϕ' . In this case ϕ' will be replaced with $\phi'^{out} (= \phi' - \phi'^{in})$ because only the outgoing wave should be absorbed on the radiating boundary. Using ϕ' and ϕ'^{in} with Equation (3.887) gives:

$$f'(\phi') = \hat{\psi}(\Psi - 2i\kappa) \left[-\kappa^2 - i \frac{\partial \kappa}{\partial n} - K^2 - \frac{\partial^2}{\partial s^2} \right] \phi' \quad (3.930)$$

$$f'(\phi'^{in}) = \hat{\psi}(\Psi - 2i\kappa) \left[-\kappa^2 - i \frac{\partial \kappa}{\partial n} - K^2 - \frac{\partial^2}{\partial s^2} \right] \phi'^{in} \quad (3.931)$$

Expansion of Equations (3.930) and (3.931) gives:

$$f'(\phi') = \left\{ \hat{\psi} \left[\begin{aligned} & -\Upsilon \kappa^2 \phi' - i \Upsilon \frac{\partial \kappa}{\partial n} \phi' - \Upsilon K^2 \phi' - \Upsilon \frac{\partial^2 \phi'}{\partial s^2} \\ & + 2i \kappa^3 \phi' - 2 \kappa \frac{\partial \kappa}{\partial n} \phi' + 2i \kappa K^2 \phi' + 2i \kappa \frac{\partial^2 \phi'}{\partial s^2} \end{aligned} \right] \right\} \quad (3.932)$$

$$f'(\phi'^{in}) = \left\{ \hat{\psi} \left[\begin{aligned} & -\Upsilon \kappa^2 \phi'^{in} - i \Upsilon \frac{\partial \kappa}{\partial n} \phi'^{in} - \Upsilon K^2 \phi'^{in} - \Upsilon \frac{\partial^2 \phi'^{in}}{\partial s^2} \\ & + 2i \kappa^3 \phi'^{in} - 2 \kappa \frac{\partial \kappa}{\partial n} \phi'^{in} + 2i \kappa K^2 \phi'^{in} + 2i \kappa \frac{\partial^2 \phi'^{in}}{\partial s^2} \end{aligned} \right] \right\} \quad (3.933)$$

Substituting Equations (3.932) and (3.933) into Equation (3.929) gives:

$$\begin{aligned} \frac{\partial \phi'}{\partial n} = & \left\{ \hat{\psi} \left[\begin{aligned} & -\Upsilon \kappa^2 \phi' - i \Upsilon \frac{\partial \kappa}{\partial n} \phi' - \Upsilon K^2 \phi' - \Upsilon \frac{\partial^2 \phi'}{\partial s^2} \\ & + 2i \kappa^3 \phi' - 2 \kappa \frac{\partial \kappa}{\partial n} \phi' + 2i \kappa K^2 \phi' + 2i \kappa \frac{\partial^2 \phi'}{\partial s^2} \end{aligned} \right] \right\} \\ & - \left\{ \hat{\psi} \left[\begin{aligned} & -\Upsilon \kappa^2 \phi'^{in} - i \Upsilon \frac{\partial \kappa}{\partial n} \phi'^{in} - \Upsilon K^2 \phi'^{in} - \Upsilon \frac{\partial^2 \phi'^{in}}{\partial s^2} \\ & + 2i \kappa^3 \phi'^{in} - 2 \kappa \frac{\partial \kappa}{\partial n} \phi'^{in} + 2i \kappa K^2 \phi'^{in} + 2i \kappa \frac{\partial^2 \phi'^{in}}{\partial s^2} \end{aligned} \right] \right\} + \frac{\partial \phi'^{in}}{\partial n} \end{aligned} \quad (3.934)$$

Equation (3.934) may now be separated into real and imaginary components using Equation (3.916):

Real:

$$\begin{aligned} \frac{\partial \phi'_1}{\partial n} = & \hat{\psi} \left[\begin{aligned} & -\Upsilon \kappa^2 \phi'_1 + \Upsilon \frac{\partial \kappa}{\partial n} \phi'_2 - \Upsilon K^2 \phi'_1 - \Upsilon \frac{\partial^2 \phi'_1}{\partial s^2} \\ & -2\kappa^3 \phi'_2 - 2\kappa \frac{\partial \kappa}{\partial n} \phi'_1 - 2\kappa K^2 \phi'_2 - 2\kappa \frac{\partial^2 \phi'_2}{\partial s^2} \end{aligned} \right] + \\ & -\hat{\psi} \left[\begin{aligned} & -\Upsilon \kappa^2 \phi'^{in}_1 + \Upsilon \frac{\partial \kappa}{\partial n} \phi'^{in}_2 - \Upsilon K^2 \phi'^{in}_1 - \Upsilon \frac{\partial^2 \phi'^{in}_1}{\partial s^2} \\ & -2\kappa^3 \phi'^{in}_2 - 2\kappa \frac{\partial \kappa}{\partial n} \phi'^{in}_1 - 2\kappa K^2 \phi'^{in}_2 - 2\kappa \frac{\partial^2 \phi'^{in}_2}{\partial s^2} \end{aligned} \right] + \frac{\partial \phi'^{in}_1}{\partial n} \end{aligned} \quad (3.935)$$

Imaginary:

$$\begin{aligned} \frac{\partial \phi'_2}{\partial n} = & \hat{\psi} \left[\begin{aligned} & -\Upsilon \kappa^2 \phi'_2 - \Upsilon \frac{\partial \kappa}{\partial n} \phi'_1 - \Upsilon K^2 \phi'_2 - \Upsilon \frac{\partial^2 \phi'_2}{\partial s^2} \\ & +2\kappa^3 \phi'_1 - 2\kappa \frac{\partial \kappa}{\partial n} \phi'_2 + 2\kappa K^2 \phi'_1 + 2\kappa \frac{\partial^2 \phi'_1}{\partial s^2} \end{aligned} \right] \\ & -\hat{\psi} \left[\begin{aligned} & -\Upsilon \kappa^2 \phi'^{in}_2 - \Upsilon \frac{\partial \kappa}{\partial n} \phi'^{in}_1 - \Upsilon K^2 \phi'^{in}_2 - \Upsilon \frac{\partial^2 \phi'^{in}_2}{\partial s^2} \\ & +2\kappa^3 \phi'^{in}_1 - 2\kappa \frac{\partial \kappa}{\partial n} \phi'^{in}_2 + 2\kappa K^2 \phi'^{in}_1 + 2\kappa \frac{\partial^2 \phi'^{in}_1}{\partial s^2} \end{aligned} \right] + \frac{\partial \phi'^{in}_2}{\partial n} \end{aligned} \quad (3.936)$$

Equation (3.935) can now be used with the boundary term of Equation (3.754) to provide a boundary condition for a radiation boundary, Γ_3 :

$$\begin{aligned} \int_S W^I \frac{\partial \phi'_1}{\partial n} dS = & \int_{\Gamma_3} W^I \left\{ \hat{\psi} \left[\begin{aligned} & -\Upsilon \kappa^2 \phi'_1 + \Upsilon \frac{\partial \kappa}{\partial n} \phi'_2 - \Upsilon K^2 \phi'_1 - \Upsilon \frac{\partial^2 \phi'_1}{\partial s^2} \\ & -2\kappa^3 \phi'_2 - 2\kappa \frac{\partial \kappa}{\partial n} \phi'_1 - 2\kappa K^2 \phi'_2 - 2\kappa \frac{\partial^2 \phi'_2}{\partial s^2} \end{aligned} \right] \right\} dS \\ & - \int_{\Gamma_3} W^I \left\{ \hat{\psi} \left[\begin{aligned} & -\Upsilon \kappa^2 \phi'^{in}_1 + \Upsilon \frac{\partial \kappa}{\partial n} \phi'^{in}_2 - \Upsilon K^2 \phi'^{in}_1 - \Upsilon \frac{\partial^2 \phi'^{in}_1}{\partial s^2} \\ & -2\kappa^3 \phi'^{in}_2 - 2\kappa \frac{\partial \kappa}{\partial n} \phi'^{in}_1 - 2\kappa K^2 \phi'^{in}_2 - 2\kappa \frac{\partial^2 \phi'^{in}_2}{\partial s^2} \end{aligned} \right] \right\} dS \\ & + \int_{\Gamma_3} W^I \left\{ \frac{\partial \phi'^{in}_1}{\partial n} \right\} dS \end{aligned} \quad (3.937)$$

3.11.4.1 Incident Potential and Gradients

It is apparent that in order to utilise the radiating boundary condition of Equation (3.937) the incident potential and its gradients must be known. Vincent *et al.* (2002) give the following formula for wave height in the surf zone:

$$H = H_0 K_R K_S \quad (3.938)$$

where H is the wave height at a downwave point, K_R is the refraction coefficient, K_S is the shoaling coefficient and H_0 is the deep-water wave height.

In the case of incident wave height Equation (3.938) becomes:

$$H^{in} = H_0^{in} K_R K_S \quad (3.939)$$

The refraction coefficient K_R relates the wave angle at a given point to the deep-water wave angle. The relationship is given by Vincent *et al.* (2002) as follows:

$$K_R = \sqrt{\frac{\cos \alpha_0}{\cos \alpha}} \quad (3.940)$$

The wave angle at any given downwave point can be obtained using Snell's law. Snell's law relates the wave angle at a downwave point with the deep-water wave angle using the wave celerity and deep-water celerity as follows:

$$\frac{\sin \alpha}{C} = \frac{\sin \alpha_0}{C_0} = \text{constant} \quad (3.941)$$

The shoaling coefficient in Equation (3.939) may be obtained from the wave celerity and deep-water celerity using the following equation from Vincent *et al.* (2002):

$$K_S = \sqrt{\frac{C_0}{2nC}}, \text{ where } n = \frac{1}{2} \left(1 + \frac{2\kappa h'}{\sinh(2\kappa h')} \right) \quad (3.942)$$

Knowing the wave height on the boundary in question it is now necessary to use the calculated wave height and known period at the boundary to the incoming velocity potential on the boundary. Using the form of velocity potential from Equation (3.870) the following can be stated:

$$\phi'^{in} = \sqrt{CC_g} A_\phi^{in} e^{iS_\phi^{in}} \quad (3.943)$$

Equation (3.118) in the absence of current and energy dissipation is:

$$i\omega\tilde{\phi} - g\zeta' = 0 \text{ at } z = \bar{\eta} \quad (3.944)$$

Equation (3.944) implies that:

$$|\zeta'| = \frac{\omega}{g} |\tilde{\phi}| \quad (3.945)$$

Therefore the amplitude of velocity potential can be related to the wave height as follows:

$$H^{in} = 2A_{\zeta}^{in} = 2\left(\frac{\omega}{g} A_{\phi}^{in}\right) \quad (3.946)$$

Manipulation of Equation (3.946) gives:

$$A_{\phi}^{in} = \frac{gH^{in}}{2\omega} \quad (3.947)$$

Substituting Equation (3.947) into Equation (3.943) gives:

$$\phi'^{in} = \sqrt{CC_g} \frac{gH^{in}}{2\omega} e^{iS_{\phi}^{in}} = \sqrt{CC_g} \frac{gH^{in}}{2\omega} e^{i\int_{x_0}^x \kappa_1 dx + \kappa_2 y} \quad (3.948)$$

The integration from x_0 to x_1 is an integration in the direction of wave propagation. For the case of the origin at the beach this amounts to an integration in the negative x direction. Equation (3.948) can be written more symbolically as:

$$\phi'^{in} = A_{\phi}^{in'} e^{iS_{\phi}^{in}} \text{ where } A_{\phi}^{in'} = \sqrt{CC_g} \frac{g}{\omega} A_{\phi}^{in} \quad (3.949)$$

The derivative of ϕ'^{in} with respect to s may be defined as follows:

$$\frac{\partial \phi'^{in}}{\partial s} = e^{iS_{\phi}^{in}} \frac{\partial A_{\phi}^{in'}}{\partial s} + iA_{\phi}^{in'} \frac{\partial S_{\phi}^{in}}{\partial s} e^{iS_{\phi}^{in}} = \frac{\partial A_{\phi}^{in'}}{\partial s} \frac{\phi'^{in}}{A_{\phi}^{in'}} + i \frac{\partial S_{\phi}^{in}}{\partial s} \phi'^{in} \quad (3.950)$$

The second derivative may be expressed as follows:

$$\begin{aligned} \frac{\partial^2 \phi'^{in}}{\partial s^2} = & i \frac{\partial S_\phi^{in}}{\partial s} \frac{\partial A_\phi^{in'}}{\partial s} e^{iS_\phi^{in}} + \frac{\partial^2 A_\phi^{in'}}{\partial s^2} e^{iS_\phi^{in}} + i \frac{\partial A_\phi^{in'}}{\partial s} \frac{\partial S_\phi^{in}}{\partial s} e^{iS_\phi^{in}} \\ & + i \frac{\partial^2 S_\phi^{in}}{\partial s^2} A_\phi^{in'} e^{iS_\phi^{in}} - \frac{\partial S_\phi^{in}}{\partial s} \frac{\partial S_\phi^{in}}{\partial s} A_\phi^{in'} e^{iS_\phi^{in}} \end{aligned} \quad (3.951)$$

Re-expressing Equation (3.951) in terms of ϕ'^{in} gives:

$$\frac{\partial^2 \phi'^{in}}{\partial s^2} = i \frac{\partial S_\phi^{in}}{\partial s} \frac{\partial A_\phi^{in'}}{\partial s} \frac{\phi'^{in}}{A_\phi^{in'}} + \frac{\partial^2 A_\phi^{in'}}{\partial s^2} \frac{\phi'^{in}}{A_\phi^{in'}} + i \frac{\partial A_\phi^{in'}}{\partial s} \frac{\partial S_\phi^{in}}{\partial s} \frac{\phi'^{in}}{A_\phi^{in'}} + i \frac{\partial^2 S_\phi^{in}}{\partial s^2} \phi'^{in} - \frac{\partial S_\phi^{in}}{\partial s} \frac{\partial S_\phi^{in}}{\partial s} \phi'^{in} \quad (3.952)$$

The derivative of ϕ'^{in} with respect to n can also be calculated:

$$\frac{\partial \phi'^{in}}{\partial n} = e^{iS_\phi^{in}} \frac{\partial A_\phi^{in'}}{\partial n} + i A_\phi^{in'} \frac{\partial S_\phi^{in}}{\partial n} e^{iS_\phi^{in}} = \frac{\partial A_\phi^{in'}}{\partial n} \frac{\phi'^{in}}{A_\phi^{in'}} + i \frac{\partial S_\phi^{in}}{\partial n} \phi'^{in} \quad (3.953)$$

A similar process may be carried out for the non-Helmholtz velocity potential. Using the form of velocity potential from Equation (3.135) the following can be stated:

$$\phi^{in} = A_\phi^{in} e^{iS_\phi^{in}} \quad (3.954)$$

Substituting Equation (3.947) into Equation (3.954) gives:

$$\phi^{in} = \frac{gH^{in}}{2\omega} e^{iS_\phi^{in}} = \frac{gH^{in}}{2\omega} e^{\left(i \int_{x_0}^x \kappa_1 dx + \kappa_2 y \right)} \quad (3.955)$$

The integration from x_0 to x_1 is an integration in the direction of wave propagation. For the case of the origin at the beach this amounts to an integration in the negative x direction. Equation (3.948) can be written more symbolically as:

$$\phi^{in} = A_\phi^{in} e^{iS_\phi^{in}} \text{ where } A_\phi^{in} = \frac{g}{\omega} A_\phi^{in} \quad (3.956)$$

The derivative of ϕ^{in} with respect to s may be defined as follows:

$$\frac{\partial \phi^{in}}{\partial s} = e^{iS_\phi^{in}} \frac{\partial A_\phi^{in}}{\partial s} + i A_\phi^{in} \frac{\partial S_\phi^{in}}{\partial s} e^{iS_\phi^{in}} = \frac{\partial A_\phi^{in}}{\partial s} \frac{\phi^{in}}{A_\phi^{in}} + i \frac{\partial S_\phi^{in}}{\partial s} \phi^{in} \quad (3.957)$$

The second derivative may be expressed as follows:

$$\begin{aligned} \frac{\partial^2 \phi^{in}}{\partial s^2} = & i \frac{\partial S_\phi^{in}}{\partial s} \frac{\partial A_\phi^{in}}{\partial s} e^{iS_\phi^{in}} + \frac{\partial^2 A_\phi^{in}}{\partial s^2} e^{iS_\phi^{in}} + i \frac{\partial A_\phi^{in}}{\partial s} \frac{\partial S_\phi^{in}}{\partial s} e^{iS_\phi^{in}} \\ & + i \frac{\partial^2 S_\phi^{in}}{\partial s^2} A_\phi^{in} e^{iS_\phi^{in}} - \frac{\partial S_\phi^{in}}{\partial s} \frac{\partial S_\phi^{in}}{\partial s} A_\phi^{in} e^{iS_\phi^{in}} \end{aligned} \quad (3.958)$$

Re-expressing Equation (3.958) in terms of ϕ'^{in} gives:

$$\frac{\partial^2 \phi^{in}}{\partial s^2} = i \frac{\partial S_\phi^{in}}{\partial s} \frac{\partial A_\phi^{in}}{\partial s} \frac{\phi^{in}}{A_\phi^{in}} + \frac{\partial^2 A_\phi^{in}}{\partial s^2} \frac{\phi'^{in}}{A_\phi^{in}} + i \frac{\partial A_\phi^{in}}{\partial s} \frac{\partial S_\phi^{in}}{\partial s} \frac{\phi^{in}}{A_\phi^{in}} + i \frac{\partial^2 S_\phi^{in}}{\partial s^2} \phi^{in} - \frac{\partial S_\phi^{in}}{\partial s} \frac{\partial S_\phi^{in}}{\partial s} \phi^{in} \quad (3.959)$$

The derivative of ϕ^{in} with respect to n can also be calculated:

$$\frac{\partial \phi^{in}}{\partial n} = e^{iS_\phi^{in}} \frac{\partial A_\phi^{in}}{\partial n} + i A_\phi^{in} \frac{\partial S_\phi^{in}}{\partial n} e^{iS_\phi^{in}} = \frac{\partial A_\phi^{in}}{\partial n} \frac{\phi^{in}}{A_\phi^{in}} + i \frac{\partial S_\phi^{in}}{\partial n} \phi^{in} \quad (3.960)$$

3.11.5 Reflecting Boundary Condition

In the case of a reflecting boundary no wave energy should be allowed exit the domain at all. This would occur in the case of a harbour wall or some other large sea-based structure that allows no energy to dissipate on it. In order for a boundary to prevent wave energy from passing through it the gradient of velocity potential must be zero:

$$\frac{\partial \phi'}{\partial n} = 0 \quad (3.961)$$

Hence both the real and imaginary components of this gradient are also zero:

$$\frac{\partial \phi'_1}{\partial n} = 0 \quad (3.962)$$

$$\frac{\partial \phi'_2}{\partial n} = 0 \quad (3.963)$$

In the case of the reflecting boundary condition, Γ_1 , the boundary term of Equation (3.754) disappears completely.

3.11.6 Full Helmholtz form of the 2d-NM-WCIM finite element solution scheme

Initially the imaginary terms of Equation (3.754) may be discarded to obtain the real equation that will be solved by the computer program:

$$\begin{aligned}
& \int_S W^I \frac{\partial \phi_1'}{\partial n} ds - \iint_A \frac{\partial N^I}{\partial x_k} \frac{\partial N^J}{\partial x_k} \phi_1'' dA + \iint_A K^2 N^I N^J \phi_1'' dA + \iint_A W^I \frac{\omega^2}{CC_g} \phi_1'' N^I N^J dA \\
& - \iint_A W^I \frac{\sigma^2}{CC_g} \phi_1'' N^I N^J dA - \iint_A \frac{U_j}{CC_g} \frac{\partial U_k}{\partial x_j} N^I \frac{\partial N^J}{\partial x_k} \phi_1'' dA + 2 \iint_A \frac{U_j U_k}{(CC_g)^{\frac{3}{2}}} \frac{\partial \sqrt{CC_g}}{\partial x_j} N^I \frac{\partial N^J}{\partial x_k} \phi_1'' dA \\
& + \iint_A \frac{U_j}{(CC_g)^{\frac{3}{2}}} \frac{\partial U_k}{\partial x_j} \frac{\partial \sqrt{CC_g}}{\partial x_k} N^I N^J \phi_1'' dA + \iint_A \frac{U_j U_k}{(CC_g)^{\frac{3}{2}}} \frac{\partial^2 \sqrt{CC_g}}{\partial x_j \partial x_k} N^I N^J \phi_1'' dA \\
& - \iint_A \frac{U_j U_k}{(CC_g)^{\frac{5}{2}}} \frac{\partial \sqrt{CC_g}}{\partial x_k} \frac{\partial (CC_g)}{\partial x_j} N^I N^J \phi_1'' dA \\
& + \iint_A \frac{U_j U_k}{CC_g} \frac{\partial N^I}{\partial x_j} \frac{\partial N^J}{\partial x_k} \phi_1'' dA + \iint_A \frac{\partial U_j}{\partial x_j} \frac{U_k}{CC_g} N^I \frac{\partial N^J}{\partial x_k} \phi_1'' dA \\
& + \iint_A \frac{U_j}{CC_g} \frac{\partial U_k}{\partial x_j} N^I \frac{\partial N^J}{\partial x_k} \phi_1'' dA + \iint_A U_k U_j \frac{\partial}{\partial x_j} \left[(CC_g)^{-1} \right] N^I \frac{\partial N^J}{\partial x_k} \phi_1'' dA \\
& + \iint_A \frac{2\omega U_k}{(CC_g)^{\frac{3}{2}}} \frac{\partial \sqrt{CC_g}}{\partial x_k} N^I N^J \phi_2'' dA - \iint_A \frac{2\omega U_k}{CC_g} N^I \frac{\partial N^J}{\partial x_k} \phi_2'' dA = 0
\end{aligned} \tag{3.964}$$

The first term of Equation (3.964) can now be replaced by the boundary terms of Equations (3.937) and (3.919)

$$\begin{aligned}
\int_S W^I \frac{\partial \phi_1'}{\partial n} ds &= \int_{\Gamma_{2,3}} W^I \left\{ \hat{\psi} \left[\begin{aligned} & -\Upsilon \kappa^2 \phi_1' + \Upsilon \frac{\partial \kappa}{\partial n} \phi_2' - \Upsilon K^2 \phi_1' - \Upsilon \frac{\partial^2 \phi_1'}{\partial s^2} \\ & -2\kappa^3 \phi_2' - 2\kappa \frac{\partial \kappa}{\partial n} \phi_1' - 2\kappa K^2 \phi_2' - 2\kappa \frac{\partial^2 \phi_2'}{\partial s^2} \end{aligned} \right] \right\} ds \\
& - \int_{\Gamma_3} W^I \left\{ \hat{\psi} \left[\begin{aligned} & -\Upsilon \kappa^2 \phi_1'^{in} + \Upsilon \frac{\partial \kappa}{\partial n} \phi_2'^{in} - \Upsilon K^2 \phi_1'^{in} - \Upsilon \frac{\partial^2 \phi_1'^{in}}{\partial s^2} \\ & -2\kappa^3 \phi_2'^{in} - 2\kappa \frac{\partial \kappa}{\partial n} \phi_1'^{in} - 2\kappa K^2 \phi_2'^{in} - 2\kappa \frac{\partial^2 \phi_2'^{in}}{\partial s^2} \end{aligned} \right] \right\} ds \\
& + \int_{\Gamma_3} W^I \left\{ \frac{\partial \phi_1'^{in}}{\partial n} \right\} ds
\end{aligned} \tag{3.965}$$

$$\begin{aligned}
\int_S W^I \frac{\partial \phi'_1}{\partial n} ds &= \int_{\Gamma_{2,3}} W^I \left\{ \hat{\psi} \left[\begin{aligned} &-\Upsilon \kappa^2 \phi'_1 + \Upsilon \frac{\partial \kappa}{\partial n} \phi'_2 - \Upsilon K^2 \phi'_1 - \Upsilon \frac{\partial^2 \phi'_1}{\partial s^2} \\ &-2\kappa^3 \phi'_2 - 2\kappa \frac{\partial \kappa}{\partial n} \phi'_1 - 2\kappa K^2 \phi'_2 - 2\kappa \frac{\partial^2 \phi'_2}{\partial s^2} \end{aligned} \right] \right\} ds + \\
&- \int_{\Gamma_3} W^I \left\{ \hat{\psi} \left[\begin{aligned} &-\Upsilon \kappa^2 \phi'^{in}_1 + \Upsilon \frac{\partial \kappa}{\partial n} \phi'^{in}_2 - \Upsilon K^2 \phi'^{in}_1 - \Upsilon \frac{\partial^2 \phi'^{in}_1}{\partial s^2} \\ &-2\kappa^3 \phi'^{in}_2 - 2\kappa \frac{\partial \kappa}{\partial n} \phi'^{in}_1 - 2\kappa K^2 \phi'^{in}_2 - 2\kappa \frac{\partial^2 \phi'^{in}_2}{\partial s^2} \end{aligned} \right] \right\} ds \\
&+ \int_{\Gamma_3} W^I \left\{ \frac{\partial \phi'^{in}_1}{\partial n} \right\} ds
\end{aligned} \tag{3.966}$$

Further expansion of Equation (3.966) gives:

$$\begin{aligned}
\int_S W^I \frac{\partial \phi'_1}{\partial n} ds &= - \int_{\Gamma_{2,3}} W^I \hat{\psi} \Upsilon \kappa^2 \phi'_1 ds + \int_{\Gamma_{2,3}} W^I \hat{\psi} \Upsilon \frac{\partial \kappa}{\partial n} \phi'_2 ds - \int_{\Gamma_{2,3}} W^I \hat{\psi} \Upsilon K^2 \phi'_1 ds \\
&- \int_{\Gamma_{2,3}} W^I \hat{\psi} \Upsilon \frac{\partial^2 \phi'_1}{\partial s^2} ds - \int_{\Gamma_{2,3}} W^I \hat{\psi} 2\kappa^3 \phi'_2 ds - 2 \int_{\Gamma_{2,3}} W^I \hat{\psi} \kappa \frac{\partial \kappa}{\partial n} \phi'_1 ds \\
&- 2 \int_{\Gamma_{2,3}} W^I \hat{\psi} \kappa K^2 \phi'_2 ds - 2 \int_{\Gamma_{2,3}} W^I \hat{\psi} \kappa \frac{\partial^2 \phi'_2}{\partial s^2} ds + \\
&+ \int_{\Gamma_3} W^I \hat{\psi} \Upsilon \kappa^2 \phi'^{in}_1 ds - \int_{\Gamma_3} W^I \hat{\psi} \Upsilon \frac{\partial \kappa}{\partial n} \phi'^{in}_2 ds + \int_{\Gamma_3} W^I \hat{\psi} \Upsilon K^2 \phi'^{in}_1 ds \\
&+ \int_{\Gamma_3} W^I \hat{\psi} \Upsilon \frac{\partial^2 \phi'^{in}_1}{\partial s^2} ds + 2 \int_{\Gamma_3} W^I \hat{\psi} \kappa^3 \phi'^{in}_2 ds + 2 \int_{\Gamma_3} W^I \hat{\psi} \kappa \frac{\partial \kappa}{\partial n} \phi'^{in}_1 ds \\
&+ 2 \int_{\Gamma_3} W^I \hat{\psi} \kappa K^2 \phi'^{in}_2 ds + 2 \int_{\Gamma_3} W^I \hat{\psi} \kappa \frac{\partial^2 \phi'^{in}_2}{\partial s^2} ds \\
&+ \int_{\Gamma_3} W^I \frac{\partial \phi'^{in}_1}{\partial n} ds
\end{aligned} \tag{3.967}$$

As discussed in Appendix A the Galerkin method consists of substituting the weighting functions W^I with a shape function; a linear one in this case L^I .

$$\begin{aligned}
\int_S W^l \frac{\partial \phi_1'}{\partial n} ds = & - \int_{\Gamma_{2,3}} L^l \hat{\psi} \Upsilon \kappa^2 \phi_1' ds + \int_{\Gamma_{2,3}} L^l \hat{\psi} \Upsilon \frac{\partial \kappa}{\partial n} \phi_2' ds - \int_{\Gamma_{2,3}} L^l \hat{\psi} \Upsilon K^2 \phi_1' ds \\
& - \int_{\Gamma_{2,3}} L^l \hat{\psi} \Upsilon \frac{\partial^2 \phi_1'}{\partial s^2} ds - \int_{\Gamma_{2,3}} L^l \hat{\psi} 2\kappa^3 \phi_2' ds - 2 \int_{\Gamma_{2,3}} L^l \hat{\psi} \kappa \frac{\partial \kappa}{\partial n} \phi_1' ds \\
& - 2 \int_{\Gamma_{2,3}} L^l \hat{\psi} \kappa K^2 \phi_2' ds - 2 \int_{\Gamma_{2,3}} L^l \hat{\psi} \kappa \frac{\partial^2 \phi_2'}{\partial s^2} ds + \\
& + \int_{\Gamma_3} L^l \hat{\psi} \Upsilon \kappa^2 \phi_1'^{in} ds - \int_{\Gamma_3} L^l \hat{\psi} \Upsilon \frac{\partial \kappa}{\partial n} \phi_2'^{in} ds + \int_{\Gamma_3} L^l \hat{\psi} \Upsilon K^2 \phi_1'^{in} ds \\
& + \int_{\Gamma_3} L^l \hat{\psi} \Upsilon \frac{\partial^2 \phi_1'^{in}}{\partial s^2} ds + 2 \int_{\Gamma_3} L^l \hat{\psi} \kappa^3 \phi_2'^{in} ds + 2 \int_{\Gamma_3} L^l \hat{\psi} \kappa \frac{\partial \kappa}{\partial n} \phi_1'^{in} ds \\
& + 2 \int_{\Gamma_3} L^l \hat{\psi} \kappa K^2 \phi_2'^{in} ds + 2 \int_{\Gamma_3} L^l \hat{\psi} \kappa \frac{\partial^2 \phi_2'^{in}}{\partial s^2} ds \\
& + \int_{\Gamma_3} L^l \frac{\partial \phi_1'^{in}}{\partial n} ds
\end{aligned} \tag{3.968}$$

Applying the Gauss divergence theorem to the second order derivatives with respect to s , the fourth term in Equation (3.967) becomes:

$$\begin{aligned}
- \int_{\Gamma_{2,3}} L^l \hat{\psi} \Upsilon \frac{\partial^2 \phi_1'}{\partial s^2} ds = & \left(-L^l \hat{\psi} \Upsilon \frac{\partial \phi_1'}{\partial s} \Big|_0^l \right)_{\Gamma_{2,3}} + \int_{\Gamma_{2,3}} \frac{\partial L^l}{\partial s} \hat{\psi} \Upsilon \frac{\partial \phi_1'}{\partial s} ds \\
& + \int_{\Gamma_{2,3}} L^l \frac{\partial \hat{\psi}}{\partial s} \Upsilon \frac{\partial \phi_1'}{\partial s} ds + \int_{\Gamma_{2,3}} L^l \hat{\psi} \frac{\partial \Upsilon}{\partial s} \frac{\partial \phi_1'}{\partial s} ds
\end{aligned} \tag{3.969}$$

The eighth term in Equation (3.968) becomes:

$$\begin{aligned}
-2 \int_{\Gamma_{2,3}} L^l \hat{\psi} \kappa \frac{\partial^2 \phi_2'}{\partial s^2} ds = & \left(-2L^l \hat{\psi} \kappa \frac{\partial \phi_2'}{\partial s} \Big|_0^l \right)_{\Gamma_{2,3}} + 2 \int_{\Gamma_{2,3}} \frac{\partial L^l}{\partial s} \hat{\psi} \kappa \frac{\partial \phi_2'}{\partial s} ds \\
& + 2 \int_{\Gamma_{2,3}} L^l \frac{\partial \hat{\psi}}{\partial s} \kappa \frac{\partial \phi_2'}{\partial s} ds + 2 \int_{\Gamma_{2,3}} L^l \hat{\psi} \frac{\partial \kappa}{\partial s} \frac{\partial \phi_2'}{\partial s} ds
\end{aligned} \tag{3.970}$$

Similarly:

$$\begin{aligned}
\int_{\Gamma_3} L^l \hat{\psi} \Upsilon \frac{\partial^2 \phi_1'^{in}}{\partial s^2} ds = & \left(L^l \hat{\psi} \Upsilon \frac{\partial \phi_1'^{in}}{\partial s} \Big|_0^l \right)_{\Gamma_3} - \int_{\Gamma_3} \frac{\partial L^l}{\partial s} \hat{\psi} \Upsilon \frac{\partial \phi_1'^{in}}{\partial s} ds \\
& - \int_{\Gamma_3} L^l \frac{\partial \hat{\psi}}{\partial s} \Upsilon \frac{\partial \phi_1'^{in}}{\partial s} ds - \int_{\Gamma_3} L^l \hat{\psi} \frac{\partial \Upsilon}{\partial s} \frac{\partial \phi_1'^{in}}{\partial s} ds
\end{aligned} \tag{3.971}$$

$$\begin{aligned}
2 \int_{\Gamma_3} L' \hat{\psi} \kappa \frac{\partial^2 \phi_2'^{in}}{\partial s^2} ds &= \left(2L' \hat{\psi} \kappa \frac{\partial \phi_2'^{in}}{\partial s} \Big|_0^l \right)_{\Gamma_3} - 2 \int_{\Gamma_3} \frac{\partial L'}{\partial s} \hat{\psi} \kappa \frac{\partial \phi_2'^{in}}{\partial s} ds \\
&\quad - 2 \int_{\Gamma_3} L' \frac{\partial \hat{\psi}}{\partial s} \kappa \frac{\partial \phi_2'^{in}}{\partial s} ds - 2 \int_{\Gamma_3} L' \hat{\psi} \frac{\partial \kappa}{\partial s} \frac{\partial \phi_2'^{in}}{\partial s} ds
\end{aligned} \tag{3.972}$$

Substituting Equations (3.970), (3.969), (3.971) and (3.972) into Equation (3.968) yields:

$$\begin{aligned}
\int_S W^I \frac{\partial \phi_1'}{\partial n} ds &= - \int_{\Gamma_{2,3}} L' \hat{\psi} \Upsilon \kappa^2 \phi_1' ds + \int_{\Gamma_{2,3}} L' \hat{\psi} \Upsilon \frac{\partial \kappa}{\partial n} \phi_2' ds - \int_{\Gamma_{2,3}} L' \hat{\psi} \Upsilon K^2 \phi_1' ds \\
&\quad \left(-L' \hat{\psi} \Upsilon \frac{\partial \phi_1'}{\partial s} \Big|_0^l \right)_{\Gamma_{2,3}} + \int_{\Gamma_{2,3}} \frac{\partial L'}{\partial s} \hat{\psi} \Upsilon \frac{\partial \phi_1'}{\partial s} ds + \int_{\Gamma_{2,3}} L' \frac{\partial \hat{\psi}}{\partial s} \Upsilon \frac{\partial \phi_1'}{\partial s} ds \\
&\quad + \int_{\Gamma_{2,3}} L' \hat{\psi} \frac{\partial \Upsilon}{\partial s} \frac{\partial \phi_1'}{\partial s} ds - \int_{\Gamma_{2,3}} L' \hat{\psi} 2\kappa^3 \phi_2' ds - 2 \int_{\Gamma_{2,3}} L' \hat{\psi} \kappa \frac{\partial \kappa}{\partial n} \phi_1' ds \\
&\quad - 2 \int_{\Gamma_{2,3}} L' \hat{\psi} \kappa K^2 \phi_2' ds + \left(-2L' \hat{\psi} \kappa \frac{\partial \phi_2'}{\partial s} \Big|_0^l \right)_{\Gamma_{2,3}} + 2 \int_{\Gamma_{2,3}} \frac{\partial L'}{\partial s} \hat{\psi} \kappa \frac{\partial \phi_2'}{\partial s} ds \\
&\quad + 2 \int_{\Gamma_{2,3}} L' \frac{\partial \hat{\psi}}{\partial s} \kappa \frac{\partial \phi_2'}{\partial s} ds + 2 \int_{\Gamma_{2,3}} L' \hat{\psi} \frac{\partial \kappa}{\partial s} \frac{\partial \phi_2'}{\partial s} ds + \int_{\Gamma_3} L' \hat{\psi} \Upsilon \kappa^2 \phi_1'^{in} ds \\
&\quad - \int_{\Gamma_3} L' \hat{\psi} \Upsilon \frac{\partial \kappa}{\partial n} \phi_2'^{in} ds + \int_{\Gamma_3} L' \hat{\psi} \Upsilon K^2 \phi_1'^{in} ds + \left(L' \hat{\psi} \Upsilon \frac{\partial \phi_1'^{in}}{\partial s} \Big|_0^l \right)_{\Gamma_3} \\
&\quad - \int_{\Gamma_3} \frac{\partial L'}{\partial s} \hat{\psi} \Upsilon \frac{\partial \phi_1'^{in}}{\partial s} ds - \int_{\Gamma_3} L' \frac{\partial \hat{\psi}}{\partial s} \Upsilon \frac{\partial \phi_1'^{in}}{\partial s} ds - \int_{\Gamma_3} L' \hat{\psi} \frac{\partial \Upsilon}{\partial s} \frac{\partial \phi_1'^{in}}{\partial s} ds \\
&\quad + 2 \int_{\Gamma_3} L' \hat{\psi} \kappa^3 \phi_2'^{in} ds + 2 \int_{\Gamma_3} L' \hat{\psi} \kappa \frac{\partial \kappa}{\partial n} \phi_1'^{in} ds + 2 \int_{\Gamma_3} L' \hat{\psi} \kappa K^2 \phi_2'^{in} ds \\
&\quad + \left(2L' \hat{\psi} \kappa \frac{\partial \phi_2'^{in}}{\partial s} \Big|_0^l \right)_{\Gamma_3} - 2 \int_{\Gamma_3} \frac{\partial L'}{\partial s} \hat{\psi} \kappa \frac{\partial \phi_2'^{in}}{\partial s} ds - 2 \int_{\Gamma_3} L' \frac{\partial \hat{\psi}}{\partial s} \kappa \frac{\partial \phi_2'^{in}}{\partial s} ds \\
&\quad - 2 \int_{\Gamma_3} L' \hat{\psi} \frac{\partial \kappa}{\partial s} \frac{\partial \phi_2'^{in}}{\partial s} ds + \int_{\Gamma_3} L' \frac{\partial \phi_1'^{in}}{\partial n} ds
\end{aligned} \tag{3.973}$$

A shape function may also be applied to the unknown value, in this case the scaled velocity potential:

$$\phi' = \phi'^J L^J \tag{3.974}$$

Using Equation (3.974) with Equation (3.973) gives:

$$\begin{aligned}
\int_S W^I \frac{\partial \phi_1'}{\partial n} dS = & - \int_{\Gamma_{2,3}} \hat{\psi} \Upsilon \kappa^2 L^I L^J \phi_1'^J dS + \int_{\Gamma_{2,3}} \hat{\psi} \Upsilon \frac{\partial \kappa}{\partial n} L^I L^J \phi_2'^J dS - \int_{\Gamma_{2,3}} \hat{\psi} \Upsilon K^2 L^I L^J \phi_1'^J dS \\
& + \left(-L^I \hat{\psi} \Upsilon \frac{\partial \phi_1'}{\partial s} \Big|_0 \right)_{\Gamma_{2,3}} + \int_{\Gamma_{2,3}} \hat{\psi} \Upsilon \frac{\partial L^I}{\partial s} \frac{\partial L^J}{\partial s} \phi_1'^J dS + \int_{\Gamma_{2,3}} \frac{\partial \hat{\psi}}{\partial s} \Upsilon L^I \frac{\partial L^J}{\partial s} \phi_1'^J dS \\
& + \int_{\Gamma_{2,3}} \hat{\psi} \frac{\partial \Upsilon}{\partial s} L^I \frac{\partial L^J}{\partial s} \phi_1'^J dS - \int_{\Gamma_{2,3}} \hat{\psi} 2\kappa^3 L^I L^J \phi_2'^J dS - 2 \int_{\Gamma_{2,3}} \hat{\psi} \kappa \frac{\partial \kappa}{\partial n} L^I L^J \phi_1'^J dS \\
& - 2 \int_{\Gamma_{2,3}} \hat{\psi} \kappa K^2 L^I L^J \phi_2'^J dS + \left(-2L^I \hat{\psi} \kappa \frac{\partial \phi_2'}{\partial s} \Big|_0 \right)_{\Gamma_{2,3}} + 2 \int_{\Gamma_{2,3}} \hat{\psi} \kappa \frac{\partial L^I}{\partial s} \frac{\partial L^J}{\partial s} \phi_2'^J dS \\
& + 2 \int_{\Gamma_{2,3}} \frac{\partial \hat{\psi}}{\partial s} \kappa L^I \frac{\partial L^J}{\partial s} \phi_2'^J dS + 2 \int_{\Gamma_{2,3}} \hat{\psi} \frac{\partial \kappa}{\partial s} L^I \frac{\partial L^J}{\partial s} \phi_2'^J dS + \int_{\Gamma_3} \hat{\psi} \Upsilon \kappa^2 L^I L^J (\phi_1'^{in})^J dS \\
& - \int_{\Gamma_3} \hat{\psi} \Upsilon \frac{\partial \kappa}{\partial n} L^I L^J (\phi_2'^{in})^J dS + \int_{\Gamma_3} \hat{\psi} \Upsilon K^2 L^I L^J (\phi_1'^{in})^J dS + \left(L^I \hat{\psi} \Upsilon \frac{\partial \phi_1'^{in}}{\partial s} \Big|_0 \right)_{\Gamma_3} \\
& - \int_{\Gamma_3} \hat{\psi} \Upsilon \frac{\partial L^I}{\partial s} \frac{\partial L^J}{\partial s} (\phi_1'^{in})^J dS - \int_{\Gamma_3} \frac{\partial \hat{\psi}}{\partial s} \Upsilon L^I \frac{\partial L^J}{\partial s} (\phi_1'^{in})^J dS - \int_{\Gamma_3} \hat{\psi} \frac{\partial \Upsilon}{\partial s} L^I \frac{\partial L^J}{\partial s} (\phi_1'^{in})^J dS \\
& + 2 \int_{\Gamma_3} \hat{\psi} \kappa^3 L^I L^J (\phi_2'^{in})^J dS + 2 \int_{\Gamma_3} \hat{\psi} \kappa \frac{\partial \kappa}{\partial n} L^I L^J (\phi_1'^{in})^J dS + 2 \int_{\Gamma_3} \hat{\psi} \kappa K^2 L^I L^J (\phi_2'^{in})^J dS \\
& + \left(2L^I \hat{\psi} \kappa \frac{\partial \phi_2'^{in}}{\partial s} \Big|_0 \right)_{\Gamma_3} - 2 \int_{\Gamma_3} \hat{\psi} \kappa \frac{\partial L^I}{\partial s} \frac{\partial L^J}{\partial s} (\phi_2'^{in})^J dS - 2 \int_{\Gamma_3} \frac{\partial \hat{\psi}}{\partial s} \kappa L^I \frac{\partial L^J}{\partial s} (\phi_2'^{in})^J dS \\
& - 2 \int_{\Gamma_3} \hat{\psi} \frac{\partial \kappa}{\partial s} L^I \frac{\partial L^J}{\partial s} (\phi_2'^{in})^J dS + \int_{\Gamma_3} L^I \frac{\partial \phi_1'^{in}}{\partial n} dS
\end{aligned} \tag{3.975}$$

The results of Equation (3.975) may now be substituted in Equation (3.964) to give:

$$\begin{aligned}
& - \int_{\Gamma_{2,3}} \hat{\psi} \Upsilon \kappa^2 L^I L^J \phi_1'^J ds + \int_{\Gamma_{2,3}} \hat{\psi} \Upsilon \frac{\partial \kappa}{\partial n} L^I L^J \phi_2'^J ds - \int_{\Gamma_{2,3}} \hat{\psi} \Upsilon K^2 L^I L^J \phi_1'^J ds \\
& + \left(-L^I \hat{\psi} \Upsilon \frac{\partial \phi_1'^I}{\partial s} \Big|_0 \right)_{\Gamma_{2,3}} + \int_{\Gamma_{2,3}} \hat{\psi} \Upsilon \frac{\partial L^I}{\partial s} \frac{\partial L^J}{\partial s} \phi_1'^J ds + \int_{\Gamma_{2,3}} \frac{\partial \hat{\psi}}{\partial s} \Upsilon L^I \frac{\partial L^J}{\partial s} \phi_1'^J ds \\
& + \int_{\Gamma_{2,3}} \hat{\psi} \frac{\partial \Upsilon}{\partial s} L^I \frac{\partial L^J}{\partial s} \phi_1'^J ds - \int_{\Gamma_{2,3}} \hat{\psi} 2\kappa^3 L^I L^J \phi_2'^J ds - 2 \int_{\Gamma_{2,3}} \hat{\psi} \kappa \frac{\partial \kappa}{\partial n} L^I L^J \phi_1'^J ds \\
& - 2 \int_{\Gamma_{2,3}} \hat{\psi} \kappa K^2 L^I L^J \phi_2'^J ds + \left(-2L^I \hat{\psi} \kappa \frac{\partial \phi_2'^I}{\partial s} \Big|_0 \right)_{\Gamma_{2,3}} + 2 \int_{\Gamma_{2,3}} \hat{\psi} \kappa \frac{\partial L^I}{\partial s} \frac{\partial L^J}{\partial s} \phi_2'^J ds \\
& + 2 \int_{\Gamma_{2,3}} \frac{\partial \hat{\psi}}{\partial s} \kappa L^I \frac{\partial L^J}{\partial s} \phi_2'^J ds + 2 \int_{\Gamma_{2,3}} \hat{\psi} \frac{\partial \kappa}{\partial s} L^I \frac{\partial L^J}{\partial s} \phi_2'^J ds + \int_{\Gamma_3} \hat{\psi} \Upsilon \kappa^2 L^I L^J (\phi_1'^{in})^J ds \\
& - \int_{\Gamma_3} \hat{\psi} \Upsilon \frac{\partial \kappa}{\partial n} L^I L^J (\phi_2'^{in})^J ds + \int_{\Gamma_3} \hat{\psi} \Upsilon K^2 L^I L^J (\phi_1'^{in})^J ds + \left(L^I \hat{\psi} \Upsilon \frac{\partial \phi_1'^{in}}{\partial s} \Big|_0 \right)_{\Gamma_3} \\
& - \int_{\Gamma_3} \hat{\psi} \Upsilon \frac{\partial L^I}{\partial s} \frac{\partial L^J}{\partial s} (\phi_1'^{in})^J ds - \int_{\Gamma_3} \frac{\partial \hat{\psi}}{\partial s} \Upsilon L^I \frac{\partial L^J}{\partial s} (\phi_1'^{in})^J ds - \int_{\Gamma_3} \hat{\psi} \frac{\partial \Upsilon}{\partial s} L^I \frac{\partial L^J}{\partial s} (\phi_1'^{in})^J ds \\
& + 2 \int_{\Gamma_3} \hat{\psi} \kappa^3 L^I L^J (\phi_2'^{in})^J ds + 2 \int_{\Gamma_3} \hat{\psi} \kappa \frac{\partial \kappa}{\partial n} L^I L^J (\phi_1'^{in})^J ds + 2 \int_{\Gamma_3} \hat{\psi} \kappa K^2 L^I L^J (\phi_2'^{in})^J ds \\
& + \left(2L^I \hat{\psi} \kappa \frac{\partial \phi_2'^{in}}{\partial s} \Big|_0 \right)_{\Gamma_3} - 2 \int_{\Gamma_3} \hat{\psi} \kappa \frac{\partial L^I}{\partial s} \frac{\partial L^J}{\partial s} (\phi_2'^{in})^J ds - 2 \int_{\Gamma_3} \frac{\partial \hat{\psi}}{\partial s} \kappa L^I \frac{\partial L^J}{\partial s} (\phi_2'^{in})^J ds \\
& - 2 \int_{\Gamma_3} \hat{\psi} \frac{\partial \kappa}{\partial s} L^I \frac{\partial L^J}{\partial s} (\phi_2'^{in})^J ds + \int_{\Gamma_3} L^I \frac{\partial \phi_1'^{in}}{\partial n} ds - \iint_A \frac{\partial N^I}{\partial x_k} \frac{\partial N^J}{\partial x_k} \phi_1'^J dA \\
& + \iint_A K^2 N^I N^J \phi_1'^J dA + \iint_A W^I \frac{\omega^2}{CC_g} \phi_1'^J N^I N^J dA - \iint_A W^I \frac{\sigma^2}{CC_g} \phi_1'^J N^I N^J dA \\
& - \iint_A \frac{U_j}{CC_g} \frac{\partial U_k}{\partial x_j} N^I \frac{\partial N^J}{\partial x_k} \phi_1'^J dA + 2 \iint_A \frac{U_j U_k}{(CC_g)^{\frac{3}{2}}} \frac{\partial \sqrt{CC_g}}{\partial x_j} N^I \frac{\partial N^J}{\partial x_k} \phi_1'^J dA \\
& + \iint_A \frac{U_j}{(CC_g)^{\frac{3}{2}}} \frac{\partial U_k}{\partial x_j} \frac{\partial (CC_g)}{\partial x_k} N^I N^J \phi_1'^J dA + \iint_A \frac{U_j U_k}{(CC_g)^{\frac{3}{2}}} \frac{\partial^2 \sqrt{CC_g}}{\partial x_j \partial x_k} N^I N^J \phi_1'^J dA \\
& - \iint_A \frac{U_j U_k}{(CC_g)^{\frac{5}{2}}} \frac{\partial \sqrt{CC_g}}{\partial x_k} \frac{\partial (CC_g)}{\partial x_j} N^I N^J \phi_1'^J dA \\
& + \iint_A \frac{U_j U_k}{CC_g} \frac{\partial N^I}{\partial x_j} \frac{\partial N^J}{\partial x_k} \phi_1'^J dA + \iint_A \frac{\partial U_j}{\partial x_j} \frac{U_k}{CC_g} N^I \frac{\partial N^J}{\partial x_k} \phi_1'^J dA \\
& + \iint_A \frac{U_j}{CC_g} \frac{\partial U_k}{\partial x_j} N^I \frac{\partial N^J}{\partial x_k} \phi_1'^J dA + \iint_A U_k U_j \frac{\partial}{\partial x_j} \left[(CC_g)^{-1} \right] N^I \frac{\partial N^J}{\partial x_k} \phi_1'^J dA \\
& + \iint_A \frac{2\omega U_k}{(CC_g)^{\frac{3}{2}}} \frac{\partial \sqrt{CC_g}}{\partial x_k} N^I N^J \phi_2'^J dA - \iint_A \frac{2\omega U_k}{CC_g} N^I \frac{\partial N^J}{\partial x_k} \phi_2'^J dA = 0
\end{aligned} \tag{3.976}$$

In the formation of any finite element matrix the known terms are entered in the right hand side vector. Hence the known terms in Equation (3.976) will be moved to the right hand side of the equals:

$$\begin{aligned}
& - \int_{\Gamma_{2,3}} \hat{\psi} \Upsilon \kappa^2 L^I L^J \phi_1'^J ds + \int_{\Gamma_{2,3}} \hat{\psi} \Upsilon \frac{\partial \kappa}{\partial n} L^I L^J \phi_2'^J ds - \int_{\Gamma_{2,3}} \hat{\psi} \Upsilon K^2 L^I L^J \phi_1'^J ds + \left(-L^I \hat{\psi} \Upsilon \frac{\partial \phi_1'^I}{\partial s} \right)_{\Gamma_{2,3}} \\
& + \int_{\Gamma_{2,3}} \hat{\psi} \Upsilon \frac{\partial L^I}{\partial s} \frac{\partial L^J}{\partial s} \phi_1'^J ds + \int_{\Gamma_{2,3}} \frac{\partial \hat{\psi}}{\partial s} \Upsilon L^I \frac{\partial L^J}{\partial s} \phi_1'^J ds + \int_{\Gamma_{2,3}} \hat{\psi} \frac{\partial \Upsilon}{\partial s} L^I \frac{\partial L^J}{\partial s} \phi_1'^J ds - \int_{\Gamma_{2,3}} \hat{\psi} 2 \kappa^3 L^I L^J \phi_2'^J ds \\
& - 2 \int_{\Gamma_{2,3}} \hat{\psi} \kappa \frac{\partial \kappa}{\partial n} L^I L^J \phi_1'^J ds - 2 \int_{\Gamma_{2,3}} \hat{\psi} \kappa K^2 L^I L^J \phi_2'^J ds + \left(-2 L^I \hat{\psi} \kappa \frac{\partial \phi_2'^I}{\partial s} \right)_{\Gamma_{2,3}} + 2 \int_{\Gamma_{2,3}} \hat{\psi} \kappa \frac{\partial L^I}{\partial s} \frac{\partial L^J}{\partial s} \phi_2'^J ds \\
& + 2 \int_{\Gamma_{2,3}} \frac{\partial \hat{\psi}}{\partial s} \kappa L^I \frac{\partial L^J}{\partial s} \phi_2'^J ds + 2 \int_{\Gamma_{2,3}} \hat{\psi} \frac{\partial \kappa}{\partial s} L^I \frac{\partial L^J}{\partial s} \phi_2'^J ds - \iint_A \frac{\partial N^I}{\partial x_k} \frac{\partial N^J}{\partial x_k} \phi_1'^J dA \\
& + \iint_A K^2 N^I N^J \phi_1'^J dA + \iint_A W^I \frac{\omega^2}{CC_g} \phi_1'^J N^I N^J dA - \iint_A W^I \frac{\sigma^2}{CC_g} \phi_1'^J N^I N^J dA - \iint_A \frac{U_j}{CC_g} \frac{\partial U_k}{\partial x_j} N^I \frac{\partial N^J}{\partial x_k} \phi_1'^J dA \\
& + 2 \iint_A \frac{U_j U_k}{(CC_g)^{\frac{3}{2}}} \frac{\partial \sqrt{CC_g}}{\partial x_j} N^I \frac{\partial N^J}{\partial x_k} \phi_1'^J dA + \iint_A \frac{U_j}{(CC_g)^{\frac{3}{2}}} \frac{\partial U_k}{\partial x_j} \frac{\partial \sqrt{CC_g}}{\partial x_k} N^I N^J \phi_1'^J dA \\
& + \iint_A \frac{U_j U_k}{(CC_g)^{\frac{3}{2}}} \frac{\partial^2 \sqrt{CC_g}}{\partial x_j \partial x_k} N^I N^J \phi_1'^J dA - \iint_A \frac{U_j U_k}{(CC_g)^{\frac{5}{2}}} \frac{\partial \sqrt{CC_g}}{\partial x_k} \frac{\partial (CC_g)}{\partial x_j} N^I N^J \phi_1'^J dA \\
& + \iint_A \frac{U_j U_k}{CC_g} \frac{\partial N^I}{\partial x_j} \frac{\partial N^J}{\partial x_k} \phi_1'^J dA + \iint_A \frac{\partial U_j}{\partial x_j} \frac{U_k}{CC_g} N^I \frac{\partial N^J}{\partial x_k} \phi_1'^J dA + \iint_A \frac{U_j}{CC_g} \frac{\partial U_k}{\partial x_j} N^I \frac{\partial N^J}{\partial x_k} \phi_1'^J dA \\
& + \iint_A U_k U_j \frac{\partial}{\partial x_j} \left[(CC_g)^{-1} \right] N^I \frac{\partial N^J}{\partial x_k} \phi_1'^J dA + \iint_A \frac{2 \omega U_k}{(CC_g)^{\frac{3}{2}}} \frac{\partial \sqrt{CC_g}}{\partial x_k} N^I N^J \phi_2'^J dA - \iint_A \frac{2 \omega U_k}{CC_g} N^I \frac{\partial N^J}{\partial x_k} \phi_2'^J dA = \\
& \int_{\Gamma_3} \hat{\psi} \Upsilon \frac{\partial \kappa}{\partial n} L^I L^J (\phi_2'^{in})^J ds - \int_{\Gamma_3} \hat{\psi} \Upsilon K^2 L^I L^J (\phi_1'^{in})^J ds - \left(L^I \hat{\psi} \Upsilon \frac{\partial \phi_1'^I}{\partial s} \right)_{\Gamma_3} + \int_{\Gamma_3} \hat{\psi} \Upsilon \frac{\partial L^I}{\partial s} \frac{\partial L^J}{\partial s} (\phi_1'^{in})^J ds \\
& + \int_{\Gamma_3} \frac{\partial \hat{\psi}}{\partial s} \Upsilon L^I \frac{\partial L^J}{\partial s} (\phi_1'^{in})^J ds + \int_{\Gamma_3} \hat{\psi} \frac{\partial \Upsilon}{\partial s} L^I \frac{\partial L^J}{\partial s} (\phi_1'^{in})^J ds - 2 \int_{\Gamma_3} \hat{\psi} \kappa^3 L^I L^J (\phi_2'^{in})^J ds \\
& - 2 \int_{\Gamma_3} \hat{\psi} \kappa \frac{\partial \kappa}{\partial n} L^I L^J (\phi_1'^{in})^J ds - 2 \int_{\Gamma_3} \hat{\psi} \kappa K^2 L^I L^J (\phi_2'^{in})^J ds - \left(2 L^I \hat{\psi} \kappa \frac{\partial \phi_2'^I}{\partial s} \right)_{\Gamma_3} + 2 \int_{\Gamma_3} \hat{\psi} \kappa \frac{\partial L^I}{\partial s} \frac{\partial L^J}{\partial s} (\phi_2'^{in})^J ds \\
& + 2 \int_{\Gamma_3} \frac{\partial \hat{\psi}}{\partial s} \kappa L^I \frac{\partial L^J}{\partial s} (\phi_2'^{in})^J ds + 2 \int_{\Gamma_3} \hat{\psi} \frac{\partial \kappa}{\partial s} L^I \frac{\partial L^J}{\partial s} (\phi_2'^{in})^J ds - \int_{\Gamma_3} L^I \frac{\partial \phi_1'^{in}}{\partial n} ds - \int_{\Gamma_3} \hat{\psi} \Upsilon \kappa^2 L^I L^J (\phi_1'^{in})^J ds
\end{aligned} \tag{3.977}$$

Equation (3.977) is the complete finite element equation for solution of the Helmholtz form of the extended elliptic mild-slope wave equation including currents but in the absence of energy dissipation. In accordance with the Galerkin method each variable will

now also be assigned a shape function for complete solution. It would be inefficient to rewrite the entire of Equation (3.977) in this form but an example will be expressed for the 19th term in the equation:

$$-\iint_A \frac{U_j}{CC_g} \frac{\partial U_k}{\partial x_j} N^I \frac{\partial N^J}{\partial x_k} \phi_1'^J dA = -U_j^K U_k^L \left(\frac{1}{CC_g} \right)^M \frac{\partial N^J}{\partial x_k} \frac{\partial N^L}{\partial x_j} \left(\iint_A N^I N^K N^M dA \right) \phi_1'^J \quad (3.978)$$

Equation (3.978) can be rewritten as follows using the formula for derivatives of shape functions from Appendix A:

$$-\iint_A \frac{U_j}{CC_g} \frac{\partial U_k}{\partial x_j} N^I \frac{\partial N^J}{\partial x_k} \phi_1'^J dA = -U_j^K U_k^L \left(\frac{1}{CC_g} \right)^M \frac{b_j^k b_L^j}{4\Delta^2} \left(\iint_A N^I N^K N^M dA \right) \phi_1'^J \quad (3.979)$$

A similar process is carried out for every term in Equation (3.977).

Examining Figure 3.13 shows that on the downstream (beach) boundary, Γ_{2d} , the following is true for a wave propagating as shown:

$$n = -x_1$$

Thus: (3.980)

$$\frac{d}{dn} = -\frac{d}{dx_1} \quad (3.981)$$

The following is also true on Γ_{2d} :

$$s = -x_2 \quad (3.982)$$

Therefore:

$$\frac{d}{ds} = -\frac{d}{dx_2} \quad (3.983)$$

Using Equation (3.981) the following can be stated:

$$\frac{\partial S_\phi}{\partial n} = -\kappa_1 \quad (3.984)$$

$$\frac{\partial^2 S_\phi}{\partial n^2} = -\frac{\partial \kappa_1}{\partial n} \quad (3.985)$$

Using Equation (3.983) the following can be stated:

$$\frac{\partial S_\phi}{\partial s} = -\kappa_2 \quad (3.986)$$

If the wave is progressing at an angle it will also be possible to apply an absorbing boundary on the side of the mesh, which will absorb the longshore component of wave propagation. Examining Figure 3.13 shows that on the side absorbing boundary, Γ_{2l} , the following is true for a wave propagating as shown:

$$n = x_2 \quad (3.987)$$

Thus:

$$\frac{d}{dn} = \frac{d}{dx_2} \quad (3.988)$$

The following is also true on Γ_{2l} :

$$s = -x_1 \quad (3.989)$$

Therefore:

$$\frac{d}{ds} = -\frac{d}{dx_1} \quad (3.990)$$

Using Equation (3.988) the following can be stated:

$$\frac{\partial S_\phi}{\partial n} = \kappa_2 \quad (3.991)$$

$$\frac{\partial^2 S_\phi}{\partial n^2} = \frac{\partial \kappa_2}{\partial n} \quad (3.992)$$

Using Equation (3.990) the following can also be stated:

$$\frac{\partial S_\phi}{\partial s} = -\kappa_1 \quad (3.993)$$

The first term of Equation (3.964) may be expressed as follows by substituting the result of Equation (3.890) gives the following:

$$\int_s W' \frac{\partial \phi'}{\partial n} ds = \int_s W' \left\{ \hat{\psi} \left(\Upsilon - 2i \frac{\partial S_\phi}{\partial n} \right) \left[- \left(\frac{\partial S_\phi}{\partial n} \right)^2 - i \frac{\partial^2 S_\phi}{\partial n^2} - K^2 - \frac{\partial^2}{\partial s^2} \right] \right\} \phi' ds \quad (3.994)$$

Expanding Equation (3.994) gives:

$$\int_s W' \frac{\partial \phi'}{\partial n} ds = \int_s W' \hat{\psi} \left[\begin{aligned} & -\Upsilon \left(\frac{\partial S_\phi}{\partial n} \right)^2 \phi' - i\Upsilon \frac{\partial^2 S_\phi}{\partial n^2} \phi' - \Upsilon K^2 \phi' - \Upsilon \frac{\partial^2 \phi'}{\partial s^2} \\ & - 2i \left(\frac{\partial S_\phi}{\partial n} \right)^3 \phi' + 2 \frac{\partial S_\phi}{\partial n} \frac{\partial^2 S_\phi}{\partial n^2} \phi' - 2i \frac{\partial S_\phi}{\partial n} K^2 \phi' - 2i \frac{\partial S_\phi}{\partial n} \frac{\partial^2 \phi'}{\partial s^2} \end{aligned} \right] ds \quad (3.995)$$

Isolating the real terms in Equation (3.995) yields:

$$\int_s W' \frac{\partial \phi'}{\partial n} ds = \int_s W' \hat{\psi} \left[\begin{aligned} & -\Upsilon \left(\frac{\partial S_\phi}{\partial n} \right)^2 \phi'_1 + \Upsilon \frac{\partial^2 S_\phi}{\partial n^2} \phi'_2 - \Upsilon K^2 \phi'_1 - \Upsilon \frac{\partial^2 \phi'_1}{\partial s^2} \\ & + 2 \left(\frac{\partial S_\phi}{\partial n} \right)^3 \phi'_2 + 2 \frac{\partial S_\phi}{\partial n} \frac{\partial^2 S_\phi}{\partial n^2} \phi'_1 + 2 \frac{\partial S_\phi}{\partial n} K^2 \phi'_2 + 2 \frac{\partial S_\phi}{\partial n} \frac{\partial^2 \phi'_2}{\partial s^2} \end{aligned} \right] ds \quad (3.996)$$

The results of Equations (3.984), (3.985), (3.991) and (3.992) can now be substituted in Equation (3.996) to give boundary conditions on the two absorbing boundaries. A radiation boundary condition will also be required for the Γ_3 boundary:

$$\begin{aligned} \int_S W^I \frac{\partial \phi'_1}{\partial n} ds = & \int_{\Gamma_{2d}} W^I \hat{\psi} \left[\begin{aligned} & -\Upsilon(-\kappa_1)^2 \phi'_1 + \Upsilon \left(-\frac{\partial \kappa_1}{\partial n} \right) \phi'_2 - \Upsilon K^2 \phi'_1 - \Upsilon \frac{\partial^2 \phi'_1}{\partial s^2} \\ & + 2(-\kappa_1)^3 \phi'_2 + 2(-\kappa_1) \left(-\frac{\partial \kappa_1}{\partial n} \right) \phi'_1 + 2(-\kappa_1) K^2 \phi'_2 + 2i(-\kappa_1) \frac{\partial^2 \phi'_2}{\partial s^2} \end{aligned} \right] ds \\ & + \int_{\Gamma_{2l}} W^I \hat{\psi} \left[\begin{aligned} & -\Upsilon(\kappa_2)^2 \phi'_1 + \Upsilon \frac{\partial \kappa_2}{\partial n} \phi'_2 - \Upsilon K^2 \phi'_1 - \Upsilon \frac{\partial^2 \phi'_1}{\partial s^2} \\ & + 2(\kappa_2)^3 \phi'_2 + 2\kappa_2 \frac{\partial \kappa_2}{\partial n} \phi'_1 + 2\kappa_2 K^2 \phi'_2 + 2\kappa_2 \frac{\partial^2 \phi'_2}{\partial s^2} \end{aligned} \right] ds + \int_{\Gamma_3} W^I \frac{\partial \phi'_1}{\partial n} ds \end{aligned} \quad (3.997)$$

Equation (3.997) can be simplified as follows:

$$\begin{aligned} \int_S W^I \frac{\partial \phi'_1}{\partial n} ds = & \int_{\Gamma_{2d}} W^I \left[\begin{aligned} & -\Upsilon \kappa_1^2 \phi'_1 - \Upsilon \frac{\partial \kappa_1}{\partial n} \phi'_2 - \Upsilon K^2 \phi'_1 - \Upsilon \frac{\partial^2 \phi'_1}{\partial s^2} \\ & - 2\kappa_1^3 \phi'_2 + 2\kappa_1 \frac{\partial \kappa_1}{\partial n} \phi'_1 - 2\kappa_1 K^2 \phi'_2 - 2\kappa_1 \frac{\partial^2 \phi'_2}{\partial s^2} \end{aligned} \right] ds \\ & + \int_{\Gamma_{2l}} W^I \left[\begin{aligned} & -\Upsilon \kappa_2^2 \phi'_1 + \Upsilon \frac{\partial \kappa_2}{\partial n} \phi'_2 - \Upsilon K^2 \phi'_1 - \Upsilon \frac{\partial^2 \phi'_1}{\partial s^2} \\ & + 2\kappa_2^3 \phi'_2 + 2\kappa_2 \frac{\partial \kappa_2}{\partial n} \phi'_1 + 2\kappa_2 K^2 \phi'_2 + 2\kappa_2 \frac{\partial^2 \phi'_2}{\partial s^2} \end{aligned} \right] ds + \int_{\Gamma_3} W^I \frac{\partial \phi'_1}{\partial n} ds \end{aligned} \quad (3.998)$$

The final term of Equation (3.998) can now be examined. Recalling Equation (3.929) for radiation boundary conditions:

$$\frac{\partial \phi'}{\partial n} = f'(\phi') - f'(\phi'^{in}) + \frac{\partial \phi'^{in}}{\partial n}$$

Equation (3.890) is an absorbing boundary equation for ϕ' . In this case ϕ' will be replaced with $\phi'^{out} (= \phi' - \phi'^{in})$ because only the outgoing wave should be absorbed on the radiating boundary. Using ϕ' and ϕ'^{in} with Equation (3.890) gives:

$$f'(\phi') = \hat{\psi} \left(\Upsilon - 2i \frac{\partial S_\phi}{\partial n} \right) \left[- \left(\frac{\partial S_\phi}{\partial n} \right)^2 - i \frac{\partial^2 S_\phi}{\partial n^2} - K^2 - \frac{\partial^2}{\partial s^2} \right] \phi' \quad (3.999)$$

$$f'(\phi'^{in}) = \hat{\psi} \left(\Upsilon - 2i \frac{\partial S_\phi}{\partial n} \right) \left[- \left(\frac{\partial S_\phi}{\partial n} \right)^2 - i \frac{\partial^2 S_\phi}{\partial n^2} - K^2 - \frac{\partial^2}{\partial s^2} \right] \phi'^{in} \quad (3.1000)$$

Expansion of Equations (3.999) and (3.1000) gives:

$$f'(\phi') = \left\{ \hat{\psi} \left[\begin{aligned} & -\Upsilon \left(\frac{\partial S_\phi}{\partial n} \right)^2 \phi' - i\Upsilon \frac{\partial^2 S_\phi}{\partial n^2} \phi' - \Upsilon K^2 \phi' - \Upsilon \frac{\partial^2 \phi'}{\partial s^2} \\ & - 2i \left(\frac{\partial S_\phi}{\partial n} \right)^3 \phi' + 2 \frac{\partial S_\phi}{\partial n} \frac{\partial^2 S_\phi}{\partial n^2} \phi' - 2i \frac{\partial S_\phi}{\partial n} K^2 \phi' - 2i \frac{\partial S_\phi}{\partial n} \frac{\partial^2 \phi'}{\partial s^2} \end{aligned} \right] \right\} \quad (3.1001)$$

$$f'(\phi'^{in}) = \left\{ \hat{\psi} \left[\begin{aligned} & -\Upsilon \left(\frac{\partial S_\phi}{\partial n} \right)^2 \phi'^{in} - i\Upsilon \frac{\partial^2 S_\phi}{\partial n^2} \phi'^{in} - \Upsilon K^2 \phi'^{in} - \Upsilon \frac{\partial^2 \phi'^{in}}{\partial s^2} \\ & - 2i \left(\frac{\partial S_\phi}{\partial n} \right)^3 \phi'^{in} + 2 \frac{\partial S_\phi}{\partial n} \frac{\partial^2 S_\phi}{\partial n^2} \phi'^{in} - 2i \frac{\partial S_\phi}{\partial n} K^2 \phi'^{in} - 2i \frac{\partial S_\phi}{\partial n} \frac{\partial^2 \phi'^{in}}{\partial s^2} \end{aligned} \right] \right\} \quad (3.1002)$$

Substituting Equations (3.1001) and (3.1002) into Equation (3.929) gives:

$$\begin{aligned} \frac{\partial \phi'}{\partial n} = & \left\{ \hat{\psi} \left[\begin{aligned} & -\Upsilon \left(\frac{\partial S_\phi}{\partial n} \right)^2 \phi' - i\Upsilon \frac{\partial^2 S_\phi}{\partial n^2} \phi' - \Upsilon K^2 \phi' - \Upsilon \frac{\partial^2 \phi'}{\partial s^2} \\ & - 2i \left(\frac{\partial S_\phi}{\partial n} \right)^3 \phi' + 2 \frac{\partial S_\phi}{\partial n} \frac{\partial^2 S_\phi}{\partial n^2} \phi' - 2i \frac{\partial S_\phi}{\partial n} K^2 \phi' - 2i \frac{\partial S_\phi}{\partial n} \frac{\partial^2 \phi'}{\partial s^2} \end{aligned} \right] \right\} \\ & - \left\{ \hat{\psi} \left[\begin{aligned} & -\Upsilon \left(\frac{\partial S_\phi}{\partial n} \right)^2 \phi'^{in} - i\Upsilon \frac{\partial^2 S_\phi}{\partial n^2} \phi'^{in} - \Upsilon K^2 \phi'^{in} - \Upsilon \frac{\partial^2 \phi'^{in}}{\partial s^2} \\ & - 2i \left(\frac{\partial S_\phi}{\partial n} \right)^3 \phi'^{in} + 2 \frac{\partial S_\phi}{\partial n} \frac{\partial^2 S_\phi}{\partial n^2} \phi'^{in} - 2i \frac{\partial S_\phi}{\partial n} K^2 \phi'^{in} - 2i \frac{\partial S_\phi}{\partial n} \frac{\partial^2 \phi'^{in}}{\partial s^2} \end{aligned} \right] \right\} + \frac{\partial \phi'^{in}}{\partial n} \end{aligned} \quad (3.1003)$$

The real component of Equation (3.1003) may now be isolated using Equation (3.916):

$$\begin{aligned} \frac{\partial \phi'_1}{\partial n} = & \left\{ \hat{\psi} \left[\begin{aligned} & -\Upsilon \left(\frac{\partial S_\phi}{\partial n} \right)^2 \phi'_1 + \Upsilon \frac{\partial^2 S_\phi}{\partial n^2} \phi'_2 - \Upsilon K^2 \phi'_1 - \Upsilon \frac{\partial^2 \phi'_1}{\partial s^2} \\ & + 2 \left(\frac{\partial S_\phi}{\partial n} \right)^3 \phi'_2 + 2 \frac{\partial S_\phi}{\partial n} \frac{\partial^2 S_\phi}{\partial n^2} \phi'_1 + 2 \frac{\partial S_\phi}{\partial n} K^2 \phi'_2 + 2 \frac{\partial S_\phi}{\partial n} \frac{\partial^2 \phi'_2}{\partial s^2} \end{aligned} \right] \right. \\ & \left. - \hat{\psi} \left[\begin{aligned} & -\Upsilon \left(\frac{\partial S_\phi}{\partial n} \right)^2 \phi'^{in}_1 + \Upsilon \frac{\partial^2 S_\phi}{\partial n^2} \phi'^{in}_2 - \Upsilon K^2 \phi'^{in}_1 - \Upsilon \frac{\partial^2 \phi'^{in}_1}{\partial s^2} \\ & + 2 \left(\frac{\partial S_\phi}{\partial n} \right)^3 \phi'^{in}_2 + 2 \frac{\partial S_\phi}{\partial n} \frac{\partial^2 S_\phi}{\partial n^2} \phi'^{in}_1 + 2 \frac{\partial S_\phi}{\partial n} K^2 \phi'^{in}_2 + 2 \frac{\partial S_\phi}{\partial n} \frac{\partial^2 \phi'^{in}_2}{\partial s^2} \end{aligned} \right] \right\} + \frac{\partial \phi'^{in}_1}{\partial n} \end{aligned} \quad (3.1004)$$

Examining Figure 3.13 shows that on the upstream radiating, Γ_{3u} , the following is true for the backscattered (i.e. absorbed wave):

$$n = x_1$$

Thus: (3.1005)

$$\frac{d}{dn} = \frac{d}{dx_1} \quad (3.1006)$$

The following is also true on Γ_{2d} :

$$s = x_2 \quad (3.1007)$$

Therefore:

$$\frac{d}{ds} = \frac{d}{dx_2} \quad (3.1008)$$

Using Equation (3.1006) the following can be stated:

$$\frac{\partial S_\phi}{\partial n} = \kappa_1 \quad (3.1009)$$

$$\frac{\partial^2 S_\phi}{\partial n^2} = \frac{\partial \kappa_1}{\partial n} \quad (3.1010)$$

Examining Figure 3.13 shows that on the side radiating boundary, Γ_{3l} , the following is true for the backscattered (i.e. absorbed wave):

$$n = -x_2 \quad (3.1011)$$

Thus:

$$\frac{d}{dn} = -\frac{d}{dx_2} \quad (3.1012)$$

The following is also true on Γ_{2d} :

$$s = x_1 \quad (3.1013)$$

Therefore:

$$\frac{d}{ds} = \frac{d}{dx_1} \quad (3.1014)$$

Using Equation (3.1012) the following can be stated:

$$\frac{\partial S_\phi}{\partial n} = -\kappa_2 \quad (3.1015)$$

$$\frac{\partial^2 S_\phi}{\partial n^2} = -\frac{\partial \kappa_2}{\partial n} \quad (3.1016)$$

Equations (3.1004), (3.1009), (3.1010), (3.1015) and (3.1016) can now be used with Equation (3.998) to give the following:

$$\begin{aligned}
\int_S W^I \frac{\partial \phi'_1}{\partial n} ds = & \int_{\Gamma_{2d}} W^I \hat{\psi} \left[\begin{array}{l} -\Upsilon \kappa_1^2 \phi'_1 - \Upsilon \frac{\partial \kappa_1}{\partial n} \phi'_2 - \Upsilon K^2 \phi'_1 - \Upsilon \frac{\partial^2 \phi'_1}{\partial s^2} \\ -2\kappa_1^3 \phi'_2 + 2\kappa_1 \frac{\partial \kappa_1}{\partial n} \phi'_1 - 2\kappa_1 K^2 \phi'_2 - 2i\kappa_1 \frac{\partial^2 \phi'_2}{\partial s^2} \end{array} \right] ds \\
& + \int_{\Gamma_{2l}} W^I \hat{\psi} \left[\begin{array}{l} -\Upsilon \kappa_2^2 \phi'_1 + \Upsilon \frac{\partial \kappa_2}{\partial n} \phi'_2 - \Upsilon K^2 \phi'_1 - \Upsilon \frac{\partial^2 \phi'_1}{\partial s^2} \\ +2\kappa_2^3 \phi'_2 + 2\kappa_2 \frac{\partial \kappa_2}{\partial n} \phi'_1 + 2\kappa_2 K^2 \phi'_2 + 2\kappa_2 \frac{\partial^2 \phi'_2}{\partial s^2} \end{array} \right] ds \\
& + \int_{\Gamma_{3u}} W^I \left\{ \hat{\psi} \left[\begin{array}{l} -\Upsilon (\kappa_1)^2 \phi'_1 + \Upsilon \left(\frac{\partial \kappa_1}{\partial n} \right) \phi'_2 - \Upsilon K^2 \phi'_1 - \Upsilon \frac{\partial^2 \phi'_1}{\partial s^2} \\ +2(\kappa_1)^3 \phi'_2 + 2(\kappa_1) \left(\frac{\partial \kappa_1}{\partial n} \right) \phi'_1 + 2(\kappa_1) K^2 \phi'_2 + 2(\kappa_1) \frac{\partial^2 \phi'_2}{\partial s^2} \end{array} \right] \right\} ds \\
& - \int_{\Gamma_{3u}} W^I \left\{ \hat{\psi} \left[\begin{array}{l} -\Upsilon (\kappa_1)^2 \phi_1'^{in} + \Upsilon \left(\frac{\partial \kappa_1}{\partial n} \right) \phi_2'^{in} - \Upsilon K^2 \phi_1'^{in} - \Upsilon \frac{\partial^2 \phi_1'^{in}}{\partial s^2} \\ +2(\kappa_1)^3 \phi_2'^{in} + 2(\kappa_1) \left(\frac{\partial \kappa_1}{\partial n} \right) \phi_1'^{in} + 2(\kappa_1) K^2 \phi_2'^{in} + 2(\kappa_1) \frac{\partial^2 \phi_2'^{in}}{\partial s^2} \end{array} \right] \right\} ds \\
& + \int_{\Gamma_{3u,3l}} W^I \frac{\partial \phi_1'^{in}}{\partial n} ds \\
& + \int_{\Gamma_{3l}} W^I \left\{ \hat{\psi} \left[\begin{array}{l} -\Upsilon (-\kappa_2)^2 \phi'_1 + \Upsilon \left(-\frac{\partial \kappa_2}{\partial n} \right) \phi'_2 - \Upsilon K^2 \phi'_1 - \Upsilon \frac{\partial^2 \phi'_1}{\partial s^2} \\ +2(-\kappa_2)^3 \phi'_2 + 2(-\kappa_2) \left(-\frac{\partial \kappa_2}{\partial n} \right) \phi'_1 + 2(-\kappa_2) K^2 \phi'_2 + 2(-\kappa_2) \frac{\partial^2 \phi'_2}{\partial s^2} \end{array} \right] \right\} ds \\
& - \int_{\Gamma_{3l}} W^I \left\{ \hat{\psi} \left[\begin{array}{l} -\Upsilon (-\kappa_2)^2 \phi_1'^{in} + \Upsilon \left(-\frac{\partial \kappa_2}{\partial n} \right) \phi_2'^{in} - \Upsilon K^2 \phi_1'^{in} - \Upsilon \frac{\partial^2 \phi_1'^{in}}{\partial s^2} \\ +2(-\kappa_2)^3 \phi_2'^{in} + 2(-\kappa_2) \left(-\frac{\partial \kappa_2}{\partial n} \right) \phi_1'^{in} + 2(-\kappa_2) K^2 \phi_2'^{in} + 2(-\kappa_2) \frac{\partial^2 \phi_2'^{in}}{\partial s^2} \end{array} \right] \right\} ds
\end{aligned} \tag{3.1017}$$

Equation (3.1017) may be expressed more explicitly as:

$$\begin{aligned}
\int_S W^I \frac{\partial \phi'_1}{\partial n} ds = & \int_{\Gamma_{2d}} W^I \hat{\psi} \left[\begin{array}{l} -\Upsilon \kappa_1^2 \phi'_1 - \Upsilon \frac{\partial \kappa_1}{\partial n} \phi'_2 - \Upsilon K^2 \phi'_1 - \Upsilon \frac{\partial^2 \phi'_1}{\partial s^2} \\ -2\kappa_1^3 \phi'_2 + 2\kappa_1 \frac{\partial \kappa_1}{\partial n} \phi'_1 - 2\kappa_1 K^2 \phi'_2 - 2i\kappa_1 \frac{\partial^2 \phi'_2}{\partial s^2} \end{array} \right] ds \\
& + \int_{\Gamma_{2l}} W^I \hat{\psi} \left[\begin{array}{l} -\Upsilon \kappa_2^2 \phi'_1 + \Upsilon \frac{\partial \kappa_2}{\partial n} \phi'_2 - \Upsilon K^2 \phi'_1 - \Upsilon \frac{\partial^2 \phi'_1}{\partial s^2} \\ +2\kappa_2^3 \phi'_2 + 2\kappa_2 \frac{\partial \kappa_2}{\partial n} \phi'_1 + 2\kappa_2 K^2 \phi'_2 + 2\kappa_2 \frac{\partial^2 \phi'_2}{\partial s^2} \end{array} \right] ds \\
& + \int_{\Gamma_{3u}} W^I \left\{ \hat{\psi} \left[\begin{array}{l} -\Upsilon \kappa_1^2 \phi'_1 + \Upsilon \frac{\partial \kappa_1}{\partial n} \phi'_2 - \Upsilon K^2 \phi'_1 - \Upsilon \frac{\partial^2 \phi'_1}{\partial s^2} \\ +2\kappa_1^3 \phi'_2 + 2\kappa_1 \frac{\partial \kappa_1}{\partial n} \phi'_1 + 2\kappa_1 K^2 \phi'_2 + 2\kappa_1 \frac{\partial^2 \phi'_2}{\partial s^2} \end{array} \right] \right\} ds \\
& + \int_{\Gamma_{3l}} W^I \left\{ \hat{\psi} \left[\begin{array}{l} -\Upsilon \kappa_2^2 \phi'_1 - \Upsilon \frac{\partial \kappa_2}{\partial n} \phi'_2 - \Upsilon K^2 \phi'_1 - \Upsilon \frac{\partial^2 \phi'_1}{\partial s^2} \\ -2\kappa_2^3 \phi'_2 + 2\kappa_2 \frac{\partial \kappa_2}{\partial n} \phi'_1 - 2\kappa_2 K^2 \phi'_2 - 2\kappa_2 \frac{\partial^2 \phi'_2}{\partial s^2} \end{array} \right] \right\} ds \\
& + \int_{\Gamma_{3u,3l}} W^I \frac{\partial \phi_1'^{in}}{\partial n} ds \\
& - \int_{\Gamma_{3u}} W^I \left\{ \hat{\psi} \left[\begin{array}{l} -\Upsilon \kappa_1^2 \phi_1'^{in} + \Upsilon \frac{\partial \kappa_1}{\partial n} \phi_2'^{in} - \Upsilon K^2 \phi_1'^{in} - \Upsilon \frac{\partial^2 \phi_1'^{in}}{\partial s^2} \\ +2\kappa_1^3 \phi_2'^{in} + 2\kappa_1 \frac{\partial \kappa_1}{\partial n} \phi_1'^{in} + 2\kappa_1 K^2 \phi_2'^{in} + 2\kappa_1 \frac{\partial^2 \phi_2'^{in}}{\partial s^2} \end{array} \right] \right\} ds \\
& - \int_{\Gamma_{3l}} W^I \left\{ \hat{\psi} \left[\begin{array}{l} -\Upsilon \kappa_2^2 \phi_1'^{in} - \Upsilon \frac{\partial \kappa_2}{\partial n} \phi_2'^{in} - \Upsilon K^2 \phi_1'^{in} - \Upsilon \frac{\partial^2 \phi_1'^{in}}{\partial s^2} \\ -2\kappa_2^3 \phi_2'^{in} + 2\kappa_2 \frac{\partial \kappa_2}{\partial n} \phi_1'^{in} - 2\kappa_2 K^2 \phi_2'^{in} - 2\kappa_2 \frac{\partial^2 \phi_2'^{in}}{\partial s^2} \end{array} \right] \right\} ds
\end{aligned} \tag{3.1018}$$

Further simplification yields:

$$\begin{aligned}
\int_S W^I \frac{\partial \phi'_1}{\partial n} ds = & - \int_{\Gamma_{2d,3u}} W^I \hat{\psi} \kappa_1^2 \phi'_1 ds - \int_{\Gamma_{2d}} W^I \hat{\psi} \Gamma \frac{\partial \kappa_1}{\partial n} \phi'_2 ds - \int_{\Gamma_{2d,3u}} W^I \hat{\psi} \Gamma K^2 \phi'_1 ds - \int_{\Gamma_{2d,3u}} W^I \hat{\psi} \Gamma \frac{\partial^2 \phi'_1}{\partial s^2} ds \\
& - 2 \int_{\Gamma_{2d}} W^I \hat{\psi} \kappa_1^3 \phi'_2 ds + 2 \int_{\Gamma_{2d,3u}} W^I \hat{\psi} \kappa_1 \frac{\partial \kappa_1}{\partial n} \phi'_1 ds - 2 \int_{\Gamma_{2d}} W^I \hat{\psi} \kappa_1 K^2 \phi'_2 ds - 2 \int_{\Gamma_{2d}} W^I \hat{\psi} \kappa_1 \frac{\partial^2 \phi'_2}{\partial s^2} ds \\
& + \int_{\Gamma_{3u}} W^I \hat{\psi} \Gamma \frac{\partial \kappa_1}{\partial n} \phi'_2 ds + 2 \int_{\Gamma_{3u}} W^I \hat{\psi} \kappa_1^3 \phi'_2 ds + 2 \int_{\Gamma_{3u}} W^I \hat{\psi} \kappa_1 K^2 \phi'_2 ds + 2 \int_{\Gamma_{3u}} W^I \hat{\psi} \kappa_1 \frac{\partial^2 \phi'_2}{\partial s^2} ds \\
& - \int_{\Gamma_{2l,3l}} W^I \hat{\psi} \Gamma \kappa_2^2 \phi'_1 ds + \int_{\Gamma_{2l}} W^I \hat{\psi} \Gamma \frac{\partial \kappa_2}{\partial n} \phi'_2 ds - \int_{\Gamma_{2l,3l}} W^I \hat{\psi} \Gamma K^2 \phi'_1 ds - \int_{\Gamma_{2l,3l}} W^I \hat{\psi} \Gamma \frac{\partial^2 \phi'_1}{\partial s^2} ds \\
& + 2 \int_{\Gamma_{2l}} W^I \hat{\psi} \kappa_2^3 \phi'_2 ds + 2 \int_{\Gamma_{2l,3l}} W^I \hat{\psi} \kappa_2 \frac{\partial \kappa_2}{\partial n} \phi'_1 ds + 2 \int_{\Gamma_{2l}} W^I \hat{\psi} \kappa_2 K^2 \phi'_2 ds + 2 \int_{\Gamma_{2l}} W^I \hat{\psi} \kappa_2 \frac{\partial^2 \phi'_2}{\partial s^2} ds \\
& - \int_{\Gamma_{3l}} W^I \hat{\psi} \Gamma \frac{\partial \kappa_2}{\partial n} \phi'_2 ds - 2 \int_{\Gamma_{3l}} W^I \hat{\psi} \kappa_2^3 \phi'_2 ds - 2 \int_{\Gamma_{3l}} W^I \hat{\psi} \kappa_2 K^2 \phi'_2 ds - 2 \int_{\Gamma_{3l}} W^I \hat{\psi} \kappa_2 \frac{\partial^2 \phi'_2}{\partial s^2} ds \\
& + \int_{\Gamma_{3u}} W^I \hat{\psi} \Gamma \kappa_1^2 \phi_1'^{in} ds - \int_{\Gamma_{3u}} W^I \hat{\psi} \Gamma \frac{\partial \kappa_1}{\partial n} \phi_2'^{in} ds + \int_{\Gamma_{3u}} W^I \hat{\psi} \Gamma K^2 \phi_1'^{in} ds + \int_{\Gamma_{3u}} W^I \hat{\psi} \Gamma \frac{\partial^2 \phi_1'^{in}}{\partial s^2} ds \\
& - 2 \int_{\Gamma_{3u}} W^I \hat{\psi} \kappa_1^3 \phi_2'^{in} ds - 2 \int_{\Gamma_{3u}} W^I \hat{\psi} \kappa_1 \frac{\partial \kappa_1}{\partial n} \phi_1'^{in} ds - 2 \int_{\Gamma_{3u}} W^I \hat{\psi} \kappa_1 K^2 \phi_2'^{in} ds - 2 \int_{\Gamma_{3u}} W^I \hat{\psi} \kappa_1 \frac{\partial^2 \phi_2'^{in}}{\partial s^2} ds \\
& + \int_{\Gamma_{3l}} W^I \hat{\psi} \Gamma \kappa_2^2 \phi_1'^{in} ds + \int_{\Gamma_{3l}} W^I \hat{\psi} \Gamma \frac{\partial \kappa_2}{\partial n} \phi_2'^{in} ds + \int_{\Gamma_{3l}} W^I \hat{\psi} \Gamma K^2 \phi_1'^{in} ds + \int_{\Gamma_{3l}} W^I \hat{\psi} \Gamma \frac{\partial^2 \phi_1'^{in}}{\partial s^2} ds \\
& + 2 \int_{\Gamma_{3l}} W^I \hat{\psi} \kappa_2^3 \phi_2'^{in} ds - 2 \int_{\Gamma_{3l}} W^I \hat{\psi} \kappa_2 \frac{\partial \kappa_2}{\partial n} \phi_1'^{in} ds + 2 \int_{\Gamma_{3l}} W^I \hat{\psi} \kappa_2 K^2 \phi_2'^{in} ds + 2 \int_{\Gamma_{3l}} W^I \hat{\psi} \kappa_2 \frac{\partial^2 \phi_2'^{in}}{\partial s^2} ds \\
& + \int_{\Gamma_{3u,3l}} W^I \frac{\partial \phi_1'^{in}}{\partial n} ds
\end{aligned} \tag{3.1019}$$

Replacing the weighting function with a shape function to follow the Galerkin method and applying the Gauss divergence theorem to the second order derivatives with respect to s gives:

$$\begin{aligned}
\int_S L' \frac{\partial \phi'}{\partial n} ds = & - \int_{\Gamma_{2d,3u}} L' \hat{\psi} \Upsilon \kappa_1^2 \phi'_1 ds - \int_{\Gamma_{2d}} L' \hat{\psi} \Upsilon \frac{\partial \kappa_1}{\partial n} \phi'_2 ds - \int_{\Gamma_{2d,3u}} L' \hat{\psi} \Upsilon K^2 \phi'_1 ds + \left(-L' \hat{\psi} \Upsilon \frac{\partial \phi'_1}{\partial s} \Big|_0 \right)_{\Gamma_{2d,3u}} \\
& + \int_{\Gamma_{2d,3u}} \frac{\partial L'}{\partial s} \hat{\psi} \Upsilon \frac{\partial \phi'}{\partial s} ds + \int_{\Gamma_{2d,3u}} L' \frac{\partial \hat{\psi}}{\partial s} \Upsilon \frac{\partial \phi'}{\partial s} ds + \int_{\Gamma_{2d,3u}} L' \hat{\psi} \frac{\partial \Upsilon}{\partial s} \frac{\partial \phi'}{\partial s} ds - 2 \int_{\Gamma_{2d}} L' \hat{\psi} \kappa_1^3 \phi'_2 ds \\
& + 2 \int_{\Gamma_{2d,3u}} L' \hat{\psi} \kappa_1 \frac{\partial \kappa_1}{\partial n} \phi'_1 ds - 2 \int_{\Gamma_{2d}} L' \hat{\psi} \kappa_1 K^2 \phi'_2 ds + \left(-2L' \hat{\psi} \kappa_1 \frac{\partial \phi'_2}{\partial s} \Big|_0 \right)_{\Gamma_{2d}} + 2 \int_{\Gamma_{2d}} \frac{\partial L'}{\partial s} \hat{\psi} \kappa_1 \frac{\partial \phi'_2}{\partial s} ds \\
& + 2 \int_{\Gamma_{2d}} L' \frac{\partial \hat{\psi}}{\partial s} \kappa_1 \frac{\partial \phi'_2}{\partial s} ds + 2 \int_{\Gamma_{2d}} L' \hat{\psi} \frac{\partial \kappa_1}{\partial s} \frac{\partial \phi'_2}{\partial s} ds + \int_{\Gamma_{3u}} L' \hat{\psi} \Upsilon \frac{\partial \kappa_1}{\partial n} \phi'_2 ds + 2 \int_{\Gamma_{3u}} L' \hat{\psi} \kappa_1^3 \phi'_2 ds \\
& + 2 \int_{\Gamma_{3u}} L' \hat{\psi} \kappa_1 K^2 \phi'_2 ds + \left(2L' \hat{\psi} \kappa_1 \frac{\partial \phi'_2}{\partial s} \Big|_0 \right)_{\Gamma_{3u}} - 2 \int_{\Gamma_{3u}} \frac{\partial L'}{\partial s} \hat{\psi} \kappa_1 \frac{\partial \phi'_2}{\partial s} ds - 2 \int_{\Gamma_{3u}} L' \frac{\partial \hat{\psi}}{\partial s} \kappa_1 \frac{\partial \phi'_2}{\partial s} ds \\
& - 2 \int_{\Gamma_{3u}} L' \hat{\psi} \frac{\partial \kappa_1}{\partial s} \frac{\partial \phi'_2}{\partial s} ds - \int_{\Gamma_{2l,3l}} L' \hat{\psi} \Upsilon \kappa_2^2 \phi'_1 ds + \int_{\Gamma_{2l}} L' \hat{\psi} \Upsilon \frac{\partial \kappa_2}{\partial n} \phi'_2 ds - \int_{\Gamma_{2l,3l}} L' \hat{\psi} \Upsilon K^2 \phi'_1 ds \\
& + \left(-L' \hat{\psi} \Upsilon \frac{\partial \phi'_1}{\partial s} \Big|_0 \right)_{\Gamma_{2l,3l}} + \int_{\Gamma_{2l,3l}} \frac{\partial L'}{\partial s} \hat{\psi} \Upsilon \frac{\partial \phi'_1}{\partial s} ds + \int_{\Gamma_{2l,3l}} L' \frac{\partial \hat{\psi}}{\partial s} \Upsilon \frac{\partial \phi'_1}{\partial s} ds + \int_{\Gamma_{2l,3l}} L' \hat{\psi} \frac{\partial \Upsilon}{\partial s} \frac{\partial \phi'_1}{\partial s} ds \\
& + 2 \int_{\Gamma_{2l}} L' \hat{\psi} \kappa_2^3 \phi'_2 ds + 2 \int_{\Gamma_{2l,3l}} L' \hat{\psi} \kappa_2 \frac{\partial \kappa_2}{\partial n} \phi'_1 ds + 2 \int_{\Gamma_{2l}} L' \hat{\psi} \kappa_2 K^2 \phi'_2 ds + \left(2L' \hat{\psi} \kappa_2 \frac{\partial \phi'_2}{\partial s} \Big|_0 \right)_{\Gamma_{2l}} \\
& - 2 \int_{\Gamma_{2l}} \frac{\partial L'}{\partial s} \hat{\psi} \kappa_2 \frac{\partial \phi'_2}{\partial s} ds - 2 \int_{\Gamma_{2l}} L' \frac{\partial \hat{\psi}}{\partial s} \kappa_2 \frac{\partial \phi'_2}{\partial s} ds - 2 \int_{\Gamma_{2l}} L' \hat{\psi} \frac{\partial \kappa_2}{\partial s} \frac{\partial \phi'_2}{\partial s} ds - \int_{\Gamma_{3l}} L' \hat{\psi} \Upsilon \frac{\partial \kappa_2}{\partial n} \phi'_2 ds \\
& - 2 \int_{\Gamma_{3l}} L' \hat{\psi} \kappa_2^3 \phi'_2 ds - 2 \int_{\Gamma_{3l}} L' \hat{\psi} \kappa_2 K^2 \phi'_2 ds + \left(-2L' \hat{\psi} \kappa_2 \frac{\partial \phi'_2}{\partial s} \Big|_0 \right)_{\Gamma_{3l}} + 2 \int_{\Gamma_{3l}} \frac{\partial L'}{\partial s} \hat{\psi} \kappa_2 \frac{\partial \phi'_2}{\partial s} ds \\
& + 2 \int_{\Gamma_{3l}} L' \frac{\partial \hat{\psi}}{\partial s} \kappa_2 \frac{\partial \phi'_2}{\partial s} ds + 2 \int_{\Gamma_{3l}} L' \hat{\psi} \frac{\partial \kappa_2}{\partial s} \frac{\partial \phi'_2}{\partial s} ds + \int_{\Gamma_{3u}} L' \hat{\psi} \Upsilon \kappa_1^2 \phi'^{in}_1 ds - \int_{\Gamma_{3u}} L' \hat{\psi} \Upsilon \frac{\partial \kappa_1}{\partial n} \phi'^{in}_2 ds \\
& + \int_{\Gamma_{3u}} L' \hat{\psi} \Upsilon K^2 \phi'^{in}_1 ds + \left(L' \hat{\psi} \Upsilon \frac{\partial \phi'^{in}_1}{\partial s} \Big|_0 \right)_{\Gamma_{3u}} - \int_{\Gamma_{3u}} \frac{\partial L'}{\partial s} \hat{\psi} \Upsilon \frac{\partial \phi'^{in}_1}{\partial s} ds - \int_{\Gamma_{3u}} L' \frac{\partial \hat{\psi}}{\partial s} \Upsilon \frac{\partial \phi'^{in}_1}{\partial s} ds \\
& - \int_{\Gamma_{3u}} L' \hat{\psi} \frac{\partial \Upsilon}{\partial s} \frac{\partial \phi'^{in}_1}{\partial s} ds - 2 \int_{\Gamma_{3u}} L' \hat{\psi} \kappa_1^3 \phi'^{in}_2 ds - 2 \int_{\Gamma_{3u}} L' \hat{\psi} \kappa_1 \frac{\partial \kappa_1}{\partial n} \phi'^{in}_2 ds - 2 \int_{\Gamma_{3u}} L' \hat{\psi} \kappa_1 K^2 \phi'^{in}_2 ds \\
& + \left(-2L' \hat{\psi} \kappa_1 \frac{\partial \phi'^{in}_2}{\partial s} \Big|_0 \right)_{\Gamma_{3u}} + 2 \int_{\Gamma_{3u}} \frac{\partial L'}{\partial s} \hat{\psi} \kappa_1 \frac{\partial \phi'^{in}_2}{\partial s} ds + 2 \int_{\Gamma_{3u}} L' \frac{\partial \hat{\psi}}{\partial s} \kappa_1 \frac{\partial \phi'^{in}_2}{\partial s} ds + 2 \int_{\Gamma_{3u}} L' \hat{\psi} \frac{\partial \kappa_1}{\partial s} \frac{\partial \phi'^{in}_2}{\partial s} ds \\
& + \int_{\Gamma_{3l}} L' \hat{\psi} \Upsilon \kappa_2^2 \phi'^{in}_1 ds + \int_{\Gamma_{3l}} L' \hat{\psi} \Upsilon \frac{\partial \kappa_2}{\partial n} \phi'^{in}_2 ds + \int_{\Gamma_{3l}} L' \hat{\psi} \Upsilon K^2 \phi'^{in}_1 ds + \left(L' \hat{\psi} \Upsilon \frac{\partial \phi'^{in}_1}{\partial s} \Big|_0 \right)_{\Gamma_{3l}}
\end{aligned}$$

cont..

$$\begin{aligned}
& - \int_{\Gamma_{3l}} \frac{\partial L^l}{\partial s} \hat{\psi} \Upsilon \frac{\partial \phi_1'^{in}}{\partial s} ds - \int_{\Gamma_{3l}} L^l \frac{\partial \hat{\psi}}{\partial s} \Upsilon \frac{\partial \phi_1'^{in}}{\partial s} ds - \int_{\Gamma_{3l}} L^l \hat{\psi} \frac{\partial \Upsilon}{\partial s} \frac{\partial \phi_1'^{in}}{\partial s} ds + 2 \int_{\Gamma_{3l}} L^l \hat{\psi} \kappa_2^3 \phi_2'^{in} ds \\
& - 2 \int_{\Gamma_{3l}} L^l \hat{\psi} \kappa_2 \frac{\partial \kappa_2}{\partial n} \phi_1'^{in} ds + 2 \int_{\Gamma_{3l}} L^l \hat{\psi} \kappa_2 K^2 \phi_2'^{in} ds + \left(2 L^l \hat{\psi} \kappa \frac{\partial \phi_2'^{in}}{\partial s} \Big|_0^l \right)_{\Gamma_{3l}} - 2 \int_{\Gamma_{3l}} \frac{\partial L^l}{\partial s} \hat{\psi} \kappa \frac{\partial \phi_2'^{in}}{\partial s} ds \\
& - 2 \int_{\Gamma_{3l}} L^l \frac{\partial \hat{\psi}}{\partial s} \kappa \frac{\partial \phi_2'^{in}}{\partial s} ds - 2 \int_{\Gamma_{3l}} L^l \hat{\psi} \frac{\partial \kappa}{\partial s} \frac{\partial \phi_2'^{in}}{\partial s} ds + \int_{\Gamma_{3u,3l}} L^l \frac{\partial \phi_1'^{in}}{\partial n} ds
\end{aligned} \tag{3.1020}$$

Applying a shape function to the velocity potential values in Equation (3.1020) gives:

$$\begin{aligned}
\int_S L' \frac{\partial \phi_1'}{\partial n} ds = & - \int_{\Gamma_{2d,3u}} \hat{\psi} \Upsilon \kappa_1^2 L' L' \phi_1'^J ds - \int_{\Gamma_{2d}} \hat{\psi} \Upsilon \frac{\partial \kappa_1}{\partial n} L' L' \phi_2'^J ds - \int_{\Gamma_{2d,3u}} \hat{\psi} \Upsilon K^2 L' L' \phi_1'^J ds + \left(-L' \hat{\psi} \Upsilon \frac{\partial \phi_1'}{\partial s} \Big|_0 \right)_{\Gamma_{2d,3u}} \\
& + \int_{\Gamma_{2d,3u}} \hat{\psi} \Upsilon \frac{\partial L'}{\partial s} \frac{\partial L'}{\partial s} \phi_1'^J ds + \int_{\Gamma_{2d,3u}} \frac{\partial \hat{\psi}}{\partial s} \Upsilon L' \frac{\partial L'}{\partial s} \phi_1'^J ds + \int_{\Gamma_{2d,3u}} \hat{\psi} \frac{\partial \Upsilon}{\partial s} L' \frac{\partial L'}{\partial s} \phi_1'^J ds - 2 \int_{\Gamma_{2d}} \hat{\psi} \kappa_1^3 L' L' \phi_2'^J ds \\
& + 2 \int_{\Gamma_{2d,3u}} \hat{\psi} \kappa_1 \frac{\partial \kappa_1}{\partial n} L' L' \phi_1'^J ds - 2 \int_{\Gamma_{2d}} \hat{\psi} \kappa_1 K^2 L' L' \phi_2'^J ds + \left(-2L' \hat{\psi} \kappa_1 \frac{\partial \phi_2'}{\partial s} \Big|_0 \right)_{\Gamma_{2d}} + 2 \int_{\Gamma_{2d}} \hat{\psi} \kappa_1 \frac{\partial L'}{\partial s} \frac{\partial L'}{\partial s} \phi_2'^J ds \\
& + 2 \int_{\Gamma_{2d}} \frac{\partial \hat{\psi}}{\partial s} \kappa_1 L' \frac{\partial L'}{\partial s} \phi_1'^J ds + 2 \int_{\Gamma_{2d}} \hat{\psi} \frac{\partial \kappa_1}{\partial s} L' \frac{\partial L'}{\partial s} \phi_1'^J ds + \int_{\Gamma_{3u}} \hat{\psi} \Upsilon \frac{\partial \kappa_1}{\partial n} L' L' \phi_2'^J ds + 2 \int_{\Gamma_{3u}} \hat{\psi} \kappa_1^3 L' L' \phi_2'^J ds \\
& + 2 \int_{\Gamma_{3u}} \hat{\psi} \kappa_1 K^2 L' L' \phi_2'^J ds + \left(2L' \hat{\psi} \kappa_1 \frac{\partial \phi_2'}{\partial s} \Big|_0 \right)_{\Gamma_{3u}} - 2 \int_{\Gamma_{3u}} \hat{\psi} \kappa_1 \frac{\partial L'}{\partial s} \frac{\partial L'}{\partial s} \phi_2'^J ds - 2 \int_{\Gamma_{3u}} \frac{\partial \hat{\psi}}{\partial s} \kappa_1 L' \frac{\partial L'}{\partial s} \phi_2'^J ds \\
& - 2 \int_{\Gamma_{3u}} \hat{\psi} \frac{\partial \kappa_1}{\partial s} L' \frac{\partial L'}{\partial s} \phi_2'^J ds - \int_{\Gamma_{2l,3l}} L' \hat{\psi} \Upsilon \kappa_2^2 L' L' \phi_1'^J ds + \int_{\Gamma_{2l}} \hat{\psi} \Upsilon \frac{\partial \kappa_2}{\partial n} L' L' \phi_2'^J ds - \int_{\Gamma_{2l,3l}} \hat{\psi} \Upsilon K^2 L' L' \phi_1'^J ds \\
& + \left(-L' \hat{\psi} \Upsilon \frac{\partial \phi_1'}{\partial s} \Big|_0 \right)_{\Gamma_{2l,3l}} + \int_{\Gamma_{2l,3l}} \hat{\psi} \Upsilon \frac{\partial L'}{\partial s} \frac{\partial L'}{\partial s} \phi_1'^J ds + \int_{\Gamma_{2l,3l}} \frac{\partial \hat{\psi}}{\partial s} \Upsilon L' \frac{\partial L'}{\partial s} \phi_1'^J ds + \int_{\Gamma_{2l,3l}} \hat{\psi} \frac{\partial \Upsilon}{\partial s} L' \frac{\partial L'}{\partial s} \phi_1'^J ds \\
& + 2 \int_{\Gamma_{2l}} \hat{\psi} \kappa_2^3 L' L' \phi_2'^J ds + 2 \int_{\Gamma_{2l,3l}} \hat{\psi} \kappa_2 \frac{\partial \kappa_2}{\partial n} L' L' \phi_1'^J ds + 2 \int_{\Gamma_{2l}} \hat{\psi} \kappa_2 K^2 L' L' \phi_2'^J ds + \left(2L' \hat{\psi} \kappa_2 \frac{\partial \phi_2'}{\partial s} \Big|_0 \right)_{\Gamma_{2l}} \\
& - 2 \int_{\Gamma_{2l}} \hat{\psi} \kappa_2 \frac{\partial L'}{\partial s} \frac{\partial L'}{\partial s} \phi_2'^J ds - 2 \int_{\Gamma_{2l}} \frac{\partial \hat{\psi}}{\partial s} \kappa_2 L' \frac{\partial L'}{\partial s} \phi_2'^J ds - 2 \int_{\Gamma_{2l}} \hat{\psi} \frac{\partial \kappa_2}{\partial s} L' \frac{\partial L'}{\partial s} \phi_2'^J ds - \int_{\Gamma_{3l}} \hat{\psi} \Upsilon \frac{\partial \kappa_2}{\partial n} L' L' \phi_2'^J ds \\
& - 2 \int_{\Gamma_{3l}} \hat{\psi} \kappa_2^3 L' L' \phi_2'^J ds - 2 \int_{\Gamma_{3l}} \hat{\psi} \kappa_2 K^2 L' L' \phi_2'^J ds + \left(-2L' \hat{\psi} \kappa_2 \frac{\partial \phi_2'}{\partial s} \Big|_0 \right)_{\Gamma_{3l}} + 2 \int_{\Gamma_{3l}} \hat{\psi} \kappa_2 \frac{\partial L'}{\partial s} \frac{\partial L'}{\partial s} \phi_2'^J ds \\
& + 2 \int_{\Gamma_{3l}} \frac{\partial \hat{\psi}}{\partial s} \kappa_2 L' \frac{\partial L'}{\partial s} \phi_2'^J ds + 2 \int_{\Gamma_{3l}} \hat{\psi} \frac{\partial \kappa_2}{\partial s} L' \frac{\partial L'}{\partial s} \phi_2'^J ds + \int_{\Gamma_{3u}} \hat{\psi} \Upsilon \kappa_1^2 L' L' (\phi_1'^{in})^J ds - \int_{\Gamma_{3u}} \hat{\psi} \Upsilon \frac{\partial \kappa_1}{\partial n} L' L' (\phi_2'^{in})^J ds \\
& + \int_{\Gamma_{3u}} \hat{\psi} \Upsilon K^2 L' L' (\phi_1'^{in})^J ds + \left(L' \hat{\psi} \Upsilon \frac{\partial \phi_1'^{in}}{\partial s} \Big|_0 \right)_{\Gamma_{3u}} - \int_{\Gamma_{3u}} \hat{\psi} \Upsilon \frac{\partial L'}{\partial s} \frac{\partial L'}{\partial s} (\phi_1'^{in})^J ds - \int_{\Gamma_{3u}} \frac{\partial \hat{\psi}}{\partial s} \Upsilon L' \frac{\partial L'}{\partial s} (\phi_1'^{in})^J ds \\
& - \int_{\Gamma_{3u}} \hat{\psi} \frac{\partial \Upsilon}{\partial s} L' \frac{\partial L'}{\partial s} (\phi_1'^{in})^J ds - 2 \int_{\Gamma_{3u}} \hat{\psi} \kappa_1^3 L' L' (\phi_2'^{in})^J ds - 2 \int_{\Gamma_{3u}} \hat{\psi} \kappa_1 \frac{\partial \kappa_1}{\partial n} L' L' (\phi_1'^{in})^J ds \\
& - 2 \int_{\Gamma_{3u}} \hat{\psi} \kappa_1 K^2 L' L' (\phi_2'^{in})^J ds + \left(-2L' \hat{\psi} \kappa_1 \frac{\partial \phi_2'^{in}}{\partial s} \Big|_0 \right)_{\Gamma_{3u}} + 2 \int_{\Gamma_{3u}} \hat{\psi} \kappa_1 \frac{\partial L'}{\partial s} \frac{\partial L'}{\partial s} (\phi_2'^{in})^J ds \\
& + 2 \int_{\Gamma_{3u}} \frac{\partial \hat{\psi}}{\partial s} \kappa_1 L' \frac{\partial L'}{\partial s} (\phi_2'^{in})^J ds + 2 \int_{\Gamma_{3u}} \hat{\psi} \frac{\partial \kappa_1}{\partial s} L' \frac{\partial L'}{\partial s} (\phi_2'^{in})^J ds + \int_{\Gamma_{3l}} \hat{\psi} \Upsilon \kappa_2^2 L' L' (\phi_1'^{in})^J ds \\
& + \int_{\Gamma_{3l}} \hat{\psi} \Upsilon \frac{\partial \kappa_2}{\partial n} L' L' (\phi_2'^{in})^J ds + \int_{\Gamma_{3l}} \hat{\psi} \Upsilon K^2 L' L' (\phi_1'^{in})^J ds + \left(L' \hat{\psi} \Upsilon \frac{\partial \phi_1'^{in}}{\partial s} \Big|_0 \right)_{\Gamma_{3l}}
\end{aligned}$$

cont..

$$\begin{aligned}
& - \int_{\Gamma_{3l}} \hat{\psi} \Upsilon \frac{\partial L^l}{\partial s} \frac{\partial L^j}{\partial s} (\phi_1'^{in})^j ds - \int_{\Gamma_{3l}} \frac{\partial \hat{\psi}}{\partial s} \Upsilon L^l \frac{\partial L^j}{\partial s} (\phi_1'^{in})^j ds - \int_{\Gamma_{3l}} \hat{\psi} \frac{\partial \Upsilon}{\partial s} L^l \frac{\partial L^j}{\partial s} (\phi_1'^{in})^j ds \\
& + 2 \int_{\Gamma_{3l}} \hat{\psi} \kappa_2^3 L^l L^j (\phi_2'^{in})^j ds - 2 \int_{\Gamma_{3l}} \hat{\psi} \kappa_2 \frac{\partial \kappa_2}{\partial n} L^l L^j (\phi_1'^{in})^j ds + 2 \int_{\Gamma_{3l}} \hat{\psi} \kappa_2 K^2 L^l L^j (\phi_2'^{in})^j ds \\
& + \left(2 L^l \hat{\psi} \kappa \frac{\partial \phi_2'^{in}}{\partial s} \bigg|_0^l \right)_{\Gamma_{3l}} - 2 \int_{\Gamma_{3l}} \hat{\psi} \kappa \frac{\partial L^l}{\partial s} \frac{\partial L^j}{\partial s} \phi_2'^j ds - 2 \int_{\Gamma_{3l}} \frac{\partial \hat{\psi}}{\partial s} \kappa L^l \frac{\partial L^j}{\partial s} \phi_2'^j ds \\
& - 2 \int_{\Gamma_{3l}} \hat{\psi} \frac{\partial \kappa}{\partial s} L^l \frac{\partial L^j}{\partial s} \phi_2'^j ds + \int_{\Gamma_{3u,3l}} L^l \frac{\partial \phi_1'^{in}}{\partial n} ds
\end{aligned} \tag{3.1021}$$

Equation (3.1021) can be substituted into Equation (3.964) to give a complete finite element equation for solution of the Helmholtz form of the extended elliptic mild-slope wave equation including currents for the given special case of a propagating wave in a domain with no obstacles:

$$\begin{aligned}
& - \int_{\Gamma_{2d,3u}} \hat{\psi} \Upsilon \kappa_1^2 L' L' \phi_1'^J ds - \int_{\Gamma_{2d}} \hat{\psi} \Upsilon \frac{\partial \kappa_1}{\partial n} L' L' \phi_2'^J ds - \int_{\Gamma_{2d,3u}} \hat{\psi} \Upsilon K^2 L' L' \phi_1'^J ds + \left(-L' \hat{\psi} \Upsilon \frac{\partial \phi_1'^J}{\partial s} \Big|_0 \right)_{\Gamma_{2d,3u}} \\
& + \int_{\Gamma_{2d,3u}} \hat{\psi} \Upsilon \frac{\partial L'}{\partial s} \frac{\partial L'}{\partial s} \phi_1'^J ds + \int_{\Gamma_{2d,3u}} \frac{\partial \hat{\psi}}{\partial s} \Upsilon L' \frac{\partial L'}{\partial s} \phi_1'^J ds + \int_{\Gamma_{2d,3u}} \hat{\psi} \frac{\partial \Upsilon}{\partial s} L' \frac{\partial L'}{\partial s} \phi_1'^J ds - 2 \int_{\Gamma_{2d}} \hat{\psi} \kappa_1^3 L' L' \phi_2'^J ds \\
& + 2 \int_{\Gamma_{2d,3u}} \hat{\psi} \kappa_1 \frac{\partial \kappa_1}{\partial n} L' L' \phi_1'^J ds - 2 \int_{\Gamma_{2d}} \hat{\psi} \kappa_1 K^2 L' L' \phi_2'^J ds + \left(-2L' \hat{\psi} \kappa_1 \frac{\partial \phi_2'^J}{\partial s} \Big|_0 \right)_{\Gamma_{2d}} + 2 \int_{\Gamma_{2d}} \hat{\psi} \kappa_1 \frac{\partial L'}{\partial s} \frac{\partial L'}{\partial s} \phi_2'^J ds \\
& + 2 \int_{\Gamma_{2d}} \frac{\partial \hat{\psi}}{\partial s} \kappa_1 L' \frac{\partial L'}{\partial s} \phi_1'^J ds + 2 \int_{\Gamma_{2d}} \hat{\psi} \frac{\partial \kappa_1}{\partial s} L' \frac{\partial L'}{\partial s} \phi_1'^J ds + \int_{\Gamma_{3u}} \hat{\psi} \Upsilon \frac{\partial \kappa_1}{\partial n} L' L' \phi_2'^J ds + 2 \int_{\Gamma_{3u}} \hat{\psi} \kappa_1^3 L' L' \phi_2'^J ds \\
& + 2 \int_{\Gamma_{3u}} \hat{\psi} \kappa_1 K^2 L' L' \phi_2'^J ds + \left(2L' \hat{\psi} \kappa_1 \frac{\partial \phi_2'^J}{\partial s} \Big|_0 \right)_{\Gamma_{3u}} - 2 \int_{\Gamma_{3u}} \hat{\psi} \kappa_1 \frac{\partial L'}{\partial s} \frac{\partial L'}{\partial s} \phi_2'^J ds - 2 \int_{\Gamma_{3u}} \frac{\partial \hat{\psi}}{\partial s} \kappa_1 L' \frac{\partial L'}{\partial s} \phi_2'^J ds \\
& - 2 \int_{\Gamma_{3u}} \hat{\psi} \frac{\partial \kappa_1}{\partial s} L' \frac{\partial L'}{\partial s} \phi_2'^J ds - \int_{\Gamma_{2l,3l}} L' \hat{\psi} \Upsilon \kappa_2^2 L' L' \phi_1'^J ds + \int_{\Gamma_{2l}} \hat{\psi} \Upsilon \frac{\partial \kappa_2}{\partial n} L' L' \phi_2'^J ds - \int_{\Gamma_{2l,3l}} \hat{\psi} \Upsilon K^2 L' L' \phi_1'^J ds \\
& + \left(-L' \hat{\psi} \Upsilon \frac{\partial \phi_1'^J}{\partial s} \Big|_0 \right)_{\Gamma_{2l,3l}} + \int_{\Gamma_{2l,3l}} \hat{\psi} \Upsilon \frac{\partial L'}{\partial s} \frac{\partial L'}{\partial s} \phi_1'^J ds + \int_{\Gamma_{2l,3l}} \frac{\partial \hat{\psi}}{\partial s} \Upsilon L' \frac{\partial L'}{\partial s} \phi_1'^J ds + \int_{\Gamma_{2l,3l}} \hat{\psi} \frac{\partial \Upsilon}{\partial s} L' \frac{\partial L'}{\partial s} \phi_1'^J ds \\
& + 2 \int_{\Gamma_{2l}} \hat{\psi} \kappa_2^3 L' L' \phi_2'^J ds + 2 \int_{\Gamma_{2l,3l}} \hat{\psi} \kappa_2 \frac{\partial \kappa_2}{\partial n} L' L' \phi_1'^J ds + 2 \int_{\Gamma_{2l}} \hat{\psi} \kappa_2 K^2 L' L' \phi_2'^J ds + \left(2L' \hat{\psi} \kappa_2 \frac{\partial \phi_2'^J}{\partial s} \Big|_0 \right)_{\Gamma_{2l}} \\
& - 2 \int_{\Gamma_{2l}} \hat{\psi} \kappa_2 \frac{\partial L'}{\partial s} \frac{\partial L'}{\partial s} \phi_2'^J ds - 2 \int_{\Gamma_{2l}} \frac{\partial \hat{\psi}}{\partial s} \kappa_2 L' \frac{\partial L'}{\partial s} \phi_2'^J ds - 2 \int_{\Gamma_{2l}} \hat{\psi} \frac{\partial \kappa_2}{\partial s} L' \frac{\partial L'}{\partial s} \phi_2'^J ds - \int_{\Gamma_{3l}} \hat{\psi} \Upsilon \frac{\partial \kappa_2}{\partial n} L' L' \phi_2'^J ds \\
& - 2 \int_{\Gamma_{3l}} \hat{\psi} \kappa_2^3 L' L' \phi_2'^J ds - 2 \int_{\Gamma_{3l}} \hat{\psi} \kappa_2 K^2 L' L' \phi_2'^J ds + \left(-2L' \hat{\psi} \kappa_2 \frac{\partial \phi_2'^J}{\partial s} \Big|_0 \right)_{\Gamma_{3l}} + 2 \int_{\Gamma_{3l}} \hat{\psi} \kappa_2 \frac{\partial L'}{\partial s} \frac{\partial L'}{\partial s} \phi_2'^J ds \\
& + 2 \int_{\Gamma_{3l}} \frac{\partial \hat{\psi}}{\partial s} \kappa_2 L' \frac{\partial L'}{\partial s} \phi_2'^J ds + 2 \int_{\Gamma_{3l}} \hat{\psi} \frac{\partial \kappa_2}{\partial s} L' \frac{\partial L'}{\partial s} \phi_2'^J ds - \iint_A \frac{\partial N^I}{\partial x_k} \frac{\partial N^J}{\partial x_k} \phi_1'^J dA + \iint_A K^2 N^I N^J \phi_1'^J dA \\
& + \iint_A W^I \frac{\omega^2}{CC_g} \phi_1'^J N^I N^J dA - \iint_A W^I \frac{\sigma^2}{CC_g} \phi_1'^J N^I N^J dA - \iint_A \frac{U_j}{CC_g} \frac{\partial U_k}{\partial x_j} N^I \frac{\partial N^J}{\partial x_k} \phi_1'^J dA \\
& + 2 \iint_A \frac{U_j U_k}{(CC_g)^{\frac{3}{2}}} \frac{\partial \sqrt{CC_g}}{\partial x_j} N^I \frac{\partial N^J}{\partial x_k} \phi_1'^J dA + \iint_A \frac{U_j}{(CC_g)^{\frac{3}{2}}} \frac{\partial U_k}{\partial x_j} \frac{\partial \sqrt{CC_g}}{\partial x_k} N^I N^J \phi_1'^J dA \\
& + \iint_A \frac{U_j U_k}{(CC_g)^{\frac{3}{2}}} \frac{\partial^2 \sqrt{CC_g}}{\partial x_j \partial x_k} N^I N^J \phi_1'^J dA - \iint_A \frac{U_j U_k}{(CC_g)^{\frac{5}{2}}} \frac{\partial \sqrt{CC_g}}{\partial x_k} \frac{\partial (CC_g)}{\partial x_j} N^I N^J \phi_1'^J dA
\end{aligned}$$

cont..

$$\begin{aligned}
& + \iint_A \frac{U_j U_k}{CC_g} \frac{\partial N^I}{\partial x_j} \frac{\partial N^J}{\partial x_k} \phi_1'^J dA + \iint_A \frac{\partial U_j}{\partial x_j} \frac{U_k}{CC_g} N^I \frac{\partial N^J}{\partial x_k} \phi_1'^J dA \\
& + \iint_A \frac{U_j}{CC_g} \frac{\partial U_k}{\partial x_j} N^I \frac{\partial N^J}{\partial x_k} \phi_1'^J dA + \iint_A U_k U_j \frac{\partial}{\partial x_j} \left[(CC_g)^{-1} \right] N^I \frac{\partial N^J}{\partial x_k} \phi_1'^J dA \\
& + \iint_A \frac{2\omega U_k}{(CC_g)^{\frac{3}{2}}} \frac{\partial \sqrt{CC_g}}{\partial x_k} N^I N^J \phi_2'^J dA - \iint_A \frac{2\omega U_k}{CC_g} N^I \frac{\partial N^J}{\partial x_k} \phi_2'^J dA = \\
& - \int_{\Gamma_{3u}} \hat{\psi} \Upsilon \kappa_1^2 L^I L^J (\phi_1'^{in})^J ds + \int_{\Gamma_{3u}} \hat{\psi} \Upsilon \frac{\partial \kappa_1}{\partial n} L^I L^J (\phi_2'^{in})^J ds - \int_{\Gamma_{3u}} \hat{\psi} \Upsilon K^2 L^I L^J (\phi_1'^{in})^J ds \\
& - \left(L^I \hat{\psi} \Upsilon \frac{\partial \phi_1'^{in}}{\partial s} \Big|_0^l \right)_{\Gamma_{3u}} + \int_{\Gamma_{3u}} \hat{\psi} \Upsilon \frac{\partial L^I}{\partial s} \frac{\partial L^J}{\partial s} (\phi_1'^{in})^J ds + \int_{\Gamma_{3u}} \frac{\partial \hat{\psi}}{\partial s} \Upsilon L^I \frac{\partial L^J}{\partial s} (\phi_1'^{in})^J ds \\
& + \int_{\Gamma_{3u}} \hat{\psi} \frac{\partial \Upsilon}{\partial s} L^I \frac{\partial L^J}{\partial s} (\phi_1'^{in})^J ds + 2 \int_{\Gamma_{3u}} \hat{\psi} \kappa_1^3 L^I L^J (\phi_2'^{in})^J ds + 2 \int_{\Gamma_{3u}} \hat{\psi} \kappa_1 \frac{\partial \kappa_1}{\partial n} L^I L^J (\phi_1'^{in})^J ds \\
& + 2 \int_{\Gamma_{3u}} \hat{\psi} \kappa_1 K^2 L^I L^J (\phi_2'^{in})^J ds - \left(-2 L^I \hat{\psi} \kappa_1 \frac{\partial \phi_2'^{in}}{\partial s} \Big|_0^l \right)_{\Gamma_{3u}} - 2 \int_{\Gamma_{3u}} \hat{\psi} \kappa_1 \frac{\partial L^I}{\partial s} \frac{\partial L^J}{\partial s} (\phi_2'^{in})^J ds \\
& - 2 \int_{\Gamma_{3u}} \frac{\partial \hat{\psi}}{\partial s} \kappa_1 L^I \frac{\partial L^J}{\partial s} (\phi_2'^{in})^J ds - 2 \int_{\Gamma_{3u}} \hat{\psi} \frac{\partial \kappa_1}{\partial s} L^I \frac{\partial L^J}{\partial s} (\phi_2'^{in})^J ds - \int_{\Gamma_{3l}} \hat{\psi} \Upsilon \kappa_2^2 L^I L^J (\phi_1'^{in})^J ds \\
& - \int_{\Gamma_{3l}} \hat{\psi} \Upsilon \frac{\partial \kappa_2}{\partial n} L^I L^J (\phi_2'^{in})^J ds - \int_{\Gamma_{3l}} \hat{\psi} \Upsilon K^2 L^I L^J (\phi_1'^{in})^J ds - \left(L^I \hat{\psi} \Upsilon \frac{\partial \phi_1'^{in}}{\partial s} \Big|_0^l \right)_{\Gamma_{3l}} \\
& + \int_{\Gamma_{3l}} \hat{\psi} \Upsilon \frac{\partial L^I}{\partial s} \frac{\partial L^J}{\partial s} (\phi_1'^{in})^J ds + \int_{\Gamma_{3l}} \frac{\partial \hat{\psi}}{\partial s} \Upsilon L^I \frac{\partial L^J}{\partial s} (\phi_1'^{in})^J ds + \int_{\Gamma_{3l}} \hat{\psi} \frac{\partial \Upsilon}{\partial s} L^I \frac{\partial L^J}{\partial s} (\phi_1'^{in})^J ds \\
& - 2 \int_{\Gamma_{3l}} \hat{\psi} \kappa_2^3 L^I L^J (\phi_2'^{in})^J ds + 2 \int_{\Gamma_{3l}} \hat{\psi} \kappa_2 \frac{\partial \kappa_2}{\partial n} L^I L^J (\phi_1'^{in})^J ds - 2 \int_{\Gamma_{3l}} \hat{\psi} \kappa_2 K^2 L^I L^J (\phi_2'^{in})^J ds \\
& - \left(2 L^I \hat{\psi} \kappa_2 \frac{\partial \phi_2'^{in}}{\partial s} \Big|_0^l \right)_{\Gamma_{3l}} + 2 \int_{\Gamma_{3l}} \hat{\psi} \kappa_2 \frac{\partial L^I}{\partial s} \frac{\partial L^J}{\partial s} \phi_2'^J ds + 2 \int_{\Gamma_{3l}} \frac{\partial \hat{\psi}}{\partial s} \kappa_2 L^I \frac{\partial L^J}{\partial s} \phi_2'^J ds \\
& + 2 \int_{\Gamma_{3l}} \hat{\psi} \frac{\partial \kappa_2}{\partial s} L^I \frac{\partial L^J}{\partial s} \phi_2'^J ds - \int_{\Gamma_{3u,3l}} L^I \frac{\partial \phi_1'^{in}}{\partial n} ds
\end{aligned} \tag{3.1022}$$

3.12 Wave Breaking in the One-Dimensional and Two-Dimensional Wave-Current Interaction Models

Section 2.3.2 discusses the inclusion of wave breaking effects in numerical wave models. Where simple linear breaking will be implemented in the NM-WCIM it is possible to solve the model with no energy dissipation (i.e. unbroken waves) and apply a scaling factor afterwards based on the similarity method discussed in Section 2.3.2. This will involve the selection of an appropriate insipience depth and a specific relationship between wave height in the breaking zone and water depth. Using the wave ray post-processing method discussed in Section 5.6 it is possible to apply the same methodology to more complex non-linear breaking processes.

As shown in Equation (3.527) it is also possible to include a dissipative term in the basic equations of the NM-WCIM. Zhao *et al.* (2001) and Clyne (2008) are among the authors who include an energy dissipation term based on eddy viscosity in their model equations. This same process has been applied to the NM-WCIM. All the non-dissipative terms in Equation (3.527) have already been accounted for and thus to include energy dissipation in the previously derived finite element equations it is only necessary to carry out integration of the dissipative terms over the finite element and isolate the real portion.

3.12.1 Energy Dissipation in 1d-NM-WCIM

Due to the constant nature of the one-dimensional model in the longshore direction only one of the dissipative terms will interact with the one-dimensional model. Equation (3.535) becomes the following in the one dimensional:

$$\begin{aligned} \frac{\partial}{\partial x_1} \left(CC_g \frac{\partial \hat{\phi}}{\partial x_1} \right) - \kappa_2^2 CC_g \hat{\phi} + \hat{\phi} \sigma^2 Q' + \kappa^2 CC_g \hat{\phi} - \sigma^2 \hat{\phi} \\ - g \frac{\partial \hat{\phi}}{\partial x_1} \left(\frac{\partial \bar{\eta}}{\partial x_1} \right) + \omega^2 \hat{\phi} - 2\omega \kappa_2 U_2 \hat{\phi} + \kappa_2^2 U_2^2 \hat{\phi} + i\omega \gamma \hat{\phi} + \gamma U_2 \frac{\partial \hat{\phi}}{\partial x_2} = 0 \end{aligned} \quad (3.1023)$$

In the presence of energy dissipation Equation (3.693) therefore becomes:

$$\begin{aligned}
& \int_0^l 2\omega\kappa_2 U_2 L' L' \hat{\phi}^J dx - \int_0^l \kappa_2^2 U_2^2 L' L' \hat{\phi}^J dx + \int_0^l CC_g \frac{\partial L'}{\partial x_1} \frac{\partial L'}{\partial x_1} \hat{\phi}^J dx + \int_0^l \kappa_2^2 CC_g L' L' \hat{\phi}^J dx \\
& + \int_0^l \sigma^2 L' L' \hat{\phi}^J dx - \int_0^l \omega^2 L' L' \hat{\phi}^J dx - \int_0^l \kappa^2 CC_g L' L' \hat{\phi}^J dx - \int_0^l \sigma^2 Q' L' L' \hat{\phi}^J dx \\
& + \int_0^l g \frac{\partial \bar{\eta}}{\partial x_1} L' \frac{\partial L'}{\partial x_1} \hat{\phi}^J dx - CC_g \left. \frac{\partial \hat{\phi}}{\partial x_1} L' \right|_l + CC_g \left. \frac{\partial \hat{\phi}}{\partial x_1} L' \right|_0 + \int_0^l i\omega\gamma L' L' \hat{\phi}^J dx + \int_0^l \gamma U_2 L' \frac{\partial L'}{\partial x_2} \hat{\phi}^J dx = 0
\end{aligned} \tag{3.1024}$$

Isolating the real terms in Equation (3.1024) yields:

$$\begin{aligned}
& \int_0^l 2\omega\kappa_2 U_2 L' L' \hat{\phi}_1^J dx - \int_0^l \kappa_2^2 U_2^2 L' L' \hat{\phi}_1^J dx + \int_0^l CC_g \frac{\partial L'}{\partial x_1} \frac{\partial L'}{\partial x_1} \hat{\phi}_1^J dx + \int_0^l \kappa_2^2 CC_g L' L' \hat{\phi}_1^J dx \\
& + \int_0^l \sigma^2 L' L' \hat{\phi}_1^J dx - \int_0^l \omega^2 L' L' \hat{\phi}_1^J dx - \int_0^l \kappa^2 CC_g L' L' \hat{\phi}_1^J dx - \int_0^l \sigma^2 Q' L' L' \hat{\phi}_1^J dx \\
& + \int_0^l g \frac{\partial \bar{\eta}}{\partial x_1} L' \frac{\partial L'}{\partial x_1} \hat{\phi}_1^J dx - CC_g \left. \frac{\partial \hat{\phi}_1^J}{\partial x_1} L' \right|_l + CC_g \left. \frac{\partial \hat{\phi}_1^J}{\partial x_1} L' \right|_0 + \int_0^l \omega\gamma L' L' \hat{\phi}_2^J dx + \int_0^l \gamma U_2 L' \frac{\partial L'}{\partial x_2} \hat{\phi}_1^J dx = 0
\end{aligned} \tag{3.1025}$$

3.12.2 Energy dissipation in 2d-NM-WCIM

Similarly the two-dimensional finite element solution of Equation (3.977) becomes the following when the energy dissipation terms are included:

$$\begin{aligned}
& - \int_{\Gamma_{2,3}} \hat{\psi} \Upsilon \kappa^2 L^I L^J \phi_1'^J dS + \int_{\Gamma_{2,3}} \hat{\psi} \Upsilon \frac{\partial \kappa}{\partial n} L^I L^J \phi_2'^J dS - \int_{\Gamma_{2,3}} \hat{\psi} \Upsilon K^2 L^I L^J \phi_1'^J dS + \left(-L^I \hat{\psi} \Upsilon \frac{\partial \phi_1'}{\partial s} \Big|_0 \right)_{\Gamma_{2,3}} \\
& + \int_{\Gamma_{2,3}} \hat{\psi} \Upsilon \frac{\partial L^I}{\partial s} \frac{\partial L^J}{\partial s} \phi_1'^J dS + \int_{\Gamma_{2,3}} \frac{\partial \hat{\psi}}{\partial s} \Upsilon L^I \frac{\partial L^J}{\partial s} \phi_1'^J dS + \int_{\Gamma_{2,3}} \hat{\psi} \frac{\partial \Upsilon}{\partial s} L^I \frac{\partial L^J}{\partial s} \phi_1'^J dS - \int_{\Gamma_{2,3}} \hat{\psi} 2\kappa^3 L^I L^J \phi_2'^J dS \\
& - 2 \int_{\Gamma_{2,3}} \hat{\psi} \kappa \frac{\partial \kappa}{\partial n} L^I L^J \phi_1'^J dS - 2 \int_{\Gamma_{2,3}} \hat{\psi} \kappa K^2 L^I L^J \phi_2'^J dS + \left(-2L^I \hat{\psi} \kappa \frac{\partial \phi_2'}{\partial s} \Big|_0 \right)_{\Gamma_{2,3}} + 2 \int_{\Gamma_{2,3}} \hat{\psi} \kappa \frac{\partial L^I}{\partial s} \frac{\partial L^J}{\partial s} \phi_2'^J dS \\
& + 2 \int_{\Gamma_{2,3}} \frac{\partial \hat{\psi}}{\partial s} \kappa L^I \frac{\partial L^J}{\partial s} \phi_2'^J dS + 2 \int_{\Gamma_{2,3}} \hat{\psi} \frac{\partial \kappa}{\partial s} L^I \frac{\partial L^J}{\partial s} \phi_2'^J dS - \iint_A \frac{\partial N^I}{\partial x_k} \frac{\partial N^J}{\partial x_k} \phi_1'^J dA \\
& + \iint_A K^2 N^I N^J \phi_1'^J dA + \iint_A W^I \frac{\omega^2}{CC_g} \phi_1'^J N^I N^J dA - \iint_A W^I \frac{\sigma^2}{CC_g} \phi_1'^J N^I N^J dA - \iint_A \frac{U_j}{CC_g} \frac{\partial U_k}{\partial x_j} N^I \frac{\partial N^J}{\partial x_k} \phi_1'^J dA \\
& + 2 \iint_A \frac{U_j U_k}{(CC_g)^{\frac{3}{2}}} \frac{\partial \sqrt{CC_g}}{\partial x_j} N^I \frac{\partial N^J}{\partial x_k} \phi_1'^J dA + \iint_A \frac{U_j}{(CC_g)^{\frac{3}{2}}} \frac{\partial U_k}{\partial x_j} \frac{\partial \sqrt{CC_g}}{\partial x_k} N^I N^J \phi_1'^J dA \\
& + \iint_A \frac{U_j U_k}{(CC_g)^{\frac{3}{2}}} \frac{\partial^2 \sqrt{CC_g}}{\partial x_j \partial x_k} N^I N^J \phi_1'^J dA - \iint_A \frac{U_j U_k}{(CC_g)^{\frac{5}{2}}} \frac{\partial \sqrt{CC_g}}{\partial x_k} \frac{\partial (CC_g)}{\partial x_j} N^I N^J \phi_1'^J dA \\
& + \iint_A \frac{U_j U_k}{CC_g} \frac{\partial N^I}{\partial x_j} \frac{\partial N^J}{\partial x_k} \phi_1'^J dA + \iint_A \frac{\partial U_j}{\partial x_j} \frac{U_k}{CC_g} N^I \frac{\partial N^J}{\partial x_k} \phi_1'^J dA + \iint_A \frac{U_j}{CC_g} \frac{\partial U_k}{\partial x_j} N^I \frac{\partial N^J}{\partial x_k} \phi_1'^J dA \\
& + \iint_A U_k U_j \frac{\partial}{\partial x_j} \left[(CC_g)^{-1} \right] N^I \frac{\partial N^J}{\partial x_k} \phi_1'^J dA + \iint_A \frac{2\omega U_k}{(CC_g)^{\frac{3}{2}}} \frac{\partial \sqrt{CC_g}}{\partial x_k} N^I N^J \phi_2'^J dA - \iint_A \frac{2\omega U_k}{CC_g} N^I \frac{\partial N^J}{\partial x_k} \phi_2'^J dA \\
& - \iint_A \frac{\gamma}{CC_g} \frac{\partial U_j}{\partial x_j} N^I N^J \phi_1'^J dA - \iint_A \frac{\gamma U_j}{CC_g} N^I \frac{\partial N^J}{\partial x_j} \phi_1'^J dA + \iint_A \frac{\omega \gamma}{CC_g} N^I N^J \phi_2'^J dA \\
& - \iint_A \gamma U_j \frac{\partial}{\partial x_j} \left[(CC_g)^{-1} \right] N^I N^J \phi_1'^J dA = \\
& \int_{\Gamma_3} \hat{\psi} \Upsilon \frac{\partial \kappa}{\partial n} L^I L^J (\phi_2'^{in})^J dS - \int_{\Gamma_3} \hat{\psi} \Upsilon K^2 L^I L^J (\phi_1'^{in})^J dS - \left(L^I \hat{\psi} \Upsilon \frac{\partial \phi_1'^{in}}{\partial s} \Big|_0 \right)_{\Gamma_3} + \int_{\Gamma_3} \hat{\psi} \Upsilon \frac{\partial L^I}{\partial s} \frac{\partial L^J}{\partial s} (\phi_1'^{in})^J dS \\
& + \int_{\Gamma_3} \frac{\partial \hat{\psi}}{\partial s} \Upsilon L^I \frac{\partial L^J}{\partial s} (\phi_1'^{in})^J dS + \int_{\Gamma_3} \hat{\psi} \frac{\partial \Upsilon}{\partial s} L^I \frac{\partial L^J}{\partial s} (\phi_1'^{in})^J dS - 2 \int_{\Gamma_3} \hat{\psi} \kappa^3 L^I L^J (\phi_2'^{in})^J dS \\
& - 2 \int_{\Gamma_3} \hat{\psi} \kappa \frac{\partial \kappa}{\partial n} L^I L^J (\phi_1'^{in})^J dS - 2 \int_{\Gamma_3} \hat{\psi} \kappa K^2 L^I L^J (\phi_2'^{in})^J dS - \left(2L^I \hat{\psi} \kappa \frac{\partial \phi_2'^{in}}{\partial s} \Big|_0 \right)_{\Gamma_3} + 2 \int_{\Gamma_3} \hat{\psi} \kappa \frac{\partial L^I}{\partial s} \frac{\partial L^J}{\partial s} (\phi_2'^{in})^J dS \\
& + 2 \int_{\Gamma_3} \frac{\partial \hat{\psi}}{\partial s} \kappa L^I \frac{\partial L^J}{\partial s} (\phi_2'^{in})^J dS + 2 \int_{\Gamma_3} \hat{\psi} \frac{\partial \kappa}{\partial s} L^I \frac{\partial L^J}{\partial s} (\phi_2'^{in})^J dS - \int_{\Gamma_3} L^I \frac{\partial L^J}{\partial n} (\phi_1'^{in})^J dS - \int_{\Gamma_3} \hat{\psi} \Upsilon \kappa^2 L^I L^J (\phi_1'^{in})^J dS
\end{aligned}$$

(3.1026)

3.12.3 Expressing energy dissipation in terms of the parameters of wave breaking

The energy dissipation term γ in Equations (3.1025) and (3.1026) above must be obtained prior to running the wave model. As discussed in Section 2.3.2 there is a wide variety of different wave breaking models that link wave breaking to energy dissipation. Zhao *et al.* (2001) examines a number of these different models. The various formulae for energy dissipation listed by Zhao *et al.* (2001) are described below:

3.12.3.1 Battjes and Janssen (1978) breaking solution

Both Zhao *et al.* (2001) and Clyne (2008) provide a monochromatic wave version of the Battjes and Janssen (1978) energy dissipation factor for spectral waves. The equation varies slightly between authors. Clyne (2008) provides a full derivation starting with the spectral wave basis and hence this equation is chosen here:

$$\gamma = \frac{\alpha}{\pi} \omega Q_b \frac{1}{r^2} \quad (3.1027)$$

α is a constant, taken by Zhao *et al.* (2001) as unity. Clyne (2008) describes the Q_b term as the probability of a wave height being equal to H_m (within the Rayleigh wave height distribution).

$$Q_b = e^{\frac{-(1-Q_b)}{r^2}} \quad (3.1028)$$

$$r = \frac{H}{\sqrt{2}H_m} \quad (3.1029)$$

Where H_m is the maximum sustainable wave height (insipience height) and H is the wave height obtained from the monochromatic wave solution of Equation (3.1026). Zhao *et al.* (2001) uses the criterion of Miche (1954) to select the maximum height, H_m . This Miche (1954) criterion has also been used by other wave breaking models to define the insipience point as described in Section 5.7.2.

$$H_m = \frac{0.88}{\kappa} \tanh \left[\frac{\gamma_0}{0.88} \kappa d \right] \quad (3.1030)$$

However, in shallow water Zhao *et al.* (2001) state that this may be reduced to:

$$H_m = \gamma_0 d \quad (3.1031)$$

Battjes and Janssen (1978) state that Equation (3.1030) was selected in such a way that it would reduce to Equation (3.1031) in shallow water. Equation (3.1031) is used by various wave models as a breaking model within its own right to give a linear decrease in wave height within the breaking zone. This approach is discussed further in Section 5.7.1. Zhao *et al.* (2001) suggest a value of 0.8 for γ_0 . Newell and Mullarkey (2007a) use a value of 0.78. The Clyne (2008) model also uses the solution of Battjes and Janssen (1978) for energy dissipation due to wave breaking. It is obvious that this breaking criteria includes the use of wave height. As such it is necessary to run the wave model iteratively to obtain a solution for the broken wave heights within a domain.

To carry out the iterative process successfully both Zhao *et al.* (2001) and Clyne (2008) suggest the application of a lower limit to the use of the Battjes and Janssen (1978) criterion to prevent γ for having a negative value. Clyne (2008) relates H_m to the root mean squared wave height and Zhao *et al.* (2001) relates it to the significant wave height, hence the selected lower limit varies between the authors. Clyne (2008) suggests:

$$H_b = 0.3H_m \quad (3.1032)$$

Zhao *et al.* (2001) use:

$$H_b = 0.3\sqrt{2}H_m \quad (3.1033)$$

Throughout the implementation of wave breaking in this project γ was maintained above or equal to zero using the Zhao *et al.* (2001) method.

3.12.3.2 Massel (1992) breaking solution

An alternative to Equation (3.1027) is the equation of Massel (1992). This equation also examines an energy dissipation factor caused by wave breaking. Zhao *et al.* (2001) reproduces the equation of Massel (1992):

$$\gamma = \left[\left(1 + 0.65 \frac{H}{d} \right) \left(1 - 0.35 \frac{H}{d} \right) \right]^{-1} \frac{\sigma H}{\pi C_g d} \quad (3.1034)$$

In order to prevent the energy dissipation factor from going below zero it is also necessary to apply an upper limit to this formula. Zhao *et al.* (2001) states that if H from

one step in the iterative procedure is greater than $2.85d$ then γ for the next iterative step would be less than zero. In order to avoid this a limit of $2.85d$ was imposed upon H . Massel (1992) breaking solution has no insipience point and is active throughout the domain. The results of Newell and Mullarkey (2007a) show that this has an effect on the suitability of this method for use alongside wave-driven hydrodynamic models.

Zhao *et al.* (2001) introduces an improvement to the Massel (1992) methodology to alleviate this issue. Zhao *et al.* (2001) suggests the application of a lower limit to broken wave height similar to that described in Section 3.12.3.1 above could be appropriate. The results of The results of Newell and Mullarkey (2007a) confirm this.

3.12.3.3 Chawla *et al.* (1998) breaking solution

A second alternative to Equation (3.1027) is the Chawla *et al.* (1998) breaking solution, based on the work of Thornton and Guza (1983). This work is based on spectral wave analysis and hence may not be strictly applicable to linear wave theory. Zhao *et al.* (2001) give the following equation for the energy dissipation factor due to wave breaking created for a monochromatic wave by Chawla *et al.* (1998):

$$\gamma = \frac{3\sqrt{\pi}}{2} \frac{\sigma B^3}{C_g \lambda^4 d^5} H^5 \quad (3.1035)$$

Chawla *et al.* (1998) suggest values of 1.0 and 0.6 for B and λ respectively.

The Chawla *et al.* (1998) breaking solution has no insipience point and is active throughout the domain. The results of Newell and Mullarkey (2007a) show that this has an effect on the suitability of this method for use alongside wave-driven hydrodynamic models.

3.13 NM-WCIM in Operation

3.13.1 Iteration of NM-WCIM for Solution of Wave Current Interaction

This chapter has presented the various equations used in the NM-WCIM. In the case of a simple wave in the absence of currents and energy dissipation the finite-element solution to Equation (3.1026) is a one step procedure with no iteration. In the presence of a current it is impossible to solve the dispersion relation (Equation (3.189)) in one step so an iterative process is required. Equation (3.189) may be re-expressed as follows:

$$\sigma^2 = \left[\omega - \kappa \left(\mathbf{U} \cdot \frac{\boldsymbol{\kappa}}{|\boldsymbol{\kappa}|} \right) \right]^2 \quad (3.1036)$$

At this stage the following substitution can be made to generalise the equation.

$$\boldsymbol{\kappa} = \nabla S_\phi \quad (3.1037)$$

Therefore Equation (3.1036) becomes:

$$\sigma^2 = \left[\omega - \kappa \left(\mathbf{U} \cdot \frac{\nabla S_\phi}{|\nabla S_\phi|} \right) \right]^2 \quad (3.1038)$$

An iterative process can be used with Equation (3.1038) by initially solving in the absence of a current and on successive iterations updating the value of ∇S_ϕ . ∇S_ϕ can be obtained from the velocity potential results of the previous step. An equation to do this is derived in Section 5.8. Experience with the NM-WCIM has shown that it converges in 4 to 5 iterations for wave-current interaction.

3.13.2 Iteration of NM-WCIM for Energy Dissipation

In the case of energy dissipation, iteration is also required. The model is initially calculated in the absence of energy dissipation and this provides an initial value for wave height in the next iteration. The wave heights calculated from this first step are used to obtain a γ value using one of the breaking methods described in Section 3.12. The finite element solution is then re-run using the calculated γ value to get new wave heights. This allows for the calculation of a new γ value for the second iteration. Iteration continues until convergence of wave heights occurs. Usually this takes approximately 10 to 20 iterations.

Chapter 4: Wave-Driven Hydrodynamic Model

“The cure for anything is salt water: sweat, tears or the sea,” Isak Dinesen.

4.1 Introduction

In order to examine the effects of wave generated set-up/set-down and currents it is necessary to create a hydrodynamic model (NM-WDHM) using driving terms from the NM-WCIM developed in Chapter 3. The derivation of this wave-driven current model closely follows the methodology adopted by Mei *et al.* (2005) to obtain conservation laws of mass and horizontal momentum for a current field in the presence of waves.

The progression of Chapter 4 is as follows:

- Depth and time averaged equations for the mean motion of the water body are developed. The conservation of mass and conservation of momentum equations are developed into a depth integrated form – Section 4.3
- A unique equation is developed to express the radiation stress driving force term of the momentum equation as a function of velocity potential – Section 4.5
- A bottom friction term is developed for the momentum equation – Section 4.6
- A turbulent diffusion term is developed for the momentum equation – Section 4.7
- The NM-WDHM finite element equations are formed from the conservation of mass equation and the conservation of momentum equation including radiation stress, bottom friction and turbulent diffusion – Section 4.8

4.2 Initial Definitions

It will be useful to distinguish the vertical coordinate and vertical component of velocity from the horizontal components.

Horizontal velocity: u_1, u_2

Vertical velocity: w

Horizontal coordinates: x_1, x_2

Vertical coordinate: z

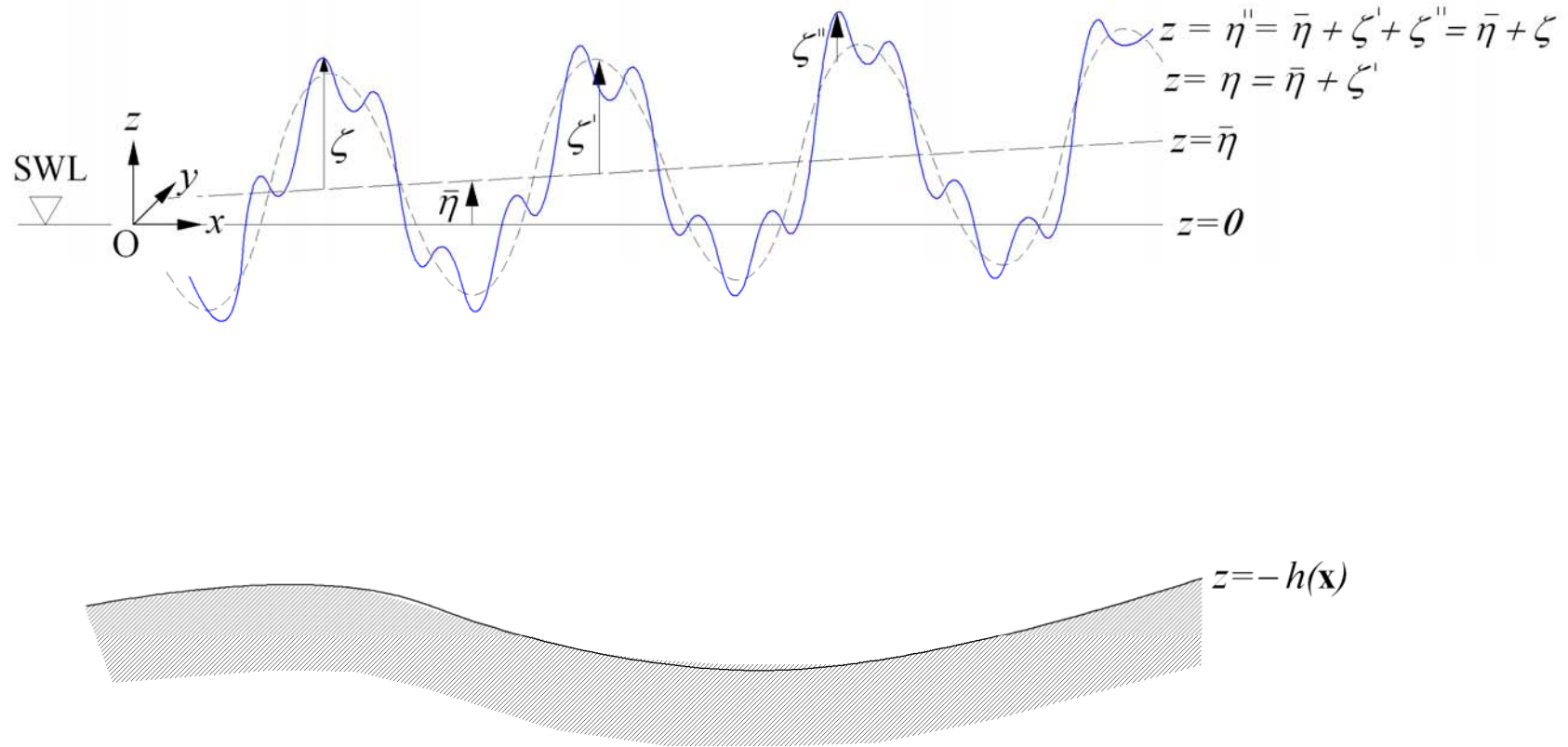


Figure 4.1 – Full Definition of Surface Measurements including Turbulence

4.3 Depth and Time-Averaged Equations for Mean Motion of Water Body

In order to examine wave-generated behaviour a set of equations must be developed to describe the mean motion of the water body. This section develops a set of depth and time averaged equations of motion that will be used with a finite element solution scheme to model wave-generated behaviour.

For this project an overbar indicates integration and averaging over a wave-period:

$$\frac{1}{T} \int_0^T x dt = \bar{x} \quad (4.1)$$

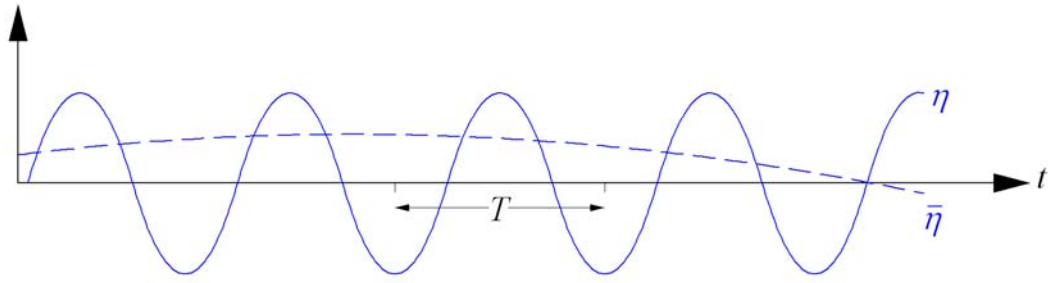


Figure 4.2 – Variation of Free Surface and Mean Surface over Short and Long Time Scales

In order to obtain mean horizontal velocity, the instantaneous velocity is integrated over the depth and also integrated and averaged over the time period T , which is the wave period.

$$U_i = \frac{1}{\eta + h} \overline{\int_{-h}^{\eta''} u_i dz} \quad \text{for } i = 1, 2 \quad (4.2)$$

$$W_v = \frac{1}{\eta + h} \overline{\int_{-h}^{\eta''} w_i dz} \quad \text{for } i = 1, 2 \quad (4.3)$$

Equation (4.2) can be rearranged as:

$$U_i (\bar{\eta} + h) = \overline{\int_{-h}^{\eta''} u_i dz} \quad \text{for } i = 1, 2 \quad (4.4)$$

Similarly Equation (4.3) can be rearranged as:

$$W_v (\bar{\eta} + h) = \overline{\int_{-h}^{\eta''} w_i dz} \quad \text{for } i = 1, 2 \quad (4.5)$$

Separating the instantaneous horizontal velocity into its steady component (long time scale) and oscillatory component (short time scale) as in Equation (3.42) gives:

$$u_i = U_i + \tilde{u}_i(x, y, z, t) \text{ for } i = 1, 2 \quad (4.6)$$

Similarly separating the instantaneous vertical velocity into its steady component (long time scale) and oscillatory component (short time scale) gives:

$$w = W_v + \tilde{w}(x, y, z, t) \text{ for } i = 1, 2 \quad (4.7)$$

Examining Equation (4.6) gives the following:

$$\tilde{u}_i = u_i - U_i \text{ for } i = 1, 2 \quad (4.8)$$

The time averaged integral of Equation (4.8) is:

$$\overline{\int_{-h}^{\eta''} \tilde{u}_i dz} = \overline{\int_{-h}^{\eta''} u_i dz} - \overline{\int_{-h}^{\eta''} U_i dz} \text{ for } i = 1, 2 \quad (4.9)$$

Acknowledging the slowly varying nature of U_i over a short time scale gives:

$$\overline{\int_{-h}^{\eta''} \tilde{u}_i dz} = \overline{\int_{-h}^{\eta''} u_i dz} - U_i \overline{\int_{-h}^{\eta''} dz} \text{ for } i = 1, 2 \quad (4.10)$$

Equation (4.10) becomes:

$$\overline{\int_{-h}^{\eta''} \tilde{u}_i dz} = \overline{\int_{-h}^{\eta''} u_i dz} - \overline{U_i [z]_{-h}^{\eta''}} \text{ for } i = 1, 2 \quad (4.11)$$

Simplifying Equation (4.11) gives:

$$\overline{\int_{-h}^{\eta''} \tilde{u}_i dz} = \overline{\int_{-h}^{\eta''} u_i dz} - \overline{U_i [\eta'' + h]} \text{ for } i = 1, 2 \quad (4.12)$$

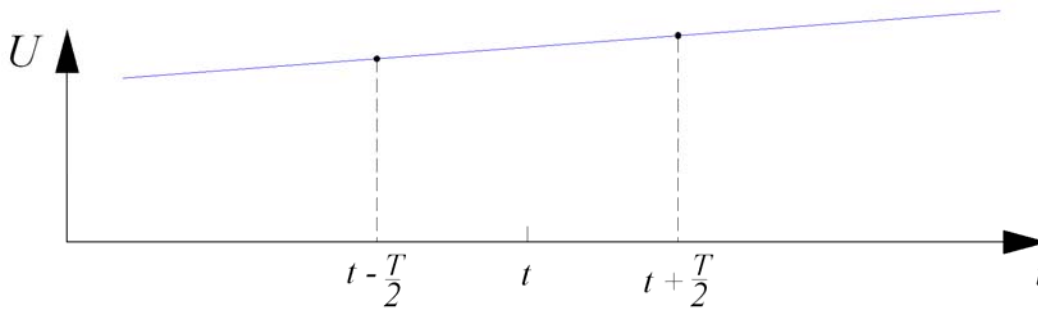


Figure 4.3 – Function of long time scale plotted over short time period

When a time averaged integral over a short time period is obtained for a function of a long time scale the original function is returned. As shown in Figure 4.3 over a single wave-period U varies only slightly yielding the following:

$$\bar{U} = \frac{1}{T} \int_{t-\frac{T}{2}}^{t+\frac{T}{2}} U dt = \frac{U}{T} T = U \text{ for } i = 1, 2 \quad (4.13)$$

Using Equation (4.13) with Equation (4.12) gives:

$$\overline{\int_{-h}^{\eta^*} \tilde{u}_i dz} = \overline{\int_{-h}^{\eta^*} u_i dz - U_i [\overline{\eta''} + h]} \text{ for } i = 1, 2 \quad (4.14)$$

h is not a function of time so Equation (4.14) becomes:

$$\overline{\int_{-h}^{\eta^*} \tilde{u}_i dz} = \overline{\int_{-h}^{\eta^*} u_i dz - U_i [\bar{\eta} + h]} \text{ for } i = 1, 2 \quad (4.15)$$

Using Equation (4.2) with Equation (4.15) gives:

$$\overline{\int_{-h}^{\eta^*} \tilde{u}_i dz} = \overline{\int_{-h}^{\eta^*} u_i dz} - \overline{\int_{-h}^{\eta^*} u_i dz} \text{ for } i = 1, 2 \quad (4.16)$$

Hence:

$$\overline{\int_{-h}^{\eta^*} \tilde{u}_i dz} = 0 \text{ for } i = 1, 2 \quad (4.17)$$

Using the definitions above it is now possible to derive an equation for conservation of mass.

4.3.1 Averaged Equation for Conservation of Mass

Equation (3.41) states that:

$$\nabla \cdot \mathbf{u} = 0$$

This can be re-written as:

$$\frac{\partial u_i}{\partial x_i} + \frac{\partial w}{\partial z} = 0 \quad \text{for } i = 1, 2 \quad (4.18)$$

Integrating Equation (4.18) over the depth gives:

$$\int_{-h}^{\eta'} \left[\frac{\partial u_i}{\partial x_i} + \frac{\partial w}{\partial z} \right] dz = 0 \quad \text{for } i = 1, 2 \quad (4.19)$$

Equation (4.19) may be expressed more explicitly as:

$$\int_{-h}^{\eta'} \frac{du_i}{dx_i} dz + [w]_{\eta} - [w]_{-h} = 0 \quad \text{for } i = 1, 2 \quad (4.20)$$

Leibniz's rule as stated in Equation (3.399) can now be applied:

$$D \int_b^a Y dz = \int_b^a D Y dz + (Da) Y_{z=a} - (Db) Y_{z=b}$$

$$\text{where } D = \frac{\partial}{\partial x} + \frac{\partial}{\partial y} + \frac{\partial}{\partial t}$$

Using Leibniz's rule Equation (4.20) becomes:

$$\frac{d}{dx_i} \int_{-h}^{\eta'} u_i dz + \left[-u_i \frac{\partial \eta''}{\partial x_i} + w \right]_{\eta} - \left[u_i \frac{\partial h}{\partial x_i} + w \right]_{-h} = 0 \quad \text{for } i = 1, 2 \quad (4.21)$$

The kinematic boundary condition, Equation (3.73) is:

$$\frac{\partial F}{\partial t} + \mathbf{u} \cdot \nabla F = 0 \quad (4.22)$$

Where Equation (3.70) states:

$$F(\mathbf{x}, t) = z - \eta''(\mathbf{x}, t) = 0$$

Substituting Equation (3.70) into Equation (3.73) gives:

$$\frac{\partial (z - \eta'')}{\partial t} + \mathbf{u} \cdot \nabla (z - \eta'') = 0 \quad (4.23)$$

Expressing Equation (4.23) in tensor form yields:

$$\frac{\partial(z-\eta'')}{\partial t} + u_i \frac{\partial}{\partial x_i}(z-\eta'') = 0 \text{ for } i=1,2,3 \text{ at } z=\eta \quad (4.24)$$

Equation (4.24) may be expanded as follows:

$$\frac{\partial z}{\partial t} - \frac{\partial \eta''}{\partial t} + u_i \frac{\partial z}{\partial x_i} - u_i \frac{\partial \eta''}{\partial x_i} = 0 \text{ for } i=1,2,3 \text{ at } z=\eta \quad (4.25)$$

Acknowledging that $\frac{\partial z}{\partial t} = 0$ and $\frac{\partial \eta''}{\partial z} = 0$ gives:

$$\frac{\partial \eta''}{\partial t} + u_i \frac{\partial \eta''}{\partial x_i} - w = 0 \text{ for } i=1,2 \text{ at } z=\eta'' \quad (4.26)$$

Equation (4.26) can be re-written as:

$$\frac{\partial \eta''}{\partial t} + u_i \frac{\partial \eta''}{\partial x_i} = w \text{ for } i=1,2 \text{ at } z=\eta'' \quad (4.27)$$

at $z=-h$ a rigid seabed is assumed leading to:

$$u_i = w = 0 \text{ for a real fluid} \quad (4.28)$$

So Equation (3.105) becomes:

$$\left[u_i \frac{\partial h}{\partial x_i} + w \right]_{-h} = 0 \text{ for } i=1,2 \text{ at } z=-h \text{ for an inviscid fluid} \quad (4.29)$$

Using Equations (4.27), (4.28) and (4.29) with Equation (4.21) gives:

$$\frac{\partial}{\partial x_i} \int_{-h}^{\eta} u_i dz + \frac{\partial \eta''}{\partial t} = 0 \text{ for } i=1,2 \quad (4.30)$$

Integrating the last term of Equation (4.30) over time gives:

$$\overline{\frac{\partial \eta}{\partial t}} = \frac{1}{T} \int_{t-\frac{T}{2}}^{t+\frac{T}{2}} \frac{\partial \eta''}{\partial t} dt \quad (4.31)$$

Equation (4.31) may be simplified as:

$$\overline{\frac{\partial \eta}{\partial t}} = \frac{1}{T} [\eta'']_{t-\frac{T}{2}}^{t+\frac{T}{2}} \quad (4.32)$$

Expanding Equation (4.32) yields:

$$\frac{\partial \bar{\eta}}{\partial t} = \frac{1}{T} \left[\eta''_{t+\frac{T}{2}} - \eta''_{t-\frac{T}{2}} \right] \quad (4.33)$$

Equation (4.33) may be written as:

$$\frac{\partial \bar{\eta}}{\partial t} = \frac{1}{T} \left[\bar{\eta}_{t+\frac{T}{2}} + \zeta'_{t+\frac{T}{2}} + \zeta''_{t+\frac{T}{2}} - \bar{\eta}_{t-\frac{T}{2}} - \zeta'_{t-\frac{T}{2}} - \zeta''_{t-\frac{T}{2}} \right] \quad (4.34)$$

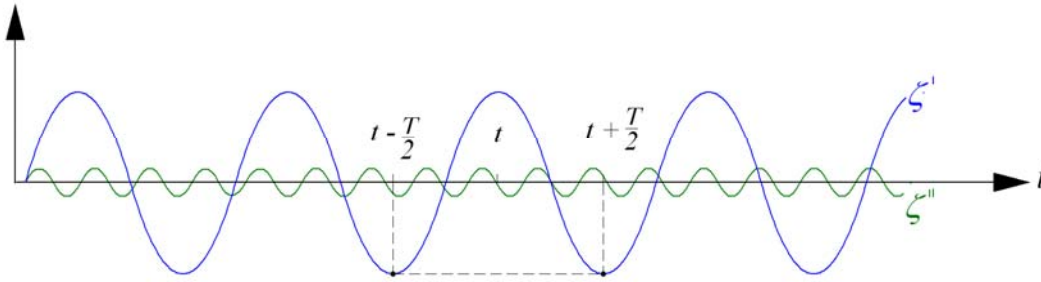


Figure 4.4 – Diagram showing relative orders of magnitude and time scales of oscillatory and turbulent fluctuations of wave surface

As shown in Figure 4.4 the order of magnitude of the turbulent terms is minor compared to the oscillatory component. It is hence valid to disregard the effects of the turbulent terms in Equation (4.34). Figure 4.4 also shows that for a periodic wave $\zeta_{t+\frac{T}{2}} \approx \zeta_{t-\frac{T}{2}}$ so

assuming the variation of $\bar{\eta}$ is assumed to be linear over a wave period:

$$\frac{\partial \bar{\eta}}{\partial t} = \frac{1}{T} \left[\bar{\eta}_{t+\frac{T}{2}} - \bar{\eta}_{t-\frac{T}{2}} \right] \approx \frac{\partial \bar{\eta}}{\partial t} \quad (4.35)$$

Therefore averaging Equation (4.30) over time gives:

$$\frac{\partial}{\partial x_i} \int_{-h}^{\bar{\eta}'} u_i dz + \frac{\partial \bar{\eta}}{\partial t} = 0 \text{ for } i = 1, 2 \quad (4.36)$$

Substituting Equation (4.4) into Equation (4.36) gives:

$$\frac{d}{dx_i} \left[U_i (\bar{\eta} + h) \right] + \frac{d \bar{\eta}}{dt} = 0 \text{ for } i = 1, 2 \quad (4.37)$$

Equation (4.37) is the equation for conservation of mass within a system.

4.3.2 Averaged Equation for Conservation of Momentum

4.3.2.1 Complete Momentum Balance Equation including time

The equation for conservation of momentum within a system may be rewritten as follows in the absence of the energy dissipation term (for wave breaking). Recalling Equation (3.37):

$$\frac{\partial \mathbf{u}}{\partial t} + \mathbf{u} \cdot (\nabla \mathbf{u}) + \nabla gz + \frac{\nabla p}{\rho} = \frac{\nabla \cdot (\boldsymbol{\sigma}')}{\rho}$$

Equation (3.37), the equation for conservation of momentum within a system, may be rewritten as follows:

$$\rho \frac{\partial \mathbf{u}}{\partial t} + \rho \mathbf{u} \cdot (\nabla \mathbf{u}) + \rho \nabla gz + \nabla p = \nabla \cdot (\boldsymbol{\sigma}') \quad (4.38)$$

Expressing Equation (4.38) in tensor notation yields:

$$\rho \frac{\partial u_j}{\partial t} + \rho u_i \frac{\partial u_j}{\partial x_i} = -\frac{\partial}{\partial x_j}(p) - \rho \frac{\partial}{\partial x_j}(gz) + \frac{\partial}{\partial x_i} \sigma'_{ij} \text{ for } i, j = 1, 2, 3 \quad (4.39)$$

Equation (4.39) can be expressed as follows:

$$\rho \frac{\partial u_j}{\partial t} + \rho u_i \frac{\partial u_j}{\partial x_i} = -\frac{\partial}{\partial x_i} (p \delta_{ij} + \rho g z \delta_{ij} + \sigma'_{ij}) \text{ for } i, j = 1, 2, 3 \quad (4.40)$$

In the case of the wave-driven current model the predominant energy losses are due to bed friction. Mei *et al.* (2005) express this as the gradient of the stress tensor. This corresponds to the gradient of the $\boldsymbol{\sigma}'$ stress tensor in Equation (4.40) .

It is known from simple calculus that:

$$\rho u_i \frac{\partial u_j}{\partial x_i} + \rho u_j \frac{\partial u_i}{\partial x_i} = \rho \frac{\partial u_i u_j}{\partial x_i} \text{ for } i, j = 1, 2, 3 \quad (4.41)$$

Recalling Equation (3.41) and from continuity:

$$\frac{\partial u_i}{\partial x_i} = 0 \text{ for } i = 1, 2, 3 \quad (4.42)$$

Therefore:

$$\rho u_i \frac{\partial u_j}{\partial x_i} = \rho \frac{\partial u_i u_j}{\partial x_i} \text{ for } i, j = 1, 2, 3 \quad (4.43)$$

Hence Equation (4.40) can be rewritten as:

$$\rho \frac{\partial u_j}{\partial t} + \rho \frac{\partial u_i u_j}{\partial x_i} = -\frac{\partial}{\partial x_i} (p \delta_{ij} + \rho g z \delta_{ij} - \sigma'_{ij}) \text{ for } i, j = 1, 2, 3 \quad (4.44)$$

Acknowledging that $u_3 = w$ and changing the subscript i to only include 1 and 2 and no longer 3 yields:

$$\rho \frac{\partial u_j}{\partial t} + \rho \frac{\partial u_i u_j}{\partial x_i} + \rho \frac{\partial u_j w}{\partial z} = -\frac{\partial}{\partial x_i} (p \delta_{ij} - \sigma'_{ij}) - \frac{\partial}{\partial z} (p \delta_{3j} + \rho g z \delta_{3j} - \sigma'_{3j})$$

for $i = 1, 2, j = 1, 2, 3$ (4.45)

The horizontal component of the equation for conservation of momentum can be obtained by examining $j = 1, 2$ from Equation (4.45):

$$\rho \frac{\partial u_j}{\partial t} + \rho \frac{\partial u_i u_j}{\partial x_i} + \rho \frac{\partial u_j w}{\partial z} = \frac{\partial}{\partial x_i} (-p \delta_{ij} + \sigma'_{ij}) + \frac{\partial \sigma'_{3j}}{\partial z} \text{ for } i, j = 1, 2 \quad (4.46)$$

The vertical component of the equation for conservation of momentum can be obtained by examining $j = 3$ in Equation (4.45) (recalling that $u_3 = w$):

$$\rho \frac{\partial w}{\partial t} + \rho \frac{\partial u_i w}{\partial x_i} + \rho \frac{\partial w^2}{\partial z} = -\frac{\partial}{\partial z} (p + \rho g z) + \frac{\partial \sigma'_{i3}}{\partial x_i} + \frac{\partial \sigma'_{33}}{\partial z}, \text{ for } i = 1, 2 \quad (4.47)$$

4.3.2.2 Horizontal Momentum Balance Equation including Time Integrated over Depth

Vertical integration can be carried out on Equation (4.46). Integration will be carried out from $-h$ to η'' . After vertical integration and using the Leibniz rule, Equation (3.399), the first term of Equation (4.46) becomes:

$$\int_{-h}^{\eta''} \rho \frac{\partial u_j}{\partial t} dz = \frac{\partial}{\partial t} \int_{-h}^{\eta''} \rho u_j dz - \rho [u_j]_{\eta''} \frac{\partial \eta''}{\partial t}, \text{ for } j = 1, 2 \quad (4.48)$$

Similarly the second term in Equation (4.46) becomes:

$$\int_{-h}^{\eta''} \rho \frac{\partial u_i u_j}{\partial x_i} dz = \frac{\partial}{\partial x_i} \int_{-h}^{\eta''} \rho u_i u_j dz - \rho [u_i u_j]_{\eta''} \frac{\partial \eta''}{\partial x_i} - \rho [u_i u_j]_{-h} \frac{\partial h}{\partial x_i} \text{ for } i, j = 1, 2 \quad (4.49)$$

Integration yields the following for the third term in Equation (4.46):

$$\int_{-h}^{\eta''} \rho \frac{\partial u_j w}{\partial z} dz = \rho [u_j w]_{\eta''} - \rho [u_j w]_{-h} \quad \text{for } j = 1, 2 \quad (4.50)$$

Summing up Equations (4.48), (4.49) and (4.50) gives the following for the left hand side (LHS) of Equation (4.46):

$$\begin{aligned} LHS = & \frac{\partial}{\partial x_i} \int_{-h}^{\eta''} \rho u_i u_j dz - \rho [u_i u_j]_{\eta''} \frac{\partial \eta''}{\partial x_i} - \rho [u_i u_j]_{-h} \frac{\partial h}{\partial x_i} \\ & + \frac{\partial}{\partial t} \int_{-h}^{\eta''} \rho u_j dz - \rho [u_j]_{\eta''} \frac{\partial \eta''}{\partial t} + \rho [u_j w]_{\eta''} - \rho [u_j w]_{-h} \end{aligned} \quad (4.51)$$

for $i, j = 1, 2$

$$LHS = \frac{\partial}{\partial x_i} \int_{-h}^{\eta''} \rho u_i u_j dz + \frac{\partial}{\partial t} \int_{-h}^{\eta''} \rho u_j dz + \rho \left[u_j w - u_j \frac{\partial \eta''}{\partial t} - u_i u_j \frac{\partial \eta''}{\partial x_i} \right]_{\eta''} - \rho \left[u_j w + u_i u_j \frac{\partial h}{\partial x_i} \right]_{-h} \quad (4.52)$$

for $i, j = 1, 2$

$$LHS = \frac{\partial}{\partial x_i} \int_{-h}^{\eta''} \rho u_i u_j dz + \frac{\partial}{\partial t} \int_{-h}^{\eta''} \rho u_j dz + \rho \left[u_j w - u_j \left(\frac{\partial \eta''}{\partial t} + u_i \frac{\partial \eta''}{\partial x_i} \right) \right]_{\eta''} - \rho \left[u_j w + u_i u_j \frac{\partial h}{\partial x_i} \right]_{-h} \quad (4.53)$$

for $i, j = 1, 2$

Using Equations (4.28) and (4.26) with Equation (4.53) gives:

$$LHS = \frac{\partial}{\partial x_i} \int_{-h}^{\eta''} \rho u_i u_j dz + \frac{\partial}{\partial t} \int_{-h}^{\eta''} \rho u_j dz + \rho [u_j w - u_j w]_{\eta''} - \rho [0]_{-h} \quad \text{for } i, j = 1, 2 \quad (4.54)$$

$$LHS = \frac{\partial}{\partial x_i} \int_{-h}^{\eta''} \rho u_i u_j dz + \frac{\partial}{\partial t} \int_{-h}^{\eta''} \rho u_j dz \quad \text{for } i, j = 1, 2 \quad (4.55)$$

The right hand side of Equation (4.46) can also be integrated vertically:

$$RHS = \int_{-h}^{\eta''} \frac{\partial}{\partial x_i} (-p \delta_{ij} + \sigma'_{ij}) dz + \int_{-h}^{\eta''} \frac{\partial \sigma'_{j3}}{\partial z} dz \quad \text{for } i, j = 1, 2 \quad (4.56)$$

Using Leibniz's rule on Equation (4.56) gives:

$$RHS = \frac{\partial}{\partial x_i} \int_{-h}^{\eta'} (-p\delta_{ij} + \tau_{ij}) dz - \frac{\partial \eta''}{\partial x_i} [-p\delta_{ij} + \sigma'_{ij}]_{\eta''} - \frac{\partial h}{\partial x_i} [-p\delta_{ij} + \sigma'_{ij}]_{-h} + \int_{-h}^{\eta'} \frac{\partial \sigma'_{j3}}{\partial z} dz \quad (4.57)$$

for $i, j = 1, 2$

$$RHS = \frac{\partial}{\partial x_i} \int_{-h}^{\eta'} (-p\delta_{ij} + \sigma'_{ij}) dz - \frac{\partial \eta''}{\partial x_i} [-p\delta_{ij} + \sigma'_{ij}]_{\eta''} - \frac{\partial h}{\partial x_i} [-p\delta_{ij} + \sigma'_{ij}]_{-h} + [\sigma'_{j3}]_{\eta''} - [\sigma'_{j3}]_{-h} \quad (4.58)$$

On the free surface of a fluid the atmospheric force per unit area must balance the stresses in the fluid in order to satisfy equilibrium. Using Cauchy's theorem the following relationship can be defined where τ_j^F is the j th component of atmospheric force per unit area:

$$(-p\delta_{ij} + \sigma'_{ij})n_i = \tau_j^F \quad \text{at } z = \eta'', \text{ for } i, j = 1, 2, 3 \quad (4.59)$$

Examining the horizontal externally applied horizontal stress component only (i.e. $j = 1, 2$) yields:

$$(-p\delta_{ij} + \sigma'_{ij})n_i + \sigma'_{3j}n_3 = \tau_j^F \quad \text{at } z = \eta'', \text{ for } i, j = 1, 2 \quad (4.60)$$

because $\delta_{3j} = 0$ for $j = 1, 2$

Examining the vertical externally applied horizontal stress component only (i.e. $j = 3$) yields:

$$(-p\delta_{i3} + \sigma'_{i3})n_i + (-p\delta_{33} + \sigma'_{33})n_3 = \tau_3^F \quad \text{at } z = \eta'', \text{ for } i = 1, 2 \quad (4.61)$$

The unit normal \mathbf{n} pointing out of the fluid body is defined as:

$$\mathbf{n} = (n_1, n_2, n_3) \quad (4.62)$$

At the free surface $z = \eta''$ and therefore a function for the free surface can be defined as in Equation (3.70):

$$F(x, y, z, t) = z - \eta'' = 0 \quad (4.63)$$

Differentiation of F leads to:

$$\nabla F = \left(-\frac{\partial \eta''}{\partial x}, -\frac{\partial \eta''}{\partial y}, 1 \right) \quad (4.64)$$

The outward unit normal at the free surface is then defined as follows acknowledging that the z -axis points upwards out of the fluid column as shown in Figure 4.1:

$$\mathbf{n} = \frac{\nabla F}{|\nabla F|} \quad (4.65)$$

Equation (4.60) can then be rewritten using the results of Equations (4.64) and (4.65):

$$-\left(-p\delta_{ij} + \sigma'_{ij}\right)\frac{\partial \eta''}{\partial x_i} + \sigma'_{3j} = \tau_j^F |\nabla F| \text{ at } z = \eta'' \text{ for } i, j = 1, 2 \quad (4.66)$$

A similar relationship to Equation (4.60) can be developed for the sea-bed and bottom stress. The pressure term on the left hand side of the Cauchy equation is dropped here because the τ_j^B term on the right hand side only measures additional stress caused by fluid movement:

$$\sigma'_{ij}n_j + \sigma'_{i3}n_3 = \tau_j^B \text{ at } z = -h, \text{ for } i, j = 1, 2 \text{ and } j = 1, 2 \quad (4.67)$$

At the seabed $z = -h$ and therefore a function for the seabed can be defined as follows similar to the F' function of Equation (3.99):

$$B(x, y, z, t) = z + h = 0 \quad (4.68)$$

Differentiation of B leads to:

$$\nabla B = \left(\frac{\partial h}{\partial x}, \frac{\partial h}{\partial y}, 1 \right) \quad (4.69)$$

In the case the outward pointing normal from the fluid column is in the negative z -direction. The outward unit normal at the seabed is therefore:

$$\mathbf{n} = -\frac{\nabla B}{|\nabla B|} \quad (4.70)$$

Equation (4.67) can then be rewritten using the results of Equations (4.69) and (4.70):

$$\sigma'_{ij} \frac{\partial h}{\partial x} + \sigma'_{i3} = -\tau_j^B |\nabla B| \text{ at } z = -h \quad (4.71)$$

Substituting Equations (4.66) and (4.71) into Equation (4.58) gives:

$$\begin{aligned} RHS = & \frac{\partial}{\partial x_i} \int_{-h}^{\eta'} (-p\delta_{ij} + \sigma'_{ij}) dz - \frac{\partial \eta''}{\partial x_i} [-p\delta_{ij} + \sigma'_{ij}]_{\eta'} - \frac{\partial h}{\partial x_i} [-p\delta_{ij} + \sigma'_{ij}]_{-h} \\ & + [\sigma'_{j3}]_{\eta'} - [\sigma'_{j3}]_{-h} \end{aligned} \quad (4.72)$$

for $i, j = 1, 2$

$$RHS = \frac{\partial}{\partial x_i} \int_{-h}^{\eta'} (-p\delta_{ij} + \sigma'_{ij}) dz + \tau_j^F |\nabla F| + [p]_{-h} \delta_{ij} \frac{\partial h}{\partial x_i} + \tau_j^B |\nabla B| \quad (4.73)$$

for $i, j = 1, 2$

$$RHS = \frac{\partial}{\partial x_i} \int_{-h}^{\eta'} (-p\delta_{ij} + \sigma'_{ij}) dz + [p]_{-h} \frac{\partial h}{\partial x_j} + \tau_j^F |\nabla F| + \tau_j^B |\nabla B| \quad (4.74)$$

for $i, j = 1, 2$

Putting Equations (4.55) and (4.74) together gives:

$$\begin{aligned} \frac{\partial}{\partial x_i} \int_{-h}^{\eta'} \rho u_i u_j dz + \frac{\partial}{\partial t} \int_{-h}^{\eta'} \rho u_j dz = & \frac{\partial}{\partial x_i} \int_{-h}^{\eta'} (-p\delta_{ij} + \sigma'_{ij}) dz + [p]_{-h} \frac{\partial h}{\partial x_j} + \tau_j^F |\nabla F| + \tau_j^B |\nabla B| \end{aligned} \quad (4.75)$$

Equation (4.75) is the horizontal momentum balance equation. It is for a column of fluid with unit area and height $\eta'' + h$. The terms on the left hand side of the equation are the net momentum flux and the acceleration through the sides of the column of fluid. The terms on the right hand side are the net stresses on the sides of the column, the pressure exerted by the seabed to the fluid and the surface stresses at the free surface and the seabed.

4.4.3 Vertically Integrated Horizontal Momentum Balance Equation averaged over time

The left hand side of Equation (4.75) can be averaged over time.

$$\overline{\frac{\partial}{\partial x_i} \int_{-h}^{\eta'} \rho u_i u_j dz} + \overline{\frac{\partial}{\partial t} \int_{-h}^{\eta'} \rho u_j dz} = \rho \overline{\frac{\partial}{\partial x_i} \int_{-h}^{\eta'} u_i u_j dz} + \rho \overline{\frac{\partial}{\partial t} \int_{-h}^{\eta'} u_j dz} \text{ for } i, j = 1, 2 \quad (4.76)$$

Using Equation (3.45) the following can be stated:

$$\int_{-h}^{\eta'} u_j dz = \int_{-h}^{\eta'} U_j dz + \int_{-h}^{\eta'} u'_j dz + \int_{-h}^{\eta'} u''_j dz \text{ for } i, j = 1, 2 \quad (4.77)$$

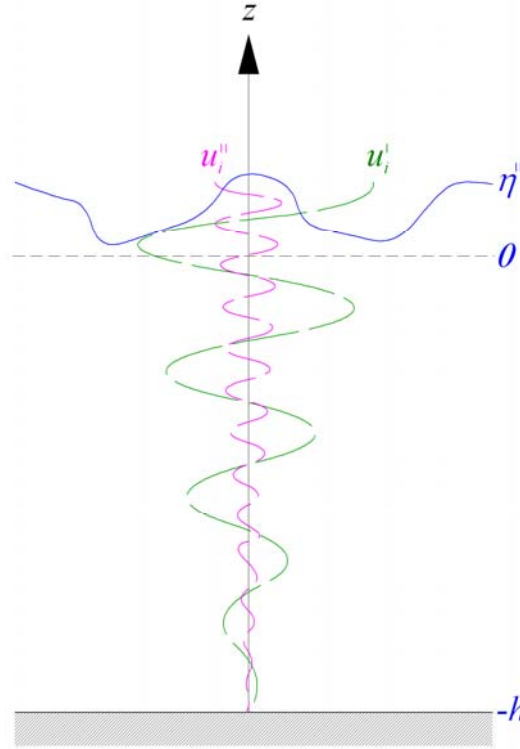


Figure 4.5 – Plot of wave particle velocity and turbulent velocity over depth

It can be seen from Figure 4.5 that the positive and negative portions of both the wave particle velocity and turbulent velocity plots over the depth are roughly equal. This shows that the integrals of u'_j and u''_j from $-h$ to η'' are approximately zero. This gives the following:

$$\int_{-h}^{\eta'} u_j dz \approx \int_{-h}^{\eta'} U_j dz \text{ for } i, j = 1, 2 \quad (4.78)$$

Hence the following can be stated:

$$\overline{\rho \frac{\partial}{\partial t} \int_{-h}^{\eta'} u_j dz} = \overline{\rho \frac{\partial}{\partial t} \int_{-h}^{\eta'} U_j dz} \quad \text{for } i, j = 1, 2 \quad (4.79)$$

Equation (4.79) can now be expanded as follows:

$$\overline{\rho \frac{\partial}{\partial t} \int_{-h}^{\eta'} u_j dz} = \overline{\rho \frac{\partial}{\partial t} U_j [h + \eta'']} \quad \text{for } i, j = 1, 2 \quad (4.80)$$

Examining the time averaged integral of a function f gives:

$$\overline{\frac{\partial f}{\partial t}} = \frac{1}{T} \int_{t-\frac{T}{2}}^{t+\frac{T}{2}} \frac{\partial f}{\partial t} dt \quad (4.81)$$

Equation (4.81) becomes:

$$\overline{\frac{\partial f}{\partial t}} = \frac{1}{T} f \Big|_{t-\frac{T}{2}}^{t+\frac{T}{2}} \quad (4.82)$$

Equation (4.82) can be expressed more explicitly as:

$$\overline{\frac{\partial f}{\partial t}} = \frac{f_{t+\frac{T}{2}} - f_{t-\frac{T}{2}}}{T} \quad (4.83)$$

Therefore:

$$\overline{\frac{\partial f}{\partial t}} \approx \frac{\partial \bar{f}}{\partial t} \quad (4.84)$$

Using Equation (4.84) with Equation (4.80) gives:

$$\overline{\rho \frac{\partial}{\partial t} \int_{-h}^{\eta'} u_j dz} = \rho \frac{\partial}{\partial t} \overline{U_j [h + \eta'']} \quad \text{for } i, j = 1, 2 \quad (4.85)$$

Equation (4.13) can now be used to re-express Equation (4.85) as follows:

$$\overline{\rho \frac{\partial}{\partial t} \int_{-h}^{\eta'} u_j dz} = \rho \frac{\partial}{\partial t} U_j [\overline{h + \eta''}] \quad \text{for } i, j = 1, 2 \quad (4.86)$$

The depth, h , does not vary over time so Equation (4.86) becomes:

$$\overline{\rho \frac{\partial}{\partial t} \int_{-h}^{\eta'} u_j dz} = \rho \frac{\partial}{\partial t} U_j [h + \bar{\eta}] \text{ for } i, j = 1, 2 \quad (4.87)$$

Using Equation (4.87) with Equation (4.76) gives:

$$\frac{\partial}{\partial x_i} \overline{\int_{-h}^{\eta'} \rho u_i u_j dz} + \frac{\partial}{\partial t} \overline{\int_{-h}^{\eta'} \rho u_j dz} = \rho \frac{\partial}{\partial x_i} \overline{\int_{-h}^{\eta'} u_i u_j dz} + \rho \frac{\partial}{\partial t} [U_j (\bar{\eta} + h)] \text{ for } i, j = 1, 2 \quad (4.88)$$

Explicitly expressing the steady and unsteady terms in Equation (4.88) gives:

$$\begin{aligned} \frac{\partial}{\partial x_i} \overline{\int_{-h}^{\eta'} \rho u_i u_j dz} + \frac{\partial}{\partial t} \overline{\int_{-h}^{\eta'} \rho u_j dz} = \rho \frac{\partial}{\partial x_i} \left[\overline{\int_{-h}^{\eta'} U_i U_j dz} + \overline{\int_{-h}^{\eta'} \tilde{u}_i \tilde{u}_j dz} + \overline{\int_{-h}^{\eta'} U_i \tilde{u}_j dz} + \overline{\int_{-h}^{\eta'} U_j \tilde{u}_i dz} \right] \\ + \rho \frac{\partial}{\partial t} [U_j (\bar{\eta} + h)] \end{aligned} \quad \text{for } i, j = 1, 2 \quad (4.89)$$

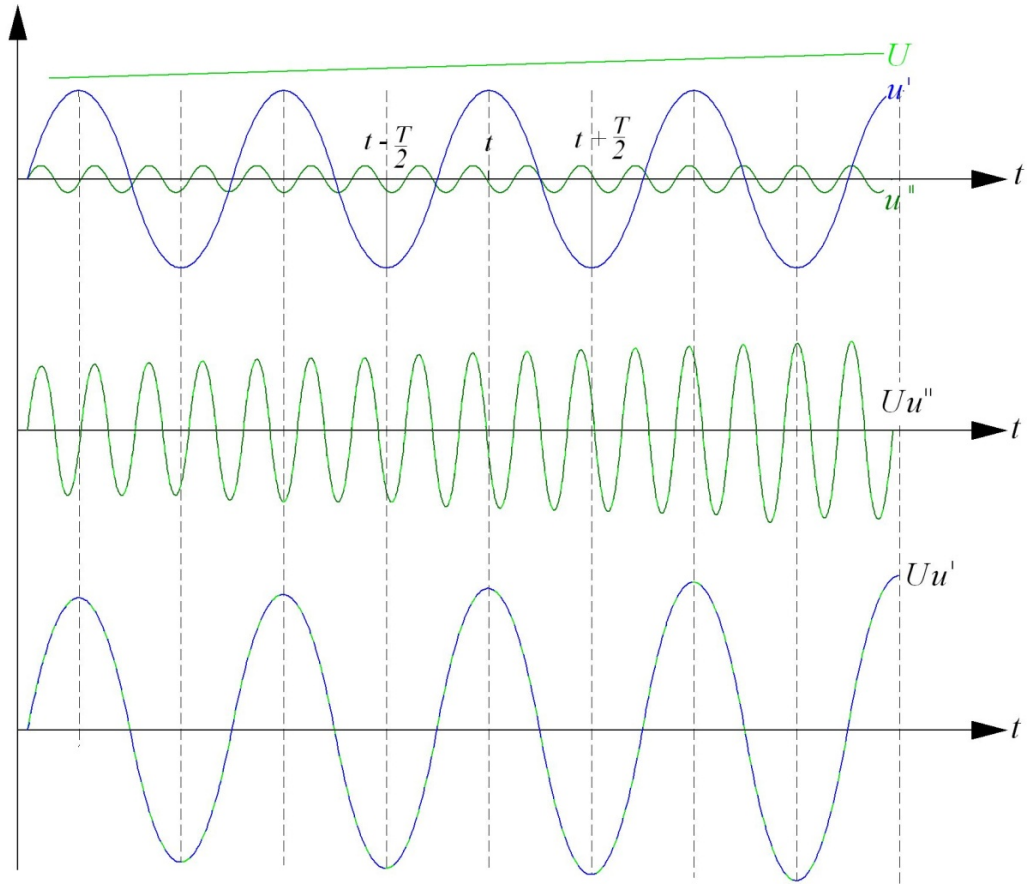


Figure 4.6 – Variation in velocity terms and their products over time

Examining Equation (4.17) and Figure 4.6 shows that the time averaging of a single unsteady velocity term is zero. Hence Equation (4.89) becomes:

$$\overline{\frac{\partial}{\partial x_i} \int_{-h}^{\eta''} \rho u_i u_j dz} + \overline{\frac{\partial}{\partial t} \int_{-h}^{\eta''} \rho u_j dz} = \rho \frac{\partial}{\partial x_i} \overline{\int_{-h}^{\eta''} U_i U_j dz} + \rho \frac{\partial}{\partial x_i} \overline{\int_{-h}^{\eta''} \tilde{u}_i \tilde{u}_j dz} + \rho \frac{\partial}{\partial t} [U_j (\bar{\eta} + h)]$$

for $i, j = 1, 2$ (4.90)

Equation (4.90) may be expanded as follows:

$$\overline{\frac{\partial}{\partial x_i} \int_{-h}^{\eta''} \rho u_i u_j dz} + \overline{\frac{\partial}{\partial t} \int_{-h}^{\eta''} \rho u_j dz} = \rho \frac{\partial}{\partial x_i} [U_i U_j (\bar{\eta} + h)] + \rho \frac{\partial}{\partial x_i} \overline{\int_{-h}^{\eta''} \tilde{u}_i \tilde{u}_j dz} + \frac{\partial}{\partial t} [U_j (\bar{\eta} + h)]$$

for $i, j = 1, 2$ (4.91)

A further expansion of Equation (4.91) yields:

$$\begin{aligned} \overline{\frac{\partial}{\partial x_i} \int_{-h}^{\eta''} \rho u_i u_j dz} + \overline{\frac{\partial}{\partial t} \int_{-h}^{\eta''} \rho u_j dz} &= \rho U_i U_j \frac{\partial}{\partial x_i} (\bar{\eta} + h) + \rho U_i (\bar{\eta} + h) \frac{\partial U_j}{\partial x_i} + \rho U_j (\bar{\eta} + h) \frac{\partial U_i}{\partial x_i} \\ &+ \rho \left[(\bar{\eta} + h) \frac{\partial U_j}{\partial t} + U_j \frac{\partial \bar{\eta}}{\partial t} \right] + \rho \frac{\partial}{\partial x_i} \overline{\int_{-h}^{\eta''} \tilde{u}_i \tilde{u}_j dz} \end{aligned}$$

for $i, j = 1, 2$ (4.92)

Equation (4.92) may be rewritten as:

$$\begin{aligned} \overline{\frac{\partial}{\partial x_i} \int_{-h}^{\eta''} \rho u_i u_j dz} + \overline{\frac{\partial}{\partial t} \int_{-h}^{\eta''} \rho u_j dz} &= \rho U_j \frac{\partial}{\partial x_i} [U_i (\bar{\eta} + h)] + \rho U_i (\bar{\eta} + h) \frac{\partial U_j}{\partial x_i} \\ &+ \rho (\bar{\eta} + h) \frac{\partial U_j}{\partial t} + \rho U_j \frac{\partial \bar{\eta}}{\partial t} + \rho \frac{\partial}{\partial x_i} \overline{\int_{-h}^{\eta''} \tilde{u}_i \tilde{u}_j dz} \end{aligned}$$

for $i, j = 1, 2$ (4.93)

Using Equation (4.37) with Equation (4.93) gives:

$$\begin{aligned} \overline{\frac{\partial}{\partial x_i} \int_{-h}^{\eta''} \rho u_i u_j dz} + \overline{\frac{\partial}{\partial t} \int_{-h}^{\eta''} \rho u_j dz} &= -\rho U_j \frac{\partial \bar{\eta}}{\partial t} + \rho U_i (\bar{\eta} + h) \frac{\partial U_j}{\partial x_i} \\ &+ \rho (\bar{\eta} + h) \frac{\partial U_j}{\partial t} + \rho U_j \frac{\partial \bar{\eta}}{\partial t} + \rho \frac{\partial}{\partial x_i} \overline{\int_{-h}^{\eta''} \tilde{u}_i \tilde{u}_j dz} \end{aligned}$$

for $i, j = 1, 2$ (4.94)

Simplification of Equation (4.94) yields:

$$\overline{\frac{\partial}{\partial x_i} \int_{-h}^{\eta''} \rho u_i u_j dz} + \frac{\partial}{\partial t} \int_{-h}^{\eta''} \rho u_j dz = \rho (\bar{\eta} + h) \left[\frac{\partial U_j}{\partial t} + U_i \frac{\partial U_j}{\partial x_i} \right] + \rho \frac{\partial}{\partial x_i} \int_{-h}^{\eta''} \tilde{u}_i \tilde{u}_j dz \quad \text{for } i, j = 1, 2 \quad (4.95)$$

The right hand side of Equation (4.75) is now examined.

Initially the various symbols for pressure at the seabed will be examined:

$[p]_{-h}$ is the total pressure at the seabed.

$\rho g(\eta + h)$ is the hydrostatic pressure at the seabed.

p_b is the dynamic pressure at the seabed.

Hence the mean dynamic pressure at the seabed may be defined as:

$$\bar{p}_b = [p]_{-h} - \rho g(\bar{\eta} + h) \quad (4.96)$$

Therefore:

$$[\bar{p}]_{-h} \frac{\partial h}{\partial x_j} = \bar{p}_b \frac{\partial h}{\partial x_j} + \rho g(\bar{\eta} + h) \frac{\partial h}{\partial x_j} \quad \text{for } i, j = 1, 2 \quad (4.97)$$

The following identity will now be useful:

$$\frac{\partial}{\partial x_j} \left[\frac{1}{2} \rho g(\bar{\eta} + h)^2 \right] = \rho g(\bar{\eta} + h) \frac{\partial}{\partial x_j} (\bar{\eta} + h) \quad \text{for } j = 1, 2 \quad (4.98)$$

$$\frac{\partial}{\partial x_j} \left[\frac{1}{2} \rho g(\bar{\eta} + h)^2 \right] = \rho g(\bar{\eta} + h) \frac{\partial \bar{\eta}}{\partial x_j} + \rho g(\bar{\eta} + h) \frac{\partial h}{\partial x_j} \quad \text{for } j = 1, 2 \quad (4.99)$$

$$\rho g(\bar{\eta} + h) \frac{\partial h}{\partial x_j} = \frac{\partial}{\partial x_j} \left[\frac{1}{2} \rho g(\bar{\eta} + h)^2 \right] - \rho g(\bar{\eta} + h) \frac{\partial \bar{\eta}}{\partial x_j} \quad \text{for } j = 1, 2 \quad (4.100)$$

Using Equation (4.100) with Equation (4.97) gives:

$$[\bar{p}]_{-h} \frac{\partial h}{\partial x_j} = \bar{p}_b \frac{\partial h}{\partial x_j} + \frac{\partial}{\partial x_j} \left[\frac{1}{2} \rho g(\bar{\eta} + h)^2 \right] - \rho g(\bar{\eta} + h) \frac{\partial \bar{\eta}}{\partial x_j} \quad \text{for } j = 1, 2 \quad (4.101)$$

Using Equations (4.95) and (4.101) to obtain a time averaged version of (4.75) gives:

$$\begin{aligned} \rho(\bar{\eta}+h) \left[\frac{\partial U_j}{\partial t} + U_i \frac{\partial U_j}{\partial x_i} \right] + \rho \frac{\partial}{\partial x_i} \overline{\int_{-h}^{\eta'} \tilde{u}_i \tilde{u}_j dz} &= \frac{\partial}{\partial x_i} \overline{\int_{-h}^{\eta'} (-p \delta_{ij} + \sigma'_{ij}) dz} + \overline{p_b} \frac{\partial h}{\partial x_j} \\ &+ \frac{\partial}{\partial x_j} \left[\frac{1}{2} \rho g (\bar{\eta}+h)^2 \right] - \rho g (\bar{\eta}+h) \frac{\partial \bar{\eta}}{\partial x_j} \\ &+ \overline{\tau_j^F |\nabla F|} + \overline{\tau_j^B |\nabla B|} \end{aligned}$$

for $i, j = 1, 2$ (4.102)

Rewriting Equation (4.102) gives:

$$\begin{aligned} \rho(\bar{\eta}+h) \left[\frac{\partial U_j}{\partial t} + U_i \frac{\partial U_j}{\partial x_i} \right] &= \overline{p_b} \frac{\partial h}{\partial x_j} - \rho g (\bar{\eta}+h) \frac{\partial \bar{\eta}}{\partial x_j} \\ &+ \frac{\partial}{\partial x_i} \left[- \overline{\int_{-h}^{\eta'} p \delta_{ij} dz} + \overline{\int_{-h}^{\eta'} \rho \tilde{u}_i \tilde{u}_j dz} + \overline{\int_{-h}^{\eta'} \sigma'_{ij} dz} \right] + \frac{\partial}{\partial x_j} \left[\frac{1}{2} \rho g (\bar{\eta}+h)^2 \right] \\ &+ \overline{\tau_j^F |\nabla F|} + \overline{\tau_j^B |\nabla B|} \end{aligned}$$

for $i, j = 1, 2$ (4.103)

This may be rewritten as follows:

$$\begin{aligned} \rho(\bar{\eta}+h) \left[\frac{\partial U_j}{\partial t} + U_i \frac{\partial U_j}{\partial x_i} \right] &= \overline{p_b} \frac{\partial h}{\partial x_j} - \rho g (\bar{\eta}+h) \frac{\partial \bar{\eta}}{\partial x_j} \\ &+ \frac{\partial}{\partial x_i} \left[- \overline{\int_{-h}^{\eta'} (p \delta_{ij} + \rho \tilde{u}_i \tilde{u}_j) dz} + \delta_{ij} \left[\frac{1}{2} \rho g (\bar{\eta}+h)^2 \right] + \overline{\int_{-h}^{\eta'} \sigma'_{ij} dz} \right] \\ &+ \overline{\tau_j^F |\nabla F|} + \overline{\tau_j^B |\nabla B|} \end{aligned}$$

for $i, j = 1, 2$ (4.104)

Introducing the term R_{ij} in Equation (4.104) gives:

$$\rho(\bar{\eta}+h) \left[\frac{\partial U_j}{\partial t} + U_i \frac{\partial U_j}{\partial x_i} \right] = \overline{p_b} \frac{\partial h}{\partial x_j} - \rho g (\bar{\eta}+h) \frac{\partial \bar{\eta}}{\partial x_j} + \frac{\partial}{\partial x_i} \left[-R_{ij} + \overline{\int_{-h}^{\eta'} \sigma'_{ij} dz} \right] + \overline{\tau_j^F |\nabla F|} + \overline{\tau_j^B |\nabla B|}$$

for $i, j = 1, 2$ (4.105)

Where:

$$R_{ij} = \overline{\int_{-h}^{\eta'} (p \delta_{ij} + \rho \tilde{u}_i \tilde{u}_j) dz} - \delta_{ij} \left[\frac{1}{2} \rho g (\bar{\eta}+h)^2 \right] \text{ for } i, j = 1, 2 \quad (4.106)$$

Examining the following term:

$$\rho g \int_{-h}^{\bar{\eta}} (\bar{\eta} - z) dz = \rho g \int_{-h}^{\bar{\eta}} \bar{\eta} dz - \rho g \int_{-h}^{\bar{\eta}} z dz \quad (4.107)$$

$$\rho g \int_{-h}^{\bar{\eta}} (\bar{\eta} - z) dz = \rho g [\bar{\eta} z]_{-h}^{\bar{\eta}} - \rho g \left[\frac{z^2}{2} \right]_{-h}^{\bar{\eta}} \quad (4.108)$$

$$\rho g \int_{-h}^{\bar{\eta}} (\bar{\eta} - z) dz = \rho g [\bar{\eta}^2 + \bar{\eta} h] - \rho g \left[\frac{\bar{\eta}^2}{2} - \frac{h^2}{2} \right] \quad (4.109)$$

$$\rho g \int_{-h}^{\bar{\eta}} (\bar{\eta} - z) dz = \rho g \bar{\eta}^2 + \rho g \bar{\eta} h - \frac{\rho g \bar{\eta}^2}{2} + \frac{\rho g h^2}{2} \quad (4.110)$$

$$\rho g \int_{-h}^{\bar{\eta}} (\bar{\eta} - z) dz = \frac{\rho g}{2} [\bar{\eta}^2 + 2\bar{\eta} h + h^2] \quad (4.111)$$

$$\rho g \int_{-h}^{\bar{\eta}} (\bar{\eta} - z) dz = \frac{\rho g}{2} (\bar{\eta} + h)^2 \quad (4.112)$$

Equation (4.106) can be rewritten using the result of Equation (4.112):

$$R_{ij} = \overline{\int_{-h}^{\eta^*} (p \delta_{ij} + \rho \tilde{u}_i \tilde{u}_j) dz} - \delta_{ij} \rho g \int_{-h}^{\bar{\eta}} (\bar{\eta} - z) dz \quad \text{for } i, j = 1, 2 \quad (4.113)$$

$$R_{ij} = \left[\overline{\int_{-h}^{\eta^*} p dz} - \rho g \int_{-h}^{\bar{\eta}} (\bar{\eta} - z) dz \right] \delta_{ij} + \rho \overline{\int_{-h}^{\eta^*} \tilde{u}_i \tilde{u}_j dz} \quad \text{for } i, j = 1, 2 \quad (4.114)$$

4.3.3 Some Simplifications of the Horizontal Momentum Balance Equation

4.3.3.1 Preliminary Orders of Magnitude

In order to use the equations derived in Section 4.3.2 in an engineering model it is necessary to carry out some simplifications. Firstly to solve to a steady state for wave generated set-up/set-down and currents it is acceptable to state the following for the steady state solution:

$$\frac{\partial U_j}{\partial t} = \frac{\partial \bar{\eta}}{\partial t} = 0 \text{ for } j = 1, 2 \quad (4.115)$$

If atmospheric disturbance of the free surface is discounted the following simplification can also be applied:

$$\overline{\tau_j^F} = 0 \text{ for } j = 1, 2 \quad (4.116)$$

It is noted by Mei (2005) that the transient effects such as wind could have a “very direct influence on short-term evolution of beaches.” However Mei (2005) goes on to comment that very little research has been carried out into this topic.

Examining Equation (4.105) we can assume that viscosity, bottom slope and wave slope are all small quantities. Clearly viscosity would be of the order of μ . Wave steepness would be of the order κA as shown below:

$$\text{Wave Steepness} = \frac{H}{L} \sim O\left(\frac{A_\xi}{L}\right) \quad (4.117)$$

$$\kappa = \frac{2\pi}{L} \quad (4.118)$$

Hence:

$$\kappa \sim O\left(\frac{1}{L}\right) \quad (4.119)$$

$$\text{So } \frac{H}{L} \sim O(\kappa A_\xi) \quad (4.120)$$

Examination of beach properties would also lead to the conclusion that the order of the bottom slope would be less than or equal to the order of magnitude of the wave slope:

$$|\nabla h| \leq O(\kappa A_\xi) \quad (4.121)$$

4.3.3.2 Viscous Stress Terms

It is known from kinematics that any particle on the free surface remains on the free surface. Hence a water particle undergoing wave orbital velocity will have an orbit with a radius of approximately the same size as the wave height which in turn is of the same order as the wave amplitude. The horizontal displacement that a particle undergoes per wave period will be approximately equal to the radius and hence wave amplitude. Hence it is possible to say that:

$$\text{Horizontal velocity, } |\tilde{u}_i| \sim O\left(\frac{A_\xi}{T}\right) \sim O(\omega A_\xi) \quad (4.122)$$

If the assumption is made that velocity varies at the same rate as a wave length then the horizontal gradient of horizontal particle velocity $\sim O\left(\frac{\omega A_\xi}{L}\right) \sim O(\kappa \omega A_\xi)$.

The order of magnitude of the viscous stress term in Equation (4.105) is now examined. The viscous stress term is a product of viscosity $[O(\mu)]$ and the gradients of horizontal velocity $[O(\kappa \omega A_\xi)]$. This leads to the following order of magnitude expression for the vertical integration of the viscous stress term:

$$\overline{\int_{-h}^{\eta^*} \sigma'_{ij} dz} \sim O(\mu \kappa \omega A_\xi h) \quad (4.123)$$

Similarly Equation (4.114) can be examined with respect to orders of magnitude leading to the following expression:

$$R_{ij} = O\left[\overline{\rho \int_{-h}^{\eta} \tilde{u}_i \tilde{u}_j dz}\right] \text{ for } i, j = 1, 2 \quad (4.124)$$

Using Equation (4.122) with Equation (4.124) yields:

$$R_{ij} \sim O\left(\rho (\omega A_\xi)^2 h\right) \text{ for } i, j = 1, 2 \quad (4.125)$$

Using Equations (4.123) and (4.125) the following can be obtained:

$$\frac{\overline{\int_{-h}^{\eta^*} \sigma'_{ij} dz}}{R_{ij}} \sim O\left[\frac{\mu \kappa \omega A h}{\rho (\omega A_\xi)^2 h}\right] \sim O\left[\frac{\mu \kappa}{\rho \omega A_\xi}\right] \sim O\left[\frac{\nu \kappa}{\omega A_\xi}\right] \text{ for } i, j = 1, 2 \quad (4.126)$$

Where $\nu = \frac{\mu}{\rho}$. It is known that the Reynolds number based on wave orbital velocity and wavelength is:

$$R_E \equiv \frac{\omega A_\xi}{\nu \kappa} = \frac{A_\xi}{\kappa \delta^2} \quad (4.127)$$

Where δ is the boundary layer thickness.

Equation (4.126) can then be related to the Reynolds Number, R_E :

$$\frac{\overline{\int_{-h}^{\eta'} \sigma'_{ij} dz}}{R_{ij}} \sim O\left[\frac{\nu \kappa}{\omega A_\xi}\right] \sim O[R_E^{-1}] \text{ for } i, j = 1, 2 \quad (4.128)$$

Under practical circumstances the ratio expressed in Equation (4.128) is very small and hence the integral of viscous stress can be assumed to be negligible with respect to radiation stress for present purposes.

4.3.3.3 Bottom Stress Terms

The bottom stress term, τ_i^B , however, cannot be assumed to be negligible. Mei (2005) uses the assumption that the square of the slope of the seabed is small. Using Equation (4.69) the following can be stated:

$$|\nabla B| = \sqrt{\left(\frac{\partial h}{\partial x}\right)^2 + \left(\frac{\partial h}{\partial y}\right)^2 + 1} \quad (4.129)$$

Equation (4.129) can also be expressed as:

$$|\nabla B| = \sqrt{1 + (\nabla h)^2} \quad (4.130)$$

Hence:

$$|\nabla B| = 1 + O(\nabla h)^2 \quad (4.131)$$

Therefore:

$$\overline{\tau_j^B |\nabla B|} = \overline{\tau_j^B} \left[1 + O(\nabla h)^2 \right] \quad (4.132)$$

4.3.3.4 Integration of Vertical Momentum Equation

In order to examine the mean dynamic pressure of Equation (4.96) it is necessary to integrate the vertical momentum equation. Equation (4.47) becomes:

$$\int_z^{\eta'} \left[\frac{\partial}{\partial z} (p + \rho g z) \right] dz = -\rho \int_z^{\eta'} \frac{\partial w}{\partial t} dz - \rho \int_z^{\eta'} \frac{\partial u_i w}{\partial x_i} dz - \rho \int_z^{\eta'} \frac{\partial w^2}{\partial z} dz + \int_z^{\eta'} \frac{\partial \sigma'_{i3}}{\partial x_i} dz + \int_z^{\eta'} \frac{\partial \sigma'_{33}}{\partial z} dz$$

for $i = 1, 2$ (4.133)

Equation (4.133) can be expanded to give the following:

$$\begin{aligned} [p]_{\eta} - [p]_z + \rho g (\eta - z) &= \int_z^{\eta'} \frac{\partial \sigma'_{i3}}{\partial x_i} dz + [\sigma'_{33}]_{\eta} - [\sigma'_{33}]_z - \rho \int_z^{\eta'} \frac{\partial w}{\partial t} dz \\ &\quad - \rho \int_z^{\eta'} \frac{\partial u_i w}{\partial x_i} dz - \rho [w^2]_{\eta} + \rho [w^2]_z \end{aligned}$$

for $i = 1, 2$ (4.134)

Using the Leibniz Rule, Equation (3.399), Equation (4.134) becomes:

$$\begin{aligned} [p]_{\eta} - [p]_z + \rho g (\eta - z) &= \frac{\partial}{\partial x_i} \int_z^{\eta'} \sigma'_{i3} dz - \frac{\partial \eta}{\partial x_i} [\sigma'_{i3}]_{\eta} + [\sigma'_{33}]_{\eta} - [\sigma'_{33}]_z \\ &\quad - \rho \frac{\partial}{\partial t} \int_z^{\eta'} w dz + \rho \frac{\partial \eta}{\partial t} [w]_{\eta} - \rho \frac{\partial}{\partial x_i} \int_z^{\eta'} u_i w dz \\ &\quad + \rho \frac{\partial \eta}{\partial x_i} [u_i w]_{\eta} - \rho [w^2]_{\eta} + \rho [w^2]_z \end{aligned}$$

for $i = 1, 2$ (4.135)

Equation (4.135) can be rearranged to give:

$$\begin{aligned} [p]_z &= \rho g (\eta - z) + \rho \left[\frac{\partial}{\partial t} \int_z^{\eta'} w dz + \frac{\partial}{\partial x_i} \int_z^{\eta'} u_i w dz \right] \\ &\quad - \rho \left[w \left(\frac{\partial \eta}{\partial t} + u_i \frac{\partial \eta}{\partial x_i} - w \right) \right]_{\eta} - \rho [w^2]_z - \frac{\partial}{\partial x_i} \int_z^{\eta'} \tau_{i3} dz \\ &\quad - \left[-p + \sigma'_{33} - \frac{\partial \eta}{\partial x_i} \sigma'_{i3} \right]_{\eta} + [\sigma'_{33}]_z \end{aligned}$$

for $i = 1, 2$ (4.136)

The boundary terms of Equation (4.136) are now examined.

Examining the case of $j = 3$ from Equation (4.59) gives:

$$(-p\delta_{i3} + \sigma'_{i3})n_i = \tau_3^F \text{ at } z = \eta', \text{ for } i = 1, 2, 3$$

(4.137)

Expressing Equation (4.137) more explicitly gives:

$$(-p\delta_{13} + \sigma'_{13})n_1 + (-p\delta_{23} + \sigma'_{23})n_2 + (-p\delta_{33} + \sigma'_{33})n_3 = \tau_3^F \text{ at } z = \eta'' \quad (4.138)$$

Equation (4.138) can be expanded as follows using Equation (4.65) :

$$(-p\delta_{13} + \sigma'_{13})\left(-\frac{\partial\eta}{\partial x_1}\right) + (-p\delta_{23} + \sigma'_{23})\left(-\frac{\partial\eta}{\partial x_2}\right) + (-p\delta_{33} + \sigma'_{33}) = |\nabla F| \tau_3^F \text{ at } z = \eta'' \quad (4.139)$$

This may be simplified as:

$$\left(-\sigma'_{13} \frac{\partial\eta}{\partial x_1}\right) + \left(-\sigma'_{23} \frac{\partial\eta}{\partial x_2}\right) + (-p\delta_{33} + \sigma'_{33}) = |\nabla F| \tau_3^F \text{ at } z = \eta'' \quad (4.140)$$

Equation (4.140) may be rewritten as follows:

$$-\sigma'_{i3} \frac{\partial\eta}{\partial x_i} - p + \sigma'_{33} = |\nabla F| \tau_3^F \text{ at } z = \eta'' \text{ for } i = 1, 2 \quad (4.141)$$

If the atmospheric pressure is zero the Equation (4.141) becomes:

$$-p + \sigma'_{33} - \sigma'_{i3} \frac{\partial\eta}{\partial x_i} = 0 \text{ at } z = \eta'' \text{ for } i = 1, 2 \quad (4.142)$$

Using Equations (4.27) and (4.142) with Equation (4.136) and acknowledging an atmospheric pressure of zero at the free surface gives:

$$\begin{aligned} [p]_z &= \rho g (\eta - z) + \rho \left[\frac{\partial}{\partial t} \int_z^{\eta'} w dz + \frac{\partial}{\partial x_i} \int_z^{\eta'} u_i w dz \right] \\ &\quad - \rho [w^2]_z - \frac{\partial}{\partial x_i} \int_z^{\eta'} \sigma'_{i3} dz + [\sigma'_{33}]_z \end{aligned} \quad \text{for } i = 1, 2 \quad (4.143)$$

Obtaining the time average of the terms in Equation (4.143) yields:

$$\begin{aligned} [\bar{p}]_z &= \rho g (\bar{\eta} - z) + \rho \left[\overline{\frac{\partial}{\partial t} \int_z^{\eta'} w dz} + \overline{\frac{\partial}{\partial x_i} \int_z^{\eta'} u_i w dz} \right] \\ &\quad - \rho [\bar{w}^2]_z - \overline{\frac{\partial}{\partial x_i} \int_z^{\eta'} \sigma'_{i3} dz} + [\bar{\sigma}'_{33}]_z \end{aligned} \quad \text{for } i = 1, 2 \quad (4.144)$$

Using the result of Equation (4.84) with Equation (4.144) gives:

$$\begin{aligned} \left[\overline{p} \right]_z = & \rho g (\bar{\eta} - z) + \rho \left[\overline{\frac{\partial}{\partial t} \int_z^{\eta''} w dz} + \frac{\partial}{\partial x_i} \overline{\int_z^{\eta''} u_i w dz} \right] \\ & - \rho \left[\overline{w^2} \right]_z - \frac{\partial}{\partial x_i} \overline{\int_z^{\eta''} \sigma'_{i3} dz} + \left[\overline{\sigma'_{33}} \right]_z \end{aligned} \quad \text{for } i = 1, 2 \quad (4.145)$$

The time average of the vertical velocity is zero:

$$\overline{\int_z^{\eta''} w dz} = 0 \quad (4.146)$$

Giving the following simplification of Equation (4.144):

$$\left[\overline{p} \right]_z = \rho g (\bar{\eta} - z) + \rho \frac{\partial}{\partial x_i} \overline{\int_z^{\eta''} u_i w dz} - \rho \left[\overline{w^2} \right]_z - \frac{\partial}{\partial x_i} \overline{\int_z^{\eta''} \sigma'_{i3} dz} + \left[\overline{\sigma'_{33}} \right]_z \quad \text{for } i = 1, 2 \quad (4.147)$$

4.3.3.5 Use of Dimensional Analysis to Simplify the Mean Water Pressure

Equation (4.128) shows that the integrated viscosity term is of the order $O(R_E^{-1})$ relative to the other terms in the equation. Using Equation (4.18), the continuity equation, the order of $\left[\overline{\sigma'_{33}} \right]_z$ can be obtained. Rearranging Equation (4.18) gives:

$$\frac{\partial u_i}{\partial x_i} = - \frac{\partial w}{\partial z} \quad \text{for } i = 1, 2 \quad (4.148)$$

Therefore:

$$\frac{\partial u_i}{\partial x_i} \sim O \left[\frac{\partial w}{\partial z} \right] \quad \text{for } i = 1, 2 \quad (4.149)$$

It is clear from Equation (4.149) that the following is true:

$$\frac{\partial \overline{u_i}}{\partial x_i} \sim O \left[\frac{\partial \overline{w}}{\partial z} \right] \quad \text{for } i = 1, 2 \quad (4.150)$$

Hence the following is true:

$$\left[\overline{\sigma'_{33}} \right]_z = \mu \frac{\partial \overline{w}}{\partial z} \sim O \left(\mu \frac{\partial \overline{u_i}}{\partial x_i} \right) \quad \text{for } i = 1, 2 \quad (4.151)$$

The magnitude of $\overline{\sigma'_{33}}$ is hence negligible leading to the following expression of Equation (4.147) when examined using Equation (4.128):

$$\left[\overline{p}\right]_z \equiv \left[\rho g (\overline{\eta} - z) + \rho \frac{\partial}{\partial x_i} \int_z^{\overline{\eta'}} u_i w dz - \rho \left[\overline{w^2}\right]_z \right] \left(1 + O(R_E^{-1})\right) \text{ for } i = 1, 2 \quad (4.152)$$

Examining Equation (4.152) at the seabed, where $z = -h$, and using Equation (4.28) yields:

$$\left[\overline{p}\right]_{-h} \equiv \left[\rho g (\overline{\eta} + h) + \rho \frac{\partial}{\partial x_i} \int_{-h}^{\overline{\eta'}} u_i w dz \right] \left(1 + O(R_E^{-1})\right) \text{ for } i = 1, 2 \quad (4.153)$$

Equations (4.152) and (4.153) yield the conclusion that viscosity does not have a direct influence on the time averaged pressure at any point in the fluid depth.

Using Equation (4.96) with Equation (4.153) yields:

$$\overline{p_b} \equiv \left[\rho \frac{\partial}{\partial x_i} \int_{-h}^{\overline{\eta'}} u_i w dz \right] \left(1 + O(R_E^{-1})\right) \text{ for } i = 1, 2 \quad (4.154)$$

Therefore:

$$\overline{p_b} \frac{\partial h}{\partial x_j} \equiv \left[\rho \frac{\partial h}{\partial x_j} \frac{\partial}{\partial x_i} \int_{-h}^{\overline{\eta'}} u_i w dz \right] \left(1 + O(R_E^{-1} |\nabla h|)\right) \text{ for } i, j = 1, 2 \quad (4.155)$$

Examination of Equation (4.155) shows that its order of magnitude is:

$$\overline{p_b} \frac{\partial h}{\partial x_j} = O(|\nabla h| \rho (\omega A)^2 \kappa h) \text{ for } j = 1, 2 \quad (4.156)$$

Assuming the length scale of variables $U, \overline{\eta}$ and R_{ij} is of the same order of magnitude as the wavelength: examination of other terms in Equation (4.105) for orders of magnitude gives the following results:

$$\rho (\overline{\eta} + h) U_i \frac{\partial U_j}{\partial x_i} = O(\rho h (\omega A)^2 \kappa) \text{ for } i, j = 1, 2 \quad (4.157)$$

$$\rho g (\overline{\eta} + h) \frac{\partial \overline{\eta}}{\partial x} = O(\rho g h A \kappa) \quad (4.158)$$

$$\frac{\partial R_{ij}}{\partial x_i} = O(\rho h (\omega A)^2 \kappa) \text{ for } i, j = 1, 2 \quad (4.159)$$

Equation (4.156) is at least an order of magnitude lower than the terms in Equations (4.157), (4.158) and (4.159) under the assumption that the slope of the seabed $|\nabla h|$ is small. Hence the term $\overline{p_b} \frac{\partial h}{\partial x_j}$ is unimportant and can be ignored.

Equation (4.105) may now be rewritten as follows using the results of Equations (4.116), (4.127), (4.132) and (4.156):

$$\rho(\overline{\eta} + h) \left[\frac{\partial U_j}{\partial t} + U_i \frac{\partial U_j}{\partial x_i} \right] = -\rho g (\overline{\eta} + h) \frac{\partial \overline{\eta}}{\partial x_j} - \frac{\partial R_{ij}}{\partial x_i} + \overline{\tau_j^B} \quad \text{for } i, j = 1, 2 \quad (4.160)$$

4.3.4 Radiation Stress

For the purposes of further examination it will be helpful to split the velocity and free surface variables into two separate components caused by wave and turbulent fluctuations respectively as in the case of Equation (3.43):

$$\tilde{u}_i = u'_i + u''_i \text{ for } i = 1, 2, 3 \quad (4.161)$$

$$\zeta = \zeta' + \zeta'' = \eta'' - \bar{\eta} \quad (4.162)$$

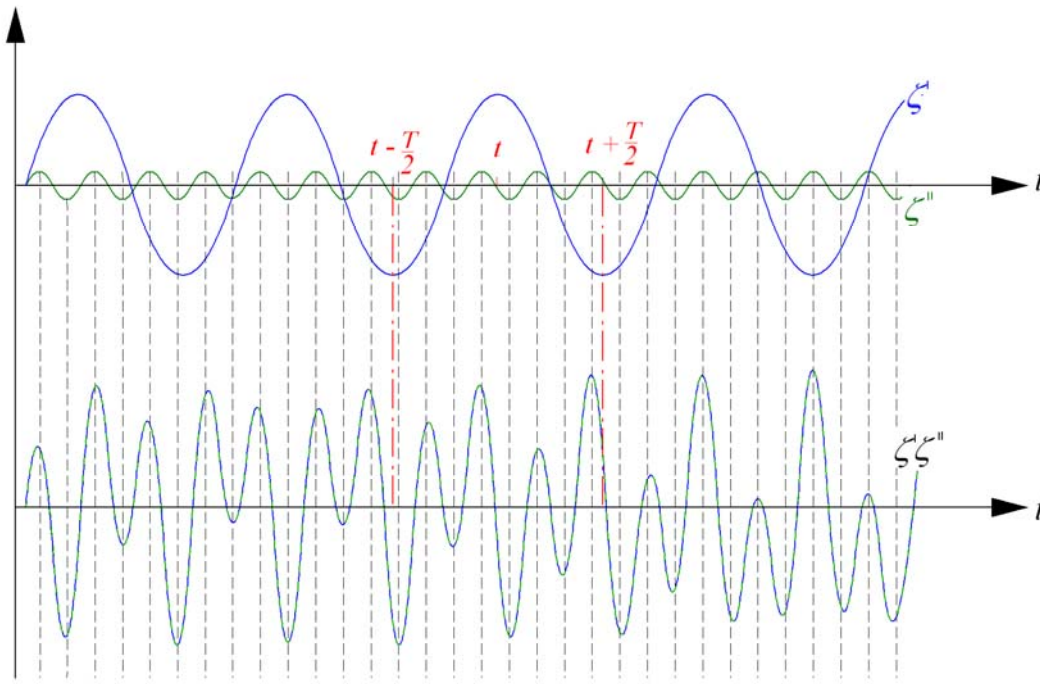


Figure 4.7 – Diagram showing different Time Scales of Wave and Turbulent Fluctuations

It is appropriate to make the assumption in this case that the characteristic time scales of the two components are not close and hence there is no relationship between the two. Figure 4.7 shows that the product of two terms with different characteristic time scales produces a function that when integrated over time will produce a result close to zero. This leads to the following results:

$$\overline{u'_i u''_i} = 0 \text{ for } \overline{\zeta' \zeta''} = 0 \quad (4.163)$$

$$\overline{\zeta' \zeta''} = 0 \quad (4.164)$$

The last term in Equation (4.114) can now expanded as follows:

$$\overline{\rho \int_{-h}^{\eta''} \tilde{u}_i \tilde{u}_j dz} = \overline{\rho \int_{-h}^{\bar{\eta} + \zeta' + \zeta''} \tilde{u}_i \tilde{u}_j dz} \text{ for } i, j = 1, 2, 3 \quad (4.165)$$

Equation (4.165) may be expanded as follows:

$$\overline{\rho \int_{-h}^{\eta''} \tilde{u}_i \tilde{u}_j dz} = \overline{\rho \left[\int_{-h}^{\bar{\eta}} \tilde{u}_i \tilde{u}_j dz + \int_{\bar{\eta}}^{\bar{\eta} + \zeta' + \zeta''} \tilde{u}_i \tilde{u}_j dz \right]} \text{ for } i, j = 1, 2, 3 \quad (4.166)$$

Re-expressing this yields:

$$\overline{\rho \int_{-h}^{\eta''} \tilde{u}_i \tilde{u}_j dz} = \overline{\rho \int_{-h}^{\bar{\eta}} \tilde{u}_i \tilde{u}_j dz} + \overline{\rho \int_{\bar{\eta}}^{\bar{\eta} + \zeta' + \zeta''} \tilde{u}_i \tilde{u}_j dz} \text{ for } i, j = 1, 2, 3 \quad (4.167)$$

Expanding the final term of Equation (4.167) gives:

$$\overline{\rho \int_{-h}^{\eta''} \tilde{u}_i \tilde{u}_j dz} = \overline{\rho \int_{-h}^{\bar{\eta}} \tilde{u}_i \tilde{u}_j dz} + \overline{\rho \int_{\bar{\eta}}^{\bar{\eta} + \zeta' + \zeta''} (u'_i + u''_i)(u'_j + u''_j) dz} \text{ for } i, j = 1, 2, 3 \quad (4.168)$$

Further expansion of the final term gives the following:

$$\overline{\rho \int_{-h}^{\eta''} \tilde{u}_i \tilde{u}_j dz} = \overline{\rho \int_{-h}^{\bar{\eta}} \tilde{u}_i \tilde{u}_j dz} + \overline{\rho \int_{\bar{\eta}}^{\bar{\eta} + \zeta' + \zeta''} (u'_i u'_j + u'_i u''_j + u''_i u'_j + u''_i u''_j) dz} \text{ for } i, j = 1, 2, 3 \quad (4.169)$$

Using Equation (4.163) with Equation (4.169) and assuming that the turbulent setup is an order of magnitude less than the wave set up yields:

$$\overline{\rho \int_{-h}^{\eta''} \tilde{u}_i \tilde{u}_j dz} = \overline{\rho \int_{-h}^{\bar{\eta}} \tilde{u}_i \tilde{u}_j dz} + \overline{\rho \int_{\bar{\eta}}^{\bar{\eta} + \zeta' + \zeta''} u'_i u'_j dz} \text{ for } i, j = 1, 2, 3 \quad (4.170)$$

Using Equation (4.122) the order of magnitude of each term of Equation (4.170) can be given as follows:

$$\overline{\rho \int_{-h}^{\bar{\eta}} \tilde{u}_i \tilde{u}_j dz} \sim O(\rho)(\omega A_\xi)(\omega A_\xi)(h') \sim O(\rho \omega^2 A_\xi^2 h') \text{ for } i, j = 1, 2, 3 \quad (4.171)$$

$$\overline{\rho \int_{\bar{\eta}}^{\bar{\eta} + \zeta' + \zeta''} u'_i u'_j dz} \sim O(\rho)(\omega A_\xi)(\omega A_\xi)(A_\xi) \sim O(\rho \omega^2 A_\xi^3) \text{ for } i, j = 1, 2, 3 \quad (4.172)$$

Using the assumption that the amplitude of the wave is significantly less than the water depth shows that the second term in Equation (4.122) is an order of magnitude less than the first term. This leads to the following equation:

$$\overline{\rho \int_{-h}^{\eta''} \tilde{u}_i \tilde{u}_j dz} = \rho \int_{-h}^{\bar{\eta}} \tilde{u}_i \tilde{u}_j dz + O(\rho \omega^2 A_\xi^3) \text{ for } i, j = 1, 2, 3 \quad (4.173)$$

So:

$$\overline{\rho \int_{-h}^{\eta''} \tilde{u}_i \tilde{u}_j dz} \cong \rho \int_{-h}^{\bar{\eta}} \overline{u'_i u'_j} dz + \rho \int_{-h}^{\bar{\eta}} \overline{u''_i u''_j} dz \text{ for } i, j = 1, 2, 3 \quad (4.174)$$

Ignoring the viscous stresses in Equation (4.143) due to their small order of magnitude gives:

$$[p]_z = \rho g (\eta - z) + \rho \left[\frac{\partial}{\partial t} \int_z^{\eta''} w dz + \frac{\partial}{\partial x_i} \int_z^{\eta''} u_i w dz \right] - \rho [w^2]_z \text{ for } i = 1, 2 \quad (4.175)$$

Integrating Equation (4.175) vertically and carrying out a time average gives the following:

$$\overline{\int_{-h}^{\eta''} p dz} = \rho g \overline{\int_{-h}^{\eta''} (\eta - z) dz} + \rho \overline{\int_{-h}^{\eta''} \left(\frac{\partial}{\partial t} \int_z^{\eta''} w dz \right) dz} + \rho \overline{\int_{-h}^{\eta''} \left(\frac{\partial}{\partial x_i} \int_z^{\eta''} u_i w dz \right) dz} - \rho \overline{\int_{-h}^{\eta''} w^2 dz} \quad (4.176)$$

for $i = 1, 2$

Evaluating the first integral on the right hand side of Equation (4.176) gives:

$$\overline{\int_{-h}^{\eta''} p dz} = \rho g \left(\overline{[\eta z]_{-h}^{\eta''}} - \overline{\left[\frac{z^2}{2} \right]_{-h}^{\eta''}} \right) + \rho \overline{\int_{-h}^{\eta''} \left(\frac{\partial}{\partial t} \int_z^{\eta''} w dz \right) dz} + \rho \overline{\int_{-h}^{\eta''} \left(\frac{\partial}{\partial x_i} \int_z^{\eta''} u_i w dz \right) dz} - \rho \overline{\int_{-h}^{\eta''} w^2 dz} \quad (4.177)$$

for $i = 1, 2$

Simplification of Equation (4.177) yields the following:

$$\overline{\int_{-h}^{\eta''} p dz} = \frac{\rho g}{2} \overline{(\eta'' + h)^2} + \rho \overline{\int_{-h}^{\eta''} \left(\frac{\partial}{\partial t} \int_z^{\eta''} w dz \right) dz} + \rho \overline{\int_{-h}^{\eta''} \left(\frac{\partial}{\partial x_i} \int_z^{\eta''} u_i w dz \right) dz} - \rho \overline{\int_{-h}^{\eta''} w^2 dz} \quad (4.178)$$

for $i = 1, 2$

The first term on the right hand side of Equation (4.178) will now be split into its wave and turbulent components:

$$(\eta'' + h)^2 = (\bar{\eta} + \zeta' + \zeta'' + h)^2 \quad (4.179)$$

$$(\eta'' + h)^2 = (\bar{\eta} + \zeta' + \zeta'')^2 + 2h(\bar{\eta} + \zeta' + \zeta'') + h^2 \quad (4.180)$$

$$(\eta'' + h)^2 = (\bar{\eta} + \zeta')^2 + 2(\bar{\eta} + \zeta')\zeta'' + \zeta''^2 + 2h\bar{\eta} + 2h\zeta' + 2h\zeta'' + h^2 \quad (4.181)$$

$$(\eta'' + h)^2 = \bar{\eta}^2 + 2\bar{\eta}\zeta' + \zeta'^2 + 2\bar{\eta}\zeta'' + 2\eta'\zeta'' + \zeta''^2 + 2h\bar{\eta} + 2h\zeta' + 2h\zeta'' + h^2 \quad (4.182)$$

$$(\eta'' + h)^2 = (\bar{\eta} + h)^2 + \zeta'^2 + \zeta''^2 + 2\bar{\eta}\zeta' + 2\bar{\eta}\zeta'' + 2\zeta'\zeta'' + 2h\zeta' + 2h\zeta'' \quad (4.183)$$

The first term of Equation (4.178) becomes:

$$\frac{\rho g}{2} \overline{(\eta'' + h)^2} = \frac{\rho g}{2} \overline{(\bar{\eta} + h)^2 + \zeta'^2 + \zeta''^2 + 2\bar{\eta}\zeta' + 2\bar{\eta}\zeta'' + 2\zeta'\zeta'' + 2h\zeta' + 2h\zeta''} \quad (4.184)$$

Equation (4.184) can then be simplified as follows using the assumption that the time scales of the wave and turbulent components are very different and after removal of terms negated by time integration:

$$\frac{\rho g}{2} \overline{(\eta'' + h)^2} = \frac{\rho g}{2} \overline{(\bar{\eta} + h)^2 + \zeta'^2 + \zeta''^2} \quad (4.185)$$

$$\frac{\rho g}{2} \overline{(\eta'' + h)^2} = \frac{\rho g}{2} \overline{(\bar{\eta} + h)^2 + \overline{\zeta'^2} + \overline{\zeta''^2}} \quad (4.186)$$

Using Leibniz's rule, Equation (3.399), the second term on the right hand side of Equation (4.178) yields:

$$\rho \int_{-h}^{\eta'} \left(\frac{\partial}{\partial t} \int_z^{\eta'} w dz' \right) dz = \rho \frac{\partial}{\partial t} \int_{-h}^{\eta'} \left(\int_z^{\eta'} w dz' \right) dz - \rho \frac{\partial \eta}{\partial t} \int_{\eta'}^{\eta'} w dz' + \rho \frac{\partial h}{\partial t} \int_{-h}^{\eta'} w dz' \quad (4.187)$$

$$\rho \int_{-h}^{\eta'} \left(\frac{\partial}{\partial t} \int_z^{\eta'} w dz' \right) dz = \rho \frac{\partial}{\partial t} \int_{-h}^{\eta'} \left(\int_z^{\eta'} w dz' \right) dz - \rho \frac{\partial \eta}{\partial t} (0) + \rho (0) \int_{-h}^{\eta'} w dz' \quad (4.188)$$

$$\rho \int_{-h}^{\eta'} \left(\frac{\partial}{\partial t} \int_z^{\eta'} w dz' \right) dz = \rho \frac{\partial}{\partial t} \int_{-h}^{\eta'} \left(\int_z^{\eta'} w dz' \right) dz \quad (4.189)$$

Hence acknowledging the result of Equation (4.146):

$$\rho \int_{-h}^{\eta'} \left(\frac{\partial}{\partial t} \int_z^{\eta'} w dz' \right) dz = \rho \frac{\partial}{\partial t} \int_{-h}^{\eta'} \left(\int_z^{\eta'} w dz' \right) dz = 0 \quad (4.190)$$

Using Equation (4.2) the time averaged vertical velocity is:

$$W = \frac{1}{\bar{\eta} + h} \int_{-h}^{\bar{\eta}''} w dz = \frac{1}{\bar{\eta} + h} \left(\int_{-h}^{\bar{\eta}} \bar{w} dz + \int_{\bar{\eta}}^{\bar{\eta}''} w dz \right) \quad (4.191)$$

The third and fourth terms on the right hand side of Equation (4.178) are examined with a view to splitting them into their wave and turbulent components.

$$\rho \int_{-h}^{\bar{\eta}''} \left(\frac{\partial}{\partial x_i} \int_z^{\bar{\eta}''} u_i w dz \right) dz = \rho \int_{-h}^{\bar{\eta}} \left(\frac{\partial}{\partial x_i} \int_z^{\bar{\eta}} \overline{[(U_i + u_i' + u_i'')(W + w' + w'')]} dz \right) dz \text{ for } i = 1, 2 \quad (4.192)$$

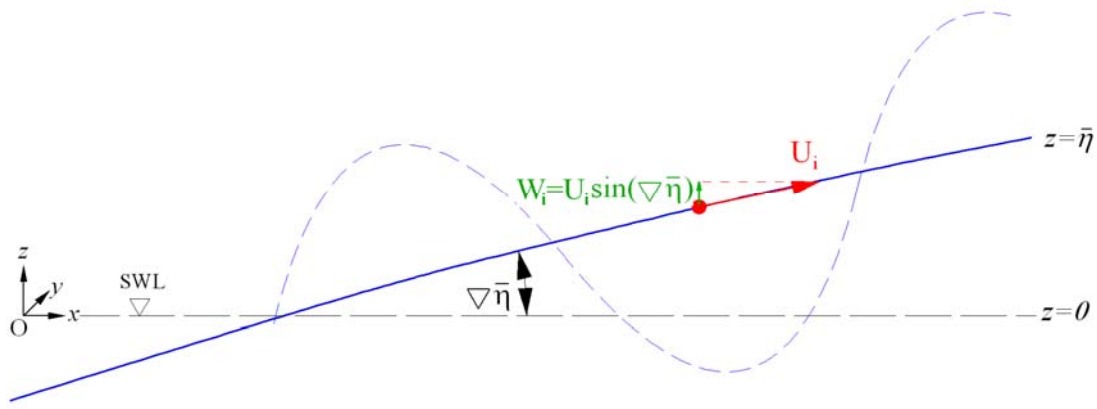


Figure 4.8 – Vertical Component of Total Steady Particle Velocity

The total steady particle velocity at the surface may be split into the horizontal and vertical component. The vertical component is equal to the overall velocity multiplied by the sine of the slope of the mean position of the water surface. The slope of the water surface is considered to be very small and hence its sine will also be small. This means the vertical steady particle velocity at the surface is small. The vertical steady particle velocity within the fluid column is considered to be at a maximum at the surface so therefore the vertical component of steady velocity and its products are small everywhere and can be ignored. This gives the following expression of Equation (4.192):

$$\rho \int_{-h}^{\bar{\eta}''} \left(\frac{\partial}{\partial x_i} \int_z^{\bar{\eta}''} u_i w dz \right) dz = \rho \int_{-h}^{\bar{\eta}} \left(\frac{\partial}{\partial x_i} \int_z^{\bar{\eta}} \overline{[(U_i + u_i' + u_i'')(w' + w'')]} dz \right) dz \text{ for } i = 1, 2 \quad (4.193)$$

Equation (4.193) can be expressed more explicitly as:

$$\rho \int_{-h}^{\eta''} \left(\frac{\partial}{\partial x_i} \int_z^{\eta''} u_i w dz \right) dz = \rho \int_{-h}^{\bar{\eta}} \left(\frac{\partial}{\partial x_i} \int_z^{\bar{\eta}} \left[\overline{U_i w' + u_i' w' + u_i'' w'} + \overline{U_i w'' + u_i' w'' + u_i'' w''} \right] dz \right) dz \quad \text{for } i = 1, 2 \quad (4.194)$$

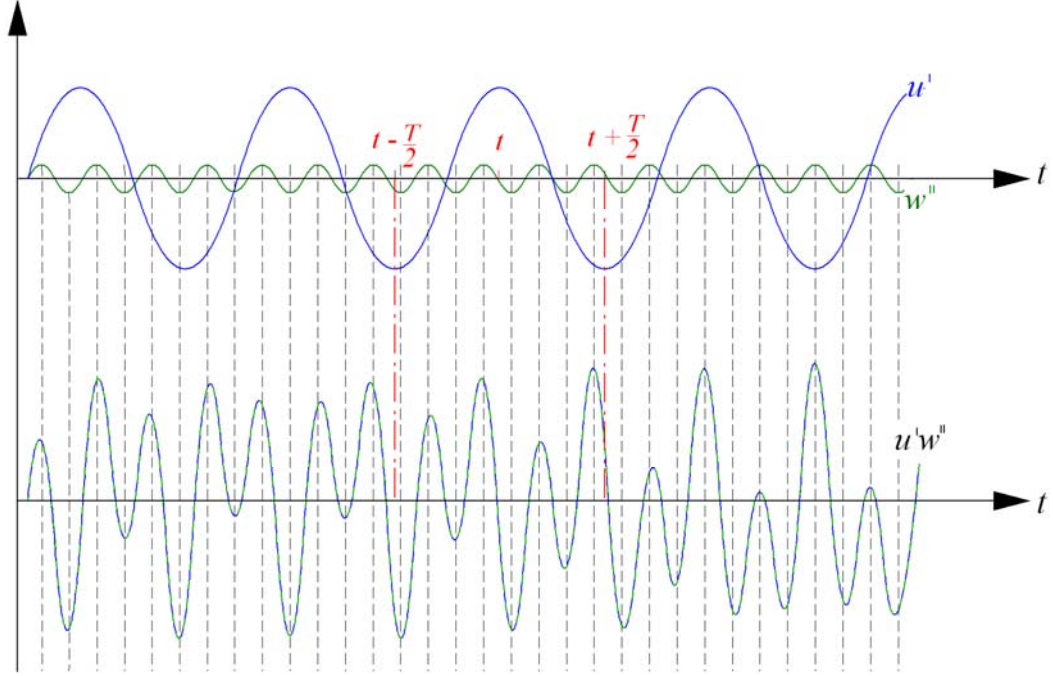


Figure 4.9 – The product of velocity functions with different time scales over time

Figure 4.9, shows that the product of velocity functions with different time scales produce a function that integrates to zero over time. Hence Equation (4.194) becomes:

$$\rho \int_{-h}^{\eta''} \left(\frac{\partial}{\partial x_i} \int_z^{\eta''} u_i w dz \right) dz \cong \rho \int_{-h}^{\bar{\eta}} \left(\frac{\partial}{\partial x_i} \int_z^{\bar{\eta}} \left[\overline{u_i' w'} + \overline{u_i'' w''} \right] dz \right) dz \quad \text{for } i = 1, 2 \quad (4.195)$$

and:

$$\rho \int_{-h}^{\eta''} w^2 dz \cong \rho \int_{-h}^{\bar{\eta}} \left[\overline{w'^2} + \overline{w''^2} \right] dz \quad (4.196)$$

Substituting Equations (4.186), (4.190), (4.195) and (4.196) into Equation (4.178) gives:

$$\int_{-h}^{\eta''} p dz = \frac{\rho g}{2} \left[(\bar{\eta} + h)^2 + \overline{\eta'^2} + \overline{\eta''^2} \right] + \rho \int_{-h}^{\bar{\eta}} \left(\frac{\partial}{\partial x_i} \int_z^{\bar{\eta}} \left[\overline{u_i' w'} + \overline{u_i'' w''} \right] dz \right) dz - \rho \int_{-h}^{\bar{\eta}} \left[\overline{w'^2} + \overline{w''^2} \right] dz \quad (4.197)$$

for $i = 1, 2$

Substituting Equations (4.174) and (4.197) into (4.106) yields:

$$R_{ij} = \delta_{ij} \left[\begin{aligned} & \frac{\rho g}{2} \left[(\bar{\eta} + h)^2 + \bar{\zeta}'^2 + \bar{\zeta}''^2 \right] \\ & + \rho \int_{-h}^{\bar{\eta}} \left(\frac{\partial}{\partial x_i} \int_z^{\bar{\eta}} \left[\overline{u'_i w'} + \overline{u''_i w''} \right] dz \right) dz \\ & - \rho \int_{-h}^{\bar{\eta}} \left[\overline{w'^2} + \overline{w''^2} \right] dz \end{aligned} \right] - \delta_{ij} \left[\frac{\rho g}{2} (\bar{\eta} + h)^2 \right] + \rho \int_{-h}^{\bar{\eta}} \overline{u'_i u'_j} dz + \rho \int_{-h}^{\bar{\eta}} \overline{u''_i u''_j} dz$$

for $i, j = 1, 2$ (4.198)

Expressing wave and turbulent portions of Equation (4.198) separately yields:

$$R_{ij} = \delta_{ij} \left[\frac{\rho g \bar{\zeta}'^2}{2} + \rho \int_{-h}^{\bar{\eta}} \left(\frac{\partial}{\partial x_l} \int_z^{\bar{\eta}} \overline{u'_l w'} dz \right) dz - \rho \int_{-h}^{\bar{\eta}} \overline{w'^2} dz \right] + \rho \int_{-h}^{\bar{\eta}} \overline{u'_i u'_j} dz$$

for $i, j, l = 1, 2$ (4.199)

$$+ \delta_{ij} \left[\frac{\rho g \bar{\zeta}''^2}{2} + \rho \int_{-h}^{\bar{\eta}} \left(\frac{\partial}{\partial x_l} \int_z^{\bar{\eta}} \overline{u''_l w''} dz \right) dz - \rho \int_{-h}^{\bar{\eta}} \overline{w''^2} dz \right] + \rho \int_{-h}^{\bar{\eta}} \overline{u''_i u''_j} dz$$

$$R'_{ij} + R''_{ij} = \delta_{ij} \left[\frac{\rho g \bar{\zeta}'^2}{2} + \rho \int_{-h}^{\bar{\eta}} \left(\frac{\partial}{\partial x_l} \int_z^{\bar{\eta}} \overline{u'_l w'} dz \right) dz - \rho \int_{-h}^{\bar{\eta}} \overline{w'^2} dz \right] + \rho \int_{-h}^{\bar{\eta}} \overline{u'_i u'_j} dz$$

for $i, j, l = 1, 2$

$$+ \delta_{ij} \left[\frac{\rho g \bar{\zeta}''^2}{2} + \rho \int_{-h}^{\bar{\eta}} \left(\frac{\partial}{\partial x_l} \int_z^{\bar{\eta}} \overline{u''_l w''} dz \right) dz - \rho \int_{-h}^{\bar{\eta}} \overline{w''^2} dz \right] + \rho \int_{-h}^{\bar{\eta}} \overline{u''_i u''_j} dz$$

(4.200)

Where:

$$R'_{ij} = \rho \delta_{ij} \left[\frac{g \bar{\zeta}'^2}{2} + \rho \int_{-h}^{\bar{\eta}} \left(\frac{\partial}{\partial x_l} \int_z^{\bar{\eta}} \overline{u'_l w'} dz \right) dz - \int_{-h}^{\bar{\eta}} \overline{w'^2} dz \right] + \rho \int_{-h}^{\bar{\eta}} \overline{u'_i u'_j} dz \text{ for } i, j, l = 1, 2 \quad (4.201)$$

$$R''_{ij} = \delta_{ij} \rho \left[\frac{g \bar{\zeta}''^2}{2} + \rho \int_{-h}^{\bar{\eta}} \left(\frac{\partial}{\partial x_l} \int_z^{\bar{\eta}} \overline{u''_l w''} dz \right) dz - \int_{-h}^{\bar{\eta}} \overline{w''^2} dz \right] + \rho \int_{-h}^{\bar{\eta}} \overline{u''_i u''_j} dz \text{ for } i, j, l = 1, 2 \quad (4.202)$$

R'_{ij} and R''_{ij} are the excess momentum flux tensors due to wave and turbulent components respectively. Longuet-Higgins and Steward (1962, 1964) call R'_{ij} the Radiation Stress.

4.4 Summary of Approximate Equations of Motion

The approximate version of the equation for conservation of mass that is used in the finite element hydrodynamic model may be obtained from Equation (4.37):

$$\frac{\partial \bar{\eta}}{\partial t} = \frac{\partial}{\partial x_i} \left[U_i (\bar{\eta} + h) \right] \text{ for } i = 1, 2 \quad (4.203)$$

The approximate equations of conservation of momentum that are used in the finite element hydrodynamic wave-driven model can be obtained from Equations (4.160) and (4.200):

$$\frac{\partial U_j}{\partial t} = -U_i \frac{\partial U_j}{\partial x_i} - g \frac{\partial \bar{\eta}}{\partial x_j} - \frac{1}{\rho(\bar{\eta} + h)} \frac{\partial (R'_{ij} + R''_{ij})}{\partial x_i} + \frac{\bar{\tau}_j^B}{\rho(\bar{\eta} + h)} \text{ for } i, j = 1, 2 \quad (4.204)$$

4.5 Radiation Stress expressed in terms of Velocity Potential

At this stage it is useful to examine the equation for Radiation Stress with a view to expressing it exclusively in terms of velocity potential. This allows it to be used directly with the results of the NM-WCIM described in Chapter 3.

4.5.1 Expression of wave orbital velocity in terms of velocity potential

Expressing Equation (3.40) using Equation (3.109) gives:

$$u'_i = \text{Re} \left(e^{-i\omega t} \frac{\partial \tilde{\phi}}{\partial x_i} \right) \text{ for subscript } i = 1, 2, 3 \quad (4.205)$$

Substituting the results of Equations (3.130) and (3.197) into Equation (4.205) gives:

$$u'_i = \text{Re} \left[e^{-i\omega t} \frac{\partial}{\partial x_i} \left(\phi \frac{\cosh[\kappa(h' + z')]}{\cosh[\kappa h']} \right) \right] \text{ for subscript } i = 1, 2, 3 \quad (4.206)$$

Examining horizontal velocities only limits the variable subscript i to 1 and 2. An examination of Equation (3.216) shows that if κ and h' are considered to vary slowly in the horizontal direction the gradients of the vertical function may be discounted. This is considered an appropriate assumption in the case of this derivation. Therefore for horizontal coordinates Equation (4.206) becomes:

$$u'_i = \text{Re} \left[e^{-i\omega t} \frac{\cosh[\kappa(h' + z')]}{\cosh[\kappa h']} \frac{\partial \phi}{\partial x_i} \right] \text{ for subscript } i = 1, 2 \quad (4.207)$$

Splitting ϕ into its real and imaginary components, $\phi = \phi_1 + i\phi_2$, yields:

$$u'_i = \text{Re} \left(e^{-i\omega t} \frac{\cosh[\kappa(h' + z')]}{\cosh[\kappa h']} \left[\frac{\partial \phi_1}{\partial x_i} + i \frac{\partial \phi_2}{\partial x_i} \right] \right) \text{ for subscript } i = 1, 2 \quad (4.208)$$

This may be expressed more explicitly as:

$$u'_i = \frac{\cosh[\kappa(h' + z')]}{\cosh[\kappa h']} \text{Re} \left((\cos \omega t - i \sin \omega t) \left[\frac{\partial \phi_1}{\partial x_i} + i \frac{\partial \phi_2}{\partial x_i} \right] \right) \text{ for } i = 1, 2 \quad (4.209)$$

Equation (4.209) may be simplified as:

$$u'_i = \frac{\cosh[\kappa(h' + z')]}{\cosh[\kappa h']} \left[\cos \omega t \frac{\partial \phi_1}{\partial x_i} + \sin \omega t \frac{\partial \phi_2}{\partial x_i} \right] \text{ for } i = 1, 2 \quad (4.210)$$

Using Equation (3.184) and (3.195) the following can be stated:

$$h' + z' = h + z \quad (4.211)$$

Using Equation (4.211) and examining vertical velocity alone leads to the following result of Equation (4.206):

$$w' = \text{Re} \left[e^{-i\omega t} \frac{1}{\cosh[\kappa h']} \frac{\partial}{\partial x_i} \left(\phi \cosh[\kappa(h+z)] \right) \right] \text{ for } i = 1, 2 \quad (4.212)$$

This may be simplified as:

$$w' = \text{Re} \left[e^{-i\omega t} \frac{\kappa \sinh[\kappa(h+z)]}{\cosh[\kappa h']} \phi \right] \text{ for } i = 1, 2 \quad (4.213)$$

Using Equation (4.211) again yields:

$$w' = \text{Re} \left[e^{-i\omega t} \frac{\kappa \sinh[\kappa(h'+z')]}{\cosh[\kappa h']} \phi \right] \text{ for } i = 1, 2 \quad (4.214)$$

Splitting ϕ into its real and imaginary components, $\phi = \phi_1 + i\phi_2$, yields:

$$w' = \text{Re} \left(e^{-i\omega t} \frac{\kappa \sinh[\kappa(h'+z')]}{\cosh[\kappa h']} (\phi_1 + i\phi_2) \right) \quad (4.215)$$

Expanding the exponential term yields:

$$w' = \frac{\kappa \sinh[\kappa(h'+z')]}{\cosh[\kappa h']} \text{Re}((\cos \omega t - i \sin \omega t)(\phi_1 + i\phi_2)) \quad (4.216)$$

Equation (4.216) may be simplified as:

$$w' = \frac{\kappa \sinh[\kappa(h'+z')]}{\cosh[\kappa h']} (\phi_1 \cos \omega t + \phi_2 \sin \omega t) \quad (4.217)$$

4.5.2 First term of Equation (4.201) in terms of velocity potential

Initially an expression will be derived for the time averaged integral of ζ' .

Examining the free-surface gives:

$$\zeta' = \text{Re}(\tilde{\zeta}) \quad (4.218)$$

This may be expanded as follows:

$$\zeta' = \text{Re}(\xi e^{-i\omega t}) \quad (4.219)$$

Expanding the exponential term in Equation (4.219) gives:

$$\zeta' = \text{Re}[(\xi_1 + i\xi_2)(\cos \omega t - i \sin \omega t)] \quad (4.220)$$

Examining only the real terms of Equation (4.220) yields:

$$\zeta' = \xi_1 \cos \omega t + \xi_2 \sin \omega t \quad (4.221)$$

Squaring Equation (3.59) gives:

$$\zeta'^2 = \xi_1^2 \cos^2 \omega t + \xi_2^2 \sin^2 \omega t + 2\xi_1 \xi_2 \cos \omega t \sin \omega t \quad (4.222)$$

Obtaining a time averaged integral of Equation (4.222) gives the following:

$$\frac{\int_0^T \zeta'^2 dt}{T} = \overline{\zeta'^2} = \frac{\xi_1^2 \int_0^T \cos^2 \omega t dt + \xi_2^2 \int_0^T \sin^2 \omega t dt + 2\xi_1 \xi_2 \int_0^T \cos \omega t \sin \omega t dt}{T} \quad (4.223)$$

but:

$$2\xi_1 \xi_2 \int_0^T \cos \omega t \sin \omega t dt = 0 \quad (4.224)$$

so:

$$\overline{\zeta'^2} = \frac{\xi_1^2 \int_0^T \cos^2 \omega t dt + \xi_2^2 \int_0^T \sin^2 \omega t dt}{T} \quad (4.225)$$

$$T = \frac{2\pi}{\omega} \quad (4.226)$$

Examining the first integral in Equation (4.225):

An appropriate substitution is firstly selected:

$$u = \omega t \quad (4.227)$$

Therefore:

$$du = \omega dt \quad (4.228)$$

$$\frac{1}{\omega} du = dt \quad (4.229)$$

With the substitution of Equation (4.227) the upper limit $\frac{2\pi}{\omega}$ changes to 2π and the lower limit remains 0 giving the following for the first integral in Equation (4.225):

$$\int_0^T \cos^2 \omega t dt = \frac{1}{\omega} \int_0^{2\pi} \cos^2 u du \quad (4.230)$$

The following mathematical identity can now be used:

$$\int \cos^2 u du = \frac{1}{2} \left(u + \frac{1}{2} \sin u \right) \quad (4.231)$$

Using Equation (4.231) with Equation (4.230) gives:

$$\int_0^T \cos^2 \omega t dt = \frac{1}{\omega} \left[\frac{1}{2} \left(u + \frac{1}{2} \sin u \right) \right]_0^{2\pi} \quad (4.232)$$

After evaluation of the upper and lower limits Equation (4.232) becomes:

$$\int_0^T \cos^2 \omega t dt = \frac{1}{\omega} \left[\frac{1}{2} \left(2\pi + \frac{1}{2} \sin 2\pi \right) \right] \quad (4.233)$$

$$\int_0^T \cos^2 \omega t dt = \frac{\pi}{\omega} \quad (4.234)$$

Examining the second integral in Equation (4.225):

An appropriate substitution is firstly selected:

$$u = \omega t \quad (4.235)$$

Therefore:

$$du = \omega dt \quad (4.236)$$

$$\frac{1}{\omega} du = dt \quad (4.237)$$

With the substitution of Equation (4.235) the upper limit $\frac{2\pi}{\omega}$ changes to 2π and the lower limit remains 0 giving the following for the first integral in Equation (4.225):

$$\int_0^T \sin^2 \omega t dt = \frac{1}{\omega} \int_0^{2\pi} \sin^2 u du \quad (4.238)$$

The following mathematical identity can now be used:

$$\int \sin^2 u du = \frac{1}{2} \left(u - \frac{1}{2} \sin u \right) \quad (4.239)$$

Using Equation (4.239) with Equation (4.238) gives:

$$\int_0^T \sin^2 \omega t dt = \frac{1}{\omega} \left[\frac{1}{2} \left(u - \frac{1}{2} \sin u \right) \right]_0^{2\pi} \quad (4.240)$$

After evaluation of the upper and lower limits Equation (4.240) becomes:

$$\int_0^T \sin^2 \omega t dt = \frac{1}{\omega} \left[\frac{1}{2} \left(2\pi - \frac{1}{2} \sin 2\pi \right) \right] \quad (4.241)$$

$$\int_0^T \sin^2 \omega t dt = \frac{\pi}{\omega} \quad (4.242)$$

Using Equations (4.226), (4.234) and (4.242) in Equation (4.225) gives:

$$\overline{\zeta'^2} = \frac{\frac{\xi_1^2 \pi}{\omega} + \frac{\xi_2^2 \pi}{\omega}}{\frac{2\pi}{\omega}} \quad (4.243)$$

Simplification of Equation (4.243) gives:

$$\overline{\zeta'^2} = \frac{\xi_1^2}{2} + \frac{\xi_2^2}{2} \quad (4.244)$$

4.5.3 Second term of Equation (4.201) in terms of velocity potential

The product of Equations (4.210) and (4.217) is:

$$u_l' w' = \frac{\kappa \cosh[\kappa(h' + z')]}{\cosh^2(\kappa h')} \left[\frac{\partial \phi_1}{\partial x_l} \cos \omega t + \frac{\partial \phi_2}{\partial x_l} \sin \omega t \right] (\phi_1 \cos \omega t + \phi_2 \sin \omega t)$$

for $l = 1, 2$ (4.245)

Integrating Equation (4.245) over time and expressing it more explicitly gives:

$$\int_0^T u_l' w' dt = \frac{\kappa \sinh(2\kappa(h' + z'))}{\cosh^2(\kappa h')} \int_0^T \left[\phi_1 \frac{\partial \phi_1}{\partial x_l} \cos^2 \omega t + \phi_2 \frac{\partial \phi_2}{\partial x_l} \sin^2 \omega t + \frac{\partial \phi_1}{\partial x_l} \phi_2 \cos \omega t \sin \omega t + \frac{\partial \phi_2}{\partial x_l} \phi_1 \sin \omega t \cos \omega t \right] dt$$

for $l = 1, 2$ (4.246)

It can be seen that the following is true:

$$\int_0^T \frac{\partial \phi_1}{\partial x_l} \phi_2 \cos \omega t \sin \omega t dt = 0 \text{ for } l = 1, 2 \quad (4.247)$$

$$\int_0^T \frac{\partial \phi_2}{\partial x_l} \phi_1 \sin \omega t \cos \omega t dt = 0 \text{ for } l = 1, 2 \quad (4.248)$$

Hence Equation (4.246) can be simplified using the results of Equations (4.247) and (4.248):

$$\int_0^T u_l' w' dt = \frac{\kappa \sinh(2\kappa(h' + z'))}{\cosh^2(\kappa h')} \int_0^T \left[\phi_1 \frac{\partial \phi_1}{\partial x_l} \cos^2 \omega t + \phi_2 \frac{\partial \phi_2}{\partial x_l} \sin^2 \omega t \right] dt \text{ for } l = 1, 2 \quad (4.249)$$

Using the result of Equation (4.234) gives:

$$\int_0^T \phi_1 \frac{\partial \phi_1}{\partial x_l} \cos^2 \omega t dt = \frac{\partial \phi_1}{\partial x_l} \phi_1 \frac{\pi}{\omega} \text{ for } l = 1, 2 \quad (4.250)$$

Similarly using the result of Equation (4.242) gives:

$$\int_0^T \phi_2 \frac{\partial \phi_2}{\partial x_l} \sin^2 \omega t dt = \frac{\partial \phi_2}{\partial x_l} \phi_2 \frac{\pi}{\omega} \text{ for } l = 1, 2 \quad (4.251)$$

Using Equations (4.250) and (4.251) with Equation (4.249) gives the following:

$$\int_0^T u'_l w' = \frac{\kappa \sinh(2\kappa(h' + z'))}{\cosh^2(\kappa h')} \left(\frac{\partial \phi_1}{\partial x_l} \phi_1 \frac{\pi}{\omega} + \frac{\partial \phi_2}{\partial x_l} \phi_2 \frac{\pi}{\omega} \right) \text{ for } l = 1, 2 \quad (4.252)$$

Division of Equation (4.252) by the wave period gives:

$$\overline{u'_l w'} = \frac{1}{T} \left[\frac{\kappa \sinh(2\kappa(h' + z'))}{\cosh^2(\kappa h')} \left(\frac{\partial \phi_1}{\partial x_l} \phi_1 \frac{\pi}{\omega} + \frac{\partial \phi_2}{\partial x_l} \phi_2 \frac{\pi}{\omega} \right) \right] \text{ for } l = 1, 2 \quad (4.253)$$

Equation (4.253) may be simplified as follows:

$$\overline{u'_l w'} = \frac{\omega}{2\pi} \left[\frac{\pi \kappa \sinh(2\kappa(h' + z'))}{\cosh^2(\kappa h')} \left(\frac{\partial \phi_1}{\partial x_l} \phi_1 + \frac{\partial \phi_2}{\partial x_l} \phi_2 \right) \right] \text{ for } l = 1, 2 \quad (4.254)$$

$$\overline{u'_l w'} = \frac{\kappa \sinh(2\kappa(h' + z'))}{2 \cosh^2(\kappa h')} \left(\frac{\partial \phi_1}{\partial x_l} \phi_1 + \frac{\partial \phi_2}{\partial x_l} \phi_2 \right) \text{ for } l = 1, 2 \quad (4.255)$$

Integration of Equation (4.255) over the depth yields:

$$\int_z^{\bar{\eta}} \overline{u'_l w'} dz = \frac{\kappa}{2 \cosh^2(\kappa h')} \left(\frac{\partial \phi_1}{\partial x_l} \phi_1 + \frac{\partial \phi_2}{\partial x_l} \phi_2 \right) \int_z^{\bar{\eta}} \sinh(2\kappa(h' + z')) dz \text{ for } l = 1, 2 \quad (4.256)$$

An examination of the integration on the right hand side of Equation (4.256) can be carried out.

Using Equation (4.211) an appropriate substitution is selected:

$$u = \sinh(2\kappa(h + z)) \quad (4.257)$$

Therefore:

$$\frac{du}{dz} = 2\kappa \quad (4.258)$$

$$\frac{1}{2\kappa} du = dz \quad (4.259)$$

With the substitution of Equation (4.257) the upper limit $\bar{\eta}$ changes to $2\kappa h'$ and the lower limit z changes $2\kappa(z + h)$ to giving the following for the integral under examination:

$$\int_z^{\bar{\eta}} \sinh(2\kappa(h' + z')) dz = \frac{1}{2\kappa} \int_{2\kappa(z+h)}^{2\kappa h'} \sinh u du \quad (4.260)$$

Evaluation of the integral may now be carried out as follows:

$$\int_z^{\bar{\eta}} \sinh(2\kappa(h' + z')) dz = \frac{1}{2\kappa} [\cosh u]_{2\kappa(z+h)}^{2\kappa h'} \quad (4.261)$$

After calculating the limits of Equation (4.261) the following is obtained:

$$\int_z^{\bar{\eta}} \sinh(2\kappa(h' + z')) dz = \frac{1}{2\kappa} [\cosh(2\kappa h') - \cosh(2\kappa(h' + z'))] \quad (4.262)$$

Using Equation (4.211) again this becomes:

$$\int_z^{\bar{\eta}} \sinh(2\kappa(h' + z')) dz = \frac{1}{2\kappa} [\cosh(2\kappa h') - \cosh(2\kappa(h' + z'))] \quad (4.263)$$

Combining Equations (4.263) and (4.256) gives

$$\int_z^{\bar{\eta}} u'_l w'_l dz = \frac{\kappa}{2 \cosh^2(\kappa h')} \left(\frac{\partial \phi_1}{\partial x_l} \phi_1 + \frac{\partial \phi_2}{\partial x_l} \phi_2 \right) \left[\frac{1}{2\kappa} [\cosh(2\kappa h') - \cosh(2\kappa(h' + z'))] \right] \quad (4.264)$$

for $l = 1, 2$

Obtaining the horizontal derivative of Equation (4.264) in the x direction yields:

$$\frac{\partial}{\partial x} \int_z^{\bar{\eta}} u'_l w'_l dz = \frac{[\cosh(2\kappa h') - \cosh(2\kappa(h' + z'))]}{4 \cosh^2(\kappa h')} \frac{\partial}{\partial x} \left(\frac{\partial \phi_1}{\partial x_l} \phi_1 + \frac{\partial \phi_2}{\partial x_l} \phi_2 \right) \text{ for } l = 1, 2 \quad (4.265)$$

Expressing Equation (4.265) more explicitly yields:

$$\frac{\partial}{\partial x} \int_z^{\bar{\eta}} u'_l w'_l dz = \frac{[\cosh(2\kappa h') - \cosh(2\kappa(h' + z'))]}{4 \cosh^2(\kappa h')} \left(\phi_1 \frac{\partial^2 \phi_1}{\partial x_l \partial x_l} + \left(\frac{\partial \phi_1}{\partial x_l} \right)^2 + \phi_2 \frac{\partial^2 \phi_2}{\partial x_l \partial x_l} + \left(\frac{\partial \phi_2}{\partial x_l} \right)^2 \right) \quad (4.266)$$

for $l = 1, 2$

Integrating Equation (4.266) over the depth gives:

$$\int_{-h}^{\bar{\eta}} \frac{\partial}{\partial x} \int_z^{\bar{\eta}} u'_l w'_l dz dz = \frac{1}{4 \cosh^2(\kappa h')} \left(\phi_1 \frac{\partial^2 \phi_1}{\partial x_l \partial x_l} + \left(\frac{\partial \phi_1}{\partial x_l} \right)^2 + \phi_2 \frac{\partial^2 \phi_2}{\partial x_l \partial x_l} + \left(\frac{\partial \phi_2}{\partial x_l} \right)^2 \right) \int_{-h}^{\bar{\eta}} [\cosh(2\kappa h') - \cosh(2\kappa(h' + z'))] dz \quad (4.267)$$

for $l = 1, 2$

Examining the integral on the right hand side of Equation (4.267) and using Equation (4.211) gives:

$$\int_{-h}^{\bar{\eta}} \left[\cosh(2\kappa h') - \cosh(2\kappa(h' + z')) \right] dz = \int_{-h}^{\bar{\eta}} \cosh(2\kappa h') dz - \int_{-h}^{\bar{\eta}} \cosh(2\kappa(h + z)) dz \quad (4.268)$$

Equation (4.268) can be expressed as:

$$\int_{-h}^{\bar{\eta}} \left[\cosh(2\kappa h') - \cosh(2\kappa(h' + z')) \right] dz = [\bar{\eta} + h] \cosh(2\kappa h') - \int_{-h}^{\bar{\eta}} \cosh(2\kappa(h + z)) dz \quad (4.269)$$

$$\int_{-h}^{\bar{\eta}} \left[\cosh(2\kappa h') - \cosh(2\kappa(h' + z')) \right] dz = h' \cosh(2\kappa h') - \int_{-h}^{\bar{\eta}} \cosh(2\kappa(h + z)) dz \quad (4.270)$$

An examination of the remaining integration on the right hand side of Equation (4.270) can be carried out.

An appropriate substitution is selected:

$$u = 2\kappa(z + h) \quad (4.271)$$

Therefore:

$$\frac{du}{dz} = 2\kappa \quad (4.272)$$

$$\frac{1}{2\kappa} du = dz \quad (4.273)$$

With the substitution of Equation (4.271) the upper limit $\bar{\eta}$ changes to $2\kappa h'$ and the lower limit $-h$ changes 0 to giving the following for the integral under examination:

$$\int_{-h}^{\bar{\eta}} \cosh(2\kappa(h + z)) dz = \frac{1}{2\kappa} \int_0^{2\kappa h'} \cosh u du \quad (4.274)$$

Evaluation of the integral may now be carried out as follows:

$$\int_{-h}^{\bar{\eta}} \cosh(2\kappa(h + z)) dz = \frac{1}{2\kappa} \int_0^{2\kappa h'} [\sinh u] \quad (4.275)$$

After calculating the limits of Equation (4.275) the following is obtained:

$$\int_{-h}^{\bar{\eta}} \cosh(2\kappa(h+z)) dz = \frac{\sinh(2\kappa h')}{2\kappa} \quad (4.276)$$

Combining Equations (4.270) and (4.276) gives

$$\int_{-h}^{\bar{\eta}} \left[\cosh(2\kappa h') - \cosh(2\kappa(h' + z')) \right] dz = h' \cosh(2\kappa h') - \frac{\sinh(2\kappa h')}{2\kappa} \quad (4.277)$$

Now combining Equation (4.277) with (4.267) gives:

$$\int_{-h}^{\bar{\eta}} \frac{\partial}{\partial x} \int_z^{\bar{\eta}} u'_l w' dz dz = \frac{1}{4 \cosh^2(\kappa h')} \left(\phi_l \frac{\partial^2 \phi_l}{\partial x_l \partial x_l} + \left(\frac{\partial \phi_l}{\partial x_l} \right)^2 \right) \left[h' \cosh(2\kappa h') - \frac{\sinh(2\kappa h')}{2\kappa} \right] \quad (4.278)$$

for $l = 1, 2$

4.5.4 Third term of Equation (4.201) in terms of velocity potential

Squaring Equation (4.217) gives

$$w'^2 = \frac{\kappa^2 \sinh^2(\kappa(h' + z'))}{\cosh^2(\kappa h')} (\phi_1^2 \cos^2 \omega t + \phi_2^2 \sin^2 \omega t + 2\phi_1 \phi_2 \sin \omega t \cos \omega t) \quad (4.279)$$

Integrating Equation (4.279) over a wave period with respect to time gives:

$$\int_0^T w'^2 dt = \frac{\kappa^2 \sinh^2(\kappa(h' + z'))}{\cosh^2(\kappa h')} \int_0^T (\phi_1^2 \cos^2 \omega t + \phi_2^2 \sin^2 \omega t + 2\phi_1 \phi_2 \sin \omega t \cos \omega t) dt \quad (4.280)$$

An examination of the integration on the right hand side of Equation (4.280) can be carried out.

$$\begin{aligned} \int_0^T (\phi_1^2 \cos^2 \omega t + \phi_2^2 \sin^2 \omega t + 2\phi_1 \phi_2 \sin \omega t \cos \omega t) dt = \\ \frac{2\pi}{\omega} \int_0^{\frac{\omega}{2}} \phi_1^2 \cos^2 \omega t dt + \int_0^{\frac{\omega}{2}} \phi_2^2 \sin^2 \omega t dt + 2 \int_0^{\frac{\omega}{2}} \phi_1 \phi_2 \sin \omega t \cos \omega t dt \end{aligned} \quad (4.281)$$

An appropriate substitution is selected:

$$u = \omega t \quad (4.282)$$

Therefore:

$$du = \omega dt \quad (4.283)$$

$$\frac{1}{\omega} du = dt \quad (4.284)$$

With the substitution of Equation (4.282) the upper limit $\frac{2\pi}{\omega}$ changes to 2π and the

lower limit remains zero to giving the following for the integral under examination:

$$\begin{aligned} \int_0^T (\phi_1^2 \cos^2 \omega t + \phi_2^2 \sin^2 \omega t + 2\phi_1 \phi_2 \sin \omega t \cos \omega t) dt = \\ \frac{\phi_1^2}{\omega} \int_0^{2\pi} \cos^2 u du + \frac{\phi_2^2}{\omega} \int_0^{2\pi} \sin^2 u du + 2\phi_1 \phi_2 \int_0^{2\pi} \sin u \cos u du \end{aligned} \quad (4.285)$$

Evaluation of the integral may now be carried out as follows:

$$\int_0^T \left(\phi_1^2 \cos^2 \omega t + \phi_2^2 \sin^2 \omega t + 2\phi_1 \phi_2 \sin \omega t \cos \omega t \right) dt =$$

$$\frac{\phi_1^2}{2\omega} \left[u + \frac{1}{2} \sin 2u \right]_0^{2\pi} + \frac{\phi_2^2}{2\omega} \left[u - \frac{1}{2} \sin 2u \right]_0^{2\pi} - \frac{\phi_1 \phi_2}{\omega} [\cos 2u]_0^{2\pi} \quad (4.286)$$

After calculating the limits of Equation (4.286) the following is obtained:

$$\int_0^T \left(\phi_1^2 \cos^2 \omega t + \phi_2^2 \sin^2 \omega t + 2\phi_1 \phi_2 \sin \omega t \cos \omega t \right) dt =$$

$$\frac{\phi_1^2}{2\omega} \left[2\pi + \frac{1}{2} \sin 4\pi \right] + \frac{\phi_2^2}{2\omega} \left[2\pi - \frac{1}{2} \sin 4\pi \right] - \frac{\phi_1 \phi_2}{\omega} [0] \quad (4.287)$$

$$\int_0^T \left(\phi_1^2 \cos^2 \omega t + \phi_2^2 \sin^2 \omega t + 2\phi_1 \phi_2 \sin \omega t \cos \omega t \right) dt = \frac{\phi_1^2 \pi}{\omega} + \frac{\phi_2^2 \pi}{\omega} \quad (4.288)$$

Combining Equation (4.288) with Equation (4.280) gives:

$$\int_0^T w'^2 dt = \frac{\kappa^2 \sinh^2 (\kappa(h' + z'))}{\cosh^2 (\kappa h')} \left[\frac{\phi_1^2 \pi}{\omega} + \frac{\phi_2^2 \pi}{\omega} \right] \quad (4.289)$$

Division of Equation (4.289) by the wave period gives:

$$\overline{w'^2} = \frac{1}{T} \frac{\kappa^2 \sinh^2 (\kappa(h' + z'))}{\cosh^2 (\kappa h')} \left[\frac{\phi_1^2 \pi}{\omega} + \frac{\phi_2^2 \pi}{\omega} \right] \quad (4.290)$$

Expressing Equation (4.290) more explicitly yields:

$$\overline{w'^2} = \frac{\omega}{2\pi} \frac{\kappa^2 \sinh^2 (\kappa(h' + z'))}{\cosh^2 (\kappa h')} \left[\frac{\phi_1^2 \pi}{\omega} + \frac{\phi_2^2 \pi}{\omega} \right] \quad (4.291)$$

Equation (4.291) may be simplified as follows:

$$\overline{w'^2} = \frac{\kappa^2 \sinh^2 (\kappa(h' + z'))}{2 \cosh^2 (\kappa h')} [\phi_1^2 + \phi_2^2] \quad (4.292)$$

Vertical integration of Equation (4.292) gives:

$$\int_{-h}^{\bar{\eta}} \overline{w'^2} dz = \frac{\kappa^2}{2 \cosh^2 (\kappa h')} [\phi_1^2 + \phi_2^2] \int_{-h}^{\bar{\eta}} \sinh^2 (\kappa(h' + z')) dz \quad (4.293)$$

An examination of the integration on the right hand side of Equation (4.293) can be carried out.

Using Equation (4.211) an appropriate substitution is selected:

$$u = \kappa(h + z) \quad (4.294)$$

Therefore:

$$\frac{du}{dz} = \kappa \quad (4.295)$$

$$\frac{1}{\kappa} du = dz \quad (4.296)$$

With the substitution of Equation (4.294) the upper limit $\bar{\eta}$ changes to $\kappa h'$ and the lower limit $-h$ changes 0 to giving the following for the integral under examination:

$$\int_{-h}^{\bar{\eta}} \sinh^2(\kappa(h' + z')) dz = \frac{1}{\kappa} \int_0^{\kappa h'} \sinh^2 u du \quad (4.297)$$

Evaluation of the integral may now be carried out as follows:

$$\int_{-h}^{\bar{\eta}} \sinh^2(\kappa(h' + z')) dz = \frac{1}{\kappa} \left[\frac{1}{2} \left(-u + \frac{1}{2} \sinh 2u \right) \right]_0^{\kappa h'} \quad (4.298)$$

After calculating the limits of Equation (4.298) the following is obtained:

$$\int_{-h}^{\bar{\eta}} \sinh^2(\kappa(h' + z')) dz = \frac{1}{\kappa} \left[\frac{1}{2} \left(-\kappa h' + \frac{1}{2} \sinh 2\kappa h' \right) \right] \quad (4.299)$$

$$\int_{-h}^{\bar{\eta}} \sinh^2(\kappa(h' + z')) dz = -\frac{h'}{2} + \frac{\sinh 2\kappa h'}{4\kappa} \quad (4.300)$$

Combining Equation (4.293) and (4.300) gives:

$$\int_{-h}^{\bar{\eta}} \frac{1}{w'^2} dz = \frac{\kappa^2 (\phi_1^2 + \phi_2^2)}{2 \cosh^2(\kappa h')} \left[-\frac{h'}{2} + \frac{\sinh 2\kappa h'}{4\kappa} \right] \quad (4.301)$$

4.5.5 Fourth term of Equation (4.201) in terms of velocity potential

Using Equation (4.210) the following can be calculated:

$$u_i' u_j' = \frac{\cosh^2(\kappa(h' + z'))}{\cosh^2(\kappa h')} \left[\frac{\partial \phi_1}{\partial x_i} \cos \omega t + \frac{\partial \phi_2}{\partial x_i} \sin \omega t \right] \left[\frac{\partial \phi_1}{\partial x_j} \cos \omega t + \frac{\partial \phi_2}{\partial x_j} \sin \omega t \right]$$

for $i, j = 1, 2$ (4.302)

Expressing Equation (4.302) more explicitly yields:

$$u_i' u_j' = \frac{\cosh^2(\kappa(h' + z'))}{\cosh^2(\kappa h')} \left[\begin{aligned} &\frac{\partial \phi_1}{\partial x_i} \frac{\partial \phi_1}{\partial x_j} \cos^2 \omega t + \frac{\partial \phi_2}{\partial x_i} \frac{\partial \phi_2}{\partial x_j} \sin^2 \omega t \\ &+ \frac{\partial \phi_1}{\partial x_i} \frac{\partial \phi_2}{\partial x_j} \sin \omega t \cos \omega t + \frac{\partial \phi_2}{\partial x_i} \frac{\partial \phi_1}{\partial x_j} \sin \omega t \cos \omega t \end{aligned} \right]$$

for $i, j = 1, 2$ (4.303)

Integrating Equation (4.303) with over a wave period with respect to time gives:

$$\int_0^T u_i' u_j' dt = \frac{\cosh^2(\kappa(h' + z'))}{\cosh^2(\kappa h')} \int_0^T \left[\begin{aligned} &\frac{\partial \phi_1}{\partial x_i} \frac{\partial \phi_1}{\partial x_j} \cos^2 \omega t + \frac{\partial \phi_2}{\partial x_i} \frac{\partial \phi_2}{\partial x_j} \sin^2 \omega t \\ &+ \frac{\partial \phi_1}{\partial x_i} \frac{\partial \phi_2}{\partial x_j} \sin \omega t \cos \omega t + \frac{\partial \phi_2}{\partial x_i} \frac{\partial \phi_1}{\partial x_j} \sin \omega t \cos \omega t \end{aligned} \right] dt$$

for $i, j = 1, 2$ (4.304)

It is clear that:

$$\int_0^T \frac{\partial \phi_1}{\partial x_i} \frac{\partial \phi_2}{\partial x_j} \sin \omega t \cos \omega t dt = 0 \text{ for } i, j = 1, 2$$

(4.305)

$$\int_0^T \frac{\partial \phi_2}{\partial x_i} \frac{\partial \phi_1}{\partial x_j} \sin \omega t \cos \omega t dt = 0 \text{ for } i, j = 1, 2$$

(4.306)

Equation (4.304) can be rewritten with the aid of Equations (4.305) and (4.306):

$$\int_0^T u_i' u_j' dt = \frac{\cosh^2(\kappa(h' + z'))}{\cosh^2(\kappa h')} \int_0^T \left[\frac{\partial \phi_1}{\partial x_i} \frac{\partial \phi_1}{\partial x_j} \cos^2 \omega t + \frac{\partial \phi_2}{\partial x_i} \frac{\partial \phi_2}{\partial x_j} \sin^2 \omega t \right] dt \text{ for } i, j = 1, 2$$

(4.307)

An examination of the integration on the right hand side of Equation (4.307) can be carried out.

$$\int_0^T \left[\frac{\partial \phi_1}{\partial x_i} \frac{\partial \phi_1}{\partial x_j} \cos^2 \omega t + \frac{\partial \phi_2}{\partial x_i} \frac{\partial \phi_2}{\partial x_j} \sin^2 \omega t \right] dt = \frac{\partial \phi_1}{\partial x_i} \frac{\partial \phi_1}{\partial x_j} \int_0^{\frac{2\pi}{\omega}} \cos^2 \omega t dt + \frac{\partial \phi_2}{\partial x_i} \frac{\partial \phi_2}{\partial x_j} \int_0^{\frac{2\pi}{\omega}} \sin^2 \omega t dt$$

for $i, j = 1, 2$ (4.308)

An appropriate substitution is selected:

$$u = \omega t \quad (4.309)$$

Therefore:

$$du = \omega dt \quad (4.310)$$

$$\frac{1}{\omega} du = dt \quad (4.311)$$

With the substitution of Equation (4.309) the upper limit $\frac{2\pi}{\omega}$ changes to 2π and the

lower limit remains 0 to giving the following for the integral under examination:

$$\int_0^T \left[\frac{\partial \phi_1}{\partial x_i} \frac{\partial \phi_1}{\partial x_j} \cos^2 \omega t + \frac{\partial \phi_2}{\partial x_i} \frac{\partial \phi_2}{\partial x_j} \sin^2 \omega t \right] dt = \frac{\partial \phi_1}{\partial x_i} \frac{\partial \phi_1}{\partial x_j} \frac{1}{\omega} \int_0^{2\pi} \cos^2 u du + \frac{\partial \phi_2}{\partial x_i} \frac{\partial \phi_2}{\partial x_j} \frac{1}{\omega} \int_0^{2\pi} \sin^2 u du$$

for $i, j = 1, 2$ (4.312)

Evaluation of the integral may now be carried out as follows:

$$\int_0^T \left[\frac{\partial \phi_1}{\partial x_i} \frac{\partial \phi_1}{\partial x_j} \cos^2 \omega t + \frac{\partial \phi_2}{\partial x_i} \frac{\partial \phi_2}{\partial x_j} \sin^2 \omega t \right] dt =$$

$$\frac{\partial \phi_1}{\partial x_i} \frac{\partial \phi_1}{\partial x_j} \frac{1}{2\omega} \left[u + \frac{1}{2} \sin 2u \right]_0^{2\pi} + \frac{\partial \phi_2}{\partial x_i} \frac{\partial \phi_2}{\partial x_j} \frac{1}{2\omega} \left[u - \frac{1}{2} \sin 2u \right]_{2\pi}^{2\pi} \quad \text{for } i, j = 1, 2 \quad (4.313)$$

After calculating the limits of Equation (4.313) the following is obtained:

$$\int_0^T \left[\frac{\partial \phi_1}{\partial x_i} \frac{\partial \phi_1}{\partial x_j} \cos^2 \omega t + \frac{\partial \phi_2}{\partial x_i} \frac{\partial \phi_2}{\partial x_j} \sin^2 \omega t \right] dt =$$

$$\frac{\partial \phi_1}{\partial x_i} \frac{\partial \phi_1}{\partial x_j} \frac{1}{2\omega} \left[2\pi + \frac{1}{2} \sin 4\pi \right] + \frac{\partial \phi_2}{\partial x_i} \frac{\partial \phi_2}{\partial x_j} \frac{1}{2\omega} \left[2\pi - \frac{1}{2} \sin 4\pi \right] \quad \text{for } i, j = 1, 2 \quad (4.314)$$

$$\int_0^T \left[\frac{\partial \phi_1}{\partial x_i} \frac{\partial \phi_1}{\partial x_j} \cos^2 \omega t + \frac{\partial \phi_2}{\partial x_i} \frac{\partial \phi_2}{\partial x_j} \sin^2 \omega t \right] dt = \frac{\partial \phi_1}{\partial x_i} \frac{\partial \phi_1}{\partial x_j} \frac{\pi}{\omega} + \frac{\partial \phi_2}{\partial x_i} \frac{\partial \phi_2}{\partial x_j} \frac{\pi}{\omega} \quad \text{for } i, j = 1, 2 \quad (4.315)$$

Combining Equations (4.307) and (4.315) gives:

$$\int_0^T u_i' u_j' dt = \frac{\cosh^2(\kappa(h' + z'))}{\cosh^2(\kappa h')} \left[\frac{\partial \phi_1}{\partial x_i} \frac{\partial \phi_1}{\partial x_j} \frac{\pi}{\omega} + \frac{\partial \phi_2}{\partial x_i} \frac{\partial \phi_2}{\partial x_j} \frac{\pi}{\omega} \right] \text{ for } i, j = 1, 2 \quad (4.316)$$

Division of Equation (4.316) by the wave period gives:

$$\overline{u_i' u_j'} = \frac{1}{T} \frac{\cosh^2(\kappa(h' + z'))}{\cosh^2(\kappa h')} \frac{\pi}{\omega} \left[\frac{\partial \phi_1}{\partial x_i} \frac{\partial \phi_1}{\partial x_j} + \frac{\partial \phi_2}{\partial x_i} \frac{\partial \phi_2}{\partial x_j} \right] \text{ for } i, j = 1, 2 \quad (4.317)$$

Expressing Equation (4.317) more explicitly yields:

$$\overline{u_i' u_j'} = \frac{\omega}{2\pi} \frac{\cosh^2(\kappa(h' + z'))}{\cosh^2(\kappa h')} \frac{\pi}{\omega} \left[\frac{\partial \phi_1}{\partial x_i} \frac{\partial \phi_1}{\partial x_j} + \frac{\partial \phi_2}{\partial x_i} \frac{\partial \phi_2}{\partial x_j} \right] \text{ for } i, j = 1, 2 \quad (4.318)$$

Equation (4.318) may be simplified as follows:

$$\overline{u_i' u_j'} = \frac{\cosh^2(\kappa(h' + z'))}{2 \cosh^2(\kappa h')} \left[\frac{\partial \phi_1}{\partial x_i} \frac{\partial \phi_1}{\partial x_j} + \frac{\partial \phi_2}{\partial x_i} \frac{\partial \phi_2}{\partial x_j} \right] \text{ for } i, j = 1, 2 \quad (4.319)$$

Vertical integration of Equation (4.319) gives:

$$\int_{-h}^{\bar{\eta}} \overline{u_i' u_j'} dz = \frac{1}{2 \cosh^2(\kappa h')} \left[\frac{\partial \phi_1}{\partial x_i} \frac{\partial \phi_1}{\partial x_j} + \frac{\partial \phi_2}{\partial x_i} \frac{\partial \phi_2}{\partial x_j} \right] \int_{-h}^{\bar{\eta}} \cosh^2(\kappa(h' + z')) dz \text{ for } i, j = 1, 2 \quad (4.320)$$

An examination of the integration on the right hand side of Equation (4.293) can be carried out.

Using Equation (4.211) an appropriate substitution is selected:

$$u = \kappa(h + z) \quad (4.321)$$

Therefore:

$$\frac{du}{dz} = \kappa \quad (4.322)$$

$$\frac{1}{\kappa} du = dz \quad (4.323)$$

With the substitution of Equation (4.321) the upper limit $\bar{\eta}$ changes to $\kappa h'$ and the lower limit $-h$ changes 0 to giving the following for the integral under examination:

$$\int_{-h}^{\bar{\eta}} \cosh^2(\kappa(h' + z')) dz = \frac{1}{\kappa} \int_0^{\kappa h'} \cosh^2 u du \quad (4.324)$$

Evaluation of the integral may now be carried out as follows:

$$\int_{-h}^{\bar{\eta}} \cosh^2(\kappa(h' + z')) dz = \frac{1}{\kappa} \int_0^{\kappa h'} \left[\frac{1}{2} \left(u + \frac{1}{2} \sinh 2u \right) \right] \quad (4.325)$$

After calculating the limits of Equation (4.325) the following is obtained:

$$\int_{-h}^{\bar{\eta}} \cosh^2(\kappa(h' + z')) dz = \frac{1}{\kappa} \left[\frac{1}{2} \left(\kappa h' + \frac{1}{2} \sinh 2\kappa h' \right) \right] \quad (4.326)$$

$$\int_{-h}^{\bar{\eta}} \cosh^2(\kappa(h' + z')) dz = \frac{h'}{2} + \frac{\sinh(2\kappa h')}{4\kappa} \quad (4.327)$$

Combining Equations (4.320) and (4.327) gives:

$$\int_{-h}^{\bar{\eta}} \overline{u'_i u'_j} dz = \frac{\left(\frac{\partial \phi_1}{\partial x_i} \frac{\partial \phi_1}{\partial x_j} + \frac{\partial \phi_2}{\partial x_i} \frac{\partial \phi_2}{\partial x_j} \right)}{2 \cosh^2(\kappa h')} \left[\frac{h'}{2} + \frac{\sinh(2\kappa h')}{4\kappa} \right] \text{ for } i, j = 1, 2 \quad (4.328)$$

4.5.6 Complete Expression of Radiation Stress in terms of Velocity Potential

Replacing terms in Equation (4.201) with those from (4.244), (4.278), (4.301) and (4.328) gives the following:

$$\begin{aligned}
 R'_{ij} = & \rho \frac{\left(\frac{\partial \phi_1}{\partial x_i} \frac{\partial \phi_1}{\partial x_j} + \frac{\partial \phi_2}{\partial x_i} \frac{\partial \phi_2}{\partial x_j} \right)}{2 \cosh^2(\kappa h')} \left[\frac{h'}{2} + \frac{\sinh(2\kappa h')}{4\kappa} \right] \\
 & + \delta_{ij} \left[\begin{aligned} & \frac{\rho g}{2} \left(\frac{\xi_1^2}{2} + \frac{\xi_2^2}{2} \right) \\ & + \frac{\rho}{4 \cosh^2(\kappa h')} \left(\phi_1 \frac{\partial^2 \phi_1}{\partial x_i \partial x_i} + \left(\frac{\partial \phi_1}{\partial x_i} \right)^2 \right. \\ & \quad \left. + \phi_2 \frac{\partial^2 \phi_2}{\partial x_i \partial x_i} + \left(\frac{\partial \phi_2}{\partial x_i} \right)^2 \right) \left[\frac{h' \cosh(2\kappa h')}{2\kappa} \right] \\ & - \left[\frac{\rho \kappa^2 (\phi_1^2 + \phi_2^2)}{2 \cosh^2(\kappa h')} \left[-\frac{h'}{2} + \frac{\sinh 2\kappa h'}{4\kappa} \right] \right] \end{aligned} \right] \text{ for } i, j = 1, 2 \quad (4.329)
 \end{aligned}$$

Equation (4.329) may be rearranged as follows to give an equation for Radiation Stress explicitly in terms of the velocity potential:

$$\begin{aligned}
 R'_{ij} = & \rho \frac{\left(\frac{\partial \phi_1}{\partial x_i} \frac{\partial \phi_1}{\partial x_j} + \frac{\partial \phi_2}{\partial x_i} \frac{\partial \phi_2}{\partial x_j} \right)}{2 \cosh^2(\kappa h')} \left[\frac{h'}{2} + \frac{\sinh(2\kappa h')}{4\kappa} \right] \\
 & + \frac{\delta_{ij} \rho g}{2} \left(\frac{\xi_1^2}{2} + \frac{\xi_2^2}{2} \right) \\
 & + \delta_{ij} \left[\begin{aligned} & \frac{\rho}{4 \cosh^2(\kappa h')} \left(\phi_1 \frac{\partial^2 \phi_1}{\partial x_i \partial x_i} + \left(\frac{\partial \phi_1}{\partial x_i} \right)^2 \right. \\ & \quad \left. + \phi_2 \frac{\partial^2 \phi_2}{\partial x_i \partial x_i} + \left(\frac{\partial \phi_2}{\partial x_i} \right)^2 \right) \left[\frac{h' \cosh(2\kappa h')}{2\kappa} \right] \\ & - \delta_{ij} \left[\frac{\rho \kappa^2 (\phi_1^2 + \phi_2^2)}{2 \cosh^2(\kappa h')} \left[-\frac{h'}{2} + \frac{\sinh 2\kappa h'}{4\kappa} \right] \right] \end{aligned} \right] \text{ for } i, j = 1, 2 \quad (4.330)
 \end{aligned}$$

Equation (4.330) allows Radiation Stress values for the NM-WDHM computer model to be obtained directly from the results of velocity potential obtained using the wave model.

4.6 Bottom Friction

Equation (4.204) contains a time averaged bottom friction term, $\overline{\tau_i^B}$. In order to use the equation for modelling wave-driven currents in any direction it is necessary to obtain an expression for $\overline{\tau_i^B}$ that is valid in all directions. Mei (2005) suggests the following expression for the instantaneous bottom friction:

$$\tau_i^B = -\frac{\rho f_B}{2} |\mathbf{u}| u_i \text{ for } i = 1, 2 \quad (4.331)$$

Where f is a friction coefficient. Ignoring the effects of turbulence and the minor contribution of turbulent fluctuations; Equation (4.331) can be expanded as follows using Equation (3.42):

$$\tau_i^B = -\frac{\rho f_B}{2} |\mathbf{U} + \mathbf{u}'| (U_i + u_i') \text{ for } i = 1, 2 \quad (4.332)$$

The bottom friction term means that the wave particle velocity need only be examined at the sea bed. Examining Equation (4.208) at $z' = -h'$ yields:

$$u_i' = \text{Re} \left(\frac{e^{-i\omega t}}{\cosh(\kappa h')} \left[\frac{\partial \phi_1}{\partial x_i} + i \frac{\partial \phi_2}{\partial x_i} \right] \right) \text{ for } i = 1, 2 \quad (4.333)$$

Expansion of Equation (4.333) gives:

$$u_i' = \text{Re} \left(\frac{1}{\cosh(\kappa h')} (\cos \omega t - i \sin \omega t) \left[\frac{\partial \phi_1}{\partial x_i} + i \frac{\partial \phi_2}{\partial x_i} \right] \right) \text{ for } i = 1, 2 \quad (4.334)$$

Further expansion of Equation (4.334) gives:

$$u_i' = \text{Re} \left[\frac{1}{\cosh(\kappa h')} \left(\frac{\partial \phi_1}{\partial x_i} \cos \omega t - i \frac{\partial \phi_1}{\partial x_i} \sin \omega t + i \frac{\partial \phi_2}{\partial x_i} \cos \omega t + \frac{\partial \phi_2}{\partial x_i} \sin \omega t \right) \right] \text{ for } i = 1, 2 \quad (4.335)$$

It is only necessary to examine the real components of Equation (4.335) which gives:

$$u_i' = \frac{\cos \omega t}{\cosh(\kappa h')} \frac{\partial \phi_1}{\partial x_i} + \frac{\sin \omega t}{\cosh(\kappa h')} \frac{\partial \phi_2}{\partial x_i} \text{ for } i = 1, 2 \quad (4.336)$$

Hence:

$$\left| \mathbf{U} + \mathbf{u}' \right| = \left| \left(U_i + \frac{\cos \omega t}{\cosh(\kappa h')} \frac{\partial \phi_1}{\partial x_i} + \frac{\sin \omega t}{\cosh(\kappa h')} \frac{\partial \phi_2}{\partial x_i} \right) \hat{\mathbf{e}}_i \right| \text{ for } i = 1, 2 \quad (4.337)$$

Where $\hat{\mathbf{e}}$ is the unit vector. Equation (4.331) can now be rewritten using the results of Equations (4.336) and (4.337):

$$\tau_i^B = -\frac{\rho f_B}{2} \left[\left(U_j U_j + 2U_j \frac{\cos \omega t}{\cosh(\kappa h')} \frac{\partial \phi_1}{\partial x_j} + \frac{\cos^2 \omega t}{\cosh^2(\kappa h')} \left(\frac{\partial \phi_1}{\partial x_j} \frac{\partial \phi_1}{\partial x_j} \right) \right)^{\frac{1}{2}} \left(U_i + \frac{\cos \omega t}{\cosh(\kappa h')} \frac{\partial \phi_1}{\partial x_i} + \frac{\sin \omega t}{\cosh(\kappa h')} \frac{\partial \phi_2}{\partial x_i} \right) + 2 \frac{\sin \omega t \cos \omega t}{\cosh^2(\kappa h')} \frac{\partial \phi_1}{\partial x_j} \frac{\partial \phi_2}{\partial x_j} + 2U_j \frac{\sin \omega t}{\cosh(\kappa h')} \frac{\partial \phi_2}{\partial x_j} + \frac{\sin^2 \omega t}{\cosh^2(\kappa h')} \left(\frac{\partial \phi_2}{\partial x_j} \frac{\partial \phi_2}{\partial x_j} \right) \right] \quad (4.338)$$

for $i, j = 1, 2$

A time integral may now be obtained of Equation (4.338) to give the time averaged bottom friction term required for Equation (4.204):

$$\overline{\tau_i^B} = -\frac{\rho f_B}{2T} \int_0^T \left[\left(U_j U_j + 2U_j \frac{\cos \omega t}{\cosh(\kappa h')} \frac{\partial \phi_1}{\partial x_j} + \frac{\cos^2 \omega t}{\cosh^2(\kappa h')} \left(\frac{\partial \phi_1}{\partial x_j} \frac{\partial \phi_1}{\partial x_j} \right) \right)^{\frac{1}{2}} \left(U_i + \frac{\cos \omega t}{\cosh(\kappa h')} \frac{\partial \phi_1}{\partial x_i} + \frac{\sin \omega t}{\cosh(\kappa h')} \frac{\partial \phi_2}{\partial x_i} \right) + 2 \frac{\sin \omega t \cos \omega t}{\cosh^2(\kappa h')} \frac{\partial \phi_1}{\partial x_j} \frac{\partial \phi_2}{\partial x_j} + 2U_j \frac{\sin \omega t}{\cosh(\kappa h')} \frac{\partial \phi_2}{\partial x_j} + \frac{\sin^2 \omega t}{\cosh^2(\kappa h')} \left(\frac{\partial \phi_2}{\partial x_j} \frac{\partial \phi_2}{\partial x_j} \right) \right] dt \quad (4.339)$$

for $i, j = 1, 2$

For the purposes of the NM-WDHM the integration of the bottom friction term over a wave period is carried out using numerical integration.

4.7 Turbulent term in Hydrodynamic Equation

The term R''_{ij} in Equation (4.204) represents turbulent diffusion or lateral mixing due to wave breaking. It tends to cause a spreading out and smoothing of wave-driven effects across a larger area than would be expected for non-turbulent conditions. Kraus and Larson (1991) explain that lateral mixing is not well understood in the surf zone and is hence usually modelled using an eddy viscosity term. Mei *et al.* (2005) give a simpler specification based on the work of Longuet-Higgins (1970a). This method, however, is only appropriate for use in areas where the seabed slopes at a constant slope away from the beach on which the waves are shoaling.

4.7.1 Turbulent Diffusion Term in NM-WDHM

Kraus and Larson (1991) gives the following formulae for lateral mixing terms:

$$L_x = \frac{1}{h'} \left[\frac{\partial}{\partial x} \left(\varepsilon_{xx} h' \frac{\partial U}{\partial x} \right) + \frac{\partial}{\partial y} \left(\varepsilon_{xy} h' \frac{\partial U}{\partial y} \right) \right] \quad (4.340)$$

$$L_y = \frac{1}{h'} \left[\frac{\partial}{\partial x} \left(\varepsilon_{yx} h' \frac{\partial V}{\partial x} \right) + \frac{\partial}{\partial y} \left(\varepsilon_{yy} h' \frac{\partial V}{\partial y} \right) \right] \quad (4.341)$$

where:

$$L_j = \frac{1}{\rho(\bar{\eta} + h)} \left[\frac{\partial R''}{\partial x_i} \right] \quad (4.342)$$

Equations (4.340) and (4.341) can be expressed in tensor notation, using the nomenclature of the current project, as:

$$L_j = \frac{1}{(\bar{\eta} + h)} \left[\frac{\partial}{\partial x_i} \left(\varepsilon_{ij} (\bar{\eta} + h) \frac{\partial U_j}{\partial x_i} \right) \right] \quad (4.343)$$

Where ε_{ij} is the eddy viscosity. Battjes (1975) associates lateral mixing with wave orbital velocities as opposed to distance offshore. The methodology of Haas *et al.* (2003) can be followed where ε_{ij} is considered the same in every direction:

$$\varepsilon_{ij} = \varepsilon_{11} = \varepsilon_{22} = \varepsilon_{12} = \varepsilon_{21} = \varepsilon \quad (4.344)$$

Hence Equation (4.343) becomes:

$$L_j = \frac{1}{(\bar{\eta} + h)} \left[\frac{\partial}{\partial x_i} \left(\varepsilon (\bar{\eta} + h) \frac{\partial U_j}{\partial x_i} \right) \right] \quad (4.345)$$

Equation (4.345) can be multiplied above and below the line by the density to give:

$$L_j = \frac{1}{\rho (\bar{\eta} + h)} \left[\frac{\partial}{\partial x_i} \left(\rho \varepsilon (\bar{\eta} + h) \frac{\partial U_j}{\partial x_i} \right) \right] \quad (4.346)$$

The R_{ij}'' term of Equation (4.204) can now be obtained from Equation (4.346):

$$R_{ij}'' = \rho \varepsilon (\bar{\eta} + h) \frac{\partial U_j}{\partial x_i} \quad (4.347)$$

The result of Equation (4.347) is used for turbulent diffusion in the NM-WDHM.

4.7.2 Relating lateral mixing to Wave Breaking

An equation for ε , the eddy viscosity, must be developed. From the work of Battjes (1975) it can be seen that:

$$\varepsilon = M^3 \left(\frac{D}{\rho h} \right) \quad (4.348)$$

Where M is an empirical coefficient that defines the degree of spread of the turbulent mixing effects spread. Battjes (1975) states that the values of M are expected to be of the order of unity. D is defined as follows:

$$D = -\frac{\partial}{\partial s}(EnC) \quad (4.349)$$

Where s increases in the direction of wave propagation and E is the wave energy.

It is apparent from Equations (4.348) and (4.349) that to adequately model lateral dispersion in the NM-WDHM it will be necessary to obtain the variable D from the NM-WCIM. The process for obtaining values of D for the model domain from the wave data of the NM-WCIM is discussed in Chapter 5.

It is acknowledged at this point that in the case where wave direction is altered by wave-current interaction the direction of energy propagation is not the exact same as the direction of wave propagation. In the case of the relatively weak currents being examined in this project it is considered that the effect of this on the calculated eddy viscosity would be very small especially considering the empirical nature of the formula. This assumption is further backed up by the widespread use of the Battjes (1975) eddy viscosity methodology to obtain a diffusion coefficient. Many modern computer models such as the MIKE-21 model, discussed by Danish Hydraulic Institute (2008a), consider the use of a constant diffusion coefficient not to be inaccurate for most cases. This is a considerably larger assumption than the aligning of energy propagation and wave propagation for the calculation of eddy viscosity.

4.8 Finite Element Solution of NM-WDHM

In order to utilise the depth and time averaged conservation of mass and momentum equations to examine wave-generated behaviour a solution scheme must be chosen. Pinder and Gray (1977) present a solution scheme for hydrodynamic equations that solves for unknown variables using a finite element technique over the area of the domain and iterates to a solution using a finite difference iterative technique. The process outlined below follows the overall methodology of Pinder and Gray (1977) while using the particular equations of this project.

Applying a weighting function (equal to a shape function in the Galerkin method) to Equation (4.204) and integrating over the area of a triangular finite element yields:

$$\begin{aligned} \iint_A \frac{\partial U_j}{\partial t} N^I dA = & - \iint_A U_i \frac{\partial U_j}{\partial x_i} N^I dA - \iint_A g \frac{\partial \bar{\eta}}{\partial x_j} N^I dA - \iint_A \frac{1}{\rho(\bar{\eta}+h)} \frac{\partial R'_{ij}}{\partial x_i} N^I dA \\ & - \iint_A \frac{1}{\rho(\bar{\eta}+h)} \frac{\partial R''_{ij}}{\partial x_i} N^I dA + \iint_A \frac{\bar{\tau}_i^B}{\rho(\bar{\eta}+h)} N^I dA \end{aligned} \quad (4.350)$$

Applying a shape function to the unknown gradient of U_j with respect to time yields:

$$\begin{aligned} \left(\frac{dU_j}{dt} \right)^J \iint_A N^I N^J dA = & - \iint_A U_i U_j N^I \frac{\partial N^J}{\partial x_i} dA - \iint_A g \bar{\eta}^J N^I \frac{\partial N^J}{\partial x_j} dA - \iint_A \frac{1}{\rho(\bar{\eta}+h)} R'_{ij}{}^J N^I \frac{\partial N^J}{\partial x_i} dA \\ & - \iint_A \frac{1}{\rho(\bar{\eta}+h)} R''_{ij}{}^J N^I \frac{\partial N^J}{\partial x_i} dA + \iint_A \frac{\bar{\tau}_i^B{}^J}{\rho(\bar{\eta}+h)} N^I N^J dA \end{aligned} \quad (4.351)$$

Expressing Equation (4.351) in matrix form yields:

$$[KI] \left\{ \frac{dU_j}{dt} \right\} = \{ E_{U_j} \} \quad (4.352)$$

A similar process may now be undertaken for the equation of conservation of mass within the system. Equation (4.203), after applying a weighting function (equal to a shape function in the Galerkin method) and integration over the area of a triangular finite element, becomes the following:

$$\iint_A \frac{\partial \bar{\eta}}{\partial t} N^I dA = - \iint_A \frac{\partial}{\partial x_i} \left[U_i (\bar{\eta}+h) \right] N^I dA \quad (4.353)$$

Applying a shape function to the unknown gradient of $\bar{\eta}$ with respect to time yields:

$$\left(\frac{\partial \bar{\eta}}{\partial t}\right)^J \iint_A N^I N^J dA = - \iint_A \bar{\eta}^J \frac{\partial}{\partial x_i} [U_i N^J + U_i h] N^I dA \quad (4.354)$$

Expressing Equation (4.353) in matrix form yields:

$$[KI] \left\{ \frac{d\bar{\eta}}{dt} \right\} = \{E_{\bar{\eta}}\} \quad (4.355)$$

Equations (4.352) and (4.355) now provide the three simultaneous equations that must be solved for the NM-WDHM:

$$[KI] \left\{ \frac{dU_1}{dt} \right\} = \{E_{U_1}\}$$

$$[KI] \left\{ \frac{dU_2}{dt} \right\} = \{E_{U_2}\}$$

$$[KI] \left\{ \frac{d\bar{\eta}}{dt} \right\} = \{E_{\bar{\eta}}\}$$

The solutions examined by this process are steady state problems where the driving force of the radiation stress terms in the hydrodynamic equations is balanced by the magnitude of set-up/set-down and currents. Hence an iterative solution scheme is set up using Equations (4.352) and (4.355) to obtain steady state values of U_1 , U_2 , $\bar{\eta}$ that balance the radiation stress driving term. A finite difference iterative scheme discussed by Pinder and Gray (1977) is chosen. The time derivatives in Equations (4.352) and (4.355) are expressed using a finite difference scheme over the time period Δt and the $\{E\}$ vectors are averaged over the same time period to yield:

$$[KI] \{U_j\}_{t+\Delta t} = [KI] \{U_j\}_t + \frac{1}{2} \Delta t \{E_{U_j}\}_{t+\Delta t} + \frac{1}{2} \Delta t \{E_{U_j}\}_t \quad (4.356)$$

$$[KI] \{\bar{\eta}\}_{t+\Delta t} = [KI] \{\bar{\eta}\}_t + \frac{1}{2} \Delta t \{E_{\bar{\eta}}\}_{t+\Delta t} + \frac{1}{2} \Delta t \{E_{\bar{\eta}}\}_t \quad (4.357)$$

Using the iterative scheme of Equations (4.356) and (4.357) iteration is carried out on successive time steps until the values of U_1 , U_2 and $\bar{\eta}$ converge. Values of U_1 , U_2 and $\bar{\eta}$ at $t = 0$ can be set to any value but for this project zero values are always used.

Boundary conditions for U_1 , U_2 and $\bar{\eta}$ are applied using the big number method. Where the solution value at a particular node is known this value is multiplied by a large number and the resulting product is inserted in the vector of unknowns for the $t + \Delta t$ term. The large number is inserted in the corresponding diagonal of the stiffness matrix hence ensuring that when the finite element calculation is completed the known value at the node is maintained.

Various boundary conditions are used in the NM-WDHM depending on the particular circumstances being examined. This project utilises a no-slip boundary condition on the beach shore (i.e. U_1 and U_2 are set equal to zero on the beach boundary). For a model where longshore currents are not significant or where the side boundaries of the model are sufficiently far away from the portion of the domain where interest lies it is also possible to implement a non-slip boundary condition on these boundaries. In other cases where longshore current must pass through the boundary the longshore current values at the centre of the domain from the t timestep works very well as the boundary conditions at the edge of the domain for the $t + \Delta t$ timestep.

Values of $\bar{\eta}$ are also used as boundary conditions particularly in the case of linear or rectangular meshes. If the deep water boundary is remote from the breaking zone it is possible to apply a boundary condition for $\bar{\eta}$. In most other cases no boundary conditions are applied to $\bar{\eta}$.

The solution is deemed to converge when the difference between two successive iterations is equal to zero or reaches a specified lower limit. The length of time taken for convergence to occur depends on the chosen time step. Experience with the NM-WDHM

has shown that the more complex meshed areas and more stringent boundary conditions as well as the inclusion of turbulent diffusion require smaller time steps and hence take longer to converge. Time scales of 2 to 36 hours have been experienced on desktop computers depending on model complexity.

Chapter 5: Wave Energy Rays

“Energy and persistence alter all things,” Benjamin Franklin.

5.1 Introduction

Clyne (2008) developed a new method to plot wave rays and hence calculate wave heights and breaking heights with a post-processing methodology based on the velocity potential solution of an elliptic mild-slope wave model. A similar process will be applied for this project to calculate wave heights and breaking heights as well as to obtain energy values from which eddy viscosity values can be obtained. These eddy viscosity values can be used for the lateral mixing terms of the NM-WDHM. The Clyne (2008) wave ray approach did not include the effects of current. The approach of this project will include these effects.

The progression of this chapter is as follows:

- A wave energy equation is developed – Section 5.2
- A relationship is developed between amplitude and phases of velocity potential and physical waves – Section 5.3
- The results of Section 5.2 and 5.3 are combined to obtain a wave energy equation in terms of wave components – Section 5.4
- A methodology to obtain eddy viscosity values from wave energy rays is developed – Section 5.5
- A methodology to obtain wave heights from wave energy rays is developed – Section 5.6
- Insipience criterion for wave breaking using energy rays is examined – Section 5.7
- Input terms required for the Wave Energy Ray method are examined – Section 5.8

5.2 Development of Wave Energy Equation

The elliptic mild-slope equation including currents is examined. The extended terms in the mild-slope equation will be discarded for this process due to their limited effect on the results. It will also be necessary in order to obtain an energy equation to disregard the effects of diffraction (i.e. use a plane wave solution) at some points during the derivation of the energy equation. This is considered acceptable because the energy equation will only be used within the breaking zone to obtain broken wave heights and turbulent coefficients. The majority of diffraction within the models being examined by this project occurs outside the breaking zone.

Equation (3.528) is the Mild-Slope Equation including the effects of current and energy dissipation:

$$\begin{aligned} & \frac{\partial^2 \phi}{\partial x_k \partial x_k} CC_g + \frac{\partial \phi}{\partial x_k} \frac{\partial (CC_g)}{\partial x_k} + \phi \kappa^2 CC_g - \phi \sigma^2 + \omega^2 \phi \\ & + \left[2i\omega U_k \frac{\partial \phi}{\partial x_k} + i\omega \frac{\partial U_j}{\partial x_j} \phi - U_k \frac{\partial U_j}{\partial x_j} \frac{\partial \phi}{\partial x_k} - U_j \frac{\partial U_k}{\partial x_j} \frac{\partial \phi}{\partial x_k} - U_j U_k \frac{\partial^2 \phi}{\partial x_j \partial x_k} \right] \\ & = \gamma \frac{\partial}{\partial x_j} (U_j \phi) - i\omega \gamma \phi \end{aligned}$$

The velocity potential may be described as follows using Equation (3.135):

$$\phi = A_\phi e^{iS_\phi}$$

Initially it is necessary to examine the derivatives of Equation (3.135).

First Derivative:

$$\frac{\partial \phi}{\partial x_j} = e^{iS_\phi} \frac{\partial A_\phi}{\partial x_j} + iA_\phi \frac{\partial S_\phi}{\partial x_j} e^{iS_\phi} \quad (5.1)$$

Second derivative:

$$\frac{\partial^2 \phi}{\partial x_j \partial x_j} = \frac{\partial}{\partial x_j} \left(e^{iS_\phi} \frac{\partial A_\phi}{\partial x_j} \right) + \frac{\partial}{\partial x_j} \left(iA_\phi \frac{\partial S_\phi}{\partial x_j} e^{iS_\phi} \right) \quad (5.2)$$

Equation (5.2) may be expanded to give:

$$\frac{\partial^2 \phi}{\partial x_j \partial x_j} = i \frac{\partial A_\phi}{\partial x_j} \frac{\partial S_\phi}{\partial x_j} e^{iS_\phi} + e^{iS_\phi} \frac{\partial^2 A_\phi}{\partial x_j \partial x_j} - A_\phi \frac{\partial S_\phi}{\partial x_j} \frac{\partial S_\phi}{\partial x_j} e^{iS_\phi} + iA_\phi \frac{\partial^2 S_\phi}{\partial x_j \partial x_j} e^{iS_\phi} + i \frac{\partial S_\phi}{\partial x_j} \frac{\partial A_\phi}{\partial x_j} e^{iS_\phi} \quad (5.3)$$

Second cross-derivative:

$$\frac{\partial^2 \phi}{\partial x_j \partial x_k} = i \frac{\partial A_\phi}{\partial x_j} \frac{\partial S_\phi}{\partial x_k} e^{iS_\phi} + i A_\phi \frac{\partial^2 S_\phi}{\partial x_j \partial x_k} e^{iS_\phi} - A_\phi \frac{\partial S_\phi}{\partial x_k} \frac{\partial S_\phi}{\partial x_j} e^{iS_\phi} + i \frac{\partial S_\phi}{\partial x_j} \frac{\partial A_\phi}{\partial x_k} e^{iS_\phi} + e^{iS_\phi} \frac{\partial^2 A_\phi}{\partial x_j \partial x_k} \quad (5.4)$$

Substituting the results of Equations (5.1), (5.3), and (5.4) into Equation (3.532) gives:

$$\begin{aligned} & 2i\omega U_j \left(e^{iS_\phi} \frac{\partial A_\phi}{\partial x_j} + i A_\phi \frac{\partial S_\phi}{\partial x_j} e^{iS_\phi} \right) + i\omega A_\phi e^{iS_\phi} \frac{\partial U_j}{\partial x_j} - U_k \frac{\partial U_j}{\partial x_k} \left(e^{iS_\phi} \frac{\partial A_\phi}{\partial x_j} + i A_\phi \frac{\partial S_\phi}{\partial x_j} e^{iS_\phi} \right) \\ & - U_k U_j \left(i \frac{\partial A_\phi}{\partial x_j} \frac{\partial S_\phi}{\partial x_k} e^{iS_\phi} + i A_\phi \frac{\partial^2 S_\phi}{\partial x_j \partial x_k} e^{iS_\phi} - A_\phi \frac{\partial S_\phi}{\partial x_k} \frac{\partial S_\phi}{\partial x_j} e^{iS_\phi} + i \frac{\partial S_\phi}{\partial x_j} \frac{\partial A_\phi}{\partial x_k} e^{iS_\phi} + e^{iS_\phi} \frac{\partial^2 A_\phi}{\partial x_j \partial x_k} \right) \\ & - U_j \frac{\partial U_k}{\partial x_k} \left(e^{iS_\phi} \frac{\partial A_\phi}{\partial x_j} + i A_\phi \frac{\partial S_\phi}{\partial x_j} e^{iS_\phi} \right) + \frac{\partial (CC_g)}{\partial x_j} \left(e^{iS_\phi} \frac{\partial A_\phi}{\partial x_j} + i A_\phi \frac{\partial S_\phi}{\partial x_j} e^{iS_\phi} \right) - (\sigma^2 - \omega^2 - \kappa^2 CC_g) A_\phi e^{iS_\phi} \\ & + CC_g \left(i \frac{\partial A_\phi}{\partial x_j} \frac{\partial S_\phi}{\partial x_j} e^{iS_\phi} + e^{iS_\phi} \frac{\partial^2 A_\phi}{\partial x_j \partial x_j} - A_\phi \frac{\partial S_\phi}{\partial x_j} \frac{\partial S_\phi}{\partial x_j} e^{iS_\phi} + i A_\phi \frac{\partial^2 S_\phi}{\partial x_j \partial x_j} e^{iS_\phi} + i \frac{\partial S_\phi}{\partial x_j} \frac{\partial A_\phi}{\partial x_j} e^{iS_\phi} \right) \\ & = \gamma A_\phi e^{iS_\phi} \frac{\partial U_j}{\partial x_j} + \gamma U_j \left(e^{iS_\phi} \frac{\partial A_\phi}{\partial x_j} + i A_\phi \frac{\partial S_\phi}{\partial x_j} e^{iS_\phi} \right) - i\omega \gamma A_\phi e^{iS_\phi} \end{aligned} \quad (5.5)$$

Further expanding Equation (5.5) gives:

$$\begin{aligned} & 2i\omega U_j e^{iS_\phi} \left(\frac{\partial A_\phi}{\partial x_j} + i A_\phi \frac{\partial S_\phi}{\partial x_j} \right) + i\omega A_\phi e^{iS_\phi} \frac{\partial U_j}{\partial x_j} - U_k \frac{\partial U_j}{\partial x_k} e^{iS_\phi} \left(\frac{\partial A_\phi}{\partial x_j} + i A_\phi \frac{\partial S_\phi}{\partial x_j} \right) \\ & - U_k U_j e^{iS_\phi} \left(i \frac{\partial A_\phi}{\partial x_j} \frac{\partial S_\phi}{\partial x_k} + i A_\phi \frac{\partial^2 S_\phi}{\partial x_j \partial x_k} - A_\phi \frac{\partial S_\phi}{\partial x_k} \frac{\partial S_\phi}{\partial x_j} + i \frac{\partial S_\phi}{\partial x_j} \frac{\partial A_\phi}{\partial x_k} + \frac{\partial^2 A_\phi}{\partial x_j \partial x_k} \right) \\ & - U_j \frac{\partial U_k}{\partial x_k} e^{iS_\phi} \left(\frac{\partial A_\phi}{\partial x_j} + i A_\phi \frac{\partial S_\phi}{\partial x_j} \right) + \frac{\partial (CC_g)}{\partial x_j} e^{iS_\phi} \left(\frac{\partial A_\phi}{\partial x_j} + i A_\phi \frac{\partial S_\phi}{\partial x_j} \right) - (\sigma^2 - \omega^2 - \kappa^2 CC_g) A_\phi e^{iS_\phi} \\ & + CC_g e^{iS_\phi} \left(i \frac{\partial A_\phi}{\partial x_j} \frac{\partial S_\phi}{\partial x_j} + \frac{\partial^2 A_\phi}{\partial x_j \partial x_j} - A_\phi \frac{\partial S_\phi}{\partial x_j} \frac{\partial S_\phi}{\partial x_j} + i A_\phi \frac{\partial^2 S_\phi}{\partial x_j \partial x_j} + i \frac{\partial S_\phi}{\partial x_j} \frac{\partial A_\phi}{\partial x_j} \right) \\ & = \gamma A_\phi e^{iS_\phi} \frac{\partial U_j}{\partial x_j} + \gamma U_j e^{iS_\phi} \frac{\partial A_\phi}{\partial x_j} + i \gamma U_j A_\phi \frac{\partial S_\phi}{\partial x_j} e^{iS_\phi} - i\omega \gamma A_\phi e^{iS_\phi} \end{aligned} \quad (5.6)$$

All the terms in Equation (5.6) can now be multiplied by the complex conjugate of the velocity potential $\phi^* = A_\phi e^{-iS_\phi}$:

$$\begin{aligned}
& 2i\omega U_j A_\phi \left(\frac{\partial A_\phi}{\partial x_j} + iA_\phi \frac{\partial S_\phi}{\partial x_j} \right) + i\omega A_\phi^2 \frac{\partial U_j}{\partial x_j} - A_\phi U_k \frac{\partial U_j}{\partial x_k} \left(\frac{\partial A_\phi}{\partial x_j} + iA_\phi \frac{\partial S_\phi}{\partial x_j} \right) \\
& - A_\phi U_k U_j \left(i \frac{\partial A_\phi}{\partial x_j} \frac{\partial S_\phi}{\partial x_k} + iA_\phi \frac{\partial^2 S_\phi}{\partial x_j \partial x_k} - A_\phi \frac{\partial S_\phi}{\partial x_k} \frac{\partial S_\phi}{\partial x_j} + i \frac{\partial S_\phi}{\partial x_j} \frac{\partial A_\phi}{\partial x_k} + \frac{\partial^2 A_\phi}{\partial x_j \partial x_k} \right) \\
& - A_\phi U_j \frac{\partial U_k}{\partial x_k} \left(\frac{\partial A_\phi}{\partial x_j} + iA_\phi \frac{\partial S_\phi}{\partial x_j} \right) + A_\phi \frac{\partial (CC_g)}{\partial x_j} \left(\frac{\partial A_\phi}{\partial x_j} + iA_\phi \frac{\partial S_\phi}{\partial x_j} \right) - A_\phi^2 (\sigma^2 - \omega^2 - \kappa^2 CC_g) \\
& + A_\phi CC_g \left(i \frac{\partial A_\phi}{\partial x_j} \frac{\partial S_\phi}{\partial x_j} + \frac{\partial^2 A_\phi}{\partial x_j \partial x_j} - A_\phi \frac{\partial S_\phi}{\partial x_j} \frac{\partial S_\phi}{\partial x_j} + iA_\phi \frac{\partial^2 S_\phi}{\partial x_j \partial x_j} + i \frac{\partial S_\phi}{\partial x_j} \frac{\partial A_\phi}{\partial x_j} \right) \\
& = \gamma A_\phi^2 \frac{\partial U_j}{\partial x_j} + \gamma U_j A_\phi \frac{\partial A_\phi}{\partial x_j} + i\gamma U_j A_\phi^2 \frac{\partial S_\phi}{\partial x_j} - i\omega \gamma A_\phi^2
\end{aligned} \tag{5.7}$$

Examining only the imaginary components of Equation (5.7) gives:

$$\begin{aligned}
& 2\omega U_j A_\phi \frac{\partial A_\phi}{\partial x_j} + \omega A_\phi^2 \frac{\partial U_j}{\partial x_j} - A_\phi^2 U_k \frac{\partial U_j}{\partial x_k} \frac{\partial S_\phi}{\partial x_j} \\
& - A_\phi U_k U_j \frac{\partial A_\phi}{\partial x_j} \frac{\partial S_\phi}{\partial x_k} - A_\phi^2 U_k U_j \frac{\partial^2 S_\phi}{\partial x_j \partial x_k} - A_\phi U_k U_j \frac{\partial S_\phi}{\partial x_j} \frac{\partial A_\phi}{\partial x_k} \\
& - A_\phi^2 U_j \frac{\partial U_k}{\partial x_k} \frac{\partial S_\phi}{\partial x_j} + A_\phi^2 \frac{\partial (CC_g)}{\partial x_j} \frac{\partial S_\phi}{\partial x_j} + A_\phi CC_g \frac{\partial A_\phi}{\partial x_j} \frac{\partial S_\phi}{\partial x_j} \\
& + A_\phi^2 CC_g \frac{\partial^2 S_\phi}{\partial x_j \partial x_j} + A_\phi CC_g \frac{\partial S_\phi}{\partial x_j} \frac{\partial A_\phi}{\partial x_j} = \gamma U_j A_\phi^2 \frac{\partial S_\phi}{\partial x_j} - \omega \gamma A_\phi^2
\end{aligned} \tag{5.8}$$

Simplification of Equation (5.8) yields:

$$\begin{aligned}
& 2\omega U_j A_\phi \frac{\partial A_\phi}{\partial x_j} + \omega A_\phi^2 \frac{\partial U_j}{\partial x_j} - A_\phi^2 U_k \frac{\partial U_j}{\partial x_k} \frac{\partial S_\phi}{\partial x_j} - 2A_\phi U_k U_j \frac{\partial A_\phi}{\partial x_j} \frac{\partial S_\phi}{\partial x_k} \\
& - A_\phi^2 U_k U_j \frac{\partial^2 S_\phi}{\partial x_j \partial x_k} - A_\phi^2 U_j \frac{\partial U_k}{\partial x_k} \frac{\partial S_\phi}{\partial x_j} + \frac{\partial}{\partial x_j} \left(A_\phi^2 CC_g \frac{\partial S_\phi}{\partial x_j} \right) = \gamma U_j A_\phi^2 \frac{\partial S_\phi}{\partial x_j} - \omega \gamma A_\phi^2
\end{aligned} \tag{5.9}$$

Using Equation (3.189) in the absence of diffraction gives:

$$\omega = \sigma + U_k \frac{\partial S_\phi}{\partial x_k} \tag{5.10}$$

It is acknowledged that the use of Equation (5.10) somewhat limits the developed energy equation by neglecting diffractive effects. However, this assumption was necessary to obtain an energy equation in the form of Booij (1981).

Substituting Equation (5.10) into Equation (5.9) gives:

$$\begin{aligned}
 & 2U_j A_\phi \frac{\partial A_\phi}{\partial x_j} \left(\sigma + U_k \frac{\partial S_\phi}{\partial x_k} \right) + A_\phi^2 \frac{\partial U_j}{\partial x_j} \left(\sigma + U_k \frac{\partial S_\phi}{\partial x_k} \right) - A_\phi^2 U_k \frac{\partial U_j}{\partial x_k} \frac{\partial S_\phi}{\partial x_j} \\
 & - 2A_\phi U_k U_j \frac{\partial A_\phi}{\partial x_j} \frac{\partial S_\phi}{\partial x_k} - A_\phi^2 U_k U_j \frac{\partial^2 S_\phi}{\partial x_j \partial x_k} - A_\phi^2 U_j \frac{\partial U_k}{\partial x_k} \frac{\partial S_\phi}{\partial x_j} + \frac{\partial}{\partial x_j} \left(A_\phi^2 C C_g \frac{\partial S_\phi}{\partial x_j} \right) \\
 & = \gamma U_j A_\phi^2 \frac{\partial S_\phi}{\partial x_j} - \gamma A_\phi^2 \left(\sigma + U_k \frac{\partial S_\phi}{\partial x_k} \right)
 \end{aligned} \tag{5.11}$$

Expanding Equation (5.11) gives:

$$\begin{aligned}
 & 2\sigma A_\phi U_j \frac{\partial A_\phi}{\partial x_j} + 2A_\phi U_j U_k \frac{\partial A_\phi}{\partial x_j} \frac{\partial S_\phi}{\partial x_k} + A_\phi^2 \sigma \frac{\partial U_j}{\partial x_j} + A_\phi^2 U_k \frac{\partial U_j}{\partial x_j} \frac{\partial S_\phi}{\partial x_k} - A_\phi^2 U_k \frac{\partial U_j}{\partial x_k} \frac{\partial S_\phi}{\partial x_j} \\
 & - 2A_\phi U_k U_j \frac{\partial A_\phi}{\partial x_j} \frac{\partial S_\phi}{\partial x_k} - A_\phi^2 U_k U_j \frac{\partial^2 S_\phi}{\partial x_j \partial x_k} - A_\phi^2 U_j \frac{\partial U_k}{\partial x_k} \frac{\partial S_\phi}{\partial x_j} + \frac{\partial}{\partial x_j} \left(A_\phi^2 C C_g \frac{\partial S_\phi}{\partial x_j} \right) \\
 & = \gamma U_j A_\phi^2 \frac{\partial S_\phi}{\partial x_j} - \gamma A_\phi^2 \left(\sigma + U_k \frac{\partial S_\phi}{\partial x_k} \right)
 \end{aligned} \tag{5.12}$$

Equation (5.12) simplifies to become:

$$\begin{aligned}
 & 2\sigma A_\phi U_j \frac{\partial A_\phi}{\partial x_j} + A_\phi^2 \sigma \frac{\partial U_j}{\partial x_j} - A_\phi^2 U_k \frac{\partial}{\partial x_k} \left(U_j \frac{\partial S_\phi}{\partial x_j} \right) + \frac{\partial}{\partial x_j} \left(A_\phi^2 C C_g \frac{\partial S_\phi}{\partial x_j} \right) \\
 & = \gamma U_j A_\phi^2 \frac{\partial S_\phi}{\partial x_j} - \gamma A_\phi^2 \left(\sigma + U_k \frac{\partial S_\phi}{\partial x_k} \right)
 \end{aligned} \tag{5.13}$$

Equation (5.10) can be utilised in Equation (5.13) to obtain:

$$\begin{aligned}
 & 2\sigma A_\phi U_j \frac{\partial A_\phi}{\partial x_j} + A_\phi^2 \sigma \frac{\partial U_j}{\partial x_j} - A_\phi^2 U_k \frac{\partial}{\partial x_k} (\omega - \sigma) + \frac{\partial}{\partial x_j} \left(A_\phi^2 C C_g \frac{\partial S_\phi}{\partial x_j} \right) \\
 & = \gamma A_\phi^2 \left[U_j \frac{\partial S_\phi}{\partial x_j} - \left(\sigma + U_k \frac{\partial S_\phi}{\partial x_k} \right) \right]
 \end{aligned} \tag{5.14}$$

The angular frequency ω is a constant non-varying value. Hence Equation (5.14) becomes:

$$2\sigma A_\phi U_j \frac{\partial A_\phi}{\partial x_j} + A_\phi^2 \sigma \frac{\partial U_j}{\partial x_j} - A_\phi^2 U_k \frac{\partial \sigma}{\partial x_k} + \frac{\partial}{\partial x_j} \left(A_\phi^2 C C_g \frac{\partial S_\phi}{\partial x_j} \right) = \gamma A_\phi^2 \left[U_j \frac{\partial S_\phi}{\partial x_j} - \left(\sigma + U_k \frac{\partial S_\phi}{\partial x_k} \right) \right] \quad (5.15)$$

Equation (5.15) can be further simplified as:

$$\frac{\partial}{\partial x_j} (\sigma A_\phi^2 U_j) + \frac{\partial}{\partial x_j} \left(A_\phi^2 C C_g \frac{\partial S_\phi}{\partial x_j} \right) = \gamma A_\phi^2 \left[U_j \frac{\partial S_\phi}{\partial x_j} - \sigma - U_k \frac{\partial S_\phi}{\partial x_k} \right] \quad (5.16)$$

$$\frac{\partial}{\partial x_j} \left[A_\phi^2 \left(C C_g \frac{\partial S_\phi}{\partial x_j} + \sigma U_j \right) \right] = -\gamma A_\phi^2 \sigma \quad (5.17)$$

5.3 Relating Amplitudes and Phases of Velocity Potential and Physical Waves

At this point it is beneficial to change Equation (5.17) into a form expressed in terms of physical quantities. This may be accomplished by replacing the amplitude of velocity potential, A_ϕ , with the physical wave amplitude, A_ξ , and determining a relationship between the phase of velocity potential, S_ϕ , and the wave phase, S_ξ .

The difference between mean set-up and wave set-up has been defined as ζ' , as shown in Figure 3.4. A harmonic difference between mean and instantaneous set-up may be expressed as follows:

$$\zeta' = \text{Re}(\xi e^{-i\omega t}) \quad (5.18)$$

Utilising the same plane wave method as discussed in Section 3.9.2 for this harmonic term gives the following:

$$\xi = A_\xi e^{iS_\xi} \quad (5.19)$$

Using Equation (3.109) with the Dynamic Free Surface Boundary Condition of Equation (3.91), yields:

$$\frac{\partial}{\partial t}(\tilde{\phi} e^{-i\omega t}) + U_j \frac{\partial}{\partial x_j}(\tilde{\phi} e^{-i\omega t}) + g(\xi e^{-i\omega t}) = 0 \text{ at } z = \bar{\eta}, j = 1, 2 \quad (5.20)$$

Simplification of Equation (5.20) gives:

$$-i\omega \tilde{\phi} + U_j \frac{\partial \tilde{\phi}}{\partial x_j} + g\xi = 0 \text{ at } z = \bar{\eta}, j = 1, 2 \quad (5.21)$$

Using the vertical function from Equation (3.130) with Equation (5.21) gives:

$$-i\omega f\phi + U_j \frac{\partial(f\phi)}{\partial x_j} + g\xi = 0 \text{ at } z = \bar{\eta}, j = 1, 2 \quad (5.22)$$

Acknowledging the fact that $f=1$ at $z = \bar{\eta}$ gives:

$$-i\omega \phi + U_j \frac{\partial \phi}{\partial x_j} + U_j \phi \frac{\partial f}{\partial x_j} + g\xi = 0 \text{ at } z = \bar{\eta}, j = 1, 2 \quad (5.23)$$

Using Equations (3.135) and (5.19) with Equation (5.23) gives:

$$-i\omega A_\phi e^{iS_\phi} + U_j \frac{\partial(A_\phi e^{iS_\phi})}{\partial x_j} + U_j A_\phi e^{iS_\phi} \frac{\partial f}{\partial x_j} + g A_\xi e^{iS_\xi} = 0 \quad (5.24)$$

$$-i\omega A_\phi e^{iS_\phi} + U_j e^{iS_\phi} \frac{\partial A_\phi}{\partial x_j} + U_j A_\phi i e^{iS_\phi} \frac{\partial S_\phi}{\partial x_j} + U_j A_\phi e^{iS_\phi} \frac{\partial f}{\partial x_j} + g A_\xi e^{iS_\xi} = 0 \quad (5.25)$$

For a plane wave solution on a constant depth, in the absence of diffraction, the following identities hold true

$$\frac{\partial A_\phi}{\partial x_j} = 0 \quad (5.26)$$

$$\frac{\partial f}{\partial x_j} = 0 \quad (5.27)$$

Using Equations (5.26) and (5.27) with Equation (5.25) gives:

$$-i\omega A_\phi e^{iS_\phi} + U_j A_\phi i e^{iS_\phi} \frac{\partial S_\phi}{\partial x_j} + g A_\xi e^{iS_\xi} = 0 \quad (5.28)$$

Equation (5.28) may be rewritten as follows to separate the terms containing velocity potential and wave components.

$$\left(i\omega A_\phi - U_j A_\phi i \frac{\partial S_\phi}{\partial x_j} \right) e^{iS_\phi} = g A_\xi e^{iS_\xi} \quad (5.29)$$

Equation (5.29) may be expressed as follows:

$$\left(\omega A_\phi - U_j A_\phi \frac{\partial S_\phi}{\partial x_j} \right) e^{i\left(S_\phi - \frac{\pi}{2}\right)} = g A_\xi e^{iS_\xi} \quad (5.30)$$

Equation (5.30) gives the relationship between wave amplitude and amplitude of velocity potential for a plane wave:

$$\frac{\omega A_\phi - U_j A_\phi \frac{\partial S_\phi}{\partial x_j}}{g} = A_\xi \quad (5.31)$$

Using Equation (5.10) this relationship may be expressed as:

$$A_\phi = \frac{gA_\xi}{\sigma} \quad (5.32)$$

Equation (5.30) also shows that the relationship between wave phase and phase of velocity potential is:

$$S_\phi - \frac{\pi}{2} = S_\xi \quad (5.33)$$

Substituting Equations (5.33) and (5.31) into Equation (5.19) gives:

$$\xi = \left[\frac{\omega A_\phi - U_j A_\phi \frac{\partial S_\phi}{\partial x_j}}{g} \right] e^{i\left(S_\phi - \frac{\pi}{2}\right)} \quad (5.34)$$

Using Equation (3.135) with Equation (5.34) yields:

$$\xi = \left[\frac{\omega - U_j \frac{\partial S_\phi}{\partial x_j}}{g} \right] \left(\frac{\phi}{e^{iS_\phi}} \right) e^{i\left(S_\phi - \frac{\pi}{2}\right)} \quad (5.35)$$

Simplifying Equation (5.35) gives the following:

$$\xi = \left[\frac{\omega - U_j \frac{\partial S_\phi}{\partial x_j}}{g} \right] \phi e^{\frac{i\pi}{2}} \quad (5.36)$$

The exponential function in Equation (5.36) can be expanded to give the following equation:

$$\xi = -i \left[\frac{\omega - U_j \frac{\partial S_\phi}{\partial x_j}}{g} \right] \phi \quad (5.37)$$

Taking the minus inside the brackets in Equation (5.37) yields:

$$\xi = \left[\frac{U_j \frac{\partial S_\phi}{\partial x_j} - \omega}{g} \right] i\phi \quad (5.38)$$

Using Equation (5.18) and Equation (5.38) an expression can be given for the wave fluctuation of the free surface:

$$\zeta' = \text{Re} \left(\xi e^{-i\omega t} \right) = \text{Re} \left[i\phi \left(\frac{U_j A_\phi \frac{\partial S_\phi}{\partial x_j} - \omega}{g} \right) e^{-i\omega t} \right] \quad (5.39)$$

5.4 Expression of Energy Equation in terms of Wave Components

The results of Sections 5.2 and 5.3 can now be combined to obtain an energy equation in terms of wave components.

Equation (5.17) may now be rewritten using Equation (5.32):

$$\frac{\partial}{\partial x_j} \left[\frac{g^2 A_\xi^2}{\sigma^2} \left(CC_g \frac{\partial S_\phi}{\partial x_j} + \sigma U_j \right) \right] = -\gamma \sigma \frac{g^2 A_\xi^2}{\sigma^2} \quad (5.40)$$

Equation (5.40) may also be written as:

$$\frac{\partial}{\partial x_j} \left[\frac{A_\xi^2}{\sigma} \left(\frac{CC_g}{\sigma} \frac{\partial S_\phi}{\partial x_j} + U_j \right) \right] = -\gamma \frac{A_\xi^2}{\sigma} \quad (5.41)$$

But we know that:

$$E = \frac{1}{8} \rho g H^2 = \frac{1}{2} \rho g A_\xi^2 \quad (5.42)$$

Rewriting this in terms of the wave amplitude gives:

$$\frac{2E}{\rho g} = A_\xi^2 \quad (5.43)$$

Using Equation (5.43) with Equation (5.41) gives:

$$\frac{\partial}{\partial x_j} \left[\frac{2E}{\sigma \rho g} \left(\frac{CC_g}{\sigma} \frac{\partial S_\phi}{\partial x_j} + U_j \right) \right] = -\gamma \frac{2E}{\sigma \rho g} \quad (5.44)$$

Equation (5.44) can be simplified as:

$$\frac{\partial}{\partial x_j} \left[\frac{E}{\sigma} \left(\frac{CC_g}{\sigma} \frac{\partial S_\phi}{\partial x_j} + U_j \right) \right] = -\gamma \frac{E}{\sigma} \quad (5.45)$$

5.5 Obtaining Eddy Viscosity from Wave Energy Equation

The development of an equation for eddy viscosity is carried out for a plane wave solution in order to compare the terms with the breaking methodology of Battjes (1975). The resulting equation, however, will be readily adaptable to the more general case necessary for this project.

Further examination of Equation (5.45) for a plane wave gives:

$$\frac{\partial}{\partial x_1} \left[\frac{E}{\omega} \left(\frac{CC_g}{\omega} \frac{\partial S_\phi}{\partial x_1} \right) \right] + \frac{\partial}{\partial x_2} \left[\frac{E}{\omega} \left(\frac{CC_g}{\omega} \frac{\partial S_\phi}{\partial x_2} \right) \right] = -\gamma \frac{E}{\omega} \quad (5.46)$$

$$\frac{\partial}{\partial x_1} \left(\frac{ECC_g}{\omega^2} \frac{\partial S_\phi}{\partial x_1} \right) + \frac{ECC_g}{\omega^2} \frac{\partial^2 S_\phi}{\partial x_2^2} = -\gamma \frac{E}{\omega} \quad (5.47)$$

Equation (3.136) says for a plane wave:

$$S_\phi = \kappa_1 x + \kappa_2 x_2$$

Hence;

$$\frac{\partial S_\phi}{\partial x_2} = \kappa_2 \quad (5.48)$$

$$\frac{\partial^2 S_\phi}{\partial x_2^2} = 0 \quad (5.49)$$

$$\frac{\partial S_\phi}{\partial x_1} = \kappa_1 \quad (5.50)$$

Using Equation (5.49) with Equation (5.47) gives:

$$\frac{\partial}{\partial x_1} \left(\frac{ECC_g}{\omega^2} \frac{\partial S_\phi}{\partial x_1} \right) = -\gamma \frac{E}{\omega} \quad (5.51)$$

Using Equation (5.50) with Equation (5.51) gives:

$$\frac{\partial}{\partial x_1} \left(\frac{ECC_g}{\omega^2} \kappa_1 \right) = -\gamma \frac{E}{\omega} \quad (5.52)$$

For a plane wave the equations defined in Section 3.7.5.2 reduce to:

$$C_g = nC \quad (5.53)$$

$$C = \frac{\omega}{\kappa} \quad (5.54)$$

Using Equations (5.53) and (5.54) with Equation (5.52) yields:

$$\frac{\partial}{\partial x_1} \left(\frac{EnC}{\omega^2} \frac{\omega}{\kappa} \kappa_1 \right) = -\gamma \frac{E}{\omega} \quad (5.55)$$

Expressing the κ_1 component of the plane wave in terms of κ and wave direction θ gives:

$$\frac{\partial}{\partial x_1} \left[\frac{EnC}{\omega} \frac{(-\kappa \cos \theta)}{\kappa} \right] = -\gamma \frac{E}{\omega} \quad (5.56)$$

$$-\frac{\partial}{\partial x_1} \left[\frac{EnC}{\omega} \cos \theta \right] = -\gamma \frac{E}{\omega} \quad (5.57)$$

Expressing Equation (5.57) in terms of wave direction s gives:

$$-\frac{\partial}{\partial s} \left[\frac{EnC}{\omega} \right] = -\frac{\gamma E}{\omega} \quad (5.58)$$

$$-\frac{\partial}{\partial s} [EnC] = -\gamma E \quad (5.59)$$

Using Equation (4.349) it can be seen that:

$$D = -\gamma E \quad (5.60)$$

Although this development is carried out for a plane wave solution in order to compare the terms with the breaking methodology of Battjes (1975) the result of Equation (5.60) can be used for the full solution of Equation (5.45).

Thus using Equation (4.348) ε , the eddy viscosity, may be linked with γ the energy dissipation term as follows:

$$\varepsilon = -M^3 \left(\frac{\gamma E}{\rho h} \right) \quad (5.61)$$

5.6 Obtaining Wave Heights using Wave Energy Rays

In order to use Equation (5.61) to obtain eddy viscosity, it is necessary to know the energy at any point. In order to calculate energy values the wave height must be known. Wave energy rays can be used to calculate the wave height.

Examining Equation (5.45) in the absence of energy dissipation yields:

$$\frac{\partial}{\partial x_j} \left[\frac{E}{\sigma} (C_{Gj} + U_j) \right] = 0 \quad (5.62)$$

Where:

$$C_{Gj} = \frac{CC_g}{\sigma} \frac{\partial S_\phi}{\partial x_j} \quad (5.63)$$

Figure 5.1 below shows energy rays following the direction of energy propagation through a domain where A_D is the area between the energy rays and the two perpendicular lines to the rays.

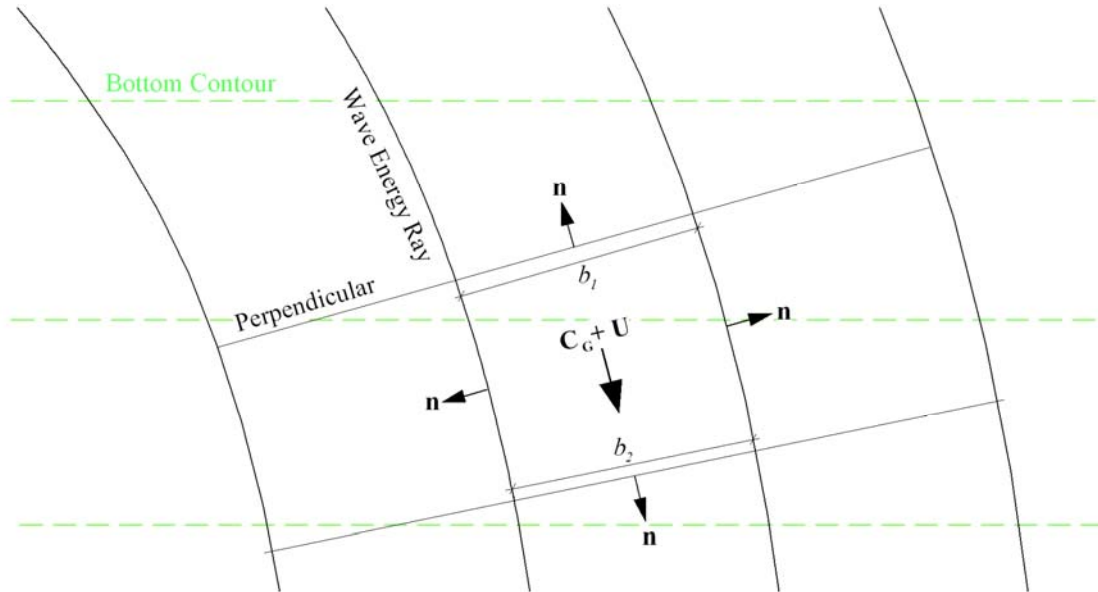


Figure 5.1 – Geometry of Wave Energy Rays

If Equation (5.62) is integrated over the area A_D the following result is obtained:

$$\iint_{A_D} \frac{\partial}{\partial x_j} \left[\frac{E}{\sigma} (C_{Gj} + U_j) \right] dA_D = \int_s \frac{E}{\sigma} (C_{Gj} + U_j) n_j ds \quad (5.64)$$

The term on the right hand side of Equation (5.64) can be expressed more explicitly as the sum of the energy equation along each side of the area in question:

$$\int_s \frac{E}{\sigma} (\mathbf{C}_{G_j} + \mathbf{U}_j) n_j ds = \sum_{s_j}^{i=4} \left[\frac{E}{\sigma} (\mathbf{C}_{G_j} + \mathbf{U}_j) \right] n_j ds \quad (5.65)$$

It is obvious from Figure 5.1, however, that the integral over s_3 and s_4 is zero because the normals to sides 3 and 4 (n_3 and n_4) are perpendicular to the $\mathbf{C}_G + \mathbf{U}$ vector. Hence the following can be expressed using Equations (5.64) and (5.65):

$$\iint_{A_D} \frac{\partial}{\partial x_j} \left[\frac{E}{\sigma} (\mathbf{C}_{G_j} + \mathbf{U}_j) \right] dA_D = \int_{s_1} \frac{E}{\sigma} (\mathbf{C}_{G_j} + \mathbf{U}_j) n_j ds + \int_{s_2} \frac{E}{\sigma} (\mathbf{C}_{G_j} + \mathbf{U}_j) n_j ds = 0 \quad (5.66)$$

$$\iint_{A_D} \frac{\partial}{\partial x_j} \left[\frac{E}{\sigma} (\mathbf{C}_{G_j} + \mathbf{U}_j) \right] dA_D = -\frac{E_1}{\sigma_1} |\mathbf{C}_G + \mathbf{U}|_1 b_1 + \frac{E_2}{\sigma_2} |\mathbf{C}_G + \mathbf{U}|_2 b_2 = 0 \quad (5.67)$$

Where b_1 and b_2 are the distance between the rays along the first and second perpendicular lines.

Rearranging Equation (5.67) yields:

$$E_2 = \frac{\frac{E_1}{\sigma_1} |\mathbf{C}_G + \mathbf{U}|_1 b_1}{\frac{1}{\sigma_2} |\mathbf{C}_G + \mathbf{U}|_2 b_2} \quad (5.68)$$

Using Equation (5.42) with Equation (5.68) gives the following formula for wave height at the second perpendicular using a known wave height at the first:

$$H_2 = \sqrt{\frac{\frac{H_1^2}{\sigma_1} |\mathbf{C}_G + \mathbf{U}|_1 b_1}{\frac{1}{\sigma_2} |\mathbf{C}_G + \mathbf{U}|_2 b_2}} \quad (5.69)$$

Where:

$$|\mathbf{C}_G + \mathbf{U}| = \sqrt{\left(\frac{CC_g}{\sigma} \frac{\partial S_\phi}{\partial x_1} + U_1 \right)^2 + \left(\frac{CC_g}{\sigma} \frac{\partial S_\phi}{\partial x_2} + U_2 \right)^2} \quad (5.70)$$

The wave height can be calculated along any set of wave rays within a domain using Equation (5.69) and the results of the NM-WCIM for the same domain. An appropriate

wave height is chosen at the first point along a wave ray channel and the calculation process can then be carried forward in a step by step manner obtaining the wave height at each perpendicular line to the ray channel using the height at the previous perpendicular line. The spacing of these perpendiculars can be varied to aid computational efficiency but they must be sufficiently frequent to describe the wave profile accurately over a wavelength . When an incipient wave height is reached it is necessary to use a different formula that will account for breaking. Section 3.12.3.1 discusses the Battjes and Janssen (1978) wave breaking solution. The application of this breaking methodology to the wave energy ray method is discussed below.

5.6.1 Battjes and Janssen (1978) Wave Breaking Solution in the Wave Energy Ray Method

Using Equation (3.1027) with Equation (5.45) gives:

$$\frac{\partial}{\partial x_j} \left[\frac{E}{\sigma} \left(\frac{CC_g}{\sigma} \frac{\partial S_\phi}{\partial x_j} + U_j \right) \right] = - \frac{\omega \alpha E Q_b}{r^2 \sigma \pi} \quad (5.71)$$

Equation (5.71) can be rewritten as:

$$\frac{\partial}{\partial x_j} \left[\frac{E}{\sigma} (C_{Gj} + U_j) \right] = - \frac{\omega \alpha E Q_b}{r^2 \sigma \pi} \quad (5.72)$$

Equation (5.72) can be integrated over the area between two rays and intersecting perpendiculars as before:

$$\iint_{A_D} \frac{\partial}{\partial x_j} \left[\frac{E}{\sigma} (C_{Gj} + U_j) \right] dA_D = - \frac{\omega \alpha}{\pi} \iint_{A_D} \frac{E Q_b}{r^2 \sigma} dA_D \quad (5.73)$$

The resulting Equation is similar to that of Equation (5.67) with the inclusion of energy dissipation terms:

$$-\frac{E_1}{\sigma_1} |C_G + U|_1 b_1 + \frac{E_2}{\sigma_2} |C_G + U|_2 b_2 = - \frac{\omega \alpha \Delta_c}{2\pi} \left[\left(\frac{E Q_b}{r^2 \sigma} \right)_1 + \left(\frac{E Q_b}{r^2 \sigma} \right)_2 \right] \quad (5.74)$$

Where Δ_c is the area of the cell under consideration.

Isolating the energy at the second point along the ray channel gives:

$$E_2 \left[\frac{1}{\sigma_2} |\mathbf{C}_G + \mathbf{U}|_2 b_2 + \frac{\Delta_c \omega \alpha}{2\pi} \frac{Q_{b2}}{r_2^2 \sigma_2} \right] = \left[-\frac{\Delta_c \omega \alpha}{2\pi} \frac{Q_{b1}}{r_1^2 \sigma_1} + \frac{1}{\sigma_1} |\mathbf{C}_G + \mathbf{U}|_1 b_1 \right] E_1 \quad (5.75)$$

$$E_2 = \frac{\left[\frac{1}{\sigma_1} |\mathbf{C}_G + \mathbf{U}|_1 b_1 - \frac{\Delta_c \omega \alpha}{2\pi} \frac{Q_{b1}}{r_1^2 \sigma_1} \right] E_1}{\frac{1}{\sigma_2} |\mathbf{C}_G + \mathbf{U}|_2 b_2 + \frac{\Delta_c \omega \alpha}{2\pi} \frac{Q_{b2}}{r_2^2 \sigma_2}} \quad (5.76)$$

Introducing the result of Equation (5.42) in Equation (5.76) gives the following equation for the wave height at the second perpendicular interceptor of the wave rays knowing the wave height at the first:

$$H_2 = \sqrt{\frac{\left[\frac{1}{\sigma_1} |\mathbf{C}_G + \mathbf{U}|_1 b_1 - \frac{\Delta_c \omega \alpha}{2\pi} \frac{Q_{b1}}{r_1^2 \sigma_1} \right] H_1}{\frac{1}{\sigma_2} |\mathbf{C}_G + \mathbf{U}|_2 b_2 + \frac{\Delta_c \omega \alpha}{2\pi} \frac{Q_{b2}}{r_2^2 \sigma_2}}} \quad (5.77)$$

It should be noted at this point that r_2 and hence Q_{b2} are initially unknown, hence a degree of iteration is required to obtain a result in the breaking zone. Clyne (2008) uses the same iterative process.

5.6.2 Dally *et al.* (1985) Wave Breaking Solution in the Wave Energy Ray Method

Dally *et al.* (1985) proposed a closed form solution to wave breaking based on energy dissipation. This method had the advantage of not requiring iteration on the wave heights of the solution. Authors such as Clyne (2008), Smith (2003) and Zhao *et al.* (2001) all examine this method. Dally *et al.* (1985) suggest that when a wave breaks it will continue breaking until its height becomes less than some stable wave height, which Dally *et al.* (1985) express as a percentage of the water depth. When this lower boundary for wave breaking is passed the breaking process stops.. Hence the Dally *et al.* (1985) method allows for the recovery of wave height where areas of shoaling are interrupted by areas of breaking. The ability to model this process is rare in wave breaking models.

Using the wave energy equation of this project to express the methodology of Dally *et al.* (1985) gives:

$$\frac{\partial}{\partial x_j} \left[\frac{E}{\sigma} (\mathbf{C}_{Gj} + U_j) \right] = -\frac{K_D}{h} \left[\frac{E}{\sigma} |\mathbf{C}_G + \mathbf{U}| - \left\{ \frac{E}{\sigma} |\mathbf{C}_G + \mathbf{U}| \right\}_{st} \right] = -\frac{K_D C'_G}{\sigma h} [E - E_{st}] = -\frac{\gamma}{\sigma} E' \quad (5.78)$$

Where the subscript st denotes the value of a property for the stable wave height. Hence:

$$H_{st} = \Gamma h \quad (5.79)$$

Where Γ is an empirical parameter relating wave height to water depth after Dally *et al.* (1985).

Using Equation (5.78) with Equation (5.45) yields the following energy equation including the energy dissipation methodology of Dally *et al.* (1985):

$$\frac{\partial}{\partial x_j} \left[\frac{E}{\sigma} \left(\frac{CC_g}{\sigma} \frac{\partial S_\phi}{\partial x_j} + U_j \right) \right] = -\frac{K_D |\mathbf{C}_G + \mathbf{U}|}{\sigma h} [E - E_{st}] \quad (5.80)$$

To benefit the further development of Equation (5.80) the result of Equation (5.42) may be included to give:

$$\frac{\partial}{\partial x_j} \left[\frac{H^2}{\sigma} \left(\frac{CC_g}{\sigma} \frac{\partial S_\phi}{\partial x_j} + U_j \right) \right] = -\frac{K_D |\mathbf{C}_G + \mathbf{U}|}{\sigma h} [H^2 - \Gamma^2 h^2] \quad (5.81)$$

Using Figure 5.1 it is once again possible to integrate over the area between two rays and intersecting perpendiculars as before:

$$\iint_{A_D} \frac{\partial}{\partial x_j} \left[\frac{H^2}{\sigma} (\mathbf{C}_{Gj} + U_j) \right] dA_D = -K_D \iint_{A_D} \frac{H^2 |\mathbf{C}_G + \mathbf{U}|}{\sigma h} dA_D + K_D \iint_{A_D} \frac{\Gamma^2 h^2 |\mathbf{C}_G + \mathbf{U}|}{\sigma h} dA_D \quad (5.82)$$

$$\iint_{A_D} \frac{\partial}{\partial x_j} \left[\frac{H^2}{\sigma} (\mathbf{C}_{Gj} + U_j) \right] dA_D = -K_D \iint_{A_D} \frac{H^2 |\mathbf{C}_G + \mathbf{U}|}{\sigma h} dA_D + K_D \Gamma^2 \iint_{A_D} \frac{h |\mathbf{C}_G + \mathbf{U}|}{\sigma} dA_D \quad (5.83)$$

Equation (5.83) can be expressed in a more discrete manner as:

$$\begin{aligned} -\frac{H_1^2}{\sigma_1} |\mathbf{C}_G + \mathbf{U}|_1 b_1 + \frac{H_2^2}{\sigma_2} |\mathbf{C}_G + \mathbf{U}|_2 b_2 = & -\frac{\Delta_c K_D}{2} \left[\frac{H_1^2 |\mathbf{C}_G + \mathbf{U}|_1}{\sigma_1 h_1} + \frac{H_2^2 |\mathbf{C}_G + \mathbf{U}|_2}{\sigma_2 h_2} \right] \\ & + \frac{\Delta_c K_D \Gamma^2}{2} \left[\frac{h_1 |\mathbf{C}_G + \mathbf{U}|_1}{\sigma_1} + \frac{h_2 |\mathbf{C}_G + \mathbf{U}|_2}{\sigma_2} \right] \end{aligned} \quad (5.84)$$

Isolating the wave height at the second point along the ray channel gives:

$$H_2^2 \left[\frac{1}{\sigma_2} |\mathbf{C}_G + \mathbf{U}|_2 b_2 + \frac{\Delta_c K_D |\mathbf{C}_G + \mathbf{U}|_2}{2\sigma_2 h_2} \right] = -\frac{\Delta_c K_D H_1^2 |\mathbf{C}_G + \mathbf{U}|_1}{2\sigma_1 h_1} + \frac{\Delta_c K_D \Gamma^2 h_1 |\mathbf{C}_G + \mathbf{U}|_2}{2\sigma_1} \quad (5.85)$$

$$+ \frac{\Delta_c K_D \Gamma^2 h_2 |\mathbf{C}_G + \mathbf{U}|_2}{2\sigma_2} + \frac{H_1^2}{\sigma_1} |\mathbf{C}_G + \mathbf{U}|_1 b_1$$

$$H_2^2 = \frac{\frac{H_1^2}{\sigma_1} |\mathbf{C}_G + \mathbf{U}|_1 b_1 - \frac{\Delta_c K_D H_1^2 |\mathbf{C}_G + \mathbf{U}|_1}{2\sigma_1 h_1} + \frac{\Delta_c K_D \Gamma^2 h_1 |\mathbf{C}_G + \mathbf{U}|_1}{2\sigma_1} + \frac{\Delta_c K_D \Gamma^2 h_2 |\mathbf{C}_G + \mathbf{U}|_2}{2\sigma_2}}{\frac{1}{\sigma_2} |\mathbf{C}_G + \mathbf{U}|_2 b_2 + \frac{\Delta_c K_D |\mathbf{C}_G + \mathbf{U}|_2}{2\sigma_2 h_2}} \quad (5.86)$$

The following equation for the wave height at the second perpendicular interceptor of the wave rays knowing the wave height at the first is now obtained:

$$H_2 = \sqrt{\frac{\frac{H_1^2}{\sigma_1} |\mathbf{C}_G + \mathbf{U}|_1 b_1 - \frac{\Delta_c K_D H_1^2 |\mathbf{C}_G + \mathbf{U}|_1}{2\sigma_1 h_1} + \frac{\Delta_c K_D \Gamma^2 h_1 |\mathbf{C}_G + \mathbf{U}|_1}{2\sigma_1} + \frac{\Delta_c K_D \Gamma^2 h_2 |\mathbf{C}_G + \mathbf{U}|_2}{2\sigma_2}}{\frac{1}{\sigma_2} |\mathbf{C}_G + \mathbf{U}|_2 b_2 + \frac{\Delta_c K_D |\mathbf{C}_G + \mathbf{U}|_2}{2\sigma_2 h_2}}} \quad (5.87)$$

$$H_2 = \sqrt{\frac{\frac{|\mathbf{C}_G + \mathbf{U}|_1}{\sigma_1} \left(H_1^2 b_1 - \frac{\Delta_c K_D H_1^2}{2h_1} + \frac{\Delta_c K_D \Gamma^2 h_1}{2} \right) + \frac{\Delta_c K_D \Gamma^2 h_2 |\mathbf{C}_G + \mathbf{U}|_2}{2\sigma_2}}{\frac{1}{\sigma_2} |\mathbf{C}_G + \mathbf{U}|_2 \left(b_2 + \frac{\Delta_c K_D}{2h_2} \right)}} \quad (5.88)$$

Equation (5.88) can be used to progressively calculate broken wave height in the surf zone starting at the insipience point where the wave height is known. The selection of an appropriate insipience point is examined in Section 5.7. If the wave height at any stage drops below the stable wave height the breaking terms are deactivated. In contrast to Equation (5.77) no iteration is required on Equation (5.88).

5.7 Selection of Insipience Criterion for Wave Breaking In Wave Energy

Methodology

A number of authors including Weggel (1972) have examined criterion for selection of the insipience point. Four such methods for obtaining the insipient wave height are discussed in this section.

5.7.1 Simple relationship between Water Depth and Wave Height

The simplest form of equation to describe maximum wave height is a linear relationship between water depth and wave height. This method enjoys widespread use because of its simplicity. It has been discussed and used by authors such as Mei *et al.* (2005), Zhao *et al.* (2001), Péchon *et al.* (1997), Mei and Angelides (1977), Liu and Mei (1976), Newell *et al.* (2005b) and Newell and Mullarkey (2007b). Newell and Mullarkey (2007a) examine this among other methods in a sensitivity analysis of wave-driven current models. The relationship may be described as follows:

$$H_m = \gamma_0 d \quad (5.89)$$

A value of approximately 0.78-0.8 has gained widespread acceptance as an appropriate value for γ_0 in the absence of available measured data.

5.7.2 Miche (1954) Insipience Criterion

Weggel (1972) and Zhao *et al.* (2001) present the criteria of Miche (1954). In Section 3.12.3.1 this criteria was introduced to define the maximum stable wave height for the Battjes and Janssen (1978). Weggel (1972) also presents the same formula for use in selection of an insipience point for other methods of wave breaking such as that of Dally *et al.* (1985). The Miche (1954) formula is also based on the selection of a parameter γ_0 . Equation (3.1030) gives the relationship between the wave height and depth as:

$$H_m = \frac{0.88}{\kappa} \tanh \left[\frac{\gamma_0}{0.88} \kappa d \right]$$

Zhao *et al.* (2001) suggest a value of 0.8 for γ_0 . Newell and Mullarkey (2007a) use a value of 0.78. As stated in Section 5.7.1, above, values in the region of approximately 0.78-0.8 have gained widespread acceptance as appropriate in the absence of available measured data.

5.7.3 Miche (1954) Insipience Criterion including the effects of Wave Steepness

Battjes and Stive (1985) present an empirical formula to obtain a breaker index $\hat{\gamma}$ based on the steepness of the wave in question. The formula for this breaker index proposed by Battjes and Stive (1985) is as follows:

$$\hat{\gamma} = 0.5 + 0.4 \tanh(33s_0) \quad (5.90)$$

Where s_0 is the deep-water wave steepness defined as:

$$s_0 = \frac{H_0}{L_0} \quad (5.91)$$

Incorporating this wave steepness dependant breaker index into the Miche (1954) formula gives:

$$H_m = \frac{0.88}{\kappa} \tanh\left[\frac{\hat{\gamma}}{0.88} \kappa h\right] \quad (5.92)$$

5.7.4 Dally (1990) Insipience Criterion

Dally (1990) proposes a different breaking criterion also based on wave steepness. The expression is described as follows:

$$\hat{\gamma} = b(m_b) - 0.0827a(m_b)s_0^{4/5} \quad (5.93)$$

$$H_m = \hat{\gamma}h \quad (5.94)$$

Where m_b is the slope of the beach and $b(m_b)$ and $a(m_b)$ are functions of wave steepness. They are defined as follows by Smith (2003):

$$a(m_b) = 43.8(1 - e^{-19m}) \quad (5.95)$$

$$b(m_b) = \frac{1.56}{1 + e^{-19.5m}} \quad (5.96)$$

5.8 Calculation of Input Terms Required for Wave Energy Methodology

In order to carry out the wave energy method described above it is necessary to have certain initial data. The following data is readily obtainable for the domain:

- The Current, U
- The Depth, h
- The Chosen Width between Rays, b
- The Dally *et al.* (1985) empirical parameters, Γ , K_D
- The Battjes and Janssen (1978) empirical parameter, α

The following data can be obtained using the NM-WCIM:

- CC_g
- σ

This leaves one unknown input parameter; $\frac{\partial S_\phi}{\partial x}$. This can be readily obtained using the velocity potential results of the NM-WCIM as shown by Clyne (2008). Starting with Equation (3.135):

$$\phi = A_\phi e^{iS_\phi}$$

The gradient of Equation (3.135) is:

$$\nabla \phi = \nabla A_\phi e^{iS_\phi} + i \nabla S_\phi A_\phi e^{iS_\phi} \quad (5.97)$$

Isolating the gradient of S_ϕ yields:

$$\nabla S_\phi = \frac{\nabla \phi - \nabla A_\phi e^{iS_\phi}}{i A_\phi e^{iS_\phi}} \quad (5.98)$$

$$\nabla S_\phi = \frac{\nabla \phi - \nabla A_\phi A_\phi^{-1} \phi}{i \phi} \quad (5.99)$$

Splitting the velocity potential into its real and imaginary components gives:

$$\phi = \phi_1 + i \phi_2 \quad (5.100)$$

Using Equation (5.100) with Equation (5.99) gives:

$$\nabla S_\phi = \frac{\nabla \phi_1 + i \nabla \phi_2 - \nabla A_\phi A_\phi^{-1} \phi_1 - i \nabla A_\phi A_\phi^{-1} \phi_2}{i \phi_1 - \phi_2} \quad (5.101)$$

Multiplying above and below the line by the complex conjugate of the denominator yields:

$$\nabla S_\phi = \frac{(-i \phi_1 - \phi_2) [\nabla \phi_1 + i \nabla \phi_2 - \nabla A_\phi A_\phi^{-1} \phi_1 - i \nabla A_\phi A_\phi^{-1} \phi_2]}{\phi_1^2 + \phi_2^2} \quad (5.102)$$

$$\nabla S_\phi = \frac{\begin{bmatrix} -i \phi_1 \nabla \phi_1 + \phi_1 \nabla \phi_2 + i \phi_1^2 \nabla A_\phi A_\phi^{-1} - \phi_1 \phi_2 \nabla A_\phi A_\phi^{-1} \\ -\phi_2 \nabla \phi_1 - i \phi_2 \nabla \phi_2 + \phi_1 \phi_2 \nabla A_\phi A_\phi^{-1} + i \phi_2^2 \nabla A_\phi A_\phi^{-1} \end{bmatrix}}{\phi_1^2 + \phi_2^2} \quad (5.103)$$

Expanding the magnitude of the velocity potential in Equation (3.135) gives:

$$|\phi| = A_\phi \left| e^{i S_\phi} \right| \quad (5.104)$$

Using Equation (5.100) with Equation (5.104) gives:

$$\sqrt{\phi_1^2 + \phi_2^2} = A_\phi \sqrt{\cos^2 S_\phi + \sin^2 S_\phi} \quad (5.105)$$

Therefore:

$$\sqrt{\phi_1^2 + \phi_2^2} = A_\phi \quad (5.106)$$

Squaring both sides of Equation (5.106) gives:

$$\phi_1^2 + \phi_2^2 = A_\phi^2 \quad (5.107)$$

Equation (5.103) can be written as follows using the result of Equation (5.107):

$$\nabla S_\phi = \frac{\phi_1 \nabla \phi_2 - \phi_2 \nabla \phi_1}{\phi_1^2 + \phi_2^2} + \frac{[-i \phi_1 \nabla \phi_1 - i \phi_2 \nabla \phi_2 + i \nabla A_\phi A_\phi^{-1} (A_\phi^2)]}{A_\phi^2} \quad (5.108)$$

Carrying out a derivation on Equation (5.107) gives:

$$2 \phi_1 \nabla \phi_1 + 2 \phi_2 \nabla \phi_2 = 2 A_\phi \nabla A_\phi \quad (5.109)$$

$$\phi_1 \nabla \phi_1 + \phi_2 \nabla \phi_2 = A_\phi \nabla A_\phi \quad (5.110)$$

Using Equation (5.110) with Equation (5.109) yields the following:

$$\nabla S_\phi = \frac{\phi_1 \nabla \phi_2 - \phi_2 \nabla \phi_1}{\phi_1^2 + \phi_2^2} + \frac{[-i(A_\phi \nabla A_\phi) + iA_\phi \nabla A_\phi]}{A_\phi^2} \quad (5.111)$$

$$\nabla S_\phi = \frac{\phi_1 \nabla \phi_2 - \phi_2 \nabla \phi_1}{\phi_1^2 + \phi_2^2} \quad (5.112)$$

Equation (5.112) represents an equation using which the gradient of wave phase can be obtained from the velocity potential results of the NM-WCIM. (Acknowledging that, from Equation (3.721), in the case of the Helmholtz version of the model $\frac{\phi'}{\sqrt{CC_g}} = \phi$).

The magnitude of ∇S_ϕ can be obtained from Equation (5.112):

$$|\nabla S_\phi| = \frac{|\phi_1 \nabla \phi_2 - \phi_2 \nabla \phi_1|}{\phi_1^2 + \phi_2^2} \quad (5.113)$$

Equation (5.113) can be expanded as follows:

$$|\nabla S_\phi| = \frac{\left| \left(\phi_1 \frac{\partial \phi_2}{\partial x_1} - \phi_2 \frac{\partial \phi_1}{\partial x_1}, \phi_1 \frac{\partial \phi_2}{\partial x_2} - \phi_2 \frac{\partial \phi_1}{\partial x_2} \right) \right|}{\phi_1^2 + \phi_2^2} \quad (5.114)$$

Further expansion yields:

$$|\nabla S_\phi| = \frac{\sqrt{\left(\phi_1 \frac{\partial \phi_2}{\partial x_1} - \phi_2 \frac{\partial \phi_1}{\partial x_1} \right)^2 + \left(\phi_1 \frac{\partial \phi_2}{\partial x_2} - \phi_2 \frac{\partial \phi_1}{\partial x_2} \right)^2}}{\phi_1^2 + \phi_2^2} \quad (5.115)$$

Expanding the squared terms in Equation (5.115) gives:

$$|\nabla S_\phi| = \frac{\sqrt{\phi_1^2 \left(\frac{\partial \phi_2}{\partial x_1} \right)^2 - 2\phi_1 \phi_2 \frac{\partial \phi_1}{\partial x_1} \frac{\partial \phi_2}{\partial x_1} + \phi_2^2 \left(\frac{\partial \phi_1}{\partial x_1} \right)^2 + \phi_1^2 \left(\frac{\partial \phi_2}{\partial x_2} \right)^2 - 2\phi_1 \phi_2 \frac{\partial \phi_1}{\partial x_2} \frac{\partial \phi_2}{\partial x_2} + \phi_2^2 \left(\frac{\partial \phi_1}{\partial x_2} \right)^2}}{\phi_1^2 + \phi_2^2} \quad (5.116)$$

Equation (5.116) can be written as follows:

$$|\nabla S_\phi| = \frac{\sqrt{\phi_1^2 \left[\left(\frac{\partial \phi_2}{\partial x_1} \right)^2 + \left(\frac{\partial \phi_2}{\partial x_2} \right)^2 \right] - 2\phi_1\phi_2 \left[\frac{\partial \phi_1}{\partial x_1} \frac{\partial \phi_2}{\partial x_1} + \frac{\partial \phi_1}{\partial x_2} \frac{\partial \phi_2}{\partial x_2} \right] + \phi_2^2 \left[\left(\frac{\partial \phi_1}{\partial x_2} \right)^2 + \left(\frac{\partial \phi_1}{\partial x_1} \right)^2 \right]}}{\phi_1^2 + \phi_2^2} \quad (5.117)$$

Using Equation (5.117) the following can be stated:

$$\frac{\nabla S_\phi}{|\nabla S_\phi|} = \frac{\frac{\partial S_\phi}{\partial x_j} \phi_1 \frac{\partial \phi_2}{\partial x_j} - \phi_2 \frac{\partial \phi_1}{\partial x_j}}{\left| \frac{\partial S_\phi}{\partial x_i} \hat{\mathbf{e}}_i \right| \sqrt{\phi_1^2 \left[\left(\frac{\partial \phi_2}{\partial x_1} \right)^2 + \left(\frac{\partial \phi_2}{\partial x_2} \right)^2 \right] - 2\phi_1\phi_2 \left[\frac{\partial \phi_1}{\partial x_1} \frac{\partial \phi_2}{\partial x_1} + \frac{\partial \phi_1}{\partial x_2} \frac{\partial \phi_2}{\partial x_2} \right] + \phi_2^2 \left[\left(\frac{\partial \phi_1}{\partial x_2} \right)^2 + \left(\frac{\partial \phi_1}{\partial x_1} \right)^2 \right]}} \quad (5.118)$$

Section 5.7 has shown that all the required values for implementation of the Wave Energy Ray method can be obtained from an non-breaking run of the NM-WCIM.

Chapter 6: Results and Discussion

“Perfect numbers, like perfect men, are very rare,” René Descartes.

6.1 Introduction

This chapter examines the results of the one-dimensional and two-dimensional NM-WCIM and NM-WDHM for a selection of scenarios. The particular scenarios chosen are designed to examine the accuracy of the developed models in comparison with analytical formulae, measured data and published data from other numerical models. The chapter examines both the one-dimensional and two-dimensional versions of the NM-WCIM and NM-WDHM in comparison with published data. The final section of this chapter utilises the NM-WCIM and NM-WDHM for a case study of Casheen Bay situated on the west coast of Ireland.

For the purposes of this chapter a convention has been chosen for the direction of wave propagation. Unless otherwise stated, for models presented in this chapter, waves will propagate from right to left. The main exception to this convention is the case study of Casheen Bay where the plots are aligned to correspond with a northerly direction being towards the top of the page. In some cases it has been necessary to rotate or mirror results from other authors to match the convention used here.

6.2 Wave Height vs. Analytical

6.2.1 Introduction

The NM-WCIM is initially run for various waves propagating towards a beach of uniform slope. The results of these runs prove the accuracy of the basic wave model created. The diagrams below show a selection of these results displaying the accuracy of the NM-WCIM for waves propagating in the absence of a current.

6.2.2 Results

Figure 6.1 and Figure 6.2, below, show the amplitude of two different waves approaching a beach with a slope of 1 in 50. No breaking is evident on the graphs because in order to compare with the analytical shoaling formula of Mei *et al.* (2005) breaking effects are ignored. The effects of breaking are discussed in Section 3.12.3 above and are also examined in Section 6.4. Figure 6.3 and Figure 6.4 show a further two waves approaching a beach with a slope of 1 in 20. Similarly, breaking is neglected for this check of accuracy.

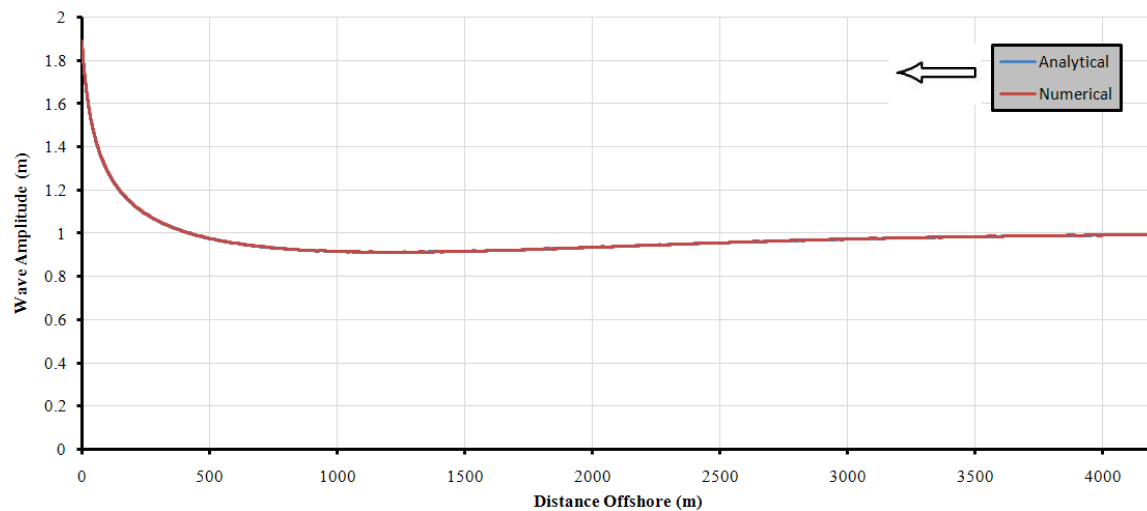


Figure 6.1 – Plot of Analytical vs. Numerical Wave Amplitude for a 1m wave of 10 second period at a deep-water angle of 0 degrees on a slope of 1 in 50. Waves propagate from right to left.

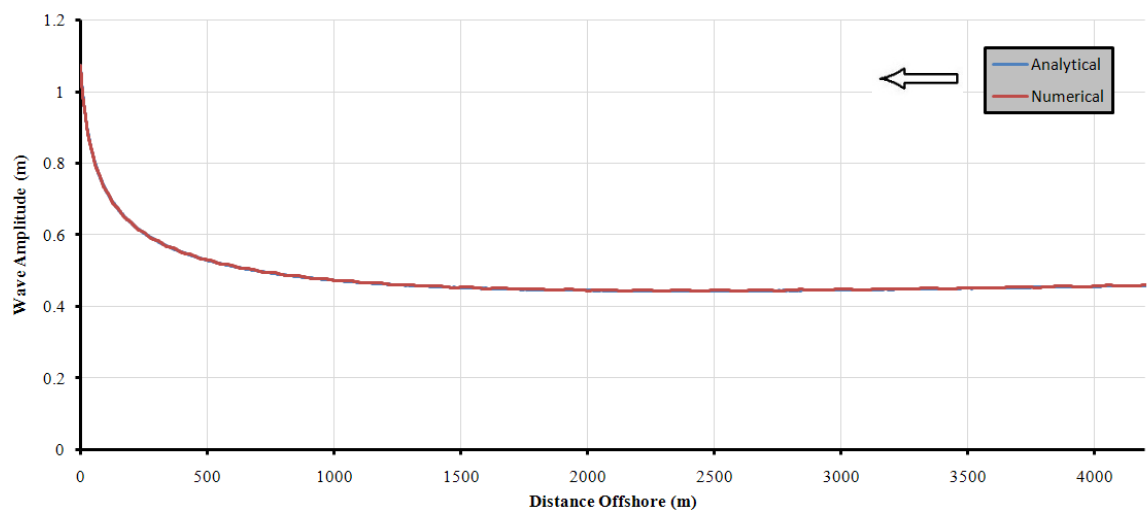


Figure 6.2 – Plot of Analytical vs. Numerical Wave Amplitude for a 0.5m wave of 15 second period at a deep-water angle of 30 degrees on a slope of 1 in 50. Waves propagate from right to left.

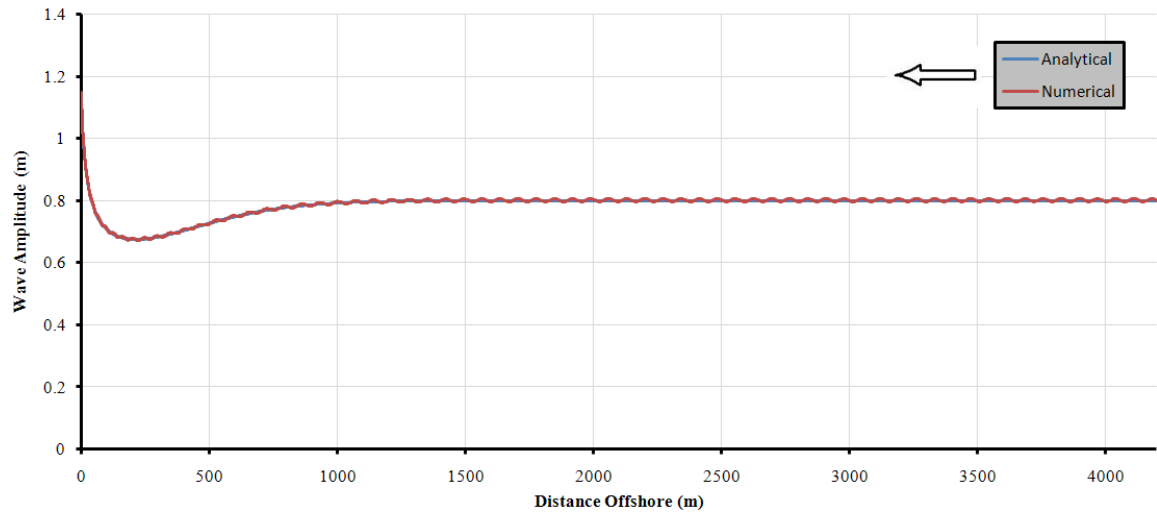


Figure 6.3 – Plot of Analytical vs. Numerical Wave Amplitude for a 0.8m wave of 8 second period at a deep-water angle of 45 degrees on a slope of 1 in 20. Waves propagate from right to left.

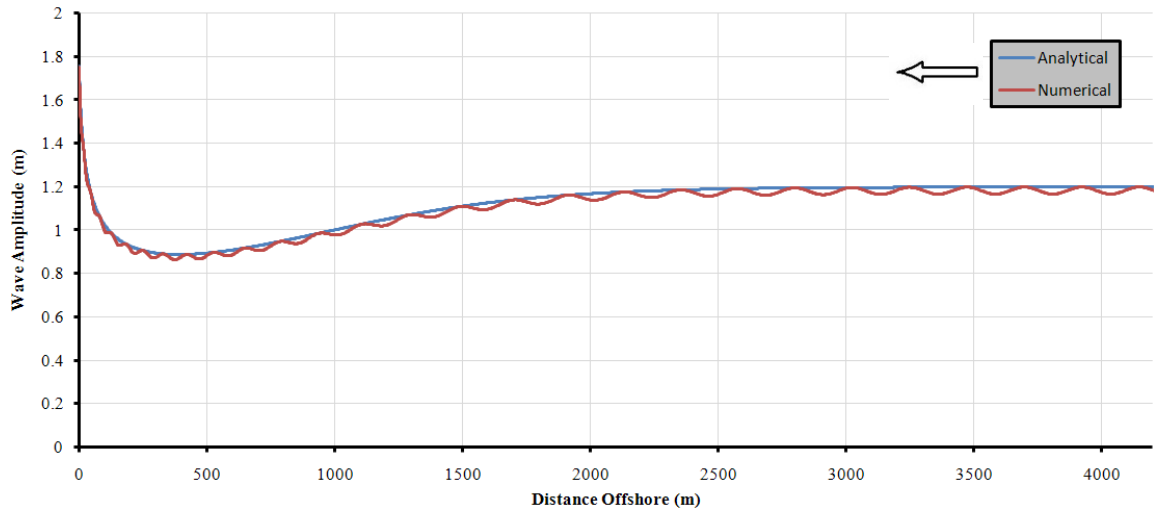


Figure 6.4 – Plot of Analytical vs. Numerical Wave Amplitude for a 1.2m wave of 12 second period at a deep-water angle of 60 degrees on a slope of 1 in 20. Waves propagate from right to left.

6.2.3 Discussion

The figures presented in this section show that the results of the NM-WCIM for wave propagation are in line with those expected from analytical theory. Figure 6.1 and Figure 6.2 above show that for small deep-water angles on gentle slopes the analytical and numerical results are indistinguishable. Figure 6.3 and Figure 6.4 show a slight degree of numerical variation in the results of the NM-WCIM caused by the quite large deep-water angle. This variation however is well within an acceptable range even up to the large angle of sixty degrees.

6.3 Wave Current Interaction vs. Mei *et al.* (2005) and Brevik and Aas (1980)

6.3.1 Introduction

Mei *et al.* (2005) and Brevik and Aas (1980) published plots showing the effective change of wave amplitude caused by wave-current interaction. These plots provided a good opportunity to test the accuracy of the NM-WCIM for wave propagation in the presence of a current. Section 6.3.2 examines the first plot of Mei *et al.* (2005) for waves at an angle to an assisting current and Section 6.3.3 examines the Brevik and Aas (1980) plots for waves with a collinear current. Newell *et al.* (2005a) compare an early version of the NM-WCIM with these results.

6.3.2 Waves approaching a current at an angle

Mei *et al.* (2005) examine waves approaching an assisting current at an angle. Figure 6.6 shows the effect on wave amplitude of various magnitudes of current for eight different prevailing wave scenarios. Figure 6.5 shows a sketch of the model scenario to which Figure 6.6 relates. Figure 6.7 shows the results of this author versus those analytically obtained by Mei *et al.* (2005). Figure 6.9 shows the author's results extended to include the effects of a retarding current.

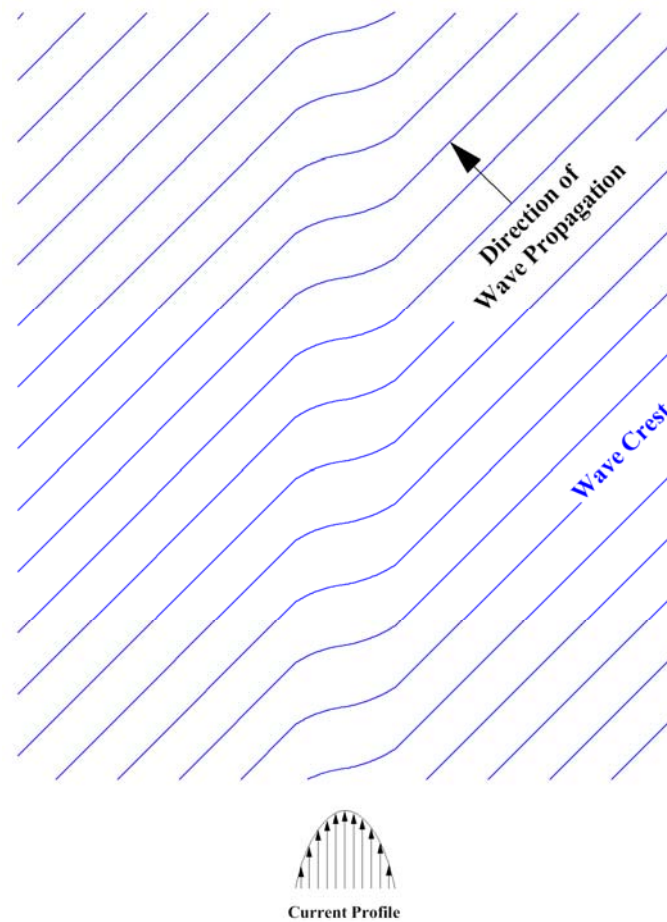


Figure 6.5 – Sketch of Wave Scenario Under Examination in Figure 6.6 for Current Assisting Wave Propagation

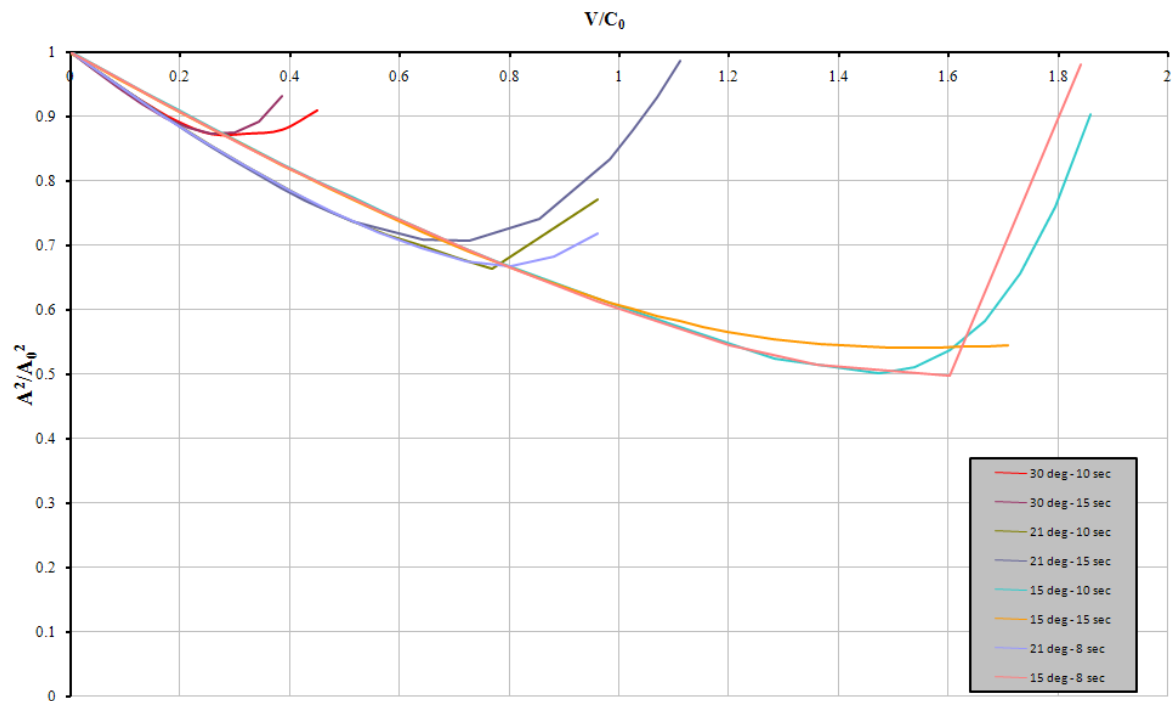


Figure 6.6 – Dimensionless Amplitude vs. Dimensionless Velocity values for Waves of Various Deep-Water Angle and Period.

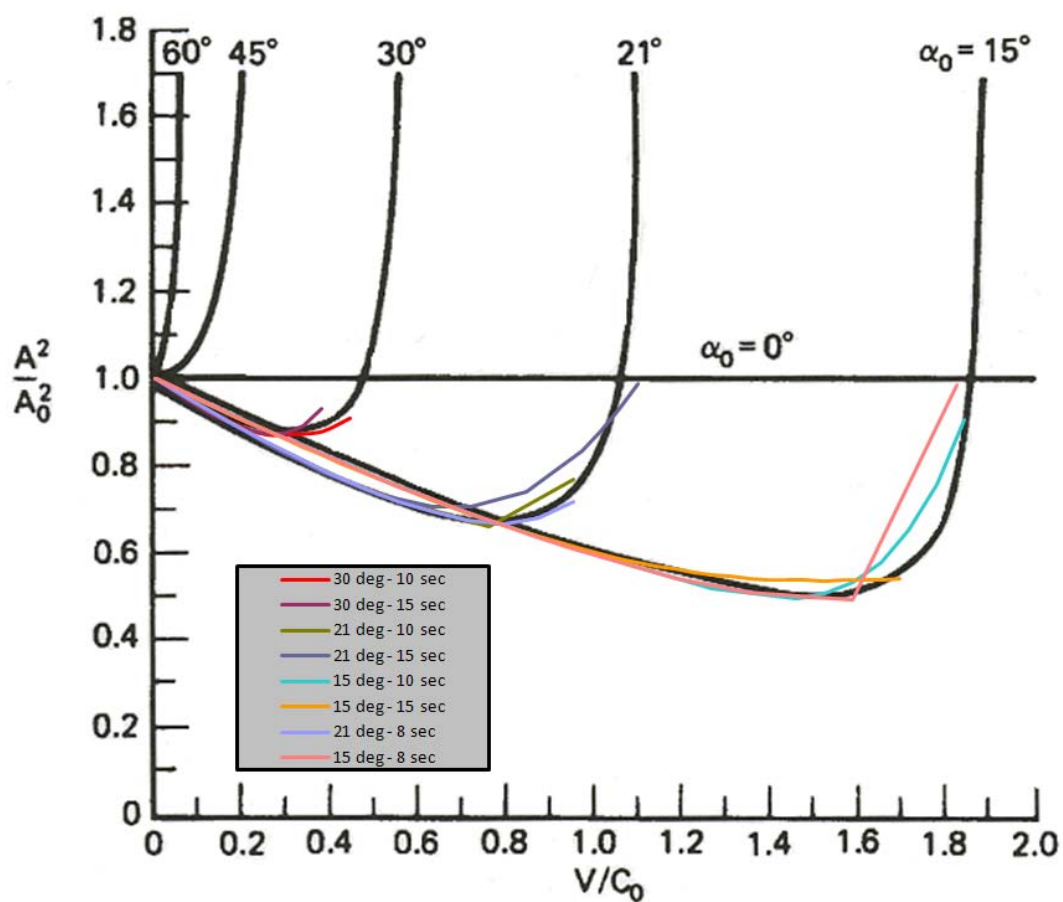


Figure 6.7 – Dimensionless Amplitude vs. Dimensionless Velocity values for Waves of Various Deep-Water Angle and Period plotted against similar results by Mei *et al.* (2005)

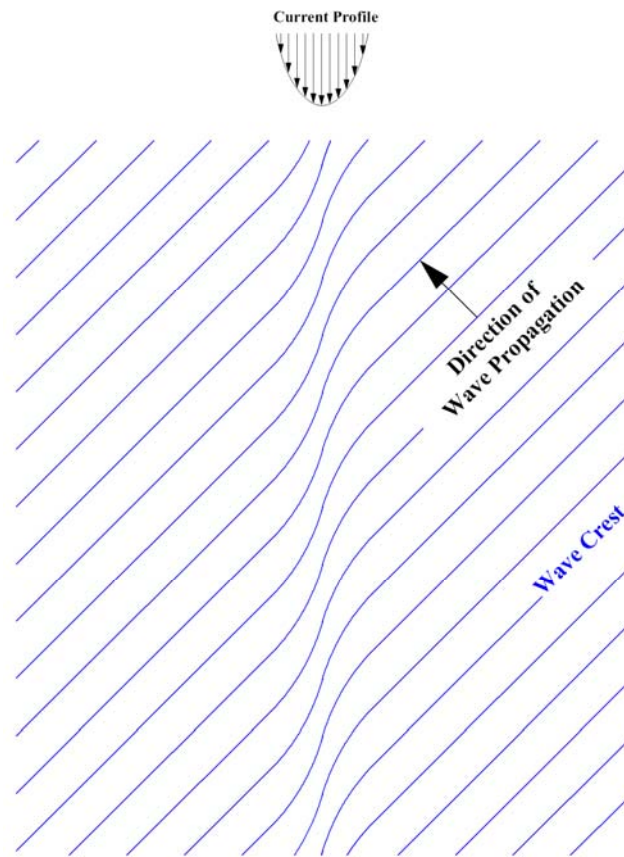


Figure 6.8 – Sketch of Wave Scenario with Current Retarding Wave Propagation leading to the Upper Left Portion of Figure 6.9

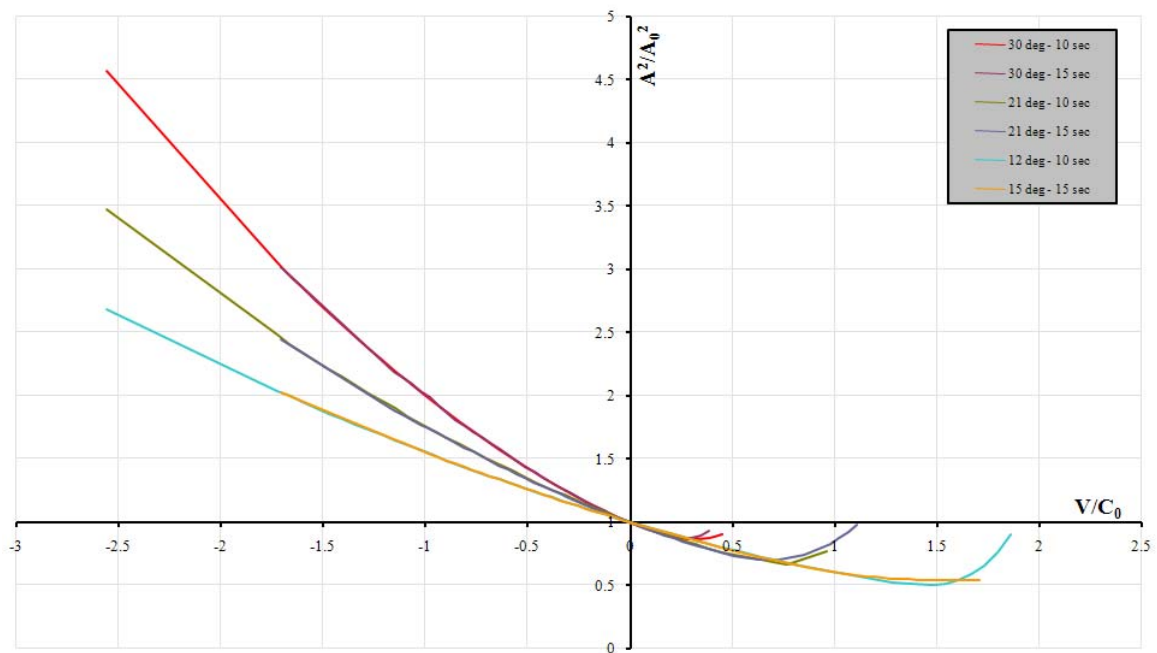


Figure 6.9 - Dimensionless Amplitude vs. Dimensionless Velocity values for Waves of various Deep-Water Angles and Periods extended to include Retarding Currents.

6.3.3 Waves with a Co-linear Current

Brevik and Aas (1980) examined the effect of co-linear currents on wavelength and amplitude. Sketchs of this scenario are showing in Figure 6.10 and Figure 6.11. Current both directly in line with the direction of wave propagation and exactly against the direction of wave propagation are examined. Figure 6.12 shows the effect on wavelength of various magnitudes of current for three different wave scenarios obtained numerically by this author and analytically by Brevik and Aas (1980). Figure 6.13 shows the effect on wave amplitude of various magnitudes of current for the same wave scenarios, again obtained numerically by this author and analytically by Brevik and Aas (1980).

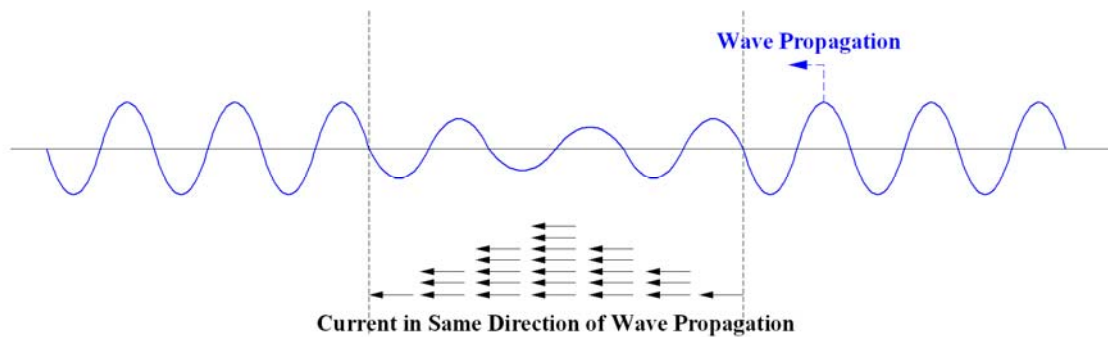


Figure 6.10 – Sketch of Wave Propagation in the Presence of a Co-linear Assisting Current

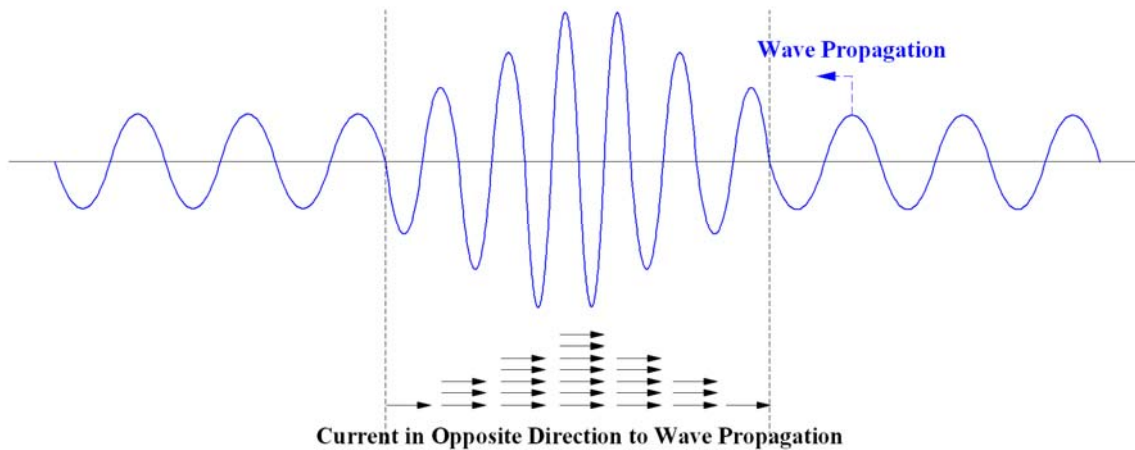


Figure 6.11 – Sketch of Wave Propagation in the Presence of a Co-linear Retarding Current

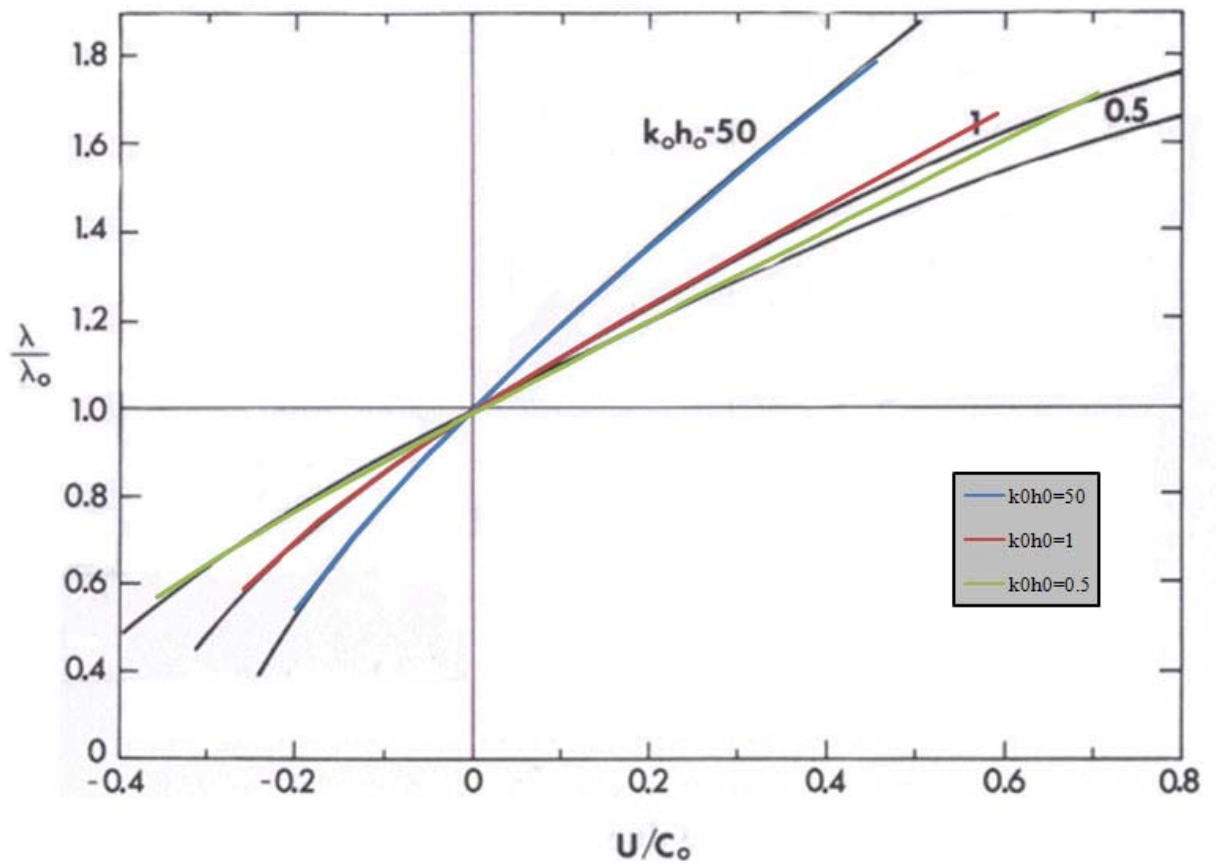


Figure 6.12 – Dimensionless Wavelength versus Dimensionless Co-linear Current for three different waves compared with the results of Brevik and Aas (1980)

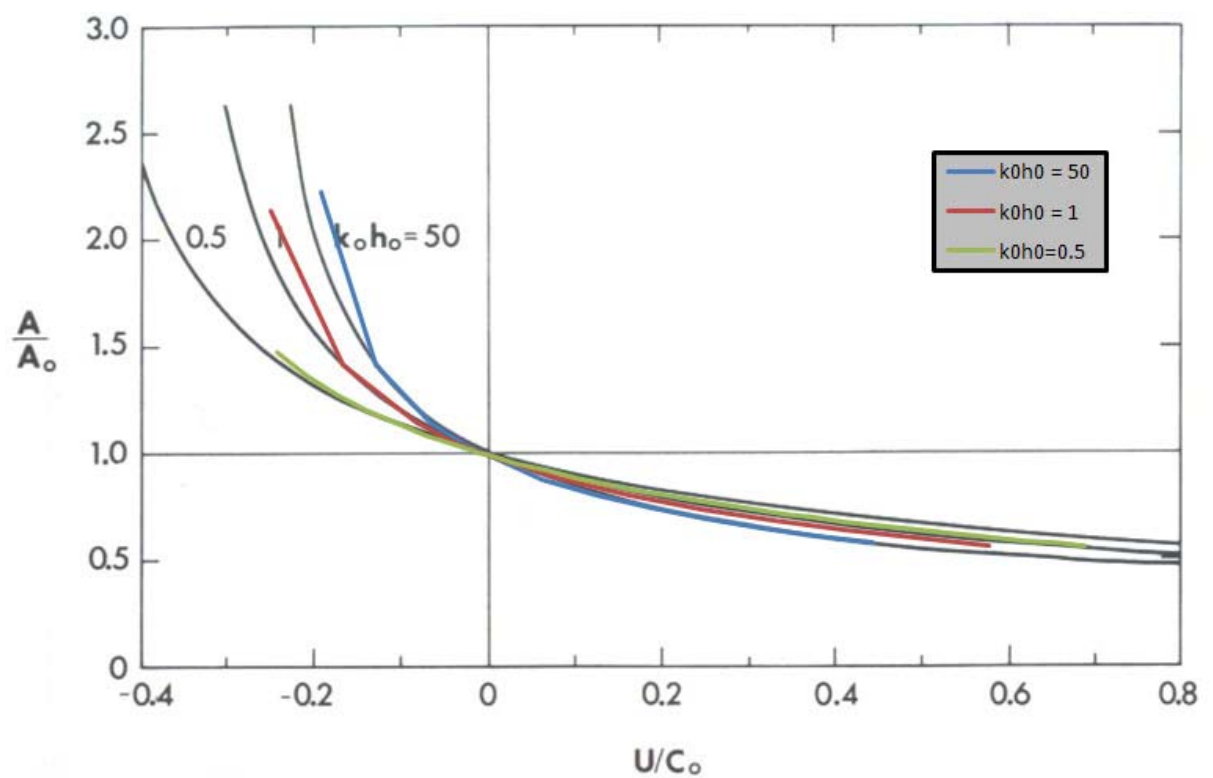


Figure 6.13 - Dimensionless Wave Amplitude versus Dimensionless Co-linear Current for three different waves compared with the results of Brevik and Aas (1980)

6.3.4 Discussion

Figures Figure 6.6 and Figure 6.7 show a good comparison between the numerical results of the NM-WCIM and the analytical solution of Mei *et al.* (2005). There is some variation in results when the plotted lines return towards a scaled amplitude of unity. This is to be expected because in this region the magnitude of the current with respect to the wave direction and size is very large. This particular scenario would be a very rare occurrence in nature and is at the outer bounds of what would be expected from a numerical model. It should also be pointed out that the section of the plot from the Mei *et al.* (2005) that extends above a scaled amplitude of unity represents a mathematically obtained asymptote and hence could not be obtained with a numerical model. The type of wave-current interaction scenario that would cause a result in this region is very unique. Figure 6.9 shows an extension of the plot, using the NM-WCIM, to include the effects of a retarding current on the wave train. As expected the magnitude of wave amplitude increases as the retarding effect of the current increases.

Figure 6.12 is a plot by Brevik and Aas (1980) showing the effects of a co-linear current on the wave-length of three different wave trains. The results of the NM-WCIM for the same currents and wave-train are also plotted on this graph. In the presence of the retarding current there is good comparison between the values of the NM-WCIM and Brevik and Aas (1980). In the presence of an assisting current there is good comparison between the values for weaker currents. Figure 6.13 shows that in the presence of stronger assisting currents the results of the NM-WCIM and the Brevik and Aas (1980) analytical solution compare well for the $k_0 h_0 = 50$ solution. Some difference is evident in this region for the other two cases. In the case of a numerical model this would not be unexpected towards the extremities of the results. For a common wave period the case of $k_0 h_0 = 0.5$ represents a shallow water depth.

6.4 Different Breaker Methods

6.4.1 Introduction

Newell and Mullarkey (2007a) examine the sensitivity of the NM-WDHM to various breaking models, after Zhao *et al.* (2001), that are applied to the NM-WCIM. The results of Newell and Mullarkey (2007a) indicated that in order to get a clearly defined result of set-up/set-down it is necessary to use a breaking formula that gives a defined insipience point. The figures below examine breaking using a simple linear breaking relationship, the energy dissipation method of Battjes and Janssen (1978) discussed in Section 3.12.3.1 and the Dally *et al.* (1985) method of Section 5.6.2. In the case of the Dally *et al.* (1985) breaking methodology a number of different methods are examined for selection of the insipience point. The radiation stress for each scenario is calculated from the velocity potential results of the NM-WCIM with the appropriate breaking methodology implemented. The radiation stress values are used in the NM-WDHM to calculate set-up and set-down for the various breaking methodologies.

6.4.2 Results

Figure 6.14 shows the broken wave height for a wave with a deep-water wave height of 0.5m breaking on a beach slope of 1 in 50. The wave is propagating perpendicularly to the beach throughout. The six different breaking methodologies employed are detailed in Table 6.1 below. Figure 6.15 shows the set-up and set-down resulting from the wave heights plotted in Figure 6.14. Figure 6.16 examines the Miche (1954) formula for maximum stable wave height with a view to explaining why the third method in this section falls almost exactly in line with the second method.

Table 6.1 – Table of Different Breaking Methodologies used in Section 6.4

Method Number	Breaking Methodology	Insipience Point
1	Linear Relationship between Wave Height and Water Depth	$\gamma_0 = 0.78$
2	Dally <i>et al.</i> (1985)	$\gamma_0 = 0.78$
3	Dally <i>et al.</i> (1985)	Miche (1954) Criterion with $\gamma_0 = 0.78$
4	Dally <i>et al.</i> (1985)	Miche (1954) Criterion including Battjes and Stive (1985) Wave Steepness Criterion
5	Dally <i>et al.</i> (1985)	Dally (1990) criterion including Wave Steepness Criterion
6	Dally <i>et al.</i> (1985)	Average of Insipience points for Methods 3 & 4
7	Battjes and Janssen (1978)	<i>No Defined Insipience Point – Maximum Stable Height using Miche (1954) Criterion</i>

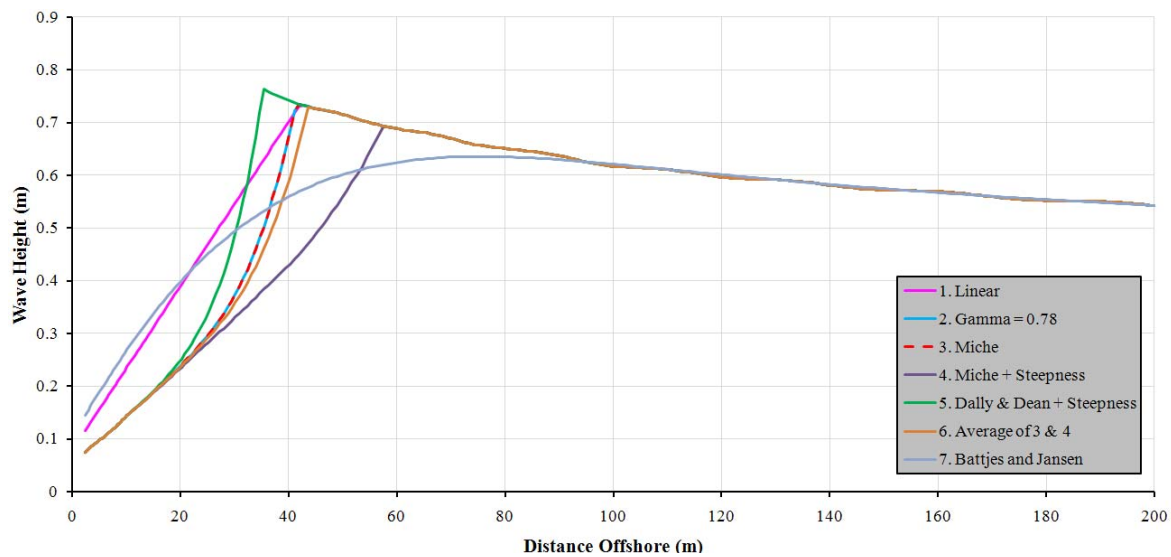


Figure 6.14 – Wave Height for different breaking methods on a wave of 0.5m Deep-Water Height breaking on a 1 in 50 slope. Waves propagate from right to left.

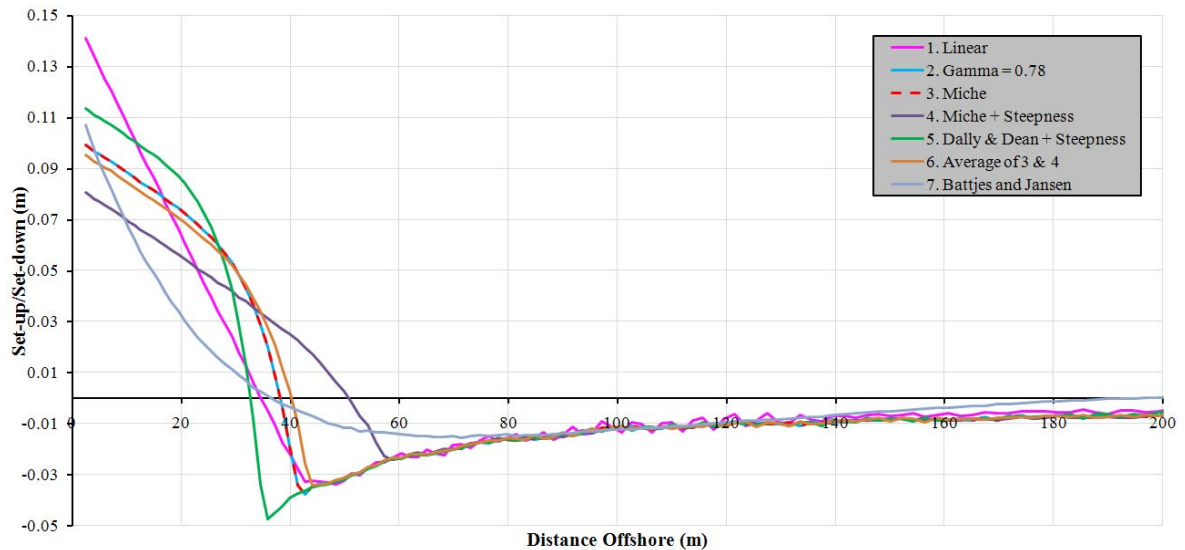


Figure 6.15 – Set-up/Set-down for different breaking methods for a wave of 0.5m Deep-Water Height breaking on a 1 in 50 slope

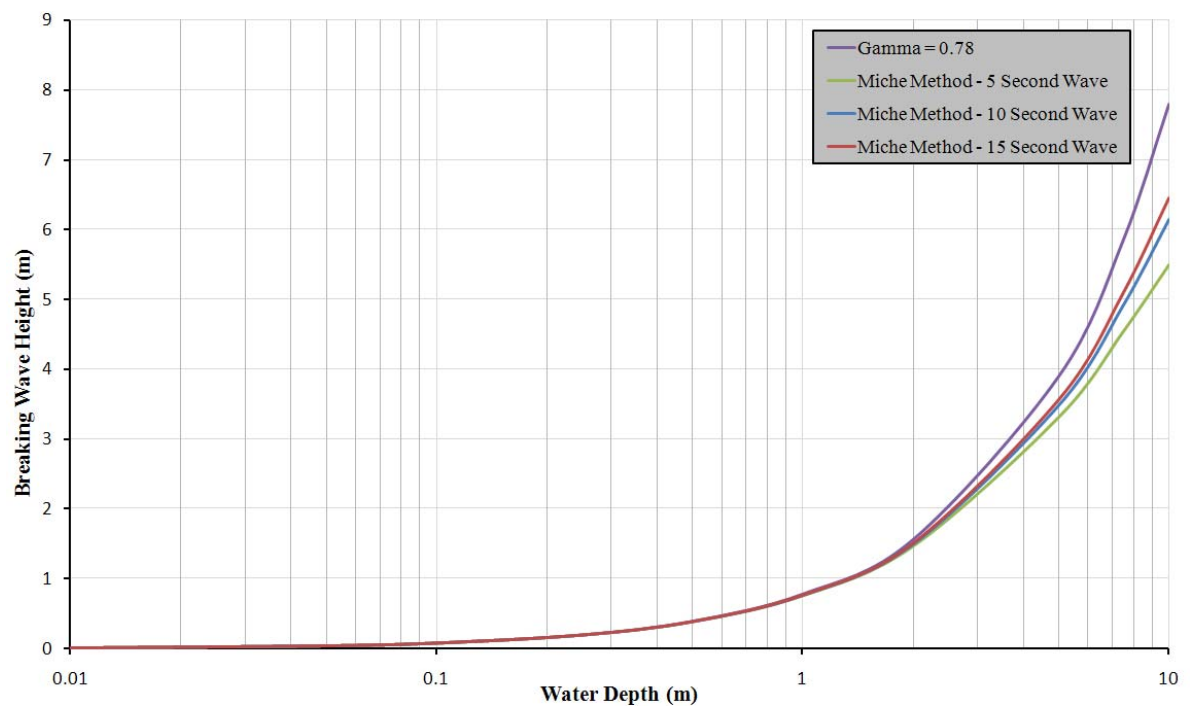


Figure 6.16 – Comparison of Breaking Wave height obtained for a given wave using the simple $\Gamma = 0.78$ formula and the Miche criterion for different Wave Periods.

6.4.3 Discussion

It is evident from the figures in this section that the choice of breaking methodology and maximum stable wave height has a significant effect on wave height obtained in the breaking zone. The results of Figure 6.15 show the corresponding difference caused in the set-up/set-down results though significant are not as dissimilar as the wave results in

Figure 6.14. It is evident in Figure 6.14 that in the majority of the breaker zone the wave height obtained using the linear breaking methodology is quite similar to that of the Battjes and Janssen (1978) method. The main difference being the defined peak in wave height using the linear method that is absent in the gentle change in wave height of the Battjes and Janssen (1978) method. The Dally *et al.* (1985) breaking methodology provides a concave effect on the wave heights in the surf-zone in contrast to the more convex approach of the Battjes and Janssen (1978) method. Considering the different types of breaking that can occur in a given situation (as discussed in Section 2.2.2.5) a decision on which breaking model to use should be guided by conditions at the site being examined. With regards to the insipience points it is clear that the Dally *et al.* (1985) method provides the highest sustainable wave height and the Miche (1954) criterion including Battjes and Stive (1985) wave steepness criterion provides the lowest. The Miche (1954) formula provides an incipient point very similar to the value of $\gamma_0 = 0.78$. Figure 6.16 shows why this is the case. The difference between the Miche (1954) formula and the simple linear relationship is very small for water depths below 1.5m and hence for waves with heights of up to 1m. This encompasses a large portion of waves in coastal regions.

Figure 6.15 shows the various shapes of set-up/set-down obtained using the breaking methods described above. It is clear that the maximum set-up and the maximum set-down are affected by the breaking model chosen. However, considering the overall accuracy expected from any model of this type the difference between any of the methods is not large with the possible exception of set-down driven by the Battjes and Janssen (1978) breaking method. The degree of set-down obtained by this method is quite small due to the lack of a defined insipience point. Radiation stress calculations are based on the gradients of velocity potential. The rapid change in gradient caused by a defined insipience point produces a much more significant set-down than the gradual change caused by breaking methods such as that of Battjes and Janssen (1978). Newell and Mullarkey (2007a) examine some other breaking models discussed by Zhao *et al.* (2001). The results of Newell and Mullarkey (2007a) suggest that the Battjes and Janssen (1978), Dally *et al.* (1985) and linear breaking methods are the most useful for obtaining radiation stress driving forces for a hydrodynamic model.

6.5 Turbulent Diffusion in NM-WDHM

6.5.1 Introduction

As discussed in Section 4.8 the two prevalent methods for energy dissipation due to turbulence in wave-driven current models are the simplified Longuet-Higgins (1970a) method which is suitable only for uniformly sloping beaches and the method of Battjes (1975) based on eddy viscosity which is useful in a more general context for varying bathymetry. The NM-WDHM has been developed to utilise either of these methodologies. Both the Longuet-Higgins (1970a) and the Battjes (1975) breaking methodologies contain an empirical parameter. The empirical parameter of Longuet-Higgins (1970a) has been titled N after Mei *et al.* (2005) and that of Battjes (1975) is M , as discussed in Section 4.7.2. The figures in this section demonstrate the effects of turbulence on a longshore current with varying values of the empirical parameter of each method. Also presented is an analytical plot by Longuet-Higgins (1970b) of similar data. Results of both the Longuet-Higgins (1970a) and the Battjes (1975) breaking methodologies are also compared with measured results from published data.

6.5.2 Results

Figure 6.17 shows a profile of longshore current for a wave of 1m deep-water height and 30° deep water angle on a slope of 1 in 50 in the presence of varying intensities of Longuet-Higgins (1970a) type turbulent diffusion. A thirty degree angle was used for the results in Figure 6.17 to Figure 6.20. (The intensity was altered by altering the empirical parameter, N .) Figure 6.18 shows a non-dimensional plot of the same scenario. Figure 6.19 shows a profile of longshore current for a wave of 1m deep-water height on a slope of 1 in 50 in the presence of varying intensities of Battjes (1975) type turbulent diffusion. (The intensity in this case was altered by altering the empirical parameter, M .) Figure 6.20 shows a non-dimensional plot of the same scenario.

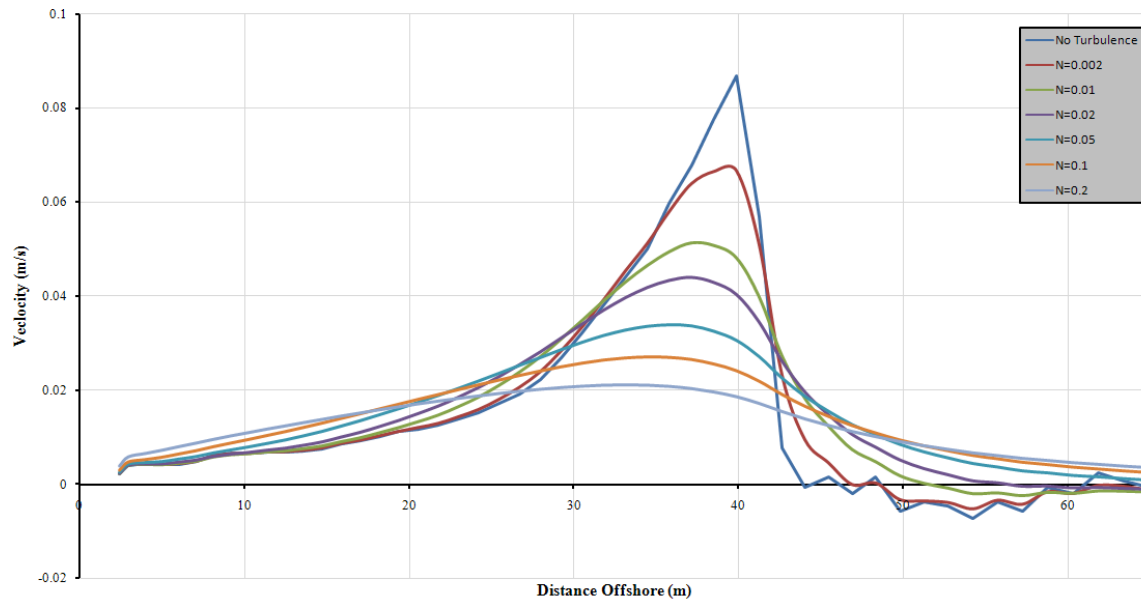


Figure 6.17 – Plot of Longshore Velocity versus Distance Offshore for a wave of 1m Deep-Water Height on a 1 in 50 slope with 30 degree incidence angle in the presence of Turbulent Diffusion after Longuet-Higgins (1970a)

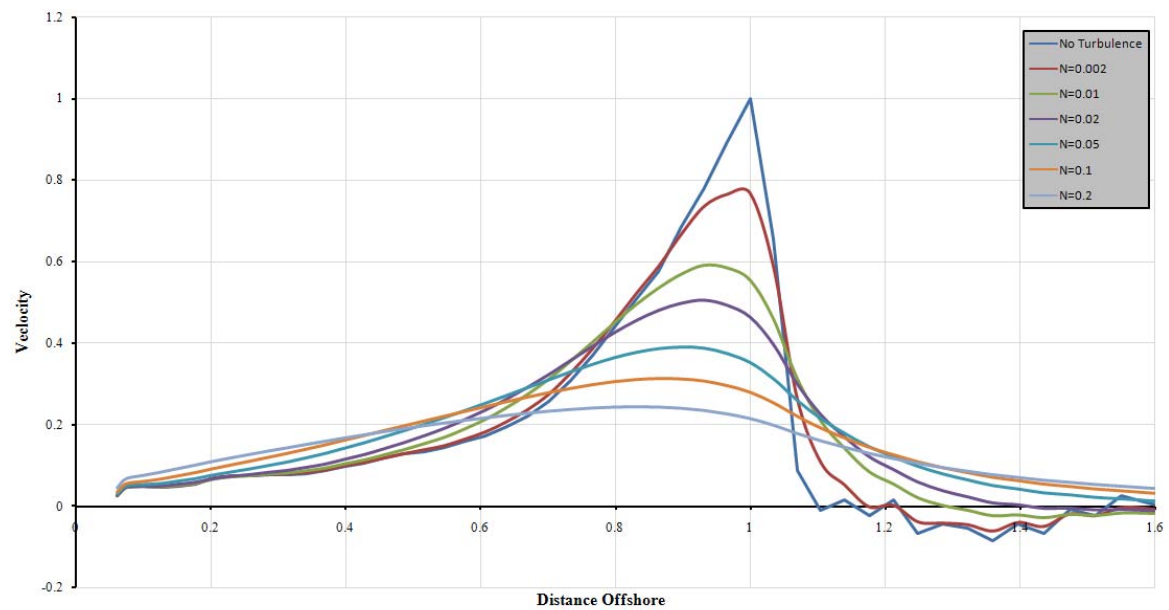


Figure 6.18 – Plot of Non-Dimensional Longshore Velocity versus Non-Dimensional Distance Offshore for a wave of 1m Deep-Water Height on a 1 in 50 slope with 30 degree incidence angle in the presence of Turbulent Diffusion after Longuet-Higgins (1970a)

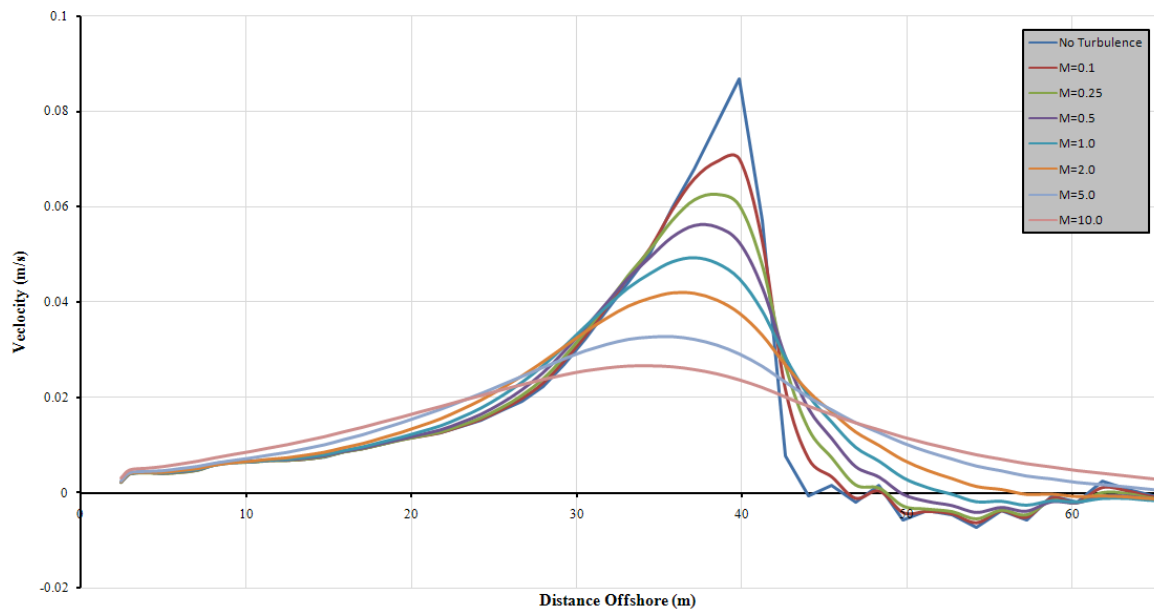


Figure 6.19 – Plot of Longshore Velocity versus Distance Offshore for a wave of 1m Deep-Water Height on a 1 in 50 slope with 30 degree incidence angle in the presence of Turbulent Diffusion after Battjes (1975)

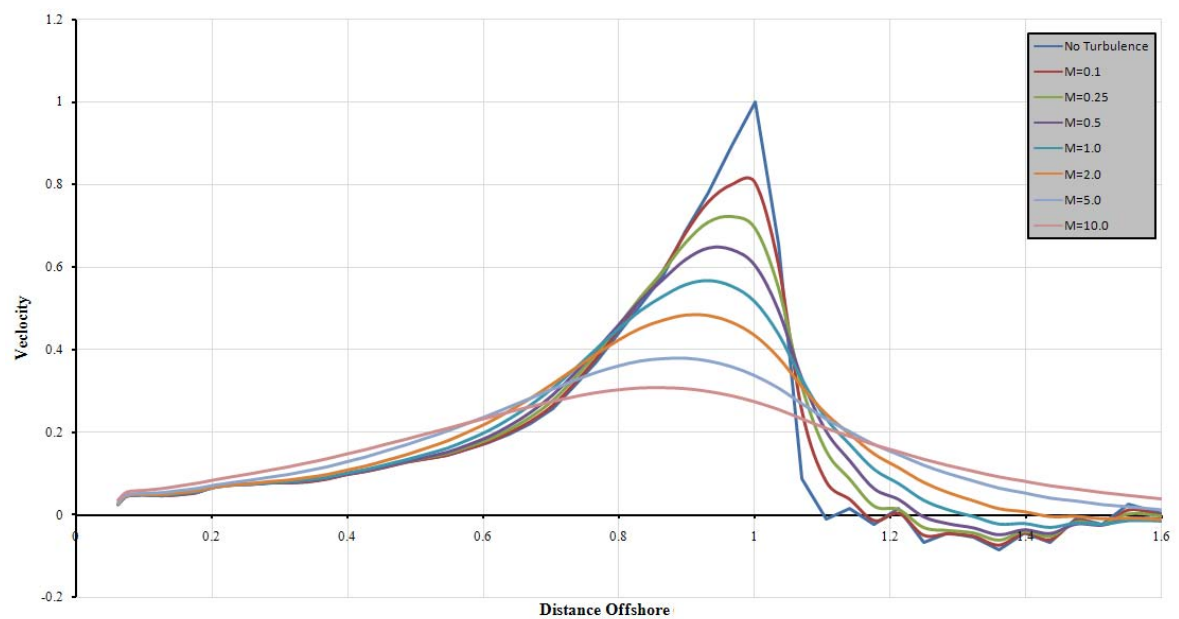


Figure 6.20 – Plot of Non-Dimensional Longshore Velocity versus Non-Dimensional Distance Offshore for a wave of 1m Deep-Water Height on a 1 in 50 slope with 30 degree incidence angle in the presence of Turbulent Diffusion after Battjes (1975)

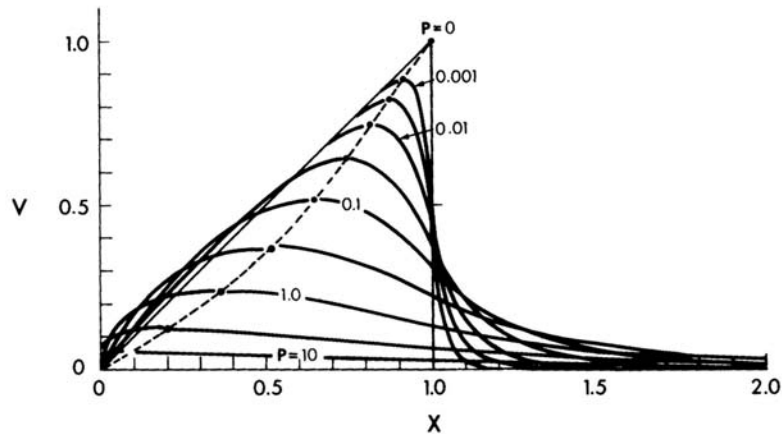


Figure 6.21 – Theoretical Form of Longshore Current from Longuet-Higgins (1970b)

Figure 6.22 to Figure 6.26 shows a similar set of non-dimensional results with an angle of incidence of five degrees. The results are compared with measured data from Kim (2004) after Sonu (1975) and with measured laboratory results of Hamilton and Ebersole (2001) for both the Longuet-Higgins (1970a) and the Battjes (1975) breaking methodologies.

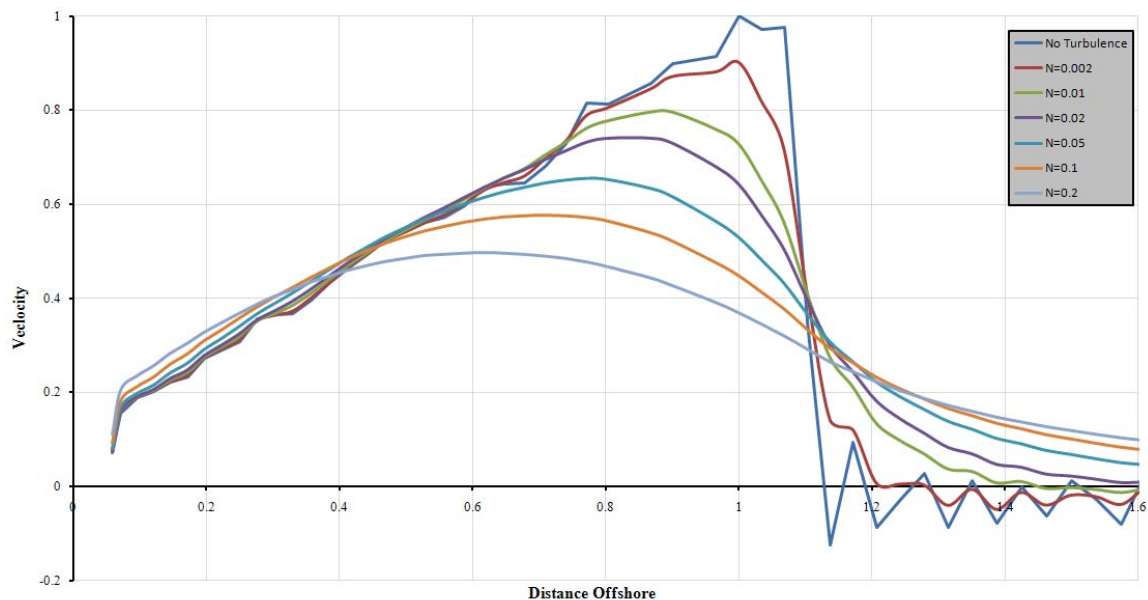


Figure 6.22 – Plot of Non-Dimensional Longshore Velocity versus Non-Dimensional Distance Offshore for a wave of 1m Deep-Water Height on a 1 in 50 slope with 5 degree incidence angle in the presence of Turbulent Diffusion after Battjes (1975)

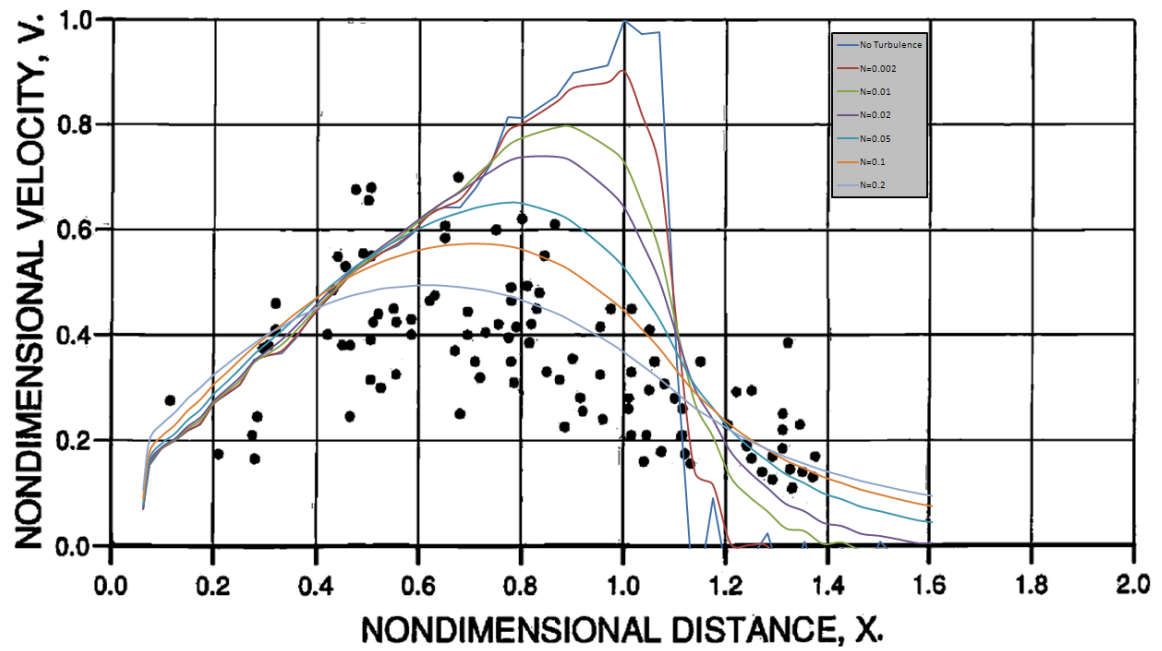


Figure 6.23 – Comparison of Non-Dimensional Longshore Velocity after Longuet-Higgins (1970a) and measured Longshore Velocity Values after Kim (2004) and Sonu (1975).

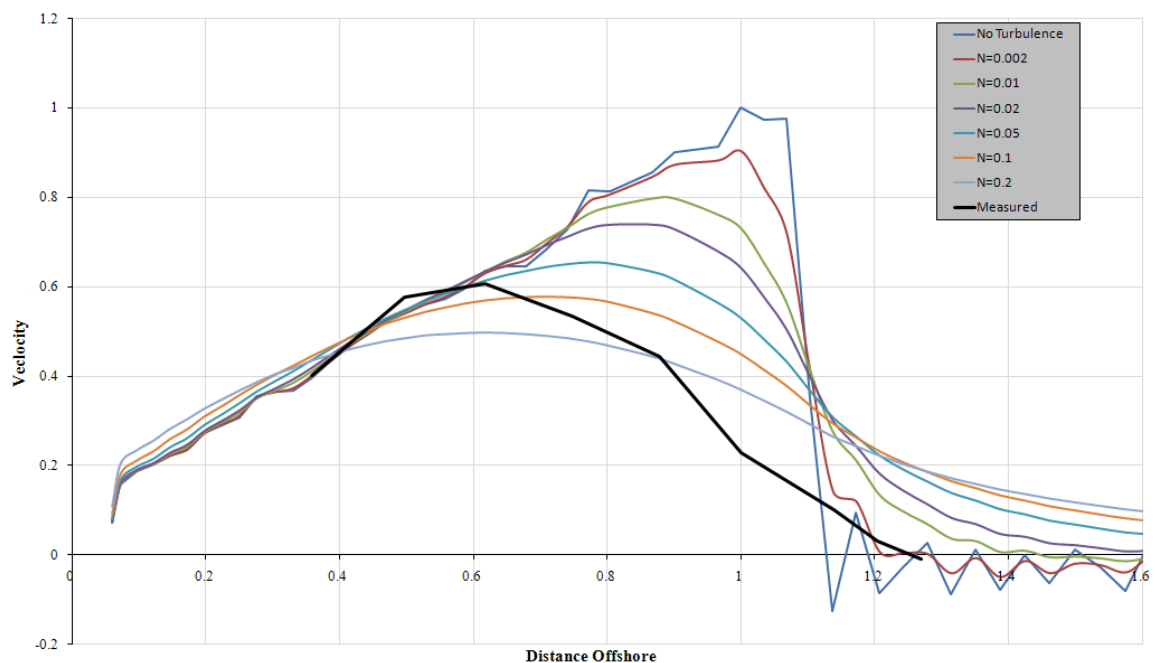


Figure 6.24 – Comparison of Non-Dimensional Longshore Velocity after Longuet-Higgins (1970a) and measured Longshore Velocity Values after Hamilton and Ebersole (2001)

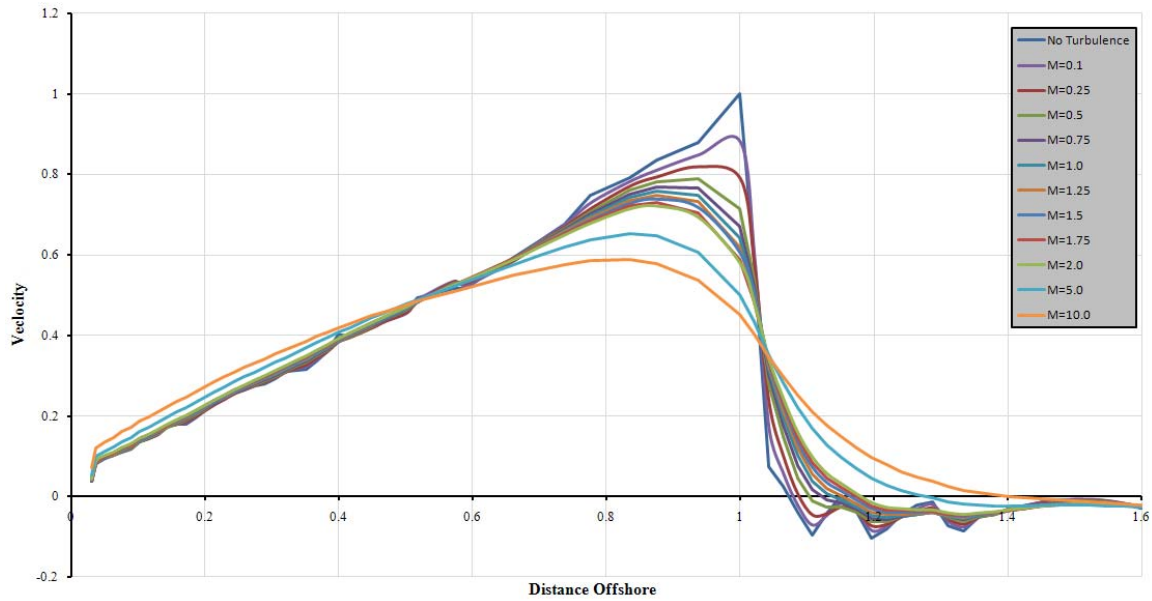


Figure 6.25 – Plot of Non-Dimensional Longshore Velocity versus Non-Dimensional Distance Offshore for a wave of 1m Deep-Water Height on a 1 in 50 slope with 5 degree incidence angle in the presence of Turbulent Diffusion after Battjes (1975)

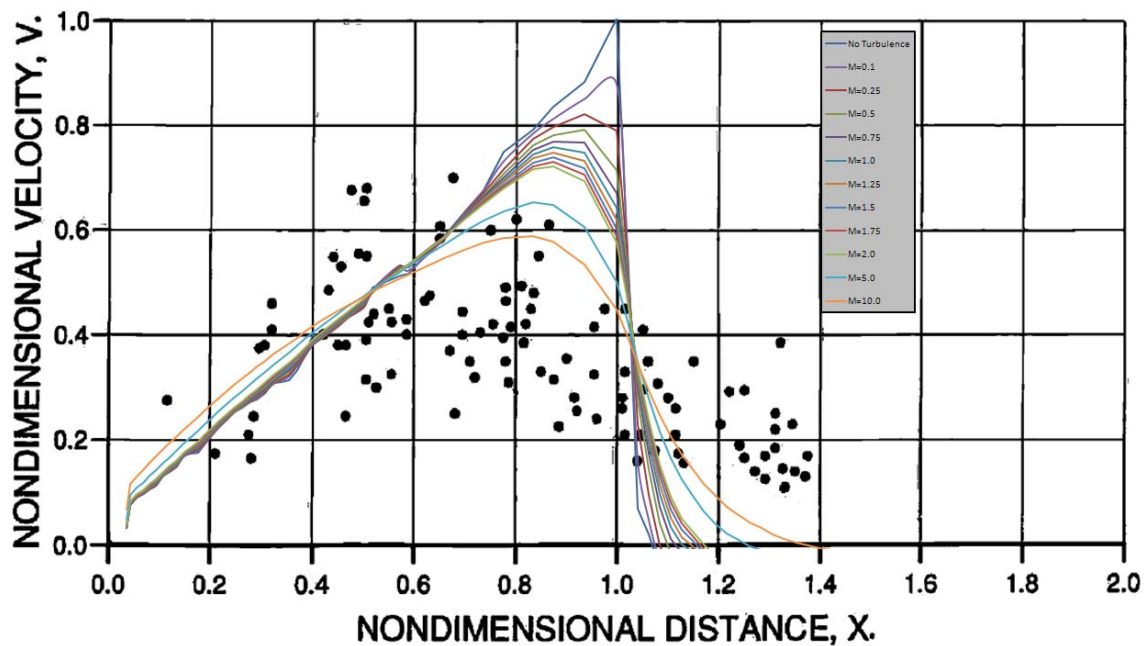


Figure 6.26 – Comparison of Non-Dimensional Longshore Velocity after Battjes (1975) and measured Longshore Velocity Values after Kim (2004) and Sonu (1975)

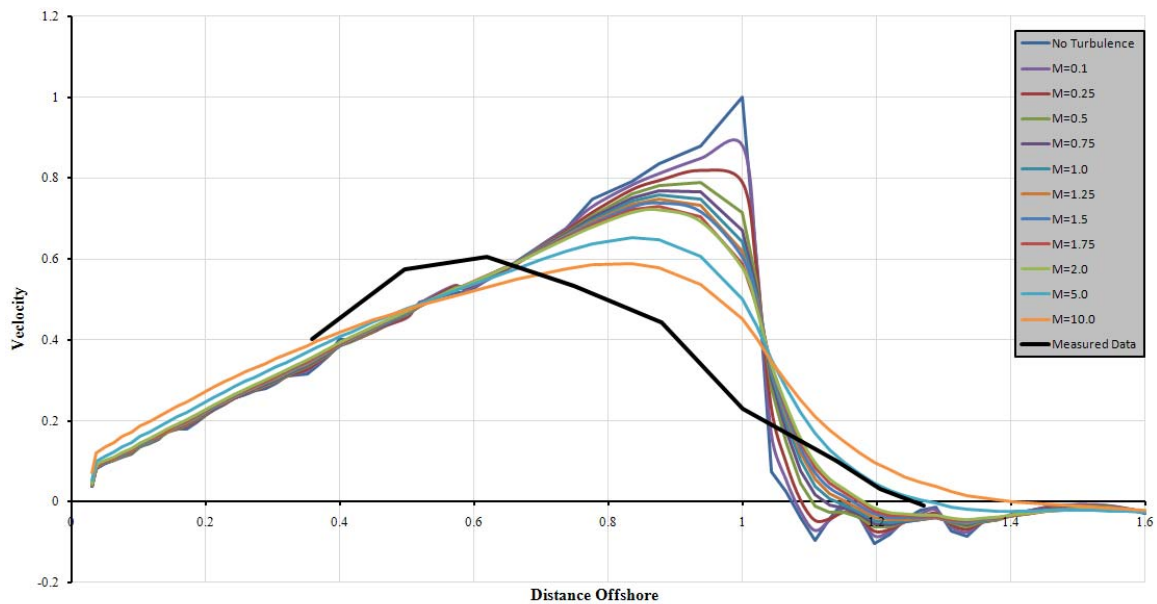


Figure 6.27 – Comparison of Non-Dimensional Longshore Velocity after Battjes (1975) and measured Longshore Velocity Values after Hamilton and Ebersole (2001)

6.5.3 Discussion

There is an apparent difference between the almost linear rise to peak velocity in Figure 6.21 and the more curved rise in the results in Figure 6.18 and Figure 6.20. This difference is not as apparent in Figure 6.22 or Figure 6.25. This would tend to indicate the angle of incidence of the wave has an effect on the obtained cross-shore profile of longshore current. The effect of varying the empirical factors in both the Longuet-Higgins (1970a) and the Battjes (1975) method provides the same spreading of lateral dispersion as that discussed by Longuet-Higgins (1970b). From inspection of Figure 6.20 and Figure 6.25 it is clear that for different angles of incidence the spreading effect of each empirical parameter is different. Similar empirical parameters appear to cause a larger degree of spread for higher angles of wave incidence. This effect is also apparent to a lesser degree when comparing Figure 6.18 and Figure 6.22.

In practice it is necessary to select an empirical factor that best matches the prevailing conditions. For a coastal site where measured longshore current data is available it is possible to calibrate the model against measured data to select an appropriate empirical factor. In the absence of such data the best estimate based on similar measurements elsewhere is chosen. Battjes (1975) suggests the value of M to be “of order one.” It is

further discussed by Battjes (1975) that most measured profiles of longshore current fell in the range of $0.0024 < N < 0.0096$ with M values approximately 27 times greater.

The comparisons between measured data and the results of this section show that the overall trend of spreading and reduction in peak of the idealised longshore current profile is in line with that experienced in nature. The results, however, further underline the necessity to choose appropriate empirical parameters for any given model. Figure 6.26 and Figure 6.27 show that a relatively high value of M is appropriate in the circumstances under examination. Similarly, appropriate N values for the same circumstances, shown in Figure 6.23 and Figure 6.24, are comparatively high.

6.6 Comparison of Set-up/Set-down with Bowen *et al.* (1968)

6.6.1 Introduction

Bowen *et al.* (1968) published measured set-up/set-down values for a laboratory wave. Newell and Mullarkey (2007b) published results of the NM-WDHM for the same scenario based on radiation stress values from the NM-WCIM. This result is reproduced below.

6.6.2 Results

Figure 6.28 below shows the set-up/set-down results for a measured wave of period 1.14 seconds and with a deep-water wave height of 6.45cm. The slope of the beach is 0.082. Included in the plot are the measured values of Bowen *et al.* (1968) as well as the results of the Bowen *et al.* (1968) theory. The results of the NM-WDHM for the same set of wave data is plotted in red. A linear breaking methodology was used and it was found for the case of this laboratory model that an insipience point of 1.1 provided the most accurate result. In this case waves propagate from left to right.

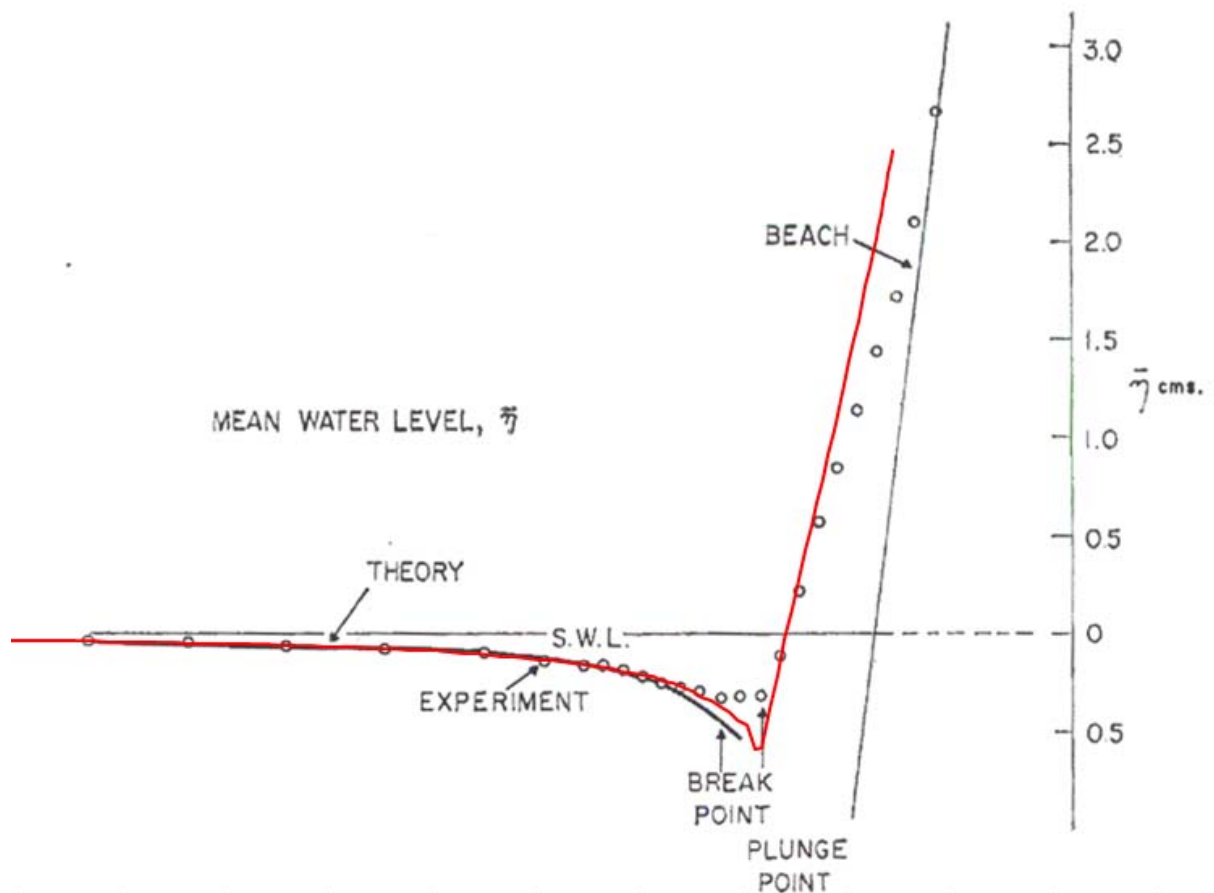


Figure 6.28 – Comparison of Measured and Calculated Set-up/Set-down for a laboratory wave after Bowen *et al.* (1968) and Newell and Mullarkey (2007b). Waves propagate from left to right.

6.6.3 Discussion

Figure 6.28 shows a close correspondence between the measured results of Bowen *et al.* (1968) and the results of the NM-WDHM. It is believed that the slightly higher than usual insipience point was required to compensate for the laboratory nature of the sea-bed and the scale of the wave. Measured values of set-up are difficult to obtain for real coastal situations so the availability of the Bowen *et al.* (1968) measured data is quite useful for examining the accuracy of the NM-WDHM.

6.7 Iteration between NM-WCIM and NM-WDHM

6.7.1 Introduction

The development of the coupled NM-WCIM and NM-WDHM for this project allows for the examination of the circular nature of the relationship between waves and wave-generated effects. Newell and Mullarkey (2007b) provides an examination of the effect of iteration between the NM-WCIM and the NM-WDHM for the purposes of examining a wave-generated current and set-up/set-down.

6.7.2 Results

Figure 6.29 shows the results for set-up/set-down obtained from the first and second steps of the iterative procedure. A wave of 0.6m deep-water height and ten second period with a deep-water angle of 30 degrees is examined on a beach of 1 in 50 slope. The NM-WCIM is initially run in the absence of a current and radiation stress values from this model are used in the NM-WDHM to calculate the first set-up/set-down results as well as the magnitude of longshore current. A second iteration of the NM-WCIM is then carried out using the values of current to obtain a second set of radiation stress values. The second iteration of the NM-WDHM is then carried out to obtain a second set of results for set-up/set-down.

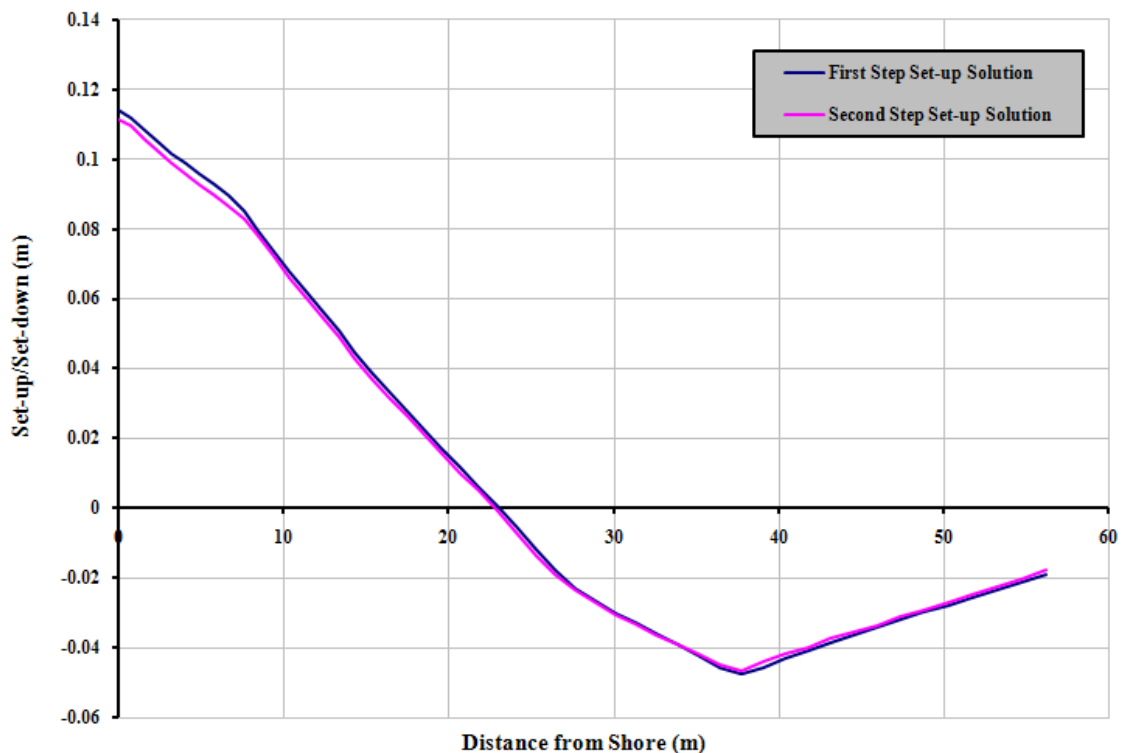


Figure 6.29 – Plot of Set-up/Set-down for the first and second steps of an iterative use of the NM-WCIM and NM-WDHM. Waves propagate from right to left.

6.7.3 Discussion

The maximum difference between the plotted results in Figure 6.29 is of the order of 2%. Considering the level of accuracy expected of numerical wave-current interaction and hydrodynamic models this would be considered a very small difference and would tend to indicate that in the presence of purely wave-generated currents iteration of the NM-WCIM and NM-WDHM would not usually be necessary unless there was some indication that the bathymetry would be such to cause an amplified wave-generated current. Obviously in the case of strong currents, that may not be generated by waves, iteration of the model to obtain appropriate wave-current interaction results is essential.

6.8 Wave Breaking and Recovery over an Offshore Bar

6.8.1 Introduction

As discussed in Section 5.6.2 the Dally *et al.* (1985) wave breaking solution allows for recovery of wave height when a wave train initially breaks over an offshore bar and continues into deeper water following this initial breaking. The Dally *et al.* (1985) breaking solution is unique in this regard among the breaking solutions examined by this project. The figures below show the effects of this wave recovery on both wave height and wave generated set-up/set-down and currents.

6.8.2 Results

The figures below present the results of the NM-WCIM and NM-WDHM for a wave of 2m deep-water height and ten second period approaching an offshore bar at a deep-water angle of 30 degrees. Figure 6.30 shows the bathymetry of the offshore bar including the initial 1 in 20 slope, the 1 in 20 slope of the beach and the 1 in 20 slope in the opposite direction on the downwave side of the bar. A small flat area is provided at the crest of the bar and at the base of the trough. Figure 6.31 shows the results obtained using unbroken wave heights from the NM-WCIM and the Ray Energy Method as a post-processing method to obtain broken wave heights using the Dally *et al.* (1985) wave breaking solution. Figure 6.32 shows the longshore current obtained using the NM-WDHM with radiation stress values obtained from the broken wave heights and similarly Figure 6.33 shows the set-up/set-down for the same scenario.

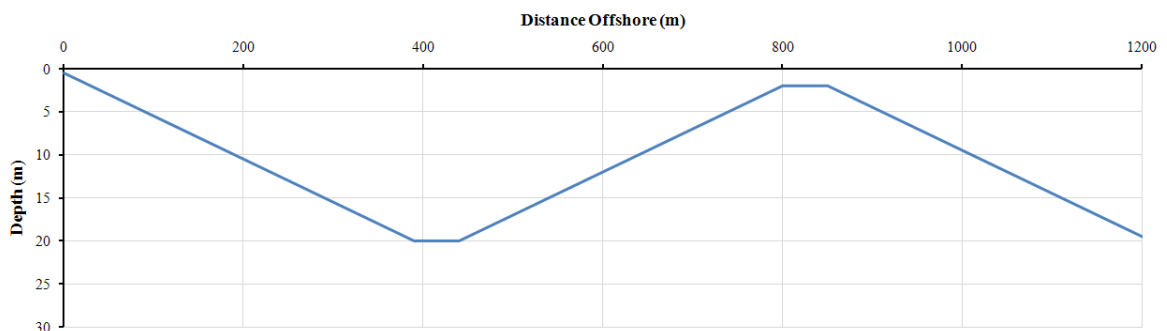


Figure 6.30 – Bathymetry of Offshore Bar

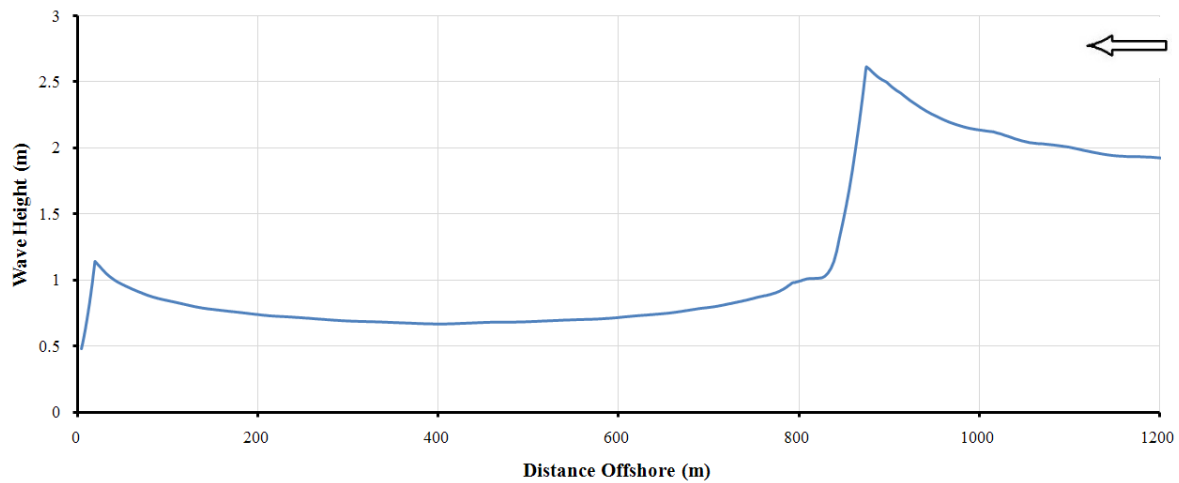


Figure 6.31 – Wave Height in the presence of an Offshore Bar. Waves propagate from right to left.

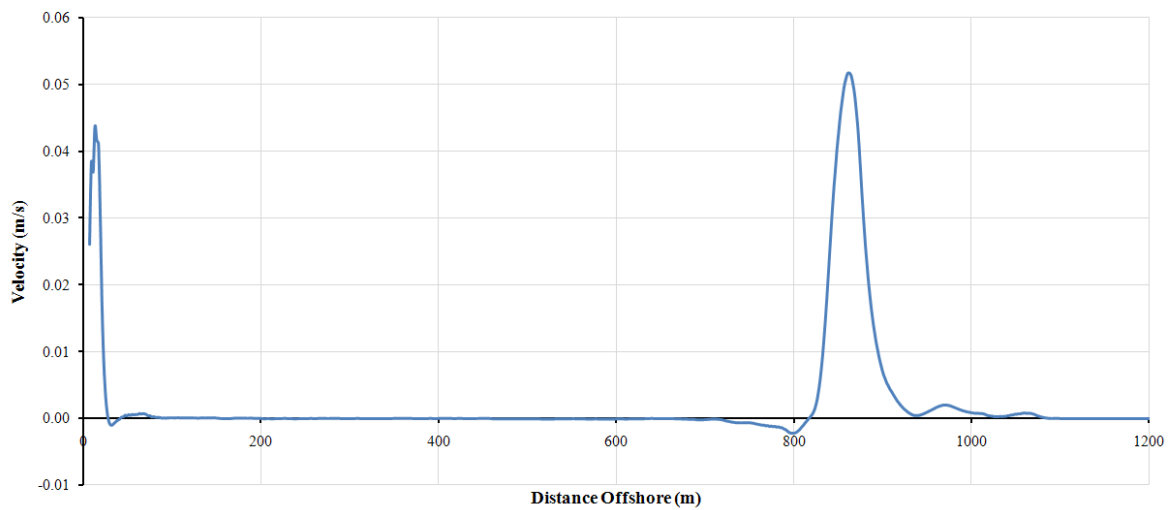


Figure 6.32 – Magnitude of Longshore Current in the presence of an Offshore Bar

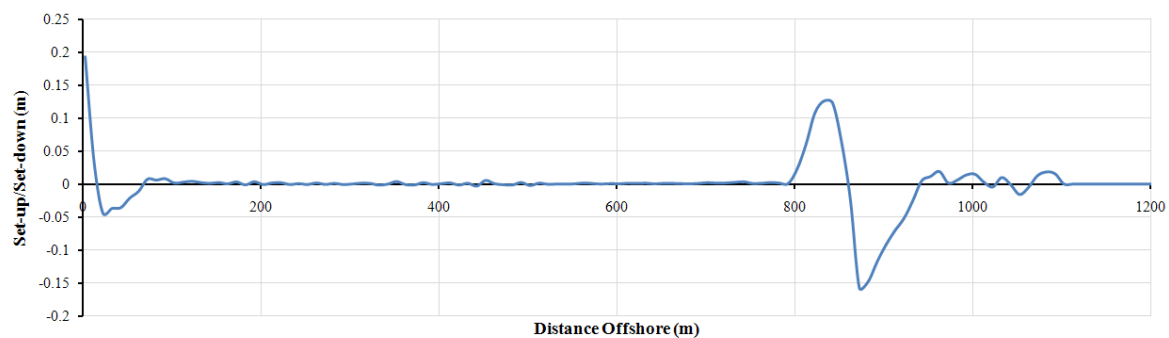


Figure 6.33 – Set-up/Set-down in the presence of an Offshore Bar

6.8.3 Discussion

Figure 6.31 shows a reduction in wave height caused by breaking over the offshore bar. As the wave train progresses over the downwave side of the bar and the deeper section of the trough there is a region of gradual small change in the wave height before shoaling recommences on the 1 in 20 beach section to provide a recovered wave height. Breaking then occurs again on the recovered wave height in the vicinity of the beach. Figure 6.32 shows the profile of longshore current caused by the wave breaking over the longshore bar and at the beach. The magnitude of current caused by the offshore bar is of the same order as that caused by breaking at the beach. Figure 6.33 shows the set-up/set-down caused by both the breaking on the offshore bar and the breaking on the beach. There is a noticeable region of set-down at the point of initial wave breaking and set-up on the bar side of this region. The set-up in this region decays quickly over the top of the bar. The set-up caused by the beach is of the same order as that caused by the bar but the set-down caused by breaking waves at the beach is approximately three times smaller than the magnitude of that caused by the bar. This difference is thought to be due to the relative magnitudes of the initial and recovered breaking waves.

The shallowness of the bar examined in this case, at 2m, would be considered quite shallow and the NM-WCIM and NM-WDHM address this depth very well. There is a degree of numerical noise on the upwave side of the set-down and longshore current at the breakwater. However, this noise does not affect the overall trend of the results.

6.9 Detached Breakwater of Liu and Mei (1976)

6.9.1 Introduction

In the presence of complicated bathymetry or offshore obstacles one-dimensional versions of the NM-WCIM and NM-WDHM would not provide sufficient results. In cases such as this the NM-WCIM and NM-WDHM are run in two-dimensional form. In this case the effect of a detached breakwater upon shoaling waves on a beach is examined using both the NM-WCIM and NM-WDHM. Liu and Mei (1976) examine a detached breakwater and the same bathymetry and layout have been chosen for the model in question to allow comparison.

6.9.2 Results

Figure 6.34 shows the scenario under examination. A detached breakwater is situated 350m offshore on a beach of 1 in 50 slope. A wave of 10 second period and 1m deep-water height approaches the beach perpendicularly. Because of the symmetry of the situation it was only necessary to model half the breakwater. Liu and Mei (1976) used the same process to produce results with a smaller domain. A circular boundary is applied to the open water side of the domain to allow backscattered waves to exit the domain. The water surface is shown in Figure 6.34 for unbroken waves. The same scenario is plotted in Figure 6.35 for broken waves. It is worth noting that Liu and Mei (1976) use an insipience criterion of $\gamma_0 = 0.4$. Although this would be considered quite low it was utilised in the NM-WCIM in this case to ensure the comparison of like with like.

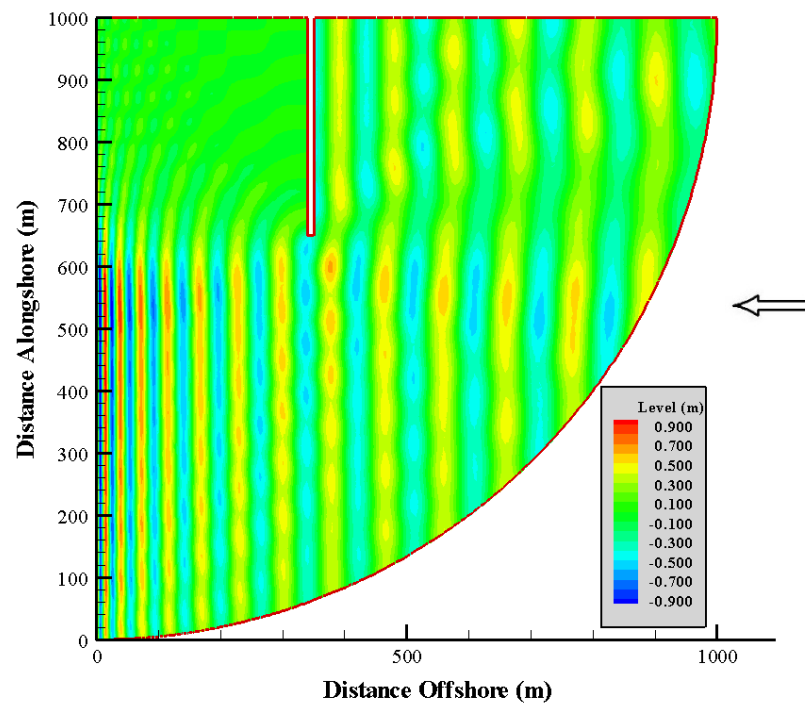


Figure 6.34 – Water surface in the presence of a Detached Breakwater with Unbroken Waves. Waves propagate from right to left.

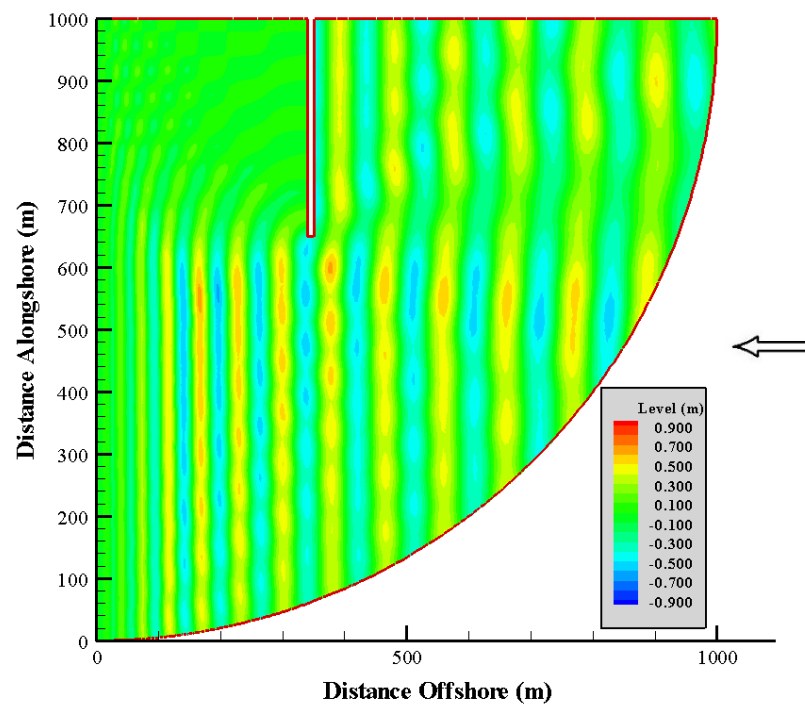


Figure 6.35 – Water Surface in the presence of a Detached Breakwater with Broken Waves. Waves propagate from right to left.

Figure 6.36 shows contour lines of where the water surface height is zero. These lines provide an ideal method of envisaging the wave phase. Figure 6.37 shows a three-dimensional plot of the same results as Figure 6.35.

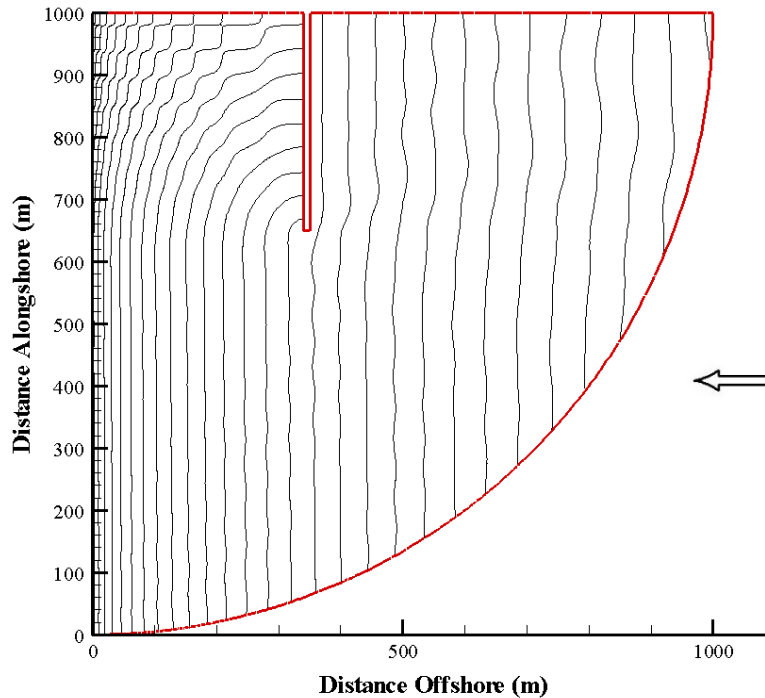


Figure 6.36 – Contours of Water Surface = 0 to indicate Wave Phase. Waves propagate from right to left.

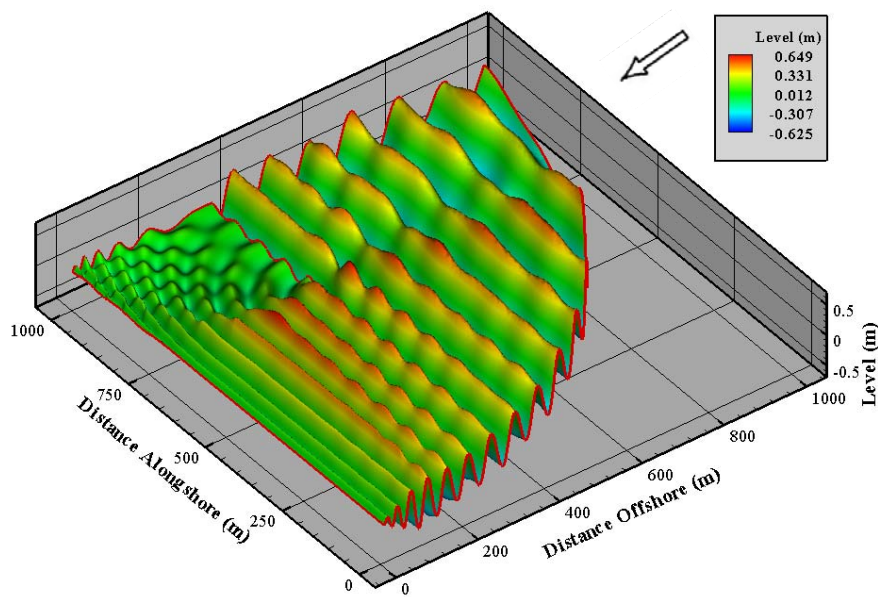


Figure 6.37 – Three dimensional plot of Water Surface for Broken Waves

Figure 6.38 and Figure 6.39 show plots of unbroken and broken wave heights respectively for the same scenario as the wave surfaces plotted above.

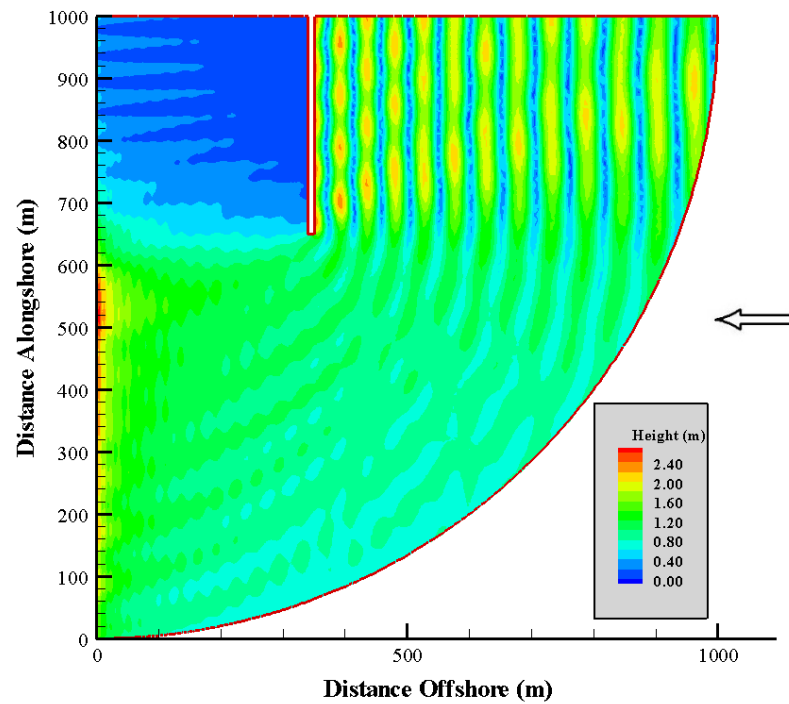


Figure 6.38 – Unbroken Wave Height in the presence of a Detached Breakwater. Waves propagate from right to left.

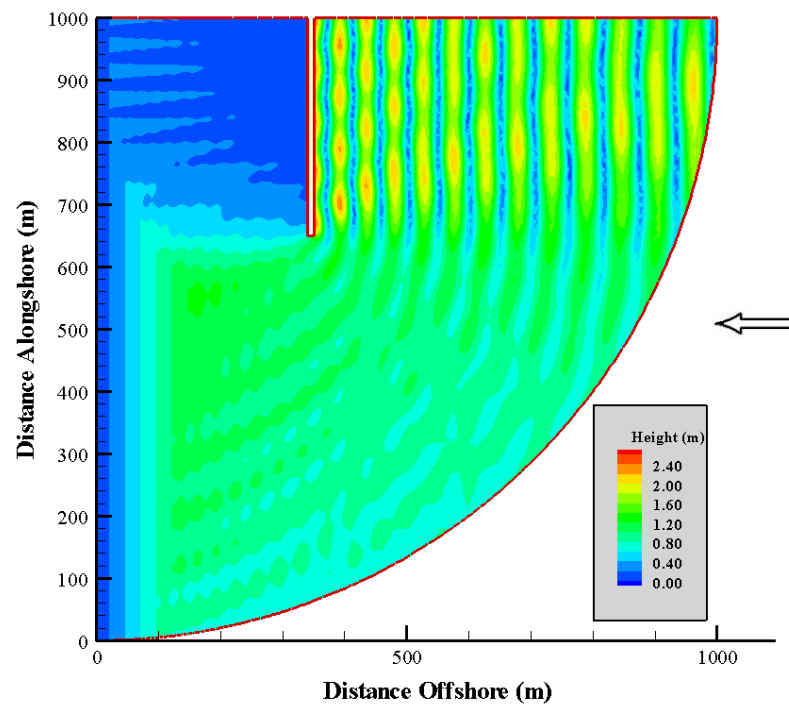


Figure 6.39 – Broken Wave Height in the presence of a Detached Breakwater. Waves propagate from right to left.

Figure 6.40 shows the set-up and set-down obtained from the NM-WDHM both in the region unaffected by the breakwater and the region behind the breakwater. Figure 6.41 shows velocity vectors for the same area in the absence of any turbulent terms. Figure 6.42 and Figure 6.43 show the effect on the vectors of including turbulence based on eddy viscosity. Figure 6.42 shows the results of the NM-WDHM using an empirical parameter of $M=1.1$ whereas Figure 6.43 shows the results in the case of an empirical parameter of $M=2.0$. The inclusion of turbulent terms can cause numerical noise in the velocity results at the tip of the breakwater therefore this region has been removed from the results plotted in Figure 6.42 and Figure 6.43.

The next figures show a more magnified view of approximately 4.3 hectares of the model. This allows for a more detailed examination of the velocity components in this area. Figure 6.44 shows the velocity components in this area in the absence of any turbulent terms. Figure 6.45 and Figure 6.46 show the velocity components in this area with the use of turbulent parameters of $M=1.1$ and $M=2.0$ respectively. The eddy viscosity values and breaking wave heights for turbulent diffusion were obtained using the wave energy ray method discussed in Chapter 5.

Figure 6.47 shows the velocity components in the same area plotted along with the set-up/set-down results to allow examination of the effects of set-up and set-down on the velocity components. Figure 6.48 and Figure 6.49 show the velocity streamline and set-up/set-down results obtained by Liu and Mei (1976) for the same scenario. Figure 6.50, that follows, shows a cross-section of longshore current along a line of $y = 610\text{m}$. This plot allows the examination of the effects of turbulent diffusion within the NM-WDHM.

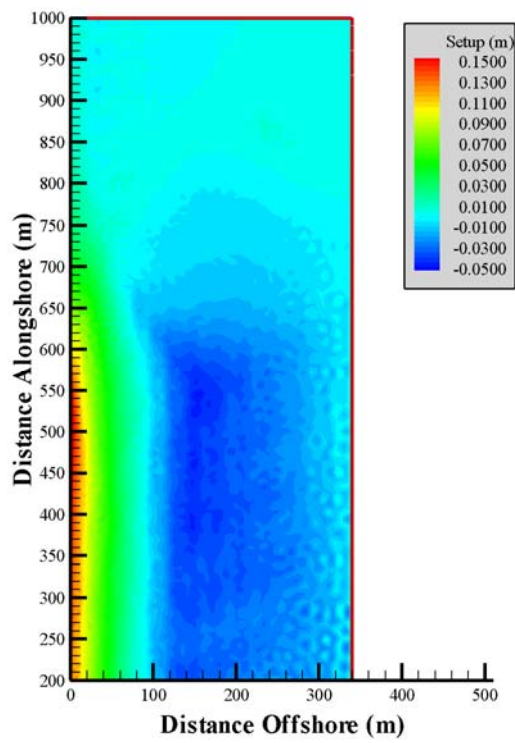


Figure 6.40 – Set-up/Set-down in region behind Breakwater

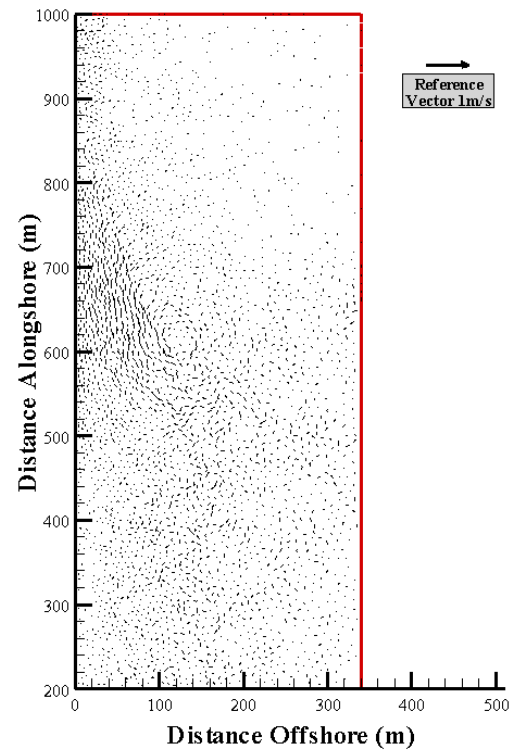


Figure 6.41 – Velocity behind Breakwater in the absence of turbulence

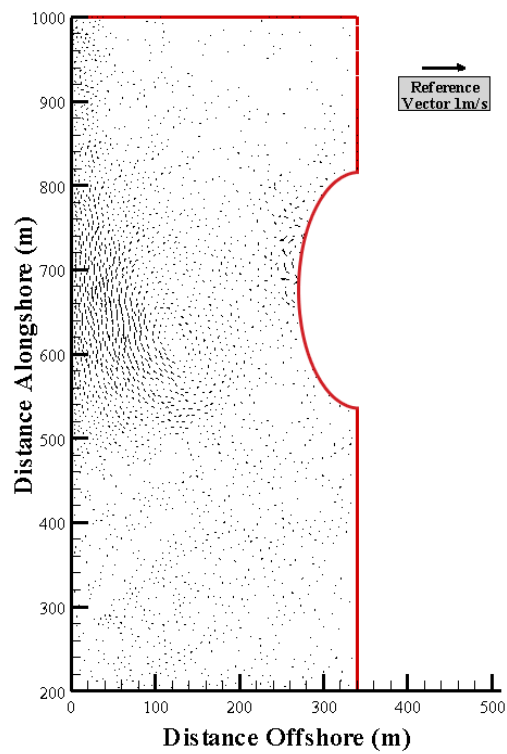


Figure 6.42 – Velocity behind Breakwater with Turbulent Parameter $M=1.1$

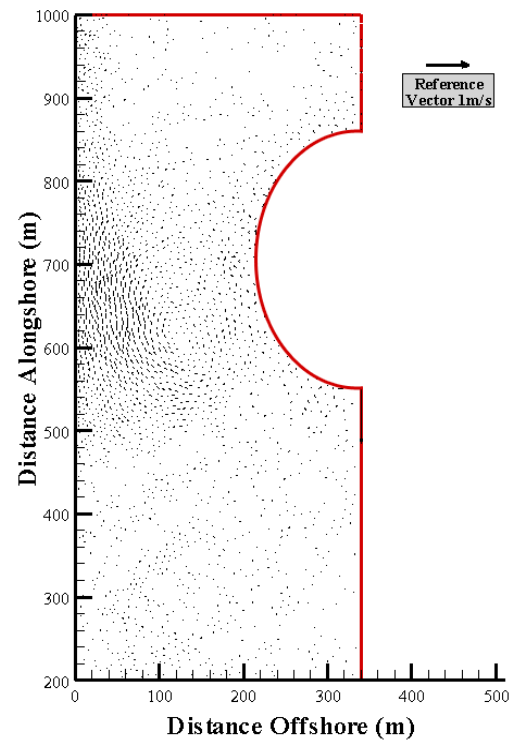


Figure 6.43 – Velocity behind Breakwater with Turbulent Parameter $M=2.0$

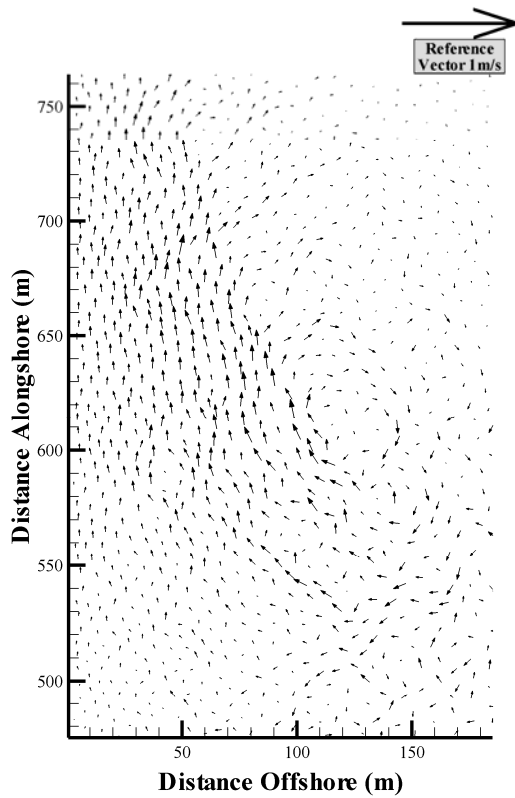


Figure 6.44 – Velocity Plot in the absence of Turbulence

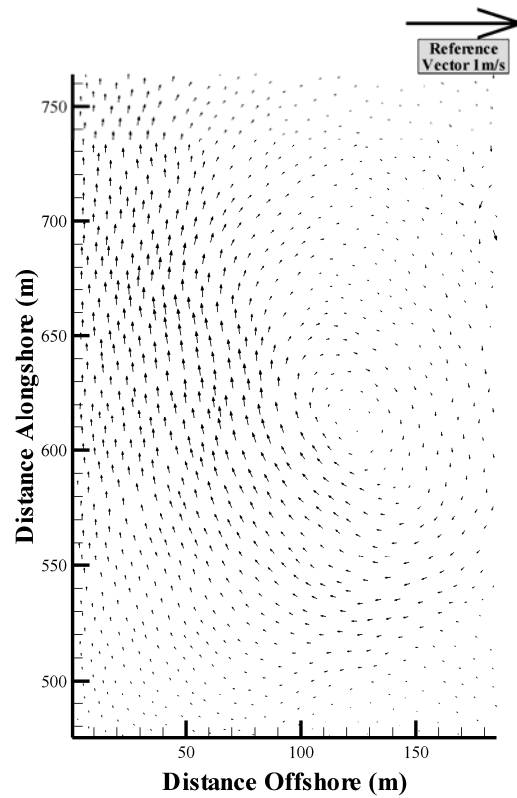


Figure 6.45 – Velocity Plot with Turbulent Parameter $M=1.1$

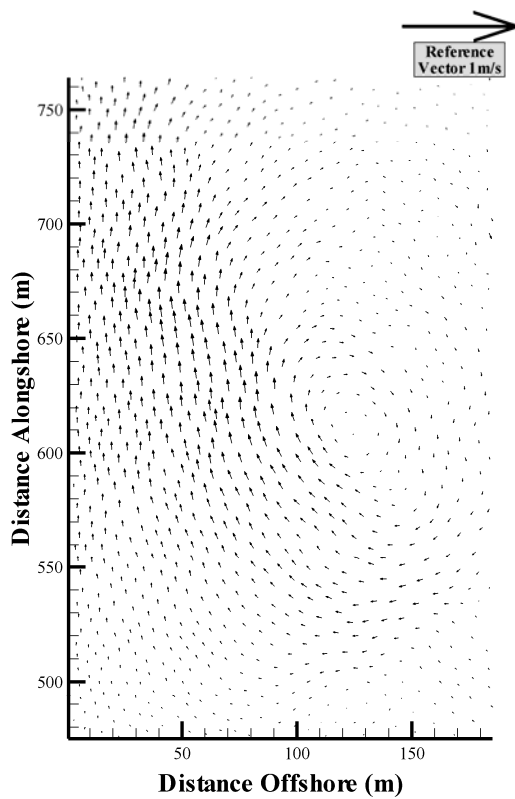


Figure 6.46 – Velocity Plot with Turbulent Parameter $M=2.0$

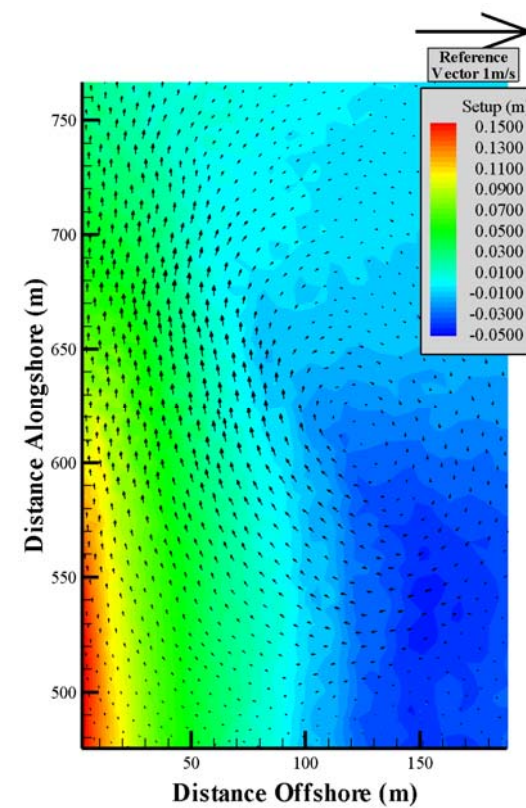


Figure 6.47– Velocity Plotted alongside Set-up/Set-down

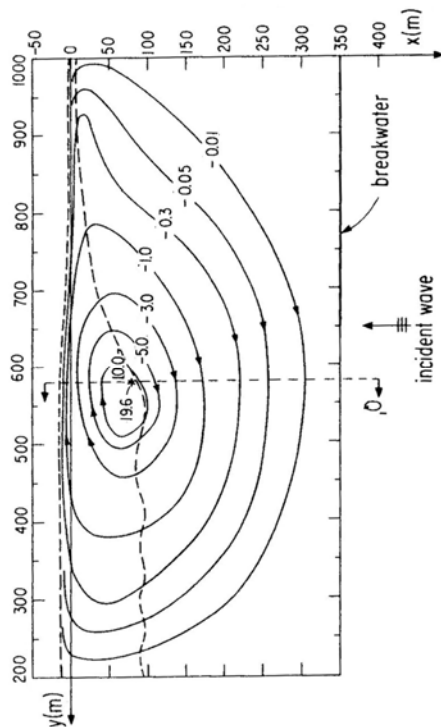


Figure 6.48 – Streamlines showing direction and magnitude of vortex from Liu and Mei (1976). Values indicated on the plot are magnitudes of a streamline function. This plot has been mirrored to provide results for the same location as this project.

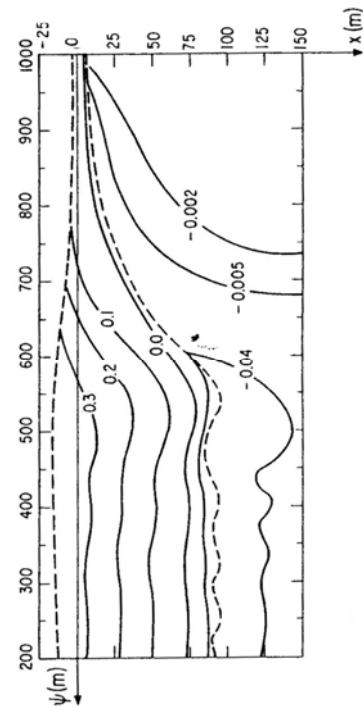


Figure 6.49 – Contours of set-up/set-down from Liu and Mei (1976). This plot has been mirrored to provide results for the same location as this project.

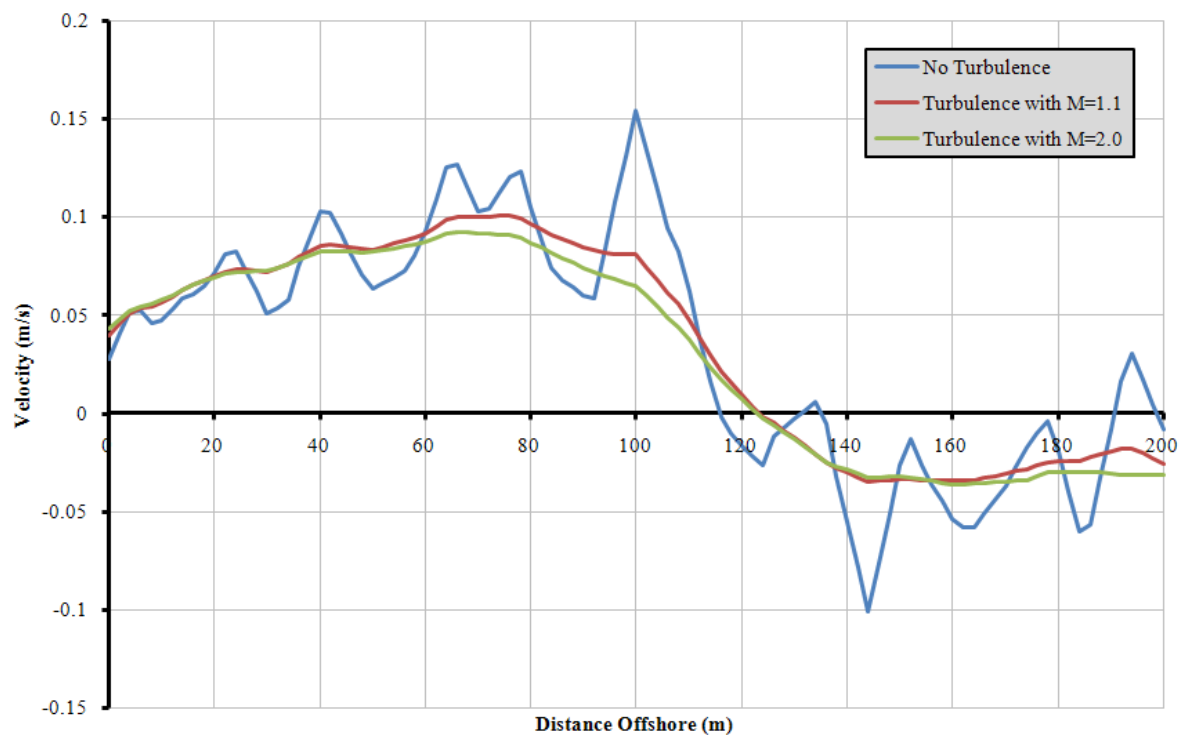


Figure 6.50 – Profile of Longshore Current at $y = 610\text{m}$ showing the effect of Turbulence in the NM-WDHM

6.9.3 Discussion

It is evident from the results of the NM-WCIM that the presence of a breakwater has a sheltering effect. The wave heights behind the breakwater are quite low. Diffraction is also evident behind the breakwater. Figure 6.36 shows how the waves diffract around the back of the breakwater after the wave train passes it. Figure 6.39, however, shows that the height of these waves behind the breakwater is significantly lower than those in the unsheltered region to the side of the breakwater. The presence of a standing wave on the deep-water side of the breakwater is also easily visible from the wave heights plotted in Figure 6.39. The fact that these standing waves do not affect the results elsewhere in the domain is a good indication that the radiation boundary condition on the open water boundary allows the backscattered wave energy to exit the domain effectively.

The results of the NM-WDHM show that any noticeable set-up and set-down is confined to unsheltered region to the side of the breakwater. This is due to the magnitude of the waves behind the breakwater being too small to cause a strong radiation stress. It is evident from Figure 6.41, Figure 6.42 and Figure 6.43 that the inclusion of turbulent diffusion has a significant effect on the results of the NM-WDHM. Many previous wave-driven hydrodynamic models ignore turbulent diffusion for the sake of speed of solution. The results of this model show that turbulent diffusion smoothens the results of the model and gives a more realistic view of the vortex created in the region behind the breakwater tip. This is further proved by the magnified plots of Figure 6.44, Figure 6.45 and Figure 6.46. The cross-section of longshore velocity in Figure 6.50 clearly shows the smoother results of the models including turbulent diffusion when compared with the jagged results of the model run without turbulent effects. Liu and Mei (1976) ignore the effects of turbulent diffusion. Figure 6.47 shows the relationship between set-up/set-down and wave driven currents. It is evident from this plot that the vortex formed behind the breakwater is caused by the difference in set-up and set-down between the shadow region behind the breakwater and the unsheltered region to the side of it. The hydrostatic difference between the two causes a vortex to be created with flow from regions of higher pressure to regions of lower pressure.

The results of the Liu and Mei (1976) model shown in Figure 6.48 and Figure 6.49 are comparable in trend with those of the NM-WDHM model. The set-up of the Liu and Mei (1976) model is approximately 0.15m higher than that predicted by the NM-WDHM

model. The reason for this difference is not clear. In Sections 6.6 and 6.11 the set-up predicted by the NM-WDHM compares favourably with that of experimental tests and existing numerical models. Using an approximate method for prediction of set-up from Smith (2003) for a wave of 10 second period and 1m height breaking on a beach with a slope of 1 in 50 gives a value of approximately 0.14m. In this model it is reasonable to expect that in regions remote from the breakwater the set-up would behave as it would in the absence of the obstacle. The set-up obtained by the NM-WDHM in this region is approximately 0.15m. The overall trend of the velocity vortex is shown to be comparable between the NM-WDHM and Liu and Mei (1976). The streamline solution of Liu and Mei (1976) makes it difficult to compare magnitudes of velocities.

6.10 Detached Breakwater of Liu and Mei (1976) – Waves at an Angle

6.10.1 Introduction

This section examines the same bathymetry and dimensions as Section 6.9 but in this case the wave approaching the beach has a deep-water angle of 30 degrees to the beach. This process has also been examined by Liu and Mei (1976). Due to the wave direction in this model there was no symmetry about the centre of the breakwater and hence a larger semi-circular domain was examined.

6.10.2 Results

Figure 6.51 shows the scenario under examination. A detached breakwater is situated 350m offshore on a beach of 1 in 50 slope. A wave of 10 second period and 1m deep-water height approaches the beach with a deep-water angle of 30 degrees. A circular boundary is applied to the open water side of the domain to allow backscattered waves to exit the domain. The water surface is shown in Figure 6.51 for unbroken waves. The same scenario is plotted in Figure 6.52 for broken waves. As previously discussed in Section 6.9.4 Liu and Mei (1976) use an insipience criterion of $\gamma_0 = 0.4$ and the same is used in this case.

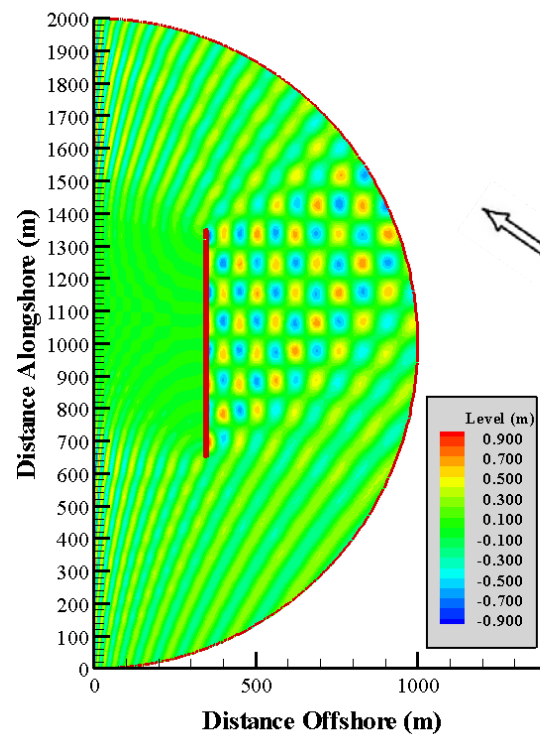


Figure 6.51 – Water surface in the presence of a Detached Breakwater with Unbroken Waves at an Angle. Waves propagate as indicated by the arrow.

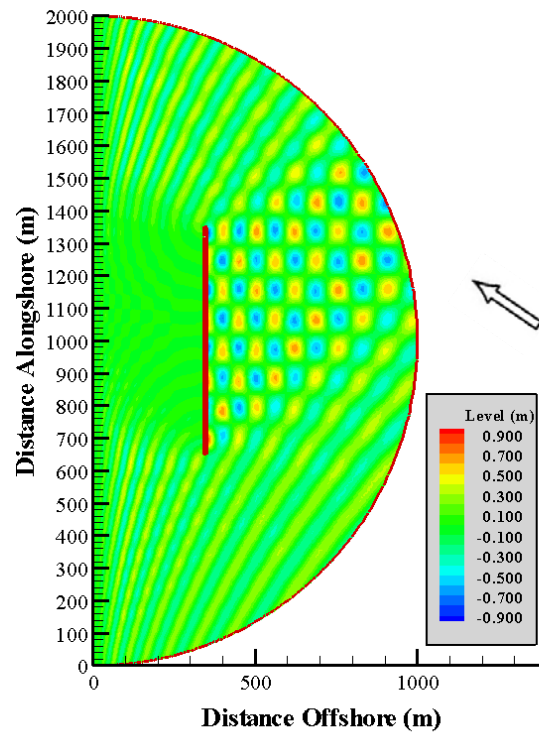


Figure 6.52 – Water Surface in the presence of a Detached Breakwater with Broken Waves at an Angle. Waves propagate as indicated by the arrow.

Figure 6.53 shows contour lines of where the water surface height is zero to aid the envisaging of wave phase. Figure 6.54 shows a three-dimensional plot of the same results as Figure 6.52 to demonstrate the modelled results.

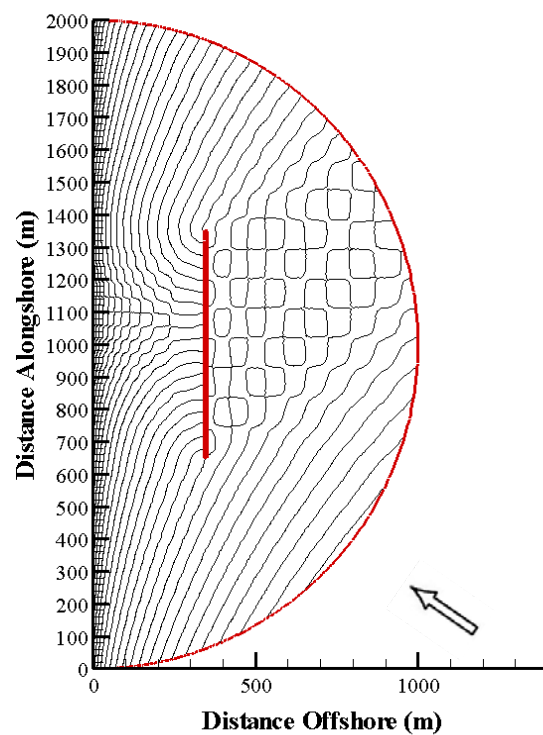


Figure 6.53 – Contours of Water Surface = 0 to indicate Wave Phase for Waves approaching a Breakwater at an Angle. Waves propagate as indicated by the arrow.

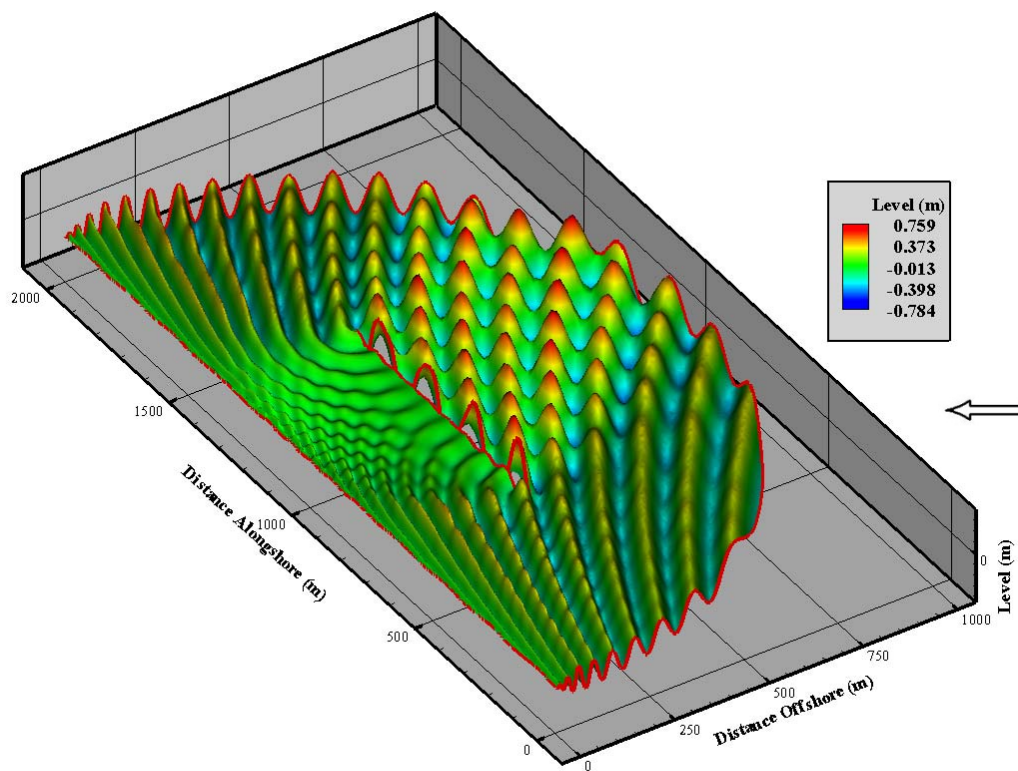


Figure 6.54 – Three dimensional plot of Water Surface for Broken Waves for waves at an Angle. Waves propagate as indicated by the arrow.

Figure 6.55 and Figure 6.56 show plots of unbroken and broken wave heights respectively for the same scenario as the wave surfaces plotted above.

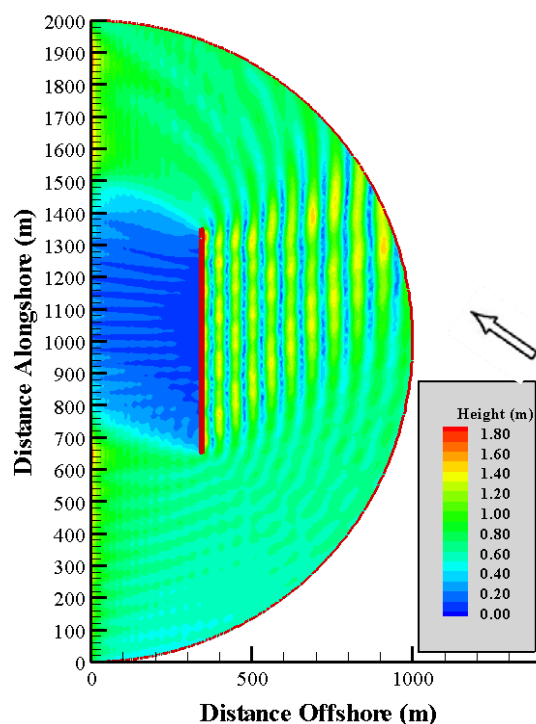


Figure 6.55 – Unbroken Wave Height in the presence of a Detached Breakwater for waves at an Angle. Waves propagate as indicated by the arrow.

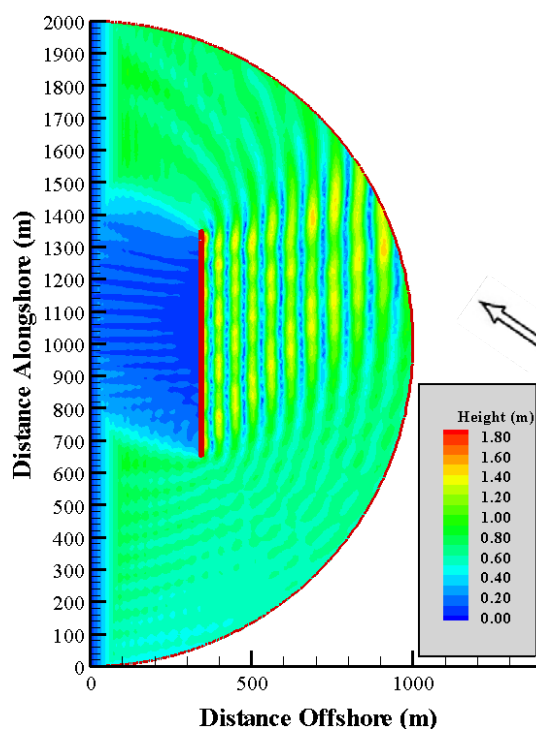


Figure 6.56 – Broken Wave Height in the presence of a Detached Breakwater for Waves at an Angle. Waves propagate as indicated by the arrow.

Figure 6.57 shows the set-up and set-down obtained from the NM-WDHM both in the region unaffected by the breakwater and the region behind the breakwater. Figure 6.58 shows the same plot but with differing x-axis and y-axis scales for comparison with the similar plot of Liu and Mei (1976) in Figure 6.65. Figure 6.59 shows velocity vectors and set-up/set-down from the NM-WDHM for the lower area of the modelled region in the absence of any turbulent diffusion. Figure 6.60 shows a plot of the same area with an empirical turbulent parameter of $M=1.1$ used for eddy viscosity in the turbulent diffusion terms. Figure 6.61 shows velocity vectors and set-up/set-down from the NM-WDHM for the upper area of the modelled region in the absence of any turbulent diffusion. Figure 6.62 shows a plot of the same area with an empirical turbulent parameter of $M=1.1$ used for eddy viscosity in the turbulent diffusion terms. Where the NM-WDHM included the effects of turbulent diffusion; breaking wave heights and eddy viscosity values were obtained using the wave ray method discussed in Chapter 5 above. Figure 6.63, that follows, shows a cross-section of longshore current along a line of $y = 270\text{m}$. This plot allows the examination of the effects of turbulent diffusion within the NM-WDHM.

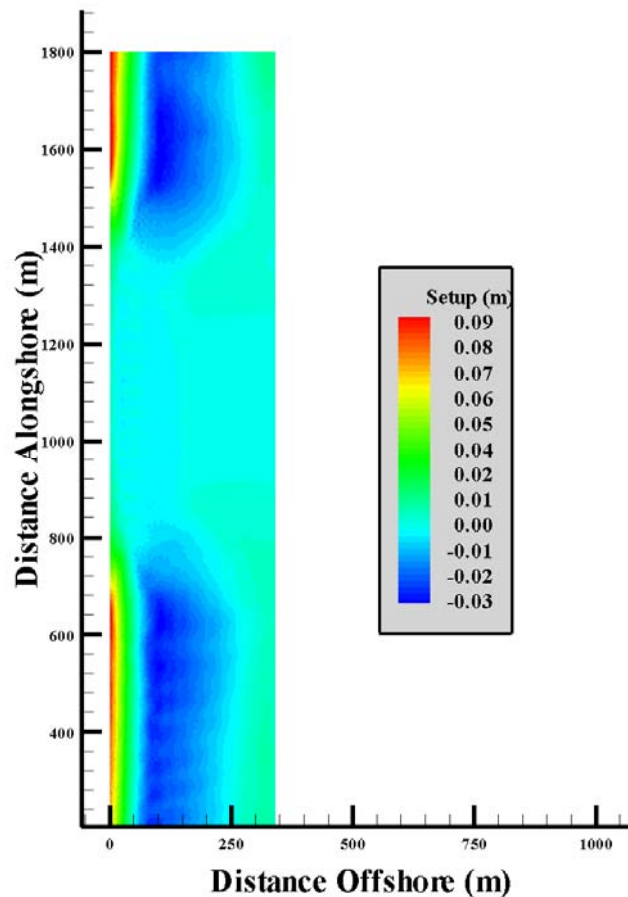


Figure 6.57 – Plot of Set-up and Set-down for Waves approaching a Breakwater at an Angle

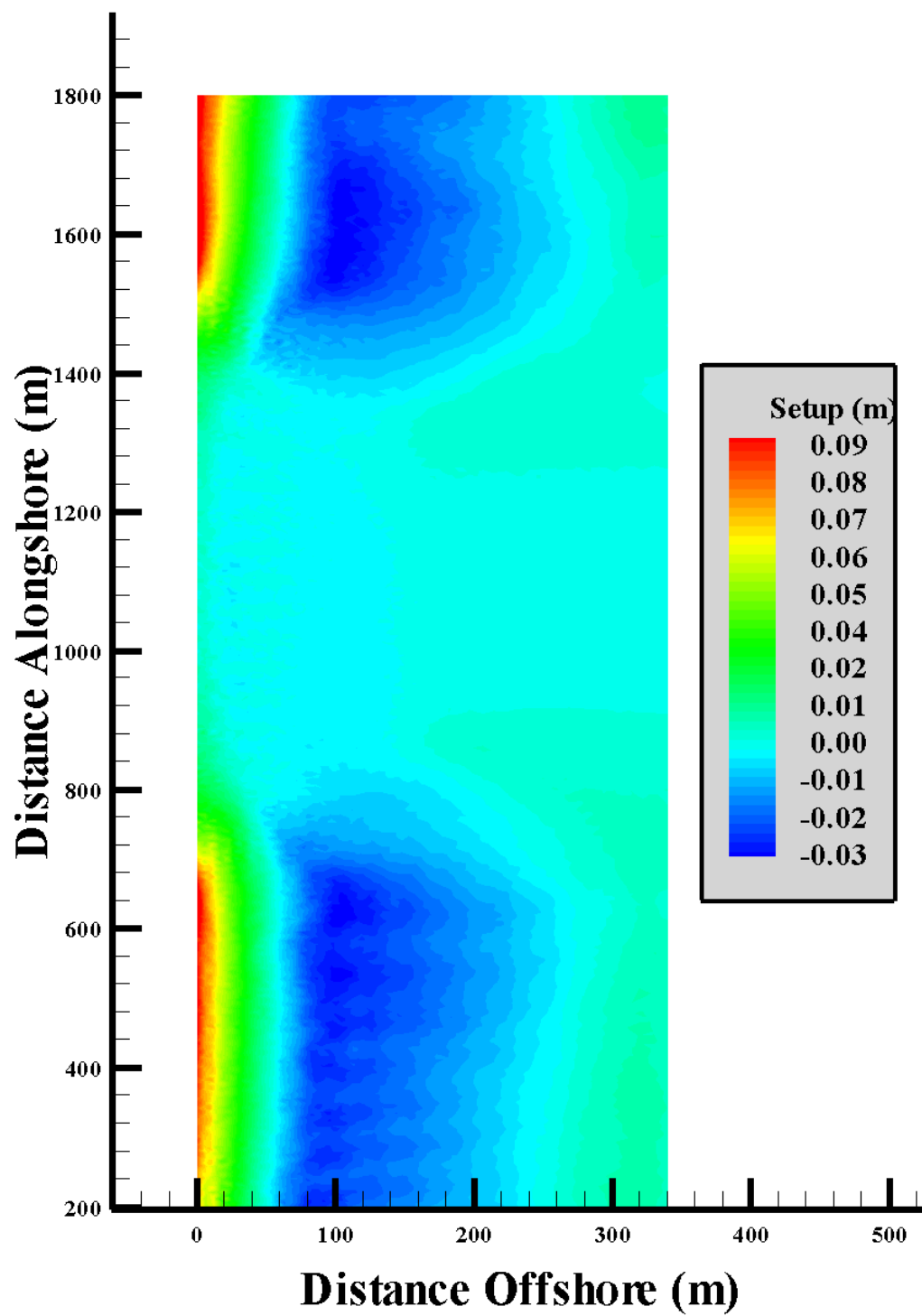


Figure 6.58 – Plot of Set-up and Set-down for Waves approaching a Breakwater at an Angle with exaggerated x-axis for comparison with Liu and Mei (1976) solution

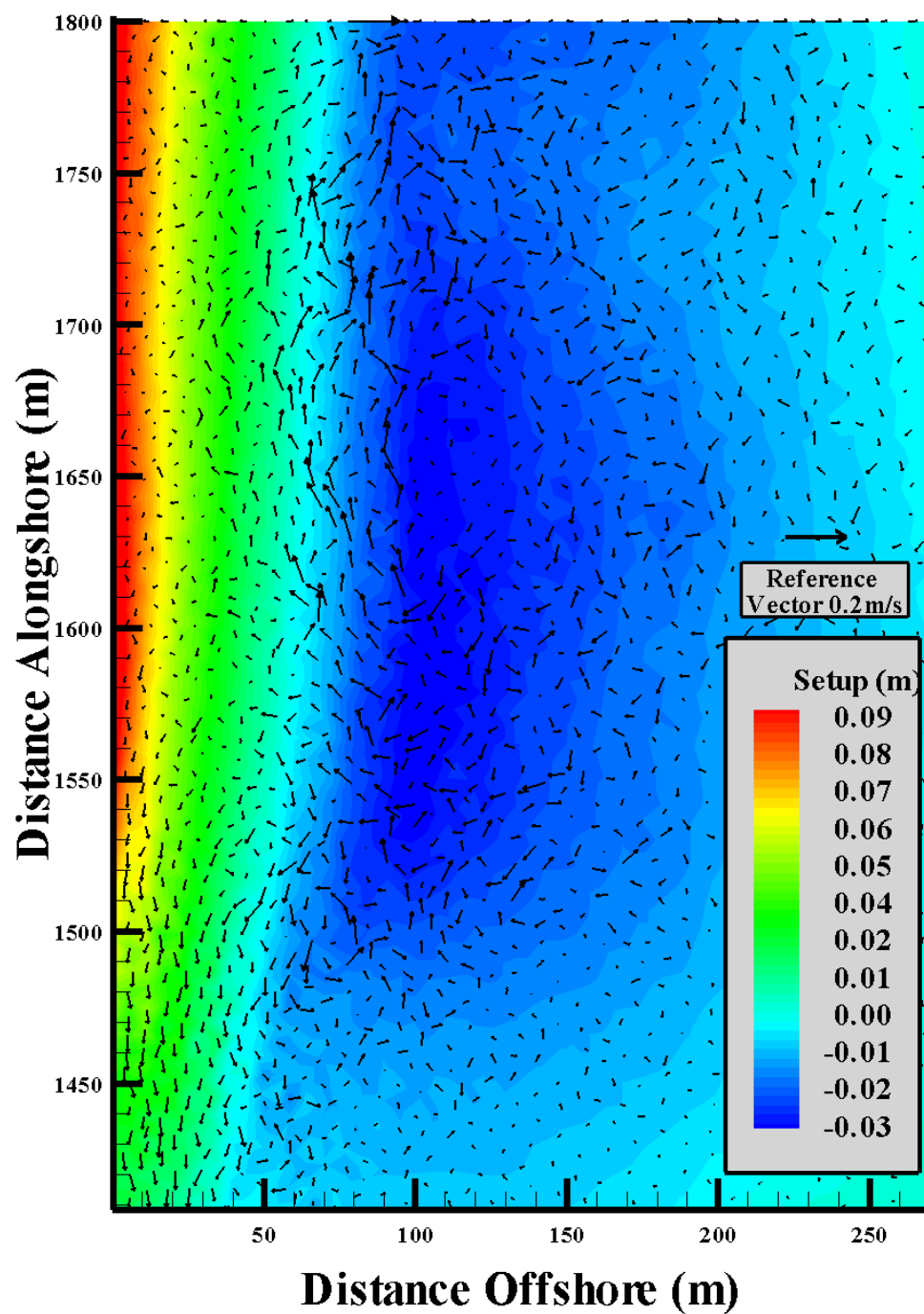


Figure 6.59 – Set-up/Set-down and Currents in region above Breakwater with no turbulence

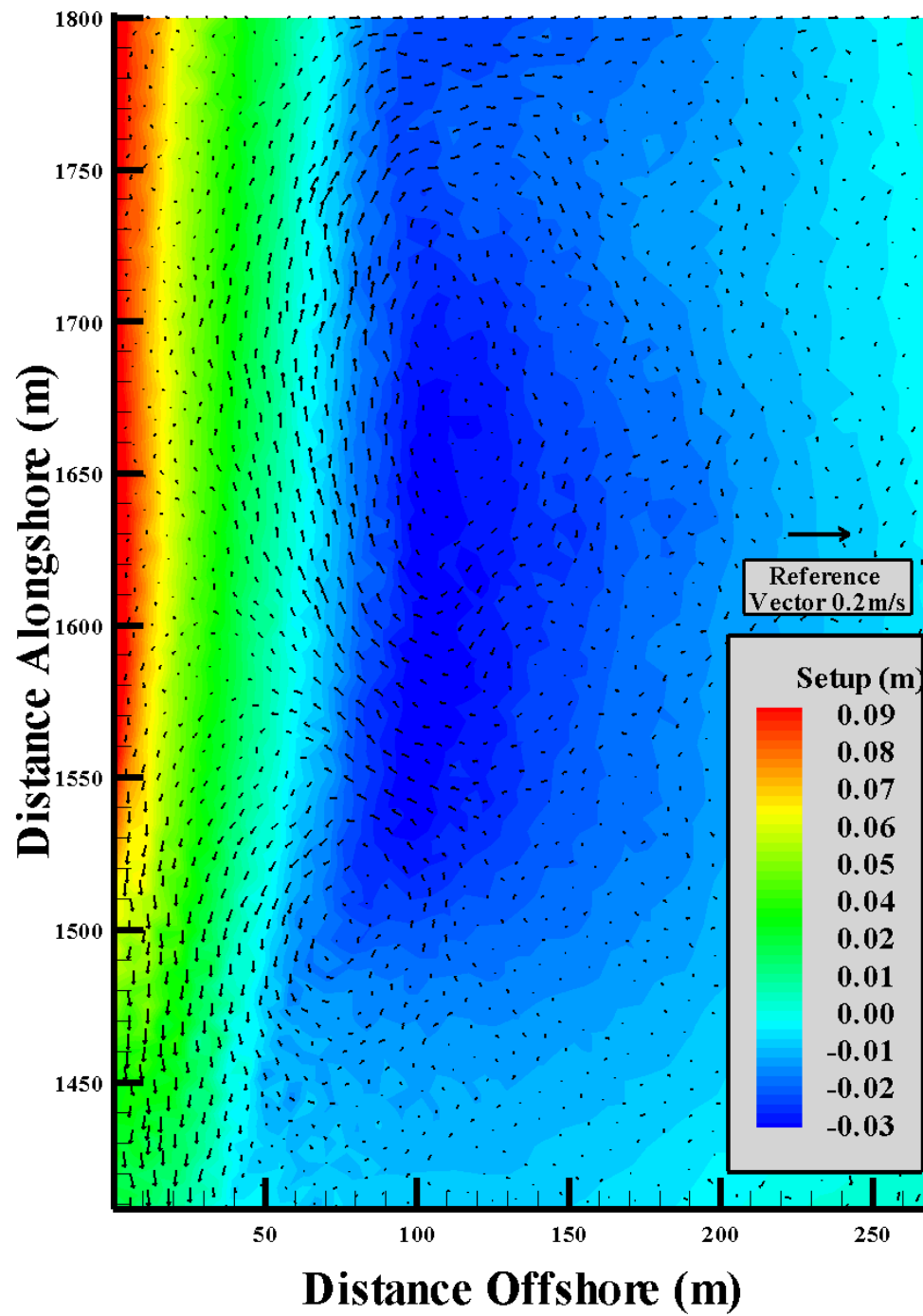


Figure 6.60 – Set-up/Set-down and Currents in region above Breakwater with turbulence

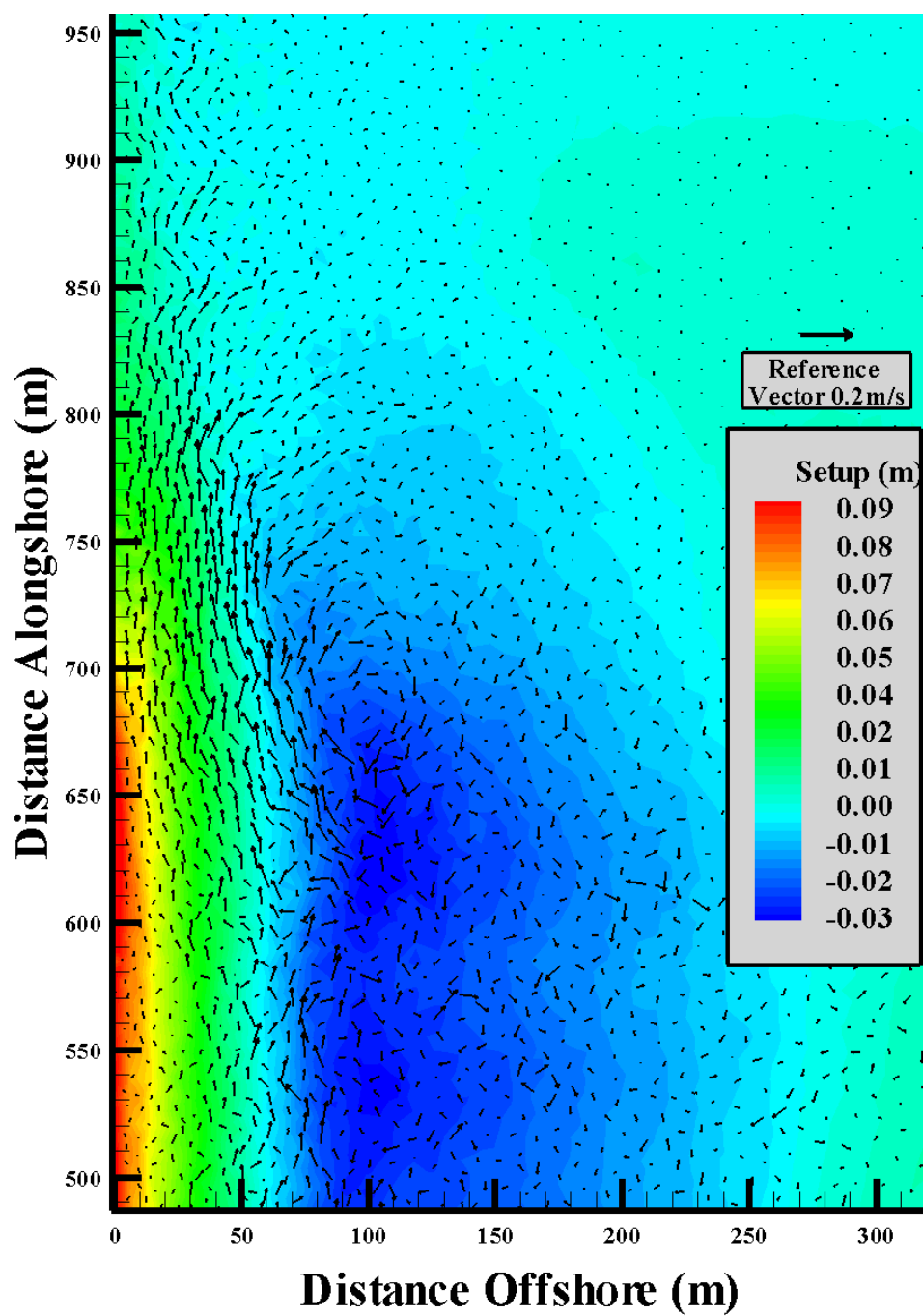


Figure 6.61 – Set-up/Set-down and Currents in region below Breakwater with no turbulence

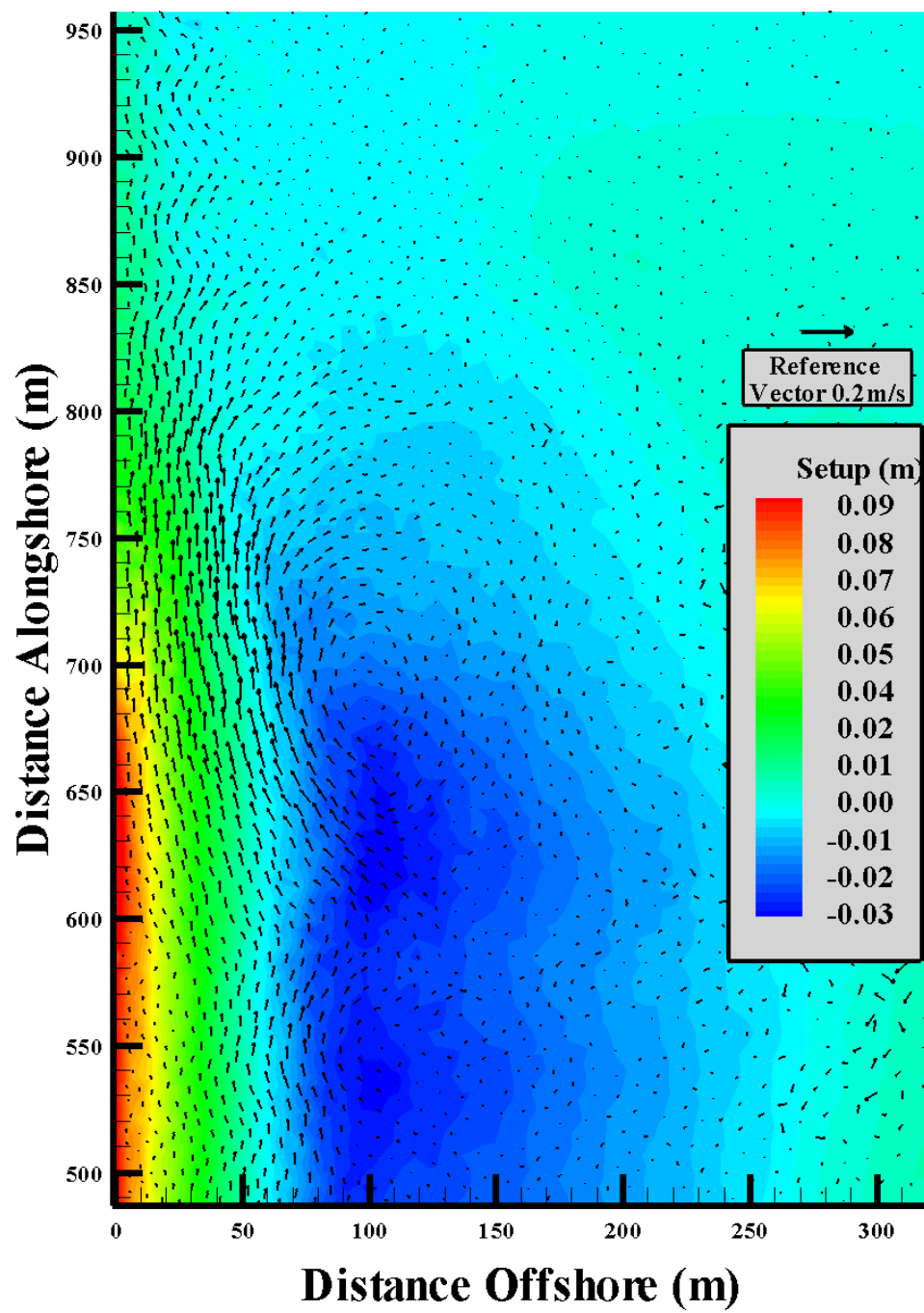


Figure 6.62 – Set-up/Set-down and Currents in region below Breakwater with turbulence

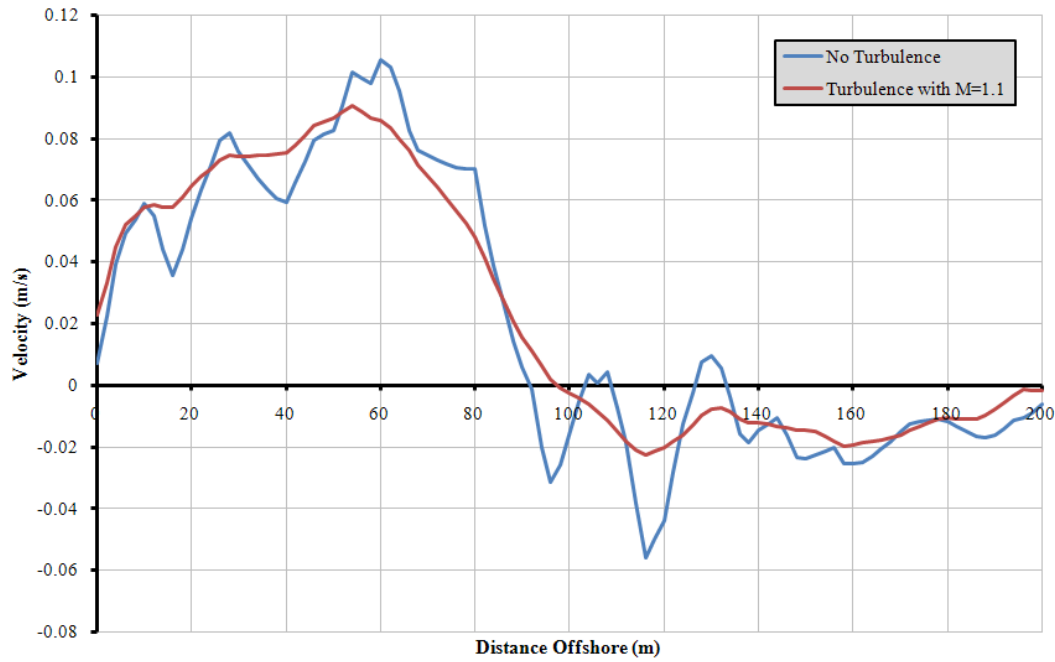


Figure 6.63 – Profile of Longshore Current at $y = 270\text{m}$ showing the effect of Turbulence in the NM-WDHM

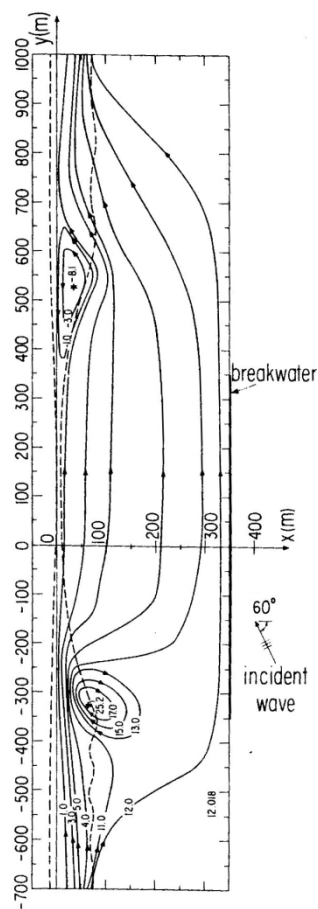
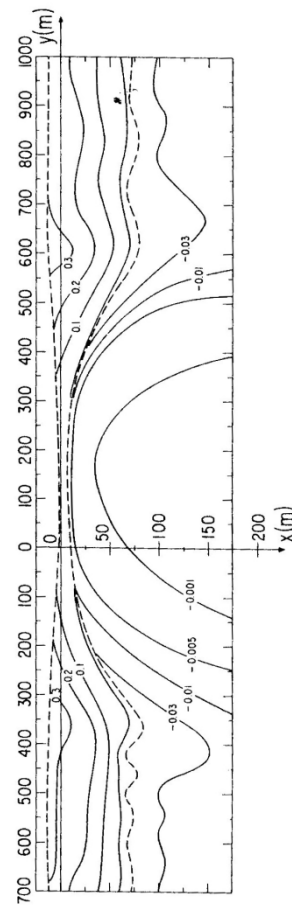


Figure 6.64 – Streamlines showing direction and magnitude of vortex from Liu and Mei (1976). Values indicated on the plot are magnitudes of a streamline function.



6.10.3 Discussion

The difference between the results in this section and Section 6.9 are clear. Due to the wave approaching the breakwater from an angle the shadow zone is shifted towards the upper end of the modelled area. Figure 6.52 and Figure 6.56 both display this shadow zone very well. Diffraction of waves behind the breakwater is also apparent in these results. The shape of the diffracted waves shown in Figure 6.53 and Figure 6.54 is slightly different to those in the previous section. Again, this is due to the deep-water angle of the examined wave. There is a standing wave field behind the breakwater. This field can be seen in Figure 6.52 and Figure 6.56 as well as in three-dimensional form in Figure 6.54. The interesting set of peaks and troughs in this wave field is caused by the interaction of an incoming wave at a positive angle and the corresponding reflected (outgoing) wave having the reciprocal angle. As before the radiating boundary condition on the open water boundary efficiently deals with these backscattered waves and allows them to exit the domain thus not affecting any other modelled wave data in the domain.

The results of the NM-WDHM for this scenario are further proof of the angled shadow zone visible in the wave results. Figure 6.57 shows how a certain amount of the set-up towards the lower portion of the modelled area is actually behind the breakwater because the angle of the incoming waves means this area, although behind the breakwater, is not in the shadow zone. Figure 6.59 and Figure 6.60 show the set-up/set-down and currents in the region just above the shadow zone caused by the breakwater. The set-up/set-down results of the NM-WDHM are not affected greatly by the inclusion or neglecting of the turbulence terms. However, as displayed in Section 6.9, earlier, the velocity field is described more realistically when the effect of turbulent diffusion is included. As before the vortex in this area is driven mainly by hydrostatic forces with flow from regions of higher pressure into regions of lower pressure. Figure 6.61 and Figure 6.62 show similar circumstances for set-up/set-down and currents in the region towards the lower end of the modelled area. Figure 6.63 shows a cross-section of longshore current velocities along a line at $y = 270\text{m}$. This plot shows the smoothing effect brought about by the inclusion of turbulent diffusion within the model.

Figure 6.64 shows the streamlines obtained by Liu and Mei (1976) for velocity in the vicinity of a detached breakwater with waves approaching from an angle. The x-axis for the Liu and Mei (1976) results is at $x = 1000\text{m}$ in the notation of this project. The

streamlines show a concurrence with the trend of the vortices obtained in the NM-WDHM results. The method of streamline plotting by Liu and Mei (1976) makes it difficult to compare the values of velocity quantitatively. The streamlines are closer together in the locations where higher velocity values are predicted by the NM-WDHM.. Figure 6.65 shows contours of the set-up and set-down obtained by Liu and Mei (1976). The values of set-down obtained by Liu and Mei (1976) compare favourably with those of the NM-WDHM. Although the general trend of set-up contours are similar, the results of Liu and Mei (1976) predict a higher set-up at the shoreline than that of the NM-WDHM. A similar difference was evident in the results of Section 6.9 and it is discussed in Section 6.9.3.

6.11 Detached Breakwater after P  chon *et al.* (1997)

6.11.1 Introduction

P  chon *et al.* (1997) examine a number of different wave-driven hydrodynamic models and their corresponding wave models. The title and origin of each of these models are detailed in Table 6.2. Each of the models is examined for the same set of wave data and bathymetry. Newell *et al.* (2005b) examine the NM-WCIM and NM-WDHM for the same set of circumstances. The current version of the NM-WCIM and NM-WDHM are examined in this section for comparison with the results of the other wave-driven current models examined by P  chon *et al.* (1997). In order to provide measured results for the scenario in question P  chon *et al.* (1997) chose a small experimental sized domain with an experimental wave height.

6.11.2 Results

The experimental domain is 30m by 30m in size with a half detached breakwater of 0.87m width and 6.66m long situated approximately 10m offshore. The underwater beach slope is 1 in 50 until a depth of 0.33m is reached and then a flat seabed continues to the outer end of the domain. The side walls of the experimental tank are reflective, hence in the NM-WCIM a radiation boundary is not be used on the sides. A wave of 1.7 second period and 7.5cm height at the outer end of the domain approaches the beach perpendicularly. Figure 6.66 shows the water surface results obtained using the NM-WCIM for this scenario in the case of unbroken waves. The same scenario is plotted in Figure 6.67 for broken waves.

Table 6.2 - Table of computer models examined by P  chon *et al.* (1997)

Wave Model		Hydrodynamic Model		Developed by
W1	ARTEMIS	C1	TELEMAC-3D	EDF-LNH, France
W2	PROPS	C2	CIRCO	LIM-UPC, Spain
W3	MIKE 21 PMS	C3	MIKE 21 HD	DHI, Denmark
W4	FDWAVE	C4	TIDEFLOW-2D	HR Wallingford Ltd., UK
W5	<i>Wave Model</i>	C5	<i>Hydrodynamic Model</i>	Maritime Group, University of Liverpool, UK
W6	<i>Wave Model</i>	C6	<i>Hydrodynamic Model</i>	STCPMVN, France
W7	<i>Wave Model</i>	C7	<i>Hydrodynamic Model</i>	Aristotle University of Thessaloniki, Greece

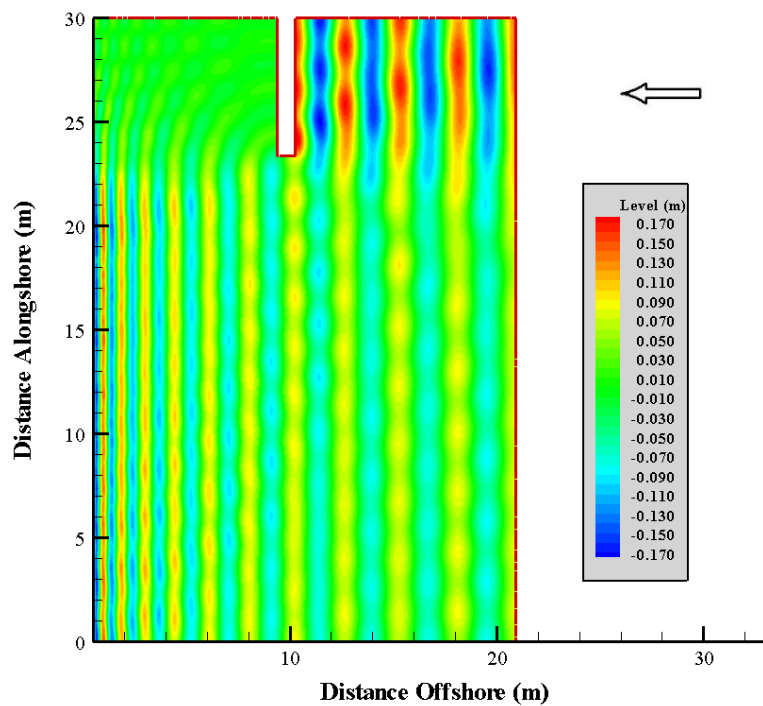


Figure 6.66 – Water surface in the presence of the Detached Breakwater of Péchon *et al.* (1997). Waves propagating from right to left.

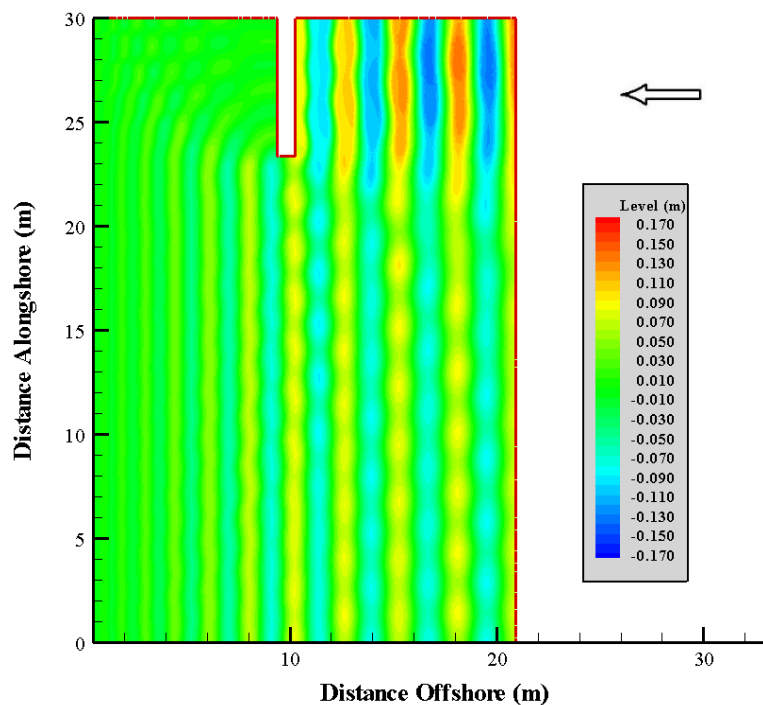


Figure 6.67 – Water Surface in the presence of the Detached Breakwater of Péchon *et al.* (1997). Waves propagating from right to left.

Figure 6.68 shows contour lines of where the water surface height is zero to describe wave phase. Figure 6.69 shows a three-dimensional plot of the same results as Figure 6.67.

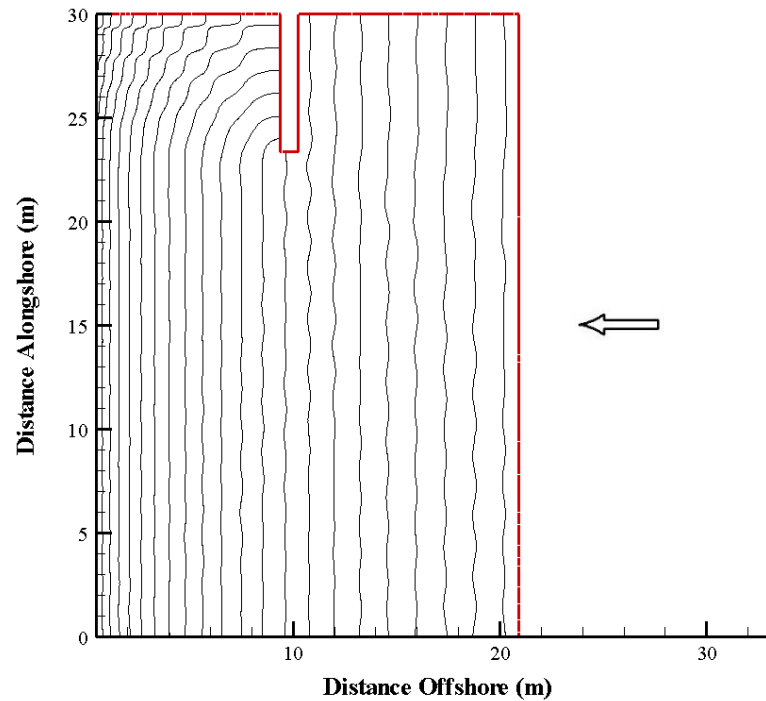


Figure 6.68 – Contours of Water Surface = 0 to indicate Wave Phase for Waves approaching a Breakwater at an Angle. Waves propagating from right to left.

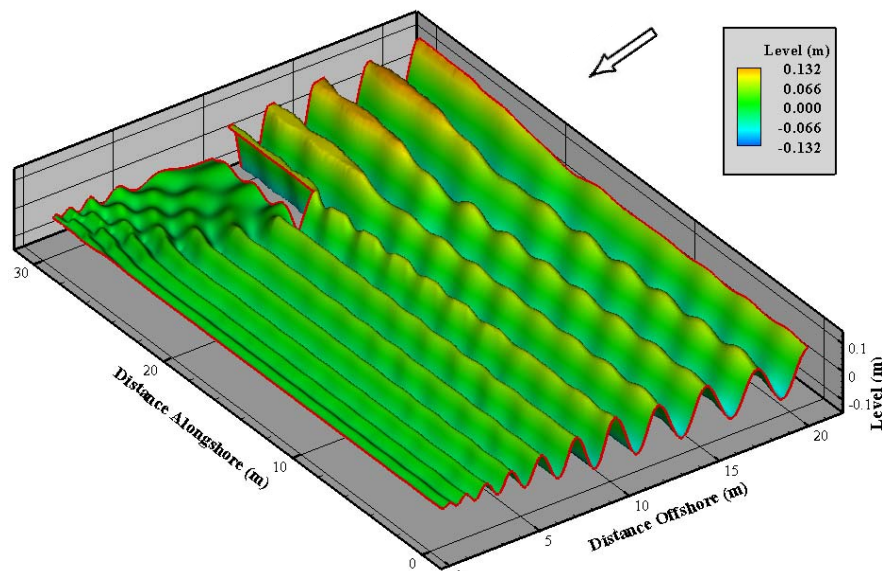


Figure 6.69 – Three dimensional plot of Water Surface for Broken Waves in the presence of the Detached Breakwater of Péchon *et al.* (1997).

Figure 6.70 and Figure 6.71 show plots of unbroken and broken wave heights respectively for the same scenario as the wave surfaces plotted above. Figure 6.72 is a plot of the breaker lines from various wave models reproduced from P  chon *et al.* (1997) and adapted to include the results of the NM-WCIM. Similarly Figure 6.73 is a plot of wave heights obtained from various wave models by P  chon *et al.* (1997) at $x = 20\text{m}$ and the results of the NM-WCIM have been included. For the NM-WCIM in this case a simple linear relationship between water depth and maximum wave height (with $\gamma_0 = 0.78$) proved appropriate to decide the insipience point.

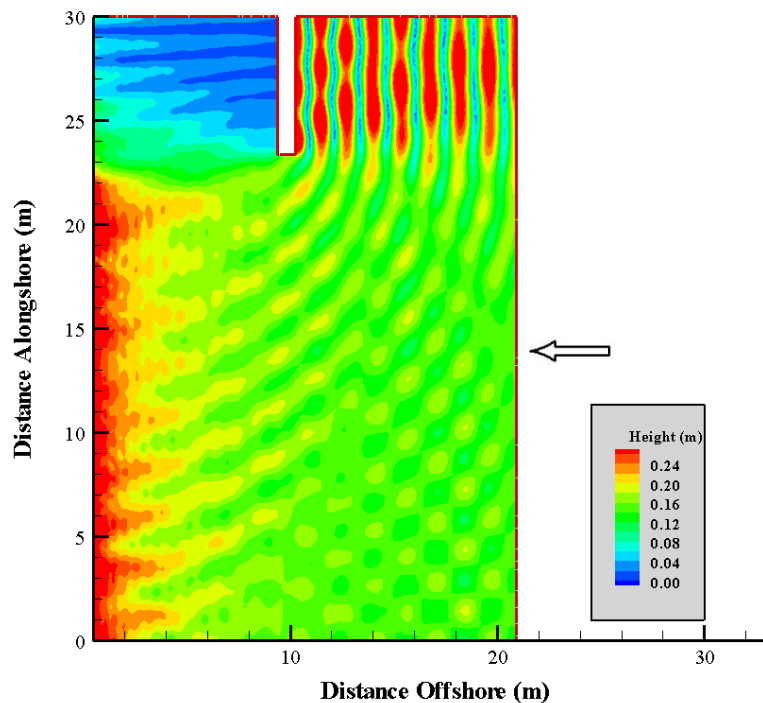


Figure 6.70 – Unbroken Wave Height in the presence of the Detached Breakwater of P  chon *et al.* (1997). Waves propagating from right to left.

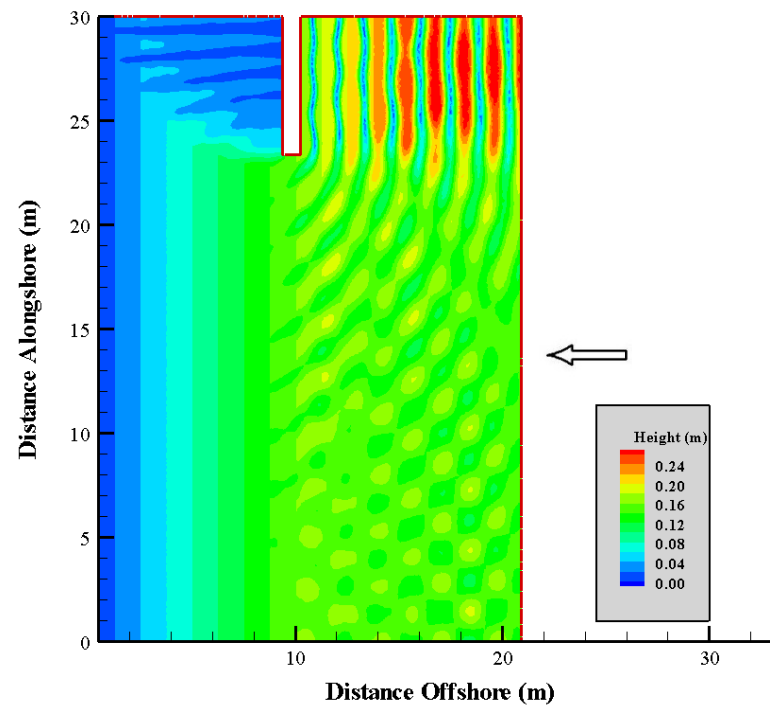


Figure 6.71 – Broken Wave Height in the presence of the Detached Breakwater of Péchon *et al.* (1997). Waves propagating from right to left.

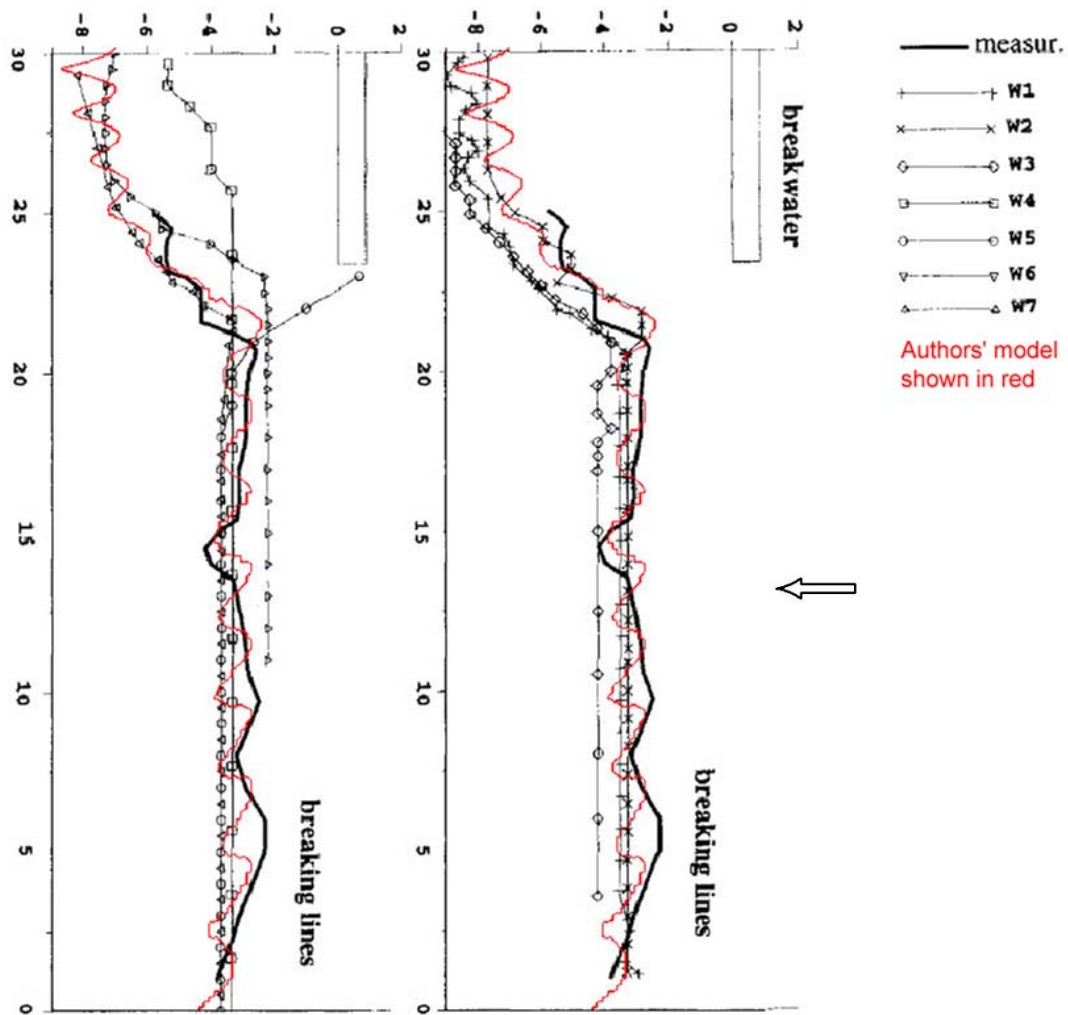


Figure 6.72 – Comparison of breaking line for NM-WCIM and models examined by Pechon *et al.* (1997). Waves propagating from right to left.

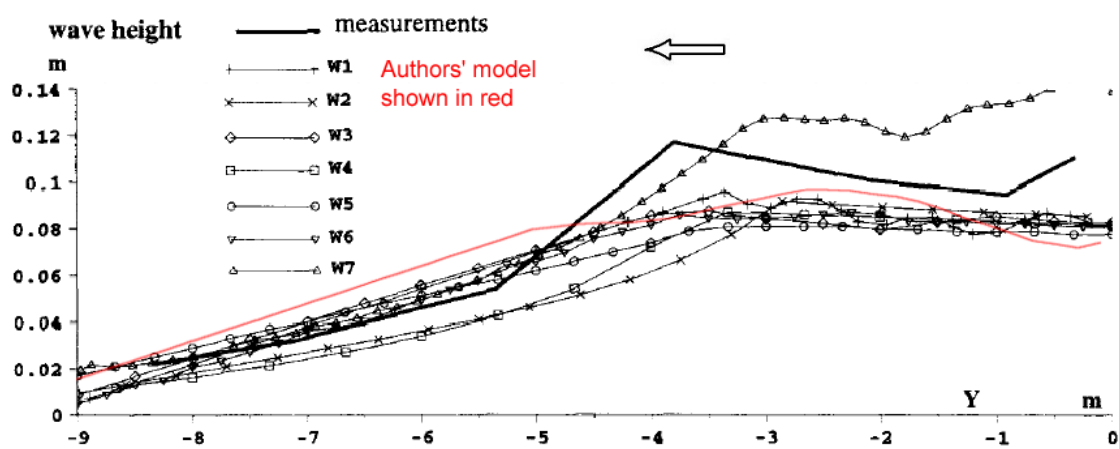


Figure 6.73 – Comparison of Wave Height for NM-WCIM and models examined by Pechon *et al.* (1997) at $x = 20\text{m}$. Waves propagating from right to left.

Figure 6.74 shows the set-up/set-down obtained from the NM-WDHM both in the region unaffected by the breakwater and the region behind the breakwater in the absence of turbulent diffusion. Figure 6.75 shows results in the same region when turbulent diffusion is included in the NM-WDHM. A turbulent parameter of $M=1.1$ is used for eddy viscosity in the turbulent diffusion terms. Eddy viscosity values are obtained along with broken wave heights for the turbulent model using the wave ray method described in Chapter 5 above. Figure 6.76 shows velocity vectors and set-up/set-down from the NM-WDHM for the upper area of the modelled region (behind the breakwater) in the absence of any turbulent diffusion. Figure 6.77 shows a plot of the same area with an empirical turbulent parameter of $M=1.1$ used for eddy viscosity in the turbulent diffusion terms. Figure 6.78, that follows, shows a cross-section of longshore current along a line of $y = 20\text{m}$. This plot allows the examination of the effects of turbulent diffusion within the NM-WDHM. Similarly Figure 6.79 shows a cross-section along a line at $y = 27\text{m}$.

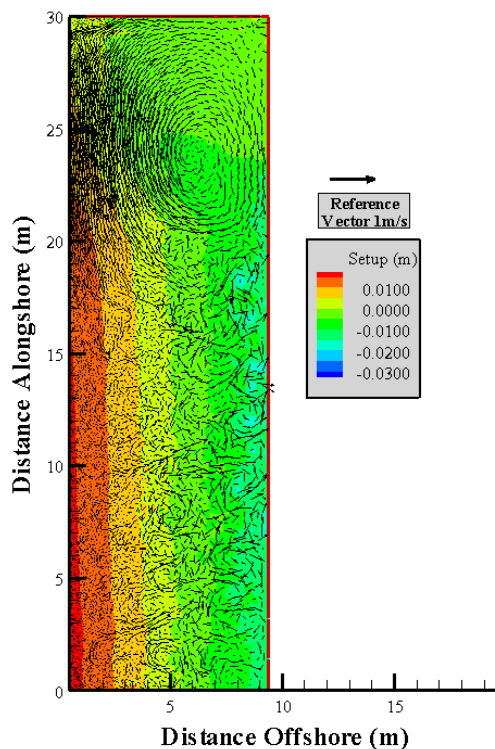


Figure 6.74 – Set-up/Set-down and Currents for Péchon *et al.* (1997) model using NM-WDHM with no turbulence

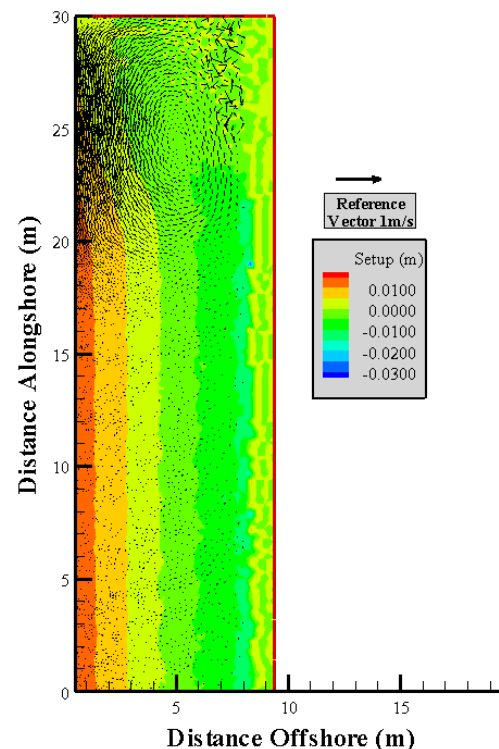


Figure 6.75 – Set-up/Set-down and Currents for Péchon *et al.* (1997) model using NM-WDHM with turbulence

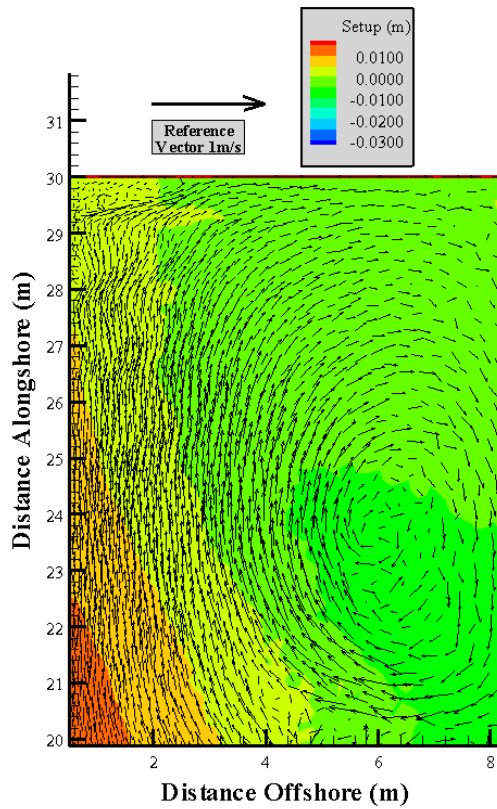


Figure 6.76 – Set-up/Set-down and Currents behind Breakwater with no turbulence

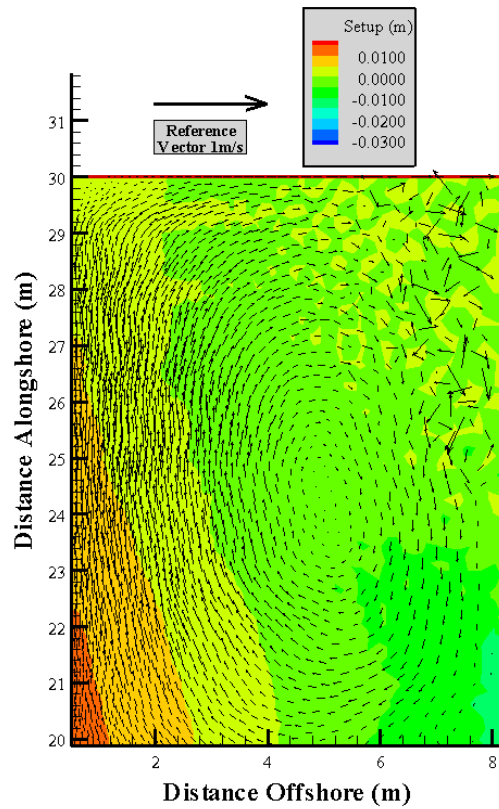


Figure 6.77 – Set-up/Set-down and Currents behind Breakwater with turbulence

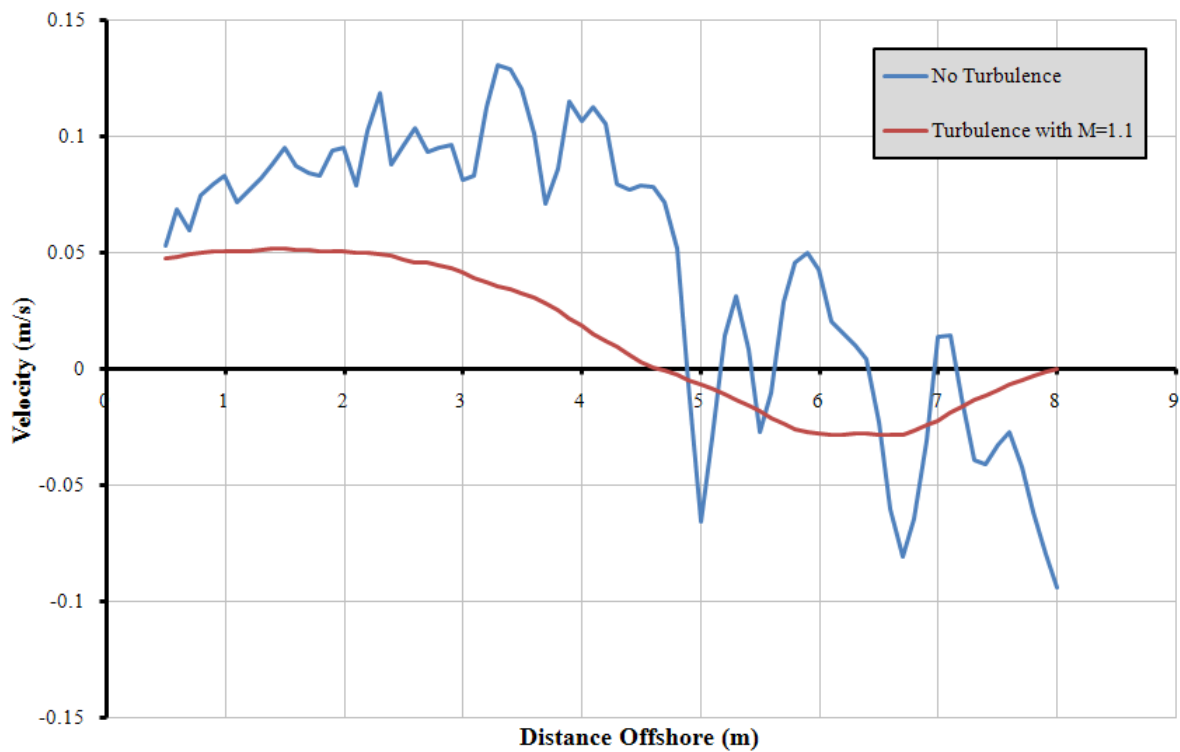


Figure 6.78 – Profile of Longshore Current at $y = 20\text{m}$ showing the effect of Turbulence Diffusion

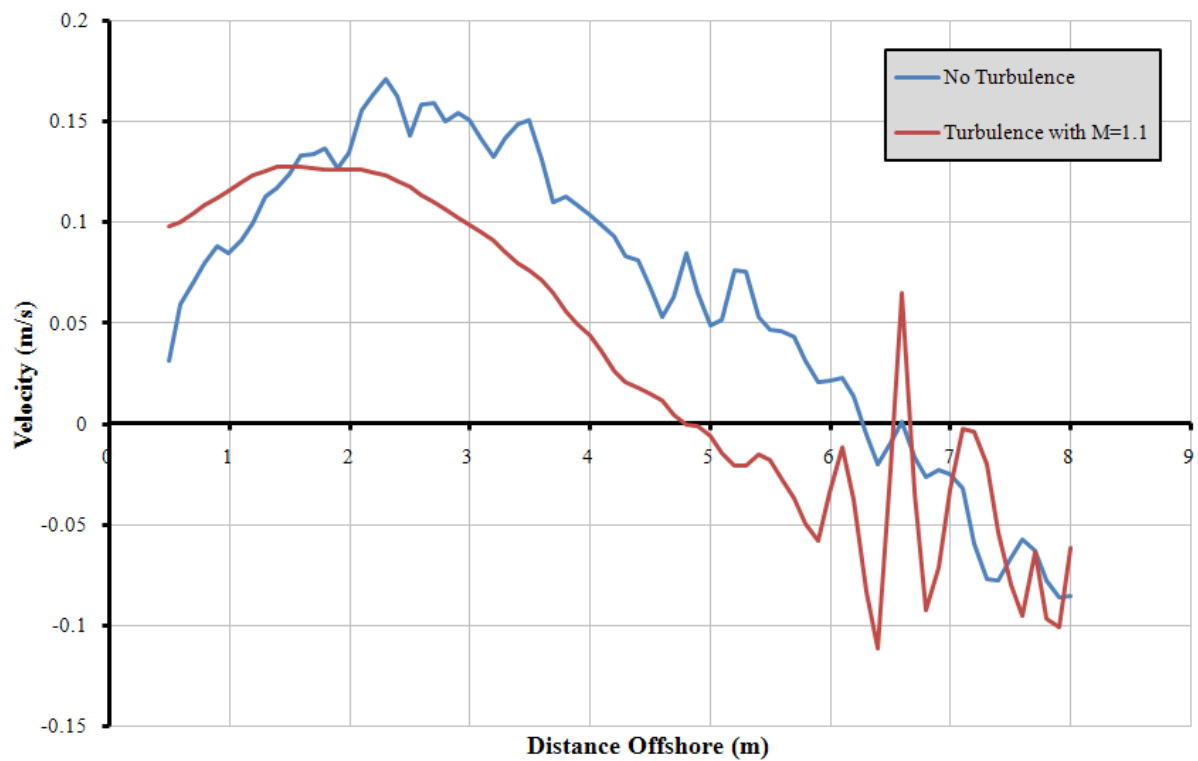


Figure 6.79 – Profile of Longshore Current at $y = 27\text{m}$ showing the effect of Turbulent Diffusion

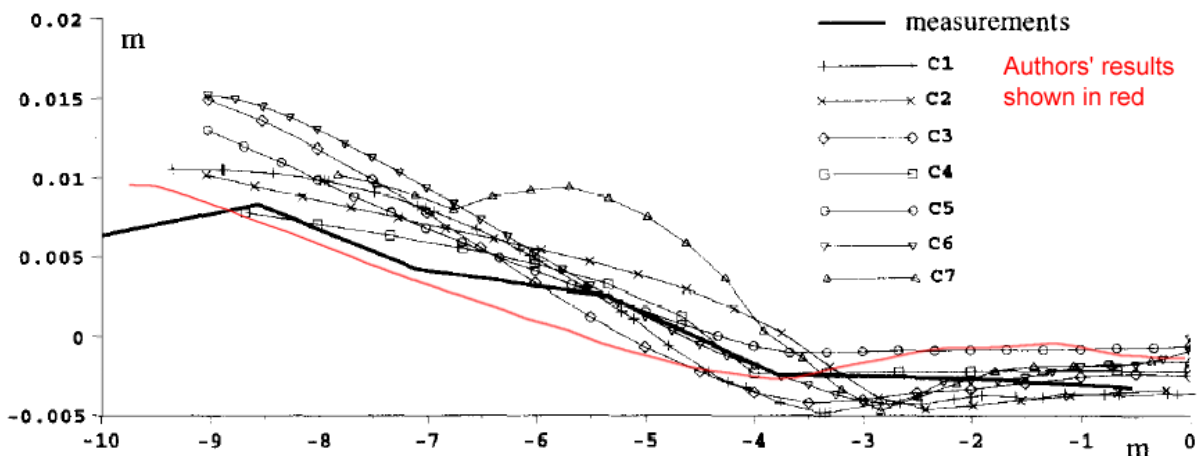


Figure 6.80 – Comparison of Set-up/Set-down for NM-WCIM and models examined by P  chon *et al.* (1997) at $x = 21\text{m}$

6.11.3 Discussion

The results of the NM-WCIM compare well with both the measured results of P  chon *et al.* (1997) and the results of other numerical models presented. The varying breaking criterion chosen by different models does not appear to have a large effect in this scenario and indeed a simple linear relationship between water depth and wave height allows the

NM-WCIM to give a result similar to the other models. Similarly the linear breaking relationship applied in the NM-WCIM predicts a similar broken wave height to the other methods examined by Péchon *et al.* (1997). These results reiterate the need to select appropriate breaking and insipience criteria based on measured data from the site being considered.

The NM-WDHM also provides results that compare well with the measured results of wave-generated effects presented by Péchon *et al.* (1997). The NM-WDHM does not appear to over-predict the set-up as much as some of the other models. Figure 6.76 and Figure 6.77 show some interesting results in this case. In the case of an experimental sized domain with a small wave of very short period the inclusion of turbulent effects in the NM-WDHM has a significant effect. Turbulence has a noticeable decreasing effect on the magnitude of the velocity vectors and it also appears to cause a change in the location of the centre of the developed vortex. This is further displayed by the differing x-intercepts visible in Figure 6.79. (It should be noted that the unsteadiness of the velocity values in the region of the breakwater in Figure 6.79 is caused by numerical noise which is a function of turbulent interactions near the closed boundary of the domain. It only occurs near the breakwater tip and does not affect other results in the domain. This is demonstrated by the steady results of Figure 6.78.)

6.12 Comparison of Radiation Stress with Watanabe and Maruyama (1986)

6.12.1 Introduction

Watanabe and Maruyama (1986) present calculated radiation stress values for an experimental sized domain with small waves of short period. Newell *et al.* (2005b) compare radiation stress values calculated using the results of the NM-WCIM for this scenario. Similar results are presented here for the current version of the NM-WCIM.

6.12.2 Results

The experimental domain is 4m by 5m in size with a half detached breakwater 3.3m long situated approximately 3m offshore. The slope of the seabed is 1 in 50. A wave of 1.6 second period and 4.2cm deep-water height approaches the beach perpendicularly. Figure 6.81 shows the water surface results obtained using the NM-WCIM for this scenario in the case of unbroken waves. The same scenario is plotted in Figure 6.82 for broken waves.

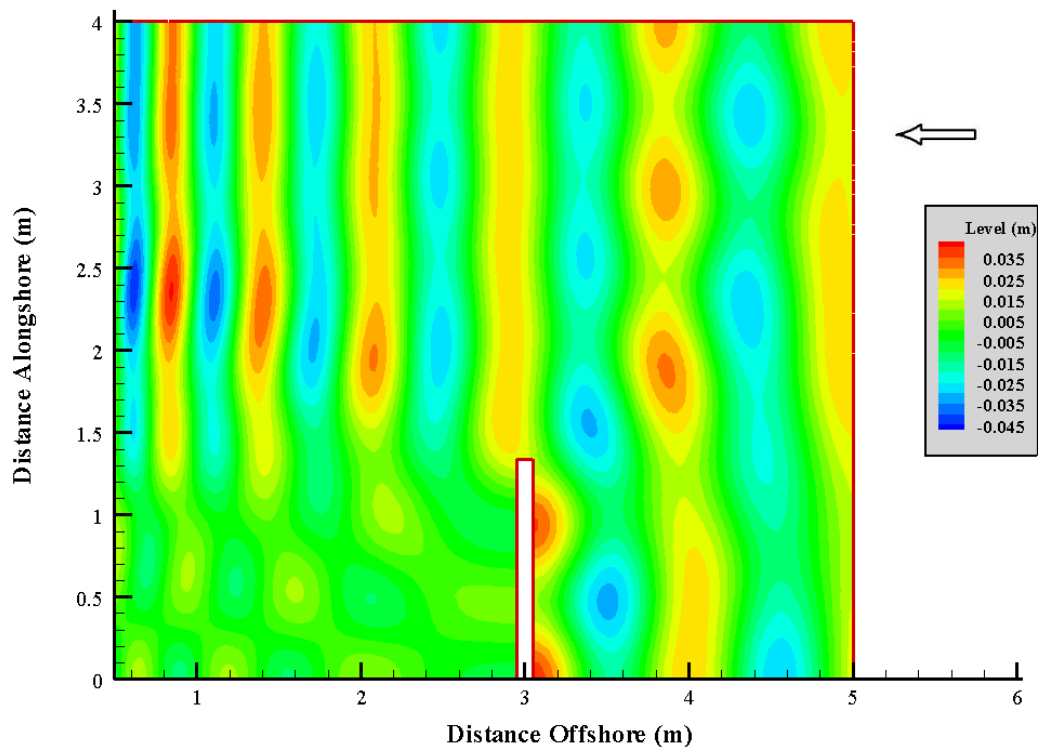


Figure 6.81 – Water surface in the presence of the Watanabe and Maruyama (1986) Detached Breakwater with Unbroken Waves. Waves propagating from right to left.

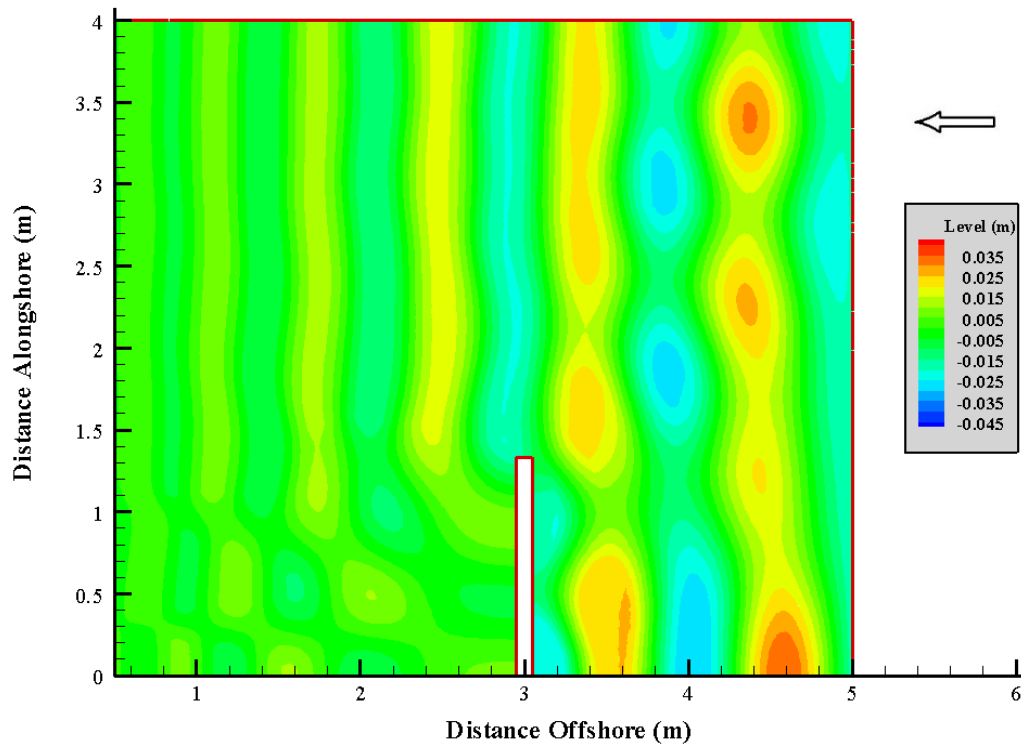


Figure 6.82 – Water Surface in the presence of the Watanabe and Maruyama (1986) Detached Breakwater with Broken Waves. Waves propagating from right to left.

Figure 6.83 shows contour lines of where the water surface height is zero. Figure 6.84 shows wave rays obtained using the wave ray method of Chapter 5 plotted alongside the contours of Figure 6.83. Figure 6.85 shows a three-dimensional plot of the same results as Figure 6.81.

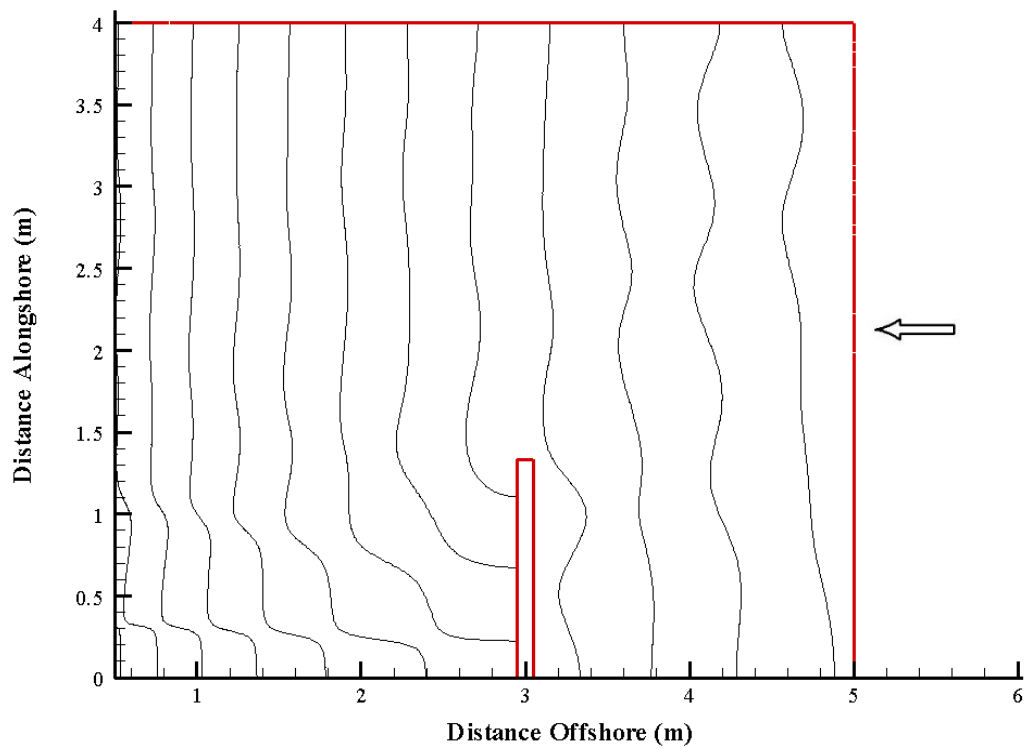


Figure 6.83 – Contours of Water Surface = 0 to indicate Wave Phase for Waves approaching the Watanabe and Maruyama (1986) Detached Breakwater. Waves propagating from right to left.

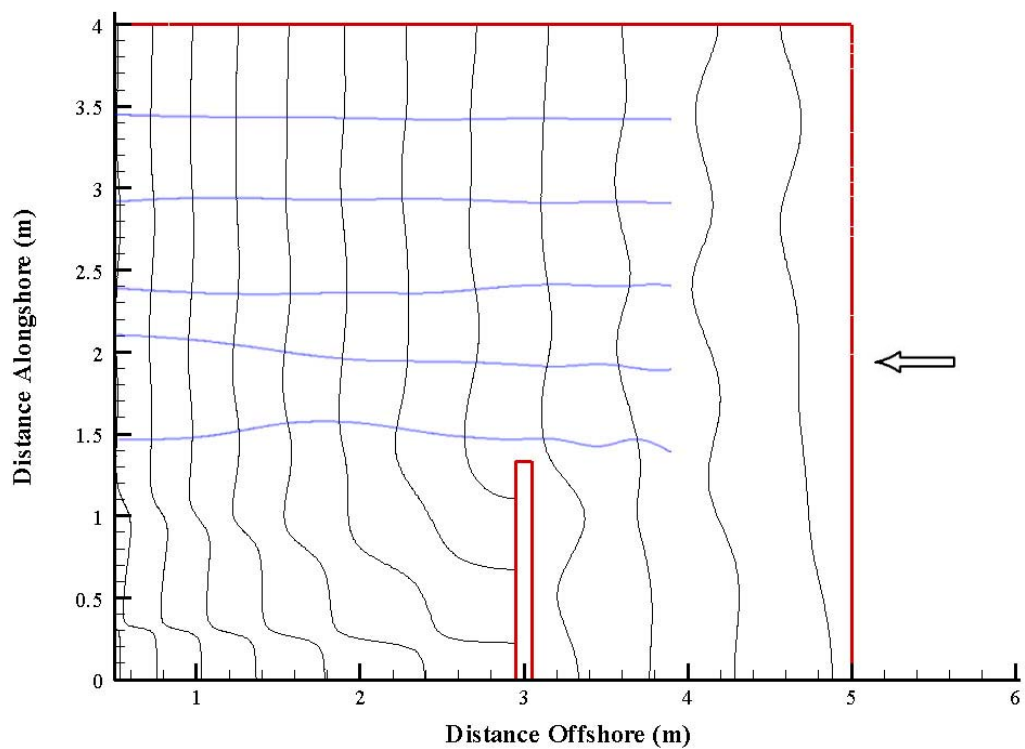


Figure 6.84 – Wave Rays (in blue) plotted alongside contours of Water Surface = 0 for Waves approaching the Watanabe and Maruyama (1986) Detached Breakwater. Waves propagating from right to left.

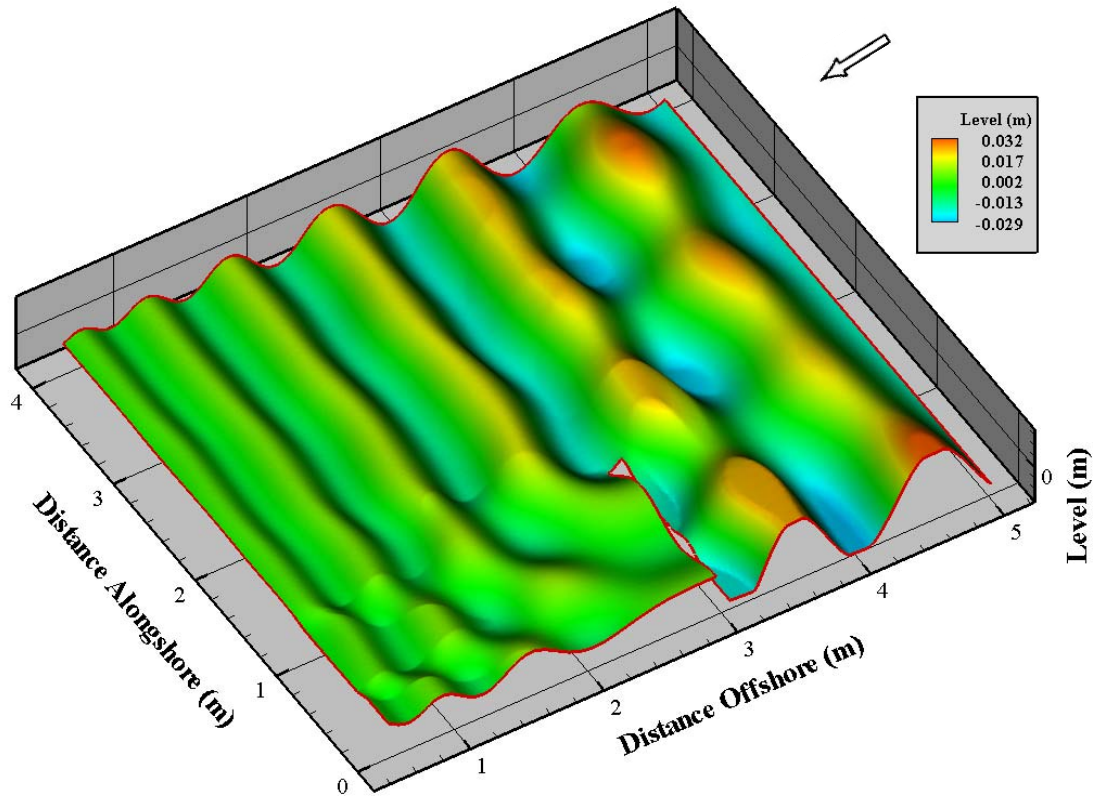


Figure 6.85 – Three dimensional plot of Water Surface in the vicinity of the Watanabe and Maruyama (1986) Detached Breakwater for Broken Waves

Figure 6.86 and Figure 6.87 show plots of unbroken and broken wave heights respectively for the same scenario as the wave surfaces plotted above. Linear breaking has been used in this case with $\gamma_0 = 0.78$. Watanabe and Maruyama (1986) do not provide wave-driven currents or set-up/set-down results for this domain, however in the interests of completeness the NM-WDHM has been used to examine set-up/set-down and wave driven currents for the Watanabe and Maruyama (1986) scenario. These results of the NM-WDHM are shown in Figure 6.88.

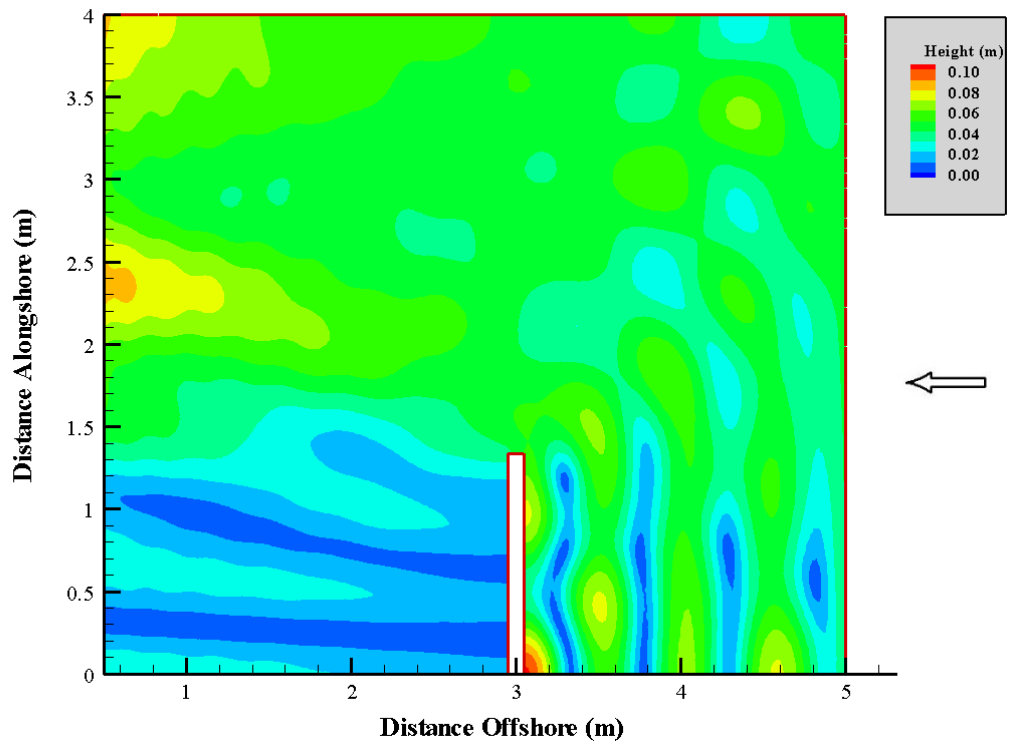


Figure 6.86 – Unbroken Wave Height in the presence of the Watanabe and Maruyama (1986) Detached Breakwater. Waves propagating from right to left.

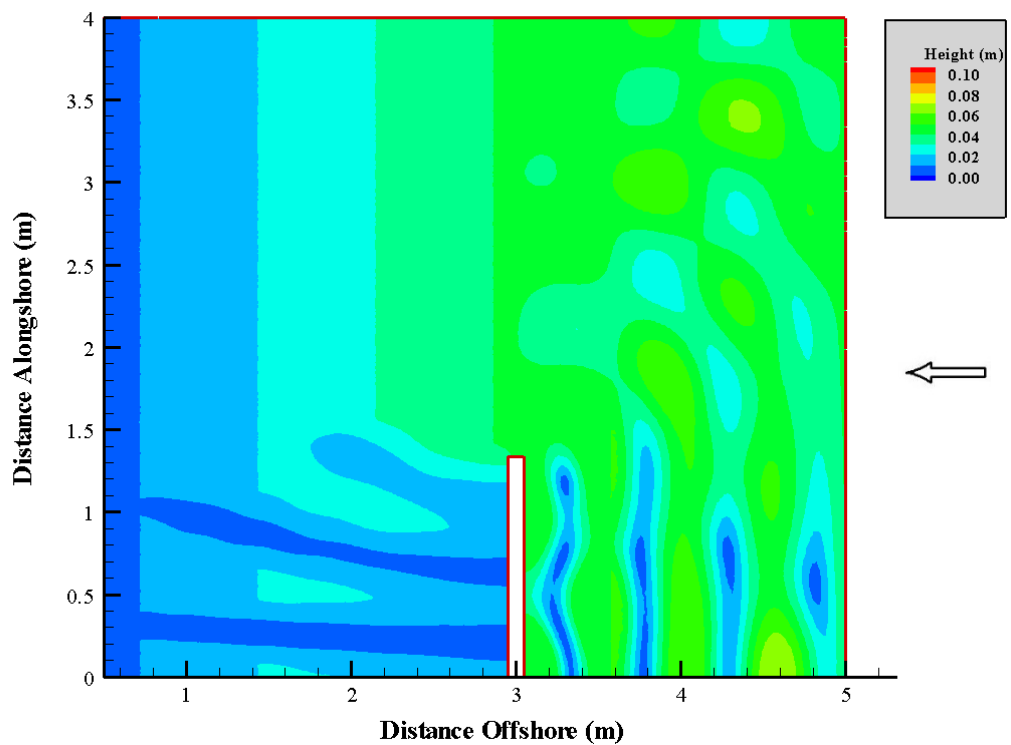


Figure 6.87 – Broken Wave Height in the presence of the Watanabe and Maruyama (1986) Detached Breakwater. Waves propagating from right to left.

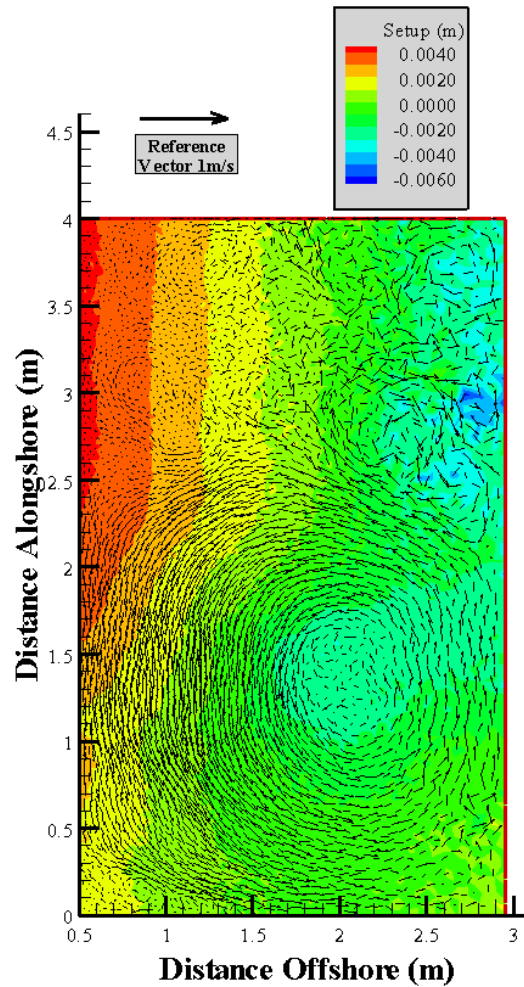


Figure 6.88 – Set-up/Set-down and Wave-Driven Currents from NM-WDHM for Watanabe and Maruyama (1986)

Radiation stress values calculated using the method described in Section 4.5 are plotted below for comparison with radiation stress values presented by Watanabe and Maruyama (1986). Figure 6.89 and Figure 6.90 show the component of radiation stress in the longshore direction from the NM-WCIM and Watanabe and Maruyama (1986) respectively, Figure 6.91 and Figure 6.92 show the shear component of radiation stress from the NM-WCIM and Watanabe and Maruyama (1986) respectively and Figure 6.93 and Figure 6.94 show the component of radiation stress in the crossshore direction from the NM-WCIM and Watanabe and Maruyama (1986) respectively.

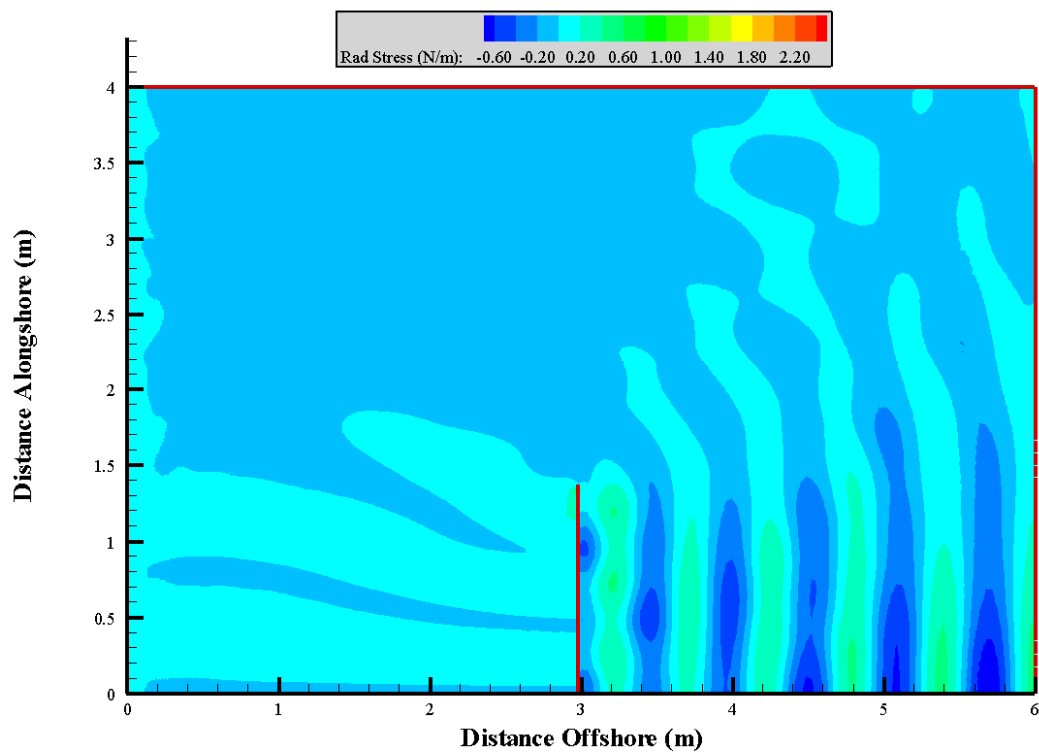


Figure 6.89 – R'_{22} from NM-WCIM

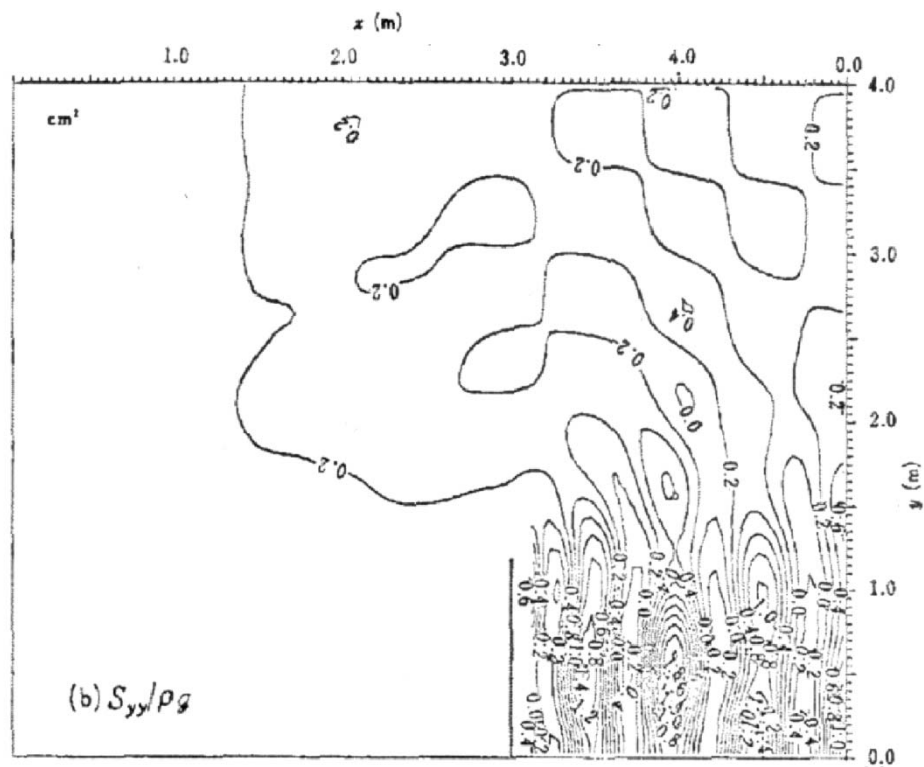
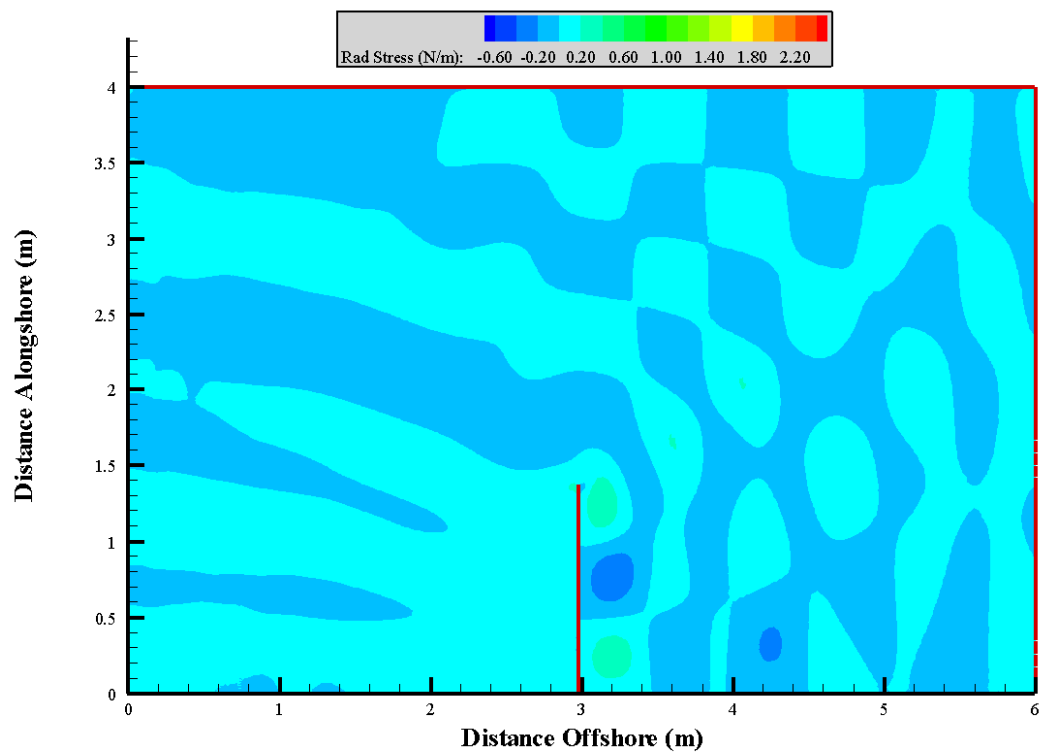
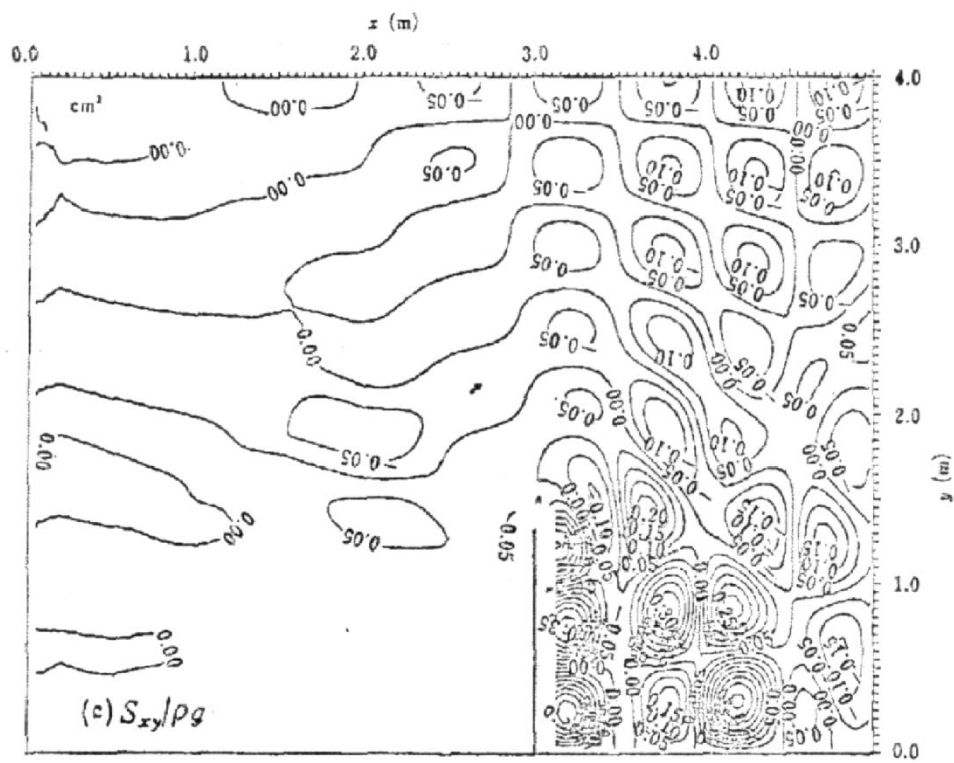


Figure 6.90 – S_{yy} from NM-WCIM Watanabe and Maruyama (1986)

Figure 6.91 – R'_{12} from NM-WCIMFigure 6.92 - S_{xy} from NM-WCIM Watanabe and Maruyama (1986)

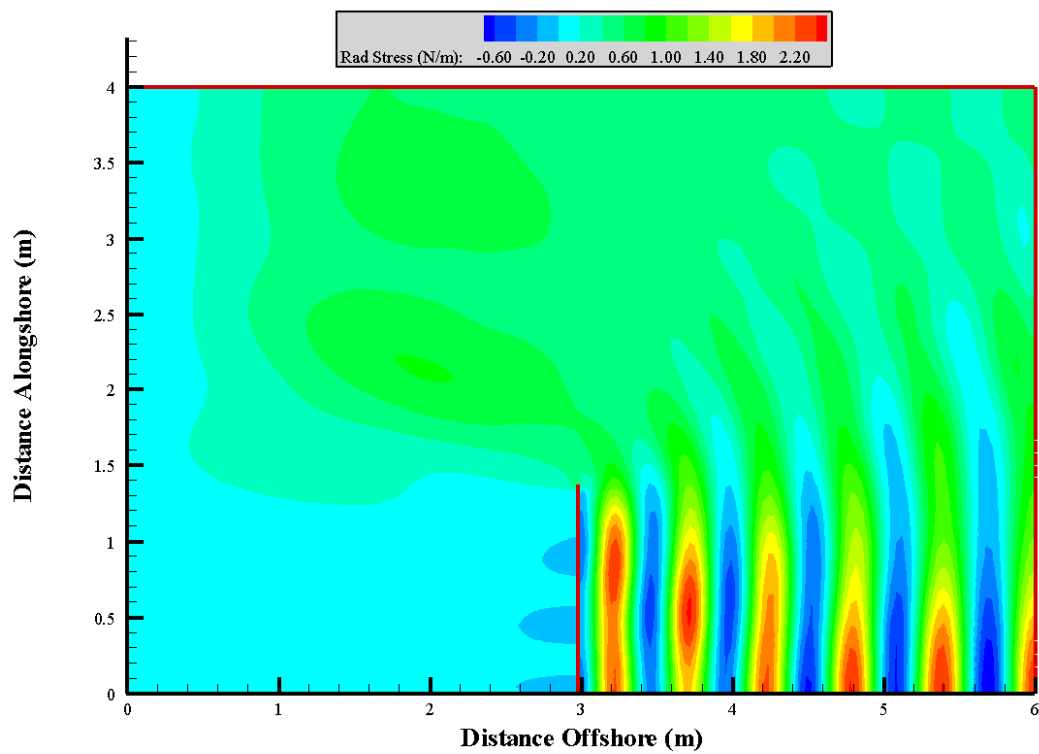


Figure 6.93 – R'_{11} from NM-WCIM

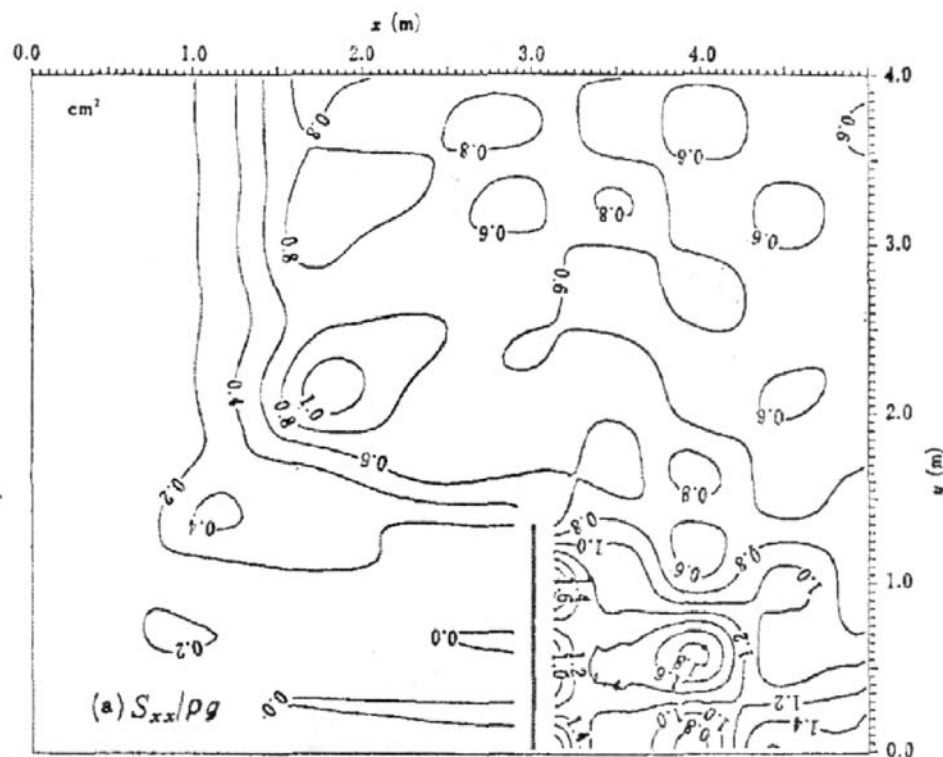


Figure 6.94 - S_{xx} from NM-WCIM Watanabe and Maruyama (1986)

6.12.3 Discussion

The results of the NM-WCIM for the Watanabe and Maruyama (1986) scenario are as expected with the wave shoaling and breaking on the beach and a shadow zone with diffracted waves behind the breakwater. Figure 6.88 shows the development of a vortex behind the breakwater as experienced in other models with detached breakwaters. There is also a defined set-up and set-down in the region to the side of the breakwater and only a minor degree of set-up and set-down in the shadow zone behind the breakwater.

The trend and contour plots of the radiation stress values presented in Figure 6.89 for the longshore direction compare well with those of Watanabe and Maruyama (1986) in Figure 6.90. The peak values in the surf zone and on the downwave side of the breakwater are in close agreement. There is a slight difference evident in the lower values at the nadir points up-wave of the breakwater. Similarly, the values for the shear component of radiation stress calculated from the results of the NM-WCIM and shown in Figure 6.91 compare well with those published by Watanabe and Maruyama (1986) for the same direction, as shown in Figure 6.92. The peak values are approximately the same but, as before, there is a slightly lower prediction of the nadir values on the upwave side of the breakwater by the NM-WCIM. Interestingly, in the same region, the radiation stress values calculated from the NM-WCIM for the cross-shore direction (Figure 6.93) show a larger degree of difference from those of the same direction published by Watanabe and Maruyama (1986) (Figure 6.94). As before, the results in other regions of the model appear to compare favourably with those of Watanabe and Maruyama (1986).

Wave-driven effects such as set-up and set-down only become evident in the surf-zone and the results of the NM-WCIM and Watanabe and Maruyama (1986) compare favourably with each other in this region for the three components of radiation stress. The presence of a standing wave field upwave of the breakwater may be the cause of the difference in results in that region. For the NM-WCIM a radiation boundary condition is applied to the open boundary to address the reflected waves from the breakwater. For the Watanabe and Maruyama (1986) model “flow rate” values are applied to the open boundary to address this issue. These may cause the model to yield different results to the NM-WCIM upwave of the breakwater.

6.13 Comparison with Attached Breakwater of Liu and Mei (1976)

6.13.1 Introduction

In addition to the detached breakwater examined in Section 6.9 and 6.10 Liu and Mei (1976) also examine the effects of an attached breakwater on wave-driven hydrodynamics. The NM-WCIM and NM-WDHM have been used to examine the same set of circumstances for further validation of the created models.

6.13.2 Results

Figure 6.95 shows the scenario under examination. An attached breakwater of 400m length is situated on a beach with a slope of 1 in 10. A wave of 10 second period and 1m deep-water height approaches the beach at a deep-water angle of 45 degrees. A semi-circular boundary is applied to the open water side of the domain to allow backscattered waves to exit the domain. The water surface is shown in Figure 6.95 for unbroken waves. The same scenario is plotted in Figure 6.96 for broken waves. As in Sections 6.9 and 6.10 Liu and Mei (1976) use an insipience criterion of $\gamma_0 = 0.4$. The same is used in this case for the purposes of comparison.

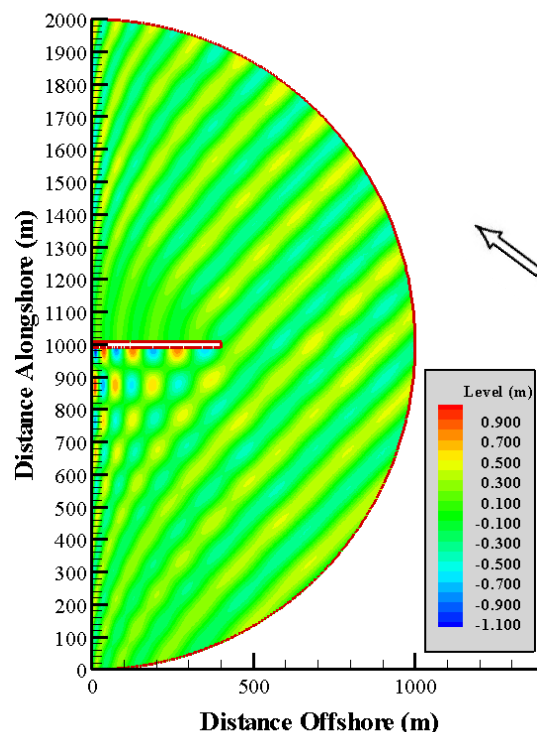


Figure 6.95 – Water surface in the presence of an Attached Breakwater with Unbroken Waves at an Angle

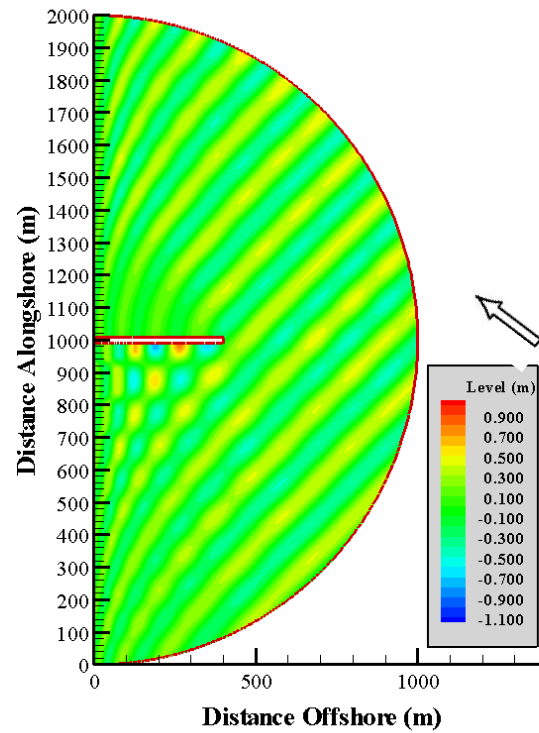


Figure 6.96 – Water Surface in the presence of an Attached Breakwater with Broken Waves at an Angle

Figure 6.97 shows contour lines of where the water surface height is zero to demonstrate the wave phase. Figure 6.98 shows a series of wave rays to illustrate the direction of wave propagation in the model. The wave rays are also used as described in Chapter 5 above to give breaking wave heights and eddy viscosity terms for use in the NM-WDHM. Figure 6.99 shows a three-dimensional plot of the same results as Figure 6.96.

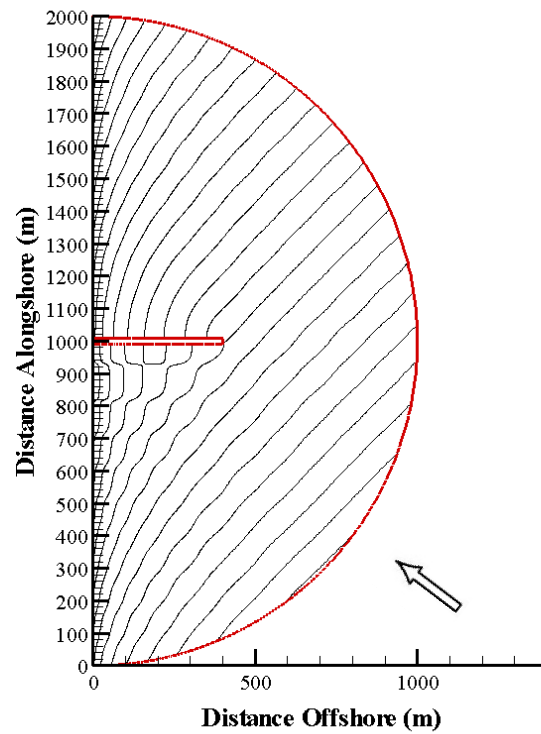


Figure 6.97 – Contours of Water Surface = 0 to indicate Wave Phase for Waves approaching an Attached Breakwater at an Angle

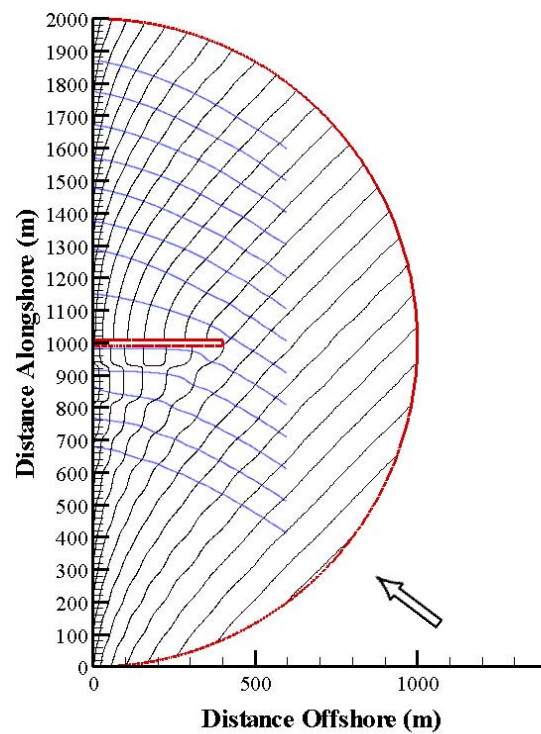


Figure 6.98 – Wave Rays (in blue) plotted alongside contours of Water Surface = 0 for Waves approaching an Attached Breakwater at an Angle

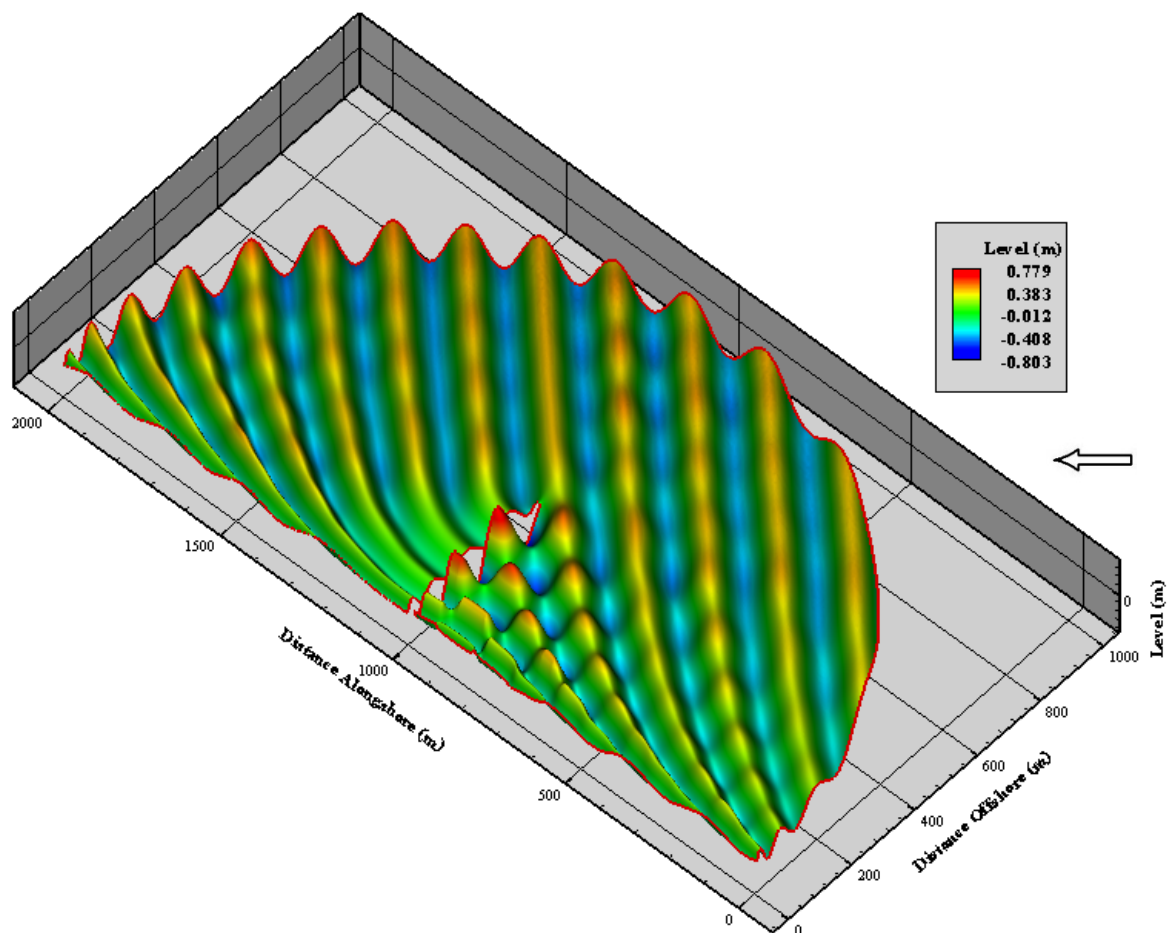


Figure 6.99 – Three dimensional plot of Water Surface for Broken Waves for waves at an Angle

Figure 6.100 and Figure 6.101 show plots of unbroken and broken wave heights respectively for the same scenario as the wave surfaces plotted above.

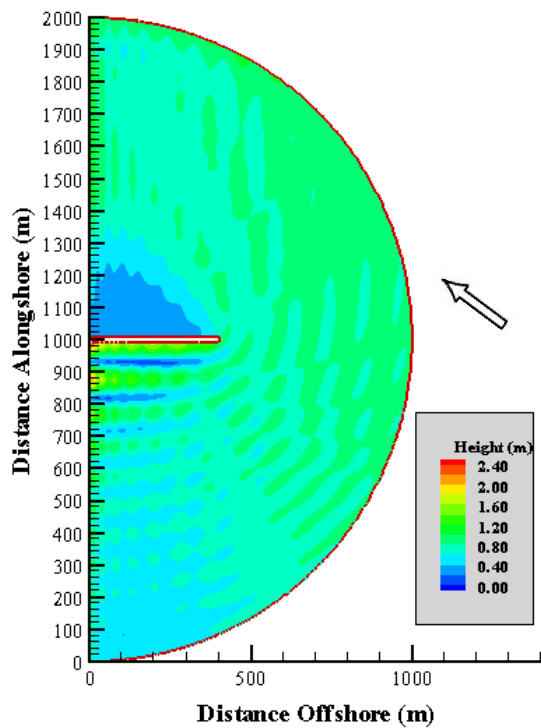


Figure 6.100 – Unbroken Wave Height in the presence of a Detached Breakwater for waves at an Angle

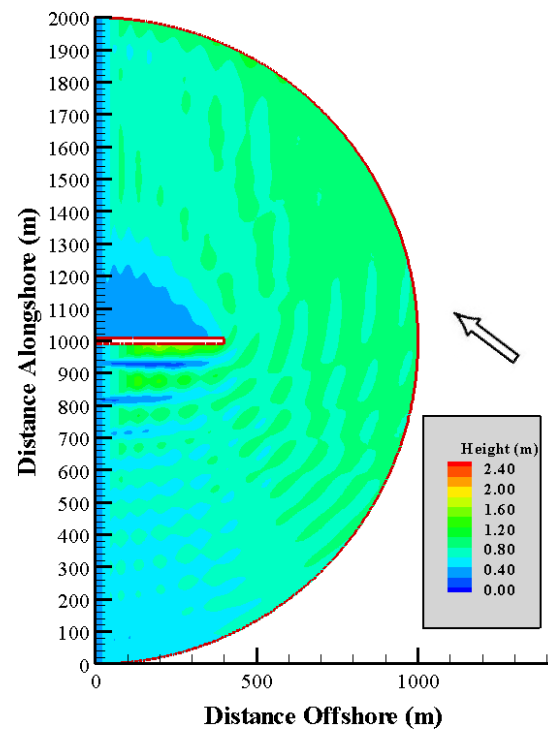


Figure 6.101 – Broken Wave Height in the presence of an Attached Breakwater for Waves at an Angle

Figure 6.102 shows the set-up and set-down obtained from the NM-WDHM both in the region unaffected by the breakwater and the region behind the breakwater. Figure 6.103 shows velocity vectors and set-up/set-down from the NM-WDHM. Figure 6.104 to Figure 6.107 show the set-up and set-down and currents in the region in proximity to, and just upwave the attached breakwater. These include figures with increased scales in the cross-shore direction in order to compare with Figure 6.108 and Figure 6.109 of Liu and Mei (1976). Figure 6.110 to Figure 6.113 show similar data in the region downwave of the breakwater. As before figures with increased scales in the cross-shore direction are included in order to compare with results of Liu and Mei (1976), as shown in Figure 6.114 and Figure 6.115. Figure 6.108 and Figure 6.114 show velocity streamlines obtained by Liu and Mei (1976). Figure 6.109 and Figure 6.115 show contours of set-up and set-down obtained by Liu and Mei (1976) downwave and upwave of the breakwater respectively.

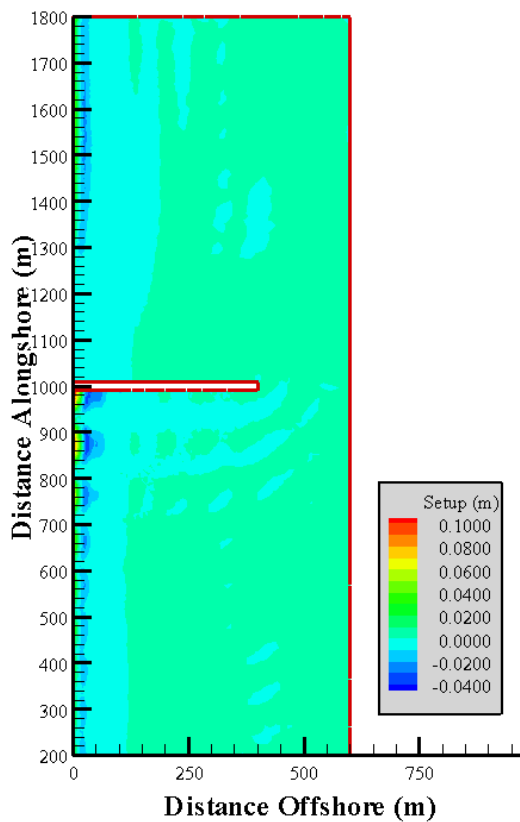


Figure 6.102 – Set-up/Set-down from NM-WDHM for an Attached Breakwater

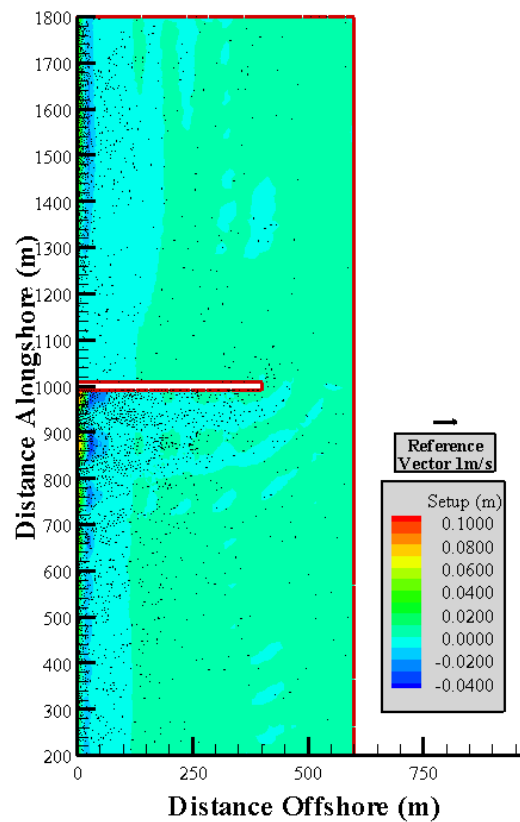


Figure 6.103 – Set-up/Set-down and Currents from NM-WDHM for an Attached Breakwater

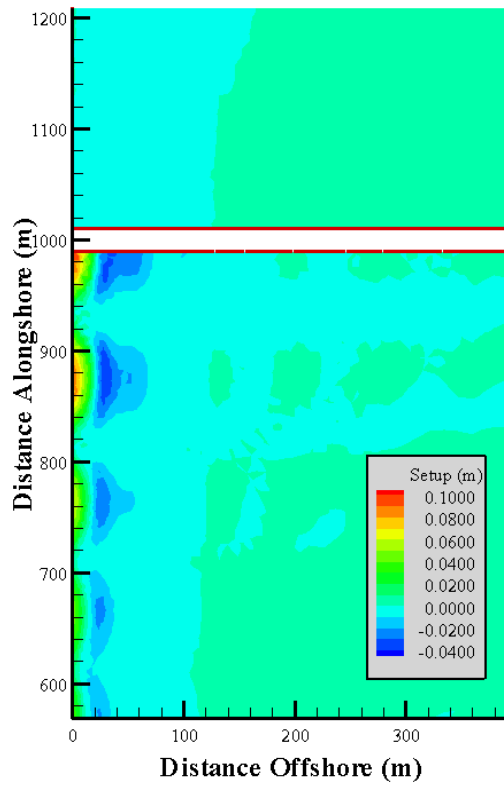


Figure 6.104 – Set-up/Set-down in the vicinity of the Attached Breakwater

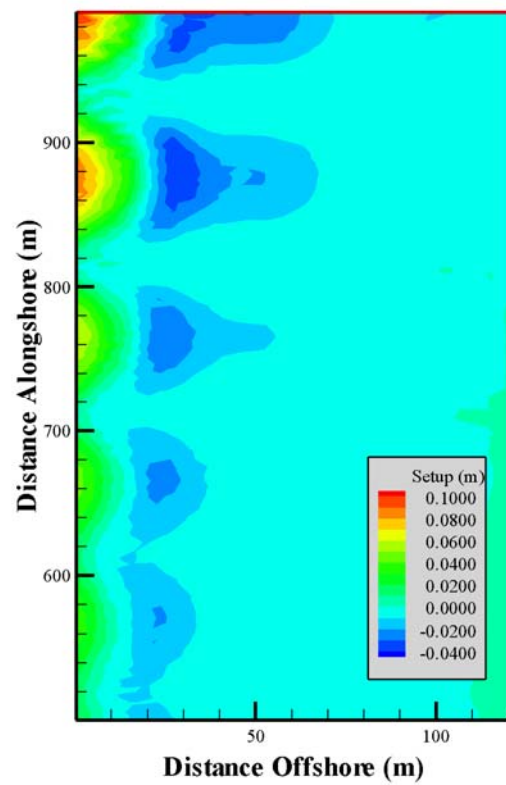


Figure 6.105 – Set-up/Set-down upwave of the Attached Breakwater with increased scale in x-direction

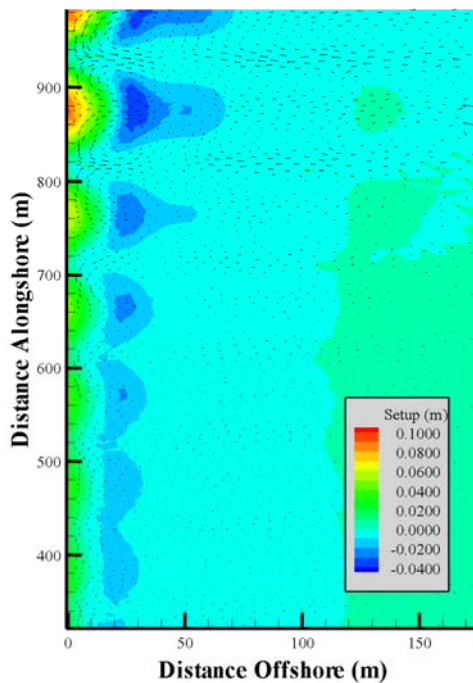


Figure 6.106 – Set-up/Set-down and Currents upwave of the Attached Breakwater with increased scale in x-direction in the presence of turbulent diffusion

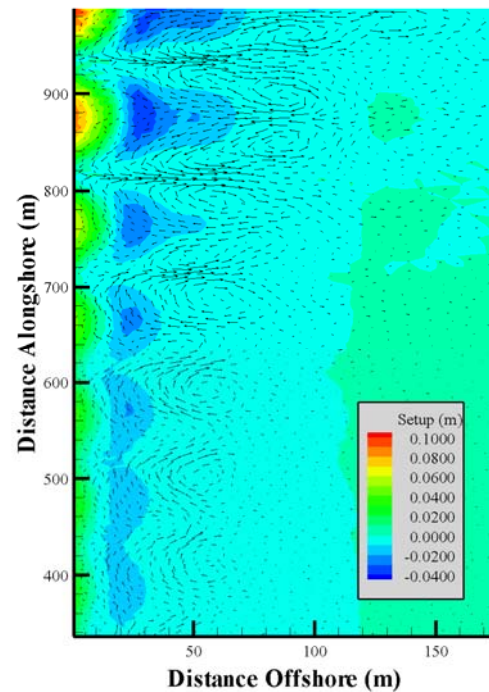


Figure 6.107 – Set-up/Set-down and Currents upwave of the Attached Breakwater with increased scale in x-direction in the absence of turbulent diffusion

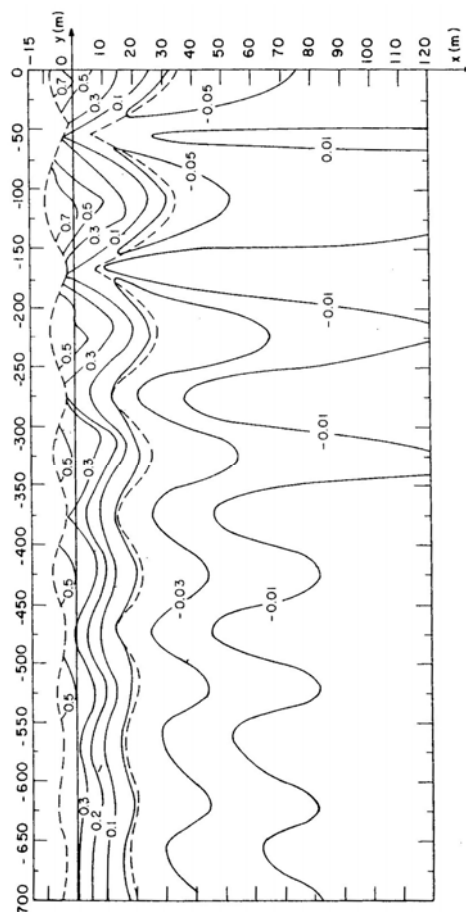


Figure 6.109 – Contours of set-up/set-down downwave of the Attached Breakwater from Liu and Mei (1976).

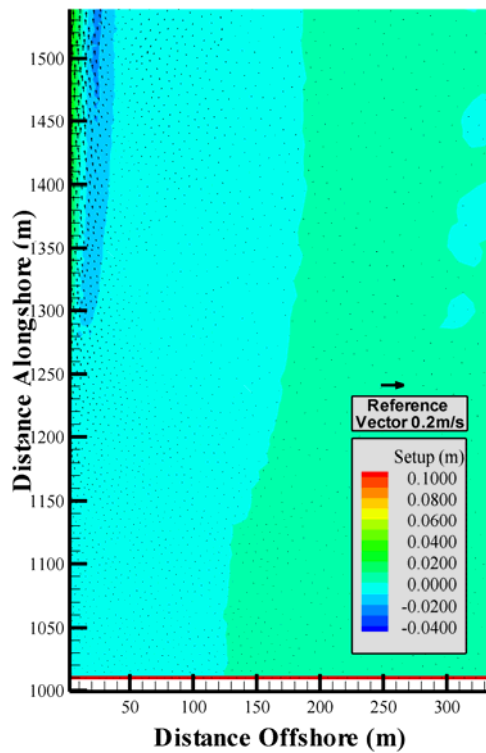


Figure 6.110 – Set-up/Set-down and Currents downwave of the Attached Breakwater

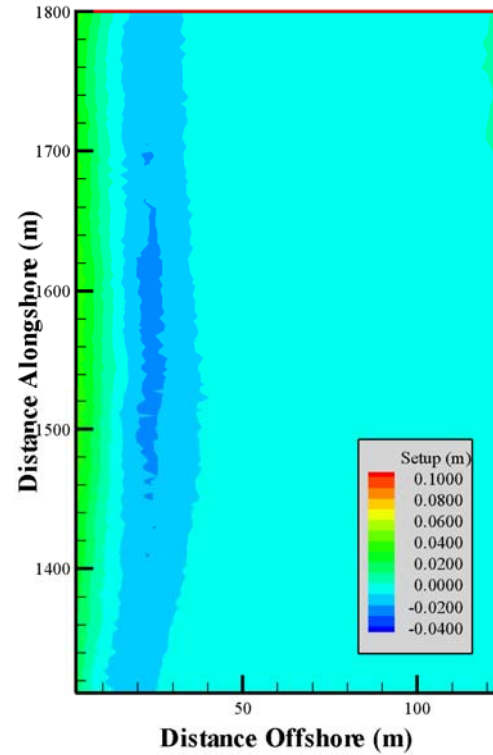


Figure 6.111 – Set-up/Set-down downwave of the Attached Breakwater with increased scale in x-direction

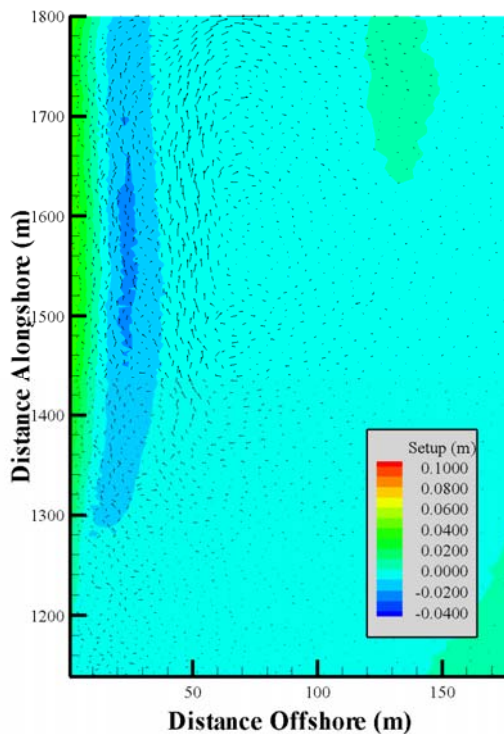


Figure 6.112 – Set-up/Set-down and Currents downwave of the Attached Breakwater with increased scale in x-direction in the presence of turbulent diffusion

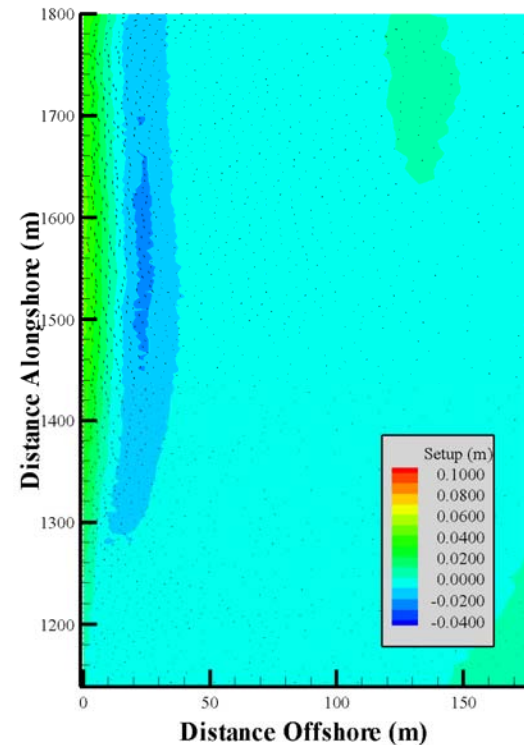


Figure 6.113 – Set-up/Set-down and Currents downwave of the Attached Breakwater with increased scale in x-direction in the absence of turbulent diffusion

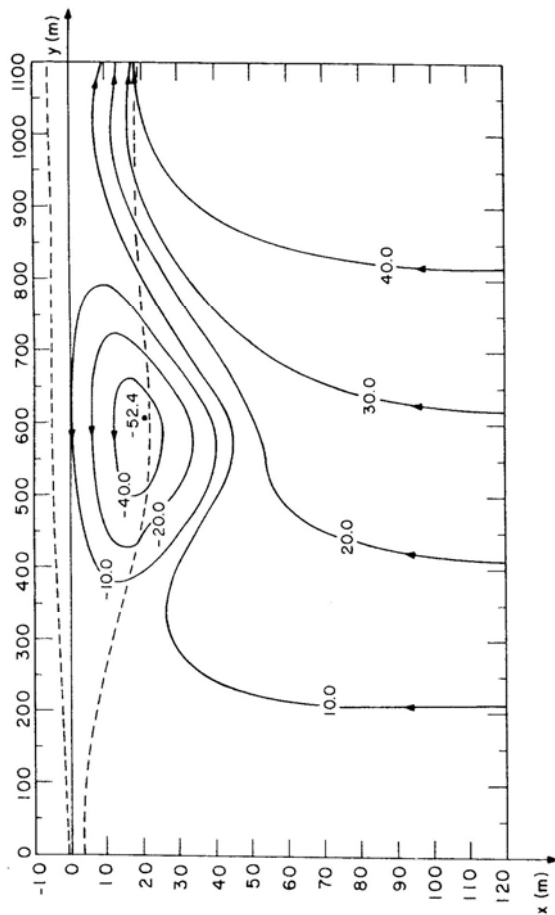


Figure 6.114 – Streamlines showing Direction and Magnitude of Velocities downwave of the Attached Breakwater from Liu and Mei (1976). Values indicated on the plot are magnitudes of a streamline function.

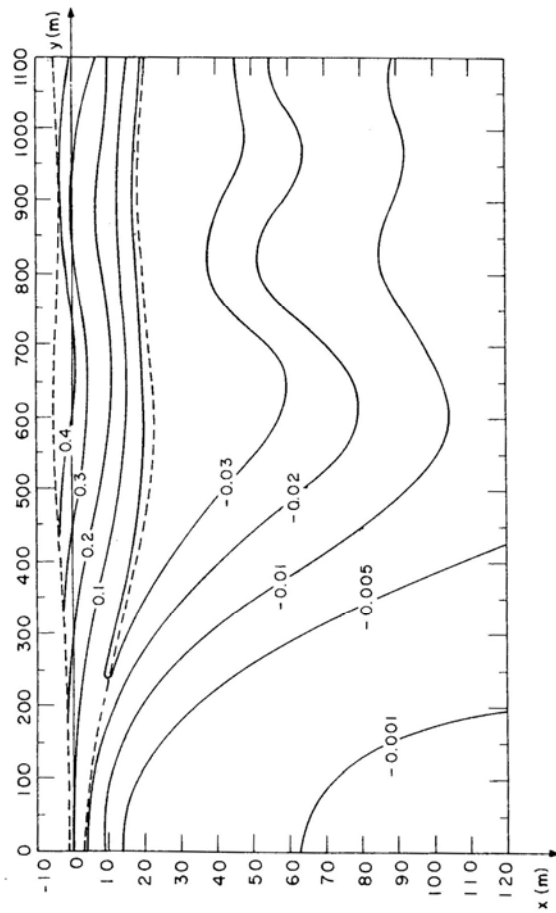


Figure 6.115 – Contours of set-up/set-down upwave of the Attached Breakwater from Liu and Mei (1976).

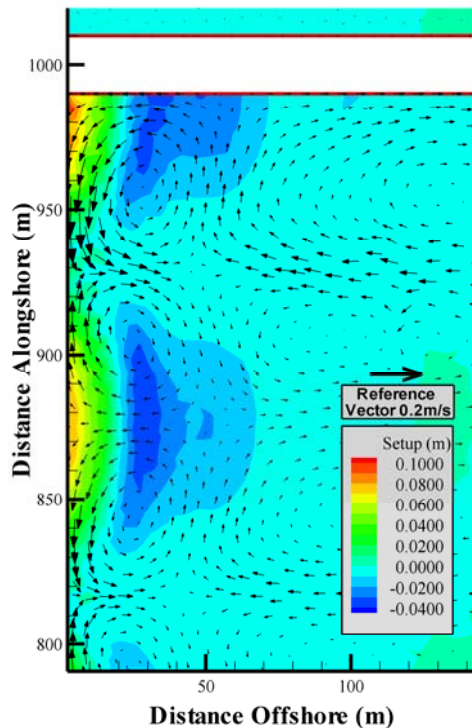


Figure 6.116 – Magnified View of Set-up/Set-down and Currents upwave of the Attached Breakwater

6.13.3 Discussion

The plotted results of the NM-WCIM show an approximately triangular shaped shadow zone downwave of the attached breakwater as expected. Figure 6.96 and Figure 6.99 both show a zone of wave field interaction where the wave reflected off the breakwater interacts with the incoming wave resulting in the unique peak and trough effect seen before. As before the semi-circular radiating boundary on the open water sides of the domain is used to address the removal of this backscattered wave energy from the domain. Figure 6.98 shows an interesting phenomenon with respect to the closest wave ray to the breakwater. Once it reaches the breakwater it travels along the downwave impermeable face to the shore.

Figure 6.102 shows the set-up/set-down for the entire region under examination. As expected there is a region of very little set-up in the shadow zone downwave of the breakwater. A less expected result is the region of intermittent set-up and set-down on the upwave side of the breakwater. This corresponds in trend with the set-up/set-down results of the Liu and Mei (1976) model, shown in Figure 6.109. The magnitude of peak set-up

presented by Liu and Mei (1976) is larger than that calculated by the NM-WDHM. This is similar to the difference seen in Sections 6.9 and 6.10. The reason for this difference is not clear. Sections 6.6 and 6.11 also examine set-up values calculated by the NM-WDHM and the results are comparable with measured and modelled data.

The intermittent set-up and set-down can be explained by examination of the velocity vectors of Figure 6.116. The regular rip currents that form prevent set-up from occurring in some regions. These rip-currents obtained using the NM-WDHM shown in Figure 6.106, Figure 6.107 and Figure 6.116 occur in similar locations to those of Liu and Mei (1976), shown in Figure 6.108. The velocity results of Liu and Mei (1976) are presented in the form of streamlines which makes quantitative comparison with the values of the NM-WDHM difficult. The velocity streamlines of Liu and Mei (1976) appear to disagree in direction with the vectors obtained by the NM-WDHM shown in Figure 6.116. The rip-current calculated by the NM-WDHM meets an incoming current in the region just upwave of the set-down area, the velocity streamlines of Liu and Mei (1976) are continuous in this region. Figure 6.107 shows that if the NM-WDHM is run in the absence of turbulent diffusion the direction of the vectors agree with the streamlines of Liu and Mei (1976). Liu and Mei (1976) state that their model does not include turbulent diffusion.

Downwave of the attached breakwater the set-up and set-down results of the NM-WCIM are shown in Figure 6.110 to Figure 6.113 and those of Liu and Mei (1976) are shown in and Figure 6.115. As was noted upwave of the breakwater there is a difference in the magnitude of set-up obtained by each model. The same comments apply here. It is worth noting that Liu and Mei (1976) obtain a slight vortex in the area just upwave of the breakwater. This is shown in Figure 6.114. The same vortex is not immediately evident in the NM-WDHM results. It is considered that the low magnitude of the currents in this area combined with the turbulent diffusion terms and the size of the finite elements may explain this difference.

6.14 Currents around a Conical Island after Mei and Angelides (1977)

6.14.1 Introduction

Mei and Angelides (1977) and Mei *et al.* (2005) examine the occurrence of a longshore current on a conical island. The dimensions of the island in question and hence the surrounding coastal waters are on quite a large scale thus challenging the NM-WCIM and NM-WDHM models to produce wave data and currents on a much larger scale than the previous examples.

6.14.2 Results

Presented below are the NM-WCIM and NM-WDHM results for the conical island labelled “Case I” by Mei and Angelides (1977). The emergent radius of the island is 10,000ft (approx. 3048m) and the seabed slope of 1 in 20 continues until the seabed is at a depth of 100ft (approx. 30.48m) at a total radius of 12,000ft (approx. 3657.6m). The wave approaching the island has a 10 second period and a deep-water height of 3ft (approx. 0.9144m). The water surface is shown in Figure 6.117 for unbroken waves. The same scenario is plotted in Figure 6.118 for broken waves. Both of these sets of results have been obtained using the NM-WCIM. Mei and Angelides (1977) use classic wave ray theory to examine wave behaviour around the island.

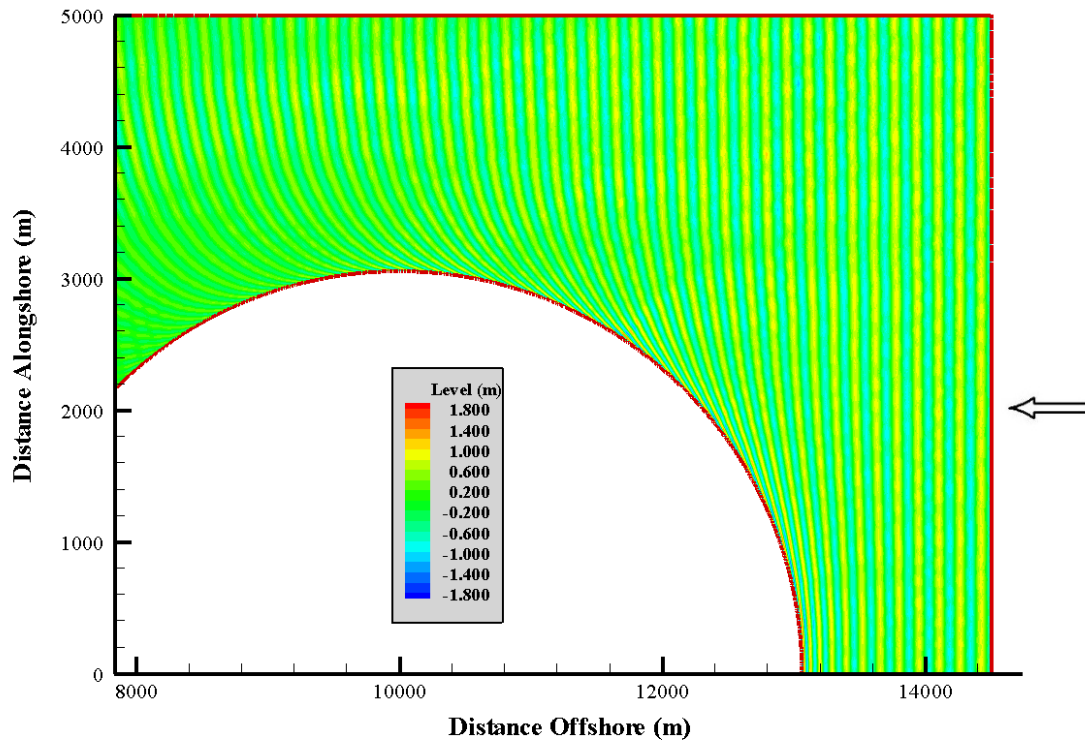


Figure 6.117 – Water surface for Waves approaching a Conical Island in the absence of Breaking. Waves Propagating from Right to Left.

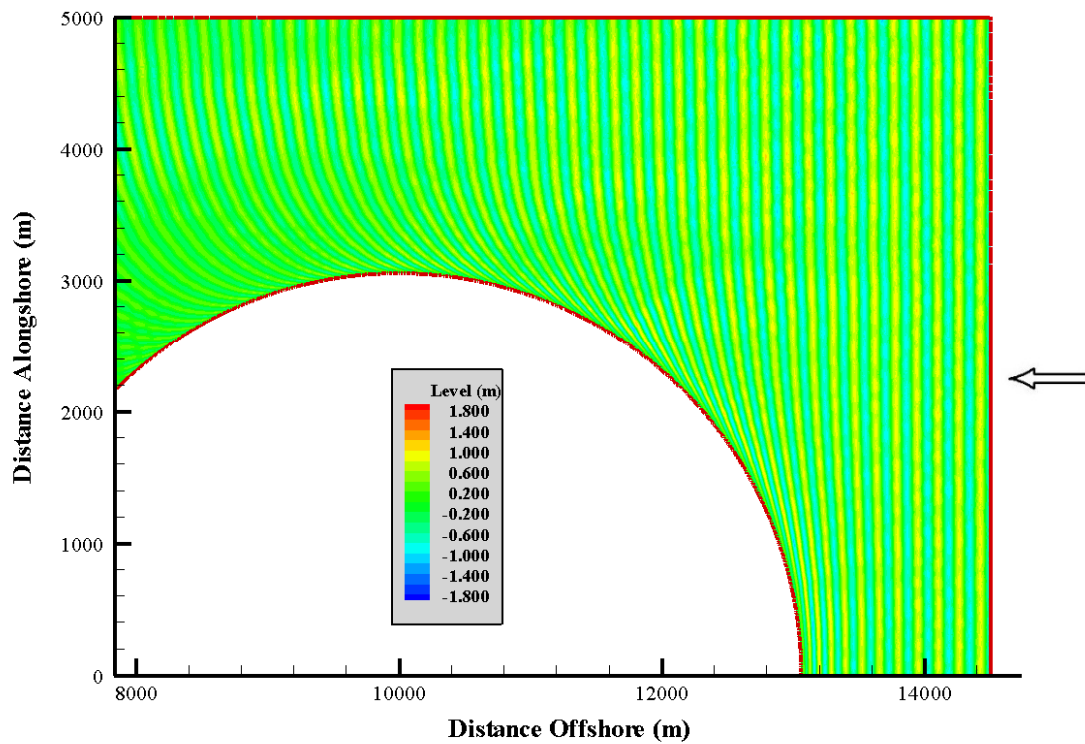


Figure 6.118 – Water surface for Waves approaching a Conical Island with Breaking. Waves Propagating from Right to Left.

Figure 6.119 shows contour lines of where the water surface height is zero. Figure 6.120 shows a series of wave rays obtained using the wave ray methodology of Chapter 5. This post processing wave ray process provides the same rays as Mei and Angelides (1977) obtained. Wave heights were calculated along these rays (in a denser form) and hence eddy viscosity and breaking wave heights were obtained. Figure 6.121 shows a three-dimensional plot of the same results as Figure 6.118.

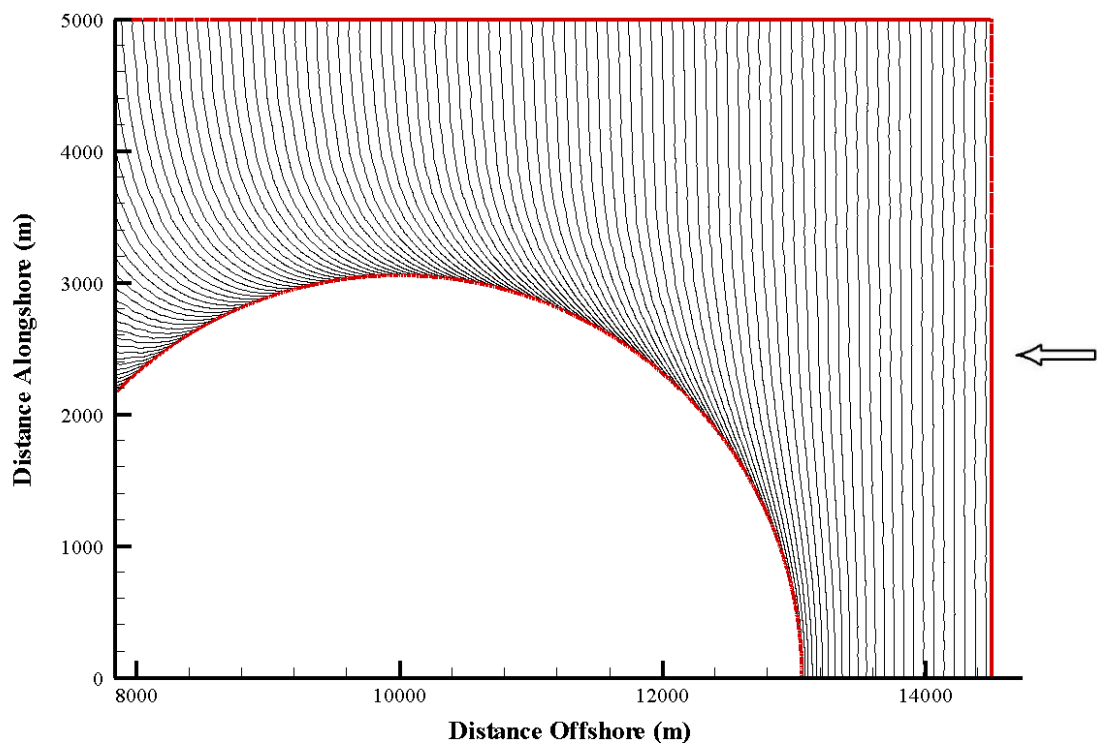


Figure 6.119 – Contours of Water Surface = 0 to indicate Wave Phase for Waves approaching a Conical Island. Waves Propagating from Right to Left.

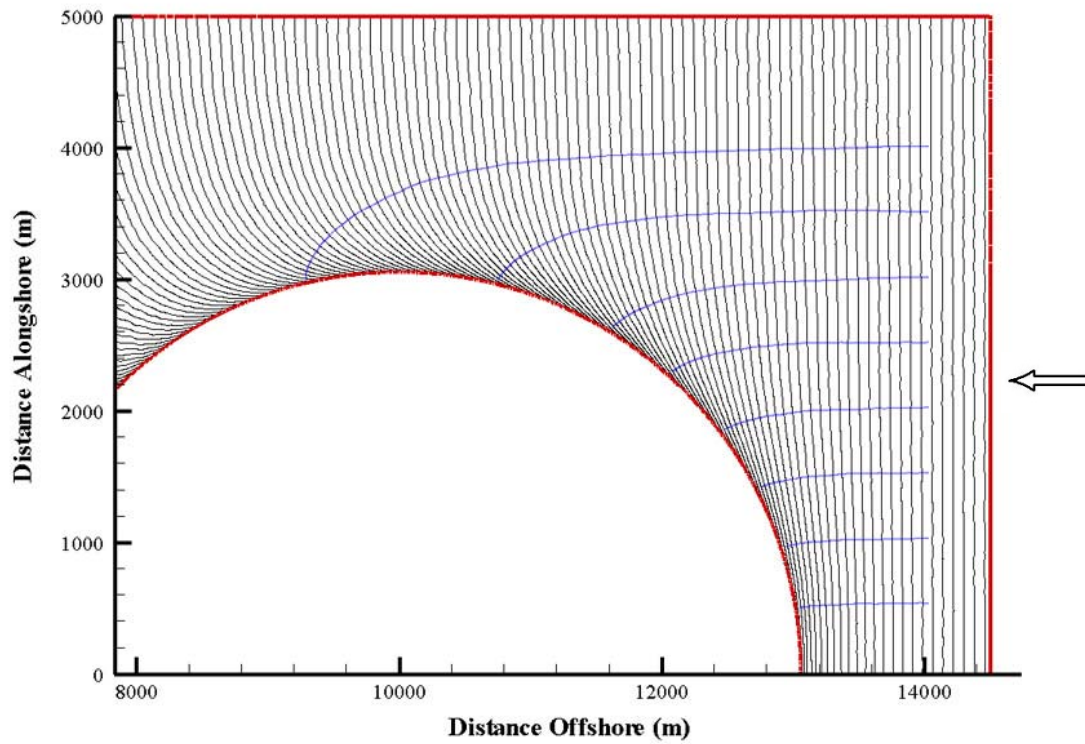


Figure 6.120 – Wave Rays (in blue) plotted alongside contours of Water Surface = 0 for Waves approaching a Conical Island. Waves Propagating from Right to Left.

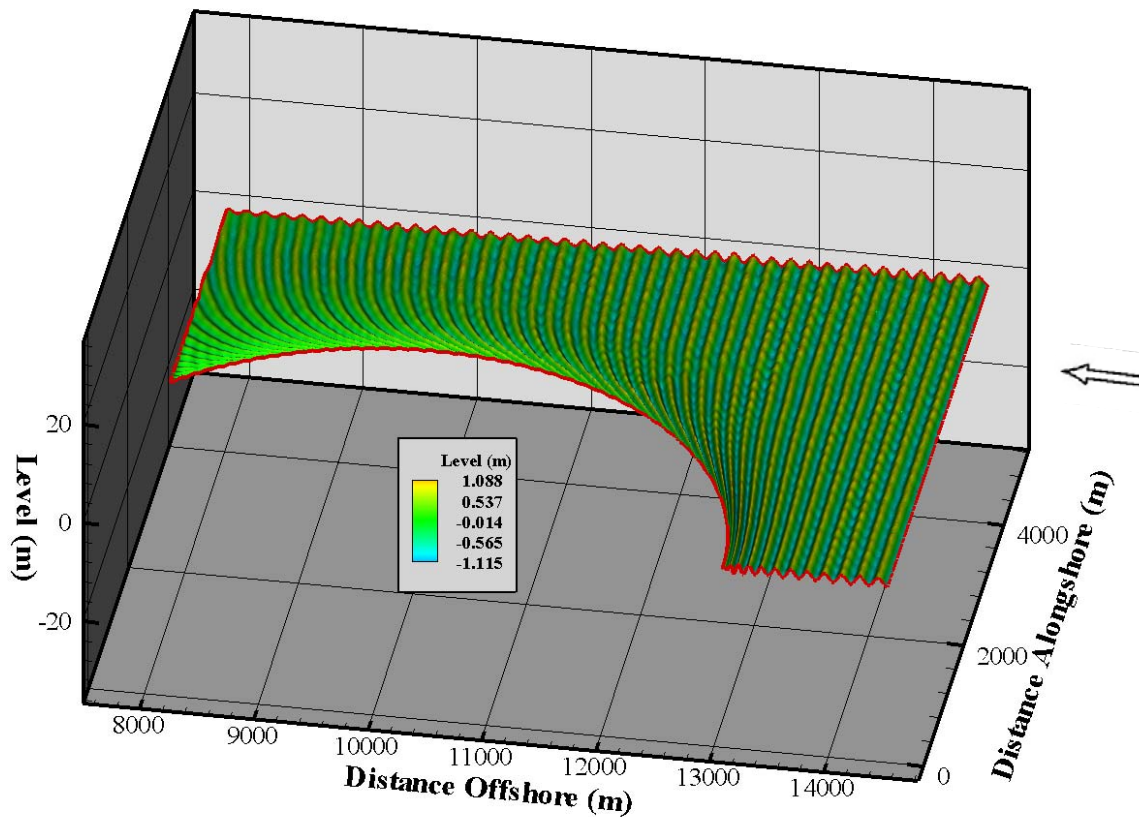


Figure 6.121 – Three dimensional plot of Water Surface for Breaking Waves approaching a Conical Island. Waves Propagating from Right to Left.

Figure 6.122 and Figure 6.123 show plots of unbroken and broken wave heights respectively for the same scenario as the wave surfaces plotted above. Figure 6.124 and Figure 6.125 show a closer view of broken and unbroken wave heights for a section of the conical island's coast.

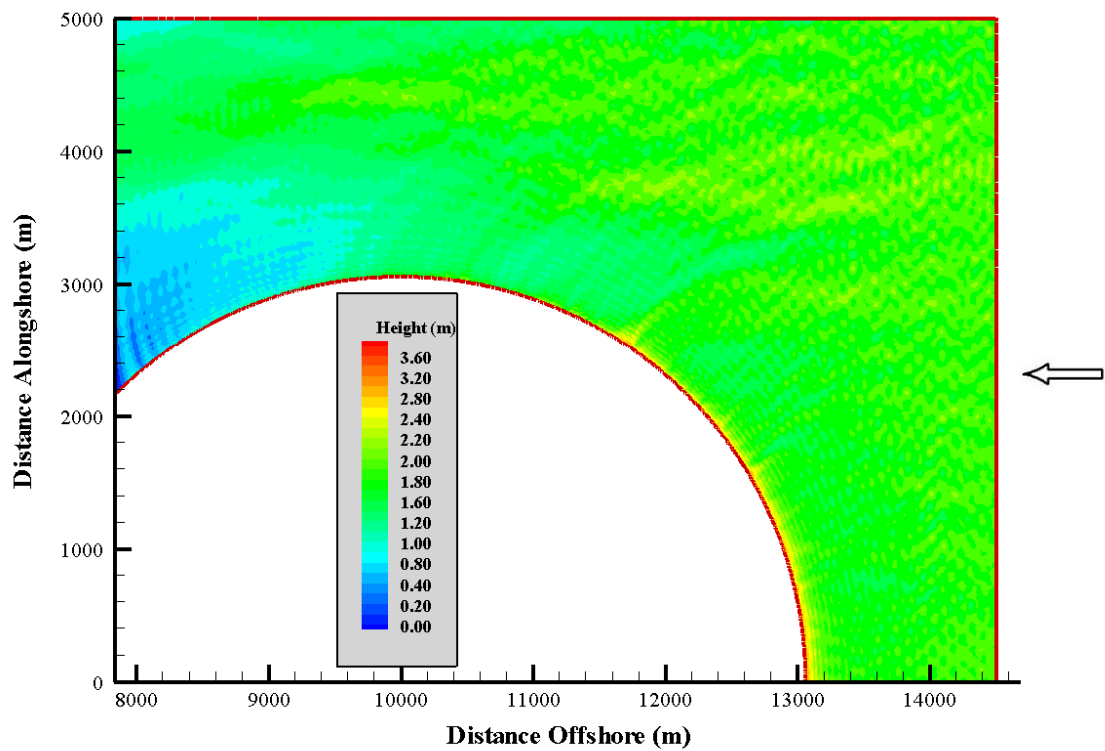


Figure 6.122 – Unbroken Wave Height for Waves approaching a Conical Island. Waves Propagating from Right to Left.

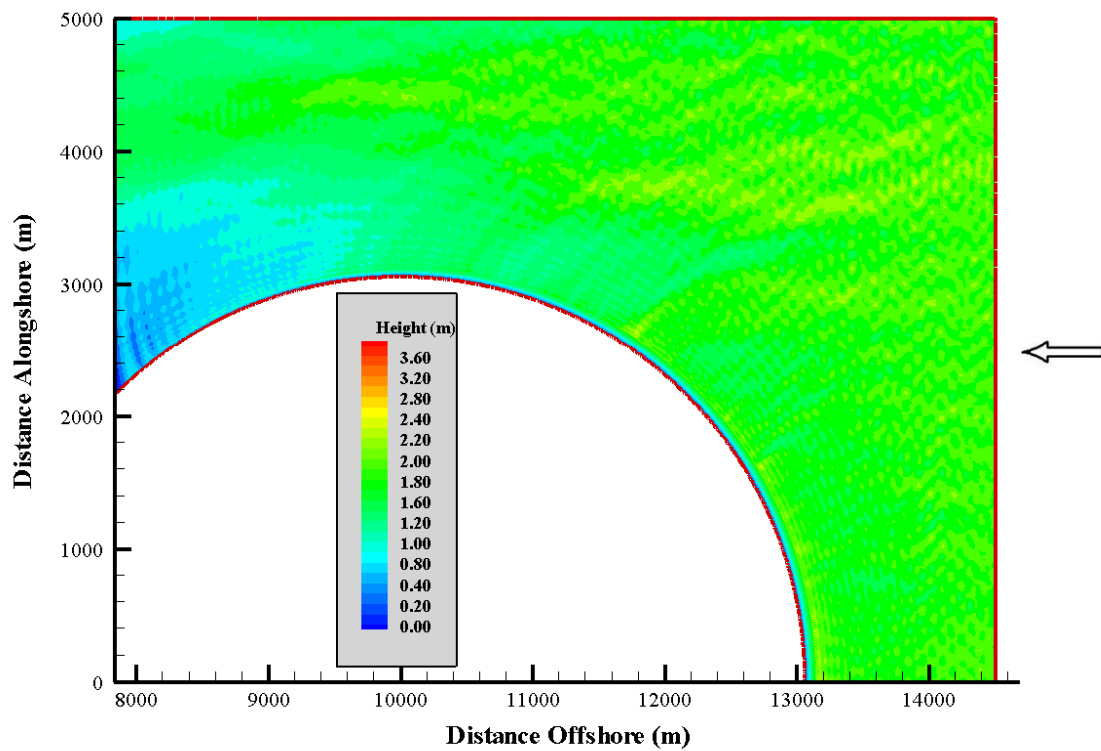


Figure 6.123 – Broken Wave Height for Waves approaching a Conical Island. Waves Propagating from Right to Left.

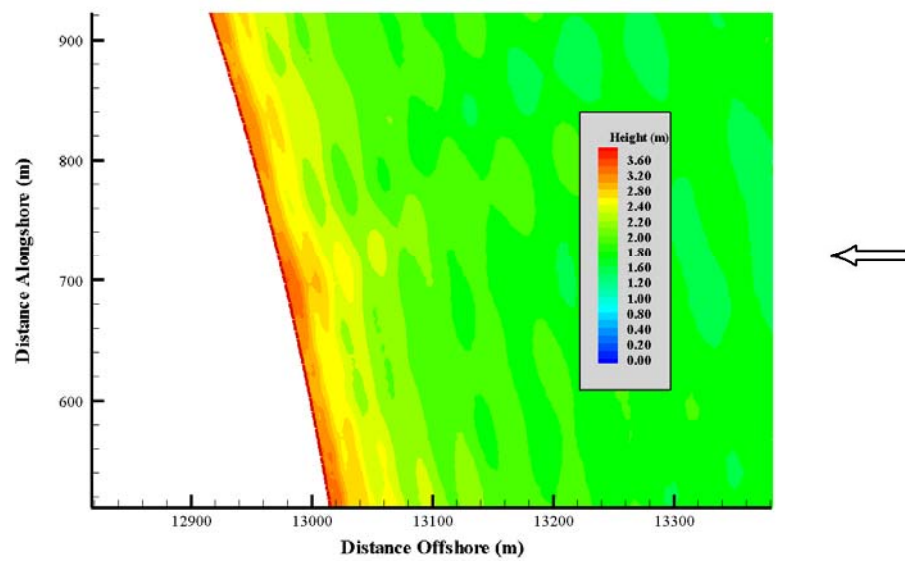


Figure 6.124 – Unbroken wave height for a section of coast on a Conical Island. Waves Propagating from Right to Left.

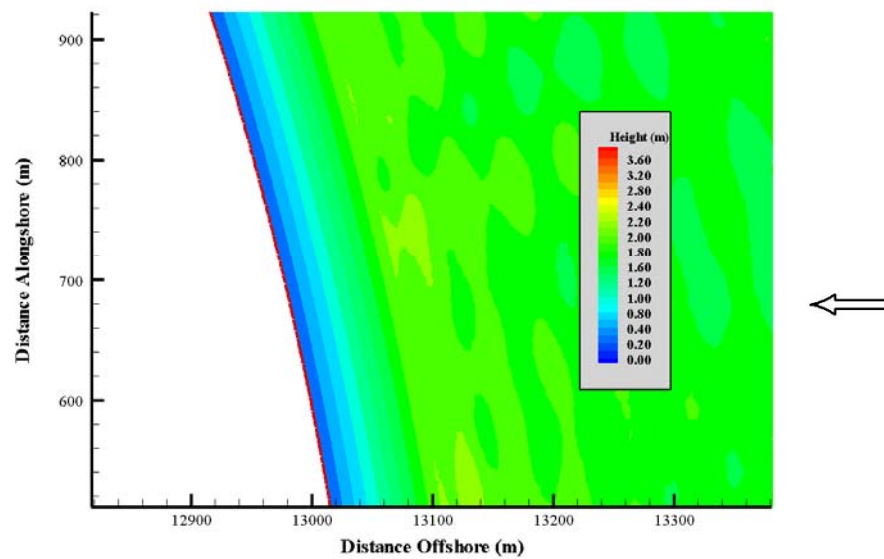


Figure 6.125 – Broken wave height for a section of coast on a Conical Island. Waves Propagating from Right to Left.

Figure 6.126 shows the set-up and set-down obtained from the NM-WDHM. Figure 6.127 and Figure 6.128 show set-up, set-down and velocity vector results for a portion of island coast with and without the inclusion of turbulent diffusion in the NM-WDHM respectively. Figure 6.129 and Figure 6.130 show a similar comparison between the hydrodynamic results of the NM-WDHM with and without turbulent diffusion for a more exposed section of coast towards the east of the island as plotted. Figure 6.131 shows the streamlines obtained by Mei and Angelides (1977) for the conical island in question.

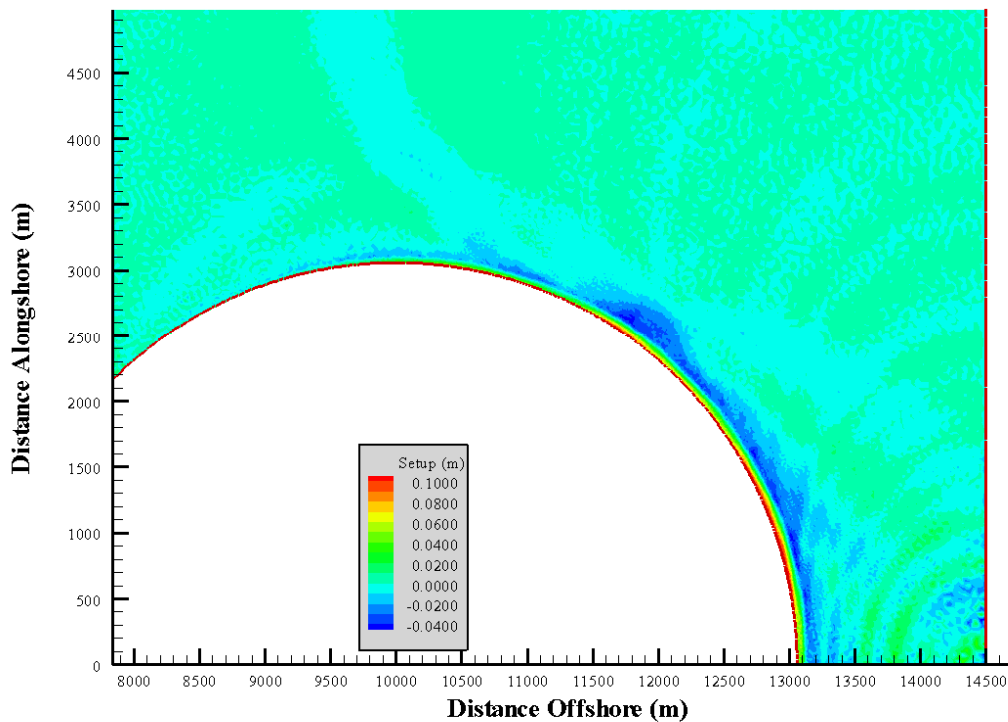


Figure 6.126 – Plot of Set-up and Set-down for Waves approaching a Conical Island

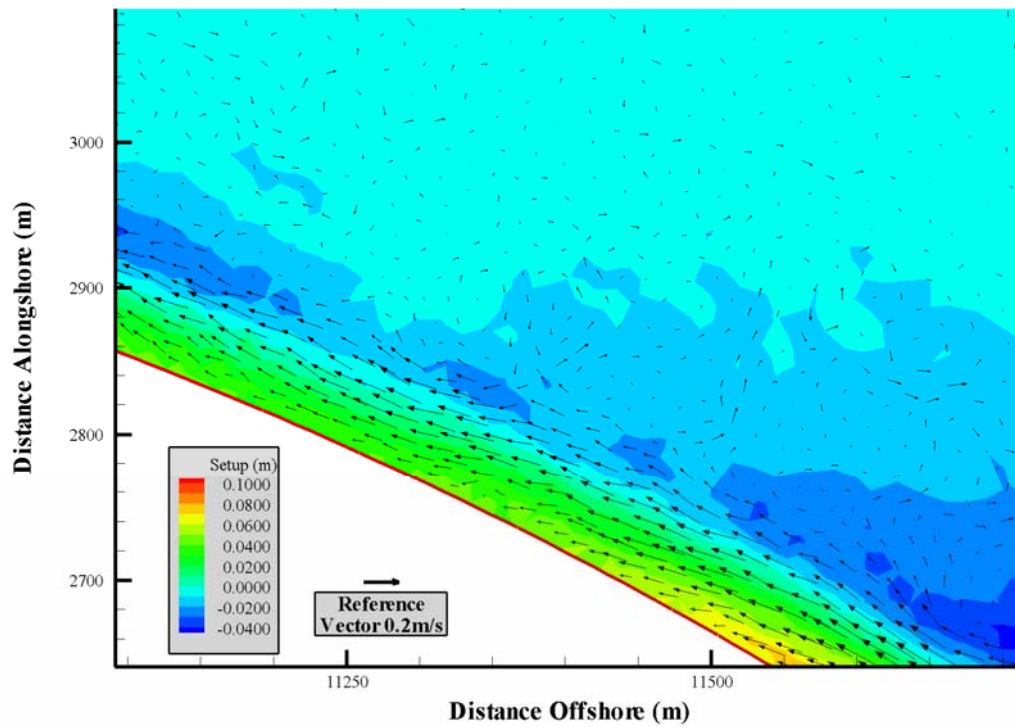


Figure 6.127 – Set-up/Set-down and Currents towards the Lee Coast of a Conical Island Including Turbulence

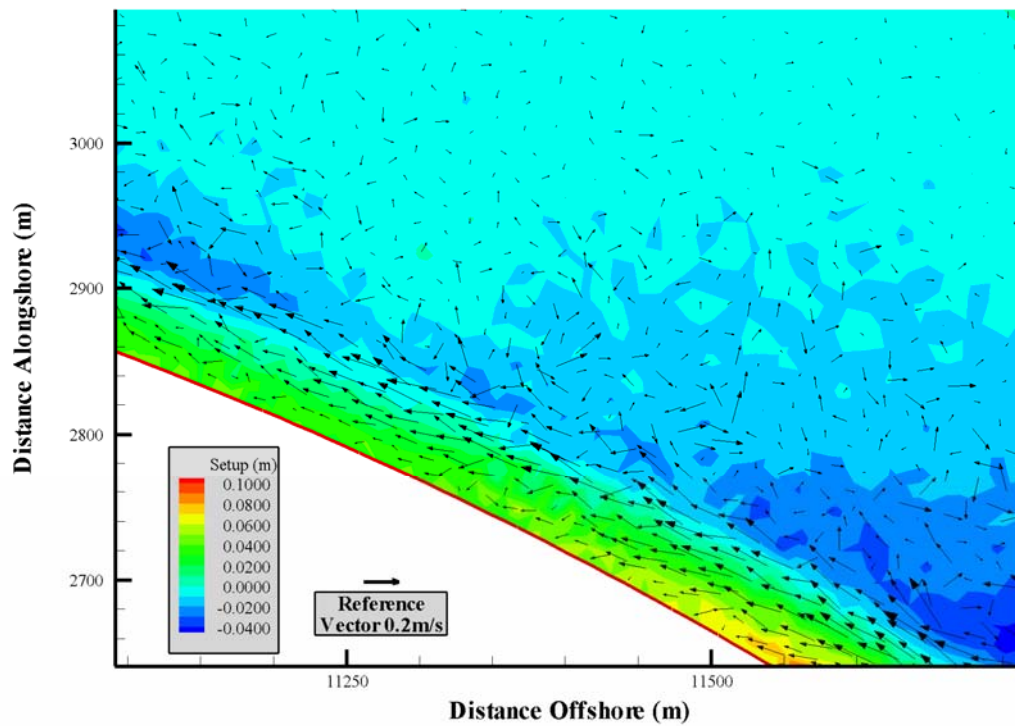


Figure 6.128 – Set-up/Set-down and Currents towards the Lee Coast of a Conical Island with No Turbulence

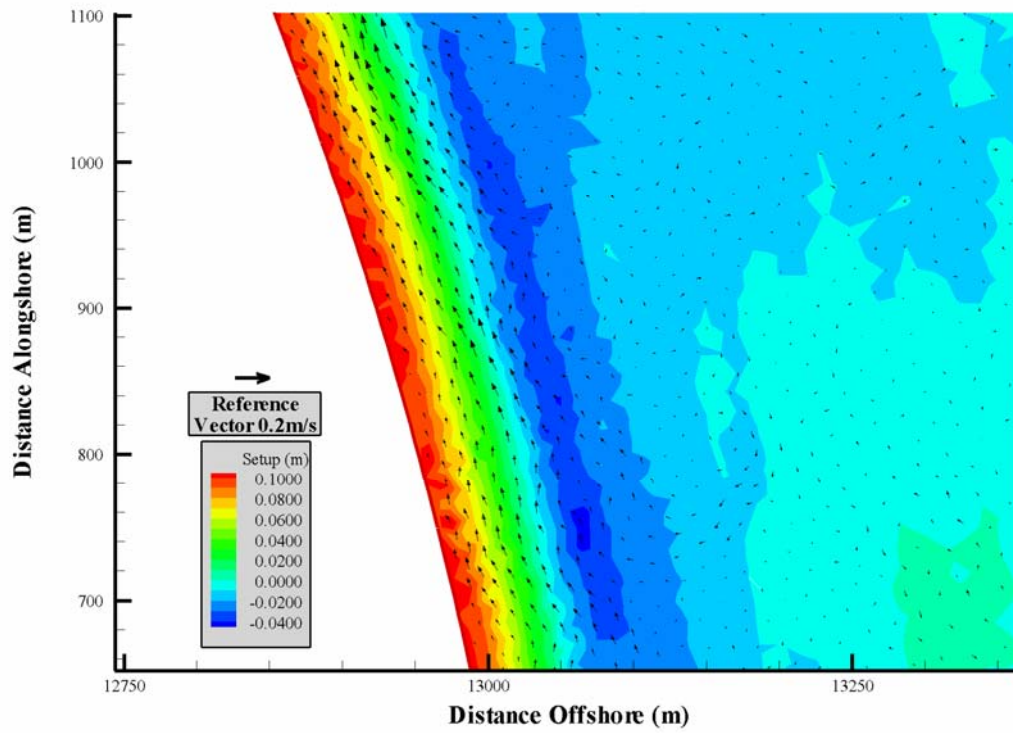


Figure 6.129 – Set-up/Set-down and Currents along the Exposed Coast of a Conical Island Including Turbulence

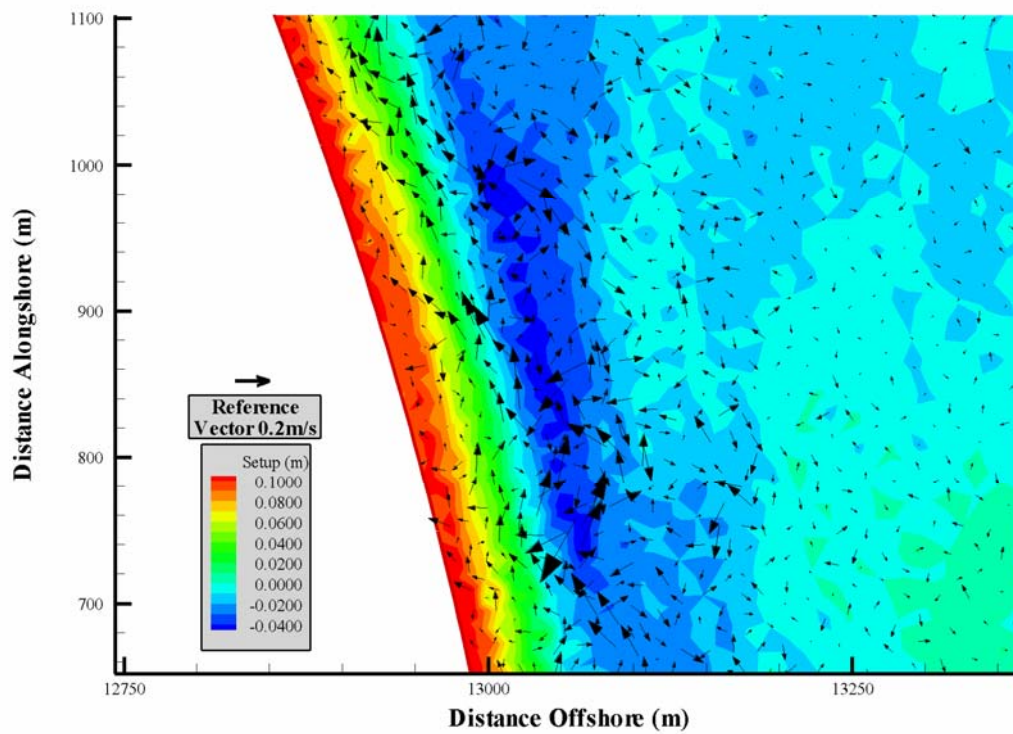


Figure 6.130 – Set-up/Set-down and Currents along the Exposed Coast of a Conical Island with No Turbulence

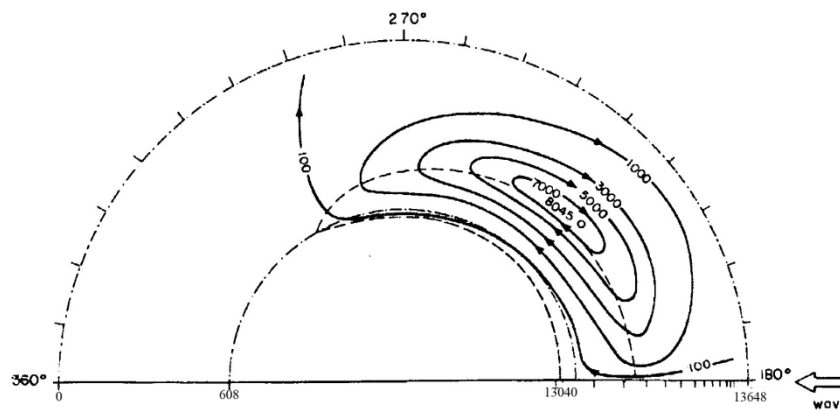


Figure 6.131 – Streamlines showing direction and magnitude of Longshore Currents for a Conical Island from Mei and Angelides (1977). Values indicated on the plot are magnitudes of a streamline function.

6.14.3 Discussion

The plotted results from both the NM-WCIM and NM-WDHM show that the models can accommodate the larger scale scenario presented here. The finite element size needed to allow results for the domain to be computed on a desktop computer is larger than that needed for the models discussed in previous sections. The NM-WCIM and NM-WDHM do not appear to display a significant degree of sensitivity to this enlarged element size.

It is evident from Figure 6.118, Figure 6.119 and Figure 6.121 that the island creates a shadow zone on the downwave side into which waves diffract. Figure 6.126 shows the effect this shadow zone has on wave-driven hydrodynamics. There is negligible set-up, set-down or longshore current created in this shadow zone. The magnitude of set-up/set-down gradually decreases along the shore of the island as the degree of exposure to waves decreases. The velocity values obtained from the NM-WDHM appear to be in good agreement with the trend of the streamlines of Mei and Angelides (1977) in Figure 6.131. The use of streamlines by Mei and Angelides (1977) make it difficult to examine values of longshore velocity but the streamlines appear to be closer together in the regions where the NM-WDHM predicts the strongest currents. It is considered that for the scale of the scenario in question some of the streamlines shown in Figure 6.131 are far enough apart to indicate a current too small to be effectively modelled using a numerical finite element model such as the NM-WDHM.

6.15 Wave-Current Interaction of Chen *et al.* (2005) and Kostense *et al.* (1988)

6.15.1 Introduction

Chen *et al.* (2005) and Kostense *et al.* (1988) present the results of a wave-current interaction model for the analytical rip-current of Arthur (1950). The NM-WCIM model was examined for the same set of circumstances to examine similarities between the results. The Chen *et al.* (2005) and Kostense *et al.* (1988) models are quite similar to the NM-WCIM. They are both finite element wave-current interaction models that iterate to a solution for velocity potential. The Chen *et al.* (2005) model contains a modified form of the dispersion relation for waves in the shallow water zone.

6.15.2 Results

The results in this section compare the NM-WCIM with the Chen *et al.* (2005) and Kostense *et al.* (1988) models of wave-current interaction. Arthur (1950) provides a formula for analytical longshore and cross-shore velocities at any point in the domain. The formula is also used by this project, Chen *et al.* (2005) and Kostense *et al.* (1988) with appropriate adjustment for the differing coordinate regime. The wave affected by the calculated current is an 8 second wave with a unit height in deep-water. The wave approaches the beach perpendicularly. The data below is presented for unbroken wave heights throughout. Figure 6.132 and Figure 6.133 show the wave results for the NM-WCIM interacting with the given current. Figure 6.138 shows a three-dimensional plot of the same scenario for conceptualisation. Figure 6.134 and Figure 6.135 show contours of wave height equal to zero obtained by the NM-WCIM for the given situation. Figure 6.136 and Figure 6.137 show plots of wave height for the given wave-current interaction scenario. Figure 6.139 and Figure 6.140 show the results of Chen *et al.* (2005) and Kostense *et al.* (1988) respectively for the same wave-current interaction. Figure 6.141 shows a plot of Chen *et al.* (2005) comparing the results of Yoon and Liu (1989) with those of Chen *et al.* (2005). The NM-WCIM results have been added to this plot and this author has endeavoured to include an approximation of the results of Kostense *et al.* (1988). The Kostense *et al.* (1988) approximation is hampered by the lack of dimensions on the Kostense *et al.* (1988) plot and the poor quality of the reproductions available.

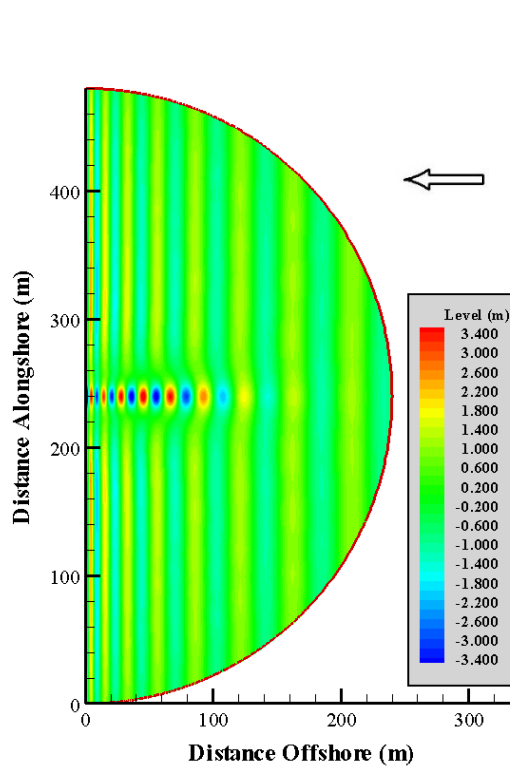


Figure 6.132 – Water Level for Wave-Current Interaction of Chen *et al.* (2005). Waves Propagating from Right to Left.

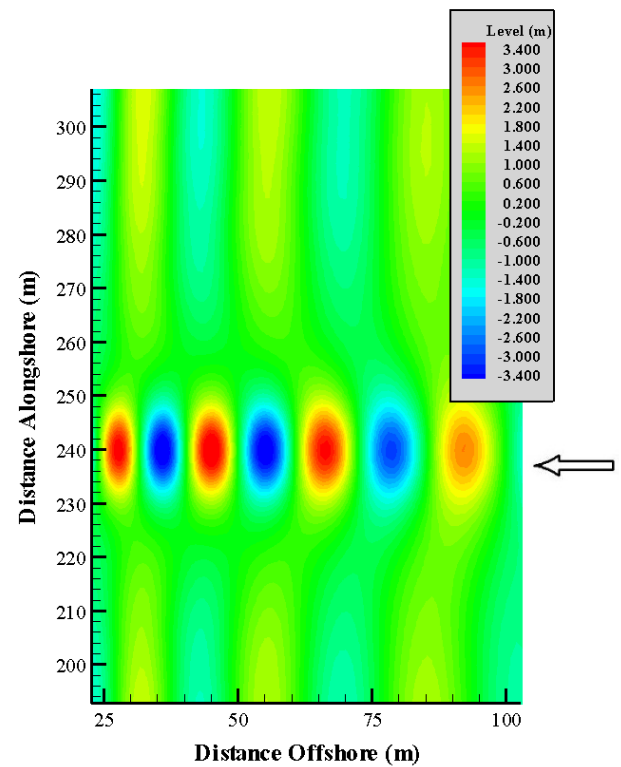


Figure 6.133 – Water Level in region of strong current for Wave-Current Interaction of Chen *et al.* (2005). Waves Propagating from Right to Left.

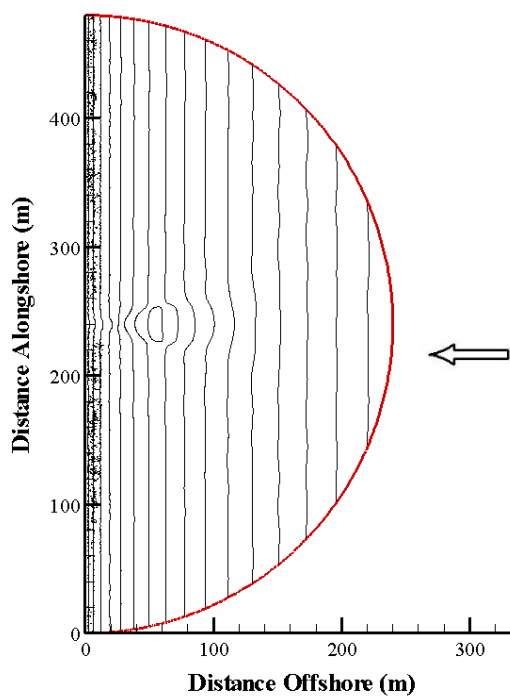


Figure 6.134 – Contours of Zero Amplitude for Wave-Current Interaction of Chen *et al.* (2005). Waves Propagating from Right to Left.

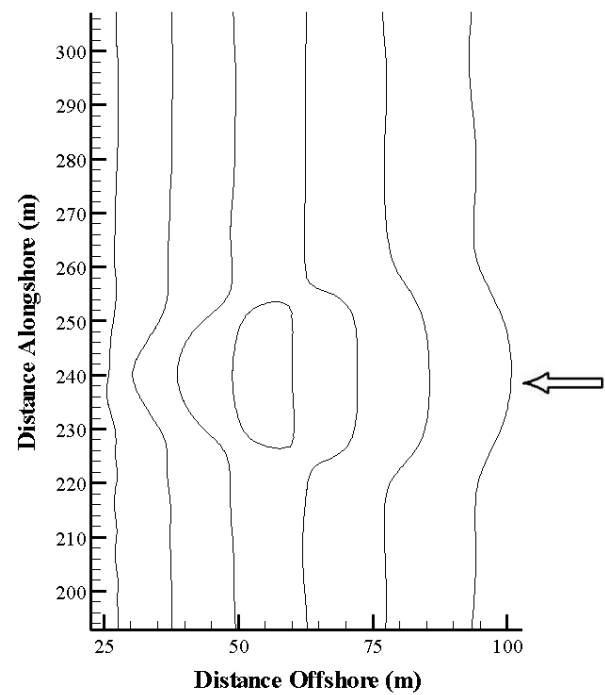


Figure 6.135 – Contours of Zero Amplitude in region of strong current for Wave-Current Interaction of Chen *et al.* (2005). Waves Propagating from Right to Left.

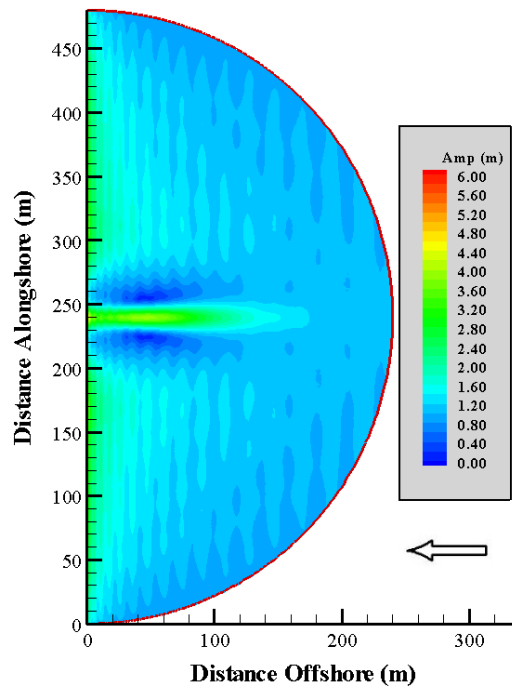


Figure 6.136 – Wave Amplitude for Wave-Current Interaction of Chen *et al.* (2005). Waves Propagating from Right to Left.

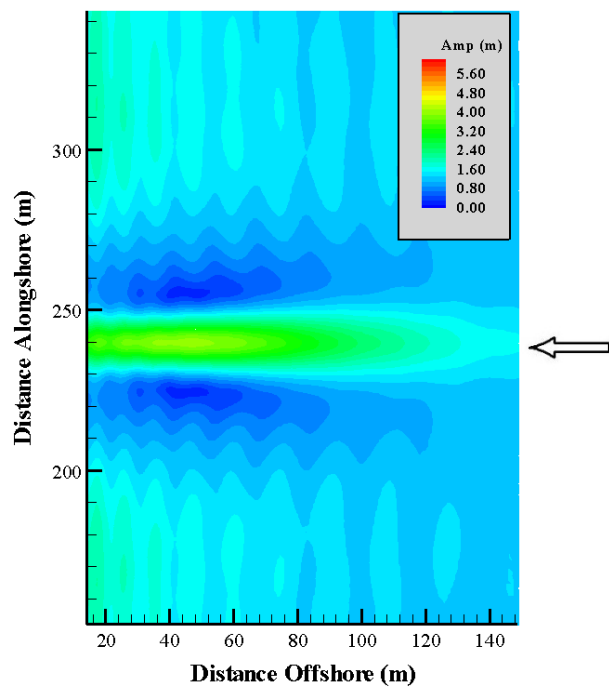


Figure 6.137 – Wave Amplitude in region of strong current for Wave-Current Interaction of Chen *et al.* (2005). Waves Propagating from Right to Left.

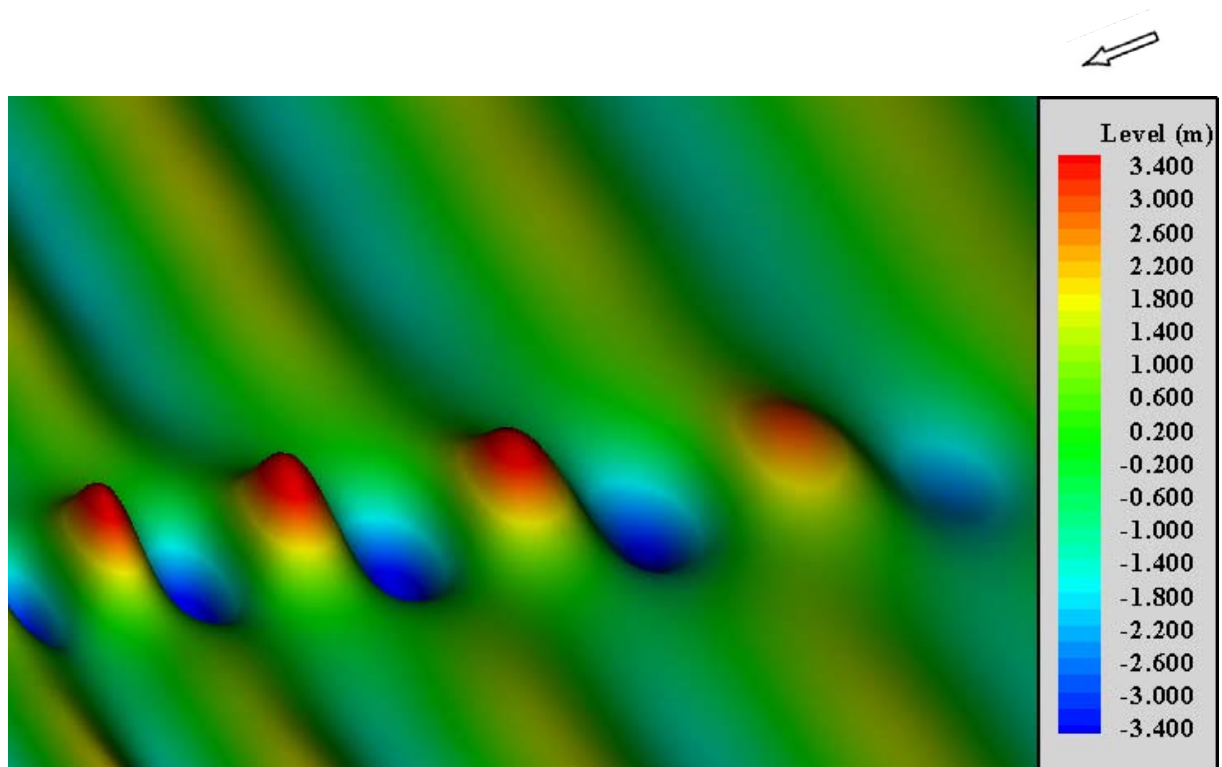


Figure 6.138 – Three-dimensional view of Water Surface in the presence of Wave-Current Interaction of Chen *et al.* (2005). Waves propagating in the direction shown by the arrow.

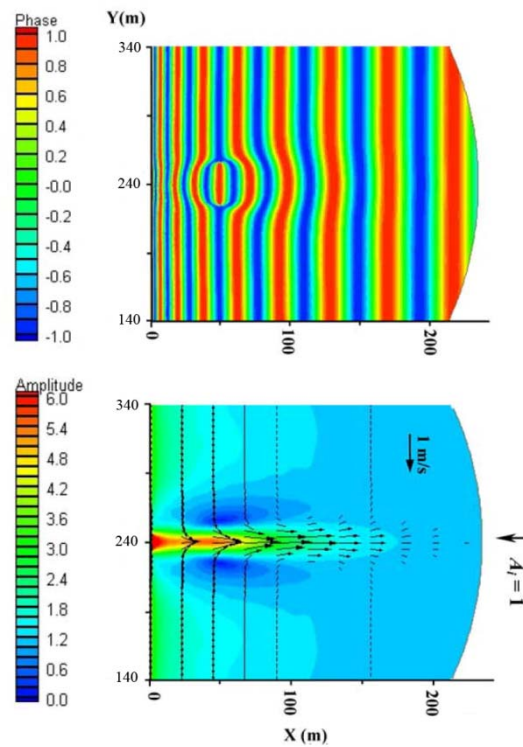


Figure 6.139 – Results of Chen *et al.* (2005) for Wave Phase and Amplitude during Wave-Current Interaction

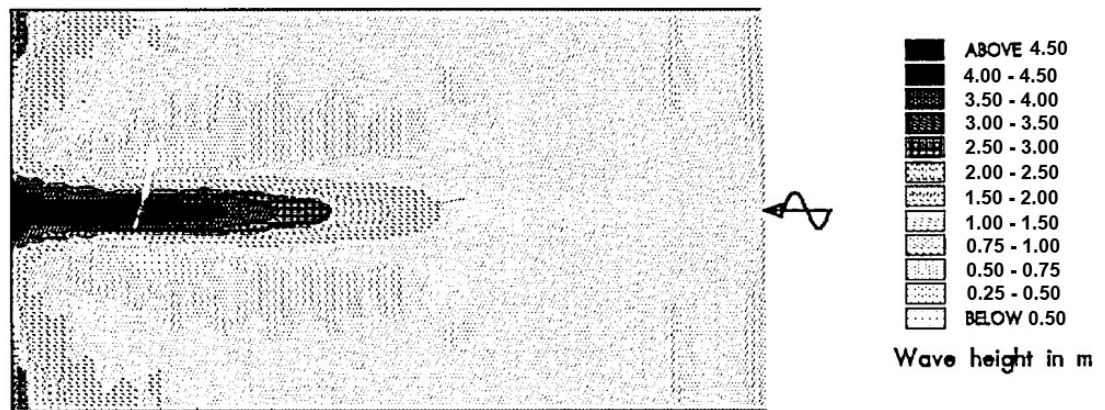


Figure 6.140 – Results of Kostense *et al.* (1988) for Wave Phase and Amplitude during Wave-Current Interaction (Adjusted to produce Height Values for Unit Deep-Water Wave Height)

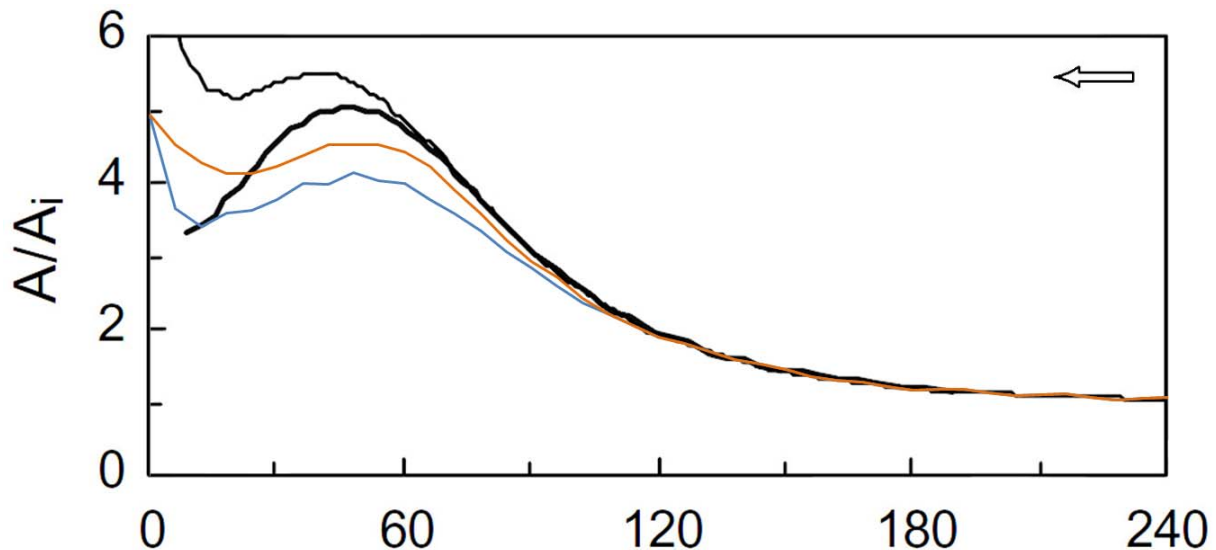


Figure 6.141 – Cross-Section of Wave Amplitude at $y = 240\text{m}$ showing results of Chen *et al.* (2005) (Thin Black), NM-WCIM (Blue), Kostense *et al.* (1988) (Orange) and Yoon and Liu (1989) (Thick Black). Waves Propagating from Right to Left.

6.15.3 Discussion

It is clear from Figure 6.135 and Figure 6.139 that the phase obtained by the NM-WCIM is similar to that of Chen *et al.* (2005). This indicates a good degree of agreement between the phase of the velocity potential results obtained from both models.

It is noticeable that the factor to which the incoming wave height is amplified by the current is greater in the Chen *et al.* (2005) results. The Chen *et al.* (2005) model shows a peak change due to current of about 5.5 times the deep-water amplitude whereas the NM-WCIM shows a peak change due to current of 4.15 times the deep-water amplitude. The Kostense *et al.* (1988) model while slightly higher than the NM-WCIM, at 4.5 is within the same range. The Yoon and Liu (1989) method is based on a parabolic model and although in the correct range cannot obtain the increase in unbroken wave height towards the shore obtained by the elliptic models. It is possible that the different dispersion relation used in the shallow water zone by the Chen *et al.* (2005) may be the factor that causes the apparent difference between results. The correspondence of phase results between the Chen *et al.* (2005) model and the NM-WCIM tends to indicate that the implementation of the elliptic equation is similar in the two models. Kostense *et al.* (1988) use the same dispersion relation as the NM-WCIM and iterate on the gradient of phase in a similar way. The wave height results of Kostense *et al.* (1988) are comparable to the NM-WCIM results.

The results of Section 6.3 of this project also examine the effect of currents on the wave height obtained by the NM-WCIM. Section 6.3 shows that in the presence of a co-linear current the NM-WCIM gives an increase in wave height similar to the analytically predicted increase.

6.16 Energy Rays vs. Wave Rays

6.16.1 Introduction

Chapter 5 of this thesis discusses a post-processing method to obtain wave energy rays. Clyne (2008) introduced wave rays obtained as a post-processing technique on a wave model whose results were in terms of velocity potential. Clyne (2008) used the wave rays as a means of calculating broken wave height, especially in cases where recovery of wave height was necessary. This thesis uses the same methodology to assess broken wave height in a variety of the models discussed so far in Chapter 6. The wave ray technique can also be used to obtain eddy viscosity values necessary for the inclusion of turbulent diffusion in the NM-WDHM. However, as shown in Chapter 5 the wave rays of Clyne (2008) cannot be directly applied to the results of the NM-WCIM due to the presence of currents. Hence the wave energy ray technique of Chapter 5 was developed. This section shows the difference between the standard wave rays of Clyne (2008) method and the wave energy rays of this thesis.

6.16.2 Results

Plotted below are the phase lines for a 10 second wave of 1m height propagating in deep-water. The wave encounters a hindering current of varying magnitude between 500m and 1500m off the artificial deep-water shore. The blue lines on the plot are wave rays obtained using the Clyne (2008) method and the pink rays are the energy rays of this project.

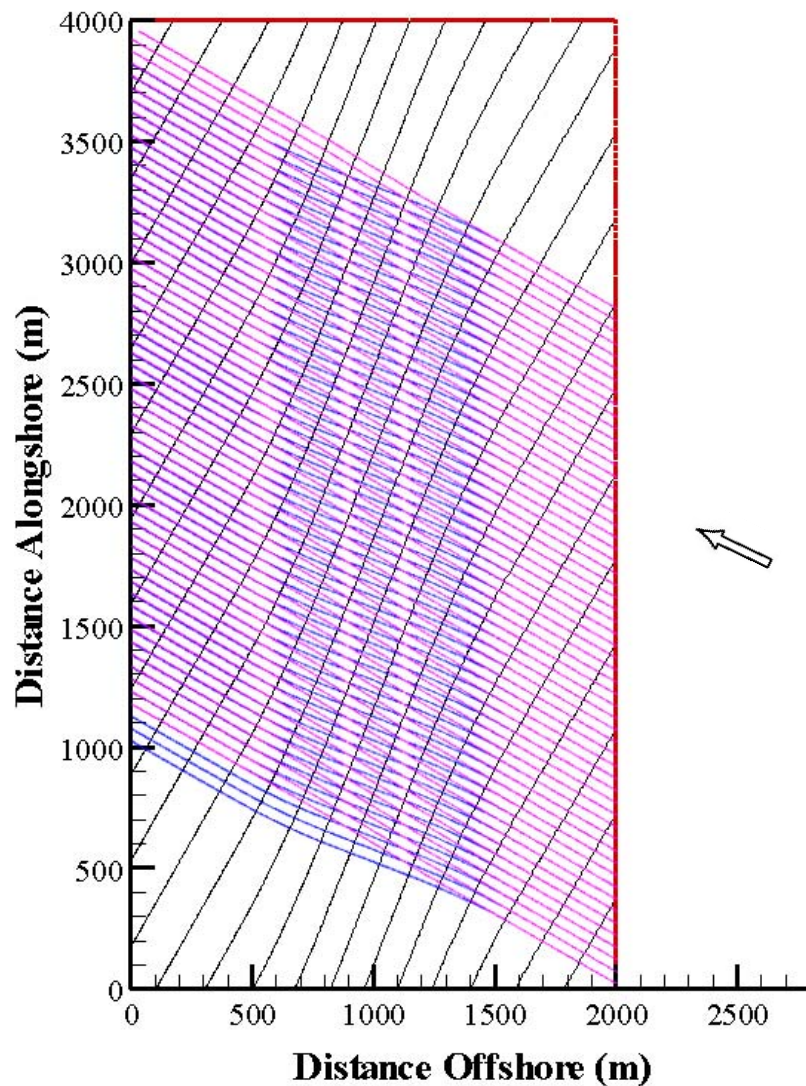


Figure 6.142 – Wave Rays using Clyne (2008) method (blue) vs. Wave Energy Rays (pink) plotted against Wave Crests (black)

6.16.3 Discussion

The plot above shows that the rays of the Clyne (2008) method are perpendicular to the direction of wave propagation, as they are supposed to be in the absence of a current. Figure 6.142 shows that as the waves change direction due to the crossing current the wave rays also change direction. However, the wave energy rays of this project follow the transmission of energy through the domain as opposed to the direction of wave propagation. The results of this section indicate that energy transmission continues in the direction of original wave propagation and is unaffected by the presence of a current.

The results of this section have interesting implications and could prove useful for any process that involves the identification of areas of focused wave energy. A classic example would be the selection of an appropriate location for a wave energy device in a bay. To position the device in an area of high energy one would look for a region where energy rays concentrate. If the traditional wave rays were utilised the region may not be selected appropriately due to the rays being affected by currents.

6.17 Case Study – Casheen Bay

6.17.1 Introduction

In order to fully utilise the NM-WCIM and NM-WDHM it was deemed necessary to carry out a case study of a real location. It was necessary to chose a location where there are reasonably strong currents so the effect of wave-current interaction in the NM-WCIM could be examined. Dr. Tomasz Dabrowski and Dr. Michael Hartnett of NUI, Galway generously provided measured data of bathymetry and modelled data of tidal currents for Casheen Bay, in Galway Bay on the west coast of Ireland. Casheen Bay proved to be an ideal case study for the NM-WCIM and NM-WDHM.

6.17.2 Casheen Bay – Location and Bathymetry

Casheen Bay is located on the West Coast of Ireland in the Galway Bay area as shown in Figure 6.143. It is situated approximately 45km west of Galway City as shown in Figure 6.144. Figure 6.145 shows an overhead photograph of the Casheen Bay area. The measured bathymetry of Casheen Bay is shown in Figure 6.146 and a three-dimensional plot of the same is shown in Figure 6.147 for visualisation purposes. It was necessary to create an artificial zone at the outer edge of the modelled area to allow appropriate radiation of backscattered wave energy and allow the modelled incoming waves to settle before approaching any rapid changes of depth. The depth of this region was set at 15m.



Figure 6.143 – Approximate Location of Casheen Bay, in Galway Bay, on the West Coast of Ireland



Figure 6.144 – Location of Casheen Bay with respect to Galway City and Galway Bay

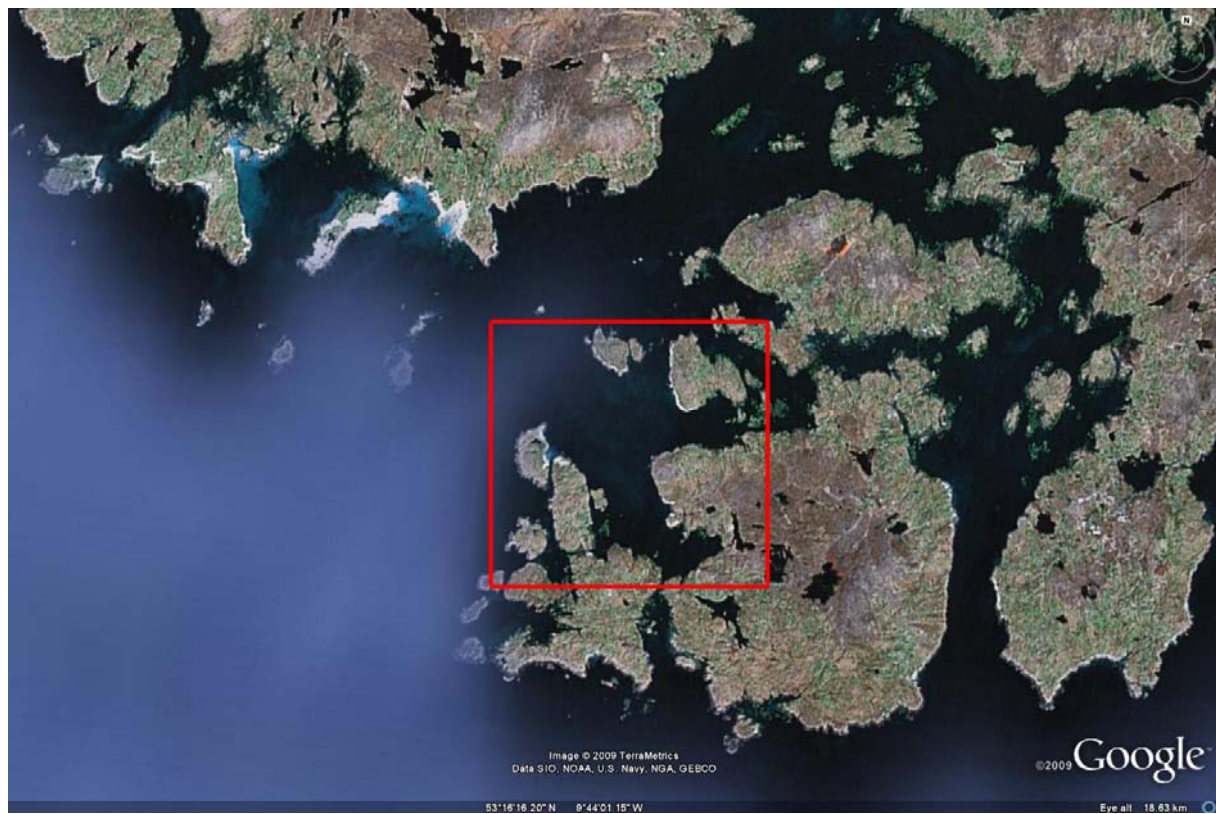


Figure 6.145 – Overhead Photograph of Casheen Bay

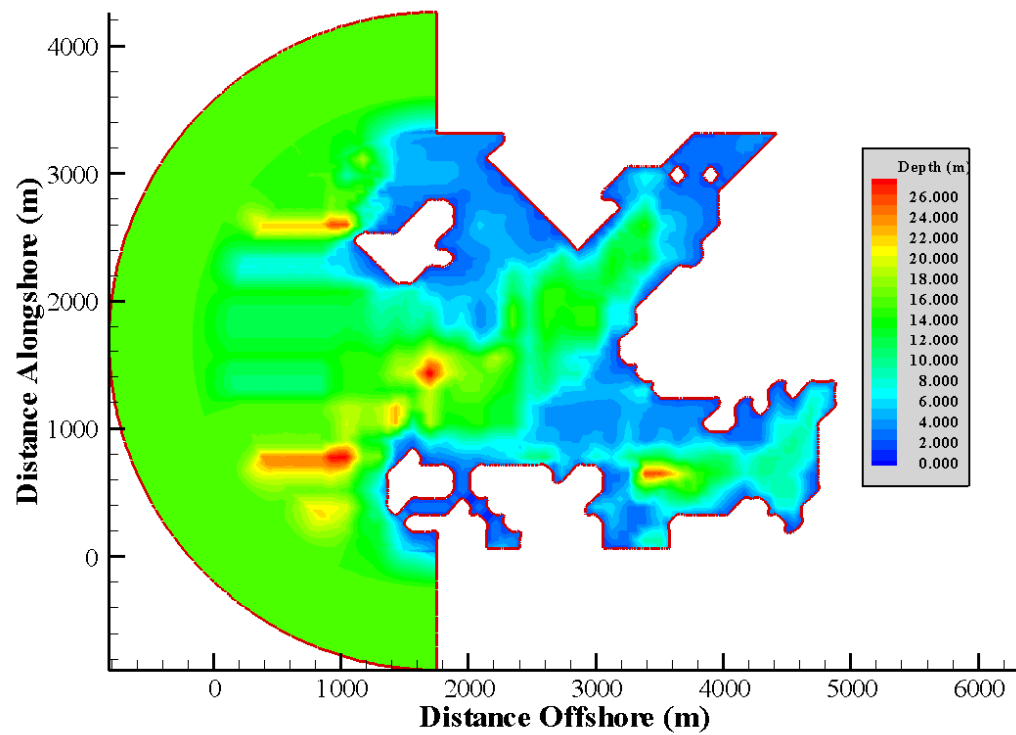


Figure 6.146 – Bathymetry of Casheen Bay

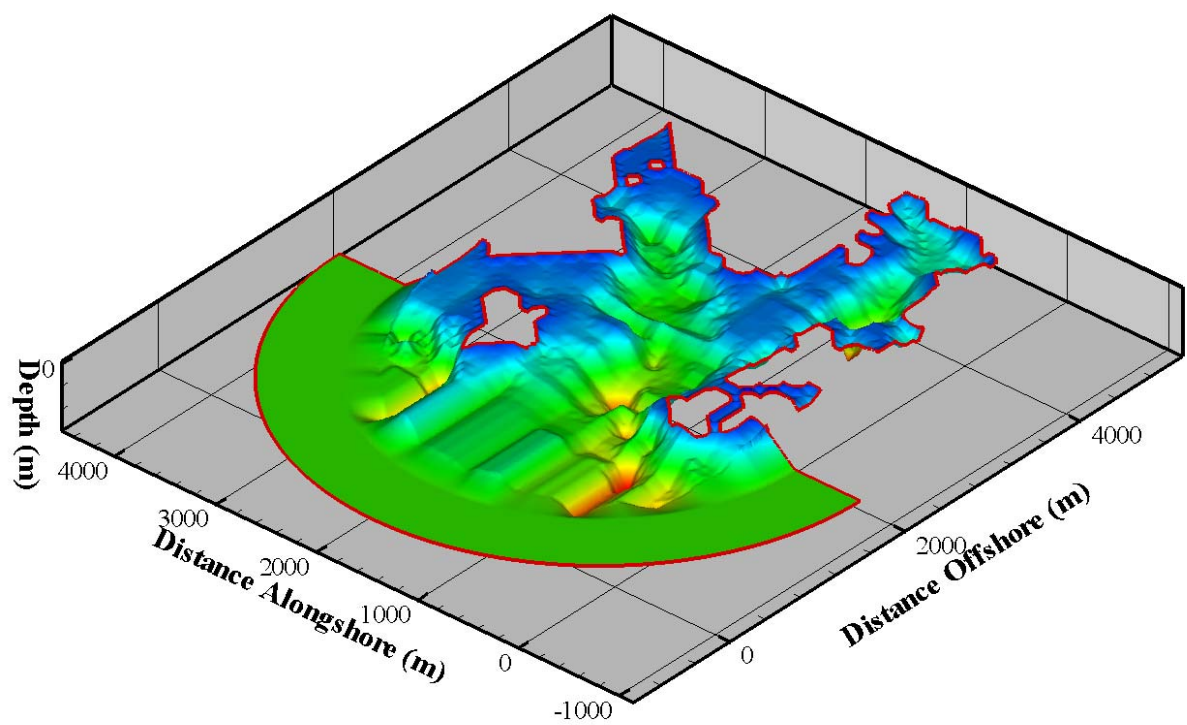


Figure 6.147 – Three Dimensional Plot of Casheen Bay Bathymetry

6.17.3 Wave Propagation in Casheen Bay

The prevailing wave direction on the west coast of Ireland is approximately south west. Although there is no measured wave data for Casheen Bay it is not unreasonable to assume the same is true especially considering the aerial photograph of Figure 6.145 indicates that this direction is the most exposed part of Casheen Bay to the main body of the Atlantic Ocean. The NM-WCIM was used to model waves approaching Casheen Bay from the south-west. Waves approaching from the west were also modelled for comparison purposes. In each case a wave height of 1m at the open boundary was chosen. The chosen period was 10 seconds.

Figure 6.148 and Figure 6.149 show the finite element mesh used for the NM-WCIM in this model. The mesh was made dense in areas where the wave behaviour is expected to be intricate and less dense where a simple wave solution is expected. Figure 6.149 shows a range of element sizes and the increase in mesh density near the island. The figures between Figure 6.150 and Figure 6.157 examine water surface, wave height and phase for each of the waves. Figure 6.158 is also included to show the wave rays obtained for the domain in the case of the south-westerly wave.

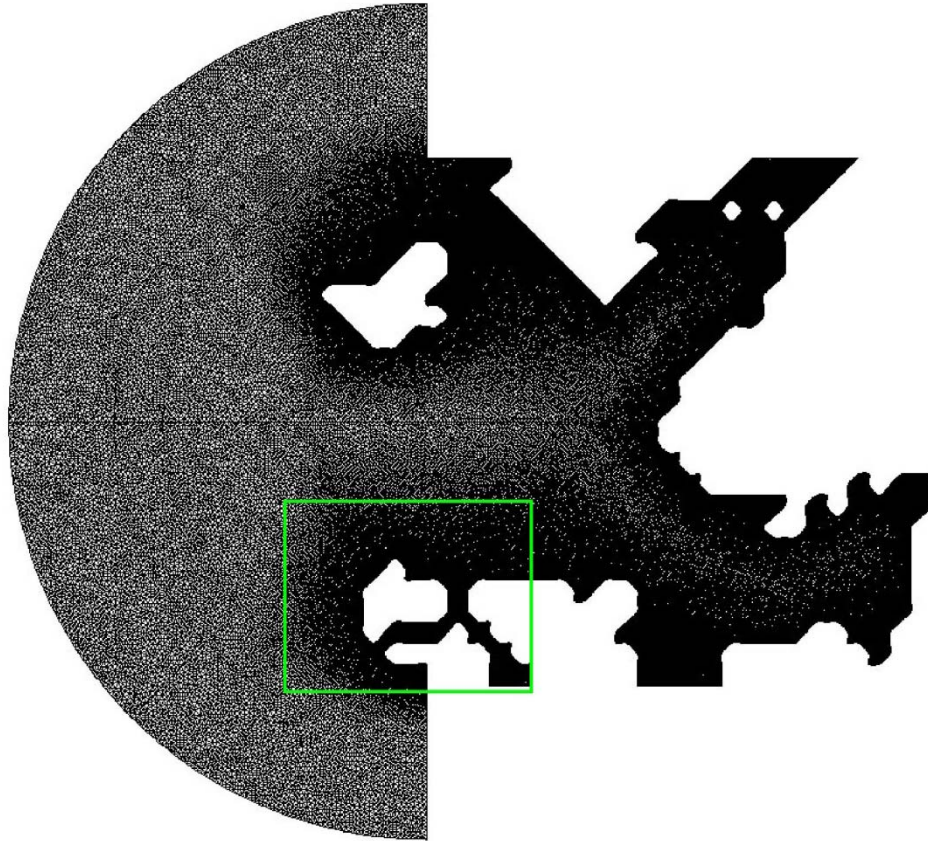


Figure 6.148 – Diagram of Finite Element Mesh for NM-WCIM of Casheen Bay. Section Highlighted in Green expanded in Figure 6.149.

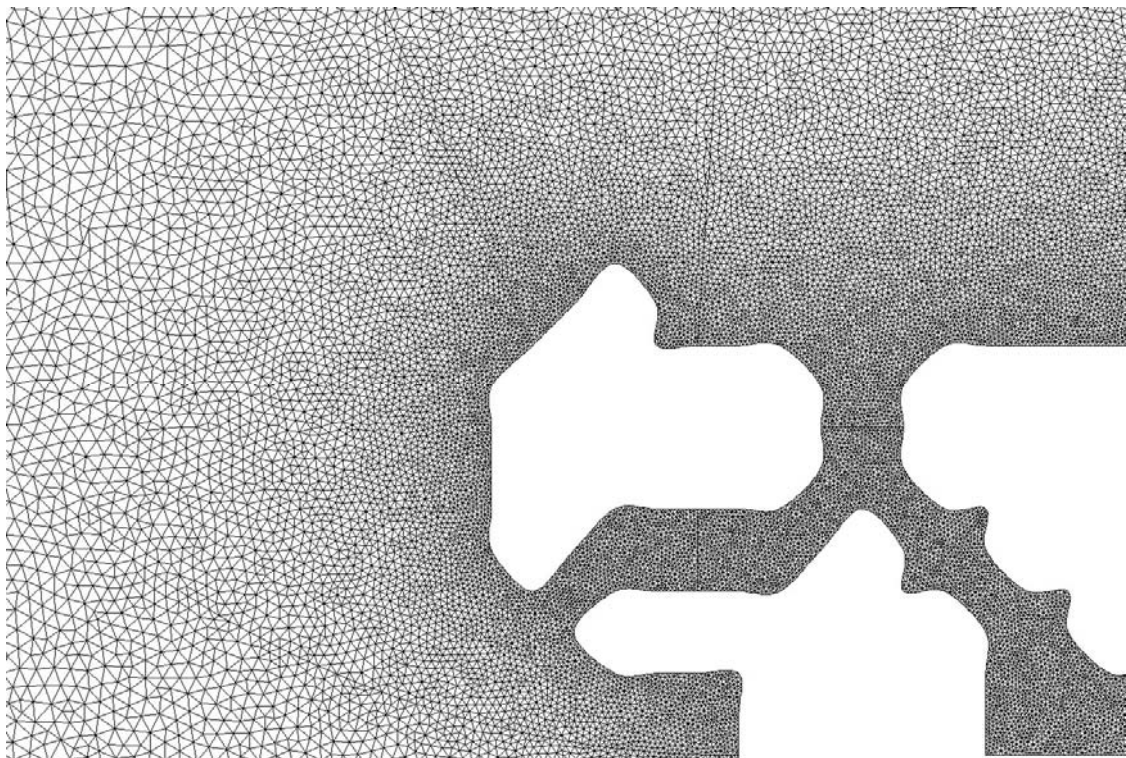


Figure 6.149 – Section of Finite Element Mesh for NM-WCIM of Casheen Bay as highlighted in Figure 6.148.

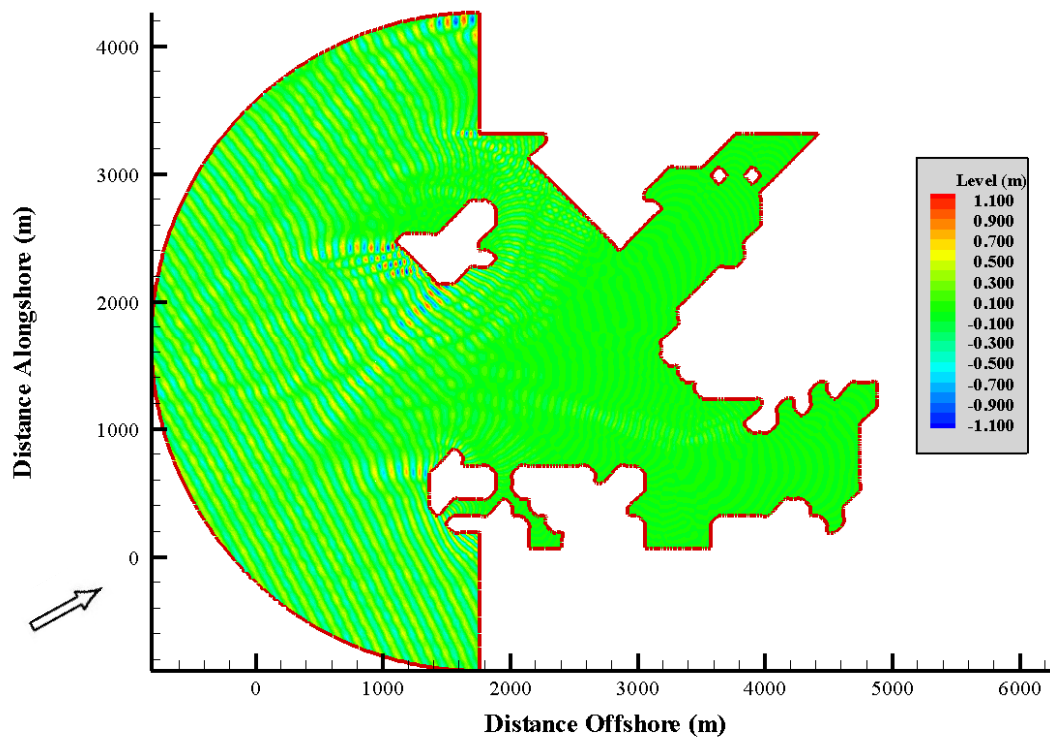


Figure 6.150 – Water Surface in Casheen Bay for Waves approaching from South-West

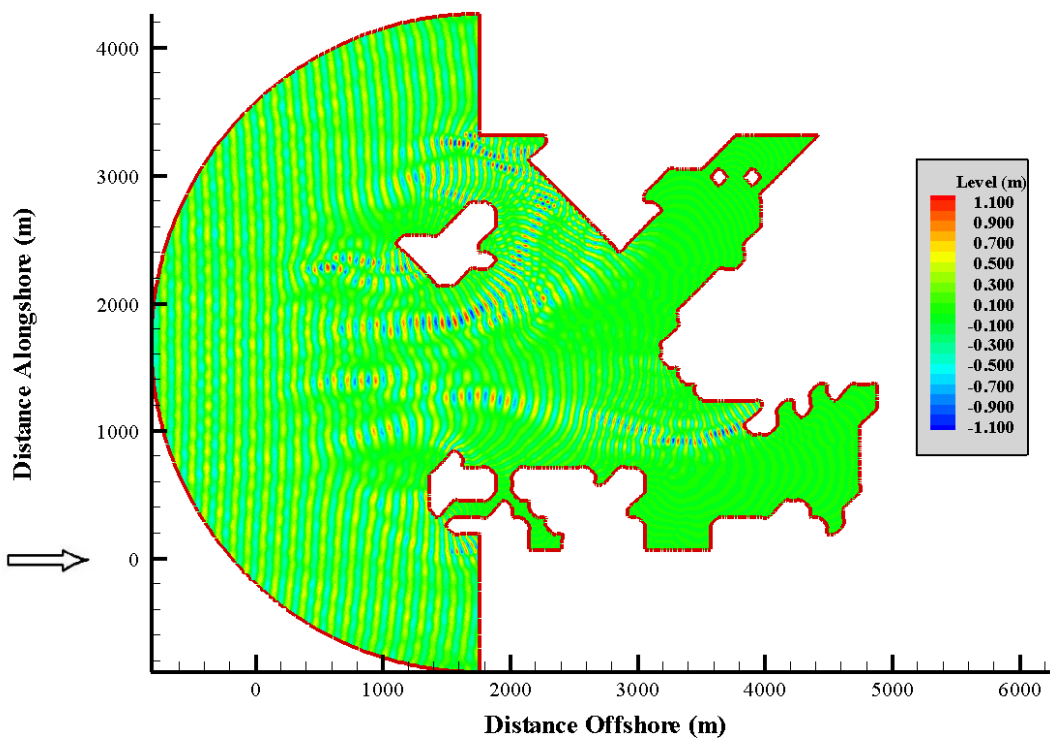


Figure 6.151 – Water Surface in Casheen Bay for Waves approaching from West

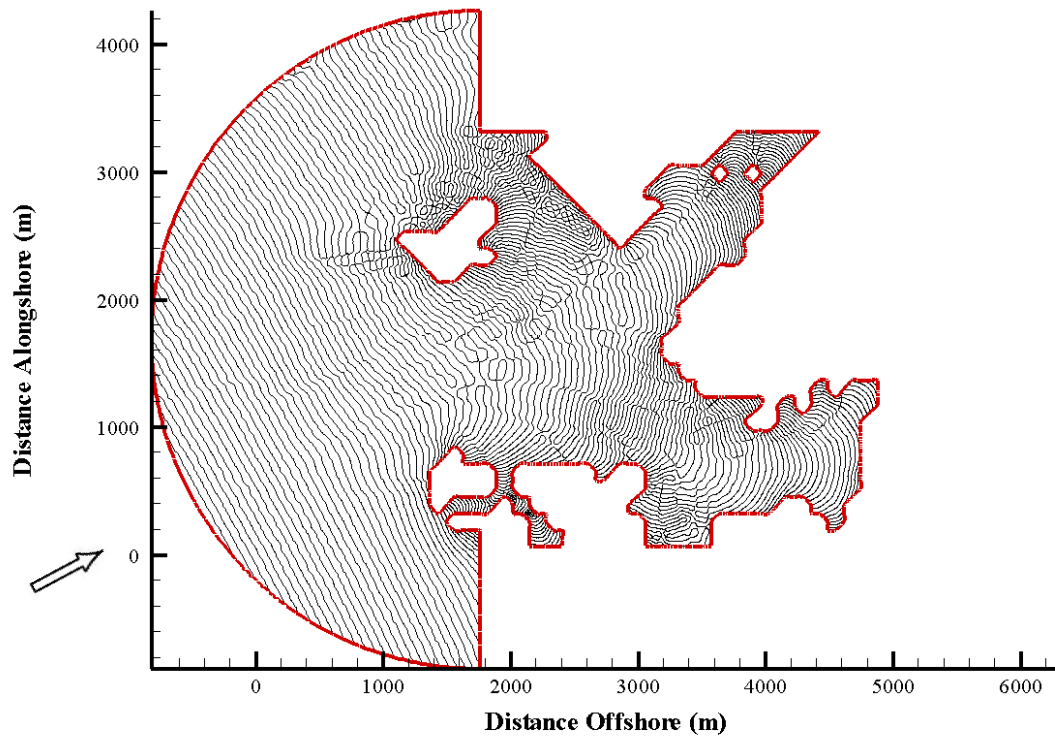


Figure 6.152 – Plot of Water Level = 0 in Casheen Bay for Waves approaching from South-West

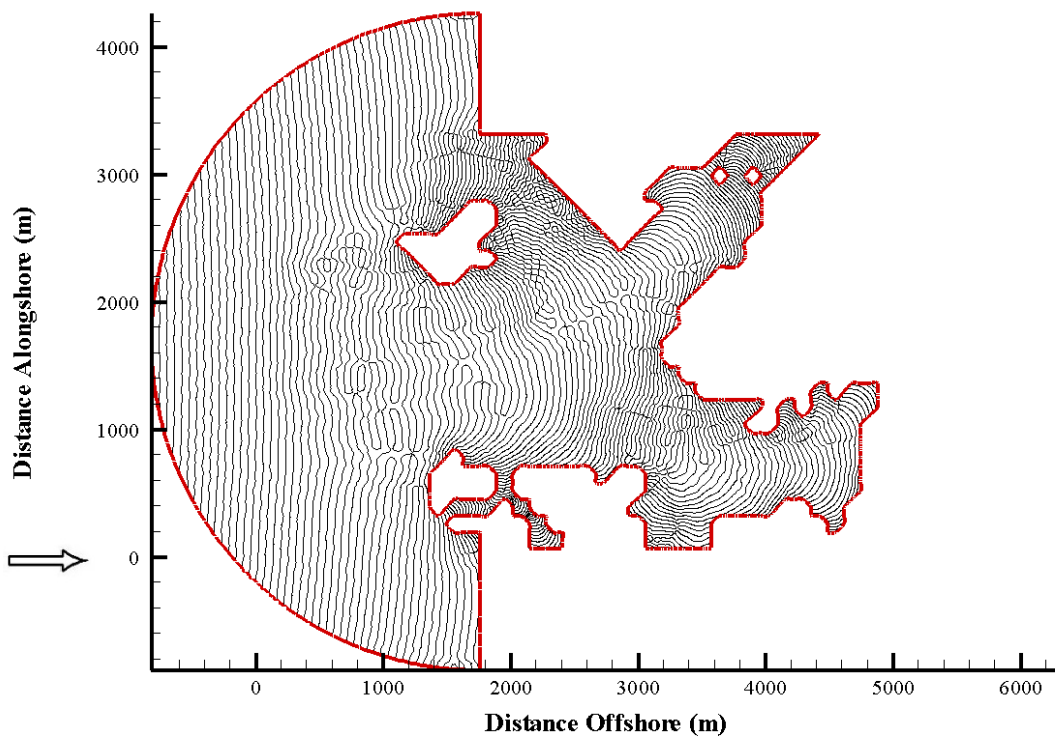


Figure 6.153 – Plot of Water Level = 0 in Casheen Bay for Waves approaching from West

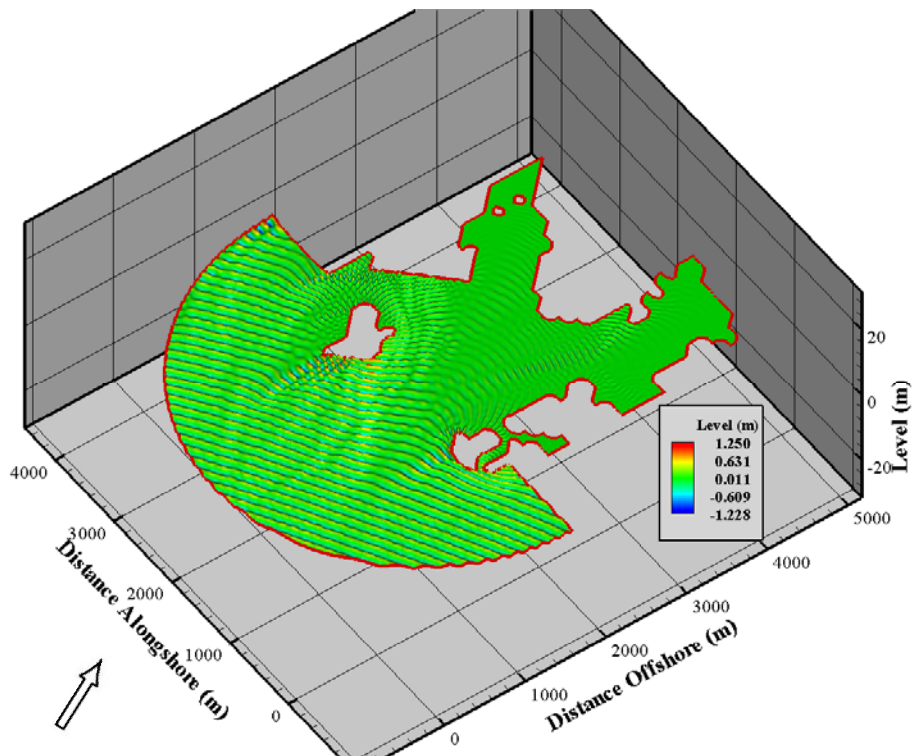


Figure 6.154 – Three Dimensional Plot of Water Surface in Casheen Bay for Waves approaching from South-West

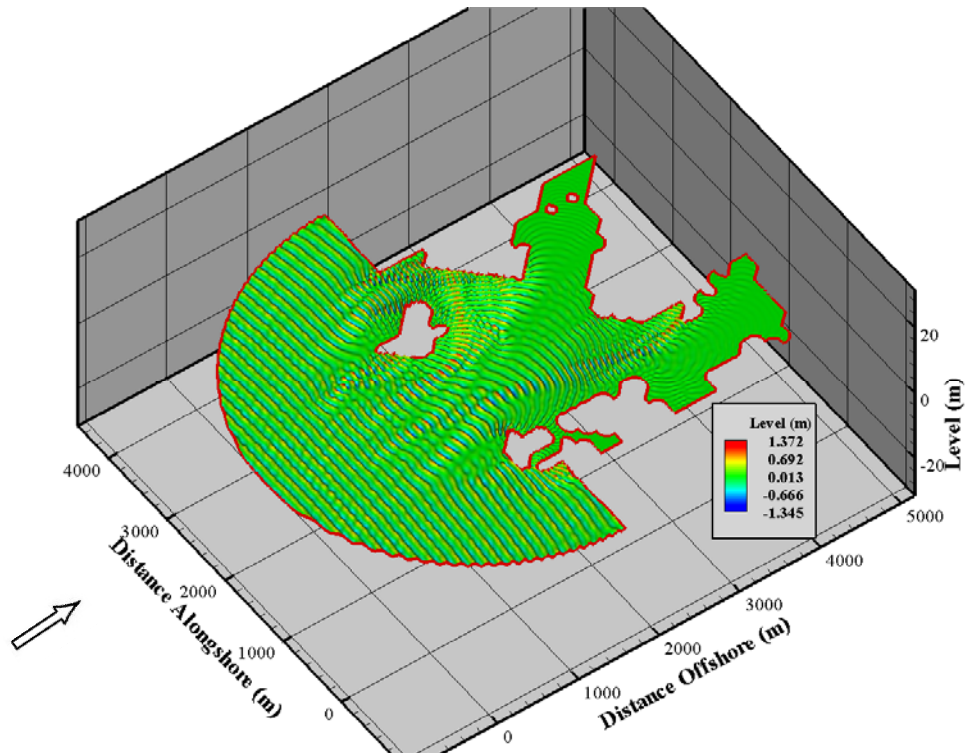


Figure 6.155 – Three Dimensional Plot of Water Surface in Casheen Bay for Waves approaching from West

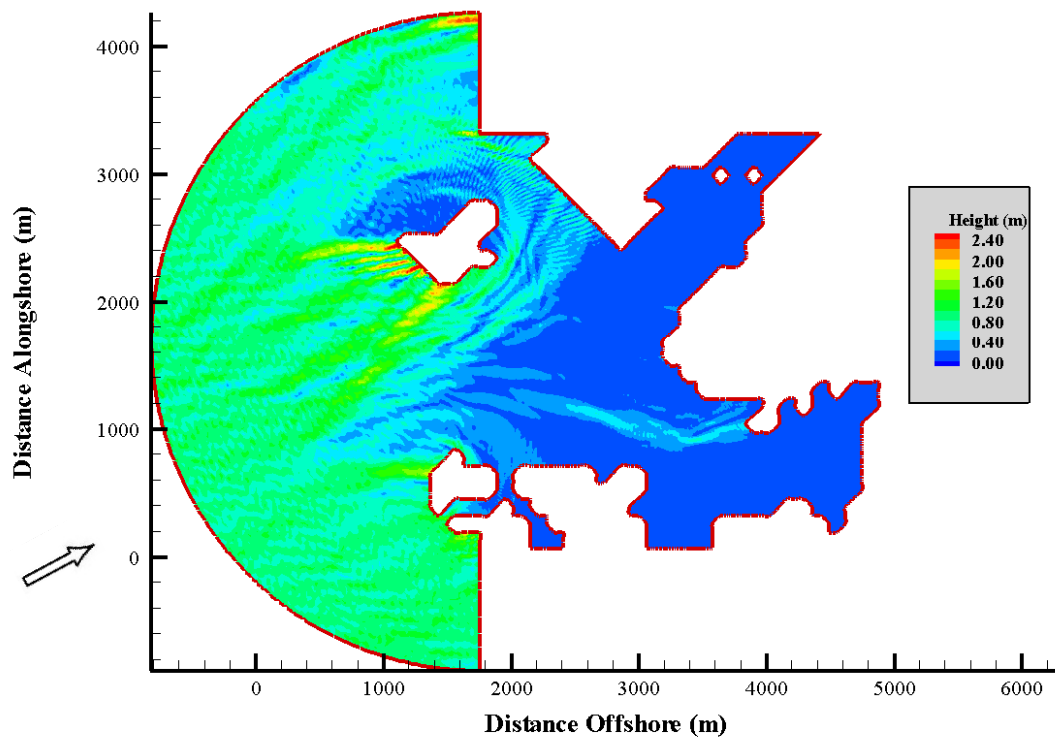


Figure 6.156 –Plot of Wave Height in Casheen Bay for Waves approaching from South-West

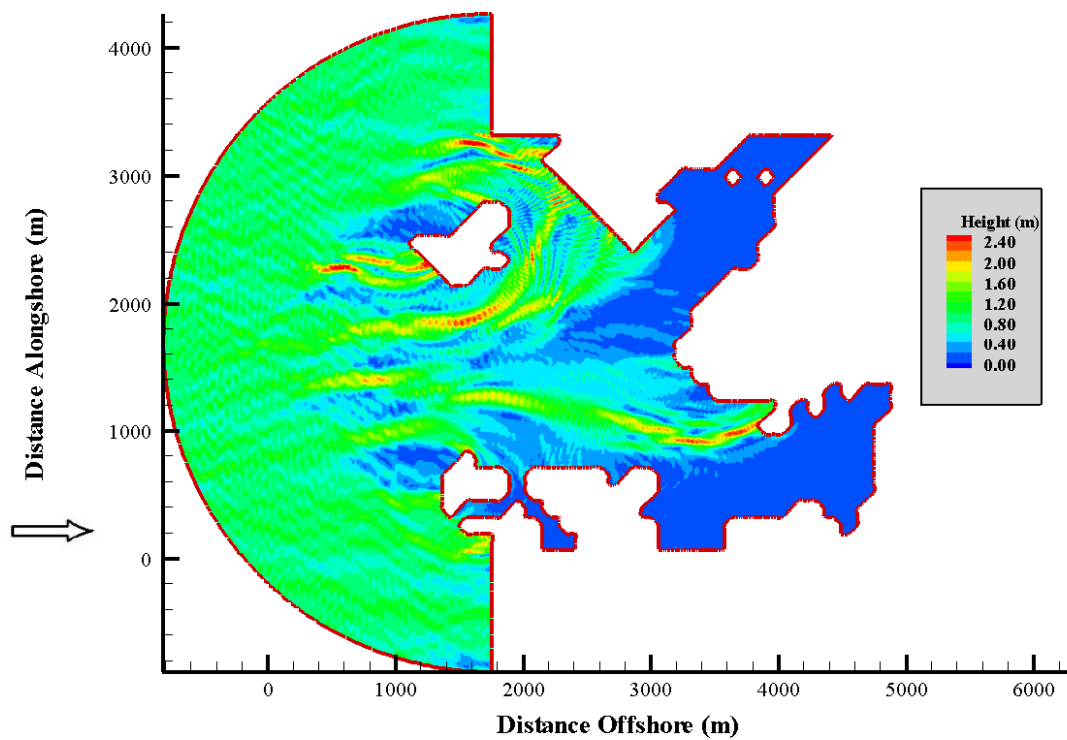


Figure 6.157 – Plot of Wave Height in Casheen Bay for Waves approaching from West

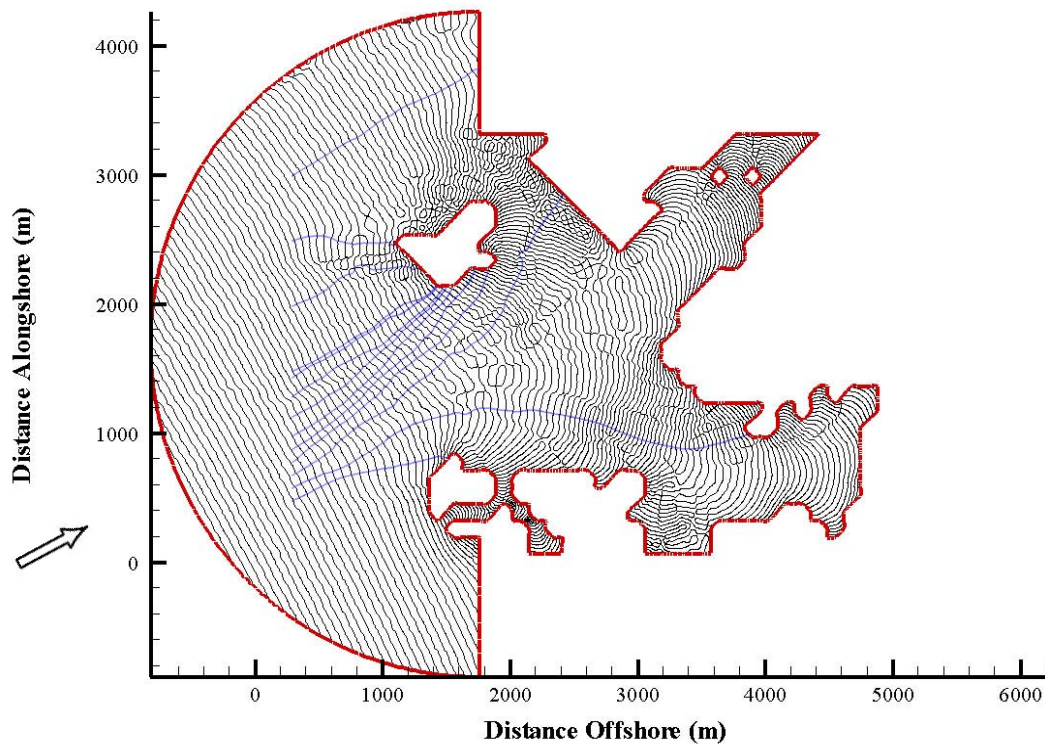


Figure 6.158 – Plot of Wave Rays (in blue) in Casheen Bay for Waves approaching from South-West

6.17.4 Wave-Current Interaction in Casheen Bay

Using modelled tidal flood and ebb velocities obtained from Dr. Dabrowski and Dr. Hartnett of NUI, Galway wave-current interaction in Casheen Bay can be examined. The NM-WCIM was run with a wave approaching from the south-west for both the maximum tidal flood velocity and the maximum tidal ebb velocity. The data presented below examines the changes in wave phase brought about by this wave-current interaction. A wave of 10 second period with a height of 1m at the boundary of the domain was once again chosen. Figure 6.159 and Figure 6.160 show the magnitude of modelled velocity distributed throughout Casheen Bay at maximum ebb tidal flow and maximum flood tidal flow respectively.

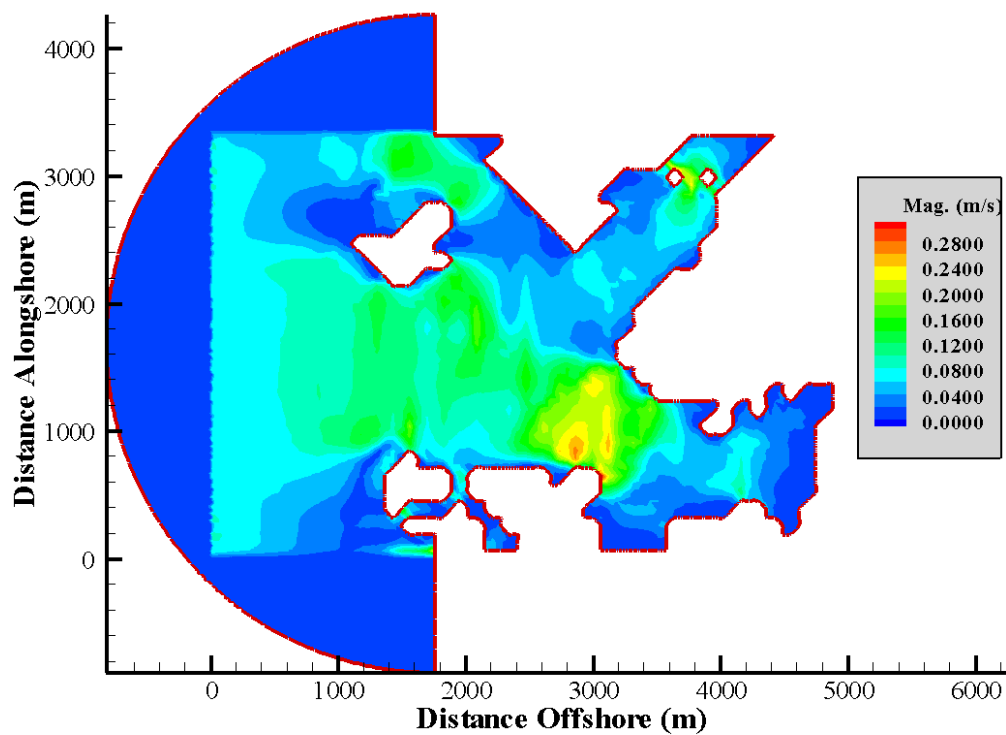


Figure 6.159 – Plot of Modelled Velocity Magnitude in Casheen Bay for Maximum Ebb Tidal Flow

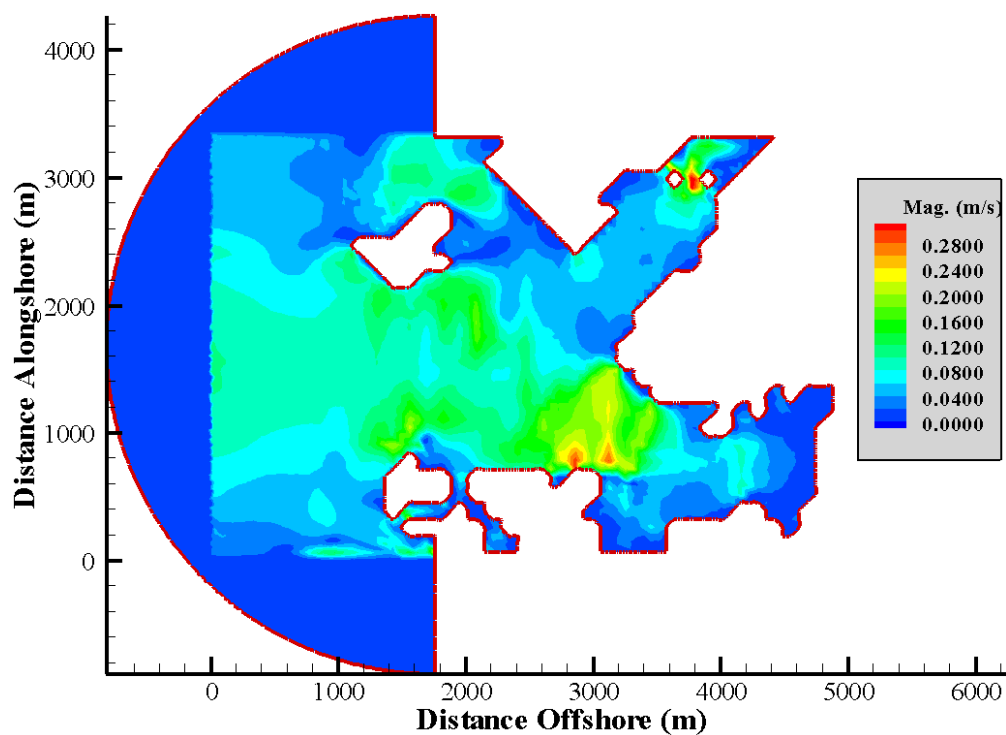


Figure 6.160 – Plot of Modelled Velocity Magnitude in Casheen Bay for Maximum Flood Tidal Flow

Using Figure 6.159 and Figure 6.160 it was possible to select three locations to examine wave-current interaction in detail. The selected locations were between the two islands in the north-east of the bay, in the narrow channel between the coast and the southernmost island and in the triangular shaped inlet on the north edge of the southern inlet. The next series of plots present the coordinates and velocity values at each of these locations.

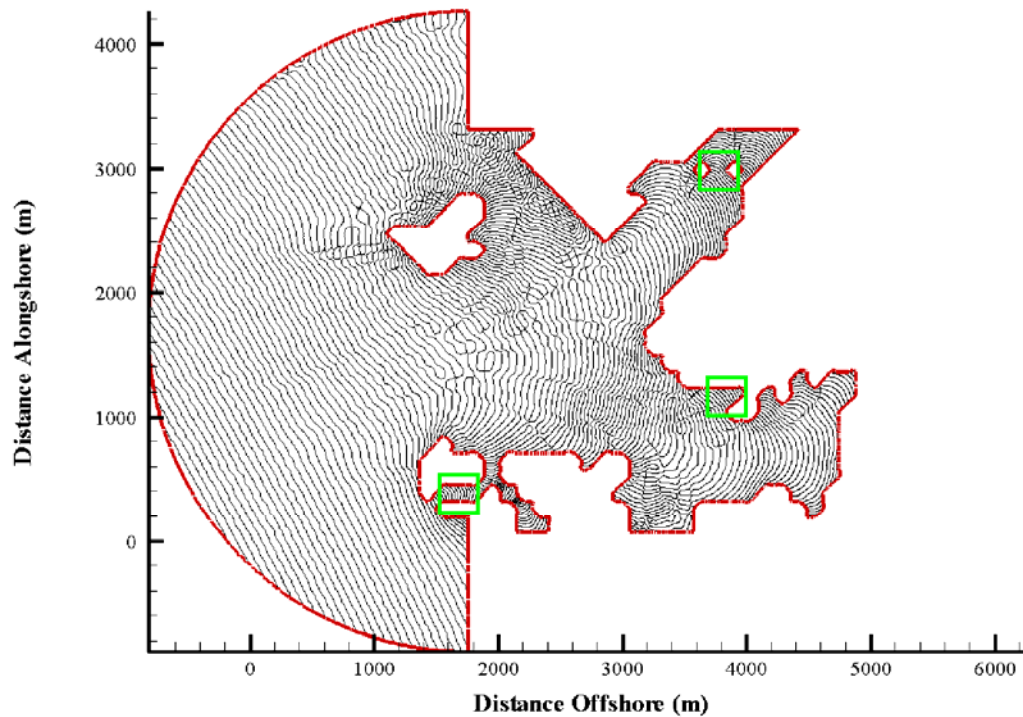


Figure 6.161 – Diagram showing Locations of detailed Wave-Current Interaction Analysis

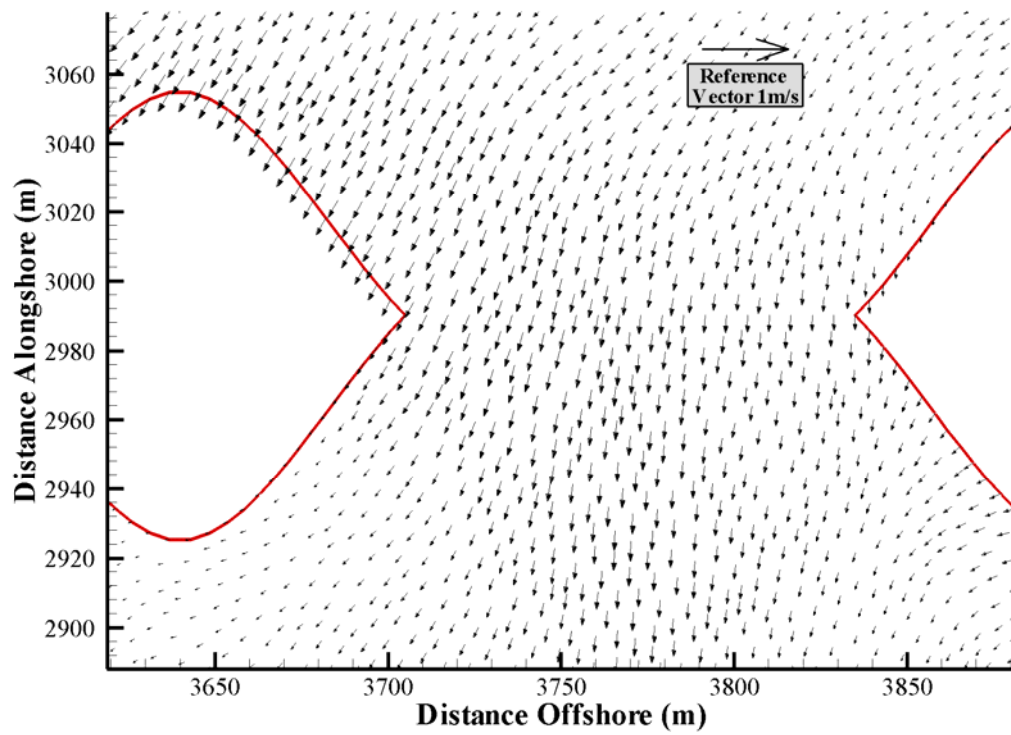


Figure 6.162 – Maximum Ebb Flow between two islands in Casheen Bay

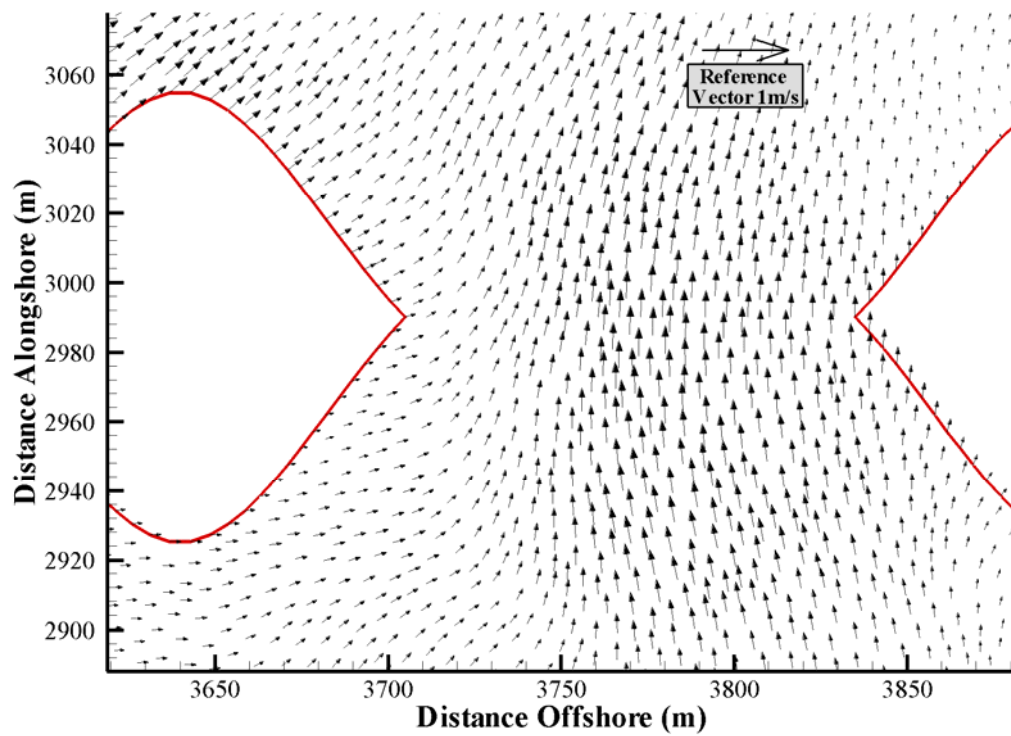


Figure 6.163 – Maximum Flood Flow between two islands in Casheen Bay

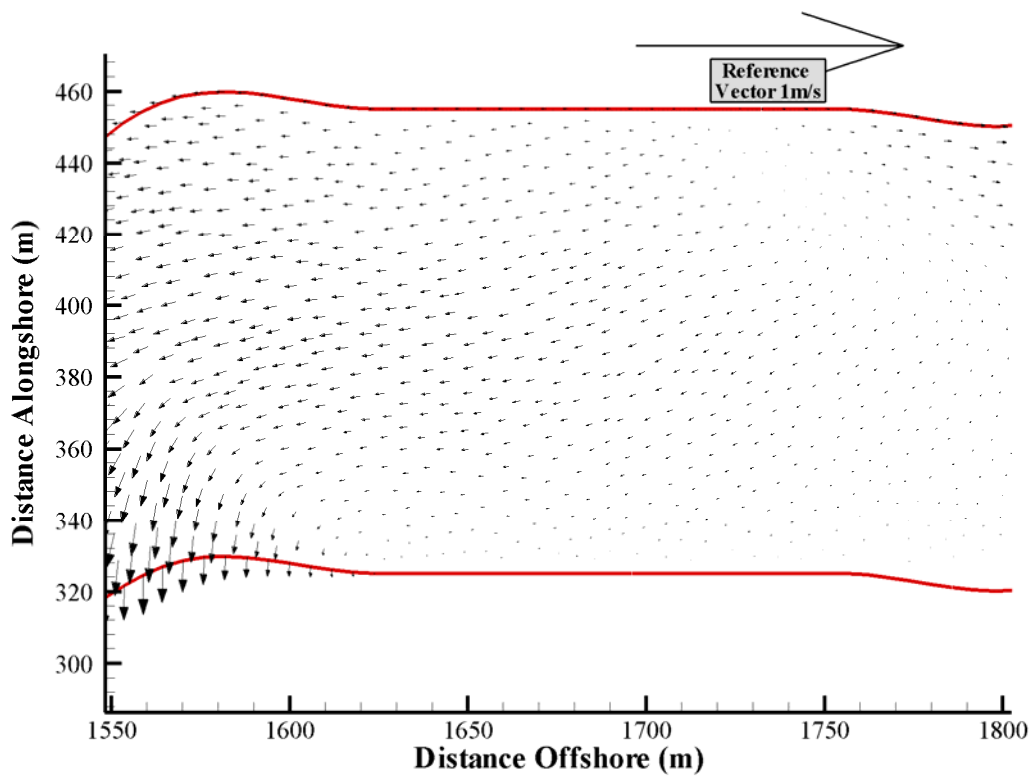


Figure 6.164 – Maximum Ebb Flow South of Southerly Island Casheen Bay

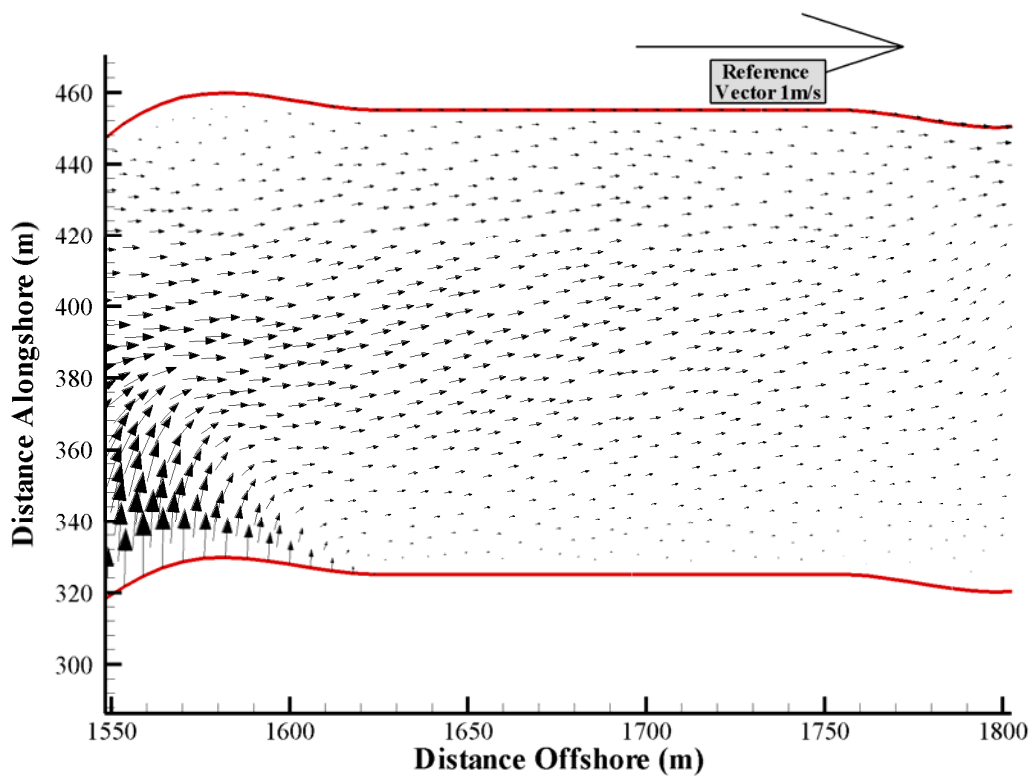


Figure 6.165 – Maximum Flood Flow South of Southerly Island Casheen Bay

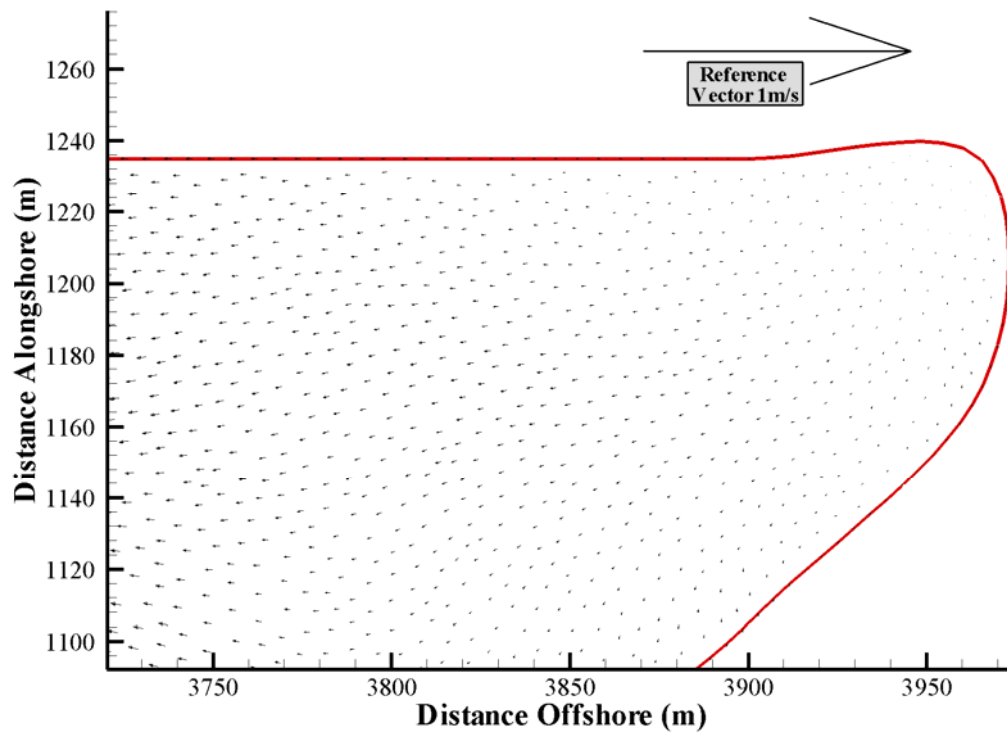


Figure 6.166 – Maximum Ebb Flow in an Inlet Casheen Bay

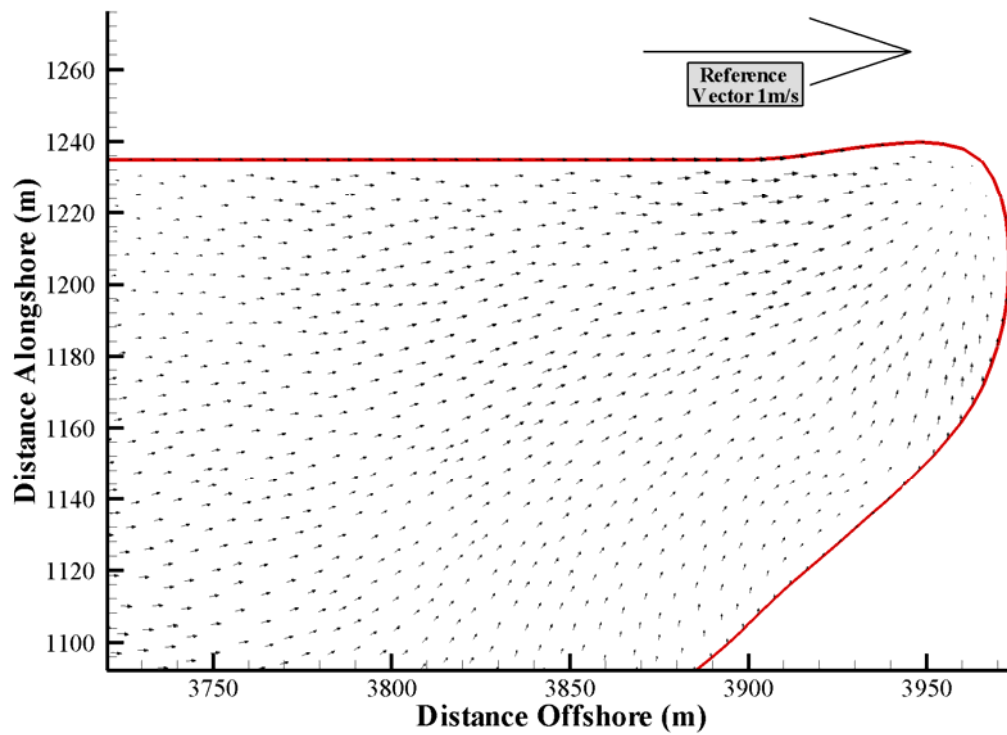


Figure 6.167 – Maximum Flood Flow in an Inlet Casheen Bay

Using the velocity values shown, the NM-WCIM was run for both maximum ebb tidal flow and maximum flood tidal flow. Plots of wave phase lines for the identified locations are shown below. The plots include phase lines for maximum ebb flow, maximum flood flow and in the absence of any current.

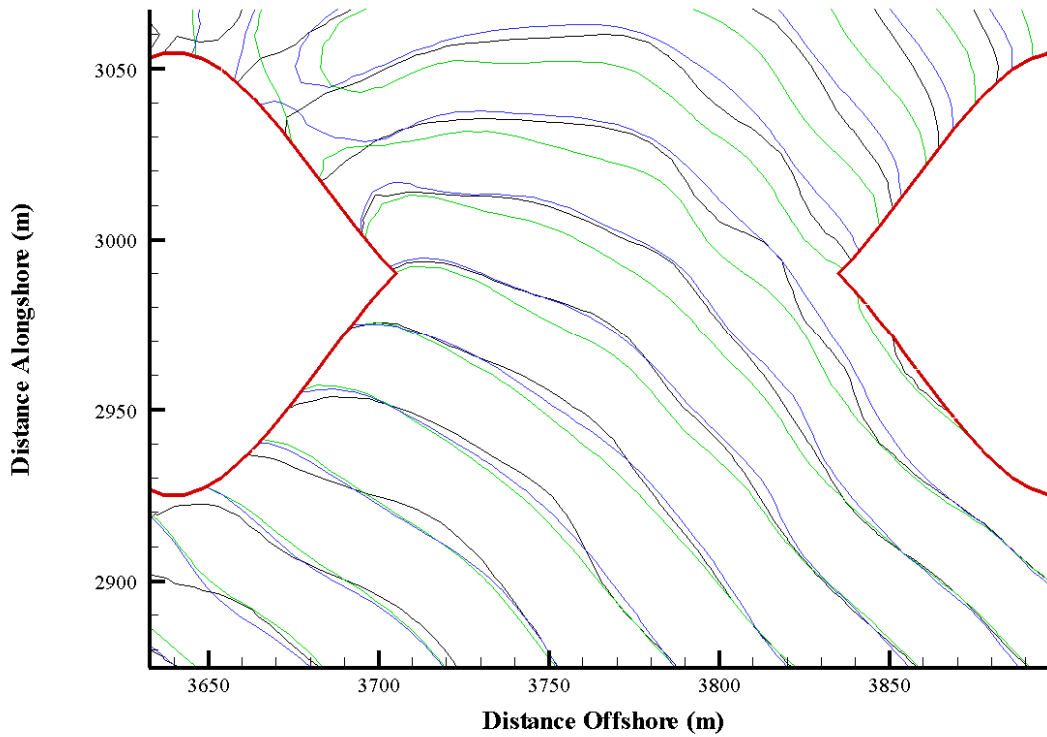


Figure 6.168 – Plot of Wave Phase between two islands in Casheen Bay. Blue Lines represent Maximum Flood, Green Lines represent Maximum Ebb & Black lines represent No Current.

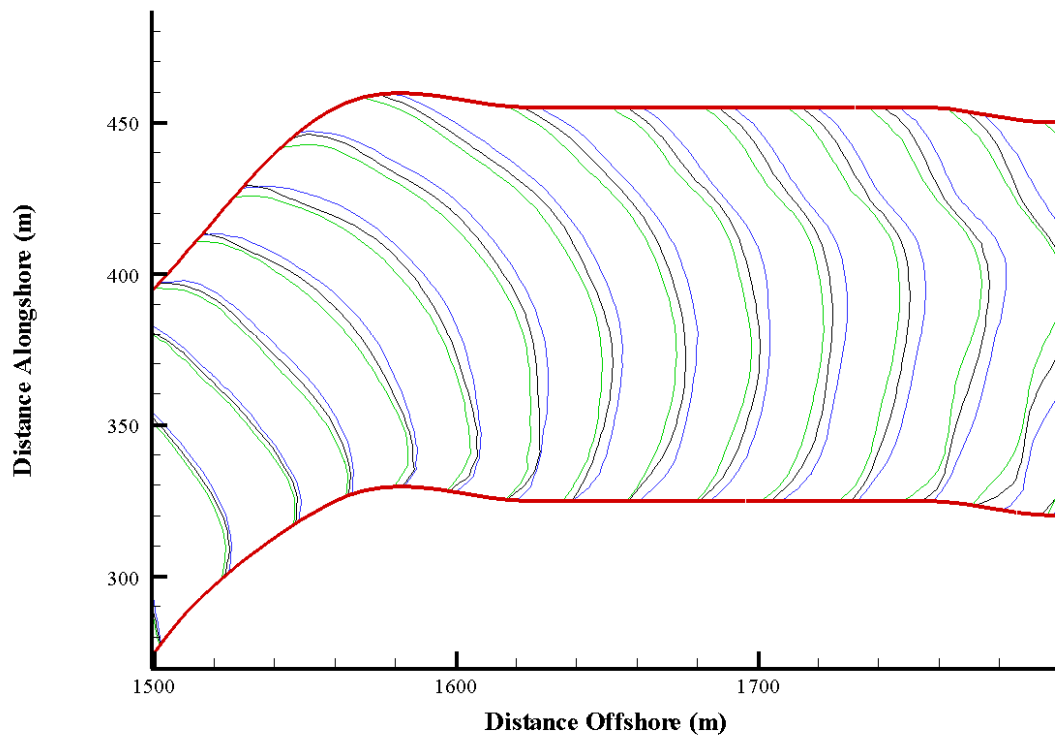


Figure 6.169 – Plot of Wave Phase south of Southerly Island in Casheen Bay. Blue Lines represent Maximum Flood, Green Lines represent Maximum Ebb & Black lines represent No Current.

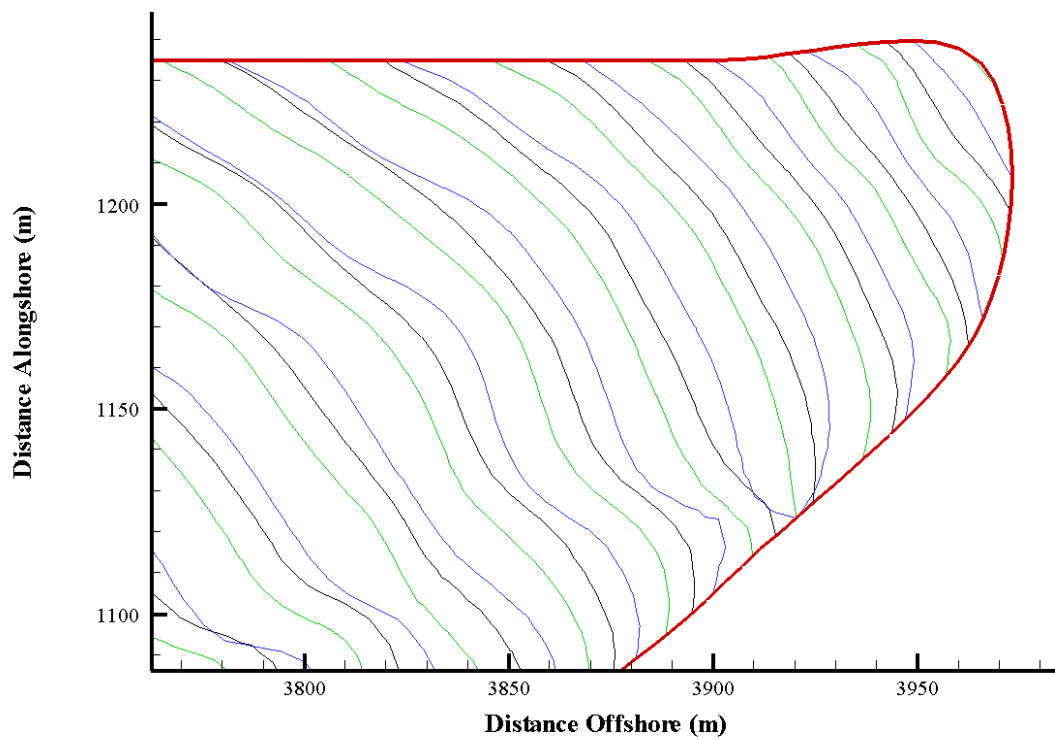


Figure 6.170 – Plot of Wave Phase in an Inlet in Casheen Bay. Blue Lines represent Maximum Flood, Green Lines represent Maximum Ebb & Black lines represent No Current.

The figures below examine the effect of the presence of a current on wave height between the two islands previously examined. Figure 6.171 and Figure 6.172 show the wave height at the location for maximum flood and maximum ebb flow respectively. Figure 6.173 shows the percentage difference between the two.

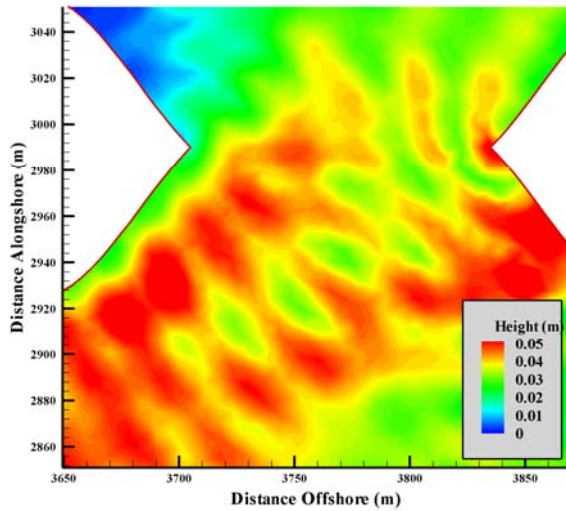


Figure 6.171 – Wave Height between Two Islands in Casheen Bay in the Presence of Max Flood Flow

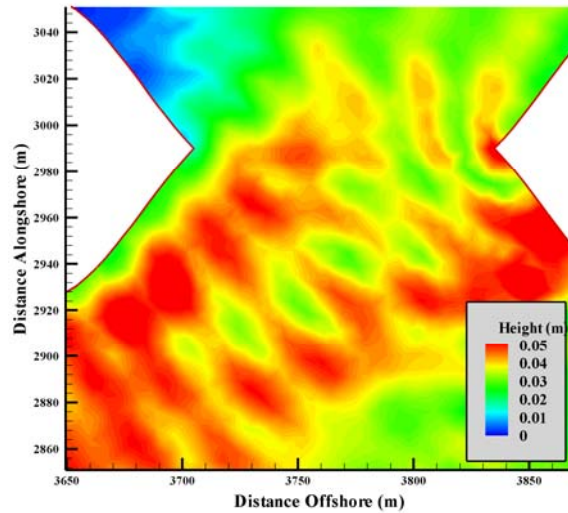


Figure 6.172 – Wave Height between Two Islands in Casheen Bay in the Presence of Max Ebb Flow

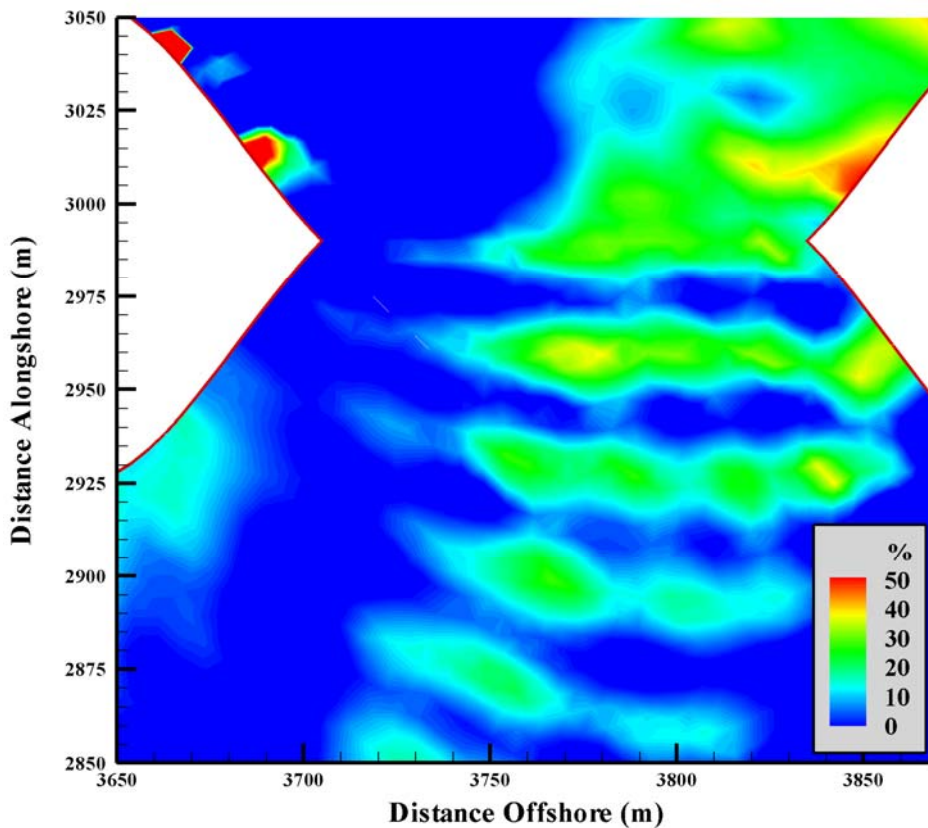


Figure 6.173 – Percentage Difference in Wave Height at Flood and Ebb Flow between Two Islands in Casheen Bay

6.17.5 Wave-Driven Hydrodynamic Behaviour In Casheen Bay

The NM-WDHM was run also run to examine wave-driven hydrodynamic effects in Casheen Bay. The NM-WDHM was run using the results of the initial NM-WCIM in the absence of a current both for a westerly approaching wave and a south-westerly approaching wave. Figure 6.175 and Figure 6.176 show the set-up and set-down in Casheen Bay for a wave approaching from a south-westerly and westerly direction respectively. Figure 6.177 and Figure 6.178 show the set-up/set-down and longshore currents generated on the exposed coast of the largest island in Casheen Bay for both the south-westerly and westerly approaching waves. Similarly Figure 6.179 and Figure 6.180 show the same data for the exposed coast of the southerly island within Casheen Bay.

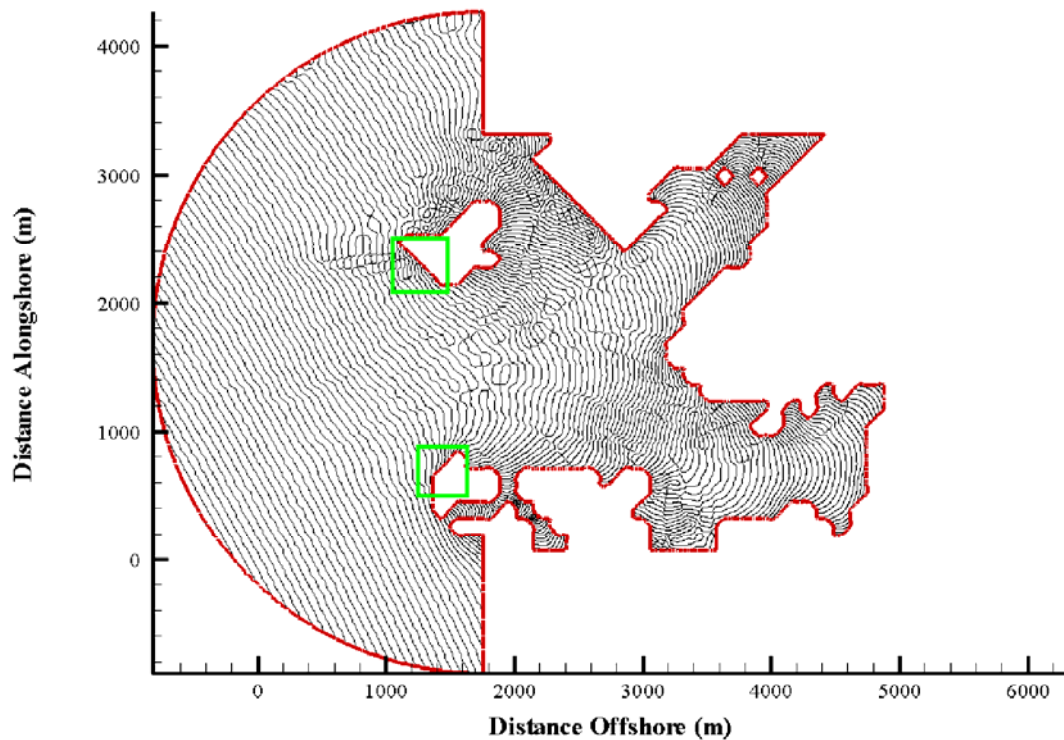


Figure 6.174 – Diagram showing the Locations of Detailed Wave-Driven Current and Set-up/Set-down Analysis

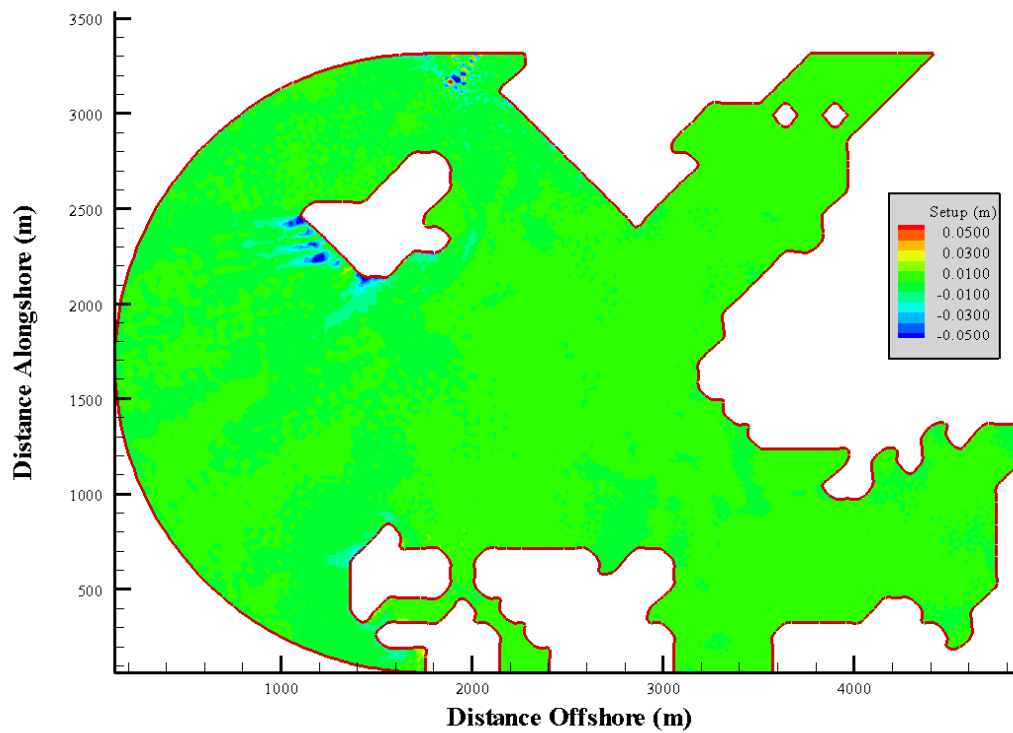


Figure 6.175 – Set-up/Set-down in Casheen Bay for a Wave Approaching from the South-West

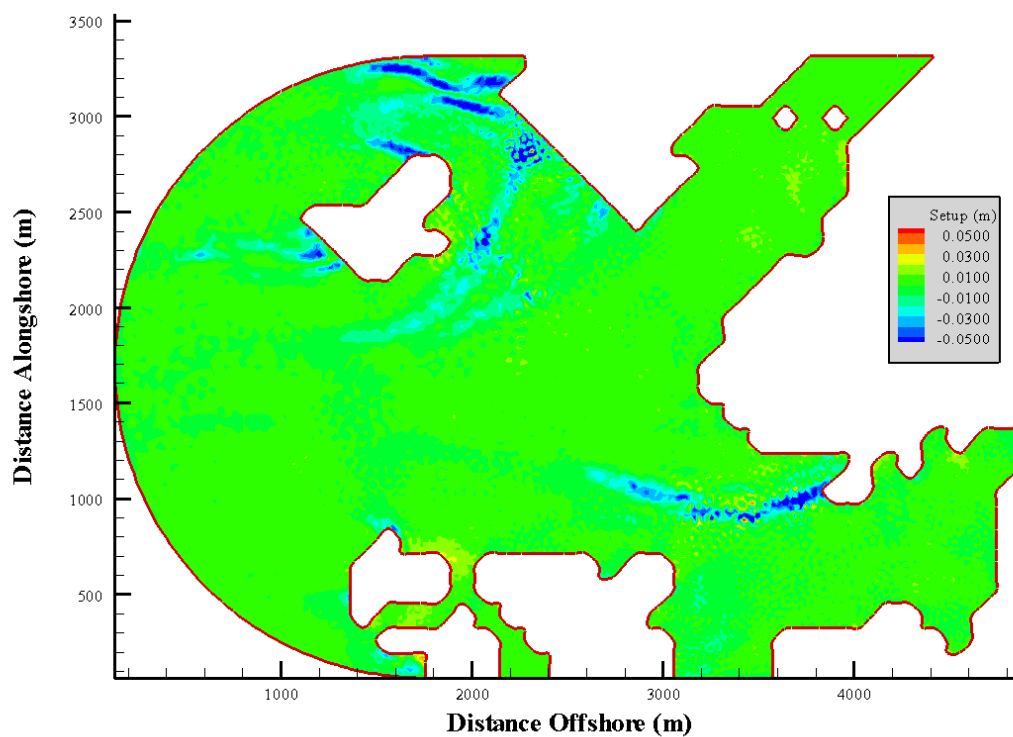


Figure 6.176 – Set-up/Set-down in Casheen Bay for a Wave Approaching from the West

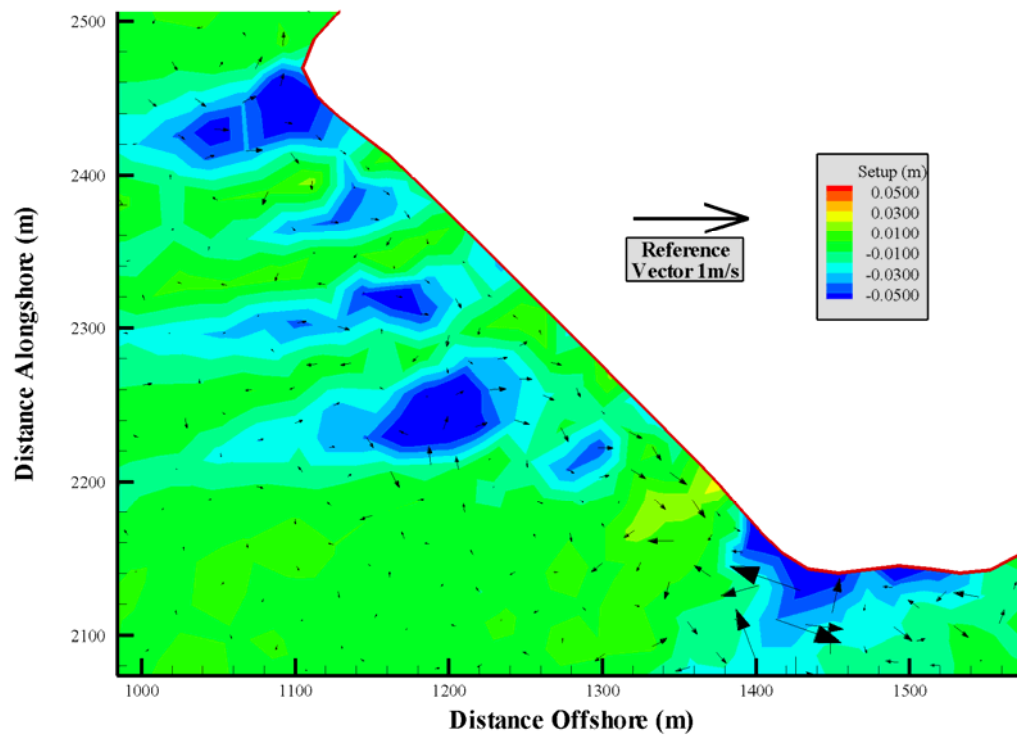


Figure 6.177 – Set-up/Set-down and Wave-Generated Currents on the coast of Large Island in Casheen Bay – South-West Wave

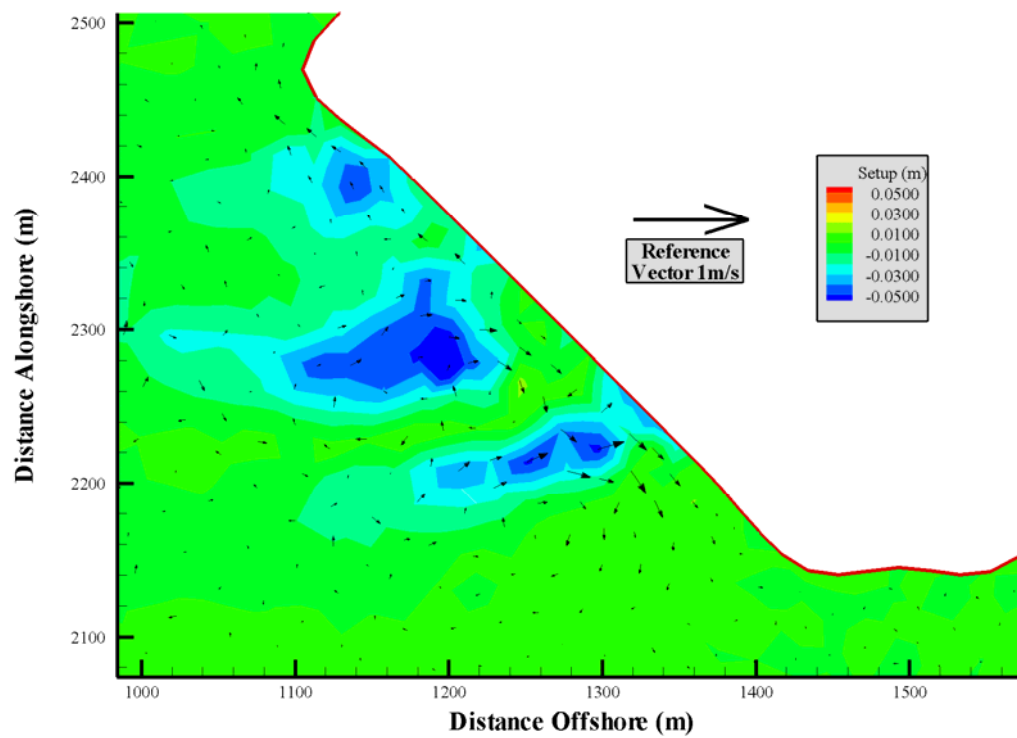


Figure 6.178 – Set-up/Set-down and Wave-Generated Currents on the coast of Large Island in Casheen Bay – West Wave

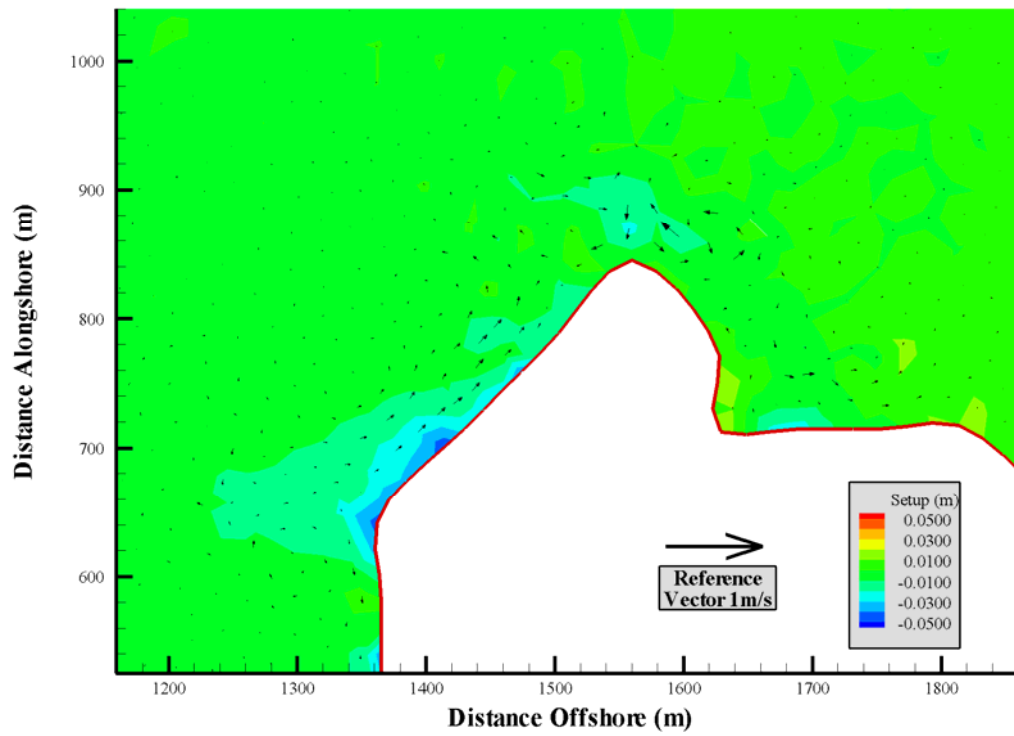


Figure 6.179 – Set-up/Set-down and Wave-Generated Currents on the coast of Southerly Island in Casheen Bay – South-West Wave

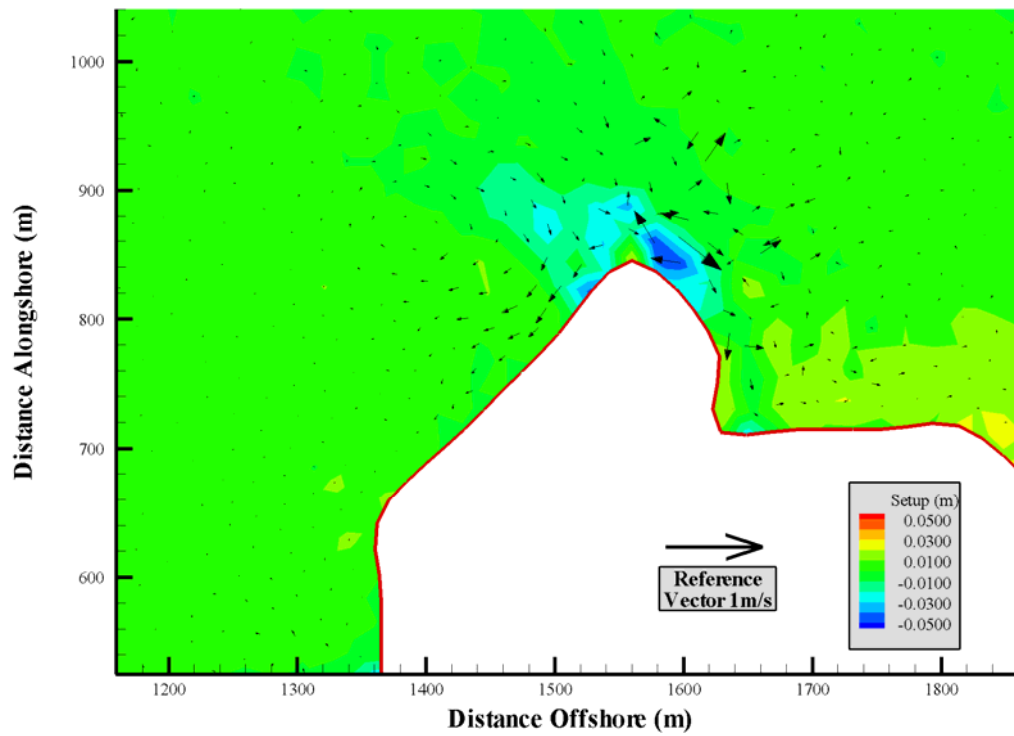


Figure 6.180 – Set-up/Set-down and Wave-Generated Currents on the coast of Southerly Island in Casheen Bay – West Wave

The figures plotted below show the wave-generated currents at the locations discussed in Section 6.17.4. They are shown to give an indication of the relative magnitudes of wave generated currents and tidal currents in a real bay. Figures Figure 6.181, Figure 6.183 and Figure 6.185 show wave-generated currents for a south-westerly approaching wave and Figure 6.182, Figure 6.184 and Figure 6.186 show the same data in the case of waves approaching from a westerly direction.

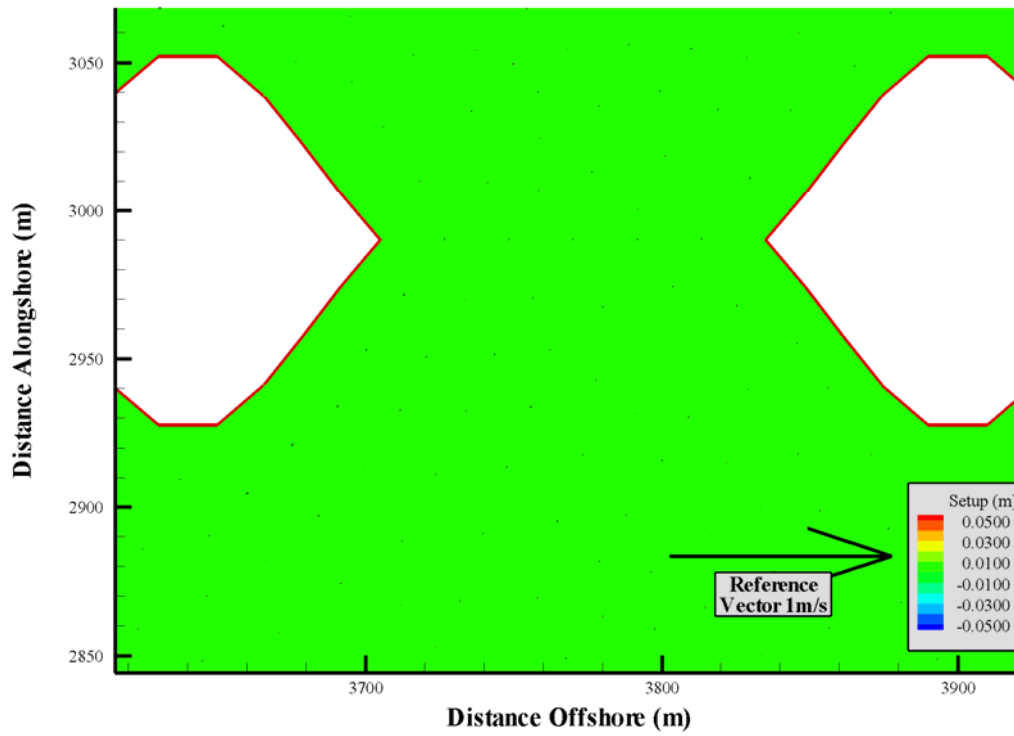


Figure 6.181 – Wave-Generated Currents for region between two Islands in Casheen Bay – South-West Wave

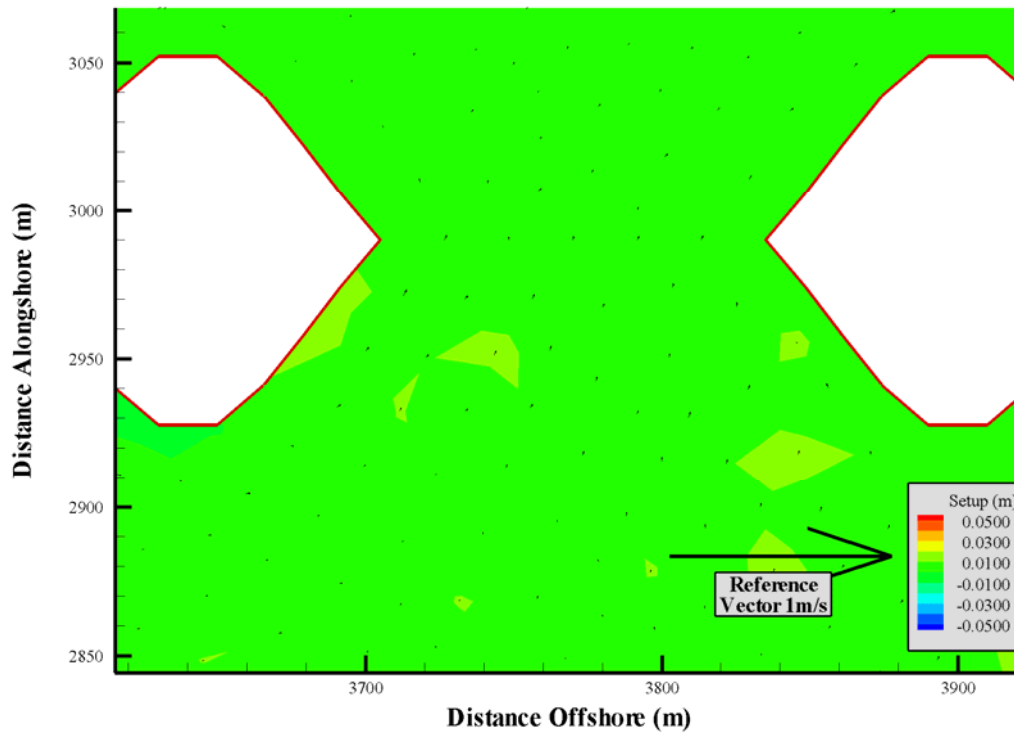


Figure 6.182 – Wave-Generated Currents for region between two Islands in Casheen Bay – West Wave

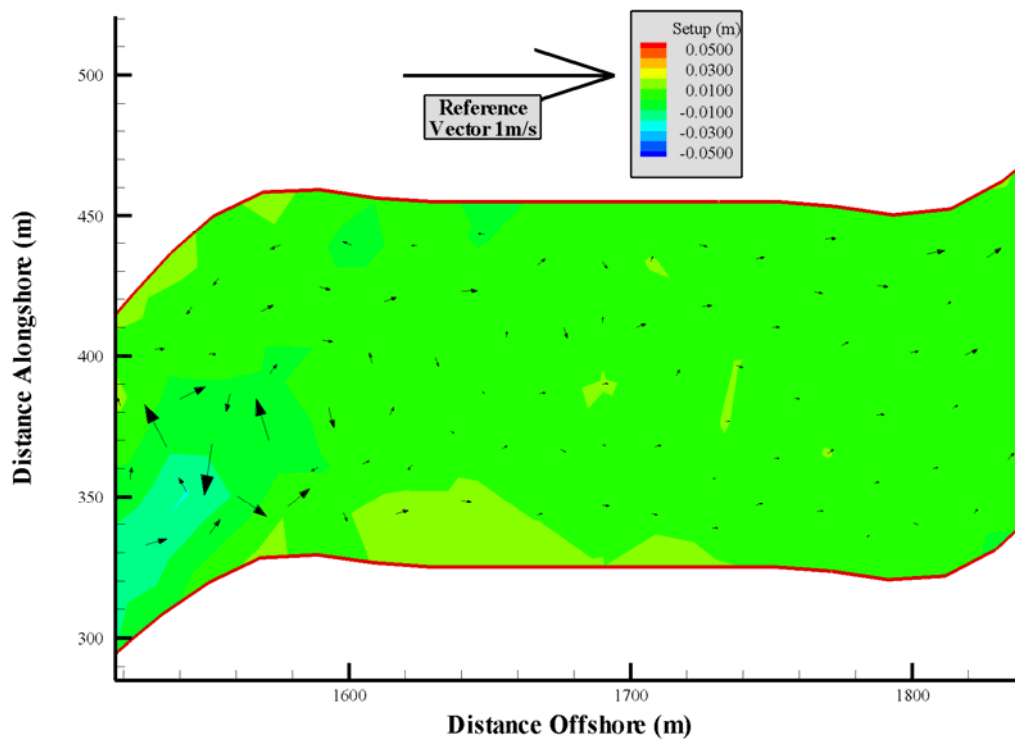


Figure 6.183 – Wave-Generated Currents for region South of Southerly Island in Casheen Bay – South-West Wave

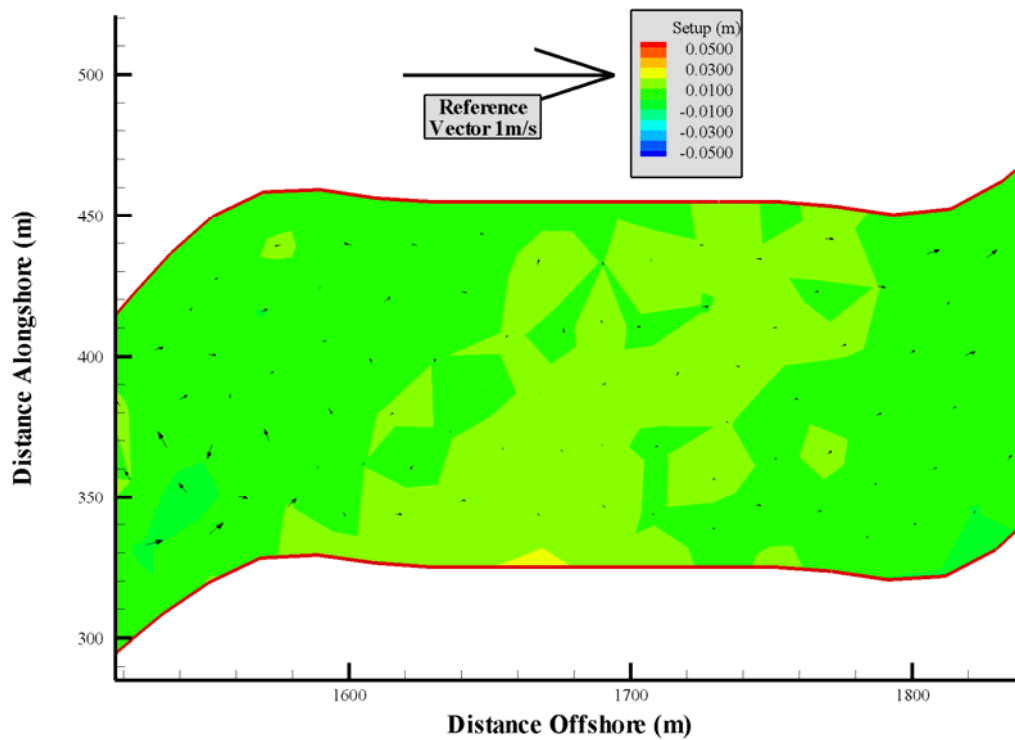


Figure 6.184 – Wave-Generated Currents for region South of Southerly Island in Casheen Bay – West Wave

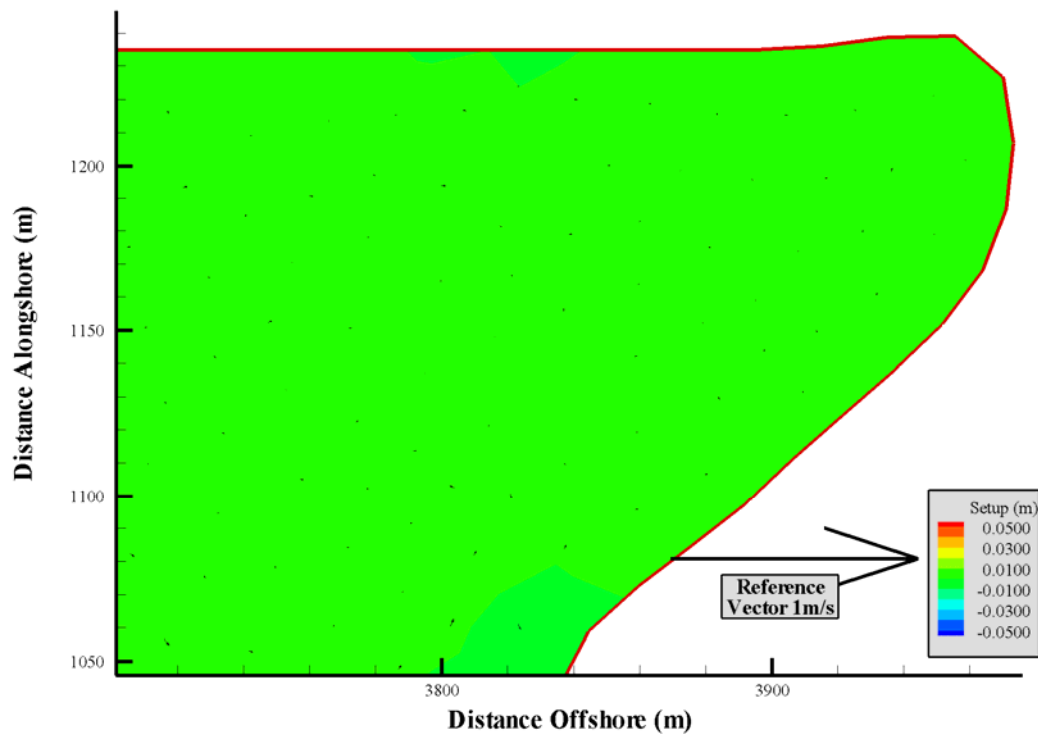


Figure 6.185 – Wave-Generated Currents for an Inlet in Casheen Bay – South-West Wave

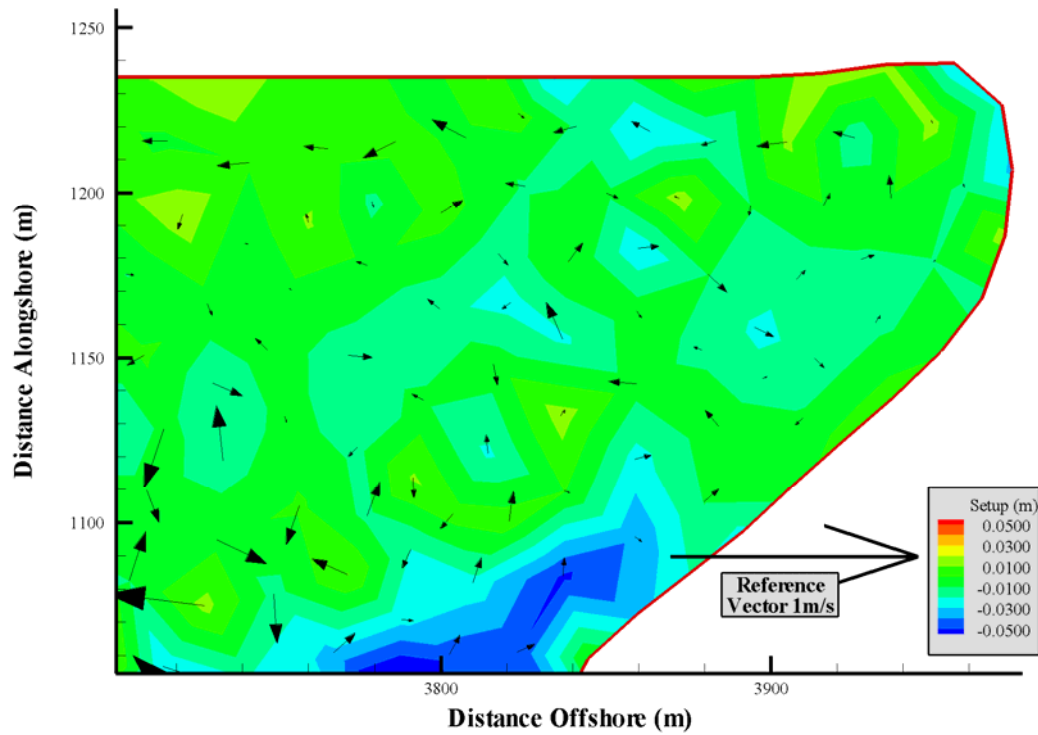


Figure 6.186 – Wave-Generated Currents for an Inlet in Casheen Bay – West Wave

6.17.6 Discussion

The results of the NM-WCIM for waves approaching Casheen Bay are interesting. It is obvious from Figure 6.157 that waves approaching Casheen Bay penetrate the depth of the bay to a much greater degree if they approach from the west (an unlikely event) than if they approach from the south-west as shown in Figure 6.156. A visual examination of the shape and bathymetry of the bay would tend to suggest that the bay developed as it did partially because of the prevailing wave direction. If the high wave heights shown deep in the bay for the westerly approaching wave occurred much in reality it is not unreasonable to believe that the shape of the bay would be different. This is further backed up by evidence from the NM-WDHM. Figure 6.176 shows strong wave generated effects deep in the bay for a wave approaching from a westerly direction whereas Figure 6.175 shows lesser wave-generated affects in the same area.

The wave-current interaction results of the NM-WCIM are as expected. The results show a small degree of variation in the wave phase due to the differing tidal currents. The areas where this change is most evident is where flow is concentrated, such as at the bottleneck between the two small islands in the north-east of the bay. The percentage difference of wave heights in this area between maximum flood and ebb flows is shown in Figure 6.173. Variation of up to 30% is evident. Larger variations are also evident but localised to small areas of coast where wave phase changes significantly for the different currents. This is caused by one of the more interesting results of the wave-current interaction model, that in some cases the change in wave behaviour due to wave-current interaction has a greater effect on the wave phase at the coastline even though the velocity there is of the same magnitude and indeed in some cases smaller. This effect is shown quite well in Figure 6.168.

The NM-WDHM shows how a small change in the direction of wave propagation can have quite a large effect on hydrodynamics within a specific area. For example Figure 6.179 and Figure 6.180 show how the longshore current along the exposed shore of the island occurs in almost opposite directions for the two wave scenarios examined despite the fact that the waves in question are only separated by a relatively small angle. An inspection of the wave fields in Figure 6.150 and Figure 6.151 shows why this is the case. It is evident that the change in direction of waves approaching the island in question can cause high waves to approach the island towards the middle of its western coast or

towards the top, thus influencing the direction of longshore current. Figure 6.146 shows the bathymetry in this region is quite complex thus causing the difference in waves approaching the island. Figure 6.177 shows how at the southern tip of the large island in the bay there is a good degree of wave generated disturbance for a wave approaching from the south-west in contrast to the lack of any significant effects at the same area in Figure 6.178 for waves approaching from the west.

Chapter 7: Conclusion & Recommendations

*“Ask, and it shall be given you; seek; and you shall find; knock and it shall be opened unto you.”
Matthew 7:7-8*

7.1 Conclusion

The stated aim of this thesis is to examine wave-current interaction and wave-generated hydrodynamics in the surf-zone. The preceding chapters do this in detail and in the process the NM-WCIM and NM-WDHM are derived and utilised effectively. They have been shown to provide results that compare well with expected values and trends and represent a step forward in the modelling of waves, wave-current-interaction and wave-driven hydrodynamics both within and outside the surf-zone.

Chapter 3 of this thesis develops a basic set of equations for the examination of wave-current interaction in the surf-zone. This derivation is carried out using a Galerkin-Eigenfunction method to obtain an extended elliptic mild-slope equation for waves and wave-current interaction including energy dissipation. The derivation of such an equation has not been presented previously using a Galerkin-Eigenfunction method. The use of this method gives an improvement in the quality of the final equations by including terms, such as extended current terms, that are neglected in previous derivations of similar formulae. The wave-current interaction equation is derived with the inclusion of energy dissipation from the outset, thus leading to an equation containing a more complete set of energy dissipation terms than many previously published equations. The equation is also presented in Helmholtz form to ensure adequate comparison with existing formulae. The usefulness of the formula derived is demonstrated effectively by its use in the finite element model whose results are presented in Chapter 6. The results compare favourably with both measured values and previously published numerical results.

Chapter 3 also presents the development of the extended elliptic mild-slope equation for waves and wave-current interaction including energy dissipation into a form that can be solved using the finite element method on a desktop computer. This development uses the Galerkin finite element method where shape functions and weighting functions are set to equal one another. The model uses two-dimensional triangular finite elements. The scalability of the mesh elements allows the model domain to be created in such a way as to maximise computer efficiency. Many existing computer models of a similar nature

utilise the finite difference methodology. Many of those that utilise finite elements do not include all the terms included in the basic equations for the NM-WCIM. Results from the NM-WCIM are shown in Chapter 6 of this thesis. The results obtained compare well with both measured data and results of previous similar models. The scalability and efficiency of the model are also demonstrated by the range of scenarios and scale of domains examined; from simple waves approaching a uniform beach to complex real-world bathymetry and large scale problems.

The iterative technique chosen to obtain convergence for wave-current interaction in the NM-WCIM is also effective. Convergence is achieved in quite a small number of iterative steps by inspecting the changes in the gradient of phase. Iteration on the gradient of phase is an effective and succinct method of examining wave-current interaction.

Chapter 4 of this thesis develops a numerical model for the examination of wave-driven hydrodynamics (NM-WDHM). The basic equations for this model are widely used but the driving forces for wave-driven effects selected by this project are unique. Chapter 4 presents the development of an equation to calculate radiation stress driving forces for the NM-WDHM based on the velocity potential results of the NM-WCIM. The development of a radiation stress formula directly in terms of velocity potential is an advance in the field of wave-driven hydrodynamics. The NM-WDHM also contains a state of the art bottom friction term and includes a turbulent diffusion term based on eddy viscosity values. The inclusion of such features ensure it performs well when compared with existing similar models. Chapter 6 presents the results of the NM-WDHM and comparison with measured data and the results of previous models. The results compare favourably with previously published modelled and measured results. The NM-WDHM is a finite-element areal model that iterates to a converged solution using a finite difference scheme. It is used on a desktop computer to solve problems with complex bathymetry.

Chapter 5 of this thesis continues the examination of Clyne (2008) of an new method for obtaining wave rays. This post-processing method using velocity potential results of a wave model or wave-current interaction model holds a lot of potential for the continued use of wave rays as an investigative tool for engineers. This project develops a wave energy ray that can be used for waves in the presence of a current. The wave energy rays are used to obtain breaking wave heights, particularly in regions where breaking waves

may recover due to complex bathymetry. Wave energy rays are also used in this project to obtain values of eddy viscosity, which are useful for the modelling of turbulent diffusion in the wave-driven hydrodynamic model. The fact that the wave ray process can be applied as a post-processing technique to any set of velocity potential results means that it is very computationally efficient. This technique is demonstrated in the results of Chapter 6 of this thesis.

This thesis has developed a new coupled model for the examination of wave-current interaction and wave-generated hydrodynamics both within and outside the surf-zone. The mathematical methods used to develop these models are innovative and succinct and the results of the models themselves compare well with published results and measurements.

7.2 Recommendations for Future Work

In the general area of investigation of waves and wave-current interaction it is apparent from the results of this project that further mathematical investigation is needed into the processes involved in wave breaking. Current formulae for wave breaking and energy dissipation due to wave breaking vary widely and are based largely on empirical evidence. Although wave breaking is a difficult field to investigate it is probable that a formula can be developed to link the various breaker types to bathymetry and wave conditions and hence provide a more universal equation for energy dissipation due to wave breaking.

The NM-WCIM could be modified to perform various extra functions. A possible future enhancement would be the inclusion of a subroutine to examine wave forces imparted on structures. A subroutine such as this could lead to the NM-WCIM being used for design of coastal structures such as breakwaters and jetties. This may or may not be coupled with an extension of the model to three dimensions.

The NM-WDHM could be enhanced to carry out various other functions with the addition of extra subroutines. Due to its basis in the overall equations of hydrodynamics any hydrodynamic behaviour of a fluid could be added to the model. Examples include subroutines to examine tidal effects, shipping wakes or sediment suspension and dispersion.

Appendix A: Finite Element Methodology

A.1 Introduction

This appendix gives a brief description of the finite element method as it is applied to the NM-WCIM and NM-WDHM. The description is not intended to be a complete discussion of the finite element technique. It is a specification of the particular type of finite element technique used in this thesis. For a complete discussion of the finite element technique the reader is referred to Zienkiewicz (1977).

A.2 Finite Element Technique

The finite element technique in general terms is a method of solving a set of equations for a series of unknown variables throughout a given domain. At the boundaries of said domain boundary conditions must be applied using known variables or relations to allow for the solution of the unknown variables across the domain. The domain is discretised into a number of different elements. A matrix of equations is then calculated for each individual element and combined into one overall “stiffness” matrix for the domain. This stiffness matrix multiplied by a vector of the unknown variables is equal to a vector of known boundary conditions. Hence the inverse of this mass matrix multiplied by the vector of known boundary conditions gives the solution to the vector of unknown variables.

A.3 Method of Weighted Residuals

Following the methodology of Pinder and Gray (1977); consider an operator Π that acts on an unknown function v_v in a domain B to generate a known function f_v .

$$\Pi v_v = f_v \text{ in a domain } B \quad (\text{A.1})$$

A function $\hat{v}_v(x)$ is made up of a linear combination of functions that satisfy the known conditions of v_v and the boundary.

$$\hat{v}_v(x) = \sum_{J=1}^M a^J N^J(x) \quad (\text{A.2})$$

Where $N_J(x)$ are shape functions and a^J are a series of constants chosen to ensure the boundary conditions of the domain B are satisfied.

Substituting Equation (A.2) in Equation (A.1) yields:

$$\mathfrak{R}(x) = \Pi \widehat{v}_v(x) - f_v(x) = \Pi \left[\sum_{J=1}^M a^J N^J(x) \right] - f_v(x) \quad (\text{A.3})$$

Where $\mathfrak{R}(x)$ is a residual.

The method of weighted residuals is a method through which the residual $\mathfrak{R}(x)$ is forced to equal zero in an average sense through the selection of appropriate values of a^J :

$$\int_B \mathfrak{R}(x) W^I(x) dx = 0, \quad I = 1, 2, \dots, M \quad (\text{A.4})$$

Where $W^I(x)$ is a weighting function.

Equation (A.4) for the method of weighted residuals can be expressed more explicitly as:

$$\int_B \left[\Pi \left(\sum_{J=1}^M a^J N^J(x) \right) - f_v(x) \right] W^I(x) dx = 0, \quad I = 1, 2, \dots, M \quad (\text{A.5})$$

A.3 Galerkin Method

A wide variety of functions may be chosen for the weighting function of the method of weighted residuals. The Galerkin Method is a special case of the method of weighted residuals where the weighting function W^I is set equal to the shape functions N^I . Thus the following version of Equation (A.5) is obtained for the Galerkin Method:

$$\int_B \left[\Pi \left(\sum_{J=1}^M a^J N^J \right) - f_v \right] N^I dx = 0, \quad I = 1, 2, \dots, M \quad (\text{A.6})$$

$$\int_B \Pi \left(\sum_{J=1}^M a^J N^J \right) N^I dx - \int_B f_v N^I dx = 0, \quad I = 1, 2, \dots, M \quad (\text{A.7})$$

$$\int_B \Pi \sum_{J=1}^M a^J N^J N^I dx = \int_B f_v N^I dx, \quad I = 1, 2, \dots, M \quad (\text{A.8})$$

The series of equations in Equation (A.8) can be expressed in matrix form as:

$$[B]\{A\} = \{F_v\} \quad (\text{A.9})$$

Where the elements of $[B]$ are made up using the shape functions and Π . The vector $\{A\}$ is constructed from the unknown variables a^j and the vector $\{F_v\}$ from the known function f_v .

The unknown variables a^j can then be solved as follows:

$$\{A\} = \{F_v\}[B]^{-1} \quad (\text{A.10})$$

Equation (A.10) shows the final form of the Galerkin Method as used in the NM-WCIM.

A.4 Shape Functions

A.4.1 Introduction

For this project a linear shape function was deemed appropriate for describing the behaviour of unknowns within a domain. This was chosen because of its simplicity and the fact that the elements chosen were deemed small enough that a linear shape function would provide an accurate result.

A.4.2 One-Dimensional Linear Shape Function

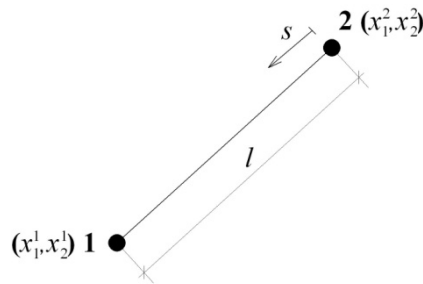


Figure A.1 – Linear One-Dimensional Finite Element

The chosen linear shape function, $N^I(s)$, for the one-dimensional models of this project is:

$$L^1(s) = 1 - \frac{s}{l} \quad (\text{A.11})$$

$$L^2(s) = \frac{s}{l} \quad (\text{A.12})$$

Where l is the length of the element.

The derivatives of this shape function are as follows:

$$\frac{d}{ds} [L^1(s)] = -\frac{1}{l} \quad (\text{A.13})$$

$$\frac{d}{ds} [L^2(s)] = \frac{1}{l} \quad (\text{A.14})$$

The integral of the one-dimensional shape function is:

$$\int_s (L^1)^\alpha (L^2)^\beta ds = \frac{\alpha! \beta!}{(\alpha + \beta + 1)!} l \quad (\text{A.15})$$

A.4.3 Two-Dimensional Linear Shape Function

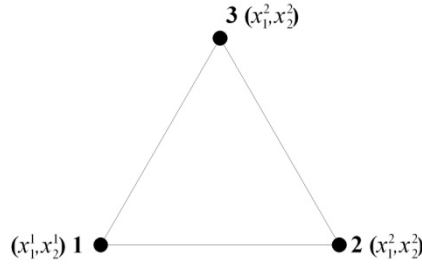


Figure A.2 – Triangular Two-Dimensional Finite Element

The chosen areal shape function, $L^I(s)$, for the two-dimensional models of this project is:

$$N^I = \frac{1}{2A} (a^I + b_j^I x_j), \quad I = 1, 2, 3, \quad j = 1, 2 \quad (\text{A.16})$$

Where I is the local node number and j denotes the coordinate direction. A is the area of the triangular element.

a^I and b^I are obtained using the determinants of the matrix as follows:

$$a^1 = x_1^1 x_2^3 - x_1^3 x_2^2 \quad (\text{A.17})$$

$$a^2 = x_1^3 x_2^1 - x_1^1 x_2^3 \quad (\text{A.18})$$

$$a^3 = x_1^1 x_2^2 - x_1^2 x_2^1 \quad (\text{A.19})$$

$$b_1^1 = x_2^2 - x_2^3 \quad (\text{A.20})$$

$$b_1^2 = x_2^3 - x_2^1 \quad (\text{A.21})$$

$$b_1^3 = x_2^1 - x_2^2 \quad (\text{A.22})$$

$$b_2^1 = x_1^2 - x_1^3 \quad (\text{A.23})$$

$$b_2^2 = x_1^3 - x_1^1 \quad (\text{A.24})$$

$$b_2^3 = x_1^1 - x_1^2 \quad (\text{A.25})$$

The derivative of the shape function is as follows:

$$\frac{dN^I}{dx_j} = \frac{b_j^I}{2A}, \quad I = 1, 2, 3, \quad j = 1, 2 \quad (\text{A.26})$$

The integral of the two-dimensional shape function is:

$$\iint_A (N^1)^\alpha (N^2)^\beta (N^3)^\gamma dA = \frac{\alpha! \beta! \gamma!}{(\alpha + \beta + \gamma + 2)!} 2A \quad (\text{A.27})$$

Appendix B: Comparison of Nomenclature with Clyne (2008)

Newell	Clyne
A = Area	Δ
A = Wave Amplitude	
A_D = Area between Energy Rays and Perpendicular Lines to Rays	
A_ξ = Amplitude of Instantaneous Set-Up (Wave Amplitude)	
A_ϕ = Amplitude of Velocity Potential	A_ϕ
a_m^m = Divergence of the Vector A	a_m^m
B = Empirical Wave Breaking Constants	
b = Width between Rays	b_1, b_2
C = Constant	
C = Relative Wave Celerity	C
$C_{precise}$ = Absolute Wave Celerity	
C_g = Relative Wave Group Velocity	C_g
$\mathbf{C}_{Gj} = CC_g \sigma \frac{\partial S_\phi}{\partial x_j}$	\mathbf{C}_G No Current
cn = Jacobian Elliptic Function	
$D = -\frac{\partial}{\partial s}(EnC)$	

E	= Energy	E
\mathbf{E}_x	= Basis Vector	\mathbf{E}_x
$\hat{\mathbf{e}}$	= Unit Vector	$\hat{\mathbf{e}}$
$\{E_{U_1}\}$	$= [KI] \left\{ \frac{dU_1}{dt} \right\}$	
$\{E_{U_2}\}$	$= [KI] \left\{ \frac{dU_2}{dt} \right\}$	
$\{E_{\eta}\}$	$= [KI] \left\{ \frac{d\bar{\eta}}{dt} \right\}$	
\mathbf{F}	= External Force per unit Volume	
f_B	= Friction Coefficient	
f	= Vertical Function such that $\tilde{\phi}(x, y, z) = f(z)\phi(x, y)$	Z
$G^{\alpha(i)}$	= The Cofactor of $g_{\alpha\beta}$	
g	= Gravitational Acceleration	\mathbf{g}
g_{xx}	= Metric Tensor	g_{xx}
g^{ij}	= Conjugate Metric Tensor	g^{ij}
g	= Determinant of the Metric Tensor Matrix	\mathfrak{g}
H_{st}	= Stable Wave Height	
H_0	= Deep-Water Wave Height	H_0
H_b	= Breaking Height	H_b
H_m	= Maximum Sustainable Wave Height	H_m
H	= Wave Height	H
h	= Depth	h
h'	$= h + \bar{\eta}$	

I	=	Integral of Various Functions	\mathcal{I}
i	=	$\sqrt{-1}$	i
K	=	Effective Wave Number	K
\mathbf{K}	=	Pressure Vector	
K_{cn}	=	Parameter of Jacobian Elliptic Function	
$[KI]$	=	Mass Matrix	
L^I	=	One-Dimensional Shape Function	L^I
L	=	Wave Length	L
L_j	=	Lateral Mixing Term	
L_0	=	Deep-Water Wave Length	L_0
l	=	Length of Element	l_D
M	=	Mass	M
M	=	Empirical Turbulence Coefficient	
m_b	=	Slope of Beach	
N	=	Empirical Turbulence Coefficient	
N^I	=	Two-Dimensional Shape Function	N^I
\mathbf{n}	=	Outward Unit Normal to Surface	\mathbf{n}
NM-WCIM	=	Newell Mullarkey Wave-Current Interaction Model	
NM-WDHM	=	Newell Mullarkey Wave-Driven Hydrodynamic Model	
p	=	Pressure	p
\mathbf{p}	=	Momentum	\mathbf{p}

$Q_b = e^{\frac{-(1-Q_b)}{r^2}}$	Q_b
$R_{ij} =$ Radiation Stress	
$\partial R =$ Boundary Curve	
$R_E =$ Reynolds Number	
$\mathbf{r}(s) =$ Positional Vector	$\mathbf{r}(s)$
$r = \frac{H}{\sqrt{2}H_m}$	r
$\{R_{U_j}\}$ and $\{R_{\eta_j}\} =$ Residual Vectors	
$S =$ Surface	
$S_\phi =$ Phase of Velocity Potential	
$s_0 =$ Wave Steepness	s_0
$T =$ Period	T
$t =$ Time	t
$\mathbf{t} =$ Tangent	\mathbf{t}
$\Delta t =$ Time Step	
$\mathbf{U} =$ Steady Component of Instantaneous Velocity	
$\mathbf{u} = (u_1, u_2, u_3) =$ Instantaneous Velocity	
$\tilde{\mathbf{u}} =$ Unsteady Component of Instantaneous Velocity	
$\mathbf{u}' =$ Wave Fluctuation of Velocity	
$\mathbf{u}'' =$ Turbulent Fluctuation of Velocity	
$u_1, u_2 =$ Horizontal Velocity	

V = Volume	V
W^I = Weighting Function	
W_v = Steady Component of Instantaneous Vertical Velocity	
w = Vertical Velocity = u_3	w
\tilde{w} = Unsteady Component of Instantaneous Vertical Velocity	
w' = Wave Fluctuation of Vertical Velocity	
w'' = Turbulent Fluctuation of Vertical Velocity	
$\mathbf{x} = (x, y)$ = Horizontal Coordinates	
x_1, x_2 = Horizontal Coordinates	x_1, x_2
z = Vertical Coordinates	
$z' = z - \bar{\eta}$	
$A_x, B_x, C_x, D_x, E_x, H_x, J_x,$ $M_x, P_x, W_x, Q_x, Q', Q'', Q_U, \tilde{Q}''$ = Various Functions of $h', \lambda',$ $\kappa, \bar{\eta}, I$ and z'	
α = An Empirical Wave Breaking Constant	

Γ	= Empirical Parameter Relating Wave Height to Water Depth	Γ
Γ_x	= Boundary	Γ_x
γ	= Energy Dissipation Factor	γ
γ_0	= Wave Breaking and Insipience Constant	
$\hat{\gamma}$	= Breaker Index	$\hat{\gamma}$
δ_{ij}	= Kroneker Delta	δ_{ij}
δ	= Boundary Layer Thickness	
ε_{ij}	= Eddy Viscosity	
$\tilde{\zeta}$	= Complex Wave Set-up	
ζ'	= Wave Fluctuation of Free Surface = $\text{Re}(\tilde{\zeta}) = \text{Re}(\xi e^{-i\omega t})$	
ζ''	= Turbulent Fluctuation of Free Surface	
$\eta(x, y, t)$	= Free Surface in the absence of turbulence = $\zeta' + \bar{\eta}$	
$\eta(x, y, t)$	= Free Surface	$\tilde{\eta}$
$\eta''(x, y, t)$	= Free Surface = $\zeta' + \zeta'' + \bar{\eta} = \zeta'' + \eta$	
$\bar{\eta}(x, y)$	= Steady Component of Free Surface	
κ	= Wave Number	κ

λ	= Empirical Wave Breaking Constants	
λ'	= $\frac{\sigma^2}{g}$	
μ	= Viscosity	
ν	= $\frac{\mu}{\rho}$	
ξ	= Complex Instantaneous Set-Up	η
ρ	= Density	ρ
σ	= Intrinsic/Relative Frequency	
σ'_{ij}	= A Stress Tensor	
τ_j^B	= Bottom Stress	
τ_j^F	= Stress at the Free Surface	
Υ	= $\mathbf{t} \cdot \frac{d\mathbf{n}}{ds}$	

$\tilde{\Phi}(x, y, z, t)$	= Velocity Potential in Three-Dimensional and Time Space $= \text{Re}(\tilde{\phi}(x, y, z)e^{-i\omega t})$	Φ
$\tilde{\phi}(x, y, z) = \tilde{\phi}_1 + i\tilde{\phi}_2$	= Velocity Potential in Three-Dimensional Space $= f(z)\phi(x, y)$	ϕ
$\phi(x, y) = \phi_1 + i\phi_2$	= Velocity Potential in Two-Dimensional Space	ϕ
$\phi' = \phi\sqrt{CC_g}$	= Scaled Helmholtz Style Velocity Potential	$\hat{\phi}$
$\hat{\phi} = A_\phi e^{iS_\phi}$	= One-Dimensional Velocity Potential	$\frac{\tilde{\phi}}{\sqrt{CC_g}}$
ψ	$= \frac{1}{\left(\mathbf{t} \cdot \frac{d\mathbf{n}}{ds}\right)^2 + 4\left(\frac{\partial S_\phi}{\partial n}\right)^2}$	ψ
$\hat{\psi}$	$= \frac{1}{\Upsilon^2 + 4\kappa^2}$	$\hat{\psi}$
Ω	= External Force Potential	
ω	= Angular Frequency (in rad/s)	
$\nabla = \frac{\partial}{\partial x} + \frac{\partial}{\partial y} + \frac{\partial}{\partial z}$		∇
$\nabla_h = \frac{\partial}{\partial x} + \frac{\partial}{\partial y}$		∇_h

References

Primary References

- Arthur, R.S., 1950.** Refraction of shallow water waves: the combined effect of currents and under water topography. EOS Trans, 31: 549-552.
- Battjes, 1975.** Modeling of Turbulence in the Surf Zone, Symposium on Modeling Techniques. American Society of Civil Engineers, San Francisco, pp. 1050-1061.
- Battjes, J.A. and Janssen, J., 1978.** Energy Loss and set-up due to breaking of random waves, 16th International Conference on Coastal Engineering. ASCE, New York, pp. 569-587.
- Battjes, J.A. and Stive, M.J.F., 1985.** Calibration and verification of a dissipation model for random breaking waves. Journal of Geophysical Research, 90(C5): 9159-9167.
- Berkhoff, J.C.W., 1972.** Computation of combined refraction-diffraction, 13th International conference on Coastal Engineering. ASCE, New York, Vancouver, pp. 471-490.
- Berkhoff, J.C.W., 1976.** Mathematical models for simple harmonic linear water waves - wave diffraction and refraction, Publication No. 163.
- Berkhoff, J.C.W., Booij, N. and Radder, A.C., 1982.** Verification of numerical wave propagation models for simple harmonic linear water waves. Coastal Engineering, 6: 255-279.
- Booij, N., 1981.** Gravity waves on water with non-uniform depth and current. Doctoral Thesis published as Communications on Hydraulics Report no. 81-1, Delft University of Technology, Dept. Civil Eng.
- Booij, N., 1983.** A note on the accuracy of the mild-slope equation. Coastal Engineering, 7: 191-203.
- Booij, N., Ris, R.C. and Holthuijsen, L.H., 1999.** A third-generation wave model for coastal regions, Part I, Model description and validation. Journal of Geophysical Research, 104(C4): 7649-7666.
- Bowen, A.J., 1969.** The Generation of Longshore Currents on a Plane Beach. Journal of Marine Research, 27(1): 206-215.
- Bowen, A.J., Inman, D.L. and Simmons, V.P., 1968.** Wave "Set-Down" and Set-Up. Journal of Geophysical Research, 73(8): 2569-2577.
- Brevik, I. and Aas, B., 1980.** Flume experiments on waves and currents, I. Rippled bed. Coastal Engineering, 3: 149-177.
- Briggs, M., Demirbilek, Z. and Green, D., 1996.** Wave-current Interaction at Inlets, 25th International Coastal Engineering Conference, pp. 1219-1232.
- Chamberlain, P.G. and Porter, D., 1995.** The Modified Mild-Slope Equation. Journal of Fluid Mechanics, 291: 393-407.
- Chawla, A., Ozkan-Haller, H.T. and J.T., K., 1998.** Spectral model for wave transformation and breaking over irregular bathymetry. Journal of Waterway, Port, Coastal and Ocean Engineering, 124: 189-198.
- Chen, H.S., 1986.** Effects of Bottom Friction and Boundary Absorption on Water Wave Scattering. Applied Ocean Research, 8(2): 99-104.
- Chen, H.S. and Houston, J.R., 1987.** Calculation of Water Level Oscillation in Coastal Harbors: HARBS and HARBD User's Manual, Instructional Report CERC-87-2, Coastal Engineering Research Center, WES, Vicksburg, MS.

- Chen, W., Panchang, V. and Demirbilek, Z., 2005.** On the modeling of wave-current interaction using the elliptic mild-slope wave equation. *Ocean Engineering*(32): 2135-2164.
- Church, J.C. and Thornton, E.B., 1993.** Effects of breaking wave induced turbulence within a longshore current model. *Coastal Engineering*, 20: 1-28.
- Clyne, M., 2008.** An Elliptic-Parabolic Coastal Wave Model Incorporating Shorelines of Varying Curvature Using Tensors and Incorporating Breaking with Recovery Using Rays. PhD Thesis, National University of Ireland, Galway, Galway.
- Clyne, M. and Mullarkey, T., 2004.** Parabolic Absorbing and Radiating Boundary Conditions with Diffraction and Wave Breaking, The fourteenth international offshore and polar engineering conference (ISOPE), Toulon, France., pp. 594-601.
- Clyne, M. and Mullarkey, T., 2008.** Simulating wave reflection using radiation boundary. *Journal of Coastal Research*, 24(1A): 24-40.
- Cokelet, E.D., 1977.** Steep Gravity Waves in Water of Arbitrary Uniform Depth. *Phil. Trans. Roy. Soc.*, London, 286(Series A): 183-230.
- Dally, W.R., 1990.** Random breaking waves: a closed-form solution for planar beaches. *Coastal Engineering*, 14: 233-263.
- Dally, W.R., Dean, R.G. and Dalrymple, R.A., 1985.** Wave height variation across beaches of arbitrary profile. *Journal of Geophysical Research*, 90(C6): 11917-11927.
- Dalrymple, R.A., Kirby, J.T. and Hwang, P.A., 1984.** Wave Diffraction Due to Areas of High Energy Dissipation. *Journal of Waterway, Port, Coastal and Ocean Engineering*, 110(1): 67-79.
- Danish Hydraulic Institute, 2008a.** MIKE 21 Flow Model, Hydrodynamic Model, Scientific Documentation (Edition 2008), Danish Hydraulic Institute, DK-2970 Hørsholm, Denmark.
- Danish Hydraulic Institute, 2008b.** MIKE 21 Flow Model, Hydrodynamic Model, User Guide (Edition 2008), Danish Hydraulic Institute, DK-2970 Hørsholm, Denmark.
- Danish Hydraulic Institute, 2008c.** MIKE 21, Elliptic Mild Slope Wave Model, Scientific Documentation (Edition 2008), Danish Hydraulic Institute, DK-2970 Hørsholm, Denmark.
- De Girolamo, P., Kostense, J.K. and Dingemans, M.W., 1988.** Inclusion of Wave Breaking in a Mild Slope Model. In: B.A. Schrefler and O.C. Zienkiewicz (Editors), *Computer Modelling in Ocean Engineering: Proceedings of an International Conference on Computer Modelling in Ocean Engineering*. Aa Balkema; Rotterdam, Venice.
- Dean, R.G., 1965.** Stream Function Representation of Nonlinear Ocean Waves. *Journal of Geophysical Research*, 70: 4561-4572.
- Dean, R.G., 1974.** Evaluation and Development of Water Wave Theories for Engineering Applications, Coastal Engineering Research Center, U.S. Army Engineer Waterways Experiment Station.
- Dean, R.G. and Dalrymple, R.A., 1991.** *Water Wave Mechanics for Engineers and Scientists*. World Scientific Publishing Company, Teaneck, NJ.
- Demirbilek, Z. and Vincent, L., 2002.** Water Wave Mechanics. In: Z. Demirbilek (Editor), *Coastal Engineering Manual, Part 2, Coastal Hydrodynamics*. Chapter 1 , Engineer Manual 1110-2-1100,. U.S. Army Corps of Engineers, Washington, DC. .
- Demirbilek, Z. and Panchang, V., 1998.** CGWAVE: A coastal surface water wave model of the mild slope equation, Technical Report CHL-TR-98-26.

- Demirbilek, Z. and Webster, W.C., 1992a.** Application of the Green-Naghdi Theory of Fluid Sheets to Shallow-Water Wave Problems; Report 1: Model Development, Technical Report CERC-92-11, U.S. Army Engineer Waterways Experiment Station, Vicksburg, MS.
- Demirbilek, Z. and Webster, W.C., 1992b.** User's Manual and Examples for GNWAVE, Final Report, "Technical Report CERC-92-13, U.S. Army Engineer Waterways Experiment Station, Vicksburg, MS.
- Dingemans, M.W., Radder, A.C. and Vriend, J.J.D., 1987.** Computation of the Driving Forces and Wave-Induced Currents. *Coastal Engineering*, 11: 539-563.
- Divoky, D., Le Méhauté, B. and Lin, A., 1970.** Breaking waves on gentle slopes. *Journal of Geophysical Research*, 75(9): 1681-16921.
- Dobson, R.S., 1967.** Some Applications of a Digital Computer to Hydraulic Engineering Problems, Technical Report No. 80, Department of Civil Engineering, Stanford University, Stanford, CA.
- Ebersole, B.A., 1985.** Refraction-Diffraction Model for Linear Water Waves. *Journal of Waterways, Port, Coastal, and Ocean Engineering*, III(WW6): 939-953.
- Ebersole, B.A., Cialone, M.A. and Prater, M.D., 1986.** Regional Coastal Processes Numerical Modeling System, Report 1, RCPWAVE - A Linear Wave Propagation Model for Engineering Use, Technical Report CERC-86-4, U.S. Army Engineer Waterways Experiment Station, Vicksburg, MS., Vicksburg, MS.
- Fenton, J.D., 1985.** A Fifth-Order Stokes Theory for Steady Waves. *Journal of Waterway, Port, Coastal and Ocean Engineering*, 111: 216-234.
- Fenton, J.D., 1988.** The Numerical solution of Steady Water Wave Problem. *Jour. Comp. and Geo*, 14: 357-368.
- Galvin, C.J., 1968.** Breaker Type Classification on Three Laboratory Beaches. *Journal of Geophysical Research*, 73(12): 3651-3659.
- Haas, K.A., Svendsen, I.A., Haller, M.C. and Zhao, Q., 2003.** Quasi-three-dimensional modeling of rip current systems. *Journal of Geophysical Research*, 108(C7): 3217.
- Hamilton, D.G. and Ebersole, B.A., 2001.** Establishing uniform longshore currents in a large-scale sediment transport facility. *Coastal Engineering*, 42: 199-218.
- Harrison, W. and Wilson, W.S., 1964.** Development of a Method for Numerical Calculation of Wave Refraction, Technical Memorandum No. 6, Coastal Engineering Research Center, U.S. Army Engineer Waterways Experiment Station, Vicksburg, MS.
- Hedges, T.S., 1976.** An Empirical Modification to Linear Wave Theory. *Proceedings of the Institute of Civil Engineers*, 61: 575-579.
- Heinbockel, J.H., 2001.** Introduction to Tensor Calculus and Continuum Mechanics, <http://www.math.odu.edu/~jh/h/counter2.html>. Trafford.
- Houston, J.R., 1981.** Combined refraction and diffraction of short waves using the finite element method. *Applied Ocean Research*, 3(4): 163-170.
- Isaacson, M. and Qu, S., 1990.** Waves in a harbour with partially reflecting boundaries. *Coastal Engineering*, 14: 193-214.
- Isobe, M., 1999.** Equation for Numerical Modeling of Wave Transformation in Shallow Water. In: J.B. Herbich (Editor), *Developments in Offshore Engineering*. Gulf Publishing Company, pp. 101-162.

- Jensen, R.E., Vincent, C.L. and Abel, C.E., 1987.** SHALWV - Hurricane Wave Modeling and Verification; User's Guide to SHALWV: Numerical Model for Simulation of Shallow-Water Wave Growth, Propagation, and Decay," Instruction Report CERC-86-2, No. 2, U.S. Army Engineer Waterways Experiment Station, Coastal Engineering Research Center, Vicksburg, MS.
- Jonsson, I.G., Skovgaard, O. and Jacobsen, T.S., 1974.** Computation of Longshore Currents, 14th Coastal Engineering Conference. American Society of Civil Engineers.
- Kim, H., 2004.** Practical spreading of driving forces for wave-driven currents. *Ocean Engineering*, 31: 435-453.
- Kirby, J.T., 1984.** A Note on Linear Surface Wave-Current Interaction Over Slowly Varying Topography. *Journal of Geophysical Research*, 89(C1): 745-747.
- Kirby, J.T., 1986.** Higher order approximations in the parabolic equation method for water waves. *Journal of Geophysical Research*, 91(C1): 933-952.
- Kirby, J.T., 1989.** A note on parabolic radiation boundary conditions for elliptic wave calculations. *Coastal Engineering*, 13: 211-218.
- Kirby, J.T. and Dalrymple, R.A., 1984.** Verification of a Parabolic Equation for Propagation of Weakly-Nonlinear Waves. *Coastal Engineering*, 8: 219-232.
- Kirby, J.T. and Dalrymple, R.A., 1986a.** An Approximate Model for Nonlinear Dispersion in Monochromatic Wave Propagation Models. *Coastal Engineering*, 9: 545-561.
- Kirby, J.T. and Dalrymple, R.A., 1986b.** Modeling Waves in Surfzones and Around Islands. *Journal of Waterway, Port, Coastal and Ocean Engineering*, 112: 78-93.
- Kirby, J.T., Dalrymple, R.A. and Kaku, H., 1994.** Parabolic approximations for water waves in conformal coordinate systems. *Coastal Engineering*, 23: 185-213.
- Komar, P.D., 1998.** Beach Processes and Sedimentation. Prentice Hall.
- Komar, P.D. and Inman, D.L., 1970.** Longshore Sand Transport on Beaches. *Journal of Geophysical Research*, 75(30): 5914-5927.
- Korteweg, D.J. and de Vries, G., 1895.** On the Change of Form of Long Waves Advancing in a Rectangular Canal, and on a New Type of Stationary Waves. *Phil. Mag. 5th Series*, 39: 422-443.
- Kostense, J.K., Dingemans, M.W. and van den Bosch, P., 1988.** Wave-Current Interaction in Harbours, Proceedings of 21st International Conference on Coastal Engineering. ASCE, New York, pp. 32-46.
- Kraus, N.C. and Larson, M., 1991.** NMLONG: Numerical Model for Simulating the Longshore Current. Report 1: Model Development and Tests. Technical Report DRP-91-1, US Army Engineer Waterways Experiment Station, Vicksburg, MS.
- Kuriyama, Y. and Nakatsukasa, T., 2000.** A one-dimensional model for undertow and longshore current on a barred beach. *Coastal Engineering*, 40: 39-58.
- Larson, M. and Kraus, N.C., 1991.** Numerical Model of Longshore Current for Bar and Trough Beaches. *Journal of Waterway, Port, Coastal and Ocean Engineering*, 117(4): 326-347.
- Larson, M. and Kraus, N.C., 2002.** NMLONG: Numerical Model for Simulating Longshore Current. Report 2: Wave-Current Interaction, Roller Modeling, and Validation of Model Enhancements ERDC/CHL TR-02-22, U.S. Army Engineer Research and Development Center, Coastal and Hydraulics Laboratory, Vicksburg, MS.

- Leont'yev, I.O., 1997.** Short-term shoreline changes due to cross-shore structures: a one-line numerical model. *Coastal Engineering*, 31: 57-75.
- Liu, P.L.-F., 1994.** Model Equations for Wave Propagation from Deep to Shallow Water. *Advances in Coastal and Ocean Engineering*, 1. World Scientific.
- Liu, P.L.-F. and Mei, C.C., 1976.** Water Motion on a Beach in the Presence of a Breakwater 2. Mean Currents. *Journal of Geophysical Research*, 81(18): 3085-3094.
- Longuet-Higgins, M.S., 1970a.** Longshore Currents Generated by Obliquely Incident Sea Waves, 1. *Journal of Geophysical Research*, 75(33): 6778-6789.
- Longuet-Higgins, M.S., 1970b.** Longshore Currents Generated by Obliquely Incident Sea Waves, 2. *Journal of Geophysical Research*, 75(33): 6790-6801.
- Longuet-Higgins, M.S. and Stewart, R.W., 1963.** A Note on Wave Setup. *Journal of Marine Research*, 21(1): 4-10.
- Longuet-Higgins, M.S. and Stewart, R.W., 1964.** Radiation stresses in water waves: A physical discussion with applications. *Deep Sea Research*, 11: 529-562.
- Madsen, P.A., Murray, R. and Sorenson, O.R., 1991.** A new form of the Boussinesq equations with improved linear dispersion characteristics. *Ocean Engineering*, 15: 371-388.
- Madsen, P.A. and Sorenson, O.R., 1992.** A New Form of Boussinesq Equations with Improved Linear Dispersion Characteristics: Part 2. A Slowly-Varying Bathymetry. *Coastal Engineering*, 18: 183-204.
- Massel, S.R., 1992.** Inclusion of wave-breaking mechanism in a modified mild-slope model. In: M.L. Banner and R.H.J. Grimshaw (Editors), *Breaking Waves IUTAM Symposium 1991*, Sydney, Australia. Springer-Verlag, Berlin, pp. 319-324.
- Massel, S.R., 1993.** Extended refraction-diffraction equation for surface waves. *Coastal Engineering*, 19: 97-126.
- Massel, S.R., 1994.** Measurement and Modeling of Waves Incident on Steep Islands or Shoals, *International Symposium: Waves - Physical and Numerical Modeling*, University of British Columbia, Vancouver, Canada. August 21-24, 1994.
- McCowan, A.D., 1987.** The Range of Application of Boussinesq Type Numerical Short Wave Models, 22nd IAHR Congress, Laussane, pp. 378-384.
- Mei, C.C. and Angelides, D., 1977.** Longshore Circulation Around a Conical Island. *Coastal Engineering*, 1: 31-42.
- Mei, C.C. and LeMehaute, B., 1966.** Note on the Equations of Long Waves Over an Uneven Bottom. *Journal Geophysical Research*, 71: 393.
- Mei, C.C., Stiassnie, M. and Yue, D.K.-P., 2005.** Theory and Applications of Ocean Surface Waves. *Advanced Series on Ocean Engineering*, 23. World Scientific.
- Munk, W.H., 1949.** The Solitary Wave Theory and Its Application to Surf Problems. *Annals New York Academy of Science*, 51: 376-423.
- Newell, C. and Mullarkey, T., 2007a.** The Sensitivity of Set-up/Set-down and Wave-Driven Currents to Different Breaking Models, 26th International Conference on Offshore and Arctic Engineering. American Society of Mechanical Engineers, San Diego, CA, USA.

- Newell, C. and Mullarkey, T., 2007b. Wave-Current Interaction Involving Iteration between Finite Element Wave and Current Models. *Journal of Coastal Research*(SI 50).
- Newell, C., Mullarkey, T. and Clyne, M., 2005a. The Development of a Finite Element Wave-Current Interaction Model, Canadian Coastal Conference, Dartmouth, Nova Scotia.
- Newell, C., Mullarkey, T. and Clyne, M., 2005b. Radiation Stress due to ocean waves and the resulting currents and set-up/set-down. *Ocean Dynamics*, 55: 499-514.
- Noda, E.K., Sonu, C.J., Rupert, V.C. and Collins, J.I., 1974. Nearshore Circulations Under Sea Breeze Conditions and Wave-Current Interactions in the Surf Zone, Technical Report No. 4, Tetra Tech, Inc., Pasadena, CA.
- Nwogu, O., 1993. Alternative form of Boussinesq equations for nearshore wave propagation. *Journal of Waterway, Port, Coastal and Ocean Engineering*, 119(6): 618-638.
- Nwogu, O. and Demirbilek, Z., 2001. BOUSS-2D: A Boussinesq wave model for coastal regions and harbors, ERDC/CHL TR-01-25, U.S. Army Engineer Research and Development Center, Vicksburg, MS.
- Panchang, V., Chen, W., Xu, B., Schlenker, K., Demirbilek, Z. and Okihiro, M., 2000. Exterior bathymetric effects in elliptic harbour wave models. *Journal of Waterway, Port, Coastal and Ocean Engineering*, 126(2): 71-78.
- Panchang, V.G., Pearce, B.R., Wei, G. and Cushman-Roisin, B., 1991. Solution of the mild-slope wave problem by iteration. *Applied Ocean Research*, 13(4): 187-199.
- Panchang, V.G., Xu, B. and Demirbilek, Z., 1999. Wave Prediction Models for Coastal Engineering Applications. In: J.B. Herbich (Editor), *Developments in Offshore Engineering*. Gulf Publishing Company, pp. 163-194.
- Péchon, P., Rivero, F., Johnson, H., Chesher, T., O'Connor, B., Tanguy, J.-M., Karambas, T., Mory, M. and Hamm, L., 1997. Intercomparison of wave-driven current models. *Coastal Engineering*, 31: 199-215.
- Peregrine, D.H., 1967. Long waves on a beach. *Journal of Fluid Mechanics*, 27: 815– 827.
- Pinder, G.F. and Gray, W.G., 1977. *Finite Element Simulation in Surface and Subsurface Hydrology*. Academic Press, Inc.
- Porter, D. and Staziker, D.J., 1995. Extensions of the Mild-Slope Equation. *Journal of Fluid Mechanics*, 300: 367-382.
- Putnam, J.A. and Johnson, J.W., 1949. The dissipation of wave energy by bottom friction. *Trans. Am. Geoph. Union*, 30: 67-74.
- Radder, A.C., 1979. On the parabolic equation method for water-wave propagation. *Journal of Fluid Mechanics*, 95(1): 159-176.
- Smith, J.M., 2003. Surf Zone Hydrodynamics. In: Z. Demirbilek (Editor), *Coastal Engineering Manual, Part 2, Coastal Hydrodynamics*. Chapter 4 , Engineer Manual 1110-2-1100,. U.S. Army Corps of Engineers, Washington, DC. .
- Sorenson, R.M., 2006. *Basic Coastal Engineering*. Springer.
- Steward, D.R. and Panchang, V.G., 2000. Improved coastal boundary condition for surface water waves. *Ocean Engineering*, 28: 139-157.
- Sukardi, Y., 2008. Boussinesq Equation. <http://boussinesq-equation.blogspot.com/feeds/posts/default>.

- Sverdrup, H.U. and Munk, W.H., 1947.** Wind, Sea and Swell: Theory of Relations for Forecasting, U.S. Navy Hydro. Office, Publication No. 601.
- Thompson, E.F., Chen, H.S. and Hadley, L.L., 1996.** Validation of numerical model for wind waves and swell in harbors. *Journal of Waterway, Port, Coastal and Ocean Engineering*, 122(6): 245-257.
- Thornton, E.B., 1970.** Variation of Longshore Current Across the Surf Zone, 12th Coastal Engineering Conference. American Society of Civil Engineers, pp. 291-308.
- Thornton, E.B. and Guza, R.T., 1983.** Transformations of wave height distribution. *Journal of Geophysical Research*, 88: 5925-5938.
- Tsay, T.-K. and Liu, P.L.-F., 1983.** A Finite Element Model for Wave Refraction and Diffraction. *Applied Ocean Research*, 5(1): 30-37.
- Vincent, L., Demirbilek, Z. and Weggel, J.R., 2002.** Estimation of Nearshore Waves. In: Z. Demirbilek (Editor), *Coastal Engineering Manual, Part 2, Coastal Hydrodynamics*. Chapter 3, Engineer Manual 1110-2-1100,. U.S. Army Corps of Engineers, Washington, DC. .
- Watanabe, A. and Maruyama, K., 1986.** Numerical Modeling of Nearshore Wave Field Under Combined Refraction Diffraction and Breaking. *Coastal Engineering in Japan*, 29: 19-39.
- Weggel, J.R., 1972.** Maximum Breaker Height. *Journal of the Waterways, Harbors and Coastal Engineering Division, Proceedings of the ASCE*, 98(WW4): 529-548.
- Wei, G., Kirby, J.T., Grilli, S.T. and Subramanya, R., 1995.** A Fully Nonlinear Boussinesq Model for Surface Waves, Part I, Highly Nonlinear Unsteady Waves. *Journal of Fluid Mechanics*, 294: 71-92.
- Wiegel, R.L., 1960.** A Presentation of Cnoidal Wave Theory for Practical Application. *Journal of Fluid Mechanics*, 7: 273-286.
- Xu, B. and Panchang, V., 1993.** Outgoing boundary conditions for finite difference elliptic water-wave models. *Proceedings, Royal Society of London, Series A, London, UK*, 441: 575-588.
- Xu, B., Panchang, V. and Demirbilek, Z., 1996.** Exterior reflections in elliptic harbour wave models. *Journal of Waterway, Port, Coastal and Ocean Engineering*, 122(3): 118-126.
- Yoon, S.B. and Liu, P.L.-F., 1989.** Interactions of currents and weakly nonlinear water waves in shallow water. *Journal of Fluid Mechanics*, 205: 397-419.
- Zhao, L., Panchang, V., Chen, W., Demirbilek, Z. and Chhabra, N., 2001.** Simulation of wave breaking effects in two-dimensional elliptic harbour wave models. *Coastal Engineering*, 42: 359-373.
- Zienkiewicz, O.C., 1977.** *The Finite Element Method*. McGraw Hill, London; New York, 787 pp.

Secondary References

- Airy, G.B., 1845.** On Tides and Waves, Article 192, *Encyclopaedia Metropolitana*, London, pp. 241-396.
- Boussinesq, J., 1871.** Theorie de L'intumescence Liquide Appelee Onde Solitaire ou de Translation se Propageant dans un Canal Rectangulaire. *Comptes Rendus Acad. Sci. Paris*, 72: 755-759.
- Boussinesq, J., 1872.** Théorie des ondes et des remous qui se propagent le long d'un canal rectangulaire horizontal, en communiquant au liquide contenu dans ce canal des vitesses sensiblement pareilles de la surface au fond". *Journal de Mathématique Pures et Appliquées, Deuxième Série* (17): 55-108.

-
- Demirbilek, Z., 1994.** Comparison Between REFDIFS and CERC Shoal Laboratory Study, Unpublished Report, Waterways Experimentation Station, Vicksburg, MS.
- Korteweg, D.J. and de Vries, G., 1895.** On the Change of Form of Long Waves Advancing in a Rectangular Canal, and on a New Type of Stationary Waves. *Phil. Mag. 5th Series*, 39: 422-443.
- Masch, F.D. and Wiegel, R.L., 1961.** Cnoidal waves, tables of functions, Council on Wave Research, Engineering Foundation, Richmond: Calif.
- Miche, R., 1954.** Mouvements Ondulatoires des Mers en Profondeur Constante en Decroissant (translation by Lincoln and Chevron), University of California at Berkley, Wave Research Laboratory, Series 3, Issue 363.
- Resio, D.T., 1993.** STWAVE: Wave Propagation Simulation Theory, Testing and Application, Department of Oceanography, Ocean Engineering, and Environmental Science, Florida Institute of Technology.
- Sonu, C.J., 1975.** COmputer prediction of nearshore and surf zone statistics: final report. Report TC-394, Tetra Tech, Inc., Pasadena, California.
- Stokes, G.G., 1847.** On the Theory of Oscillatory Waves. *Trans. Camb. Phil. Soc.*, 8: 441-455.
- Stokes, G.G., 1880.** *Math. Phys. Papers*, 1. Camb. Univ. Press.
- Szuwalski, A., 1970.** Littoral Environment Observation Program in California - Preliminary Report. Miscellaneous Publication 2-70, U.S. Army Coastal Engineering Research Center, Washington, DC.

Derive Continuity Derive Momentum



Flowchart of Mathematical Derivations

C. Newell